# Environmental Science and Technology

# (2012)

## Volume 2

Edited by

## George A. Sorial
## Jihua Hong

# Environmental Science and Technology

## (2012)

**Volume 2**

Edited by

George A. Sorial
Jihua Hong

# TABLE OF CONTENTS

## LAND (SOIL, SOLID WASTE) POLLUTION AND REMEDIATION

### *Contaminants in the Subsurface*

### *Natural Attenuation of Contaminants*
### */In-Situ Remediation*

### *Solid Waste Management / Polymer Waste Recycling and Management*

### *Phytoremediation of Organic Pollutants*

### *Polymer Waste Recycling and Management*

## BIO-ASSESSMENT AND TOXICOLOGY

### *Human Exposure*

### *Bio-response and Ecotoxicology*

*Bioavailability and Bio-accumulation*

*Microbiology and Microbisl Degradation*

**WETLANDS AND SEDIMENTS**

*Wetlands for Wastewater Treatment*

*Wetland Conservation*

*Assessment of Sediments*

*Remediation of Contaminated Sediments*

## GLOBAL CHANGE

*Global Warming and its Impacts*

*Carbon Discharge Reduction*

## METALS

*Metal Distribution*

## *Metal Removal and Remediation*

## *Speciation, Bioavailability and Accumulation*

## *Phytoremediation*

# CHLORINATED AND OTHER PERSISTENT ORGANIC COMPOUNDS

## *Degradation of Persistent Organic Pollutants*

### *Characterization of Organic Pollutants*

## MODELING

### *Environmental Simulation*

### *Water Quality Modeling*

## GIS, DATABASE, AND REMOTE SENSING

### *GIS for Environmental Assessment*

### *Data Management and Statistics*
### */Environmental Remote Sensing Applications*

## ENVIRONMENTAL ANALYSIS AND MEASUREMENTS

### *Environmental Analysis*

### *New Method Applications*

## *Environmental Monitoring*

# SOCIETY AND THE ENVIRONMENT

## *Society and the Environment*

## *Environmental Education*

# ENVIRONMENTAL PLANNING AND MANAGEMENT

## *Environmental Quality and Planning*

## *Energy-related Environmental Problems*

### *Environmental Policy and Management*

## RENEWABLE ENERGY DEVELOPMENT

### *Water Energy Nexus*

### *Wind Energy* / **Solar Energy**

### *Bio-fuels*

### Special Energy Development

# LAND (SOIL, SOLID WASTE) POLLUTION
# AND
# REMEDIATION

# ASSESSMENT OF HEAVY METAL LEACHING RATES FROM TOPSOILS ON REGIONAL SCALE (PART I)

J. Schmidt, A. Steinz, M. Schindewolf (Technical University Freiberg, Germany)

**ABSTRACT:** The leaching rate of heavy metals with drainage water is a significant criterion for assessing heavy metal concentrations of soils and associated risks of ground water pollution. However, the transport rates of heavy metals in soils are difficult to quantify. First of all monitoring is limited to small lysimeter plots and results are hardly transferable. Secondly the solid-liquid-transfer conditions in soils are highly variable, primarily due to the fluctuating retention time of percolating soil water.

This paper aims to introduce a new method that allows to estimate the leaching rate of heavy metals from contaminated top soils for standardised transfer conditions. The method should provide an effective and easy to use tool for the assessment of contaminated soils on regional scale. The developed method is based on metal specific transfer functions which have to be determined experimentally. For laboratory tests 16 undisturbed soil columns were taken at different highly contaminated sites in the German States of Saxony and Baden-Wuerttemberg. Parallel to the column tests the mobilizable metal contents of each of the tested soils were determined using different standardised extraction methods (DIN 38414, 19730, 19735). Measured metal concentrations of percolating soil water at unsaturated, steady-state flow conditions were plotted as a function of corresponding mobilizable metal contents of the tested soils. This comparison results in a set of empirical functions - one for each extraction method respectively metal species. Best fit was obtained using the $NH_4NO_3$-extraction (DIN 19730), where correlation coefficients range between r=0,62 and r=0,85. Since $NH_4NO_3$ mobilizable metal contents are available on regional scale in Germany the empirical transfer functions allow to calculate metal concentration of percolating soil water based on mobilizable metal contents as determined by simple extraction methods. As a first example heavy metal concentrations were calculated for the State of Saxony based on available $NH_4NO_3$ monitoring data of about 4600 topsoil samples. Leaching rates were calculated by multiplying the resulting metal concentrations with local groundwater recharge rates. In order to assess subsurface retention the calculated topsoil losses for Zn and Pb were compared with measured metal discharge rates of a selected river catchment resulting in a much greater retention of Pb than Zn.

## INTRODUCTION

On the background of soil and groundwater conservation particular attention has been focused on the leaching of heavy metals from contaminated topsoils for many years. There are various reports referring to laboratory methods (e.g. Davidson et al. 2006), field experiments (e.g. Beesley et al. 2010) and modelling approaches (e.g. Dijkstra et al. 2004) in order to assess the mobility of heavy metals in soils. However, only a few attempts have been made to evaluate the fate of heavy metals in soils on regional scale (e.g. Bontena et al. 2008).

Since total concentrations of heavy metals in soils are poor indicators for the risk of ground water pollution leaching rates are significant criterions for the assessment of contaminated soils. The mobility of heavy metals in soils is usually tested by standardized leaching experiments. Legal regulations in many countries (e.g. BBodSchV 1999) are based on this kind of extraction procedures. Generally accepted are batch tests using a 24 h elution procedure at a liquid/solid ratio of 10 : 1. This kind of experiments represents a worst case (Hirner et al. 1998), which means that each soil particle is circulated by the leaching agent. However, under natural conditions the liquid/solid ratio is usually less than 1 : 1 and soil water percolates most commonly along preferential flow paths (Beven and Germann 1982, Camobreco et

al. 1996). Consequently certain parts of the soil matrix won't get in contact with percolating water under unsaturated and even under saturated conditions. Accordingly standard batch tests are not capable to estimate natural leaching rates. Instead of that these tests might be an adequate method in order to quantify the pool of mobilizable metals under standardized conditions. Quantifying this pool is helpful in terms of an overall risk assessment but provides no answer regarding actual leaching rates.

Alternatively soil water concentrations (and fluxes) of heavy metals could be measured in the field using lysimeters or suction cups in order to sample the percolating pore water directly (e.g. Tiensing et al. 2001). However, this kind of field based techniques have only a minor potential for risk assessment because the various parameters influencing the leaching processes are highly variable under natural weather conditions. Furthermore field based monitoring is very laborious and thus limited to a few number of small plots. As a consequence results are hardly transferable. This is especially true for the retention time of the percolating soil water, which is one of the most sensitive parameters affecting the solid-liquid transfer. Hence metal concentrations of in situ soil water samples will be highly variable as Fig. 1 shows. In order to assess mean leaching rates long term monitoring is essential.

The aim of the present study is to assess the leaching rates of heavy metals from contaminated top soils on regional scale. The newly developed method is based on metal specific transfer functions which are derived from undisturbed soil column leaching experiments under controlled water transport conditions. The transfer functions allow to calculate metal concentrations in soil water depending on mobilizable metal fractions under standardised transfer conditions. The method should provide an effective and easy to use GIS-tool for the assessment of contaminated soils.
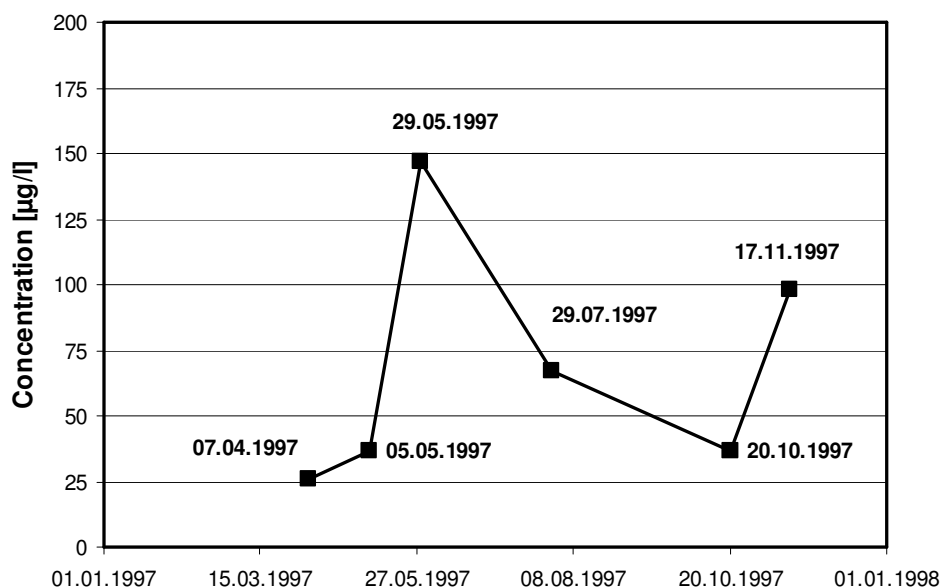
Fig. 1: Temporal variation of zink concentration of in situ water samples taken at Hilbersdorf monitoring station in a depth of 0,4m  (Source: Sächsisches Landesamt für Umwelt und Geologie)

## MATERIALS AND METHODS

**Sampling sites.** For laboratory tests 16 undisturbed soil columns were taken at different highly contaminated sites in the German Federal States of Sachsen and Baden-Wuerttemberg (see Fig. 2). The experimental data selected for presentation in this paper refer to an agricultural site located south of the village Hilbersdorf close to the city of Freiberg/Saxony (50° 55′ N, 13° 21′ E, 425 m above sea level). Besides the high geologic content of heavy metals the pollution of top soils with metals and metalloids at this site results from emissions of local lead and silver mines and smelter plants over more than eight

centuries culminating in the first half of the last century. The mining complex "Muldenhuetten" was the main source for pollution in that area with high levels of zinc, cadmium, arsenic, and lead emissions. In 1991 the Saxonian Environmental Report stated an immission of lead in the Hilbersdorf area of 40mg/(m²*30d). Referring to cadmium an immission of 0.8mg/(m²*30d) was reported. The Saxonian agency for Environment and Geology (Saechsisches Landesamt für Umwelt und Geologie) is using this site as a long-term soil monitoring station. These investigations include the sampling of soil solution in the time period between April and November. The sampling is performed by using ceramic suction cells at a constant vacuum of 200hPa. Some results from these samples are presented in Fig. 1.
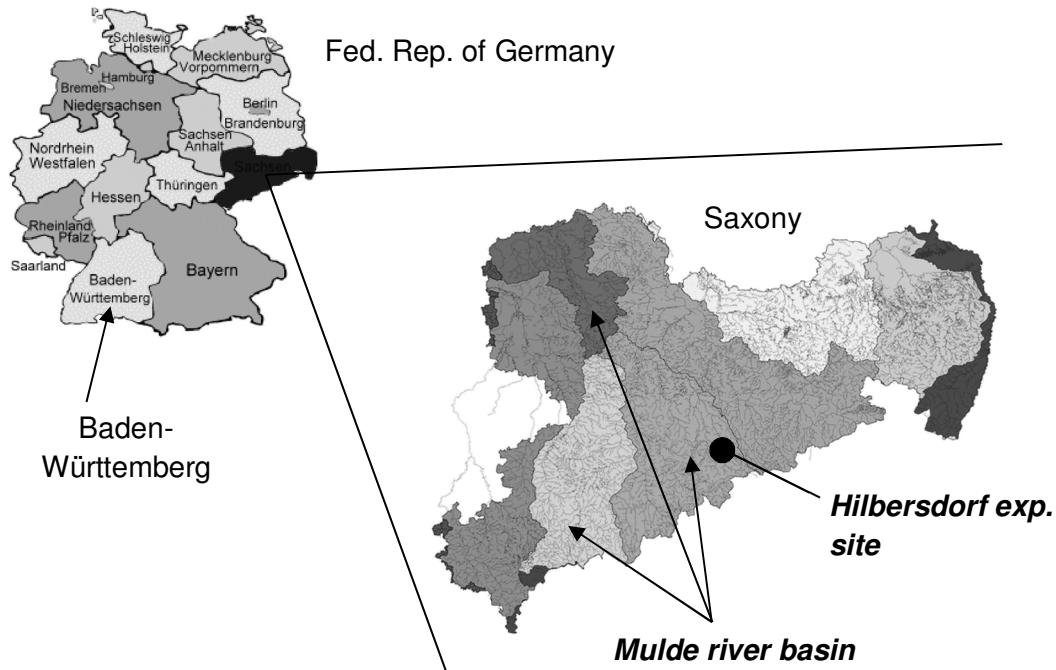


Fig. 2: Study areas

Experimental results are used for the assessment of heavy metal leaching on regional scale referring to the State of Sachsen (18400 km$^2$) with special respect to the Mulde river basin (7400km$^2$). Topsoils of the Mulde catchment (Cambisols, Luvisols, Stagnosols and Fluvisols) have arisen predominantly from loess deposits except the upper mountain range where weathered rock soils are distributed. Mean yearly precipitation varies between 500mm/a in the northern lowlands up to1200mm/a in the southern mountain range.

Intensive mining activities and metal processing during the last centuries cause severely contaminated topsoils in some parts of the saxonian mountain range. Most important contaminants are Zn, Cu, Pb, Cd, Ni, Cr, Hg, and As.

**Soil sampling.** Undisturbed soil columns (length: 50cm; diameter: 12.5cm) were taken using stainless steel tubes which were pressed carefully into the soil and excavated manually. In order to press the tubes strongly vertical into the soils a specially designed duct was applied. To avoid any damages at the front of the tubes during penetration a removable cutting ring was positioned at the lower end of the tubes. Additionally, bulk soil samples were taken from each site.

**Soil properties.** The properties of the soils were determined referring to the following parameters: particle size distribution (determination with pipette by KOEHN), soil moisture suction curve, pH of the soil solution, content of organic carbon (burning with oxygen, STROEHLEIN Cmat 550). The results are compiled in Table 1. The pH of the soil was determined for CaCl2 (0,01M), KCl (0,1M) and deionized water as solvents. A 10g sample of air-dried soil has been mixed with 25ml of the solvent at room temperature. The pH was measured twice, once after 4 hours and again after 24 hours.

Table 1:  Particle size fractions, organic matter content, bulk density, pH for $CaCl_2$ (0,01M), KCl (0,1M) and $H_2O$ after 4 hours and after 24 hours

| sample depth [cm] | Stones M% | fine soil particles (yields 100 M.%) | | | bulk density [g/cm³] | organic matter content [M%] | pH after 4 hours (21.7 °C) | | | pH after 24 hours (22.2 °C) | | |
|---|---|---|---|---|---|---|---|---|---|---|---|---|
| | | Sand M% | Silt M% | Clay M% | | | $CaCl_2$ (0,01M) | KCL (0,1M) | deion. $H_2O$ | $CaCl_2$ (0,01M) | KCL (0,1M) | deion. $H_2O$ |
| 0-25 | 34.0 | 43.5 | 43.1 | 14.4 | 1.18 | 2.49 | 4.71 | 4.01 | 5.00 | 5.02 | 5.08 | 5.48 |
| 25-40 | 56.3 | 55.6 | 35.9 | 9.0 | 1.6 | 0.51 | 4.80 | 4.48 | 5.29 | 4.92 | 4.66 | 5.54 |

**Extraction of heavy metals.** Different batch tests (DEV-S4/DIN 38414, DIN 19730) have been used in order to quantify the pool of mobilizable metals under standardized conditions. The DEV-S4/DIN 38414-4 method uses 50g of air-dried soil which is mixed with 500ml deionised water. The mixture is shaken in an over-head-mixer for 24 hours. The extract is obtained by centrifugation at 2500rpm or vacuum filtration (filter pore size 0.45µm). The soil equilibrium extract according to DIN V19735 is obtained using 200g air-dried soil. The sample (<2mm) is mixed with deionised water added drop by drop under constant kneading until field capacity is reached. Avoiding evaporation the sample is kept at 5°C for 24 hours. The extract can be obtained by vacuum filtration (filter pore size 0.45µm). The NH4NO3 extraction method as described by DIN 19730 uses 50 ml of 1M NH4NO3 solution which is added to 20g of soil material (<2mm). The suspension is shaken in an over-head-mixer for 2 hours. Similar to the above mentioned methods the extract is obtained by centrifugation or filtration. The mass-related extractable concentration [µg/kg] can be calculated by multiplication of the resulting dissolved element concentration with the soil/extraction solution ratio.

**Column leaching experiments.** The laboratory setup consists of 4 vacuum-controlled workstations comprising the following components:
- stainless steel cylinders coated inside with Teflon (length: 50cm; diameter: 12.5cm) each housing an undisturbed soil column with a porous plate/membrane closures at the bottom
- an electronically controlled rainfall simulator
- two separate sample cells for each soil column; the lower cell is coupled with a balance in order to measure the volume rate of percolating soil water
- an electronically controlled vacuum in order to adjust flow rates and retention times of percolating soil water
- micro-tensiometers and TDR sensors for the measurement of capillary water tension (pressure head) and soil moisture
- a data logging system.

The experimental set-up is similar to the design described by Rambow and Lennartz (1993) which allows to study the leaching of heavy metals in undisturbed soil columns under vadose zone conditions.
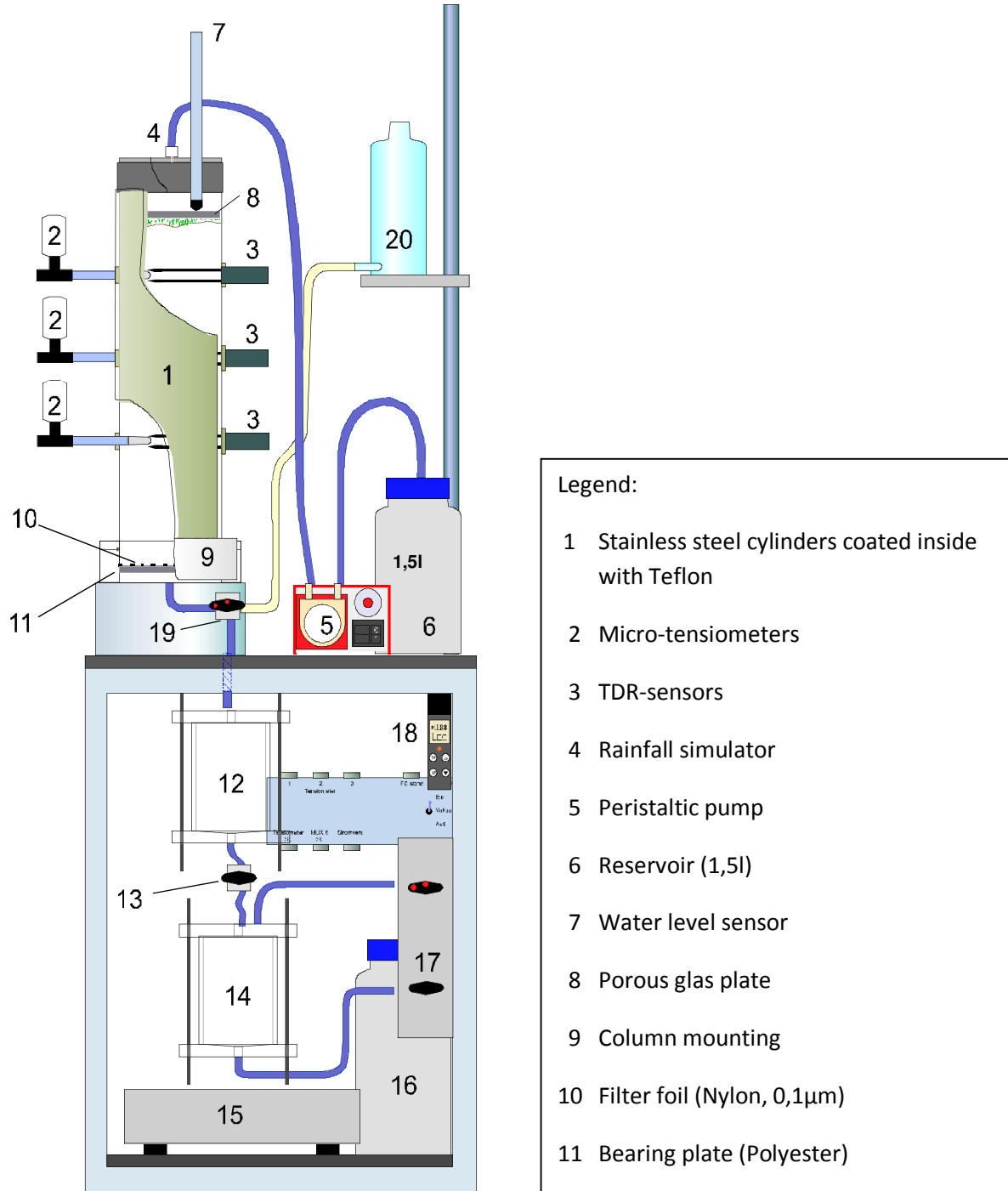


Fig. 3: Schematic view of the experimental setup (Schmidt & Kaltschmidt 2001)

Soil water tension and volume rate respectively retention time of percolating water could be varied according to natural water flow conditions (Fig.4). Soil water tension, soil water content, applied vacuum, and the amount of precipitation are controlled continuously over the entire experiment which can

last up to several months. By using two separate sample cells for each soil column a constant vacuum at the bottom end of the soil column can be maintained during the sampling of the percolate (for details see Fig. 3). Sample cells are placed on a balance to register the volume rate of percolating water continuously. The experimental setup was placed in an air conditioned room with a constant temperature of 20 °C.
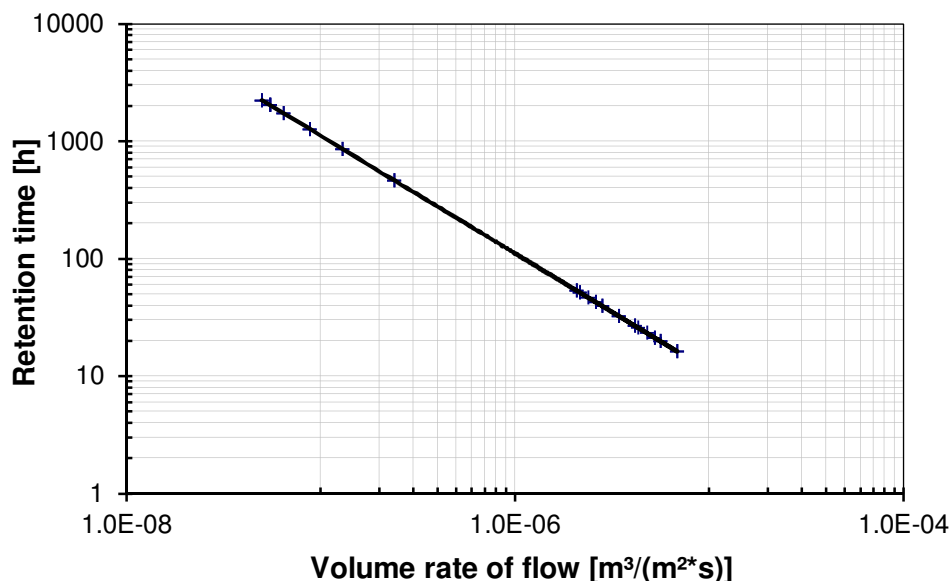


Fig. 4: Retention time of percolating soil water as a function of volume rate of flow

A "synthetic rain water" is used in order to simulate natural rainfall conditions (Table 2). After adjusting the predefined flow rate of percolating soil water by means of the vacuum at the column bottom water samples were taken for unsaturated (pF=1.4) and saturated steady-state flow conditions. Simulated rainfall intensity was set to 1ml/h in case of unsaturated flow respectively 100 ml/h in case of saturated flow. Sampling was continued until heavy metal concentrations in the percolates are constant, which requires up to 3 months of continuous percolation depending on retention time and volume rate of flow (Fig. 4). Water conductivity was used as an indicating sum parameter. The heavy metal concentrations in the percolates have been determined for the following elements: As, Cd, Cr, Cu, Hg, Ni, Pb, Sb and Zn using an ICP-MS analyser. In addition, pH and redox potential are measured.

Table 2: Ionic concentrations of synthetic rain water [µg/l]

| $Na^+$ | $K^+$ | $Mg^{2+}$ | $Ca^{2+}$ | $Cl^-$ | N | S |
|---|---|---|---|---|---|---|
| 219,1 | 121,7 | 83,1 | 548,0 | 459,0 | 43,6 | 137,7 |

The soil column tests have been performed according to the following procedure:

1. Drainage of field moisture from the soil columns at a vacuum of 630hPa in order to remove remaining soil water that has not been exchanged since the samples were taken.
2. Watering of the columns from the bottom in order to avoid trapped air in the columns
3. Adjustment of the precipitation rate to 1ml/h (1st step)
4. Optimising of the vacuum for the adjusted precipitation rate up to the establishment of the desired soil moisture tension (pF=1.4) as an average of the three tensiometers in each soil column.
5. The sampling of percolating water starts as soon as the desired soil moisture tension is established within the soil column.

6. Continual sampling until the heavy metal concentrations in the percolates are constant. The conductivity of the percolate is used as a sum parameter. Also, pH and redox potential are measured. Samples were stored at 4 °C until metal concentrations are analysed.
7. The heavy metal concentrations in the percolates has been determined for the following elements: As, Cd, Cr, Cu, Hg, Ni, Pb, Sb and, Zn.

This procedure assures comparable results over all test runs.

## RESULTS AND DISCUSSION

**Experimental results.** As example for all investigated heavy metals Fig. 5 shows the topsoil zinc concentrations for the Hilbersdorf experimental site as obtained by the different extraction methods.
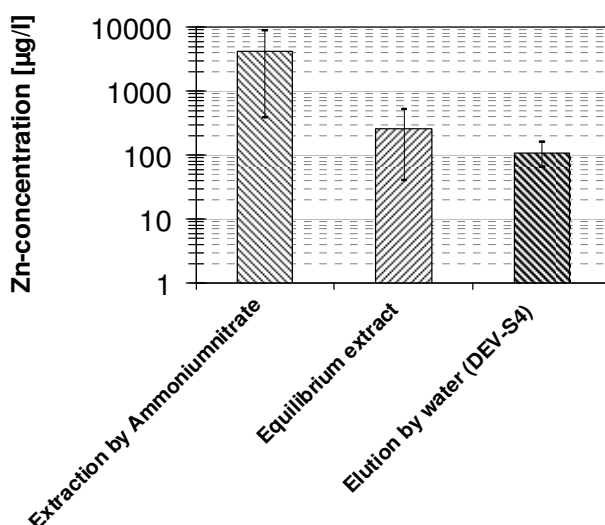


Fig. 5: Topsoil zinc concentrations for the Hilbersdorf experimental site as obtained by the different extraction methods

The by far highest concentrations are gained using the NH4NO3 extraction method because ammonium nitrate is a much more aggressive extraction agent than water. The difference in concentration amounts to more than one order of magnitude compared to the water based methods. The equilibrium extract yields somewhat higher concentrations because of the closer liquid/solid ratio.

Zinc concentrations determined in the percolates of the column tests vary over time until initial soil water is entirely substituted by continuous supplied rainwater. Theoretically concentrations should reach an approximately constant value when the ratio of the volume of percolated water and the watered pore volume is greater than 1. Actually concentrations approach the constant level at a ration of 1.2 as Fig. 6 shows. Precautionally only concentrations measured for rations >1.5 are taken into account for further analyses.

In Fig. 7 zinc concentrations in the percolates of undisturbed soil columns are compared to in-situ pore water samples with respect to water content (unsaturated versus saturated) and volume rate of flow (respectively rainfall intensity). Taking the mean in-situ pore water concentration as reference the best correlation can be determined for the unsaturated column tests at a rainfall intensity of 1ml/h which equals 713 mm/a. Therefore only the unsaturated test variant is evaluated for further analysis.

In Fig. 8 measured zinc concentrations of percolating soil water at unsaturated, steady-state flow conditions were plotted as a function of corresponding mobilizable metal contents. This comparison results in a set of curves respectively empirical functions - one for each extraction method. Taking account of all investigated metal species the respective functions are compiled in Table 3. This set of transfer functions allow to calculate metal concentrations of percolating soil water based on mobilizable metal contents as determined by simple extraction methods. Best fit was obtained using the $NH_4NO_3$-extraction (DIN 19730), where correlation coefficients range between r=0,62 and r=0,85.
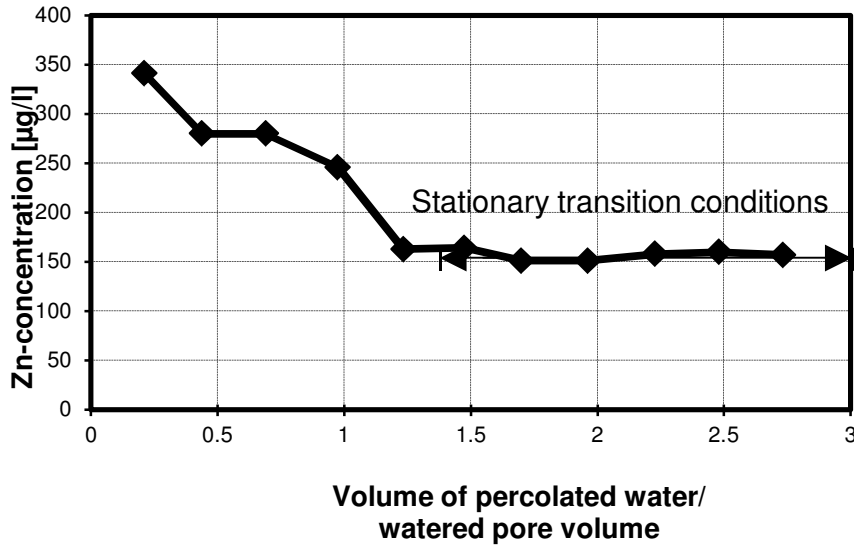


Fig. 6: Variability of zinc concentrations during percolation of a undisturbed soil column under unsaturated conditions
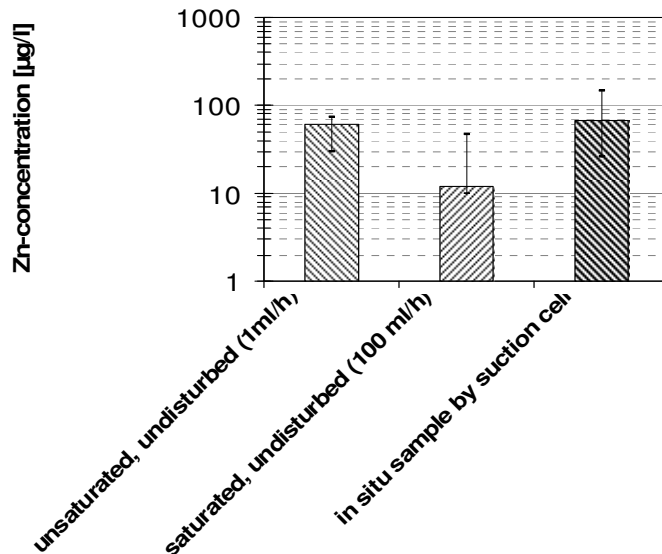


Fig. 7: Comparison of zinc concentrations of percolates from soil column tests with in-situ samples (all data related to Hilbersdorf test site)

Tab. 3: Regression equations for the conversion of mobilizable metal contents into leachate concentrations

| based on DIN 38414 (DEV S4) extraction: | | |
|---|---|---|
| Element | equation | correlation coefficient r |
| Cd | y = 0,487 x | 0,49 |
| As | y = 0,017 x | 0,48 |
| Cu | y = 0,048 x | 0,78 |
| Pb | y = 0,021 x | 0,54 |
| Zn | y = 0,584 x | 0,60 |
| | | |
| based on DIN V 19735 extraction: | | |
| Cd | - | - |
| As | - | - |
| Cu | y = 0,558 x | 0,50 |
| Pb | - | - |
| Zn | y = 2,219 x | 0,70 |
| | | |
| based on DIN 19730 ($NH_4NO_3$-) extraction: | | |
| Cd | y = 0,018 x | 0,64 |
| As | y = 0,181 x | 0,62 |
| Cu | y = 0,177 x | 0,77 |
| Pb | y = 0,006 x | 0,85 |
| Zn | y = 0,032 x | 0,74 |
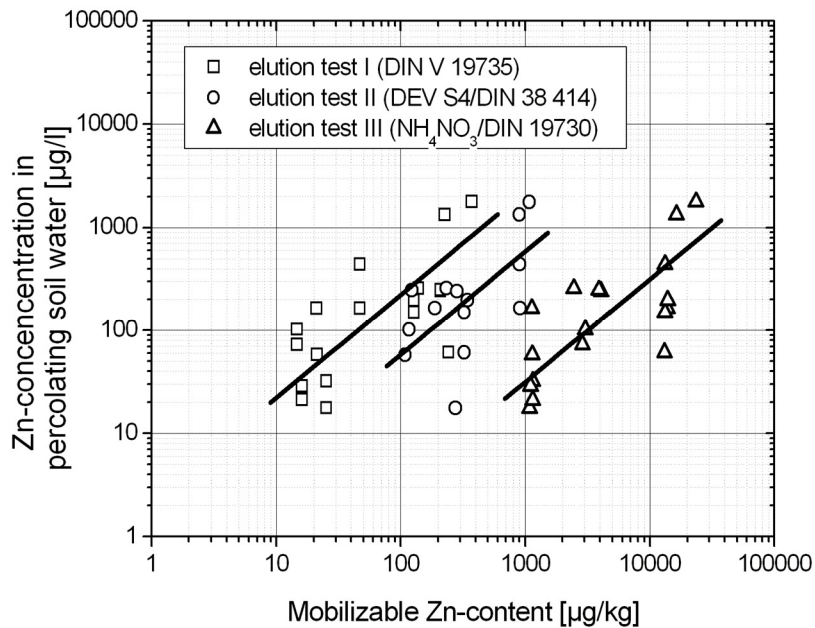


Fig. 8: Zinc concentrations of percolating soil water at unsaturated, steady-state flow conditions as a function of corresponding mobilizable metal contents.

**Transfer on regional scale.** The Saxonian agency for Environment and Geology (Saechsisches Landesamt für Umwelt und Geologie) conducted a comprehensive measuring program in the years 1993-2004 in order to evaluate the heavy metal load of saxonian soils. Based on a 4x4km grid total as well as $NH_4NO_3$ mobilizable metal contents were determined for topsoil and subsoil samples. Altogether 2584 samples were taken at 1164 locations (Sächsisches Landesamt für Umwelt und Geologie 2000). By adding further monitoring data available at the agency a total of 4600 topsoil samples are available referring to topsoil $NH_4NO_3$ mobilizable metal contents.
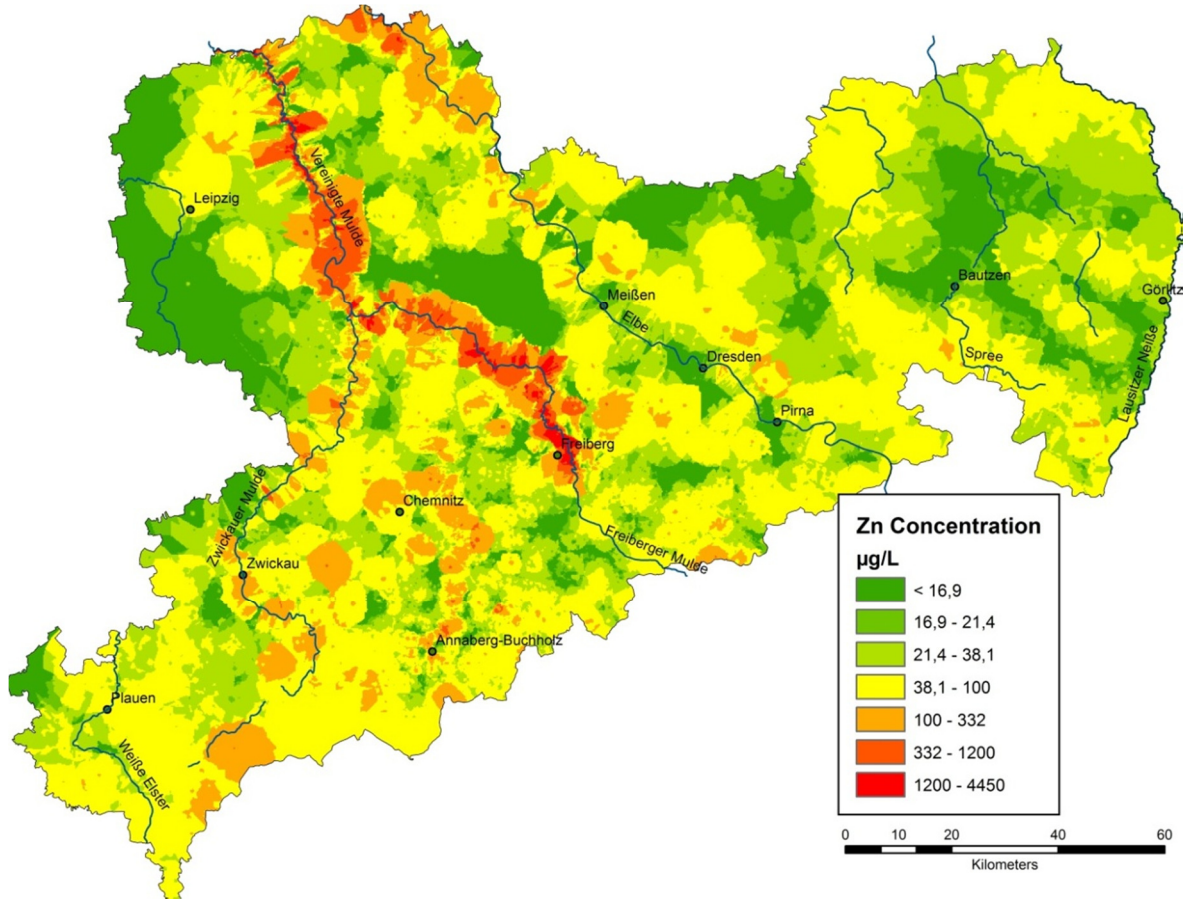


Fig. 9: Calculated concentration of Zinc in topsoil percolating water

Applying the regression equations as compiled in table 2 to the bulk of topsoil $NH_4NO_3$ mobilizable contents the resulting soil water concentrations are aggregated to a set of maps showing the topsoil metal concentrations for the entire state of Saxony. As an example Fig. 9 plots the calculated zinc concentrations which vary between 0.4µg/l and 4450 µg/l. Mean concentration accounts for 63.6 µg/l. Due to the former lead and silver mines and smelter plants highest zinc concentrations are found around the city of Freiberg and along the downstream section of the Freiberger Mulde river where eroded soils including particle bound metals are deposited within the flood plane. According to the respective German legislation (BBodSchV 1999) a zinc concentration of >500 µg/l is associated to a considerable risk of groundwater pollution. Taking the calculated topsoil zinc concentrations as reference this threshold might be exceeded around the city of Freiberg and the downstream Mulde flood plain.

In a subsequent step leaching rates were calculated by multiplying the calculated metal concentrations with spatially distributed groundwater recharge rates which are also provided by the Saxonian state agency (Sächsisches Landesamt für Umwelt und Geologie 2007). Fig. 10 presents the

resulting map for the leaching of zinc. Calculated losses of zinc approach a maximum of 10000 g/(ha ·a). However, mean loss amounts to 95 g/(ha ·a). As expected highest losses occur in the area of Freiberg and the downstream flood plane of the Mulde river.

With regard to the calculated topsoil losses the question arises to which extent the leached metals enters the surface water system by subsurface respectively groundwater transport. To answer that question the topsoil losses were added up for the Mulde river basin and compared to the long-term mean metal discharges measured at the catchment outlet. Some results are compiled in Fig. 11. Total mass rates (output) of Zn and Pb are provided by the Elbe River Council (Flussgebietsgemeinschaft Elbe). Although anthropogenic contaminants in surface waters (point sources) have been reduced by more than 90% during the past decades the total output from the Mulde basin has to be reduced by the population related inputs which amount to less than 6 t/a Zn and less than 1 t/a Pb. Comparing the resulting geogenic output with the calculated sum of topsoil losses reveals that subsoil retention amounts to 27% of topsoil losses for Zn respectively 84% for Pb. Actually the expected subsoil retention for Pb should be much higher than for Zn because the mobility of Zn in soils is substantially higher than those of Pb as commonly known (Li & Shuman 1996). Therefore received results seem to be plausible with respect to subsurface retention.
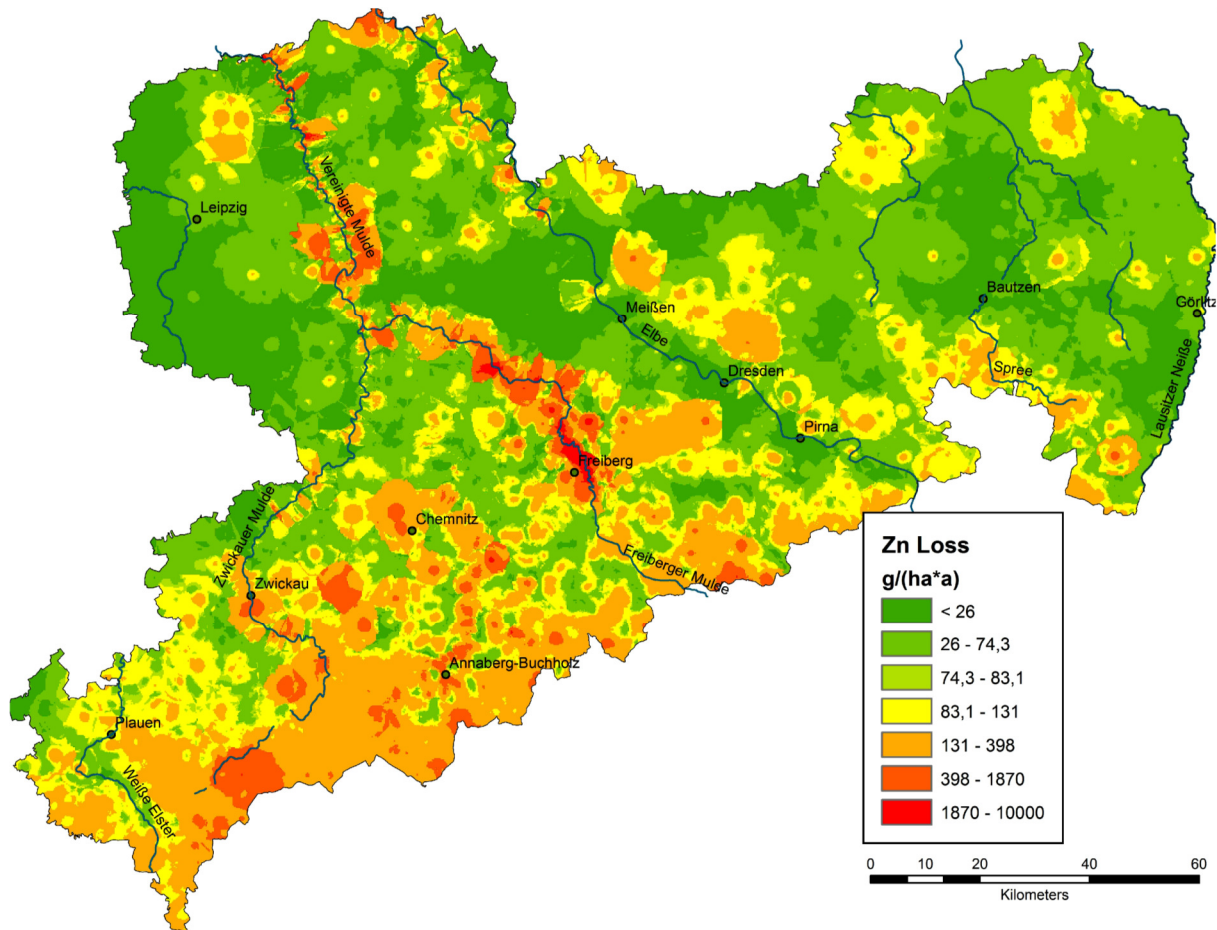


Fig. 10: Loss of Zinc by leaching of topsoils

**CONCLUSIONS**

In contrast to in-situ soil water sampling laboratory tests of heavy metal mobility are only an incomplete reproduction of natural conditions. Their advantage, however, is the reduction of the various natural impacts (e.g. weather conditions) to a small number of parameters that can be controlled and varied systematically. Simple standard methods such as the NH4NO3 – extraction cover the pool of mobile element fractions of a soil. Those methods are very well adapted for surveying heavy metals on regional scale.

Unsaturated steady-state column tests using undisturbed samples are capable to reproduce mean long term heavy metal concentrations in percolating soil water adequately. These tests provide the best representation of natural conditions under laboratory conditions, but they are time consuming and expensive. Using both - standard extraction methods and soil column tests - this study derives a set of empirical relationships that are successfully used to estimate top soil heavy metal concentrations and leaching losses on regional scale. The transport of heavy metals to ground respectively surface waters was assessed by comparing the calculated top soil metal losses with the metal discharge at the outlet of an exemplary river catchment. Results prove different retention losses dependent on metal species. Retention of Pb is much higher than that for Zn.
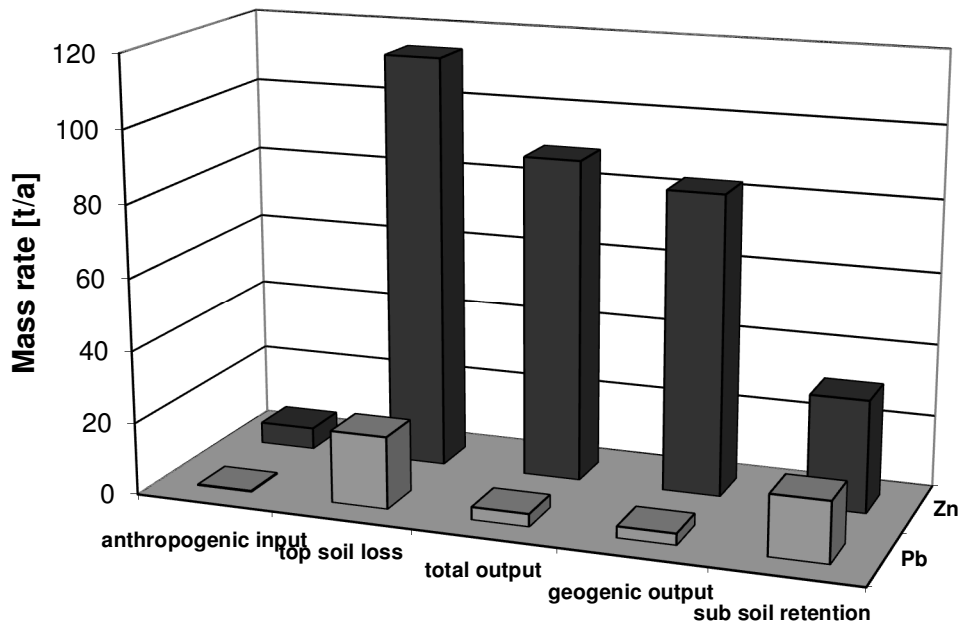


Fig. 11: Mass rates of Zn and Pb related to the Mulde river basin assign to different sources
(Source: Flussgebietsgemeinschaft Elbe 2012)

**ACKNOWLEDGEMENTS**

**REFERENCES**

BBodSchV 1999: Bundes-Bodenschutz- und Altlastenverordnung vom 16. Juli 1999, Bundesgesetztblatt, Teil I, Nr. 36, S. 1554-1682

Beesley, L., Moreno-Jiménez, E., Clemente, R., Lepp, N., Dickinson, N. 2010: Mobility of arsenic, cadmium and zinc in a multi-element contaminated soil profile assessed by in-situ soil pore water sampling, column leaching and sequential extraction, Environmental Pollution, Volume 158, Issue 1, pp. 155-160

Beven K., and Germann P. 1982: Macropores and Water Flows in Soils. Water Resources

Research 18(5): pp. 1311-1325.

Bontena, L.T.C., Römkensa, P. F. A. M. & Brusa, D. J. 2008. Contribution of Heavy Metal Leaching from Agricultural Soils to Surface Water Loads. Environmental Forensics

Volume 9, Issue 2-3, pp. 252-257

Camobreco, V.J., B.K., Richards, T.S. Steenhuis, J.H. Peverly, McBride, M.B. 1996: Movement of Heavy Metals Through Undisturbed and Homogenized Soil Columns. Soil Science 161(11), pp. 740-750.

Davidson, C. M, Urquhart, G. J., Ajmone-Marsan, F., Biasoli, M., Duarte, A. C., Díaz-Barrientos, E., et al. 2006: Fractionation of potentially toxic elements in urban soils

from five European cities by means of a harmonised sequential extraction procedure. Analytica Chimica Acta, 565, pp. 63–72.

Dijkstra, J.J., Meeussen, J.C.L., Rob N.J. Comans, R.N.J. 2004: Leaching of heavy metals from contaminated soils: An experimental and modelling study. Environ. Sci. Technol. 38 (16), pp. 4390-4395

DIN 19730 1997: „Extraktion von Spurenelementen mit Ammoniumnitrat", Berlin

DIN V19735 1999: „Ableitung von Konzentrationen im Bodenwasser aus ammoniumextrahierbaren Gehalten oder Eluatgehalten", Berlin

DIN 138414-4 (1984): „Schlamm und Sedimente (Gruppe S) Bestimmung der Eluierbarkeit mit Wasser (S 4)", Berlin

Hirner, A.V., Pestke, F.M. ,Busche, U., Eckelhoff A. 1998: Testing contaminant mobility in soils and waste materials. Journal of Geochemical Exploration 64, pp. 127–132

Li, Z. and Shuman, L. M. 1996: Heavy Metal Movement in Metal-Contaminated Soil Profiles. Soil Science Vol. 161, Issue 10, pp. 656-666

Rambow, J., Lennartz, B. 1993: Laboratory method for studying pesticide dissipation in the vadoze zone. Soil Sci. Soc. Am. J., 57 (1993), pp. 1476–1479

Sächsisches Landesamt für Umwelt und Geologie 2000: Bodenatlas des Freistaates Sachsen - Teil 3: Bodenmeßprogramm

Sächsisches Landesamt für Umwelt und Geologie 2007: Bodenatlas des Freistaates Sachsen -Teil 4: Auswertungskarten zum Bodenschutz

Schmidt, J. & Kaltschmidt, T. 2001: Methodenvergleich zur Abschätzung des Schwermetallaustrages für die Elemente As, Cd, Pb und Zn aus Böden mit dem Sickerwasser. In: Cyffka, B. u. Härtling, J. W. (ed.): Bodenmanagement. Berlin, Heidelberg, New York

Tiensing, T., Preston, S., Strachan, N., Paton, G.I., 2001: Soil solution extraction

techniques for microbial ecotoxicology testing: a comparative evaluation.

J. Environ. Monit. 3, pp. 91–96.

# FATE OF ARSENATE ADSORBED ON NANO-TiO2 WITH SULFATE REDUCING BACTERIA

*Chuanyong Jing*, Ting Luo and Suqin Liu
(Chinese Academy of Sciences, Beijing, China)

**ABSTRACT :** Arsenic (As) removal using nanomaterials has attracted increasing attention worldwide, whereas the potential release of As from spent nanomaterials to groundwater in reducing environments is presently underappreciated. To investigate the fate of As(V) adsorbed on nano-TiO2 in the presence of sulfate reducing bacteria (SRB) *Desulfovibrio vulgaris* (ATCC 7757) and *Desulfovibrio vulgaris* DP4, multiple complimentary techniques were employed including batch incubation tests, synchrotron-based X-ray scanning transmission X-ray microscopy (STXM) and X-ray absorption near edge structure (XANES) spectroscopy. The incubation results demonstrated that As(V) was desorbed from nano TiO2, and subsequently reduced to As(III) in aqueous solution. Reduction of As(V) to As(III) was coupled to the conversion of sulfate to sulfide and lactate to acetate. STXM results revealed that As(V) reduction also occurred on the TiO2 surface. The release of adsorbed As(V) was promoted substantially by SRB relative to abiotic controls. XANES analysis at the end of 98 d incubation indicated that As(V) was the predominant species for As loads of 150-300 mg/g, while 15~28% As precipitated as orpiment for a high As load of 5700 mg/g. The insight gained from this study furthers our understanding of the key role of SRB in the fate of As adsorbed at the mineral-water interface.

## INTRODUCTION

Naturally-occurring and anthropogenic arsenic (As) pollution poses a severe threat to public health worldwide. Recently, metal oxide nanomaterials such as nano-$TiO_2$, zero valent iron, and iron oxy-hydroxides, have been successfully applied in As removal from groundwater and industrial wastewater. As a result, As-laden nanomaterials may accumulate and have a potential to release As and re-contaminate surface and groundwater if not safely disposed of. Moreover, the high mobility of nanoparticles may exacerbate the transport and fate of the adsorbed As compared with bulk adsorbents. Quantifying the relative influence of microbial activities and the spatial distribution of As species represents a major challenge in the biogeochemical cycling of As.

The fate and transport of As are mainly controlled by microorganisms, redox potential, and pH, as well as adsorption, desorption, and coprecipitation reactions on a variety of natural and engineered nanoparticles in the environment. Sulfate-reducing bacteria (SRB) play a dominant role in determining whether dissolved As could accumulate to hazardous levels in anaerobic conditions. Previous laboratory studies explored the correlation between sulfate reduction and As mobilization in reducing conditions. The sulfide produced during microbial sulfate reduction can form As-sulfide minerals, such as orpiment ($As_2S_3$) and realgar (AsS), which sequester As from the water. Under conditions where sulfide is stable, the concentration of dissolved As at equilibrium is controlled by the solubility of sulfide phases and therefore depends on the rate of microbially mediated sulfate reduction. However, there is a paucity of data regarding biogeochemical processes leading to As release from spent nano $TiO_2$ in anoxic surroundings, and the relevant mechanisms remain unresolved.

Recently, synchrotron-based techniques such as soft X-ray scanning transmission X-ray microscopy (STXM) have been developed for imaging and spectroscopic characterization of metal-microbe-mineral interfaces. STXM combines high spatial resolution (<50 nm) with the chemical sensitivity of near-edge X-ray absorption fine structure (NEXAFS) spectroscopy, and enables characterization of the elemental composition of the adsorbent and speciation of adsorbed metals.

In this study, we combined synchrotron-based techniques including STXM and XANES and incubation experiments to explore the redox transformation and mobility of adsorbed As(V) on nano $TiO_2$ in association with SRB. The objectives of our study were therefore to (1) evaluate the desorption and reduction of adsorbed As(V) on nano $TiO_2$, and (2) quantify the contribution of SRB to As release in reducing conditions

## MATERIALS AND METHODS

**Incubation Experiments**: Nano-$TiO_2$ was synthesized via the hydrolysis of titanium sulfate. The details of the synthesis and basic properties of $TiO_2$ were described in our previous work (Luo et al., 2010). The adsorption experiment of As(V) on $TiO_2$ was performed in a glovebox (100% $N_2$). The loads of As(V) on $TiO_2$ were approximately 150 mg/g, 300 mg/g, and 5700 mg/g by mass balance calculation with the soluble As concentrations, and the samples were denoted as As-150, As-300, and As-5700, respectively.

The artificial groundwater at pH 7.8 was composed of 0.02 mM $NH_4Cl$, 0.07 mM KCl, 9 mM Na-lactate, 4.5 mM $MgSO_4$, 0.5 mM $NaHCO_3$, 1.5 mM $CaCO_3$, and 0.1 mL/L Wolfe's Minerals. An electron acceptor was added as sulfate ($MgSO_4$), and the electron donor was lactate (Na-lactate). The artificial groundwater was autoclaved prior to addition of pre-sterilized $NaHCO_3$ solution, and was maintained in anoxic condition in the glovebox.

Incubation experiments were conducted in serum bottles in the glovebox. Abiotic control experiments were also conducted for $TiO_2$-As(V) solids in artificial groundwater without an electron donor. Cell counts using microscopy were conducted at the beginning (initial cell density 8×107 cells/L for As-150, As-300, and As-5700) and during the period of incubation by extracting suspension samples of As-5700.

Eh and pH were monitored with an interval of 1-2 d for about 10 days, then at 7 d intervals over a period of 97 d. At the same time, homogenized samples were extracted using a pre-sterilized syringe and passed through a 0.22 μm filter in the glovebox.

**Sulfate Reducing Bacteria:** Two SRB, one isolated from soil and the other obtained from ATCC, were used in the incubation experiments. A bacterium was isolated from a soil sample collected at a naturally-occurring As-contaminated site in China, and was identified as *Desulfovibrio vulgaris* DP4 (99% similarity, GeneBank accession number: CP000527). To compare with the SRB isolated from the environment, *Desulfovibrio vulgaris* strain 7757 was purchased from ATCC. The two SRB were grown to the late-exponential phase under anaerobic conditions in modified Baar's medium at 37°C. Cells were harvested by centrifugation (6000 g, 8 min, 25°C), then the bacteria were rinsed with artificial groundwater before being added to the $TiO_2$-As(V) suspension.

**STXM Study:** Approximately 1 μL suspension sample containing As, bacteria, and $TiO_2$ (1 g/L) was taken after 4 d incubation. The sample was sandwiched between two 100 nm thick $Si_3N_4$ windows, and then sealed with high vacuum adhesive to prevent water evaporation during the STXM analysis. STXM experiments were performed at the soft X-ray beamline (BL08U) at the Shanghai Synchrotron Radiation

Facility (SSRF), China. The STXM images were taken by scanning in the x-y direction of selected sample areas about 20×20 μm over the energy range of interest (1334-1360 eV). The dual-energy ratio-contrast image method was used to analyze the STXM data.

**Analysis:** The concentrations of total dissolved As were determined using a furnace atomic absorption spectrometer (AAS-800, Perkin Elmer, US). The As speciation determination was performed by high performance liquid chromatography atomic fluorescence spectrometry (HPLC-AFS, Jitian, China). Sulfate, lactate, and acetate concentrations were determined using a DX-1100 ion chromatograph (Dionex, US) with an AS11-HC Ion Pac column. Sulfide concentrations were measured using the methylene blue method immediately following the sample collection.

**Arsenic XANES Analysis:** The $TiO_2$ solid samples were sealed between two layers of Kapton tape. The As k-edge XANES spectra were collected at beamline 01C1 at the National Synchrotron Radiation Research Center (NSRRC), Taiwan. Spectra were acquired from -150 to 300 eV relative to the As K-edge of 11,867 eV at cryogenic temperature (77 K) using a cryostat to prevent the oxidation of As(III) by X-rays. The fluorescence signals were collected using a Lytle detector. The spectra were analyzed with the Athena program in the IFEFFIT computer package for energy calibration, averaging of multiple scans, background subtraction, normalization, and linear combination fit. No energy shifts was allowed during fitting. The weighting of single species was constrained between 0 and 1, and the sum of species was constrained to be 1.

**RESULT AND DISCUSSION**

**Changes of SRB Substrates**: The sulfate concentrations decreased over time driven by SRB, and sulfide accumulated accordingly due to the reduction of sulfate (Figure 1). For all three As load levels (150, 300, and 5700 mg/g), sulfide was detected in the aqueous phase in the presence of strain 7757 and DP4 and its concentrations increased to about 70 mg/L. Sulfate levels fell from about 160 mg/L to 10~13 mg/L for strain 7757 compared with 11~12 mg/L for strain DP4 for the three As loads during 97 d incubation. The sulfate decrease was delayed in As-5700 sample compared with As-150 and As-300. In line with our observations, Kocar et al. (2010) reported that sulfate reduction occurred more slowly at high As load on ferrihydrite (50% of maximum As adsorption) than at low As load (10% of maximum As adsorption) with Desulfovibrio vulgaris (Hildenborough).

**Desorption and Reduction of As(V) with SRB:** The adsorbed As(V) on nano $TiO_2$ was reduced to As(III) in the presence of strain 7757 and DP4, while As(III) was not observed in abiotic controls. As(III) was detected with soluble concentrations ranging from 0.03 to 7 mg/L, accounting for 0.1-3.3% of total adsorbed As for the three As loads on $TiO_2$. The desorption of As(V) from nano $TiO_2$ was promoted by SRB relative to abiotic controls, as evidenced by the two to three times greater As(V) concentrations observed . Among biotic samples, dissolved As(III) concentrations were 40% and 26% higher in As-5700 than in As-150 and As-300 samples, respectively, and As(V), 46% and 26% higher.

　　*Desulfovibrio vulgaris* used in this study cannot directly metabolize As(V), whereas the biogenic sulfide can reduce As(V) to As(III). However, where the reduction of As(V) to As(III) occurs, whether in the aqueous or solid phase, is a controversial issue. A previous study found that the As(V) adsorbed on iron oxyhydroxides was reduced to As(III) on solid surfaces (Masscheleyn et al., 1991). To the contrary, Huang et al. (2011) demonstrated that As(V) desorbed from iron oxides before its reduction by *Shewanella putrefaciens* strain CN-32. The authors concluded that the reduction of adsorbed As(V) is

insignificant or at least much slower than that of dissolved As(V). These studies concentrated on the As-Fe oxides-bacteria system. To the best of our knowledge, no investigation of As fate and transformation has been reported in the presence of redox insensitive $TiO_2$ nanoparticles and SRB.
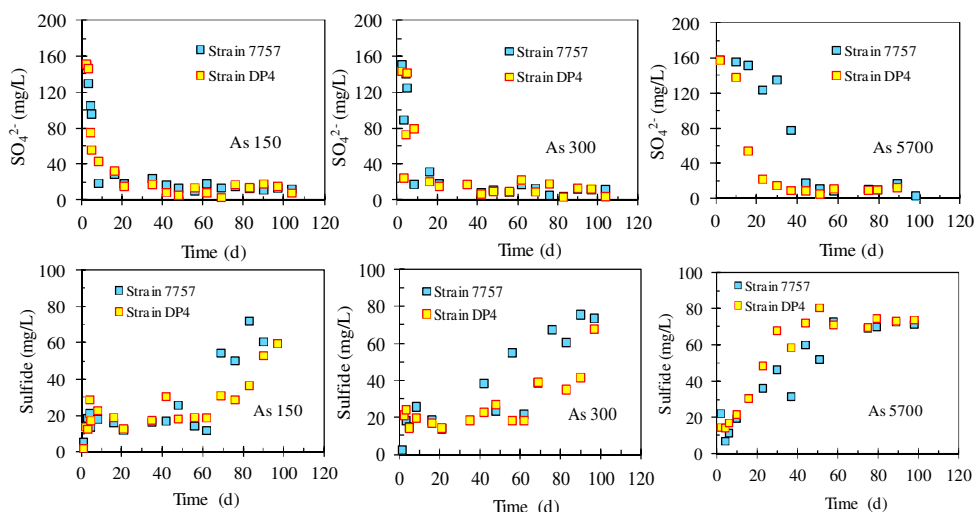


**FIGURE 1.** Dissolved sulfate and sulfide concentrations as a function of incubation time for As-150, As-300, As-5700 samples. Two sulfate reducing bacteria strains: *Desulfovibrio vulgaris* (strain 7757) obtained from ATCC, and *Desulfovibrio vulgaris* (strain DP4) isolated from an As contaminated soil.

As speciation and mobility largely depends on sulfide concentrations. The sharp drop of As(III) concentrations in As-5700 in the initial incubation stage might be ascribed to the As sulfide precipitation coincident with biogenic sulfide production. Due to the presence of sulfide, the formation of As sulfide precipitates such as orpiment is readily possible and should control the transport and fate of As under sulfate-reducing conditions. For example, at high ratios of As:S, $As_2S_3$ precipitates were observed in *Desulfotomaculum auripigmentum* cultures by Newman et al. (1997). The authors not only reported the formation of $As_2S_3$ but emphasized that the $As_2S_3$ precipitation occurred only at high ratios of As(III):S. Therefore, the As-S precipitate was observed in high As(III) concentration with As-5700 only, and not in low As(III) with As-150 and As-300.

**STXM Image Analysis of As(V) on TiO$_2$ Solids:** STXM is a recent addition to the third generation synchrotron-based techniques in studying interactions of As at mineral-water interfaces. Our study shows that the As $L_3$-edge provides clear information on As oxidation state in the samples of As-containing $TiO_2$ with SRB. In such complex assemblages, simultaneous observation of As speciation and distribution on minerals accompanied by microbes on the submicron scale may provide insightful knowledge about As behavior on mineral interfaces.

**As Speciation in the Solid Phase:** The As speciation on $TiO_2$ solids at the end of the incubation experiments was determined with XANES analysis. XANES results reveal that As(V) was the predominant species on $TiO_2$ solids for As-150 and As-300 samples. The XANES spectra of the high As load sample (As-5700) demonstrated the formation of orpiment in the presence of strain 7757 and DP4. According to the linear combination fitting of the XANES spectra, the As-5700 sample contained 67% As(V), 4% As(III), and 29% orpiment for strain 7757, and included 80% As(V), 5% As(III), and 15%

orpiment for strain DP4. Mass balance results show that the total dissolved As released from $TiO_2$ was higher than that in abiotic controls, though over 83% As remained in the TiO2 solid phase.

## CONCLISIONS

With the increasing application of nanomaterials in the removal of As from contaminated waters, the amount of spent nanomaterials with elevated As content has increased. However, the release of pre-adsorbed As from nanomaterials is underappreciated. In stark contrast to previous findings that dissimilatory sulfate reduction alone would not lead to As contamination in the presence of ferrihydrite, our results reveal that milligram levels of As may be released to aqueous solution from spent nano $TiO_2$ adsorbent. With the high mobility of nanomaterials, the fate and transport of associated pollutants would be greatly changed compared with bulk minerals and adsorbents. The potential risks associated with engineered nanomaterials experiencing redox changes should be considered before their environmental application.

Our results demonstrate that SRB could facilitate desorption, as well as reduction of As(V) under reducing conditions. The anoxic environment in groundwater aquifers can be caused by microbial activity and reduction of dissolved oxygen by biogenic sulfide. Under such reducing conditions, in situ characterization of As speciation and its spatial distribution at the mineral-water interface presents a major challenge in As biogeochemistry. The results highlight the key role of SRB in the fate of As in the presence of nanomaterials and the need for further exploration on interactions of anaerobic bacteria and As at the mineral-water interface.

## REFERENCES

Huang, J. H., A. Voegelin, S. A. Pombo, A. Lazzaro, J. Zeyer, R. Kretzschmar. 2011. "Influence of arsenate adsorption to ferrihydrite, goethite, and boehmite on the kinetics of arsenate reduction by shewanella putrefaciens strain CN-32." *Environ. Sci. Technol*. 45: 7701-7709.

Kocar, B. D., T. Borch, S. Fendorf. 2010. "Arsenic repartitioning during biogenic sulfidization and transformation of ferrihydrite." *Geochim. Cosmochim. Acta* 74: 980-994.

Luo, T., J. Cui, S. Hu, Y. Huang, C. Jing. 2010. "Arsenic removal and recovery from copper smelting wastewater using $TiO_2$." *Environ. Sci. Technol*. 44: 9094-9098.

Masscheleyn, P. H., R. D. Delaune, W. H. Patrick. 1991. "Effect of redox potential and pH on arsenic speciation and solubility in a contaminated soil." *Environ. Sci. Technol*. 25: 1414-1419.

Newman, D. K., T. J. Beveridge, F. M. M Morel. 1997. "Precipitation of arsenic trisulfide by *Desulfotomaculum auripigmentum*." *Appl. Environ. Microbiol*. 63: 2022-2028.

# EXPERIMENTAL STUDY ON DENSE GAS TRANSPORT IN POROUS MEDIA

*Chiu-Shia Fen* and Yuen Cheng
(Feng Chia University, Taichung, Taiwan, ROC)

**ABSTRACT:** This paper presents an experimental study on density-driven and gravity-induced gas phase transport in a soil column. A substantial pressure variation responding to the migration of dense gas mixture along the column was observed. Based on various flux components computed from the pressure and density measurements, the slip and gravity-induced diffusions given in the dusty gas model (DGM) equation may account for more than 10% of the total diffusive flux component. The diffusive flux, if in terms of component mass fraction gradient for the Fickian-type diffusion, is in magnitude smaller than those with other gradient expressions, which may predict total flux two times in magnitude greater than the DGM result.

## INTRODUCTION

Gas phase chemical contaminants in soils possess a threat to human health once they continuously evaporate from industrial solvents, gasoline or agricultural chemicals residing in soils or dissolved in groundwater. As the popularity of monitoring natural attenuation as a subsurface remediation strategy increases, a complete understanding of gas phase transport under natural conditions is needed. It is recognized that gas phase transport in porous systems is driven by concentration difference, pressure variation and gravity. Fick's law is usually employed for gas phase diffusion. As one knows, chemical vapors mixed with soil gases may greatly alter total density of the gas mixture from the air density, so as to induce additional transport component, which is not considered in the Fickian-type diffusion. Besides, gravitational force may induce not only advection but also diffusion as included in the dusty gas model (DGM) equations, which may more comprehensively describe multicomponent gas diffusion in porous systems than the Fickian-type diffusion. Altevogt et al. (2003) conducted experiments for dense gas transport in a soil column. They observed pressure variation along the soil column when a dense gas mixture enters into the column and addressed it as slip. Then, they introduced a slip-induced flux component according to Jackson (1977) in the standard advective-diffusive transport equation as density-driven diffusion. Hamamoto et al. (2008) also investigated dense gas transport in two different soils with considering only Fickian-type diffusion in their modeling work.

This paper presents an experimental study on density-driven and gravity-induced transport of dense gas mixture along a soil column. Pressure and density variations along the column were measured in the experiment and used to determine various flux components with using the DGM equations and the Fickian-type diffusion, respectively.

## MATERIALS AND METHODS

An experimental setup for investigating dense gas transport in a porous system was constructed according to the setting presented in Altevogt et al. (2003). The transport system is a soil column packed with sea sand and connected at each end with a chamber, hereafter called inlet chamber (IC) and outlet chamber (OC), respectively. These components are all filled with nitrogen gas firstly and an amount of $SF_6$ was then injected into the IC to form a dense gas mixture in the chamber with a plunger cover the entrance to the soil column. Pressure transmitters are responsible for recording pressure differences between the outside and inside of the chambers and between sampling ports at the soil column and the inside of the OC. Before the plunger is pulled for allowing the gas mixture to enter the soil column, the whole system is maintained at atmospheric pressure by vent tubing on the IC and OC. Once the plunger

is pulled, pressure differences were recorded every half an hour and gas samples were taken every one hour from the ports at the IC and OC and four sampling ports along the soil column (5, 15, 25, 35 cm from the column entrance) for 4.5 to 5 hours. Concentration of $SF_6$ of each sample was measured using a gas chromatograph (GC-17A, Shimadzu Corp., Kyoto, Japan) equipped with an electron-capture detector (ECD) with a molecular sieve 5A GC PLOT capillary column (Supelco). The experiment was conducted with different initial $SF_6$ densities in the IC ranging from 0.8 to 1.55 $Kg/m^3$. The transport system has three different configurations: horizontally, vertically with the IC on the ground (transport in the vertically upward direction) or with the OC on the ground (transport in the vertically downward direction) to investigate gravitational effect on the migration of the gas mixture.

Before the transport experiment, batch study was carried out to assess sorptive effect of $SF_6$ onto sea sand. Result shows that the amount of $SF_6$ sorption onto sea sand is negligibly small. Effective diffusion coefficient and air permeability for gas phase transport in a soil column were also measured separately to assess diffusive and advective flux components of gas transport. These coefficients were determined from gas flow and diffusion experiments in which the setups and methodologies can be referred to Fen et al. (2009) and (2011). Soil columns used in different experiments were all packed with sea sand with a porosity of 0.3676.

**TABLE** 1 Expressions of various flux components with different formulation bases

| Flux component | Molar basis | Mass basis |
|---|---|---|
| Total diffusive flux of species $i$ | two-component DGM[&]: $$N_i^D = -\frac{D_{ij}^e D_i^K C}{D_{ij}^e + D_i^K(1-a_iX_i)}\frac{\partial X_c}{\partial z} - \frac{D_i^K(D_{ij}^e+D_i^K)X_i}{D_{ij}^e + D_i^K(1-a_iX_i)}\frac{\partial C}{\partial z}$$ $$-\frac{D_i^K(D_{ij}^e M_i + D_i^K M)X_i}{D_{ij}^e + D_i^K(1-a_iX_i)}\frac{Cg}{RT} \qquad (1)$$ | |
| | Fickian-type diffusion[%]: $$N_i^D = -D_{ij}^e\frac{\partial C_i}{\partial z} \qquad (2a)$$ $$N_i^D = -CD_{ij}^e\frac{\partial X_i}{\partial z} \qquad (2b)$$ | Fick's: $$G_i^D = -D_{ij}^e\frac{\partial \rho_i}{\partial z}$$ (2c) $$G_i^D = -\rho D_{ij}^e\frac{\partial w_i}{\partial z}$$ (2d) |
| Viscous flux of species $i$ [$] | $$N_i^v = -\frac{k_e}{\mu_m}X_i(RTC\frac{\partial C}{\partial z} - C^2 Mg) \quad (3a)$$ | $$G_i^v = -\frac{k_e}{\mu_m}\rho_i(\frac{\partial P}{\partial z} - \rho g)$$ (3b) |

[&] $X_i$ is mole fraction of species $i$; $C(=C_1+C_2)$ is total molar concentration ($mol/L^3$); $R$ is the universal gas constant ($ML^2/t^2 Tmol$); $T$ is the absolute temperature (°$K$); $g$ is the gravitational constant ($L/t^2$); $D_{ij}^e$ and $D_i^K$ are the "effective" binary molecular diffusion coefficient ($L^2/t$) and the Knudsen diffusion coefficient ($L^2/t$); $a_1 = 1-(M_1/M_2)^{1/2}$; $M = X_1M_1 + X_2M_2$.

[%] $\rho = \rho_1 + \rho_2$; $\omega_i$ is mass fraction of species $i$

[$] $k_e$ is effective air permeability of the medium ($L^2$); $\mu_m$ is dynamic viscosity of the gas mixture ($M/Lt$); $P(=RTC)$ is total gas pressure ($M/Lt^2$);

One-dimensional gas phase transport equation is generally applied to describe gas transport in a soil column. Two kinds of formulation basis are usually applied: molar and mass basis. Total flux of gas transport is divided into two components: total diffusive and viscous flux components. Expressions for

the total diffusive flux given in the dusty gas model (DGM) equations and in the Fickian-type diffusion are different as shown in Table 1 in which the DGM equation is expressed for gas diffusion system comprised of two gases. Various flux components for different formulation bases are also presented in the table. The Fickian-type diffusion expressions can be one of equation (2a)- (2d).

## RESULTS AND DISCUSSION

One set of the experimental results is presented in Figure 1 for transport in the vertically downward direction at an initial $SF_6$ density ($\rho_o$) of 0.8 kg/m$^3$ in the IC (about 0.13 mole fraction of $SF_6$). The pressure difference presented in the figure is a pressure value relative to the outside pressure of the system. It shows a negative pressure difference with the highest (-0.7 Pa) at beginning for the IC and a negligible difference for the OC throughout the measurement period. The four sampling ports at the soil column, however, respond with positive pressure differences quickly in half an hour once the transport starts. Specifically, the highest difference (1.3Pa) is located at 5 cm from the entrance and lasts for the rest measurement period. The results for transport in the horizontal direction are similar to those presented in the figure, but with lower pressure differences in the IC and in the column. For transport in the vertically upward direction, a reversed trend in pressure difference was observed, i.e., positive pressure differences measured from the IC and negative ones from the soil column. These pressure responses in the IC in our experiment are opposite to the result presented in Altevogt et al. (2003). Moreover, they observed a gradually increased pressure difference in the column.

**TABLE** 2 Various flux components of $SF_6$ determined from the DGM equation and the Fickian-type diffusion using the experimental measurements

| Flux unit in mol/m$^2$sec | | | Flux between the IC and 5cm port | | | Flux between the 5cm and 15 cm ports | | |
|---|---|---|---|---|---|---|---|---|
| | | | H[&] | VU[&] | VD[&] | H[&] | VU[&] | VD[&] |
| **DGM** | | First term in Eq. (1)* | 5.5903E-05 | 2.1544E-04 | 1.4383E-04 | 7.0585E-05 | 8.6899E-05 | 1.0931E-05 |
| | | Second term in Eq. (1)* | -6.2446E-06 | 1.8266E-05 | -1.0930E-05 | 4.2232E-07 | 2.2000E-08 | 3.9067E-07 |
| | | Third tern in Eq. (1)* | 0.0000E+00 | -1.0450E-05 | 7.1427E-06 | 0.0000E+00 | -3.5217E-06 | 3.4586E-06 |
| | | $N_i^{D\,!}$ | 4.9659E-05 | 2.2326E-04 | 1.4004E-04 | 7.1008E-05 | 8.3500E-05 | 1.4781E-05 |
| | | First term in Eq. (3a)[@] | -1.0114E-04 | 3.0123E-04 | -1.7107E-04 | 9.5523E-06 | 4.8512E-07 | 8.6004E-06 |
| | | Second term in Eq. (3a)[@] | 0.0000E+00 | -1.7220E-04 | 1.1169E-04 | 0.0000E+00 | -7.7538E-05 | 7.6021E-05 |
| | | $N_i^{v\,\%}$ | -1.0114E-04 | 1.2903E-04 | -5.9384E-05 | 9.5523E-06 | -7.7052E-05 | 8.4621E-05 |
| | | $N_i^{T\,\$}$ | **-5.1486E-05** | **3.5229E-04** | **8.0660E-05** | **8.0560E-05** | **6.3475E-06** | **9.9402E-05** |
| **Fick's** | $N_i^{D}$ | Eq.(2a) - (2c) | 6.7777E-05 | 2.6581E-04 | 1.6854E-04 | 8.1959E-05 | 9.8290E-05 | 1.2343E-05 |
| | | Eq.(2d) | 4.0032E-05 | 1.6231E-04 | 1.1429E-04 | 5.4086E-05 | 6.5325E-05 | 8.6959E-06 |
| | $N_i^{T}$ $\$ | Eq.(2a) - (2c) | **-3.3368E-05** | **3.9485E-04** | **1.0916E-04** | **9.1511E-05** | **2.1237E-05** | **9.6964E-05** |
| | | Eq.(2d) | **-6.1112E-05** | **2.9134E-04** | **5.4904E-05** | **6.3639E-05** | **-1.1727E-05** | **9.3317E-05** |

[&] H=transport in the horizontal direction ($\rho_o$ =1.14 kg/m$^3$); VU=transport in the vertically upward direction ($\rho_o$ =1.26 kg/m$^3$); VD=transport in the vertically downward direction ($\rho_o$ =0.8 kg/m$^3$)

[!] $N_i^{D}$ =Eq. (1); [%] $N_i^{v}$ =Eq. (3a); [$] $N_i^{T} = N_i^{D} + N_i^{v}$ ;

* First term=mole fraction gradient term; Second term=total concentration gradient term; Third term=gravity-induced diffusion term in Eq. (1)

[@] First term=total concentration gradient term; Second term=gravity-induced advection term in Eq. (3a)

Variation of the SF$_6$ density in the system corresponding to the pressure variation shown in Figure 1 is also presented in the same figure. It shows that the SF$_6$ density at the 5cm port is almost half of that in the IC in half an hour once the transport starts. Similar trends are also observed for transport in other directions. However, the density variation at the 35cm port and in the OC is almost negligibly small for transport in all directions in the 4.5-hr measurement period.

Various flux components of SF$_6$ for different transport configurations were determined according to the measurements obtained from our experiment. They are assessed between the IC and the 5cm port and between the 5cm and 15cm ports at a transport time of 4.5 hours. Gas permeability ($k_e$) and effective molecular diffusion coefficient of the N$_2$/SF$_6$ gas pair ($D_{ij}^e$) were determined to be $2.1 \times 10^{-11}$ m$^2$ and $3.53 \times 10^{-6}$ m$^2$/sec, respectively. The Knudsen diffusion coefficient of SF$_6$ ($D_j^K$) is consequently computed to be in the range of $2.67\text{-}3.89 \times 10^{-3}$ m$^2$/sec from the method presented in Fen et al. (2011). The transport system is therefore addressed to be dominated by molecular diffusion as $D_{ij}^e << D_j^K$. The parameters determined above were then used for assessing different flux components as shown in Table 2 in which the DGM equation, i.e., Eq. (1), and the Fickian-type diffusion expressions, i.e., Eqs. (2a)-(2d), were used for determining the total diffusive flux component and Eq. (3a) for the viscous flux component of SF$_6$.
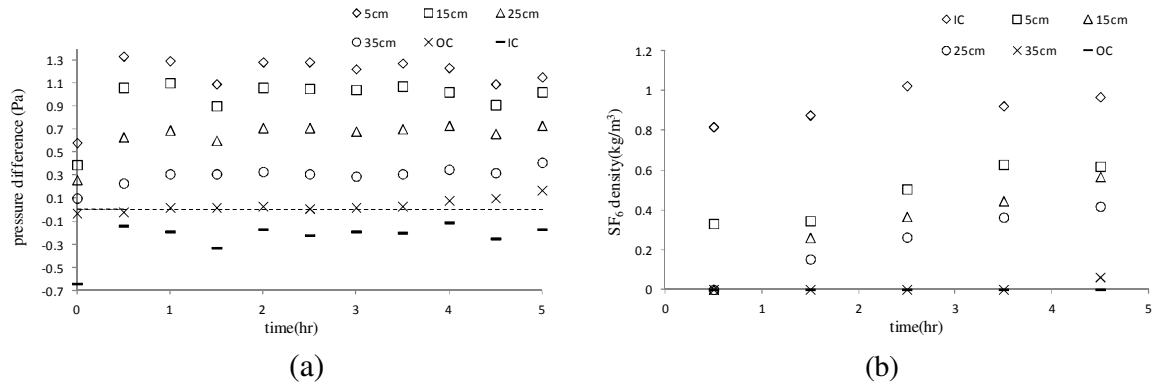


**FIGURE** 1 (a) Pressure difference and (b)SF$_6$ density measured at sampling ports for dense gas transport in the vertically downward direction at $\rho_o = 0.8$ kg/m$^3$ in the IC

For the two-component DGM equation, three terms are shown in the total diffusive flux expression, as in Eq. (1), including mole fraction gradient, total concentration gradient and gravity-induced diffusion terms in which the last two terms are not included in any Fickian-type diffusion expression. Note that slip is included in the total concentration gradient term with a sum of the effective molecular and Knudsen diffusion coefficients in the numerator. As a result, the diffusive flux component determined from the mole fraction gradient term is generally more than one order of magnitude greater than those from the other terms. As shown in the table, the gravity-induced diffusion term may account for 23% of the total diffusive flux component for vertical transport between the 5cm and 15cm ports; the total concentration gradient term (include slip) may account for 13% of the total diffusive flux component for transport between the IC and 5cm port. The same diffusive flux values were obtained with the component molar concentration, mole fraction and mass concentration gradient expressions for the Fickian-type diffusion, i.e., Eqs. (2a)-(2c), and are greater than those obtained with the component mass fraction gradient expression, i.e., Eq. (2d). Overall, the total diffusive flux value of SF$_6$ obtained with the DGM lies between the results with the Fickian-type diffusion, except for the VD result between the 5cm and 15cm ports.

The table further shows that the gravity-induced advection, i.e., the second term in Eq. (3a), is generally more than one order of magnitude greater than the advection induced by total concentration

variation (density-driven flow) for the vertical transport systems between the 5cm and 15cm ports. However, between the IC and the 5cm port, these advective components are of the same order of magnitude. Note that for the horizontal transport system the direction of advection is opposite to that of total diffusive flux component between the IC and the 5cm port, resulting in a total flux at the entrance of the dense gas mixture to the soil column in direction opposite to that in the soil column. Finally, it is found that the total flux of $SF_6$ assessed by the Fickian-type diffusion may be two times in magnitude greater than the DGM result for transport in the vertically upward direction.

## CONCLUSIONS

The experimental measurements show that pressure variation for dense gas transport along a soil column is substantial. Based on various flux components computed according to the pressure and $SF_6$ density measurements along the column, the slip and gravity-induced diffusions determined from the DGM may account for 13% and 23% of the total diffusive flux component, respectively. Different expressions for the Fickian-type diffusion are consistent in assessing the diffusive flux component, except for the expression in terms of component mass fraction gradient. The total diffusive flux and total flux obtained with the DGM generally lie between those given from different Fickian-type diffusion expressions, which, however, may result in total flux prediction two times greater than the DGM result.

## ACKNOWLEDGEMENTS

## REFERENCES

Altevogt, A.S., D.E. Rolston, and R.T. Venterea. 2003. "Density and pressure effects on the transport of gas phase chemicals in unsaturated porous media." *Water Resources Reserach* 39(3): 1061, doi:10.1029/2002WR001338.

Jackson, R.. 1977. *Transport in porous catalysts*, New York: Elsevier

Fen, C.-S., Y. Huang, and J.-L. Chen. 2009. "Experimental study of gas transport parameters in unsaturated silica flour." *Vadose Zone Journal* 8(2): 373-382.

Fen, C.-S., W. Liang, P. Hsiesh, and Y. Huang. 2011. "Knudsen and Molecular Diffusion Coefficients for Gas Transport in Unconsolidated Porous Media." *Soil Science Society of America Journal* 75(2): 456-467.

Namamoto, S., T. Tokida, T. Miyazaki, and M. Mizoguchi. 2008. "Dense gas flow in Volcanic ash soil: effect of pore structure on density-driven flow." *Soil Science Society of America Journal* 72(2): 480-486.

# POLYCYCLIC AROMATIC HYDROCARBONS DEGRADATION MODEL IN THE MARSH WETLAND SEDIMENT

***Doorce S. Batubara***, Ronald F. Malone, and Donald D. Adrian
(Louisiana State University, Baton Rouge, LA, USA)

Oil spilled in the U.S. Gulf of Mexico will accumulate over time while mobility, biological uptake, and degradation processes take place. Crude oil contains a significant amount of polycyclic aromatic hydrocarbons (PAHs) which can damage coastal areas and also can be toxic to many marine species, such as: marine diatoms, mussels, crustaceans, and fish. The degree to which those habitats and their species are impacted by the oil depends on a number of factors such as: amount of oil; degree of weathering before it reaches the coast; inundation rate onto the coastal area including marsh wetland; frequency of inundation; and rate of degradation or cleanup of the oil within these habitats. Some of the PAHs do not reach coastal areas or have been degraded significantly after undergoing some weathering processes such as: evaporation and dilution. The PAHs of concern that reach marsh wetland after being weathered are phenanthrene, pyrene, and benzo(e)pyrene. Knowing the level of these PAHs concentration in marsh wetland over a long time helps predict how much the aquatic species are exposed to PAHs contaminant.

Mathematical models are developed to show the degradation of PAHs, particularly phenanthrene, pyrene, and benzo(e)pyrene in a marsh wetland sediment over time. Numerical modeling using Stella Modeling Software is developed from mass balance equations for two levels of sediment: the top is for aerobic sediment and the bottom one is for the anaerobic sediment.

The long term impact of PAHs in crude oil to some aquatic species is relatively difficult to evaluate since exposure rates of the oil are largely unknown. Gulf coast habitats have experienced a wide range of inundation and exposure rates of the released oil making it difficult to assess the overall impacts to the coast and its fauna. Mesocosms allow replicated looks at different scenarios of long-term exposure and study of the biodegradation of contaminants of concern in crude oil (phenanthrene, pyrene, and benzo(e)pyrene), especially by mimicking important features related to their degradation in a marsh wetland sediment system. The designed recirculating mesocosm for the marsh wetland consists of two mud oil modules (MOMs) with different elevation to enable evaluation of sediment that is intermittently emerged by tidal movement or constantly submerged. The top or the emerged MOM is facultative since it is intermittently exposed to the air and the submerged MOM is anaerobic. The MOMs are put in a tank above an air chamber filled with water. The water level (tidal movement) is controlled by filling the air chamber with air (the water level goes up) and letting the water back to the air chamber (the water level goes down) periodically.

The modeling effort and ongoing mesocosm work is expected to show that degradation of PAHs is higher in the intermittently emerged sediment (subject to facultative degradation reactions and physical exchange processes) than the submerged sediments.

# GEOTECHNICAL PROPERTIES OF SOILS AFFECTED BY ACID MINE DRAINAGE FROM THE GOLDFIELDS OF SOUTH AFRICA

*Stephen O. Ekolu* (University of the Witwatersrand, Johannesburg, South Africa)
Firehiwot Azene (Council for Geoscience, Pretoria, South Africa)
Vivek Madhav (University of the Witwatersrand, Johannesburg, South Africa)

The acid mine drainage (AMD) flowing from abandoned mines may adversely affect soil characteristics both at the surface and underground. This paper is based on an investigation undertaken following field observation of soils contamination by acid mine drainage. Experiments were conducted using AMD water taken from field sources of the goldfields of South Africa. Two sets of experimental studies were done by: (a) testing of AMD-contaminated and non-contaminated soils obtained from field sources, (b) laboratory treatment involving soaking of two types of non-contaminated soils (taken from abandoned mines) in acid mine water, followed by testing of soil properties. Three types of AMD water from field sources, one synthetic AMD solution, and sulphuric acid to pH 1 were used in the experiments. The tests conducted include grain size analyses, physico-chemical properties, consistency, and strength. Also, microstructural analysis of the sheared soil samples was done by scanning electron microscopy. It was found that, generally, alteration (deterioration) of soil quality occurs when exposed to the acidic water. The characteristics of deterioration are associated with reduction of the pH of the soils, change of grain sizes to fine fractions, significant reduction in shear strength and bearing capacity.

# EMERGING CONCRETE MATERIAL TECHNOLOGIES FOR INSITU TREATMENT OF ACID MINE DRAINAGE – ISSUES AND LIMITATIONS

*Stephen O. Ekolu* (University of the Witwatersrand, Johannesburg, South Africa)
Firehiwot Azene (Council for Geoscience, Pretoria, South Africa)

**ABSTRACT:** Two emerging and innovative treatment techniques of employing cementitious material technologies i.e. coal ash and pervious concrete for insitu treatment of acid mine drainage (AMD) have been examined with a view of developing understanding of their effectiveness and feasibility. Field experience with the use of coal ash as AMD treatments by mine filling has yielded mixed results but the inadequacy may be related to flaws in the system design. Pervious concrete shows enormous potential as a permeable reactive material with the ability to remove contaminant elements from AMD water and from the environment altogether, moreover, at remarkable levels of efficiency. The main limitation however is the likely short lifespan of the filter. This and other related properties require improvement.

## INTRODUCTION

This article is focussed on potential use of cementitious material systems and pervious concrete technology as new approaches to insitu treatment of acidic mine water. Field data from the literature are examined and issues of interest discussed. This work in conducted against the background of relatively recent acid mine drainage problems experienced in South Africa, which highlight the need to develop cost effective, sustainable AMD remedial options with long-term viability. The oxidation of pyrites, usually from abandoned mining activity causes the formation of acidic mine water containing high concentrations of heavy metals. The oxidation process occurs upon exposure of the sulphidic ores to atmospheric oxygen and moisture in a chemical reaction process that eventually results in formation of sulphuric acid effluent given as (Petrik el al., 2006):

$$2\,FeS_2 + 7.5O_2 + 7H_2O \longrightarrow 2Fe(OH)_3 + 4H_2SO_4$$
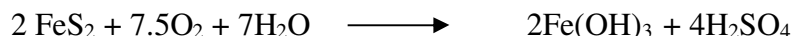
But it is the discharge of the acid mine drainage from its source of formation to the surrounding water courses that amplifies the problem causing diverse adverse effects. For underground mines, the acid mine water may pollute ground water aquifers that usually provide quality water for urban supply and human consumption. Underground mines may also discharge the polluted water to the surface as has been the case in the goldfields of the Witwatersrand, South Africa. Surface mines and tailings cause discharge of acid mine drainage at the earth's surface level, directly impacting the environment and its habitation.

## ABATEMENT TECHNIQUES FOR ACIDIC MINE WATER

The three necessary conditions responsible for the geochemical process of acid mine drainage formation are the presence of pyritic ore rock, the availability of sufficient oxygen, and the availability of sufficient moisture. Absence of anyone of these conditions would hinder formation of acidic mine water. Additionally, the presence of iron and sulphate oxidising bacteria is essential when the pH drops below 3.5. The approaches available for mitigation of acid mine drainage can be divided into four categories (Blowes et al., Younger):

- Prevention of the geochemical process
- Active treatment with lime or other chemical agents

- Passive wetland treatment
- Passive reactive barrier treatment

In each approach, there are a suit of possible methods that have in the past been proposed, used or attempted for abatement of the AMD problem under specific mine considerations. Table 1 gives the techniques available under the various approaches. The applicability of these methods is dependant on the physical site setting, the hydraulic conditions and water quality. But practical considerations have shown that just about every one of the methods has limitations, to the extent that some of these techniques have not gained consideration for full-scale field application. Nonetheless, insights can be obtained by examining the potential in the various methods.

TABLE 1 Techniques for control and mitigation of acid mine drainage

| Approach | Classification | Methods | Types |
|---|---|---|---|
| Prevention | | Physical barriers to oxygen and/or moisture | i) Dry /soil covers |
| | | | ii) Synthetic covers |
| | | | ii) Flooding |
| | | b) Oxygen consuming | iii)Organic covers |
| | | c) Coatings | |
| | | d) Bactericides | |
| Prevention and treatment | | Mine filling | Coal combustion products |
| Chemical treatment | Active | Lime | Others: soda ash, ammonia, limestone etc. |
| Wetland treatment | Passive | Wetlands | |
| Permeable reactive barriers (PRBs) treatment | Passive | Barriers | Limestone, municipal wastes, wood wastes etc. |

Neutralisation of acid mine water with lime is the conventional active treatment system, mainly suited as a short-time measure while better and sustainable options are being sought. Lime treatment is not only expensive, it is also unable to remove sulphates and it generates sludge waste by-product which has to be separated out and disposed of independently. It is normally expensive to set up a lime treatment plant and the process involves high maintenance costs which continue for an indefinite future of continuous AMD generation. Yet in all these, there are no income returns of any sort arising from operation of the plant. Lime treatment is therefore viewed as a non-sustainable operation but may serve well for emergency treatments. In South Africa, there are lime treatment plants situated in the West Rand goldfields and in some collieries of Mpumalanga coalfields. Their performance and efficiency has often been criticized on grounds of poor maintenance, high cost and lack of sustainability.

## USE OF CEMENTITIOUS WASTES FOR INSITU AMD-TREATMENT

The alkaline nature of cementious materials provides the basis for their effectiveness as neutralizing agents in the treatment of acidic mine water. Examples of cementitious wastes that have been found to be quite effective include cement kiln dust (Mackie and Walsh, 2011), paper waste (Bellaloui et al., 1998), fly ash (Vadapalli et al., 2008) or coal combustion by-products (CCPs) in general. While mine filling is an old art of land reclamation and restoration, its use as treatment to restore water quality is a new focus that has recently gained interest with regard to acid mine drainage. Over the past decades, some research efforts have been devoted along this application of using CCPs for AMD amelioration at its source. However, the efficacy of the technique is not fully established. Murarka (2006) lists 106 mines in US where CCPs have been used in mine filling applications. But most of these cases were carried out to structurally stabilise the mine void for underground mines or for land reclamation in the case of surface mines. Only few cases have been done deliberately as treatments for AMD water quality improvement.

Some understanding of the effectiveness and the limitations of using cementitious /coal ash wastes in mine filling has been acquired from field experience and research in the recent years.

**Impact of CCP Injection on AMD Water Quality.** Monitoring of water quality following injection of CCPs have yielded mixed results. In some cases (e.g Clinton County mine), pH increased temporarily from 2.3 to 9 while element concentrations reduced for a short time before returning to pre-injection quality. In others (e.g Arnold Willis mine) there was no significant change in pH and acidity but alkalis (Na, K, Ca, Mg) increased in the water effluent. However, there are other mine injection treatments where marked improvement in water quality has been reported. In the Universal Mine, a dry fill of bottom ash /fly ash to reclaim an open pit mine 576m long x 97.5m wide x 2.7m deep was monitored for 13.5 years. The water pH increased from initial 3.5 pH to a level of 6.4-7.2 pH accompanied by a decrease in Fe, Mn, $SO_4$. One year of monitoring was also reported after injection of 415 tons of coal ash in a 45.6-acre Red Oak "rat hole" coal mine. The pH increased from 4.4 to 6.3, while the concentrations of 200 mg/l Fe, 7 mg/l Mn, 6 mg/l Al in AMD water all decreased to 120 mg/l, 4.8 mg/l, 2.3 mg/l respectively. It may be expected that water quality will likely return to pre-injection levels after depletion of the alkalinity of CCP treatment. The Winding Ridge Project /Frazee Mine is a grout filling project that was reportedly conducted to demonstrate beneficial use of CCPs for remediation of AMD. The 10-acre coal mine which was operated in the 1930s to 60's, consisted of two underground tunnels connected by cross-cuts. A grout mixture of 60% bottom ash + 20%Class F fly ash + 20%FGD mixed with mine water was injected in 1996 and afterwards monitored for 10 years. It was reported that the pH of water effluent increased from initial 2.6-3.4pH to steady 3.0-3.6 pH i.e an increase of about 1 unit. Average acidity decreased by 80% while Fe, Al, $SO_4$ concentrations all decreased. Some of the contributing factors to the effectiveness of the insitu treatments seem to be the mix design of grout mixtures, mineralogy of the CCP wastes, initial AMD water quality, and perhaps also the method of grout injection.

**Longevity of Insitu CCP Injection Treatment**. In those treatments where the injection of CCPs have improved the effluent water, there is presently no clear indication of the lifespan to which the treatment may continue to maintain improved water quality. Data from field experience shows that at least 10 years can be expected from some effective treatments. However, a continuous generation of AMD will deplete the neutralising capacity of the grouts, causing the water quality to degrade and eventually return to initial poor quality. But there are no complete studies that may provide answers to this question, and extensive research is needed to deal with the issue of the durability and lifespan of CCP insitu treatment (Murarka, 2006).

**Mechanism of AMD Remedial Actions by Alkaline Reagents.** Multiple processes appear to be involved in the use of alkaline reagents for insitu treatment of AMD:- (a) The *dissolution* and *adsorption* chemical processes emanate from the high alkalinity of treatment reagents. The calcium (and other alkalis) present in them dissolve and react with hydrogen ions in the AMD water, causing neutralisation of the latter. As alkalinity increases, the Fe and Al precipitate out of the water solution at pH levels of 6 to 8, while other ions can precipitate at higher pH values. But the dissolution process does not account for the elements that are not affected by pH increase, especially sulphates. Adsorption has been proposed as another possible mechanism that may explain the reduction of ion concentrations in water, when acid mine water is exposed to cementitious systems. The highly alkaline concrete or grout surface is negatively charged and the cations (mainly metals) in water are attracted and chemically adsorbed onto the cementious surface. The adsorption occurs at specific sites at the surface. Since there are limited adsorption sites at any given surface, it is expected that the process can be efficient initially, reducing the metal concentrations significantly. But as time progresses and further fresh AMD comes in contact with the surface, its adsorption capacity will be exhausted. Consequently, the concentration of metal ions in the solution will rise asymptotically approaching the levels of untreated water, in a manner referred to as the "breakthrough curve". Figure 1 represents the development of events described and the shape of the breakthrough curve pattern (Gynn et al., 2007). Results from field investigations, however, do not fully

agree with the breakthrough pattern of changes in metal concentrations. It has been reported that certain field sites where grouts had been applied, exhibited initial rise in metal concentrations before decreasing significantly. Furthermore, the adsorption mechanism should be incapable of affecting the concentration of sulphate ions, since these are negatively charged. In contrast, field results show that sulphate concentrations are reduced by as much as 50% due to insitu treatment of AMD by using grouts. (b) When properly applied, grouting can also provide sealing of reactive surfaces, cutting off their exposure to oxygen and thereby preventing pyritic oxidation from occurring. Consequently, the AMD discharge from the reactive surfaces may reduce, leading to improvement in the quality of water effluent from the mine.
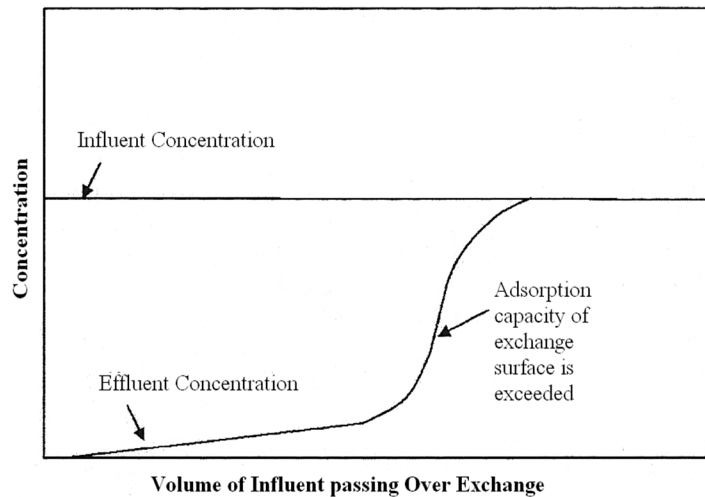


FIGURE 1 Breakthrough curve of adsorption at the AMD water-grout interface (Gynn et al., 2007)

## PERVIOUS CONCRETE WATER PURIFICATION TECHNOLOGY

It has been shown that pervious concrete on its own contains water purification qualities but very limited work has been done to scientifically establish the essence of this property. Experimental studies (Park and Tia, 2004; Majersky 2009; Brown) have found that properly designed pervious concrete can be effective in purifiying polluted or acidic water, not only raising its pH but also efficiently removing most of the undesireable chemical elements including sulphate, iron, zinc, sodium, magnesium, manganese and most other metals. Furthermore, reported water quality improvements in field applications of pervious concrete involving pavements include reduction in oil and grease, and petroleum products (PAH's – Polycyclic Aromatic Hydrocarbons) from the water effluent drained through pervious concrete (Brown). The use of different cementitious material systems and mixture designs also influence the quality of the purification attainable.

Figure 2 shows results of a demonstration pervious concrete pavement which was monitored for changes in pH and water quality under stormwater run-off. Typically, the suitable range of pH for domestic water use is 5 to 9. Pervious concrete can raise the pH of water to higher levels beyond this range, depending on the mixture designs. It is reported that the pH surges immediately upon contact with water, before stabilizing within 15 to 20 minutes (Brown). Conflicting results have been reported as to whether the use of fly ash and/or slag extenders may raise the pH any greater than plain Portland cement (PC) mixtures. Park and Tia (2004) show fly ash concrete giving higher pH than plain PC concretes, at least initially, while Brown's results indicated quite the opposite (see Figures 2 and 3). Brown's results also suggest 20 to 30% incorporation of fly ash to be the most suitable range, with higher proportions in the range of 50% showing less effective results in raising the pH. Majersky (2009) reported significant element removal efficiency from AMD water by using pervious concrete, as shown in Figure 4.

In terms of field application, pervious concrete can potentially be used as a Permeable Reactive Barrier (PRB) for AMD treatment. PRB's are insitu treatments constructed by excavating the flow path of the acidic mine water and filling it with the reactive material. Figure 5 shows an installation of a reactive barrier in combination with different treatments. The main limitation of pervious concrete for use as a PRB material is associated with its service lifespan. Research shown in Figures 2 to 4 all show that the efficiency levels of the filter will reduce within a short time period (of up to three months). While there has been no comprehensive research work done to establish the mechanisms responsible for the loss in efficiency of the filter, it may be attributed to depletion of neutralizing ions in association with the adsorption mechanism. Accordingly, the "breakthrough" curve (shown in Figure 1) may also represent the functioning of a pervious concrete filter.
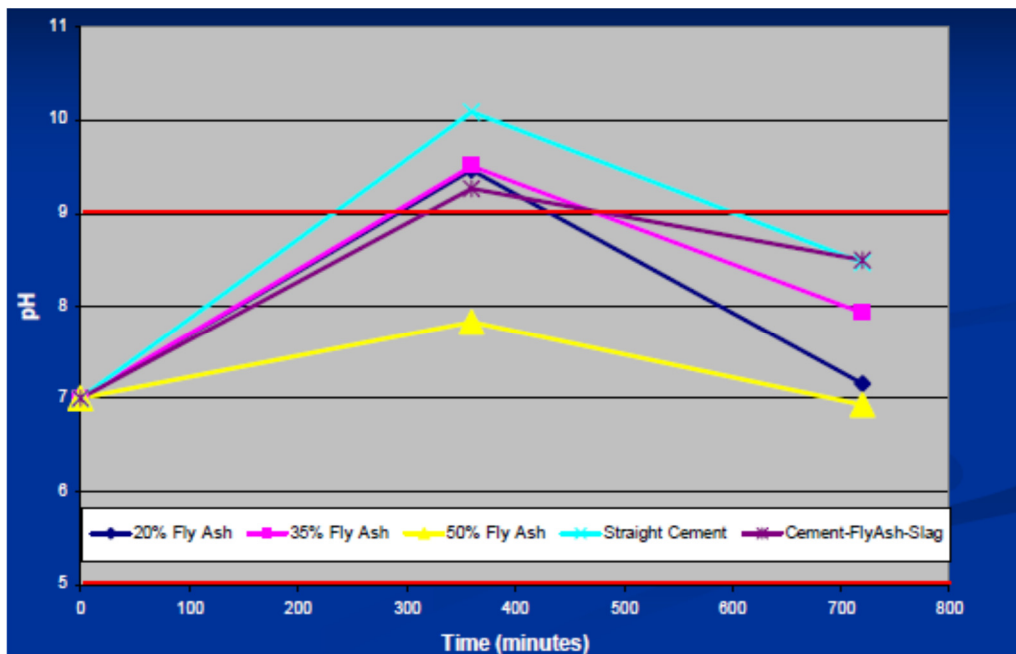


FIGURE 2 Change in pH of storm water passing through pervious concrete pavement of varied mixtures (Brown)
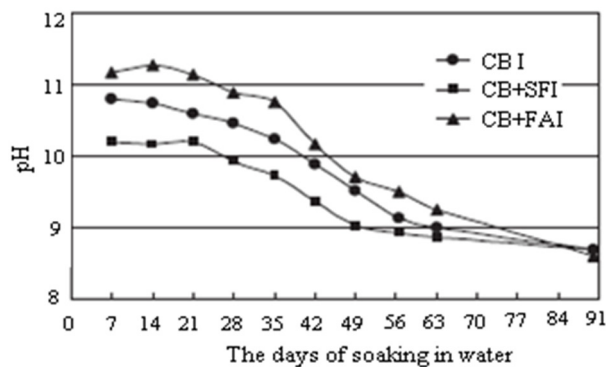


FIGURE 3 Change in pH of water used to soak pervious concrete; CB = Portland blast-furnace slag cement, SF = silica fume 10%, FA = fly ash 20% (Park and Tia, 2004)
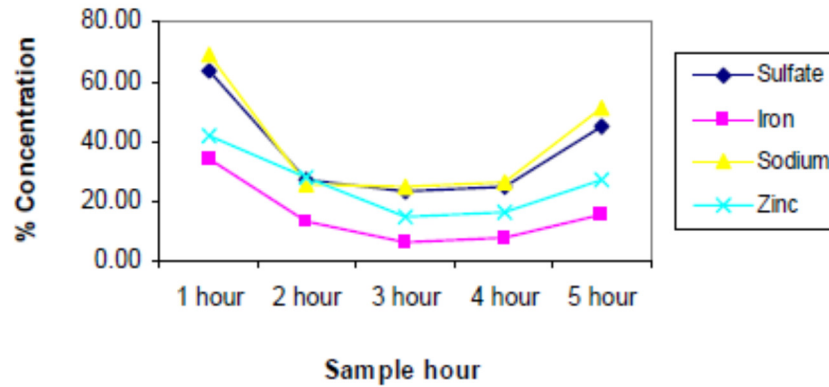
FIGURE 4 Removal of elements from AMD water using a pervious concrete filter (Majersky, 2009)
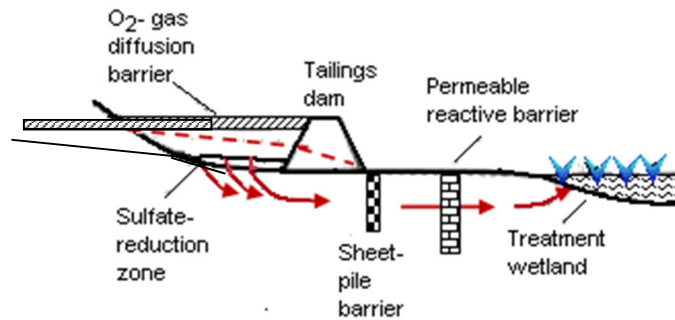


FIGURE 5 Permeable reactive barrier installation (Blowes et al.)

## SUMMARY

The purpose of the article was to examine the concrete material technologies of utilizing cementitious wastes and pervious concrete as remedial insitu treatments for acid mine drainage. Field experience from the use of coal ash indicates mixed results but it appears that a properly designed system can produce an effective insitu treatment system. Pervious concrete has tremendous potential for use as a permeable reactive barrier material. The paramount value in pervious concrete filter treatment is its ability to remove contaminant agents from the environment, which other treatment systems are unable to achieve. Pervious concrete increases pH of acid mine water and has been found to reduce element concentrations significantly. But the innovation is still premature and further research is needed to develop the technology further for AMD treatment. A major concern for both treatment systems is their limited lifespan, which appears to range from few months to years. Longer life spans are indeed desireable in order to enhance the viability of the technologies for application as insitu treatment systems.

## REFERENCES

Bellaloui A., Chtaini A., Ballivy G., Narasiah S. 1998, "Laboratory Investigation of the Control of Acid Mine Drainage using Alkaline Paper Mill Waste", *Dept of Civil Engrg, University of Sherbrooke*, Quebec, Canada, 17p.

Blowes D.W, Ptacek C.J, Jambor J.L, Weisener C.G, *The Geochemistry of Acid Mine Drainage*, University of Waterloo, Canada, 196p

Guynn R.L., Rafalko L.G, Petzrick P. 2007, "Use of a CCP Grout to Reduce the Formation of Acid Mine Drainage: 10-year Update on the Winding Ridge Project", *World of Coal Ash (WOCA)*, May 7-10, Nothern Kennedy, USA, 20p

Mackie Allison L., Walsh Margret E. 2011, "Bench-Scale Study of Active Mine Water Treatment using Cement Kiln Dust (CKD) as a Neutralization Agent", *Water Research* (2011) 1-8

McCarthy T. (2011), "The Impact of Acid Mine Drainage in South Africa", *The South Africa Journal of Science*, 107(5/6), 7p

Murarka Ishwar P. 2006, *Use of Coal Combustion Products in Mine-Filling Applications: A review of Available Literature and Case Studies*, Final report, DOE Award No. 99-CBRC, 44p

Park S-B and Tia M. 2004, "An Experimental Study on Water Purification Properties of Porous Concrete", *Cement and Concrete Research*, 34, 177-184

Vadapalli V.R.K, Klink M.J, Etchebers O., Petrick L.F, Gitari W., White R.A, Key D., Iwuoha E. (2008), "Neutralization of Acid Mine Drainage using Fly Ash, and Strength Development of the Resulting Residues", *Research Letters, South African Journal of Science*, 104, July/August 2008, 317-322

Younger Paul L.," The Mine Water Pollution Threat to Water Resources and its Remediation in Practice, *School of Civil Engrg and Geosciences, University of Newscatle*, Newcastle Upon Tyne, NE1 7RU, UK, 48p

# REDUCTION OF LEAD PAINT BIOAVAILABILITY IN SOIL THROUGH ADDITION OF APATITE II

*A. **Hunt***, D.S. Alkandary, and R.W. Brown
(University of Texas – Arlington, TX, USA)

Building line soils around older residences can contain highly elevated levels of lead (Pb) as a result of flaking of old Pb-based paint applied historically to the outside of the structure. Old Pb-paint can contain variable quantities of Pb, ranging from those that consist mostly Pb-pigment (usually basic lead carbonate), to low Pb-pigment concentrations in vehicles (e.g., linseed oil, alkyd resin) that contain substantial quantities of extender components (inexpensive inorganic pigment substitutes).

A potentially useful method of *in situ* reduction of bioaccessible Pb in soil utilizes a phosphate amendment to convert the soil Pb to a sparingly soluble Pb-phosphate form. Here we explore the application of phosphate amendments to soils to which we have added Pb-paint in a variety of forms. We examined phosphate-induced immobilization of paint-Pb through addition of the biogenic (from fish bones) phosphate product Apatite II ($Ca_{10-x}Na_x(PO4)_{6-x}(CO3)_x(OH)_2$ where $x < 1$).

In a series of soil column trials, a commercially available "A" horizon soil was spiked with Pb-paint of different compositions, and amended with phosphate in the form of Apatite II. Ten Pb-paints were utilized, that contained Pb-pigment in various crystalline forms ($PbCO_3$, Pb-oxide, Pb-phosphate, and $PbSO_4$), and a wide variety of extenders and other pigments (e.g. Zn-oxide, Ti-oxide, quartz, dolomite, calcium carbonate, Ba-sulfate, Cr, Fe). Dried paints were ground and screened to $< 250\,\mu m$ and mixed with soil on a 2% w/w basis. Apatite II was added and mixed at 5% w/w. Two and three replicates were prepared for each Pb paint sample type for apatite and no apatite additions. Select samples had iron sulfate added to reduce soil pH. Control soils were included that were either unmodified or contained Apatite II. In all, a set of sixty-seven soil columns were monitored. Three times a week 10 ml of Milli-Q water was added to the surface of each soil column. Subsamples from each column were collected at baseline (time zero), and at three-, six-, and twelve-months for *in vitro* bioaccessibilty testing.

An *in vitro* bioaccessibility assay was employed that utilized a simulated gastric fluid extraction to determine the amount of Pb that could potentially be mobilized in the human stomach if the soil were ingested. In the first instance Pb bioaccessibility was determined from soil samples taken from the soil columns at times zero and twelve-months. X-ray diffraction (XRD) was used to determine the crystalline form of the Pb in the paints. Scanning electron microscopy (SEM) and energy dispersive X-ray spectroscopy (EDS) was used to obtain information on the associations between Pb and other inorganic constituents at the individual particle level at both time points. The determination of the quantity of Pb mobilized in the *in vitro* assay was accomplished using a hand-held X-ray fluorescence (XRF) detector with the extraction fluid being retained in a mylar window cup, and placed on the window of the detector.

We found that there was a general reduction in the amount of bioaccessible Pb in the soils at twelve months compared to time zero. This was supported by the identification of Pb-phosphate particle phases in the soil samples at twelve months (by SEM/EDS). We also found that in the control soils (Apatite II not added) there was a general increase in the amount of bioaccessible Pb at twelve months. The effectiveness of using apatite II to remediate Pb-paint contaminated soil, through the immobilization of Pb through the formation of the sparingly soluble Pb-phosphate mineral pyromorphite ($Pb_5(PO_4)_3(Cl)$) appeared to be justified.

# APATITE II IMMOBILIZATION OF LEAD IN SOIL – A NEW ORLEANS FIELD TRIAL

*A. Hunt*, B. Shirtcliff, D. Alkandary, R.W. Brown
(University of Texas – Arlington, TX, USA)

Low-level, inadvertent, pediatric ingestion of lead (Pb) contaminated soil can produce sub-clinical adverse health effects. The problem posed by Pb in soil is that it is relatively abundant in urban-industrial areas with long-duration occupancy (e.g., older inner-city areas). In this context, effective risk reduction requires an appropriate form of mitigation. While many remediation strategies have been advocated and implemented, there is no consensus on what constitutes a "cost-effect" intervention that can be widely used to address a problem that can be very expensive to remediate. Here, we focus on the addition of phosphorus to soil as a way of converting the Pb to a sparingly soluble (less bioaccessible) form.

The Contaminated Urban-yard Restoration: Testing Apatite II Immobilization of Lead in Soil (CURTAILS) - A New Orleans Field Trial, is a study where we are testing the proposition that the bioaccessible Pb in residential soil can be limited by adding the biogenic (from fish bones) phosphate product Apatite II ($Ca_{10-x}Na_x(PO4)_{6-x}(CO3)_x(OH)_2$ where x < 1). The effectiveness of Apatite II is being tested in side-by-side plot trials with a variety of other types of phosphate products that have been used in previous studies. These other phosphates are: Triple Super Phosphate ($Ca(H_2PO_4)_2 \cdot H_2O$), rock phosphate ($Ca_5(PO_4)_3F$), hydroxyapatite (calcium apatite; $Ca_{10}(PO_4)_6(OH)_2$), bone-char fertilizer (poorly crystalline apatite, $[Ca_{10}(PO_4)_6OH_2]$), bone-meal fertilizer (typically, 90% hydroxyapatite and 10% carbon) and phosphoric acid ($H_3PO_4$). The appropriateness of these phosphates for treatment of Pb contaminated soil in New Orleans, LA, is being tested at three residential sites. The goal of adding phosphate to the soils is to supply phosphorus which can combine with the resident Pb to form a lead phosphate mineral from (pyromorphite). This mineral form has an extremely low solubility product (Ksp) of approximately $10^{-80}$. Pyromorphite is thus highly insoluble and when consumed should be bio-persistent in physiological gastric fluid. The transformation process in the soil involves the dissolution of the Apatite II followed by precipitation of pyromorphite phases.

Apatite dissolution: $Ca_5(PO_4)_3OH + 7H^+ \leftrightarrow 5Ca^{2+} + 3H_2(PO_4)- + H_2O$
Lead Precipitation: $5Pb^{2+} + 3H_2(PO_4)^- + H_2O \leftrightarrow Pb_5(PO_4)_3OH + 7H^+$
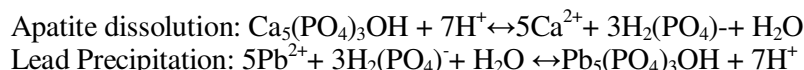
Here we present initial results from an in vitro bioaccessibility assay used to assess changes in the likely bio-persistence of soil Pb at various time points following phosphate addition. The residential sites under investigation in this study are located in the St Roch and Treme neighborhoods of New Orleans. Tests of surface soils collected at various locations in each yard revealed soil Pb concentrations typically in excess of 1,000 mg/kg. Each of the three study yards was divided into eight plots 10' x 10' in size, two of which were each amended with three of the phosphate products with the remaining two reserved as controls. The pre-amendment soils did not exhibit 100% Pb bioaccessibility following the in vitro dissolution. Microscopic analysis of the pre-amendment soil revealed Pb in the form of classic Pb-paint pigment particles. In addition, prior to the amendment, some fraction of the Pb in the soil was found to be associated at the individual particle level with phosphorus (as determined by scanning electron microscopy and energy dispersive X-ray spectroscopy). This analysis suggested that a transformation of the soil Pb to a Pb-phosphate form was occurring in the soils before the addition of the phosphates.

We suggest, that Apatite II, because of its low cost, can be used to accelerate the conversion of the soil Pb to a Pb-phosphate form which appeared to be already underway in the New Orleans soils. Because Pb contamination of soil is widespread in New Orleans, we posit that Apatite II could be widely used in the city as a way of reducing the toxic levels of Pb in the soils

# PHYTOREMEDIATION OF ARSENIC CONTAMINATED SOIL BY FUNGI INOCULATED RUDBECKIA HIRTA

*Haydn A. "Chip" Fox* and Beth Felix

(Texas A&M University-Commerce, Commerce TX, USA)

A feasible method for using phytoremediation of arsenic contaminated soil was investigated. *Rudbeckia hirta* (black-eyed susan) has shown potential in previous studies and arbuscular mycorrhizal fungi is known to take up phosphorous which is similar in chemistry to arsenic. Several groups of *R. hirta* were planted in both arsenic-contaminated soil and arsenic free soil to determine the fungi-inoculated plants' effectiveness in removing arsenic from the soil. It was concluded that R. hirta does have phytoremediation potential that may aid in the cleanup of arsenic contaminated areas. There was no statistically significant increase in the rate of absorption between the fungi inoculated group and the arsenic control group.

# DEMONSTRATION OF IN-SITU REMEDIATION USING A LOW CONCENTRATION SURFACTANT IN A SHALLOW AQUIFER

*Lee, G.S.*, Uhm, J.Y., Kim, Y.I. (Rural Research Institute, Gyunggi, R.O. Korea)
Kam, S.I. (Louisiana State University, Baton Rouge, LA, USA)

This research demonstrates in-situ remediation of LNAPLs, consisting of oils, benzene, toluene, ethyl benzene, and xylene, at a military base located in the Western part of South Korea, by using a low concentration non-ionic surfactant. The military base has been used as a major hydrocarbon storage and distribution focal point for gasoline and diesel fuels since 1991. During the investigation, it was found that as much as 6,374 $m^2$ of soils were contaminated by leaked oils, especially concentrated near and underneath oil distribution facilities and buildings. The contaminants were shown to be present approximately 3.5 m below the ground, exceeding the Korean soil contamination countermeasure standard at a military base. These oil distribution facilities and buildings sitting on a concrete and cement foundation were still in operation, and therefore the use of in-situ remediation method were selected as the most viable and practical means not to disrupt on-going activities.

In order to conduct the small-scale in-situ remediation pilot tests, three injection and three extraction wells were drilled in parallel to about 5 m depth. The distance between injection and extraction wells was approximately 5.0 m, and the distance between adjacent injection or extraction wells was 2.5 m. The well diameters were about 50 mm. Tween-80 surfactant was selected because of a low toxicity and a low critical micelle concentration (CMC) value, in addition to well-investigated fate characteristics. Two cycles of injection, each cycle consisting of surfactant followed by water, were performed. The first injection cycle was conducted in three injection wells during 9 days in which extraction wells were pumping out ground water simultaneously. This operation was carried out only during the day time (about 10 hours per day) because of the military regulations prohibiting any non-military activities during the night time. The concentration of injected surfactant solution was 0.1 ~ 0.2 % (v/v), and a total of 7,800 L of solution was injected during first 5 days. Bromide at the concentration of 671 mg/L was also injected together with surfactant as a tracer during first 1,200 L injection. After the 5 days surfactant injection, groundwater injection was followed for 4 days to induce the migration of surfactant solution toward the extraction wells. The second injection cycle was conducted for another 5 days, again during day time only, 25 days after the end of first injection cycle. Approximately 4,200 L of surfactant solution was injected at the concentration of 0.3 % (v/v) during 5 days.

When the concentrations of tracer and LNAPLs were continuously monitored and measured from 3 extraction wells, the results from these tests showed that (i) there was some level of heterogeneity between the injection and extraction wells, evidenced by early breakthrough of the tracer; (ii) the concentration of LNAPLs increased sharply for the extraction well along the high-conductivity path, while the concentration of LNAPLs increased much gradually for the extraction well along the low-conductivity path, implying the operation time for remediation depends on heterogeneity.

In addition, the results from soil sampling tests after the first and second injection cycles at the locations roughly half-way between injection wells and extraction wells showed that (i) for the high-conductivity path, the LNAPL concentration in soils increased at the end of first cycle, but decreased after second cycle; and (ii) for the low-conductivity path, the response was similar, but the change in LNAPL concentration was a lot smaller. These results indicated that the injection of surfactant solution migrated LNAPL towards the extraction wells, if the process was continued long enough. After two cycles of surfactant and water treatments, the entire site was shown to have LNAPL concentration below the Korea regulatory standard. It is believed that the use of mobility-control agent, such as foams, can be used to accelerate the remediation process or to treat larger contaminated areas more efficiently, which remains as our future research topic.

---

# THE EFFECT OF COMPOSTING ON THE SURVIVAL OF *ESCHERICHIA COLI* O157:H7 IN BOVINE MANURE.

***Itelima Janet*** and Agina Samuel
(University of Jos, Jos, Nigeria)

**ABSTRACT:** Raw animal manure can lead to serious pollution problems, by fouling water ways, disrupting the flora and fauna in the soil and spreading of pathogens into the environment. Outbreaks of *Escherichia coli* O157:H7 infections associated with vegetables, fruits and root crops have occurred with increasing frequency in the recent years. Contaminated manure has been recognised as one of the probable vehicles for the pathogen in many outbreaks. In this study, the effect of composting on the survival of *E. coli* O157:H7 in bovine manure was determined. Two different types of bovine manure, bovine feces and bovine slurry were inoculated with *E. coli* O157:H7. The pathogen concentration was $10^5$ CFU/g of manure. The contaminated manure was mixed with saw dust to obtain carbon nitrogen ratio (C:N) of 30. The composting procedures were carried out in the windrows and plastic bins, while the control experiments (bovine feces and bovine slurry not mixed with saw dust) were kept at fluctuating environmental conditions. *E. coli* O157:H7 survived for 4 months and 6 months in manure composted in windrows and plastic bins respectively. The bacterium persisted in manure kept at fluctuating environmental conditions for up to eight months, and the percentage recovery of the organism ranged from 27% to 124% at different times over the course of the experiments. No significant difference ($p > 0.05$) was observed in *E. coli* O157:H7 survival based on the manure types alone, but significant differences ($p < 0.05$) existed in the survival of the organism with regard to the composting methods. The long-term survival of *E. coli* O157:H7 in raw manure emphasizes the need for appropriate farm waste management to curtail environmental spread of this bacterium. Raw animal manure must be composted if it is to be applied to the land used for a crop intended for human consumption.

## INTRODUCTION

Animal manure use is well accepted among farmers and demand for manure is projected to increase as organically grown vegetables and fruits gain in popularity. In most countries, however, animal manure is often viewed as a waste management problem (Eghball and Power, 1994) due to the availability of inexpensive man made commercial fertilizer and the prohibitive handling cost of manure from the confinement to the agricultural fields. This results in manure disposal at excessive rates on agricultural field nearby the feed lot or disposed on crop fields without consideration to nutrient values. Lack of storage space is also one of the waste management problems encountered by farmers. In addition, raw cattle manure may not only led to serious pollution problems by fouling water ways and disrupting the flora and fauna in the soil but may play an important role in the persistence and dissemination of pathogens on agricultural environment. Vegetable plants can become contaminated with pathogens before harvest when grown in fields fertilized with fresh or aged manure (Islam *et al*., 2004). This in no doubt has spelt out clearly the need for intervention strategies such as composting of raw manure to prevent contamination of food and water supplies. Composting is the process of decomposing organic matter, whether manure, crop residue or municipal wastes, by mixed microbial population in a warm, moist aerobic environment. Composted manure is not only a potential source of nutrient needed for organically grown plants, it is free of pathogenic organisms.

*Escherichia coli* is a normal number of the gastrointestinal microflora of humans and animals, however *E. coli* serotype O157:H7 can severe hemorrhagic disease, and in some cases lead to serious complications, even death (Buchanan and Doyle, 1997). *Escherichia coli* O517 H7 has been a public health concern to food processors and consumers since its first recognition in 1982, with incidents of food

borne associated with this pathogen occurring in most countries (CDC, 2006). Healthy cattle sporadically harbour *E. coli* O157:H7 in their gastrointestinal tract and shed the pathogen asymptomatically in their feces (Kudva *et al*., 1998). Previous studies have revealed long term survival of *E. coli* O157 H7 in manure held under a variety of conditions (Kudva *et al*., 1998; Grewal *et al*., 2006; Franz *et al*., 2007). In addition, *E. coli* O157 H7 can survive, replicate, and move with in soil, and the presence of manure increase the pathogen's survival time (Gagliardi *et al*., 2000).

In most developed countries, raw manure must be composted if it to be applied to land used for a crop intended for human consumption. However, in Plateau States, Nigeria – the experimental area, organic manure farmers rarely apply composted manure to their farms. They use aged manure that has been kept for about one month under fluctuating environmental conditions. The application of raw manure or aged manure on agricultural fields has been found to increase the risk of pathogen contamination of farmland and agricultural produce (Armstrong *et al*., 1996). Research work done on composting of animal in is very limited. Therefore, there is dearth of information on the effect of composting on the destruction pathogens in animal manure. The objective of this research is to evaluate the effect of composting on the survival of *E. coli* O157:H7 in bovine manure.

## MATERIALS AND METHODS

Composting of bovine manure inoculated with *E. coli* O157:H7 was carried out in windrows and plastic bins. Manure samples kept under fluctuating environmental conditions to serve as control experiments. The major materials used in this experiment included the following: bovine slurry (BS), bovine feces (BF) and saw dust (S). The composting process was carried out between the months of October 2009 to April 2010.

**Collection of Compost Materials.** Manure and sawdust were collected from abattoir and timber market respectively in Jos Plateau State, Nigeria. These materials were loaded in big sacks and transported to the Botanical Garden of the Department of Plant Science and Technology University of Jos, the experimental sites. The manures were sundried to reduce microbial load and moisture content and then re-bagged prior to use.

**Construction of Windrow.** Ten freestanding windrows were constructed at the Botanical Garden of the Department of Plant Science and Technology University of Jos. The size of the windrow was adopted from Larney *et al*. (2003).

**Preparation of inocula.** *E. coli* O157:H7 isolated from bovine feces was subcultured on three successive days to reactivate the cells after storage in refrigeration (Sutherland *et al*., 1995). *E. coli* O157:H7 was inoculated into portions of the manure with pathogen concentration of $10^5$ cfu/g of manure to serve as inocula.

**Experimental Protocol.** Saw dust was added to different manure types (BS and BF) to obtain carbon to nitrogen ratio (C: N) of 30 according to the method prescribed by Alberta Government Agriculture and Food Agency (AGAFA) (2005). The (C:N) of manure is a very important factor that affects the whole composting process because microbes need 25 to 30 times more carbon than nitrogen. The manure–sawdust mixture was inoculated with *E. coli* positive manure (inoculum) and composted in the windrows and plastic bin in replicates of five for each manure types. The amount of manure used in each window and plastic bin was 20kg. The manure saw dust mixture was watered to obtain the recommended moisture content of 60% needed for active composting. Bovine manure types without saw dust comprised of bovine feces and bovine slurry (BF and BS) was each inoculated with *E. coli* O157:H7 positive manure and kept outside the Botany Garden under fluctuating environmental conditions and used as control experiments as earlier stated. The different types of compost manure were replicated five times and samples were collected from them on weekly basis and taken to the laboratory for analysis. The *E. coli* O157:H7 counts were determined for each manure types weekly by culturing on selective agar medium – Sorbitol MacConkey agar (March and Ratnam, 1986) and then confirmed both biochemically and serologically as described by Cheesbrough (1991) and Nataro and Kaper (1998) respectively. The temperature in the different manure types were recorded weekly using a thermometer which was inserted inside the manure piles. The pH of the manure samples was determined during each sampling period by homogenizing 5g of the manure with 45ml distilled water. The pH of the resulting homogenate was

measured with pH-meter (Model 320). Moisture content was determined by drying 5g portions to constant weight in a hot air oven at $80^O$C.

**Statistical Analysis.** The statistical analyses employed in this study were one way analysis of variance and correlation coefficient analysis.

**RESULTS AND DISCUSSION**

   The results of the effect of composting on the percentage recovery of *E. coli* O157:H7 from various compost manures are depicted in Fig.1. As the composting process progressed, all the manure began to show a steady decrease in the percentage recovery of *E. coli* O157:H7 with the windrow compost manure having a significantly higher ($p<0.05$) death rate of the organism than those of the plastic bin and the controls. *E. coli* O157:H7 positive manure-saw dust mixtures composted in windrows (BFSw and BSSw) and those composted in plastic bins (BFSp and BSSp) remained culture positive for up to 4 and 6 months respectively. Manure samples without saw dust which served as the controls (BF and BS) and kept at fluctuating environmental conditions remained culture positive throughout the eight months of the composting process. There was no significant difference ($p>0.05$) was observed in *E. coli* O157:H7 survival based on the manure types alone, but significant differences ($p<0.05$) existed in the survival of the organism with regard to the composting methods.
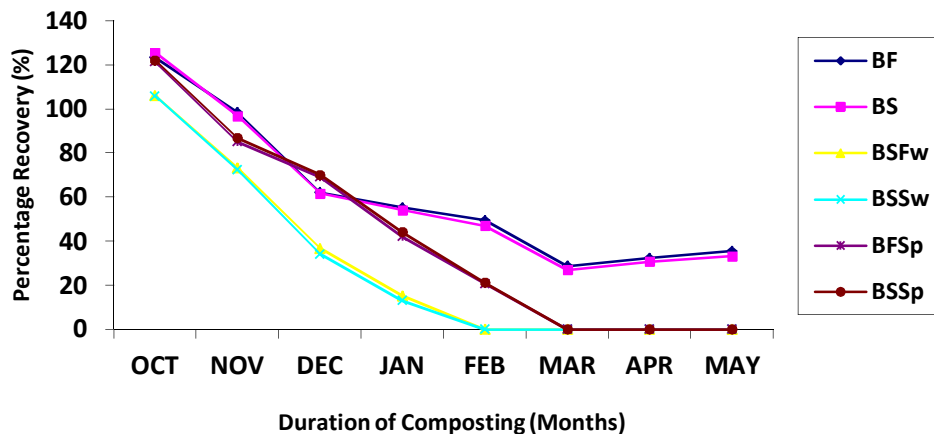


Fig. 1: Effect of Composting on the Percentage Recovery of *E. coli* O157:H7 from Manure Types Kept at Different environments for Eight Months.

BF = Bovine Faeces, BS = Bovine Slurry, BFSw = Bovine Faeces-Saw Dust in Windrow, BSSw = Bovine Slurry-Saw Dust in Windrow, BFSp = Bovine Faeces-Saw Dust in Plastic Bin and BSSp = Bovine Slurry-Saw Dust in Plastic Bin.

   The results of changes in the composting parameters such as temperature, pH and moisture content of the various compost manures which are likely to affect the percentage recovery of *E.coli* O157:H7 from the various manures during the eight months of composting process are presented in Figures 2-4. The range between the maximum and the minimum temperatures of the bovine manure composted in windrows ($61^O$C and $26^O$C respectively for BFSw and $60^O$C and $25^O$C respectively for BSSw) was higher than those composted in plastic bins ($56^O$C and $32^O$C respectively for BFSp and $55.5^O$C and $32^O$C respectively for BSSp). The results also revealed that the range between the maximum and the minimum temperatures of the manure samples that served as controls was the lowest ($30^O$C and $25^O$C respectively for BF and $30^O$C and $26^O$C respectively for BS).

   Fig.3 shows that the various compost manures rapidly decreased in pH at the initial stage of the composting. The windrow manures (BFSw and BSSw) developed ultimate low pH (5.4 and5.5 respectively) within 3 months of composting process. Beyond this time a rise in pH was recorded for each of the windrow composting manures with the pH of BFSw rising to 7.6, while that of BSSw rose to 7.2 at the end of the composting. Meanwhile, the compost manures of the plastic bins and those of the control

experiments continued to maintain low pH throughout the composting period. A slight rise in the controls (BF and BS) was observed as a result of dilutions caused by early rains of April and May.
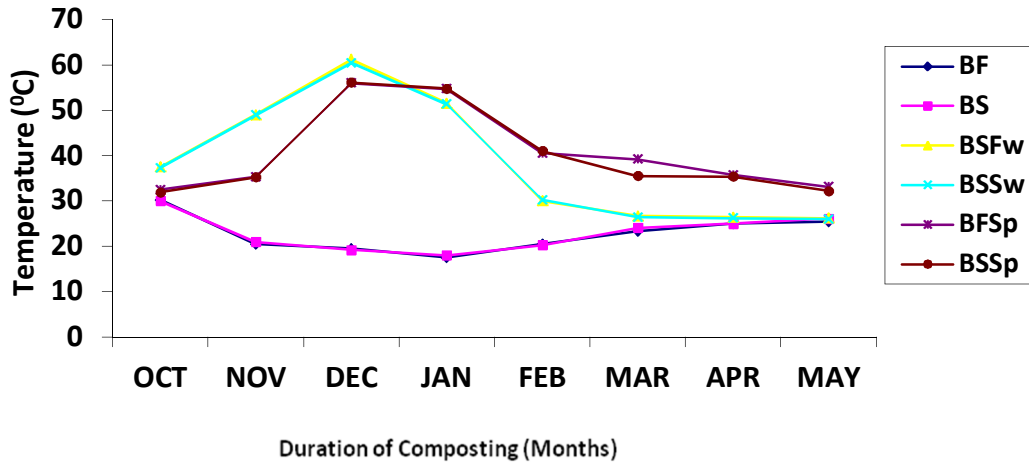


Fig. 2: Changes in Temperature ($^o$C) of the Manure Types Kept at Different Environments During Eight Months of Composting.
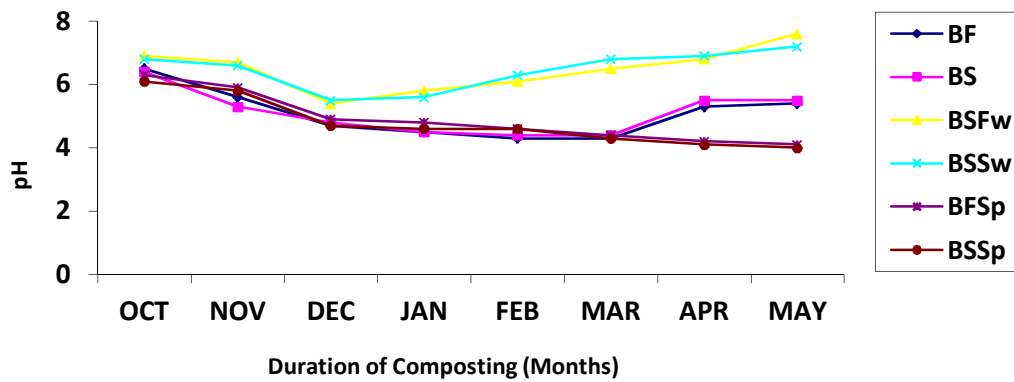


Fig. 3: Changes in pH Values of the Manure Types Kept at Different Environments During Eight Months of Composting.

Fig.4 reveals that the manure kept at the various environments decreased in moisture content as the compost process progressed. However, the plastic bin manure retained a significantly higher ($P<0.05$) moisture content than those of the windrows and the controls.

The correlation coefficients between *E. coli* O157:H7 population recovered from the compost manure types and the composting variables (temperature, pH and moisture content) within eight months indicate that among the periods of composting, the 3$^{rd}$ month (December) had the highest significant correlation coefficients in the various compost manure and was chosen to further explain the relationship between the organism and the composting parameters (Table 1). High temperatures and low pH values recorded during the 3$^{rd}$ month of composting period in windrow and plastic bin manure were positively associated with decline in the percentage recovery of *E. coli* O157:H7. During this period, low moisture contents of the windrow manure piles were also positively correlated with low percentage recovery of the organism. The moderate moisture contents of the plastic bin compost manures correlated negatively with decline in the percentage recovery of the pathogen. The results of the correlation analysis showed that there was no significant correlation ($p>0.05$) between the percentage recovery of *E. coli* O157 H7 from the manure and the composting independent variables in the control experiments.
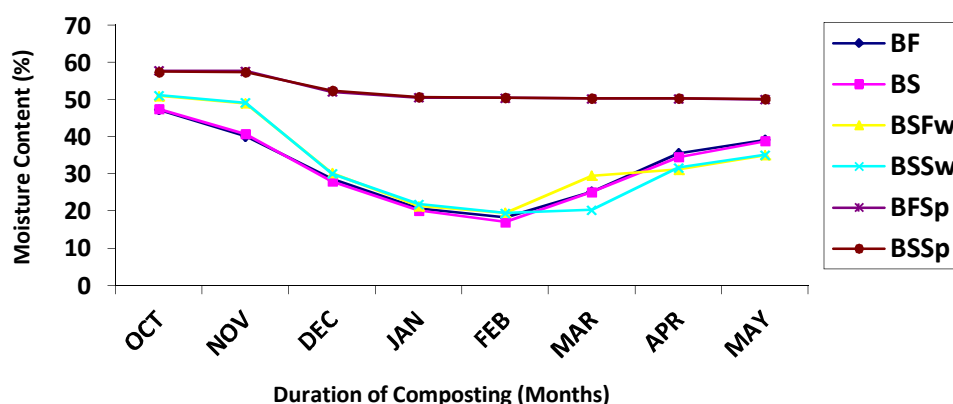
Fig. 4: Changes in Moisture Content (%) of the Manure Types Kept at Different Environments During Eight Months of Composting.

Table 1: Correlation Coefficients between *E. coli* O157:H7 Population and Composting Parameters at the 3rd Month Period of Composting in various types of Manure

| Parameter | BF | BS | BFSw | BSSw | BFSp | BSSp |
|---|---|---|---|---|---|---|
| Temperature $^O$C | -0.31 | -0.32 | 0.97** | 0.98** | 0.87* | 0.85* |
| pH | 0.50 | 0.63 | 0.88* | 0.85* | 0.83* | 0.80* |
| Moisture Content % | 0.55 | 0.60 | 0.63 | 0.67 | -0.81* | -0.84* |

*Significant at 0.05, **Significant at 0.01*

The findings of this study revealed that in all the compost manure in windrow, plastic bin and the control experiments, the numbers of *E. coli* O157.H7 cells decreased during composting. This may be attributed to the production of toxic metabolites from other microorganisms in the various types of manure, which may be deleterious to *E. coli* O157.H7 (Martin *et al.*, 1986). There was no significant difference in the percentage recovery of *E. coli* O157:H7 based on the manure types alone (i.e. BFS and BSS). This may be due to the fact that the C:N ratios of both manure types were balanced before composting thereby making equal nutrient available to the decomposing microorganisms for metabolic activities (Eghball and Power,1994). Proper blending of carbon and nitrogen also helped to ensure that composting temperatures were high enough for the process to work efficiently. This also explains why bovine manure without saw dust did not generate sufficient heat needed to destroy *E. coli* O157:H7. It was observed from this study that significant differences existed in the rate of death of *E. coli* O157:H7 cells in the manure based on the method of composting. Hence, the windrow composting method had a more rapid death rate of the pathogen than that of the plastic bin and the control experiments. This report agrees with the work of Kudva *et al.* (1998). They reported that pathogenic bacteria survived in shorter period of time in manure composted in windrow and periodically aerated by mixing than in manure kept in anaerobic environment; similar to the plastic bins used in the present study. The reason for the high death rate of *E. coli* O157:H7 observed in the windrow compost manure piles could be due to the presence of indigenous soil microorganism found in the windrow which may be antagonistic to *E. coli* O157: H7, which is of intestinal origin (Pelczar *et al.*, 2003). Another reason for faster decline of *E. coli* 0157:H2 recorded in the windrow than in the plastic bin is that *E. coli* O157:H7 is an anaerobic bacterium and it has the ability to survive longer in plastic bins without aeration. In windrows with sufficient supply of oxygen, the aerobic bacteria are likely to dominate the anaerobes (Martin, 1986).

The results of this study revealed that the manure composted in windrows and plastic bins became *E. coli* O157:H7 negative before the end of the composting process, while that kept under fluctuating environmental conditions (controls) remained *E. coli* O157:H7 positive throughout the composting process. This report is in agreement with the findings of Davis and Kendall (2007). The

authors reported that raw manure (not composted) deposited on farms and garden soil may serve as a long- term reservoir of *E. coli* O157:H7 on such environments and may also be a source of infection for humans when it contaminates produce. The long–term survival of *E. coli* O157:H7 in the manure kept at fluctuating environmental conditions in this study is also supported by the reports of Kudva *et al.* (1998) and AGAFA (2005). This explains the reason why animal manure should be properly composted in order eliminate or reduce to a minimal level the numbers of pathogenic microorganisms resident in such manure before applying them on the farm land or garden soil.

The association between *E. coli* O157:H7 population in composting manure and composting parameters (independent variables) such as temperature, pH and moisture content was also determined in this study. The high variances of the composting parameters recorded from windrow and plastic bin compost piles seem to indicate that the pathogen is strongly influenced by these environments. This report agrees with that of Hussein (2000) who reported that the survival and growth of *E. coli* O157:H7 in any environment, like all bacteria are dependent on the interactions of various factors such as temperature, pH and water availability. The findings of the present investigation showed that high temperature recorded in bovine manure-saw dust mixture composted in windrow and plastic bin correlated positively with decline in the population density of *E. coli* O157:H7. The population of *E. coli* O157: H7 cells in the various compost piles at any given time are directly proportional to the moisture contents of the environments. This is because the microbial population in any environment is directly related to the level of moisture content (Pelczar *et al.*, 2003). Water is the major component of bacterial protoplasm and an adequate supply must be available for vegetative development. The findings of this study showed that in all cases low pH exerted negative effect on *E. coli* O157:H7 cells by reducing the numbers of the organism. This finding agrees with the report of Buchanan and Klawitter (1992) who reported that the growth rate of *E. coli* O157:H7 declined at low pH level. This study has shown that of the three composting variables, high temperature had the highest correlation coefficient thus suggesting that it may be the major composting variable that inhibited the growth of *E. coli* O157: H7. This was in agreement with the work of Buchanan and Doyle (1997) who revealed that *E. coli*: O157: H7 is quite tolerant of acid and dry conditions but can easily be destroyed by high temperature.

## CONCLUSIONS

The present finding emphasizes the importance of balancing the C:N ratio of the manure using saw dust and other carbon rich materials before composting. This is to facilitate the composting process which consequently helps to destroy the pathogens. The long–term survival of *E. coli* O157:H7 in manure samples used as the control experiments emphasizes the need for appropriate farm waste management to curtail environmental spread of this bacterium. This study showed that among the composting methods evaluated, the windrow method was found to be the best, as the pathogen was eliminated at a shorter period of time in windrow manure piles. Surprisingly, the best temperatures needed to destroy the pathogen at a very short time were attained in the windrow environment. The present experiment can be extrapolated to farm environment in which poor farmers in Nigeria, who cannot afford inorganic fertilizer, can fall back on windrow method to compost organic manure before using it on their farms.

## REFERENCES

Alberta Government Agriculture and Food Agency (AGAFA). 2005. *Manure composting manual*.http://www.agric.gov.ab.ca/app19/calc/manure/manure.jsp.(retrievedon7/16/ 2008).

Armstrong, G. l., J. Hollingswort, and G. Morris. 1996. Emerging Food-borne Pathogen. *Escherichia coli* O157:H7 as a Model of Entry of a New Pathogen into the Food Supply of the Developed World. *Epidemiol. Rev*. 18(1): 29-51.

Buchanan, R. C., and L. A. Klawitter. 1992. The Effect of Incubation Temperature, Initial pH, and Sodium Chloride on the Growth Kinetics of *Escherichia coli* O157:H7. *Food Microbiol*. 9:185 – 196.

Buchanan, R. L., and M. P. Doyle. 1997. Food Borne Disease Significance of *Escherichia coli* O157:H7 and other Enterohemorragic *Escherichia coli*. *Food Technol*. 51(10): 69 – 76.

Centres for Disease Control and Prevention. 2006. Questions and Answers: Sickness caused by *Escherichia coli* O157:H7. http://www.cdc.gov/ ncidod/dbmd/diseaseinfo/escherichia coli-g.htm. (Retrieved on 7/16/ 2007).

Cheesbrough, M. A. (1991). *Medical Laboratory Manual for Tropical Countries.* Vol.11. Butterworth and Company Limited London.

Davis, D.  G. and P. Kendall. 2007. Preventing *Escherichia coli* from garden to plate. *Food Science and Human Nutrit*. 6:1 – 6.

Eghball, B. and, J. Power. 1994. Beef cattle feedlot manure management. *J. of Soil and Water Conserv*. 49:113 – 122.

Franz, E., A. D. O. J., Van Diepeningen de Vos, and A. H. C. Van Bruggen. 2007. Effects of Cattle Feeding Regimen and Soil Management Type on the Fate of *Escherichia coli* O157:H7 and *Salmonella enterica* in Manure, Manure-amended Soil and Lettuce. *Appl. and Environ Microbiol.* 1:6165 – 6174.

Gagliardi, J.V., and  J. S. Karns. 2000. Leaching of *Escherichia coli* O157:H7 in Diverse Soils under Various Agricultural Managemnt Practices. *Appl. and Environ. Microbiol.* 66:877 – *883*.

Grewal, S. K., S. Rajeev, S., Sreevatsan, F. C. Jr. Michel. 2006. Persistence of *Mycobacterium avium*, Paratuberculosis and other Zoonotc Pathogens during Simulated Composting, Manure Packing, and Liquid Storage of Dairy Manure. *Appl. and Environ. Microbiol.* 72:565 – 574.

Hussein, H. S. 2000 . On farm factors can decrease risk of *Escherichia coli* contamination feedstuffs. *Newsletter.*18 – 23.

Islam, M., F. C. Jr ., Morgan, M. P.,Doyle, S. C., Phatak, P.  Millner, and X. Jiang. 2004.  Persistence Of *Salmonella Enterica* Servovar *Typhimurium* Sp. on Lettuce And Parsley and in Soils on which they were Grown and in Fields Treated with Contaminated Manure Composts or Irrigation Water. *Food borne Pathol. and Dis.* 1:27 – 36.

Kudva, I.T., K. Blanch, and J. Houde. 1998. Analysis of *Escherichia coli* O157:H7 survival in ovine or bovine manure slurry. *App. Eviron. Microbiol*. 64: 3166-3174

Larney, F, J., Yanke, L. J., Miller, J. J., McAllister, T. A. (2003). Fate of coliform bacteria in composted feed lot manure. *J. of Environ Quality*. 32: 1508 – 1515.

March, S. B., and S. Ratnam. 1986. Sorbitol Macconkey Medium for Detection of *Escherichia coli* O157:H7 Associated with Hemorrhagic Colitis. *J. of Clin. Microbiol*. 23:869 – 872.

Martin, L. M., L. D. Shipman, J. G. Wells, I. K. Wachsmuth, R.V. Tauxe, J. P. Davis, J.  Arnoldi, and J. Tillehi.  1986. Isolation of *Escherichia coli* O157:H7 from Dairy Cattle Associated with Two Cases of Hemolytic uremic Syndrome. *Lancet*. 11:1043.

Nataro, J. P.  and Kaper, J. B. (1998). Diarrhoegenic *Escherichia coli*. *Journal of Clinical Microbiology Review.*  11: 142 – 20.

Pelczar, M. J., E. C. S. Chan, and N. R. Krieg. 2003. *Microbiology* . (5th ed). Tata Mc Graw-Hill Publishing Company Limited. New Delhi.

Sutherland, J. P., Bayliss, A. J. and Braxtox, D.S. (1995). Predictive modeling of growth of *Escherichia coli* O157:H7. The effects of temperature, pH and sodium nitrite. *Internal J of Food Microbiol*. 25:29 – 49.

# SITE EVALUATION FOR OLIVE MILLS WASTE COMPOSTING FACILITY

Amal Iaaly and *Mervat El-Hoz*
(University of Balamand, Tripoli, Lebanon)

**ABSTRACT:** The site selection process for a sustainable composting plant to manage olive mills waste was studied based on a set of technical and non-technical criteria or constraints produced by the Ministry of Environment and EU. The GIS approach was used where five constraints maps layers (slope, roads, rivers and watershed, residential areas, and olive zones) were produced. Furthermore, an evaluation stage was undertaken to combine the information from the various constraints. The Weighted Linear Combination method of multi-criteria evaluation within raster GIS environment was applied to reclassify these constraint maps and derive the weights associated with them by applying the pairwise comparison method. Then, the Raster Arithmetic Addition tool in ArcView was used to overlay the reclassified maps where areas with the highest values reflect best scenarios of the analysis. Lastly, a query was conducted to define the grouped areas that met the size and locational constraints previously identified which helped in the selection of the most suitable site. This created the final map showing the location of the scientific decision site that was approved by all concerned parties.

## INTRODUCTION

The Governorate of Akkar is located in north Lebanon. It has a total surface area of 798km², and is divided into two agricultural regions where the mountainous region is cultivated with olive trees and all kinds of fruit trees. The agricultural land represents 56.6 % of the total surface area (MOE and FAO, 1999). There are 222 Olive mills in North Lebanon. The olive oil mill wastes (OMW) are characterized by high organic load and a substantial quantity of plant nutrients that could increase both soil fertility and crops production (Montemurro et al., 2006). The improper disposal of these wastes cause negative environmental impacts to soil, water and air. As a result, the UNDP, Nahr El-Bared Conflict (NBC) Program, the supporter of the olive mills waste composting (OMWC) project decided to construct a composting plant to manage olive mills wastes from the traditional olive oil extraction mills for 9 villages in Akkar region. The aim of this study is to find a suitable site for this composting plant (CP).

## STUDY AREA AND METHODOLOGY

The cultivated area with olive trees in the NBC 9 villages is 5.5 km$^2$, with a density varies between 100-300 olive trees per 10,000 m$^2$. Demand of land for CPs depends on various factors. Waste quantity was used to determine type, size, and design of the CP facility. The proposed pilot project will handle up to 500 tons of waste per year, and will be located in Bkarzala village, the most production olives in the studied area. The surface area required for the proposed project is 5,000 m$^2$. The particular approach proposed for OMWC is open windrow that has the advantage of being relatively less expensive than other alternatives, more flexible to accommodate wider variation in feedstock and being adaptable to different operating conditions (El-Hoz, 2011).

There are a number of examples in the world of GIS application for locating suitable sanitary landfilld sites (Despotakis and Economopoulos 2007; and Yahaya et.al. 2010) but very few for CPs. The site selection process for CP is usually the most critical steps in the entire decision making cycle. Inappropriate allocation can lead to environmental damages, social and political conflicts and economic inefficiency. Therefore, the technical criteria used in this study have been identified based on the guideline produced by the Ministry of Environment and EU site selection that are constraints for an ideal

CP siting. The non-technical aspects are very important for considering all criteria which influence the planning and design of the composting facility such as access road, availability of appropriate utilities (water, power and other services), space for future expansion of the facility, and anticipated growth and development near the facility. Table 1 presents the technical and non-technical aspects used in this study. Furthermore, to ensure that the composting operation is environmentally and socially acceptable, additional two requirements for the site were also considered, the site has approval from all surrounding land users and be accessible to all individuals who want to use it.

The study undertook a review of available records and conducted site reconnaissance visits to develop an initial potential CP site list. During investigation, many knowledge gaps existed for the facility siting since it is very difficult to satisfy social, environmental, economic and political factors to the fullest extent. Therefore, a GIS-based approach is used to determine the ideal location for the composting plant based on the MOE and EU identified criteria that were set as restricted areas.

**Table 1. Ministry of Environment and EU Site Selection Criteria**

| Criteria | | Value |
|---|---|---|
| Siting | Distance to development zone, rural townships | 1,000 m |
| Access Road | Distance to arterial road networks | 500 m |
| Floodplain | Not within designated area as a '100-year floodplain' | 100m |
| Slope | Areas with slopes | < 10% |
| Water Supply | Distance away from surface water, whether permanent or intermittent | 100m |
| Design Area | Room for future expansion of the facility | 5,000 m$^2$ |
| Utilities | Availability of appropriate utilities (water, power and other services) | |
| Sensitive Areas | Distance from environmentally sensitive or protected areas | 1,000 m$^2$ |

In order to satisfy all specified criteria, five constraint maps were produced and converted into weighted geographical raster layers along the Spatial Extent of Akkar governorate to represent the regions which are suitable and unsuitable for development of the CP. Those constraints maps were: (1) slope, (2) distance from rivers, (3) distance from residential zones, (4) distance from roads, and (5) distance from olive zones. Then, a reclassification tool from ArcGIS Spatial Analyst Expansion is used in order to rearrange the results as it provides a broad range of powerful spatial modeling and analysis features. It is important to note that the philosophy of the Analytical Hierarchy Process (AHP) and environmental criteria for site selection are not rigid and limited to only two values 0 and 1 where 0 is the rejected region and 1 is the accepted one. The reclassification method used in this study is the weighted Linear Combination (WLC) comparison model of multi-criteria evaluation (MCE) to reclassify these constraints maps created on the binding criteria to limit the alternatives, convert the raster layers into decision and derive the weights associated with them. Ratings for reclassification are provided on a 10-point continuous scale based on pairwise comparison method. Once they are produced, an evaluation stage was undertaken. The Raster Arithmetic Addition Operation in ArcView was used where results are obtained (calculation) based on overlay the reclassified maps in order to achieve a desired result. Lastly, a query was conducted to define the grouped areas that met the size and locational constraints previously identified which helped in the selection of the most suitable site. The model used for the production of the final constraint map for the most suitable site is illustrated in Figure 1.

**ANALYSIS AND DISCUSSION OF SITE SELECTION CRITERIA**

The site requirements for specific waste disposal technologies vary, as do their site-specific impacts on the environment. To start the analysis, the GIS map of Lebanon was prepared where the region under study is highlighted. The above criteria or constraints are briefly explained in the following paragraphs:
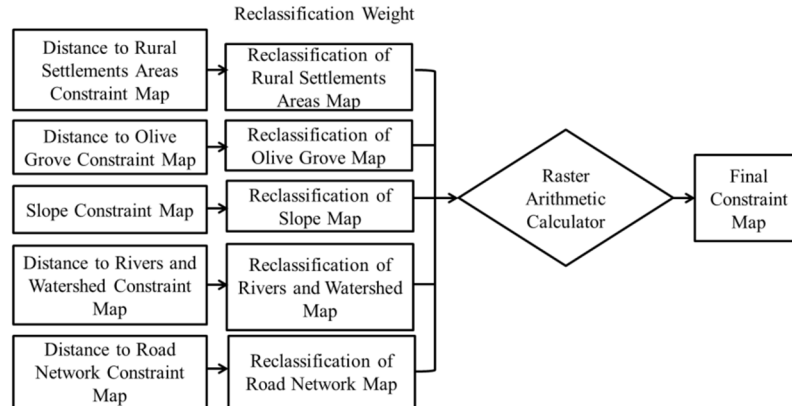


Figure 1: Model for Final Constraint Map Production for Site Selection



| Figure 1:Map ofLebanon | Figure 2: Topographic Map ofAkkar |
|---|---|
| Figure 3. Slope Governorate of Akkar | Figure 4: Reclassification Slope |
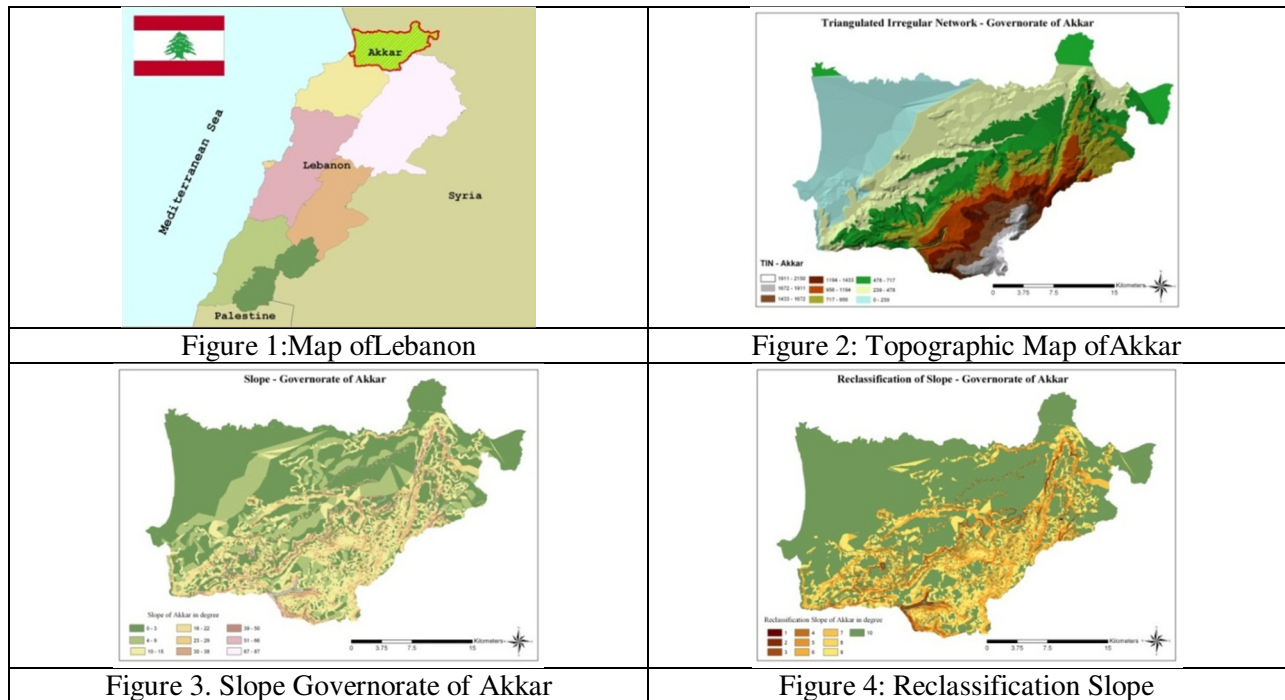
**Slope.** The topographic Triangulated Irregular Network (TIN) layer in GIS environment for Akkar region was used. Based on this map and criteria, the GIS Spatial Analyst Distance Tool is used to generate a slope surface map that reflects regions with various slope degree values. Concerning the CP, only areas with slopes < 10% are listed as candidates. Figure 3 shows the slope analysis varying from 0 to $87^o$. The first and second region 0-$3^o$ and 4-$9^o$ represent the flat and small slope areas whereas the last region (67-$87^o$) represents the steepest one. In order to select a region with a slope < 10%, a reclassification of the constraints maps was used to limit the alternatives. According to Figure 4, it is worth nothing that the value 10 was given to slope values <10% and the value 1 to 90-100% slope.

**Land Use.** The Land use and Land cover must be known in order to determine which areas are more suitable for a CP. The land use map of Akkar region is used as a reference. Again, based on this map and criteria, the Spatial Analyst Distance Tool is used to create a surface showing the distance from the populated areas and olive grove zones. Due to the same conflicts relating to the NIMBY syndrome, development of CP shall be prohibited within 1000 meters from village settlements. According to Figure 5, 0-981 values belong to distance more than 1km of area, the most suitable locations, and the least value of importance with distances 8831-9811, the farthest ones. Then, the reclassification method is implemented with the same ranges as in slope criterion. In this case, the value 10 describes the farthest location and 1 the closest to the populated areas. As shown in Figure 6, the values ranging from 2-10 are all acceptable in this case as they represent a distance greater than1000 m from population areas.
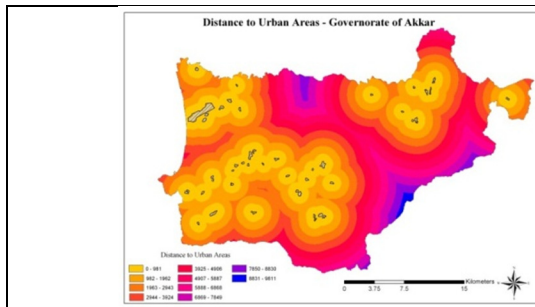


| | |
|---|---|
| Figure 5. Distance to Urban Area | Figure 6. Reclassification Distance To Urban Area |
| Figure 7. Distance to Olive Zone Map | Figure 8. Reclassification Distance to Olive Zone Map |
| Figure 9: Distance to Rivers and Watershed | Figure 10: Reclassification of Rivers and Watershed |
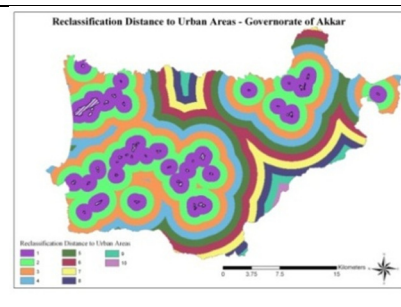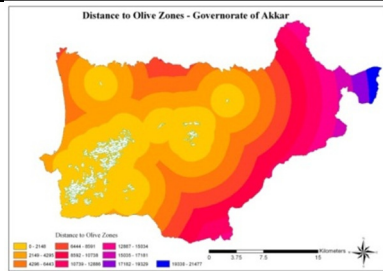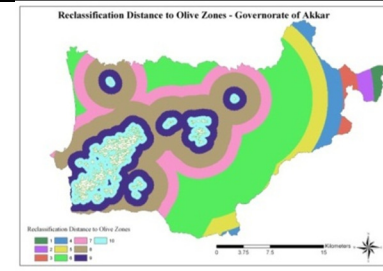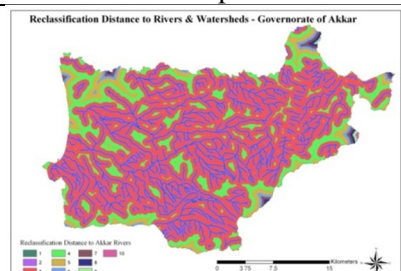
**Distance to Olive Zone.** Figure 7 shows the distance of olive grove zone map. Values between 0-2148 represent areas close to olive grove zone. Concerning the reclassification of the distance to olive zone, the value 10 represents the nearest area and zeros the farthest one (opposite to the previous case) as shown in Figure 8. In this case, only regions 9 and 10 are the most suitable areas for the CP.

**Rivers and Watershed.** Farther lands from streams and river banks get more preferences for being selected. A map representing rivers and their watersheds for Akkar region is created based on a 100-meter

buffer to further analysis with zoning process schematically shown in Figure 9. High values belong to distances < 314 meters of area and less value belong to distance between 2,830 - 3,144 meters to the watershed river. Again reclassification of rivers was made where value of 10 represents the ideal value for acceptable regions (Figure 10).

**Distance from Roads.** Road Network was created to show the various distances from roads centerline. Aesthetically and logically a buffer of 500 meter has been considered in this study for access roads. According to Figure 11, high value is belong to distance between 0-500 meters and less value is belong to distance more than 1439 meters of total study area. Moreover, a reclassification weight of the road was done where value of 10 represents the 500m distance of the access road (Figure 12).

**Raster Arithmetic Addition tool.** Furthermore, in order to come up with potential areas across the governorate of Akkar, the Raster Arithmetic Addition tool is used to overlay all the reclassified surfaces where areas with the highest values reflect best scenarios of the analysis. The given lands were overlaid on top of the analysis surface in order to compare scientifically their geographical location with the environmental criteria. Based on this map, someone can visually explore the compatibility of the locations with the GIS spatial analysis. A query was then conducted to determine the largest clustered areas that met the size and locational constraints previously stated which aided in the selection of the most suitable site.
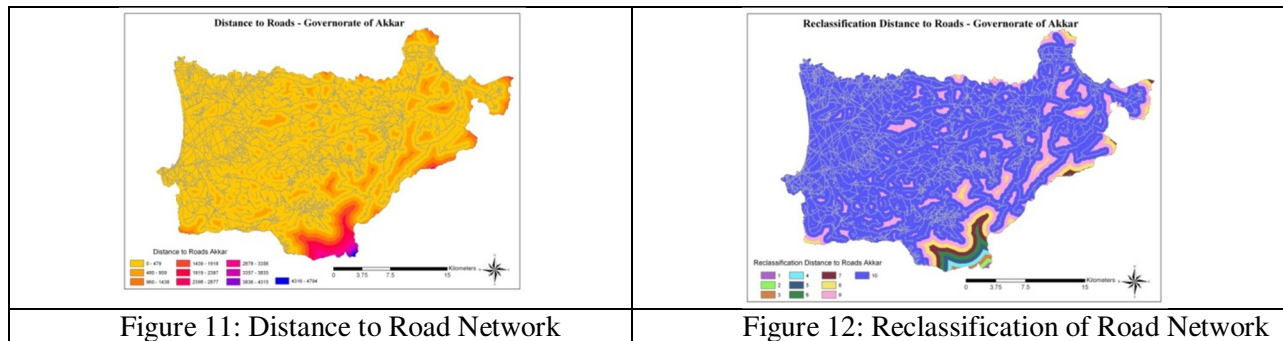


| Figure 11: Distance to Road Network | Figure 12: Reclassification of Road Network |
| --- | --- |

**Additional Criteria.** Moreover, additional constraints were taken into consideration:

*Distance from environmentally sensitive or protected areas.* The location of a CP in close proximity to sensitive areas was excluded.

*Minimum Design Area.* This project will be extended in the future to become a full scale project and will include additional 25 villages of the region for 25 years lifetime of the facility. Therefore, it was determined that the CP would require a minimum of 5000 m$^2$ taking into consideration that the design factor would account for adequate buffers between surrounding land use activities and on-site facilities and similar requirements (El-Hoz, 2010). Consequently, as small and scattered areas would not be suitable for CP development, a further screening is done masking out all the scattered areas and those having an area less than 5000m$^2$.

Likewise, to ensure that the composting operation is environmentally and socially acceptable, additional requirements were also considered, future residential growth and the site has approval from all surrounding land users. All of these aspects were also studied to narrow the proposed potential land areas.

After scoping and analysis of the technical and non-technical aspects, two alternative sites were feasible. Table 2 presents the characteristics of these two alternative sites. Based on the GIS scientific decision, Site 2 was chosen to be used for the pilot project and also recommended by most of the participants (mayor and members of the municipal council of Bkarzela, and some presidents and members of the concerned agricultural cooperatives).

**RESULTS AND CONCLUSION**

The site selected is located in Bkarzela town, in a strongly preferred area which met all environmental, social, economic and political criteria examined in the study. The final site selection map is illustrated in graphical form in Figure 13.The best location is indicated by the black circle around the site.

The evaluation of a CP site is a complicated process. The outlined GIS model integration methodology did produce the expected result using constraint mapping techniques in the ArcView 11, multiple criteria decision evaluation, weighted overlay analysis and Raster Arithmetic calculator and is of uttermost importance to effective, reliable and efficient site selection. It is easy to understand, can illustrate which areas are better or less suitable for composting plant site selection in the shortest probable time and least costs, and can assist in getting full support from the concerned parties and public for locating one of the most difficult issue of the planning process in solid waste management.

**Table 2. Comparison of the two Alternative Sites**

| Parameters | Site 1 | Site 2 |
|---|---|---|
| large land for the construction of the project | 7,200 $m^2$ | 117,000 $m^2$ |
| Least excavation work | Almost flat | Need little excavation work |
| Near-by access to the major highway | 2.8 km | 410m |
| Distance from the nearest residence | 450m | >250m |
| Proximity to the olive orchards sources | Agricultural area | Agricultural area |
| Flood plain | N/A | N/A |
| Convenient utilities | Telephone | Electricity, telephone, well |
| A rectangular or square site | Rectangular site | Desired shape can be obtained |
| Public acceptance | Not accepted by major participants | Accepted by all participants |



Figure 13. Final Results with Location of Composting Plant

## ACKNOWLEDGEMENTS

**REFERENCES**

El-Hoz, M. (2011). "Sustainable Environmental Management for Olive Mill Waste in Rural Areas". *The Twenty-Sixth International Conference, On Solid Waste Technology and Management, Philadelphia, Pa U.S.A., March 27 – 30*, 1164-1175

FAO and Ministry of Agriculture (1997). "The 1996 Agricultural Statistics, Study on Villages".

Montemurro, F., M. Maiorana, G. Convertini, and D. Ferri. (2006). "Compost Organic Amendments in Fodder Crops: Effects on Yield, Nitrogen Utilization and Soil Characteristics". *J. Compost Sci Util.* 14(2): 114–123

Yahaya, S., Ilori, C., Whanda, S., and J. Edicha. (2010). "Land Fill Site Selection for Municipal Solid Waste Mangement Using Geographic Information System and Multicriteria Evaluation. *Am J Sci. Res.* 10 (2010): 34-49

# EXPERIMENTAL STUDY ON ANAEROBIC THERMOPHILIC DIGESTION OF PRE-THICKENED WASTE ACTIVATED SLUDGE

***Zifu Li**, Fubin Yin, Lei Xun, Xuan Liu, Shikun Cheng*

(School of Civil and Environmental Engineering, University of Science and Technology Beijing, China)

**ABSTRACT:** Compared to conventional low solid anaerobic mesophilic digestion, high solid anaerobic thermophilic digestion may offer attractive advantages such as lower viscosity value, higher volatile solid destruction efficiency, higher biogas generation, higher disinfection effect and better dewater ability, then lower reactor volume demand. In this study, two experiments of high solid waste activated sludge were conducted using one liter glass jars and 6 liter CSTR to evaluate the biogas production and thermophilic anaerobic process stability. The sludge was taken from the secondary sedimentation tank of a wastewater treatment plant in Beijing. The sludge should be thickened before anaerobic experiment. In first experiment, the biogas production of 4 one-liter glass jarred actors with solid concentration of 6%, 8%, 10% and 12% respectively at thermophilic (55±1)℃ temperatures was observed. The biogas productions in 4 jar reactors were 4,444.00mL, 4,891.00mL, 5,573.00mL and 6,327.00mL respectively and the methane content in biogas of each reactor was kept about 70%. In second experiment, 6 liter CSTR was employed for 12% solid concentration sludge. For 40 days operation, total biogas production was about 52.7L, the methane content of biogas was about 69%, biogas production per gram volatile substance was about 0.34L/g VS. In first 30 days, the cumulative produced biogas amount could reach more than 90% of total biogas production. The results showed that high solid anaerobic thermophilic digestion process for waste activated sludge could be operated steadily. This process could reduce the volume demand of anaerobic reactor dramatically, which could make anaerobic sludge treatment process more attractive and economic.

**Keywords:** high solid waste activated sludge; anaerobic thermophilic digestion; biogas production; thermophilic anaerobic process stability.

## INTRODUCTION

Mass reduction, stabilization, methane production and improved dewatering properties are the main features of the process (Mata-Alvarez et al., 2000).However, low TS concentration and the relatively low volatile solids (VS) removal (30% - 40%) are often the disadvantages of the process as the digesters are rarely optimized for biogas production and are operated with too low organic loading rate and very large digester volume, which often causes high investment and operation costs (Murto et al.,2004. Climent et al., 2007).To enhance the process and reduce the digester volume, waste activated sludge would be pre-thickened to 8% -12% TS before anaerobic digestion. The pre-treated waste activated sludge by thermophilic digestion could produce more biogas with high organic load rate (OLR) and low viscosity, which can also reduce the demanded digester volume (Ahring, 1994).

This study aims to systematically and comprehensively evaluate the impact of combined thermophilic and high solid on the process stability of anaerobic digestion of waste activated sludge. The influence of different conditions were evaluated in terms of (a) biogas production, (b) organic matter degradation, (c) gas production per unit VS digested, (d) methane concentration in biogas, and (e) process stability of a thermophilic sludge digester during operating.

## MATERIALS AND METHODS

**Seed and anaerobic inoculum.** The raw excess sludge used as substrate was obtained from a C-TECH biological treatment system of a wastewater treatment plant in Beijing. Before the anaerobic experiment, the sludge was dewatered and thickened by filter cloth and natural ventilation to achieve TS concentration between 8% and 10%, and no coagulant was added in this process. In order to reduce the influence of temperature, the pre-thickened sludge was put into a water bath for preheating (55±1)°C before digestion. The digested sludge used as inoculums was collected from a digester of a wastewater treatment plant in Shijiazhuang city. The main characteristics of the digested thermophilic sludge used as inoculum and the average feed composition are summarized in table 1.

TABLE 1. Initial characterization of raw sludge and inoculum used

| Analytical parameters | Raw sludge | Inoculum |
|---|---|---|
| TN/TS | 0.024 | 0.00055 |
| TOC/TS | 0.35 | 0.011 |
| C/N | 14.6 | 20 |
| TS | 1% | 1% |
| pH | 6.8-7.1 | 7.4 |
| TOM/TS | 60.34% | 56.37% |

**Analytical Methods.** The reactor was monitored by analyzing daily samples of the influent and effluent streams. Main parameters were measured in order to study the process stability. The parameters of total solids (TS) and volatile solids (VS) concentration were determined according to the APHA standard methods (APHA, 1998). The pH and Oxidation-Reduction Potential (ORP) were measured using a pH/ORP meter (HI 9125N). Total alkalinity and volatile fatty acids (VFAs) were measured by chemical titration. Total organic carbon (TOC) was analyzed by potassium dichromate volumetric method. Total nitrogen (TN) was analyzed by Kjeldahl method. Biogas yield was measured by water displacement method. And the methane content was obtained by the biogas analyzer (Geotech-Biogas check).
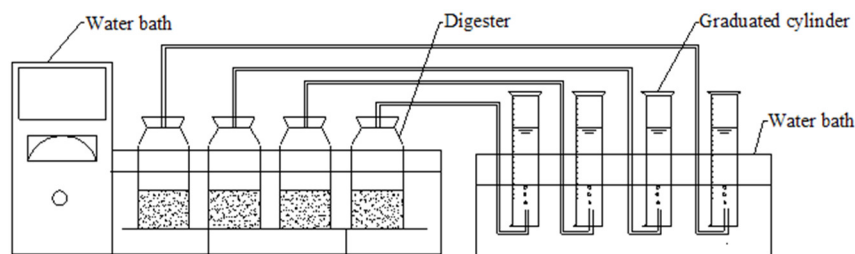


FIGURE 1. The experimental setup of 1 liter jar digestion

**Experimental setup and procedures.** Experimental setup shown in figure 1 consists of 4 pieces of 1L jars as digesters and 4 pieces of 1L graduated cylinders as biogas collectors. The digesters were kept in the thermostat water bath with a constant temperature of (55±1)°C to maintain constant reaction temperature, and the reactors were shaken manually once a day to get the materials fully mixed. Biogas generated in the digesters was led by a rubber pipe into graduated cylinders which pressed the same volume water out of the graduated cylinders into the water tank. The biogas production yields were

monitored at the same time once a day and the methane gas content analysis was conducted once three to five days.

Continuous stirred tank reactors (CSTR) with the effective volume of 5 L were employed as thermophilic anaerobic digesters of excess activated sludge (figure 2). The raw sludge was pumped into the digesters through inlet ports and the digested sludge flows out from outlet by gravity. There is a sampling port at the central wall of the tank through which sampling was conveniently taken and analyzed. The tank was equipped with pH, ORP and temperature meters that could promptly on-line measure these values and demonstrate them on the monitoring control panel. To ensure the temperature constant of anaerobic fermentation process, the reactor was also equipped with a temperature regulation device and heated by an electric heater. The mixing device installed inside the reactor adopts speed adjustable mixer which is controlled by the PLC system. In the first day of experimental operation, the stirrer of the reactor rotated at 120rpm for 24h in order to ensure that the sludge and anaerobic microbes were completely mixed. Then after the first day, the reactor was stirred at 60rpm for 2h every day until the end of the anaerobic digestion experiment. The biogas outlet was equipped with a condense water trap and biogas flow rate was measured with a wet type flow meter (accuracy of 0.01 ml, Ritter-MGC-1 V3.0 PMMA). And reactor biogas generated from the test through a bag collection. Biogas composition (vol. % of $CH_4$) was determined with a special biogas analyzer.
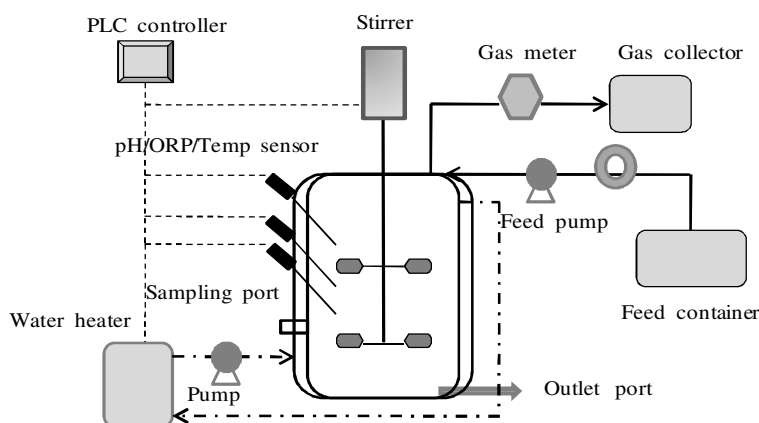


FIGURE 2. Schematic diagram of CSTR experiment

**RESULTS AND DISCUSSION**

**Anaerobic thermophilic digestion test of different TS concentration sludge in Jar-test.** According to the sludge concentrations after dehydration, 4 groups of testing with solid concentration in the range of 6% - 12% were conducted, with a blank (0%) test as a control shown in Table 2. High temperature (55±1)℃ anaerobic digestion test was conducted with a seed sludge ratio of 25%.

**Biogas production.** The cumulative biogas productions in 4 reactors were 4,444mL, 4,891mL, 5,573mL and 6,327mL respectively (as shown in Figure 3). With the increase of the concentration of sludge (TS), the organic load rate increased and the cumulative biogas output was also gradually increased till the digestion was completed (Harikishan et al., 2003). In the second day after inoculation, each reactor reached the first daily biogas production peak (the highest 416 mL/d); this was because the initial hydrolysis acidification produced more carbon dioxide (Liu et al., 2011. Appels et al., 2008). Subsequently, the biogas production appeared low ebb, after 3-6 days, microorganisms gradually adapted to anaerobic environment as well as the high sludge organic load (Forster-Carneiro et al., 2008).

The daily biogas production began to increase on 10th day and reached the second biogas production peak (figure 3). With higher sludge concentration, the biogas production peak appeared relatively higher (Dumas et al., 2010). In the reactor with total solid (TS) of 12%, the biogas production peak reach 520mL/d; this was because the sludge with higher concentration, the anaerobic microbes needed more time to adapt to the environment (Forster-Carneiro et al., 2008). However, when this happened, the biogas production was rapidly stable. The daily biogas production stayed stable for about two weeks and then began to decline, the biogas production of each reactor almost stopped in about one month after inoculation.

TABLE 2. Uniform design and experimental data

| NO. | 1 | 2 | 3 | 4 | 5 |
|---|---|---|---|---|---|
| TS/% | 6.0 | 8.0 | 10.0 | 12.0 | 0 |
| Sludge/g | 30 | 40 | 50 | 60 | 0 |
| Inoculum/ml | 125 | 125 | 125 | 125 | 125 |
| Water/ml | 345 | 335 | 325 | 315 | 375 |
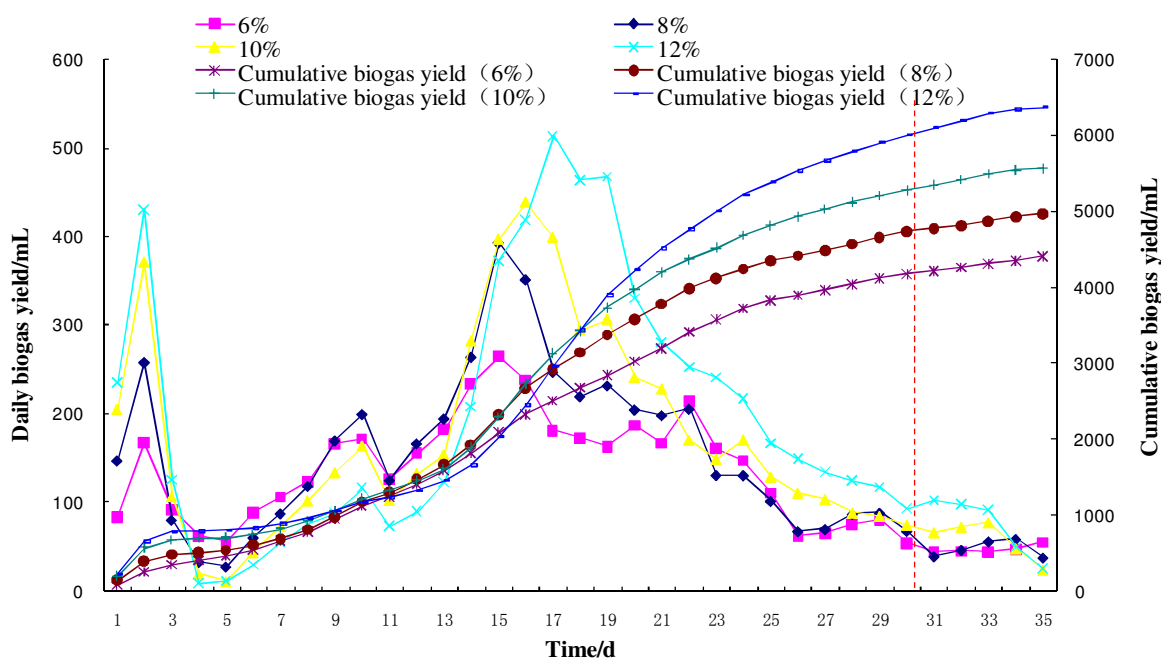


FIGURE 3. The effect of TS on the cumulative biogas yield

**Anaerobic thermophilic digestion of pre-thickened waste activated sludge in CSTR.** Anaerobic thermophilic (55±1)℃ digestion methane production test was conducted in CSTR with onetime high concentration sludge cast (TS of 12%, inoculums concentration was 30%).

As shown in figure 4, at the beginning of the daily biogas production, an obvious wave-like change was first increased and later decreased. In the second day after inoculation, sludge reached the first biogas production peak (4.05 L/d); this was because the initial hydrolysis acidification produced more carbon dioxide (Liu et al., 2011, Ferrer et al., 2010). Subsequently, the biogas production appears low ebb, and went to 4 days adapt stage in which microorganisms gradually adapted to anaerobic

environment as well as the high sludge organic load (Forster-Carneiro et al., 2008). The daily biogas production began to increase at 7 days and reached the second biogas production peak (2.7 L/d), after that the daily biogas production had gradually begun to stabilize at a higher level. Due to the easily degradable organic matter continuously consumed, nutritional deficiencies of anaerobic microorganisms occurred and biogas production began to decline at 32 days. For 40 days operation, total biogas production was about 52.7L. Under high temperature conditions, methanogens activities increased and consumed organic matter more thoroughly with a biogas production per gram volatile substance about 0.34L/g.
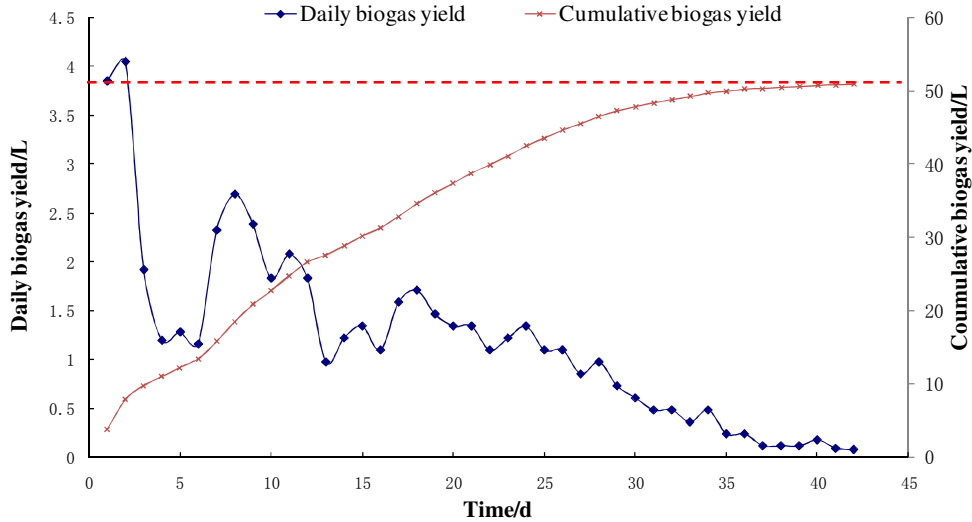


FIGURE 4. Biogas production with digestion time
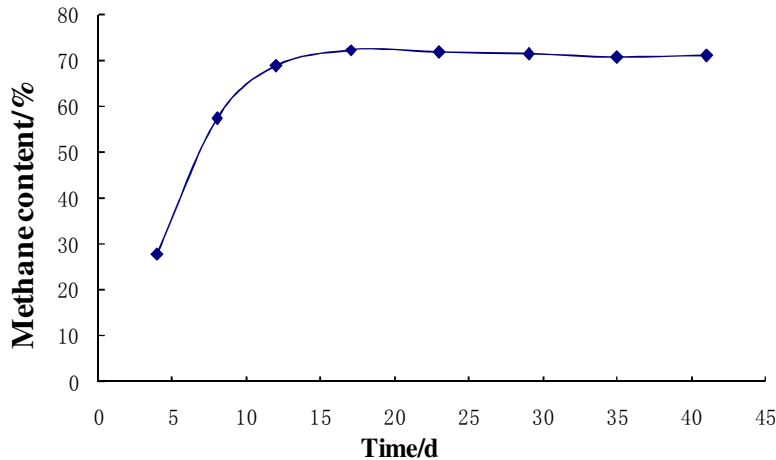


FIGURE 5. Methane content of biogas with digestion time

Also in figure 5, anaerobic microbe had not adapted to the reactor environment yet (Ferrer et al., 2008), and the activities of methanogens were low, making the methane content in the initial biogas production lower than normal. As the anaerobic digestion process continued, the activity of methanogens gradually increased (Shim et al., 2003), prompted the methane content to elevate. After about 7 days, the methane content reached 58% and then remained stable at about 69%. This indicated that the anaerobic microorganisms in the sludge had fully adapted to the anaerobic environment within the reactor (Palatsi et

al., 2009), which also proved that sludge with higher concentration would produce biogas with better quality.

## CONCLUSIONS

• Comparing anaerobic digestion effects of different concentration sludge test, it can be deduced that the increasing of sludge concentration did not inhibit the biogas production process; Moreover, anaerobic digestion of high concentration sludge can significantly improve the biogas production rate of per effective reactor volume and the organic matter degradation rate. But it does not mean that higher sludge concentrations have better effect. Further comprehensive economic benefits study is needed.

• The biogas production per unit VS digested of high concentration sludge are all between 300 mL/g to 350 mL/g and the organic matter degradation rate were about 48% on average.

• The biogas production quality was good, methane content of high temperature anaerobic digestion were on average between 60% - 70%, methanogens were able to adapt to the environment within the reactor quickly, making methane content in the biogas production achieved higher content in a short time, which was helpful for further purification, burning or to electricity producing usage.

• The system was stable. In 40 days of anaerobic digestion cycle, thermophilic anaerobic digestion of high concentrations sludge system has the stability and reliability in practical engineering application.

## REFERENCES

Ahring B.K. 1994. Status on science and application of thermophilic anaerobic digestion. *Water Science and Technology*. 30(12): 241-249.

APHA-AWWA-WPCF. 1998. *Standard methods for the examination of water and wastewater*, 20th ed. Washington, DC.

Appels L, Baeyens J, Degreve J, et al. 2008. Principles and potential of the anaerobic digestion of waste activated sludge. *Progress in Energy and Combustion Science*. 34(6): 755-781.

Climent Mavi, Ferrer Ivet, Ma del Mar Baeza, et al. 2007. Effects of thermal and mechanical pretreatments of secondary sludge on biogas production under thermophilic conditions. *Chemical Engineering Journal*. 133(1): 335-342.

Dumas C., Perez S., Paul E., et al. 2010. Combined thermophilic aerobic process and conventional anaerobic digestion: Effect on sludge biodegradation and methane production. *Bioresource Technology*. 101(8): 2629-2636.

Ferrer Ivet, Felicitas Vazquez, Xavier Font. 2010. Long term operation of a thermophilic anaerobic reactor: Process stability and efficiency at decreasing sludge retention time. *Bioresource Technology*. 101(9): 2972-2980.

Ferrer Ivet., Ponsa Sergio., Vazquez Felicitas, et al. 2008. Increasing biogas production by thermal (70℃) sludge pre-treatment prior to thermophilic anaerobic digestion. *Biochemical Engineering Journal*. 42(2): 186-192.

Forster-Carneiro, T, Pérez, M., Romero, L.I.2008.Anaerobic digestion of municipal solid wastes: dry thermophilic performance. *Bioresource Technology*. 99(1): 8180-8184.

Harikishan S, Shihwu Sung. 2003. Cattle waste treatment and Class A biosolid production using temperature-phased anaerobic digester. *Advances in Environmental Research*. 7(3): 701-706.

Liu Xiaoling, Li Shizhong, Liu Jianshuang, etal. 2011. Evaluation of high-solids anaerobic digestion process for converting excess sludge to biogas. *Acta Scientiae Circumstantiae*. 31(5): 955-963.

Mata-AlvarezJ, MaceS, LlabresP.2000.Anaerobic digestion of organic solid wastes. An over view of research achievements and perspectives. *Bioresource Technology*. 74(1): 3-16.

MurtoM,BjornssonL, MattiassonB. 2004. Impact of food industrial waste on anaerobic co-digestion of sewage sludge and pig manure. *Journal of Environmental Management*. 70(2): 101-107.

Palatsi J, Gimenez-Lorang A, Ferrer I, etal. 2009. Start-up strategies of thermophilic anaerobic digestion of sewage sludge. *Water Science and Technology*. 59(9): 1777-1784.

Shim H S, Kang S T. 2003. Characteristics and fates of soluble microbial products in ceramic membrane bioreactor at various sludge retention times. *Water Research*. 37(1): 121-127.

# CHARACTERISTICS CHANGES OF BY-PRODUCTS ORIGIN SAND-ALTERNATIVES IN SEAWATER AND SEDIMENT

Satoshi ASAOKA[1], Tetsuji OKUDA*[1], Hitomi YANO[2],
Kouji YOSHITSUGU[2], Satoshi NAKAI[2], Wataru NISHIJIMA[1], Kenji SUGIMOTO[3], Daijirou MATSUNAMI[4], Yorihide ASAOKA[4], Mitsumasa OKADA[5]

1) Environmental Research and Management Center, Hiroshima University
2) Faculty of engineering, Hiroshima University
3) Ube National College of Technology
4) Chugoku-Shikoku Defense Bureau
5) Open University of Japan
* aqua@hiroshima-u.ac.jp, 1-5-3 Kagamiyama, Higashi-Hiroshima, Hiroshima, JAPAN, 739-8513

**ABSTRACT:** Seagrass beds and tidal flats are facing in danger of disappearing, therefore it is desired to restore them. Steel slag from steelmaking processes, its granulated agglomerates, clinker ash from thermal power stations, its granulated agglomerates and molten slag from municipal solid waste incineration plant are one of the promising alternative materials for marine sands in the restoration. The release of calcium and alkaline caused by the hydrolysis and elution of calcium oxide from the sand-alternatives was considered as main reaction though their aging processes in marine environment. However, the quantitative changes during aging in seawater are not fully understood. Therefore, this study is aiming to reveal the aging of sand-alternatives by targeting at calcium and alkaline elution. The maximum elution potential of calcium and the depth of its elution of these sand-alternatives were investigated in order to quantify their maximum elution potential in the sea. Sand-alternatives were submerged in a real sea at over 500 days. After the regular intervals, the in-depth profile of elements were measured using X-ray analysis. Under the marine environment, the depth where calcium concentration was decreased by its elution increased through its aging periods. The depth was difference in increase rate among sand-alternatives. It is considered that pozzolanic reaction and the carbonization of calcium eluted on the surface of the sand-alternatives would be prevented their aging. The maximum elutable amount of calcium from the sand-alternatives in the seawater was calculated by the maximum elution depth and the maximum calcium elution potential determined by the batch experiments.

**Key Words:** aging; calcium; elution; marine environment; pH; sand-alternative.

## INTRODUCTION

Seagrass beds and tidal flats have important function for marine ecosystem, however a number of tidal flats and eelgrass beds have been disappeared throughout the world due to harbor improvements and others. For example, 40% of tidal flats (33,120 ha) was disappeared within 60 years in Japan[1-5]. Therefore, it is necessary to create and restore the seagrass beds and tidal flats in order to maintain healthy marine ecosystems. Accordingly, restoration projects and studies for the recovery of sea grass beds and tidal flats have been conducted all over the world[6,7]. However, a large amount of sand is required to construct them, and the extraction of sand from sea bottom or river bottom may blame for disturbing aquatic ecosystems therein. Therefore, some alternative material of sand or sand alternatives (hereinafter referred to as "SAs") is required.

Iron and steel slag from steelmaking processes, coal ash from thermal power stations and molten

ash from incineration plants for domestic wastes all are byproducts, and these are produced approximately 36, 10, 0.8 million ton per year in Japan, respectively[8-10]. Commonly, they have been utilized for roadbed construction material, coarse aggregate in concrete and raw material of cement[8, 11]. However, their outputs are still enough to create coastal ecosystems such as tidal flat and eelgrass bed.

The iron and steel slags are mainly classified into two categories, i.e. blast furnace slag and steelmaking slag (steel slag) including converter slag. The former is produced from the conversion process of iron ore into pig iron, and the latter is produced with CaO added through purification processes from pig iron into steel. The steel slags are further subdivided into desiliconized slag, dephoshorized slag, decarburized slag and others, according to the purification process of pig iron. There is granulated agglomerate using cement and fly ash of coal ash in order to add value for its recycling[12]. The coal ash from thermal power stations can be mainly classified into clinker ash and fly ash. The fly ash would contain CaO caused from original coal[13], and its granulated agglomerates using about 10% of cement containing calcium is produced in order to make granule[14]. Molten slag is the fused ash from incineration plants, molten slag of municipal solid waste is produced in order to decrease elution of added calcium during incineration and gas purification process and contaminated heavy metals and to promote its recycling[15].

From the standing point of environmental safety, the environmental regulated substances form the SAs were verified based on the soil pollution standards under the law on the prevention of marine pollution and maritime disaster for using a marine environment[15,16]. For the target SAs, the environmental regulated substances such as heavy metals are obviously below these environmental criterions[7,14-16]. These SAs with the particles sizes of 0.5~4.0 mm are almost the same size of natural sand in sandy beaches. In addition, some of them had several advantages in terms of environmental remediation[11,14,17-19]. For example, it is reported that steel slag could suppress phosphate liberation from sediment and decrease acid volatile sulfide in organically enriched sediment, and also it can create reef-like habitat for fishes and promote growth of some marine phytoplankton.

However, it is commonly reported that they have hydraulic properties which are mainly caused by CaO called 'free lime'. The free lime increases the pH in interstitial water by the elution of alkaline and calcium and triggers various chemical reactions between the SAs and seawater or sediment[20-23]. The calcium ion derived from the CaO also reacts with silicate and aluminate and accordingly forms lime-pozzolan[24,25] which causes solidification. While the pH increase would be temporal because of neutralization capacity of seawater and the solidification of sediment might be qualified by the mixing with soils and/or the streaming movement with seawater flow, it is important to understand the calcium and alkaline behavior in marine environments. Their behavior depends on the liquid phase, namely seawater in marine environment and its flow conditions. Therefore, it is important to understand of their chemical changes after submerged into the sea so as to apply these SAs to contract seagrass bed and tidal flats. Especially, to quantify the maximum elutable amounts of calcium with consideration to elution depth and its elution kinetics in each SAs under the real marine environment are important in order to evaluate their environmental impacts. However, their aging behaviors in the sea are not fully understood.

In this study, the quantitative chemical changes of SAs, namely, two kinds of steel slag, decarburized slag and dephosphorized slag, its granulated agglomerates, clinker ash and its granulated agglomerates and molten slag, were investigated under the sea environment. We quantified their maximum elutable amount of calcium from the SAs and its kinetics in seawater was also quantified.

## MATERIALS AND METHODS

**Target sand-alternatives(SAs).** The slags and its granulated agglomerates used in this study were provided by a steelmaking plant in Japan. The slag is generated through decarburization and dephosphorization processes from pig iron into steel, which was discharged from steelmaking processes. The clinker ash and granulated agglomerates of coal ash was obtained from a thermal power stations in Japan. The molten slag was obtained from a municipal solid waste incineration plant in Chugoku-Shikoku region.

The chemical composition analyzed by an energy dispersive X-ray fluorescence Spectroscopy (EDX-720, Shimadu), with the semi-quantitative mode on the surface (several dozen micro-meter depth) of each SAs used in this study are shown in Table 1. Hereinafter, each SA was respectively referred to as abbreviated name in Table 1.

For this analysis, each SAs were powdered by a high-energy planetary ball-mill (Fritsch Japan Co., Ltd, Pulverisette-7) with zirconium ball and sieved to obtain less than 250 µm diameter particles. Although they generally exist as oxide, they are shown as atom ratio without taking account of other light elements. "Others" in the Table 1 represents mainly phosphate, Mg, Al and Ti. Calcium, iron and silicon were main components for these 6 materials. The Ca content was relatively higher than other reports[12-15, 26, 27].

Table 1  Chemical composition of surface of SAs. Data of powdered SAs were shown in parentheses.

| Elements (%) | Decarburized slag (DCSlag-SM) | Dephosphori-zed slag (DPSlag-SM) | Granulated Slag (GranulSlag-SM) | Clinker Ash (Clinker-TP) | Granulated fly ash (GranulAsh-TP) | Molten slag (MSlag-MSW) |
|---|---|---|---|---|---|---|
| Ca | 58 | 52 | 60 | 8 | 50 | 55 |
| Fe | 28 | 30 | 19 | 37 | 16 | 15 |
| Mn | 6 | 6 | 4 | 0 | 0 | 1 |
| Si | 4 | 5 | 9 | 31 | 16 | 13 |
| P | 0.8 | 0.9 | 1 | 0 | 0 | 2 |
| S | 0.4 | 0.6 | 1 | 3 | 4 | 3 |
| Al | 0.7 | 2 | 3 | 13 | 7 | 5 |
| others | 2.1 | 3.5 | 3 | 8 | 7 | 6 |

**Continuous extraction to determine maximum calcium elution potential.** The maximum calcium elution potential of the SAs was determined with replacing artificial seawater by batch elution experiment. The powdered SA with less than 250 µm diameter was used for the each elution test on the basis of JIS K 0058-1 (Test method for chemicals in slags Part 1: Leaching test method). A 20 g of the powdered sample was stirred in 200 mL of artificial seawater (SEALIFE, Marinetech, Japan, at 30‰) at $25\pm1^{o}C$ in a 700 mL of vessel. Thereafter, it was mixed at 100 rpm by a rotary shaker. The artificial seawater was replaced to new one at every 6 hours with the sold–liquid separation by a membrane filter with 0.47 µm of pore size (Millipore, HAWPO470). Thereafter, the amount of eluted calcium in each fraction was determined by ICP-AES (VARIAN, 720-ES).
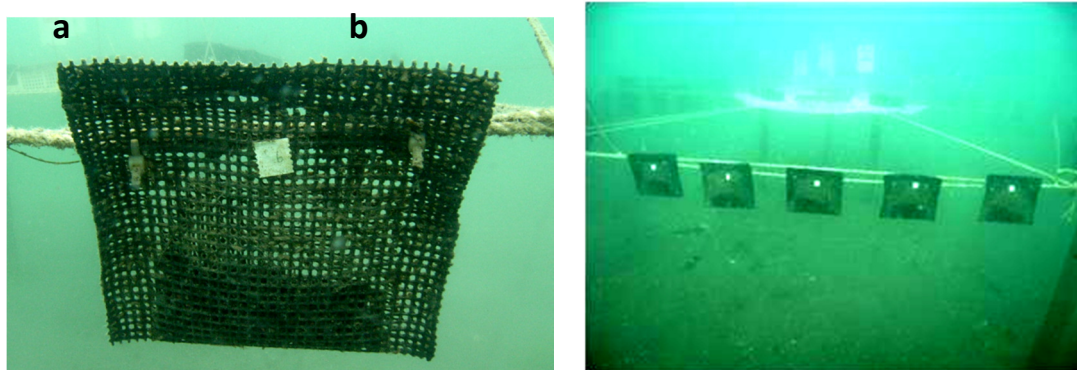


Figure 1  Submerged and aging situation in seawater (Samples are in the black net).

**Aging experiments in the sea to determine maximum elution depth.** The maximum elution depth of calcium in each SAs was determined by the aging in the sea over 500 days. The aging site is located on

the coast of Iwakuni area, Seto inland sea, Japan. The submerged depth ranges from D.L. −1.0 to −3.0 m. The aging experiment started from spring in 2010. The averages of major water quality of the seawater were pH 8.2, COD 2.4 mg/L and DO 8.9 mg/L, respectively. The SAs with 0.5~2.0 cm diameter was used for this aging test. About 10 pieces of sample was put into polypropylene net with 3 mm mesh (Fig. 1a), and submerged into seawater with hooking on a rope (Fig. 1b) to simulate the surface condition of sediment. The net were collected at certain aging period by a diver.

**Column elution experiments to determine the calcium elution rate.** In order to evaluate the calcium elution rate and the time required for the chemical stabilization of SAs in sea environment, a column experiment was conducted by using real seawater at Takehara area in Seto inland sea. Table 2 shows operational parameters for the column experiments. The particle sizes in the range 0.85~4.75 mm were selected for this experiment, and its empty bed contact time (EBCT) was set to 0.022~1.5 min on the basis of 72~4,800 ml/min of flow velocity. Elution of calcium was indirectly checked by measuring pH, because the difficulty of calcium detection in seawater having high concentration of calcium.

Table 2  Operational parameters of column experiments.

| | |
|---|---|
| Length (Depth) (cm) | 10 |
| Cross-sectional area (cm$^2$) | 86 |
| Particle size of ash (mm) | 0.85~4.75 |
| Empty bed (ml) | 95 |
| Flow rate (ml/min) | 72, 900, 4,800 |
| Rate of exchange (1/min) | 0.68, 8.5, 45 |
| (EBCT (min)) | (1.5, 0.12, 0.022, respectively) |
| Volume of SA (ml) | 700 |

**Analytical methods.** The pH was measured by a pH meter (F-51, Horiba). Sand-alternative was beforehand dried under nitrogen gas over than 24 h for these analyses. The elemental mapping of calcium and vertical distribution from surface of SA were observed by an electron probe micro-analyser, EPMA (JXA-8200, JEOL) after cutting off at the center of SAs and grinding the cross-section of each SA in order to determine the depth of calcium eluted. Total pore volume was measured by an automatic vapor adsorption analyzer (BELSOrP-aqua[3], BEL JAPAN, INC.) followed by the BET method.

To determine the calcium composition of surface, calcium K-edge XANES spectra (range 4030-4090 eV) were measured using the BL11 in the Hiroshima Synchrotron Research Center, HiSOR. The synchrotron radiation from a bending magnet was monochromatized with a Si(111) double-crystal monochromator. The sample chamber was filled with He gas, and XAFS spectra were measured by the conversion electron yield (CEY) mode. Pieces of relatively flat samples were mounted on a double-sided stick tape (NW-K15; Nichiban) and placed in the central hole (15 mm in diameter) of a copper plate.

**RESULTS AND DISCUSSION**

**Maximum calcium elution potential.** The cumulative calcium elution from the SAs into artificial seawater is shown in Fig. 2. The major calcium elution was observed until around 10 times replacement (100 ml of cumulative volume) of seawater. The maximum calcium elution potential of the decarburized and dephosphorized slag, its granulated slag, clinker ash, granulated ash and molten slag was 204, 75, 26, 6, 19 and 5 mg/g-SA, respectively. The maximum calcium elution potential of the decarburized is slightly low compared to other report (250~500 mg/g[20]). Two kinds of slag contain limestone, which added during oxidation refining stage, might increase the maximum calcium elution potential. The elution potential of granulated slag and granulated ash is attributed to mixed cement component. The elution of calcium from clinker ash and molten slag was less than 10 mg/g-SA of detection limit, indicating that their elution potential was almost negligible.

**Maximum elution depth in sea environment.** Calcium distribution mapping on center cross-section of DCSlag-SM sample before aging and after 504 days was shown in Fig. 3 as an example. The left black colored area of both pictures represents the outside of the slag, and the interface with black colored area and colored area shows the slag surface. The color bar represents relative calcium concentration, namely, red color represents high concentration, while blue and black represents low concentration, respectively. Both before (a) and after aging (b), the concentrations of calcium in the slag surface were lower than those in the deep area (right side). It indicates that the calcium eluted from the slag surface into seawater. Approximately until 70 μm of depth, approximately half of calcium was eluted from decarburized slag even before submersing since they are exposed to rain or artificial water spray for cooling them through producing and conditioning processes. From this element map, the depth of calcium eluted can be determined for each SAs. The change in average elution depth of calcium determined from the calcium mapping was summarized in Fig. 4. Since the elution depth was not identified (less than 5 μm of detection limit) in clinker ash and molten slag of municipal solid waste, their results was not shown in Fig. 4. Increase of calcium elution depth by aging was observed for all SAs under seawater condition except for clinker ash and molten slag.
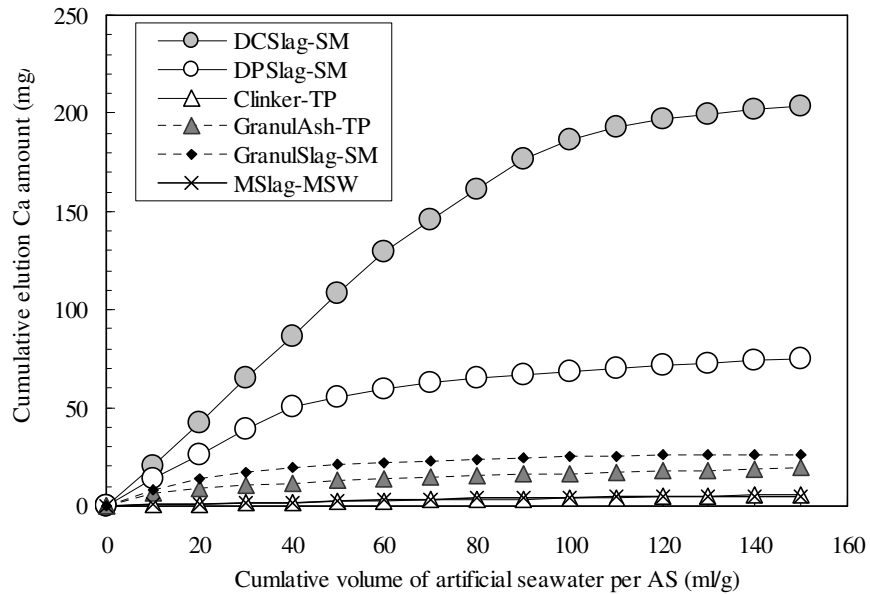


Figure 2  Cumulative amount of eluted calcium from the SAs by artificial seawater.



a) Before aging             b) After aging
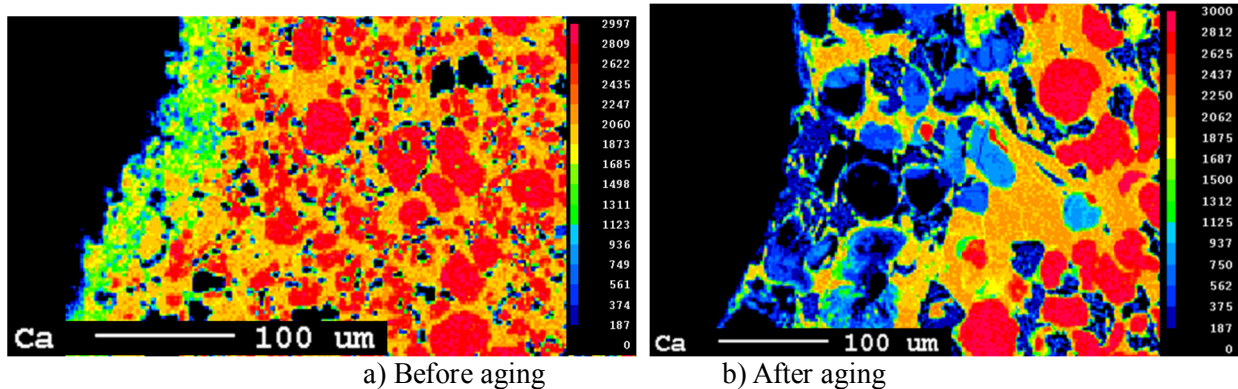
Figure 3  Ca distribution map of decarburized slag before aging (a) and after 504 days (b) obtained by EPMA (Left side is the surface. They are different particle.).

The maximum depth of calcium eluted in the seawater was 140, 300, over 3,000 and over than 5,000 µm after 504 days aging for decarburized slag, dephosphorized slag, granulated slag and granulated ash, respectively. The maximum calcium elution depth for the two granulated materials was over the measuring limit, i.e. the radius of its particle, indicating that all elutable calcium could be elutable in the size rage as sand alternative. Because both the granulated materials ash were mixture of several materials (blast-furnace slag, ordinary Portland cement, fly ash, admixtures and about 60% slag for the granulated slag[12], and blast furnace cement, Bentonite and about 90% of fly ash from thermal power station for the granulated ash[17]), seawater would penetrate into the interspace in each hetero-phase. The total pore volume of granulated slag and granulated ash was higher than that of other SA as summarized in Table 3, which is supported that the granulated slag and granulated ash had greater amount of interspace compared to other SAs.
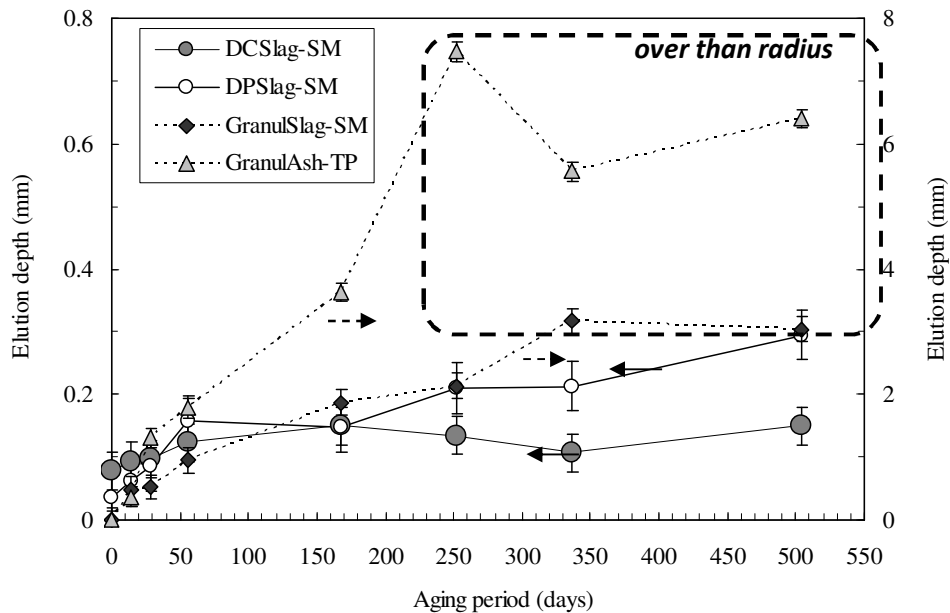


Figure 4  Depth change of Ca eluted for each SA during 504 days submersed period.

Table 3  Total pore volume of each SA in BET analysis.

|  | DCSlag-SM | DPSlag-SM | GranulSlag-SM | Clinker-TP | GranulAsh-TP | MSlag-MSW |
|---|---|---|---|---|---|---|
| Total pore volume ($mm^3$/g) | 12 | 7 | 19 | 19 | 4 | 1 |

On the other hand, the reason why there was limitation of calcium elution in the two slags would be blocking reactions at the pore where calcium eluted. The calcium ion released can react with silicate and aluminate and accordingly forms lime-pozzolan[24,25]. The formation lime-pozzolan in the surface of slag at the calcium eluted area might block the further elution of calcium from its inside. Fig. 5 shows the composition change of calcium species on the surface of DPSlag-SM during aging of 288 days. As is the case with other analysis, sample has heterogeneous structure (refer to Fig. 3) and there was large dispersion. During aging of 504 days, the calcium spices changed to $Ca(OH)_2$ and $CaCO_3$ from CaO. It would be derived from the hydrolysis of CaO with high solubility (1.4 g/L). The accumulation of $CaCO_3$ with low solubility (0.015 g/L) on the surface or in the calcium eluted space in SAs can block the percolation of seawater and stop the increase of depth calcium eluted (Fig. 4).

**Maximum elutable amount of calcium.** The maximum elutable amount of calcium in the sea

environment can be calculated following by the maximum calcium elution potential, maximum calcium elution depth, density and size of SA. The diameter of SA was supposed to be 5 mm in here and the density of each SA was measured for the aging samples at before section. As previously mentioned, the maximum calcium elution potential and maximum elution depth were obtained with summarized in Table 4. The maximum elutable amount of calcium calculated was almost same in DCSlag-SM, DPSlag-SM, SolidSlag-SM and SolidAsh-TP (32, 24, 26, 19, respectively) and 0 in ClinkAsh-TP and MeltSlag-MSW. These values will provide useful information to evaluate the environmental impact of each SA by the combination with further reaction of the calcium released.
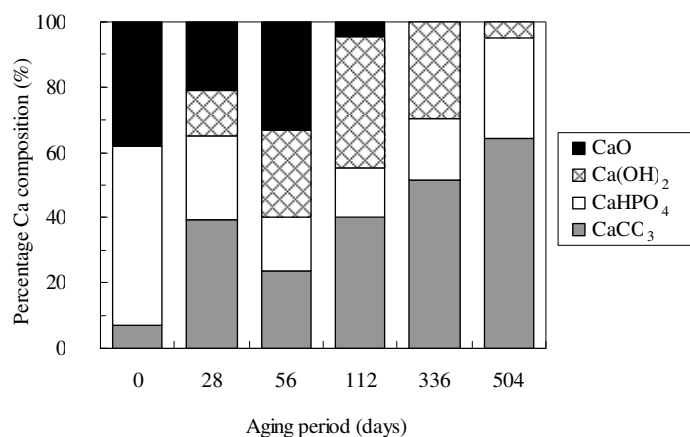


Figure 5  The change of Ca species on the surface of DPSlag-SM during 504 days.

Table 4  Maximum elutable amount of calcium from SAs in the seawater. (*Initial eluted depths was not removed.)

| | DCSlag-SM | DPSlag-SM | SolidSlag-SM | ClinkAsh-TP | SolidAsh-TP | MeltSlag-MSW |
|---|---|---|---|---|---|---|
| Density* (g/cm$^3$) | 3.6 | 3.6 | 2.3 | 1.7 | 1.8 | 3.1 |
| Maximum Ca elution Potential (mg/g) | 204 | 75 | 26 | 6 | 19 | 5 |
| Maximum elution depth (mm) | 0.14* | 0.30* | 2.50 | 0.00 | 2.50 | 0.00 |
| Maximum elutable amount of Ca (mg/g) | 32 | 24 | 26 | 0 | 19 | 0 |

**Elution kinetics in sea water.** The elution amount of calcium in seawater should be controlled by the exchange rate of surrounding seawater, because its equilibrium would be fast. Fig. 6 shows the pH variation of effluent of column from DCSlag-SM packed in column at each flow velocity of seawater, and it is recalculated by the exchange rate of pore volume. X-axis shows the number of exchanged pore volume of column filled by DCSlag-SM. The initial effluent pH was over than 10 because the hydrolysis of CaO and release of Ca ion and alkaline as mentioned previously. The pH decrease less than 9 after 10,000 times exchange of pore volume, and it decreased to 8.3, which is same value with influent seawater, at around 100,000 pore volumes.

In here, the decrease trend was almost similar in three exchange rate of seawater, from 0.7 to 45

min$^{-1}$ which represents from 72 to 4,800 ml/min to 0.7 L of filled slag. It indicates that the main factor of CaO reaction is the rate of exchange of seawater, therefore the calcium elution rate in each SAs could be expressed by the exchange rate of seawater.

Fig. 7 shows the pH decrease of four SAs at around 8.5 min$^{-1}$, while ClinkAsh-TP and MeltSlag-MSW was not examined in here on the basis of the 0 of maximum elutable amount of calcium (Table 4). The initial pH of DPSlag-SM, SolidSlag-SM and SolidAsh-TP was over than 9, but they are decreased to lower than 9 after 200 pore volume exchanged. The pH decrease to 8.3 was at around 100,000 times exchange in DPSlag-SM, SolidSlag-SM and SolidAsh-TP as like DCSlag-SM.
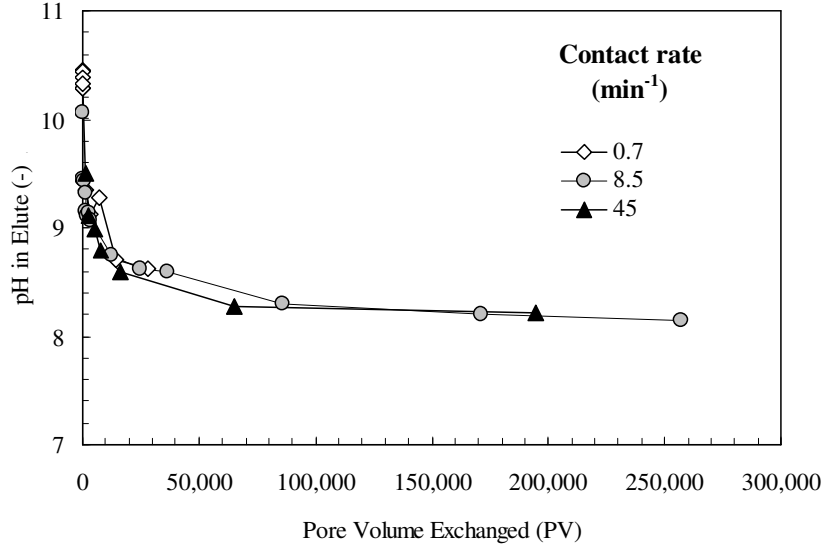


Figure 6  pH variation of effluent solution from column filled with DCSlag-SM against exchanged time of pore volume.
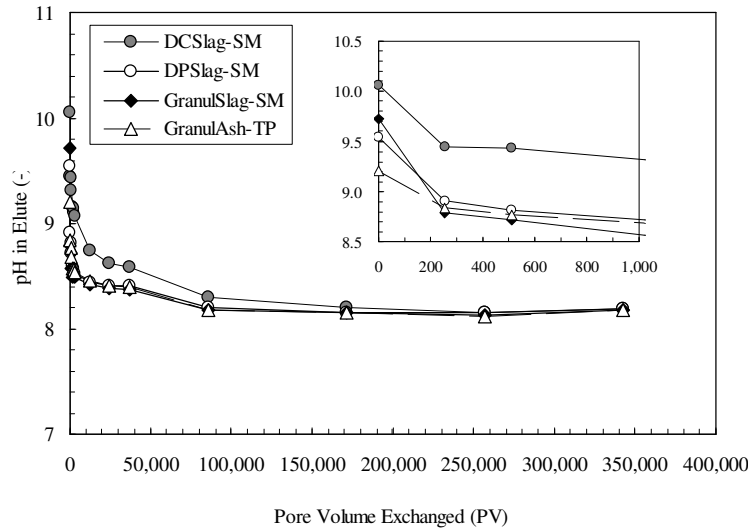


Figure 7  pH variation of effluent solution from column filled with four SAs against exchanged time of pore volume. (8.5 min$^{-1}$)

**CONCLUSION**

The behaviors of six sand alternatives during aging in sea environment are investigated by targeting at calcium and alkaline elution. The rate of alkaline elution and the maximum elutable amount

of calcium in sea environment from each sand alternative were determined.

The maximum elutable amount of calcium was almost same in decarburized slag, dephosphorized slag, granulated slag and granulated fly ash was 32, 24, 26, 19, respectively, and 0 in clinker ash and molten slag. It is found that the pH of contacted seawater with decarburized slag, dephosphorized slag, granulated Slag and granulated fly ash can be decreased to lower than 9 after the exchange of 1,000, 200, 200 and 200 of pore volume of seawater respectively. The pH can be decrease to 8.3 by around 100,000 pore volume of seawater exchanges.

**ACKONWLEDGEMENTS**

**REFERENCES**

1) F.T. Short and S. Wyllie-Echeverria (1996) Natural and human-induced disturbance of eelgrass, Environment Conservation, 23, 17–27.

2) Yao Jianting, Duan Delin, Jiang Hongtao (2010) Artificial enhancement of sea-forest for reducing the Isoyake degree along the north coast of China, 32, 19-24.

3) R. Inoue and H. Suito (2002) Behavior of Fluorine Dissolution from Hot Metal Pretreatment Slag, Tetsu-to-Hagané, 88, 340-347.

4) Shinichi Hanawa (2006) Status and future of Tidal flats in Japan (Nihon no Higata no Genjyoyu to Mirai), Global Environment (Chikyu Kankyou), 11, 2, 235-244 (in Japanese).

5) H. Suito and R. Inoue (2002) Fluorine-containing Mineral Phases in Iron Making and Steelmaking Slags and Their Solubilities in Aqueous Solution, ISIJ Int., 42, 785-793.

6) Toshinobu Terawaki, Goro Yoshida, Motoharu Uchida, Masami Hamaguchi (2005) Present State of the Tidal Zone Environment ad Adaptive Management in Seto Inland Sea, Japan, Proceedings of Civil Engineering in the Ocean, 21, 83-88 (in Japanese).

7) Ealey T., Baca B., Livesey S., Al-Jamali F., Jones D. A. (2007) Gulf desert developments encompassing a marine environment, a compensatory solution to the loss of coastal habitats by infill and reclamation: The case of the Pearl City Al-Khiran, Kuwait, Aquat Ecosyst Health Manag., 10, 3, 268-276.

8) Tatsuhiko Tanaka, Seiji Inoba, Satoshi Kawada, Akiko Kida, Kazuhiko Kurusu, Masaru Furusaki, Takao Tanosaki, Norihiko Nishida, Toshihisa Maruta, Yoshifumi Watanabe, Akihiro Ono, Mamoru Sakata, Kazutoshi Kakita, Ken-Ichi Takimoto (2010) Development of Coal Ash Certified Reference Materials JSAC 0521 and 0522 for Determination of Inorganic Constituents, Bunseki Kagaku, 59, 2, 137-150 (in Japanese).

9) The Japan Society of Industrial Machinery Manufactures (2012) The numerical statement of eco-slag production in Japan, http://www.jsim.or.jp/ecoslag/pdf/toukei_seisan1222.pdf (at 2012.5.25) in Japanese.

10) Tekko Sulagu Kyokai (2010) Statistical Yearbook of Steel Slag (Tekko Sulagu Toukeinennpou), http://www.slg.jp/statistics/report.html (accessed at 2012.5.25).

11) J. H. Martin (1990) Glacial-interglacial $CO_2$ change: The Iron Hypothesis, Paleoceanography, 5, 1.

12) Udagawa Etsuro and Matsunaga Hisahiro (2008) "Frontier rock$^{TM}$" an Artificial Stone Made by Steel Slag Hydrated Matrix.

13) Norihiro Murayama, Yousuke Yamakawa, Kazuo Ogawa, Hideki yamamoto and Junji Shibata (2001) Evaluation of Coal Fly Ash and Incineration Ash as Raw Material for Zeolite Synthesis, Shigen-to-Sozai, 117, 501-505 (in Japanese).

14) Satoshi Asaoka, Tamiji Yamamoto, Kyoko Yamamoto (2008) A Preliminary Study of Coastal Sediment Amendment with Granulated Coal Ash -Nutrient Elution Test and Experiment on Skeletonema costatum Growth-, Journal of Japan Society on Water Environment, 31, 8, 455-462.

15) Jun Kobayashi, Ryoichi Kizau, Kazuyuki Torii (2004) Physical Properties and Metal Elutions of the Thirteen Molten Slags Produced from Incinerated Ash, Yakugaku Zasshi, 124, 9 (in Japanese).

16) Amelia B. Hizon-Fradejas, Yoichi Nakano, Satoshi Nakai, Wataru Nishijima, Mitsumasa Okada (2009) Anchorage and resistance to uprooting forces of eelgrass (Zostera marina L.) shoots planted in slag substrates, Journal of Water and Environment Technology, 7, 2.

17) Satoshi Asaoka, Tamiji Yamamoto, Shinjiro Hayakawa (2009) Removal of Hydrogen Sulfide Using Granulated Coal Ash, Journal of Japan Society on Water Environment, 32, 7, 363-368 (in Japanese).

18) Akio Hayashi, Hirokazu Tozawa, Katsuya Shimada, Katunori Takahashi, Ryoko Kaneko, Fumitaka Tsukihashi, Ryo Inoue and Tatsuro Ariyama (2011) Effects of the Seaweed Bed Construction Using the Mixture of Steelmaking Slag and Dredged Soil on the Growth of Seaweeds, ISIJ Int., 51, 11, 1919-1928.

19) Tamiji Yamamoto, Masami Suzuki, Seok Jin Oh and Osamu Matsuda (2003) Release of Phosphorus and Silicone from Steelmaking Slag and Their Effects on Frowth of Natural Phytoplankton Assemblages, Tetsu-to-Hagané, 89, 482-488 (in Japanese).

20) T. Futatsuka, K. Shitogiden, T. Miki, T. Nagasaka and M. Hino (2003) Dissolution Behavior of Elements in Steelmaking Slag into Artificial Seawater, Tetsu-to-Hagané, 89, 382-388 (in Japanese).

21) Takayuki Futatsuka, Kiyoteru Shitogiden, Takahiro Miki, Tetsuya Nagasaka, Mitsutaka Hino (2004) Dissolution Behavior of Nutrition Elements from Steelmaking Slag into Seawater, ISIJ Int., 44, 753-761.

22) Takahiro Miki, Kiyoteru Shitogiden, Yusuke Samada and Mitsutaka Hino (2004) Elution Mechanism of Fluorine from Steelmaking Slag into Seawater, ISIJ Int., 44, 5, 935-939.

23) Takahiro Miki, Takayuki Futatsuka, Kiyoteru Shitogiden, Tetsuya Nagasaka and Mitsutaka Hino (2004) Dissolution Behavior of Environmentally Regulated Elements from Steelmaking Slag into Seawater, ISIJ Int., 44, 4, 762-769.

24) Shi, S. and Day, R. L. (2000a) Pozzolanic reaction in the presence of chemical activators Part I. Reaction kinetics, Cement and Concrete Research 30, 51-58.

25) Shi, S. and Day, R. L. (2000b) Pozzolanic reaction in the presence of chemical activators Part II. Reaction products and mechanism, Cement. and Concrete Research 30, 607-613.

26) Hisahiro Matsunaga, Masato Takagi and Fumio Kogiku (2003) Fundamental Properties of Blocks which Set Steel Slag by Hydration Reaction and Biofouling Build-up Properties on Exposure to Marine Environment, Tetsu-to-Hagané, 89, 454-460 (in Japanese).

27) Kouji Sugawara, Akio Kondo, Katsuya Akiyamaa and Haeyang Pak (2010) Evaluation of Ash Deposition and Clinker Generation in Boiler of Coal Fired Power Plant, R・D Kobe Steel Engineering Reports, 60,1.

# THE USE OF FUZZY COGNITIVE MAPS IN MODELING
# REGIONAL WASTE MANAGEMENT SYSTEMS

*Adrienn Buruzs* and Miklós Bulla PhD (Széchenyi István University, Győr, Hungary)

**ABSTRACT:** One of the priorities of EU waste management strategy is to reduce the amount of waste; and the reuse and recycling of produced waste. In order to comply with EU legislation, Hungary has to fulfil requirements, which essentially influences the former waste management practices in the country. The main target is to develop regional waste management systems (RWMS) with the involvement of local governments. System dynamics principles and analytical tools have the potential to alleviate several deficiencies in current management analytical techniques. This paper investigates a new theory, Fuzzy Cognitive Maps (FCM), and the initiations of its implementation in solid waste management modelling systems. First the current Hungarian waste management situation is presented, then the description and the methodology of FCM is examined, finally the application of FCM in a waste management system is presented. The paper indicates how effective FCMs are in waste management modelling and presents a casual loop diagram (CLD) of a generic project management system.

## INTRODUCTION

In this paper the main objective is to define and construct FCM for modelling regional waste management system (RWMS). The organisation of this paper is as follow: first the current Hungarian waste management situation is presented, then the description and the methodology of FCM is examined, finally the application of FCM in a waste management system is presented. The paper indicates how effective FCMs are in waste management modelling and presents a casual loop diagram (CLD) of a generic project management system. It is intended that the paper be of interest to all project management researchers in the field of environment and sustainability, not just those interested in waste management projects.

## MATERIALS AND METHOD

**Regional Waste Management System in Europe and Hungary:** The European Union's approach to waste management is based on three principles: (1) waste prevention, (2) recycling and reuse, and (3) improving final disposal and monitoring (Waste Framework Directive 2008). Waste management refers to various interlinked activities such as collection, transportation, processing, recycling, disposal, reduction and monitoring of waste materials. Sustainable waste management must go beyond the mere safe disposal or recovery of wastes that are generated and must seek to address the root cause of the problem by attempting to change unsustainable patterns (United Nations Environment Programme). In recent years, a variety of material and energy recovery technologies have been devised and are now included in modern systems. Global efforts are now in force to reorient solid waste management systems toward sustainability. Additionally, it should be realized by using the technical, organizational and financial resources available in a particular locality, followed by waste policy, waste planning, regulatory framework, and enforcement of the law.

The most important areas related to the developing projects of municipal solid waste treatment in Hungary were: increasing the capacity of landfills, accomplishment of the infrastructure of selective waste collection, building of new composting plants. It follows that the main methods currently employed are landfilling, recycling, composting and energy from waste plants. In Hungary the deposition of waste is the determining treatment manner and it is likely to stay in the future. The main problems to the next

years will be the lack of reprocessing industry. The high number of to-be-recultivated landfills and the attainability of necessary financial sources are also serious problems (Orosz Z., Fazekas I. 2008).

The amount of solid wastes that society produces seemed to move together with economic growth over the last century. Predictions indicate to double the generation of certain wastes by 2025. In addition, there is a clear correlation between the concentration of populations and generation of municipal waste. In Hungary about 4.7 million tons municipal solid waste generates per year and 85% of this quantity gets to landfills. The ratio of disposal has to reduce to 50% by 2013 (Orosz Z., Fazekas I. 2008).

According to the 1999/31/EK directive on waste deposition the quantity of deposited biodegradable organic waste has to be decreased by 35%, 50% and 65% by the year 2006, 2009 and 2016 compared to the level of deposited organic waste in 1995. To achieve this goal, in the country new capacities were realized in 2009 and 2010. The projects were designed to establish EU-compliant waste management by introducing a selective waste collection strategy and optimizing logistics systems. Only 57 dumpsites of former landfills (2667) operate after 2009.

These regional projects significantly contribute to the fulfilment of the aims of waste management. Due to the building-up of selective collection systems and treatment plants of biodegradable organic waste, the quantity of material recovered waste will increase, hereby the quantity of deposited waste will decrease. Moreover, the system provides services to the public, employs a sizable number of people and requires significant resources in various forms. Over the years, it has been realized that it is necessary to design an integrated system as a whole rather than selecting individual component subsystems that may not work well together (Shekdar, A. 2009). In Hungary, the concept of integrated solid waste management systems on regional level have gained acceptance. The resulting system configuration ensures improving overall performance. RWMSs has also been defined as the selection and application of suitable techniques, technologies and management approaches to achieve specific objectives and goals.

Waste management in Hungary is primarily controlled through legal regulations. In case of municipal waste, the municipal governments are responsible for organising municipal services, ensuring the treatment of municipal waste, so that the responsibility of the inhabitants can be enforced. Urban and rural municipalities can join together to form a RWMS and delegate their waste management responsibilities to a central authority. The authority is a separate legal entity, governed by a board, with representatives from the communities and rural municipalities.

General features of RWMS can be as follows:
- establish or up-to-date one or two centralized municipal landfills (depending on region size) used by all municipalities belonging to the regional system;
- operation of transfer stations;
- collection of municipal waste;
- operation of recycling programs for the entire region; and
- joint public education programs.

In addition to being less costly to operate than individual landfills, RWMSs have other advantages such as:
- improve environmental performance;
- improve landfill operations;
- promote waste minimization;
- reduce equipment requirements to run waste and recycling collection and processing systems; and
- provide better waste handling prices.

In a RWMS, all users have to share the cost of building the basic infrastructure. Keeping everyone informed is a constant and crucial part of a successful regional system. Moreover, the one of the very first steps which must be taken prior to introduction of new waste management systems is to establish the structure of information flow towards users, and a two-way communications system among citizens, municipalities and the public utility company. To realize this, it is necessary to streamline functionality by integrating many elements that govern performance within the system.

In order to achieve the above mentioned goals, in many Hungarian settlements as part of different RWMSs, each householder is provided with two bins for recycling. The citizens deposit kitchen and garden waste into the – usually – brown top bin. The other, grey top bin is for collection of the materials which are not recyclable. Then the bins are collected separately, on different days of the week by the recycling collections crews and taken to the regional waste treatment facility. In addition, householders are expected to make special trips to dedicated waste collection points in order to dispose of particular items, such as plastic, glass, paper and metal. Some regions have introduced the possibility of fining residents by the polluter-pays-principle (PPP) that do not take part in the waste selection program and/or do not use the recycling facilities. The essence of the PPP is the billing on the basis of the numbers of bin emptied which is monitored by the collection vehicle. Thereby this figure composes the basis for billing.

**Fuzzy Cognitive Maps:** It is widely recognized that the contribution of conventional methods in modelling waste management systems due to their complexity is limited (Stylios, C. D. et al 1997). The most important component in defining an FCM is the determination of the concepts that best describe the system and the directions and grade of causality between concepts. The next step is to express the relationship among these factors. These concepts must be connected with each other. First it must be decided for each concept to which another concept is connected Then the sign of the connection is decided, and the weight of each connection is determined. Interconnections of concepts can easily be changed. A concept can be added or removed if this improves the system's description (Stylios C. D. and Groupmos P. P. 1999).

The theory of Fuzzy Cognitive Maps (FCMs) uses a symbolic representation for the description and modelling of the system. Nodes of the graph stand for the concepts of the system that are connected by signed and weighted arcc representing the causal relationships that exist between the concepts (Stylios, C. D. et al 1997). Involving some elements of the RWMS, a FCM is developed (Figure 1). For the modelling of a RWMS, the crucial elements can be the follows:

- amount of generated waste (*C1*)
- amount of recycled waste (*C2*)
- strictness of legal regulation (*C3*)
- motivation of users (*C4*)
- activity of municipalities' consortium (*C5*)
- payment for waste handling (*C6*)
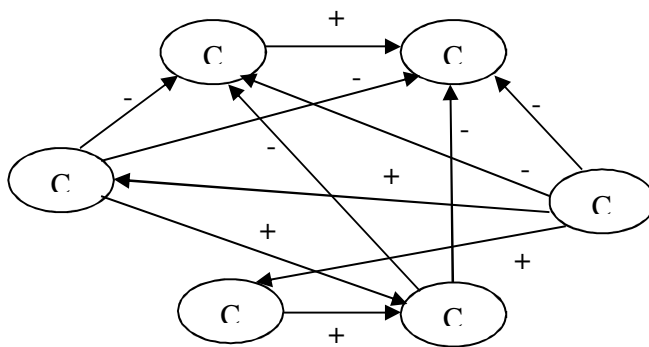


FIGURE 1: An initial FCM is developed for the main elements of RWMS

Each concept of the FCM takes a value which ranges in the interval [0,1] and the weights of the interconnections belong to the interval [-1,1]. From simple observation of FCMs, it becomes clear, which concept influences which other concepts, showing the interconnections among concepts and it permits thoughts and suggestions for the reconstruction of the graph. Building an FCM model of a system depends on human experts who have knowledge on the structure of the operation (Stylios, C. D. et al 1997). First of all, we have to determine the relevant factors of our system that should be present in the

map, which has been done above. The next step is to express the relationship among these factors. Then the sign of the connection is decided, and then the weight of each connection is determined. Interconnections of concepts can easily be changed. A concept can be added or removed if this improves the system's description (Stylios, C. D. et al 1997).

As it can be seen from the graph of Figure 1, in a RWMS – as in every environment-related system – each element is connected with the other – more than one – element. In this graph, we can state, that the most influential element is 'legal regulation', the second one is 'motivation of users'. Furthermore, the most effected item is 'amount of recycled waste' and the second one is 'amount of generated waste'.

Between the concepts, there are two possible types of casual relationship that express the type of influence from one concept to the other. The weights of the arcs between concept $C_i$ and concept $C_j$ could be positive ($W_{ij}>0$) which means that an increase in the value of concept $C_i$ leads to the increase of the value of concept $C_j$, and a decrease in the value of concept $C_i$ leads to the decrease of the value of $C_j$. Or there is a negative causality ($W_{ij}<0$) which means that an increase in the value of concept $C_i$ leads to the decrease of the value of concept $C_j$ and vica versa (Stylios C. D. and Groupmos P. P. 1999). The adjacency matrix representations of the above described cognitive map is presented in Figure 2. In the matrix, $e_{ij}=e(C_i, C_j)$ is the causal edge function value, the causality causal concept node $C_i$ imparts to $C_j$. $C_i$ causally increases $C_j$ if $e_{ij}=1$, causally decreases $C_j$ if $e_{ij}=-1$ and imparts no causality if $e_{ij}=0$ (Kosko B. 1985).

|       | $C_1$ | $C_2$ | $C_3$ | $C_4$ | $C_5$ | $C_6$ |
|-------|-------|-------|-------|-------|-------|-------|
| $C_1$ | 0     | 1     | 0     | 0     | 0     | 0     |
| $C_2$ | 0     | 0     | 0     | 0     | 0     | 0     |
| $C_3$ | -1    | -1    | 0     | 0     | 1     | 1     |
| $C_4$ | -1    | -1    | 0     | 0     | 0     | 0     |
| $C_5$ | 0     | 0     | 0     | 1     | 0     | 0     |
| $C_6$ | -1    | -1    | 0     | 1     | 0     | 0     |

FIGURE 2. The adjacency matrix representation of an initial FCM
developed for the main elements of RWMS

**Causal Loop Diagrams:** System thinking is a science based on understanding connections and relations between seemingly isolated things. In technical terms system thinking is ; understanding relationships and patterns between components in a network of relationship (Capra F. 1997). In all planning and modelling procedure there is a need to predict and assess the possible effects a project has on development issues. This is not only restricted to environmental aspects but also to socio-economic issues since these are closely integrated. In a world where resources are becoming scarce, the marginal for errors is diminishing. There exists less and less space for manoeuvring in long-term planning. The key tenant of system thinking is that all elements within a system are related (Haraldsson H. V. 2000). One reason project goals are often not met is that the project management concepts and tools used today are too complex and volatile and contain too much apparent randomness to be managed effectively by the linear, deterministic tools that focus on one portion of the system at a time (Toole T. M. 2005). The CLD is a tool for systematically identifying, analysing and communicating feedback loop structures (Haraldsson et al. 2006).

For example, Figure 3 presents a portion of the RWMS. We have designed a CLD as a system thinking tool in order to get a better picture about the amount of collected and treated bio and green waste.

The quantity of deposited biodegradable organic waste has to be decreased by 35%, 50% and 65% by the year 2006, 2009 and 2016 compared to the level of deposited organic waste in 1995. So it is crucial to distract bio and green waste from the landfills, and produce high-quality compost which can be sold on the market.

To create a causal loop diagram, we had to identify which of the variables of the system are causally related to other variables, and decide whether the effect of one variable on another is positive or

negative. A plus sign indicates that when the variable next to the tail of an arrow increases, the variable next to the head of the arrow also increases. A minus sign indicates that when one variable increases, the other variable decreases.

The reader may note the numbers of the negative and positive causalities. If the feedback loop includes even number of negative causal relationships, this is therefore positive (self-reinforcing) feedback loop. In the case of the odd number of negative causal relationships, this is a negative (balancing) feedback loop.
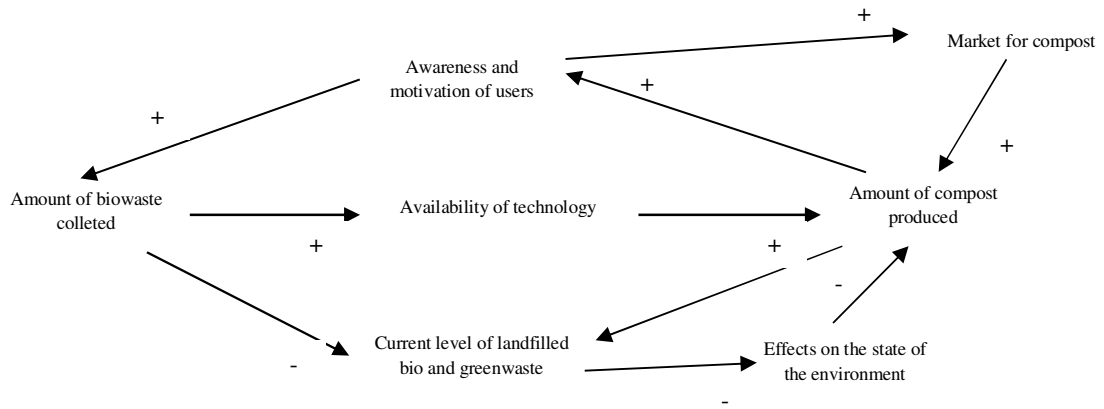


FIGURE 3. A CLD designed to get a better picture about the amount of collected and treated bio and green waste

## RESULTS AND DISCUSSION

The use of system analysis involves tools like FCM and CLD. Fuzzy Cognitive Maps (FCMs) is a new approach in modelling the behaviour and operation of complex systems. FCMs are proposed to be used in the modelling of various systems. Efficient FCMs are in expressing qualitative information and knowledge about the process structure. Any procedures include uncertain description and can have subtle variations in relation to time and space; for such situations FCMs seem to be capable to deal with (Stylios, C. D. et al 1997; Kosko B. 1985).

FCM is a model for representing and decoding the expert's knowledge and experience. For large and complex systems it is extremely difficult to describe the entire system by precise mathematical model. Thus, it is more attractive and useful to represent it, in a graphical abstract way showing the causal relationships between concepts. This symbolic method of modelling and control of a system is easily adaptable and relies on expert experience. Fuzzy Cognitive Map seems to be a useful modelling method, which can be used to control complex systems. In this paper, an initial FCM is constructed that can be used to model and simulate the behaviour of the RWMS. The FCM is a powerful tool that can be used for modelling RWMS systems.

The engineering analytical process always begins with a conceptual model where thinking is translated from an idea onto a paper. Communication can only be done if the participants speak the same language using the same terminology and expressions for describing the systems. Therefore, the CLD concepts was developed and it was soon discovered that a CLD could be used as an aid for conceptualizing a hypothesis for a problem (Haraldsson et al. 2006).

## CONCLUSION

This paper has summarized the situation of waste management systems on regional level in Hungary, has introduced the basic theory of FCM and CLD and presented a FCM and a CLD for regional

waste management systems. It is not suggested that the FCM and CLD presented here accurately depicts all project contexts. It is intended to serve as a initial system thinking tools for sustainability-related projects and practitioners can use as a starting point to think about their own projects.

## CLOSING

Beyond the graphical representation of the FCM there is its mathematical model which the authors intend to apply to a real regional waste management system in the near future. In this case, the modelling of a practical problem will be examined. Furthermore, the CLD presented in this paper will be applied to other aspects of regional systems, and not only on waste issues.

## REFERENCES

Cornelissen, A. M. G. (2003): *The Two Faces of Sustainability. Fuzzy Evaluation of Sustainable Development.* PhD thesis. Wageningen University, The Netherlands.

Directive 2008/98/EC on waste (Waste Framework Directive)

Haraldsson H. V. (2000): *Introduction to Systems and Causal Loop Diagrams.* System Analysis Course. Lumes. Lund University

Haraldsson H. V., Belyazid S. and Sverdrup H. U. (2006): *Causal Loop Diagrams – Promoting Deep Learning of Complex Systems in Engineering Education.* 4th Pedagogical Inspiration Conference. Lund University, Sweden

Kosko B. (1986): *Fuzzy Cognitive Maps.* Int. J. Man-Machine Studies. 24, 65-75.

Orosz Z. and Fazekas I. (2008): *Challenges of Municipal Waste Management in Hungary.* AGD Landscape & Environment 2 (1) 2008. 78-85.

Shekdar A. V. (2009): *Sustainable solid waste management: An integrated approach for Asian countries.* Waste Management, Volume 29, Issue 4, Pages 1438-1448

Stylios C. D., Geirgopolus V. C. and Groumpos P. P. (n.d.): *The Use of Fuzzy Cognitive Maps in* Modeling Systems. 5th IEEE Mediterranean Conference on Control and Systems (MED '97), Paphos, Cyprus

Stylios C. D. and Groumpos P. P. (1999). *Fuzzy Cognitive Maps: a Model for Intelligent Supervisory Control Systems.* Elsevier Science. Computer in Industry. 229-238.

Toole T. M. (2005): *A Project Management Causal Loop Diagram.* ARCOM Conference, London, UK

United Nations Environment Programme: *Environmentally Sound Management of Solid Wastes and Sewage-related Issues.*
http://www.unep.org/Documents.Multilingual/Default.asp?DocumentID=52&ArticleID=69

# BRIQUETTING: THE SOLUTION TO AGRO-WASTE MANAGEMENT

D.R. Naron (Department of Chemistry, University of Jos-Nigeria)
and *Juliet M Yakubu*
(Department of Biological Sciences, Federal University, Wukari-Nigeria)

**ABSTRACT:** This study investigates the usefulness of Agro-wastes (rice husk, sawdust, sugar cane waste and groundnut shells as an alternative fuel for household energy.  Briquettes were produced from each material with the aid of cassava starch as a binder in the ratio of 5:1 and compressing machine. Water Boiling Test (WBT) was carried out using an improved stove to test the performance of these briquettes. Proximate analysis shows that the produced briquettes have good properties and burned well in the stove and could serve as substitute for fire wood besides keeping the environment clean.

**Key words:** Agro-wastes, Briquettes, Water Boiling Test (WBT)

## INTRODUCTION

The continuous increase in concern over environmental pollution has resulted in greater negative cost values of wastes and hence has increased their potential as substrates for bio-derived energy. Agro-wastes are biomass materials: organic carbon based materials that react with oxygen in combustion and natural metabolic process to release heat.

The briquetting of agro-residues is of relatively origin in developing countries. The technique was adapted for organic wastes about 50years ago in industrial countries, having been first developed to briquette low-grade coal, but interest waned in the 60s. It has only been revived in the 80s on any significant scale in most developing countries (Anonymous, 2006).

Briquetting is one of the several densification techniques by which wood residues and other forestry products and agricultural residues are agglomerated to become denser to enable their expanded use in energy production (Sambo, 1996). Briquetting the wastes improve their burning characteristics and also produce fuel pieces that is similar in size and weight. At the same time, problems of dust are reduced during handling, transportation and combustion and handling and storage problems are alleviated. Briquette making exemplifies the potential of appropriate technology. It saves trees and prevents problems like soil erosion and desertification by providing an alternative to burning wood for heating and cooking. It substitutes agricultural waste like hulls, husks, corn stocks, grass, leaves, food and animal garbage for a valuable resource. It improves health by providing a cleaner burning fuel. The briquettes are also designed for holding, growing, and protecting seedlings. It tackles the problem on both ends by giving a better alternative to firewood (40% more efficient, longer burning, and hotter) as well as helping with reforestation. Briquette production is well known in many manufacturing nations of the world.

As of April 1969, there were 638 plants in Japan engaged in the manufacture of sawdust briquettes Known as 'Ogalite', amounting to a production of 0.81megaton per year (MTY) (Sadakichi, 1969). Aside from sawdust itself, other wood wastes as briquetting materials include bark dust, planer waste, sander dust, and chip dust, all of which are accumulated and available in powder form.

Nigeria has abundant supplies of agro-forested residues whose potentials are yet to be fully tapped for energy generation (Orunnisola, 2006). Briquettes can be made from bagasse (sugar cane waste). Surplus bagasse presents a disposal problem for many sugar factories. Large acreages of land have been cultivated for cane sugar production and excess tonnes of bagasse have been produced from this cane sugar in Nigeria.  This by-product of the sugar industry can be utilize to produce all the energy required for the manufacturing of sugar and other end uses such as lime-burning, brick burning and cement kiln.

Saw dust is a renewable energy source of great potential value in Nigeria. It is waste material from all types of primary and secondary wood processing (Jocob et. al., 2007 ). Between 1983-1987 the average annual output of forest wood processed into log splits and plywood stood at $4.39 \times 10^6 \text{m}^3$/annum

(Ekechukwu, 1999). It is generally estimated that for every 100 metric tones of lumber produced, about 42 tonnes of saw dust are generated. Nigeria is therefore estimated to generate between $1.91 \times 10^6$-$1.25 \times 10^6$ tonnes of saw dust annually. Presently this large quantity of saw dust is grossly underutilized and constitutes a real problem in most wood processing centers.

Apart from the environmental hazard posed by these wastes, investigations show that Millers in one timber in Enugu state Nigeria spent between N16, 000-N24, 000 monthly to cart away the waste products from the location of the mill to designated spot where they are burnt uncontrollably. In Nigeria, the saw dust stove, using saw dust is the last resort during periods of scarcity of domestic fuel such as kerosene and Liquefied Petroleum Gas (LPG).

Rice husk is another renewable source available in large quantity in Nigeria. In 1994, about $3.62 \times 10^6$ tonnes of rice residue were produced in Nigeria (Ekechukwu, 1999). The utilization of rice husks as an energy source in Nigeria is very insignificant. In all the rice producing communities across the nation, mountains of these are seen decorating the sites constituting serious environmental problems. It is a common phenomenon all over the world where often times piles of this waste material is stacked for disposal or some are thrown and burnt on road sides to reduced its volume (Alex, 2005). If this waste can be converted into fuel for domestic cooking, there will be a lot of households that can be benefited, and more money saving for the country can be achieved. Studies on the pyrolysis of rice husks utilization has its greatest potential as a substitute fuel in rice milling operating and in a domestic energy use. Pyrolysis of rice husks yields combustible char, oil and gas products. The char can be briquetted and utilized as both domestic and industrial solid fuel with a heating value of 3,930kcal/kg on a dry basis. As a smokeless fuel which is easy to transport, rice husks char can serve as replacement for fire wood. It has also been noted that with some modification of the furnace, it can replaced the fuel oil used in cement kilns. From an environmental point of view, rice husks char has very low sulphur content therefore, causing no sulphur dioxide pollution.

## MATERIALS AND METHODS

**Materials**. Sawdust was collected from saw mill industry; groundnut shell was collected from a nearby Agricultural Institution to Abubakar Tafawa Balewa University (ATBU) Bauchi, sugar cane wastes (bagasse) was collected from sugar cane processing spot in Bauchi metropolis, rice husk was collected from the rice millers at Yelwa Tudu in Bauchi town, and cassava starch was purchased from local market. A cubic steel mould was fabricated at Center for Industrial Studies (CIS) of (ATBU) Bauchi. Also with the mould was a cubic wooden block carved to fit into the mould for compression. Ele-Budenberg compressing machine of Model El: 31-347010 was used to compact the materials.

**Methods.** Materials for the briquettes making were sorted to remove impurities or foreign bodies and reduced to smaller sizes through hammer milling. The materials were then sieved to obtained overall uniform particle size of 2000µm (2mm mesh). These materials were mixed with starch as a binder in the ratio 5:1 and compressed in a cubic mould to a pressure of $40kN/m^2$ to form the briquettes with the aid of a compressing machine. The cubic-shaped briquettes obtained were sun-dried for one week before the commencement of the Water Boiling Test (WTB).

**Water boiling tests.** What is interesting concerning the energy content of a briquette is how much of the energy in the briquette that can actually be used. The useful energy is the energy transferred into the pot that is used while cooking. This test is performed on each briquette and on fire wood for good comparison. The Water Boiling Test was used for comparing:
- The briquettes with each other
- The briquettes with fire wood

**Apparatus for water boiling test.**

- A standard pot with a lid
- A pyrometer for measuring flame temperature
- A digital balance for measuring the weight of briquette, water and pot
- A stop watch to take the time from the start to the boiling point of water
- A Thermometer for measuring the ambient and boiling water temperature.

**Procedure.** 1.5kg of each sample of the produced briquettes was weighed and equivalent weight of firewood was also weighed for each weighed briquettes. The apparatus for the test which are stopwatch, pot and water, a balance and thermometer were assembled and prepared. Empty pot was weighed and filled with 3liters of water. The pot and water was weighed and the initial temperature of the water was estimated. The briquettes were placed inside the stove and small amount of kerosene was poured on top of the briquettes. The pot was mounted on the stove and was covered with its lid that had a hole for insertion of thermometer. The briquettes were ignited on top with a single match and the water was brought to boiling while temperatures reading were taken at 5minutes interval

## RESULTS AND DISCUSSION

The produced briquettes were strong after drying except for the minor cracks on the surface of most of the briquettes. These cracks could be as a result of the applied force up and below the mould without a corresponding application at the sides during densification.

**Table 1:** Proximate Analysis of the Briquette fuels.

| Sample | Rice Husk Briquettes (RHB) | Groundnut Shell Briquettes (GSB) | Bagasse Briquettes (BB) | Sawdust Briquettes (SDB) |
|---|---|---|---|---|
| % Moisture Content | 7.71 | 8.59 | 4.14 | 4.89 |
| % Volatile Matter | 67.92 | 63.33 | 65.66 | 75.23 |
| % Ash | 20.04 | 17.45 | 16.82 | 5.51 |
| % Fixed Carbon | 4.33 | 10.63 | 13.38 | 14.37 |
| Calorific Value (cal/g) | 3406.3 | 3882.6 | 3612.8 | 4070.4 |

**TABLE2:** Time and Temperature of Boiling of Briquettes and Firewood

| Time (minutes) | SDB (°C) | GSB (°C) | BB (°C) | RHB (°C) | FW (°C) |
|---|---|---|---|---|---|
| 0 | 27 | 28 | 28 | 28 | 27 |
| 5 | 44 | 32 | 32 | 36 | 40 |
| 10 | 85 | 43 | 38 | 55 | 90 |
| 15 | 98 | 57 | 55 | 71 | 98 |
| 20 | (12) | 68 | 78 | 82 | (15) |
| 25 | | 77 | 93 | 94 | |
| 30 | | 83 | 98 | 98 | |
| 35 | | 98 | (26) | (28) | |
| 40 | | (32) | | | |

The Water Boiling Tests revealed that while the sawdust briquettes burnt slightly ahead of the fire wood, other briquettes boiled water slightly below firewood. Groundnut shell had the longest time to boiled water. The flame given out by groundnut shell briquettes slowed down until a steady state was attained due to poor feedback. This could be due to the difference in densities of the biomass fuels as well as the chemical composition of the fuels since rate of combustion depends on it.

It was also observed that fire wood burnt with more smoke than the briquettes from all the Agro-waste materials and their flames were luminous for fire wood and less luminous with intense glow for briquettes.

Briquettes were also observed to maintain their shapes as they burnt compared to fire wood.
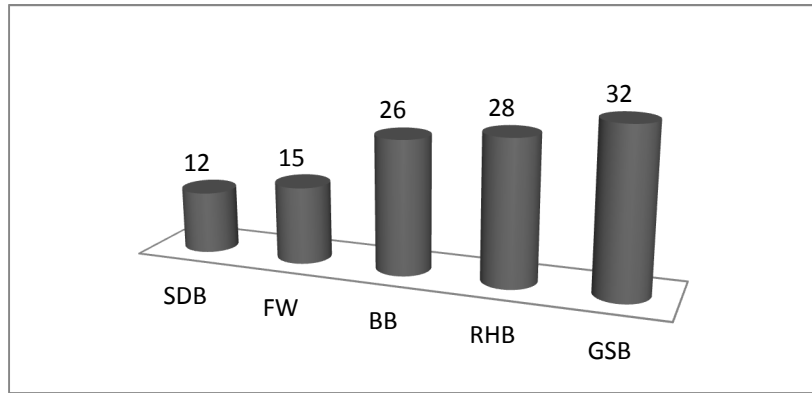


**Figure1: Plot of Time until Boiling using Briquettes and Firewood**

**CONCLUSION**

Agro- wastes or residues can be converted to briquettes to provide process heat for a variety of end use. Briquetting of Agro-wastes makes them cleaner and easier to transport. Conversion of wastes to briquettes is one promising strategy to curtail the dumping of agricultural wastes in many cities and rural areas, to improve energy efficiency, reduce pollution and desertification. Utilization of Agro-wastes as fuel entails replacement of firewood and hence improves the living condition of the rural women and children, who spend most of their time collecting fuel wood instead of engaging in other income generating activities or attending school. Briquettes represent an alternative source of cooking energy and viable opportunities for income generation while at the same time contribute to environmental preservation.

**REFERENCES**

**Akpabio, I.O. and Illalu, A.** (1997) The Conversion of Sugar cane Waste into Solid Fuel. Nigeria Journal of Renewable Energy. **5:**83-87.

**Alex, T. B**. (2005). Rice Husk Gas Stove Handbook, Appropriate Technology Centre, Department of Agricultural Engineering and Environmental Management, College of Agriculture Central Philippine University Iloilo City, Philippines. Retrieved December 6, 2007 from http:www.crest.org /discussion/group /resources/stoves /belnio/belniogasifier.pdf.

**Ekechukwu, O.V.** (1999). Promotion of Renewable Energy Supply in Nigeria. A paper presented at the National Seminar on Sustainable Energy Development and the Nigerian Environment: Challenges of the New Millennium, 3 August, Abuja, Nigeria.

**Eriksson, S. and Prior. M.** Briquetting Technology, an Overview of the Densification Process, chapter 6. Retrieved July 10, 2007 from http://www.fao.org/gocrep/T0275E/T0275E04.htm.

**Jacob, K. K., Simon, N.M., Jonothan, M., Canon, N. S. and Wanyonyi E.** Recycling Waste into Fuel Briquette. Organic Resource Management in Kenya (Perspectives and Guidelines) Chapter 15. Retrieved October 26, 2007 from http://www.formatkenya.org/ormbook/chapters /chapter15.htm.

**Olorunnisola, A.** Production of Fuel Briquettes from Waste Paper and Coconut Husk Admixtures. Retrieved September 20, 2007.

**Sadakichi, K.** (1996). The Sawdust Briquetting and Agglomerating Industry in Japan. Proceeding of the 11th Briquetting Conference. Sun Valley, Idaho, pp. 43-49.

**Saglam, M., Yulsel, M., Yanik, J., Tutas, M., Karadun, M. and Ustun, G.** (1990)**.** Production of Water-resistant Briquettes from Turkish Lignites using Sulphite Liquor Binders. Department of Chemical Engineering, Ege University, Bornova-Izmin, Turkey. **69:** 60-63.

**Sambo, A.S.** (1996). Energy Option for National Development. Resources, issues and Position of Renewable Energy Technology. An Inaugural Lecture held at Abubakar Tafawa Balewa University, Bauchi.

**Sanu, K. S.** Fuel Briquettes from Wastes. Foundation for Sustainable Technologies (FOST). Galkopakha, Thamel,Kathmandu, Nepal. Retrieved September 20, 2007 from http://www.hedon.info/goto.php/FuelBriquettesfromwastes**.**

**UNIDO-RMRDC Forum Nigeria.** (2003). Agro-waste Briquettes making Machines for Rural Energy and Pollution Reduction in Nigeria. Abuja, Nigeria. Retrieved March 21, 2007 from (http://www.unido.org/doc/12469).

# UTILIZATION METHOD OF MANURE AND SLAUGHTERING WASTES IN REARING OF GEESE ON THE MINERAL-ORGANIC FERTILIZERS – PILOT PLANT INVESTIGATION

*Radosław Wilk*, Helena Górecka, Henryk Górecki and Katarzyna Chojnacka
(Wrocław University of Technology. Wrocław. Poland)

**ABSTRACT:** The method of mineral-organic fertilizer production from geese slaughterhouse wastes and topsoil, from rearing geese is presented. This method was tested in pilot plant scale in big geese slaughterhouse. In order to reduce ammonia losses from manure, the top-soil for rearing geese was formed from brown coal and mixtures with magnesite. Saturated subsoil is then sanitized by the addition of acidic mineralizate, which is the result of disposal of slaughterhouse waste of geese with concentrated sulfuric acid with micronutrient salts. The composition of the fertilizer was corrected by the addition of ammonia and granulated with ash from the combustion of biomass containing more than 6% $K_2O$. In pilot plant investigation, the next form of fertilizer was obtained: mineral- organic fertilizer on the base of manure sorbent topsoil and suspension obtained from mineralization of slaughtering waste and biomass ash, suspension NP fertilizer with micronutrients, and granulated mineral-organic fertilizer obtained only from slaughterhouse wastes, biomass ash and magnesite. Fertilizers produced in pilot plant from slaughterhouse wastes were tested in agricultural investigations.

## INTRODUCTION

The production of poultry meat last year accounted for about 33.4 % of the world meat production, an increase by over 12% compared to 1990 and 3.8% to 2000. The European Union annual production of poultry meat is approximately 12 million tons and the average consumption amounts to about 23 kilos per capita per year [1].

**Table 1. Global picture of the poultry sector. Revised from [1].**

|  | EU-27 | USA | BRAZIL | CHINA | RUSSIAN FEDER. | UKRAINE | POLAND | WORLD |
|---|---|---|---|---|---|---|---|---|
| Production (μ 2009-'10) kton | 11.677 | 19.174 | 11.903 | 15.751 | 2.541 | 742 | 1.250 | 95.019 |
| % prod. Growth 2001-2010 | 0.68 | 1.53 | 6.53 | 2.34 | 13.79 | 14.11 | 23.8 | 3.30 |
| Consumption (μ 2008-'10) kton | 11.570 | 15.885 | 8.357 | 16.057 | 3.435 | 1.056 | - | 95.156 |
| Consumption per head kg | 20.5 | 44.4 | 38.0 | 10.5 | 21.5 | 20.3 | 23.5 | 12.3 |
| % growth per head 2001-2010 | 0.65 | 0.26 | 3.98 | 1.96 | 6.45 | 15.22 | 2.53 | 2.12 |

The daily slaughter of poultry in a medium-sized slaughterhouse is shown in Table 2.

Expensive and limited by restrictive environmental regulations justifies the implementation of the complex utilization slaughterhouse waste to fertilizer product/ costs of waste disposal for such companies is accounted for about $1 million per year/. Another troublesome problem to be dealt with is the

utilization of manure from big farms in local agriculture company. The poultry branch needs solution to reduce emissions of nitrogen from geese manure and migration of these compounds into groundwater. The presented method of mineral-organic fertilizer production from geese slaughterhouse waste and topsoil from geese rearing. can be a solution to poultry waste management.

**Table. 2 Daily slaughter of poultry in a medium-sized slaughterhouses.**

| Type of poultry | Daily slaughter | Waste generated (Mg) | | |
| --- | --- | --- | --- | --- |
| | | Blood | Mixture of slaughter wastes | Feathers |
| Geese | 35 000 | 6 | 15 | 4 |
| Ducks | 35 000 | 6 | 15 | 4 |
| Chickens | 50 000 | 6-7 | 15 | 13-15 |

## TECHNOLOGICAL AND ENVIRONMENTAL GOALS AND OBJECTIVES [2.3.4]

-Method ensuring complete utilization of slaughterhouse wastes from poultry industry. in particular geese slaughter wastes by decomposition them with concentrated sulfuric acid. Proposed technology is prepared to implement in plant scale of capacity of slaughterhouse up to 40 thousands geese/ day allowing to utilize 20-30 Mg organic solid wastes (raw feather, bones, skin, intestines, adipose and muscle tissue) and 6-7 Mg blood.

-Presented technology allows to recover fertilizer components contained in wastes in the form suspension fertilizer for fertilization in spring and winter season and in solid form produced and stored in summer and winter.

-Total concentration of fertilizer nutrients /NPK/ of the obtained products is 2-4 times less than in commercial fertilizers produced in industrial plants using expensive raw materials.

The fundamentals of the project include using wastes from different industrial branches: cheap waste sulfuric acid without heavy metals from cooper industry**,** ash from the combustion of biomass containing high concentration of potassium and magnesium, phosphate sludge from purification of wet process phosphoric acid, additionally increasing an economy impact.

**-**The experience and knowledge from the pilot plant investigation allows to design and optimize industrial installations for utilization wastes from poultry industry, so that they can be applied at lowest costs and the highest efficiency of the process. It also fulfill the conditions assessed by the Directive of European Commission WE 1774/2002. stating the sanitary rules concerning by-products of animal origin not devoted for consumption by human.

-The method should further decrease negative environmental impact of process of breeding geese by reducing ammonia emission from their manure by using a top-soil formed from brown carbon and mixtures with magnesite for rearing and using it after saturation for mineral fertilizers production.

## TECHNOLOGICAL FUNDAMENTALS OF THE PROCESS

The technological concept of the method is based on decomposition all slaughtering wastes obtained in big geese slaughterhouse by concentrated sulfuric acid />90%/ [ 3.4.5.6.7 ]. In this process natural substances are decomposed to the simple compounds e.g., keratine to ammonia ion and mixtures amino acids. The heat of dilution concentrated sulfuric acid is sufficient to ensure the reaction temperature 80-90 $^0$C.To obtain the desired fertilizer formula /N-P-K/ tailored to the needs of particular species of plans composition of the mineralizate is modified by addition wet process phosphoric acid/ or sludge from purification wet process phosphoric acid/, aqueous ammonia. potassium hydroxide and micronutrients /B.Fe.Mn.Zn.Co.Mo/.This process occurs in periodic system with retention time 2-4 hours, depending on composition of slaughtering waste.

Obtained acidic suspension may be processed to several fertilizers products:

**Fert.1**. Stabilizing agent for manure storage, decreasing emission of nitrogen / crude mineralizate without additives/

**Fert.2**. Suspension NPS fertilizer with micronutrients / mineraliazate modified by addition wet process phosphoric acid, aqueous ammonia, potassium hydroxide, micronutrients salts/

**Fert.3**. Granulated mineral-organic fertilizer obtained from mineralizate of slaughterhouse wastes neutralized and granulated with biomass ash and magnesite

**Fert.4**.Liquid NPS fertilizer on the base of fresh blood from slaughterhouse produced from mineralizate neutralized by ammonia with addition of micronutient salts

**Fert.5**.Mineral-organic fertilizer on the base of manure absorbent topsoil and suspension obtained from mineralization of slaughtering waste and ash.

## PILOT PLANT INVESTIGATION OF FERTILIZER PRODUCTION FROM SLAUGHTERHOUSE WASTE

**Semi-technical plant.** The aim of semi-technical tests was verification of technological concept, identification of technical problems in production scale and obtaining fertilizer products for agricultural research in big scale. Semi technical pilot plant was built in slaughter geese AMI Co Mikstat, the largest Polish exporter geese. The plant consist of :

- digestion reactor / $V=2.6$ m$^3$/ with enamel interior equipped with slow speed stirrer /N=4kW/ and water jacket produced by Fagaras Co.
- drum mixer granulator /V=5m$^3$/
- twin-shaft mixer
- feather chopper and auger
- centrifugal pumps, feed conveyors, liquid raw material tanks

In the Fig. 1 technological scheme of pilot plant, used to fertilizers (1-5) production and in the fig 2 the photos of pilot plant are presented.
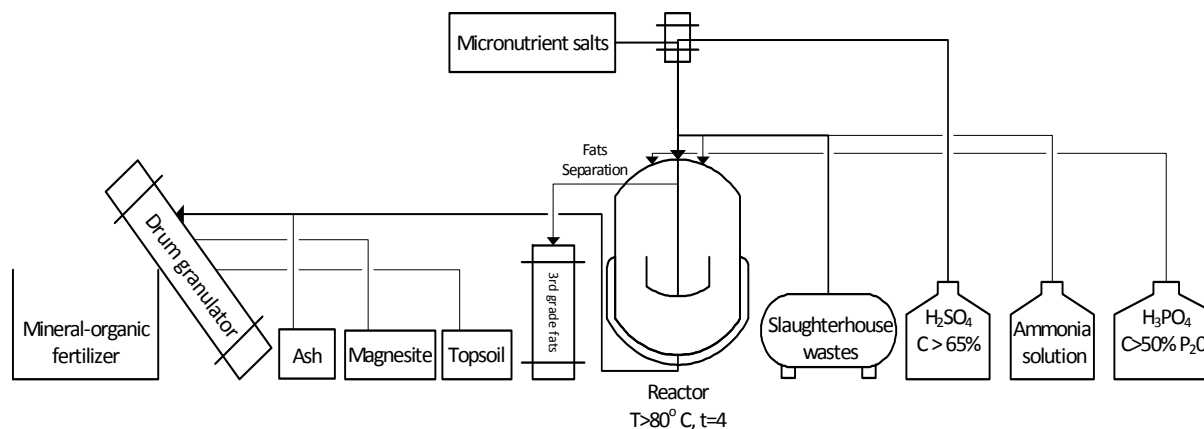


**Figure. 1 Scheme of the production of mineral-organic fertilizers.**

**Semi-technical fertilizers production.** The above mentioned fertilizer products were are presented in Table.3

Raw geese feathers were used to production fertilizer products Fert. 1.2.3 and 5. and geese raw blood for production Fer.4 .These wastes were delivered to plant directly from slaughterhouse. Aqueous ammonia/20%N/potassium hydroxide and micronutrient salts such as: $ZnSO_4.H_2O$, $CuSO_4.5H_2O$, $MnSO_4.H_2O$, $CoSO_4.7H_2O$, $FeSO_4.7H_2O$, $(NH_4)_6Mo_7O_{24.}4H_2O$, $Na_2B_4O_7.10H_2O$ were used to complete

fertilizer composition according agricultural suggestions. The special raw material for production Fert.5 was topsoil consisted of brown coal with geese manure deposited during outdoor free-range geese breeding in large livestock units. For decreasing about 50% of ammonia emission and collection manure 10 cm layer of mixture brown coal and magnesite in proportion 100/1 was formed. After 3 weeks this synthetic topsoil was removing and next mixed with ash containing potassium salts and mineralizate obtained in the process decomposition of feather wastes by sulfuric acid /Fert.1/[4.8]



**Figure. 2 The pilot plant for the production suspension and solid of mineral-organic fertilizers based on waste from poultry industry.**

**Table 3. Raw materials used for fertilizer production.**

| Waste material | Poultry feather / dry mass/ | Biomass ash | Magnesite | Blood | Wet process phosphoric acid | Sulfuric acid |
|---|---|---|---|---|---|---|
| Macronutrients. % | | | | | | |
| N | 10-15 | 0.21 | <0.001 | 1.5-2.6 | | |
| $P_2O_5$ | 0.457 | 2.56 | 0.0069 | 2.56 | 51.7 | 0.0006 |
| $K_2O$ | 0.331 | 7.18 | 0.0036 | 0.14 | 0.038 | <0.0001 |
| S | 2.60 | 1.62 | 0.014 | 0.145 | 0.47 | |
| Mg | 0.018 | 1.32 | 16.2 | 0.067 | 0.46 | <0.0001 |
| Ca | 0.12 | 4.89 | 0.57 | 0.0613 | 0.14 | 0.0005 |
| Na | 0.15 | 1.06 | 126 | 0 | 0.12 | 0.0011 |
| Micronutrients, mg/kg | | | | | | |
| B | 6.61 | 9.21 | <5.0 | | 42.4 | 2.06 |
| Co | 0.647 | 24.7 | 44.5 | 1.55 | 10.24 | 0.137 |
| Cu | 10.097 | 10.6 | 2.78 | 2.71 | 13.33 | 0.169 |
| Fe | 167 | 1940 | 14304 | 585.2 | 6371 | 11.59 |
| Mn | 16.34 | 998 | 518 | 15.3 | 178 | 0.077 |
| Mo | 0.757 | 11.2 | <0.1 | 0.14 | 5.23 | 0.047 |
| Zn | 84.07 | 350 | 15.1 | 27.3 | 251.2 | 0.287 |
| Toxic components, mg/kg | | | | | | |
| As | 0.12 | <1.0 | 4.82 | 0.02 | 9.61 | 1.43 |
| Cd | 0.29 | 3.63 | 0.24 | 0.75 | 17.73 | 0.025 |
| Pb | 8.30 | 132 | 5.28 | 2.97 | 8.44 | 2.12 |
| Hg | 0.32 | 0.006 | 0.014 | 0.012 | 0.12 | 2.90 |

Raw material feedstock for production fertilizer covered for one charge:

- Fert.1 / mineralizate 1500 kg/- feathers -1000kg. sulfuric acid -500 kg

-Fert.2 /suspension NPKS 2000 kg/-feathers-900kg.sulfuric acid- 660kg, wet process phosphoric acid-300kg, aqueous ammonia 40 kg, potassium hydroxide 100kg

-Fert.3 /granular fertilizer NPKS 2240kg/-feathers-1000kg, sulfuric acid- 380 kg, wet process phosphoric acid-180 kg, aqueous ammonia -80 kg, biomass ash-1000kg, magnesite-100 kg

-Fert.4 /suspension NPS 1380 kg/-geese blood-1000kg, sulfuric acid-190 kg, wet process phosphoric acid-150 kg, aqueous ammonia 40 kg.

-Fert.5 /solid NPKSMg fertilizer -1350 kg / brown coal topsoil manure-1000kg. coal ash-300 kg. magnesite-50 kg, mineralizate /Fert.1/-100 kg

## RESULTS AND DISCUSSION

The raw materials and obtained fertilizer product were analyzed by chemical. biological and agricultural methods. The fertilizer products presented in table 4 were determined by Chemical Laboratory of Multielemental Analysis – Wrocław. Poland. accredited by Polish Centre for Accreditation (number of accreditation: AB696 according ISO 17025). using the methods: macronutrients – inductively coupled plasma optical emission spectrometry (Spectrometer ICP-OES VISTA MPX. VARIAN. Australia); micronutrients and trace metals (except for Hg) - inductively coupled plasma optical emission spectrometry (Spectrometer ICP-MS ThermoScientific X series) ; total nitrogen and carbon - elemental analysis method (Elemental Analyzer CN Vario MACRO Cube. ELEMENTAR Analysensysteme, Germany); Hg - atomic absorption spectrometry (Mercury Analyzer AMA-254. Altec Ltd.. Czech Republic).

The main intermediate in production presented fertilizers was acidic mineralizate /Fert.1/ obtained in the process of decomposition organic substance by concentrated sulfuric acid causing decomposition of keratinous materials to amino acid. In the mixture amino acids we determined 18, such as: cysteine, methionine, serine, proline, glicyne, valine, leucine, methionine, serine, aspartic acid, arginine, glutamic acid phenyloamine. The contents these amino acids in mineralizate was higher then 1%[8]. Hydrolized keratinous materials is the source of bioavailable nutrients in cultivating plants as source of nitrogen and as chelating agent of micronutrients. According to analysis of nitrogen form in obtained mineralizates:

$$N_{total}- 2.5-5.0\ \%.N-NH_4 - 0.8-1.8\ \%.\ N-NO_3 -0.2-0.4\%.N-organic -1.8-2.4\%.$$

All produced fertilizers manufactured in pilot plant in spring 2012 now are tested and were used in standard agricultural investigations on big area. We are expecting the results of this cultivation research in September, but already we have at the moment results biological and agricultural tests of fertilization effect the similar fertilizers obtained in large laboratory scale using the same raw materials and similar technological parameters.

The germination tests carried out on seeds of chess and radish fertilized with fertilizers produced indicated that these products showed no biological toxicity. In these tests carried out according international standards germination efficiency was in the range 80-92 /amount od germinated plant from 100 seeds [9]. Microbiological tests indicate that produced fertilizers on the base of topsoil sanitized by addition acidic mineralizate / Fert.5/ fertilizer not included bacteria *Salmonella eggs Ascarsis* sp*., Trichuris* sp*., Toxacara* sp. Results of these research were negative for bacterial and fungal pathogen presence limited by EU sanitary directive [10].

All produced fertilizers were also tested in field experiments by Institute of Soil Science and Plant Cultivation State Research Institute (IUNG-PIB). Poland [11] in order to validate their fertilizer properties and efficiency. The examination of fertilizers included yield and quality of experimental crop and nutrients uptake in comparison to commercially available fertilizer products. The following experiments were carried out: - field with white mustard and corn for seed, micro - field with vegetables: cucumber, beetroot and radish, productive with corn for seed. Experiments at different levels, micro-scale ($3m^2$) and field-scale ($15m^2$), were carried out in four repeated randomized trials. Field experiments with White Corn were conducted at area of 1ha. Produced fertilizers showed increase in crop yield and enhancement of N, P, K, Mg and S uptake.

Table 4. Chemical composition of manufactured fertilizers in pilot plant

| Komponent | Feather mineralizate /manure stabilizing agent/ Fert.1 | NPS-suspension fertilizer with micronutrients Fert.2 | Granulated fertilizer slaughterhouse mineralizate . biomass ash and magnesite Fert.3 | NPS-suspension fertilizer from fresh blood from slaughterhouse Fert.4 | Granulated topsoil with manure with ash. and slaughterhouse mineralizate Fert.5 |
|---|---|---|---|---|---|
| Macronutrients. % | | | | | |
| $N_{total}$ | 3.12 | 2.55 | 2.0 | 2.95 | 0.95-1.84 |
| $P_2O_5$ | 0.39 | 7.20 | 3.32 | 5.42 | 0.49-1.1 |
| $K_2O$ | 0.16 | 4.54 | 3.42 | 0.20 | 1.2-1.28 |
| S | 6.42 | 8.86 | 4.86 | 4.68 | 2.19-3.28 |
| Mg | 0.03 | 0.14 | 0.52 | 0.032 | 0.51-0.97 |
| Ca | 0.13 | 0.13 | 5.33 | 0.12 | 1.54-1.55 |
| Na | 0.15 | | 0.12 | 0.48 | 1.02-1.26 |
| Micronutrients. mg/kg | | | | | |
| B | 6.23 | 620 | 65.7 | 8.12 | 44-646 |
| Co | 7.34 | 0.92 | 3.42 | 3.12 | 3.54-31.4 |
| Cu | 3.62 | 5.0 | 374 | 170 | 27.5-55.4 |
| Fe | 27.6 | 1200 | 3760 | 478 | 5935-9575 |
| Mn | 6.64 | 43 | 358 | 11 | 386-689 |
| Mo | 0.14 | 44 | 75-85 | 28 | 3.08-81 |
| Zn | 22.3 | 71 | 275-346 | 127 | 325-628 |
| Toxic components. mg/kg | | | | | |
| | | | | | |
| As | 6.4 | 9.35 | 4.6-8.5 | 8.9-22 | <1.0 |
| Cd | 0.1 | 0.29 | 0.53-1.6 | 0.73-0.98 | 1.18-2.11 |
| Pb | 8.3 | 3.6 | 9.7-16 | 1.5 | 29.2-31.9 |
| Hg | 0.01 | 0.02 | 0.67 | 0.07 | 0.0381-0.141 |

**SUMMARY**

The presented method guarantees complete utilization of slaughterhouse wastes and geese manure, on variant products / suspension, solid fertilizer, agent for stabilizing liquid manure storage/. Financial profits including savings on expensive biological wastes disposal and environmental impact we estimate for about 1 mln Euro and for recovery about 400 t fertilizer nutrients about 0.2 mln Euro in the slaughterhouse of capacity 40 th geese/day. The method was developed in full R&D cycle including agricultural tests.

**ACKNOWLEDGMENTS**

**REFERENCES**

[1] A.V.E.C Annual Report 2011. Association of Poultry Processors and Poultry Trade in the EU Countries. available at: http://www.avec-pultry.eu

[2] Polish Patent No. 205666 (2010)

[3] Polish Patent No. 197609 (2010)

[4]Polish Patent Application NoP-393 752 (2011)

[5]Górecki H..Górecka H..Chojnacka K..Dobrzański Z.. Artmańska M. Barańska M.. Przem.Chem.89/4.360-365(2011)

[6] Górecki H.. Artmańska M.. Górecka H.. Dobrzański Z.. Chojnacka K.. Barańska M.. Baśladyńska S.. Przem. Chem. 90/5. 769-773 (2011) (In Polish)

[7] Mironiuk M.. Górecki H.. Górecka H.. Dobrzański Z.. Chojnacka K.. Wilk R.. Rusek P.. Sienkiewicz-Cholewa U. Przem. Chem. 91/5.900-905. (2012) (in Polish)

[8]International Rules of Seed Testing ed.IRST 2011

[9]Regulation EU (WE) No1774/2002

[10] Górecka H.. Sztuder H.. Sienkiewicz-Cholewa U.. Zeszyty problemowe postępów nauk rolniczych. 2009 z. 537: 125-133

# DEVELOPMENT AND IMPLEMENTATION OF A RECYCLING PROGRAM IN AN ELEMENTARY SCHOOL

*Vasil Diyamandoglu* Miriam N. Ward**,** and Blake Wells
(City College of the City University of New York, NY, USA)

New York City provides many of the educational tools to integrate responsible waste management into elementary school operations, yet implementation has fallen short. To address this endemic shortcoming, this project assisted in the development and implementation of a recycling program in a local school. After identifying an elementary school looking to build a recycling program, extensive effort was put into developing a relationship with personnel and building the internal support required to change habits. To assess existing habits, a waste audit was conducted, material flows were calculated, and the habits of the custodial staff, faculty and students were documented. The existing diversion rate was found to be significantly below municipal mandates. From this analysis, a recycling plan was developed which takes into consideration major waste flows and social barriers. In addition to a purchasing and deployment plan, maps and flow diagrams were developed and used to communicate the necessary changes in behavior to initiate implementation. A waste audit was conducted two months after commencement of program implementation to gauge the success of the recycling plan. From the lessons learned, potentially successful waste handling approaches and recommendations for NYC school waste management were proposed.

# FACTORS AFFECTING THE SELECTION BETWEEN DEMOLITIONS VERSUS DECONSTRUCTION IN BUILDING REMOVAL

*Vasil Diyamandoglu* Bishoy Takla and Wojciech Bzdyra
(City College of the City University of New York, NY, USA)

The demolition process removes a building by completely destroying it using heavy machinery and equipment in time and cost efficient manner. The demolition debris are scooped out and hauled to C&D recycling facilities or a landfill. Deconstruction focuses on the salvage of reusable building materials from building removal or remodeling and can involve selective salvage of materials or whole structure removal. Deconstruction can replace demolition, but can also be part of a building removal process, which includes partial demolition following early deconstruction. The present study examined the structural and non-structural deconstruction processes and the materials typically recovered in such processes. Materials obtained from structural deconstruction are bricks, wood products, steel and architectural components. Non-structural deconstruction refers to the stripping down of buildings and usually is followed by some level of demolition. Limitations of the applicability of deconstruction include project time constraints, housing preservation policies, material contamination, salvaged materials perception, and requirements of building codes. The study compares the two alternatives using examples from different States in the United States. The results showed mixed results, with deconstruction being competitive in wood structures, but not as much when the main construction material are brick and/or concrete.

# EFFECTIVENESS OF MATERIAL RECOVERY DURING COMPLETE DECONSTRUCTION OF WOOD FRAMED HOUSES - A CASE STUDY

*Vasil Diyamandoglu* Bishoy Takla and Wojciech Bzdyra
(City College of the City University of New York, NY, USA)

The group participated in the actual deconstruction of the building shown and described below. The deconstruction site was in the State of Vermont. The pre- and post-deconstruction work was carried out in New York, in close collaboration with the staff of the contractor undertaking the deconstruction project. The objectives of this study were to (a) layout process sequence, tools and labor requirements for specific deconstruction activities, (b) identify major problems in deconstruction as an alternative to demolition, (c) determine reclaimed materials value, (d) investigate the marketability of reclaimed materials. The study revealed that in complete deconstruction of wood framed buildings the process can be broken down to the following distint parts: (1) Preparing the site, (2) Soft-stripping, (3) Removing interior wall finishes, (4) Removing the roof, (5) Removing exterior doors and windows, (6) Removing the interior walls, (7) Removing the exterior walls, and (8) Processing the materials. The process steps will be described in detail and supported with photographic documentation, while the results of the study objectives will be presented in detail. The broad conclusions of this study in terms of factors of sustainability are: **Social Benefits:** The project created 532 person hours of work during 4 weeks in comparison to demolition which could be done in a day or two, **Environmental Benefits:** Material inventory revealed recovery in excess of 80 percent of construction materials, and **Economic Benefits:** Deconstruction saved $3929.59 in addition to the value of the reclaimed materials.

# DEGRADATION OF LIGNOSULFONATE BY A *SPHINGOBACTERIUM SP.* STRAIN HY-H

Dongqi Wang, *Yanling He*, Jidong Liang, Wenjing Du and Guanfei Huang
(Xi'an Jiaotong University, Xi'an, Shaanxi, China)

Six aerobic bacterial species, originating from activated sludge in a wastewater treatment system of a pulp and paper mill, were isolated on a mineral salt medium utilizing lignosulfonate (LS) as the sole carbon and energy source. By comparing the results of the biodegradability tests, strain HY-H, identified as *Sphingobacterium sp.*, was selected for subsequent tests on the optimization and mechanism of LS degradation. The optimum growth conditions for the strain HY-H were determined by orthogonal layout method to be pH 7.0, temperature 30°C, and LS/ammonium chloride ratio of 5. Under the optimum conditions, the maximum degradation capacity of the strain HY-H reached to 30%. Through spectroscopic, elemental and functional groups analysis, it was speculated that the strain HY-H partially oxidized the side chain, cleaved the aromatic ring and further transformed LS to carbon dioxide. Results of this study showed that, if properly optimized and controlled, *Sphingobacterium sp.* strain HY-H may play a role in the treatment of pulp and paper wastewater containing a high concentration of LS.

# ASSESSMENT OF RURAL ALASKAN SOLID WASTE LEACHATE

*Edda Mutter*

(University of Alaska Fairbanks, Fairbanks, Alaska, USA)

In Alaska, rural communities are highly sensitive to changes in the surrounding ecosystem and its effects upon subsistence activities. In turn, ecosystems themselves are highly sensitive to perturbations brought about by ineffective solid waste management practices. In the state of Alaska, most rural communities have insufficient waste disposal practices to guarantee human and ecosystem health. In instances, untreated waste material, including household waste, chemical compounds, such as pharmaceutical, personal hygiene products, potential hazardous material (i.e. lead batteries, electrical waste, etc.), and frequently human waste is disposed in unpermitted landfills, underlying permafrost or on the wet ground surface. A two-year study was performed to evaluate the prevalence and diversity of landfill leachate pollutants, and their potential impacts on drinking water resources. Shallow ground and surface waters were tested in and around five rural Alaskan solid waste sites for the presence of inorganics, waste-derived organic chemicals, and pathogenic indicator organisms. Microbial indicator analysis was performed using most probable number methods (i.e., Colilert® for E.coli, and Enterolert® for ENT; ICP-MS instrumentation for metal analysis; and extraction methods were developed for HPLC-MSMS analysis to detect low-level concentrations of phthalates, alkyl phenols, and pharmaceuticals. The obtained biophysical and chemical results demonstrate the need of state regulation to diverge potential disposal and toxic components from the waste stream, as well as monitor and assess present and closed landfills.

# IMPLEMENTATION OF GLOBAL PRODUCT CLASSIFICATION BY THE REUSE SECTOR IN NEW YORK CITY

**Lorena Fortuna\*, David Hirschler\*\*, *Vasil Diyamandoglu\****
*\*Doctoral Student* and Assistant Professor Department of Civil Engineering, The Grove School of Engineering, City College of New York, New York, NY 10031, USA
\*\*Deputy Director, Waste Prevention Unit, New York City Department of Sanitation, Bureau of Waste Prevention Reuse and Recycling*, 44 Beaver Street, 5th Floor, New York, NY 10031, USA

Product classification systems are tools created to organize information in classes according to common properties relations or affinities. The objective of this study was to review common product classification systems, evaluate their applicability in the product reuse sector and select the most suitable PCS for adoption in the analysis of the New York City Reuse Sector.

Product reuse extends the life of unwanted products that would otherwise be discarded in a landfill, following minor refurbishing while holding the original product characteristics. Reused products diverted from the waste stream provide savings in disposal and material costs, and contribute the urban sustainability.

Many organizations that promote reuse locally or worldwide, handle products such as furniture, appliances, textiles, construction and demolition products, books, and a variety of specialized items that suit their mission. Preliminary surveys carried out in New York City by the Materials Exchange Development Program revealed that record keeping and product classification/ categorization is as varied as the number of organizations that participated in the surveys. Furthermore, the inventory and operating data tracking systems such organizations use are selected to meet their specific needs or budgetary constraints and range from sophisticated custom designed systems to inexpensive downloadable software or even phone based manual data tracking thus creating widespread incompatibility among the systems.

The Data Management Project initiated by NYCMEDP aimed at exploring the possibility of using an existing and internationally accepted product classification system to unify all product reuse activities in the New York City area, and use the information obtained to describe the products in terms of the materials they consist of. This process would enable one to describe the effectiveness of product reuse efforts in New York City in terms of quantity of "materials" diverted from the waste stream.

Extensive research was carried out to identify and examine the available product classification system. The classification systems included in the evaluation were: (a) Global Product Classification (GPC), (b) Harmonized System (HS), (c) Harmonized Tariff System (HTS), (d) Schedule B, (e) Central Product Classification (CPC), (f) Standard International Trade Classification (SITC), (g) Standard Classification of Transported Goods (SCTG) and (h) the North American Product Classification System (NAPCS). Comparative analysis of the selected classification systems revealed that the Global Product Classification (GPC) is the most appropriate system to the reuse sector. Justification of the final selection and examples of implementation of the characterization methodology will be presented.

# EFFECT OF STRAW RETURN ON DOC AND CADMIUM BEHAVIOR IN POLLUTED SOIL

*Bai Yanchao*, Feng Ke, Shan Yuhua

(College of Environmental Science and Engineering, Yangzhou University, Yangzhou, China)

A pot experiment was carried out to study the effect of straw returning on dissolved organic carbon (DOC) in percolating water and cadimium (Cd) availability in a polluted rice soil. Wheat straw was added to Cd-polluted soil with the rates of 0.1%, 0.2% and 0.4% (on the base of dried soil), respectively, and DOC in percolating water and Cd content in soil and rice plant were measured during the experiment. The results showed that DOC concentration in percolating water in rice soil increased with the increase of the amount of straw returned. After rice harvest, total and available Cd in the soil decreased (or decreased significantly in some treatments) with the amount of straw added to the soil, due to the loss of Cd through percolating water enhanced by addition of wheat straw. Under experimental conditions, Cd uptake by rice plants responded to the rate of straw added. The peak Cd concentration and accumulation in rice plants appeared in the treatment with 0.5% straw returned, with the values of 45.10 mg·kg$^{-1}$ and 1858.1 μg·pot$^{-1}$, respectively. Straw returning elevated DOC concentration in percolating water and the activity of soil Cd in polluted rice field.

# STUDY ON CHARACTERISTIC OF ELECTROLYSIS MANGANESE SLAG

*Changbo ZHOU,* Bing DU and Qianqian PEI

(Chinese Research Academy of Environmental Sciences, Beijing, China)

The electrolysis manganese holds the pivotal status in our country national economy. For many years, the electrolysis manganese industry's fast development has caused and accumulated the massive environment problem, especially the electrolysis manganese slag. In this paper, it focuses on the study of physical and chemical characteristic and leaching characteristic. The electrolysis manganese slag was analyzed by using X-ray fluorescence spectrometry (XRF), X-ray diffraction (XRD), scanning electron microscopy (SEM) and laser particle size analyzer. The chemical components, mineral compositions, mineral morphology, particle size distribution were investigated. And a leaching column model was used to study the leaching process of manganese and ammonium with the simulated acid rain. The results showed that the electrolysis manganese slag was a kind of Calcium-rich slag and the particle size of 83.33% was smaller than 30μm. The main minerals were gypsum (~64%), quartz (~13%), mica (~7%), albite(~4%) and a spot of green mudstone, pyrite. Gypsum is the primary mineral.

After leaching for a certain amount of the rainfall, the accumulated mobility quality of manganese and ammonium increased with the increase of rainfall. For the release process of manganese or ammonium, it can be divided into two stages of fast leaching and slow leaching. The release density of manganese increased along with the increase of acid rain's acidity, while that of ammonium had no obvious relation with acid rain's acidity.

# TECHNOLOGY DEVOID OF HUMAN APROACH BRINGS MISERY FOR MASSES: A CASE STUDY

*Binayak Rath*
(Indian Institute of Technology, Kanpur, India)

The rapid industrilization and its concurrent urbanization in India has not only brought significant rise in urban population, but owing to the new consumerism culture and changing life styles, the waste generations have gone up rapidly in almost all urban conglomerations . The handling of these urban wastes has not only posed a serious threat to physical environment but also for sustenance of man. The pollution loads are also rising steadily and posing many managerial challenges in the urban areas. However, with the advancement of science and technology, the policy makers have always looked forward to some scientific solutions to the urban infrastructure problems. The urban planners and managers have attempted to use of scientific knowledge and technologies to tackle the twin problems of solid and liquid waste handling. Though science and technology responses to these problems have been positive, but these problems and issues are growing day by day due to lack of a human approach in use of new technologies. In order to tackle those problems, different technological and managerial solutions are suggested to the urban planners. Most of these planners being influenced by Western capitalist model of developments have tried to borrow imported ideas and technologies, such as, setting up of Effluent Treatment Plants (ETPs) to handle liquid urban wastes and power generation from solid wastes.  As far as the waste management issues are concerned, one of the oldest Municipal Authorities of India, viz.,  the Kanpur Municipal Corporation, Kanpur,Uttar Pradesh have always attempted to imitate the western practices and one such case is  setting up of a centralised ETP at Jajmau under the Ganga Action Plan that was undertaken in mid 1980 with Dutch collaboration. In this paper, an attempt is made to critically examine the various issues involved in sewage water treatment at Kanpur, its utilization and also to gauge the environmental impacts of the new technology on both the physical and socio-economic environment in the villages which have been using the sewage irrigation water of Kanpur city for more than last 50 years. Our field survey results have proved that the sewage farming practices have undergone significant changes after introduction of the new water treatment practices. It has been established that the new sewage irrigation system has proved to be a bane for the farmers. Not only agricultural productivity has declined by 30%-40%, the floriculture that was very remunerative for the farmers of the area has been almost vanished in the area. Besides, the health hazards have posed serious threats to the lives of both human beings and animals owing to high level of contamination of the treated water. The societal perspectives and values have also undergone significant changes; even many villagers are being ostracized on the count that their progeny will suffer from deformities. On this count, the girls and boys of some of these villages are facing problems in finding their spouses. In view of these serious problems, we have drawn the conclusion that the new technology, which is devoid of holistic human values, in stead of helping the society, has heralded doom for the villagers in the surrounding areas of the CETP at Kanpur and has led to unsustainable development.  Hence, there is an urgent need to review the long term technological implications of setting up of the CETP and more particularly, the implications of using the imported technologies in our existing environment.

# EVALUATION OF BACTERIA AND METALS IN SEWAGE DUMP SITE IN JOS-NIGERIA

*Yakubu, Juliet M* (Federal University, Wukari-Nigeria)
Agarry O. O (University of Abuja, Nigeria)

The bacterial load and heavy metal content was carried out on a domestic sewage dump to determine the suitability of the soil for agricultural use as is the current practice. The total viable mean colony of the 17 bacterial species detected ranged from 214.3-229.7 for soil sample; 709-779 for soil-sewage sample and 406.3-451 for deep-pit sample cells/plate. All the isolates were mesophilic showing a decrease in number below and above $31^{o}$C. Inductively coupled Plasma Optical Emission Spectrum was used to detect 11 metals including As, Cr, Cu, Fe, K, Na, P, Sb, Se and Zn in the sludge in order to determine the suitability of the soil for agricultural purposes. The data generated showed no hazard so far for the direct use of such domestically generated sewage for agricultural use as biofertiliser.

# POTASSIUM SILICATE DRILLING FLUID AS A LAND RECLAMATION AMENDMENT

*Linjun Yao* and M. Anne Naeth
(University of Alberta, Edmonton, AB, Canada)

Potassium silicate drilling fluid (PSDF) is a new water based mud used in the oil and gas industry. Whether potassium silicate, the major component of PSDF, serves the same purpose as potassium fertilizer is not known since the properties and environmental impacts of PSDF have not been fully studied. Therefore, the goal of this research is to evaluate the environmental impacts of PSDF to the soil-plant-water system to determine whether it can be used as a soil amendment in reclamation.

Both greenhouse and laboratory approaches are being used to quantify the impacts of PSDF on soil properties. The impacts on plants are being measured in the greenhouse only. Preliminary results showed both slender wheatgrass (*Agropyron trachycaulum* (Link) Malte ex H.F. Lewis) and common barley (*Hordeum vulgare* L.) established in all PSDF treatments. Compared to the control, 82% of the raw PSDF treatments did not have negative influences on plant density. Plant above ground biomass was impacted by soil texture and positively correlated to available potassium and phosphate in soil and was negatively correlated to soil salinity. However, both available potassium and EC in soil increased with increased PSDF application rates. PSDF disposal methods and rates did have an effect on plant and soil properties measured, and we will investigate the mechanisms of the impacts in subsequent laboratory experiments.

# GROUNDWATER PROTECTION PROGRAM AT SAUDI ARAMCO

Humoud W. Al-Utaibi, Philip E. Reed, Jr., Mansour A. Kashir, Namir F. Najjar, and ***Ramzi F. Hejazi***
(Environmental Engineering Division, Environmental Protection Department, W-912, Al-Midra Tower, Saudi Aramco, Dhahran, 31311, Saudi Arabia)

**ABSTRACT:** In the early 1990s, Saudi Aramco operations in the downstream sector were expanded when the Company acquired bulk plant and refinery assets located throughout the Kingdom. In response to environmental due-diligence requirements following the acquisition, the Company's Environmental Protection Department (EPD) developed a Groundwater Contaminant Monitoring Program (GCMP). The objective of the program was to monitor groundwater quality through hundreds of groundwater monitoring wells at facilities that are located throughout the entire country. The GCMP elements consisted of installation of groundwater monitoring wells, groundwater detailed monitoring and sampling activities, and laboratory analysis.

The second milestone in the evolution of our groundwater protection program occurred in 2001 when unleaded gasoline was introduced to the Kingdom; replacing TEL by MTBE. Compared to the BTEX components in gasoline, MTBE has certain unique characteristics in groundwater, specifically its relatively high solubility in water and low taste and odor thresholds.

In response to emerging groundwater regulations, expanding corporate operations, and groundwater protection best-practice development, in 2003 EPD expanded the GCMP into a more comprehensive groundwater protection program entitled "Saudi Aramco Groundwater Protection Program (SAGPP)." Incorporating elements of the GCMP, the SAGPP also included conducting more detailed site characterizations and risk assessments

## STRATEGY

The strategic aspiration of the program is to protect employee health and the environment, prevent impacts to neighbors, and optimize investment in remediation efforts. The program has the following three main initiatives: Prevention, Monitoring & Assessment, and Remediation.

The Prevention element essentially involves controlling leak sources to groundwater. This is achieved through engineering controls (establishing standards/procedures and conducting design reviews) and periodic inspection and consultation to proponents to identify and stop leaks.

The Monitoring & Assessment element consists of four technical facets:

1. Conduct vulnerability assessments at each facility to determine risk and prioritize monitoring.

2. Conduct groundwater contaminant monitoring by collecting and analyzing groundwater samples from a network of 850 groundwater monitoring wells installed at 55 facilities.

3. Conduct facility-specific risk assessments to identify potential risks to our employees, neighbors and the environment.

4. Develop remedial action plans to mitigate the identified risks, if any.

Once an action plan for a specific facility is developed, the third element is initiated and follows a phased approach, as follows:

Phase I: Implement any interim action required (e.g., identify and control new leak sources).

Phase II: Implement a detailed site characterization and risk assessment evaluation to identify cost effective risk reduction measures. Based on assessed risk, appropriate remedial methods are selected that protects human health and the environment but avoids unnecessary clean-up – optimizing the corporate remedial investment portfolio.

Phase III: Pilot test identified remedial methods to evaluate and validate performance for full-scale design and implementation.

Phase IV: Develop full-scale remediation system requirements for inclusion in the Environmental Master Plan.
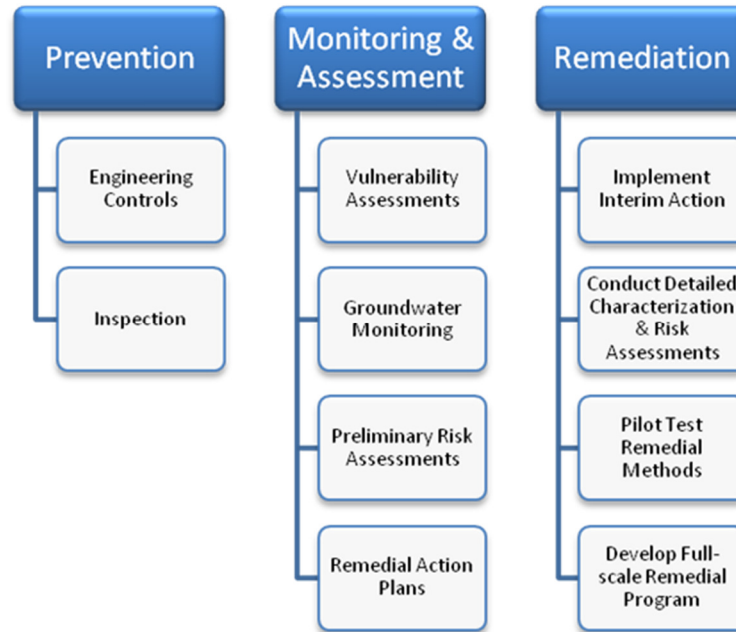


Figure 1: Groundwater Protection Strategy Chart

## SAUDI ARAMCO STANDARDS

Saudi Aramco has developed internal corporate standards for groundwater protection. The company has a general environmental protection policy that states "the Company will assure that its operations do not create undue risks to the environment or public health, and will conduct its operations with full concern for the protection of the land, air, and water from harmful pollution."

Groundwater protection requirements have also been established in several corporate engineering standards and procedures. These are essentially pollution prevention measures. Some examples include:

- SAEP-327: Hydrotest Water Disposal procedures for disposal of water used to hydrotest pipelines, tanks and vessels.
- SAES-A-104: Wastewater Management design standard including the construction of ponds and oily water pipelines.
- SAES-D-116: Standard for installation of secondary containment and leak detection systems for storage tanks.
- SAES-A-115: Groundwater Monitoring Well Design

## PROGRAM COMPONENTS

The following are the six main components of the Saudi Aramco Groundwater Protection Program:
- Monitoring well installation.
- Groundwater Sampling and Laboratory analysis.

-   Site Characterization and Risk-based Assessments.
-   Corrective Action Evaluation.
-   Technology development to enhance the program.
-   Facility Specific Projects and Special Initiatives.

## MONITORING WELL INSTALLATION

The groundwater monitoring wells are installed by pre-qualified local contractors according to Saudi Aramco specifications (SAES-A-115: Groundwater Monitoring Well Design), which is based on ASTM D5299 protocols. EPD facilitates the well installation; however the individual facilities or proponents actually fund the work.

Since the early 1990s Saudi Aramco has been installing groundwater monitoring wells at its facilities throughout the Kingdom. The number of monitoring wells is increasing dramatically since the commission of the SAGPP (Figure 2). Over 850 monitoring wells have been installed to date.
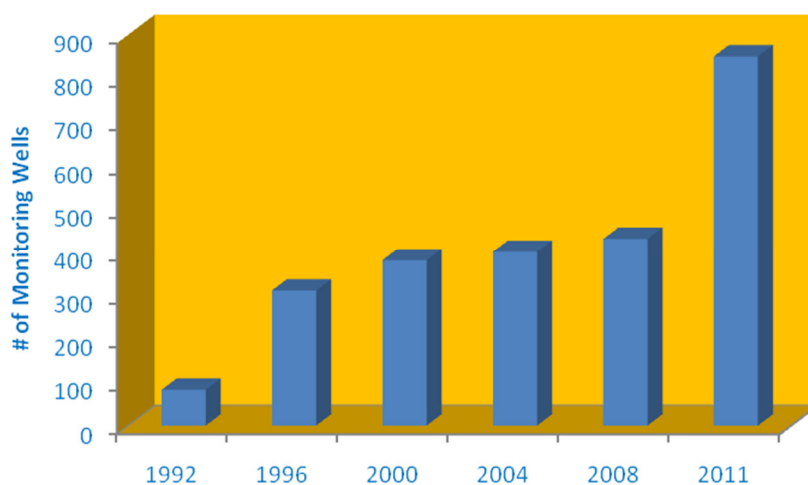


Figure 2: Groundwater monitoring well history

## GROUNDWATER SAMPLING AND LABORATORY ANALYSIS

Most of the sampling of monitoring wells is conducted by in-house staff. International best-practice sampling protocols are followed, and include sampling by dedicated bailers, low-flow sampling, or no-purge sampling. Selection of the sampling method depends on hydrogeologic conditions groundwater chemistry. The following are the main goals of groundwater monitoring in Saudi Aramco:

-   Assess shallow water-bearing zones (typically the first aquifer encountered) beneath Saudi Aramco facilities.
-   Collect baseline groundwater quality data.
-   Define facilities with major impact for further detailed site characterization, risk assessment, remedial pilot testing and remedial action plan development.
-   Provide input to departmental annual reports on the status of the groundwater conditions at Saudi Aramco facilities.

Field measurement, sampling collection, and laboratory analysis are the main components of the sampling and monitoring program which are described below:

**Field measurements.**
- o The measurement of the groundwater level in a well is frequently conducted in conjunction with groundwater sampling to determine the static water surface. The measurements are made relative to the top of well riser casing, which has been previously surveyed for UTM position and Mean Sea Level elevation. This potentiometric surface measurement can be used to establish groundwater direction and gradients. Groundwater level and well depth measurements are needed to determine the volume of water in the well casing prior to purging the well for sampling purposes.
- o Light Non-Aqueous Phase Liquid (LNAPL)-water interface probes are used to determine the free product thickness, if any. In addition, a bottom-loading bailer is used to confirm the LNAPL-water interface probe readings.

**Sample Collection.** In addition to the primary contaminants of concern at Saudi Aramco facilities, which are Volatile Organic Carbons (VOCs) and Semi-VOCs associated with hydrocarbons, the groundwater samples are analyzed for trace elements and general water chemistry.

**Purging.** Depending on the sampling methodology used (dedicated bailers, low-flow sampling, or no-purge sampling), removal of non-representative or stagnant water by "purging" prior to sample collection may be required. When purging is conducted, certain indicator parameters are measured in the field, including pH, specific conductance, temperature, dissolved oxygen, and oxidation-reduction potential.

Purging is conducted until the field-measured indicator parameters stabilize. Stabilization occurs when, for at least three consecutive measurements, indicator parameters meet the following criteria:

- Temperature ± 3% in °C
- pH ± 0.1 unit
- Specific Conductance ± 3% in µS/cm
- DO ± 10% in mg/L

**Sampling Vials and Preservation.** Groundwater samples for VOC analysis are collected in 40 ml glass vials fitted with Teflon® septa caps. The vial may be either preserved with concentrated hydrochloric acid or they may be unpreserved. Preserved samples have a two week holding time, whereas unpreserved samples have only a seven day holding time. In the great majority of cases, the preserved vials are used to take advantage of the extended holding time. In some situations, however, it is necessary to use the unpreserved vials or use of a different preservative (e.g., for MTBE analysis).

Efforts are made to reduce the flow from either the pump discharge line or the bailer during sample collection to minimize sample agitation. The vial should be completely filled to prevent volatilization. The samples are carefully poured down the side of the bottle to minimize turbulence and avoid bubbles or headspace forming in the vial after it is capped.

**Laboratory Analysis.** All collected groundwater samples are analyzed for VOCs and Semi-VOCs, in addition to trace elements and general water chemistry as required. The analyses are performed by participating Saudi Aramco Laboratories and ISO certified In-Kingdom Laboratories adhering to US EPA analytical protocols.

The results of well measurement and analytical data are managed in a web-based GIS. The data is evaluated to determine Risk-Based Corrective Action requirements and compliance with applicable and standards of Saudi Aramco, Presidency of Meteorology and Environment (PME) and Royal Commission requirements.

**Site Characterization and Risk Assessment.** Characterization and Risk Assessment is the heart of our program and is the most important component of a groundwater protection program aimed to evaluate the degree of impact and the areas of concern within a site and the associated risk, if any, based on the monitoring data. EPD undertakes detailed site characterizations and risk assessments at Saudi Aramco facilities to develop appropriate remedial alternatives, if warranted.

**Conceptual Site Model development.** The characterization element of our program involves developing conceptual site models (CSMs) for each facility. Typical CSMs (see Figure 3) integrate information on a plot plan of the facility that shows well locations, depth to groundwater, groundwater flow direction and gradient, and laboratory analytical results for the constituents of concern including any historical trends extracted from our GIS database.
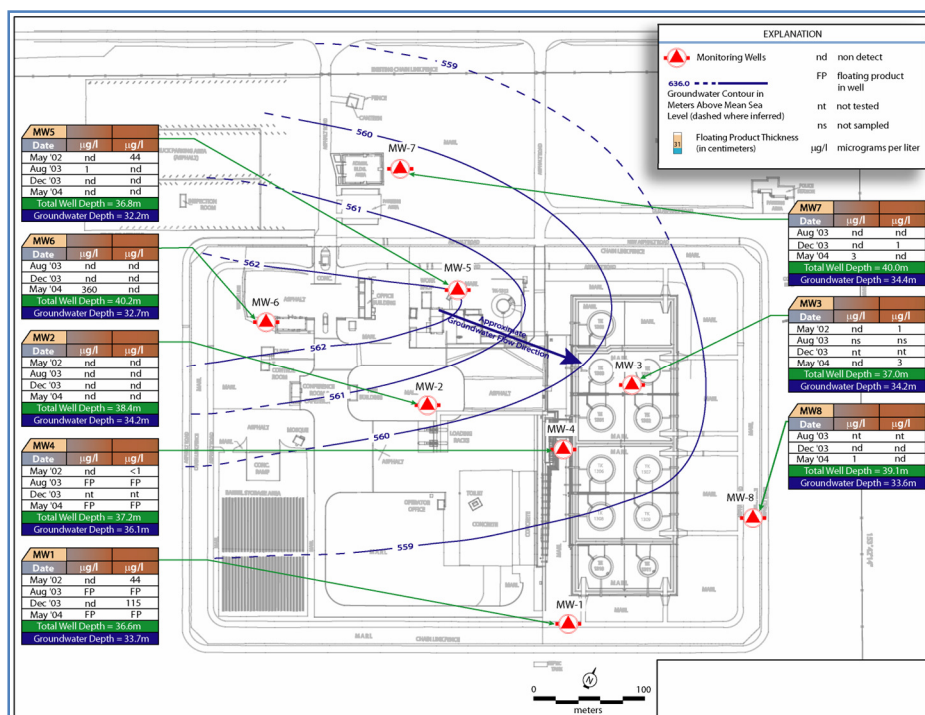


Figure 3:  an example of the conceptual site model

**Risk Assessment.** Once the conceptual site model is developed, we evaluate our sites using the concept of risk-based assessment, which involves the evaluation of human health hazards and potential adverse consequences related to environmental or occupational exposures.

In risk assessment, we look for 1) who may be affected – or the receptors, and 2) what the potential leak sources could be.

For a receptor to be affected by a given source, a pathway must also be present. In the case of groundwater, typical pathways are:
- Ingestion, either of contaminated drinking water or through fruits or vegetables that may be irrigated with contaminated water.
- Inhalation, if a plume of highly contaminated groundwater or product floating on groundwater is present at shallow depths underneath a building where people are working.
- Dermal contact, if people are using the water for washing.

Site-specific risks are quantified using protocols formulated under ASTM E 1739-95 and is known as Risk Based Corrective Action (RBCA). This step-by-step or "tiered" approach begins with development of the conceptual site models and works successively through more detailed data collection and analysis steps.

The RBCA process incorporates analytical fate and transport models. For more complex sites, we have applied numerical fate and transport models using software available in the marketplace.

The results of the RBCA assessments are presented in reports that include identification of potential receptors and pathways, the analysis results, and detailed discussion and justifications of remedial alternatives selected, if needed. Each potential remedial alternative will be evaluated for:

   a. Ability to meet the remedial objectives as determined by the RBCA assessment.
   b. Long-term reliability of the alternative.
   c. Short-term reliability of the alternative.
   d. Applicability of the alternative to the facility (in consideration of any operational impacts) and the surrounding community.
   e. Cost effectiveness of the alternative.
   f. Operation and maintenance requirements.
   g. Order of magnitude costs for the alternative.

**Corrective Action (Remediation).** The SAGPP includes a remediation or corrective action component. The corrective action typically occurs in a phased approach beginning first with source control, then, if necessary to source reduction and plume treatment based on the results of the risk assessment.

For source control, it is important to identify and stop any leaks as soon as possible and to prevent offsite migration of any impacted groundwater. We actively promote source control as a prevention tool to be the first step in groundwater remediation. Following source control implementation, if the results of the risk assessment indicate that further work is necessary to reduce whatever risks are present, the next logical step is to implement a source reduction program. In cases around the world, this involves either containing or removing accumulated product from the leak that is floating on top of groundwater. If the risk assessment requires some level of groundwater clean-up to be conducted, then we would next proceed to the plume treatment phase, once source control and source reduction has taken place.

Based on the findings of the site evaluations and selected remedial alternatives, detailed work plans are prepared for conducting remedial investigations and feasibility studies. The work plans include scope of work items for any additional investigation work recommended, any required remedial bench scale and field pilot tests required to evaluate the proposed remedial alternatives, and cost estimates and completion schedule for each item.

**Enhancement Technologies.** Part of our program is to evaluate and promote technologies to enhance groundwater protection here in the Kingdom; as they apply in our environment. Examples include:

**Soil Vapor Surveys.** Collection of soil vapor samples in the unsaturated or "vadose" zone in soil and analysis for indicator compounds such as BTEX or $CO_2$ can provide information to identify and delineate source areas. There are two categories of soil vapor surveying methods: passive and active. Conventional or active approaches involve inserting a hollow-stemmed probe into the subsurface and "actively" removing a relatively small sample of soil gas from the pore spaces. This sample is moved to a container for later analysis, or analyzed at the site using field analytical equipment. The active soil gas sampling method uses vacuum methods to collect soil gas samples at discrete depth intervals, and provides a "snapshot" of the soil vapor environment at a particular moment and at a specific depth.

Passive soil gas sampling involves use of collectors or "modules" housing adsorbent materials that are placed in the subsurface, and left for a specified period, typically several days or weeks. Organic vapors migrating through the subsurface encounter the collector and are "passively" collected onto the

adsorbent material. The collectors are retrieved and analyzed in a laboratory following the field survey. Passive sampling techniques rely on diffusion and adsorption and are more representative of in-situ conditions.

Saudi Aramco has successfully tested and evaluated both active and passive sampling technologies, and the results of this technology given the geological conditions prevalent in the Kingdom will allow us to roll-out this survey technique to other Saudi Aramco facilities, as required. The advantage of this technology is to identify the location and source of any potential contaminant instead of drilling many wells.

**Membrane Interface Probes (MIPs).** MIP is an investigative tool developed to detect volatile organic compounds (VOCs) within the subsurface. The MIP is advanced using direct push technology (DPT) in unconsolidated geologic materials and is advanced at a rate of approximately 0.3 m per minute thus allowing for quick assessment of potentially impacted sites (Figure 4). The MIP heats the surrounding soil and groundwater to approximately 100 to 120 degrees Celsius, which causes VOCs within the soil and groundwater to volatilize. The VOCs migrate across a semi-permeable film polymer impregnated into a stainless steel screen and then are transported to detectors above ground via a carrier gas. Above ground, the MIP is attached to three detectors; a photoionization detector (PID), a flame ionization detector (FID), and a halogen specific detector (XSD). These detectors are employed in series with each detector providing sensitivity to a particular group or type of contaminant. The XSD is highly specific to halogenated compounds and is the best detector when the MIP is used for logging chlorinated solvent plumes, whereas the PID provides sensitivity to aromatic compounds (BTEX) as well as confirmation of chlorinated ethylene compounds detected by the XSD. The FID is a general detector useful for hydrocarbon detection as well as confirmation of high concentration of all compounds seen on the other two detectors.

The MIP probe is also equipped with an electrical conductivity probe that allows for the electrical conductivity of the soil to be measured at the same time. This provides data on the geology of the subsurface, which can be used to correlate with the readings from the three detectors.



Figure 4: Membrane Interface Probes (MIPs)

**Compound Specific Isotopic Analysis (CSIA).** This enhancement technology evaluates the predictive capability of CSIA in hydrocarbon contaminated groundwater where high salinity and elevated ambient

temperatures exist, as is prevalent in Saudi Arabia. CSIA is a technique to provide knowledge and predictions of the extent and efficacy of degradation and/or natural attenuation of organic contaminants in groundwater. The feasibility of this technique under the high groundwater temperature and salinity conditions prevalent in Saudi Arabia will be evaluated. The majority of available data and studies on CSIA are related to North America and Europe where the groundwater characteristics are different.

**MTBE Removal Using Advanced Oxidation.** Saudi Aramco is currently testing a novel groundwater remediation technology that will evaluate the removal efficiency of MTBE and its degradation by-products. A pilot-scale treatment unit is being developed that utilizes a combination of advanced oxidation processes involving ultraviolet and hydrogen peroxide at varying circulation rates. A treatment unit and UV-photoreactor has been fabricated to treat groundwater "spiked" with MTBE at varying concentrations to evaluate treatment efficacy. The main goals of this study is (1) demonstrating the removal efficiency of MTBE and its degradation by-product by the pre-fabricated pilot unit; (2) determining the optimum treatment conditions for different water sources; (3) redesigning the pilot unit to be applied in the field based on the optimization results achieved; (4) determining the optimum treatment conditions of the modified field unit.

**ACKNOWLEDGEMENT**

# *EX SITU* MEASUREMENTS OF DIOXIN BIOAVAILABILITY IN *IN SITU* REMEDIATED DEEP FJORD SEDIMENTS

*Morten T. Schaanning* and Ian Allan (Norwegian Institute for Water Research, Oslo, Norway),
Sarah Josefsson, (University of Umeå, Umeå, Sweden)
Espen Eek (Norwegian Geotechnical Institute, Oslo, Norway)

Thin capping with or without active carbon (AC) amendment has been proposed for *in situ* remediation of contaminated sediment areas which are too large or beyond reach of common dredging operations or isolation capping. The Grenlandfjords, SE Norway, received emissions of dioxins from a magnesium production plant operated during 1951-2002, and the sediments, 10 km$^2$ of which are located below 50 m depth, have later become a major secondary source of dioxins for fish and shellfish caught in the area. Food chain modelling has indicated that levels of dioxins in cod liver will remain high for another 4-5 decades.

In this area in September 2009, thin caps were placed on four experimental plots at 30 and 100 m depth by discharging cap materials suspended in sea water into the water column 5-20 m above the bottom. The materials used were 500 m$^3$ of gravel supplied from a terrestrial limestone quarry, 1600 m$^3$ of suspended clay dredged from a nearby fjord location and 80 tons of activated carbon. During discharge, the vessel moved slowly in predefined patterns across each plot. A few weeks after cap placement, sediment profile images showed fairly even 1-4 cm thin layers of cap materials covering the seabed. Thus, one 4 ha plot at 100 m depth was covered with dredged clay and AC, and three 1 ha plots at 30 m depth were covered with, respectively, limestone gravel, dredged clay and dredged clay and AC. One adjacent plot at each depth was left uncapped for control.

The main objective of the work presented here was to determine cap efficiency with regard to reducing the bioavailability of dioxins in the old sediment. This was done by transferring intact seabed sections from the experimental plots to a mesocosm laboratory in October 2009 and November 2010, using a 0.1m$^2$ box-corer with internal liners. In the mesocosm, 20 individuals each of the surface dwelling gastropod *Hinia reticulata* and the deep burrowing polychaete *Nereis (Hediste) diversicolor* were added and allowed to find their way down to their respective niches within the sediment. In addition, passive samplers (LDPE-membranes) were installed in the overlying water about 10 cm above the sediment surface to extract bioavailable fractions leaking out from the sediments. After three months exposure, membranes and organisms were sampled, carefully rinsed and sent to Miljökemiska Laboratoriet, University of Umeå, for extraction and chemical analyses of dioxins and other chlororganic compounds.

The boxes transferred in 2009 were used as a pilot test for exposure of gastropods, only. This test showed that the concentration of dioxins (given as toxicity equivalents PCDD/F-TEQ), was reduced from 4.3-5.2 pg/g wet tissue in boxes from control plots, to 0.5-1.4 pg/g in capped plots. In the boxes transferred one year later, concentrations were essentially unchanged in control and clay/AC plots, but had increased significantly in the clay and limestone gravel plots. Analyses of the polychaetes and the LDPE membranes confirmed the low efficiency of the limestone gravel and clay plots one year after cap placement and the good performance of the clay/AC plots. Considering all matrixes (polychaetes, gastrodpods and LDPE membranes), dioxin toxicity equivalents in the clay/AC plots were reduced to between 14 and 28% of those determined in uncapped control sediments.

The results obtained here have demonstrated the efficiency of field applications of AC amendment, but further investigations on long-term efficiency maintenance and effects on benthic organisms are needed before the method can be recommended for large areas with high ecological status.

# QUANTIFICATION OF WATER ADSORPTION CAPACITY OF BIOLOGICALLY ACTIVE SOIL AND WOODCHIPS

*Sagar Chitre*, Sergio Santos, David Ramirez and Kim Jones
(Texas A & M University-Kingsville, Kingsville, TX, USA)

**ABSTRACT:** Biologically active cover (biocover) materials are proposed to mitigate the fugitive methane emissions from landfill sites by oxidizing methane to carbon dioxide. The efficiency of the methane oxidation has been found to be a function of the biocover material's moisture content (MC). In-column experiments were conducted to determine and quantify the water adsorption capacity of the proposed biocover material (organically rich soil and woodchips) obtained from the McCommas Bluff Landfill site in the City of Dallas, Texas. Bench scale in-column tests were conducted by humidifying a dry air stream and passing it through a column containing the biocover media. Breakthrough curves were obtained for as-received organically rich soil samples, woodchip samples and mixture of as-received organically rich soil samples and woodchip samples, respectively, for relative humidity (RH) ranging from 75% to 95%. Additional tests were conducted with organically rich soil pre-humidified at 25% MC. The MC of the as-received organically rich soil and woodchips increased by 5 % (from 9% to 14% MC) and 5% (from 10% to 15%), respectively, when the air stream was at 95% RH. The pre-humidified biocover soil sample observed an 8 % MC decrease (from 25% to 17%) when the air stream was at 95 % RH. When the organically rich soil sample and woodchip sample was mixed in the volumetric ratios of 1:1 the water adsorption capacity of the media was considerably affected and the increase in the MC was 1% (from 11% to 12%) when the air stream was at 95 % RH.

## INTRODUCTION

Traditional approach towards designing a landfill was mainly focused and restricted towards leachate containment and prevention of landfill fire that can occur due to methane emissions from landfills. However, recent research in the field of global climate change has listed methane emission from the landfills as a potent contributor to the global warming (Huber-Humer, Gebert et al. 2008). Although carbon dioxide ($CO_2$) and methane ($CH_4$) are the two main principal greenhouse gases, the infrared activity of methane is about 25 times more than that of $CO_2$. The atmospheric concentration of methane has increased by a factor of 2 since the last century (Abichou, Powelson et al. 2006). Amongst all the long-lasting greenhouse gases responsible for climate change forcing, the contribution of $CH_4$ is 18.0% of the total radiative forcing. Along with the $CH_4$ emissions, the nonmethane organic compounds (NMOC) emitted from landfills possess a grave and serious environmental threat as many of them are toxic and contribute to global climate change. Even though the concentrations of NMOC are in parts per million by volume or parts per trillion by volume, there is a concern regarding the emissions of NMOC from landfills as some of the species like benzene and vinyl chloride are known for their carcinogenic properties whereas compound like chlorofluorocarbons deplete upper atmospheric ozone (Bogner 2003; Scheutz, Pedersen et al. 2009).

Landfills are the third largest contributors of the anthropogenic atmospheric methane in the United States and its share in the anthropogenic atmospheric methane budget of the United States is at

astounding 30.0% (Abichou, Chanton et al. 2006; Albanna 2009). The spatial distribution of methane emission from landfills is highly variable. The methane flux can vary from 0.4 mg per $m^2$ per day to 4 kg per $m^2$ per day. In terms of the global budget, the disparity amongst the sources and sinks of methane is below 6%. As a result, a minor reduction in the $CH_4$ source can facilitate an appreciable decline in the concentration of atmospheric $CH_4$. Also, the residence time of $CO_2$ in atmosphere (100 years) is relatively very high compared to the atmospheric residence time of $CH_4$ (7 to 10 years), which implies that any effort towards $CH_4$ mitigation would be observed rapidly. Hence lowering the atmospheric concentration of $CH_4$ is a practical and noteworthy goal (Abichou, Chanton et al. 2006).

An engineered biocover system offers a comprehensive and cost-effective solution towards mitigation of fugitive methane emissions from landfills. The materials that are used in the construction of biocover are mostly recovered from waste products, residues and by-product generated from sewage sludge, composts or biologically and mechanically treated waste (Huber-Humer, Tintner et al. 2011). Biocovers are the biotic systems that can mitigate landfill methane emissions by microbial oxidation of $CH_4$ to $CO_2$ in the presence of methanotrophic bacteria. Biocovers can be used effectively to mitigate the fugitive methane emissions from the landfills that are equipped with LFG collection system. They can also be employed effectively and economically at the landfill sites where LFG collection is technically and economically not feasible due to the weak methane fluxes (Huber-Humer, Gebert et al. 2008).

Results from a recent research related to mitigation of landfill NMOC using engineered biocovers has proved the potential capacity of biocovers to attenuate landfill NMOC emissions (Scheutz, Pedersen et al. 2009). Some of the NMOC can be degraded biologically when aerobic conditions exist. Hence, the biocover that can enhance the oxidation of $CH_4$ can also bring down the emissions of NMOC (Barlaz, Green et al. 2004). Intergovernmental Panel on Climate Change (IPCC), in its working group III assessment report, has identified biocovers as a prominent mitigation technology for mitigating the greenhouse LFG emissions (Gebert, Groengroeft et al. 2011; Gebert, Röwer et al. 2011).

Landfill cover soil is known to harbor a high population of methanotrophic bacteria. Methanotrophic bacteria contain a methane mono-oxygenase enzyme that allows them to consume methane to yield energy, producing $CO_2$ and water as by-products. Hence, it is extremely important that the methanotrophic bacteria found in the landfill cover soil are able to oxidize the landfill methane to $CO_2$. However, the methanotrophic bacteria will be effective only if they have favorable environmental conditions and this is where biocovers comes into picture. Biocover media is engineered in such a way that it provides favorable environmental conditions to the methanotrophic bacteria so that their methane oxidation potential can attain extremely high values (Albanna 2009; Gebert, Groengroeft et al. 2011).

Microbial uptake rate of methane in the biocover depends upon various environmental factors such as temperature, soil composition and characteristics, moisture content, pH, concentration of oxygen($O_2$), nutrient content and water retaining capacity (Stern, Chanton et al. 2007). One of the most crucial parameters affecting the $CH_4$ oxidation is the MC of the biocover soil media. The efficiency of $CH_4$ consumption by biocover follows a parabolic trend. There is considerable reduction in the efficiency at low and high MC (Einola, Kettunen et al. 2007). Many column and batch studies have shown that the optimum MC for efficient $CH_4$ oxidation is in the range of 10.0% - 20.0% (w/w) at a temperature ranging from 25º-30º C. In one of the study where municipal solid waste was employed as landfill biocover, high methane oxidation was observed at MC of 45%(w/w) (Stern, Chanton et al. 2007).

Soil texture and compaction decides the pore size distribution responsible for controlling the water withholding capacity and gas transport in the biocover soil. Pore size distribution determines the rate at which atmospheric oxygen and landfill methane becomes available to methanotrophic bacteria.

For efficient mitigation of $CH_4$, the materials should be selected in such way that the pores should contain sufficient space devoid of pore water that can allow the diffusion of atmospheric oxygen into the biocover at optimum MC and prevalent atmospheric conditions (Gebert, Groengroeft et al. 2011). Biocover should have good moisture retaining capacity and permeability for oxygen diffusion. The depth and thickness of biocover is a function of depth of up to which atmospheric oxygen can penetrate and diffusion. More the depth of the biocover, more will be the stability for regimes of moisture and temperature (Stern, Chanton et al. 2007).

The main objective of this study was to quantify the water adsorption capacity of the biocover material that has been proposed for the McCommas Bluff Landfill. The information obtained from this study was useful in designing a system that could maintain the biocover media at the desired MC. The main goal of this research work was to: (1) investigate and quantify the water adsorption capacity of the as-received soil and woodchip samples at 75% and 95% RH, respectively and (2) investigate and quantify the changes in the water adsorption capacity of the as-received soil and woodchip samples when they are combined in a volumetric proportion of 1:1 at 95% RH.

## MATERIALS AND METHODS

**Experimental Design and Setup** The bench scale experimental setup shown in figure 1 was used for the determination of the water adsorption capacity of as-received soil and woodchip samples. The compressed air form the header was regulated at 23 psi and the flow rate was adjusted to 0.5 LPM. The air stream was then passed through a silica gel column where it dries out to a RH of 5.5%. The air stream was then humidified with water vapor at the desired % RH using an automated syringe pump (Genie Plus). The calibration of water injection relative to %RH is shown in table 1.
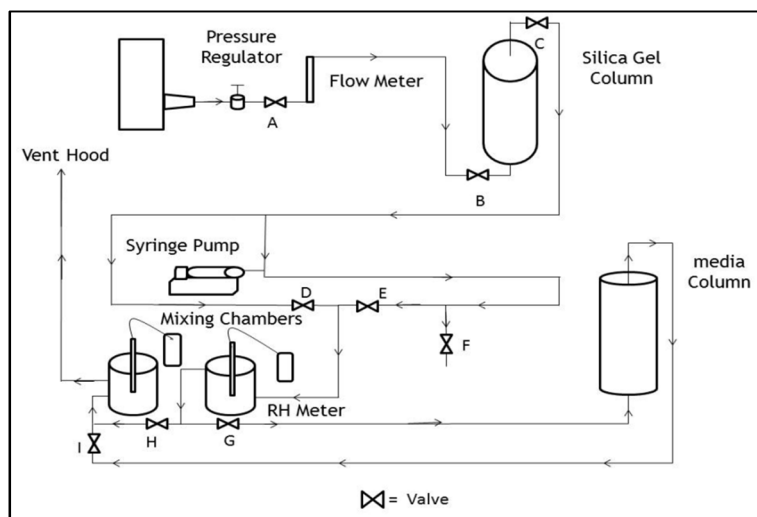


**FIGURE 1** Schematic of Experimental Setup

Valve E was always kept open and valve D and valve F was always kept closed throughout the experiment. Valve D was only opened if dry air stream was required for cleaning and drying of the system in case of condensation due to saturation of water vapor at high RH. Valve F acted like a drainage system in case of heavy condensation and was always kept closed unless drying of system was required.

Hence, with valve E open and valve D and F closed, the humidified air stream entered the first mixing chamber (inlet) holding a RH meter (OMEGA-ETTE HH311) and then to the second mixing chamber (outlet) holding the similar RH meter. The RH meter was equipped with inbuilt data logging ability thus making it possible to records the RH data at every 30 seconds throughout the operation. At this point, valve I and G were kept closed while valve H was kept open. Valve H was kept open until the RH values in the inlet and outlet mixing chamber achieved equilibrium.

**TABLE 1** Calibration of Water Injection Relative to %RH

| RH (%) | $P/P_0$ | ppmv | Water Injection µL/hr |
|--------|---------|------|-----------------------|
| 60 | 0.6 | 12,533.02 | 419.00 |
| 70 | 0.7 | 14,621.86 | 489.00 |
| 75 | 0.75 | 15,666.28 | 524.00 |
| 80 | 0.8 | 16,710.70 | 559.00 |
| 85 | 0.85 | 17,755.12 | 594.00 |
| 90 | 0.9 | 18,799.53 | 629.00 |
| 95 | 0.95 | 19,843.95 | 664.00 |

Once RH equilibrium between the inlet and outlet mixing chamber was attained, the valve H was closed and valve I and G were opened so that the air stream from the inlet mixing chamber could enter the media column and from the media column to the outlet mixing chamber. The media (soil/woodchips) in the media column would either adsorb or desorb the MC from the humidified air stream or to the humidified air stream, respectively. The RH meter at the inlet chamber recorded the RH which was at a constant pre-determined value. However, the RH meter in the outlet mixing chambers recorded the changes in the RH values corresponding to whether media adsorbs or desorbs water. From the outlet chamber the air stream finally escaped out through the fume hood.

The experiment was continued till breakthrough was achieved. After the breakthrough the sample from the media column was analyzed for the MC using ASTM-D2974-1987 standard. Data from the RH meter was downloaded to a spreadsheet and breakthrough curves were plotted. Quantification of the water adsorption by the media was calculated using the expression (1)

$$\text{Mass}_{adsorbed} = \text{mass}_{in} - \text{mass}_{out}$$
$$= Q_{in} C_{in} \Delta T - Q_{out} C_{out} \Delta T \tag{1}$$

Where $Q_{in, out}$ = flow rate, $C_{in, out}$ = concentration in ppmv = $(0.031333*(P_{H2O}/P))*10^6$, $P_{H2O}/P$ = RH/100 and T = Time interval. Concentration C in ppmv can be converted to g/m$^3$ using expression

$$C(g/_{m^3}) * \frac{10^3 * R * T}{P * MW} = C(ppmv) \tag{2}$$

where, R = 0.0821 L·atm/K·mol, T = 295.37 K, P = 1.5 atm, MW = 18 g/mol.

**Material Characterization** The biocover material (organically rich soil and woodchips) used in this research was obtained from the McCommas Bluff Landfill site in the City of Dallas, Texas. The soil and woodchips had an average initial MC of 11.1% and 8.2% with a standard deviation of 0.9 and 0.51, respectively. The test was conducted using the ASTM-D2974-1987 standard. The pH of soil and woodchips was determined using ASTM-D4972-01 standard. The average pH of soil and woodchips was 7.79 and 6.33 with a standard deviation of 0.023 and 0.159, respectively. The pore size and the surface area of the soil were determined using NOVA 2000e High Speed Surface Area and Pore Size Analyzer-Quantachrome Instruments. The surface area and pore size of as-received soil sample was 70 sq. /g and 4 e+01 Å, respectively.

The bulk density of soil and woodchips was determined by using calibrated cylinder filled with known mass of sample. The cylinder was vibrated for a few seconds to remove air voids. The volume of the sample in the cylinder was noted. Bulk density was then given by mass of sample divided by the volume of sample. The average bulk density of as-received sample was 1.089 g/ml with standard deviation of 0.083. In the case of woodchip sample the average bulk density was 0.364 g/ml with standard deviation of 0.031.

The engineering classification of soil was conducted using ASTM-D2487-90 standard and the as-received soil was classified as organic clay. The liquid limit (LL) and plastic limit (PL) tests were conducted on the soil samples using ASTM D-431-84 standard. The average LL and PL of soil sample was found to be 57.7 and 24.85 with a standard deviation of 5.23 and 2.47, respectively. ASTM-D422 hydrometer analysis was conducted to determine the particle size distribution of the as-received soil sample. The as-received soil sample had particle size ranging from 71 µm to 1µm.

**Experimental Methods** The water adsorption capacity of the as-received soil and woodchip samples was tested at relative RH of 75% and 95%, respectively. A separate test was also performed at 95% RH on the as-received soil samples pre-humidified at 25% MC. This test was conducted to determine whether the water adsorption capacity of the as-received soil can be increased to around 20% to 25% MC by pre-humidifying the soil sample.

The proposed biocover will be designed using a combination of soil and woodchips, mixed in a definite proportion by volume. Hence, for understanding the effect of combination of soil and woodchips on the water adsorption capacity of the biocover media, a volumetric combination of soil and woodchips in the ratio of 1:1 was tested at 95% RH.

**RESULTS AND DISCUSSION**

The as-received soil sample desorbed when the air stream was at 75% RH. Figure 2 shows the breakthrough curve for the as-received soil sample at 75% RH. The soil sample desorbed 31.67 mg water/ mg soil. The soil lost 2 % MC from initial MC of 9% to final MC of 7%. However, at 95% RH, the soil sample adsorbed 38.66 mg water/ mg soil. The gain in the MC was 5% from initial MC of 9% to final MC of 14%. Figure 3 shows the breakthrough curve at 95% RH. The limiting RH was found to be 77%. At RH below 77% soil desorbed moisture and at RH above 77% the soil adsorbed moisture from the air stream. Table 2 summarizes the experimental conditions and results.

The as-received woodchip sample behaved quiet differently at 75% RH (Fig 4). Unlike the soil sample, the woodchip sample did adsorb 2.31 mg water/ mg woodchips at RH of 75%. The gain in MC was 1% from initial MC of 10% to final MC of 11%. Similarly, at 95% RH, the woodchips gained 5% MC from initial MC of 10% to final MC of 15%(Fig 5). The amount of water adsorbed in this case was 24.87 mg water/ mg woodchips.
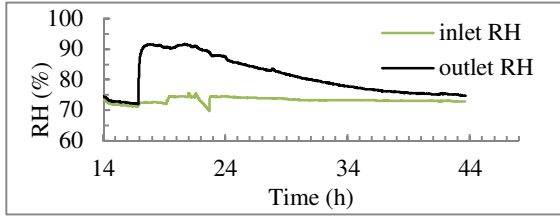


**FIGURE 2** Soil Moisture Breakthrough Curve at 75% RH
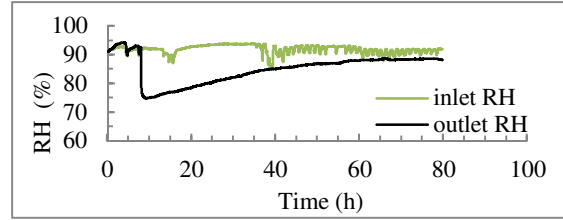


**FIGURE 3** Soil Moisture Breakthrough Curve at 95% RH
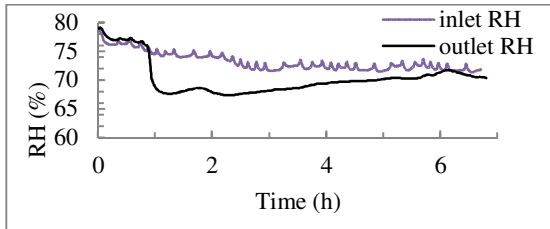


**FIGURE 4** Woodchip Moisture Breakthrough Curve at 75% RH
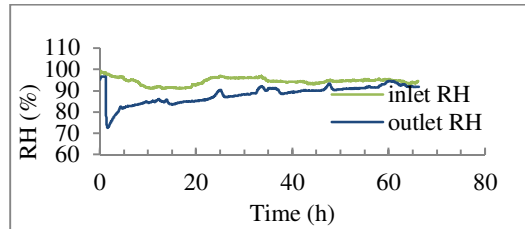


**FIGURE 5** Woodchip Moisture Breakthrough Curve at 95% RH
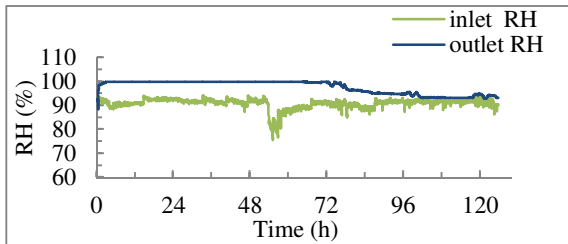


**FIGURE 6** Soil Moisture Breakthrough Curve at 95% RH for as-received Soil sample Pre-humidified at 25% MC
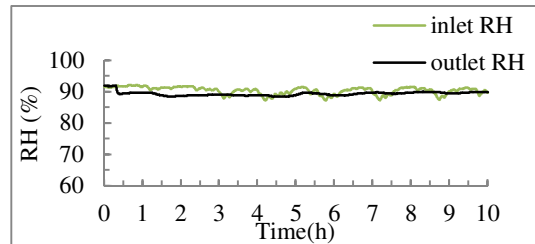


**FIGURE 7** Moisture Breakthrough Curve at 95% RH for as-received soil and woodchip sample mixed in volumetric ratio of 1:1

When the as-received soil sample was pre-humidified at 25% MC, the air stream saturated 95% RH was able to sustain the MC of the pre-humidified soil at 17% MC. Figure 6 shows the moisture breakthrough curve for the pre-humidified soil sample. Although, there was a drop of 8% in the MC of the pre-humidified soil, the air stream at 95% RH was able to maintain the soil at 17% MC. The water desorbed in this case was 118.26 mg water/mg soil. Hence, this concept can be effectively used to bring the soil at optimum MC in any of the biocover in-column experiments.

When a combination of soil and woodchips was used mixed in a volumetric ratio of 1:1, the water adsorption capacity of media was drastically affected. Figure 7 shows the moisture breakthrough curve for this case. The media could just adsorb 4.39 mg water/mg media even at 95% RH. The increase in MC was just 1% from initial MC of 11% to final MC of 12%.

**TABLE 2** Experimental Conditions and Results for Biocover Water Adsorption Tests

| Media | Mass (g) | Air Flow Rate (Lpm) @ 23psi | Water Injection Rate (μL/h) | Target RH of Air Stream (%) | Observed RH of Air Stream (%) | Initial Soil MC (%) | Final Soil MC (%) | Water Adsorbed mg water/mg soil | Water Desorbed mg water/mg soil |
|---|---|---|---|---|---|---|---|---|---|
| Soil | 50 | 0.5 | 524 | 75 | 73-75 | 9 | 7 | 0 | 31.67 |
| Soil | 50 | 0.5 | 664 | 95 | 90-95 | 9 | 14 | 38.66 | 0 |
| Soil Prehumidified | 50 | 0.5 | 664 | 95 | 90-95 | 25 | 17 | 0 | 118.26 |
| Woodchips | 27 | 0.5 | 524 | 75 | 73-78 | 10 | 11 | 2.31 | 0 |
| Woodchips | 31 | 0.5 | 664 | 95 | 92-97 | 10 | 15 | 24.87 | 0 |
| Soil + woodchip 1:1 Vol. ratio | 12.5 | 0.5 | 664 | 95 | 90-95 | 11 | 12 | 4.39 | 0 |

## CONCLUSION

**O**rganically rich soil and woodchips that were proposed as biocover materials in this research could gain 5% moisture content (MC), respectively, when the air stream was saturated at 95% relative humidity (RH). On pre-humidifying the organically rich soil at 25% MC, the air stream at 95% RH could retain the MC at 17%. When the woodchips and organically rich soil was mixed in the volumetric ratio of 1:1, the water adsorption capacity was decreased and the media could gain only 1% MC even at 95% RH.

The results obtained from this research can be used for designing a system that will maintain the biocover media at the 14% MC in the column experiments where biocover efficiency will be tested in the simulated the landfill conditions. The research highlights the challenges in maintain the biocover media at 20% to 25% MC when organically rich soil and woodchips are used as biocover materials. Pre-humidifying the biocover media at the optimum MC level of 25% can be an effective option towards maintaining the MC of the media close to 20%. However, when a mixture of organically rich soil and woodchips are used as biocover media, the water adsorption capacity of the media can be adversely affected.

## ACKNOWLEDGEMENT

## REFERENCES

Abichou, T., J. Chanton, et al. (2006). "Methane flux and oxidation at two types of intermediate landfill covers." Waste Management **26**(11): 1305-1312.

Abichou, T., D. Powelson, et al. (2006). "Characterization of Methane Flux and Oxidation at a Solid Waste Landfill." Journal of Environmental Engineering **132**(2): 220-228.

Albanna, M. (2009). "Effects of Temperature, Moisture Content, and Fertilizer Addition on Biological Methane Oxidation in Landfill Cover Soils." Pract. Period. Hazard. Toxic Radioact. Waste Manage. **13**(3): 187.

Barlaz, M. A., R. B. Green, et al. (2004). "Evaluation of a Biologically Active Cover for Mitigation of Landfill Gas Emissions." Environmental Science & Technology **38**(18): 4891-4899.

Bogner, J. (2003). "FIELD MEASUREMENT OF NON-METHANE ORGANIC COMPOUND EMISSIONS FROM LANDFILL COVER SOILS " Ninth International Waste Management and Landfill Symposium S. Margherita di Pula, Cagliari, Italy; 6 - 10 October 2003 **Environmental Sanitary Engineering Centre, Italy**

Einola, J.-K. M., R. H. Kettunen, et al. (2007). "Responses of methane oxidation to temperature and water content in cover soil of a boreal landfill." Soil Biology and Biochemistry **39**(5): 1156-1164.

Gebert, J., A. Groengroeft, et al. (2011). "Relevance of soil physical properties for the microbial oxidation of methane in landfill covers." Soil Biology and Biochemistry **43**(9): 1759-1767.

Gebert, J., I. U. Röwer, et al. (2011). "Can soil gas profiles be used to assess microbial CH4 oxidation in landfill covers?" Waste Management **31**(5): 987-994.

Huber-Humer, M., J. Gebert, et al. (2008). "Biotic systems to mitigate landfill methane emissions." Waste Management & Research **26**(1): 33-46.

Huber-Humer, M., J. Tintner, et al. (2011). "Scrutinizing compost properties and their impact on methane oxidation efficiency." Waste Management **31**(5): 871-883.

Scheutz, C., G. B. Pedersen, et al. (2009). "Biodegradation of Methane and Halocarbons in Simulated Landfill Biocover Systems Containing Compost Materials." J. Environ. Qual. **38**(4): 1363-1371.

Stern, J. C., J. Chanton, et al. (2007). "Use of a biologically active cover to reduce landfill methane emissions and enhance methane oxidation." Waste Management **27**(9): 1248-1258.

563,1125,1277,1308, #563

# SELECTIVE MONITORING OF GROUNDWATER PARAMETERS FOR POST CLOSURE CARE MONITORING AT CLOSED LANDFILLS

***Banu Sizirici Yildiz*** (Case Western Reserve University, Cleveland, OH, USA)

Berrin Tansel (Florida International University, Miami, FL, USA)

The transport of leachate from landfills can have impact on groundwater quality. After the contaminants reach the groundwater, all leachate pollutants will be subjected to dilution as the leachate mixes with the aquifer. After mixing, contaminants can undergo a series of reactions and changes such as sorption, biodegradation, hydrolysis, redox reactions, ion exchange, and precipitation. The purpose of this study is to characterize the mobility of leachate contaminants through groundwater system and to optimize groundwater monitoring based on concentration and spatial mobility characteristics of groundwater (GW). A case study landfill in South Florida, USA was selected in this study. Higher contaminant concentrations were detected consistently in two monitoring wells due to southerly groundwater direction. The monitored parameters such as, iron, sodium, ammonia as nitrogen, chlorobenzene, and 1,4-dichlorobenzene had decreasing trends in groundwater system due to soil absorption and retardation factors. Metals were retarded by sorption, and concentration levels increased by depth. VOCs levels did not show a clear trend and did not change significantly with depths. The monitoring program can be modified based on groundwater direction, retardation factor, groundwater well depth, and concentration trends. Monitoring frequncy change will contribute to landfill management in better utilization of post closure monitoring.

# EMISSION OF FORMALDEHYDE IN AIR AND LEACHATE FROM MDF BURIED IN LANDFILLS

*Min Lee*, Lynn Prewitt and Hamid Borazjani
(Mississippi State University, Mississippi State, MS, USA)
Sung Phil Mun
(Chonbuk National University, Jeonju, South Korea)

Wood composites are wood materials that have been bonded together and compressed with glue or adhesives. Adhesives commonly used for bonding wood are melamine-formaldehyde (MF), phenol-formaldehyde (PF), melamine-urea-formaldehyde (MUF), and urea-formaldehyde (UF). Formaldehyde is not only widely used in the manufacture of wood products such as medium density fiberboard (MDF), oriented strand board (OSB), plywood, laminated beam, and furniture but also in the chemical and paper industries as well as in textile processing. Formaldehyde is toxic in high concentrations and causes health issues such as watery eyes, burning sensations in the eyes and throat, nausea, difficulty in breathing and cancer in humans. Approximately 14 million tons of wood waste containing formaldehyde based resins are generated yearly and disposed in large pits and landfills or burned. No regulations however exist for formaldehyde emission from formaldehyde bonded wood waste buried in landfills. Therefore, more information is needed about the environmental impact of formaldehyde released by air and water from formaldehyde bonded wood waste buried in landfills. The objective of this study is to determine the amount of formaldehyde released into the air and leached from MDF buried in a simulated landfill. Simulated landfills were constructed in cylindrical plastic containers with alternating layers of silty clay soil (2.54 cm) and milled or small pieces of MDF (2.54 cm) for a total of five layers. Soil without MDF was used as a control. Leachate and air were sampled weekly for 5 weeks. Formaldehyde in leachate was determined by derivatizing with pentafluorbenzylhydroxylamine and analyzing by gas chromatography while formaldehyde in air was determined by first collecting and derivatizing on a dinitrophenylhydrazine (DNPH) cartridge and analyzing by high-performance liquid chromatography. Preliminary results indicate that formaldehyde released in the leachate was reduced by 99% at the end of the study. The initial pH of the leachate from soil without MDF was 5.87 and increased to 6.18 at the first week's sampling time and remained at approximately 6.22 through week five, while the leachate from soil with added MDF had an initial pH of 4.66 and increased weekly to 6.40 on week 5. Dissolved oxygen and microbial enumeration in leachate will be conducted for determination of aerobic microbial activity at the beginning and end of the study.

# METHANE RECOVERY FROM LANDFILL GAS: A CASE STUDY IN CHINA

*Lei ZHENG*, Wei WANG, Zhou DENG (School of Environment, Tsinghua University, Beijing 100084, China)
Hong CHEN, Bo QU(Beijing Sustainable Development Centre,Beijing 100084, China)
Juan DU(Tsinghua Urban Planning & Design Institute, Beijing 100084, China)
Jidong CHEN(Shenzhen Sanitation Department, Shenzhen 518026, China)

In China, there are 372 modern, sanitary landfills for domestic waste currently in operation, located in 297 Chinese cities, with a total capacity of 194,600 tons per day. By the end of 2010, the output of methane from LFG in China will account for 5% of total GHG emissions of the country, reach 12 billion Nm3 a year, equivalent to 8 million tons of standard coal. To date, most methane from the Chinese landfills/dump-sites is not recovered, thus representing a significant emission source of GHG and potential of renewable energy.

Due to the complicated composition of LFG, the extraction and purification is a key process on LFG recovery. In 2005, the PSA technique on LFG extraction and purification developed by Tsinghua University was applied in Xiaping MSW landfill, Shenzhen, Southeast China, and the first domestic LFG purification and compression demonstration project with vehicle fuel production was set up as well. This subject aims to carry out systematic research on the application of LFG purification for industries, with the technique of adopting two-stage PSA system to produce high–purity methane and CO2 products, and finally realizing low emission of the whole system. Pressure swing adsorption technology was used in LFG purification, and laboratory experiment, pilot-scale test, and on-site demonstration were carried out in Shenzhen, China. The operation conditions were optimized, such as adsorption pressure, adsorption time, product gas flow, blowback flow, number of operating towers and the air content in feed gas. The recovery rate of CH4 and its concentration in the product gas reached 90% and 90%, respectively. Three kinds of commonly used vehicles were chosen to test the performance of CPLG as a vehicle fuel. The drive performance, environmental protection performance, and economy of the reformed vehicles were compared with those of un-reformed vehicles.

# MODELING OF DIFFERENT LANDFILL DAILY COVER USING HYDRUS- 2D/3D –JORDAN

Mohammad Aljaradin, Kenneth M Persson and Tarek Selim
(Lund University, Water Resources Engineering, P.O.Box:118, 221 00 LUND, SWEDEN)

The most important trends in landfill management policy over the last decade have been the universal adoption of the containment approach to emission control and the increasing legal requirement to install artificial membranes as bottom liners and caps to landfills which is now mandatory in many countries. The landfill cover is one of the most important aspects when designing and constructing landfills. The cover should minimize the quantity of water that infiltrates to the body of the solid waste landfills, reduce the rate of leachate generation, segregate solid waste from the surrounding environment, and control the risk of additional groundwater contamination and gas migration. Landfill covers are not standardized. Different covers have been proposed and executed all over the world. The selection of the suitable cover type is a big challenge especially in arid and semi-arid countries. Jordan is considered to be a semi-arid country. In Jordan, more than 20 landfills are in operation. Landfilling practiced in Jordan is generally dumping the waste in trenches with leveling and compacting by trash compactors to reduce the size and the thickness of the layers, and finally covering the waste with 0.5 m from the landfill soil in daily basis. This cover usually ends to be the cap during landfill working time and sometimes after closing.

To assess the efficiency of a certain cover with particular concentration on landfills in arid and semi-arid areas, many field studies should be adopted along an extensive time period, confirming the efficiency of the landfill cover. Cost, time, and labor demands are still the major obstacles for conducting such field studies. Other methods should be considered for evaluation of the landfill cover efficiency and also supporting correct evaluation of the performance of landfill covers. Numerical simulation with appropriate soil parameters is an inexpensive, fast, and labor saved tool for modeling water flow and solute transport in saturated and unsaturated media.

# EXPERIMENTAL INVESTIGATION OF FREE HYDROCARBON RECOVERY IN LAYERED POROUS MEDIA

*M.S. Al-Suwaiyan* (King Fahd University of Petroleum & Minerals, Dhahran, Saudi Arabia)
M. M. Rahman (University of Western Sydney)
S. Lukman & M. H. Essa (King Fahd University of Petroleum & Minerals, Dhahran, Saudi Arabia)

**ABSTRACT:** Leaking underground storage tanks are major sources for groundwater pollution. Cleanup after such incident is a complex process often having low success, mainly due to the inherited subsurface heterogeneity. A physical model was fabricated to examine the influence of uniform heterogeneity in the form of a layer of different aquifer material on the subsurface cleanup, represented by the rate and volume recovered after a controlled crude oil spill is introduced at the left of the tank. A steady one dimensional flow toward the right of the tank was created before a controlled spill was introduced. After equilibrium, the free crude was skimmed from a collection reservoir causing further crude flow towards the reservoir. As the flow of the crude became negligible, further product recovery was attained by increasing the hydraulic gradient forcing further flow towards the collection reservoir. Several experiments were carried out for different porous media combination and the volume collected and its rate were compared to examine the influence of uniform heterogeneity on the remediation process. It was possible to collect 91% of the total spill for the case where the porous media was glass beads. This collected amount was reduced significantly (62%) when a uniform sand layer was present. The results also indicate the even with small thickness of the sand layer, significant reduction in the rate and free product volume collected still existed. Finally the results showed the complication of flow at the micro scale due to layering which was apparent by the presence of irregular free product pockets, smearing and fingering.

## INTRODUCTION

Accidental spills and leakage from storage tanks are among the common sources for groundwater and subsurface pollution. According to the Office of Technology Assessment, the number of leaking underground storage tanks in the United States is between 300,000 and 400,000 which represent 80% of the contaminated sites (NRC, 1995). This clearly indicates the significance of this source and the need to deal with it. Petroleum products are mixtures of many organic compounds most of them are regulated and will obviously affect the quality of groundwater. As a tank leaks, the free product starts to spread in the subsurface and if the release is significant it could overcome capillarity and reach the water table where it will distribute according to the hydraulic properties like residual saturation, displacement head and pore size distribution index (Al-Suwaiyan et al., 2002 & Charbeneau, 2000) In their report, NRC (NRC, 1997), the Committee on Innovative Remediation Technologies reiterated the inadequacy of conventional subsurface treatment technologies and that previous research indicated that only 10% success rate was achieved. Since the first step in the remediation process involves estimating the extent and amount of contaminant, several studies were conducted to relate easily measurable quantities to the extent and amount of contamination. Several of these studies are reviewed by Saleem et al., 2004. The easiest remediation stage should be the removal of the free product, which typically represent about 60% of medium size contamination in a medium size aquifer (Sutherson, 1997). Free product recovery can be achieved by skimming it from monitoring well or trenches within the contaminated zone. Heterogeneity is a very important factor that affects subsurface remediation (Al-Suwaiyan, 2011). A comprehensive study of the influence of heterogeneity on the spread of free phase as well as dissolved contaminant is underway and the initial phase of this study is discussed in this article. The objective of this part of the study is to

examine the influence of layering on subsurface remediation, represented by free product recovery, through experimental investigation.

## MATERIALS AND METHODS

The experimental set up which is a controlled spill tank was fabricated using transparent Plexiglas, screens, monitoring wells and pumps. The fabrication resulted in a tank 135 cm in length and 45 cm high. The tank thickness was 10 cm. The tank consisted of controllable constant water level reservoirs and both ends which are hydraulically connected to the main body which is filled with porous media. Next to the left reservoir, a controlled spill will be initiated at the beginning of each experiment. A sump for collecting the free product is situated just before the right constant head reservoir. Thee fully screened monitoring wells equally spaced are also places on the side wall in order to monitor the free product thickness at various times. Figure 1 shows a front view of the spill tank.
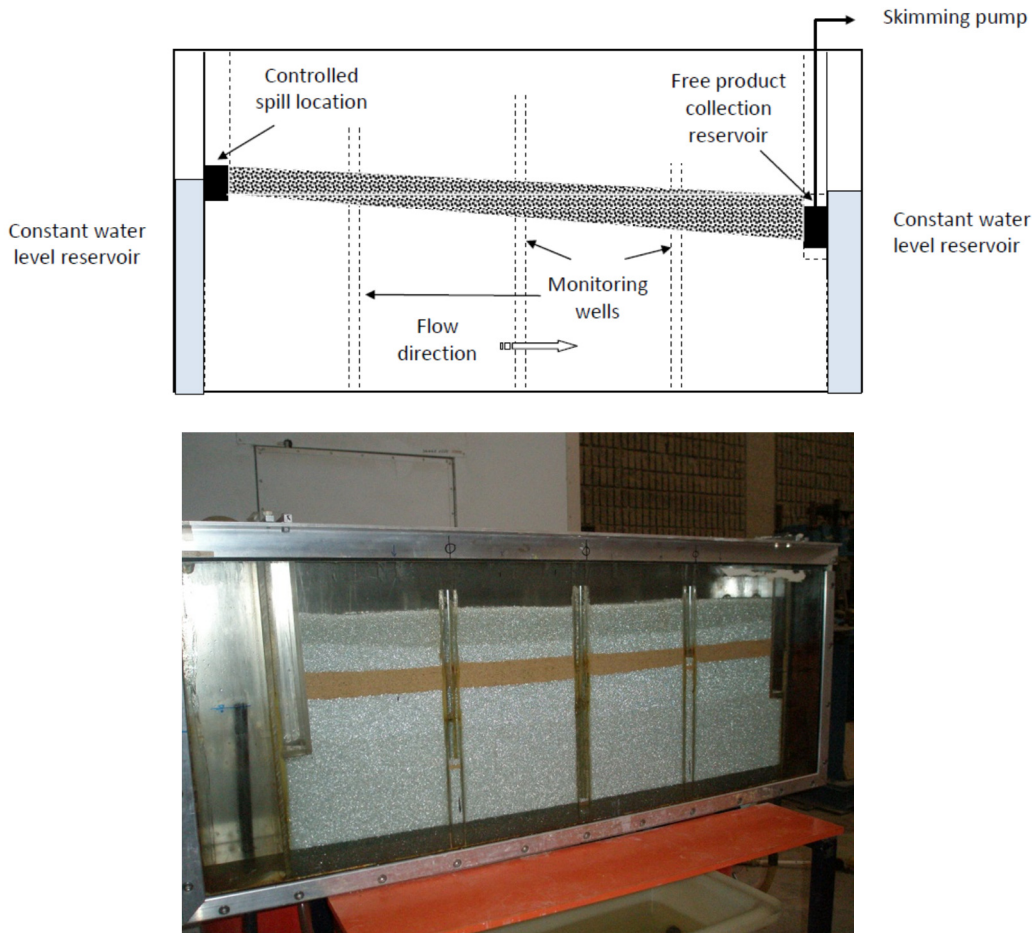


**FIGURE 1.**Experimental setup.

**Porous Media and Contaminant:** Two types of porous media considered in this study: glass beads having a size that passes sieve # 8 and retained on # 12 resulting in a size range between 2.38 and 1.68 mm and uniform sand which is retained on sieve # 16 giving an approximate diameter of 1.18 mm. The contaminant used in the study was Arabian light crude obtained from Saudi Aramco. It is classified as medium density hydrocarbon having a specific gravity of 0.86.

**Description of Experiments:** The first step was to place the proper porous media in the tank using a funnel assuring uniform distribution after which water was added through the bottom so as to prevent any air entrapment. When the desired water thickness, which was about 30 cm, was achieved a hydraulic gradient of about 0.01 was created through the two sides controllable water reservoirs. In a few minutes, this procedure results in steady from towards the right. Crude oil was spilled near the left reservoir of the setup by means of a peristaltic pump. The crude was added intermittently at every 2-3 hours. Certain amount of oil was applied in the left reservoir and waited till oil travels from reservoir to the porous media during the mentioned duration. The flow rate of the pump was maintained at 25 ml/min.

**Experiments:** Four categories of experiments were conducted in order to investigate the effect of layering on the free product collection process. For the first set of experiments, the porous media was homogeneous consisting of glass beads. In the second and third sets, the media was glass beads with horizontal layers of uniform sand of thicknesses 4 cm and 2 cm respectively. Finally the fourth experiments, the porous media was uniform sand.

## RESULTS AND DISCUSSION

During and after the controlled crude spill it formed a visible layer above the original water table which was flowing towards the right reservoir as a result of the original gradient of the water table eventually reaching the skimming reservoir. After reaching equilibrium, the free product recovery was started by skimming the product from the reservoir at approximately constant intervals. Figure 2 show the cumulative volume recovered as a function of time for the four experimental phases. This figure clearly shows the significant difference between the volume collected from homogeneous glass beads and uniform sand which can be attributed to the difference in hydraulic properties related to pore sizes and their distribution. The residual saturation is expected to be the main parameter causing the noticeable difference. The figure also shows that the presence of a sand layer reduces the volume that can be collected which results in more difficulty for subsurface restoration. The figure also indicates that even if the sand layer thickness is reduced it will still have big influence on the volume collection.
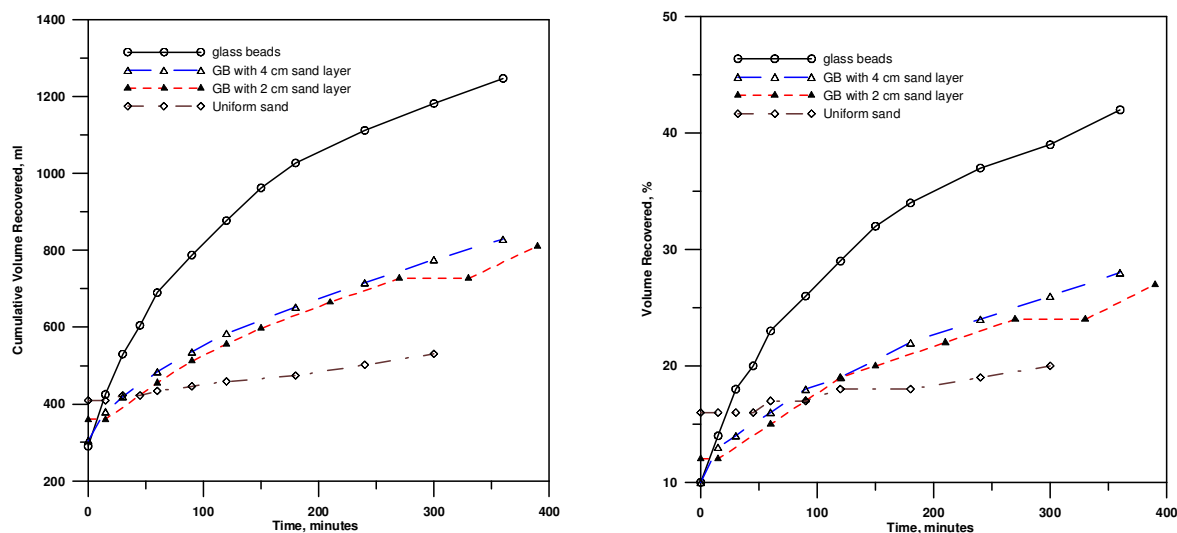


**FIGURE 2**.Recovered volume versus time, first phase.

The second phase of free product recovery involved lowering the water head in the right reservoir in order to increase the hydraulic gradient and invited the free product towards the collection reservoir. Figures 3 shows the cumulative volume collected as a function of time after increasing the hydraulic

gradient. It is clear that increasing the gradient resulted in significant flow of crude when the media was glass beads for the first three hours after which negligible volume was collected. For the other cases, uniform sand and glass beads with sand layers, the figure clearly shows that increasing the hydraulic gradient has small effect in layered glass beads (about 15%) and negligible effect in the case of uniform sand (about 5%). This can be attributed to capillarity and product smearing.
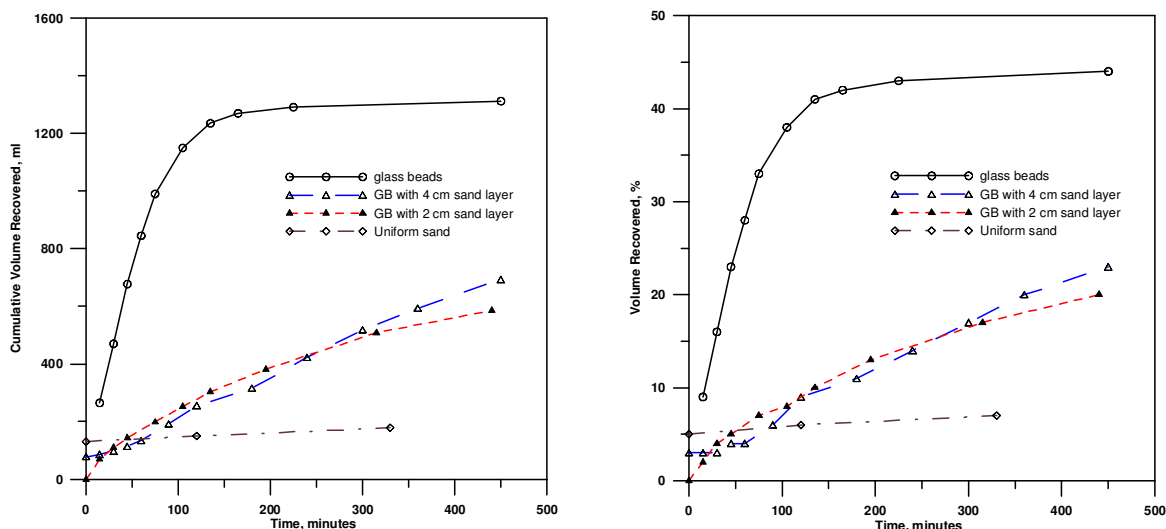


**FIGURE 3**.Recovered volume versus time, second phase.

The various experiments revealed the significant effect of layering on the flow and its pattern which clearly visible in figures 4 and 5, which show the shape and path of the crude oil for two situations. For homogeneous porous media clearly uniform distribution and lack of fingering is clearly missing. On the other hand unpredictable flow configuration and preferential flow paths become the norm as layering is introduced.



**FIGURE 4**.Distribution of free product, uniform media.

After final equilibrium conditions were reached, it was possible to recover 91% of the total spilled volume for the first set of experiments when the porous media was glass beads. On the other hand for the fourth set of experiments where the media consisted of uniform sand only 60% of the total spilled volume was recovered. The effect of the presence of a horizontal sand layer in the glass beads is significant since 4cm layer reduced the collected volume from 91% to 62% which was observed at the end of second set of experiments. Finally it was possible to collect only 64% of the spilled volume in the third set of experiments showing that reducing the thickness of the sand layer to 2 cm did not change the collected volume. This clearly shows that even small layering or heterogeneity will lead to significant reduction in the free product that can be collected which makes subsurface remediation much more difficult.



**FIGURE 5**.Distribution of free product, layered media.

## SUMMARY AND CONCLUSIONS

A comprehensive study of the influence of heterogeneity on the spread of free phase as well as dissolved contaminant is underway and the finding from the initial phase of this study were presented. The objective of this part of the study was to examine the influence of layering on subsurface remediation, represented by free product recovery, through several experimental investigations carried out for different porous media combination. The results indicated that while it was possible to collect significant volume of the initial spill when the porous media was glass beads, the collected volume was reduced significantly when a uniform sand layer was present. The results also indicated the even with small thickness of the sand layer, significant reduction in the rate and free product volume collected still existed. Finally the results showed the complication of flow at the micro scale layering which was apparent by the presence of irregular free product pockets and smearing and fingering

## ACKNOWLEDGEMENTS

## REFERENCES

Al-Suwaiyan, M.S., Bashir, K., Aiban, S.A. and Ishaq, A.M. 2002. "Analytical Model to Quantify Crude Oil Spills in Sandy Layered Aquifer." *Journal of Environmental Engineering, ASCE*, 128(4) :320-326

Al-Suwaiyan, M.S. 2011. "Role of heterogeneity in hindering assessment and cleanup of polluted groundwater aquifers". *IJCEE: International Journal of Civil & Environmental Engineering*, 11(4) :55-67.

Charbeneau, R.J. 2000. *Groundwater Hydraulics and Pollutant Transport*. Upper Saddle River, New Jersey: Prentice –Hall.

National Research Council (NRC). 1995. *Alternatives for Ground Water Cleanup*. National Academy Press, Washington, D.C.

National Research Council (NRC). 1997. *Innovations in Ground Water and Soil Cleanup*. National Academy Press, Washington, D.C.

Saleem, M. Al-Suwaiyan, M., Aiban, S., Ishaq, A.M., Al-Malack, M. and M. Hussain. 2004. "Estimation of spilled hydrocarbon volume-the state-of-the-art." *Environmental Technology*, 25(9) :1077-1090.

Suthersan, S.S. 1997. *Remediation Engineering Design Concepts*. Boca Raton, Florida, CRC Press.

# COMPARATIVE STUDY OF CONCRETE MIXES BY REPLACING AGGREGATES (COARSE & FINE) WITH SLAG

*Arun Pophale* and Mohammed Nadeem
(Visvesvaraya National Institute of Technology, Nagpur, Maharashtra State, India)

**ABSTRACT:** Present study highlights upon suitability of steel slag a waste industrial by-product as alternative to conventional aggregate (Coarse & fine) in concrete constructions. Concrete mixes of M20, M30 & M40 grade (control mixes) cast by replacing aggregates with Slag in 0, 30, 50, 70 & 100%. Properties like density, workability, compressive, split tensile, flexure strengths & soundness were studied. Investigation revealed that compressive strength increased by 4 to 6 % and concrete split tensile and flexure strengths increased by 5 to 8 % at 50% replacements. The replacement of 100% coarse aggregate increased concrete density by 5 to 7 % and split and flexure strength by 6 to 8% over control mixes. The improvement in concrete strength was due to rough surface and higher crushing strength of Slag which improved the bond, flexural & split strength. The higher unit weight of Slag enhanced density of concrete by 7% which could be utilized in special applications. Hence, it could be recommended that Slag could be effectively utilized as aggregates (coarse & fine) in all the concrete constructions like plain concrete and reinforced cement concrete including pavement concrete either as partial or full replacements over a range of 50 to 100%.

## INTRODUCTION

Rapid growth in industrialization and uncontrolled use of natural resources gave birth to numerous kinds of wastes and management of these waste materials has become one of the most complex and challenging problem in the world, which is affecting the environment. The construction industry which is the largest consumer of natural resources has always been at forefront in consuming these waste products helping to curb further damage to our earth & the environment. The consumption of Slag which is waste generated by steel industry, in concrete not only helps in reducing green house gases but also helps in making environmentally friendly material. During the production of iron and steel, fluxes (limestone and/or dolomite) are charged into blast furnace along with coke for fuel. The coke is combusted to produce carbon monoxide, which reduces iron ore into molten iron product. Fluxing agents separate impurities and slag is produced during separation of molten steel. Slag is a nonmetallic inert byproduct primarily consists of silicates, aluminosilicates, and calcium-alumina-silicates. The molten slag which absorbs much of the sulfur from the charge comprises about 20 percent by mass of iron production.

## RESEARCH SIGNIFICANCE IN INDIAN CONTEXT

The availability of good quality normal aggregates (Coarse & fine) is depleting day by day due to tremendous growth in Indian construction industry. A need is felt to identify a potential alternative source of aggregate to fulfill the future growth aspiration of Indian construction industry. Use of slag as an aggregates provides great opportunity to utilize this waste material as an alternative to normally available aggregate and river sand (fine aggregate). Presently, total steel production in India is about 72.20 Million Metric Tonnes and the waste generated annually is around 18 Million Metric Tonnes but hardly 25 % is being used mostly in cement production. Hence, the focus of present research is targeted upon feasibility & use of such a waste slag in developing country like India.

## STUDY SCOPE

In this study, concrete of M20, M30 & M40 grades were considered for a W/C ratio of 0.55, 0.45 & 0.40 respectively with the targeted slump of 100±25 mm for the replacement of 0, 30, 50, 70 & 100 %

of aggregates (Coarse & fine) with that of slag aggregate. These concrete mixes were studied for the properties like density, workability (slump & compaction factor), compressive, split tensile and flexure strengths & soundness.

## EXPERIMENTAL INVESTIGATION

**Raw Materials:** In this investigation, Slag from the local steel making plant, normal crushed coarse aggregate from Panchgaon Basalt query, natural sand from the local Kanhan river and Portland Pozzolana cement were used as shown in Figure 1.



**FIGURE 1 – View Of Slag, Normal Crushed Coarse Aggregate & Natural Sand**

**Mix Proportions:** The mix proportions were made for a control mix of slump 100 ± 25 mm for M20, M30 & M40 grade of concrete for w/c ratio of 0.55, 0.45 & 0.40 respectively by using IS-10262-2009 method of mix design. For each grade of concrete, total five mixes were made by replacing normal crushed coarse aggregate with slag aggregate, keeping w/c ratio as constant (control mix) by 0, 30, 50, 70 & 100 % replacements given in Table 1 is repetitive for all the grade of mixes M20, M30 & M40.

**TABLE 1 – Replacement Proportions of Aggregates**

| Mix No. | Normal Crushed Coarse Aggregate -% | Slag Aggregate-% | Natural sand-% | Slag sand-% |
|---|---|---|---|---|
| Control Mix | | | | |
| 1 | 100 | 0 | 100 | 0 |
| Replacement of Coarse aggregate | | | | |
| 2 | 70 | 30 | 100 | 0 |
| 3 | 50 | 50 | 100 | 0 |
| 4 | 30 | 70 | 100 | 0 |
| 5 | 0 | 100 | 100 | 0 |
| Replacement of Fine aggregate (Natural Sand) | | | | |
| 2 | 100 | 0 | 70 | 30 |
| 3 | 100 | 0 | 50 | 50 |
| 4 | 100 | 0 | 30 | 70 |
| 5 | 100 | 0 | 0 | 100 |

The final mix proportions for control mixes of M20, M30 & M40 grade of concrete obtained as per I.S. 10262-2009 guidelines were arrived given in Table 2

**TABLE 2 – Mix Proportions Of Control Mixes**

| Mix Proportions of Control Mixes | | | |
|---|---|---|---|
| Ingredients (Kg/cum) | M20 | M30 | M40 |
| Cement | 348 | 362 | 407 |
| Water (W/C ratio, 0.55,0.45 &0.40) | 192 | 163 | 163 |
| Mass of normal coarse aggregate | 1187 | 1225 | 1198 |
| Mass of fine aggregate | 725 | 748 | 731 |
| Super Plasticizer (PC based) | 0.00 | 2.17 | 3.26 |
| **Total Weight** | **2452** | **2500** | **2502** |

**Test Set-up:** The 4 in.(100 mm) cubes with a set of 3 cubes, each were cast for compressive strength .and split strength at 7, 28, 56, 91 & 119 days time. Beam moulds of size 4in x4in x20in i.e.(100x100x500mm) for flexure strength and 4 in.(100 mm) cubes for soundness test for 7 & 28 days time respectively. After the cast, all the test specimens were put into the water tank for curing maintaining temperature of 89.6±35 °F (27±2 °C) as per IS requirements. The concrete was tested for slump cone test, compaction factor test and wet density as per the IS-1199 –Methods of sampling and analysis of concrete, for each mix of concrete. To check effect of Sulfate attack on concrete strength properties, concrete cubes (M20, M30 & M40 grade) were kept in normal water as well as in solution of $MgSO_4$ (6% concentration) for 28 & 119 days and later tested for compressive strength and checked for cube weights. In addition to this, 150 mm cubes were cast for all the grades for 7 & 28 days time for comparison & co-relation observed between 85 to 90%. The test-set-up is shown in Figure 2.



**FIGURE 2 – Concreting Test Set-Up**

## RESULTS AND DISCUSSIONS

The results on strength of concrete mixes (M20, M30 & M40 grades) made by 0, 30, 50, 70 & 100%  replacement of aggregates (coarse & fine) for the w/c ratio of 0.55, 0.45 & 0.40 respectively were obtained and discussed as given below,

**Compressive Strength with Coarse Aggregate Replacements.** The results indicated that compressive strength was higher by 2 to 4% in all the mixes at 30 to 50 % replacements. The strength improvement was notably observed at 100 % replacement level in the range of 5 to 7% compared to the control mixes. The improvement was due to good adhesion between crystallized slag aggregate and cement paste due to rough surface of slag aggregate, results shown in Figure 3.
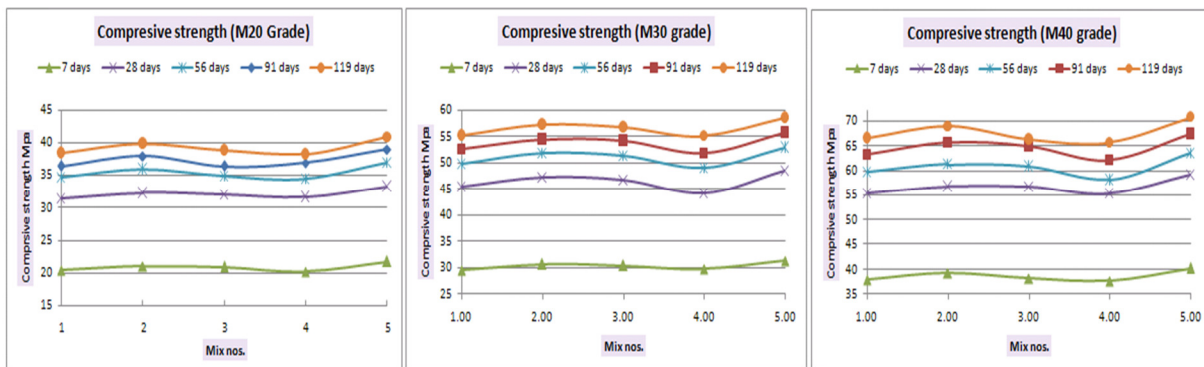


**FIGURE 3 – Concrete Compressive Strength**

**Compressive Strength with Fine Aggregate Replacements.** The results indicated that compressive strength was higher by 4 to 6 % in all the mixes at all ages for the replacement level inbetween 30 to 50%. Strength reduction was observed at 100 % replacements of fine aggregate with granular slag by 7 to 10%

which was attributed to the coarser particles affected on cohesive properties of concrete shown in Figure 4.
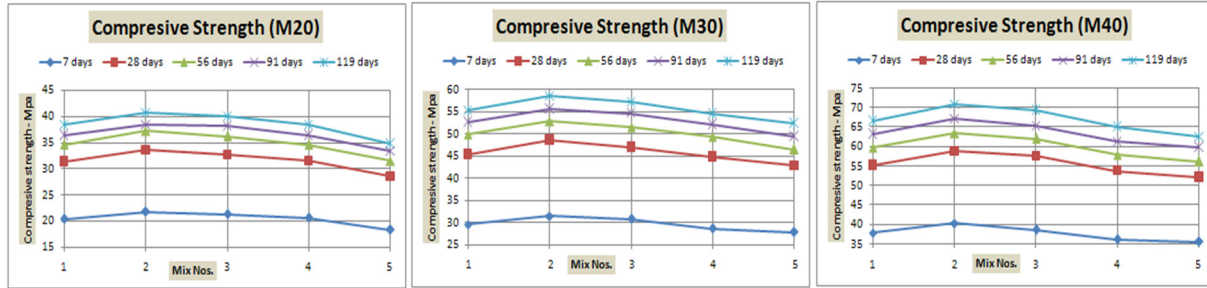


**FIGURE 4 – Concrete Compressive Strength**

**Split Tensile & Flexure Strengths with coarse aggregate replacements.** The split tensile & flexure strength at 7 & 28 days time for all the concrete mixes reported higher strength results in the range of 6 to 8 % over control mixes at all ages. The increase in strength was due to the excellent rugosity of slag aggregate which ensured strong bonding and adhesion between aggregate particles and cement paste shown in Figure 5.
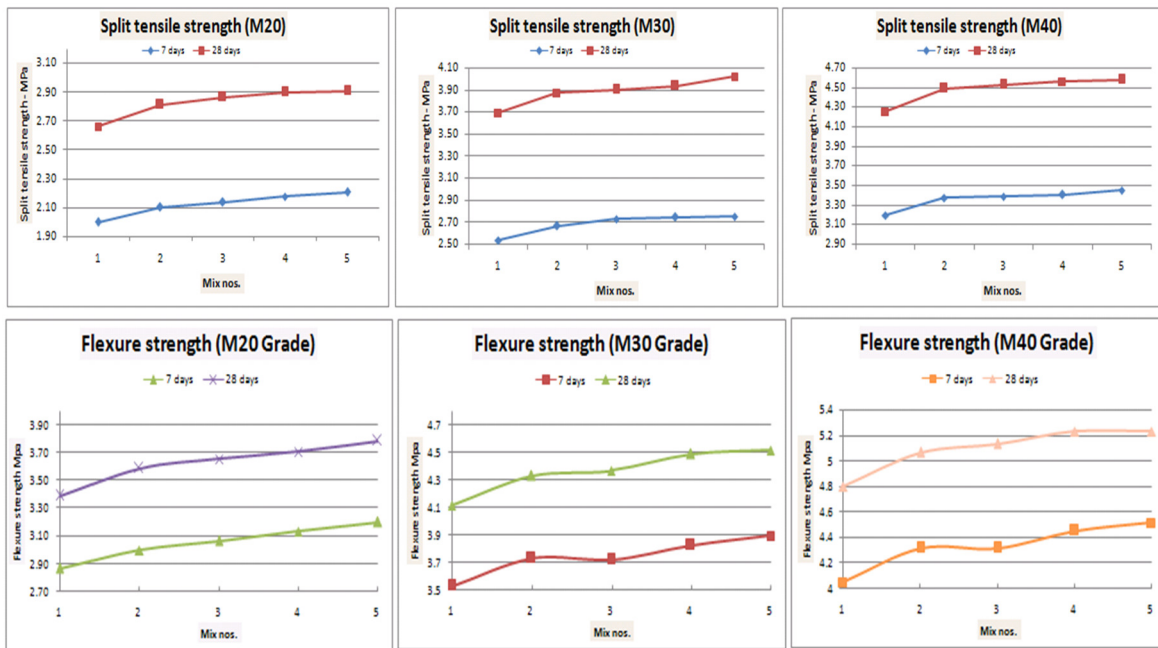


**FIGURE 5 – Concrete Split Tensile & Flexure Strength**

**Split Tensile & Flexure Strengths with Fine Aggregate Replacements.** The split tensile & flexure strengths found improved by 5 to 6 % at 30 to 50% replacement levels but it reduced by 6 to 8 % at 100 replacements as shown in Figure 6.

**Soundness Test in MgSO$_4$ Solution.** The comparative results of concrete compressive strength after 28 & 119 days for M20, M30 & M40 (Coarse & Fine aggregate replacements) showed no significant change on cubes kept in MgSO$_4$ solution as compared to cubes cured in normal water. The maximum variations in strength are found to be ± 2 % which is insignificant from Figure 7.

**Workability.** The workability of concrete decreased from 0 % to 100 % replacement level in M20 grade concrete by about 33% but in M30 & M40 grade of concrete it improved upto 30 to 50 % replacement level and later dropped at 100 % replacements by about 8 % in case of replacing coarse aggregate with slag shown in Figure 8. The phenomenon could be due to the rough surface of slag aggregated requiring more finer material to overcome the frictional forces. The workability improved in higher grades of concrete (M30 & M40) due to potential availability of finer materials. In case of replacing fine aggregate with slag the workability improved upto 50 % replacement level by 20 % and later dropped at 100 % replacement level but remained almost equal to control mix shown in Figure 8.
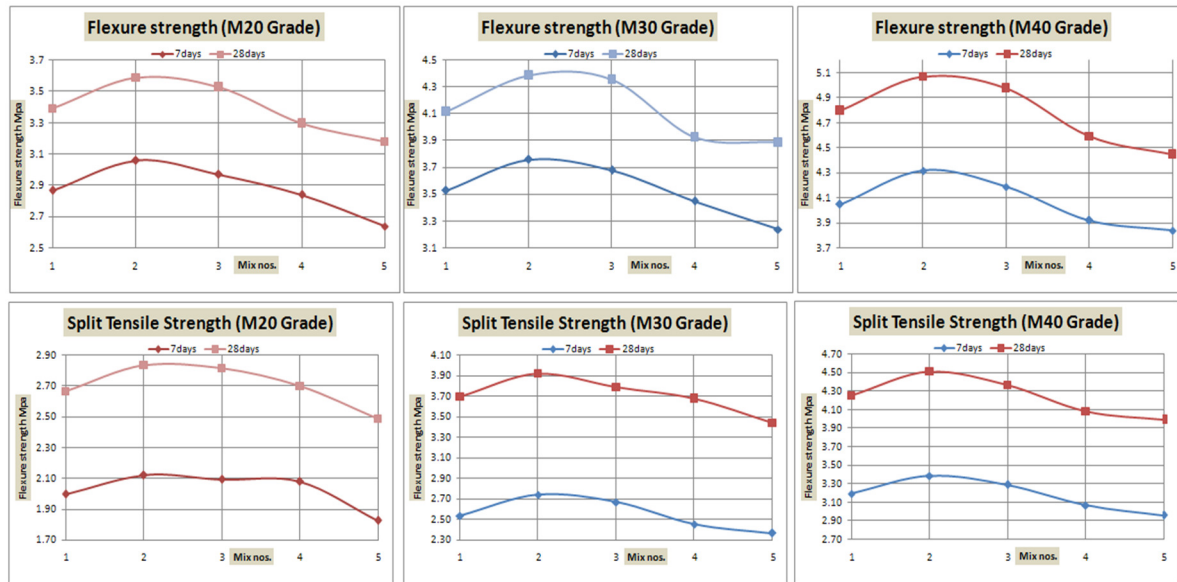


**FIGURE 6 – Concrete Split Tensile & Flexure Strength**
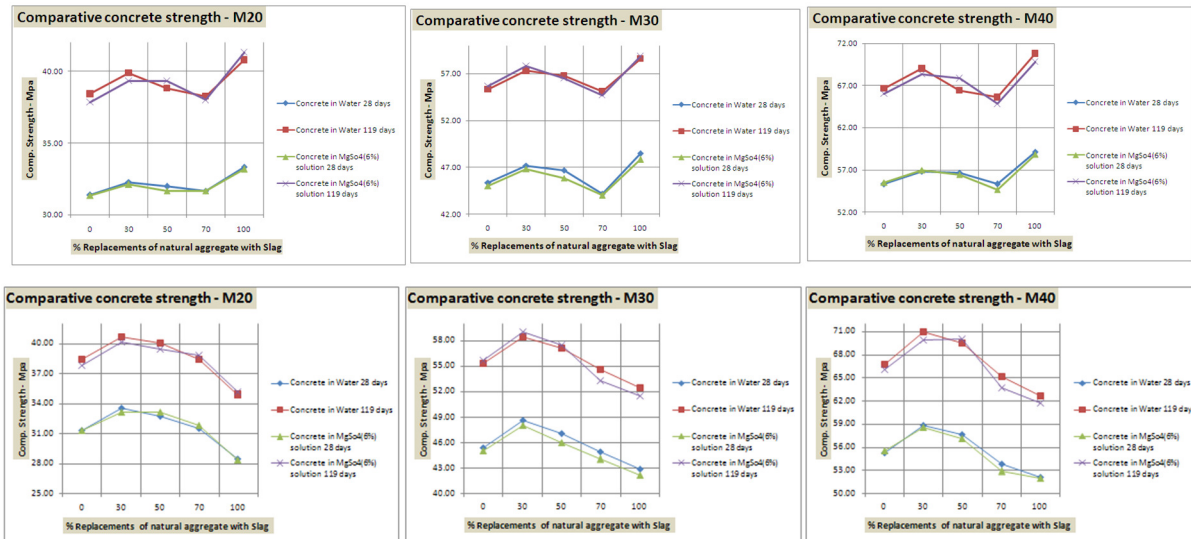


**FIGURE 7 – Comparison Of Compressive Strength In Mgso₄ Solution Vs Normal Water**

**Concrete Density.** The bulk density of slag aggregate was found to be 9.83 % higher than normal crushed aggregate which enhanced density of concrete. The concrete density achieved was higher by 5 to 7 % than control mix concrete using slag aggregate. The highest density was found in M30 grade of

concrete at 100 % replacement of slag aggregate. The bulk density of granular slag was 27 % lighter than naturally fine aggregate which was reflected in the concrete density also by 3 % shown in Figure 9.

## SUMMARY, CONCLUSIONS AND FUTURE SCOPE

The conclusions are drawn as below:

1. The compressive strength of concrete increased by 4 to 6% for replacements of both coarse & fine aggregates from 30 to 50%. However, in case of coarse aggregate the compressive strength increased by 5 to 7% and decreased in case of fine aggregate by 7 to 10% at 100% replacement over control mixes in M20, M30 & M40 grade of concrete.
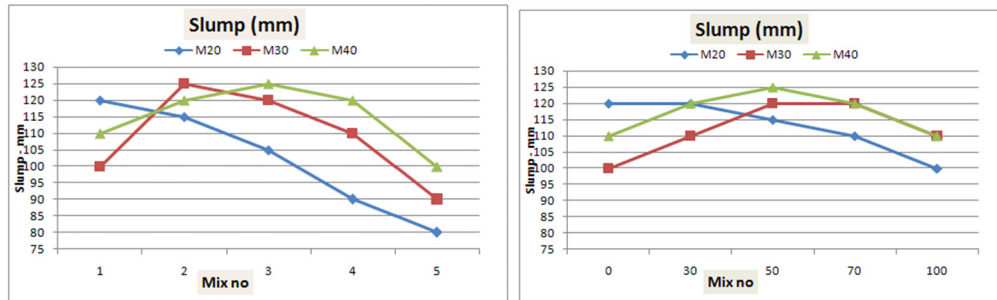


**Figure 8 – Workability (Slump – mm)**
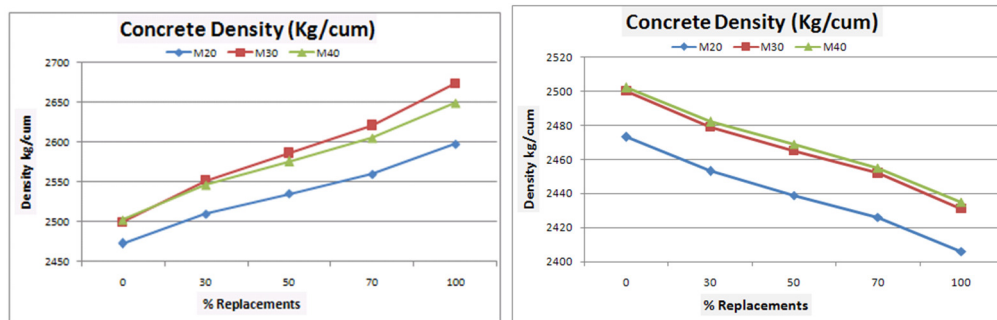


**Figure 9 – Concrete Density**

2. It could be said that 100% replacement of normal crushed coarse aggregate with slag aggregate, improved the flexure and split tensile strength by about 6 to 8 % in all mixes. The improvement in strength was attributed to the rough surface texture which ensured strong bonding and adhesion between aggregate particles and cement paste. In case of natural fine aggregate replacement with Slag fine aggregate the strength increased was for 50% by 5 to 6 % but reduced at 100% replacements by 6 to 8 %. The reason for reduction in strength for 100 % replacement could be attributed to the presence of coarser particle sizes which could be overcome by addition of finer materials.

3. The results of soundness test of concrete indicated no significant negative impact on the concrete strength properties, the strength variation was observed to be ± 2%.

4. The workability of concrete decreased with 100 % replacements of normal crushed coarse aggregate with slag by about 30 % in M20 grade and about 8 % in M30 & M40 grade of concrete compared to control mix of concrete. The drop in workability could be attributed to porous and rough surface of slag aggregate which improved in higher grade of concrete due to availability of more fine contents. In case of fine aggregate replacement the workability improved by 20% upto 50 % replacements and at 100% replacement it was similar with control mixes.

5. It could be said that 100 % replacements of coarse aggregate with slag enhanced concrete density by about 5 to 7 % in all the concrete mixes. The improvement in density was due to the higher

unit weight of Crystallized slag which is 9 % higher than the natural aggregate. The density of concrete reduced by 3% in case of replacing fine aggregate with granular slag.

Based on the above summary and conclusions, it could be recommended that Slag due to its chemical composition and its chemical inertness (soundness of aggregate & concrete) could be effectively utilized as aggregates (coarse & fine) in all the concrete constructions like plain concrete and reinforced cement concrete including pavement concrete either as partial or full replacements over an observed range of 50 to 100%. Since such Slags have compatible performance at par with conventional aggregates, their immediate use in Plain concrete & Reinforced concrete including pavements shall reduce the construction cost significantly.

Future Scope - collection of data for characterization of such slag wastes generated from all the steel making plants is of extreme importance & could be taken up immediately and study of environmental problems created by such wastes remaining without recycling and proper utilization.

**REFERENCES:**

Isa Yuksel, Omer Ozkan, turhan Bilir. 2006. "Use of granulated blast furnace slag in concrete as fine aggregate." *ACI materials journal*, May-June:203-208.

Isa yuksel, Ayten Genc. 2007. "Properties of concrete containing nonground ash and slag as fine aggregate." *ACI materials journal*, July-August:397-403.

Juan M. Manso, Javier J. Gonzalez, Juan A. Polanco. 2004. "Electric arc furnace slag in concrete." *Journal Of Materials In Civil Engineering © ASCE*, November/December:639-645.

Keun Hyeok Yang, Jin Kyu Song, Jae-Sam Lee. 2010. "Properties of alkali activated mortar and concrete using lightweight aggregates." *Materials and structures,* 43:403-416.

Li Yun-feng, Yao Yan, Wang Liang. 2009. "Recycling of industrial waste and performance of steel slag green concrete." *J cent. South university technology*, 16:768-773.

Lun Yunxia, Zhou Mingkai, Cai Xiao, Xu Fang. 2008. "Methods for improving volume stability of steel slag as fine aggregate." *Journal of Wuhan University of Technology-Mater. Sci. Ed.*, 3, October:737-742.

L. Zeghichi.2006."The effect of replacement of naturals aggregates by Slag products on the strength of concrete." *Asian Journal of Civil Engineering (Building and Housing)*. Vol. 7:27-35.

Tarun R Naik, Shiw S Singh, Mathew P Tharaniyil, Robert B Wendfort. 1996. "Application of foundry by product materials in manufacture of concrete and masonry products.", *ACI Materials Journal*, 93:41-50.

Xu Delong, Li hui. 2009. "Future resources for eco building materials – Metallurgical slag." *Journal of wuhan university of technology-Mater.Sci edi.,* June:451-456.

# HIGH STRENGTH CONCRETE BY RECYCLED AGGREGATE AND MIXING BLAST FURNACE SLAG

*S. U Hong*, Y. S Cho, S .K Back, H. S Jang (Hanyang University, Seoul, KOREA) and
Yong Taeg Lee (Hanbat National University, Daejeon, KOREA)

**ABSTRACT:** The aim of this paper is to increase of the utilization and improve of recognition and to provide reliable data and basic date for maintenance of building that will be built of recycled aggregate. By using the high strength concrete (40, 50, 60MPa), we analyzed how to change the strength by the substitution. And the addition rates are 0%, 30%, 50% and 100%. In the compressive strength test of the age of 28days, the concrete in which the recycled aggregate is mixed could know that it was nearly equal or it showed the a little bit low strength as the natural aggregate concrete. In case of substituting the recycled aggregate in the specimen, the intensity increased the average 0.93% and 0.1% more than the specimen using the natural aggregate in the specimen of 40 and 50MPa. But the intensity decreased the average 3.03% in the specimen of 60MPa. It is considered in being the thing due to the material generated by the latent hydraulic reactivity because of the powder of the recycled aggregate which it generates when producing the high quality cyclic aggregate and blast furnace slag.

## INTRODUCTION

Driven by economic development, buildings are increasingly growing in size and the number of stories. In this accord, natural aggregates are increasingly in demand, and thus the amount of natural aggregates in the nation is in decreasing trend. Also as existing buildings are running out in life span, more and more construction wastes are generated through building demolition each year, and the more construction wastes, the more pollutions and damaged are being inflicted to natural environment. Therefore, use of recycled aggregates from construction wastes is inevitable both in economical aspect and in environmental aspect. For such reason, the government also is promoting use of recycled aggregates legally.

However, recycling of construction wastes as aggregates involves many problems presently. One of the problems is that it is not easy to apply recycled aggregates immediately to concrete structure due to the consciousness that recycled aggregates fall slightly behind general natural aggregates in strength. Due to the negative view on such recycled aggregates and the few structure recycled aggregate is not actively utilized despite the impending necessity for use of it. Therefore, in this study, an analysis was done on how compressive strength changes depending on substitution rate when recycled coarse aggregates were substituted to 40MPa, 50MPa and 60MPa high strength concrete instead of normal strength concrete, and the correlation with compressive strength by wave velocity was compared and analyzed with the use of ultrasonic pulse velocity method among nondestructive test methods to predict compressive strength the major indicator of concrete quality evaluation and defects ultimately in order to increase the use of recycled aggregates and improve recognition of it.

Therefore, this study has the purpose to provide reliable data for the maintenance of structures by analyzing the correlation with compressive strength by wave velocity with the use of the compressive strength characteristics of high strength concrete in which recycled aggregates was mixed and ultrasonic

pulse velocity method among nondestructive test methods. To recycled aggregates produced from waste concretes which are demolished from concrete structure, components hazardous to concrete quality may be added, causing alkaline aggregates reaction etc, and it is very difficult to remove such components completely in practice. In addition, recycled aggregates extracted from concretes which were produced in the past with the use of cements with massive alkaline may include more content of alkaline than general natural aggregates. Therefore, as a countermeasure to this problem, blast furnace slag fine powers were mixed in for use. As for recycled aggregates, the study was conducted by substituting recycled coarse aggregates by 0%, 30%, 50% and 100% to high strength concretes of 40MPa, 50MPa and 60MPa design standard strength according to aged days.

## MATERIAL AND METHODS

As for cement, ordinary Portland cements of density 3.15g/cm$^3$ were used, and blast furnace slag was used as admixture to produce recycled aggregates concrete that includes blast furnace slag. As blast furnace slag, ones that meet KS F 2563 quality requirement were used, and Table 1 shows the physical property.

**TABLE 1.** Property of Furnace Slag

| $SiO_2$ (%) | $AlO_3$ (%) | MgO (%) | $SO_3$ (%) | CaO (%) | SPECIFIC GRAVITY | FINENESS (cm2/g) |
|---|---|---|---|---|---|---|
| 25.74 | 8.09 | 2.95 | 2.19 | 55.24 | 3.09 | 4,295 |

As for the coarse aggregates used in combining recycled aggregates concrete, the 20mm crushed stones produced in Namyangjucity of Gyeonggido in Korea province were used, where sea sands were used as general fine aggregates, and as for recycled aggregates, class I recycled coarse aggregates by KS F 2573 produced in high class treatment method by a company with production certification were used. This falls under the allowed scope of the quality for concrete recycled aggregates proposed by recycled aggregates quality standard and shows outstanding quality as to confidently be applied as the quality standard of natural aggregates.

**TABLE 2.** Experiment Factor and Level

| FACTOR | LEVEL | | |
|---|---|---|---|
| Design Strength(MPa) | 40 | 50 | 60 |
| W/B(%) | 35.6 | 30.3 | 26.0 |
| S/a(%) | 49.7 | 48.0 | 47.7 |
| Slump flow value(mm) | 600 | | |
| Natural coarse aggregate max size(mm) | 20 | | |
| Recycled coarse aggregate max size (mm) | 20 | | |
| | 100/0 | 100/0 | 100/0 |
| | 70/30 | 70/30 | 70/30 |
| Substitution Ratio (%) | 50/50 | 50/50 | 50/50 |
| | 0/100 | 0/100 | 0/100 |

The experiment factors and levels by each design standard are shown in Table 2. Blast furnace slag fine powder the admixture were mixed in with reference to slump flow value 600mm of 40MPa, 50MPa and 60MPa the design standard strengths for use of natural coarse aggregate 20mm, and recycled aggregates(0%, 30%, 50% and 100%) by each design standard strength were substituted to produce 12 cases. Also through measurement of compressive strength and nondestructive test with strength and substitution rate as parameters, the changes of compressive strength were identified.

**TABLE 3.** Mixing ratio of concrete specimen

| MPa | RATIO (%) | | UNIT WEIGHT (kg/m³) | | | | | | AE |
|---|---|---|---|---|---|---|---|---|---|
| | Natural | Recycled | W | C | BS | S | G | RG | |
| 40 | 100 | 0 | 167 | 328 | 141 | 850 | 870 | 0 | 5.16 |
| | 70 | 30 | | | | | 609 | 61 | |
| | 50 | 50 | | | | | 435 | 435 | |
| | 0 | 100 | | | | | 0 | 870 | |
| 50 | 100 | 0 | 167 | 386 | 165 | 788 | 863 | 0 | |
| | 70 | 30 | | | | | 604 | 59 | |
| | 50 | 50 | | | | | 432 | 431 | |
| | 0 | 100 | | | | | 0 | 863 | |
| 60 | 100 | 0 | 169 | 487 | 163 | 733 | 813 | 0 | |
| | 70 | 30 | | | | | 569 | 244 | |
| | 50 | 50 | | | | | 407 | 406 | |
| | 0 | 100 | | | | | 0 | 813 | |

Concrete mixing ratios are shown in Table 3. Experiment was conducted by selecting a mixture that includes blast furnace slag fine powder suitable for high strength concrete mixture and poly carboxylic acid admixture in compliance with the condition of 280kg/m³ or above and unit quantity or 185kg/m³ below specified by Quality Standard for Recycled Aggregates, 2009. As for other amounts excluding the aggregates by recycled coarse aggregates substitution rates, cement amount, blast furnace slag amount, fine aggregate amount and high performance AE admixture amount etc, the combination ratios were set as shown in Table 3 in similar conditions by each strength.

With reference to mixture table, 240 specimens for compressive strength test and 12 specimens of nondestructive test were produced. The specimens for non-destructive test were produced in box shape of 600mm width, 600mm length and 200mm height for measurement of ultrasonic pulse velocity one of non-destructive test methods. Ø100mm holes were punched at the bottom of molds to measure ultrasonic pulse velocity by ages respectively on the 1st day, 3rd day, 7th day and 28th day. That way the plan to pile high strength concrete in which recycled aggregates are combined in specimen mold was established.

## RESULTS AND DISCUSSION

Measuring compressive strengths by 5 specimens by ages respectively on the 1st day, 3rd day, 7th day and 28th day, the average of the measured values was selected as result value. The measurement results are shown in Table 4. According to Table 4, as of age 28th day, the compressive strengths of each specimen show varying rate of increase and decrease depending on substitution rate. Specimen of strength 40MPa increased slightly by about 0.6% in strength at 30% substitution rate over natural aggregate

concrete, decreased by 1.2% at 50% substitution rate, and increased slightly by 4.5% at 100% substitution rate. 60MPa strength specimen increased slightly by 0.8% in strength at 30% substitution rate over natural aggregate concrete, decreased by 4.4% at 50% substitution rate and decreased by 5.5% at 100% substitution rate. Such results indicated that recycled aggregates increase in general in strength over specimen that used general natural aggregates only when substitution rate is 30%.

**TABLE 4.** Results of Compressive Strength

| MPa | RATIO (%) | | COMPRESSIVE STRENGTH (MPa) | | | |
|---|---|---|---|---|---|---|
| | Natural | Recycled | 1day | 3day | 7day | 28day |
| 40 | 100 | 0 | 10.86 | 20.40 | 30.57 | 33.84 |
| | 70 | 30 | 9.16 | 18.16 | 31.46 | 34.04 |
| | 50 | 50 | 8.92 | 17.62 | 32.04 | 33.44 |
| | 0 | 100 | 8.58 | 18.94 | 31.42 | 34.98 |
| 50 | 100 | 0 | 11.70 | 28.14 | 46.02 | 47.56 |
| | 70 | 30 | 12.54 | 32.22 | 46.46 | 52.00 |
| | 50 | 50 | 9.94 | 25.98 | 42.92 | 45.44 |
| | 0 | 100 | 11.48 | 22.52 | 41.48 | 45.42 |
| 60 | 100 | 0 | 22.24 | 32.88 | 54.36 | 61.36 |
| | 70 | 30 | 19.44 | 33.26 | 49.06 | 61.86 |
| | 50 | 50 | 20.90 | 37.32 | 52.96 | 58.68 |
| | 0 | 100 | 20.40 | 33.42 | 49.12 | 57.98 |

It is contrary to the general recognition that use of recycled aggregates only drops strength. This is presumed to be a phenomenon caused by recycled aggregates powders which were generated when recycled aggregates were produced and attached to recycled aggregates. Recycled aggregates are produced by shocking and crushing waste concrete, and in this course, 1mm or less powders are created. In general production course, these powders are created at about 20% to 30%, and in particular, in case high quality recycled aggregates are produced, powders of recycled aggregates are created by 40% or so. Since these powders of recycled aggregates include $CaO$, $SiO_2$, $Al_2O_3$, $Fe_2O_3$ etc which are used as raw material of cement, it is known that they may be used as raw material of cement as well. Based on this point, it is judged that the more the substitution rate of recycled aggregates, the more calcium hydroxide the powders attached to recycled aggregates produce through reaction with water in combining, leading to more latent hydraulic activity reaction. Thus it is presumed that the substances created in this course fill the fine cracks inside the aggregates that occurred while recycled aggregates were produced through crushing process, and also the fine textures of cement composed through hydration, so they complement the strength by solidifying combination.

However, it appears that in case the substitution rate of recycled aggregates increases by 50% and 100%, strength decreases largely. That is presumably because the cement amount and blast furnace slag amount that react are limited regardless the substitution rate of recycled aggregates compared with the amount recycled aggregates powders that change according to substitution rate, and thus the amount of substance created after reaction also is limited that much. Therefore, it is anticipated that there are substitution rate of recycled aggregates and the critical amount of reaction for cement and blast furnace slag, and further study must be done on it.

Ultrasonic Pulse Velocity method was performed on members by ages on the 1st day, 3rd day, 7th day and 28th day by each member. As for the results of non-destructive test, wave velocity was measured 20 times in each test, and average was taken as result value. The results are shown in Table 5. As for the change of ultrasonic pulse velocity of specimen as of the 28th day in Table 5, strength 40MPa specimen decreased in strength by 0.29% or so at 30% substitution rate over natural aggregate concrete, by 0.76% at 50% substitution rate, and by 1.02% at 100% substitution rate. Strength 50MPa specimen decreased in strength by 2.34% or so at 30% substitution rate over natural aggregate concrete, by 3.35% at 50% substitution rate, and by 3.24% at 100% substitution rate. Strength 60MPa specimen decreased in strength by 2.51% or so at 30% substitution rate over natural aggregate concrete, increased by 0.75% at 50% substitution rate, and decreased by 1.54% at 100% substitution rate. Therefore, with reference to age 28th day, it is shown that the more recycled aggregates are substituted, the more ultrasonic pulse velocity of each specimen decreases than specimen of general natural aggregates.

**TABLE 5.** Results of Ultrasonic Pulse Velocity

| MPa | RATIO (%) | | ULTRASONIC PULSE VELOCITY (m/sec) | | | |
|---|---|---|---|---|---|---|
| | Natural | Recycled | 1day | 3day | 7day | 28day |
| 40 | 100 | 0 | 3737.13 | 3945.54 | 4147.45 | 4194.85 |
| | 70 | 30 | 3707.98 | 3896.11 | 4161.16 | 4182.65 |
| | 50 | 50 | 3707.78 | 3893.59 | 4160.00 | 4162.96 |
| | 0 | 100 | 3592.31 | 3848.99 | 4095.44 | 4152.23 |
| 50 | 100 | 0 | 4037.86 | 4112.29 | 4282.78 | 4369.13 |
| | 70 | 30 | 3950.00 | 4071.11 | 4249.14 | 4267.03 |
| | 50 | 50 | 3954.35 | 4060.26 | 4202.00 | 4222.65 |
| | 0 | 100 | 3886.41 | 3973.79 | 4197.13 | 4227.55 |
| 60 | 100 | 0 | 4079.74 | 4178.78 | 4219.54 | 4335.91 |
| | 70 | 30 | 3958.29 | 4113.65 | 4183.33 | 4227.09 |
| | 50 | 50 | 4075.61 | 4173.83 | 4308.09 | 4368.13 |
| | 0 | 100 | 3875.18 | 4142.2 | 4236.43 | 4269.08 |

**CONCLUSION**

In the test of compressive strength of age 28th day, the concretes in which recycled aggregates are mixed showed strength nearly equivalent to or slightly lower than natural aggregates. In case recycled aggregates are substituted to specimen, 40MPa specimen increased in strength by average 0.93% over specimens that used natural aggregates only, 50MPa specimen increased in strength by average 0.1%, and 60MPa specimen decreased in strength by average 3.03%. This is presumed to be due to the recycled aggregate powder that occur during production of high quality recycled aggregates and the substance created by latent hydraulic activity of blast furnace slag. Also, it was found that if recycled aggregates are substituted through nondestructive test method by ultrasonic pulse velocity, pulse velocity decreases slightly. However, it is also found that ultrasonic pulse velocity does not change significantly by the substitution rate of recycled aggregates. In case recycled aggregates are substituted as of the 28th day of age, 40MPa specimen showed average 0.69% decrease of pulse velocity, 50MPa specimen average 2.98% decrease of wave velocity, and 60MPa specimen average 1.1% decrease of wave velocity.

**ACKNOWLEDGMENTS**

**REFERENCES**

Jang, Hyun-Suk, Hong, Seong-Uk, Baek, Sang-Ki, Cho, Young Sang and Lee, Yong-Taeg. 2011. "Compressive Strength Estimation System of Concrete Specimens according to Replacement ratio of Recycled Aggregate using Nondestructive tests". AIK. 27.11 : 21-28

Yong Taeg, Seong Uk Hong, Hyun Suk Jang, Sang Ki Baek and Young Sang Cho. 2012. "Compressive Strength Estimation of Recycled Coarse Aggregate Concrete Using Ultrasonic Pulse Velocity". Applied Mechanics and Materials 147: 288-292

# LEACHING CHARACTERISTICS OF SCRAP CRT GLASSES AND LEAD SEPARATION BY A SHS PROCESS

*Jianxin Zhu*, Yu Wang

(Research Center for Eco-Environmental Sciences, Chinese Academy of Sciences, Beijing, China)

**ABSTRACT:** The amount of e-waste or waste electric and electronic equipment (WEEE) in the word is increasing ultimately. Among them, computer monitor and television cathode ray tubes (CRTs) that account for about 70 wt.% of the total mass are one of the key for WEEE recycling. Toxic characteristic leaching procedure (TCLP) was used to assess the environmental risk of lead contained glass of CRTs, and the feasibility to reuse hazardous waste CRT glass by self-propagating high-temperature synthesis(SHS) was investigated, where Mg and $Fe_2O_3$ was adopted as reagents. It was shown that the maximum CRT glass content is about 70%, combustion wave velocity is 0.5-6.5 mm/s and combustion temperature is 1000-2000 $^o$C. Both of the combustion wave velocity and temperature decrease linearly with the increase of CRT glass content. We found that self-propagating reaction in the presence of Mg and $Fe_2O_3$ could separate lead preferentially and superfine lead oxide nano-particles were obtained from a collecting chamber. The separation ratio was related closely to the amount of funnel glass added in the original mixture. At funnel glass addition of no more than 40 wt.%, over 90 wt.% of lead was recovered from funnel glass. The PbO nano-particles collected show good dispersion and morphology with a mean grain size of 40 - 50 nm. Results of XRD and SEM showed that samples after SHS are mainly consisted with glass ceramic composite, in which Pb and Ba could be solidified and stabilized effectively. The concentration of Pb and Ba samples after SHS according to the TCLP are much lower than the threshold values for hazardous wastes regulated by domestic and international environmental standards.

## INTRODUCTION

Wasted cathode ray tube (CRT) glass from television or computer monitors is growing at an escalating rate. According to a study, a sharp rise of obsolete personal computers and televisions may occur between 2008 and 2012, with the amount of discarded PCs and TVs reaching 93.36 million units and 74.31 million units, respectively in 2012. In response to the growing volume of CRTs, the development of recycling or disposing is a very important and urgent issue.

The self-propagating high-temperature synthesis (SHS) method is well known as an attractive alternative to the conventional methods for manufacturing advanced materials. The underlying characteristic of SHS relies on the highly exothermic reaction could be ignited in the form of self-sustaining combustion wave quickly from one side to another without additional energy, thus energetically efficient and procedurally short.

The objective of this study is to evaluate the possibility of extracting lead from CRT funnel glass by the self-propagating process. Firstly, we investigate the effects of added funnel glass content and boiling points on the extraction behavior of lead. Then, we examine the lead evaporation velocity of the SHS process. Finally, we examine the toxicity of the residues after treatment of SHS reactions.

## MATERIALS AND METHODS

Funnel glass of wasted CRTs from Huaxing Environmental Protection Corporation (Beijing, China), whose chemical composition was presented in Table 1, was pulverized by the planetary ball-milling (through 80 sieve mesh) and dried at 105 $^o$C for 24 hours piror to use. Commercial ferric oxide

(purity 99%, particle size < 5μm) and magnesium (purity 99%, particle size 200 mesh) were used as the SHS reactants. According to the experience criteria proposed by Merzhanov, this thermite reaction satisfies the high-temperature self-propagation condition of $\Delta H_{298}/C_{p298} \geq 2000K$.

**TABLE 1.** Chemical composition (wt.%) of investigated CRT funnel glass by XRF

| Composition | wt.% |
|---|---|
| $SiO_2$ | 52.45 |
| PbO | 22.89 |
| $K_2O$ | 8.66 |
| $Na_2O$ | 5.67 |
| $Al_2O_3$ | 3.68 |
| CaO | 2.74 |
| MgO | 2.43 |
| $Fe_2O_3$ | 0.57 |

A summary of the mixtures investigated is reported in TABLE 1. Parallelepiped shaped samples with dimensions 40×8×7 mm and green densities in the range from 2.19 to 2.32 g/cm3 were prepared by uniaxial pressing into a steel die with a pressure of 10 MPa for approximately two minutes. Each sample was located vertically in a small reaction chamber with dimensions 100×100×100 mm, an electrically heated graphite rod at the top of the pellet initiated the reaction.

Each sample self-propagated through the medium immediately after ignition in the form of a bright combustion front as a consequence of high energy generated from the exothermic reaction between $Fe_2O_3$ and Mg. Two solid products, residue and extract, were obtained. The extract was condensed on the reaction chamber walls due to the evaporation occurring during the SHS process while the residue remained where the original compact was placed inside the vessel.

Chemical and physical analyses of ash samples and the residues after VAHT were conducted as follows:

- Chemical composition: X-ray fluorescence (XRF) was performed with an SXF-1200 equipped with Rh X-ray tube, 40 kV, 70 mA. Fusion method was used for sample preparation to reduce the affection of graininess and mineral effects.
- Heavy metal concentration: The heavy metal concentrations in the ash and residue after VAHT were determined by a PerkinElmer OPTIMA-2000 Inductively Coupled Plasma Optical Emission Spectrometer (ICP-OES). The wavelength for the element Pb is 220.353 nm. The samples were extracted by a 4-acid ($HNO_3$-$HClO_4$-HF-HCl) digestion procedure.
- Leaching Test: Leaching test procedures regulated in the USEPA SW846-1311 were used in the study. The extraction fluids were de-ionized water and glacial acetic acid solution; and ratio of solid to liquid were 1:10 and 1:20, respectively. After agitation the sample slurry was filtered using 6 μm millipore filter. The leachates were preserved in 2% $HNO_3$.

**RESULTS AND DISCUSSION**

FIGURE 1 shows the dependence of extraction ratio of lead and combustion temperature ($T_c$) on various amount of funnel glass added in the original mixture. It is clearly apparent that the self-propagating reaction in the presence of Mg and $Fe_2O_3$ could remove lead from funnel glass, and the separation ratio is related closely with added funnel glass amount. Specifically, the separation ratio of lead was constant at over 90 wt.% when the added amount of funnel glass was either equal to or less than 40 wt.%. In addition, the extraction behavior of lead exhibited a tendency related to that of combustion temperature, which was found to have a significant negative correlation with the funnel glass content.

This result indicates that the extraction of lead from funnel glass arose from the extreme high

temperature achieved during the SHS reaction process, so that the lead could be evaporated from funnel glass. However, in the case of funnel glass added amount of more than 40 wt.%, the extraction ratio drastically decreased. This phenomenon could be explained by the thermodynamic properties of the SHS reaction process.
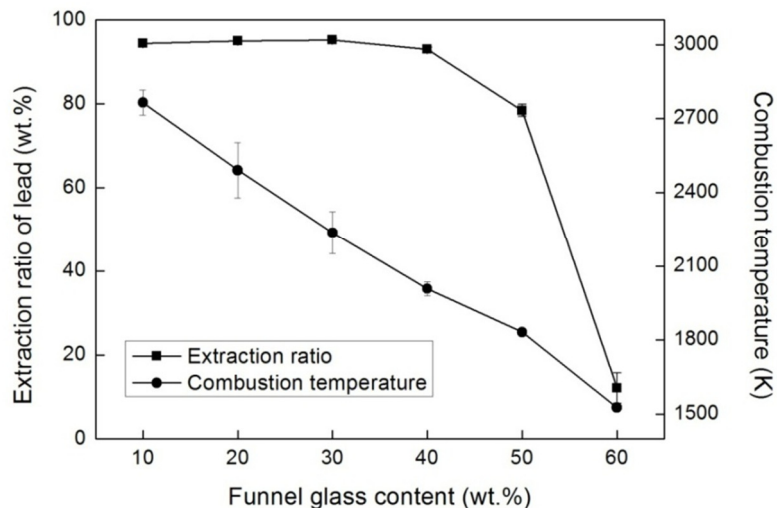


**FIGURE 1.** Effect of SHS reactant addition on the lead extraction ratio and combustion temperature
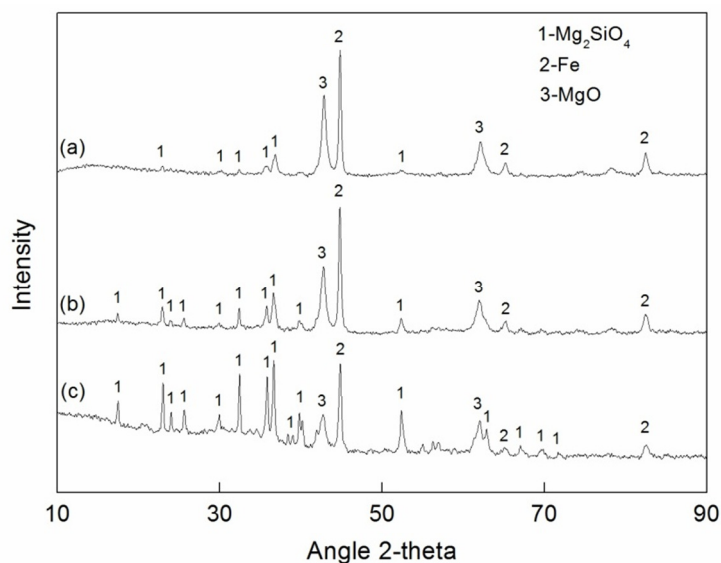


**FIGURE 2.** XRD patterns of the residues in the cases of funnel glass content ranging: (a) 10 wt. %, (b) 30 wt. %, (c) 50 wt. %

On one hand, the exothermicity of SHS reactions decreased for higher funnel glass content, with a consequent reduction in the combustion temperature. And lead is difficult to be extracted when the combustion temperature is below the boiling point of lead oxide, which is the main phase of lead in funnel glass, i.e., the extraction ratio of lead was about 12.14 wt.% in the situation of added funnel glass content equal to 60 wt.% with the combustion temperature of 1527 K. On the other hand, relatively shorter cooling time at higher funnel glass content conditions give rise to the gasified lead encapsulated in

the residue again after SHS reaction before escaping from the funnel glass. Thus, it is worth noting that the addition of funnel glass as a diluent can be used to control the SHS lead extraction behavior.

It is important to note that the SHS extraction process is analogous to the vacuum metallurgy separation method, which utilizes the difference of boiling points of various metals to separate the mixture of metals. That is to say, the composition with high vapor pressure and low boiling point can be separated through evaporation or sublimation from other components which were still remained in the residue during the SHS process.

FIGURE 2 shows the XRD patterns of the residues obtained after self-propagating in the cases of funnel glass content ranging within 10 wt.% , 30 wt.% and 50 wt.%, respectively. As is shown in Figure 2, no significant differences were observed among residues with different funnel glass content added in original mixtures, and the main crystalline phases contain $Mg_2SiO_4$, MgO and Fe. Accordingly, Mg was oxidized to $Mg_2SiO_4$ and MgO which are not easy to evaporate as their high boiling points. In addition, $Fe_2O_3$ was reduced into Fe which is also difficult to volatilize because it is prone to enrich and contact with each other during the SHS melting process.

FIGURE 3 shows the dependence of the evaporation velocity of lead on the funnel glass content. It is observed that evaporation velocity firstly increased with increasing the funnel glass, to a maximum value in the case of added funnel glass equal to 40 wt.%, then decreased when funnel glass amount is more than 40 wt.%. The maximum evaporation velocity of lead is about $2.02 \times 10^{-3}$ $g/cm^2 \cdot s$, which approaches the evaporation velocity of pure metallic lead when the temperature and pressure are 1073 K and 0.1 Pa. However, the percentage of lead in the original mixture of 40 wt.% added funnel glass amount is 10.63 wt.%, indicating SHS evaporation process is efficient and the lead extraction velocity is high enough to meet the production requirement.

Furthermore, the simple exothermic character of the SHS process , which avoids the need for expensive processing facilities and equipment, it is effective to dispose small scale of hazardous wastes in situ which could not be easily transported from one place to another. Moreover, the present separation process might be also applicable for recycling of not only funnel glass but also other materials containing heavy or precious metal resources.
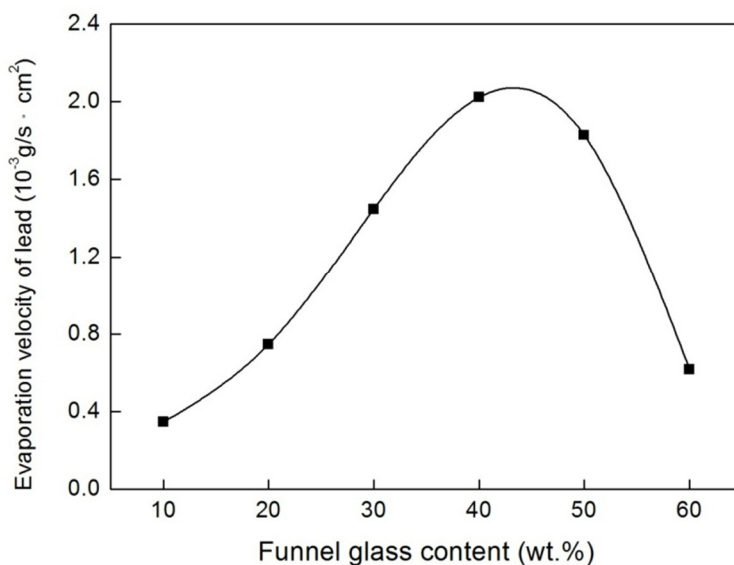


FIGURE 5. Lead extracting velocities from waste CRT funnel glass with different SHS reactant addition

It is important to note that although most of lead was separated from funnel glass when the added funnel glass amount was no more than 40 wt. % after SHS process, the residues containing a little amount

of leachable lead might still leach sufficient concentration of lead and would be regulated as hazardous wastes unless otherwise exempted. Thus, lead leachability was measured using the TCLP method and results are presented in TABLE 2. It's worth noting that all the determined leaching concentrations were well within the current regulatory despite the various funnel glass ratios, which indicates that the obtained residues were environmental safe in heavy metal leaching.

**TABLE 2.** TCLP Results and Pb Content Remained in the Residue

| Funnel glass content (wt.%) | Pb in the residue (g/kg) | TCLP of Pb (mg/L) |
| --- | --- | --- |
| 10 | 1.288 | 0.098 |
| 20 | 2.424 | 0.089 |
| 30 | 3.280 | 0.175 |
| 40 | 6.363 | 0.017 |
| 50 | 23.488 | 0.067 |
| 60 | 113.560 | 0.095 |
| | | 5.0[a] |

[a]Maximum allowable concentrations according to the EPA regulations

**CONCLUSIONS**

This study tries to demonstration a novel process of recovering lead from spent CRT funnel glass based upon self-propagation high-temperature synthesis (SHS) method. We found that self-propagating reaction in the presence of Mg and $Fe_2O_3$ could separate lead preferentially and superfine lead oxide nano-particles were obtained from a collecting chamber. The separation ratio was related closely to the amount of funnel glass added in the original mixture. At funnel glass addition of no more than 40 wt.%, over 90 wt.% of lead was recovered from funnel glass. High extraction yield reveals that the network structure of funnel glass was fractured due to the dramatic energy generated during the SHS melting process.

The concentration of Pb in the samples after SHS according to the TCLP are much lower than the threshold values for hazardous wastes regulated by the international environmental standards. Lead was preferentially separated during the process and the optimal lead removal condition is under the case of the funnel glass added amount equal to 40 wt.% which is when we succeeded in recovering over 90 wt. % of lead from funnel glass with relatively high extraction velocity.

**ACKNOWLEDGMENT**

**REFERENCES**

Chi X.W., Streicher-Porte M., Wang M.Y.L., Reuter M.A. 2011, Informal electronic waste recycling: A sector review with special focus on China, ***Waste Management***, 31: 731-742.

Jang Y.C., Townsend T.G. 2003, Leaching of lead from computer printed wire boards and cathode ray tubes by municipal solid waste landfill leachates, ***Environ. Sci. Technol***, 37:4778-4784.

Musson S.E., Jang Y.-C., Townsend T.G., Chung I.-H. 2000, Characterization of Lead Leachability from Cathode Ray Tubes Using the Toxicity Characteristic Leaching Procedure, ***Environ. Sci. Technol***, 34: 4376-4381.

Mear F., Yot P., Cambon M., Ribes M. 2006, The characterization of waste cathode-ray tube glass, ***Waste Management***, 26: 1468-1476.

Wang Y.C., Ru Y.H., Veenstra A., Wang R.J., Wang Y. 2010, Recent developments in waste electrical and electronics equipment legislation in China, ***Int. J. Adv. Manuf. Technol.***, 47: 437-448.

Wang Y. , Zhu J.X. 2012, Preparation of lead oxide nanoparticles from cathode-ray tube funnel glass by self-propagating method, ***Journal of Hazardous Materials*** 215– 216: 90-97

# KINETIC STUDY OF DUAL-CORE OXYGEN CARRIERS USING SOL-GEL FOR CHEMICAL LOOPING

*Jie Zhu*, Wei Wang, Shoudu Wang and Yue Hu
(Tsinghua University, Beijing, China)

**ABSTRACT:** The application of perfect oxygen carriers, is imperative to address the practical feasibility of chemical looping combustion. The objective of this study was to release the kinetic of the reduction process using Fe-based dual-core oxygen carriers (OCs). Particles composed of 68 wt % $Fe_2O_3$ and 30% $Al_2O_3$, together with 2wt% different additions, the oxides of Ni, Cu, Co, Ce, Mn, have been prepared by sol-gel method. The kinetic experimental tests were carried out in a thermal gravimetrical analyzer by exposing to the reducing gas CO and the oxidizing gas $O_2$ at 1075-1223K. Activation energies of the reduction stage are 22.8 kJ/mol, 20.9 kJ/mol, 19.1 kJ/mol, 15.6 kJ/mol, 21.8 kJ/mol, 30.9 kJ/mol for Fe-Al, Fe-Ni-Al, Fe-Cu-Al, Fe-Co-Al, Fe-Ce-Al, Fe-Mn-Al, respectively. The addition of Ni, Cu, Co was found to promote the reactivity in the reduction stage. From the crystal theory point, material characters have been investigated using X-ray diffraction (XRD) spectrum. Different extent of the interactions between the main atoms was found in all the dual-core OCs. Spinel phases were created in Fe-Ni-Al, Fe-Cu-Al and Fe-Co-Al system. Spinel structures had more possibility to create crystal defects and provided more channels for the lattice oxygen in the body phase to transfer outward to the surface, which definitely helped reduce the activation energy. The results of the reduction kinetic and XRD analysis came with consistency.

## INTRODUCTION

Chemical looping combustion （CLC） is a novel type of energy utilization and regarded as the fourth generation CCS technology by the developed countries for its character of high efficiency in fuel transformation, cost-effective carbon dioxide separation, low NOx and POPs emission. The CLC system is consist of two reactors, an air and a fuel reactor, where the oxidation and reduction of the oxygen carriers happens, separately. Oxygen carriers, as the medium between the two reactors, transfer oxygen from the air to the fuel, and then back to air reactor.

To realize the advantages of CLC technology, the oxygen carriers play significant roles. Iron oxides have been widely recommended for the character, high oxygen capacity, low cost and low toxicity to the environment compared with other common oxygen carriers, such as the oxides of Ni, Cu, Mn and Co. However, the reaction rate of iron oxides has to be developed. Previous studies from other researchers have given some clues through the production of complex dual-core oxygen carriers. Anders Lyngfelt[1] has found that significant improvement of the reaction between $Fe_2O_3$ and $CH_4$ can be reached by the addition of 3wt% NiO within $Fe_2O_3$. Jae-Chun Ryu[2] has found that the existing of small amount of Ce will lower the activated energy of the reaction between $Fe_2O_3$ and $H_2$. What's more, similar results has also been released in NiO-CuO[3] and NiO-CoO[4] system. Therefore, the addition of the components which are more active than $Fe_2O_3$ into the $Fe_2O_3$ system is a feasible way to promote the activity of $Fe_2O_3$. It is of great necessities to study dual- core iron based oxygen carriers systematically.

In addition, the progress of the micro reaction mechanism in chemical looping process has also made recently. In the beginning, specific surface areas and pore structures of oxygen carriers are the only things to focus on which is same as the regular gas-solid reaction. However, L.-S. Fan[5] has

found that the significant decrease in pore volume after the first redox cycle does not affect the reactivity of the Fe-Ti-O particle. He suggests a different gas-solid micro reaction mechanism, that is ion diffusion mechanism, and points out that the excellent recyclability of the Fe-Ti-O particles may be attributed to the increased ionic diffusivities for both the oxygen ion and the iron ion. As a result of his approval, the structures good for ion diffusion seems more important than specific surface areas and pore structures of oxygen carriers. However, more studies has to be carried out to further confirm the structure character of other dual-core or complex oxygen carriers and whether it is good for ion diffusion or not.

In this study, the oxide of Ni, Cu, Mn, Ce and Co has added into $Fe_2O_3$/ $Al_2O_3$ system and the reduction kinetic of them has been investigated. Moreover, the crystal structure character of them has been discussed to supply more evidences of the gas-solid micro reaction mechanism during chemical looping process.

## MATERIALS AND METHODS

**Material Preparation Method**. The common sol-gel method was used to produce dual-core oxygen carriers [6]. The precursors in this method are the nitrates of the active components and aluminum isopropoxide with water as the solvent. The mixture is then placed under an oven at 80℃ for curing to form gel and dry the gel. The gel is subsequently heated in a muffle furnace using a temperature programmed way, 100℃ for 5h, 150℃ for 5h, 200℃ for 5h, 450℃ for 3h, 600℃ for 3h, and finally 1000℃ for 10h under the atmosphere condition. The resulting particles are ground into powder form and sieved for the 100-200μm. Finally the particles should composed of 68 wt % $Fe_2O_3$ and 30% $Al_2O_3$, together with 2wt% different additions, the oxides of Ni, Cu, Co, Ce, Mn. The samples with different additives in them are named as follows : Fe-O/$Al_2O_3$ , Fe-Co-O/$Al_2O_3$ , Fe-Cu-O/$Al_2O_3$ , Fe-Ni-O/$Al_2O_3$, Fe-Ce-O/$Al_2O_3$ , Fe-Mn-O/$Al_2O_3$ .

**Thermal Gravimetrical Analysis Tests (TGA).** Thermal Gravimetrical Analysis Tests were carried out in a synchronous thermal gravimetrical analysis/ differential scanning calormetry (TGA/DSC) analyzer by exposing the samples to alternating reducing (100% CO) and oxidizing (100% $O_2$) conditions with the temperature scale from at 1075-1223K. The flow rate of CO and $O_2$ was 80ml/min and the reaction time lasted about 10min. $N_2$ was the inert gas to blow out the reactants and productions for nearly 10min with the same flow rate. The oxygen carrier was about 20mg. From the relationship between reactivity constant and temperature, the activated energy can be solved.

**Structure Tests by X-ray diffraction (XRD).** The compositions and weight content of the different fresh samples were obtained using a X-ray diffractometer with Cu K radiation. The scanning rate was 6°/min with the scope from 10° to 90°. α

## RESULTS AND DISCUSSION

**Reduction Kinetic Study Under TGA Condition.** The apparent activated energy is one of the most important kinetic parameters to release the reactivity for the reaction. The apparent activated energy of the oxygen carrier reduction is tested at the temperature scale from1075 to 1223K in TGA. Table 1 shows the results.

As shown in table 1, the addition of Ni, Cu, Co was found to decrease the activated energy and promote the reactivity in the reduction stage, especially for Co that significantly reached 30% off for the activation energy compared with Fe-Al. The activated energy of the oxygen carrier with Ce in it has the similar value with Fe-Al. However, the reactivity of Fe-Mn-Al has decreased. For most of the additives, that are more active than Fe during the chemical looping reduction process, the result indicates they have better performances compared with Fe-Al.

As shown in table 1, the addition of Ni, Cu, Co was found to decrease the activated energy and promote the reactivity in the reduction stage, especially for Co that significantly reached 30% off for the activation energy compared with Fe-Al. The activated energy of the oxygen carrier with Ce in it has the similar value with Fe-Al. However, the reactivity of Fe-Mn-Al has decreased. For most of the additives, that are more active than Fe during the chemical looping reduction process, the result indicates they have better performances compared with Fe-Al.

TABLE 1: Apparent activated energy of all the dual-core oxygen carriers

| Samples | Apparent Activated Energy (kJ/mol) | $R^2$ |
|---|---|---|
| $Fe-O/Al_2O_3$ | 22.8 | 0.9921 |
| $Fe-Co-O/Al_2O_3$ | 15.6 | 0.9923 |
| $Fe-Cu-O/Al_2O_3$ | 19.1 | 0.9529 |
| $Fe-Ni-O/Al_2O_3$ | 20.9 | 0.9994 |
| $Fe-Ce-O/Al_2O_3$ | 21.8 | 0.9947 |
| $Fe-Mn-O/Al_2O_3$ | 30.9 | 0.9770 |

**Crystalline Phase Analysis of the Fresh Oxygen Carriers.** The reactivity of the material is determined by its structure. L.-S. Fan[5] has suggested the ion diffusion mechanism during the reduction process in chemical looping combustion and points out that the increased ionic diffusivities for both the oxygen ion and the iron ion are good for the reactivity and recyclability of the oxygen carriers. As the result of the previous study, the detailed analysis of the crystalline phase is of great importance to release the micro mechanism.

Figure 1 shows the XRD results of $Fe-Ni-O/Al_2O_3$ in the important scale for example. Table 1 generalizes the XRD results of different fresh oxygen carriers. The weight content of each phases are also given.
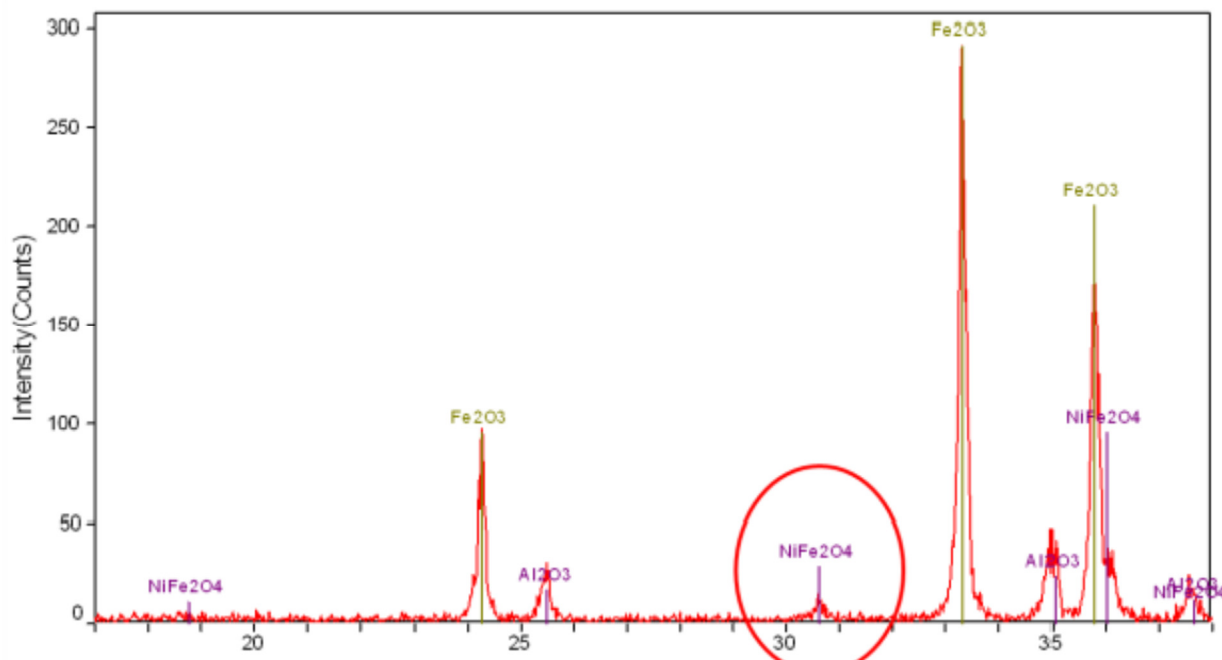


**FIGURE 1**: XRD results of $Fe-Ni-O/Al_2O_3$ in the important scale

As shown in Table 2, all the dual-core oxygen carriers can be divided into three kinds. Fe-Co-O/Al$_2$O$_3$, Fe-Cu-O/Al$_2$O$_3$ and Fe-Ni-O/Al$_2$O$_3$ is the first type which are consist of XFe$_2$O$_4$ phase. Fe-Ce-O/Al$_2$O$_3$ is the second one that only has the independent oxide phases. Fe-Mn-O/Al$_2$O$_3$ is the third type where there is no track of Mn oxides or anything else.

**TABLE** 2: Crystalline phase analysis of all the dual-core oxygen carriers

| Samples | Crystalline Phase | Weight Content wt% |
|---|---|---|
| Fe-O/Al$_2$O$_3$ | Fe$_2$O$_3$ | 69.97 |
|  | Al$_2$O$_3$ | 30.03 |
| Fe-Co-O/Al$_2$O$_3$ | Fe$_2$O$_3$ | 66.95 |
|  | Al$_2$O$_3$ | 28.47 |
|  | CoFe$_2$O$_4$ | 4.58 |
| Fe-Cu-O/Al$_2$O$_3$ | Fe$_2$O$_3$ | 63.52 |
|  | Al$_2$O$_3$ | 30.21 |
|  | CuFe$_2$O$_4$ | 6.27 |
| Fe-Ni-O/Al$_2$O$_3$ | Fe$_2$O$_3$ | 62.73 |
|  | Al$_2$O$_3$ | 28.85 |
|  | NiFe$_2$O$_4$ | 8.42 |
| Fe-Ce-O/Al$_2$O$_3$ | Fe$_2$O$_3$ | 68.54 |
|  | Al$_2$O$_3$ | 29.42 |
|  | CeO$_2$ | 2.04 |
| Fe-Mn-O/Al$_2$O$_3$ | Fe$_2$O$_3$, | 69.02 |
|  | Al$_2$O$_3$ | 30.98 |

Of all the samples, the content of Al$_2$O$_3$ is quite stable and near the designed value 30%. However, the interaction between the additive oxides and Fe$_2$O$_3$ has happened in different way. In the first type, the additive oxides reacted with Fe$_2$O$_3$ and formed the spinel phases. Through the XRD general quantity analysis of the particles, XFe$_2$O$_4$ phase weight content is almost 4%-8%. Independent oxide CeO$_2$ has found in the second type without reacting with Fe$_2$O$_3$ and its content is consistent to designed value 2%. However, there is no observation of spinel phases or independent oxide in the Fe-Mn-O/Al$_2$O$_3$ system and the result infers that the atom Mn could be into the Fe$_2$O$_3$ phase without affecting the former structure.

Compared the results mentioned in TGA section, the first type of the oxygen carriers has the ability to decrease the activated energy of the reduction solid-gas reaction. The second one has not significant effect on it while the third type even increases the activated energy. From the crystal theory, the spinel phase is one of the three type solid solutions. The micro structures of the solid solutions have their own characters that they have more opportunities to create defects and vacancies in the materials when atoms substitution happens. These defects and vacancies are related closely to improved ionic diffusivity while such diffusion will be limited severely in pure Fe$_2$O$_3$ when such vacancies in the crystal phase are absent. As a result, these defects and vacancies in spinel phase enhances the reactivity of the oxygen carriers while Fe-Ce-O/Al$_2$O$_3$ and Fe-Mn-O/Al$_2$O$_3$ system failing to form this kind of solid solution so that they affects the activated energy slightly or even to the opposite direction. To some extent, our study supplies more supports to the previous study from L.-S. Fan et al. For more confirmed conclusion, more direct evidences, such as the vacancy concentration and ion diffusion velocity, should be further studied.

**CONCLUSIONS AND SUGGESTION**

This study demonstrates some interesting conclusions as follows:

(1) The dual core oxygen carrier is an efficient way to enhance the reduction reactivity of $Fe_2O_3$. In this study, the addition of Ni, Cu, Co has positive effect, especially for Co that significantly reached 30% off for the activated energy compared with $Fe_2O_3/Al_2O_3$.

(2) Compared with TGA and XRD result, the reason why the additives can reduce the activated energy is quite close to the structure character of spinel phase which can offer more defects and vacancies as the tunnels for ion diffusion. This result will be helpful for essential understanding, targeted designing and efficient selecting of the oxygen carriers from a new point of view.

(3) Our study supplied more facts to the ion diffusion mechanism in different oxygen carriers' reduction of chemical looping process. However, more evidences directly to the ion and vacancy themselves should be studied.

## REFERENCES

[1] Johansson M., Mattisson T., Lyngfelt A. 2004. "Investigation of $Fe_2O_3$ with $MgAl_2O_4$ for chemical-looping combustion". Industrial&Engineering Chemistry Research. 43(22):6978-6987.

[2] Jae-Chun Ryu, Dong-Hee Lee, Kyoung-Soo Kang, Chu-Sik Park,Jong-Won Kim, Young-Ho Kim. 2008. "Effect of additives on redox behavior of iron oxide for chemical hydrogen storage Journal of Industrial and Engineering Chemistry". 14:252–260.

[3] Adanez J., Garcia-Labiano F., de Diego L. F., et al. 2006. "Nickel-Copper oxygen carriers to reach zero CO and $H_2$ emissions in chemical-looping combustion". Industrial & Engineering Chemistry Research. 45(8):2617-2625.

[4] Hossain M. M., de Lasa H. I. 2007. "Reactivity and stability of $Co-Ni/Al_2O_3$ oxygen carrier in multicycle CLC". AIChE Journal. 53(7):1817-1829.

[5] Fanxing Li, Zhengchao Sun et al. 2011. "Ionic diffusion in the oxidation of iron-effect of support and its implications to chemical looping applications". Energy & Environment. 4:876-880.

[6] Fanxing Li, Hyung Ray Kim, Deepak Sridhar, Fei Wang, Liang Zeng, Joseph Chen, L.-S. Fan. 2009. "Syngas Chemical Looping Gasification Process: Oxygen Carrier Particle Selection and Performance". Energy&Fuels. 23, 4182-4189

# AUTOCLAVING TREATMENT OF MUNICIPAL SOLID WASTE FOR THE RECOVERY OF BIOMASS AND ITS REUTILIZATION

Chia-Chi Chang[1], Y.C. Wang[1], Z.S. Hung[1], S.W. Chiang[1], J.L. Shie[2], Y.S. Li[2], Y.H. Chen[3], C.F Ho[4], ***C.Y. Chang**[1]*

1. Graduate Institute of Environmental Engineering, National Taiwan University, Taipei 106, Taiwan.
2. Graduate Institute of Environmental Engineering, National I-Lan University, I-Lan 260, Taiwan.
3. Department of Chemical Engineering and Biotechnology, National Taipei University of Technology, Taipei 106, Taiwan
4. Department of International Business ,Chung Yuan Christian University, Chung Li City 320, Taiwan

Autoclaving treatment of municipal solid waste (MSW) for the recovery of organic fibre material (OFM) and its reutilization was investigated in this study. High-temperature and high-pressure saturated steam was used to hydrolyze the OFM of MSW, and break the long chain structure of hemicllulose and cellulose into small fragments. Meanwhile, the plastics were softened and shrunken into small lumps by the heating of steam. Therefore, autoclaving process can effectively reduce the volume of MSW. Besides, the heating value of autoclaved MSW (noted as AMSW) only decreased slightly. Thus the energy density of AMSW per volume increased. After autoclaving, the OFM can be easily separated from the AMSW by a vibratory screen according to the size diference between OFM, plastics and the other inorganic contents, obtaining the homogenous OFM.

The autoclaving experiments were conducted at 135, 155 and 165 ℃ with various operating times of 15, 30 and 60 minutes. The results indicated that the energy of steam at 135 ℃ was not enough to reduce the volume of MSW sufficiently, while slightly decreased the heating value of AMSW, therefore reducing the energy density. At 155 ℃, the volume of MSW reduced significantly, so the energy density increased effectively. Comparing with 155 ℃, 165 ℃ did not further increase the energy density of AMSW. Hence, autoclaving at a higher temperature of 165 ℃ was not suitable because it consumed more energy without further improvement.

In order to achieve an effective volume reduction, the operating time must be at least 60 minutes incorporation with rotational shredding at proper rotating speed, say, 7 rpm. The rotational shredding can provide a shear stress to break down the OFM into small size. Therefore, the suitable operating conditions of autocalving of MSW is 155 ℃, 60 minutes with 7 rpm rotation.

The moisture content of the AMSW was 72 ~ 77%, while the proper moisture content of materials for screening is 50 ~ 60%. Thus, a decrease of the moisture content of AMSW before screening is required. After the dehydration using a centrifuge, the moisture content of dewatered AMSW (DAMSW) decreased to 56%, suitable for screening.

About 46 wt.% of DAMSW, which is OFM can be separated from the DAMSW employing 1 cm x 1 cm sieve.

The separated OFM obtained was further pelleted to reduce the volume, while increase the energy density. The proper moisture content of OFM for pelleting was found to be about 20 ~ 25 wt.%. The pelleted OFM with dry-basis heating value of 3,891 kcal kg$^{-1}$ and density of 1,346 kg m$^{-3}$ can be used as fuel for the combustion device, coal-fired boiler and co-firing cement furnace. Further torrefaction of the OFM obtained did not increase its energy density, suggesting no need of subsequent torrefaction. The information obtained is useful for the proper design and operation of autoclaving of MSW and the subsequent treatments for the better recovery and reutilization of the biomass of OFM from MSW.

---

# EVALUATION OF WASTE CONCRETE MATERIALS FOR USE IN OYSTER AQUACULTURE

Dong Hee Kang and   Kelton L. Clark (Estuarine Research Center, St. Leonard, MD, USA)
James G. Hunter (Morgan State University, Baltimore, MD, USA)
Z. Andrew Farkas (National Transportation Center, Baltimore, MD, USA)

Native oyster populations in the Chesapeake Bay are at less than 1% of historic levels due to the two protozoan diseases (MSX disease caused by Haplosporidium nelsoni and Dermo disease caused by Perkinsus marinus), overharvesting, and pollution (CRC, 1999). This tremendous decline in the oyster population has dramatically changed the Bay ecosystem as well as the oyster industry.  Individual oysters filter 4-34 liters of water per hour, removing phytoplankton, sediments, pollutants, and microorganisms from the water column (CERP, 2007). Historic oyster populations of Chesapeake Bay could filter excess nutrients from the estuary's entire water volume every three to four days. Today, that would take nearly a year.

There are two popular ways of culturing oysters in the Chesapeake region, spat-on-shell on bottom and in cages. Spat on shell is the most ecologically friendly and the most traditional method. To make new areas ready for on bottom spat-on-shell aquaculture, the barren Bay bottom needs to be built-up with a hard material that will support the spat-on-shell and prevent it from sinking into soft muddy bottoms (a process known as bottom conditioning). Historically, old oyster shell was used for this purpose. However, the decline of the Chesapeake Bay region's oyster industry has led to the scarcity of available oyster shell and using them for bottom building is no longer practical. A lack of availability of oyster shell in the Bay has required the investigation of alternative materials.

This study endeavors to examine the use of recycled concrete aggregate (RCA) to support oyster aquaculture.  To use recycled concrete as bottom conditioning material for oysters, we need to ensure that inundation of RCA in the Bay does not result in the leaching of compounds that may adversely impact growing oysters or the Bay's aquatic ecosystem.  This project will determine the type and quantity of these compounds and evaluate the impacts of these compounds on the growth of oyster, survivability, growth and disease resistance. Based on the findings of these evaluations, recommendations may be made for field testing the concrete material on oyster bottom in the Patuxent River.

# FGD GYPSUM UTILIZATION FOR PREPARATION OF ALPHA-CALCIUM SULFATE HEMIHYDRATES WITH SOLUTION METHOD

Bao Kong, Li Yang, and **Baohong Guan\*** (Zhejiang University, Hangzhou, China)

Coal is the most important fuel for power generation in the world. Lime/limestone wet flue gas desulfurization (FGD) technology is increasing to control $SO_2$ emission for its high efficiency and cost-effectiveness. Consequently, a large amount of FGD gypsum has been produced. In China, FGD gypsum is increasing dramatically, and many environmental concerns has been raised because of potential environmental impacts, resulting a great demand to the utilization of FGD gypsum. Apart from the application in the production of wallboard, cement additives, and aerated concrete block, **p**reparation of α-calcium sulfate hemihydrate (α-HH), one of the most wide-use cementitious materials, is a promising reuse of FGD gypsum. We have carried out a series of lab scale experiments and pilot scale tests for the production of α-HH from FGD gypsum based upon a Ca-K-Mg chloride solution method under atmospheric pressure on a 500-1000 kg/batch setup. α-HH with high purity of 95% was successfully prepared within 5-6 hr reaction. The product also shows high bending strength and compressive strength no less than that produce from natural gypsum. This work provides very useful process for the industrial production in the future.

# PILOT PLANT CONSTRUCTED TO GENERATE MINERAL FIBBER FROM INCINERATOR ASH AND APPLICATION AS FIREPROOF MATERIAL

***Sheng-Fu Yang***, To-Mai Wang, Wen-Cheng Lee, Kin-Seng Sun and Chin-Ching Tzeng
(Institute of Nuclear Energy Research, Taoyuan County, Taiwan, R.O.C.)

This study used products obtained from the plasma melting of municipal waste incineration ashes as raw materials for the production of mineral fiber using a fiber blowing method. Pilot plant with capacity of 50 kg/h was constructed to produce mineral fiber and the fibers were blended with cement to manufacture fireproof material. The mineral fibers belong to the short fiber which the characteristics are presented as follow: (1) fiber diameter range from 0.5 to 4.0 μm; (2) shot content less than 16 wt%; (3) temperature resistance up to 700 $^{\circ}$C; and (4) possession of a good alkali resistance. When the amount of fiber added is at 43 wt. % in fireproof material, the density, porosity and flexural strength are 0.8 g/cm$^3$, 66 % and 15 kgf, respectively. After undergoing the test for flammability and incombustibility, the fireproof specimen had good performance on anti-flame and fire-retardant ability.

# THE STUDY OF USING TEMPERATURE-PHASED ANAEROBIC DIGESTION FOR BIOFERTILIZER PRODUCTION

***Wen-Hsing Chen*** (National I-Lan University, Yilan, Taiwan)
Wei-Lun Jhuang, Jih-Gaw Lin (National Chiao Tung University, Hsinchu, Taiwan)

Compared to composting, a time-consuming bioprocess, anaerobic digestion has been examined great flexibility in treating different types of organic wastes, and can efficiently recover nutrients from the wastes. Temperature-phased anaerobic digestion (TPAD), a proven biotechnology, is demonstrated to produce Class A biosolids, the highest ranked stabilized sludge for surface disposal regulated by U.S.EPA 40 CFR Part 503. The Class A biosolids have been documented as pathogen-free biosolids for straight land-based application. The objective of the study is to evaluate the potential of using TPAD system for converting agricultural and livestock wastes into biofertilizers. The volatile solid (VS) concentration of 20 g/L from swine waste and rice straw with various mixed ratio (S/R) by mass are fed to the TPAD system. The thermophilic and mesophilic digesters of the TPAD system are operated at 4- and 10-day hydraulic retention times (HRTs), respectively, resulting in a total 14-day HRT. The results of the system performance show that the VS removal of $61\pm6\%$, methane production of $17\pm2$ L/day, and methane contents of $52\pm3\%$ in the thermophilic digester and $56\pm7\%$ in the mesophilic digester were achieved at the swine waste to rice straw ratio of 4 to 1. The levels of kjeldahl-nitrogen via temperature-phased anaerobic digestion were remained consistently, whereas the ammonium-nitrogen concentration increased from $82\pm9$ to $361\pm32$ mg/L. It is apparent that the nitrogen in organic form was converted to inorganic form. In addition, the levels of coliform bacteria after anaerobic digestion were less than 10 CFU/100 mL, below the standards of bio-fertilizer. It exhibits that the TPAD system efficiently pasteurized the mixture of the swine waste and rice straw to destroy pathogens. However, it is found that the heavy metal concentrations after anaerobic digestion could not satisfy the requirement for bio-fertilizers. The results indicate that the levels of chromium, copper, nickel, lead, and zinc were $198\pm22$, $400\pm49$, $71\pm1$, $54\pm34$, and $3480\pm111$ mg/kg dry weight, respectively, and cadmium could not be determined during the study. Notice that the high levels of copper and zinc were mainly from the swine waste. The result elucidates that the level of heavy metal will be the pivotal parameter to determine the potential of using the effluent of temperature-phased anaerobic digestion as a bio-fertilizer. The future investigations on the S/R ratios of 1 to 1 and 1 to 4 will be accomplished for evaluating the effects of the S/R ratios on the heavy metal concentrations. Thereafter, all results will be included and the conclusion will be summarized in the conference paper.

# DEVELOPMENT OF A METHODOLOGY TO TRANSPOSE COMMERCIAL PRODUCTS TO MATERIALS

***Lorena Fortuna*,** David Hirschler**, Vasil Diyamandoglu *
Department of Civil Engineering, The Grove School of Engineering, City College of New York, New York, NY 10031, USA
** Waste Prevention Unit, New York City Department of Sanitation, Bureau of Waste Prevention Reuse and Recycling, 44 Beaver Street, 5th Floor, New York, NY 10031, USA

Product reuse involves locating new users for pre-owned products in good condition. National organizations in the United States such as Goodwill and the Salvation Army as well as many regional organizations and local thrift stores, broadly identified as "product reuse organizations", receive such products from donations and channel them to new users thus contributing to the diversion of the products from landfill disposal. In order to use existing methodologies (USEPA/WARM or equivalent) to quantify the environmental social and economic benefits of product reuse, it is necessary to identify the material composition of each product. This is a difficult process as in most cases only the major materials of a product are possible to identify while minor materials remain unaccounted for. Product reuse organizations have different capabilities for tracking reused products but generally do not track material composition. The economic, social and environmental benefits of reuse can be estimated using existing models, mainly attributed to the USEPA, provided that each transacted product can be described in terms of the materials it consists of, at least the major ones. The objective of this study was to develop a systematic methodology to "transform" products into their corresponding materials. The proposed methodology consists of classifying reused products according to major product categories and material composition. Consistency in product nomenclature and product inventory (in each organization over time) would allow the application of "mapping". The product name was mapped into the industry segment (group of similar type of businesses like Building Products or Baby Care) and {product name + product attribute} was mapped into material composition. This methodology is currently being tested with data from the reuse organizations of New York City. Examples of preliminary results will be presented. The study was carried out by the New York City Materials Exchange Development Program located at the City College of New York and funded by the Bureau of Waste Prevention Reuse and Recycling of the New York City Department of Sanitation.

# PHYTOREMEDIATION OF DIESEL CONTAMINATED SOIL WITH *D. reflexa* AND *P.polystachyus*

## *Agamuthu P* and Dadrasnia A.

(Institute of Biological Sciences, Faculty of Science, University of Malaya, Kuala Lumpur, Malaysia)

**ABSTRACT:** In this work, *Dracaena reflexa* and *Podocarpus polystachyus* were investigated for their potential to remove hydrocarbon from 2.5 and 1% diesel fuel contaminated soil amended individually with 5% organic wastes [Tea Leaf (TL), Soy Cake (SC) and Potato Skin (PS)] for a period of 270 days. Loss of 90 % and 99% oil was recorded in soil contaminated with 2.5 and 1% oil with SC amendment, respectively, compared with 52 % and 62% in unamended soil with *D. reflexa* at the end of 270 days. However, 84 and 91% oil loss was recorded for *P. polystachyus* amended with organic wastes in 2.5 and 1% oil, respectively. Diesel fuel disappeared more rapidly in the soil amendment with SC than in other organic wastes supplementation. The plants did not accumulate hydrocarbon from the soil, but the number of hydrocarbon utilizing bacteria was high in the rhizosphere, thus suggesting that the mechanism of the oil degradation was rhizodegradation. A positive relationship was observed between diesel hydrocarbon degradation with plant biomass production. *D. reflexa* with organic wastes amendment has a greater potential of restoring hydrocarbon-contaminated soil compared to *P. polystachyus* plant.

**Keywords**: Phytoremediation, Organic wastes, Diesel fuel, *D. reflexa, P. polystachyus.*

## INTRODUCTION

The industrial revolution of the past century has resulted in significant damage to environmental resources such as air, water and soil. Healthy survival of human beings depends on the quality of physical environment (Riaz *et al*., 2002). Using plants to store, remove, degrade and metabolize environmental contaminants including metals, hydrocarbons and other toxic organic compounds is a bioprocess called phytoremediation. Recent increase in the application of organic and inorganic wastes as soil amendments has raised concerns about their effects on the environment. Interaction between microorganisms associated with plants and plants is the main feature of this phenomenon. Several studies serve as examples of rhizosphere effect in phytoremediation of petroleum hydrocarbons. Gunther *et al*. (1996) found higher microbial numbers and activity coupled with increased degradation in hydrocarbon-contaminated-soil planted with ryegrass, compared to un-planted soil. They suggested that plant roots stimulated the microbial growth, which enhanced the degradation of hydrocarbon mixture. Plants provide root exudates of carbon, energy, nutrients, enzymes and sometimes oxygen to microbial populations in the rhizosphere (Cunningham *et al*., 1996). Root exudates of sugars, alcohols and acids can amount to 10 to 20% of plant photosynthesis annually (Schnoor *et al*., 1995) and provide sufficient carbon and energy to support large numbers of microbes (e.g., approximately 108 - 109 vegetative microbes per gram of soil in the rhizosphere (Erickson *et al*., 1995). Dominguez-Rosasdo *et al*. (2004) reported that seed germination of several grass, legume and cereal species declined with an increase in used oil concentration, at oil rates grater than 1% (w/w). Merkl and Schultze-Kraft (2005) reported that legumes died within 6 to 8 weeks in heavily crude-oil contaminated soil, whilst the grasses showed reduced biomass production. Furthermore, a positive correlation between root biomass production and oil degradation was found. White *et al*. (2006) evaluated the effect of vegetation establishment on the biodegradation of alkylated polycyclic aromatic hydrocarbons in a crude oil contaminated soil and reported that there was greater degradation of the longer three-ring alkylated phenanthrenes-anthracences

and dibenzothiophenes, in the vegetated fertilized plots compared to the non-vegetated non-fertilized plots.

## MATERIALS AND METHODS

Soil was obtained from the Nursery section of the Asia–Europe Institute, University of Malaya, Kuala Lumpur in a sack and transported to the laboratory. Soil samples were air-dried in a dark room, mixed well, sieved through a 2 mm sieve for analysis. The diesel fuel was purchased from a petrol station in Petaling Jaya, Malaysia. As N and P are usually the limiting inorganic nutrients for oil-degrading bacteria, we used organic wastes as a nutrient source. Organic wastes used in this study were collected from different locations, for example, tea leaf (TL) and potato skins (PS) were collected from the Institute of Graduate Studies (IGS) canteen, University of Malaya and soy cake (SC) was prepared in the laboratory.

*D. reflexa* (Song of India) with a strong root system and *P. polystachyus* were used for phytoremediation assays. It is more tolerant than most plants, of dry soil and irregular watering and is widely cultivated in India and Malaysia. In this experiment we used small plants of the same age and size. Physico and chemical analysis of soil and organic wastes were carried out with standard methods. The experimental design was a randomized complete block with triplicate replication.

Two kilograms of unsterilized, air-dried soil was placed into each plastic bag. Soils were artificially contaminated with 1 and 2.5% (w/w) diesel fuel and thoroughly mixed. 5% (w/w) of different organic wastes (TL, SC and PS) were also mixed individually with the fuel-contaminated soil. The polluted soil with organic wastes, were allowed to stabilize for 5 days before transplanting the plants into the contaminated soil. Control treatments consisting bags of plants without diesel fuel or organic wastes were also set up. An additional control treatment comprising of autoclaved soil (at 121◦C and 15 psi for 1 h) containing 0.5% (w/w) $NaN_3$, was also set up to determine non-biological loss of diesel fuel from the soil. In total, 54 microcosms were set-up at room temperature (30 ± 2 ◦C) with 24 h fluorescent light. The plants were watered moderating every two days with tap water.

Soil samples from the phytoremediation experiments were collected monthly for nine months. Soil samples were taken within the rhizosphere zone of plants from each plastic bag every 30 days for analysis for total petroleum hydrocarbon (TPH), pH, total organic carbon and hydrocarbon utilizing bacterial (HUB) counts. At the completion of the experiment (270 days), the plants were uprooted. The root tissue was extracted with 1:1 hexane/acetone in a Soxhlet extractor for 10 h to determine if the roots had absorbed the hydrocarbon from the soil. To assess hydrocarbon content removal, the extracts were analyzed for hydrocarbons using gas chromatography (2010A) with a mass-selective detector (QP2010A). The GC was equipped with cross-linked 5% phenyl methyl siloxane capillary column. Helium was used as the carrier gas. The temperature was set at 40 ◦C and raised by 10 ◦C min$^{-1}$ until 300 ◦C, which was maintained for 8min. The metabolism kinetics of enzymatic reactions can be described by the *Michaelis-Menten* kinetics, and is given by the following equation (Cornish-Bowden, 1995).

$$v = v_{max} \times C / K_m + C$$

where $v$ [mg d$^{-1}$] is the oil removal rate per plant mass of the substrate concentration C (mg L$^{-1}$), $v_{max}$ is the maximal removal velocity and $K_m$ (mg L$^{-1}$) is the half-saturation constant. The model estimated the overall removal velocity by plant in soil relative to treatments applied. Analysis of variance (ANOVA) with SPSS (version 18) was used to evaluate if plant/soil treatments accelerated removal of diesel fuel.

## RESULTS AND DISCUSSION

Low N content (0.24%) and P content (0.08%) was recorded for the soil used (Table 1). Of the organic wastes used, SC had higher amount of N (1.3%) compared to PS (1.1%) and TL (1.02%).

**Degradation and phytoremediation of soil TPHs by plants.** The response of plants to 1% and 2.5% concentration of diesel were monitored throughout the 270 days of the experiment. No plant death was

recorded in the 1% diesel fuel; however some of the plants in the 2.5% fuel showed signs of phytotoxicity such as yellowing of leaves and stunted growth compared with the control. The results are in line with the findings of Vouillamoz and Mike (2009), who reported reduced growth rate in ryegrass planted in diesel contaminated soil. By the end of the experiment, removal of TPHs by plants with the treatments of SC, PS and TL were statistically significant as compared with the natural degradation in the uncontaminated soils and autoclaved soils. The degradation of TPHs at 1% diesel by *D. reflexa* with SC addition was 3.6 fold higher than by natural attenuation (Fig 1, 2). Approximately 46–59% of the diesel fuel was lost within the first two months by soil amendment with SC and 1% fuel in *D. reflexa*, presumably by volatilization and sorption in soil.

**TABLE 1.** Physical and chemical Properties of Soil and Organic Wastes Used for phytoremediation

| Parameters | Soil | TL | SC | PS |
|---|---|---|---|---|
| Total nitrogen (%) | 0.2± 0.5 | 1.0± 0.1 | 1.3± 0.1 | 1.1±0.1 |
| Phosphorus (mg/kg) | 825± 1.5 | 0.8± 0.7 | 0.9±0.9 | 0.7±0.1 |
| Moisture content (%) | 8±0.6 | 34.3±0.5 | 75.9±1.6 | 62.1 ±2.0 |
| Organic C (%) | 0.7± 0.9 | 0.9±1.2 | 1.2± 0.9 | 1.1±1.1 |
| pH | 6.4 ± 0.6 | 6.5±1.2 | 6.2±1.2 | 6.9±0.5 |
| Iron (mg/kg) | 18400 ± 1.8 | - | - | - |
| Lead(mg/kg) | 19.2 ± 1.8 | - | - | - |
| Zinc (mg/kg) | 18.1± 1.6 | - | - | - |

TL: Tea Leaf, SC: Soy Cake, PS: Potato Skin
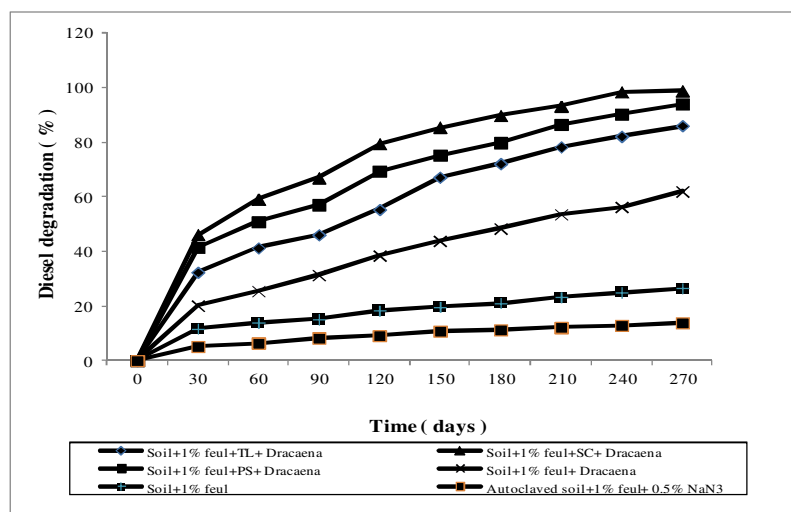


**FIGURE 1**- Biodegradation of 1% diesel fuel in contaminated soil with *D. reflexa*.

This TPH loss rate was similar to that reported by Dibble and Bertha (1979), which showed that in drummed oily waste approximately 50% of TPH would be lost after 6-weeks, mainly due to volatilization. High loss of oil in soil treated with SC and *Dracaena* plants may be due to the presence of appreciable amounts of N (1.3%) in SC (Table 1). This was also recorded in a previous work, where soil amended with SC recorded 67 – 78% loss of diesel fuel in bioremediation process in diesel contaminated soil (Dadrasnia and Agamuthu, 2010). It was also noticed that *D. reflexa* plant amended with SC grew better and taller (about 25% than other treatments) with lots of fibrous roots than other treatments in the experimental set up as compared to *P. polystachyus*. The result is similar to that of Palmroth et al., (2002),

who recorded 60% loss of diesel fuel in 30 days in diesel contaminated soil planted with pine tree and amended with NPK fertilizer, and also related to the findings of Dominguez-Rosado and Pichtel (2005) who recorded 67% degradation of used motor oil in oil contaminated soil planted with sunflower and mustard plants. Statistical analysis showed that there was significant differences between the soil treated with different organic wastes, soil with only plants and soil without plants, and also between the soil treated with SC and soil amendment with TL ($P < 0.05$).
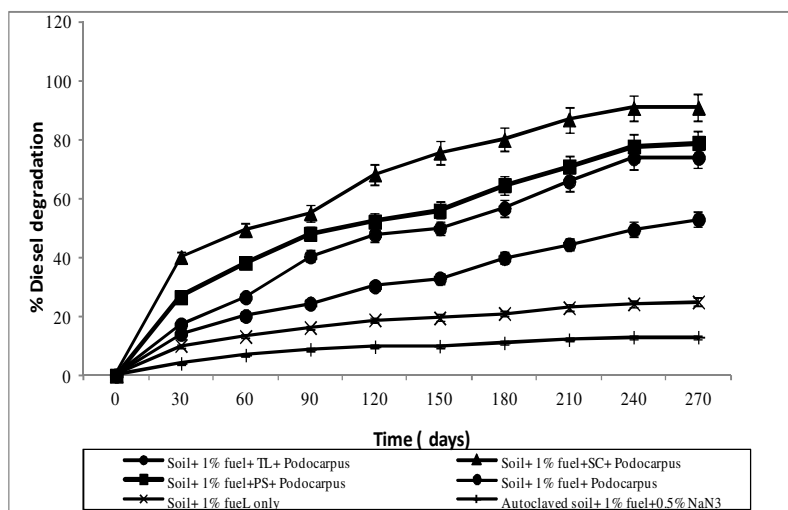


**FIGURE 2**- Biodegradation of 1% diesel fuel in contaminated soil with *P. polystachyus*.

After 180 days, 80% of added diesel fuel remained in the non-vegetated treatment with no waste amendment (control treatment) and it showed that diesel concentration decreased in the control treatment slowly as compared to other soil amendments. Degradation of 11% of oil at the end of the experiment in autoclaved control might be due to photolysis, evaporation loss or maybe amount of sodium azide (0.5%) used did not effectively sterilize the soil. Namkoong et al., (2002) found that a concentration of 1% sodium azide affected the evaporation of chlorobenzene in sludge-amended soil and the structure of the soil.

**Bacterial counts.** Contaminated soil treated with SC and *Dracaena* remediation shows high counts of hydrocarbon utilizing bacteria (HUB) ($355 \times 10^5$ CFU g$^{-1}$ and $378 \times 10^5$ CFU g$^{-1}$) in both soil contaminated with 2.5% and 1% oil, respectively. This is similar to the findings of Agamuthu et al.,(2010) whereas the treatment with only *Dracaena* and *Podocarpus* plant without organic wastes amendment recorded low counts of HUB ($163 \times 10^5$ CFU g$^{-1}$ and $202 \times 10^5$ CFU g$^{-1}$) and ($150 \times 10^5$ CFU g$^{-1}$ and $185 \times 10^5$ CFU g$^{-1}$) in 2.5% and 1% pollution, respectively. The reason for the increase in bacteria population in contaminated soil amended with organic wastes might be due to the presence of nutrients in the organic wastes especially, N and P, which enhanced the proliferation of bacteria in the soil. The HUB isolated from the contaminated soil was identified as species of *Pseudomonas, Bacillus amyloliquefaciens, Microbacterium barkeri,* and *Micrococcus*.

**Plant uptake of diesel hydrocarbons.** Hydrocarbon concentrations in shoot and root tissue were analyzed to determine if phytoaccumulation and phytodegradation played a role for diesel fuel removal. GC/MS analysis of the plant extract did not show presence of hydrocarbons for all the treatments. This is in sharp contrast with the results of Palmroth et al., (2002), who observed an uptake of diesel oil by grass root. The differences might be due to the different plants used in the studies; it might also be due to differences in the weather condition. The result suggests that the mechanism of hydrocarbon removal by

these two plants may be via rhizodegradation which has been well documented (Abhilash et al., 2009; Gerhardt et al., 2009). Also, the removal of the oil may be the result of root exudates produced by plants which enhanced the activities of soil microorganisms in mineralizing the oil in the soil. This is supported by the findings of different authors, who stated that flavonoids and other compounds released by roots can stimulate growth and activity of hydrocarbon degrading bacteria (Chaudhry et al., 2005; Leigh et al., 2006). In addition, root growth and death are known to promote soil aeration which can enhance oxidative degradation of organic contaminants  (Kuiper et al., 2004; Leigh et al., 2002).

**Biomass production.** After 270 days' exposure, the highest of *D. reflexa* longitudinal growth was observed in the amendment with SC contaminated soils with 1% and 2.5 % of petroleum hydrocarbons which was 20% and 36% higher than that of the plants growing in clean soil, respectively. However, there was no significant difference among the amendments with *P. polystachyus.* The development of the plants during the 270 day culture period was also evaluated by measuring the dry weight of the plants.

**Metabolism Kinetics of Plant.** Michaelis-Menten kinetics was used to determine the plant enzymes metabolism in the phytoremediation process (Cornish-Bowden, 1995). Soil amended with SC had the highest enzymatic reaction rate of 0.00172 mg/d, 0.00242 mg/d, 0.00132 mg/d and 0.00184 mg/d in *D. reflexa* and *P. polystachyus* at 1% and 2.5 % diesel fuel contaminated soil, respectively. The result also shows that when pollution level is high, bacteria would need longer time to complete oil degradation. Adesodun and Mbagwu (2008) showed highest biodegradation rate in oil contaminated soil amended with pig wastes.

## CONCLUSION

*D. reflexa*  has higher potential to remediate hydrocarbon from contaminated soil compared to *P. polystachyus*. No accumulation of hydrocarbon was detected in the plant tissues and the use of *D. reflexa* and *P. polystachyus* would serve as an alternative method in removing oil contaminants. Addition of organic waste, especially SC to the contaminated soil further enhanced the growth of *Dracaena* and proliferation of bacteria in the soil. Oil loss from the soil might be through rhizodegradation mechanism. This affords an alternative method in removing oil contaminants from soil while promoting growth of economically viable plant like *D. reflexa* (Song of India) which is used in NASA clean air study and has shown to help to remove formaldehyde, xylene and trichloroethylene.

## ACKNOWLEDGEMENTS

## REFERENCES

Abhilash, P.C., Jamil, S., Singh, N. 2009. Transgenic plants for enhanced biodegradation and phytoremediation of organic xenobiotics. Biotechnology Advances 27, 472-488.

Adesodun, J.K., Mbagwu, J.S.C. 2008. Biodegradation of waste-lubricating petroleum oil in a tropical alfisol as mediated by animal droppings. Bioresource Technology 99, 5659-5665

Agamuthu P, Abioye OP, Abdul Aziz A. 2010. Phytoremediation of soil contaminated with used lubricating oil using Jatropha curcas. J Hazard Mater 179:891–894

Chaudhry, Q., Blom-Zandstra, M., Gupta, S., Joner, E.J. 2005. Utilizing the synergy between plants and rhizosphere microorganisms to enhance breakdown of organic pollutants in the environment. Environmental Science Pollution Research 12, 34-48.

Cornish-Bowden, A. 1995. Fundamentals of enzyme kinetics. Portland Press, London, UK. Edwards VH (1970): The influence of high substrate concentration on microbial kinetics. Biotechnol. Bioeng. 12, 679-712.

Cunningham, S.D. Anderson, T.A. Schwab, A.P. and Hsu, F.C. 1996. Phytoremediation soils contaminated with organic pollutants. Adv. Agron., 56: 55–114.

Dadrasnia, A., Agamuthu, P., 2010. Enhanced Degradation of Diesel-Contaminated Soil using Organic Wastes. Malaysian Journalof Science 29, 225-230.

Dibble, J., Bartha, R. 1979. Effect of environmental parameters on the biodegradation of oil sludge. Appl Environ Microbiol 37.

Erickson, L.E. Davis L.C. and Muralidharan, N. 1995. Bioenergetics and bioremediation of contaminated soil. Thermochimica Acta, 250: 353–8.

Gerhardt, K.E., Huang, X.D., Glick, B.R., and Greenberg, B.M. 2009. Phytoremediation and rhizoremediation of organic soil contaminants: potential and challenges. Plant Science 176, 20-30.

Gunther, T., Dornberger U.and Fritsche, W.1996. Effects of ryegrass on biodegradation of hydrocarbons in soil. Chemosphere, 33: 203–15.

Kuiper, I., Lagendijk, E.L., Bloemberg, G.V., and Lugtenberg, B.J.J. 2004. Rhizoremediation: a beneficial plant–microbe interaction. Molecular Plant and Microbe Interaction 17, 6-15.

Leigh, M.B., Fletcher, J.S., Fu, X., and Schmitz, F.J. 2002. Root turnover: an important source of microbial substrates in rhizosphere remediation of recalcitrant contaminants. Environmental Science and Technology 36, 1579–1583.

Leigh, M.B., Prouzova, P., Mackova, M., Macek, T., Nagle, D.P., and Fletcher, J.S. 2006. Polychlorinatedbiphenyl (PCB)-degrading bacteria associated with trees in a PCBcontaminated site. Applied Environmental Microbiology 72, 2331–2342.

Namkoong, W., Hwang, E.-Y., Park, J.-S., and Choi, J.-Y., 2002. Bioremediation of diesel-contaminated soil with composting. Environmental Pollution 119, 23-31.

Palmroth, M.R.T., Pichtel, J., Puhakka, J.A., 2002. Phytoremediation of subarctic soil contaminated with diesel fuel. Bioresource Technology 84, 221-228.

Riaz, A., Batool, Z., Younas A., and Abid, L. 2002. Green areas: source of healthy environment for people and value addition to property. Int. J.Agric. Biol., 4: 478–81.

Schnoor, J.L., Licht, L.A. McCutcheon, S.C. Wolf N.L., and Carreira, L.H. 1995. Phytoremediation of organic and nutrient contaminants. Environ. Sci. Technol., 29: 318–23.

Merkl, N., Schultze-Kraft, R.,and Infante, C. 2005. Phytoremediation in the tropics-influence of heavy crude oil on root morphological characteristics of graminoids. Environ. Pollut., 138: 86–91.

Vouillamoz, J., and Milke, M.W. 2009. Effect of compost in phytoremediation of dieselcontaminated soils. Water Science Technology 43, 291 – 295.

White, P.L. Jr., Wolf, D.C., Thoma, G.J., and Reynolds, C.M. 2006.Phytoremediation of alkylated polycyclic aromatic hydrocarbons in a crude oil-contaminated soil. Water Air Soil Pollut., 169: 207–20.

# BIOLOGICAL FENTON'S DEGRADATION OF CHLORINATED ENDOCRINE DISRUPTING CHEMICALS BY AQUATIC PLANTS

*Andre Rodrigues dos Reis*, Yukako Kyuma, Masaki Atarashi and Yutaka Sakakibara

(Waseda University, Tokyo, Japan)

**ABSTRACT:** Fenton reaction has been proven to rapidly degrade many persistent organic compounds via the hydroxyl radical formation. A study was performed to propose a new treatment method to decompose persistent chemicals such as dichlorodiphenyldichloroethane (p,p'-DDD) and pentachlorophenol (PCP) in water, utilizing endogenous hydrogen peroxide present in aquatic plants to proceed the biological Fenton reaction. Batch experiments were conducted using duckweeds (*Spirodela polyrhiza* and *Lemma aoukikusa*) as aquatic model plants and PCP and p,p'-DDD as persistent chemicals, respectively. Aquatic plants showed a small impact in removing PCP and p,p'-DDD. However, by adding 2.8 mM of iron ($Fe^{2+}$), there was a rapid removal of both chlorinated EDCs while at the same time consumption of endogenous hydrogen peroxide occurred. It was found that when the initial concentration of EDCs was low (100 µg/L), all EDCs were rapidly removed from water. Also, when the initial PCP concentration was high (5 mg/L), more than 80% of PCP was removed within two days. In addition, the concentration of endogenous hydrogen peroxide in duckweed plants decreased in parallel with PCP removal, as well as the increase of chloride ions formation in water – confirming the degradation of PCP. These results demonstrated that PCP and p,p'-DDD were oxidized through a biological Fenton reaction, and the hydrogen peroxide in aquatic plants was a key endogenous substance in treatment of refractory toxic pollutants.

## INTRODUCTION

The introduction in agriculture of the organochlorine insecticide p,p′-DDT led to important benefits regarding crop production and the elimination of some disease related vectors (Mitton et al., 2011). However, due to its physicochemical characteristics, high hydrophobicity, bioaccumulation, biomagnification on food chain, and persistence, its use was forbidden in most countries (Wayland et al., 1991). Moreover, PCP is also one of the most recalcitrant chemical pollutants in the environment, which has been introduced by human as a pesticide and wood preservative (Bollag, 1992). Owing to its toxicity, and the widespread distribution in the environment, PCP has been listed as a priority pollutant by the Environmental Protection Agency (EPA) of USA and in many other countries (Cooper and Jones, 2008; Dams et al., 2007). However, PCP continues to be widely used for the treatment of utility poles, wharf pilings, and railroad ties and other uses, so it still represents and remain an environmental hazard (Terry and Elisa, 2005). In addition, PCP and its salts were used extensively as pesticides in the last decades (Zhao et al., 2011), resulting in wide occurrence at low to relatively high concentrations in aquatic environment (Wen et al., 2008).

Regarding the toxicity of PCP and p,p'-DDD, effective methods for removing these organic compounds from wastewater and/or other contaminated sites are required. Current methods proposed for the removal of organic compounds from water include microbiological degradation, membrane filtration, adsorption on activated carbon, and different types of oxidation and advanced oxidation processes (Sei et al., 2008). In most cases, physicochemical treatment processes, such as adsorption on activated carbon and membrane filtration are applicable for drinking water supply, but such cases require special attention

to sustain and maintain the performance through operation and maintenance procedures such as regeneration, cleaning, or replacement. In addition, economical feasibility should be considered if the processes were applied to wastewater treatment (Sakakibara et al., 2010).

We focused on a phytoremediation process, which does not require any anthropogenic energy or resources to be carried. Former studies showed that phytoremediation is superior to conventional technology, especially in terms of cost performance and environmental burdens (Pilon-Smits, 2005). In addition, it was reported that plants can be used to treat most classes of contaminants, including petroleum hydrocarbons, chlorinated solvents, pesticides, metals, explosives, and nutrients (Schröder, 2007). Among the metals, iron is an essential trace element for plants, being involved in many processes of metabolisms (Mori, 1999). Its excess in concentration can result in high dangerous toxic levels, especially by altering synthesis of chlorophyll and protein, enzyme activities, photosynthesis and respiration, water content and plant biomass yield (Mori, 1999). In addition, duckweed plants show high accumulation of iron (Xing et al., 2009), which can react with hydrogen peroxide ($H_2O_2$) through Fenton reaction. According to our former study (Reis and Sakakibara, 2011), PCP was not effectively removed by different types of aquatic plants. However, the endogenous $H_2O_2$ produced through photochemical or respiration reaction in mitochondria (Campa, 1991) may proceed a biological Fenton reaction in the presence of ferrous ion. Fenton's reaction generates hydroxyl-radicals by means of the reaction of $H_2O_2$ with ferrous iron, which can oxidize almost every class of organic compound (Zimbron and Reardon 2009). The aim of the present study was try to degrade persistent pollutants such as PCP and p,p'-DDD through Bio-Fenton reaction in aquatic plants.

## MATERIALS AND METHODS

**Aquatic plants.** Duckweeds (*Spirodela polyrhiza* and *Lemma aoukikusa*) were cultivated in glass vessels containing 10% Hoagland nutrient solution (pH 6.0), with light intensity kept at 350 µmol photons/m$^2$/s. Hoagland solution, which contains 295 mg/L Ca(NO$_3$)$_2$.4H$_2$O, 126 mg/L KNO$_3$, 123 mg/L MgSO$_4$.7H$_2$O, 34 mg/L KH$_2$PO$_4$, 11.3 mg/L Fe-EDTA, 0.9 mg/L MnCl$_2$.4H$_2$O, 0.051 mg/L ZnCl$_2$, 0.027 mg/L CuCl$_2$.2H$_2$O, 0.025 mg/L Na$_2$MoO$_4$.2H$_2$O, and 1.43 mg/L H$_3$BO$_3$ was prepared and changed every five days. These plants were acclimatized to laboratory conditions for more than 30 days to avoid lag phase, prior to the experiments.

**Endogenous $H_2O_2$ assay.** $H_2O_2$ concentrations in aquatic plants were measured based on former studies (Okuda et al., 1991). The aquatic plant samples (0.3 g fresh weight) were crushed thoroughly into powder form, using a mortar and pestle in liquid nitrogen, and then was mixed with 1 mL of 0.2 M perchloric acid. The mixture was centrifuged at 12000×g and 4°C for 15 min. A reaction mixture was then prepared by mixing 1 mL of the eluate with 400 µL of 12.5 mM 3-dimethyl aminobenzoic acid (Sigma) in 0.375 M sodium phosphate buffer (pH 6.5), 80 µL of 1.3 mM 3-methyl-2-benzothiazolinone hydrazone and 20 µL of 5 U horseradish peroxidase. This reaction mixture was incubated at 25°C for 5 min and then left at 0°C for 15 min allowing to cool down. Supernatant absorbance was measured in triplicate at $A_{590}$ nm against a sample without the eluate. A standard calibration curve was prepared with known concentration of $H_2O_2$ using the same method.

**Biological Fenton treatment.** The biological Fenton treatment was carried out using 10 g-FW(fresh weight)/L of duckweeds in 100 µg/L and 5 mg/L of PCP, both in distilled water. A control experiment containing no aquatic plant was set as a reference. Iron sulfate used as a source of Fe$^{+2}$ was added in

vessels. The time course changes of PCP concentration, chloride ion formation in water and endogenous $H_2O_2$ concentrations of duckweeds were measured in triplicate.

In order to establish an optimum level of $Fe^{2+}$ to produce a biological Fenton reaction in duckweed plants, solutions of PCP and p,p'-DDD (100 µg/L) were treated with variable levels of $Fe^{+2}$ (0; 0.28; 1.4; 2.8; 14 and 28 mM) and the time course change of PCP or p,p'-DDD in water solutions were measured. The iron content in water and duckweed samples were measured by atomic absorption method, and the chloride ion formation in water solution was measured using the silver nitrate method by Kraemer and Stamm (1924).

**GC/MS measurements.** In the chemical analysis of PCP in solutions, 100 mL of water samples were extracted twice and each mixed with 10 mL of dichloromethane 5000 (Wako Pure Chemical Industries, Ltd.). 5 g of NaCl, 0.2 mL of 1 M HCl solution, and 5 µL of surrogate were also added. The surrogate was spiked to confirm the analytical recoveries and precision. For extraction of p,p'-DDD, water samples were extracted twice and each mixed with 10 ml of hexane. After that, the extracted samples were transferred to erlenmeyer-capped flasks, and 3 g of sodium sulfate was added and then kept for over 12 hours. Trimethylsilyl (TMS) derivatives were obtained and were measured using GC/MS (Shimadzu QP5050A). Details of the analysis were shown in our former research study (Reis and Sakakibara, 2011).

Measurements of PCP in aquatic plants were also conducted, where the extractions of PCP were carried out after the following pre-treatments. First, aquatic plants were washed with distilled water and submerged in liquid nitrogen. The samples were crushed in methanol using a mortar and pestle. After that, PCP was extracted with dichloromethane and measurements were made in the same manner for water samples.

**RESULTS AND DISCUSSION**

In our previous study (Reis and Sakakibara, 2011), we observed that different types of aquatic plants were able to produce stably endogenous $H_2O_2$ in plant tissues even under long-term continuous treatment of phenolic EDCs. These results mean that $H_2O_2$ is being produced stably in plants themselves through photochemical reaction or respiration process (Campa, 1991). In the presence of $Fe^{2+}$ and $H_2O_2$, Fenton reaction produce hydroxyl radicals ($OH^.$), which can degrade almost all organic compounds (Zimbron and Reardon, 2009). In this study, we tried to use the endogenous $H_2O_2$ in aquatic plants to decompose recalcitrant organic compounds such as PCP and p,p'-DDD. The process is shown by the following Fenton reaction equation:

$$Fe^{2+} + H_2O_2 \rightarrow Fe^{3+} + OH^. + OH^- \qquad (1)$$

In order to know the optimum $Fe^{2+}$ concentration to proceed a biological Fenton reaction using aquatic plants, a batch experiment was conducted with different concentration of $Fe^{2+}$. Figure 1 shows experimental results, where PCP and p,p'-DDD were treated by *S. polyrhiza* and *L. aoukikusa*. A control experiment without iron was conducted as reference. Therefore, $Fe^{2+}$ concentration around 2.8 mM or less seems to be suitable benchmark for the required amount of $Fe^{2+}$ for the PCP treatment. These results strongly suggested that the Fenton reaction proceeded in plant cells and decomposed PCP and p,p'-DDD regardless of the presence of aquatic plants species. To our knowledge, this result is the first experimental finding on the occurrence of a biological Fenton process for PCP and p,p'-DDD treatment.

It is evident from Figure 1 that the removal of PCP and p,p'-DDD was more effective when $Fe^{2+}$ was used taking only two days. Also endogenous $H_2O_2$ concentration decreased as shown in Figure 2.

When 2.8 mM of iron was added in the reactor, the removal efficiency of PCP was 98.2%, when the concentration of PCP almost became zero - dropping from an initial concentration of 90.6 µg/L within 48h of exposure time. On the other hand, treating without iron, the removal efficiency of PCP by aquatic plants was only 27.4% for *S. polyrhiza* and 35% for *L. aoukikusa*, indicating a considerable amount of PCP still remaining. At $Fe^{2+}$ concentration of 2.8 mM, the endogenous $H_2O_2$ concentration decreased significantly from an initial concentration of 368.7 nmol/g-FW to 100.4 nmol/g-FW within 2 days. These results suggest that endogenous $H_2O_2$ was consumed by aquatic plants through the biological Fenton reaction process. In addition, there was a rapid and significant decrease in the endogenous $H_2O_2$ levels up to iron concentration of 2.8 mM. At higher iron concentration, the consumption of $H_2O_2$ by Fenton reaction kept constant as represented by the slightly horizontal behaviour of the graph. In the absence of $Fe^{2+}$, no significant decrease or slight decrease of PCP and $H_2O_2$ were observed. On the other hand, as shown in Figure 1, when $Fe^{2+}$ concentrations were higher than 10 mM, most plants became paler losing their natural green colour whilst the removals of PCP and p,p'-DDD were ineffective.
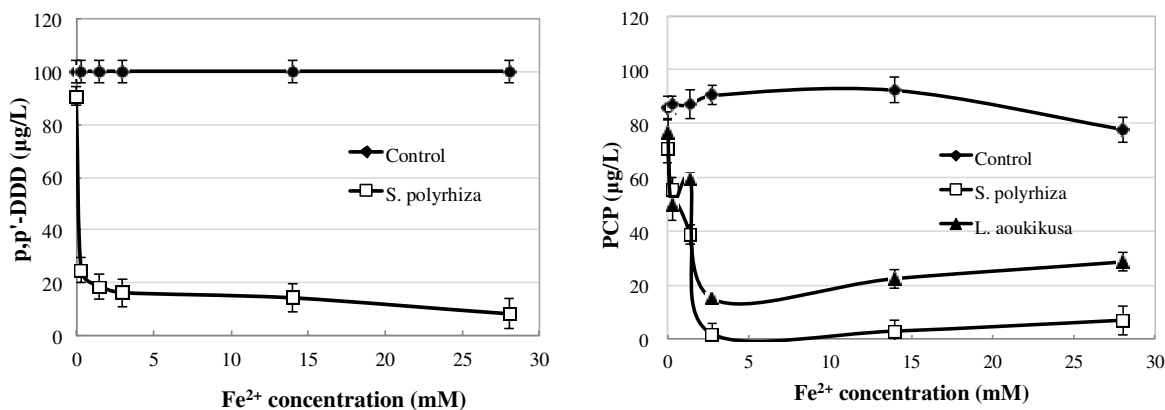


**FIGURE 1**. The effect of $Fe^{2+}$ concentration on batch treatment of p,p'-DDD and PCP. The reaction time was set at 48 hours.
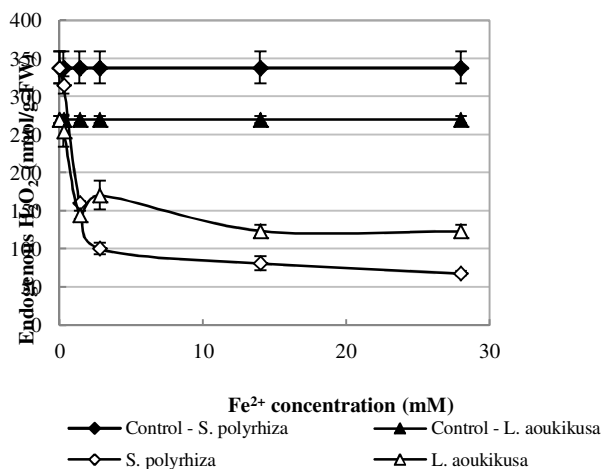


**FIGURE 2**. Course change of endogenous $H_2O_2$ in aquatic plants due to $Fe^{2+}$ concentrations.

After obtaining an adequate iron concentration (2.8mM) for PCP and p,p'-DDD oxidation by *S. polyrhiza* and *L. aoukikusa*, batch experiments were conducted with the initial concentration of PCP at 5 mg/L to evaluate the applicability of biological Fenton reaction. In addition, to confirm that PCP was completely decomposed, the chloride ions in water solutions were measured. Since PCP has five chlorine atoms in the molecule, the decomposition of PCP should result in the production of five chloride ions. Each measurements were carried out at time of exposure 0, 3, 6, 9, 12, 24 and 48 hours, where water samples were collected from the reactor and the concentrations of PCP and chloride ions were measured. As shown in Figure 3, when 2.8 mM iron was added, concentration of PCP decreased from 4.74 mg/L to 2.52 mg/L within three hours, and concentration of chloride ions increased with reaction time. The bold horizontal line in Figure 3 shows a theoretical production of chloride based on the complete dechlorination of PCP. After 24h of exposure, the amount of chlorine ions observed in the water solution was very close to theoretical values, showing a good efficiency on PCP degradation. This increase in chloride ions concentration corresponds to the 96.9% of the value calculated from the decrease of PCP. That is, PCP was almost completely decomposed and an equivalent amount of chloride ions was generated. These results suggest that biological Fenton's oxidation of PCP was achieved by aquatic plants. When a 100 □g/L PCP solution was treated, it was quickly removed by aquatic plants. However, this concentration was too low to evaluate the stoichiometric relation in the dechlorination process.
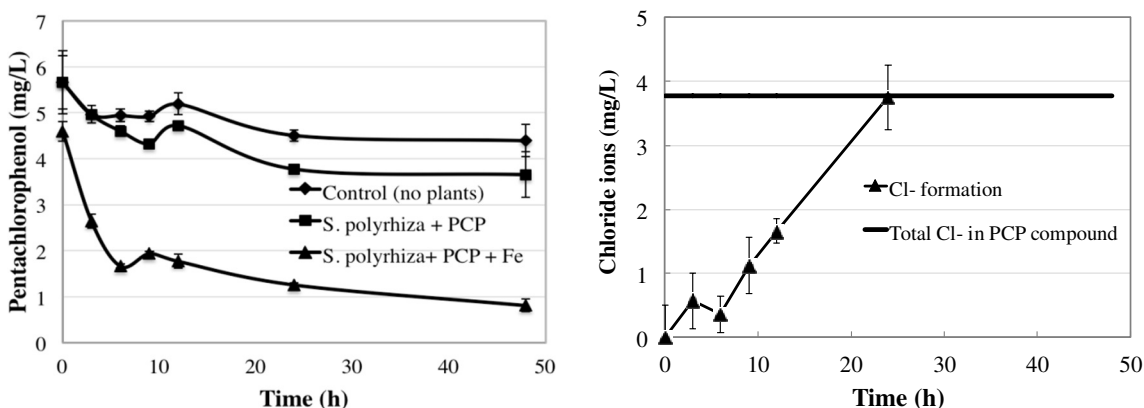


**FIGURE 3.** Batch treatment of PCP by biological Fenton reaction and chloride ions formation in water solution.

As shown in Figure 4, the uptake of iron by *S. polyrhiza* increased with time. Higher absorption of iron by duckweed plants was observed in the treatment which contained 5 mg/L of PCP. A control treatment (without PCP or $Fe^{2+}$) was conducted as a reference to confirm the biological Fenton reactions occurring inside aquatic plants. Ferrous ion is highly soluble species that exists in an aqueous phase and is easily absorbed into biological tissues (Ghaly et al., 2008). In addition, ferrous ion creates oxidative stress by inducing the formation of oxygen based radicals that may cause membrane damage. The ability of aquatic plants to absorb and accumulate metals from their aquatic environment has been demonstrated by several researches (Vlyssides and Bouranis, 1998; Galy et al., 2008; Xing et al., 2009). In addition, Figure 4 also shows the time course changes of endogenous $H_2O_2$ concentration in duckweed tissues due to iron and PCP exposure. When duckweeds were exposed to PCP in the absence of iron, the endogenous $H_2O_2$ concentration increased rapidly in comparison with the controlled experiments. Michalowicz et al., (2010)

demonstrated that PCP induces oxidative stress and hence oxidative damage in plant leaves. On the other hand, when duckweed plants are exposed to PCP and iron, the endogenous $H_2O_2$ concentration decreased quickly with exposure time. This is because, as described in equation (1), ferrous ion reacts well with endogenous $H_2O_2$ in aquatic plants, producing the highly reactive hydroxyl radical.
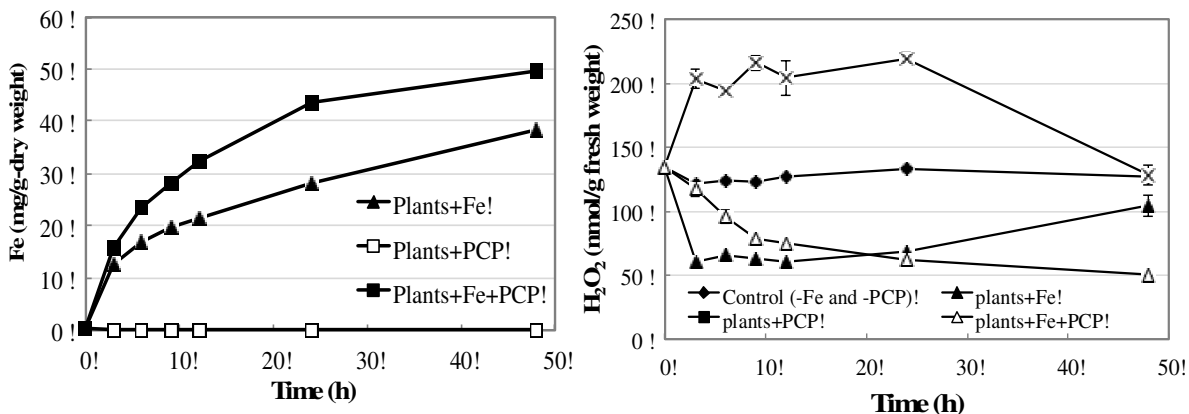


**FIGURE 4.** Iron uptake and course change of endogenous $H_2O_2$ concentration in *S. polyrhiza*. Iron concentration was set at 2.8 mM.

To evaluate the uptake and accumulation of PCP by duckweeds, samples were taken and the amount of this compound was measured (data not shown). In the control experiments, the uptake of PCP gradually increased to a steady state after around 9 hours. In contrast, when duckweeds were exposed to PCP and iron, the accumulation of PCP increased rapidly towards a peak value of around 220 microgram/gram around the same time of 9 hours, but then decreased to zero by the end of the experiment, around 2 hours after the peak. These results also strongly suggest that a biological Fenton reaction occurred inside plant cells, and oxidized the PCP molecules. Further studies will be needed to elucidate optimum operating conditions such as iron sources and different types of aquatic plants for stable treatment of refractory pollutants.

**CONCLUSIONS**

PCP and p,p'-DDD were not efficiently and effectively removed by duckweed themselves, however, when $Fe^{2+}$ was added, PCP and p,p'-DDD were quickly removed along with the consumptions of endogenous $H_2O_2$. The formation of stoichiometric amounts of chloride ion in water solution indicates the occurrence of a biological Fenton reaction in the PCP oxidation process. From these results, we concluded that water treatments by aquatic plants would be a feasible alternative to conventional processes in removing refractory pollutants. Further studies will be needed to analyze and evaluate more precise performances by different aquatic plants in the presence and absence of $Fe^{2+}$.

**ACKNOWLEDGMENT**

**REFERENCES**

Bollag, J.M. 1992. "Decontaminating soil with enzymes. An *in-situ* method using phenolic and anilinic compounds". *Environ. Sci. & Technol.* 26: 1876-1881.

Campa, A. 1991. "Biological roles of plant peroxidases: Known and potential functions". In: *Peroxidase in Chemistry and Biology*. Ed. Everse, J., Everse, K.E., Grisham, M.B., 1991, Boca Raton, Florida, CRC Press, Vol.2, pp. 25-47.

Cooper, G.S. and Jones, S. 2008. "Pentachlorophenol and cancer risk: focusing the lens on specific chlorophenols and contaminants". *Environ. Health Perspect.* 116(8): 1001–1008.

Dams R.I., Paton, G.I. and Killham, K. 2007. "Rhizoremediation of pentachlorophenol by *Sphingobium chlorophenolicum* ATCC 39723". *Chemosphere.* 68: 864–870.

Ghaly, A.E., Snow, A. and Kamal, M. 2008. "Kinetics of iron uptake by wetlands plants". *Amer. J. Biochem. Biotechnol.* 4(3): 279-287.

Kraemer, E.O. and Stamm A.J. 1924. "Mohr's Method for the Determination of Silver and Halogens in other than Neutral Solutions". *J. Am. Chem. Soc.* 46(12): 2707- 2709.

Michalowicz, J., Urbanek, H., Bukowska, B. and Duda, W. 2010. "The effect of 2,4-dichlorophenol and pentachlorophenol on antioxidant system in the leaves of *Phalaris arudinacea"*. *Biol. Plantarum.* 54(3): 597-600.

Mitton, F.M., Gonzalez, M., Pena, A., Miglioranza, K.S.B. 2011. "Effects of amendments on soil availability and phytoremediation potential of aged o,o'-DDT, p,p'-DDE and p,p'-DDD residues by willow plants (*Salix sp.*)". *J. Hazardous Materials.* (203-204): 62-68.

Mori, S. 1999. "Iron acquisition by plants". *Curr. Opin. Plant Biol.* 2: 250-253.

Okuda, T., Matsuda, Y., Yamanaka, A. and Sagisaka, S. 1991. "Abrupt increase in the level of hydrogen peroxide in leaves of winter wheat is caused by cold treatment". *Plant Physiol.* 97(3): 1265-1267.

Pilon-Smits, E. 2005. "Phytoremediation". *Annu. Rev. Plant Biol.* 56: 15-39.

Reis, A.R., and Sakakibara, Y. 2011. "Continuous treatment of endocrine disrupting chemicals by aquatic plants and biological Fenton reaction". Jap. Soc. Civil Eng., Series G (Environmental Research). 67(7):725-734.

Sakakibara, Y., Kounoike, T. and Kashimura, H. 2010. "Enhanced treatment of endocrine disrupting chemicals by a granular bed electrochemical reactor". *Water Sci. Tech.* 62(10): 2218-2224.

Schröder, P. 2007. "Exploiting plant metabolism for phytoremediation of organic xenobiotics". In: Willey, N. (Ed.), *Phytoremediation: Methods and Reviews*, Humana Press, NJ, USA.

Sei, K., Takeda, T., Soda, S., Fujita, M. and Ike, M. 2008. "Removal characteristics of endocrine disrupting chemicals by laccase from white-rot fungi". *J. Env. Sci. Health* Part A. 43: 53-60.

Terry, M. and Elisa, M.D. 2005. "[$^{C-14}$]Pentachlorophenol mineralization in the rice rhizosphere with established oxidized and reduced soil layers". *Chemosphere.* 61(1): 48–55.

Vlyssides, A.G. and Bouranis, D.L. 1998. "A kinetic approach on the estimation of iron uptake by *Apium nodiflorum* plants". *Comm. Soil Sci. Plant Anal.* 29(5&6): 561-573.

Wayland, J., Hayes, J.R., Laws, R.E. 1991. "*Handbook of Pesticides Toxicology*", vol.1, third ed., General Principles, London.

Wen, S., Hui, Y., Yang, F. X., Liu, Z. T. and Xu, Y. 2008. "Polychlorinated dibenzo-p-dioxins (PCDDs) and dibenzofurans (PCDFs) in surface sediment and bivalve from the Changjiang Estuary, China". *Chinese J. Oceanol. Limnol.* 26(1): 35-44.

Xing, W., Huang, W. and Liu, G. 2009. "Effect of excess iron and copper on physiology of aquatic plant *Spirodela polyrhiza* (L.) Schleid". *Env. Tox.* 25(2): 103-112.

Zhao, L., Zhu, C., Gao, C., Jiang, J., Yang, J. and Yang, S. 2011. "Phytoremediation of pentachlorophenol-contaminated sediments by aquatic macrophytes". *Envir. Earth Sci.* 64(2): 581-588.

Zimbron, J.A. and Reardon, K.F. 2009. "Fenton's oxidation of pentachlorophenol". *Wat. Res.* 43(7): 1831-1840.

# PHYTOEXTRACTION OF POLYCHLORINATED BIPHENYLS (PCBS) FROM CONTAMINATED SOIL BY *CHROMOLAENA ODORATA* (L) KING AND ROBINSON

Raymond Anyasi and *Harrison Atagana*
(University of South Africa, Pretoria, South Africa)

The ability of *Chromolaena odorata,* an invasive weed of tropical wastelands, propagated by stem cuttings to thrive in soil containing different concentrations of PCB and to possibly phytoextract PCB from contaminated soil was studied in a greenhouse. *Chromolaena odorata* plants were transplanted into soil containing 100, 200, and 500 µg g$^{-1}$ of Aroclor 1254 and 1260, and soil containing 100, 200, and 500 ml kg$^{-1}$ transformer oil (TO) in 1L pots. The experiments were watered daily to maintain 70% moisture at field capacity. Parameters such as fully expanded leaves per plant, shoot length, leaf colour as well as the root length at harvest were measured. *C. odorata* growth was differently affected by the different concentrations of transformer oil. The level of inhibition to plant growth increased with concentration. However, the Aroclor amended soil did not affect the plant. At the end of six weeks of growth, plants showed a diminished effect in TO amended soil to the parameters tested. Plants size was increased by 1.4, 0.46 and -1.0% in 100, 200 and 500mg/kg respectively. In Aroclor amended samples, 45.9, 39.4 and 40.0% were plants sizes at different concentrations. Such trend was observed in the leaf numbers and root length. Leaf colour was pale green in TO samples but, middle green in Aroclor amended soils. The control sample has 43.3% increase in plant size which was not significant among the values in Aroclor treated soils, an indication that *C. Odorata* could survive PCB contamination as to remediate it. The result of the GC-analysis of soil samples indicates that treatments containing Aroclor showed between 2 and 10% reduction in total PCB concentration and the treatments containing transformer oil between 2 and 100% reduction. Results from plant tissue analysis shows that PCB was present in the root, stem and leaf of plants grown in all treatments containing Aroclor while PCB was only present in roots of plants grown in transformer oil but almost completely absent in stem and leaf. The highest amount of PCB in relation to biomass found in any part of the plant was 0.5% indicating that there was a slow uptake of PCB by the plant during the six weeks of treatment. This correlates with the very large residual amounts of PCB present in the soil after the six weeks of treatment. Further studies are investigating the enhancement of the growth of rhizosphere organisms as a means of increasing degradation/removal of PCB from the contaminated soil.

# INVESTIGATING PP/LDPE/PEVA MISCIBILITY OF CARDBOARD RECYCLING'S MIXED PLASTIC WASTES BY DSC AND SEM

*Tova Sardot*, and Garon Smith
(The University of Montana, Missoula, MT, USA)

**ABSTRACT:** The feasibility of using mixed plastic wastes from cardboard recycling was investigated by looking at the miscibility of its components – 37% polyethylene-vinyl acetate hot melt adhesive (PEVA), 32% polypropylene tape (PP), 17% low density polyethylene thin film (LDPE), 9% polystyrene packing material and 5% others. The plastic mix was dried and compounded. The resulting material was subjected to characterization by differential scanning calorimetry (DSC) and scanning electron microscopy (SEM). DSC analysis revealed three principal phases corresponding to the three major components. The PEVA hot melt appears to promote miscibility between itself, the smaller granules of LDPE and some of the PP. SEM images show that the components blend into a topography with mostly small to intermediate phase regions. The large phase granules, seen in previous studies, are LDPE. Since miscibility was incomplete, the use of finer grinding and addition of compatibilizing agents is suggested.

## INTRODUCTION

Mixed commodity plastics, which account for ~ 70% of all consumed resins, are considered not recyclable on a large scale (Ajja, 2002). Rationales for this notion include: inconsistent impurities from product life, variations in day-to-day levels of polymer-type, and the debated miscibility of some polymers mixtures. The existing infrastructure that recycles plastic consumer waste (PCW) is antiquated at best. Collection and separation of polymers is costly and inefficient. There do however exist plastic wastes from industrial processes that are produced cleanly and consistently. Cardboard container recycling generates a waste stream that has a significant amount of *clean* plastic with a consistent mix of polymer-types and is the subject of this research. The plastic in the mixed waste stream is mostly commodity resins (PP, LDPE, PS) with PE-PEVA (hot melt adhesive).

Plastic wastes are a problem world-wide. As plastic generation continues to increase exponentially and land-fills decrease, recovery of polymeric wastes hovers at a mere 7% (EPA, 2009). In land-fills, plastics leach their toxic additives into waterways (Linther, 2011) and often still end up as litter in the environment. As litter, plastic migrates to waterways where birds and fish get tangled or mistakenly ingest the waste. It is estimated that over a million animals die every year due to discarded plastics (Derriak, 2002). In the oceans, we are just beginning to understand the scope of plastic litter and quantify the problem. Large plastic streams are also burned for energy recovery. Burning creates and releases toxic emissions (Simoneit, 2005). Incineration wastes an opportunity for beneficial use of a material that has a nearly endless potential to be recycled. By broadening the scale of what is recyclable, a stronger market is created for all polymers. A higher value on plastic waste means that less will end up neglected, creating problems for the environment.

Waste plastics can be converted to useful polymer alloys. This practice has been proven attainable by the wood plastic composite industry. Miscibility of mixed polymer systems is a complex issue that depends largely on processing, the percentage of each starting polymer, and interfacial tensions. Although, most combinations are considered incompatible, use in non-critical applications or

compatibilization to improve interfacial adhesion of polymer phases is possible (Ajja, 2002). Treatment by shearing is another way to achieve better mixing of otherwise immiscible polymers. This method has been successful in blending different grades of polyethylene (PE) leading to improved clarity, abrasion and stress crack resistance.

The mixed plastic waste material for this research came from the Smurfit-Stone Container Missoula mill. This mill had an Old Corrugated Container (OCC) facility that reclaimed high tear-strength fiber for reuse in their linerboard product. The OCC rejects emerged in three streams known as the hydradenser, the select purge, and the Wandel screen at a rate of 7-14 tons per day. These streams were de-watered and sent to a multi-fuel boiler for energy reclamation. Cardboard recycling facilities worldwide have analogous waste streams. In the near future these waste may have to be land-filled as EPA is reconsidering what is safe to burn. The Wandel waste stream (WWS) was chosen for this research because it had the highest plastic content of the exiting OCC streams and accounted for 75% of the total plastic rejects.

The aim of this study was to establish general miscibility/immiscibility of the identified polymers of the WWS.  An understanding of the miscibilities allows one to identify the best phases on which to concentrate for improving compatibilization. Ultimately, this will create a higher quality starting material and broaden its potential for reuse. Differential scanning calorimetry (DSC) can reveal information on phase interactions. Scanning electron microscopy (SEM) provides images from which to assess polymer identification and phase behavior. Together, the two techniques help illuminate the miscibility of the three main polymer types in the WWS.

## MATERIALS AND METHODS

The mixed plastic waste stream investigated in this research was from the Smurfit-Stone Container Corporation's OCC cardboard recycling facility in Missoula, MT. Previous studies reported that the composition of the Wandel waste stream (WWS) by weight is:  37% hot melt adhesive for boxes, 32% polypropylene (PP) carton sealing tape, 17% low density polyethylene (LDPE) thin film, 9% polystyrene (PS) packing material, and 5% other (Sardot, et al., 2012). Hot melt cardboard adhesive is composed of ~35% ethyl vinyl acetate (EVA), ~ 30% wax, and ~ 35% tackifiers. Actual percentages vary slightly based on manufacturer formulation. The 'other' category includes wood shards, low tear-strength fiber, foam, staples or any material that has a small contribution to the waste stream.

Plastic consumables were used as control sample analogues for identified plastics in the WWS mix. Woodworking hot melt glue sticks, 10 cm x 1.1 cm, from the Ace Hardware Corporation were used for comparison to cardboard box adhesive (PEVA hot melt sample). Recycled low-density polyethylene (LDPE) pellets (post-industrial thin film bags) from Rainer Plastics, Inc. were used as a control for the thin film LDPE. Two types of tapes were utilized to account for possible differences in generic brand film or adhesive thickness: Box Sealing Tape (48 mm x 10.1 m) from the 3M™ Stationary Products Division (3M™ tape sample) and Carton Sealing Tape (48 mm x 45.7 mm) from Greenbrier International, Inc (generic tape sample).

The WWS was compounded in a Lestritz 18-mm co-rotating twin-screw extruder at 100 rpm. All barrel zones were set at 180°C.  The compounded material was extruded into a rod and then ground to pass through a screen with 4-mm diameter openings. The compounded WWS was subsequently re-compounded, re-ground and re-screened.

Differential scanning calorimetry (DSC) was performed using a TA instrument model Q200 DSC coupled to a refrigerated cooling unit. The samples were cooled from room temperature to -20°C, then

subjected to a second temperature cycle from -20°C to 250 °C at heating/cooling rate of 10$^o$C/min. Data were analyzed using the Universal Analysis 2000 software (TA instruments).

Images were produced using a Tescan Mira XMU scanning electron microscope (SEM) with a resolution of 3 nm at 30 kV and an accelerating voltage of .2-30 kV detected by secondary electron back-scatter. Samples were sputtered with gold to increase their conductivity.

**RESULTS AND DISCUSSION**

*Differential Scanning Calorimetry (DSC).* DSC thermograms illuminate melt phase behavior, offering some insights into miscibility of the WWS mixture. EVA, PP and PE have low interfacial tensions and any immiscibility between them stems from differences in branching and melting temperatures (Li J., 2001). Figure 1. shows the DSC scans of the WWS mix (Curve 1) compared with control samples and isolated WWS polymer ingredients. The second and third curves in Figure 1., shows the PEVA (hot melt adhesive) samples. A typical WWS hot melt sample shows a two peak phenomenon, the first of which occurs at ~70°C and the second at ~ 112°C. The second is probably the PE copolymer of the hot melt. Formulations vary greatly among manufacturers and with product applications. The control used for this sample differs from the WWS hot melt, showing only one peak at ~ 70°C.

The wax and tackifier components of the PEVA hot melt adhesive are expected to mix well with olefins. Wax has been shown to bond well with LDPE and to increase mechanical properties (Rassiah, et al., 2010). Tackifiers are used in PP- and PE-based hot melts. The hot melt adhesive should also be compatible in the WWS. Tackifiers are most commonly terpene-phenol resins (TPR). TPRs are responsible for the adhesion of the PEVA to the substrate, forming bonds between its phenol groups and materials like aluminum, paper/fiber and glass (Nardin, et al., 1993). They remain stable in excess of 260°C and are expected retain integrity during compounding at 180°C (Ruckel, n.d.). The combination of wax and TPRs may be responsible for some of the unexpected adhesion and dispersion of polymers in the WWS.

The fourth and fifth curves in Figure 1. isolate the LDPE contribution to WWS. The appearance of two peaks suggests that this phase contains LLDPE, but it is likely that LDPE also exists in the mix. Industry does not differentiate between these two grades of PE even though they have different branch lengths that cause very different material properties. PEs of differing crystallinities (e.g., HDPE, LDPE, LLDPE), can be immiscible even though interfacial tensions are low (Li, 2001). This is due to the different melting temperatures (Tm) and extents of branching. During melting, liquefaction of the higher-Tm PEs can be impeded as they become encased by already molten material.

In the WWS mix, the first peak of the LDPE phase and the second peak of the hot melt phase have overlapping Tms and should have low interfacial tensions – a good environment for partial miscibility. Additionally, the first peak of the hot melt in the WWS is significantly smoothed over and broadened. The hot melt, some LLDPE and some PP is expected to comprise the main bulk of the polymer system. The longer branched LDPE fractions and most of the PP exist separately. The miscibility of PP and PE (of varying crystallinity) has been studied extensively, but their miscibility is debated. PP has been shown to exhibit limited miscibility with LDPE with evidence of some portions of PP dissolved in the LDPE phase (Dong, et al., 1998). Blends of PP and LLDPE, however, have been shown to achieve miscibility (Dumoulin, et al., 1989a, Dumoulin, et al., 1987b, Flaris, et al., 1992a, Flaris, et al., 1992b, Li, 2001, Ultracki, 1989). Further miscibility improvements could be attained through the use of compatibilizers.

The last four curves in Figure 1. show PP behavior. Virgin PP and two different tape control samples are included with the WWS to account for possible differences in brand, although these seem small. The PP peak of WWS is broadened over that for the other PP samples, indicative of some slight miscibility in the mix. Ethylene vinyl acetate has been employed to compatibilize PP and wood flour (Dikobe, 2009).

There may be other phases due to the PS and other trace polymers in the WWS. The occurrence of these materials is below 10% and any contribution that deviates from the three main polymer constituents will not be evident in the DSC thermograms.
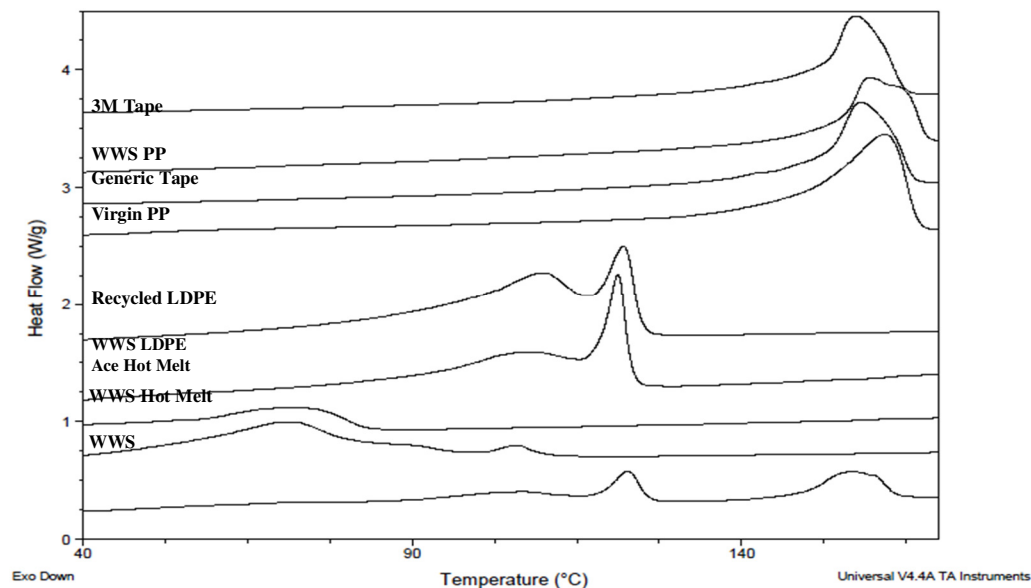


**FIGURE 1.** DSC scans of the WWS mix compared with hot melt sample from the WWS and the Ace hot melt, LDPE sample from the WWS and a recycled LDPE, tape sample from the WWS, generic packing tape, 3M packing tape and virgin PP.

***Scanning Electron Microscopy (SEM) Morphology.*** Even when polymer phases exist separately, they still can have a great effect on one another. The existence of two polymer phases can inhibit spherulite growth. Since the WWS mix is a many polymer system, the existence of very small phases may be partially due to restricted growth of the crystalline structure, as there is no discernable spherulite structure in images with ~ 1 μm resolution (Figure 2.). PEVA is likely the main matrix material. Previously reported tensile values showed that the WWS exhibited a 181% higher value for ultimate strength in comparison to hot melt adhesive values (Sardot, et al., 2012). The improved performance indicates some intermediate miscibility in the mixed polymers. Possible interactions could include: 1) miscibility of the shorter branched fractions of LLDPE with the PE copolymer of PEVA hot melt adhesive (Figure 1.); 2) miscibility of PP with LLDPE (Li, 2001); and 3) bonding of the tackifier component with the PP and PE phases. Previously published 400x micrographs of the WWS showed legging due to the visible presence of small LDPE phases (Sardot, et al., 2012).

SEM micrographs of the WWS mix are shown in Figure 2. at increasing magnifications – 500x, 4.99kx, 16.67kx and 66.67kx. Panel 2c. is the best image for viewing polymer phases. There is a smooth bulk matrix background upon which small, intermediate and larger granules are seen. There are two

possibilities for the polymer content of the smallest grains ($\leq$ 200 nm seen easily in the shaded area in the upper left corner of Panel c.) – PP and/or short-branched LLDPE. Based on WWS composition, there are nearly equal amounts of PEVA and PP (37% and 32%, respectively) in the WWS, which argues for the smallest grain phases being PP. This leaves LLDPE as the prime candidate for the intermediate phases. The largest phase granules in Panel 2c. (about 1-2 $\mu$m in dimension) are most likely LDPE. Ill-mixed LDPE rods are seen protruding from the sample face in Figure 2a. consistent with previous studies.
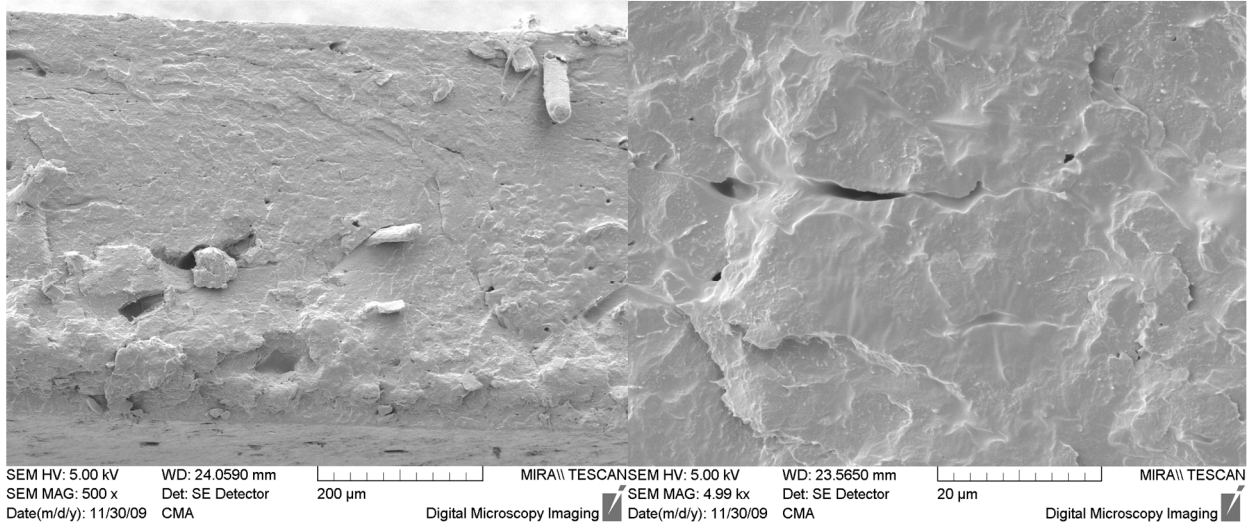


(a.)



(b.)
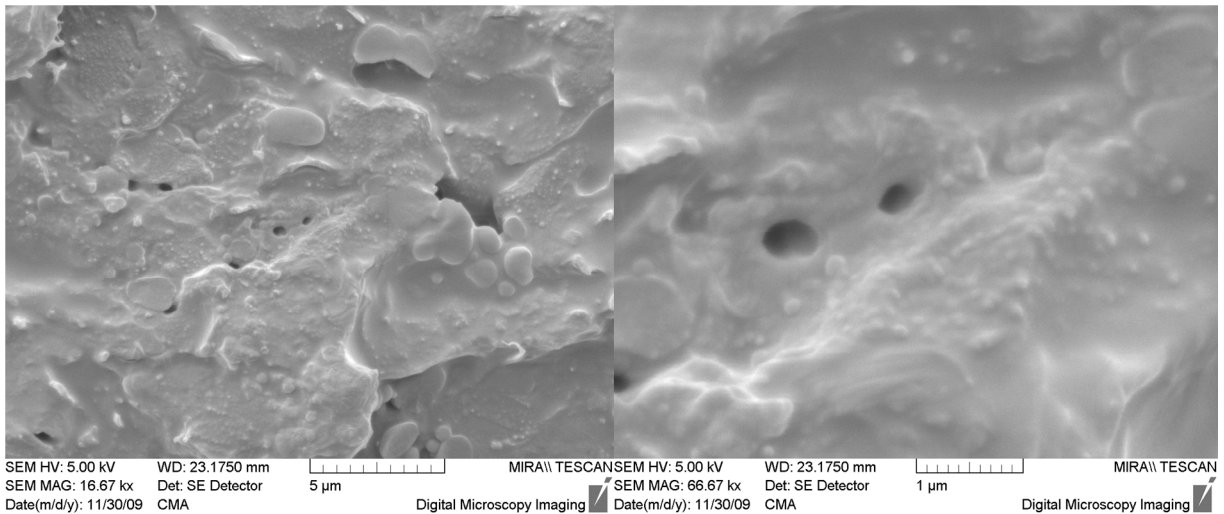


(c.)



(d.)

**FIGURE 2.** SEM images of WWS mixed plastic alloys at (a.) 500x, (b.) 4.99kx, (c.) 16.67kx, (d.) 68.67kx magnification.

A few phases may be due to PS and other trace polymers in the WWS. Identification of these minor phases was beyond the scope of this study's methodologies and instrumentation. No anomalous phase regions were noted in any SEM image, so trace polymers seem to have little influence on the final material.

**CONCLUSION**

Partial miscibility has been identified in the mixed polymer system of the WWS. Given the overall WWS composition, the PEVA hot melt seems to be promoting miscibility among other components, especially LLDPE and PP. Utilizing a compatibilizing agent geared towards increasing interactions between the two least miscible polymers in the mix, PP with PE, would be beneficial in increasing the overall properties. The WWS may also be a good candidate for a rubber additive. Many ternary PP/PE/rubber composites have been investigated that exhibited good miscibility and improved properties (Hemmati, et al., 2001). Furthermore, fine grinding and a second compounding run (with or without an additive) may enhance dispersion by decreasing phase sizes (Moreira, et al., 2001). This can also be done at an elevated temperature to entice mixing of dissimilar branched polymers.

**ACKNOWLEDGEMENTS**

**REFERENCES**

Ajji A., Dumoulin M. M., Akkapeddo K., Everaert V., Bahari K., Goettler L. A., Brown B., Hong S. G., Cowie J. M., Groeninckx G. 2002, *Polymer Blends Handbook, Volume I. L.* Ultracki (Ed.), Kluwer Academic Publishers, Dordrecht, The Netherlands.

Environmental Protection Agency. 2010. *Municipal Solid Waste Report 2009: Full Report.* http://www.epa.gov/osw/nonhaz/municipal/ msw99.htm 2009. Accessed 7 Sept 2011

Derriak J. 2002. "The Pollution of the Marine Environment by Plastic Debris: A Review". *Marine Pollution Bulletin*. 44: 842-852.

Dikobe D. 2009. "Morphology and Properties of PP/PE Vinyl Acetate Copolymer/Wood Powder Blend Composites". *Express Polymer Letters*. 3: 190-199.

Dong L., Olley R. H., Basset D. C.1998. "On Morphology and Competition Between Crystallization and Phase Separation in Polypropylene-polyethylene Blends". *J Mat Sci*. 33: 4043.

Dumoulin M. M., Farha C., Utracki L. A. 1984a. "Rheological and Mechanical Properties of Ternary Blends of Linear-low-density Polyethylene/polypropylene/ethylene-propylene Block Polymers". *Poly Eng Sci*. 24: 1319.

Dumoulin M., Carreau P. J. 1987b. "Rheological Properties of Lonear Low Density Polyethylene/polypropylene Blends. Part 2: Solid State Behavior". Polymer Eng Sci. 27: 1627-1633.

Flaris V., Stachurski Z. H. 1992a. "Effects of Processing on the Mechanical Properties of a Polyolefin Blend". *Polym Int*. 27: 267-273.

Flaris V., Stachurski Z. H. 1992b. "Mechanical Behavior of Blends of Polyethylene, Polypropylene, and an Ethylene-propylene Block Copolymer at -20°C". *J Applied Polym Sci.* 45: 1789.

Hemmati M., et al. 2001. "Study on Morphology of Ternary Polymer Blends. I. Effects of Melt Viscosity and Interfacial Interaction". J Appl Polym Sci. 82: 1139-1137.

Li J., 2001. "Miscibility and Isothermal Crystallization of Polypropylenes in Polyethylene Melts. *Polymer*. 42: 7685-7694.

Linther D., 2011, *Environmental and Health Hazards of Plastic Polymers and Products*, M.S. Thesis, University of Gothenburg, Sweden.

Moreira J., et al. 2001. "Influence of Temperature, Molecular Weight, and Molecular Weight Dispersity on the Surface Tensions of PS, PP, and PE". *J Appl Polym Sci*. 82: 1907-1920.

Nardin M., et al.1993."Effects of the Composition of Hot-melt Adhesives on their Bulk and Interfacial Properties". *J. Phys. IV France*. 3: C7 1505- C7 1510.

Rassiah K., et al. 2010. " Study of the Optimum Condition Towards the Inducing Paraffin Wax LDPE". *IJET-IJENS.* (10) 4: 9-12.

Ruckel E. R., n.d. *Terpene Phenol Resins – Tackifiers for the Next Generation of Adhesives*. Arizona Chemical Co. International Paper Corporate Research Center, Tuxedo, NY.

Sardot T., et al. 2012. "Characterization of a Cardboard Recycling Facility's Mixed Plastic Waste for Beneficial Use". *Waste Biomass Valor*. DOI: 10.1007/s12649-012-9111-0 (online only).

Simoneit B. 2005. "Combustion Products of Plastics as Indicators for Refuse Burning in the Atmosphere". *Environ. Sci. Technol.* 39: 6961-6970.

Ultracki L., 1989. "Melt Flow of Polyethylene Blend, Multiphase Polymer: Blends and Ionomers". *ACS Symp Ser.* 395: 153-210.

# BIO-ASSESSMENT
# AND
# TOXICOLOGY

# MITIGATION OF POWER LINES-PRODUCED MAGNETIC FIELDS BY OPTIMIZED ACTIVE SHIELDING

*Ayman Aboud* (Electrical Engineering Department, Fayoum University, Fayoum, Egypt)
Hussein Anis (Electric Power Department, Cairo University, Cairo, Egypt)

**ABSTRACT:** In this paper a technique for mitigating magnetic fields arising from either overhead lines or sub-transmission lines is presented, based on the use of active conductors loop (to be placed in proximity of the area where magnetic field mitigation is sought). The optimal choice of the location of conductors and currents to be driven in the loop is obtained by means of a genetic algorithm. Significant reductions of magnetic flux density into any desired target area are subsequently obtained. In this work, a novel approach is used whereby the exact extent of the targeted protected zone may be controlled.

## INTRODUCTION

Due to some epidemiological studies that have suggested an association between exposure to power frequency magnetic fields and certain diseases, especially childhood leukemia, some local and central authorities are inclined to adopt precautionary approaches and develop policies aimed at reducing, whenever possible, the risk of human exposure to magnetic fields produced by power lines (Aboud and Anis, 2009; Svendsen et al., 2007). Active shielding may be used, which involves the use of current-carrying conductors (driven by an external emf). The magnetic field induced by the injected current would effectively counter that emanating from the line conductors resulting in a reduced field in the power line vicinity. A technique for the mitigation of the magnetic due to power lines, based on active conductors and passive shields is presented in (Celozzi and Garzia, 2002). A study proposed in (Reta-Hernández and Karady.1998) of an active shielding arrangement to attenuate the 60 Hz magnetic fields produced by a transmission line at specific points.

This paper presents an efficient way to mitigate the magnetic field resulting from transmission and sub-transmission power lines in selected areas in their neighborhood. Case studies include a 500 kV single circuit overhead transmission and a 66 kV double circuit sub-transmission lines.
The location of the loop, the injected current's amplitude and phase influences the degree of field reduction. Therefore, designing the loop, i.e., determining its position and current essentially constitutes an optimization problem. The problem is constrained by the minimum allowable clearance between the loop and the line conductors. The optimization problem thus seeks the loop coordinates, the current amplitude and phase influences.

Evolutionary computation lends itself to solving this optimization problem, where it enjoys the advantage that it uses probabilistic transition rules, not deterministic rules. It uses payoff information (fitness function), not derivatives, and it works with a coding of solution set, not the solutions itself (Sivanandam and Deepa, 2008). In this paper, an optimization technique based on a genetic algorithm (GA) is presented, where the loop configuration, the current amplitude and phase that produce maximum reduction the magnetic field are sought. However, the targeted objective function to be optimized should be based on the specific protected domain, where it is desired to render the magnetic field minimal. Judgment on the part of the responsible authority at the power line site should be exercised to determine such a domain. The domain has been customarily simplified to include magnetic fields only at the edge of the right-of-way (ROW) and at mid-line span. This paper offers means of accommodating such judgment by generalizing the domain of interest in the optimization-based design of induction loops and comparing it to that confined to the single-point ROW edge.

## MATERIALS AND METHODS

**Directive Field Mitigation.** Depending on the target exposure risk area magnetic field mitigation may be classified into:

- **Unilateral field mitigation**

It is applied when –as seen in Fig. 1 - the target risk area is located on only one side of the power line.  In such cases and in order to achieve optimal mitigation one loop is used.

- **Bilateral field mitigation**

It is applied when –as seen in Fig. 1 - the target risk area is located on both sides of the power line, which is the case in many residential neighborhoods.  In such cases two inductive loops are optimally designed and placed on both sides of the line.



Unilateral field mitigation                    Bilateral field mitigation
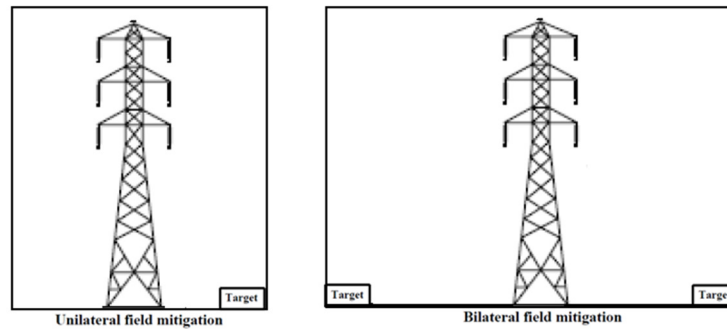
**FIGURE 1 Unilateral and Bilateral Field Mitigation**

**Zone-Based Field Mitigation.** The field mitigation process amounts to maximizing the reduction in magnetic field intensity achieved by installing the inductive loops.  This paper introduces the idea of targeting a specific zone in the power line neighborhood, in which magnetic field is desired to be mitigated.  This necessitates defining the reduction factor to suit the said approach.

**Reduction Factor.** In view of the extended mitigation approach introduced in this paper two reduction factors are defined.  Either way, the applicable reduction factor serves as the objective function in the optimization (maximization) algorithm.

***The Point Reduction Factor*** (PRF) is defined as the relative reduction in magnetic field intensity at one single critical point in the space surrounding the power line.  Such point has been customarily (and conveniently) taken by previous research as the edge of the right-of-way at the line's mid-span, where the conductors' clearance-to-ground is minimal.  It is expressed by

$$PRF = (\frac{B_p - B_t}{B_p}) \qquad (1)$$

***The Extended Reduction Factor*** (ERF), which this paper is introducing, is defined as the integrated relative reduction in magnetic field intensity over a specific distance –rather than a single point- along the mid-span plane. It may also mean the integrated relative reduction in magnetic field intensity over a specific zone in the space surrounding the power line.  Such a distance or zone, which are considered critical to people's presence and hence their welfare, are, respectively, termed here the ***Critical Mitigation Distance*** (CMD) and ***Critical Mitigation Zone*** (CMZ). The idea is that such a critical distance (or, zone) is determined based on the utility's (or, the authority's) judgment. The present paper deals with the case of a CMD measured latterly at the power line's mid-span. As a procedural example, such distance arbitrarily

extends from a point within the right-of-way to a point beyond the right-of-way's edge at the line's mid-span. The extended reduction factor based on a critical mitigation distance is expressed by

$$\text{ERF} = \int_{\text{CMD}} \left( \frac{B_p - B_t}{B_p} \right) dx, \qquad (2)$$

while that based on a critical zone is expressed by

$$\text{ERF} = \int_{\text{CMZ}} \left( \frac{B_p - B_t}{B_p} \right) dxdy \qquad (3)$$

**Optimization Problem.** Designing the field-mitigating inductive loops is essentially an optimization problem, whereby the magnetic field reduction factor is maximized.

The optimization product is an array of six variables (coordinates of the double-loop conductors & current amplitude and phase). These are subject to the following constraints:
1. To avoid flashovers, loop conductor coordinates are subject to the minimum allowable clearance between the loop and the phase conductors.
2. Other location constraints imposed by possible proximity of prospective structures in the area.
3. Current amplitude allowed to fall between 0 and active current limit.
4. Current phase allowed falling freely between 0 and 360°.

**Genetic Algorithm Application.** The authors of this paper have investigated the possible algorithms that can serve the paper's prime goal, namely, targeting a specific zone, where mitigation would be ensured to be effective. The evolutionary computational approach, customarily known as the genetic algorithm, appears to lend itself well to the problem as it inherently–during the optimization process- avoids falling into local optima and thus producing less than accurate results (Rao, 2009).

Genetic Algorithms (GAs) simulate the natural evolutionary process in searching for the best solution based on the mechanism of natural selection and natural genetic operation. The evolution starts from a population of completely random solutions and searches for the best generation by generation. In each iteration, multiple solutions are stochastically selected from the current population, modified (mutated or recombined) to form a new population, which is used in the next iteration.

The identification of the coefficients present in the reduction factor is made using a genetic algorithm, with the following characteristics:
- Population size: 100
- Fitness function: PRF or ERF, depending on the specific case study.
- Selection operator: Roulette
- Mutation operator: Adaptive feasible
- Crossover operator: Two point
- Probability of crossover: 0.8
- Stopping criteria: Stall (20 generations)

**RESULTS AND DISCUSSION**

**Case Study.** Although higher voltage power lines carry larger currents and are, therefore, expected to emanate larger magnetic fields, lower voltage distribution lines are located closer to sensitive population areas and their conductors and much closer to the ground and surrounding buildings. Therefore, lines at all levels are worthy of careful examination. In the case study, two transmission lines are subjected to the introduced procedure. The 500 kV line has single circuit towers with flat conductor configuration placed at a height of 20.5 m at the tower; the outer conductors are placed 13 m from the center. The 66 kV line uses double-circuit towers with their conductors placed symmetrically about the center and at 2.9 m from

it; their heights at the tower are 16.7, 20.5, and 22.2 m. Magnetic fields are computed at a height of 1 m from the ground. Relevant data about these lines are summarized in Table 1.

**Case Study Results.** For each of the two power lines, the lateral magnetic field's profile at mid-span was developed, while the case of unilateral field mitigation is applied. The new principle of extended mitigation is applied to an assortment of three target areas, where optimal mitigation by inductive loops is applied. These target areas are:

- Area (0) designates the traditional "point mitigation", where mitigation is optimality targeting a single point located at the edge of ROW.
- Area (1) applies the mitigation optimality to an area extending from the ROW's edge to a distance 40% beyond the ROW, i.e., CMD is 40%.
- Area (2) confines the mitigation optimality to an area extending from a point located at 80 % of ROW to a point located at 140 % of ROW, i.e., CMD is 60%.

**Active current limiting.** The effect of active current on the ERF can be shown in Figures 3 and 4 for 500 kV and 66 kV lines, respectively. At zero active current, the ERF reaches its minimal value, which represents the case of passive shielding. With increasing the active current, the ERF increases tell unlimited active current. The active current limit is determined in all cases corresponding to 10% change in ERF. The limit is equal to 20% and 30% from rated current for 500kV and 66kV respectively.

**Table 1. Case Study Data**

| Line's voltage level (kV) | 500 | 66 |
|---|---|---|
| Number of circuits per tower | 1 | 2 |
| Right-of-Way (m) | 25 | 13 |
| Minimum clearance-to ground (m) | 11 | 8.7 |
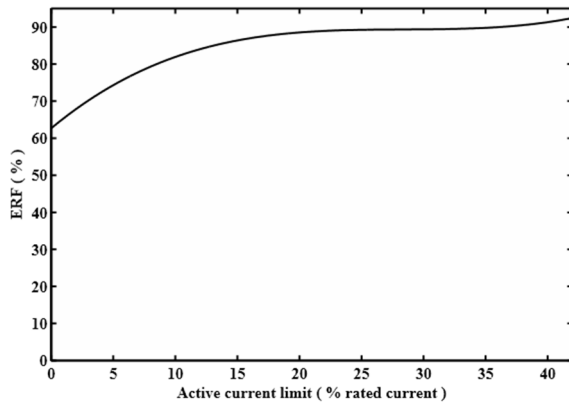


**FIGURE 2 Active Current Limits for 500 kV Line**
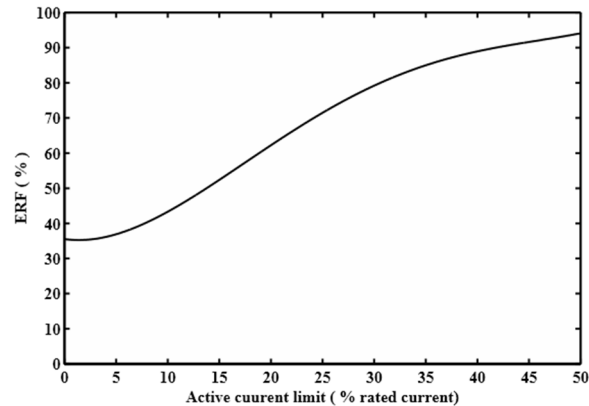


**FIGURE 3 Active Current Limits For 66 kV Line**

Figures 4 & 5 display the unilateral magnetic field profiles for the different power lines, when the new mitigation technique is applied in accordance with the above area classification, namely, [Point Mitigation, CMD 40% & CMD 60%]. Also, shown on all plots are the cases of unmitigated magnetic fields, which would allow a quick visual inspection of the effect of mitigation.

Table 2 summarizes the resulting coordinates of the shielding loop produced by the proposed algorithm. Also given are the ERF and PRF, associated with the three power lines for the three areas, as

defined earlier. It should emphasized that the listed ERF values are calculated [by equation (3)] over each corresponding shown target zone, where mitigation is applied to assess the effectiveness of the new approach in protecting that target zone.
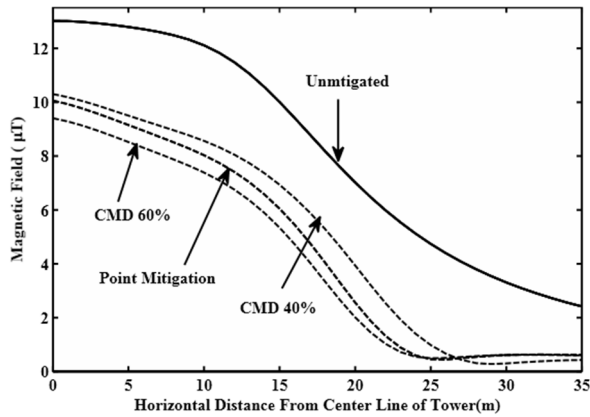


**FIGURE 4 Magnetic Field Distributions for 500 kV Line**
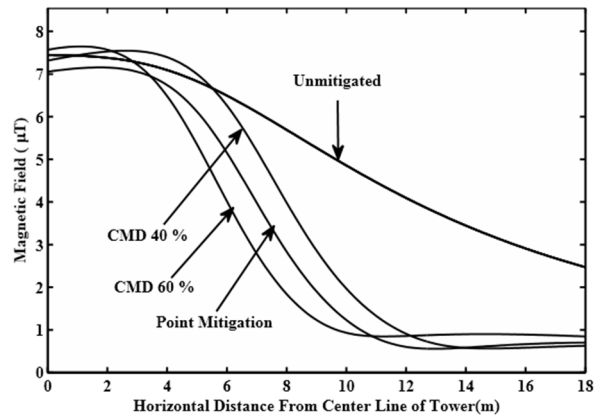


**FIGURE 5 Magnetic Field Distributions for 66 kV Line**

**Table 2. Unilateral Case Study Results**

| Line | Area / CMD ( % ) | Loop Coordinates ( m ) | | $I_{act}$ ( A ) | Relative Angle | ERF ( % ) |
|------|------------------|------------------------|---|------|---------|-----|
| | | $( X_1 , Y_1 )$ | $( X_2 , Y_2 )$ | | | |
| 500 kV | 0 / 0 | (19.4, 7.3) | (-18.7, 9.5) | 176 | -63.9$^o$ | 88.4 |
| | 1/ 40 | (20.8, 7.4) | (-20.9, 6.6) | 176 | -9.9$^o$ | 87.6 |
| | 2 / 60 | (18.5, 7.6) | (-14.3, 8.9) | 176 | -58.6$^o$ | 83.1 |
| 66 kV | 0 / 0 | (10.2, 15) | (6.1, 4.9) | 180 | -95.1$^o$ | 85.2 |
| | 1/ 40 | (10,14.6) | (6.7, 5.3) | 180 | -94.7$^o$ | 78.6 |
| | 2 / 60 | (4.7, 4.8) | (3.5, 15) | 180 | -83.4$^o$ | 74.6 |

**Table 3. Bilateral Case Study Results**

| Line | CMD ( % ) | Loop 1 | | Loop 2 | | $I_{act}$ ( A ) | Angle | ERF ( % ) |
|------|-----------|--------|---|--------|---|------|-------|-----|
| | | ( X1 , Y1 ) | ( X2 , Y2 ) | ( X1 , Y1 ) | ( X2 , Y2 ) | | | |
| 500 kV | 0 | (21.2,5.6) | (2.1,8.3) | (-20.4,5) | (-1.6,5.8) | 176 | 263.2$^o$ | 92.8 |
| | 40 | (22.3, 6.1) | (1.3, 7.5) | (-21.6, 5.2) | (-1.1, 6.2) | 176 | 259.2$^o$ | 82.7 |
| | 60 | (18.3,6.6) | (1.6,5.9) | (-17.6,6.9) | (-17.9,7.4) | 176 | 273.5$^o$ | 79.8 |

**Bilateral Versus Unilateral Field Mitigation.** The application of the zone-based mitigation using evolutionary computation was extended to the case of bilateral mitigation. Bilateral field mitigation –as demonstrated in Figure1 - is when target areas - symmetrically located on both sides of a transmission line- are declared to be at risk. Typically this is the case of farm lands and large industrial complexes. Table 3 summarizes the resulting loops coordinates obtained as a result of using the proposed algorithm. Fig. 6 shows bilateral field mitigation.
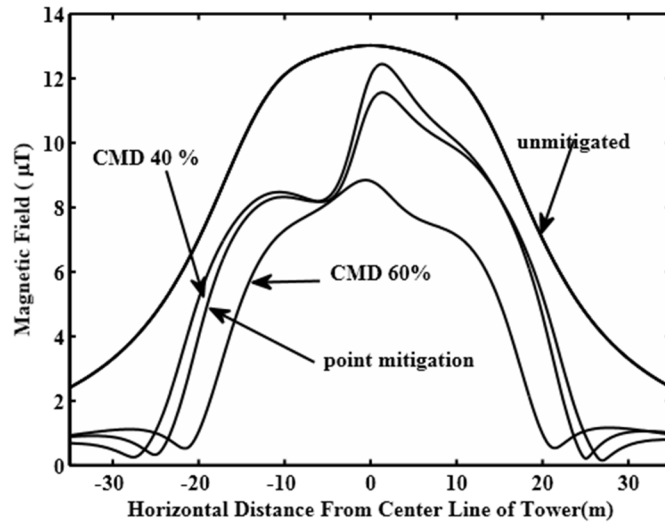


**FIGURE 6 Bilateral Magnetic Field Distributions for 500 KV Line**

## CONCLUSIONS

1. A method to locate efficient active shields of magnetic field from power lines has been presented. It consists of obtaining positions and currents of shield conductors that maximizes ERF a zone near power line by using genetic algorithms. The use of genetic algorithms allows proper application of the newly introduced zone-based mitigation technique, where it ensures finding an efficiently quasi-optimal solution that would otherwise be difficult to find due to the number of parameters involved in the optimization problem.
2. The ERF increases with the increase of the active current in shield wires.
3. The active current is limited in all cases corresponding to 10% change in ERF to decrease cost of active current source.
4. The active current limit is equal to 20% and 30% from rated current for 500kV and 66kV respectively.
5. With high voltage transmission lines (500 kV and 66 kV), the overall field reduction is substantial when zone-based mitigation targets the distance extending from the ROW's edge to a distance 40% beyond the ROW, i.e., CMD is 40%..

## REFERENCES

Aboud A., H. Anis. 2009. "Probabilistically-Based Risk of Exposure to Power Lines Magnetic Fields" *J. Electric Power Components and Systems*, 37(11): 1241-1259.

Svendsen A. L., T. Weihkopf, P. Kaatsch, and J. Schuz. 2007. "Exposure to magnetic fields and survival after diagnosis of childhood leukemia: a German cohort study". *Cancer Epidemiol Biomarkers*. 16(6): 1167-1171.

Celozzi S., and F. Garzia. 2004. "Active shielding for power-frequency magnetic field reduction using genetic algorithms optimization". *IEE Proc.-Sci. Meas. Technol.*, 151(1): 2-7.

Reta-Herna´ndez M. and G. Karady. 1998. "Attenuation of low frequency magnetic fields using active shielding". *Electric Power Systems Research*. 45(1):57-63

Sivanandam S. N., S. N. Deepa. 2008. *Introduction to Genetic Algorithms*. Springer-Verlag, Berlin.

Rao S.S. 2009. *Engineering optimization: theory and practice*. 4th ed.,Wiley.

# A HYDROLOGIC APPROACH RELATING TO THE INFLUENCES OF RADIOACTIVE SUBSTANCE IN A HUMAN BODY

*Syota Sasaki*, Hayase Yoneda, and Tadashi Yamada (Chuo University, Tokyo, Japan)
Tomohito J. Yamada (Hokkaido University, Hokkaido, Japan)

**ABSTRACT:** This study proposes a method to calculate absorbed dose emerged from radioactive substances in a human body. Previous research by specialists of radiology is too difficult and complex for non-specialists to understand. This study aims to arrive at simple understanding related to internal exposure by ingestion for general scientist and engineers. Emitted energy per radioactive decay is calculated from decay schemes and energy spectrum of $\beta^-$ decay related to individual nuclides. Accuracy of the method is proved by comparison with previously proposed method. Absorbed dose is calculated from emitted energy and total exposure dose. A coefficient of committed effective dose is calculated from absorbed dose. The calculated values are compared with those determined by previous research. Majority of nuclides are similar, the method indicates equal accuracy with previous research. Minority of those, however, does not match. Such minority of nuclides are modified to consider those tissue weighting factor and bone-seeking. Furthermore, concrete value of absorbed dose is calculated. Kalium and cesium are adopted as in point examples. It is shown that this study is useful to understand the influence of radioactive substances to a human body for general scientists and engineers. Universality of knowledge in hydrology is proved in the other field.

## INTRODUCTION

Fukushima Daiichi nuclear disaster in Mar. 2011 is greatly interested in a number of people, and throws them the excessive anxiety caused by the deficiency of fundamental information concerning radioactivity. Health damage by radiation is, however, difficult to understand not only the public but also general scientists and engineers. At the present, only very limited specialists of radiology correctly understand the information related to the disaster. The authors proposed a method to calculate storage of radioactive substances in a human body and total exposure dose by a hydrological tank model and runoff analysis [1] for non-specialists of radiology. In addition to this, the authors propose a method to calculate emitted energy per radioactive decay and absorbed dose. In the previous study [2], the absorbed energy into respective organs is calculated by computer simulation including Monte Carlo method. The method is useful to calculate accurate physical quantities. It is, however, too difficult for non-specialists of radiology to understand. This study provides better understanding related to influence of radioactive substances to a human body from the viewpoint of hydrology and nuclear physics.

## MATERIALS AND METHODS

In this paper, the authors focus attention on $\beta^-$ decay and $\gamma$ ray radiation, because of the fact that only $\beta^-$ and $\gamma$ decay are observed in the vicinity of the nuclear plant at the present. In the following, principles of nuclear physics and an estimation method the authors propose are indicated.

**Energy of radiation emerged from $\beta^-$ decay.** In $\beta^-$ decay, emission of an electron ($e^-$) and an electron antineutrino neutrino ($\overline{V}_e$) is observed per decay while at the same time converting a neutron ($n$) to a

proton ($p^+$). To put it another way, the atomic number of the substance increases one with emission of an electron. The process is expressed as the following formula (1).

$$n \rightarrow p^+ + e^- + \overline{\nu}_e \tag{1}$$

In the present study, only energy of electron is considered, interaction by neutrino is ignored. Fig.1 shows the decay scheme of $^{137}$Cs, of which decay is observed in the disaster. Approximately 94.6% of $^{137}$Cs decays to a metastable $^{137m}$Ba with electron emission of which kinetic energy is maximally 0.5120 MeV. Subsequently, $^{137m}$Ba populates stable $^{137}$Ba with radiation of γ ray of which energy is 0.6617 MeV. The other 5.4% of $^{137}$Cs directly decays to $^{137}$Ba with electron emission of which energy is maximally 1.174 MeV [3].

In the decay, it is remarkable that the energy of electron is not predicted deterministically, but stochastically. Electrons have a continuous energy spectrum such as Fig.2 [4, 5]. Assuming that the ratio ( $a$ ) of mean kinetic energy of electron ( $\overline{e}$ ) to maximum that ( $e_{max}$ ) equals 1/3, the value is known theoretically and experimentally [4, 5].
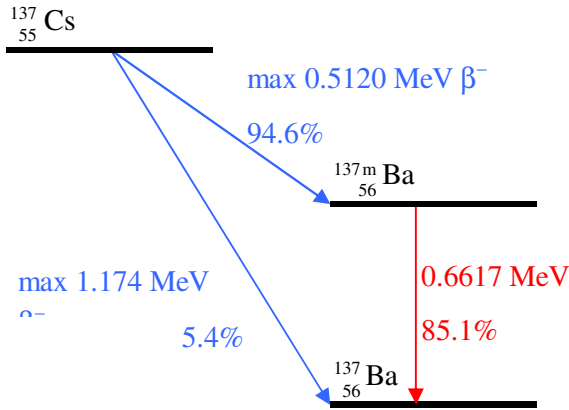


**Fig. 1** The decay scheme of $^{137}$Cs.
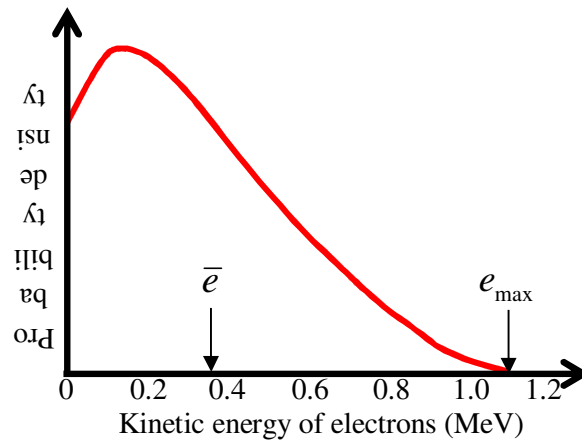
**Fig. 2** An energy spectrum of β$^-$ decay, from $^{210}$Bi as an example.

**The absorptivity of γ ray to a human body.** Estimation of the γ ray absorptivity to a human body is important for calculation of absorbed dose. In previous research [2] of Medical Internal Radiation Dose Committee (MIRD) and International Commission on Radiological Protection (ICRP), the absorptivity is assumed 40% and 60% individually. In this study, the absorptivity of γ ray ( $b$ ) equals 1/2 to take the intermediate value between researches of ICRP and MIRD.

**A calculation method of absorbed energy emerged from radioactive decay.** The energy per decay is calculated on the assumption that energy emerged from β ray is entirely absorbed to a body. Emitted energy per radioactive decay $\overline{E}$ is provided from the following expression (2). $i_{max}$, $j_{max}$, $\mu_i$, $\nu_j$ and $e_{\gamma j}$ indicate a number of arrows of β decay, that of γ decay, emission ratio of β ray, that of γ ray and radiation energy by γ ray, respectively.

$$\overline{E} = \sum_{i=1}^{i\,max} a\mu_i e_{max\,i} + \sum_{j=1}^{j\,max} b\nu_j e_{\gamma j} \tag{2}$$

The value of $\overline{E}$ is concretely calculated as follows. $^{137}$Cs decays shown as Fig.1, $\overline{E}$ is calculated as expression (3).

$$\overline{E} = 0.946 \times 1/3 \times 0.512 \text{ MeV (e}^-)$$
$$+0.054 \times 1/3 \times 1.174 \text{ MeV (e}^-) \tag{3}$$
$$+0.851 \times 1/2 \times 0.6617 \text{ MeV } (\gamma) = 0.4651 \text{ MeV}$$

$\overline{E}$ of other nuclides are also calculated with the same method. The result shows simplicity of the authors' method. Accuracy is investigated by comparison with previous research.

**Calculation of absorbed dose.** Absorbed dose $S(t)$ is calculated as below expression (4). $M(t)$ is total exposure dose.

$$S(t) = \frac{M(t) \times \overline{E} \times 1.6 \times 10^{-13}}{\text{weight}} \text{ (Gy)} \tag{4}$$

Unit conversion MeV to J $1.6 \times 10^{-13}$ (J/MeV) is adopted. The weight of a human body is assumed 70 kg supposed an average adult male. In this study, only $\beta$ and $\gamma$ decays are considered. Therefore, Gy (absorbed dose) and Sv (dose equivalent) are equivalent.

**Coefficient of committed effective dose.** Committed effective dose is total absorbed dose whole life considering effective half-life. Exposed period is assumed 50 years for convenience. Below expression (5) is employed by Nuclear Safety Commission of Japan to estimate the dose [6].

$$S \text{ (mSv)} = 0.001 \times m \times d \times p \times a \times f_1 \times f_2 \tag{5}$$

In this expression, m, d, p, a, $f_1$ and $f_2$ correspond with amount of food ingestion per day (kg/d), ingestion period (d), the coefficient of committed effective dose (mSv/Bq), radiodensity (Bq/kg), dilution factor in the market and decrease compensation caused by cooking, respectively. The values of coefficients of committed effective dose are determined by ICRP Publ.72 [7]. In this study, the authors show analytical derivation of the coefficient.

**DISCUSSION**

**Comparison of emitted energy per radioactive decay between authors' method with previously proposed method.** Accuracy of the authors' estimation method of emitted energy per decay is investigated by comparison with previous research. Fig.3 compares values of that by authors' method with those of ICRP related to individual nuclides. It is noted that both are very similar, the authors' model indicates the equal accuracy with previously proposed complex model in spite of its simplicity.

**Derivation of a coefficient of committed effective dose.** The value of coefficient of committed effective dose is provided. Expression (6) is settled.

$$S(50\text{y}) \approx S(\infty) = C_1 \times M(\infty) = C_1 \times \frac{r_0 t_m}{\alpha_e} = C_2 \times r_0 t_m \tag{6}$$

In expression (6), $C_1 = \overline{E} \times 1.6 \times 10^{-13} / 70$ and $C_2 = C_1 / \alpha_e$. $C_2$ is exactly coefficient of committed effective dose itself. It is one of the outcomes of this study that coefficient of committed effective dose is derived concisely without complex computer simulation.

**Comparison of calculated coefficient of committed effective dose values with those determined by ICRP Publ. 72.** Fig.6 compares values of coefficient of committed effective dose estimated by authors' method at with those determined by ICRP Publ. 72 [72]. Expression (6) is employed to calculate the coefficient. It is noted that majority of nuclides are similar to those of ICRP. The authors' method also indicates equal accuracy with previously research in calculation of the coefficient. Minority of those,

however, are estimated inconsistent. Sr, Zn and Fe are estimated larger, I and $^{99m}$Tc are estimated smaller. Cause for this inconsistency is considered in the followings.
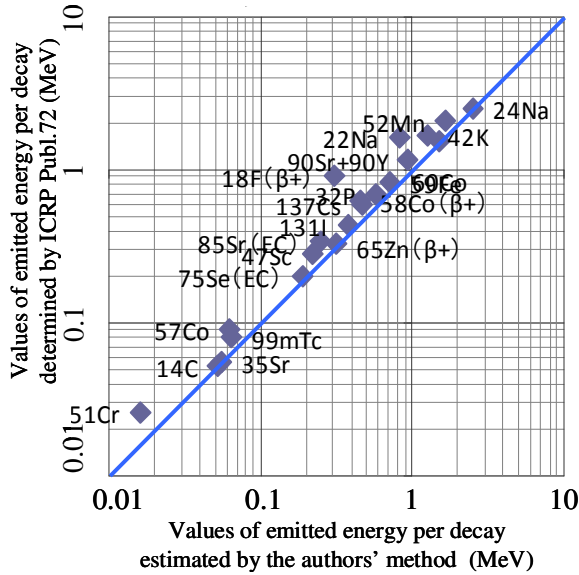


**Fig.5** Comparison of emitted energy per decay of calculated by the authors' method with determined values by ICRP Publ.72.
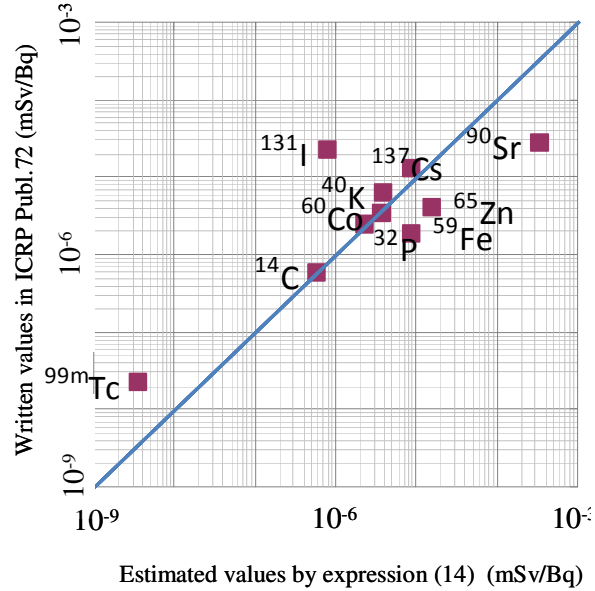
**Fig.6** Comparison of coefficient of committed effective dose of previous research with calculated by the authors' method.

It is known that Sr is one of bone-seekers, which are nuclides tend to concentrate on bone. The ratio of Sr concentrated on bone is 0.09 [8]. To multiple by the ratio, more accurate coefficient is obtained. By this modification, the coefficient of committed effective dose is estimated at $2.93\times10^{-5}$ mSv/Bq. The value determined by ICRP Publ. 72 is $2.80\times10^{-5}$ mSv/Bq. In addition, $^{131}$I tends to concentrate in a thyroid gland. ICRP recommends to employ tissue weighting factor 0.04 related to I [7]. In accordance with the recommendation, similar value with ICRP method is obtained. The authors' method indicates accuracy by above modification related to Sr and I.

**Concrete calculation of exposure dose and absorbed dose.** Some concrete values of exposure dose are introduced in the followings as examples in point from previous research [6].

Example 1: The estimation of radioactivity and internal exposure dose by K is estimated. There is K in a human body 140 g naturally, of which isotope $^{40}$K exists in percentage of 0.0118%. The radioactivity and internal exposure dose per year of the isotope is estimated. In addition, the physical half-life of $^{39}$K: $T_p=1.11\times10^{13}$ h.

Solution 1: The number of radioactive substance atoms $N(t)$ is expressed $N(t)=N_0e^{\alpha t}$ (under a condition $N(0)=N_0$), radioactivity is obtained to differentiate once $N(t)$ respect to time $t$, expressed as $\alpha N(t)$. Therefore, radioactivity (Bq) of $^{40}$K is provided as below expression (7); $N_A$ is Avogadro constant, atomic weight of K is 39.1 g/mol, $\alpha_p=\ln2/T_p$.

$$\alpha_p N(\infty) = [\frac{\ln2}{1.11\times10^{13}\,\text{h}\times3600\,\text{s/h}}][\frac{140\,\text{g}\times0.0118/100}{39.1\,\text{g}/\text{mol}}\times N_A\,\text{mol}] \approx 4411\text{Bq} \qquad (7)$$

From expression (7), total exposure dose per year $M$(1y) is provided as expression (8).

$$M(1y) \approx 3600\,\text{s/h} \times 24\,\text{h/d} \times 365\,\text{d/y} \times 4411\,\text{Bq} \tag{8}$$

The internal absorbed dose per year $S(1y)$ is provided as expression (9). The emission energy per decay of K is estimated at 0.4708 MeV as shown in expression (4), the weight of a human body is assumed 70 kg supposed an average adult male.

$$S(1y) = M(1y) \times \frac{0.4708\,\text{MeV}}{70\,\text{kg}} \times 1.60 \times 10^{-10}[\text{mJ}/\text{MeV}] = 0.1497\,\text{mSv} \tag{9}$$

The value of dose by MIRD method is estimated at 0.1773 mSv, which is very similar to that calculated in this study.

Example 2: $^{137}$Cs, of which radioactivity is roughly 1 nCi, exists in a human body in 1970's derived from nuclear testing. The internal exposure dose per year is estimated on the assumption that it evenly distributes to whole a body. In reference to the previous study [6], unit conversion that 1 nCi=37 Bq and 1 rad=0.01 Sv are a total exposure applied.

Solution 2: Estimation by MIRD method is quoted from the study. Internal exposure dose to whole a body per 1 μCi×h is $1.4 \times 10^5$ rad from MIRD Pamphlet No. 11. Exposure dose to whole a body per year is following expression (10).

$$1 \times 10^{-3}\,\mu\text{Ci} \times 8767\,(\text{h/y}) \times 1.4 \times 10^{-5}\,(\text{rad}/\mu\text{Ci}\cdot\text{h}) = 1.2 \times 10^{-4}\,(\text{rad/y}) = 1.27\,\mu\text{Sv} \tag{10}$$

The example is solved by authors' method as following. Total exposure per year $M(1y)$ and exposure dose per year $S(1y)$ are calculated as expression (11) and (12) respectively.

$$M(1y) \approx 1\,\text{y} \times N(\infty) = 3600\,(\text{s/h}) \times 24\,(\text{s/h}) \times 365\,(\text{s/h}) \times 37\,\text{Bq} \tag{11}$$

$$S(1y) = M(1y) \times \frac{0.4651\,\text{MeV}}{70\,\text{kg}} \times 1.60 \times 10^{-10}[\text{mJ}/\text{MeV}] = 1.24\,\mu\text{Sv} \tag{12}$$

The result coincides with that of MIRD, warrants its accuracy.

**CONCLUSION**

The objective of this study is to propose an approach to estimate storage of radioactive substance in a human body and absorbed dose based on hydrology and nuclear physics, which will provide better understanding of the disaster for general scientists and engineers. The results are summarized as follows.
1. Absorbed dose is provided analytically as a time-related function. The results show decrease in the ingestion period and flux lead to decrease in total exposure dose and absorbed dose.
2. Accuracy of the authors' method is indicated by comparison with previous research. Emitted energy per decay estimated by the proposed method is similar to that of previous research. As well, a coefficient of committed effective dose is compared. Majority of nuclides is similar to previous research. Minority of nuclides, however, does not match. Sr and I are modified by considering of those properties.
3. Concrete values of exposure dose and absorbed dose are calculated. This result shows that a method proposed in this study is useful for calculation of total exposure dose and absorbed dose related to individual nuclides.

Based on the above, the present study will arrive at simple understanding of the influence of radioactive substances to a human body comprehensively.

**REFFERENCES**

[1] S. Sasaki, et al., A Hydrologic Approach to Radioactive Substance in A Human Body, Global Environmental Research and Journal of Global Environment Engineering. (submitted)

[2] I. Anzai, 1980. Some explanatory notes on the practical use of the MIRD committee method for internal dose evaluation. Japanese Society of Radiological Technology 36(2), 209-225. (in Japanese)

[3] The Japan Radioisotope Association, 2011. Radioisotope Pocket Data Book, Maruzen Co., Ltd. (in Japanese)

[4] T. Sugawara et al, 2008. Fundamentals of Radiology11th edition, Kinpodo Co., Ltd. (in Japanese)

[5] E. Fermi, 1951. Nuclear Physics. The University of Chicago Press.

[6] Nuclear Safety Commission of Japan: Kankyo hoshasen monitoring ni kansuru shishin, Retrieved Apr. 9, 2012, from http://www.nsc.go.jp/housya/housya198903.pdf (in Japanese)

[7] International Commission on Radiological Protection, 1995. Age-dependent Doses to the Members of the Public from Intake of Radionuclides - Part 5 Compilation of Ingestion and Inhalation Coefficients, Ann. ICRP 26 (1).

[8] M. Izawa, et al., 1978. Hoshasen no bogo 3rd edition, Maruzen Co., Ltd. (in Japanese)

# CELLULAR PHONE EXPOSURE EFFECT ON BRAIN AND TESTICULAR PATTERN OF WISTAR RATS

**Kavindra Kumar Kesari and J. Behari** (Bioelectromagnetic Laboratory, School of Environmental Sciences, Jawaharlal Nehru University, New Delhi, India)

Recently, there have been several reports referring to detrimental effects due to radio frequency electromagnetic fields (RF-EMF) exposure. Special attention was given to investigate the effect of mobile phone exposure on reproductive and brain system. The present study investigates the effect of free radical formation due to microwave exposure effect on brain and fertility pattern in male Wistar rats (sham exposed and exposed). Exposure took place in plexiglas cages for 2 hour a day for 45 days to mobile phone. The specific absorption rate (SAR) was estimated to be 0.9 W/kg was observed. An analysis of antioxidant enzymes glutathione peroxidase, and superoxide dismutase showed a decrease while an increase in catalase was observed significant ($P< 0.05$) in brain and sperm samples. Malondialdehyde showed a significant increase and histone kinase showed a significant decrease in exposed group ($P< 0.05$) of brain and sperm samples. Change in sperm cell cycle of G0-G1 and G2/M were recorded significant ($P< 0.05$). Generation of free radicals was recorded significantly increased ($P = 0.05$). Moreover significant decrease ($P<0.05$) in the level of pineal melatonin and a significant increase ($P<0.05$) in creatine kinase and caspase 3 was also observed in exposed group of whole brain as compared with sham exposed. A significant ($P< 0.05$) decrease in serum testosterone level was also recorded in exposed group. Study concludes that the RF-EMF from commercially available cell phones might affect the fertilizing potential of spermatozoa and cause neurodegenerative deceases.

# A HYDROLOGIC APPROACH TO RADIOACTIVE SUBSTANCE IN A HUMAN BODY I

*Hayase Yoneda* [1]\*, Syota Sasaki [1], Tadashi Yamada[1], Tomohito Yamada[2]
([1] Faculty of Science and Engineering, Chuo University, Tokyo, Japan)
([2] Faculty of Engineering, Hokkaido University, Hokkaido, Japan)

"Radioactivity" is drawn great attention curse by the Fukushima Daiichi nuclear disaster in Mar. 2011. The radioactive confusion with a variety of issues should be treated by civil engineering, since civil engineering is a comprehensive academic, and supports a social infrastructure. This study aims to elucidate human, soil and biological circulation and the residual of all radioactive substance. In this paper, authors clarify residuals of radioactive substance in a human body from the view point of rainfall-runoff analysis. To analyze residual amount of remaining in a human body, regarding a human body as a single basin, tank model in runoff analysis is applied to a human body in this study. In this case, precipitation in watershed correspond to influx of radioactive substance into a human body by ingestion, evapotranspiration associates with nuclear decay radiation, and runoff in watershed is equivalent to excretion and metabolism from a human body. And half life, which determines an attenuation constant of tank model, is estimated from effective half life which is provided from physical and biological half life.

This hydrologycal approach accurately indicates the residual amount of radioactive substance in a human body in spite of its simplicity.

# CYTOTOXIC EFFECTS OF MYCOTOXIN IN HUMAN MONOCYTES AND MECHANISMS

*Ruoting Pei[±,*] and Jun Liu[±]*

[±] Department of Civil and Environment Engineering, University of Texas at San Antonio, One UTSA Circle, San Antonio, TX 78249. Tel.: (210) 458-5517, fax: (210) 458-6475. Email: ruoting.pei@utsa.edu

Fungi and their related mycotoxins in damp indoor environment and contaminated foods are known to lead to adverse health effects and even death in humans and animals. Despite the fact that mycotoxins are one of the most studied subjects in toxicology, much research is still needed to elucidate the molecular mechanism for the actions of mycotoxins. The purpose of the study is to elucidate the molecular mechanisms by which mycoxins, including deoxynivalenol, verrucarin A and ochratoxin A, regulate IL-8 gene expression in human monocytic THP-1 cells.

To study regulation of IL-8 gene expression, recombinant THP-1 cell lines were constructed that harbor the IL-8 promoters linked to an easily detectible luciferase reporter gene and treated with mycotoxins. Deoxynivalenol was found to upregulate luciferase expression, while verrucarin A upregulated at high concentration but downregulated at low concentration, and ochratoxin A did not affect luciferase expression. Mutation of the nuclear factor-$\kappa$B (NF-$\kappa$B) binding site of the IL-8 promoter significantly impaired deoxynivalenol and verrucarin A-mediated luciferase expression. In contrast, mutation of the CCAAT/enhancer-binding protein (CEBP) $\beta$ binding site of the IL-8 promoter affected verrucarin A but not deoxynivalenol-mediatedluciferase expression. Consistent with the mutation studies, the NF-$\kappa$B inhibitor caffeic acid phenethyl ester inhibited mycotoxin-mediated luciferase expression. In addition, both ochratoxin A and deoxynivalenol had weak cytotoxic effects while verrucarin A had strong cytotoxic effects for THP-1 cells. Taken together, our study in THP-1 cells indicated differential induction of IL-8 expression by deoxynivalenol, verrucarin A and ochratoxin A and suggested distinct regulatory pathways at the transcriptional level via NF-$\kappa$B and CEBP$\beta$ by these mycotoxins.

In addition, the recombinant THP-1 cells transduced with IL-8 wild type promoter-luciferase reporter gene responded differently to different mycotoxins in our research, there is potential that such THP-1 cells may be used as a biosensor for detecting mycotoxins in the field.

# PROTECTION OF ARSENIC-INDUCED THYROID OXIDATIVE STRESS BY MELATONIN

**Damore Dimple**

(Bhavan's Sheth R.A.College of Science, Ahmedabad, Gujarat, India)

Arsenic-induced tissue damage is a major concern to the human population. An impaired antioxidant defense mechanism followed by oxidative stress is the major cause of arsenic-induced toxicity, which can lead to deleterious effects in the tissues. The present study was carried out to investigate the preventive role of melatonin, against arsenic-induced thyroid damage in mice. Administration of arsenic (in the form of arsenic trioxide, $As_2O_3$, at doses of 0.5 and 1.0 mg/kg body weight) for 30 days significantly decreased the intracellular antioxidant power, the activities of the antioxidant enzymes, as well as the levels of cellular metabolites. In addition, arsenic intoxication enhanced lipid peroxidation and degeneration of the thyroid tissues. Co treatment with melatonin at a dose of 10 mg/kg body weight for 30 days could prevent the arsenic-induced oxidative stress and injury to the histological structure of the thyroid gland. In summary, the results suggest that the preventive role of melatonin against arsenic induced thyroid toxicity may be due to its intrinsic antioxidant property.

# COMPARISON OF ACUTE TOXICITY OF SIX DIFFERENT CHEMICALS WITH *EISENIA FETIDA* BIOASSAY

Laura Lomba, Diego Ballestero, Jonatan Val, Beatriz Giner and *Mª Rosa Pino*  (San Jorge University, Zaragoza, Spain)

One of the most important targets of green chemistry is the use of renewable raw materials, that is, the production of chemicals from biomass rather than fossil resources, such as oil, natural gas, or coal. The main problems of using fossil resources are that they are not renewable and their availability is diminishing rapidly. Chemicals from sustainable sources, including those from biomass, which are usually obtained by fermentation, enzymatic, or esterification processes, can be used for a number of industrial processes. This is the case of the chemicals studied in this work: levulinic acid, ethyl levulinate, propyl levulinate and butyl levulinate.

From dehydration and hydrolysis of cellulose levulinic acid and related chemicals can be obtained; they can be used in the manufacturing of synthetic fibers, pesticides, pharmaceuticals, plastics and rubber, or as an acidulant in food. Moreover, levulinic acid and its esters are used as plasticizers, odorous substances and solvents in polymers, textiles and coatings. On the other hand, compounds like lactates can be obtained from saccharose and they are used as a food additive, in perfumery, as flavor chemicals and solvent, which can dissolve acetic acid cellulose and many resins.

However, we have found that there is not a comprehensive and rigorous study about the ecotoxicology of these solvents and their environmental risk. That is why that we started a study that involves a broad characterization of these solvents from the ecotoxicological point of view. In this work, we present a part of the mentioned study in which the standardized toxicity test using earthworms *Eisenia fetida* (OECD guideline for testing of chemicals; Earthworm, acute toxicity tests 1984,  and the Spanish standard UNE 77304-1) has been used to test the environmental risk of these solvents.

The artificial soil was comprised (by dry weight) 10% sphagnum peat, 20% kaolin clay and 70% industrial fine sand. The water content of the mixture was determinate by weighing the sample, drying it to constant mass at 105ºC during 24 hours and the pH was measured with a pH meter using a KCl 1M solutions.  It was not necessary to adjust the pH because it was between 6-6.5, but the water content was too low so it was needed to add a little bit more of deionised water to get 60% of moisture. After the artificial soil was prepared, an initial study, with the different chemicals and chloroacetamide which was used as a control, was carried out to know the range of concentrations (mg/Kg) in which was the LC50. Next, ten earthworms in each vessel were added. All tests were performed with adult earthworms, with a well-developed clitellum of the species *Eisenia fetida*. The test were carried out at 20±1ºC and individual weighs were between 300-600 mg.

The results were collected at 7 and 14 days after the test was started. results were analyzed and a correlation between the results and biodisponibility of the chemical has been carried out. We can conclude that the studied compounds can be classified as low ecotoxic. Furthermore results were compared to the toxicity of other chemicals widely used in the chemistry industry.

# INHIBITORY EFFECTS OF A, B-UNSATURATED ALDEHYDES ON ALGAL PHOTOSYNTHESIS REACTION

***Chung Yuan Chen*** and Sy-Hong Lin

(Institute of Environmental Engineering, National Chiao Tung University, Taiwan)

The α,β-unsaturated aldehydes are compounds with high reactivity for nucleophilic attack. Previous studies showed that, various adverse effects including general toxicity, allergenic reactions, mutagenicity, and carcinogenicity can be induced by these chemicals. However, their effects on aquatic organisms are not yet available from existing toxicity database. Furthermore, current algal toxicity test protocols (US EPA, OECD, etc.) are basically open-system tests. Existing algal toxicity database derived by the aforementioned standard test methods has been found to be inadequate and failing to display certain important toxicological characteristics. The closed-system test technique, on the other hand, reveals much higher sensitivity and presents more realistic and meaningful concentration-response relationships of organic compounds, compared to test results from protocols.

The present study evaluated the toxicity (in terms of EC50 and NOEC values) of α,β-unsaturated aldehydes using a closed-system algal testing technique. Based on the inhibitory effects on algal photosynthesis reactions, more than 50% of the test chemicals are classified as R50 (very toxic) compounds according to the current practice for classification of new substances in the European Union. Therefore, more extensive studies are needed to quantify their impact to the aquatic environment. Quantitative-structure-activity relationships were established for predicting the toxicity of this type of compounds. Both electrophile reactivity and hydrophobicity are found to be key factors governing the toxicity of α,β-unsaturated aldehydes. The toxicity data and the quantitative structure-activity relationships (QSARs) derived from this study will be useful for risk assessment and protection of the aquatic environments.

# ECOTOXICITY TESTING OF TWO ESTONIAN SHALE FUEL OILS

***Liina Kanarbik*** (National Institute of Chemical Physics and Biophysics, Tallinn, ESTONIA)
Irina Blinova (National Institute of Chemical Physics and Biophysics, Tallinn, ESTONIA)

Estonia is the biggest oil shale processing country in the world. Oil shale is sedimentary rock containing up to 50% organic matter. Oil shale is used for the electricity and heat generation and production of different fractions of synthetic crude oil (shale fuel oil) by retorting of oil shale. Shale fuel oils are used in boilers, industrial furnaces, as ship fuels, etc. At present Estonian enterprises produce several shale fuel oil products with different physicochemical properties: density, viscosity, content of phenols, sulfur- and nitrogen-containing compounds, etc. In comparison to similar petroleum-based fuels, these oils are characterized by lower viscosity, a lower pour point, and lower sulphur content. The production of shale fuel oil in Estonia will increase up to one million tons per year in the near future. Increased production, transportation and use of shale oil entail risks of environmental contamination.

The main goal of the current investigation was to evaluate the potential hazard of Estonian shale fuel oil to soil and aquatic communities using a combined chemical and ecotoxicological approach. Samples of natural peat soil and sand were treated with two most widely used shale fuel oil fractions (VKG sweet and VKG D). The spiked soil samples were incubated for 3 months during which the mobility and oil degradation in soils was investigated. The concentrations of the hydrocarbons in the soils were measured every two weeks. At the same time toxicity of the contaminated soils to higher plants *(Sorghum saccharatum, Lepidium sativum, Sinapis alba)* and soil leachates to aquatic organisms (bacteria *Vibrio fischeri* and crustaceans *Daphnia magna*) were evaluated.

# HORMESIS INDUCED BY MIXTUES OF IONIC LIQUIDS WITH SIGMOID DOSE-RESPONSE CURVE

*Jin Zhang,* Shu-Shen Liu\*, Jin Zhang, Hui-Ping Deng (Tongji University, Shanghai, PR China)

Hormesis is a dose–response phenomenon that is characterized by low-concentration stimulation and high-concentration inhibition. The concept of hormesis has generated considerable interest in recent years. This is principally because the hormetic dose–response model challenges the linear at low-dose model employed by regulatory agencies such as the EPA and FDA in cancer risk assessment activities and the sigmoid curves employed by most of researchers when assessing the toxicities of pollutants. So, it is of vital importance to explore more hormesis within the chemicals. Room-temperature ionic liquids (ILs) are a fascinating group of new chemicals. The great interest for such compounds is the potential substitution for traditional organic solvents and their fame of "green" solvents. However, ILs is not always green. More and more studies showed that the potential (eco)-toxicological hazard and risks of ILs cannot be neglected. In our previous study, we found the IL: 1-ethyl-3-methylimidazolium bromide ([emim]Br) and tetrafluoroborate ([emim]BF4) can cause remarkable hormesis phenomenon towards the luminescent inhibition toxicity of *Vibrio qinghaiensis* sp.-Q67 (Q67). To explore more hormesis phenomenon within ILs, we investigated the single toxicity and combined toxicity of another group of IL with different alkyl-chain length on the cation, [emim]Cl, [bmim]Cl, [hmim]Cl, and [omim]Cl, to Q67 by employing the microplate toxicity analysis (MTA) procedure. The four ILs were selected as the testing materials based on our previous results, which showed the mixture rays containing the ILs exhibits antagonism and their toxicities depend on the concentration ratio of the IL, [hmim]Cl. Therefore, a series of ternary and binary IL mixture rays with or without the decisive IL were designed at different component-concentration ratio by using the uniform-design-concentration-ratio (UDCR) ray method.

The results show the concentration-response curves (CRCs) of the four ILs display sigmoid and all compounds prove to be toxic to Q67. A comparison of the observed mixture toxicity with that predicted by the reference model concentration addition shows that a good predictability was only found in the upper or lower effect range of the IL-mixture rays. In fact, strong synergisms appeared within most of the ternary and binary IL-mixture rays and antagonism within several mixture rays containing the IL ([hmim]Cl). The most interesting thing is that four ternary mixture rays composited of [emim]Cl, [bmim]Cl, and [omim]Cl and four binary mixture rays composited of [emim]Cl and [bmim]Cl provoked clearly stimulating effects (hormesis) in the relative lower effect range hampering the application of reference model. An independent repetition of the mixture experiment resulted in a principally similar concentration–response curve, again with clear hormesis effects in the lower range of test concentrations. The results suggested that hormesis can appear within IL mixture and can be induced by the mixture composites with sigmoid curves.

# TIME-DEPENDENT HORMESIS EFFECTS OF 1-ETHYL-3-METHYLIMIDAZOLIUM BROMIDE ON PHOTO-BACTERIAL LUMINESCENCE, OXIDOREDUCTASES AND ANTIOXIDASES

*Jing Zhang*, *Shu-Shen Liu*, Jin Zhang, Zhen-Yang Yu and Hai-Ling Liu
(Tongji University, Shanghai 200092, P. R. China)

Hormesis was characterized by low concentration stimulation and high concentration inhibition. The concept itself indicates its connection with concentration ranges. However, hormesis is also a time-dependent biological response, and its temporal aspect is often neglected. A series of appropriately arranged time intervals is necessary for the accurate evaluation on hormesis. Ionic liquid (IL) is a green solvent to replace traditional organic solvents with serious air pollution. The toxicities and/or hormesis effects of ILs have earned them more and more attention. Currently, the dynamic process of the hormesis of 1-ethyl-3-methylimidazolium bromide ([emim]Br) was systematically investigated on the luminescence, oxidoreductant and antioxidant systems of the photo-bacterium, *Vibrio qinghaiensis* sp.-Q67 (Q67) with multiple time intervals. All data were expressed as inhibition ratio = $(1 -$ value in concentration group/value in control group$) \times 100\%$. Inhibition ratio was positive for inhibitory effects and negative for stimulatory effects. The luminescence of Q67 was determined through a time-dependent microplate toxicity analysis. The observed hormesis was significantly related to both exposure time and concentrations. The hormesis gradually increased with time increasing (0.25 h < 2 h < 4 h < 8 h < 12 h < 16 h), reached the stimulatory peak (-277%, 20 h), and then slowly decreased (-255%, 24 h). Median effective concentration (EC50), zero effect-concentration point (ZEP) and effective concentration at the maximal stimulating effect (ECmin) were characteristic points in concentration response curves of hormesis. Their concentrations all increased with increasing exposure time. Subsequent studies investigated the oxidoreductant and antioxidant systems of Q67, and included five concentrations of 0.0710 M, 0.0430 M, 0.0260 M, 0.0150 M and 0.00600 M. Exposure containers were sterilized conical flasks, and time intervals were 2, 8, 12, 20, and 24 h. Reduced nicotinamide adenine dinucleotide (NADH) and flavin mononucleotide (FMN) were chosen to present the oxidoreductant system. Superoxide dismutase (SOD) and catalase (CAT) were chosen to indicate the antioxidant system. Two systems had different effects. NADH and FMN showed similar changes in different time intervals. At 2 h, their inhibition ratios indicated high concentration inhibition and low concentration stimulatory. From 8 h to 24 h, they showed stimulation without inhibition in five chosen concentrations. At 8 and 12 h, the maximum stimulatory effects were at 0.043 M. At 20 h, the stimulatory peaks were at 0.0710 M with -373% and -394% for NADH and FMN. At 24 h, the stimulatory effects became less than those at 20 h. Thus, they showed similar effects with the hormetic responses of luminescence, indicating their close connections with the light production system. On the other hand, the stimulatory effects of SOD and CAT increased with increasing exposure time. SOD showed stimulation without inhibition in five chosen concentrations from 8 to 24 h, while CAT showed similar phenomenon from 12 to 24 h. The stimulatory peaks of SOD and CAT were -293% and -132% at 24 h. At 12 h, SOD and CAT showed the maximal stimulation at 0.043 M. For 20 and 24 h, SOD and CAT showed the maximal stimulation at 0.0710 M. The similarities and differences between oxidoreductant and antioxidant systems and between SOD and CAT indicated different underlying mechanisms.

# NOVEL METHODS TO EXPLORE THE IMMUNE-EFFECTS OF POLLUTION ON PARASITE-HOST INTERACTIONS.

*Adam Lynch\**, Edwin Routledge, Christopher Parris and Susan Jobling (Brunel University, Uxbridge, Middlesex, UK.)
Leslie Noble (University of Aberdeen, Tillydrone Avenue, Aberdeen AB24 2TZ, UK)

The trematode *Schistosoma mansoni* is a significant human parasite with a global impact considered second only to malaria. It is transmitted to humans via tropical freshwater snails of the genus *Biomphalaria* which are often found in areas highly polluted by a range of anthropogenic contaminants. A wide range of contaminants are reported to influence the immune systems of molluscs, which in turn may alter the dynamics of the disease transmission process. We report here the novel development and adaptation of *in vitro* techniques for use in assessing the effects of various contaminants on the key immune functions in *B.glabrata* following infection with *S. mansoni*. To assess effects of chemicals on phagocytosis we have developed a novel method using imaging flow cytometry. Brightfield and fluorescent channel images were obtained from haemocytes (snail immune cells) exposed to latex flourospheres. A method for quantifying the phagocytosed beads and excluding non-internalized (free) beads was developed using the analysis software. Differences within haemolymph pools (*intra* assay) and differences between pools (*inter* assay) for the phagocytosis assay showed coefficients of variation of 3 and 9.6% respectively. The automated data analysis showed 99.8% agreement with visual observations regarding classification of phagocytosisng and non-phagocytosisng cells as well as the number of beads within each cell. Another important feature of innate immunity is chemotaxis (the ability of host immune cells to recognise and seek out parasite antigens) which can ultimately determine the success or failure of an infection. Excretory-secretory products (ESP) from *S.mansoni* sporocysts (an asexual stage of the lifecycle of the parasite when it replicates within the snail host) were used as attractants in both direct (Dunn chamber) and indirect (96-well Boyden chamber) observation chemotaxis assays for haemocytes exposed to chemical pollutants *in vitro*. Work with the chemotaxis assays has shown that both are adaptable to the addition of test chemicals *in vitro*, and preliminary results suggest that significant inhibition of motility can occur in the ng/L range with exposure to certain oestrogenic chemicals. These assays, amongst others currently under development, are being used as tools to determine the effects of various aquatic pollutants on immune function in *B.glabrata* and identify specific areas of the snail immune response toward parasites which may alter transmission rates and result in human health implications.

# EFFECT OF ACTIVE-PACKAGING COLOR AND OXYGEN PERMEABILITY ON SALMON OIL QUALITY

*Muhammad Javeed Akhtar*, Muriel Jacquot and Stéphane Desobry

(Université de Lorraine, ENSAIA, Laboratoire d'Ingénierie des Biomolécules (LIBio), 2 avenue de la Forêt de Haye, 54505 Vandœuvre-lès-Nancy Cedex, France)

Fish oil contains high levels of polyunsaturated fatty acids (PUFA) particularly eicosapentaenoic acid (EPA, omega-3) and docosahexaenoic acid (DHA, omega-3). Most of beneficial attributes of fish and fish products are due DHA and EPA presence. For instance, they have been shown to have protective effects against coronary heart disease, inflammatory processes, thrombosis, carcinomatosis, and metabolic syndrome. Such nutritional benefits have promoted significant research into methods of stabilizing unhydrogenated fish oil against oxidative deterioration. Fish oil is very sensitive to light-oxidation causing a number of unfavorable chemical changes including off-flavors formation, decrease in nutritional quality, economic losses and oxidation products formation, some of which are supposed to be against human health. These chemical changes in lipids are directly related to light source, wavelength, intensity, exposure time, and temperature, as well as packaging material characteristics such as color and oxygen barrier properties. Most appropriate way to protect lipid rich products may be oxygen removal and decrease of light exposure which is not very easy for transparent packaging, but the most harmful wavelength (400–500 nm) of light can be avoid by application of food colored packaging with high oxygen barrier properties.

The scientific aims of this study were to use HPMC films functionalized with anthocyanins as packaging materials for salmon oil and investigate effects of packaging color and improved oxygen permeability on light induced lipid oxidative deterioration.

Antioxidant food packaging films were successfully developed by incorporation of anthocyanin compound (liquid extract from natural sources) into hydroxypropyl methylcellulose (HPMC) matrix. Films color and oxygen barrier properties were measured. Red color of AC films showed good control of light transmission in comparison with control (transparent) films. Barrier properties of these films showed that addition of AC compounds decreased oxygen permeability, possibly due to hydrogen bonding between polymer OH groups and those of AC compounds. Bio-active films effectiveness was investigated by packaging applications for salmon oil. Changes in oil color, headspace oxygen consumption, conjugated dienes, polyene index and C–H stretching vibration of cis-double bond (=CH) showed that, in general AC films improved salmon oil stability. Films with 2, 3 and 4% AC offered the best protection against lipid oxidation due to improved barrier properties against light and oxygen.

# OCCURRENCE OF *ESCHERICHIA COLI* O157:H7 IN BOVINE MANURE OBTAINED FROM FARM AND ABATTOIR ENVIRONMENTS

*Itelima Janet** and Agina Samuel
(Faculty of Natural Science University of Jos, Nigeria)

**ABSTRACT:** *Escherichia coli* O157:H7 is a rare and new emerging pathogen frequently associated with the consumption of foods of bovine origin and vegetables grown in soil amended with animal manure. The severity of the infection caused by this food borne pathogen in the young and the elderly has had a tremendous impact on human health. In this study, the occurrence of pathogenic *Escherichia coli* O157:H7 in 700 bovine manure samples which comprised of 350 bovine feces and 350 bovine slurry samples were determined. The samples were obtained from cattle farm and abattoir environments located at seven different study sites in Plateau State, Nigeria, between the months of November 2008 – October 2009 and transported to the laboratory. The samples were then analyzed microbiologically for the presence of *E. coli* O157:H7 using appropriate culture methods such as enrichment broth and selective agar media. The organism was then identified based on characteristic morphological appearances of the colonies followed by biochemical and serological tests. Of the seven hundred manure samples examined 107(15.29%) were positive for *E. coli* O157:H7. A higher percentage occurrence of *E. coli* O157:H7 was recorded in bovine feces (8.86%) than in bovine slurry (6.43%). There was no significant difference ($p > 0.05$) in the occurrence of the target organism with respect to some of the experimental sites. The percentage occurrence of *E. coli* O157:H7 isolated from bovine feces from the farms and abattoirs was respectively 9.71% and 8.00%. The percentage occurrence of the organism was significantly higher ($p < 0.05$) in the wet season 68(9.72%) than in the dry season 39(5.57%). The presence of *E. coli* O157:H7 in bovine manure in Plateau State, Nigeria suggests that manure used as fertilizer or as soil amendment should be properly treated to eliminate the organism as contaminated manure are probable vehicles for the pathogen in many outbreaks.

## INTRODUCTION

*Escherichia coli* is a normal member of the gastrointestinal microfloral of humans and animals; however, *E. coli* O157:H7 can cause severe hemorrhagic disease and death in humans (Padhye and Doyle 1992; Buchanan and Doyle, 1997). Since the first outbreak of *E. coli* O157:H7 infections in 1982, there have been many outbreaks all over the world especially in developed countries (CDC, 2006). Many studies have indicated that cattle represent the main reservoir of *E. coli* O157:H7 (Hancock *et al*., 1998). According to Ohya *et al*., (2000), this organism appears to be confined to the gastrointestinal tract and is shed in feces. Numerous studies have found this organism in the feces of healthy cattle, indicating that it is usually a harmless commensal in these animals (Faith *et al*., 1996).

Although, undercooked ground beef has been identified as a leading food vehicle of *E. coli* O157:H7 infection, fresh fruits, vegetables and raw unpasteurized juice are becoming increasingly important vehicles of food borne transmission (Anon, 1999). Vegetable plants can become contaminated with pathogens before harvest when grown in fields fertilized with fresh or inadequately composted manure (Solomon *et al*., 2002). *E. coli* O157:H7 may also be introduced into soil through irrigation water contaminated with cattle feces or through contact with surface runoff from cattle production operations (Beuchat, 2002).

The increasing association of fresh vegetables with outbreaks of *E. coli* O157:H7 infection has heightened concern regarding pathogen contamination of vegetables in agricultural environment via animal manure. As understanding the ecology of *E. coli* O157:H7 in cattle manure is important to assess

the possibilities for controlling the agent at all levels, the objective of the present study, was to examine the occurrence of *E. coli* O157:H7 in bovine manure commonly utilized by farmers to fertilized garden soils and farm lands used for growing food crops and vegetables in Plateau State, Nigeria.

## MATERIAL AND METHODS

**Sample Collection.** Seven hundred samples of bovine manure, comprising of 350 samples of bovine slurry (intestinal contents from slaughtered animals in abattoirs) and 350 samples of bovine feces (feces from animals presented for slaughter in abattoirs and from animal farms) were obtained from seven selected areas of Plateau State, Nigeria. All samples were collected in sterile plastic containers and conveyed to the laboratory for bacteriological analyses between November 2009 and October 2010.

**Isolation of Organism.** A loopful of emulsified bovine manure sample was aseptically inoculated into 10ml of Tryptone Soya Broth (TSB) for the isolation of *E. coli* O157:H7. The mixture was thoroughly homogenized using a disposable sterile spatula and then treated with vacomycin to reduce the load of normal flora (Ackers *et al*., 1998) and then incubated at $37^0$C for 2 hours. The samples in TSB were further inoculated solid media, namely sorbitol MacConkey agar (SMAC) and cefixime tellurite–sorbitol MacConkey agar (CT-SMAC) and re-incubated at $37^0$C for 18 – 24 hours (March and Ratnam 1986; Chapman *et al*., 1994). This was followed by the examination of culture plates, after which *E. coli* O157:H7 was detected by both presumptive and confirmatory tests. Ten non-sorbitol fermenting colonies (NSFC), which are usually colorless colonies, were selected and gram stained for typical gram-negative rods. It was necessary to test up to 10 separate NSFC to ensure a high probability of detecting any *E. coli* O157:H7 strains which may be in mixed culture with other NSFC (Griffin, 1995). Presumptive colonies of *E. coli* O157:H7 were subjected to biochemical test as described by Cheesbrough (1991) and serological confirmation tests as described by Nataro and Kaper (1998). The serological tests consist of *E. coli* O157:H7 latex agglutination assay (Oxiod) and *E. coli* antiserum H7 assays (Difco).

**Statistical Analysis.** The data were subjected to statistical analysis using analysis of variance (ANOVA) and Chi-Square test ($X^2$). Each value presented represents a mean of five values, each consisting of 3 replicates.

## RESULTS AND DISCUSSION

The results of the occurrence of *E. coli* O157:H7 in bovine manure samples (comprising of bovine feces and bovine slurry) are shown in Table 1. Of the 700 samples of bovine manure samples examined in this study, 107 (15.29%) yielded *E. coli* O157:H7. The percentage occurrence of the bacterium isolated from bovine feces and bovine slurry was respectively 8.86% and 6.43%. Analysis of variance statistical analysis showed that there was a significant difference ($p < 0.05$) between the percent occurrences of *E. coli* O157:H7 with respect to the manure types. There was no significant difference ($p > 0.05$) in the percentage occurrence of *E. coli* O157:H7 with respect to some of the experimental sites, while significant difference $p < 0.05$ existed between others.

The effect of the two sources where samples were collected (farm and abattoir) on the percentage occurrence of *E. coli* O157:H7 isolated from bovine fecal samples alone was considered (Table 2). This is because collection of bovine slurry samples was restricted only to abattoir environment. The result show that percentage occurrence of *E. coli* O157:H7 isolated from the bovine feces samples from the farm and abattoir was respectively 9.71% and 8.00%. Chi-Square test showed that no significant difference ($p > 0.05$) existed between the two sources.

The results of the seasonal effect on the percentage occurrence of *E. coli* O157:H7 in bovine manure are shown in Figure 1. Overall, results showed that the organism occurred higher in the manure samples during the wet season 68(9.72%) than during the dry season 39(5.57%). Chi-square ($X^2$) test of the results in Figure 1 indicated that significant difference existed in the occurrence of the *E. coli* O157:H7 with regard to the two seasons.

An important finding of this study is that *E. coli* O157:H7 is present in bovine used in fertilizing farm lands and gardens used for growing vegetables and other food crops. This finding provides a better understanding of the ecology of *E. coli* O157:H7 in bovine manure. This study further confirms the fact

that cattle can harbor the bacterium in the gastrointestinal tract and be transmitted to humans via oral rout (Armstrong *et al*., 1996).

**Table 1: Occurrence of *E. coli* O157:H7 Isolated from Bovine Feces (Cow Dung) and Bovine Slurry (Cow Slurry) in the Experimental sites.**

| Experimental site | Sample size | % occurrence of *E. coli* O157:H7 in bovine manure samples | | |
| --- | --- | --- | --- | --- |
| | | Bovine feces | Bovine slurry | Total |
| A | 100 | 4/50 (0.57) | 2/50 (0.29) | 6/100 (0.86) |
| B | 100 | 11/50 (1.57) | 6/50 (0.86) | 17/100 (2.43) |
| C | 100 | 11/50 (1.57) | 8/50 (1.14) | 19/100 (2.71) |
| D | 100 | 21/50 (3.00) | 20/50 (2.86) | 41/100 (5.86) |
| E | 100 | 7/50 (1.00) | 4/50 (0.57) | 11/100 (1.57) |
| F | 100 | 7/50 (1.00) | 5/50 (0.71) | 12/100 (1.71) |
| G | 100 | 8/50 (1.14) | 6/50 (0.86) | 14/100 (2.00) |
| **Total** | **700** | **62/350 (8.86)** | **45/350 (6.43)** | **107/700 (15.29)** |

**Table 2: Effects of Various Sources on the Percentage of Occurrence of *E. coli* O157:H7 in Bovine Feces.**

| Sources | Sample Size | Number Positive % | Number Negative % | Total |
| --- | --- | --- | --- | --- |
| Farm | 175 | 34(9.71) | 141(40.29) | 175(50.00) |
| Abattoir | 175 | 28(8.00) | 147(42.00) | 175 (50.00) |
| **Total** | **350** | **62(17.71)** | **288(82.29)** | **350 (100.00)** |
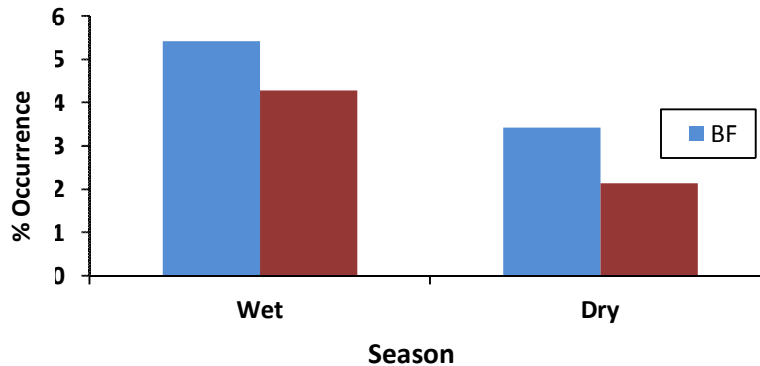


**Fig. 5. Seasonal Effect on the Percentage Occurrence of *E. coli* O157:H7 in Bovine Feces (BF) and Bovine Slurry (BS)**

Overall percentage occurrence of *E. coli* O157:H7 isolated from bovine manure (which comprised of bovine feces and bovine slurry) was about 15% a rather high value compare to that observed in Italy with values that varies from 0% to 1% (Bonardi *et al*., 1999). The high percentage occurrence of *E. coli* O157:H7 obtained in this study may be attributed to the use of more sensitive methods to detect the pathogen in environments with competitive flora. The high occurrence of *E. coli* O157:H7 in bovine manure indicates the need for intervention strategies at the point of production to prevention

contamination of food and water supplies. In this study, approximately 9% of the bovine feces and 6% of the bovine slurry had *E. coli* O157:H7. The results of the present study are also comparable with the report of Elder *et al*. (2000) who reported that percentage isolation of *E. coli* O157:H7 in bovine feces and bovine slurry were 5.0% and 2.0% respectively. In another study conducted in seven different abattoirs in northern Italy, the overall percentage occurrences of the bacterium in bovine feces and bovine slurry from intestinal content were 28% and 11% respectively (Bonardi *et al*., 2001).

In this study, it is clear that the percentage occurrence of *E. coli* O157:H7 isolated from bovine feces is higher than that of bovine slurry. The finding correlates with report of Chapman *et al*. (1994) who attributed the difference in percentage occurrence in both manure types to rumen and caecum physiology. These authors suggested that since manure slurries obtained from abattoir comprises mainly of contents from the rumen (largest of the four champers of the ruminant stomach), it is likely to be highly acidic as a result of production of large amount of fatty acid. Fatty acids are formed form cellulose fermentation by the activities of commensal bacteria and protozoan in the rumen. The very low pH level of the rumen content inhibits the growth of *E. coli* O157:H7 in that region.

The difference in the occurrence of *E. coli* O157:H7 isolated from the bovine manure among some of the experimental sites could be attributed to management factors on the farms. Faith *et al*. (1996) attributed the difference in prevalence rate of *E. coli* O157:H7 in cattle farms to be due to the fact that in some farms the cattle share the same barns, pens or water, the same feeding utensils or hard contact with pasture land that is already contaminated with feces from infected cattle, while in others modern feeding methods are used to avoid cross contamination from infected feces. Garber *et al*. (1995) found that grouping of calves prior to weaning which is being practiced in some farms may increase the risk of the infection. Le Jeune *et al*. (2001) reported that water trough sediments contaminated with feces from cattle excreting *E. coli* O157:H7 may serve as a long-term reservoir of this organism on farms and a source of infection for cattle. It has also been suggested that the increase use of manure slurries to fertilize pastures may have played a role in the dissemination of the pathogen on cattle farms (Armstrong *et al*., 1996).

The present work showed that there was no significant difference in the percentage occurrence of *E. coli* O157:H7 isolated from bovine feces obtained from the farms and those obtained from abattoirs. The present findings did not agree with the findings of Suthiekul *et al*. (1990) who in his study in Thailand found that feces of animals at slaughter houses (abattoirs) had a higher occurrence of *E. coli* O157:H7 (80%) than feces of animal farms (60%). Armstrong *et al*. (1996) suggested that the difference reported by Suthiekul *et al*. (1990) could be related to modern abattoir practices carried out in some develop countries. Example of such abattoir practices is the starvation of animals for a period of time before they are slaughtered in order to reduce their ruminal content for easy evisceration and it has observed that starvation generally causes *E. coli* O157:H7 and *Salmonella* to proliferate in cattle. In this part of the world, such modern abattoir practices hardly exist, animals are rather moved from the farms or from markets to abattoirs where they are slaughtered almost immediately. This may explain why there is no significant difference in the occurrence of *E. coli* O157:H7 with respect to the various sources.

Several authors have reported the seasonality of intestinal colonization and fecal carriage of *E. coli* O157:H7 in cattle (Kudva *et al*., 1996; Hancock *et al*., 1998; Bornardi *et al*., 2001). These authors reported high rates of *E. coli* O157:H7 isolation from cattle in various months ranging from May to September. The present study, further confirms these trends since most of the bovine manure were observed to be contaminated with the pathogen during the raining season which coincides with the months mentioned above. The high percentage occurrence of *E. coli* O157:H7 found in bovine manure during the wet season in the present study could be attributed to increased grazing area of fresh pasture favored by the rains. This increases the chances of the animals becoming infected by feeding on pasture contaminated by their fecal wastes, especially among the cattle (Bornadi *et al*. 2001). According to CDC (2006), cattle manure is regarded as an important source of *E. coli* O157:H7 since manure can contaminate the environment including streams that flow through fields used for irrigation or washing.

**CONCLUSIONS**

As a result of the findings of this study, it is reasonable to conclude that *E. coli* O157:H7 actually exists in manure commonly used for amending garden soils and farm lands used for cultivating food crops and vegetables  in Plateau State, Nigeria. In this part of the world, animal manure  used by local farmers for fertilizing the farms is usually not composted rather the farmers keep the manure under fluctuating atmospheric conditions for about a month before applying to the soil. Since previous studies have revealed long term survival of *E. coli* O157:H7 in manure, there is potential for contamination of plant produce when such manure is used to fertilize farm lands. Although, there is no report of any food borne outbreak associated with *E. coli* O157:H7 in this part of the world, there is high risk of potential outbreaks because of high isolation rate obtained in bovine manure in this study. Based on the ability of *E. coli* O157:H7 to move into ecologic niches in cattle, its virulence and low infections dose in humans, and its long term survival in bovine manure, it has become very necessary to employ appropriate environmental waste management (e.g., composting of manure used for fertilizer or as a soil amendment, suitable buffer zones should be positioned between animal grazing areas and vegetable production fields, etc.) to eliminate the pathogen. It is important also that, the Ministry of Agriculture, Nigeria and the Food Protection Agencies in Nigeria enact laws regarding the use of composted organic manure by farmers to in fertilizing the soil.

## ACKNOWLOGEMENTS

## REFERENCES

Ackers, M., B.E. Mahon, and L. Ellen. 1998. An out of *Escherichia coli* O157:H7 Infections Associated with Leafy Lettuce Consumption. *J. Infect. Dis*. 177: 1588-1593.

Anon. 1999. Microbiology Safety Evaluations and Recommendation on Fresh Produce. *Food Control*. 10:117-143.

Armstrong, G. l., J. Hollingswort, and G. Morris. 1996. Emerging Food-borne Pathogen. *Escherichia coli* O157:H7 as a Model of Entry of a New Pathogen into the Food Supply of the Developed World. *Epidemiol. Rev*. 18(1): 29-51.

Beuchat, L. R. 2002. Ecological Factors Influencing Survival and Growth of Human Pathogens on Raw Fruits and Vegetables. *Microbes Infect*. 4:413-423.

Bonardi, S., M. Emilio, P. Gisella, M. Stefano, and C. Alfredo. 2001. Faecal Carriage of Verocytotoxin – Producing *Escherichia coli* O157:H7 and Carcass Contamination in Cattle at Slaughter in Northern Italy. *Intern. J. Food Microbiol*. 66:47 – 53.

Bornardi, S., E. Maggi, A.  Bottareli, M. L. Pacciarini, A. Ansuini, G.Vellini, S. Morabito, and A. Caprioli.1999. Isolation of Verocytotoxin – Producing *Escherichia coli* O157:H7 from Cattle at Slaughter in Italy. *Vet. Microbiol*. 67: 203 – 211.

Buchanan, R. L., and M. P. Doyle. 1997. Food Borne Disease Significant of *Escherichia coli* O157:H7 and other enterohemorrahagic *E. coli*. *Food Technol*. 51(10):69-76.

Centres for Disease Control and Prevention. (2006). Questions and Answers: Sickness caused by *Escherichia coli* O157:H7. http://www.cdc.gov/  ncidod/dbmd/diseaseinfo/escherichia  coli-g.htm. (Retrieved on 7/16/ 2007).

Chapman, P.A., D. J. Wright, and C. A. Siddons. 1994. A Comparison of Immunomagnetic Seperation and Direct Culture for the Isolation of Verocytotoxin – Producing *Escherichia coli* O157:H7 from Bovine Feces. *J. Med.Microbiol*. 40: 424 – 427.

Chessbrough, M. A. 1991. *Medical Laboratory Manual for Tropical Countries*. Vol. 2. Butterworth and Company Limited. London.

Elder, R.O., A. Keen, G. R. Siragusa, G. A. Barkocy – Gallagher, M. Koohmaraie, and W.W. Laegreid. 2000. Correlation of Enterohaemorrhagic *Escherichia coli* O157:H7 Prevalence in Feces, Hides, and Carcasses of Beef Cattle during Processing. *PNASS.* 9(7): 2999 – 3003.

Faith, N.G., C.A. Shere, R. Brosch, K.W. Arnold, S. E. Ansay, M.S. Lee, J. B. Luchansky, and C.W. Kaspar. 1996. Prevalence and Clonal Nature of *Escherichia coli* O157:H7 on Dairy Farms in Wisconsin. *Appl. and Environ.* 62: 1519 – 1525.

Garber, L.P., S. J. Wells, and D. D. Hancock. 1995. Risk Factors for Fecal Shedding of *Escherichia coli* O157:H7 in Dairy Calves. *JAMA*. 207: 46 – 49.

Griffin, P. M. 1995. *Escherichia coli O157:H7 H7 and Other Enterohaemorrhagic Escherichia coli.* Raven Press. New York.

Hancock, D.D., T. E. Besser, and D. H. Rice. 1998. *Ecology of Escherichia coli in Cattle and Impact of Management Practices*. ASM Press. Washington DC.

Kudva, I.T., K. Blanch, and J. Houde. 1998. Analysis of *Escherichia coli* O157:H7 survival in ovine or bovine manure slurry. *App. Eviron. Microbiol*. 64: 3166-3174

LeJeune, J. T., T. E. Besser, and D. D. Hancock. 2001. Cattle Water Troughs as Reservoirs of *Escherichia coli*. *Appl. and Environ. Microbiol.* 67(7): 3055 – 3057.

March, S.B., and S. Ratnam. 1986. Sorbitol MacConkey Medium for Detection of *Escherichia coli* O157:H7 Associated with Hemorrhagic Colitis. *J. Clin.Microbiol*. 23: 869 – 872.

Natraro, J.P., and J. B. Kaper. 1998. Diarrhoeginic *Escherichia coli*. *J. Clin. Microbiol. Rev.* 11: 142 – 201.

Ohya, T., T. Marubashi, and H. OH. 2000. Significance of Fecal Volatile Fatty Acids in Shedding of *Escherichia coli* O157:H7 from Calves Experimental Infection and Preliminary Use of a Probiotic Product. *JAMA*. 62 (11): 1151 –1155.

Padhye, N.V., and M. P. Doyle. 1992. *Escherichia coli* O157:H7 Epidemiology, Pathogenesis and Methods for Detection in Food. *J. Food Prot*. 55:555-565.

Solomon, E.B., S. Yaron, and K.R. Matthew, S. 2002. Transmission of *Escherichia coli* O157:H7 from Contaminated Manure and Irrigation Water to Lettuce Plant Tissue and its Subsequent Internalization. *Escherichia coli* O157:H7. *Appl. Environ Microbiol*. 68:397-400

Suthienkul, O., J. E. Brown, and J. Seriwatana. (1990). Shiga- like Toxin – Producing *Escherichia* in Retail Meats and Cattle in Thailand. *Appl. and Env. Microbiol*. 56:1135 – 1139

# IDENTIFICATION OF SEA CUCUMBER SPECIES AROUND HENGAM ISLAND (PERSIAN GULF, IRAN)

*Majid Afkhami* (Yung Researches Club, Islamic Azad University, Bandar Abbas Branch, P.O.Box:79159-1311, Bandar Abbas, Iran.)

Maryam Ehsanpour (Islamic Azad University, Bandar Abbas Branch, P.O.Box:79159-1311, Bandar Abbas, Iran.)

**ABSTRACT:** Sea cucumber is one of the echinoderms belonging to the branch of (*Echinodermata)* and from the class of (*Holothuroidea)* that has appeared during the evolutionary period, 540 million years ago in the oceans. At this time 1400 species of sea cucumber have been identified and reported in the seas of the whole world Sea cucumbers have many important and useful properties known for human health. Although sea cucumber is commercially important, its biology, ecology and dynamic of population have not been known yet.With this respect and the lack of scientific knowledge about them, this study has been conducted in order to identify the species present in the Hengam Island in the Persian Gulf .Three species of sea cucumber (two species belong to genus *Holothuria* and another two species of *Stichopus*) were collected on sub tidal zone of the Hengam Island (Persian Gulf) via scuba diving on January 2011. The species identification was done through morphological keys and review of their ossicles.

## INTRODUCTION

The sea cucumbers live on rocky substrata, soft sediments and Phanerogam Sea grass beds, in depths that vary between 0 and 100 m (Fischer et al., 1987). Sea cucumber potential to be commercialized in the field of modern treatment and has good therapeutic value. They have been nominated as poly-anion reach food due to presence of glycosaminoglycans that have influence in many physiologically active function including wound healing activities (Liu et al., 2002). Since there is an expansive coastal area in Iran, most coastal cities include some sea cucumber species. In Iran, sea cucumbers are not well known and they are not consumed as food, although they have been consumed in many countries for hundreds of years. In this study sea cucumber species around Hengam Island (Persian Gulf) were identified.

## MATERIALS AND METHODS

Sea cucumber Samples have been caught around Hengam Island on March- July 2011 by scuba diving in the depths of 5-12 m .( FIGURE 1).The samples transferred to laboratory in order to photograph and extract of their ossicles. It is well-known that ossicles are the main taxonomic character in holothuroids (Thandar, 1987a). The ossicles were measured on a transect across a slide prepared from the mid–dorsal region of each specimen. For these means, samples became anaesthetized with the use of magnesium chloride ($MgCl_2$) 5% which is available in every drug stores (Jiaxin, 2003).In order to extract the ossicles a small piece made of dorsal and abdominal skin of the samples placed in to the commercial bleaching liquid for almost 30 min or less (Hickman, 1998). White sediments will accumulate at the end of test tube .One drop of liquid was spread on the glass side, and they have been taken photos in order to identify the species with valid identification keys (Samyn et al.,2006;Conand, 1993). Also, for the correct

identification some specimen was sent to Prof, Gustave   paulay at the National Museum of Florida, United States.
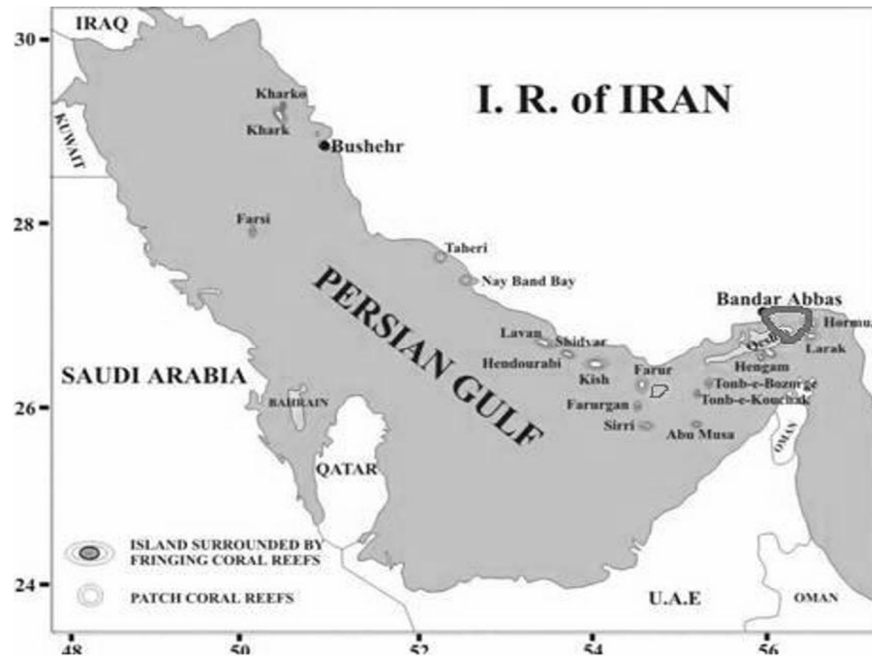


Figure 1. Sampling Site of Sea Cucumbers around Hengam Island (Persian Gulf)

**RESULTS**

This paper reports 5 species of sea cucumber in Hengam Island which is located in the south coast of the Qeshm Island (The biggest Island of the Persain Gulf). Hengam Island lies between 55°51'43''N, 26°40'86''E. This island has an area of 90 square kilometers and is 2km away from the southern part of the Qeshm Island. It is a coral island with fringing reefs.

**Table 1: Sea cucumber species identified around Hengam Island**

| (Phylum Echinodermata) | | | | |
|---|---|---|---|---|
| (Class) | (Order) | (Family) | (Genera) | (Species) |
| 1)Holothuroidea | 1)Elasipodida | 1)Holothuriidae | 1)*Holothuria* | 1)*impatines* |
| | | | | 2)*leucospilota* |
| | | | | 3)*herrmanni* |
| | | 2)Stichopodidae | 2)*Stichopus* | 4)*monotuberculatus* |
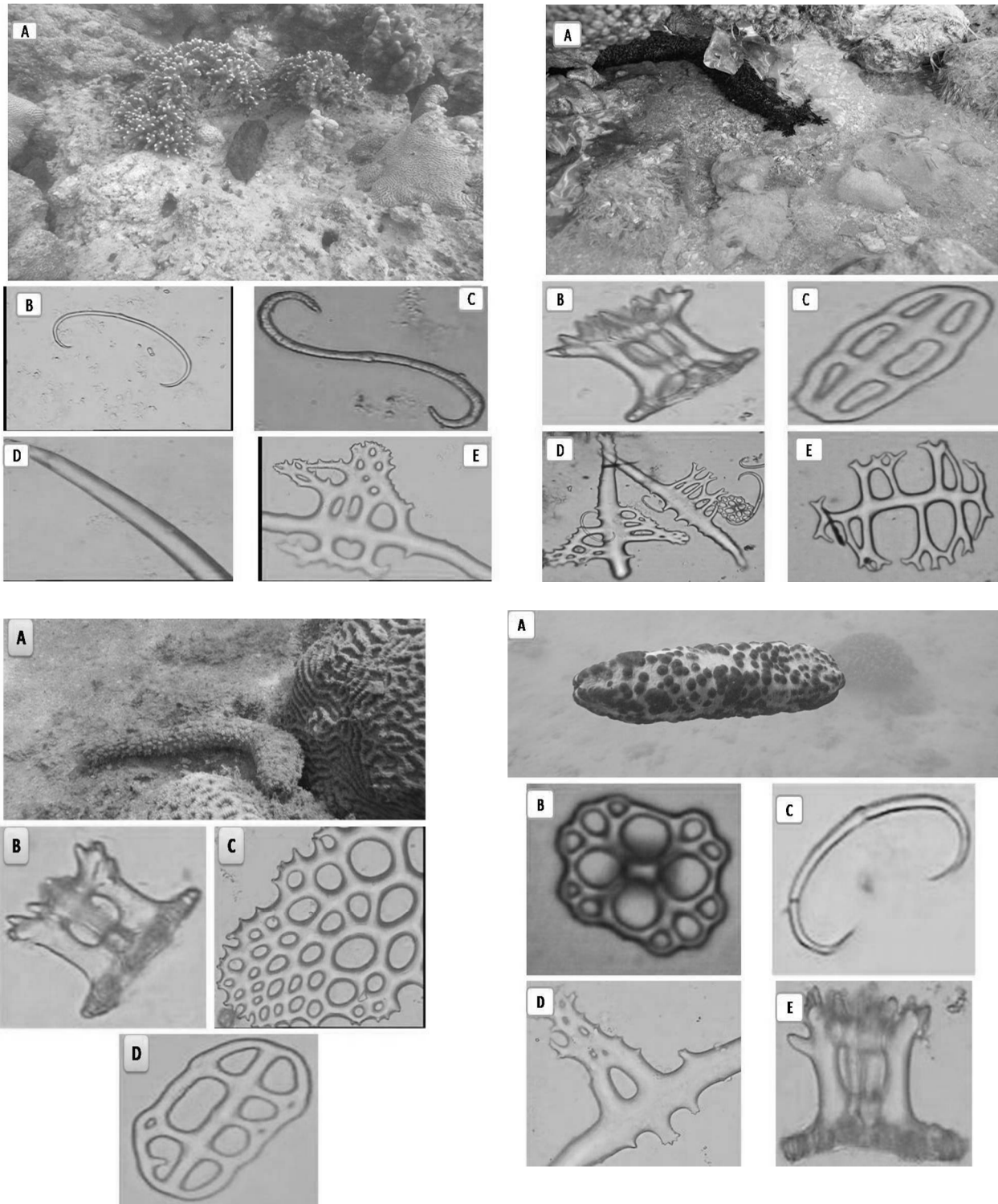
**Figure 2: Sea Cucumber Species Identified Around Hengam Island**

***Holothuria leucopilota.*** Body very elongate, narrower anteriorly than posteriorly. Mouth ventral, surrounded by 20 black tentacles. Anus subdorsal. Calcareous ring with large radial pieces and triangular interradials.Cuvierian tubules very thin and long. Colour entirely black. Spicules: dorsal and ventral tegument with tables and buttons; tables with circular large disc, having 8 holes (or more), spire with 4 pillars, and ending in a crown with large central hole; buttons regular, with 6 or 8 holes, or irregular; plates large in ventral podia, with many holes; dorsal podia also with long rods; tentacles containing few rods.

***Holothuria (Thymiosycia) impatiens.*** Ventral mouth surrounded by 20 tentacles which are in turn surrounded by a ring of very small conical papillae; anus terminal with five conical papillae. Thick Cuvierian tubules present but not readily ejected. Body wall only few mm thick and relatively smooths. In this species the body is bottle shaped with a long neck and rough surface, sandy to touch. It is covered with conical warts from which filamentous appendages emerge. It is light brown in color with 4-5 dark brown transverse bands on the upper side near the anterior end.background color beige with brown dorsal spots more or less dark. Spicules, a uniform layer of tables with almost squarish disk with eight large lllarginal holes and squat spire with numerous teeth on top, and an inner layer of buttons with three pairs of large holes

***Stichopus hermanni*(Semper,1868).** Entire body has different shades of beige to brown with irregular brown patches and fleshy tubercles projecting along the sides without cuts or small cuts across the mouth. Tentacles usually are twenty in number (non–retractile). The Body is broad, considerably flattened ventrally, and the dorsal side is slightly arched and the lateral sides are almost vertical; the body wall is fairy thick and soft; mouth sub-terminal; anus central; and tentacles usually 20 in number of moderate length and leaf – shaped. Calcareous ring slender but variable in development, which the radial plates approximately is half of the length of the inter radials. Ossicles numerous, consisting of tables with large discs having usually 7 to 15 peripheral holes, but its often irregular or incomplete, and spire of moderate height ending in a groups of spineless (sometimes in the form of a cross) about as wide as the disc, rosettes of variable development, and c – shaped rods (sometimes very few), some of which may be c–shaped or have several branches. Color of live specimens variable, it is usually brownish yellow and often mottled and with darker papillae giving a spotted appearance.

***Stichopus cf. monotuberculatus* (Quoy & Gaimard, 1833).** Dorsal side from grey green to orange-brown with dark green to black patches, ventral side grey-green with numerous small dark patches. In alcohol the colors fade to light green with patches of light brown. Ventral side flattened, dorsal side swollen, giving the animal a squarish view in cross-section. Mouth ventral surrounded by 20 large tentacles surrounded in turn by a circle of large papillae. Anus terminal, without anal teeth or papillae. Large cylindrical, yellowish brown tube feet in trivium in ambulacral areas only. Skin rather rough compared to the other *Stiehopus* species found in the region.

## DISCUSSION

Heding (1940) recorded 17 species of holothurians found in the waters around Iran. Since there is an expansive coastal area in Iran, most coastal cities include some species of holothurians (Shakouri et al., 2009). Therefore, only a few authors dealt with their taxonomy, Biology and culture (Shakouri et al.,

2009; Dabagh et al., 2011b; Amini Rad, 2004; Ehsanpour et al., 2012 and Afkhami et al., 2012). *Holothuria lecospilota* is a common shallow-water species in the area, rarely found in depths of more than 10 m; mostly on outer and inner reef flats, back reefs, and shallow coastal lagoons. Inshore, shallow-water populations are denser, composed of smaller individuals and reproduce mostly by transversal fission, while in deeper or outer reef populations the individuals are more scattered, larger, and reproduce sexually(Massin et al, 1996). The first report of successful *H. leucospilota* larval development in Iran was conducted by Dabbagh et al. (2011).*Holothuria impatiens* has long shape similar to that of *H. surinamensis* but more warty and rougher to the touch. When touched or disturbed, the animal very quickly contracts in size, an adaptive response to escape from predators and living in confined spaces. Color various shades of gray and brown with *Up* to 15 to 20 cm. long (Clark, 1942). At present it is not used for processing it is a secretive form found under dead coral stones (James, 2001). A few specimens taken at low tide but apparently most specimens live concealed among rocks a little deeper than most collectors are able to reach. At night it extends its anterior end from its hole to feed on nearby sediment. *H. impatiens* was previously recorded from Persian Gulf (Farour Island) by Hedding (1940) and Larak Island by Afkhami et al., (2012) but this is a first record of this species around Hengam Island.

Curry sea cucumber (*Stichopus hermanni*) is considered to be of low value in the export market because of the tendency of the body wall disintegrate easily, while exposed to air after harvesting and during boiling. It is reported that in the Pacific region, the intestine and gonad from this species are considered to be a delicacy among the locals and are eaten raw on the spot or squeezed into bottles and sold. Until 1995 it is almost always mentioned in the literature under the name *S. variegatus*. Since *S. variegatus* was replaced by *S. herrmanni* and *S. monotuberculatus* (Quoy & Gaimard, 1833) (Samyn et al., 2006).

The sea cucumber *Stichopus monotuberculatus* has a wide Indo-Pacific distribution and high commercial value due to its medicinal and edible properties (Massin 1996; Liao 1997). It is however an expected species since, Massin's distribution map (1996b, map 3, p. 174) shows an Indo-Pacific distribution from the Red sea and Madagascar to Eastern Islands, and from Japan to Australia. It has been demonstrated that *S. monotuberculatus* can be reared in captivity, thus the farming of this species would provide an alternative to fisheries (Hu *et al*. 2010). The spicules match the descriptions given by Cherbonnier (1952) and Massin (1996) but more specimens of different sizes from different localities are needed to clarify the identity of our specimens. *S. monotuberculatus* recently have been recorded in Persian Gulf by Ehsanpour et al., (2012).

## REFERENCES

Afkhami Majid, Ehsanpour Maryam, Khazaali Aida, Dabbagh Abdul-Reza,and maziar yahyavi. 2012. New observation of a sea cucumber, *Holothuria (Thymiosycia) impatiens*, fromLarak Island (Persian Gulf, Iran)**.** *Marine Biodiversity Records*, page 1 of 3.

Amini Rad T. 2004. Determination of the effects in co-culture between shrimp and sea cucumbers on the growth of related to lengths and weight. Pajouhesh and Sazandegi 68:19–23.

Cherbonnier G. 1952. Les holothuries de Quoy & Gaimard. *Memoire de l'Institut royal des Sciences naturelles de Belgique, Deuxieme serie* 44: 1-50 + 3 pIs.

Clark H. L.-Continued 1942. The Echinoderm Fauna of Bermuda. *Bull. Muf:' Compo ZooI.* 89: 367-394, 1 pI.

Conand, C. 1993. Reproductive biology of the holothurians from the major communities of the New Caledonia Lagoon. *Marine Biology* .116: 439-4.

Conand C. 2006. Sea cucumber biology: taxonomy; distribution; biology; conservation tatus. pp: 33–50. In The Proceedings of the CITES workshop on the conservation of sea cucumbers in the family's *Holothuriidae* and *Stichopodidae*. Bruckner, A.W. (ed.). *OAA Technical Memorandum*, 244 pp.

Dabbagh A.R. Sedaghat M.R. Rameshi H. and Kamrani E. 2011a.Breeding and larval   rearing of the sea cucumber *Holothuria leucospilota Brandt* (*Holothuria vegabunda Selenka*) from the northern Persian Gulf, Iran. *SPC Beche-de-mer Information Bulletin*, 31:35-38.

Dabagh Abdoreza and Kamrani Ehsan. 2011b.Collection of sea cucumber, *Holothuria(Mertensiothuria) Hilla* Lesson,1830 Specimen from Farour Island (Persian Gulf, Iran).*World Journal of Fish  and Marine Science*. 3(3) 214-216.

Ehsanpour Maryam,Afkhami Majid, Bahri Amir Houshang and Daryaei Abdolrasoul, 2012. First Report of a Sea cucumber, *Stichopus cf. monotuberculatus* (Quoy & Gaimard, 1833), from Hengam Island (Persian Gulf, Iran). European Journal of Experimental Biology, 2 (3):547-550.

Fischer W. Schneider M. & Bauchot M.L. 1987. Me´diterrane´e et Mer Noire (Zone de Peˆche 37). Fiches FAO. d'identification *des espe`ces pour les besoins de la peˆche*. Rev.1.

Heding S.G. 1940. Echinoderms of the Iranian Gulf. Holothuroidea. *Danish Scientific Investigations Iran*. 2:113–137.

Hickman C.J. 1998. A Field guide to sea stars and other Echinoderms of Galapagos. $1^{ST}$, *Edn., sugar spring press , Lexington ,VA, USA*. PP:83.

Hu C.Q. Xu Y.H. Wen J. Zhang L.P. Fan S.G. & Su T. 2010. Larval development and juvenile growth of the sea cucumber *Stichopus sp.* (Curry fish). *Aquaculture* **300**, 73-79.

James, D.B. 2001. Twenty sea cucumbers from seas around India, *Naga.The ICULAPM quaterly*. Vol (24):4-9.

Jiaxin c. 2003. Overview of sea cucumber farming and sea ranching practices in china. *SPC Beche-de-mer informs. Bull*., 18:1-6.

Liao Y. 1997. Fauna Sincia: *Phylum Echinodermata Class Holothuroidea*. Science Press, Beijing.

Liu H.H. W.C. Koand and M.L.Hu 2002.Hypolipidemic effect of glycosaminoglycans from the sea cucumber *metriattya scabra* in rats fed a cholesterol-supplemented diet. *J. Agric. food chem*. 50:3602-3606.

Mamelona J. Pelletier E. Girard-Lalancette K. Legault J. Karboune S. Kermasha S. 2007. Quantiication of phenolic contents and antioxidant capacity of Atlantic sea cucumber, *Cucumaria frondosa. Food Chem*; 104:1040-7.

Massin C. 1996b. The holothurians of Easter Island. *Bulletin de l'!nstitut royal des Sciences naturelles de Belgique, Biologie* 66: 151-178.

Massin C. 1996.The holothurians of Easter Island. *Bulletin de l'Institut royal des Sciences naturelles de Belgique, Biologie* **66**, 152-178

Murray A.P. Muniain C. Seldes A.M. Maier M.S. Patagonicoside A. 2001. A novel antifungal disulfated triterpene glucoside from the sea cucumber *Psolus patagonicus*. *Tetrahedron*. 57, 9563—8.

Samyn Y. and Massin C. 2003. The holothurian subgenus *Mertensiothuria* (Aspidochirotida: Holothuriidae) revisited. *Journal of Natural History* 37(20):2487–2519.

Samyn Y. VandenSpiegel D. and Massin C. (2006). *Taxonomie des holothuries des Comores*. Abc Taxa, vol 1, i-iii, 130 pp.

Shakouri A. T.aimorirad . M.B. Nbavi p. kochanian. A. savari and A. safahyie. 2009. New obsaervation of three species of sea cucumber from chabahr Bay (Sotheast coast of Iran). *J. Biol.sci*. 9:184-187.

# SPECIES OF YEAST ASSOCIATED WITH SOME NIGERIAN FRUITS

*Ogbonna, Abigail I.,* Ogbonna, Chike I. C. and Onyimba, Isaac A
(University of Jos, Plateau State , Nigeria )

**ABSTRACT:** Studies were carried out on the distribution of yeast species amongst some ripe Nigerian fruits of economic importance. The fruits examined included Anacardium occidentale, Annona muricata, Carica papaya, Citrus sinensis, Irvingia smithii, Mangifera indica, Musa sapientum and Psidium guajava . The experimental fruits were analyzed for their percentage sugar contents, percentage moisture contents and the range of pH of their juices. Twenty-three species of yeast belonging to 7 genera were isolated from the fruits. This included 9 species of Saccharomyces, 6 species of Candida, 2 species of Pichia, Rhodotorula, Hansenula respectively, 1 species of Kloeckera and Torulopsis respectively. Apart from the yeast isolates, 11 species of Fungi and 2 species of bacteria were also isolated. A. occidentale had the highest number of yeast isolates while C. papaya had the least. The fruits were found to contain appreciable amounts of sugar and the percentage moisture contents and range of pH values recorded for the fruits were within the range that will support microbial growth.
.

## INTRODUCTION

A fruit is a mature ovary and often accessory parts of the flower, enclosing the seed or seeds (Curtis and Barnes, 1984). Fruits contain a high percentage of water and are therefore low in energy value. The fruit wall at maturity may be fleshy or more commonly dry. Fleshy fruits range from soft, and juicy to hard and tough. Fleshy fruits are rarely indehiscent.

Gaman and Sherrington (1983) reported that in general fruits have a higher sugar content than vegetables and ripe fruits contain little or no starch. They said that grapes for example contain up to 15% sugar and oranges about 7%. They also said that the sugar in fruits is usually a mixture of glucose and fructose. Fruits according to Curtis and Barnes (1984) contain a variety of organic acids in particular, citric, malic and tartaric acids and that these acids are responsible for the sourness of unripe fruit. They also reported that during ripening, the concentration of these acids falls and that of sugar rises. Fruits also contain vitamins, however only certain fruits like citrus fruits contain vitamins in appreciable amounts. So the fruits apart from being a good source of vitamins to human beings could also supply the vitamin requirements of microorganisms including yeasts.

The fruits from which musts are derived could carry with them internal and external micro-flora as they are brought to the factory from the farms and markets. Yeast could be mere surface contaminants on fruits. They could also gain entry into the fruits through damaged areas on the fruits. Such fruit damages could stem from internal changes such as senescence and external factors like unfavorable environment and physical injury. Compression, like impact causes bruising or cracking which occurs primarily during or after packing.

Kunkee and Goswell (1977) reported on the species of yeast associated with grape fruits surfaces, fruit musts and wines. The implicated yeasts included species of *Brettanomyces, Candida* in South Africa, Greece and Spain, *Saccharomyces* on grapes in Czechoslovakia, Georgia, Russia, Brazil, Spain, Japan, Cognac region and Italy.

While the yeast flora of fruits of many countries have been studied and well documented, information on the yeast flora of Nigerian fruits is scanty. However, where such information exists, it is obtained indirectly and is often fragmented. Such scanty existing pieces of information on the yeast flora associated with Nigerian fruits include that of Okujagu (1970) who isolated *Candida tropicalis, Candida* species, *Saccharomyces cerevisiae, Saccharomyces* species and *Torulopsis candida* from Banana, Mango, Orange and Plantain. Olusola (1989) isolated *S. cerevisiae, S. uvarum* and *Schizosaccharomyces pombe* from natural fermenting Guava fruit must. Iketuonye (1990) isolated some species of Microorganisms including *S. cerevisiae* and *Schizosaccharomvces* species from *Xylopia aethiopica* and *Monodora brevipes.* The same author reported the presence of *S. cerevisiae* from dried stored *Piper guineense* and *X. aethiopica* treated with common salt.

The genus *Saccharomyces* is well known and the species *S. cerevisiae* commonly known as Baker's yeast is the most important representative. Brewers yeast, wine yeast and distiller's yeasts are also varieties of *S. cerevisiae* which can be used in many ways to manufacture food of different kinds. For winery, bakery, brewery, distillery industries to thrive in Nigeria and other West African countries more especially in these days of economic depression, there is need to make a proper selection of species of yeast that are adapted to the existing tropical conditions. They will also have the ability to effect efficient alcoholic fermentation of sugars, which are able to tolerate appreciable ethanol concentrations, produce organoleptically desirable compounds, which possess strain stability and viability.

The present study was therefore designed to find out the distribution of species of yeast of industrial importance amongst some selected Nigerian fruits.

## MATERIALS AND METHODS

The ripe fruits chosen for the present study included: *Anacardium occidentale.* L. (Cashew-Apple), *Annona muricata* L. (Sour-Sop), *Carica papaya* L. (Paw-Paw), *Citrus sinensis* L. (Sweet Orange), *Irvingia smithii* Hook .F. (African apple), *Mangifera indica* L. (Mango), *Musa sapientum* Schum (Banana), *Psidium guajava* L. (Guava). In the choice of the ripe fruits, attempts were made to include those healthy fruits with surface cracks.

**Yeast Isolation from the Test Fruits.** The method adopted was that described by Beech and Davenport (1971). The method of isolation from the experimental fruits involved the squeezing out of each ripe fruit juice. Such squeezed fruits juice was then enriched with small amount of sterile sugar solution. The sugar solution was obtained by dissolving 15 cubes of St. Louis sugar in 1 litre of sterile distilled water. One teaspoonful of such solution was then added to each 15ml fruit juice extract and then incubated at room temperature ($25^{o}$C) in the Laboratory for a period of 4 days in order to build up the population of the yeast cells available in each fruit juice. The yeast suspension in the fruit was then plated out on each of the growth media employed (PDA and NA). Thirty sterile Petri dishes were employed for each fruit juice extract for each medium. Such culture plates were then divided into three batches (each batch containing 10 plates). The first batch of 10 plates was incubated at $25^{o}$C, the second batch of 10 plates was incubated at $37^{o}$C while the final batch of 10 plates was incubated at $45^{o}$C. Such growth temperatures were employed in order to isolate mesophilic, thermotolerant and thermophilic yeast species respectively. In order to inhibit acid-tolerant bacteria without seriously affecting the growth of

any yeast species, Gentamycin (40mg/ml) was incorporated into the growth media which had moderately low pH (4.8).

The culture plates were incubated for a period of 24 hours and then examined for the presence of yeast species. The colonies of yeasts that so developed were sub-cultured several times until pure cultures were obtained.

**Identification of Yeast and other Microbial Isolates.** The yeast isolates were identified on the basis of a large number of features like cultural, morphological, physiological and biochemical parameters, growth temperatures, type of budding, sporulation, and film formation; the morphological nature of the ascus and ascospores, the methods involved in the ascospores germination, the appearance of colonies on various growth media, and characteristics of giant colonies. References were made to existing yeast stock cultures and (Lodder 1970; Domsch and Gams 1972; Rose 1982; Samson *et al*. 1984; Prescott *et.al*. 1996).

**pH Determination of the Fruits Musts.** The juices of the fruits were expressed with the aid of wooden wine press as reported by Okujagu (1970). The pH of each experimental fruit was then determined with the aid of Corningh pH meter (model 7). Each pH determination was replicated 3 times and the average pH reading was then recorded.

**Percentage Moisture Content of the Experimental Fruits.** he method used was that described by Sani (1985). Healthy and fresh fruits were employed for these determinations. Three of each test fruit were assembled for this particular experiment. One of such experimental fruit was then weighed intact and the result was recorded. The fruit was then crushed with the aid of a wine press and dried to constant weight in an air oven at $105^{\circ}$C. The result was then recorded. Care was taken not to lose any of the fruit particles during the process. The experiment was repeated with the remaining 2 healthy fruits of the particular test fruit. The average dry weight was taken. The percentage moisture content of the particular fruit was calculated and recorded. This particular experiment was repeated using the other experimental fruits.

**RESULTS AND DISCUSSION**

The survey as shown in Table 1 reveals that there is a wide distribution of species of yeast amongst Nigerian ripe fruits. Twenty-three species of yeast belonging to 7 genera were isolated from the experimental fruits. The highest number of yeast species was isolated from the Cashew fruits while the least number of yeast isolates was made from the Paw-Paw fruits. Of the 7 genera of yeast isolated, the genus *Saccharomyces* was found to be the most predominant, having nine (9) species with *S. cerevisiae* and *S. globosus* as the most common. They had the highest frequencies of occurrence (100%) amongst the experimental fruits. They were followed by *Rhodotorula* species and *S. delbrueckii* (75%). *H. polymorpha, S. bailii, S. bayanus, S. rosei,* and *C. parapsilosis* had the same frequencies of occurrence (62.5%). *H. anomala, K. africana, P. membranaefaciens, P. pastoria, R. aurantiaca, S.rouxii, C. albicans, C. krusei* and *C. tropicalis* had the same frequencies of occurrence (50%). The rest of the isolates had less than 50% frequencies of occurrence. *S. cerevisiae* (one of the isolates in the present study) together with *S. ellipsoideus* have been reported to represent the best known and probably most widely distributed types of yeast (Prescott *et al.,*1996). The genus *Saccharomyces* is of outstanding interest as most yeasts having any technical uses belong herein.

Almost all the yeast isolates have been reported on grapes, in musts and in wines (Kunkee and Goswell, 1977). The same authors also reported that the juices within the intact healthy grape berry is sterile and the inoculum for a natural or "spontaneous" fermentation comes from the grape skin in contrast to a fermentation initiated by inoculum with a yeast starter culture.

**TABLE 1: The distribution of yeast species amongst The experimental fruits**

| Species of Yeast Isolated | Experimental Fruits | | | | | | | | Total |
|---|---|---|---|---|---|---|---|---|---|
| | A* | B | C | G | M | O | P | S | |
| *Hansenula anomola* H. et P. Sydow | - | - | +** | -** | + | + | + | - | 4 |
| *H. polymorpha* Moraisand maia | + | - | + | + | + | - | + | - | 5 |
| *Kloeckera africana* Janke | + | - | + | - | + | - | + | - | 4 |
| *Pichia membranaefaciens* Hansen | + | - | + | + | + | - | - | - | 4 |
| *P. pastoris* Phaff | - | + | + | - | + | + | - | - | 4 |
| *Rhodotorula aurantiaca* Lodder | - | - | + | + | + | - | + | - | 4 |
| **Table 1 contd.** | + | + | + | - | + | + | + | - | 6 |
| *Saccharomyces bailii* Lindner | - | - | + | + | + | + | - | + | 5 |
| *S. bayanus* Saccardo | + | + | + | - | - | + | + | - | 5 |
| *S. cerevisiae* Hansen | + | + | + | + | + | + | + | + | 8 |
| *S. delbrueckii* Lindner | + | - | + | + | + | - | + | + | 6 |
| *S. globosus* Osterwalder | + | + | + | + | + | + | + | + | 8 |
| *S. heteroginicus* Osterwalder | - | + | + | - | + | - | - | - | 3 |
| *S. rosei* Lodder et Kreger – van Rij | - | + | + | + | - | + | + | - | 5 |
| *S. rouxii* Boutroux | - | + | + | - | - | + | - | + | 4 |
| *S. uvarum* Beijerinck | - | - | + | + | + | - | - | - | 3 |
| *Candida albicans* Berkhout | + | - | - | + | + | + | - | - | 4 |
| *C. guilliermondii* Langeron et Guerra | + | - | - | - | + | - | - | - | 2 |
| *C. krusei* Basgal | + | - | - | + | + | + | - | - | 4 |
| *C. parapsilosis Langeron et Guerra* | + | + | + | - | - | + | - | + | 5 |
| *C. stellatoidea* Langeron et Guerra | - | - | + | - | + | - | - | + | 3 |
| *C. tropicalis* Berkhout | + | - | + | - | + | + | - | - | 4 |
| *Torulopsis candida* Lodder | - | + | + | - | - | - | + | - | 3 |
| TOTAL | 13 | 10 | 20 | 11 | 18 | 13 | 11 | 7 | 103 |
| pH range of the test fruits | 4.4 | 5.2 | 3.2 | 4.7 | 4.4 | 4.2 | 6.7 | 4.2 | |
| % sugar content | 16.5 | 16.2 | 17.5 | 15.7 | 15.3 | 8.5 | 17.0 | 15.4 | |
| % moisture content | 68.7 | 70.7 | 80.5 | 77.6 | 83.0 | 86.1 | 80.4 | 80.7 | |

*A     = African apple *Irvingia smithii* L.,    B =Banana -*Musa sapientum* .L.
 C     = Cashew-*Anacardium occidentale* L.,    G=Guava -*Psidium guajava*
 M    = Mango -*Mangifera indica*           O= Orange - *Citrus sinensis*
 P     = Paw-Paw-*Carica papaya* L.,        S= Sour- sop -*Annona muricata*
** + means present        - means absent

Cashew was found to have the highest number of yeast isolates (20) and also the highest amount of sugar (17.5%) of all the fruits investigated (Table 1). It was followed by Mango which had 18 yeast isolates and (15.3%) sugar content. Gaman and Sherrington (1983) reported that fruits have a higher sugar content than vegetables and ripe fruits contain little or no starch, and that the sugar in fruit is usually a mixture of glucose and fructose. The percentage moisture contents recorded for the experimental fruits were high enough to support the growth of the yeast species especially in the cracked fruits. The experimental fruits were found to have pH range of 3.2 – 6.7.

### TABLE 2: Other Microorganisms Associated With Experimental Fruits

| Other Microbial Isolates | Experimental Fruits | | | | | | | | Total |
|---|---|---|---|---|---|---|---|---|---|
| | A* | B | C | G | M | O | P | S | |
| **PHYCOMYCETES** | | | | | | | | | |
| *Absidia corymbifera* Sacc & Trotter | + | | + | | + | | | + | 4 |
| *Circinella simplex* van Tieghem | + | + | | | + | | | | 3 |
| *Choanephora cucurbitarum* Thaxter | | | | | + | + | + | | 3 |
| *Mortierella wolfii* mehrotra & Baijal | + | + | + | | + | + | + | + | 7 |
| *Mucor pusillus* Lindt | | | + | + | | | | | 2 |
| *Rhizopus oligosporus* Saito | + | + | + | + | + | + | + | + | 8 |
| *R. nigricans* Ehrenberg | + | + | + | + | + | + | + | + | 8 |
| **HYPHOMYCETES** | | | | | | | | | |
| *Aspergillus fumigatus* Fres. | + | + | + | + | + | + | + | + | 8 |
| *A. niger* van Tieghem | | + | + | | + | | + | | 4 |
| *A. oryzae* Cohn | + | + | + | + | + | + | + | + | 8 |
| **ASCOMYCETES** | | | | | | | | | |
| *Emericella nidulans* Wint. | | | + | | + | | | | 2 |
| **BACTERIA** | | | | | | | | | |
| Bacillus sp. | | + | | + | | + | | | 3 |
| *Lactobacillus acidophilus* | + | + | + | + | + | + | + | + | 8 |
| TOTAL | 8 | 9 | 10 | 7 | 11 | 8 | 8 | 7 | 68 |

*A = African apple *Irvingia smithii* L.,    B =Banana -*Musa sapientum* .L.
 C = Cashew-*Anacardium occidentale* L.,    G=Guava -*Psidium guajava*
 M = Mango -*Mangifera indica*    O= Orange - *Citrus sinensis*
 P = Paw-Paw-*Carica papaya* L.,    S= Sour- sop -*Annona muricata*
** + means present      - means absent

The least number of species of yeast was made from paw-paw, which had pH of 6.7. The species of yeast were isolated from acidic environments moreso those ones that were isolated from the fruit juices. Ehrlich (1963) reported that several yeasts believed to resemble *Rhodotorula* have been isolated

from pH 2 copper mine wastes. Battley and Barlett (1966) reported that yeasts generally have mildly acidic pH optima of 5.5-6. They said that many species however are capable of growing down to pH 2.

Most of the yeast species isolated are being reported in Nigeria for the first time. Also two of the yeast isolate, *H. polymorph* and *T. candida* are thermophilic . These two species of yeasts are also new records for the Nigerian thermophiles.

The other microbial isolates from the experimental fruits as shown in table 2, included 11 species of fungi and two species of bacteria. Of the 11 species of fungi isolated, 7 of them belong to class phycomycetes, which are known to be sugar lovers. One of the fungal isolates *Aspergillus oryzae* has been known to ferment sugar. The significance of the association of these fungal species with the fruits is in the production of Patulin [4-hydroxy-4H-furo (3,2c) pyran-2 (6+T)-one] a toxic secondary metabolite produced by some species of fungi in several genera of fungi in fruit juices. Patulin has been found to be mutagenic to yeast cells (Mayer and Legator, 1969).

The pH ranges recorded for the various fruits were within the ranges that would support microbial growth in pure culture. The moisture contents recorded for the fruits were very adequate for the growth of microorganisms more especially when fruits were found to contain substantial amount of sugar needed for respiration including fermentation.

It is likely these species must have been carried to the ripe fruits by insects like flies or birds since these animals were seen at the area where the fruits were collected. Moreso, the fields around the houses from where these fruits were collected were found to be littered with human wastes (faeces and urine) due to the bad habits of some Nigerians who dispose their wastes in the bushes around and their inability to provide adequate toilets and other public amenities. Smeall (1932) said that yeasts occur in large numbers in vineyard soil and are spread to grapes by dust and insects. Prescott *et.al.*, (1996) reported that yeasts are of wide distribution in nature.

A detailed survey of the yeast flora of various Nigerian fruits will probably lead to the establishment of a national yeast bank. Such yeast bank will make it possible for the characterization of such yeast isolates. This will then make it possible for the biotechnological improvement of some strains of this yeast for industrial purposes.

**CONCLUSION**

This present study has shown much promises for further investigation. The yeast flora of other Nigerian fruits should be surveyed since the final out come will be very rewarding to the brewery, winery and bakery industries.

**ACKNOWLEDGEMENT**

**REFERENCES**

Battley, E.M. and E.J. Barlett. 1966. A convenient pH-gradient method for the determination of the maximum and minimum pH for microbial growth. *Antonie van Leeuwenhoek* 32: 245-255.

Beech, F.W. and R.R. Davenport. 1971. A survey of methods for the quantitative examination of the yeast flora of apple and grape leaves. In: *Ecology of leaf surface microorganisms* Publ. Academic press, London and N.Y. P. 139-157.

Curtis, H. and N.S. Barnes. 1984. *Invitation to Biology*. Publ.Worth publishers, Inc. New York. 696pp.

Domsch, K.H. and W.Gams. 1972. *Fungi in agricultural soils*. Publ. Longman group Ltd., London, 290pp.

Ehrlich, H.L. 1963. Microorganisms in Soil from a copper mine. *J. Bacteriol*. <u>86</u>: 350-352.

Gaman, P.M. and K.B. Sherrington. 1983. *The Science of food: An Introduction to food Science, Nutrition and Microbiology.*Publ. Pergamon Press, Oxford, N.Y. Toronto, Sydney, Paris, Frankfurt, 166pp.

Iketuonye, A.J.N. 1990. Microorganisms associated with some Nigerian spices. *B.Sc. Desertification, University of Jos, Nigeria*.

Kunkee, R.E. and R.W. Goswell. 1977. Table Wines. In: *Alcohol Beverages – Economic Microbiology Vol.1* Ed. A.H. Rose. Publ. Academic Press, London, N.Y. San Francisco, p. 315-386.

Lodder, J. 1970. *The Yeasts – a taxonomic study.* Publ. North-Holand publ. Co. Amsterdam, London. 1385pp.

Mayer, V.W. and M.S. Legator. 1969. Production of Petite mutants of *Saccharomyces cerevisiae by patulin. J. Agr. Food Chem. 17*: 454-456.

Okujagu, T.F. 1970. Protein enrichment of Plantain Peels by Microbiological method. *M .Sc. Dissertification, University of Jos. Nigeria.*

Olusola, O.G. 1989. Studies on the production of table wine from guava (*Psidium guajava* .L.) *M.Sc. Dissertification, University of Jos, Nigeria.*

Prescott, L.M., J.P.Harley and D.A.Klein.1996. *Microbiology.* Publ. WCB publishers Inc. N.Y. London,Chicago,Caracas p.880-930

Rose, A.H. 1982. *Fermented Foods-economic  microbiology Vol. 7.* Publ. Academic Press, Inc. London, Orlando San Diego, New York, Toronto, Montreal Sydney, Tokyo 336pp.

Samson, R.A., E.S. Hoekstra and C.A.N. Van oorschoot. (1984). *Introduction to Food-Borne Fungi.* Publ. Centraalbureau Voorschimmelcultures Baarn, Delft,  Inst. Of the royal Netherlands Academy of Arts and Sciences 249pp.

Sani, L. 1985. Species of Yeasts Associated with Commonly Eaten Fruits In Jos Metropolis *B.Sc.Dissertation,University of Jos,Nigeria*

Smeall, R. 1932. Yeasts in Vineyard Soil. *Bri. Med. J.  41*: 917-919.

# ANTIMICROBIAL ACTIVITY OF MICROORGANISMS ISOLATED FROM WASTE OIL POLLUTED MECHANIC WORKSHOPS SOILS IN PLATEAU STATE, NIGERIA.

***Ogbonna, Abigail,*** Sila, Micheal

(University of Jos, Plateau state, Nigeria)

**ABSTRACT:** The major source of oil pollution in auto-mechanic workshops soils in Jos, Nigeria is used crankcase oil from vehicles. Soil samples were collected from 3 locations (1, 2 and 3) of such crankcase oil-polluted soils and screened for the presence of microorganisms. The samples were collected from the depth of 15cm, with the aid of surface sterilized soil auger. Soil plate method was employed for the microbial isolations. Starch-casein agar, nutrient agar and malt extract agar media were used for the isolation experiments. Twenty-eight (28) species of microorganisms were isolated and these included, 3 species of actinomycetes, 5 species of bacteria, 18 species of fungi and 2 species of yeast. The highest number of microorganisms was isolated from the second experimental location (2). The growth metabolites of the microbial isolates were tested against some pathogenic bacteria (*Bacillus subtilis, Escherichia coli, Pseudomonas aeruginosa* and *Staphylococcus aureus),*pathogenic yeast (*Candida albicans)* and *Aspergillus niger* which has been implicated in some mycotic infections. The results showed that 2 of the actinomycete isolates, *Streptomyces griseus* and *Streptomyces* sp inhibited the growth of all the pathogenic test organisms. *Bacillus* sp was found to inhibit the growth of *S. aureus*. It was also observed that one of the clinical test organisms, *P. aeruginosa*, however, inhibited the growth of one of the fungal isolates, *Absidia corymbifera.* Two of the fungal isolates, *Penicillium* sp and *Paecilomyces variotii* inhibited the growth of the pathogenic yeast, *C. albicans.* Work is continuing to determine the metabolites (possibly antibiotics) that were responsible for the antimicrobial activities. It is hoped that the results would help in the development of the Nigerian antibiotics industry which is highly threatened by the rapid influx of substandard antibiotics.

## INTRODUCTION

Antibiotics first became widely available in the 1940s with the use of penicillin and sulphonamides. Since that time the pharmaceutical industry has developed more than 100 varieties of these drugs with 150million prescriptions being written for antibiotics annually in the United States alone (Levy,1998). This growth in antibiotic usage has been paralleled by the ability of bacteria to resist destruction by these agents. This has resulted in a steady decline in the number of effective antibiotics each year (Levy,1998). The acquisition of antibiotic resistance gene has been observed in at least four species of bacteria for which there are no effective forms of conventional therapy available (Jensen and Wright, 1997). In order to combat these resistance traits, new antibiotics will have to be developed. Soil bacteria and fungi have contributed immensely in the development of antibiotics and soil has been the best natural environment for the isolation of antibiotic producing microorganisms (Mah, 2003).

Petroleum is a rich source of hydrocarbons. It is readily attacked aerobically by a variety of microorganisms that can degrade such hydrocarbons. Thus it is not surprising that when petroleum is brought in contact with soil, air and moisture, it is subjected to microbial attack (Okonkwoeje, 2001). The influence of crude oil on the type and number of microorganisms in the soil has been investigated by several scientists. Michalcewics (1995) revealed that crude oil application caused changes in the total number of the investigated groups of soil microorganisms. The author further reported that crude oil-contaminated soil contained organisms such as *Pseudomonas, Arthrobacter, Bacillus, Penicillium, Aspergillus, Fusarium, Trichoderma* and *Streptomyces* species. Crude oil-contaminated soil is dominated by organisms that are antibiotic producers (Michalcewics, 1995).

The present study was designed to find out the efficacy of the metabolic substances produced by some microorganisms isolated from motor mechanic workshops soils polluted with used motor oils in Jos, Plateau State of Nigeria.

**MATERIALS AND METHODS**

Soil samples were collected from 3 mechanic workshop soils that were polluted with used motor oil in Jos, Nigeria and from the depth of 15cm with the aid of soil auger which was adequately cleaned with 90% alcohol prior to use.

Each of the said soil samples was sifted with the aid of 2mm wire mesh. For fungal isolations, soil crumbs were plated out from each of the soil samples using the method described by Ogbonna and Pugh (1982) and employing 3 culture media, Eggins & Pugh cellulose Agar, Malt extract agar and Czapek dox agar. A total of 10 culture plates were used for each soil sample from each location and for each culture medium. Suspension of each soil sample was also prepared and plated out on Starch-Casein Agar and Nutrient Agar for the isolation of species of actinomycete and bacteria respectively as described by Omemu *et al*., (2006). The resultant culture plates were then incubated at $25^0$C and examined for the presence of bacteria after 24 - 48 hours. The plates were examined after 4 –7 days for the presence of fungi. The culture plates were re-examined after 14 – 28 days for the presence of actinomycetes. The experiment was repeated twice but the resultant plates from such repetition were incubated at $37^0$C and $45^0$C respectively for the isolation of thermotolerant and thermophilic fungi respectively.

The microbial colonies that developed were sub-cultured several times until pure cultures were obtained. Such pure colonies were then examined under the microscope for their morphological characteristics. The bacterial and yeast isolates were also subjected to gram-staining and other conventional biochemical and physiological studies. The actinomycete isolates were also subjected to biochemical tests like starch hydrolysis, casein hydrolysis, urea hydrolysis, and acid production from sugar as described by Raja *et al*., (2010). References were also made to existing stock cultures and also to Domsch and Gams, (1972); Von Arx, (1974), and Cowan and Steel, (1965).

The ecological parameters of the soil samples were also determined using the method described by Ogbonna and Pugh (1982).

The microbial isolates were preliminarily tested for their antimicrobial activities against some clinical pathogens. The test pathogenic microorganisms included; *Bacillus subtilis, Escherichia coli, Pseudomonas aeruginosa, Staphylococcus aureus, Candida albicans* (pathogenic yeast) and a pathogenic fungus, *Aspergillus niger* which has been found to be involved in external mycotic keratitis. The experiment was done using the cross-streak method described by Bradshaw (1992). In this method, sterile nutrient agar was aseptically dispensed into 10 sterile Petri-dishes and then allowed to set. A seven day old culture of the test microbial isolate was used to streak each of the 10 culture plates with the aid of sterilized wire loops. An 18 hour culture of a pathogenic microorganism was then streaked at a right angle to the streak of the microbial isolate, just at the middle. The plates were then incubated at a temperature of $37^0$C for a period of 24hours and then observed for signs of antimicrobial activity. The average zone of inhibition of each microbial isolate against each test pathogen was then recorded. The experiment was repeated for each of the microbial isolates and for each of the test pathogenic microorganisms.

In another study, the metabolites of five of the microbial isolates that showed sensitivity initially were further tested against the clinical pathogens. The metabolites of the microbial isolates were obtained using the fermentation method. This was carried out in a 500ml Erlenmeyer flask for each isolate using a modified method of El-Banna and Winkelmann (1998). The pure culture of the test microbial isolate was grown in submerged culture of Potato Dextrose Broth in a rotary shaker under 130rpm at a temperature of $30^0$C for a period of 10 days. The culture was then harvested with the exclusion of spores and mycelia. The filtration was performed by passing the liquid culture through two layers of sterile cheese clothes and sterile Whatman filter paper (No.1). The clarified sap was then dried to a dark crude under reduced air and at a temperature of $50^0$C, then pulverized and kept refrigerated until needed. Similar procedures were carried out for each of the 5 microbial isolates.

For the antimicrobial determinations of the metabolites of the test isolates, the method employed was a modified agar well diffusion method described by Irobi *et.al*. (1996). In this method, agar plates were inoculated with 0.5 McFarland standard broth culture of the experimental pathogenic microorganisms. The dried, pulverized extract was then solubilized in dimethyl sulphoxide (DMSO) to a concentration of 100mg/ml. Wells of 6mm diameter were punched into the agar aseptically and then filled with 30µl of the metabolite dilution. A control experiment was set up using Gentamycin (40mg/ml). The experiment was repeated for each experimental pathogenic microorganism and for each metabolite of the microbial isolates. However, while gentamycin was employed as control for bacterial pathogens, nystatin(5mg/ml) was employed as control for fungal pathogens. The resultant plates were then incubated at $37^0$C for a period of 24hrs for bacterial pathogens and *C. albicans* and for 48-96hrs for *A. niger*. Bioactivity was determined by measuring the diameters of inhibitory zones (mm). Each experiment was repeated 3 times and the mean inhibitory zones were recorded.

## RESULTS AND DISCUSSION

A total of 28 species of microorganisms were isolated during the study. These were made up of three (3) species of actinomycetes, five (5) species of bacteria, eighteen (18) species of fungi and two (2) species of yeast. The restriction in the number of microorganisms isolated could have stemmed from the waste motor oil pollution. The species isolated may have been those that could tolerate levels of pollution. The distribution of the microbial isolates is shown in Table 1. The study has shown that some species of microorganisms can tolerate levels of pollution caused by used motor oils. This could stem from their abilities to degrade or accumulate levels of the oils in their cells or hyphae. The microbial isolates from such soils included *Streptomyces* species that have been known for their synthesis of a vast array of antibiotics (tetracycline, amphotericin B, chloramphenicol, erythromycin, neomycin, nystatin, streptomycin and others), many of which are useful in medicine and biological research (Prescott *et al*., 2005).

Ecological parameters of the soil samples are also shown in Table 1. The percentage moisture content showed variations with sites. Site 1 had the lowest value of 1.75% while sites 2 and 3 had values of 8.40% and 6.50% respectively. The waste motor oil pollution could have impacted water-proof feature to the soil, sealing off the soil pores and thereby limiting water entry into the soil.

Site 1 soil was found to be alkaline with a pH value of 8.45.The pH values of sites 2 and 3 were found to be 5.29 and 6.22 respectively. The pH values recorded were within the range that could support microbial growth in pure cultures. Drastic variations in pH values have been reported to be harmful to microorganisms as that could disrupt the plasma membrane protein transport (Prescott *et al*., 2005).

The sensitivity tests as shown in Figures 1a and 1b reveals that there were inhibitions of the metabolites on the pathogenic microrganisms. Two of the actinomycete isolates, *S. griseus* and *S.*rochei were found to have both antibacterial and antifungal activities. The metabolites inhibited both the gram negative bacteria, *E. coli* and *P. aeruginosa* and gram positive bacteria, *S. aureus* and *B. subtilis*. The results suggest that the metabolites could be antibiotics and that they have broad spectrum actions.

The metabolite of one of the isolates, *B. licheniformis* was found to inhibit the growth of *S. aureus*, a gram positive pathogen. This indicates that the metabolite could have a narrow spectrum range of activity. Pommerville (2001) reported that Bacitracin, a product of *Bacillus.* sp is effective against *S. aureus*.

The experimental pathogen, *P. aeruginosa*, was found to inhibit one of the fungal isolates *A. corymbifera* . Paul Vuillemin cited by Pommerville (2001) reported on the extraction of a substance called hemipyocyanin from *P. aeruginosa* which inhibited the growth of pathogenic fungi. Further work is needed to find out whether the substance that inhibited the *A. corymbifera* has any relationship to hemipyocyanin. It can be deduced that the hemipyocyanin could be responsible for the antifungal activity. *Aspergillus* species have been implicated in fungal infections of humans generally known as zygomycosis.

Some of the fungal isolates, *Penicillium* species and *P. variotii* were found to inhibit *A. niger* and *C. albicans* .The discovery of *P. notatum* brought about a historic breakthrough in the development of

antibiotics in 1928. It is likely that the substances produced by the *Penicillium* species and *P. variotii* which were responsible for the inhibition could be antibiotics.

**TABLE 1**: **Species of Microorganisms Isolated from the Experimental Soil samples.**

| MICROBIAL ISOLATES | 1 | 2 | 3 | Total |
|---|---|---|---|---|
| ACTINOMYCETES | | | | |
| *Actinomyces sp* | + | + | + | 3 |
| *Streptomyces rochei* | + | - | + | 2 |
| *S. griseus* | + | + | + | 3 |
| BACTERIA | | | | |
| *Bacillus licheniformis* | + | + | + | 3 |
| *Lactobacillus sp* | + | + | + | 3 |
| *Micrococcus sp* | + | + | - | 2 |
| *Pseudomonas aeruginosa* | + | + | + | 3 |
| *Staphylococcus aureus* | + | - | - | 1 |
| FUNGI | | | | |
| *Absidia corymbifera* (Cohn) Sacc & Trotter | + | + | + | 3 |
| *A. ramosa* (Lindt) Lendner | + | + | - | 2 |
| *Acremonium butyri* (V.Beyma)wigams | - | + | + | 2 |
| *Aspergillus flavus* Link | + | + | + | 3 |
| *A. fumigatus* Fres | + | + | + | 3 |
| *A. niger* Van tieghem | + | + | + | 3 |
| *A. ochraceus* Wilhelm | - | + | - | 1 |
| *A. terreus* Thom | - | - | + | 1 |
| *Alternaria alternata* Kiessler | + | + | + | 3 |
| *Curvularia sp* | + | + | + | 3 |
| *Fusarium sp* | + | + | + | 3 |
| *Humicola grisea var.thermoidea* Cooney & Emerson | - | + | - | 1 |
| *Thermomyces lanuginosus* Tsiklinski | + | + | + | 3 |
| *Penicillum sp* | + | + | + | 3 |
| *Torula thermophila* Cooney & Emerson | + | + | + | 3 |
| *Mucor pusillus* (Lindt) Schipper | + | + | - | 2 |
| *Paecilomyces variotii* Bain | - | + | - | 1 |
| *Papulospora sp* | - | + | + | 2 |
| YEAST | | | | |
| *Candida Krusei* | + | + | + | 3 |
| *Saccharomyces cerevisiae* | + | + | + | 3 |
| TOTAL 28 | 22 | 25 | 21 | 68 |
| pH | 8.45 | 5.29 | 6.22 | |
| %Moisture content | 1.75 | 8.40 | 6.50 | |
| Soil colour | Black | Brown | Dark brown | |
| Soil texture | Very coarse | Fine sand | Medium sand | |

**+ Present –Absent
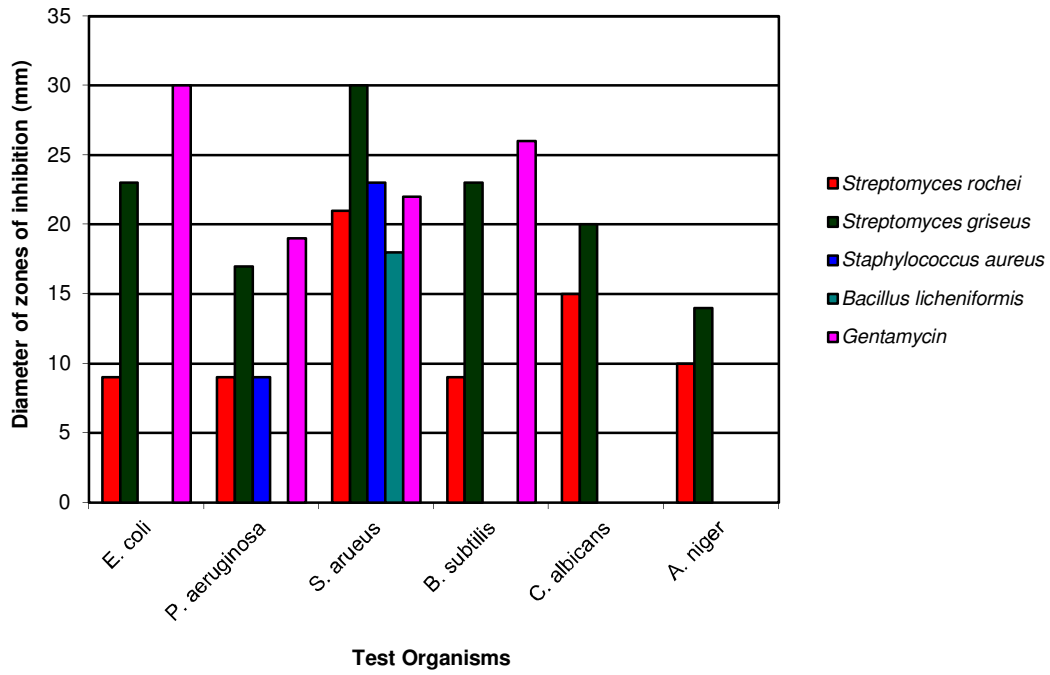
**FIGURE 1a. The effects of the metabolites of the bacterial and actinomycetes isolates on the pathogenic microorganisms.**
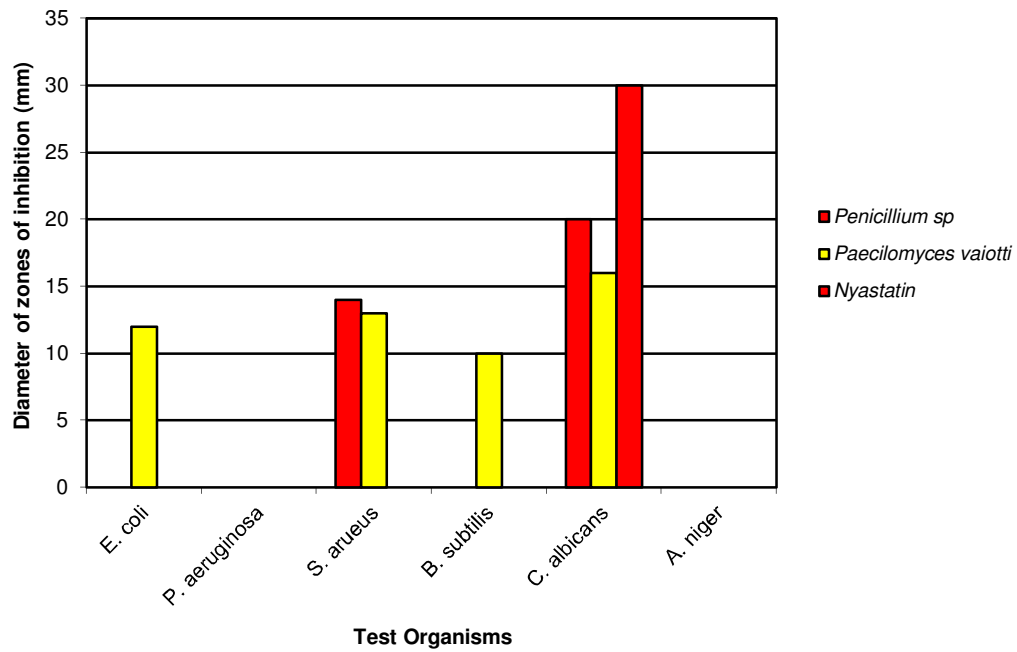


**FIGURE 1b.The effects of the test fungal metabolites on the pathogenic microorganisms.**

**CONCLUSION**

It is most likely that the various metabolites produced by the experimental microbial isolates which inhibited the test pathogenic microorganisms could be antibiotics. Work is going on to determine the constitution of the said microbial metabolites. The ability of the microbial isolates to resist waste oil pollution is also suggestive that they could play a major role in the bioremediation of crude oil spill which is a major environmental problem in Nigeria.

**ACKNOWLEDGEMENT**

**REFERENCES**

Bradshaw, L. J.1992. *Laboratory Microbiology*. Harcourt Barce, Javanorich College of  Publication. p139-193

Cowan, S.T. and K.J. Steel. 1965. *Manual for the Identification of Medical Bacteria* Cambridge. University Press. 217pp.

Domsch, K.H. and W. Gams. 1972. *Fungi In Agricultural Soils*. Publ. Longman Group Ltd. 290pp.

El-banna, N., and G. Winkelmann. 1998. Pyrrolnitrin  from *Burkholderia cepacia:* antibiotic activity against fungi and novel activities against *Streptomyces* sp. *J. Appl. Microbial.*  85:69-76.

Irobi, O.N., M. Mon-Young., and W.A. Anderson.1996. Antimicrobial activity of Annatto (*Bixa orellana*) extract. *Int. J. Pharm*. 34: 87-90.

Jensen, M.J., and N.D.Wright. 1997. *Chemotherapeutic agent: Microbiology for the health Sciences.* Publ. Prentice Hall New York p382-389.

Levy, S.B.1998.The challenge of Antibiotic Resistance.*Sci.Am*.398:451-456.

Mah, F.S. 2003. New Antibiotics For Bacterial Infections. *Ophthalmology Clinicals*. *North  America* (6): 11- 20.

Michalcewicz ,W. 1995. The influence of diesel fuel oil on the number of bacteria, fungi, actinomycetes and soil microbial biomass. *RoczPanstw Zakl Hig*. 46: 91-97.

Ogbonna, C.I.C. and G.J.F. Pugh.1982. Nigerian Soil Fungi. *Nova Hedwigia* 36:795-808.

Okonkwoeje, A.I. 2000. The Effect Of Different Soil Samples In The Remediation Of Crude Oil Polluted Nigerian Agricultural Soil. *M.Sc Dissertation University of  Jos*.

Omemu, A.M., M.O. Edema, A.O. Atayese  and A.O.Obadina. 2006. A Survey Of  The Microflora Of *Hibiscus sabdariffa* L. And The Resulting 'Zobo' Juice. *African Journal of  Biotechnology* 5(3): 254-259.

Pelczar,M. J., E.C.S.Chan, and N.R. Krieg. 1986. *Microbiology*. 5th Edition  Publ. McGraw hill Company Ltd N Y, St. Louis Sanfrancisco p543-546.

Pommerville, J.C. 2001. *Alcomo's  Fundamentals of  Microbiology*. 7th Edition Publ. Jones and Barltet publishers' lnc p 884 – 895.

Prescott, L.M., J.P. Harley, and D.A. Klein. 2005. *Microbiology* 6th Edition. Publ. McGraw Hill companies p646-792.

Raja, A., P. Prabakaran and P. Gajalakshmi. 2010. Isolation and Screening of Antibiotic Producing Psychrophilic Actinomycetes and its nature from Rothang Hill Soil Against Viridans *Streptomyces* sp. *Research Journal of Microbiology* 5(1):44-49.

Von Arx, J.A.1974. *The Genera of Fungi Sporulating In Pure Culture.* Publ. J. Grammar  In der A.R. Gantner Verlag kommanditgesellschaft. 315pp.

# CHARACTERIZATION OF MICROBIAL COMMUNITIES OF CORROSION PRODUCTS FROM SOUR AND SWEET CRUDE OIL

*Faisal M. AlAbbas*[a], Charles Williamson[b], John R. Spear[b], David L Olson[c], Brajendra Mishra[c] and Anthony Kakpovbia[a]

[a] Inspection Department, Saudi Aramco, Dhahran, Saudi Arabia, 31311
[b] Department of Civil and Environmental Engineering
[c] Department of Metallurgical and Materials Engineering
Colorado School of Mines, Golden, Colorado, USA, 80401

**ABSTRACT:** Hydrocarbon transporting pipeline networks are subject to different corrosion deterioration mechanisms, one of which is microbiologically influenced corrosion (MIC). Around 40% of the internal pipeline corrosion in the oil and gas industry has been attributed to MIC. To gain insight into the impact of microbes on corrosion in oil pipelines, the microbial diversity of samples collected from a sour oil pipeline and a sweet oil pipeline were evaluated. As cultivation-based methodologies can greatly underestimate the microbial diversity associated with an environment, the microbial diversity of sweet and sour oil pipeline samples was evaluated with a 16S rRNA gene pyrosequencing approach. The sequence results indicate that the microbial communities in the corrosion products obtained from both the sour oil pipeline and the sweet oil pipeline were dominated by bacteria; though archaeal sequences (predominately *Methanobacteriales*) were also identified in each sample. For the sour sample, the dominant phylotypes include *Synergistales* and *Thermoanaerobacterales*; while for the sweet sample, the dominant phylotypes include *Halothiobacillaceae*. This paper presents the microbial diversity and potential contribution to MIC for both samples.

## INTRODUCTION

Corrosion is a significant problem in oil and gas industry pipeline networks. In 2001, the estimated annual cost of corrosion to the oil and gas industries was $13.4 billion, of which approximately $2 billion was related to microbiologically influenced corrosion (MIC) ((Javaherdashti, 2008). The enhancement of chemical and electrochemical processes by microorganisms is known by MIC (Javaherdashti, 2008). There are many different types of microbes that cause metal deterioration. Among them are sulfate reducing bacteria (SRB), iron and $CO_2$ reducing bacteria, and iron and manganese oxidizing bacteria (Little et al., 2007). MIC often results from synergistic interactions of metabolisms of different microorganisms that coexist in the pipelines. Therefore, it is important to design and select the proper mitigation measures to control the corrosion. These measures could be reactive by treating existing MIC damages or proactive by preventing MIC in the first place. MIC could be treated by different techniques that include mechanical (i.e pigging), chemical (i.e biocides), electrochemical (i.e cathodic protection) and biological (i.e. microbial injection). Identifying the kind of micrograms present in the pipeline is a crucial step towards obtaining efficient and cost-effective mitigation programs (Javaherdashti, 2008). Traditionally, culture-based techniques have been used to investigate the microbial communities in pipelines; however this method reflects only up to 15 % of the true populations in the pipelines and underestimates the biocomplexity of microbial communities (Javaherdashti, 2008). It has been known that biodiversity in most ecosystems is dominated by uncultured microbes (Whitby et al., 2011). These limitations of culture-based methods have increased the application of molecular microbiological methods (MMM) by targeting specific genes and/or proteins. The development of sequencing technologies over the past decade has greatly increased the sequencing output compared to Sanger sequencing.

This study is part of ongoing, comprehensive research that applies molecular techniques to investigate the microbial communities associated with corrosion products collected from sour and sweet crude pipelines. The 454 Pyrosequencing technology was used to characterize the microbial communities present in these systems. This data will provide a better understanding of the microbial communities associated with corrosion in these environments and may contribute to new and improved ways to detect, monitor, study and control MIC in crude oil pipeline systems.

## MATERIALS AND METHODS

**Sample collection and characterization.** Water samples were collected from vertical outlets of sour and sweet crude pipelines as outlined by NACE standard TM0194 (2004). Immediately upon collection the samples were filtered via sterilized 0.2 μm pore size membranes and stored in sterilized glass containers for microbial evaluations. Part of the filtered solids were analyzed in the laboratory using Field Emission Environmental Scanning Electron Microscopy coupled Energy Dispersive X-ray Spectroscopy (FESEM/EDS) to investigate their morphology and the chemical composition.

**Identification of the microorganism community.** DNA was extracted using the MoBio Powersoil DNA extraction kit (MoBio, Carlsbad, CA); the 10-minute vortexing step was replaced by one minute of bead beating. DNA was prepared for sequencing as described by Osburn et al., 2011 with some exceptions: qPCR reactions were performed in duplicate and pooled prior to normalization for sequencing. Each qPCR reaction contained 5 uL of template DNA. Primers incorporated adaptor sequences for pyrosequencing on the GSFLX Titanium platform of the Roche 454 Pyrosequencing technology. Amplicons for each sample were normalized for sequencing with the SequalPrep Normalization Plate Kit (Invitrogen) and pooled amplicons were gel purified with the EZNA Gel Extraction Kit (Omega BioTek). Sequencing was completed on the Roche 454 Titanium platform. Sequence analysis was carried out using scripts available in the QIIME software package (Caporaso et al., 2010). Initial quality filtering of the sequences was conducted in accordance with findings identified by Huse et al. (2007). Sequences with errors in barcodes or primers, homopolymer runs longer than 6 nt, ambiguous base calls, or average quality scores less than 25 were removed from the data. Sequences shorter than 400 nt or longer than 500 nt were also discarded. Sequences were denoised with DeNoiser version 1.4.0 (Reeder et al., 2010). Chimeras were identified by ChimeraSlayer (Haas et al., 2011) and removed. Taxonomic classifications of sequences from each sample were assigned using QIIME's wrappers for the RDP classifier (Wang et al., 2007; Cole et al., 2009) and the Greengenes taxonomy (http://greengenes.lbl.gov/).

## RESULTS AND DISCUSSION

**Corrosion products characterizations.** The morphology observations and the EDS elemental analysis of the corrosion products collected from sour and sweet pipeline are shown in Figure 1 A & B respectively. The morphology of corrosion products for both systems showed significant differences in appearance, structure and composition (Figure 1 A & B. For the sour crude corrosion products (Figure 1A) there is evidence of thick precipitations with impeded rectangular and cylindrical crystals. The average width of the rectangular platelets was less than 1.5 µm. The EDS line analysis shown in Figure 1C reveals that the composition of the corrosion products are dominated by carbon, oxygen, sulfur, iron, chloride and sodium. This elemental analysis suggests that the corrosion products are composed of different iron oxides, iron sulfide, salts and organic compounds. In a sour crude oil environment (sulfur levels larger than 0.5 %) many types of iron sulfides may form. These iron sulfides have different structural types such as mackinawite ($Fe_{1+x}S$), pyrrhotite ($FeS_{1+x}$) and greigite ($Fe_3S_4$) (Singer et al., 2011). Among those iron sulfides, mackinawite is the predominant type that forms on the pipeline surface and usually is a precursor to other types of iron sulfides (Singer et al., 2011). In the aqueous environment enriched with hydrogen sulfide ($H_2S$), the corrosion proceeds initially by a very fast, direct, heterogeneous reaction at the steel surface forming a solid, adherent mackinawite layer (Singer et al., 2011). For the sweet crude corrosion

products, Figure 1B, there is evidence of a thick, homogenous layer of corrosion products. The EDS line analysis shown in Figure 1D shows the composition of the corrosion products are dominated by carbon, sulfur, iron, chloride and sodium. The level of sulfur for the sweet crude corrosion (Figure 1D) is lower than that for sour crude corrosion products (Figure 1C). This difference is due to the fact that sweet crude contains lower sulfur levels (less than 5%) than sour crude oil (Singer et al., 2011). The compositional difference between the two types of oil result in these significant differences in appearance, structure and composition of the corrosion products collected from both systems.
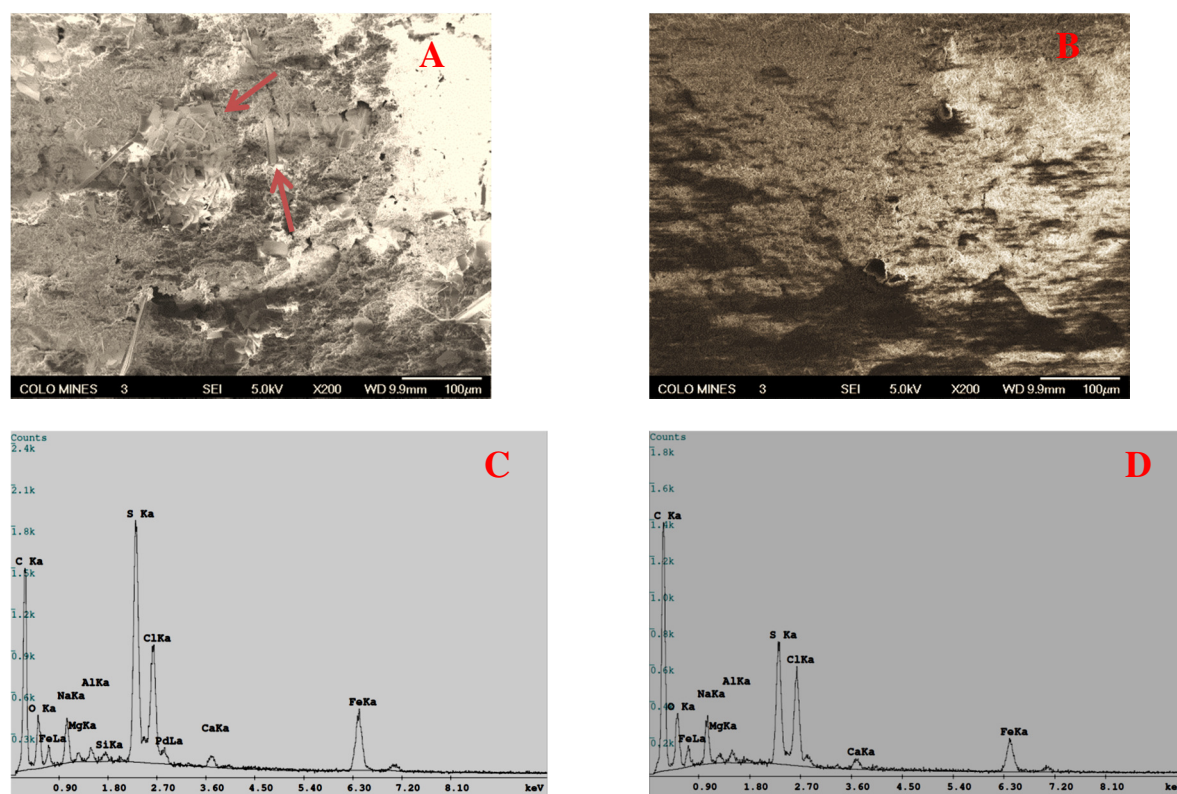


**FIGURE1**: FESEM and EDS analysis for the collected corrosion products from sour and sweet crude oil pipelines. (A) FESEM Image of corrosion products from sour crude oil pipeline, at 200X. Arrows point to rectangular and cylindrical crystals. (B) FESEM Image of corrosion products from sweet crude oil pipeline, at 200X. (C) EDS line analysis corresponding to the FESEM image shown in Fig. 1A. (D) EDS line analysis corresponding to the FESEM image shown in Fig. 1B.

**Microbial community characterizations.** The microbial diversity present in the corrosion products collected from sour and sweet crude oil pipeline was evaluated with a 16S rRNA gene pyrosequencing. Approximately 5700 sequences were obtained (~2300 sequences from the sour corrosion sample and ~3400 from the sweet corrosion sample). The composition of the microbial communities for each sample is shown in Figure 2A and B respectively.

As shown in Figure 2, the pyrosequencing results indicate that the microbial communities in the corrosion products obtained from both sour and sweet oil pipeline samples were dominated by Bacteria; though archaeal sequences (predominately *Methanobacteriales*) were also identified in each sample. There is a significant difference in the composition of the bacterial population associated with these samples. For the sour sample, Figure 2A, the dominant bacterial phylotypes include Thermoanaerobacterales (36.1%), Synergistales (28%) and Syntrophobacterales (11.8%), while for the sweet sample; Figure 2B, the dominant bacterial phylotypes include Halothiobacillaceae (82.3%),

Desulfovibrionales (6.23%) and Syntrophobacterales (3.58%). Interestingly, both samples share the presence of similar bacterial phylotypes that include Syntrophobacterales, Desulfovibrionales, and Thermotogales.
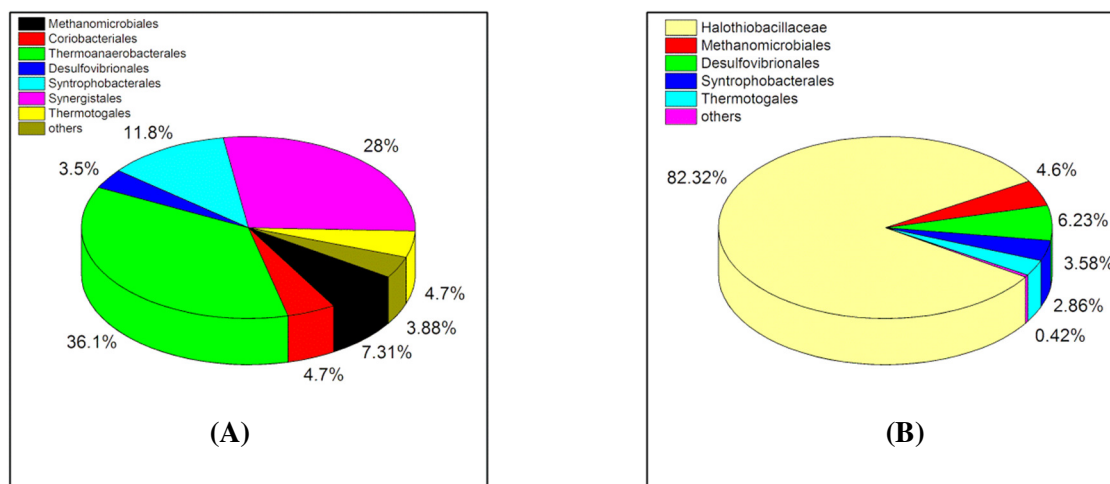


**FIGURE2**: Microbial community composition for samples as determined by 16S rRNA gene pyrosequencing: (A) the sour crude filter (B) sweet crude filter.

*Methanobacteriales* are methanogenic Archaea. This type of microbe has been identified in different oil and gas systems. Reports have identified *Methanobacteriales* in slug samples collected from gas pipelines and crude pipelines (Xiang et al., 2003). *Methanobacteriales* are capable of metabolizing hydrogen ($H_2$), carbon dioxide ($CO_2$), acetate, methylamines, and dimethylsulfides to produce methane gas ($CH_4$) (Madigan et al., 2009). They are capable of accelerating corrosion by cathodic polarization, which involved the removal of hydrogen protons from a steel surface resulting in increased anodic metal dissolution (Xiang et al., 2003). Daniels and colleagues (1987) demonstrated that methanogens can utilize iron ($Fe^0$) as an electron donor in the presence of low levels of $H_2$ and abundant of $CO_2$. This observation implies that *Methanobacteriales* could contribute significantly to MIC in anaerobic areas such as oil pipeline systems. More holistic investigations regarding the abundance, diversity and subsequent corrosive effects of methanogens in oil pipelines are needed to provide a better understanding of their role in pipeline system deterioration.

*Thermoanaerobacterales* are thermophilic, heterotrophic microbes grouped within the *Firmicutes*. They are anaerobic and exist in soil, volcanic hot springs, hydrothermal vents and oil-producing wells (Madigan et al., 2009). *Thermoanaerobacterales* have the ability to form spores under high temperature. They grow in a temperature range between 42°C and 80°C and are able to convert sugars to acetate, lactate, ethanol, $H_2$, and $CO_2$. These microbes may also reduce thiosulfate to sulfide (Fardeau et al., 1993). The production of sulfide and subsequent hydrogen sulfide will enhance biocorrosion in the pipeline systems (Fardeau et al., 1993).

*Synergistales* are Gram-negative anaerobes that are widely distributed in nature; however, they are normally only a minor constituent of the bacterial community in many environments (Vartoukian et al., 2007). *Synergistales* were reported among the communities of hot Alaskan oilfields (Vartoukian et al., 2007). Many microbes grouping within the *Synergistales* are mesophilic while some are moderately thermophilic growing at optimum temperatures of 55°C–65°C. Commonly, these microbes are fermentative acetogenic and are able to degrade amino acids (Vartoukian et al., 2007). To the researcher's best knowledge, there are no studies related to their effects on MIC.

*Syntrophobacterales* and *Desulfovibrionales* are members of the *Deltaproteobacteria*. Most species are mesophilic, with some are moderate thermophiles (Madigan et al., 2009). The members of these two orders are strictly anaerobic and sulfate-reducing. The types of microbes are commonly referred

to as sulfate reducing bacteria (SRB). SRB use sulfate ions as a terminal electron acceptor and produce sulfide. Furthermore, SRB have the ability to reduce nitrate and thiosulfate. They can manage to stay alive in an aerobic environment until the environment becomes suitably anaerobic for them to grow. SRB obtain energy from organic nutrients, such as lactate. They grow in a pH range from 4 to 9.5 and tolerate pressure up to 500 atmospheres. Most SRB exist in temperature ranges of 25-60°C (Javaherdashti, 2008). SRB can be found everywhere in oil and gas production facilities, from the well to the treatment facilities. SRB are considered the main contributor to biocorrosion. Interestingly both orders of SRB are found in the sweet and sour corrosion filters. There are different ways that SRB and the resulting biofilm produce MIC damage in the pipeline. According to the classical theory, SRB consume the cathodic hydrogen by a class of enzymes known as hydrogenases to obtain the electrons required for metabolic activities. Therefore, the removal of hydrogen from the metal surface will catalyze the activation of hydrogen and in turn will force the iron to dissolve at the anode (Little et al., 2007). Moreover, the galvanic coupling between iron/iron sulfides will further enhance corrosion. Iron sulfide will act as a cathode and absorb the molecular hydrogen, and the area beneath will be the anode site (Javaherdashti, 2008).

The predominant bacterial type found in the sweet corrosion sample is *Halothiobacillaceae*, which are aerobic members of the *Gammaproteobacteria* (Madigan et al., 2009). These microbes live in environments with high concentrations of salt and have the ability to produce sulfuric acid by oxidizing elemental sulfur, thiosulfates, metal sulfate and $H_2S$. These microbes may be referred to as sulfur oxidizing bacteria (SOB). Commonly, SOB and SRB coexist together in many environments. When the pH is low, the SOB are suspected to dominate. The role of SOB in biocorrosion has been reported in different investigations (Javaherdashti, 2008). The excreted sulfuric acids by SOB promote biocorrosion by enhancing the oxidation of different metals and preventing the formation of protective oxides (Little et al., 2007).

Both sour and sweet crude oil corrosion product samples contain *Thermotogales*. *Thermotogales* are mostly thermophilic and hyperthermophilic bacteria capable of growing at temperatures as high as 90°C. Their cells are surrounded by characteristic sheath structures, or "toga" (Madigan et al., 2009). Thermophilic isolates are becoming an exciting subject for many investigations in the oil industry because most oil reservoirs occur at depths where the temperature is extremely high (Ravot et al., 1995). *Thermotogales* were isolated from different oil fields in the Gulf of Mexico and the Troll oil formation in the North Sea (Ravot et al., 1995). They are anaerobic, fermentative chemoorganotrophs capable of metabolizing organic substrates such as hydrocarbon to produce lactate, acetate, $CO_2$ and $H_2$ (Ravot et al., 1995). They are also able to grow by using $H_2$ as an electron donor and ferric iron ($Fe^{3+}$) as an electron acceptor (Madigan et al., 2009). Some *Thermotogales* such *Thermotoga elfii sp.* can utilize thiosulfate as an electron acceptor and produce $H_2S$ (Ravot et al., 1995). The *Thermotogales* metabolic by-products (acetate, H2 and $H_2S$) have the potential to contribute to biocorrosion in oil fields (Ravot et al., 1995).

**CONCLUSIONS**

In this study the microbial communities in corrosion products collected from different pipelines was investigated. The study shows that oil fields represent a novel environment with respect to their physicochemical conditions, and diverse microbial communities exist in these systems. Synergistic interactions through co-operative microbial metabolisms may result in biocorrosion in oil pipelines. The role of some of microbes identified in this research, such as *Syntrophobacterales*, *Desulfovibrionales* and *Halothiobacillaceae* are well established in the oil industry; however, more research is required to address the role of other microorganisms identified in the oil pipeline samples (i.e. *Methanobacteriales*, *Synergistales* and *Thermotogales*) in biocorrosion processes.

**ACKNOWLEDGEMENTS**

**REFERENCES**

Cole, J. R., Q. Wang, E. Cardenas, J. Fish, B. Chai, R. J. Farris and A. S. Kulam-Syed-Mohideen. 2009. "The Ribosomal Database Project: Improved Alignments and New Tools for rRNA Analysis." Nucleic Acids Research 37 (Database) (January 1): D141–D145.

Caporaso, J. Gregory, J. Kuczynski, J. Stombaugh, K. Bittinger, F. D. Bushman, E. K. Costello and N. Fierer. 2010. "QIIME Allows Analysis of High-throughput Community Sequencing Data." *Nature Methods* 7(5):335–336.

Daniels, L., N. Belay, B. S. Rajagopal and P. J. Weimer. 1987. "Bacterial Methanogenesis and Growth From $CO_2$ With Elemental Iron as The Sole Source of Electrons", *Science*, 237:509-511.

Haas, J. Brian, D. Gevers, A. M. Earl, M. Feldgarden, D. V. Ward, G. Giannoukos and D. Ciulla. 2011. "Chimeric 16S rRNA Sequence Formation and Detection in Sanger and 454-Pyrosequenced PCR Amplicons." *Genome Research* 21(3): 494–504.

Huse, Susan, J. Huber, H. Morrison, M. Sogin and D. Welch. 2007. "Accuracy and Quality of Massively Parallel DNA Pyrosequencing." *Genome Biology* 8(7): R143.

Javaherdashti, R. 2008. *Microbiologically Influenced Corrosion- An Engineering Insight.* Springer-Verlag. London, UK, pp: 29–66 and pp: 133–155.

Little, B.J. and J.S. Lee. 2007. *Microbiologically Influenced Corrosion*. John Wiley & Sons Inc., Hoboken, NJ, USA; pp: 1–50.

Madigan, M. 2009. *Brock Biology of Microorganisms.* 12th ed., Pearson Benjamin Cummings, San Francisco, USA, Chapter 15–17.

NACE Standard (TM0194). 2004. "Field Monitoring of Bacterial Growth in Oil and Gas Systems" published by NACE, Houston, Texas.

Osburn, R. Magdalena, L. A. Sessions, C. Pepe-Ranney, and J. R. Spear. 2011. "Hydrogen-isotopic Variability in Fatty Acids from Yellowstone National Park Hot Spring Microbial Communities". *Geochimica Et Cosmochimica Acta* 75 (17): 4830–4845.

Ravot, g., M. Magot, M. Fardeau, B. K. Patel, G. Prensier, A. Egan, J. Garcia, and B. Ollivier. 1995. "*Thennotoga- elfii sp. nov.*, a Novel Thermophilic Bacterium from an African Oil-Producing Well" *Intern. J. of Systematic Bacteriology.* 45(21):308–314.

Reeder, Jens, and R. Knight. 2010. "Rapid Denoising of Pyrosequencing Amplicon Data: Exploiting the Rank-abundance Distribution" *Nature Methods.* 7(9):668–669.

Singer, M, B. Brown, A. Camancho and S. Nesic. 2011. "Combined Effect of Carbon Dioxide, Hydrogen Sulfide, and Acetic Acid on Bottom-of-the-Line Corrosion" *Corrosion* (015004):1–16.

Vartoukian, S. R., R. M. Palmer, W. G. Wade.2007. "The division ''*Synergistes*''. *Anaerobe*. 13: 99–106

Whitby, C. and T. L. Skovhus. 2009. *Proceedings from the International Symposium on Applied Microbiology and Molecular Biology in Oil Systems.* (ISMOS-2), 1st Ed., Springer, London, New York, USA. pp.63–76.

Wang, Qiong, G. M. Garrity, J. M. Tiedje, and J. R. Cole. 2007. "Naïve Bayesian Classifier for Rapid Assignment of rRNA Sequences into the New Bacterial Taxonomy" *Applied and Environmental Microbiology,* 73 (16): 5261–5267.

Xiang Y. Z., J. Lubeck, and J.J. Kilbane. 2007. "Characterization of Microbial Communities in Gas Industry Pipelines" *Applied & Environmental Microbiology*, 69(9):5354–5363.

# IRON REDUCING BACTERIA INFLUENCE ON THE CORROSION OF API 5LX52 LINEPIPE STEEL

*Faisal M. AlAbbas[a]*, Charles Williamson[b], John R. Spear[b], David L Olson[c], Brajendra Mishra[c] and Anthony Kakpovbia[1]

[a] Inspection Department, Saudi Aramco, Dhahran, Saudi Arabia, 31311
[b] Department of Civil and Environmental Engineering
[c] Department of Metallurgical and Materials Engineering
Colorado School of Mines, Golden, Colorado, USA, 80401

**ABSTRACT:** Microbiologically influenced corrosion (MIC) by microbes capable of iron reduction (iron reducing bacteria (IRB)) on API 5L grade X52 carbon steel coupons was investigated. IRB were isolated and cultivated from a water sample collected from a sour oil well located in Louisiana, USA. 16S rRNA gene sequence analysis indicated that the mixed bacterial consortium contained two phylotypes: members of the *Proteobacteria* (*Shewanella oneidensis sp.*) and *Firmicutes* (*Brevibacillus sp.*). The corrosion behavior of carbon steel coupons exposed to different media, with and without these microbes, was characterized by electrochemical impedance spectroscopy (EIS) and polarization resistance (Rp). The biofilm and pit morphology that developed with time were characterized by using field emission scanning electron microscopy (FESEM). Interestingly, IRB metabolic reactions and resulting biofilms inhibit the corrosion process. The maximum corrosion rate in the biotic system was 2 mpy while it was 20 mpy in the abiotic solution. Localized isolated pits were revealed in the biotic solution whereas extensive general pitting was found in the abiotic solution. Corrosion products were characterized by energy-dispersive X-ray spectroscopy (EDS). EDS identified the presence of carbon, iron, oxygen and salt, which were attributed to the formation of different iron oxides as well as deposited salt and organic compounds on the steel surface.

## INTRODUCTION

Microorganisms that are present in oil reservoirs are able to induce localized changes in the aqueous environment (e.g., alter the concentration of the electrolyte components pH and oxygen concentration) leading to localized corrosion known as microbiologically influenced corrosion (MIC). Microbial activities are responsible for approximately 20% of the total corrosion cost in the oil and gas industry, of which a significant part is due to anaerobic corrosion influenced by sulfate reducing bacteria (SRB) and aerobic corrosion influenced by iron-reducing and oxidizing bacteria (IRB/IOB) (Little et al., 2007). The metabolic by-products of these microorganisms found in biofilms on steel surfaces affect the kinetics of cathodic and/or anodic reactions. Moreover, these metabolic activities can considerably modify the chemistry of any protective layers, leading to either acceleration or inhibition of localized corrosion (Little et al., 2007).

The objective of this study is to investigate the impact of environmental aerobic bacteria (cultivated from oil field samples rather than obtained from a culture collection) on the corrosion behavior of low alloy high strength (API 5L X80) linepipe steel. The IRB consortium used in this study was cultivated from a sour oil well in Louisiana, USA.

## MATERIALS AND METHODS

**Organisms and Testing Medium.** The IRB consortium used in this study was cultivated from water samples obtained from a sour oil well located in Louisiana, USA. The water samples were collected and bottled at the wellhead from an approximate depth of 2200 ft. as described by NACE Standard TM0194 (2004). For IRB isolation, one milliliter of the water sample was transferred to a 250 ml of Erlenmeyer flask containing 100 ml of LB broth medium. The LB medium was composed of tryptone (10 g), sodium chloride (10 g), and yeast extract (5.0 g) added to one liter of distilled water. The pH of the medium was adjusted to 7.2 using 5M sodium hydroxide and autoclaved for 20 min. The bacteria were incubated at 30 $^o$C in a rotory shaker at 150 rpm until turbid growth was observed.

**Identification of the iron-reducing consortium.** DNA was extracted from cultivars using the MoBio Powersoil DNA extraction kit. 16S rRNA gene amplification was carried out using the 'universal' polymerase chain reaction (PCR) primers 515F and 1391R. PCR, cloning and transformation were then carried out as described by Sahl et al. (2010). Unique restriction fragment length polymorphisms (RFLP) were sequenced on an ABI 3730 DNA sequencer at Davis Sequencing, Inc. (Davis, CA). Sanger reads were called with PHRED via Xplorseq (Frank 2008). Sequences were compared to the GenBank database via BLAST (http://blast.ncbi.nlm.nih.gov/Blast.cgi).

**Specimen preparation.** Steel coupons (10 mm x 10 mm x 5 mm) were cut from a 6-inch (12.5 mm) section of API-5L X52 carbon steel pipe with chemical composition (wt.%): 0.07C, 1.05Mn, 0.008S, 0.03Cr, 0.008P and 0.195Si. The coupons were embedded in a mold of non-conducting epoxy resin, leaving an exposed area of 100 mm$^2$. For electrical connection, a copper wire was soldered at the rear of the coupons. The coupons were polished with progressively finer sand paper to a final grit size of 600 microns. After polishing, the coupons were rinsed with distilled water, ultrasonically degreased in 100% acetone followed by 100% ethanol and sterilized by exposure to 100% ethanol for 24 hours.

**Electrochemical Tests and Surface analysis of the coupons exposed to IRB.** The electrochemical measurements and subsequent surface analysis were performed per the procedure described by Al-Abbas et al. (2011) in elsewhere.

**RESULTS AND DISCUSSION**

**Identification of the iron-reducing consortium.** 16S rRNA gene analysis indicated that the mixed bacterial culture consortium contained two phylotypes: members of the *Proteobacteria* (*Shewanella oneidensis sp.*) and *Firmicutes* (*Brevibacillus sp.*). *Shewanella oneidensis* are facultative anaerobic iron-reducing bacteria that are capable of diverse metabolisms. They are able to reduce ferric iron and sulfite, oxidize hydrogen gas, and produce sulfide. It has been reported that these bacteria might be involved in biocorrosion whereas some studies suggest that *Shewanella oneidensis* may have an inhibitory effect towards corrosion (Lutterbach et al., 2009). *Brevibacillus* are aerobic spore-forming microbes. They have the ability to degrade hydrocarbons and plastics. They were used to treat part of the Daqing oil field, in which the oil production increased by 165% for about 200 days (Youssef et al., 2009).

**Morphology and composition of interfacial surfaces.** The morphology observations of corrosion products of API X52 carbon steel exposed to sterilized control medium (abiotic) and inoculated medium (biotic) are shown in Figure 1 A and B respectively. For the abiotic system, there is one homogenous layer of corrosion product (Figure 1A) formed on the surface with some deposited salt crystals. Quantitative EDS analysis, spectra not shown here, revealed peaks for oxygen, iron, chloride sodium and carbon that accumulated from the growth medium. The EDS analysis suggests that the corrosion layer is composed of iron oxides mixed with sodium chlorides and organic compounds. There is significant difference in the characteristics of the layer that developed in the presence of the IRB microbial consortium (biotic) as shown in Figure 1B. The significant amount of products observed in the biotic

system is most likely due to the production of a biofilm matrix. Figure 1C displays higher magnifications of the biofilm structure that confirms bacterial attachment to the metal surface. In the case of the biotic condition, the EDS analysis revealed peaks for nitrogen and phosphorus in addition to oxygen, iron, chloride, sodium and carbon. The presence of the nitrogen and phosphorus may be due to the microbial production of extracellular polymer substance (EPS) (Shobhana et al., 2005).

IRB cells attached to the substrate produce EPS, which results in biofilm formation. The biofilm has a heterogeneous morphology and thickness as shown in Figure 1b. The rod-shaped bacteria occupied a small volume fraction as compared to the precipitated corrosion products and EPS. The EPS and corrosion products usually occupy 75-95 % of biofilm volume, while 5-25% is occupied by the cells (Castaneda and Benetton, 2008).
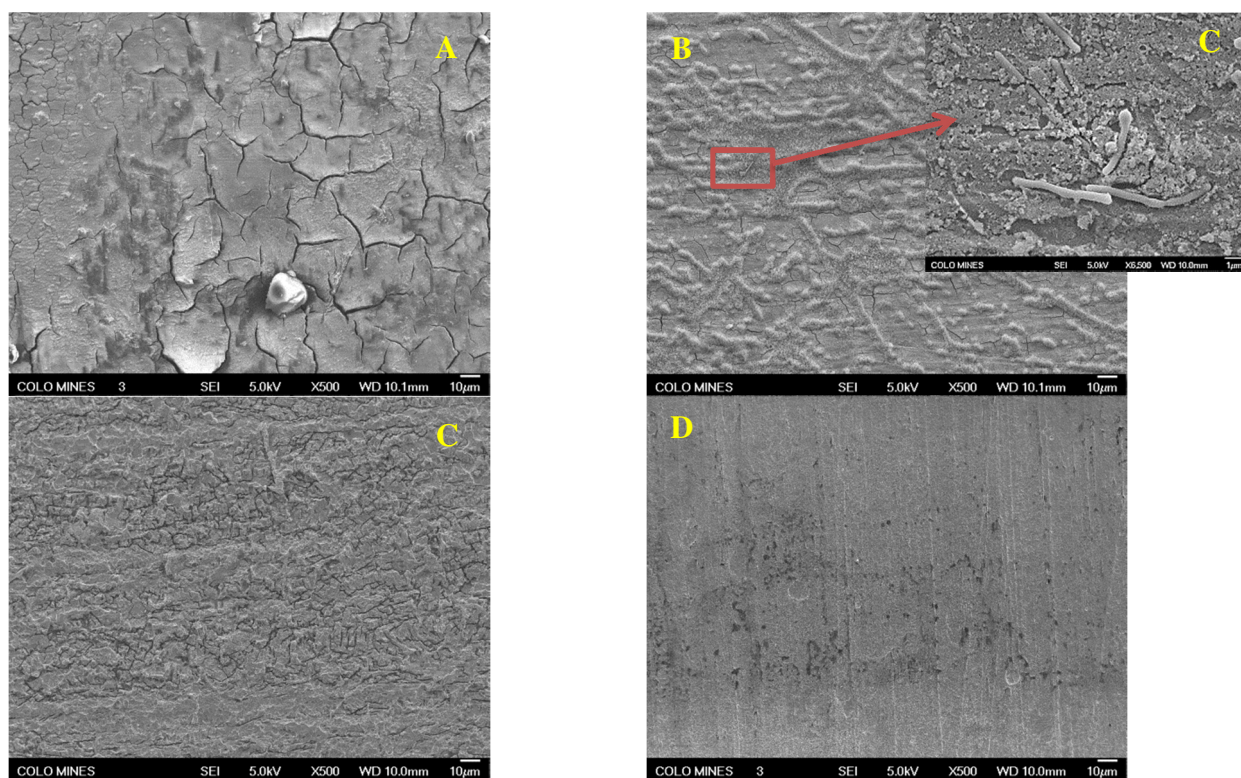


**FIGURE1**: FESEM for the API 5L X52 surface: (A) FESEM image of carbon steel exposed to sterile LB medium nutrients, at 500X. (B). FESEM Image of carbon steel exposed to LB medium inoculated with IRB at 500X. (C) Higher magnification (X6500.) of image (A) shows the bacteria cells. (D) Clean metallic surface removed from biotic system at 500X. (F) Clean metallic surface removed from biotic system.

The coupons immersed in the abiotic medium exhibit aggressive and elongated pitting (Figure 1C) in comparison with the biotic coupons that still show the polishing marks along with shallow pitting (Figure 1D). The protective effects of the biofilm in the case of biotic condition are attributed to the reduction of ferric ions to ferrous ions and increased consumption of oxygen by *Shewanella oneidensis sp* respiration. Dubiel et al. (2002) reported that *Shewanella oneidensis sp.* inhibit corrosion on stainless steel surfaces in a medium containing yeast extract and peptone. Interestingly, it has been proposed that *Shewanella oneidensis sp.* be used to control corrosion in pipeline systems. *Shewanella oneidensis sp.* may colonize the metal surface and consume oxygen molecules adjacent to the metal surface by aerobic respiration. As oxygen is depleted, the bacteria turn to $Fe^{3+}$ anaerobic respiration and produced $Fe^{2+}$ ions diffuse into the bulk fluid. In static environments, this process will create a chemical shield that reduces oxygen diffusion, which in turn, inhibits the cathodic reaction due to lower oxygen availability. By

electrochemical reaction $Fe^{2+}$ is oxidized to $Fe^{3+}$ and again reduced by bacterial respiration. Consequently, corrosion will be inhibited (Herrera and Videla, 2009).

**Polarization resistance/ Corrosion Rate.** The polarization resistance (Rp) variations for the biotic and abiotic systems are shown in Figure 2A. The LPR as a function of time data revealed that in the biotic medium a substantial increase of polarization resistance (Rp) to 7000 $\Omega.cm^2$ was followed by a decrease to 5000 $\Omega.cm^2$ at 100 hours, which then remained stable at approximately 6500 $\Omega.cm^2$ throughout the period of exposure. The polarization resistance is inversely proportional to the corrosion current, which means lower corrosion rate at higher Rp resistance. This trend confirms the corrosion inhibition effects induced by the activity of the bacterial consortium. On the other hand, in the abiotic medium, the Rp trend remained more or less steady at approximately 1500 $\Omega.cm^2$ over the entire period. When comparing the two Rp trends for the biotic and abiotic medium, the Rp values for the abiotic medium are significantly lower than those for the biotic medium. This observation suggests that the corrosion rate is substantially higher in the abiotic medium. The corrosion rate plots over time for the biotic and abiotic systems are shown in Figure 2B. The corrosion rate for the abiotic medium reached a maximum value of 20 mpy after 200 hours whereas the corrosion rate for the biotic system was around 2 mpy over the experimental period.
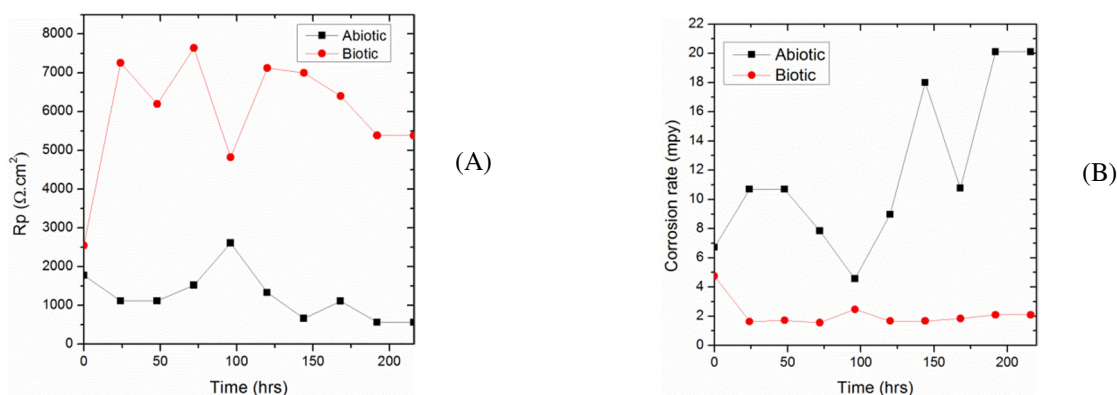


**FIGURE2** :(A) Polarization resistance (B) Corrosion rates variations for both biotic and abiotic media.

Both Rp and corrosion rate data confirm the corrosion inhibition properties of the bacterial consortium. This inhibition cannot be explained by a single mechanism (Videla and Herrera, 2009). It might be attributed to the oxygen depletion induced by bacterial respiration (Herrera and Videla, 2009). The change in oxygen concentration caused by microbial respiration can decrease the cathodic reaction rate by reducing the amount of reactants available for the cathodic reaction (Videla and Herrera, 2009). A similar inhibitory mechanism for steel in the presence of two marine isolates in saline media was reported by Pedersen and Hermansson (1991). It is also possible that the biofilm developed by the bacteria contributes to the low corrosion in the biotic medium. There have been a few reports of corrosion inhibition in the presence of biofilms (Little et al., 2007). Biofilms and attached cells may form a diffusion barrier hindering the reactants diffusion to and from the metal surface (Herrera and Videla, 2009).Another mechanism that might be responsible for the corrosion inhibition is related to the generation of a cathodic protection current by the bacterial consortium. It was reported that *Shewanella oneidensis sp.* produced electrically conductive pilus-like appendages called bacterial nanowires that can transfer electrons to the electrode. The capability of *Shewanella oneidensis sp.* to transfer electrons from organic sources to electrodes without intervening catalysts serves as the basis for electricity production in microbial fuel cells (Gorby et al., 2006). Moreover, *Brevibacillus sp.* have been investigated in microbial fuel cells for their capacity to generate electrons (Pham et al., 2008). Interestingly, previous studies show the capacity of *Brevibacillus sp.* to produce electricity increases in the presence of *Pseudomonas sp.* due to the metabolites produced by *Pseudomonas sp.*, which enable *Brevibacillus sp.* to achieve extracellular

electron transfer (Pham et al., 2008). Based on these facts, it is possible, that *Brevibacillus sp.* and *Shewanella oneidensis sp.,* through their complimentary metabolisms, produce cathodic currents that result in corrosion inhibition. The increase in corrosion rate noticed in the abiotic medium is possibly due to the effect of a formation of a mixed non-protective layer of sodium chloride, iron oxides and carbon-based compounds on the electrode surface (Castaneda and Benetton, 2008).

**Electrical Impedance Spectroscopy (EIS) results.** Figure 3A displays the Nyquist plots for the carbon steel coupon exposed to the abiotic medium over time. The steady state was reached at 120 hours. At low frequencies (LF), shown in Figure 3A, the magnitude of the capacitive loop represented by the semicircle diameter decreased with time. These LF magnitudes represent the change in charge transfer resistance (Rct) that describes the evolution of the anodic reaction that is controlled by charge transfer processes (Castaneda and Benetton, 2008). The decrease of Rct with time indicates an increase in corrosion rate, possibly due to the effect of a formation of a mixed layer of sodium chloride, sulfide, potassium and carbon-based compounds on the electrode surface. Moreover the presence of oxygen in the system enhances the cathodic reactions that drive the anodic dissolution of the metal (Castaneda and Benetton, 2008). The formation of a corrosion product layer was confirmed by the phase angle spectra (Figure 3B) that shows two time constants at 10 Hz and 0.1 Hz medium frequencies, as indicated by the arrows in Figure 3B.
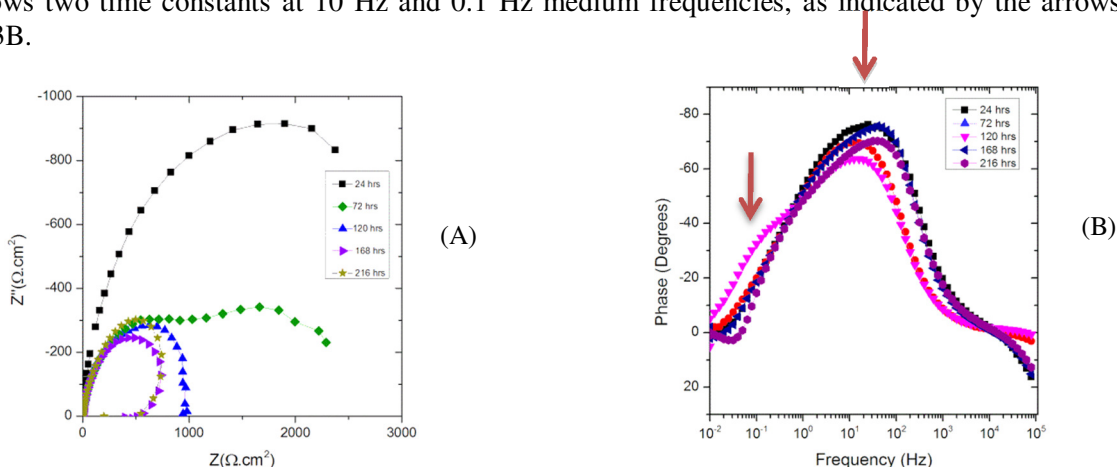


**FIGURE3**: EIS date for abiotic culture medium; (A) Nyquist Plots (B) Phase angle plots.

When the carbon steel was exposed to the inoculated culture medium (biotic), the EIS spectra varied significantly with exposure time as shown in Figure 4A. The low frequency (LF) magnitude, represented by the semicircle diameter, significantly increased with time indicating a decrease in corrosion rate and increase in charge transfer resistance (Rct) as supported by Figure 4A.
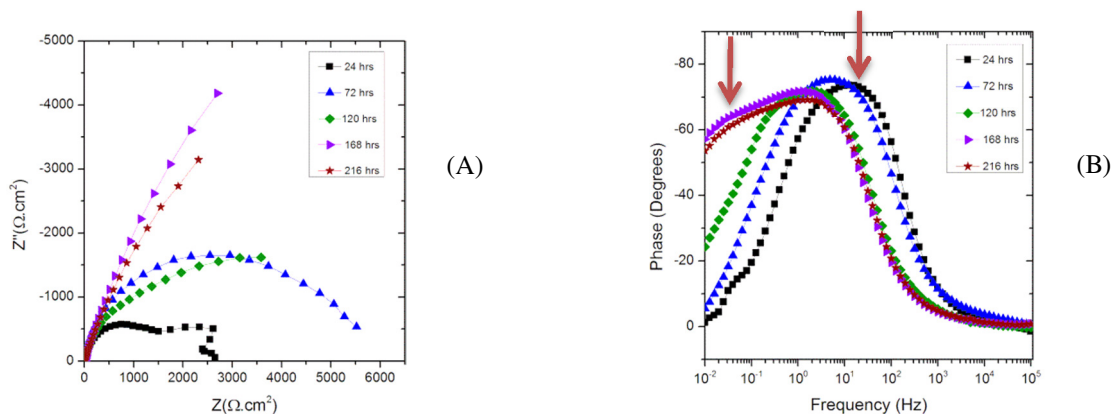


**FIGURE4**: EIS date for inoculated biotic medium; (a) Nyquist Plots (b) Phase angle plots.

For the first 72 hours, the medium frequency (10 Hz) response presented in the phase diagram in Figure 4A shows one time constant that indicates an activation control process. This behavior is attributed to the formation of an unstable conditioning layer based on a mixture of inorganic/ organic compounds (Alabbas et al., 2012). However, when stable biofilm formation was achieved at 120 hours and when steady state is reached, mass transfer limitations overcome the interfacial activation, which is reflected in a change from a semicircle behavior to a straight line shown in Figure 4A. . It is speculated that the formation of an adherent biofilm influenced the mass transfer processes in the electrochemical cell (Castaneda and Benetton, 2008). The formation of biofilm is confirmed by the two time constants indicated by arrows in Figure 4B. The EIS spectra affirm the inhibitory effect of the bacterial activities and subsequent biofilm formation described in the previous sections of this paper. Potentially the IRB consortium could be use as a strategy to combat corrosion especially in aerobic environment.

**CONCLUSIONS**

In this study the microbiologically influenced corrosion (MIC) of API 5L grade X52 carbon steel coupons by an iron-reducing consortium cultivated from a sour oil well produced water was investigated. Interestingly, IRB metabolic reactions and biofilm formation inhibit the corrosion process. The maximum corrosion rate in the biotic system was 2 mpy while it was 20 mpy in the abiotic solution. The corrosion inhibition was attributed to oxygen depletion induced by IRB bacteria respiration and the protective affect of the biofilm that formed on the metal surface.

**REFERENCES**

Alabbas, F. M., A.B. Gavanluei and J.R. Spear et al., 2011. "Effects of Sulfate Reducing Bacteria on the Corrosion of X-65 Pipeline Carbon Steel" Paper # C2012–0001140, Proceeding NACE 2012 Conference.

Castaneda, H. and X.D. Benetton. 2008. "SRB-Biofilm Influenced in Active Corrosion Sites Formed at the Steel-Electrolyte Interface When Exposed to Artificial Seawater Conditions" *Corrosion Science* 50:1169–1183.

Dubiel, M., C.H. Hsu, C.C. Chien, F. Mansfield and D.K. Newman.2002. "Microbial Iron Respiration Can Protect Steel From Corrosion" *Applied and Environmental Microbiology* 68, 1440–1445.

Frank, D., 2008. XplorSeq: a software environment for integrated management and phylogenetic analysis of metagenomic sequence data. *BMC Bioinformatics* 9: 9–420.

Gorby, Y. A. Y. Svetlana and McLean J. S. et al. 2006. "Electrically Conductive Bacterial Nanowires Produced by *Shewanella oneidensis* Strain MR-1and Other Microorganisms" *PNAS* 103: 11358-11363.

Herrera, L. K. and H.A. Videla. 2009. "Role of Iron-Reducing Bacteria in Corrosion and Protection of Carbon Steel" *International Biodeterioration & Biodegradation* 63: 891–895.

Little, B.J. and J.S. Lee. 2007. *Microbiologically Influenced Corrosion*. John Wiley & Sons Inc., Hoboken, NJ, USA; pp: 1-50.

Lutterbach, M.T, L. Contador, A. Oliveira and M. Galvão . 2009. "Iron Sulfide Production by *Shewanella* Strain Isolated From Black Powder" Paper # 09391, Proceeding NACE 2009 Conference.

NACE Standard TM0194. 2004. "Field Monitoring of Bacterial Growth in Oil and Gas Systems". Published by NACE, Houston, Texas.

Pedersen, A., M. Hermansson.1991. "Inhibition of Metal Corrosion by Bacteria" *Biofouling* 3:1–11.

Pham, T. H., Boon N. and Aelterman P. et al. 2008. "Metabolites Produced by *Pseudomonas sp.* Enable a Gram Positive Bacterium to Achieve Extracellular Electron Transfer" *Appl Microbiol Biotechnol* 77:1119–1129.

Sahl, W. Jason, F. Nathaniel, H.J. Kirk, W. David, W.C. Stone and J. R. Spear. 2010. "Novel Microbial Diversity Retrieved by Autonomous Robotic Exploration of the World's Deepest Vertical Phreatic Sinkhole" *Astrobiology*, 10(2):201–13.

Shobhana, C., G. Gunasekaran and Pradeep Kumar. 2005. "Corrosion Inhibition of Mild Steel by Aerobic Biofilm" *Electrochimica Acta*, 50 (24):4655–4665.

Videla, H. A and L. K. Herrera. 2009." Understanding Microbial Inhibition of Corrosion. A Comprehensive Overview" *International Biodeterioration & Biodegradation* 63:896–900.

Youssef, N., M.S. Elshahed and M.J. McInerney.2009. "Microbial Processes in Oil Fields: Culprits, Problems, and Opportunities", *Adv. Appl. Microbiol.* 66:141–251.

# ISOLATION AND CHARACTERIZATION OF CYANIDE AND RESORCINOL DEGRADING BACTERIUM

Preeti Parmar (Uka Tarsadia University, Surat, Gujarat, India)
Anjali Soni and *Piyush Desai* (Veer Narmad South Gujarat University, Surat, Gujarat, India)

Environmental pollution has been considered as a side effect of industrial society due to emission of various pollutants. In nature, microorganisms can effectively reduce these compounds. In this particular study, a bacterium that utilized potassium cyanide as a sole source of carbon and nitrogen was isolated after enrichment in Bushnell-Haas liquid medium embedded with 100 ppm of KCN (pH 8.5). It could also utilize resorcinol in the same medium conditions. Biodegradation studies were carried out by measuring change in pH, cyanide and resorcinol concentrations, cell biomass, ammonia production. Optimization studies with pH 7.5, 8.5, 9.5, temperatures $27^o$, $37^o$, $45^oC$, addition of 0.1%glucose, sucrose, ammonium sulphate, urea with different concentration of KCN and resorcinol were carried out to optimize the conditions for higher degradation of both the compounds. On the basis of morphological, cultural, biochemical and 16s-rDNA studies, an isolated was identified as *Pseudomonas* species, which was able to utilize 100ppm cyanide, 1000ppm resorcinol at pH 8.5 within 74 hrs at $37^oC$ in shaking conditions.

# ACQUIRED RESISTANCE ENHANCEMENT AGAINST *PLASMOPARA VITICOLA* USING DIFFERENT BIOTIC INDUCERS

## *Muneera D.F. Alkahtani*

(Faculty of Science, Prince Nora University, Kingdom of Saudi)

The different grapes (Vitis species) cultivars were attacked by downy mildew pathogen. Downy mildew disease infected the shoot full of leaves, stems, and buds, fruits, and lead to a severe shortage in the crop which may be reach the complete loss of yield. It may not be a loss in yield only but also extends to the quality of the crop due to many biochemical changes comparing to control. This investigation is based on the use of some elicitors and their biochemical effect on grape seedlings toward this disease. The enzyme activity as peroxidise, polyphenoloxidase, chitinase and β-l, 3 glucanase were determined spectroscopy as well as some of Photosynthesis pigments. Protein pattern was analysed by polyacrylamide gel electrophoresis (SDS PAGE). The most reduction for disease severity recorded by T. harzianum at 1 x 106and followed by St. plicatus at 1 x 108. Both chlorophyll and carotene were increase with T. harzianum followed by Ps. fluorescence comparing with infected control. There was diversity in enzymes activity depending on the type elicitors. SDS PAGE analysis for grape seedlings showed diversity between biotic treatments. Similarity reached to 95.76% for both St. plicatus and Ps. fluorescence in one close cluster which similar with T. harzianum at 94.25%. Alternative solutions for downy mildew disease may be occurred through enhance plant defence by safety materials and far from fungicides.

# THE OCCURRENCE OF MULTIDRUG - RESISTANT BACTERIA IN POLYCHLORINATED BIPHENYL POLLUTED SOIL-GROUNDWATER SYSTEM

*Natasha Bhutani* and Satish Walia (Oakland University, Rochester, MI)
Sandeep Walia (Oakland University, Rochester, MI and Henry Ford Hospital, Detroit, MI)
Sonia Rana (Oakland University, Rochester, MI and Kresge Eye Institute, Detroit, MI)

The purpose of this study was to assess the prevalence of antibiotic resistant heterotrophic bacteria on polychlorinated biphenyl (PCB) contaminated sites.  Environmental samples (n=56) from two PCB contaminated sites, one in Detroit, MI and the other in Syracuse, NY were studied for  the detection of antibiotic resistant opportunistic pathogens  bacteria with PCB- degrading capabilities.  Initial screening of bacteria for PCB- degrading abilities was done using biphenyl as a surrogate for PCB. PCB-degraders were detected by spraying a thin layer of ethereal solution of biphenyl on bacterial colonies and observing a yellow to brown coloration and a halo around the positive bacterial colony.   The bacteria showing a clear halo around the colony were tentatively designated as PCB - degraders and were further tested for the degradation of pure congeners of PCBs mix.  Our isolates showed 100 % biotransformation of 3,5-dichlorobiphenyl and up to 54% of  2,2',3,3'5,6,6'-heptachlorobiphenyl.   The PCB degraders were purified on tryptic soy agar plate and biochemically identified using API system.  All of the PCB-contaminated soil-water samples tested showed presence of known opportunistic pathogens.  The bacteria identified were *Pseudomonas putida, Pseudomonas aeruginosa, Pseudomonas florescence, Pseudomonas cepacia, Stenotrophomonas maltophilia*, *Pseudomonas testosterone*, *Pseudomonas avenae*, and other *Alcaligenes denitrificans, Agrobacter radiobacter*, *Acidovorax facilis, Alcaligenes xylosoxydans, Bacillus sphericus* and Rhodococcus species.   In the course of our antibiotic susceptibility assay against 8 antibiotics, our results showed PCB-degrading bacteria were resistant against several clinically effective antibiotic classes: cephalosporins, carbapenems, quinolones, aminoglycosides, chloramphenicol and tetracycline.  Thirteen out of 17 (76%) PCB-degrading bacteria were resistant to a combination of 3 or more antibiotics.  The results of our study show that multidrug resistant bacteria are not only prevalent in clinical bacteria but also present in PCB-contaminated soil-groundwater system and its natural surroundings.

# STUDY ON THE DECOMPOSITION PROCESS OF LIGNIN BY DOMESTICATED ANAEROBIC BACTERIA

Wenjing Du, *Jidong Liang*, Dongqi Wang, Jian Lin

(Department of Environmental Engineering, Xi'an Jiaotong University, Xi'an, China)

Lignin and its derivatives, a kind of complex high polymers, were the main constituents of dissolved and colloidal substances (DCS) which are a kind of harmful pollutants accumulated in the recycling water of pulp and paper making processes. So Lignin's effective decomposing is very important to the treatment of DCS in water saving pulp and paper mills. In this study, the anaerobic biodegradation processes of lignin were studied by culturing the anaerobic sludge, which had been domesticated by running a 6L UASB reactor for 118d with influent water containing lignin. The results showed that the highest COD removal of the water consist of lignin（1g/l）reached 51.85%. According to the analysis of biodegradation products by GC-MS, styrene was a possible product of the anaerobic biodegradation. And styrene could be biodegraded further to some intermediate products, such as cyclohexanone and benzal dehyde. Finally, these intermediate products were decomposed to $CO_2$, $CH_4$ and some other small organic molecules.

# ESTROGENIC ENDOCRINE DISRUPTORS ARE SUBSTRATES OF ANTIBIOTIC PUMPS IN WASTEWATER BACTERIA

***Xinhua Li***, Andrew Madsen, Otakuye Conroy-Ben
(University of Utah, Salt Lake City, UT)

Many wastewater and increasing drinking water treatment plants in the U.S. employ biological treatment to reduce contaminants. Main mechanisms at this stage are biodegradation and biosorption. However, interacting with these mechanisms are the occurrence of metal and drug resistance proteins that would lead to higher extracellular contaminant concentrations.

During export, an antibiotic (or other chemical) enters the protein complex through periplasm, and is pumped out of the bacterium. The exact method of extrusion is not yet known, but it is suspected that antibiotics and other substrates are exported entirely from the periplasm, and not the cytoplasm. This would include any interactions with hormones. When bacteria encounter a hormone in a wastewater treatment plant's secondary biological reactor, the hormone may be pumped from the cell by antibiotic resistant proteins before coming in contact with degrading enzymes.

We hypothesize that efflux pumps export endocrine disrupting chemicals from the bacterium prior to biodegradation, leading to incomplete destruction during wastewater treatment. Estrogenic endocrine disruptors ($17\beta$-estradiol, $17\alpha$-ethynylestradiol, nonylphenol, octylphenol, and bisphenol-A) are substrates of the major multi-drug resistant pumps AcrAB-TolC in *E. Coli* and MexAB-OprM in *Pseudomonas*. Since estrogens and estrogen mimics are exported from the bacterium as soon as they enter, they are not fully oxidized during biological treatment. Related metal efflux systems may contribute to liquid-phase metal concentration in wastewater. As wastewater is discharged into the environment, so are un-degraded emerging contaminants. This leads to antibiotic resistance, endocrine disruption, and metal toxicity.

Findings of this proposed work will provide insight as to why emerging contaminants such as antibiotics, endocrine disruptors, and pharmaceuticals are difficult to eliminate with conventional biological treatments.

# PRODUCTION OF EXTRACELLULAR A-AMYLASE ENZYME BY THEMOPHILIC *BACILLUS* SP. ISOLATED FROM RAJASTHAN, INDIA

*Deeksha Gaur*, Pankaj K. Jain and Vivek Bajpai

(Department of Biotechnology, MITS University, Lakshmangarh, Sikar- 332 311, Rajasthan, India)

Thermophiles are the organisms which are adapted to live at high temperatures. The enzymes from thermophiles find a number of commercial applications because of their thermostability and thermoactivity. One of the most attractive attributes of thermophiles is that they produce enzymes capable of catalyzing biochemical reactions at temperatures higher than those of mesophilic organisms. Therefore, the isolation of thermophilic bacteria from natural sources and their identification are very important in terms of discovering new industrial thermophilic enzymes. Hot Arid and Semi Arid region of Rajasthan could serve as a good source for new thermophilic microorganisms with novel industrially important properties. The aim of this research is the isolation and identification of industrially important extracellular α-amylase enzyme producing thermophilic bacteria from Arid and Semi arid Region of Rajasthan. For this study soil samples were collected from Jhunjunu, Sikar and Churu districts of Rajasthan. Total 16 bacteria were isolated from the collected soil samples. Among all isolated bacterial population 2 thermophilic bacteria were able to produce amylase enzyme. The enzyme was estimated by qualitative and quantitative experiments. The isolate was identified as *Bacillus* sp. by microscopic, biochemical and molecular characteristics. The best enzyme activity was observed at pH 7 and temperature 55°C, starch as carbon source and yeast extract as nitrogen source. So this bacterium can be potentially used in a number of industrial processes such as food (baking, brewing, dairy industries), fermentation, textile, detergent, paper industries and starch processing industries.

# FUNCTIONALITY OF THE PROBIOTICS FERMENTED RICE STRAW AND SOYBEAN MEAL HYDROLYSATES

*Li-Jung Yin* (Dept. Sea Food Science, National Kaohsiung Marine University, Kaohsiung, Taiwan)
Huei-Hung Lee (Dept. Food Science, National Taiwan Ocean University, Keelung, Taiwan)
Shann-Tzong Jiang (Dept. Food and Nutrition, Providence University, Taichung, Taiwan)

To screen the probiotics for hydrolysis of rice straw and soybean meal, the inhibition zone, acid and bile tolerance tests were employed to screen the optimal strains. The highest activity, 11.76 U/mL of cellulases, was obtained after 2 days incubation of *Bacillus subtilis* YJ1 at 37$^o$C, 150 rpm. The highest activities of mannanase and xylanase, 0.78 U/mL and 4.15 U/mL, were obtained after 4 days and 2 days incubation of *Bacillus* sp. YJ6 at 25$^o$C, 150 rpm, respectively, on the mentioned base media with 0.2% of beechwood xylan, locust bean gum (LBG), or konjac powder as carbon sources. The LAB counts increased to 8.22 log CFU/mL and 8.45 log CFU/mL, while the pHs decreased to 4.48 and 4.13 on media with 4% rice straw and 2% soybean meal, and 4% rice straw, 2% soybean meal and 2% glucose, respectively, after 18 h fermentation by 0.5% *Lactobacillus johnsonii* BCRC 17010 at 37$^o$C. The contents of reducing sugars calibrated by glucose, mannose, galactose, xylose, and arabinose decreased to 2.05, 1.51, 1.69, 1.56 and 1.62 mg/mL; and 2.11, 2.12, 1.75, 1.60 and 1.67mg/mL, while the total carbohydrates decreased to 2.53, 2.51, 3.54, 5.67 and 1.98mg/mL, and 6.95, 6.87, 9.72, 12.46 and 4.02 mg/mL, respectively, on media with 4% rice straw and 2% soybean meal, and 4% rice straw, 2% soybean meal and 2% glucose, respectively. The oligosaccharides such as manotriose and manotetraose were significantly detected on rice straw and soybean meal hydrolystaes when analyzed with thin layer chromatography (TLC). According to the data obtained, rice straw and soybean meal hydrolystaes are with high potential in the production of functional oligosaccharides.

# DEGRADATION OF HISTAMINE BY *BACILLUS POLYMAX* ISOLATED FROM SALTED SEAFOOD PRODUCTS

Yi-Chen Lee [1], Chung-Saint Lin [2], Yu-Ru Huang [3], And Yung-Hsiang Tsai [4*]

[1.] Department of Food Science, National Pingtung University of Science and Technology, Pingtung, Taiwan

[2.] Department of Food Science, Yuanpei University, Hsin-Chu, Taiwan

[3.] Department of Food Science, National Penghu University, Penghu, Taiwan

[4.] Department of Seafood Science, National Kaohsiung Marine University, Kaohsiung 811, Taiwan

Histamine is the causative agent of scombroid poisoning, a food borne chemical hazard. Some bacteria exhibit the ability to degrade histamine. In this study, eight histamine-degrading bacteria isolated from salted fish products and salted mollusk products were identified as *Rummeliibacillus stabekisii* (one strain), *Agrobacterium tumefaciens* (one strain), *Bacillus cereus* (two strains), *B. polymyxa* (one strain), *B. licheniformis* (one strain), *B. amyloliquefaciens* (one strain), *B. subtilis* (one strain). Among them, *B. polymyxa* degraded histamine up to 100% in histamine broth. The well range of temperature, pH and salt concentration for growth and histamine degradation of *B. polymyxa* were 25-37 $^{\circ}$C, pH 5-9 and 0.5-5% NaCl, respectively. However, the optimal growth and histamine dehydrogenase activity of *B. polymyxa* were at 30 $^{\circ}$C, pH 7 and 0.5% NaCl for 24 h incubation.

# BIODEGRADATION OF *N, N*-DIMETHYLFORMAMIDE BY *PSEUDOMONAS PUTIDA* MBDM-S4 AND BIOAUGMENTATION IN SBR SYSTEM

*Liwei Chen*, Tianming Cai, Shu Cai and Shiyang Liu

(Nanjing Agricultural University, Nanjing, Jiangsu, China)

*N,N*-dimethylformamide(DMF) is widely used in the pharmaceutical and chemical industries. In this study, a gram-negative, rod-shaped bacteria known as MBDM-S4, was isolated from river sediments contaminated by DMF. Strain MBDM-S4 was identified as *Pseudomonas putida*. The results of total organic carbon (TOC) and ammonia analysis indicated that strain MBDM-S4 could completely degrade 200 mg $l^{-1}$ DMF to $CO_2$, $H_2O$ and $NH_3$ in 42 h. Strain MBDM-S4 could even grow in mineral salts medium containning extremely high levels of DMF up to 10,000 mg $l^{-1}$. Degradation of DMF was strongly inhibited by $SO_4^{2-}$ (7 mM), $NH_4^+$ (30 mM) and some metal ions ($Mn^{2+}$, $Ni^{2+}$, $Cu^{2+}$ and $Ag^+$) (1.0 mM). The metabolism pathway of DMF biodegradation was proposed. In addition, bioaugmentation treatment of DMF by strain MBDM-S4 in a sequencing batch reactor (SBR) system was successfully established.

# EFFECTS OF AMINO ACIDS ON THE GROWTH AND MICROCYSTIN PRODUCTION OF *MICROCYSTIS AERUGINOSA*

***Ruihua Dai***, Yan Liu

(Fudan University, Shanghai, PR China)

A *Microcystis aeruginosa* which produced high content of microcystin -LR (MC-LR) but no microcystin-RR (MC-RR) was isolated from *Dianchi* Lake in China. In the molecular structure of MC-LR, glutamic acid, aspartic acid, leucine, alanine and arginine are the constitutional components which are abundant in natural water. In this paper, effects of six amino acids at their natural concentrations on the growth of the *Microcystis aeruginosa* and the microcystin (MC) production were studied in batch culture. *Microcystis aeruginosa* could assimilate alanine, leucine and arginine as sole nitrogen sources for growth and MC production. In the presence of glutamic acid and aspartic acid, *Microcystis aeruginosa* grew quickly and became yellow and died after 96 h. The changes of intermolecular amino acids were studied.

# WETLANDS
# AND
# SEDIMENTS

# NITROGEN DYNAMICS AND MICROBIAL COMMUNITY COMPOSITIONS IN SIX VERTICAL FLOW WETLAND COLUMNS

***Guangzhi Sun*** (James Cook University, Townsville, Australia)
Yafei Zhu (Monash University, Melbourne, Australia)
Tanveer Saeed (Ahsanullah University of Science and Technology, Dhaka, Bangladesh)

**ABSTRACT:** Two synthetic wastewaters, with mean $NH_4$ concentrations of 471±19 and 475±17 mg/L, were treated in six planted columns. Under steady hydraulic and pollutant loading, average $NH_4$ removal rate in each column was in the range of 21-47 $g/m^2d$, while average TN removal rate was 0-27 $g/m^2d$. In general, higher redox potential values benefitted ammonia removal but limited TN removal. The supply of organic carbon, by adding glucose into the synthetic wastewater, slightly reduced the rate of ammonia removal, but significantly enhanced TN removal. The seeding of microorganisms using diluted activated sludge, and submerging the columns with treated effluent for three days per week, intensified microbial activities; oxygen consumption reached 53-363 $gO_2/m^2d$ due to microbial degradations of organics and nitrogen. Fluorescence *in situ* hybridization analysis of bacterial biomass revealed the population densities of nitrifying bacteria, and specific denitrifying bacteria (*Azoarcus-Thauera*-cluster, genus *Hyphomicrobium*, genus *Paracoccus*, and family *Saprospiraceae*). Denitrifier *Azoarcus-Thauera*-cluster was found to be the dominant bacterial group (58% of all cells) when organic carbon is available. Without the supply of organic carbon, ammonium oxidising bacteria (AOB) dominate microbial populations in the planted columns.

## INTRODUCTION

Most wastewaters contain nitrogenous compounds that, if discharged without sufficient treatment, can cause adverse effects in receiving waterways. Moreton Bay and Port Philip Bay in Australia give typical examples of such effects: water quality deterioration due to insufficient removal of nitrogen from wastewaters and stormwater in upstream treatment facilities. In treatment wetlands, the efficiency of organic matter removal is often satisfactory, but sufficient removal of nitrogen often requires large treatment areas and long retention time which can be impractical for many applications. Among various nitrogenous compounds, dissolved inorganic nitrogen (e.g. ammonia, nitrate and nitrite) is predominant in most wastewaters and has the greatest impact on aquatic systems. Effective removal of inorganic nitrogen is a challenging task to wetland researchers.

It has long been assumed that single-stage constructed wetlands cannot achieve substantial removal of total nitrogen due to their inability to provide both aerobic (for nitrification) and anaerobic (for denitrification) conditions at the same time (Vymazal, 2007). To split a wetland system into different nitrification and denitrification units, however, does not necessarily resolve this dilemma. Apart from higher cost, such approach has the following problems: (1) it requires extra organic carbon input to the denitrification unit, typically a subsurface horizontal flow wetland, as the bulk of organic carbon is normally removed in the preceding nitrification unit(s); (2) it is virtually impossible to control how the added organic carbon source is used in the denitrification unit, as it may not be consumed by denitrifying bacteria; and (3) it undermines wetland character - ideally a horizontal flow wetland is used to provide both (partially) aerobic and anaerobic treatment - it loses advantage over an unplanted filter if only anaerobic condition is desired.

Functioning as a complex bioreactor, a constructed wetland removes inorganic nitrogen via various pathways that are not fully understood. To date, it is known that ammonia can be transformed in a vertical flow wetland by physicochemical processes, such as volatilisation at suitable temperature and pH,

sorption onto media (Connolly et al., 2004), assimilation into bacterial biomass and nutrient uptake by plants, and the classic nitrification-denitrification process. In addition to the heterotrophic denitrification route, removal of nitrite and nitrate in the wetland systems can also take place via Anammox process (Shipin et al, 2005).

The complexity of nitrogen removal routes has generated difficulty and unreliability in wetland design. However, it has also provided an opportunity for the development of this technology. Can the wetlands function effectively as 'one-pot' bioreactors where nitrification and denitrification occur simultaneously?

Several recent studies discovered surprisingly high ammonia removal rates. Such result has been achieved in a full-scale surface flow wetland system (Bishay and Kadlec, 2005), mesocosm and lab-scale vertical flow wetland columns (Tanner and Kadlec, 2002; Saeed et al, 2012). Significant TN removal was found, showing that simultaneous nitrification and denitrification may have taken place to transform nitrogenous pollutants into non-reactive $N_2$, which is the desired end product of nitrogen processing in the wetlands, and the only species of nitrogen cascade that is not potentially harmful to the environment. Why is nitrogen removal significantly higher in some wetlands than the others? It was speculated, based on limited evidence from mass balance stoichiometry, but without confirmation by microbiological analysis, that novel nitrogen removal routes (such as Anammox and CANON) may have contributed to the disparity between traditional nitrogen chemistry and the reality in some constructed wetland systems (Sun and Austin, 2007). Reliable achievement of such high nitrogen removal in the wetland systems, however, will depend on further understanding and modelling of nitrogen transformation processes.

With complex plant-pollutant-microorganism interactions, constructed wetland provides an ideal habitat to allow a large variety of microbial activities to take place simultaneously. These activities, if sustained under appropriate environmental conditions, can produce effective total nitrogen removal. With the overall objective of understanding nitrogen removal in vertical flow wetlands, this study was designed to investigate: (1) whether autotrophic denitrification can occur in vertical flow wetlands without the seeding of Anammox bacteria; (2) nitrogen mass removal rates under high ammonia loading; (3) the effects of several environmental factors on nitrogen degradation; and (4) identification and quantification of microbial community compositions.

## MATERIALS AND METHODS

Two synthetic wastewaters (A and B) were prepared, to study nitrogen removal and microbial community profiles with and without external organic carbon source. The wastewaters were prepared using (g in 1 L water): 1.9 $NH_4Cl$, 3.0 $NaHCO_3$, 0.066 $KH_2PO_4$, 0.13 $CaCl_2·2H_2O$, 1.0 $MgSO_4·7H_2O$, 0.001 $FeSO_4·7H_2O$, 0.001 $MnCl_2·4H_2O$, 0.0005 $CuSO_4·5H_2O$, 0.0005 $ZnSO_4·7H_2O$, and 1.16 (for A-series reactors) or 0 (for B-series) $C_6H_{12}O_6$. Thus, A-reactors received influent with moderate TOC concentration (350-450 mg/L), whereas B-reactors received zero organic carbon input from influent. It was expected that Anammox bacteria may be established in the reactors, if a suitable environment (low DO level, moderate temperature, and restricted organic carbon) is maintained.

Experiments were carried out in six vertical flow, planted column reactors with identical dimensions, namely reactor A1, A2, A3, B1, B2 and B3, as shown in Figure 1. The reactors were made of Perspex columns of 100 mm in height and 90 mm internal diameter; their bottom layer filled with 20±5.2 mm round gravel to a depth of 100 mm. The main layer, 700 mm deep, differ slightly in these reactors: A1 and B1 were filled with a mixture of 2.4-7.0 mm river pebble and 10±3.5 mm floral foam (dry weight: 0.4-0.5 g each); A2 and B2 were filled only with 2.4-7.0 mm river pebble; and A3 and B3 were filled with a mixture of 2.4-7.0 mm river pebble with 15±3.5 mm cotton ball (dry weight: 0.4-0.5 g each). A single *Phragmites australis* was planted in the main layer of each reactor. The media were arranged in such way so that different oxygen flow and redox potential conditions may be achieved in these reactors. Before experiments started, the porosity of packed media was measured as 39% in reactor A1, A2, B1, B2, and 41% in A3 and B3.

Prior to the start of experiments, all the reactors were seeded with microorganisms using active sludge (mixed liquor) collected from a domestic sewage treatment facility, according to three steps. Firstly, all the reactors were continuously dosed with diluted mixed liquor (liquor:tap water = 1:4) at 2 L/d for four weeks. This was followed by allowing all the reactors to be submerged in undiluted mixed liquor for four weeks. Finally, the reactors were rinsed twice with tap water, and submerged in tap water for one week. The total seeding period was nine weeks, before the experiments started.

During the experiments, each column was operated as a single bioreactor, with its influent flow rate controlled by a peristaltic pump and timer, as shown in Figure 1. From two feed tanks (one for A-series and the other for B-series reactors), synthetic feeds were pumped intermittently, 15 minutes per hour, onto the surfaces of the reactors. Each week, the dosing started on Monday and stopped on Friday. During weekends and experiment breaks, each column was filled with its own effluent, to support the growth of *Phragmites* and maximize the attachment of biofilms on media. Therefore, each week the reactors were operated as unsaturated vertical flow wetlands for four days (Monday to Friday), and rested as effluent-saturated packed columns for three days (Friday to Monday).
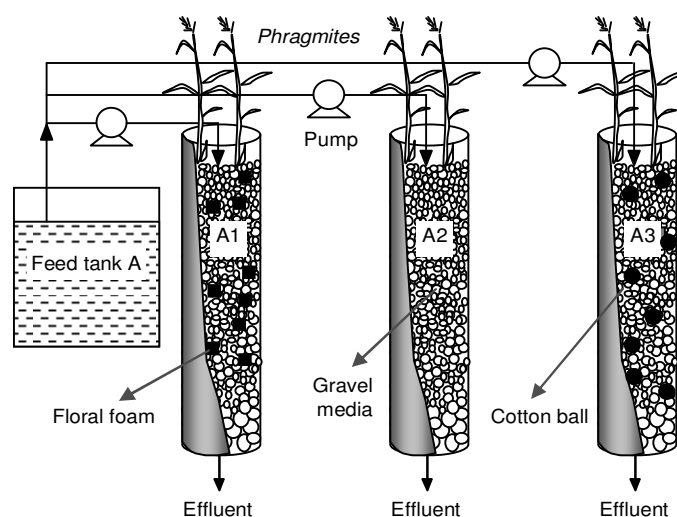


**FIGURE 1. Schematic diagram of A-series planted column reactors (same arrangement applies to B reactors)**

Wastewater samples were collected, on a weekly basis, from the feed tanks and outlet of each column; giving eight samples per week. For each sample, analysis was carried out for $NH_4$-N, $NO_3$-N, $NO_2$-N, TN, TP, TOC, COD, SS, Alkalinity (as $CaCO_3$), DO, Eh, pH, and water temperature. The values of DO, pH and water temperature were measured using a SensIon378 pH-conductivity-DO meter and electrodes. Eh value was measured with a EuTech ORPTester. Alkalinity was measured using a Hach alkalinity test kit. All other parameters were analyzed using a Hach DR5000 spectrophotometer. Ammonia, nitrate, nitrite and TN were analyzed independently.

After the completion of the experiments, biomass samples were collected (by grabbing mixtures of gravel, plant roots and sediments) from all six columns. Shortly after collection, the samples were submerged in 100% ethanol solution and sent to a commercial lab in Germany, where FISH (fluorescence *in situ* hybridization) analysis was carried out to detect, and quantify, the presence of nitrifying (AOB and NOB) and Anammox bacteria in all the samples. FISH analysis of other denitrification bacteria was only carried out for samples from reactors A3 and B3.

**RESULTS AND DISCUSSION**

**Overall Performance:** A total of ten sets of water samples were collected and analysed during the experimental period. The average performances of the column reactors, which were under different redox potential and dissolved oxygen conditions, are presented in Table 1.

**TABLE 1. Average performances of the planted column reactors (mean±SD)**

| | Influent to A reactors | A1 outlet | A2 outlet | A3 outlet | Influent to B reactors | B1 outlet | B2 outlet | B3 outlet |
|---|---|---|---|---|---|---|---|---|
| Flow rate, L/d | --- | 1.5±0.1 | 1.5±0.2 | 1.6±0.2 | --- | 1.6±0.1 | 1.4±0.2 | 1.5±0.1 |
| $NH_4$-N, mg/L | 471±19 | 320±83 | 378±64 | 350±54 | 475±17 | 302±87 | 338±58 | 280±102 |
| $NO_2$-N, mg/L | 0±1 | 27±32 | 15±32 | 1±1 | 1±1 | 152±78 | 128±54 | 58±55 |
| $NO_3$-N, mg/L | 0±0 | 11±14 | 7±11 | 0±0 | 0±0 | 43±32 | 27±17 | 30±31 |
| TN, mg/L | 472±17 | 366±81 | 399±34 | 365±47 | 479±11 | 478±23 | 479±19 | 375±36 |
| Alkalinity[*] mg/L | 1670±306 | 1138±356 | 1425±296 | 1438±189 | 1793±180 | 560±514 | 840±396 | 898±573 |
| COD, mg/L | 1216±227 | 249±153 | 331±107 | 510±138 | 164±51 | 343±102 | 314±178 | 321±148 |
| TOC, mg/L | 364±95 | 30±56 | 52±53 | 107±39 | 13±12 | 13±6 | 15±4 | 35±14 |
| $PO_4^{3-}$, mg/L | 30±11 | 18±13 | 26±20 | 18±12 | 19±5 | 15±2 | 16±2 | 11±5 |
| SS, mg/L | 108±110 | 27±26 | 55±53 | 134±66 | 7±9 | 2±3 | 3±2 | 23±25 |
| DO, mg/L | 3.5±3.2 | 2.7±2.1 | 2.4±2.0 | 0.6±0.3 | 7.4±1.2 | 6.5±1.9 | 3.1±1.9 | 3.9±2.3 |
| Eh, mV | 139±13 | 80±139 | 35±130 | -201±81 | 149±16 | 192±41 | 189±31 | 123±118 |
| pH | 7.9±0.5 | 7.4±0.4 | 7.5±0.2 | 7.4±0.3 | 8.4±0.3 | 6.8±1.0 | 7.2±0.5 | 7.0±0.6 |
| Temperature, $^0C$ | 17.3±1.7 | 17.2±1.7 | 17.2±1.8 | 17.3±1.7 | 16.9±1.7 | 16.9±1.6 | 16.8±1.7 | 17.2±1.8 |

[*]Note: alkalinity expressed as equivalence to $CaCO_3$
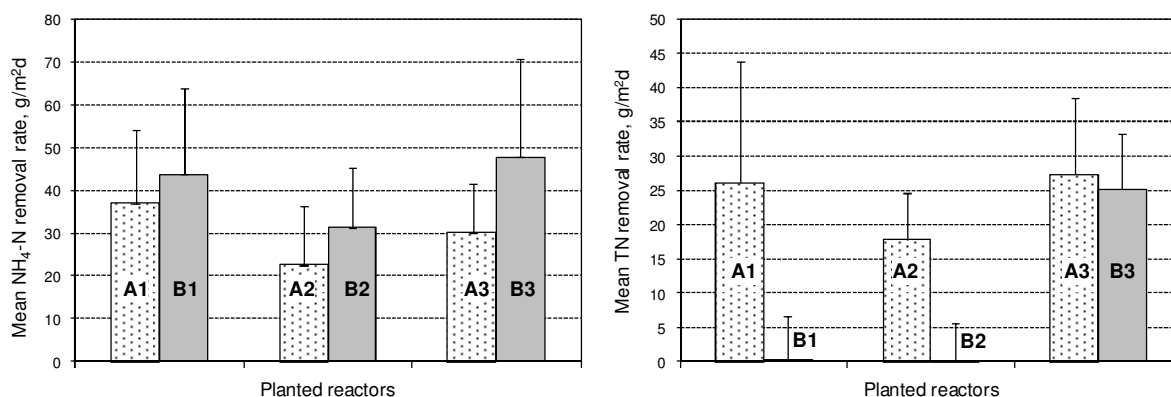


**FIGURE 2. Mean removal rates of $NH_4$-N (left) and TN (right) in all the reactors (Error bars represent standard deviations).**

**Nitrogen Removal Rate:** Figure 2 gives the average $NH_4$-N and TN removal rates obtained in the reactors. At similar nitrogen mass loading (105-118 $gNH_4$-N/$m^2$d), the availability of glucose in synthetic wastewater A allowed a significant amount of TN to be removed in reactors A1, A2 and A3. Denitrification activity was completely inhibited in B1 and B2 (i.e. zero TN removal). Surprisingly, B3 and A3 produced similar TN removal rates, around 25 gN/$m^2$d. TN removal in reactor B3 may be

attributed to: (1) carbon source within the reactor itself, such as the release of carbonaceous materials from plant roots or dead bacteria, (2) aerobic denitrification for which only preliminary evidence exists in constructed wetlands, or (3) Anammox activity or an unknown autotrophic denitrification route. The Anammox route was eliminated after microbiological analysis showed that no Anammox bacteria were present in B3.

The availability of organic carbon (COD 1216 mg/L; TOC 364 mg/L) in A-column reactors had a negative effect on ammonia removal rates. Figure 2 indicates that under similar hydraulic and ammonia mass loading, the mass removal rates of ammonia (in $g/m^2d$) in B columns are approximately 20-50% higher than those in A columns. The addition of glucose provided only carbonaceous organics (i.e. no extra nitrogen) into A columns. Therefore, the lower removal rates are believed to result from competition among different bacteria for dissolved oxygen, nutrients for cell synthesis, or spaces inside the column reactors for biofilm attachment.

**Effects of Redox Potential Value on Nitrogen Removal Rate:** The redox potential condition in these reactors, which can be influenced by media and many other factors, plays a major role in the establishment of different bacteria groups responsible for nitrogen transformation; it therefore can have a major influence on nitrogen removal efficiency. Figure 3 gives the plots of ammonia and TN removal rates vs. Eh values of the effluents from individual reactors.
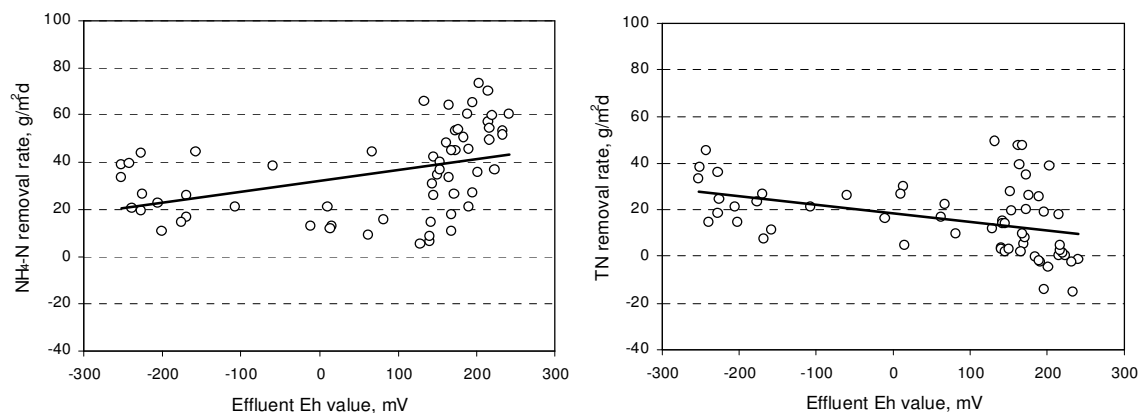


**FIGURE 3. Plots of effluent Eh values vs. $NH_4$-N (left) and TN (right) removal rates in the column reactors.**

Data in Figure 3 are highly scattered, but the overall trends indicate that $NH_4$-N removal rate generally increases with Eh, as higher Eh favours the activities of aerobic nitrifying bacteria. In contrast, TN removal rates decrease with Eh values, as aerobic condition restricts heterotrophic denitrification. It was observed during the experiments that anoxic condition (Eh between -100 mV and 100 mV) appears to be rare in the columns; redox potential condition tends to swing between extremes, aerobic (Eh above 100 mV) and anaerobic (Eh below -100 mV).

**Dissolved Oxygen Consumption:** In reactors B1 and B2, where Eh and DO levels were significantly higher than other reactors, TN removal was virtually zero, suggesting that no denitrification bacteria was active in these reactors. Similar to the profile of redox potentials vs. N removals, the correlation of DO vs. $NH_4$-N and TN removal are very scattered, but the general trends indicate that ammonia removal increases, and TN removal decreases, with higher effluent DO values.

The average oxygen consumption rates, estimated based on nitrogen and COD removal, reached 363, 283, 295, 93, 53 and 140 $gO_2/m^2d$ in A1, A2, A3, B1, B2 and B3, respectively. The high oxygen consumption figures in A-series reactors are predominately due to oxygen budget allocated to aerobic decomposition of COD (60-75%). However, because a small amount of organic carbon (i.e. glucose) may

have been consumed by heterotrophic denitrification in anaerobic zones, the actual oxygen consumption rates in A-series column reactors should be slightly lower than estimated above. The oxygen consumption rate of 53 $gO_2/m^2d$ (B2) to 363 $gO_2/m^2d$ (A1) is equivalent to upwards air flux passing through the reactors at 0.18-1.21 $m^3/m^2d$ during the experiments, considering 21% air is oxygen and the molar density of air at atmospheric pressure is 22.4 L/mol.

The range of oxygen consumption rates is comparable with those obtained in small-scale tidal flow wetland systems treating strong wastewaters (Sun et al, 2006; Wu et al, 2011). Because no forced aeration was employed, the oxygen flux in this study can only result from: (1) diffusion due to oxygen concentration gradient between the air inside and outside the reactors, (2) natural upwards air convection due to slight temperature differences inside and outside the reactors, which were caused by microbial activities, and (3) oxygen release from the roots of *Phragmites*, which is negligible in vertical flow wetland systems treating strong wastewaters. The seeding of bacteria at the start of the experiment, as well as submerging the reactors during weekends, may have produced denser population of microorganisms, and more intensive microbial activities in these reactors, compared with most vertical flow wetlands reported in literatures. Combined with the small size of the columns in this study (which implies more efficient wastewater distribution), the intensive seeding of bacteria are believed to have enhanced pollutant removal efficiencies.

**Microbial Community Composition in the Planted Columns:** Using gene probes and fluorescence microscope, qualitative and quantitative analyses of nitrifying and denitrifying bacteria in the reactors were carried out. In general, A-series reactors, where organic carbon (glucose) was supplied, contained far more viable bacterial cells than B reactors in which AOB (ammonium oxidising bacteria) dominated. No Anammox bacteria was detected in any reactor, including B3 which removed considerable amount of TN without organic carbon input; this indicating that denitrification in B3 was not caused by Anammox. Apart from Anammox bacteria, other denitrification bacteria were analysed for samples collected from A3 and B3. Table 2 summarizes the percentage bacterial populations in all the column reactors.

**TABLE 2. Percentage population of nitrification and denitrification bacteria**

| Target microbes in different reactors | A1 | A2 | A3 | B1 | B2 | B3 |
|---|---|---|---|---|---|---|
| AOB (Ammonium oxidizing bacteria) | 10% | 13% | 16% | 94% | 91% | 92% |
| NOB (Nitrite oxidizing bacteria) | 2% | 4% | 5% | 3% | 3% | 2% |
| *Azoarcus-Thauera-cluster* | n. a.[*] | n. a. | 58% | n. a. | n. a. | 1% |
| Genus *Hyphomicrobium* | n. a. | n. a. | 6% | n. a. | n. a. | < 1% |
| Genus *Paracoccus* | n. a. | n. a. | 6% | n. a. | n. a. | < 1% |
| Family *Saprospiraceae* | n. a. | n. a. | 7% | n. a. | n. a. | < 1% |

[*]Note: n. a. denotes not analysed

**CONCLUSIONS**

The effects of redox potential, dissolved oxygen, temperature and availability of organic matter on the removal of ammonia and total nitrogen were studied, when two synthetic wastewaters were treated in six planted columns. In general, higher redox potential values benefitted ammonia removal but limited TN removal. Under steady hydraulic and pollutant loading, these columns produced $NH_4$-N and TN removal in the range of 21-47 $g/m^2d$ and 0-27 $g/m^2d$, respectively. Oxygen consumption ranged 53-363 $gO_2/m^2d$, equivalent to air flux of 0.18-1.21 $m^3/m^2d$. The identity and populations density of nitrifying and denitrifying bacteria were analysed by fluorescence *in situ* hybridization. Denitrifier *Azoarcus-Thauera-cluster* was the dominant bacteria when organic carbon is present. Without organic carbon supply, AOB dominate microbial populations.

## REFERENCES

Bishay, F., and R.H. Kadlec, 2005. "Wetland Treatment at Musselwhite Mine". In: J. Vymazal (Ed.), *Nutrient Cycling and Retention in Natural and Constructed Wetlands*, pp. 176-198. Backhuys.

Connolly, R., Y. Zhao, G. Sun, and S. Allen. 2004. "Removal of Ammoniacal-Nitrogen from an Artificial Landfill Leachate in Downflow Reed Beds". *Process Biochem.*, 39: 1971-1976.

Saeed, T., R. Afrin, A. Al Muyeed, and G. Sun. 2012. "Treatment of Tannery Wastewater in a Pilot-Scale Hybrid Constructed Wetland System in Bangladesh". *Chemosphere*, in press.

Shipin O., T. Koottatep, N.T.T. Khanh, and C. Polprasert. 2005. "Integrated Natural Treatment Systems for Developing Communities: Low-Tech N-Removal through the Fluctuating Microbial Pathways". *Water Sci. Technol.,* 51(12): 299-306.

Sun, G., and D. Austin. 2007. "Completely Autotrophic Nitrogen Removal over Nitrite in Lab Scale Constructed Wetlands: Evidence from a Mass Balance Study". *Chemosphere,* 68: 1120-1128.

Sun, G., Y. Zhao, S. Allen, and D. Cooper. 2006. "Generating "Tide" in Pilot-Scale Constructed Wetlands to Enhance Agricultural Wastewater Treatment". *Eng. Life Sci.,* 6: 560-565.

Tanner, C.C., and R.H. Kadlec. 2002. "Oxygen Flux Implications of Observed Nitrogen Removal Rates in Subsurface-Flow Treatment Wetlands". *Water Sci. Technol.,* 48(5): 191-198.

Vymazal, J. 2007. "Removal of Nutrients in Various Types of Constructed Wetlands". *Sci. Total Environ.,* 380: 48-65.

Wu, S.B., D.X. Zhang, D. Austin, R.J. Dong, and C.L. Pang. 2011. "Evaluation of a Lab-Scale Tidal Flow Constructed Wetland Performance: Oxygen Transfer Capacity, Organic Matter and Ammonium Removal". *Eco. Eng.* 37: 1789-1795.

# CONSERVATION THREATS TOWARDS THE WATER BIRDS OF DEEPOR BEEL WETLAND

*Jyotismita Das* and P.K Saikia

(Department of Zoology, Gauhati University, Guwahati-14, Assam India, India)

Hemen Deka

(Department of Botany, BBK College, Nagaon, Barpeta, Assam, India)

Wetlands are the basic components for the survival of wetland birds. Water birds utilize wetlands in a various ways to fulfill their basic needs. Wetland degradation causes shrinkage of wetland habitat. This directly effects the wetland birds in performing their normal activity like feeding, breeding etc. The study was carried out in Deepor Beel from January 2007 to January 2008.The present study summarizes the different degradation processes prevailing in and within the Beel periphery and shows that human disturbance is the most prevailing degradation factor in Deepor Beel, the lone Ramsar site of Assam. This not only hampers breeding birds in selecting breeding sites but also creates a gap between their feeding and breeding sites. So, proper conservation measures should be taken to conserve the wetlands as wetland birds directly depend on them for their proper survival.

# WETLAND INDEX FOR THE ASSESSMENT OF WETLANDS ON ESKOM PROPERTIES IN MPUMALANGA

*K. Durgapersad* (Eskom, Research, Testing and Development, Johannesburg, South Africa); P. Oberholster, P. McMillan (CSIR, Natural Resources Environment, Pretoria, South Africa)

In 2008, a need for wetland management was identified by Eskom, Sustainability and Innovation, as current wetland monitoring and management was not consistent throughout Eskom. A preliminary report introduced the Wetland Classification and Risk Assessment Index (WCRAI), which has been designed and modified by CSIR senior specialist, Paul Oberholster and Peter McMillan, specifically for Eskom, to aid their environmental practitioners on the classification, assessment and management of wetlands on Eskom properties. The WCRAI is developed based on manifestations of ecological processes in natural wetland ecosystems. The index is hierarchical in structure and is designed to allow identification and rapid assessment at the broadest levels by non-experts in different disciplines. The various levels are based on broad landform types, surface morphology, hydrochemical characteristics, biological structure and external environmental stressors.

The objective of this study is to develop the WCRAI in order to classify different types of wetland, assess their ecological condition as well as identify the risks they face on Eskom properties.

Fifteen wetlands were assessed during February 2009 on Eskom's properties in Mpumalanga to streamline and test the WCRAI in order to make it user-friendly and applicable for assessment on Eskom properties. The wetland index incorporates a few but important parameters to identify wetland health. The index takes into consideration, field measurements which comprise conductivity, pH, dissolved oxygen, total dissolved solids and temperature; physical characteristics which comprise wetland zones, sediment type, pugging, bank stability, aquatic cover, aquatic organisms, algae and macrophyte layers and; overall wetland characteristics which comprise of hydroperiod, wetland shape, wetland type and size. Various Land-use impacts are evaluated as well. The index assesses four different areas of a wetland to ensure a more accurate evaluation of the entire wetland. Findings are entered into the Field Sheet. The Score Sheet identifies a Wetland Category and Land-use impact score. These can be evaluated from the Ecological Category Values determined by Department of Water Affairs and the Land-use Impact Ranges identified.

The study and workshop held has demonstrated the importance of wetland management throughout Eskom. The WCRAI is a simple and user-friendly index that can be implemented by Eskom Environmental practitioners on all wetlands on Eskom properties. The wetland field guide that has been developed provides a step-by-step guide on how to carry out the assessments, calculations and brief interpretations of the data. Wetland training on the index has been initiated in May 2011 and several more sessions have been planned for 2012. It is envisaged that the WCRAI will provide Eskom with standardized in-house skills and will contribute to responsible monitoring and management of wetlands associated with Eskom land.

# SEDIMENT QUALITY ASSESSMENT IN BOURGAS BAY, BLACK SEA

Elitza Angelova, Zvezdimira Tsvetanova, Magdalena Korsachka, Roumen Marinov, *Jordan Marinski*
(Bulgarian Academy of Sciences, Sofia, Bulgaria), Anelia Kenarova (University of Sofia "St.Kliment Ohridski", Sofia, Bulgaria)

**ABSTRACT:** Sediments content is like a database that stores crucial information about the past. Revealing the most polluted areas in the small Bourgas bay started with environmental assessment of the sediments in Bourgas Bay through testing for hydrocarbons and organic matter, measurement of elements concentration through X-ray fluorescent analysis and bio-testing the bacterial alkaline phosphatase activity. The level of the total content of hydrocarbons in most of the sediment samples was higher than 0.5 mg/g, and can be categorized as high. Some of the heavy metals (Cu, Zn) exceeded the threshold concentrations. Phosphatase activity of the sediment bacterial communities (calculated per milligram of dead organic matter) was relatively stable across the Bourgas port basins. The sediments in various points of the bay showed different level of pollution with substances of low toxicity, so that the biological species have been able to adapt and develop resistance capacity to environmental stress.

## INTRODUCTION

The Bourgas Bay is the largest bay of the Bulgarian Black Sea Coast. It cuts inland circa 31 kilometers and is 41 kilometers at its widest part, and reaches 25 m of depth. The so called Small Bourgas Bay is situated at the most western part of the bay and gives home to the Bourgas Port. The port consists of inner basins of the port terminals: terminal "East" (the old harbor); the Bulk cargo terminal (terminal 2A); terminal "Ro-Ro" and terminal "West" (Container terminal). The Oil terminal "Rossenetz" is constructed as a separate port outside the small Bourgas bay and at the moment serves "Lukoil" refinery plant.

The Bourgas Bay experienced the influence of the Bourgas Port operating for a long period of time in the near past. Together with all the inflows from the adjacent industrial zone and the Vaya Lake, this has altered the ecological status of the bay. The whole database of this exploitation is stored in the bottom sediments.

The Environmental management of transborder corridors ports, ECOPORT 8 project, funded by Transnational Cooperation Programme "South East Europe", aims to improve the quality of ports, placing the prevention of pollution and preservation of natural resources in port areas and nearby coastal zones as pivotal to the maritime system. The project involved preparation of monitoring programmes and two ports were chosen as pilot monitoring sites – the Port of Bourgas, Bulgaria and the Port of Bar, Montenegro. In order the best places for monitoring points to be chosen a preliminary monitoring had been executed before the pilot monitoring started. This study presents the results from the preliminary monitoring of the small Bourgas bay, in particular, those from the sediment analyses. The aim of the sediment quality assessment was evaluation of the current ecological status of the small Bourgas Bay providing a lead where the most polluted places are, and which the main pollution source is – the port or the adjacent industry.

## MATERIALS AND METHODS

The preliminary monitoring was conducted at the end of April 2011. The positions of the sampling points were located by GPS. Water and sediment samples were taken from 23 points: 1,3,4,6 – located in the basin of terminal East; 6,7,8,23 - in the basin of terminal 2A; 9,10,11 – in the basin of terminal Ro-Ro; 12,13,14 – in the basin of Container terminal; 15,16,17,18 – in the basin of private ports;

19 – central city beach; 20 – approach channel; 21, 22 – reference points (outside of the port); 2 – in the basin of the Oil terminal (Figure 1).

The biological analyses required three separate samples from every point to be taken in sterile bottles. Aliquot portions of each sediment sample were subjected to chemical analyses of hydrocarbons, organic matter, and bioassay for bacterial alkaline phosphatase (AP) activity.



**FIGURE 1.** Location of the sampling points in the Bourgas bay

Hydrocarbons are determined gravimetrically by threefold extraction of 5 g of sediment sample with 15 ml chloroform for 30 minutes each. The extracts are collected and vacuum evaporated at 160 rpm and 400$^o$C. The organic matter is determined by Turin's method based on its oxidation by dipotassium dichromate (Kaurichev, 1980). The results from the triple analyses are averaged.

In bacterial alkaline phosphatase (AP) bioassay, the phosphate group of p-Nitrophenylphosphate (p-NPP) is hydrolytically cleaved by sediment bacteria to orthophosphate and p-Nitrophenol (p-NP), the last is spectrophotometrically measured (Tabatabai, 1994). In a centrifuge tube 1g sediment, 4 ml of 1M Tris-hydrochloride buffer (pH 9.0) and 1 ml 0.2M p-NPP (*Sigma*) get mixed immediately for 2-3 seconds in a Vortex mixer and then incubated in dark at 22 °C for 2 hours. At the incubation end, the reaction gets stopped and color is developed by an addition of 1 ml 0.5 M $CaCl_2$ and 4 ml 0.5M NaOH. The sample is centrifuged at 3000 rpm for 10 minutes in order the sediments to be pelleted. The supernatants are measured spectrophotometrically (*CECIL 3021*) at 420 nm. Absorbance readings are converted to μg p-NP per mg dry dead organic matter per hour by means of a p-NP standard curve. A blank sample is prepared replacing the p-NPP from the reaction mixture with 1ml 0.2M Tris buffer. All samples get analyzed in triplicate and average values are calculated.

Six sediment samples, one from each of the port's basins (points 2, 5, 8, 11 and 14) and one referent point situated outside of the port area are subjected to X-ray fluorescent and XPS analyses. Energy dispersive X-ray fluorescence method is used for simultaneously detection of 32 elements in a

sediment sample. The following spectrometric systems are applied: a) Si (Li) detector with 25 μ Be window and 170 eV energy resolution at 5.9 keV Mn-Ka line (PGT); b) Si pin diode detector, Peltie cooling, with 7μ Be window and 140 eV (KETEK); c) Si pin diode detector, Peltie cooling, with 7μ Be window and 170 eV energy resolution at 5.9 keV Mn-Ka line. Specialized software (X-Ray Fit) is used for spectrum accumulation, data processing, qualitative and quantitative analyses. Calibration is performed on the base of the International Standard marine sediment GM8 (IAEA). Detection limits for the different elements are between 1 and 10 μg/g.

**RESULTS AND DISCUSSION**

The Bourgas bay is a subject to intensive human impact because of the close proximity of Bourgas town, its port and industrial complexes along the beach. The anthropogenic activities cause a significant pollution of the bay with different types of contaminants, mainly petroleum hydrocarbons, heavy metals and detritus. The hypoxia (except the old harbor), low values of ORP even negative in some stations, concentrations of $NH_3$-N exceeding the threshold, as well as high values of inorganic phosphorus forms ($PO_4$-P) are indicative for the eutrophic character of port water and the Bourgas Bay. Most nutrient loaded basin of the harbor aquatory is the Container terminal, where water and sediment quality are under the impact of the Vaya Lake and slow water mass exchange.

The sediments in the Bourgas bay memorized the pollution history of the sea water. In spite of the natural background levels of heavy metals in the sediments due to the mineral weathering and the soil erosion, the port activities could accelerate their accumulation. The data obtained show that the Bourgas bay sediments are loaded with heavy metals and the most abundant of them are copper (Cu), zinc (Zn), manganese (Mn), strontium (Sr) and lead (Pb). The sediment analyses determine high concentrations of Cu, Zn and Mn in samples 5, 11 and 14 (Figure 2 and Figure 3).
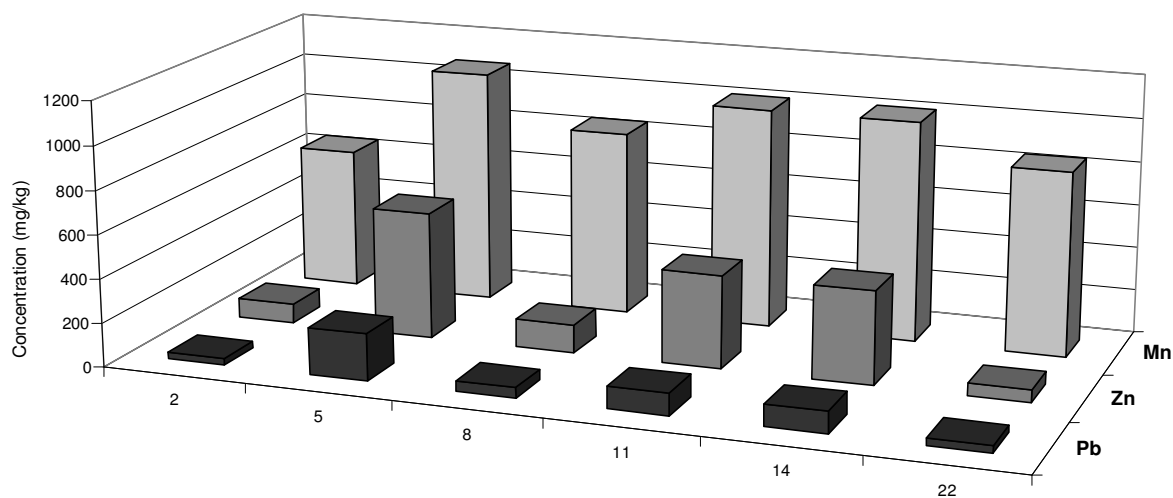


**FIGURE 2.** Concentrations of Pb, Zn and Mn in the sediments collected from the sampling points 2, 5, 8, 11, 14 and 22 of the Bourgas bay.

The concentration of Cu in the sediments of the Bourgas bay basins exceeds from 7 to 26 times that of the reference station (32 ppm), and station 11 located in the Ro-Ro terminal is the most polluted. The concentration of Zn exceeds on the average 5 time those of the control station. Most of the radionuclides recorded in the sediment samples, except Sr, have low and relatively equal concentrations across the sea bottom indicating their natural background origin, and therefore, a negligible adverse effect on benthic organisms could be expected.

The data of total petroleum hydrocarbons, presented in Figure 4, show their high level in the Bourgas bay sediments, up to 8.97 mg/g dry sediment. Concentration of total hydrocarbons higher than 0.5 mg/g sediment is indicative for petroleum pollution, while sediments containing less than 0.01 mg/g hydrocarbons could be considered as unpolluted. In accordance to this, the sediments in stations 4, 7, 10, 12, 19, 22 and 23 are considered as unpolluted, those in stations 8 and 9 as low polluted and the rest as heavily polluted. Totally, the sediment in the basin of the Container terminal is most impacted by oil pollution.

The total hydrocarbons contributed up to 8% to the total organic matter content of the sediments of the Bourgas bay, except in station 2 - 11% of the total organic matter.
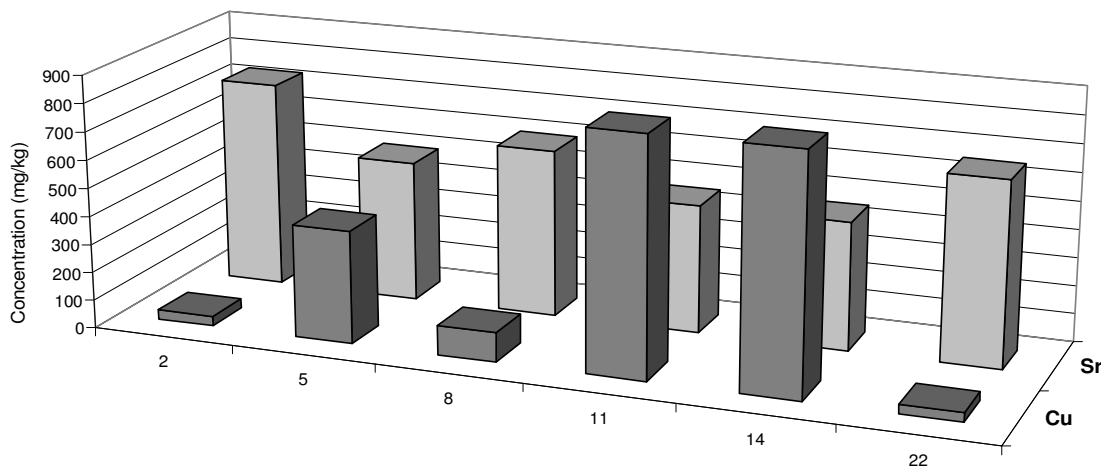


**FIGURE 3.** Concentrations of Cu and Sr in the sediments collected from the sampling points 2, 5 ,8 , 11, 14 and 22 of the Bourgas bay.
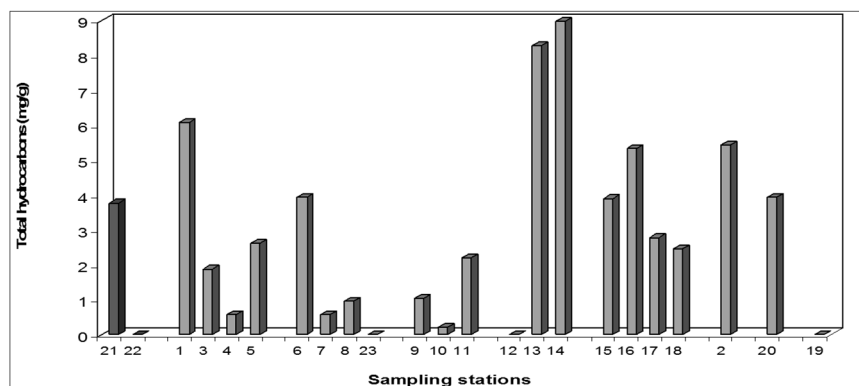


**FIGURE 4.** Concentrations of total hydrocarbons (mg/g dry weight) in the Bourgas bay sediments.

Organic matter accumulation at the sea bottom is an indicator both for organic pollution and recycling rate of nutrients turnover. Many of the sea pollutants, as well as detritus, normally deposit partially or completely unchanged, and organic matter accumulation and its nature impact on bacterial transformation activity. In most of the sampling stations of the Bourgas Bay, the sea bottom is muddy, and rich of organic matter, except stations 19 and 21 (sandy). The organic matter content varies from 28 mg/g (station 20) to 372 mg/g dry sediment (station 13), (Figure 5). The sediments of the Container terminal (stations 12 ÷ 14) are highly organic polluted, as well as station 19, where a decayed biomass of mussels is observed.

The high organic matter concentration in the sediments of the Container terminal is an indicator of the Vaya lake adverse effect and a result of the low self-purification capacity of the basin. The eutrophication and pollution of Bourgas Bay dates since the beginning of the industrialization of the region (1965-1970) and continues till the 1990's. During this long-lasting period the marine communities changed - the sensitive species reduced their numbers or completely vanished, while the resistant ones flourished being well adapted to the new environment created as a result of the human activity. Pollution and eutrophication of the Bourgas Bay, decrease in water transparency, hypoxia and reduction of hydrobiota diversity, low abundance of some species and expansion of others are reported by many researchers (Kamburska & Valcheva, 2003; Dencheva 2010; Moncheva, 2002).
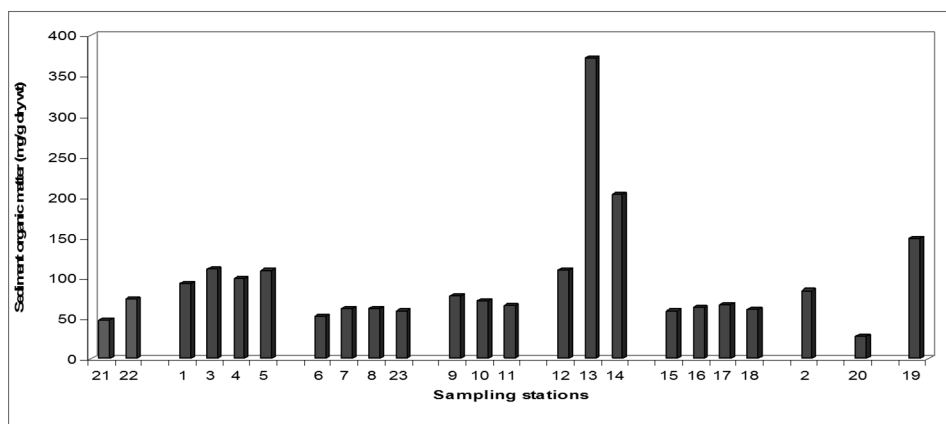


**FIGURE 5**. Organic matter content in the sediments of the Bourgas bay basins.

Because the activity of sediment bacteria is important in detritus mineralization and nutrient cycles, and in detoxication of pollutants as well, it was checked if the port and industrial activity have an impact on the transformation of the organic phosphate compounds. Alkaline phosphatase represents a key enzyme in nature, since it allows P regeneration as dissolved inorganic orthophosphate from phosphoesters. Usually AP is an inducible enzyme, however, it could be a constitutive enzyme or produced by C-limited bacteria in response to insufficiently available organic carbon and it may contribute to organic P and C cycling simultaneously. Therefore, AP activity of the sediment bacterial communities is sensitive to pollution taking into account the importance of organic matter degradation.
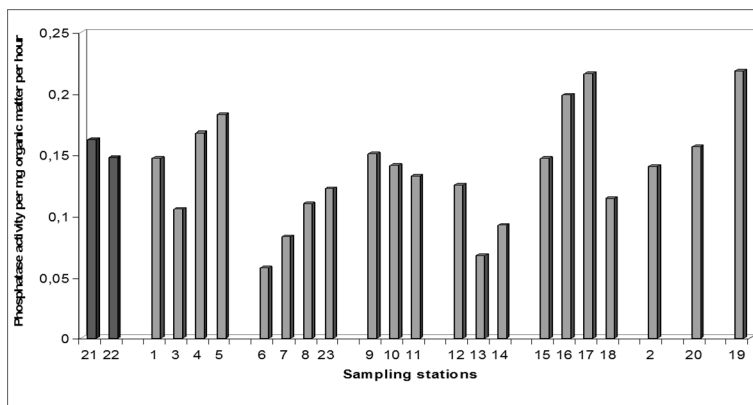


**FIGURE 6.** Bacterial phosphatase activity (μg/mg organic matter/h) in the sediments of the sampling stations.

The AP activity (μg/mg sediment organic matter/h) of the sediment bacterial communities in the basins of the Bourgas bay is relatively stable and equal to that of the reference points 21 and 22, (Figure 6). The only exceptions are the sediments in terminal 2A (points 6÷8) and the Container terminal (points 13 and 14), where bacterial AP activity is reduced circa 40%. The stability of the bacterial AP activity across the sea bottom is a result of the persistence and the long lasting history of pollution, and of the capacity of the sediment bacterial communities to adapt to the new created environment changing their structure. The sediment bacterial communities in the basins of the Container terminal and terminal 2A could not overcome the anthropogenic stress resulting in an inhibited AP activity, including the capacity to decompose organic matter and organic phosphoesters, and therefore, a reduced share in the nutrient cycles. The variability of bacterial AP activity could be a result of sea bottom heterogeneity manifested in the different rates of accumulation of organic matter and pollutants.

The data demonstrate that the sediments in the basin of the Container terminal are unfavorable for bacterial growth, while the low bacterial AP activity in the sediments of terminal 2A might be a result of the toxicity of Zn, which concentration is the highest (despite a very likely impact of some unstudied environmental/anthropogenic factors). The correlation coefficient $r = -0.62$ (p < 0.05) between bacterial AP activity and the concentration of hydrocarbons suppose a moderate adverse effects of petroleum pollution on activity of the sediment bacteria, nevertheless their capacity to utilize them as a nutrient source. The values of correlation coefficients between AP activity and the concentrations of the heavy metals varies from low (Cu, Zn, Mn) to moderate (Cr and Sr; $r$ of -0.49 ÷ -0.58). The ecological state of sediment bacterial communities (expressed by bacterial AP activity) could be assessed as moderate (Container terminal and Terminal 2A) to good (terminal East, terminal Ro-Ro, Oil terminal and private ports).

## CONCLUSIONS

The analyses of the sediments taken from various points of the Bourgas bay show a different level of pollution depending on the pollutant type. The level of total hydrocarbons in most of the sediment samples is higher than 0.5mg/g, as the sediments in the Container terminal and Oil terminal are the most polluted. The sediment in the Container terminal basin has the highest organic content. The sediments of the port basins are polluted with heavy metals. The concentration of Cu exceeds 10 times at an average those of the control station, while the Zn content – 5 times. The sediments in basins of terminal Ro-Ro and terminal East are the most polluted with Cu and Zn.

Alkaline phosphatase activity of the sediment bacterial communities is relatively stable across the Bourgas port basins. An adverse effect of anthropogenic stress on sediment bacterial communities is recorded only in the basins of the Container terminal (nutrient load) and terminal 2A, where AP activity is inhibited by 40%. The analyses of the sediments in various points of the Bourgas bay show different level of pollution with substances of low toxicity, which allows the biological species to adapt and to develop resistance capacity to environmental stress.

## ACKNOWLEDGEMENTS

## REFERENCES

Dencheva K. 2010. "State of macrophytobenthic communities and ecological status of the Varna Bay, Varna lakes and Burgas Bay", *Phytologia Balkanica,* 16(1):43-50.

Kamburska L.T. and E.Valcheva. 2003. "On the peculiarities of the zooplankton spatial distribution in Burgas Bay - May, 1996". *In Proceedings of the Institute of Oceanology, Varna*, vol. 4:124-132.

Kaurichev I.S. 1980. "Turin's method of soil organic matter analysis" (in Russian). *Manual of Pedological Practice*, Kolos, Moscow, 212-214.

Kenarova A. and G.Radeva. 2010. "Effects of copper and zinc on soil microbial enzymes", *Comptes rendus de l'Academie bulgare des Sciences*. 63(1): 105-112.

Moncheva S., V. Doncheva, G. Shtereva, L. Kamburska, A. Malej and S. Gorinstein. 2002. "Application of eutrophication indices for assessment of the Bulgarian Black Sea coastal ecosystem ecological quality". *Water Sci. Technol*., 46(8): 19-28.

Neddermann K. and M. Nausch. 2007. "Effects of organic and inorganic nitrogen compounds on the activity of bacterial alkaline phosphatase". *Aquatic Ecology*. 38(4): 475-484.

Tabatabai M.A. 1994. "Soil enzymes". Methods of Soil Analysis, Part 2. Microbiological and Biochemical Properties. (R.W.Weaver, J.S.Angle & P.S.Bottomley, Eds.). *Soil Science Society of America,* Madison, WI, pp.755.

# IN SITU REMEDIATION OF CONTAMINATED SEDIMENTS – ACTIVE CAPPING TECHNOLOGY

*Anna Sophia Knox*

(Savannah River National Laboratory, Aiken, SC, 29808, USA)

Active capping is a relatively new approach for treating contaminated sediments. It involves applying chemically reactive amendments to the sediment surface. The main role of active caps is to stabilize contaminants in contaminated sediments, lower the bioavailable pool of contaminants, and reduce the release of contaminants to the water column. In addition, downward migration of the amendments used in active caps can neutralize contaminants located deeper in the sediment profile; i.e. in the zone of influence (ZOI). Metals are common contaminants in many marine and fresh water environments as a result of industrial and military activities. The mobile, soluble forms of metals are generally considered toxic. Induced chemical precipitation of these metals can shift toxic metals from the aqueous phase to a solid, precipitated phase which is often less bioavailable. This approach can be achieved through application of sequestering agents such as rock phosphates, organoclays, zeolites, clay minerals, and biopolymers (e.g., chitosan) in active capping technology. Active capping holds great potential for a more permanent solution that avoids residual risks resulting from contaminant migration through the cap or breaching of the cap. In addition to identifying superior active capping agents, research is needed to optimize application techniques, application rates, and amendment combinations that maximize sequestration of contaminants. A selected set of active capping treatment technologies has been demonstrated at a few sites, including a field demonstration at the Savannah River Site, Aiken, SC. This demonstration has provided useful information on the effects of sequestering agents on metal immobilization, bioavailability, toxicity, and resistance to mechanical disturbance.

# GLOBAL CHANGE

# CLIMATE CHANGE VULNERABILITY ASSESSMENT BY OUTRANKING METHODS: HEAT STRESS IN SYDNEY

*Fahim Tonmoy* and Abbas El-Zein

(School of Civil Engineering, University of Sydney, NSW 2006, Australia)

**ABSTRACT:** Climate Change Vulnerability Assessment (CCVA) allows policymakers to incorporate climate futures in planning. Indicator-based vulnerability rankings are widely-used and sometimes contested forms of risk assessment. One of the challenges of indicator-based vulnerability metrics is to combine multiple indicators from both the biophysical and socioeconomic domains into indices of vulnerability for a given climatic stress, to generate a ranking of vulnerabilities. The predominant aggregation approach in the literature is based on multiple-attribute utility theory (MAUT). Scholars have critiqued this approach as theoretically flawed because a) it requires the conversion of incommensurable indicators into comparable scales; b) does not account for different types of uncertainty often present in the analysis and c) produces only a linear, threshold-free scaling of the effects of an indicator on vulnerability. In this paper, we develop an analogy between multi-criteria decision-analysis (MCDA) and Indicator-based Vulnerability Assessment (IBVA) showing that the two problems are structurally similar and share the features of incommensurability and fuzzy data. We argue that a set of techniques called Outranking Methods, based on a Condorcet approach and developed in MCDA, offer a more theoretically sound approach to aggregation. Hence, we redefine IBVA as a fuzzy problem and introduce concepts of *thresholds of vulnerability difference*, mirrored on MCDA, to quantify fuzziness. We use an outranking method, ELECTRE III (developed by Roy and his colleagues), to assess the vulnerability to heat stress of 15 local government areas in metropolitan Sydney, where heat-related mortality may be a significant public health threat. We apply different thresholds in the model, compare the resulting rankings and find that the use of dominance thresholds generates significantly different rankings compared to MAUT. Finally, we suggest further developments of the proposed methodology to integrate non-linearities in the relationship between vulnerability and indicator, and apply the outranking framework to a multi stakeholder setting of vulnerability assessment.

## INTRODUCTION

Anthropogenic climate change is projected to lead to increases in global average temperatures, a rise in sea levels, significant changes to the hydrological cycle as well as more frequent extreme events such as droughts, floods and heatwaves. Assessing the risk to populations and engineering infrastructures from exposure to these hazards has therefore emerged over the last decade as an important field of research. The purpose of such research is to provide guidance on the development of possible adaptation measures and the allocation of adaptation resources (Füssel, 2007). Concurrently, the concept of vulnerability has been used as a way of combining the physical dimensions of risk exposure with the socio-economic and institutional processes that moderate the impacts of the hazard in question, dampening or amplifying its effects. The most commonly used framework of vulnerability is the one proposed by the International Panel on Climate Change (IPCC) which recognises three dimensions of vulnerability, namely exposure, sensitivity and adaptive capacity, with the first generally referring to the

strength of the hazard, while the second and third attempt to reflect its complex repercussions in human societies (Eriksen and Kelly 2007; Parry 2007).

Indicators have been widely used as one of the simplest possible approaches to the quantification of vulnerability. However, one of the most significant methodological challenges of Indicator-based Vulnerability Assessment (IBVA) is to convert a selected set of indicators into a ranking of comparable socio-ecological systems, according to their vulnerabilities to one or more climate hazards. This process of aggregation is usually performed on the basis of multi-attribute utility theory (MAUT). It assumes complete compensation between incommensurable indicators, converts non-linear relationships into linear, monotonic ones and allocate a weight to each indicator often without recourse to scientific evidence. For further details on these methodological challenges, readers are referred to Füssel (2007), Hinkel (2011), El-Zein and Tonmoy (2012). On the other hand, the older field of Multi-Criteria Decision Analysis (MCDA) has faced similar challenges and benefited from a longer time span to develop solutions to them, including the so-called Outranking Methods.

In this paper, we build an analogy between MCDA and IBVA in order to reformulate IBVA problems within an outranking framework. We then apply an outranking method, ELECTRE-III, to assess the relative vulnerabilities to heat stress of 15 local government areas (LGA) in metropolitan Sydney.

## MCDA AND IBVA

**Analogy between MCDA and IBVA Problems:** The problem of aggregating a number of vulnerability indicators to generate vulnerability rankings in IBVA can be structured as follows. Let $s_j=\{s_1, ...., s_n\}$ be a set of n comparable socio-ecological systems (SES) (e.g., geographical areas, communities, ecosystems etc.) which need to be ranked according to the vulnerability of a valued attribute (e.g., health, economic well-being, productivity etc.) to one or more climate hazards (e.g., increase in average temperatures, rise in sea level, increased frequency of flooding etc.) based on a set of m indicators $I_i=\{I_1, ..., I_m\}$. Each indicator has a linear or non-linear relationship to vulnerability, though it is not always possible to characterize this relationship with precision. A vulnerability matrix $I_{ij}$ (i=1,m; j=1,n) is constructed with each column representing an SES, each row a given indicator and $I_{ij}$ denoting the value $I_i$ for $SES_j$.

MCDA is a process of structuring multiple-stakeholder decision-making problems involving a number of alternatives judged according to a number of conflicting criteria, in order to generate rankings of all alternatives by order of preference. Let $O_j=\{o_1, ...., o_n\}$ be a set of n decision options or alternatives (e.g., different routes for a future highway; different waste management solutions etc) which need to be ranked based on their performances relative to a set of m conflicting criteria $C_i=\{C_1, ..., C_m\}$. $C_i$ may include all the criteria selected for the analysis or may be divided into categories of criteria (e.g., financial, environmental, social etc.). A decision matrix of scores $R_{ij}$ (i=1,m; j=1,n) is constructed with each column representing an alternative and each row a given criterion, with $R_{ij}$ denoting the performance of alternative $O_j$ on criterion $C_i$.

Aggregation is required in both IBVA and MCDA. Hence, if each indicator/criterion, independently from the others, yields the same ranking of SESs/alternatives as all other indicators/criteria, we have a non-conflicting indicators/criteria problem, ranking is resolved and no aggregation is needed. This case is of course idealistic and in both IBVA and MCDA, the indicators/criteria are almost always conflicting. Depending on the type of aggregation used, a set of weights or votes $w_i=\{w_1, ...., w_m\}$ may be allocated to the set of indicators/criteria, with $w_i$ reflecting the importance of indicator $I_i$ /criteria $C_i$ relative to other indicators and criteria. Table 1 draws an analogy between the structures of MCDA and IBVA problems, as defined above and clearly shows the similarities. The ranking of alternatives/SESs is

the primary objective in both types of problems. In addition, the two problems share features of fuzziness of data and incommensurability, namely that a deficiency in one indicator/criterion cannot be compensated for by a gain in another indicator/criterion (El-Zein and Tonmoy 2012).

***Dissimilarities between MCDA and IBVA Problems:*** We have highlighted the structural similarities between MCDA and IBVA, which are strong enough to warrant cross-fertilization of approaches to the two problems. However, some fundamental differences between them must also be kept in mind. Three such dissimilarities are worth noting. First, In IBVA, the analysis framework refers to the concept of vulnerability which is difficult to define with precision and cannot be measured because it is a social construct, not a physical phenomenon (Hinkel 2011). There is no equivalent difficulty in MCDA. Second, while the outcomes of IBVA point to vulnerable socio-ecological systems, they do not necessarily yield a specific course of action, rather a narrowing down of options which requires further analysis, usually to determine suitable adaptive policy. Third, the *a priori* choice of alternatives and criteria in MCDA is often a political process and not just a technical one, because it can partly pre-determine the outcome of the analysis (e.g., which alternatives have been left out and why? how are the criteria determined and what weights are they given?).

**Table 1: Analogy between IBVA and MCDA problems:**

| | IBVA | | MCDA | |
|---|---|---|---|---|
| **Problem Definition** | To rank socio-ecological systems according to the vulnerability of a valued attribute to one or more climate hazard | | To rank decision alternatives according to their performances on a set of criteria | |
| | Socio-Ecological Systems | $s_j = \{s_1, \ldots, s_n\}$ | Decision Alternatives | $O_j = \{o_1, \ldots, o_n\}$ |
| | Indicators | $I_i = \{I_1, \ldots, I_m\}$ | Decision Criteria | $C_i = \{C_1, \ldots, C_m\}$ |
| | Vulnerability Matrix | $I_{ij}$ (i=1,m; j=1,n) | Decision Matrix | $R_{ij}$ (i=1,m; j=1,n) |
| | Indicator Weights/ Votes* | $w_i = \{w_1, \ldots, w_m\}$ | Criteria Weights/ Votes* | $w_i = \{w_1, \ldots, w_m\}$ |
| **Problem Features** | Input from multiple experts and stakeholders | | Input from multiple decision-makers, experts and stakeholders | |
| | Inconvertibility of indicators | | Incommensurability of criteria | |
| | Uncertainties (fundamental; fuzziness; data) | | Uncertainties (benefits and impacts; fuzziness; data) | |
| **Thresholds of Difference** | Indifference Threshold $q_i$ | | Indifference Threshold $q_i$ | |
| | Relative Vulnerability Threshold $p_i$ | | Preference Threshold $p_i$ | |
| | Dominance Threshold $v_i$ | | Veto Threshold $v_i$ | |

*"weights" in MAUT methods become "votes" in outranking methods

In IBVA, it is the choice of scale and boundaries of socio-ecological systems, including institutional boundaries, that may prejudice the analysis and play out in the politics of the assessment exercise (e.g., who's responsible for, and who makes decisions about, vulnerability and adaptation? how is the choice of socio-ecological units made and why?). We emphasize, therefore, that the analogy between the two problems is drawn here for the specific purpose of aggregation and ranking, and that any extension of the analogy beyond this aim would require further justification.

## OUTRANKING FRAMEWORK FOR IBVA PROBLEMS

A set of methods evolved from the late 1970s to the 1990s, called outranking procedures (OP), as an alternative to MAUT in infrastructure and environmental decision-making problems to deal with the problem of incommensurate criteria and data uncertainty. In the following sections, we build an IBVA framework using one of the widely used outranking methods ELECTRE-III developed by Roy (1968).

We assume, without loss of generality, that the higher the value of the indicator, the more vulnerable the SES. For each pair of SESs, we can define three different categories of relative vulnerability:

a) b is strictly more vulnerable than a according to criterion $I_i$ if and only if $I_{ib} - I_{ia} \geq p_i$, where $p_i \geq 0$ is the *relative vulnerability threshold for indicator $I_i$*;

b) b is indifferent to a according to criterion $I_i$ if and only if $|I_{ib} - I_{ia}| \leq q_i$, where $q_i \geq 0$ is the *indifference threshold for indicator $I_i$*;

c) b is weakly more vulnerable than a according to criterion $I_i$ if and only if $q_i < I_{ib} - I_{ia} < p_i$.

The ELECTRE III ranking process is conducted in three stages (e.g., El Hanandeh and El-Zein, 2010):

**Stage 1. Concordance and Discordance Matrices:** A concordance matrix for each indicator $I_i$ is defined by:

$$c_i(a,b) = \begin{cases} 0 & \text{if } I_{ib} - I_{ia} \geq p_i \\ \frac{p_i - (I_{ib} - I_{ia})}{p_i - q_i} & \text{if } q_i < I_{ib} - I_{ia} < p_i \\ 1 & \text{if } I_{ib} - I_{ia} \leq q_i \end{cases} \tag{1}$$

$c_i(a,b)$ is a measure of the truth of the statement that "a is at least as vulnerable as b according to indicator I". The discordance matrix for each indicator I is defined by:

$$d_i(a,b) = \begin{cases} 0 & \text{if } I_{ib} - I_{ia} \leq p_i \\ \frac{(I_{ib} - I_{ia}) - p_i}{v_i - p_i} & \text{if } p_i < I_{ib} - I_{ia} < v_i \\ 1 & \text{if } I_{ib} - I_{ia} \geq v_i \end{cases} \tag{2}$$

where $v_i$ is called *dominance threshold* for indicator $I_i$ and reflects a difference between indicator values above which b becomes more vulnerable than a, *regardless of the performances of a and b on other indicators*. We will refer to $q_i$, $p_i$ and $v_i$ collectively as *thresholds of difference* to emphasize that they provide a reference to disparities between indicators rather than the indicators themselves.

**Stage 2. Outranking Matrix:** The statement "a is at least as vulnerable as b" (denoted aVb) is true provided:

i. a "majority" of indicators supports it (concordance principle); and
ii. no single indicator vetoes it (discordance principle).

The concordance principle can be measured by the following concordance index:

$$c(a,b) = \frac{1}{\sum_{i=1}^{m} w_i} \sum_{i=1}^{m} w_i c_i(a,b) \tag{3}$$

where $w_i$ is a vote for indicator $I_i$, applied to the pair-wise comparisons, rather than a weight in a global utility function. An outranking matrix combines the concordance and discordance principles in order to quantify the degree to which aVb is true. It is given by:

$$S(a,b) = \begin{cases} c(a,b) & \text{if } d_i(a,b) \leq c(a,b) \ \forall i = 1, m \\ c(a,b) \prod_{i \in I_v(a,b)} \frac{[1-d_i(a,b)]}{[1-c(a,b)]} & \text{otherwise} \\ \quad \text{where } I_v(a,b) \text{ is the set of indicators for which } d_i(a,b) > c(a,b) \end{cases} \tag{4}$$

**Stage 3. Distillation and Ranking Procedures:** The most vulnerable SES is the one that outranks the largest number of SESs and is outranked by least. Hence, S(a,b) is used next to build two partial, descending and ascending pre-orders $D_1$ and $D_2$, and a final ranking is achieved as $D_1 \cap D_2$.

**DETERMINATION OF THRESHOLDS OF DIFFERENCE**

In aggregating indicators for an IBVA problem, we argue that an outranking approach has stronger validity than additive MAUT because, in an outranking method, no conversion of indicators into a normalized scale is performed and the analyst is compelled to spell out assumptions about compensation and uncertainties at the outset, through the definitions of $q_i$, $p_i$, $v_i$. The determination of thresholds $q_i$, $p_i$ and $v_i$, and votes $w_i$ is therefore an important part of problem definition. In vulnerability terms, they can be defined, and determined, by the following questions:

1. All other indicators being equal, what is the difference in values of indicator $I_i$ for two SESs below which the vulnerabilities of the two systems are the same? (indifference threshold $q_i$);
2. All other indicators being equal, what is the difference in values of indicator $I_i$ for two SESs above which one system is strictly more vulnerable than the other? (relative vulnerability threshold $p_i$);
3. What is the difference in values of indicator $I_i$ for two SESs above which one system is strictly more vulnerable than the other AND no advantage by any other indicator, or combination of other indicators, can compensate for it? (dominance threshold $v_i$).
4. In determining whether a 'majority' of indicators supports the statement that one SES is at least as vulnerable as another, what is the strength of a 'vote' by indicator $I_i$ relative to a reference indicator? (vote $w_i$).

**RESULTS**

We applied the outranking framework to rank 15 coastal councils of urban Sydney (Figure 1) according to their relative vulnerabilities during a heat wave. We adapted a vulnerability model from Preston et al (2008) who simulated exposure, sensitivity and adaptive capacity using a total of 22 indicators (e.g., average January maximum temperature, number of days in which temperature is greater than $30^0$C, % of vegetation in the area, % of residents over-65 or below 4 years of age, income and education status, access to information). A measure of error for each indicator was inferred or collected from data descriptors and methodologies provided by the sources, and used to derive thresholds.

Table 2 shows vulnerability rankings for the 15 LGAs for the base case (which does not include any dominance threshold). Rockdale, Botany Bay and Randwick are ranked most vulnerable and Mosman, Pittwater and Hornsby least vulnerable. The former three all have relatively low adaptive capacity, although Botany Bay and Rockdale's exposures are ranked high as well. Hornsby and Pittwater have large areas covered with vegetation and therefore low urban heat island effect.

**Table 2: Vulnerability ranking of 15 coastal councils of Sydney using ELECTRE III and the effects of changing thresholds on rankings (1: most vulnerable; SCF: Spearman Correlation Factor)**

|  | Base Case* $q_i, p_i,$ $v_i=\infty$ | $0.5q_i$ $0.5p_i$ | $2q_i$ $2p_i$ | $v_i=2p_i$ |
|---|---|---|---|---|
| SCF Relative to Base Case ELECTRE III | 1 | 0.97 | 0.96 | 0.82 |
| SCF Relative to Base Case MAUT | 0.94 | 0.93 | 0.93 | 0.73 |
| Botany Bay | 2 | 2 | 1 | 2 |
| Hornsby | 13 | 12 | 12 | 12 |
| Leichhardt | 9 | 8 | 9 | 6 |
| Manly | 11 | 11 | 9 | 6 |
| Mosman | 15 | 14 | 12 | 14 |
| North Sydney | 6 | 6 | 6 | 6 |
| Pittwater | 14 | 15 | 15 | 15 |
| Randwick | 3 | 3 | 3 | 6 |
| Rockdale | 1 | 1 | 1 | 1 |
| Sutherland | 6 | 5 | 6 | 3 |
| Sydney | 5 | 6 | 5 | 6 |
| Warringah | 8 | 9 | 8 | 6 |
| Waverley | 4 | 4 | 3 | 3 |
| Willoughby | 11 | 13 | 9 | 12 |
| Woollahra | 9 | 9 | 12 | 3 |

MAUT and ELECTRE III yield similar but not identical rankings. This is expected for the base case because the choice of $q_i$ and $p_i$ reflect a relatively small amount of uncertainty, no non-linearity and no dominance ($v_i=\infty$). The sensitivity of ELECTRE III rankings to thresholds of difference is also shown in Table 2. Correlation factors relative to the base case with summative MAUT, as well as ELECTRE III, are shown. Rankings are clearly robust under changes of up to 100% in $q_i$ and $p_i$ (columns 3 and 4 of Table 2). As expected, the introduction of dominance thresholds for all indicators has a bigger impact on rankings than changes in $q_i$ and $p_i$, with a Spearman correlation factor of 0.82 when $v_i=2p_i$.

**CONCLUSION**

IBVA is increasingly used by researchers and decision makers to guide climate change adaptation policy. However, data used to generate vulnerability indices is often a mix of qualitative, semi-

quantitative and quantitative data with high levels of incommensurability, fuzziness and nonlinearity. Building an analogy between MCDA and IBVA, we have shown that the two problems are structurally similar and that outranking methods, developed in MCDA to deal with problems of incommensurability and uncertainty can be used in IBVA as an aggregation technique with stronger scientific validity than the more widely used MAUT techniques. The application of outranking methods to a real vulnerability assessment problem in which thresholds of difference are derived from stakeholders and experts and the extension of the methods to problems of nonlinearity are important next steps that the authors are currently pursuing.
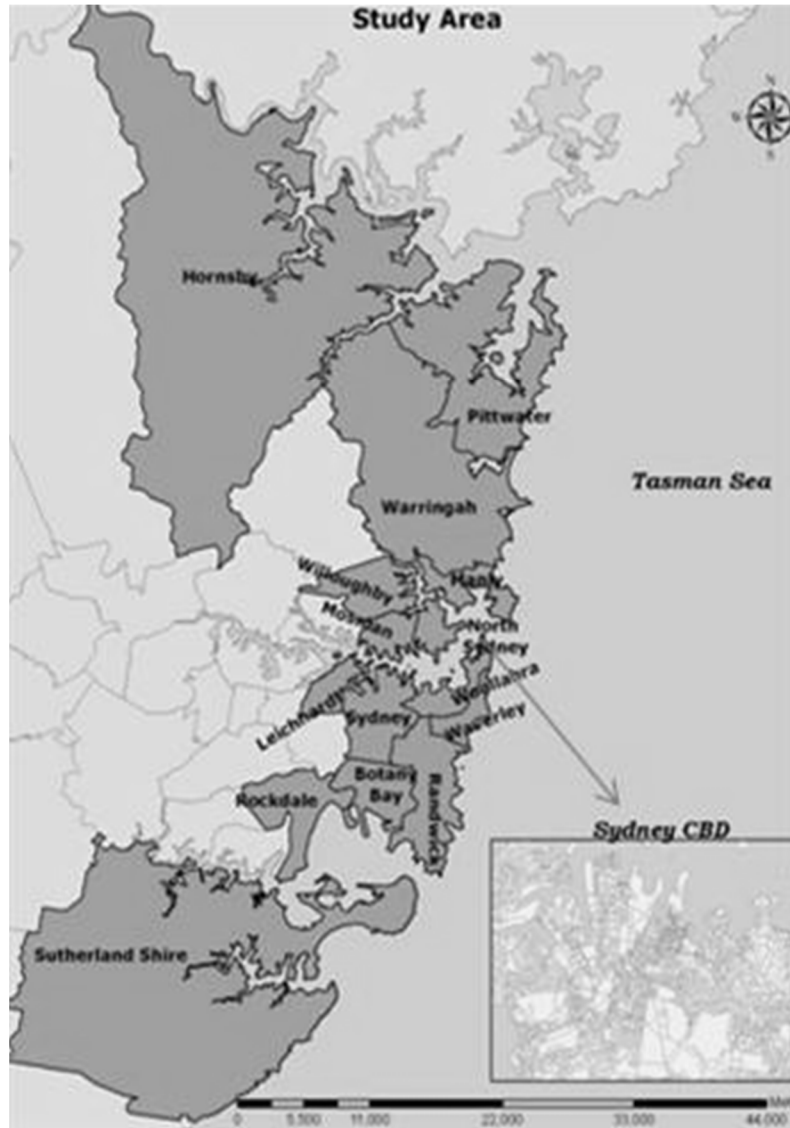


**Figure 1: Study area, 15 coastal councils of Sydney**

## ACKNOWLEDGEMENT

## REFERENCES

El-Zein, A. and F. Tonmoy (2012). "Incorporating Uncertainty and Incommensurability in Climate Change Vulnerability Assessments: An Outranking Approach." Climatic Change (Under review).

El Hanandeh, A. and A. El-Zein (2010). "The development and application of multi-criteria decision-making tool with consideration of uncertainty: The selection of a management strategy for the bio-degradable fraction in the municipal solid waste." Bioresource Technology **101**(2): 555-561.

Eriksen, S. and P. Kelly (2007). "Developing Credible Vulnerability Indicators for Climate Adaptation Policy Assessment." Mitigation and Adaptation Strategies for Global Change **12**(4): 495-524.

Füssel, H.-M. (2007). "Vulnerability: A generally applicable conceptual framework for climate change research." Global Environmental Change **17**(2): 155-167.

Hinkel, J. (2011). "" Indicators of vulnerability and adaptive capacity": Towards a clarification of the science-policy interface." Global Environmental Change **21**(1): 198-208.

Parry, M. L., O.F. Canziani, J.P. Palutikof, P.J. van der Linden and C.E. Hanson (2007). Climate Change 2007: Impacts, Adaptation and Vulnerability. Contribution of Working Group II to the Fourth Assessment Report of the Intergovernmental Panel on Climate Change. Cambridge, UK, Cambridge University Press

Preston Benjamin L. , T. F. S., Cassandra Brooke, Russell Gorddard, Tom G. Measham, Geoff Withycombe, Beth Beveridge, Craig Morrison, Kaihleen Mclnnes, Deborah Abbs (2008). Mapping Climate Change Vulnerability in Sydney Coastal Council Group. Report Available at "http://www.csiro.au/resources/SydneyClimateChangeCoastalVulnerability.html" [19th September 2011].

Roy, B. (1968). "Ranking and selection in the presence of multiple viewpoints (the ELECTRE method) (Classement et choix en présence de points de vue multiples (la méthode ELECTRE))'." RIRO **8**: 57-75.

# QUANTIFYING CLIMATE CHANGE AND SEA LEVEL RISE RISKS TO NAVAL STATION NORFOLK

*Kelly A. Burks-Copes* and Edmond J. Russo (Environmental Laboratory, US Army Engineer Research and Development Center, Vicksburg, MS)

The best available science indicates that increasing atmospheric concentrations of greenhouse gases are warming the atmosphere and the oceans at an accelerated rate. As they warm, oceans expand and glaciers melt, resulting in an overall increase in ocean volume. At the same time, many coastal shorelines are eroding and subsiding, contributing to an unprecedented rate in sea level rise. Unfortunately, coastal military operations tend to view these climate changes as strategic issues – sea level rise impacts might not be realized for several decades, uncertainties surrounding climate change cloud the issues, and appropriately-scaled tools to support risk-based decision making at the installation level are virtually nonexistent. While commanders may be situationally aware of their installation's vulnerabilities, demonstrable risk-based assessments have yet to be developed that can assist them in proactively adapting military systems, processes, and protocols to meet this pervasive challenge. To meet this challenge, the Strategic Environmental Research and Development Program (SERDP) funded an ERDC-led initiative entitled "Risk Quantification for Sustaining Coastal Military Installation Assets and Mission Capabilities (RC-1701)" to examine potential effects of sea-level rise on coastal hazards, and demonstrate the use of the ERDC's leap-ahead technology to quantify the potential risks to mission sustainability on the mid-Atlantic coast (Hampton Roads area – specifically on Naval Station Norfolk). The goal of the study is to devise a rigorous yet flexible approach to quantitatively evaluating military installation asset and mission capability risks due to a full range of sea level rise, tidal fluctuation, and storm stage-frequency hazards using probabilistic tiered risk assessments. By systematically characterizing the existing environment, predicting changes to the coastline, simulating hurricanes moving across the region, quantifying the resultant "forcings" (i.e., floodwaters, waves, winds), and constructing a dependency-based network model of the installation's assets and capabilities, the RC-1701 Team is laying the foundation to assess damages caused by tropical storms. Risk quantification is being supported by the latest innovations in storm probability analytics and high fidelity coastal wave and storm surge inundation models. These models provide robust scientific input to an innovative risk assessment analysis. Underpinning these analyses, the team has developed two independent land conversion models simulating sea level rise to capture a range of potential future long-term conditions, and has proceeded to calculate risks to mission impairment in a real-time, decision-relevant manner given these scenarios. Ultimately, these risks must be communicated to the end-users (installation planners and managers), and so the RC-1701 Team has developed a series of tables, graphics, and risk maps that transparently convey the potential not only of impairment, but duration of impairment immediately following the storms. Armed with this information, can then be communicated to the end-user in an actionable construct so that managers and policymakers can consider altering the status quo to incorporate proactive management strategies to prevent or anticipate impairments based on the risks. In effect, the capabilities developed under the RC-1701 project afford installations the opportunity to evaluate relative performance of existing conditions, future no-action conditions, as well as structural and non-structural risk mitigating alternatives to sustain military installation assets and mission capabilities at multiple scales. The final product provides a robust, scientifically defensible approach that transparently communicates risks to the end-user and helps policymakers develop guidance to promote sustainability in the face of climate change and sea level rise. Here, we provide a high-level briefing of the RC-1701 project, detailing the modeling activities underway and describing our approach to integrating these disparate metrics into a transparent, scientifically-based and robust risk assessment for the Naval Station Norfolk installation.

# RESOURCE ALLOCATION IN *BRASSICA JUNCEA* EXPOSED TO ELEVATED CO$_2$

*Neha Sharma*, Pooja Gokhale Sinha and A. K. Bhatnagar (University of Delhi, Delhi, India)
S. D. Singh (Indian Agriculture Research Institute, New Delhi, India)

Unprecedented increase in concentration of atmospheric CO$_2$ [CO$_2$] and other green house gases has led to emergence of climate change as a global environmental issue. Increased [CO$_2$] has adverse impact on the climate sensitive sectors such as agriculture and forestry. Though studies have been conducted to study the effects of elevated CO$_2$ on major crops like wheat and rice, there have been few attempts to study how oil yielding plants respond to high [CO$_2$]. Mustard, *Brassica juncea* (L.) Czern and Coss. is one of the most valued oil-yileding crops of India. In the present study, experiments were conducted on this winter crop to test the hypothesis that due to higher rate of photosynthetic product formation under CO$_2$ enrichment, and consequent higher growth rate, nitrogen demand in plant increases. Plants, therefore, are likely to allocate resources in a way to conserve nitrogen by synthesizing lesser amounts of nitrogenous compounds. Glucosinolates are important nitrogenous secondary metabolites in brassicas that play important role in plant defense. The present study was conducted to see the effects of elevated [CO$_2$] on glucosinolate concentration in mustard seeds. The study was further conducted to observe the effects of elevated CO$_2$ on plant growth and biochemical composition of seeds.

Seeds of *Brassica juncea* var. Pusa Tarak were sown in October 2010 in the Free Air CO$_2$ Enrichment (FACE) Facility at Division of Environmental Science, Indian Agriculture Research Institute (IARI), New Delhi (India). [CO$_2$] of 550 ppm was maintained in the FACE ring and control plants were grown in nearby field with all growth conditions, same as those in FACE, except for [CO$_2$]. Plants were harvested at maturity and morphological growth parameters were analyzed. Seeds obtained at harvest were analyzed for glucosinolate, protein and carbohydrate concentrations. Under elevated [CO$_2$], dry weights of shoot and root showed statistically significant increase by 97.63% and 19.3%, respectively. HPLC analysis of seeds for glucosinolates revealed statistically significant reduction in the concentration of the glucosinolates epiprogoitrin, glucoiberverin, glucobrassicanapin, glucoerucin and gluconapin by 63.74, 78.69, 53.34, 85.31 and 6.68 respectively under CO$_2$ enrichment. Spectrophotometric analysis of seeds of plant grown in CO$_2$ enriched conditions showed statistically significant higher concentration of total carbohydrates by 2.11%, whereas, concentration of soluble protein was significantly lower by 12.10%.

CO$_2$ enrichment increases the rate of carbon fixation that leads to higher carbon:nitrogen ratio in plant tissue. Further, a higher growth rate under CO$_2$ enrichment leads to increase in demand for mineral nutrients, particularly nitrogen. Decreased concentration of nitrogenous compounds observed in the present study indicates that as the C:N ratio increases, plant conserves nitrogen by reallocating its resources and reducing the synthesis of nitrogen containing compounds such as glucosinolates and protein.

# CLIMATE CHANGE SCENARIOS FOR ARAGON (SPAIN) USING A TWO-STEP ANALOG/REGRESSION DOWNSCALING METHOD

Jayme Ribalaygua[1], Mª Rosa Pino Otín[2], Luis Torres[1], Javier Pórtoles[1], Emma Gaitán[1], Esther Roldán[2]

(1) Climate Research Foundation, Madrid, Spain; (2) San Jorge University, Zaragoza, Spain

Nowadays, the Global Circulation Models (GCM) are the main tools to simulate the more relevant aspects of the future climate. These models are able to reproduce the general features of the atmospheric dynamics but their low resolution (about 200 Km) does not allow a proper simulation of lower scale meteorological effects. Downscaling techniques allow overcoming this problem by adapting the model outcomes to local scale. A statistical downscaling technique based on a two-step analogue method has been developed by the Climate Research Foundation (FIC). This methodology has been broadly tested on national (Spain) and international environments (ENSEMBLES) leading to excellent results on forecast climate models.

Several forecast climatic scenarios have been created for Aragon (Spain) by implementing the technique developed by FIC. The database utilised in these come from meteorological records provided by 267 temperature register stations and 563 precipitation register stations from the Spanish Meteorology Authority (AEMET) located in the research area, from the European re-analysis Era40 and from five different Global Circulation Models (GCMs) as follows: one form the IPCC3 (Canadian CGCM2) and four from IPCC4 (Norwegian BCM2, French CNCM3, German ECHAM5 and German EGMAM). Applying more than one GCM is one of the innovations in this project. The use of different GCMs facilitates the analysis of results when several models depart from the same forces allowing the quantification of the associated uncertainty. The atmospheric fields used are those of Surface Geopotential at 500, 850 and 1000 hPa.

Previous to the generation of scenarios we have carried out a verification (assessment of the capacity of the methodology to simulate past observed climate) and a validation (assessment of the capacity of the GCM to simulate past observed climate) of temperature and precipitation. Results for the verification process are very good for temperature and acceptable for precipitation. In the validation case, results for temperature are robust while they are more uncertain for precipitations.

Future climatic change simulation scenarios have been developed for three variables (maximum temperature, minimum temperature and precipitation). The obtained results for the regionalization average from all the GCMs studied under the emissions scenario A1B suggest that the minimum and maximum temperatures for Aragon will significantly increase along the XXI century with the increase in the maximum temperatures being higher than that for the minimum temperatures. Regarding both variables the highest increase in temperatures will occur during the summer season followed by autumn, spring and winter. The forecasted increase in the maximum temperatures towards mid century (2040-2070) will be around 3 ºC in the summer and 2-2,5 ºC the rest of the year and in the case of the minimum temperatures this increase will be around 0.5 ºC lower ( 2.5 ºC for the summer and 1.5-2 ºC the rest of the year).

# DECORATING GRAPHENE SHEET WITH PALLADIUM NANOPARTICLES FOR CARBON DIOXIDE REDUCTION

*Guang Lu* and **Hui Wang** (Beijing Forestry University, Beijing, China)
Zhaoyong Bian (Beijing Normal University, Beijing, China)

**ABSTRACT:** Pd/Graphene catalysts for electrochemical reduction of carbon dioxide were prepared by means of sodium borohydride reduction of $PdCl_2$ in a graphene oxide suspension, and characterized by X-ray diffraction (XRD), transmission electron microscopy (TEM), X-ray photoelectron spectroscopy (XPS), Fourier transform infrared spectroscopy (FTIR), Raman spectra and Cyclic Voltammetry (CV). The reaction was invested in a diaphragm electrolysis device, using Pd/Graphene gas-diffusion electrode as a cathode and a $Ti/IrO_2/RuO_2$ net anode. The main product in present system was formic acid. High electrocatalytic activity of Pd/Graphene for the $CO_2$ conversion appeared. The faradaic efficiency of formic acid was 75% in 0.5 mol/ L $KHCO_3$ electrolyte.

## INTRODUCTION

Carbon dioxide, which is believed to be the largest contributor of climate change and greenhouse efforts, is the focus of people's attention at present. Many researches have been made on the electrochemical reduction of carbon dioxide because it can not only decrease carbon dioxide release, but also produce a variety of useful organic compounds such as formic acid, CO, methane, ethylene, methanol and ethanol with high current efficiency. Since $CO_2$ is the highest oxidation stage of carbon, it is chemically stable and often seen as an inert material. Electrochemical reduction is one of the methods that can overcome the high redox potential of $CO_2/CO_2^-$, -2.21 V vs. saturated calomel electrode (SCE). The electrochemical reduction of uses water as a proton sources, produces small molecule organic compounds and $O_2$. Another advantage is high energy efficiency. Because of high Faradaic efficiencies, low energy is consumed during the reduction reaction, makes the process more feasible. However, the potential for the direct electrochemical reduction of $CO_2$ is high, at least 1-2V of overpotential. To overcome the activation barrier, high effective catalyst is need. Graphene, as a one–atom-thick two-dimensional monolayer of $sp^2$-bonded carbon, has attracted tremendous attention duo to its unique properties. Moreover, with high surface area and chemical stability, graphene is regarded as future materials for designing next-generation catalysts with enhanced activity. This paper includes the preliminary results obtained in the determination of the properties of Pd catalyst support in graphene used for carbon dioxide reduction.

## MATERIAL AND METHODS

**Preparation of Pd/Graphene Catalyst and Gas-Diffusion cathode** Graphite oxide (GO) was prepared from natural graphite flakes (99.99%, 325 mesh, Qingdao Zhongtian Company) according to modified Hummers method [1, 2]. Then the $PdCl_2$ in a graphene oxide suspension was reduced by sodium borohydride. The gas diffusion cathodes were prepared according to the reported method [3].

**Procedures** Electrolysis was conducted in a terylene diaphragm cell with a volume of 100 mL. A $Ti/IrO_2/RuO_2$ net with an area of 15 cm$^2$ was used as anode. And a self- made Pd/Graphene gas-

diffusion electrode with an area of 15 cm$^2$ was used as cathode. The distance between electrodes was 3 cm. A schematic diagram of the experimental setup has been reported before [4]. The electric power was provided by a laboratory direct current power supply with current-voltage monitor. $CO_2$ was bubbled into the electrolyte for 30 min before the reaction. The gas-diffusion electrode was fed with $CO_2$ continually during electrolysis.

**Analytical Methods** Soluble products were determined using an ion chromatograph (DIONEX ICS3000) analyses by comparing the retention time of the standard reference compounds. The separation was performed using an AS-11 column and 250 mmol/L NaOH as mobile phase at the flow rate of 1.2 mL/min. The total run time was 15 min and an injection volume was 10 μL.

## RESULR AND DISCUSSION

**XRD analysis of Pd/MWNTs catalyst** The XRD patterns of graphite GO and Pd/Graphene catalysts are shown in Figure. 1. The initial graphite powder shows the typical sharp diffraction peak at 2Ө=26.6° with the corresponding d-spacing of 3.36Å. The sharp diffraction peak shows the hexagonal system crystal structure is stable. After chemical oxidation, a lower broad peak, compared to XRD pattern of graphite, was obtained at 2Ө=12.1°, indicated the successful formation of graphite oxide. The d-spacing of graphite oxide is 7.34 Å, indicated that the ordering of layers was disrupted and oxygen functional groups insert to the interplanar crystal spacing. This larger distance between GO sheets shifts the XRD peak to smaller angles, thus explaining the low broad peak at 12.1°. After chemical reduction of GO, the XRD of the resulting graphene shows the disappearance of the 12.1° peak confirming that the reduction of the GO sheets. The appearance of a new small broad peak around 2Ө=25°with the corresponding d-spacing of 3.82Å in the Pd/CRG suggests that presence of a minor component of multilayer graphene. The peak at about 40° is characteristic diffraction peak of Pd. The average size of metal particles calculated from the Pd diffraction line by using the Scherrer formula is 3.7m.
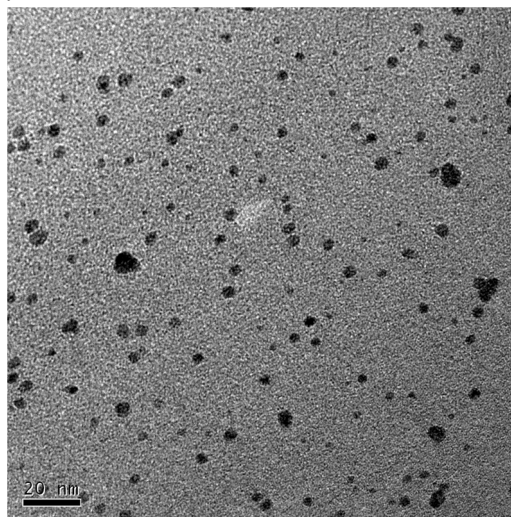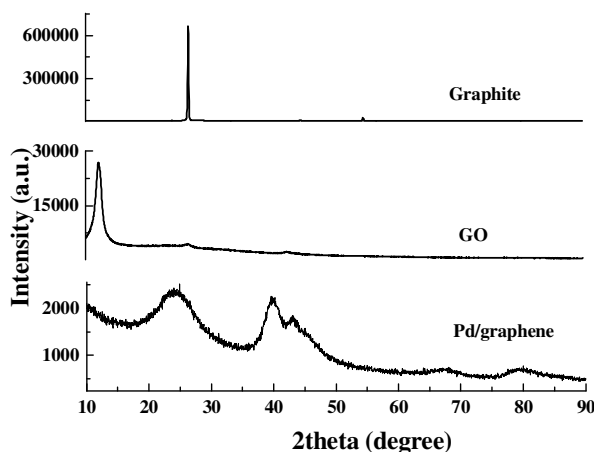


**FIGURE 1. XRD patterns of Graphite, GO and Pd/CRG catalysts**



**FIGURE 2. TM image of Pd/Graphen catalysts**

**TEM analysis of Pd/MWNTs catalyst** TEM image (Figure. 2) of Pd/CRG catalyst and its metal particle size was measured in order to estimate the geometry and the particle size of the Pd species. No obvious aggregation was detected from the image. Analysis shows a homogeneous distribution of Pd nanoparticles at graphene surface with an average particle size of 3.7nm. This conclusion agreed well with the XRD result.
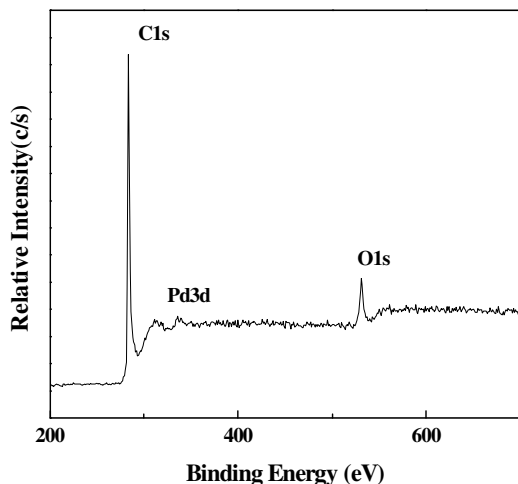
**FIGURE. 3. XPS pattern of Pd/Graphene catalysts**
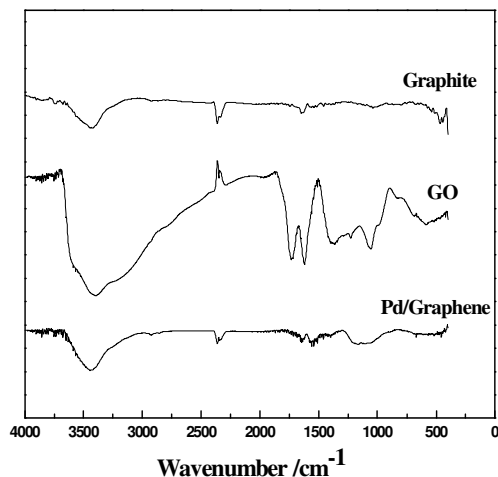


**FIGURE. 4. FTIR pattern of Pd/Graphene catalysts**

**XPS analysis of Pd/MWNTs catalyst** XPS was used to investigate the weight percentage of Pd nanoparticles in the Pd/CRG composite, as shown in Figure 3. Pd particles contented on the surface and in the interlamellar space of Pd/Graphene catalyst reached 0.3 at. %, that was 2.6 wt. %. That was comparable with the mol percentage of $K_2PdCl_4$, shows that nearly all the divalent palladium was reduced to Pd nanoparticles. The oxygen content was 8% (C: O atomic ratio 10.97:1), shows that the GO was not complete reduced to CRG. The reduction extent of GO was 82% by sodium borohydride. So FTIR was used to determination the change of functional groups in the process of preparation of the catalyst.

**FTIR analysis of Pd/MWNTs catalyst** Figure 4 shows the typical FTIR spectrums (KBr) obtain for the preparation of catalyst. Graphite has no obvious infrared absorption peak expect a small peak at 1615 corresponding to the C=C stretching vibration. The spectrum of GO are absorption bands corresponding to the C-O stretching vibration of carboxyl at 1380 $cm^{-1}$ originated from carboxylic acid, the C=O carbonyl stretching vibration at 1730 $cm^{-1}$, the C-O-C stretching vibration at 1070 $cm^{-1}$, the C=C at 1615 $cm^{-1}$ assigns to skeletal vibrations of unoxidized $sp^2$ CC bonds and 3440 $cm^{-1}$ could be due to the O-H stretching vibrations of intercalated water. In the FTIR spectra of graphene obtain after chemical treatment of GO, the C=O vibration bonds disappear, the C-O stretching bands become broader and adsorption of water was also found at 3440 $cm^{-1}$. Functional groups of O-H and C-O-C are harder to be reduced than C=O group.

**Raman spectra** Raman spectroscopy is a powerful nondestructive tool to distinguish ordered and disordered crystal structures of carbon. G band is usually assigned to the $E_{2g}$ phonon of C $sp^2$ atoms, while D band is a breathingmode of κ-point phonons of $A_{1g}$ symmetry. As shown in Figure 5, raman spectrum of the pristine graphite displays a strong G band at 1579 $cm^{-1}$, a weak D band at 1360 $cm^{-1}$, and a middle 2D band at 2700 $cm^{-1}$. The Raman spectra indicate the formation of graphene, athough there are some oxygen functionalities.

**Electrochemical analysis of Pd/Graphene catalyst** In order to elucidate the catalytic function of Pd/Graphene composites for the reduction of $CO_2$, cyclic voltammograms for graphene and Pd/Graphene by catalyst modified glassy carbon electrode in 0.5 mol/L $KHCO_3$ solution are shown in Figure 6.The cathodes currents obtain under 1 atm $N_2$ were suppressed compared with that obtained under 1 atm $CO_2$. No significant responses beyond the background current were observed for graphene and Pd/Graphene

modified glassy carbon electrode under $N_2$ purged condition. Under $CO_2$ pressure, graphene and Pd/Graphene modified glassy carbon electrode showed reduction peaks at ca. -0.65 V and -0.52 V, respectively. These results indicated that $CO_2$ could take part in the reduction reaction directly under this electrocatalytic conditions. It can be inferred from the fact that it is $CO_2$ is the key point of the reaction; $HCO_3^-$ is first decomposed to $CO_2$, and then is reduced at the electrode. It is well known that the decomposition rate of $HCO_3^-$ is slow in ambient temperature and pressure, so the decompose of $HCO_3^-$ is the rate determining step in the reaction. Carbon dioxide was fist converted into $HCO_3^-$ first, and then was transport to the surface of palladium nanoparticles in the form of $HCO_3^-$. According to the reaction redox potential, it may be inferred that HCOOH is the product [5]. The electrode potential for $CO_2$ reduction vs. standard hydrogen electrode (SHE) at pH 7.0 at 25 $^o$C is as follow [6]:

$$CO_2 + 2H^+ + 2e^- \rightarrow HCOOH \quad E = -0.43 \text{ V}$$
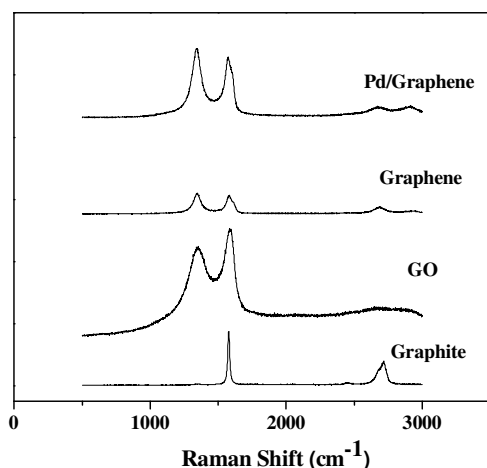


**FIGURE 5. Raman spectra pattern of Pd/Graphene catalysts**
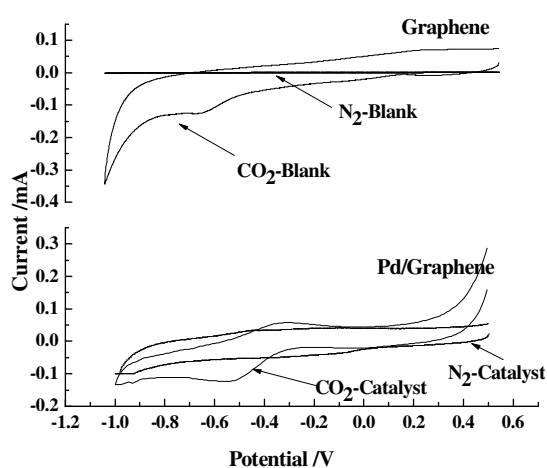


**FIGURE 6. CV for Graphene and Pd/Graphene catalysts**

**Electrochemical reduction of $CO_2$ at Pd/Graphene gas diffusion electrodes** The work is carried out in the 0.5 mol/L $KHCO_3$, the electrolysis voltage is 4 V and electrolysis time is 20 min. The products were determined by an ion chromatograph. Formic acid is the main products with 75% faradaic efficiency.

## CONCLUSIONS

A Pd/Graphene gas-diffusion electrode was prepared and used to reduce the $CO_2$. The amorphous structure Pd particles with an average size of 4 nm were highly dispersed on the surface of graphene and Pd content on the surfance of catalyst reached 0.3 at.%. FTIR shows that almost all of the oxygen functionalities on the graphite oxide ware reduced. The Raman spectra indicate the formation of graphene. The results of CV indicate that the carbion dixoide is a key point of the readction and $HCO_3^-$ took part int the reaction directly. Pd/Graphene gas-diffusion electrode show highly active and selective performance for conversation of $CO_2$ to formic acid with 75% faradaic efficiencies in 0.5 mol/L $KHCO_3$ solutions.

## ACKNOWLEDGEMENTS

**REFERENCE**

1. Hummers, W. S., and R.E. Offfeman. 1958. "Preparation of Graphite Oxide" *J. Am. Chem. Soc.* 80(6):1339–1339

2. Kovtyukhova, N. I., and P.J. Ollivier. 1999. "Layer-by-Layer Assembly of Ultrathin Composite Films from Micron-Sized Graphite Oxide Sheets and Polycations" *Chem. Mater.* 11 (3):771–778

3. Wang, H., and J.L. Wang. 2007. "Electrochemical degradation of 4-chlorophenol using a novel Pd/C gas-diffusion electrode" *Appl. Catal. B: Environ.* 77 (1-2):58-65

4. Wang, H., and D.Z. Sun. 2010, "Degradation mechanism of diethyl phthalate with electrogenerated hydroxyl radical on a Pd/C gas-diffusion electrode" *J. Hazard Mater.* 180 (1-3):710-715

5. Furuya, N., and T. Yamazaki. 1997, "High performance Ru-Pd catalysts for $CO_2$ reduction at gas-diffusion electrodes" *J. Electroanal. Chem.* 431(1): 39-41.

6. Gupta, N., and M. Gattrell. "Calculation for the cathode surface concentrations in the electrochemical reduction of $CO_2$ in $KHCO_3$ solutions" *J. Appl. Electrochem.* 36 (2):161-172.

# CARBON ABATEMENT COST OF CHINA BASED ON CO-BENEFITS ANALYSIS

***Zhou Wei*** and Mi Hong

(Zhejiang University, Hangzhou, China)

**ABSTRACT:** Carbon abatement may impact China's economy, at same time it will reduce air pollutants. The co-benefits of carbon abatement are air quality improvements and public health. Air pollution has been a growing concern for China, it brings higher economic and social cost now. The health cost caused by air pollution accounts for 3.5% of China's GDP. Carbon abatement will generate air quality improvements in China in the long-term. We calculation shows the earlier emissions mitigation, the less the economic cost. Carbon abatement in transport can bring huge economic and health co-benefits.

## INTRODUCTION

China is the largest emitter of carbon dioxide and one of world's worst polluted countries. Different from developed countries whose environmental pollution have been controlled effectively, China has not get rid of "high investment, high energy consumption, high pollution" development pattern, environmental problems in China is much more serious than that in developed countries. For example, PM2.5 (particles with diameter less than or equal to 2.5 microns that produced in coal-fired power plant, industrial production, automobile exhaust), can pass into the blood through the bronchial and alveolar, the harmful gas and heavy metals could dissolve in the blood, which can cause severe harm to the health of human beings. WHO *Air quality guidelines* mentioned that when annual mean concentration of PM 2.5 reached $35\mu g/m^3$ that the risk of death will increase 15% relative to concentration at $10\mu g/m^3$. Canadian scholar Aaron van Donkelaar et al (2010) synthesized NASA Satellite monitoring data and simulated the PM2.5 distribution. As is shown in figure 1, both the North and East of China area are the highest PM2.5 concentration area in the world.
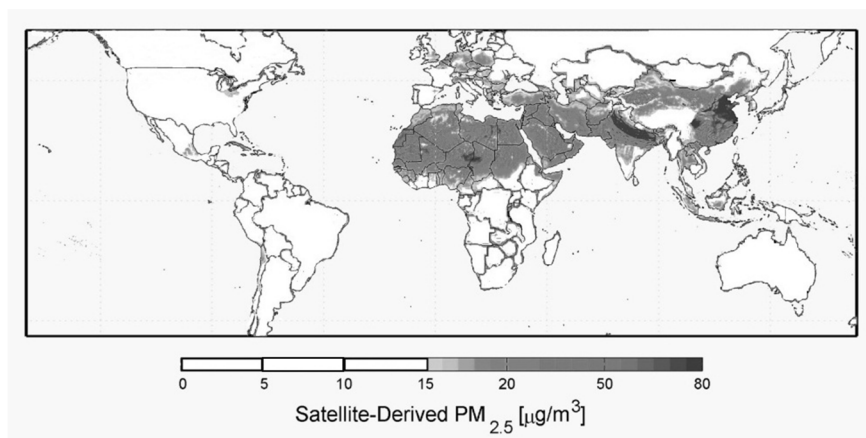


FIGURE 1 Global PM2.5 Concentrations

Apart from the direct healthy and life loss of residents, environment pollution also comes with a human capital loss, agriculture loss and ecological degeneration .Economic costs of environment pollution control is extremely high. For instance, from 2001 to 2007, China has invested 91 billion yuan of fiscal funds and bank loans in water pollution control, still failed to reached the expectation of government. Future investment in fighting against air pollution is enormous and it will take a long time for ecological improvement.

Due to the environment pollution (especially air pollution) and climate change, to a great extent, have a common source, which is mainly caused by emissions from burning fossil fuels ,so control and reduce environmental pollution and reduce greenhouse gas emissions should be consistent in action on climate protection, both existing "environment co-benefits ". IPCC (2001) defined "environment co-benefits" as following: "Profits gain while implement related policies for all sorts of reasons". Environmental co-benefits effect include two aspects: one is reducing other local pollutants (for example $SO_2$, NOx, TSP, VOCs) in the process of controlling greenhouse gas emissions ; On the other hand, reducing or absorbing $CO_2$ and other greenhouse gas emissions in the process of controlling the local pollutants and ecological construction.

## LITERATURE REVIEW

**Environmental Co-benefits** Ayers and Walter (1991)at the earliest distinguished the two kinds of effects of greenhouse gas emission reduction , defined the effect to alleviate global climate change, sea level rise as "primary benefits"; defined effect that will reduce "traditional pollutant" such as $SO_2$, $NO_x$, TSP  as "secondary benefits". IPCC (1995,2001,2007) assessment report has used concept such as the secondary benefits, ancillary benefits and then used the Co-benefits. Rypdal et al(2007) studied the co-benefits effect of atmospheric pollutants and greenhouse gas emissions reduction, environment quality, social welfare and people health under six climate change policy scene in European. Tollefsen (2009), estimated co-benefits of slowing climate change produced by the implementation of atmospheric pollution control measures in European. Chae Y. (2010)studied the correlativity of co-benefits effect of reduction measures in Seoul from the perspective of  environment economics, South Korea and performed cost-effect evaluation ,he found that no additional input is needed to achieve carbon emissions reduction and air quality improvement effect under the pollutant reduction measure considered co-benefits effect. Tian Chunxiu et al(2006) analyzed environmental co-benefits of the project "West Natural Gas Transmit to East " of China, this paper argues that the project can also reduce emissions of sulfur dioxide and carbon dioxide. Li Liping et al (2010) thought that total reduction measure have both positive and negative effect for slowing global greenhouse gas emissions, co-benefits varies form reduction technology, but in general there is a significantly positive co-benefits. Mao Xianqiang et al(2011)studied the evaluation of coordination control effect of emissions reduction technology.

**Environment Pollution Losses** Experienced environment pollution earlier in the process of industrialization, developed countries studied relevant health loss more in-depth. Concentration of atmospheric suspended particles have correlation with lung cancer incidence (Lave and Seskin, 1970; Nesnow and Lewtas, 1981), suspended particles may damage the genetic material DNA, which causes the irreversible consequences (Vineis and Husgafvel Pursiainen, 2005; Peluso et al. 2005).Xuexi Tie and Dui Wu found that there is 7 years time-lag related statistical relationship between Guangzhou lung cancer and ash haze weather. After the 1990 lung cancer incidence in Guangzhou is as high as 50-70/million, while from 1954 to 1972 the incidence is only 10/million, besides there is no significant changes of

smoking. In the years 1992 ~ 1997, the study of more than 8000 pupils from 8 elementary school in Guangzhou, Wuhan, Chongqing in Lanzhou and their families show that PM10, PM2.5 have the biggest influence among pollution factors.

In the aspect of economic loss of environment pollution, Rabl A.(1999) used the market value method to calculate the loss of building caused by the French air pollution; Delucchi M. A. et al(2002) used damage function method and value method respectively to calculate the health and visibility loss caused by the pollution of atmosphere in USA. In China, Guo Xiaomin (1990)estimated the loss caused by national atmospheric pollution in the " China environmental forecast in2000 AD and countermeasures study ".Li Ying et al (2001)studied the costs Beijing residents willing to pay to improve the environment .Environment and development research center of Chinese academy of social sciences Chinese Academy monetized  China's environmental pollution loss ,the calculation results show that in 1993, it is 108.5 billion yuan, accounting for 3% of GNP. The world bank report "Clear water blue sky: looking forward to the 21 st century Chinese environment" finds that climate change will cause certain economic loss but in the short term, the regional environmental pollution threat is more marked. The damage caused by pollution (early death, illness, resources and infrastructure loss) accounts for 8% of GDP.

To sum up, in the aspect of quantitative evaluation of co-benefits effect most existing research concerned about carbon abatement potential and the resulting environmental and health benefits, few study consider environmental co-benefits effect and carbon abatement cost together. Researched the loss of the pollution of the environment for a long time and the research findings is abundant, the developed countries at present have already solved pollution environment effectively, previous research rarely combine cost-benefit of climate change with the environment benefits of carbon abatement, especially in China.

This article adopt the willingness to pay method to calculate the health loss brought by air pollution, use the scene analysis method to study the influence to energy, environmental and economic under different highway, railway development mode.

## ENERGY CONSUMPTION OF TRANSPORT IN CHINA

With the development of economy, China transport mix has changed enormously. The proportion of railway transport continues to decline, the proportion of road transport rise quickly. Taken freight for example, in 1980, road freight volume is less than 1/4 of that of railway, but it is up to 1.5 times of railway transport in 2010 (figure 2). There is same trend in passenger transport (figure 3).

Now the development of road in China is still faster than railway because they get more investment. On the other hand, high-speed railway is given priority in railway construction. From the energy efficiency, it is not reasonable. To transport a ton of cargo, road transport consumed 14 times energy as that in railway in the same distance (figure 4); A passenger travels by highway consumes twice energy as much as by the railway (figure 5). In the railway system, as the speed increase, passenger transport energy consumption increases accordingly. High-speed railway (HSR refer the speed more than 250 km/h in China) consumed 3.4 times energy as the traditional railway. So China's transport development is more and more incline to "high energy consumption and high emissions" mode.

Before 1992, China railway system got investment more than that of highway; this trend reversed after 1992. From 1992 to 2010, total investment in highway is 2.1 times of that of railway (figure 6). From 2005, China began to develop high-speed railway. The cost of high-speed railway is more than 3 times of traditional railway in same length. And these railways can't transport freight (because of

boxcar's weight). Investment in railway increased significantly since 2008, but a large part is invested in high-speed rail system. The high cost of investment and didn't increase the railway mileage rapidly. High cost of high-speed rail increased high ticket price, for instance, Beijing-Shanghai High-speed Railway，with whole journey 1318 kilometers and speed at 300km/h, the second class seat ticket is 3 times as that of common railway while the first class seat ticket is 5 times of that.
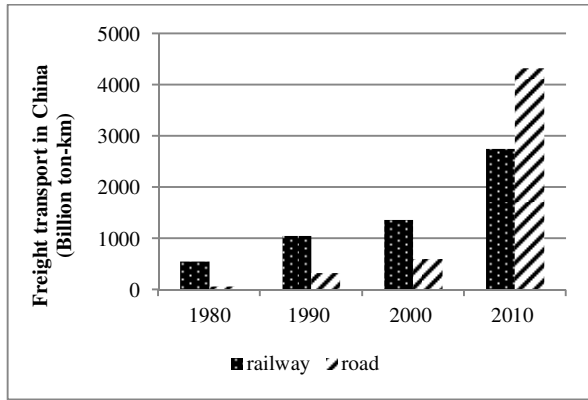


FIGURE 2 Freight Transport in China
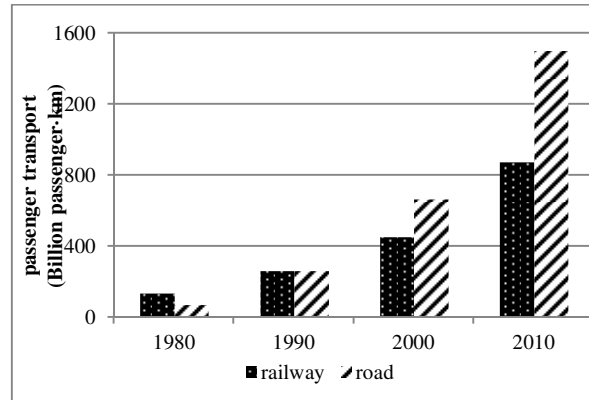


FIGURE 3 Passenger Transport in China
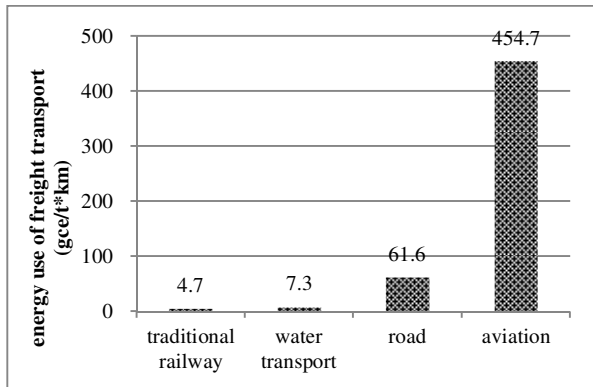


FIGURE 4 Energy Efficiency of Freight Transport
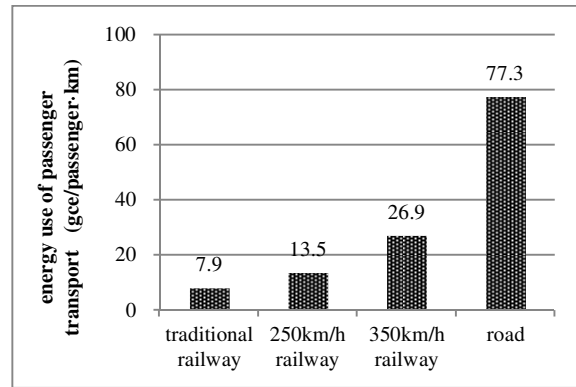


FIGURE 5 Energy Efficiency of Freight Transport

*Source:* Integrated Transport Research Center of China. Energy Consumption, Emissions and their Comparison among Different Transport Modes, 2009.

However, does the highly cost high-speed railway meet the demand of the market? In 2010, for example, road transport 30.5 billion person-trips, the average travel distance only 49 kilometers, and there is no big change nearly 20 years (figure 7); railway transport 1.68 billion person-trips, and the average travel distance for 523 kilometers (figure 7). This means that railway's passengers accounts for only of 5% the land total passengers. Because of China's population density, the distance between the city is small, most of the daily travel is short. High-speed rail can't play its speed in a shorter distance (such as within100 km). For example, from Shanghai to Nanjing, 300 km/h high-speed rail only save 25 minutes than 200 km/h train, add the commute time in two cities, high-speed train can only save 10% of the time,

but the ticket prices are 50% higher. Ticket prices rising force more passengers to choose road transport, which exacerbate energy consumption, traffic jam and air pollution.
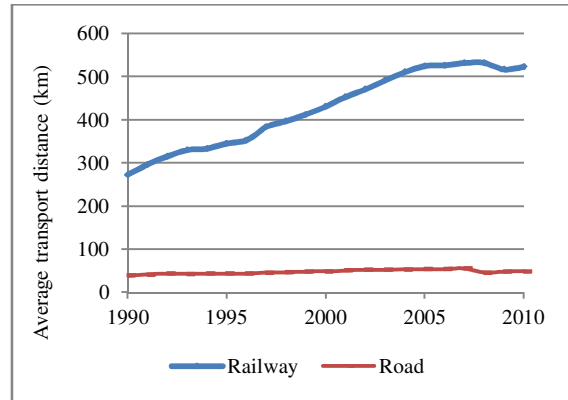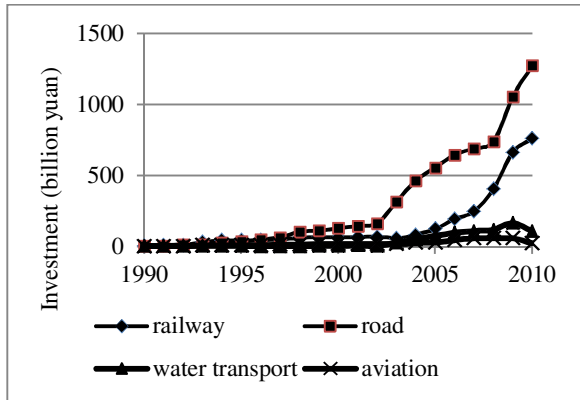


FIGURE 6 Investment in Different Transport Modes    FIGURE 7 Passengers' average travel distance

## CO-BENEFITS OF TRANSPORT OPTIMIZATION

Is there a way which can save energy to abate carbon emissions and air pollutants, at the same time transport cost can be reduced? We set up an transport optimization model as following:

$$\min L = L_1(ener) + L_2(envi) + L_3(prod) \qquad \text{L: total loss}$$

s.t.

$$ener = \sum_i P_i e_{pi} + \sum_i F_i e_{fi}$$

Value of energy consumption

$$envi = CE(ener) + POL(ener)$$

Value loss of $CO_2$ and pollution

$$prod = \varphi(uti)$$

Value loss of time

$P_i$ is passenger transport of different modes $i$, while $F_i$ is freight transport by different modes $I$;

$e_{pi}$ is energy use transport per person-trip by mode $i$;.

$e_{fi}$ is energy use per ton-kilometer in freight transport by mode $i$.

**Calculation of Result.** If the proportion of traditional railway freight keep as 40% (the level of 1990), 107 Mtce energy can be saved in 2010, and total energy consumption can be saved 764 Mtce from 1996 to 2010. While the energy saved by passenger transportation is relatively small, total energy saved is only34 Mtc in 2010e.  If in the future proportion of railway freight transportation keeps at 29% in 2010, the national total energy consumption freight will reach 475 Mtce in 2020. If the proportion of increased to 35%, the total energy consumption of freight in 2020 is 426 Mtce, energy saved during 2012-2020 is 282 Mtce; If the proportion of increased to 40%  , the total energy consumption of freight in 2020 is 339

Mtce, energy saved during 2012-2020 is 721 Mtce. Now more than 50% of China's oil depends on imports, the growth of energy consumption brought uncertainty for energy traffic safety.

**Co-benefit of Investment.** Ministry of Railway of China put huge investment in high-speed railway (special passenger railway with speed more than 250km/h), the high-cost result huge debt 2,100 billion yuan ($330 billion) in 2011, and it's net profit is not enough to pay the interest. If China develop more traditional railway rather than high-speed railway, it can transport more passengers and freight, and make more net profit and less debt.

**Co-benefit of Health and Life.** China's vehicle production was 18.26 million with an increase of 32.44%, and sale was 18.06 million with increase of 32.37% (Automobile Manufacturers Association, 2011). Till the end of August in 2011, the inventory of national vehicle fleet reached 219 million. These vehicle produce serious pollution which result in respiratory disease. Now more than 358,000 persons die of air pollution every year. Mortality rate of traffic accident is 207.5/million. Many of them can be saved if railway transport account for higher share.

Current carbon emission policy in China mainly based on the opinion that economy development requires more carbon emissions space, which put carbon emissions abatement in opposition to economy development and human living standards improvement. Public health loss, life loss and economic loss caused by pollutants come along with carbon emissions, in fact reduced welfare that economic growth brings to people. The co-benefit in carbon abatement should be taken account for future carbon abatement decision-making.

## ACKNOWLEDGEMENTS

## REFERENCES

Aaron van Donkelaar, Randall V. Martin, Michael Brauer. 2010. Global Estimates of Ambient Fine Particulate Matter Concentrations from Satellite-Based Aerosol Optical Depth: Development and Application, Environmental health perspectives, 118(6):847-855.

Allen L. Robinson, Neil M. Donahue, Manish K. Shrivastava.2007. Rethinking Organic Aerosols: Semivolatile Emissions and Photochemical Aging, Science, 315:1259-1262.

Ayers, R. and Walter, J. 1991. The Greenhouse Effect: Damages, Costs and Abatement, Environmental and Resource Economics,1(3):237-270.

Chae Y.2010. Co-benefit Analysis of An air Quality Management Plan and Greenhouse Gas Reduction Strategies in the Seoul Metropolitan Area.Environmental Science and Policy，13: 205-216．

Criquil, P., Mima, S., Viguier, L., 1999. Marginal Abatement Costs of CO2 Emission Reductions, Geographical Flexibility and Concrete Ceilings: an assessment using the POLES model. Energy Policy 27, 585–601.

David Pearce.1992.The secondary benefits of greenhouse gas control, CSERGE Working Paper GEC 92-12, The Centre for Social and Economic Research on the Global Environment, UK.

Ellerman D.A., Decaux A.. Analysis of Post-Kyoto CO2 Emission Trading Using Marginal Abatement Curves.1998. Massachusetts Institute of Technology. MIT Joint Program on the Science and Policy of Global Change, Report 40.

Hsu, G. J. Y., Chou F. Y. 2000. Integrated planning for mitigating CO2 emissions in Taiwan: A multi-objective programming approach. Energy Policy,28:519-523.

IPCC. Climate Change 1995: economic and social dimensions of climate change. Cambridge University Press,UK.

IPCC. Climate Change 2001: impacts, adaptation and vulnerability, Cambridge University Press, UK.

Jitendra J. Shah, Tanvi Nagpal. ,1997.Carter J Brandon. Urban air quality management strategy in Asia: Guidebook. The World Bank

Norwegian Central Bureau of Statistics .1991. Rapporter 91: Natural Resources and the Environment 1990, Central Bureau of Statistics, Oslo.

Peluso, M., et al., 2005. DNA adducts and lung cancer risk: a prospective study.Cancer Res. 65, 8042–8048.

Rose, A., Steven, B. 1993. The efficiency and equity of marketable permits for CO2 emissions. Resource and Energy Economics, 15: 117-146.

Rypdal K, Nordic. 2007. Air Quality Co-Benefits from European Post-2012 Climate Policies. Energy Policy,35: 6309-6322.

T.M.L. Wigley, R.Richels, J.A. 1996. Edmonds Economic and environmental choices in the stabilization of atmospheric CO2 concentrations. Nature, 379:240-243.

World Bank. 1997.Clear water Blue Skies: China's Environment in the New Century. Washington D.C.

Xuexi Tie, Dui Wu, Guy Brasseura. 2009. Lung cancer mortality and exposure to atmospheric aerosol particles in Guangzhou, China. Atmospheric Environment, 43:2375–2377(Chinese).

Zhang Z.X. 1996. Cost-Effective Analysis of Carbon Abatement Options in China's Electricity Sector. Energy Sources, 20:385-405(Chinese).

Chapter 9

# METALS

# DETERMINATION OF HEAVY METALS (CD, PB, HG, CU, FE, MN, AL, AS, NI AND ZN) IN 6 IMPORTANT COMMERCIAL FISH SPECIES IN NORTH OF HORMOZ STRAIT

***Majid Afkhami*** (Yung Researches Club, Islamic Azad University, Bandar Abbas Branch, P.O.Box:79159-1311, Bandar Abbas, Iran.)

Maryam Ehsanpour (Islamic Azad University, Bandar Abbas Branch, P.O.Box:79159-1311, Bandar Abbas, Iran.)

Zahra Khoshnood(Islamic Azad University, Dezful Branch, Dezful, Khuzestan Provionce, Iran)

**ABSTRACT:** The concentrations of 10 heavy metals (Cd, Pb, Hg, Cu, Fe, Mn, Al, As, Ni, Zn) were measured in muscle, gill and liver of 6 species from Hormoz Strait in north costal of Persian Gulf in 12 months (April 2009 – March 2010). All samples were analyzed three times for Cd, Pb, Cu, Fe, Mn, Al, As, Ni, Zn by inductively coupled plasma-atomic emission spectrometry (ICP-AES) and for Hg by LECO AMA254 Advanced Mercury Analyzer. Results of this study showed, Iron had the highest concentration (total mean concentration) in all species, and followed by Zn, Cu, Ni, Al, Pb, Mn, Cd, Hg and lowest concentration in three tissues was As. In Addition the accumulation of metals was species-dependent, and was higher in *Scomberomorous commerson* and *Scomberomorous guttatus (p<0.05)* and the lowest concentration was record in *Pampus argenteus (p<0.05)*.

## INTRODUCTION

Fishes are often at the top of the aquatic food chain and may concentrate large amount of some metals from the water (Mansour and Sidky 2002) further more fish is one of the most indicative factors in aquatic system, for the estimation of trace metals pollution and risk potential of human consumption (papagiannis et al., 2004).Heavy metals from geological and anthropogenic source are increasingly being released into natural waters (Nimmo et al., 1998).concentration of aquatic ecosystems with heavy metals has seriously increased worldwide attention, and a lot of studies have been published on the heavy metals in the aquatic environment (Wagner and Boman 2003).

Under certain environmental conditions, heavy metals may accumulate to toxic concentrations and cause ecological damage(Jefferies and Firestone 1984).Hence, it is important to determine the concentrations of Heavy metals in commercial fishes in order to evaluate the possible risk of fish consumption (Cid, Boia et al. 2001).The present study has been conducted to determine Cd,Pb,Hg,Cu,Fe,Mn,Al,As,Ni,Zn concentrations in the Gill ,Muscle and Liver, Study Area is polluted by different type of industrial agricultural drainage , Domestic waste water and oil pollution.

## METHODOLOGY

The fish species were randomly collected from commercial catches landed at local fishing ports in North side of Hormoz Strait, that's a narrow between Oman Sea and Persian Gulf. Twelve Monthly samples collections were conducted from April 2009 to March 2010. The biometrics of collected fishes samples were determined and noted. Fish samples were transported to the laboratory in a thermos flask with ice in an isolated box on the same day (Eaton et al., 1990).Approximately 5 gr samples of muscle (edible parts) two gill racers from each sample and entire Liver, were dissected, wash with De-ionized water weighed, packed in polyethylene bags and stored at $-20^0$ C prior to analysis. All of the samples were dried at 60° C for 48 h in laboratory oven (Pyle et al., 2005).All glassware's was cleaned prior using

by soaking in 10% v/v HNO3 for 12h and then rinsed with ultra-pure water. Between 0.2 to 0.4 g of dried sample material were weighted and then digested in acid-cleaned teflon beaker with 5ml of ultra-pure nitric acid (65%v/v). Typical microwave digester operated for 30-40 min at a target digestion temperature at 200°c and after then allowed for 1h to cooling. Digested samples transferred to a graduated plastic test tube and brought up to volume (50ml) with Mili-Q-water(MOOPAM 1999).All samples were analyzed three times for Cd, Pb,Cu,Fe,Mn,Al,As,Ni,Zn by inductively coupled plasma-atomic emission spectrometry (ICP-AES) (Varian Model- liberty series II) and for Hg by LECO AMA254 Advanced Mercury Analyzer.In order to assess the analytical capability of the proposed methodology, accuracy of heavy metals analyzing was tested with reference matrices of dogfish liver tissue (DORM 2), and muscle tissues (DOLT 2). Results confirms that observed and reference values have not statistically differences (P<0.05) (Table1).

**RESULTS**

Analysis of the dog fish muscle and liver standard reference material DORM 2 and DOLT 2 are shown in table 1. Table 2 show the average concentration of heavy metals in all fish samples in every month.First of all, the total concentration of Fe is very high than other metals, and Arsenic has lowest concentration. Basis on this table there is no obvious seasonal pattern to metal contamination in the fish samples. The level of 7 of the 10 metals analyzed (including Cd,Pb,Hg,Cu,Fe,Mn,As,Zn,) were higher in the May than Other month. Table 3 showed the biometry results of fish and their environment. Basis on this table the largest kind of this fish in our study was *Scomberomorous Commerson* (mean length was 68.9), and the heaviest fish was this kind too (mean weight was 10.39).the shortest of this samples was *Rastrelliger Kanagurta* (mean length was 18.2±3.4) and lightest was this kind of fish too (mean weight was 0.20±0.05).table 5 shows the total mean concentration in three tissues of every species.

**Table 1: Comparison of the Obtained and Reference Metals Concentrations (mg.mg$^{-1}$).**

| CRM | | Pb | Cd | Hg | Cu | Fe | As | Ni | Zn |
|---|---|---|---|---|---|---|---|---|---|
| DORM-2 | Certified | 0.065±0.007 | 0.043±0.008 | 4.64±0.26 | 2.34±0.16 | 142±10 | 18±1.1 | 19.4±3.1 | 25.6±2.3 |
| | Obtained | 0.049±0.003 | 0.050±0.003 | 4.31±0.39 | 2.21±0.23 | 149±13 | 16±1.6 | 19.1±1.6 | 23.1±3.5 |
| DOLT-2 | Certified | 0.16±0.04 | 24.3±0.8 | 2.58±0.22 | 31.2±1.1 | 1833±75 | 9.66±0.62 | 0.97±0.11 | 116±6 |
| | Obtained | 0.19±0.01 | 21.1±0.3 | 2.44±0.17 | 30.9±0.9 | 1813±69 | 9.30±0.42 | 0.91±0.06 | 111±3.1 |

**DISCUSSION**

The observed variability of heavy metals levels in different species depend on feeding habits(Romeoa,Siaub,1999),ecological needs, metabolism (Canli and Atli 2003),age, size and length of the fish and their habitats (Canli and Atli 2003).In our study, Iron had the highest concentration (total mean concentration) in all species, and followed by Zn (Zinc), Cu (Copper), Ni (Nickel), Al (Aluminum), Pb (Lead), Mn ( Manganese ), Cd ( Cadmium), Hg (Mercury) and lowest concentration in three tissues was As( Arsenic).The highest concentration was on dry month in this region (August and September) may be because of high evaporation rate in Persian Gulf. Basis on table 5, only in two kind of all fish species record more average concentration of metals. One of them is *Scomberomorous commerson* that had high concentration of Cadmium, Lead, Mercury, Iron, Manganese and Arsenic than other species, this

phenomenon may be arising from diet, which feed primarily on small fish, like Anchovies, Clupeids, Carangids and also Squids and penaeoid Shrimps. Another reason for this high concentration is Positive correlation between length and weight that called "Bioaccumulation".

In other species *Thannus tonggol* we record more heavy metal concentration (Copper, Aluminum, Nickel and Zinc) more than other species; this fish feeds on variety of fish Cephalopods and Crustaceans particularly steomotopod larvae and prawns. The lowest concentration was record in *Rastrelliger Kanagurta* which has the lowest weight and the shortest length.

**Table2: Heavy Metals in Fish Species from Different Month (mg.kg$^{-1}$).**

| Month/Metals | Cd | Pb | Hg | Cu | Fe | Mn | Al | As | Ni | Zn |
|---|---|---|---|---|---|---|---|---|---|---|
| April | 0.256 | 1.022 | 0.199 | 1.120 | 12.036 | 0.354 | 1.587 | 0.042 | 0.987 | 3.258 |
| May | 0.415 | 1.103 | 0.139 | 1.002 | 24.509 | 0.741 | 0.658 | 0.112 | 1.888 | 4.621 |
| June | 0.125 | 0.589 | 0.215 | 1.014 | 18.660 | 1.069 | 0.421 | 0.055 | 2.254 | 3.955 |
| July | 0.101 | 0.601 | 0.121 | 0.899 | 8.231 | 0.736 | 0.369 | 0.101 | 1.745 | 4.889 |
| August | 0.145 | 1.232 | 0.112 | 2.129 | 19.447 | 0.778 | 2.958 | 0.111 | 2.971 | 3.514 |
| September | 0.438 | 1.815 | 0.320 | 1.133 | 55.211 | 1.687 | 1.253 | 0.124 | 0.965 | 5.743 |
| October | 0.155 | 1.159 | 0.103 | 1.010 | 32.230 | 0.899 | 0.988 | 0.041 | 0.877 | 4.002 |
| November | 0.124 | 1.089 | 0.225 | 2.008 | 13.258 | 0.987 | 2.504 | 0.063 | 1.242 | 3.632 |
| December | 0.519 | 0.940 | 0.119 | 1.122 | 16.055 | 0.729 | 1.213 | 0.040 | 1.358 | 3.321 |
| January | 0.206 | 1.411 | 0.125 | 1.116 | 18.241 | 0.637 | 0.887 | 0.089 | 1.023 | 5.036 |
| February | 0.111 | 0.728 | 0.098 | 0.781 | 38.144 | 0.805 | 1.452 | 0.091 | 1.003 | 4.105 |
| March | 0.102 | 0.977 | 0.104 | 0.864 | 20.005 | 0.816 | 2.314 | 0.051 | 1.065 | 3.147 |
| **Total** | **0.224** | **1.055** | **0.157** | **1.183** | **23.002** | **0.853** | **1.384** | **0.077** | **1.448** | **4.102** |

**Table3: Results the Biometry Measurement of Fish Samples**

| Scientific name | English name | Number of Samples | Length (cm) Mean±Sd | Weight (Kg) Mean ± Sd | Environment |
|---|---|---|---|---|---|
| *Scomberomorous Commerson* | Narrow barred Spanish mackerel | 24 | 68.9±7.4 | 10.39±6.77 | Pelagic - naritic |
| *Rastrelliger Kanagurta* | Indian mackerel | 24 | 18.2±3.4 | 0.20±0.05 | Pelagic – naritic |
| *Scomberomorus guttatus* | Indo-Pacific \king mackerel | 24 | 43.1±6.9 | 0.65±0.11 | Pelagic – naritic |
| *Thannus tonggol* | Longtail tuna | 24 | 54.6±3.4 | 4.75±1.0 | Pelagic – naritic |
| *Pampus argenteus* | Silver Pomfert | 24 | 28.2±2.1 | 0.54±0.21 | Benthopelagic |
| *Acanthopagrus latus* | Yellofin seabream | 24 | 32.4±3.0 | 0.37±0.09 | Demersal |

Cd concentration generally more than other place, it was 10 times more than Adriatic Sea, 14 times more than Masan bay, Korea and 8 times more than Osaka, Japan, 9 times more than Manila, Philippines and less than recorded concentration in Gulf of California and Iskenderun bay and Arabian Sea

Pb Concentration was high than other place except in Iskenderun bay and Arabian Sea. Mean concentration of Pb in study area was 2 times more than Gulf of California, 23 times more than Adriatic

Sea, 13 times more than Mason bay, Korea, 21 times more than Osaka Japan, 7 times more than Manila bay, Philippines. About Hg concentration, our result was lower than other results except about one region including Atlantic Sea (our results 2 times more than this).Concentration of three major heavy metals including Hg, Cd, Pb comparing with standards, table 7 showed Hg and Cd concentration is below than standards and Pb concentration is exceed than standard, and there is high risk for women and children for consuming fish.

**Table 4: Concentrations of Metals in Fish Species (mg.kg$^{-1}$)**

| Species | Cd | Pb | Hg | Cu | Fe | Mn | Al | As | Ni | Zn |
|---|---|---|---|---|---|---|---|---|---|---|
| ***Scomberomorous Commerson*** | 0.673 | 1.841 | 0.403 | 2.243 | 64.461 | 2.206 | 1.411 | 0.900 | 1.962 | 3.174 |
| ***Rastrelliger Kanagurta*** | 0.190 | 0.892 | 0.107 | 2.163 | 11.744 | 0.329 | 1.494 | 0.047 | 1.278 | 4.633 |
| ***Scomberomorus guttatus*** | 0.128 | 1.194 | 0.245 | 2.577 | 51.288 | 0.176 | 1.615 | 0.088 | 1.296 | 2.888 |
| ***Thannus tonggol*** | 0.368 | 1.530 | 0.164 | 2.926 | 8.299 | 0.760 | 3.424 | 0.115 | 3.001 | 6.248 |
| ***Pampus argenteus*** | 0.175 | 1.240 | 0.100 | 1.795 | 6.131 | 2.369 | 0.509 | 0.102 | 1.467 | 4.657 |
| ***Acanthopagrus latus*** | 0.079 | 1.228 | 0.095 | 1.561 | 20.621 | 0.783 | 1.725 | 0.041 | 1.948 | 5.688 |
| **Total mean** | 0.224 | 1.055 | 0.157 | 1.831 | 23.002 | 0.853 | 1.384 | 0.077 | 1.448 | 4.102 |

**Table 5: Comparison Results with Standard**

| Standard/results | Cd | Pb | Hg |
|---|---|---|---|
| **EPA Standard** | 1 | 1 | 0.5 |
| **Italy Standard** | - | 5 | 0.7 |
| **Japan Standard** | - | - | 10 |
| **Our results** | 0.224 | 1.055 | 0.157 |

**Table 6: Comparing Between Our Results with Other Region (mg.kg$^{-1}$).**

| Location | Cd | Pb | Hg | Reference |
|---|---|---|---|---|
| **Gulf of California** | 0.46 | 0.355 | 1.6 | (Soto-Jimenze et al., 2009) |
| **Adriatic sea** | 0.022 | 0.045 | 0.515 | (Storelli 2008) |
| **Atlantic coast** | - | - | 0.073 | (Voegborlo and Akagi 2007) |
| **Iskenderun bay** | 0.950 | 2.320 | - | (Türkmen et al., 2005) |
| **Mediterranean sea** | 0.37 – 0.79 | 2.98 – 6.120 | - | (Roditi-Elasar et al., 2003) |
| **Masan Bay , Korea** | 0.015 | 0.076 | - | (Kwon and Lee 2001) |
| **Osaka, Japan** | 0.027 | 0.048 | - | (Masahiro et al., 1999) |
| **Manila bay , Philippines** | 0.024 | 0.135 | 0.289 | (Maricar et al., 1997) |
| **Arabian sea , Pakistan** | 0.320 | 4.120 | 0.133 | (Tariq et al., 1994) |
| **North side of Hormoz striate, Persian Gulf ,Iran** | 0.224 | 1.055 | 0.157 | Current study |

This study was carried out to provide information on heavy metals concentration in 6 fish species from Persian Gulf**.** The metal content is species- dependent, with some species showing high concentration of metals, and some showing low concentration. The metal concentration in the fish tissues were also time- dependent, with residues much higher during month during the rainy season. We conclude that the regular consumption of some of these fish species even during the dry season, could pose health risks, but totally have risk for human health especially for children and pregnant women. Generally, according to the results and according to regional conditions such as high evaporation, semi-closed, wastewater discharge,… and compared to other regions, Persian Gulf in the pain condition that requires more attention and control of its pollutants.

**REFERENCE**

Canli M. Atli G. 2003. "The relationships between heavy metal (Cd, Cr, Cu, Fe, Pb, Zn) levels and the size of six Mediterranean fish species." *Environ. Poll.* 121(1): 129-136.

Carpene E. Vasak M. 1989. "Hepatic Metallothionein from Goldfish (*Carassius auatus*). *Comp. Biochem. Physiol.* 92B: 463-468.

Eaton A.D. Clescend L.S. 1990. "Standard methods: For the examination of water and waste water: 17th ed. Edited by American Public Health Association, Washington, 1989, 1644 pp. *Anal Biochem.* 186(1): 183-183.

Kwon Y-T. Lee C-W. 2001. "Ecological risk assessment of sediment in wastewater discharging area by means of metal speciation. *Microchem. J.* 70(3): 255-264.

Mansour S.A. Sidky M.M. 2002. "Ecotoxicological studies: 3 heavy metals contaminating water and fish from fayoum Gov. Egypt. *Food Chem.* 78: 15-22.

Maricar P. Eun-Young K. Shinsuke T. Ryo T. (1997). "Metal levels in some commercial fish species from Manila Bay, the Philippines. *Marin Poll. Bull.* 34: 671-674.

Masahiro Y.Tomohiko I. Tomohiko F. 1999. "Heavy Metal Contents in Osaka Bay Sediments. *Kankyo Jiban Kogaku Shinpojiumu Happyo Ronbunshu* 3: 233-238.

MOOPAM .1999. Manual of oceanographic observations and pollutant analyses. 3th. Kuwait, regional organization for Protect. *Mar. Environ.* Pp.12-13.

Nimmo D.R. Willox M.J. Lafrancois T.D. Chapman P.L. Brinkman SFCGJ. 1998. "Effects of metal mining and milling on boundary waters of yellowstone National Park , USA. *Environ. Manage.* 22(6): 913-926.

Papagiannis I. Kagalou I. Leonardos J. Petridis D. Kalfakaou V. 2004. "Copper and Zinc in four freshwater fish species from Lake Pamvotis (Greece). *Environ. Int.* 30: 357-362.

Pyle G.G. Rajotte J.W. Couture P. 2005. "Effects of industrial metals on wild fish populations along a metal contamination gradient. *Ecotoxicol. Environ. Saf.* 61(3): 287-312.

Roditi-Elasar M. Kerem D. Hornung H. Kress N. Shoham-Frider F. Goffman O. Spaniera E. 2003. "Heavy metal levels in bottlenose and striped dolphins off the Mediterranean coast of Israel. *Mar. Poll. Bull.* 46: 503-512.

Roméo M. Siau Y. Sidoumou Z. Gnassia-Barelli M. 1999. "Heavy metal distribution in different fish species from the Mauritania coast. *Sci. Total Environ.* 232(3): 169-175.

Soto-Jimenze M.F. Amezcua F. González-Ledesma R. 2009. "Nonessential Metals in Striped Marlin and Indo-Pacific Sailfish in the Southeast Gulf of California, Mexico: Concentration and Assessment

of Human Health Risk. *Arch. Environ. Contam. Toxicol.* 58: 810- 818.

Storelli M.M. 2008. "Potential human health risks from metals (Hg, Cd, and Pb) and polychlorinated biphenyls (PCBs) via seafood consumption: Estimation of target hazard quotients (THQs) and toxic equivalents (TEQs). *Food Chem. Toxicol.* 46(8): 2782-2788.

Tariq J. Jaffar M. Ashraf M. Moazzam M. 1994. "Trace metal concentration, distribution and correlation in water, sediment and fish from the Ravi River, Pakistan. *Fish. Res.* 19(1-2): 131-139.

Türkmen A. Türkmen M. Tepe Y.Akyurt I. 2005. "Heavy metals in three commercially valuable fish species from Iskenderun Bay, Northern East Mediterranean Sea, Turkey. *Food Chem.* 91(1): 167-172.

Voegborlo R.B. Akagi H. 2007. "Determination of mercury in fish by cold vapors atomic absorption spectrometry using an automatic mercury analyzer. *Food Chem.* 100(2): 853-858.

Wagner A.Boman J. 2003. "Biomonitoring of trace elements in Muscle and Liver tissue of fresh water fish. *Spectrochim. Acta.* Part B 58: 2215-2226.

# GEOSPATIAL ASSESSMENT OF WIDESPREAD SOIL PB CONTAMINATION IN MEMPHIS, TN

*Ray W. Brown\**, Dhary S. Alkandary, Andrew Hunt (University of Texas – Arlington, TX, USA)

From the 1920s until 1986, when lead additives were banned from gasoline sold for non-commercial automobile fuel use, an enormous amount of Pb was emitted into urban areas. As a result, the amount of Pb in urban soils can be related to the cumulative amount of vehicular traffic that was present. Although early research suggested that the amount of Pb emitted from cars would likely not increase soil Pb concentrations to much of an extent, these early studies were flawed in the sample depths collected. Pb-contamination of soils occurs in the very top fine layer of soils and does not migrate through the soil under normal conditions for an urban or residential soil. In examination of soils along transects through urban areas, soil Pb has been shown to range from high to low moving from older parts of the city to newer parts suggesting that soil Pb is a reflection of the time spent exposed to car exhaust. This has been expanded to the development of high-resolution spatial maps of urban areas that show that proximity to freeways, highways and major arterial roads increases both total and bioavailable soil Pb in soils.

One assumption with regard to soil Pb pollution is that childhood exposure to this source is limited to outdoor activities. Unfortunately, this is a poor assumption as it has been determined that contaminated soils in yards and neighborhoods can be a major contributor to indoor dust contamination. An evaluation of the source of Pb in indoor dust has also revealed that exterior sources of Pb (e.g. soils and street dust) can contribute just as much as interior sources such as the deterioration of Pb-based paint.

Unfortunately, there is very little information with regard to the status of soil Pb pollution in many urban areas including Memphis, TN. As a result, we were interested in widespread Pb contamination of residential soils in the city from historical exposure to car exhaust.

Soil samples were collected during August 2008 and July 2009 in Memphis, Tennessee. Sample locations were chosen using a random-stratified sampling scheme in order to assess soil lead concentrations in the populations of samples defined as "residential curbside". Samples were composites of three 1 cm deep cores and stored in Zip-Loc bags until analysis. Once in the laboratory samples were processed according to EPA standard methods and analyzed using Atomic Absorption Spectroscopy.

Memphis, TN soil lead determinations from August 2008 were used to test the hypothesis: "Residential soil lead concentrations are a function of the age of the residence". This preliminary effort was conducted in order to determine whether there was an indication of the potential for city-wide patterns of soil lead distribution as a function of age of neighborhood. It was presumed that the older the residence and/or neighborhood, the longer those residential soils would have been exposed to the combustion products of leaded gasoline. Our data indicated strong evidence supporting this hypothesis so that an expanded field effort was conducted. Soil lead concentrations from the July 2009 field effort were conducted primarily to support a city-wide geospatial mapping model (Inverse Distance Weighting and Kriging). Although there were strong trends with regard to soil lead vs. residence age, limited use of residence age as a predictive model tool led us to begin looking at geographic trends for soil lead data with strong indications that elevated soil lead concentrations are focused on older, previously industrialized portions of the city that are now being converted to residential districts. This ongoing analysis is currently being coupled with evaluations of elevated childhood blood lead levels (EBLLs) in Memphis census tracts along with relevant demographic and socioeconomic characteristics that have historically been used to predict childhood blood lead levels in urban areas.

*Email: raybrown@uta.edu

# SURVEYING MERCURY RATE IN FOUR ORGANS (LIVER, KIDNEY, WING AND MUSCLE) OF WHITE CHIN SHARK (*CARCHARHINUS DUSSUMIERI*) IN NORTH OF HORMOZ STRAIT

*Aida Khazaali* (Islamic Azad University, Bandar Abbas Branch, Bandar Abbas, Iran)
Reza khoshnood(Islamic Azad University, Young reaserchers club, Tehran Central Branch)
Zahra khoshnood(Islamic Azad University, Dezful Branch, Dezful, Khuzestan Provionce, Iran)
Maryam Ehsanpour(Islamic Azad University, Bandar Abbas Branch, Bandar Abbas, Iran)

In this research we measured the rate of mercury in different organs of white chin shark (*carcharhinus dussumieri*) in the North of Hormoz strait. This took place in three stations: Bandar Abbas, Qeshm and Lengeh. The pollution level was in four organs kidney, liver, wings (caudal and dorsal) and muscle. The iteration numbers in this experiment was nine in each station. According to the data obtained, although three stations had discrepancies in pollution, it was not statistically significant. With another survey that took place on the relationship between pollution intensity and fish length, we concluded that this relationship was completely signification; it means that when length increases, pollution intensity increases, too. This statistical analysis took place via correlation test and also T-student test that yielded the above results. Another result obtained was measuring the pollution load of these aquatic resources in relation to mercury intensity in their organs. Its maximum was in a kidney sample 8834 ppb and its minimum in wing sample 255ppb. Anyway the average of mercury rate in different organs was: muscle 1338.633; kidney 1089.012; liver 1149.965; wing 705.8513ppb. The result show, except for the wings, the mercury rate in the other organs was higher than the standards of international organization like FAO and WHO.

# SPECIATION OF HEAVY METALS IN THE SEDIMENTS OF FORMER TIN MINING CATCHMENT

*Muhammad Aqeel Ashraf* , Mohd. Jamil Maah and Ismail Yusoff
(University of Malaya, Kuala Lumpur, Malaysia)

The chemical speciation of heavy metals (arsenic, chromium, copper, lead, zinc and tin) in the sediments from former tin mining catchment Bestari Jaya, Peninsular Malaysia was determined by using the latest version of the Community Bureau of Reference, usually called the BCR 3-step sequential extraction procedure. Furthermore, a fourth step was introduced for digestion and analysis of the residue. The analysis of total metal content was carried out by using micro wave acid digestion. The percentage of each metal obtained from the 4 steps extraction (acid-soluble + reducible + oxidizable + residual) is in good agreement with the percentage of total metal content obtained from microwave digestion, which implies that the accuracy of the procedure. The degree of pollution in catchment sediments was assessed using geoaccumulation index $I_{geo}$ and pollution intensity $I_{POLL}$. The results indicates that (1) the sediments have been polluted with arsenic (8.8%), chromium (12.9%), copper (17.4%), lead (19.5%), zinc (14.9%) and tin (33.8%) and have high anthropogenic influences; (2) the calculation of geo-accumulation index suggest that catchment sediments have background concentration for all studied metals (*Igeo* < 0); (3) High $I_{POLL}$ showed that all of these heavy metals pose high environmental risk. (4) the mobility order of metals in sediments at S1 and S2 was Sn>Pb>Zn>Cr >Cu >As, whereas at S3, S4 and S5 Cu>Pb>Zn>Cr>Sn>As; In conclusion, acidic pH, total organic carbon, scavenging ability and co-precipitation (inclusion, occlusion and adsorption) of studied metals with non-metals could account for change in the geo-chemistry of the catchment sediments.

# TRACE METAL AND DIOXIN DEPOSITION HISTORY IN HURRICANE KATRINA IMPACTED MARSH SEDIMENT

*Gopal Bera* and Alan Shiller (The University of Southern Mississippi, Stennis Space Center, MS, USA)
Kevin Yeager (The University of Kentucky, Lexington, KY, USA)

Increasing sea surface temperatures may lead to an increase in the frequency of major hurricanes. Major hurricanes can significantly affect the coastal landscape by eroding and re-distributing inorganic sediments. For example, more than $131 \times 10^6$ metric tons (MT) of inorganic sediment was delivered to coastal wetlands in Louisiana by storm surges from Hurricanes Katrina and Rita in 2005. Thus, it is likely that each major hurricane can leave a distinct signal in coastal wetlands. Excepting major hurricanes, salt marsh sediments generally undergo steady accumulation over time and thus are widely used to reconstruct the depositional history of anthropogenic contaminants derived from atmospheric and fluvial sources.

We collected four short (~1 m) sediment cores from the fringing marshes of St. Louis Bay, MS (located ~30 km east of Katrina's track) during 2010-2011 to investigate the impact of Hurricane Katrina on marsh sediment accumulation and if possible to reconstruct the depositional history of both trace metals and dioxin.

Initial results from Pb-210, particulate organic carbon (POC), sediment bulk density and grain size show a 10-20 cm disturbed layer in the upper 40 cm of the cores. The thickness of these disturbed layers varies from core to core depending on location. Sediment samples for trace metal analysis were digested in Teflon bombs using $HNO_3$, $HF$, and $H_2O_2$ followed by saturated $H_3BO_3$. Recovery of most elements (Pb, V, Cr, Cu, Ni, and Zn) from a standard reference material (SRM 1646a) was between 88-102%, except for Cd(67%) and As (118%). Analytical precision (RSD) was below 10%. Profiles of Cs, Nd, Pb, V, Cr and Ni showed two distinct concentration peaks (2-4 fold increase) down section while Cu, Zn and As mainly showed one peak. The first peak occurs at ~15 cm depth and second peak at ~30 cm depth. The first peak can be best explained by co-precipitation of trace metals with iron minerals (FeS) in a strongly reducing environment. A large peak in Fe concentration at this depth supports this. Also, Mn showed its highest concentration at the surface, likewise suggesting reducing conditions further down. The second peak at ~30 cm coincided with the highest percentages of silt-clay sized sediment and POC concentration in the cores. A large peak (at ~30 cm) of Cs (probably derived from a local $TiO_2$ refinery) along with Nd, Pb, V, Cr and Ni suggests deposition of contaminated sediment at this depth. High concentrations of dioxins and furans at this depth also support the idea of deposition of contaminated sediment. Initial results show concentration of 2,3,7,8 polychlorinated dibenzo dioxin (PCDD) and 2,3,7,8 polychlorinated dibenzo furans (PCDF) and toxic equivalent ( TEQ) values have two peaks in first 40 cm of the core at the same depths as the trace metal peaks. This deposition of contaminated sediment might have been caused by Hurricane Katrina storm surge.

# EXTRACTABILITY OF HEAVY METALS IN BOTTOM ASH AND FLY ASH FROM A MULTI-FUEL BOILER USING ARTIFICIAL SWEAT AND GASTRIC FLUIDS

***Risto Pöykiö*** (City of Kemi, Valtakatu 26, FI-94100 Kemi, Finland)
Kati Manskinen (Stora Enso Oyj, Heinola Fluting Mill, FI-18101 Heinola, Finland)
Olli Dahl (Aalto University, Aalto FI-00076, Finland)
Hannu Nurmesniemi (Stora Enso Oyj, Veitsiluoto Mill, FI-94800 Kemi, Finland)

**ABSTRACT:** The results indicate that most of the heavy metals in fly ash are clearly soluble in artificial gastric fluid, since the extractable heavy metal concentrations in this fluid were as follows: Al 4890 mg/kg (dry weight), As 15.0 mg/kg (d.w.), Ba 340 mg/kg (d.w.), Cr 14.8 mg/kg (d.w.), Cu 32.6 mg/kg (d.w.), Mo 33.6 mg/kg (d.w.), Ni 43.8 mg/kg (d.w.), and V 210 mg/kg (d.w.). Furthermore, Al (55.0 mg/kg; d.w.), Ba (39.0 mg/kg; d.w.) and V (39.6 mg/kg; d.w.) in the bottom ash, in particular, showed clear extractability in artificial sweat fluid. In addition, Al (753 mg/kg; d.w.), Ba (85 mg/kg; d.w.), V (129 mg/kg; d.w.) and Zn (47.6 mg/kg; d.w.) in bottom ash showed clear extractability in artificial gastric fluid. Due to the high extractability of certain heavy metals in bottom ash and fly ash using artificial sweat or gastric fluids, we recommend careful handling of these ash residues in order to prevent the ingestion and penetration of ash particles across the human gastrointestinal tract, e.g. through inadvertent wiping of the mouth with dirty hands or through the inhalation of air-borne ash particles.

## INTRODUCTION

Ash residue fractions such as bottom ash, which accumulates at the bottom of the boiler, and fly ash, which is collected from the flue gas by methods such as electrostatic precipitation, wet scrubbing, fabric filters, or a mechanical device such as a cyclone or a baghouse, constitute a major fraction of solid residues produced by power plant. Elements with low volatility concentrate in the bottom ash, while more volatile elements concentrate in fly ash. Consequently, individual ash fractions differ in their chemical composition (Lin and Yeh, 2010).

Extraction is a procedure that puts a solid and a liquid in contact with each other under defined conditions. Extractions tests are widely used as tools to estimate the potential release of constituents, for example from waste materials, over a range of possible waste management activities, including recycling, reuse or landfill disposal. One of the most frequently used extraction tests for assessing the release of heavy metals from ash (Bruder-Hubscher et al., 2002), sludge, and from other industrial waste materials is sequential extraction (Filgueiras et al., 2002), in which elements in the material are fractionated between acid soluble, reducible and oxidisable fractions. This approach provides information on the chemical conditions needed to obtain different extraction efficiencies. The goal of this method is to divide the total extractable concentration of metals into separate fractions in order to assess the form in which the metals occur in the waste material. These extraction tests are carried out in the assessment of worst-case environmental scenarios, in which the components of the sample become soluble and mobile (Filgueiras et al., 2002).

In vitro extraction tests (Intawongse and Dean, 2006) involving synthetic sweat, synthetic gastric/gastrointestinal and synthetic saliva fluids are widely used for testing metal release from consumer products such as textiles (Rezić and Steffan, 2007) and artificial (polyethylene) turf (Zhang et al., 2008) materials, and from items used in an every-day life such as coins or jewellery (Rezić et al., 2009). Furthermore, synthetic urine-like liquors are applied for studying the solubility of urinary calculi formation in clinic studies (Streit et al., 1998). Synthetic human body fluids such as sweat and gastric/gastrointestinal and saliva fluids are also used as extractants to predict the availability of metals for human absorption in a range of industrial wastes such as coal fly ash (Lu et al., 2009), contaminated soil around old mining areas (Navarro et al., 2006) and municipal solid wastes such as compost (Nunez et al., 2007). Compared to the use of real human body fluids, in tests carried out *in vivo*, testing with synthetic fluids is both rapid and inexpensive, requiring only a day to conduct and costing only a small

fraction of the amount for *in vivo* tests.

Although *in vitro* tests using synthetic fluids have been reported to have limitations, e.g. due to the fact that they cannot contain all the constituents of human fluids (e.g. proteins, enzymes, etc.), they provide an appropriate means to determine the bioaccessibility of heavy metals in various materials. Real human body fluids have also been applied to study the solubility of heavy metals (Horowitz and Finley, 1993), but the application of synthetic body fluids may be more hygienic. Furthermore, real human body fluids have reported to have an unstable nature (Leung and Darvell, 1997; Brett et al., 2002), and in the European Union (EU) their use is strictly regulated by the rules of national ethical committees.

## MATERIALS AND METHODS

**Bottom and fly ash sampling:** The bottom ash and fly ash investigated in this study originated from the large-sized (77 MW) multi-fuel boiler (MFB) at the power plant of a fluting board mill located in Finland (Pöykiö et al., 2011). In this boiler, where coal and heavy fuel oil are fired simultaneously, pressurised steam is used to excite the atomisation of heavy fuel oil into small droplets to allow stable combustion, and the pulverised combustion technique is used for the incineration of coal. The boiler started to operate in 1960, and nowadays it is only occasionally used when the main energy source of the fluting board mill, the bubbling fluidized bed boiler (BFB), is not used for the energy production. According to the environmental permit of the mill, no more than 2000 annual operational hours, starting from 1 January 2008 and ending no later than 31 December 2015, are allowed for the multi-fuel boiler, after which it is no longer permitted to use this boiler. During the sampling period, when the bottom ash was sampled from the outlet of the boiler and the fly ash from the ash silo, approximately 75-% of the energy produced by the boiler originated from the incineration of heavy fuel oil (S ~ 0.95-% by weight), and approximately 25-% from the incineration of coal. Sampling of the ashes was carried out over a period of two days, as this boiler was not needed for energy production for a longer period. During sampling, a total of two sub-samples of both ashes were collected. The weight of these individual samples was 1.5 kg. The two individual sub-samples for each ash were combined to give one composition sample with a weight of 3 kg for each ash. After sampling, the ash samples were stored in plastic bags in a refrigerator (+ 4 °C). A coning and quartering method was repeatedly applied to reduce the ash samples to a size suitable for conducting laboratory analyses.

**Determination of the physical and chemical properties of the ashes:** To determine the mineralogical composition of the bottom and fly ash, X-ray diffractograms of powdered samples were obtained with a Siemens D 5000 diffractometer (Siemens AG, Karlsruhe, Germany) using CuKα radiation. The scan was run from 2 to $80^°$ (2-theta-scale), with increments of 0.02° and a counting time of 1.5 seconds per step. The operating conditions were 40 kV and 40 mA. Peak identification was performed with the DIFFRACplus BASIC Evaluation Package PDFMaint 12 (Bruker axs, Germany) and ICDD PDF-2 Release 2006 software package (Pennsylvania, USA).

**Determination of the total heavy metal concentrations in the ashes:** For the determination of total element concentrations in the bottom and fly ash, the dried samples were digested with a mixture of HCl (3 mL) and $HNO_3$ (9 mL) in a CEM Mars 5 microprocessor-controlled microwave oven with CEM HP 500 Teflon vessels (CEM corp., Matthews, USA) using USEPA method 3051A (Yafa and Farmer, 2006). The cooled solutions were transferred to 100 mL volumetric flask and the solutions were diluted to volume with ultrapure water. The ultrapure water was generated by an Elgastat Prima reverse osmosis and Elgastat Maxima ion exchange water purification system (Elga, Ltd; Bucks, England). All reagents and acids were suprapure or pro analysis quality. The total element concentrations in the ashes were determined with a Thermo Elemental IRIS Intrepid II XDL Duo (Franklin, USA) inductively coupled plasma optical emission spectrometer (ICP-OES).

**Procedure for determining the extractability of heavy metals in ashes by artificial sweat and gastric fluids:** Artificial sweat was prepared by dissolving 5 g NaCl, 1 g lactic acid and 1 g urea in 1 L of deionized water and adjusting the pH to a value of 6.47 with ammonia (Song et al. 2007). Artificial gastric fluid was prepared by dissolving 60.06 g glycine in 2 L of deionized water and adjusting the pH to a value of 1.51 with HCl (Wang et al. 2007). The extraction was carried out in polypropylene bottles by

shaking 1 g of ash on a dry weight (d.w.) basis with 100 mL of the extract (i.e. artificial sweat or artificial gastric fluid) for 1 hour by end-over-end mixing at 37 °C. Thus, the liquid-to-solid ratio (L/S 100 L/kg) in our procedure was the same as those of Wang et al. (2007) and Kim et al (2002). In order to minimize possible chemical and/or microbiological changes in the ash during the extraction procedure, extraction was carried out using an undried ash sample instead of a dried sample, since according to Kosson et al. (2002), it is preferable to avoid sample drying before extraction. After extraction, the extract was separated from the solid residue (i.e. the undissolved ash) by filtration through a 0.45 µm membrane filter. The pH of the extract was then measured, and the metal concentrations were determined with a Thermo Fisher Scientific iCAP6500 Duo (United Kingdom) inductively coupled plasma optical emission spectrometer (ICP-OES).

## RESULTS AND DISCUSSION

**Mineralogical composition of the ashes:** The most important physical and chemical properties of the ashes are presented in our previous paper (see Pöykiö et al., 2011). Both the bottom and fly ashes were strongly alkaline (pH 9.6 and 12.4, respectively). This is a disadvantage and dermal contact with the residues should be avoided, since according to Mroueh and Wahlström (2002), the alkaline nature of the ash may cause skin irritation. An alkaline pH of the ash indicates that part of the dissolved metals occur as basic metal salts, oxides, hydroxides, and/or carbonates, although the XRD spectra (Pöykiö et al., 2011) supported the existence hematite ($Fe_2O_3$) in both ashes, which is an oxide mineral. Quartz ($SiO_2$) occurred in both ashes, and anorthite ($CaAl_2Si_2O_8$) only in the bottom ash. Both of these minerals are silicates. In addition, the fly ash contained anhydrite ($CaSO_4$). Although X-ray diffraction (XRD) analysis can be useful for identifying the mineralogical species of crystalline particles in ash, in our case only a few minerals could be identified. An XRD spectrometer is unable to identify the amorphous (glass) phase (i.e. non-crystallised matter), and its detection limit is normally 1 - 2-% (w/w). This is probably why crystalline compounds containing all the metals in Table 1 were not identified by XRD, despite the fact that concentrations of these heavy metals could be quantitatively measured by ICP-OES.

**Physical and chemical properties of the ashes:** The relatively high (9.7-% = 97.0 g/kg; d.w.) total organic carbon (TOC) value in the fly ash investigated in this study indicates the incomplete combustion of organic matter in this residue (Enell et al., 2008), although the highest incineration temperature in the boiler is between 1000 and 1100 °C. The relatively high (10.9-%; d.w.) loss on ignition value (LOI) in the fly ash also supports this. However, the low TOC (0.7-% = 7.0 g/kg; d.w.) and LOI (0.7-%; d.w.) values in the bottom ash indicates complete combustion of this residue in the boiler. This difference is due to the fact that fly ash particles rise with the flue gas into the upper zone of the boiler and so remain in the hottest zone of the combustion chamber for a shorter period than those particles that are associated with the bottom ash fraction. In this context, it is notable that although LOI is widely used to indicate the unburned material in ash, according to the findings of Payá et al. (2002), the LOI value instead indicates the volatile fractions.

Due to the very high dry matter contents of 99.9-% and 99.8-%, the bottom and fly ash are likely to cause dust problems during handling. According to the particle size distribution profile (Pöykiö et al., 2011), no particles of a diameter equal to or greater than 0.5 mm existed in the fly ash. In the fly ash, particles in the diameter range smaller than 0.075 mm accounted for 93.6 wt.-%, whereas in the bottom ash they accounted for 17.2 wt.-%. These smallest particle fractions are of greatest concern because of their dust generation potential and the inhalation exposure risks when ash is handled, e.g. in landfills (Macleod et al., 2006). The sieving losses of 0.5 wt.-% for the bottom ash and of 0.20 wt.-% for the fly ash were low.

**Total and extractable heavy metal concentrations in the ashes:** Table 1 presents the total and extractable concentrations of trace elements in the ashes. When comparing the total element concentrations in ashes, it is notable that, except for Cu and Se, they are from 1.2 (Sb) to 3.5 (Pb) times higher in the fly ash than in the bottom ash. The enrichment of trace elements in the fly ash is due to the fact that the temperature between 1000 - 1100 °C in the multi-fuel boiler is high enough to vaporize some elements.

**TABLE 1.** The total concentrations of metals (Pöykiö et al., 2011) in the bottom ash (BA) and fly ash (FA) of a multi-fuel boiler determined using USEPA method 3051A (Yafa and Farmer, 2006), and the extractable concentrations of metals in artificial sweat and gastric fluids at a liquid to solid (L/S) ratio of 100 L/kg, as well as the pH of the extract before (i.e. only extract) and after (i.e. extract + ash) extraction.

| pH and metal | Total concentration USEPA 3051A (mg/kg; d.w.) | | Extractable concentration in artificial sweat fluid (mg/kg; d.w.) | | Extractable concentration in artificial gastric fluid (mg/kg; d.w.) | |
|---|---|---|---|---|---|---|
| | BA | FA | BA | FA | BA | FA |
| pH (before) | | | 6.47 | 6.53 | 1.54 | 1.52 |
| pH (after) | | | 8.00 | 8.45 | 1.60 | 1.66 |
| Al | 14300 | 30900 | 55.0 | 110 | 753 | 4890 |
| As | 17 | 23 | 3.2 | 5.4 | 11.0 | 15.0 |
| Ba | 650 | 1200 | 39.0 | 65.0 | 85.0 | 340 |
| Be | 2.0 | 4.0 | < 0.5 | < 0.5 | < 0.5 | 1.1 |
| Cd | 0.6 | 1.2 | < 0.2 | < 0.2 | 0.4 | 0.6 |
| Co | 17 | 29 | 1.2 | < 0.5 | 2.9 | 5.1 |
| Cr | 49 | 69 | 1.7 | 3.8 | 3.5 | 14.8 |
| Cu | 120 | 110 | < 1.0 | < 1.0 | 17.5 | 32.6 |
| Mo | 27 | 63 | 16.3 | 41.1 | 14.9 | 33.6 |
| Ni | 170 | 240 | 19.1 | 4.6 | 33.0 | 43.8 |
| Pb | 26 | 91 | < 1.5 | < 1.5 | 12.6 | 18.7 |
| Sb | 6.0 | 7.0 | < 2.0 | < 2.0 | < 2.0 | < 2.0 |
| Se | < 4.0 | < 4.0 | < 2.0 | < 2.0 | < 2.0 | < 2.0 |
| V | 280 | 390 | 39.6 | 46.6 | 129 | 210 |
| Zn | 100 | 190 | < 1.5 | < 1.5 | 47.6 | 53.0 |

The final fate of volatilizable elements is determined not only by their volatilization characteristics but also by their retention in fly ash through other process (i.e. primarily the condensation process). If we disregard the metals whose concentrations were lower than the detection limits and molybdenum (Mo), the extractable concentrations of other heavy metals in artificial gastric fluid were clearly higher than those in artificial sweat fluid. These results are reasonable, as the pH of the artificial gastric fluid was extremely acidic both before (pH 1.52 - 1.54) and after (pH 1.60 - 1.66) extraction, whereas the pH of the artificial sweat fluid was slightly alkaline before (pH 6.47 - 6.53) and after extraction (pH 8.00 - 8.45). In this context, it is notable that the pH of the fly ashes was strongly alkaline (pH 12.5), the dry matter content 99.9-% and electrical conductivity 13.9 mS/cm (Pöykiö et al., 2011). However, for the fly ash, the extractable concentration of Mo was slightly higher in artificial sweat (41.1 mg/kg; dry weight) than that in artificial gastric fluid (33.6 mg/kg; d.w.). Furthermore, for the bottom ash, the extractable concentration of Mo in artificial sweat (16.3 mg/kg; d.w.) was higher than that in artificial gastric fluid (14.9 mg/kg; d.w.). The higher extractable concentration of Mo in artificial sweat is reasonable, since Mo is able to form oxyanions, which means that its extractability clearly increases from acidic pH values to neutral and alkaline conditions (Al-Abed et al., 2006). Notably, we have also observed this type of release of molybdenum from ash in our previous study (Pöykiö et al., 2009).

Mroueh and Wahlström (2002) have described the possible occupational risks to humans when industrial residues, e.g. ash, are landfilled. The main human exposure pathway is the inhalation of dust or volatile compounds, dermal contact and inhalation. Once the ash material enters the body via the respiratory and gastrointestinal tracts, it mixes with biological fluids and hence has an opportunity to be dissolved and absorbed (Twining et al., 2005). The results indicate that most of the heavy metals in fly ash are clearly soluble in artificial gastric fluid. Furthermore, Al, Ba and V in the bottom ash, in particular, showed extractability in artificial sweat fluid. Therefore, taking into consideration the toxicity of many of the heavy metals presented in Table 1 and our observation of high extractable concentrations

of certain heavy metals in artificial sweat and gastric fluids, we recommend careful handling of fly ash. In terms of human health risk assessment, we recommend the prevention of ash dusting and the penetration of ash particles across the human gastrointestinal tract, e.g. through inadvertent wiping of the mouth with dirty hands or through the inhalation of air-borne ash particles. Furthermore, due to the alkaline nature of the ashes (i.e. bottom ash pH 9.6; fly ash pH 12.4; see Pöykiö et al. 2011), according to Mroueh and Wahlström (2002), the avoidance of dermal contact with these residues is recommended to prevent skin irritation.

## CONCLUSIONS

The results indicate that most of the heavy metals in fly ash are clearly soluble in artificial gastric fluid, since the extractable heavy metal concentrations in this fluid were as follows: Al 4890 mg/kg (dry weight), As 15.0 mg/kg (d.w.), Ba 340 mg/kg (d.w.), Cr 14.8 mg/kg (d.w.), Cu 32.6 mg/kg (d.w.), Mo 33.6 mg/kg (d.w.), Ni 43.8 mg/kg (d.w.), Pb 18.7 mg/kg (d.w.), and V 210 mg/kg (d.w.). Therefore, in terms of human health risk assessment, careful handling of this residue is highly recommended since heavy metals in fly ash pose a potential human health risk, e.g. if ash particles associated with heavy metals enter the human gastrointestinal tract through inadvertent wiping the mouth with dirty hands or through the inhalation of ash particles.

## ACKNOWLEDEGEMENTS

## REFERENCES

Al-Abed, S.R., P.L. Hageman., G. Jagedeesan., N. Madhavan., and D. Allen D. 2006. "Comparative evaluation of short-term leach tests for heavy metal release from mineral processing waste." *Sci. Total Environ.* 364(1-3): 14-23

Brett, C.M.A., and L. Muresan L. 2002. "The influence of artificial body fluids on metallic corrosion." *Key Eng. Mat.* 230-232: 459-462

Bruder-Hubscher, V., F. Lagarde., and M.J.F. Leroy. 2002. "Application of a sequential extraction procedure to study the release of elements from municipal solid waste incineration bottom ash." *Anal. Chim. Acta.* 451(2): 285-295

Enell, A., F. Fuhrman., L. Lundin., P. Warfvinge., and G. Thelin G. 2008. "Polycyclic aromatic hydrocarbons in ash: Determination of total and leachable concentrations." *Environ. Poll.* 152 (2): 285-292

Filgueiras, A.V., I. Lavilla., and C. Bendicho. 2002. "Chemical sequential extraction for metal partitioning in environmental solid samples." *J. Environ. Monit.* 4(6): 823-857

Horowitz, S.B., and B.L. Finley. 1993. "Using human sweat to extract chromium from chromite ore processing residue." *J. Toxicol. Env. Heal. A.* 40(4): 585-590

Intawongse, M., and J.R. Dean. 2006. "In-vitro testing for assessing oral bioaccessibility of trace metals in soil and food samples." *Trends Anal. Chem.* 25(9): 876-886

Kim, J.Y., K.W. Kim., J.U. Lee., J.S. Lee., and J. Cook. 2002. "Assessment of As and heavy metal contamination in the vicinity of Duckum Au-Ag Mine, Korea." *Environ. Geochem. Hlth.* 24(3): 213-225

Kosson, D.S., H.A. van der Sloot., F. Sanchez., and A.C. Garrabrants. 2002. "An integrated framework for evaluating leaching in waste management and utilization of secondary materials." *Environ. Eng. Sci.* 19(3): 159-204

Leung V.W.H., and B.W. Darvell. 1997. "Artificial salivas for in vitro studies of dental materials." *J. Dent.* 25(6): 475-484

Lin, C. L., and T.Y. Yeh. 2010. "Heavy metals distribution characteristics in different particle size of

bottom ash after agglomeration/defluidization at various fluidization parameters." *Biomass Bioenerg*. 34(4): 428-437

Lu, S.G., Y.Y. Chen., H.D. Shan., and S.Q. Bai. 2009. "Mineralogy and heavy metal leachability of magnetic fractions separated from some Chinese coal fly ashes." *J. Hazard. Mater*. 169(1-3): 246-255

Macleod, C., R. Duarte-Davidson., B. Fisher., B. Ng., D. Willey., J.P. Shi., I. Martins., G. Drew., and Pollard S. 2006. "Modelling human exposures to air pollution control (APC) residues released from landfills in England and Wales." *Environ. Int.* 32(4): 500-509

Mroueh, U.M., and M. Wahlström. 2002. "By-products and recycled materials in earth construction in Finland – an assessment of applicability." *Resour. Conserv. Recy*. 35(1-2): 117-129

Mroueh, U.M., E. Mäkelä., M. Wahlström., J. Kauppila., J. Sorvari., P. Heikkinen., P. Salminen., M. Juvankoski., and M. Tammirinne. 2009. *By-products in earth construction. Assessment of acceptability. National Technology Agency*. Technology Reviewers 96/2000, pp. 39.

Navarro, M.C., C., Pérez-Sirvent., M.J. Martinez-Sánchez., J. Vidal., and J. Marimón. 2006. "Lead, cadmium and arsenic bioavailability in the abandoned mine site of Cabezo Rajao (Murcia, Se Spain)." *Chemosphere*. 63(3): 484-489

Nũñez, R.P., R.D. Rey., A.B.M. Menduiña., and M.T.B. Silva 2007. "Physiologically based extraction of heavy metals in compost: Preliminary results." *J. Trace Elem. Med. Bio*. 21(S1): 83-85

Payá, J., J. Monzó., N. Borrachero., F. Amahjour., and E. Peris-Mora 2002. "Loss on ignition and carbon content in pulverized fuel ashes (PFA): two crucial parameters for quality control." *J. Chem. Technol. Biot*. 77(3): 251-255

Pöykiö, R., K. Manskinen., H. Nurmesniemi., and O. Dahl. 2011. "Comparison of trace elements in bottom ash and fly ash from a large-sized (77 MW) multi-fuel boiler at the power plant of a fluting board mill, Finland." *Energ. Explor. Exploit*. 29(3): 217-234

Pöykiö, R., H. Rönkkömäki., H. Nurmesniemi., P. Perämäki., K. Popov., and I. Välimäki. 2009. "Release of metals from grate-fired boiler cyclone ash at different pH values." *Chem. Spec. Bioavailab*. 21(1): 23-31

Rezić, I., M. Zeiner., and I. Steffan. 2009. "Determination of allergy-causing metals from coins" *Monatsh. chem.* 140(2): 147-151

Rezić, I., and I. Steffan. 2007. "ICP-OES determination of metals present in textile materials." *Microchem. J.* 85(1): 46-51

Song, Y.W., D.Y. Shan., and H.E. Han. 2007. "Corrosion behaviours of electroless plating Ni-P coatings deposited on magnesium alloys in artificial sweat solution." *Electrochim. Acta*. 53(4): 2009-2015

Streit, J., L.C. Tran-Ho., and E. Königsberger. 1998. "Solubility of the three calcium oxalate hydrates in sodium chloride solutions and urine-like liquors." *Monatsh. chem.* 129(12): 1225-1236

Twining, J., P. McGlinn., E. Loi., K. Smith., and R. Gieré. 2005. "Risk ranking of bioaccessible metals from fly ash dissolved in simulated lung and gut fluids." *Environ. Sci. Technol*. 39(19): 7749-7756

Wang, X.S., Y. Qin, and Y.K. Chen. 2007. "Leaching characteristics of arsenic and heavy metals in urban roadside soils using a simple bioavailability extraction test." *Environ. Monit. Assess*. 129(1-3): 221-226

Yafa, C., and J.G. Farmer J.G. 2006. "A comparative study of acid-extractable and total digestion method for the determination of inorganic elements in peat material by inductively coupled plasma-optical emission spectrometry." *Anal. Chim. Acta.* 557(1-2): 296-303

Zhang, J., I. K. Han., L. Zhang., and W. Crain. 2008. "Hazardous chemicals in synthetic turf materials and their bioaccessibility in digestive fluids." *J. Exp. Sci. Env. Epid*. 18(6): 600-607

# REMOVAL OF ARSENIC BY COPRECIPITATION WITH IRON IN VERTICAL FLOW WETLAND COLUMNS

Katherine Lizama Allende (Monash University, Melbourne, Australia)
Timothy Fletcher (The University of Melbourne, Melbourne, Australia)
*Guangzhi Sun* (James Cook University, Townsville, Australia)

**ABSTRACT:** This study investigated the removal of arsenic in twenty wetland columns, planted with *Phragmites australis*, from a synthetic acidic wastewater that simulated water in a highly polluted river in northern Chile, the Azufre River. The efficiencies of four wetland media, cocopeat, zeolite, limestone, and river gravel, were investigated. A range of environmental factors, including pH, Eh, temperature and $SO_4$ level, were monitored alongside the removal rates of arsenic and iron, in order to explain the factors that must be taken into account when applying the wetland system to treat acidic wastewaters. Experimental data demonstrated that the primary route of arsenic removal is via coprecipitation with iron at increased pH level. The chemical equilibrium of arsenic-iron coprecipitation has been analysed. Also discussed are the effects of wetland media on arsenic mass removal rates, and the potential routes of arsenic removal in constructed wetland systems under oxidising condition.

## INTRODUCTION

In many countries arsenic presents a serious pollution threat to natural waterways. In Chile, for example, one of the major rivers, the Loa River, has arsenic concentration around 1,400 µg/L, due to input from runoffs and upstream geothermal activities (Romero et al., 2003). Arsenic pollution of such scale is difficult to control and remediate by conventional wastewater treatment technologies, such as adsorption, coagulation, and membrane filtration, because of high energy requirement, sludge generation, and/or transportation cost (Mohan and Pittman, 2007).

During the past two decades constructed wetlands have been increasingly used, especially in rural regions, to treat domestic and agricultural wastewaters. While constructed wetlands require large areas of space, their low energy consumption and typically low maintenance requirements make them an ideal option for treating acidic wastewaters on remote sites. The ability of constructed wetlands to remove metals and metalloids from contaminated waters has been generally recognised, but not sufficiently studied, especially concerning the removal of arsenic (Lizama Allende et al, 2011a). Most studies to date have been conducted on surface flow wetlands, with much fewer studies on subsurface flow wetlands, where contaminated waters pass through packed media, instead of flowing above, that allows more extensive contact between the contaminants and media. It may thus be hypothesised that subsurface flow wetlands should offer greater, and more reliable, treatment performance than surface flow wetlands (Buddhawong et al, 2005). However, despite the potential advantages of using the subsurface flow systems for such purpose, the lack of information about their performance hinders their ready adoption.

To assess the potential of subsurface flow wetlands for arsenic removal, experiments need to demonstrate which wetland media, or combination of different media, are most suited to remove the pollutant. Although various media have been suggested for such purposes (Ye et al, 2003), experiments are rarely carried out to verify hypothesised suitability. In a preliminary lab-scale experiment, cocopeat, zeolite and limestone were found to have the ability to remove As, Fe and B (Lizama Allende et al, 2011b) under neutral or slightly acidic environment; however, their ability to remove these pollutants under highly acidic condition, which is usually associated with contaminated waters on mining sites, was not studied.

In addition to experimental study on acid wastewater treatment, there is a need for studies that identify and quantify the environmental factors affecting the removal of As and metals in subsurface flow wetlands, as well as the links between the removal of different pollutants that result from chemical precipitation and coprecipitation. Two key factors that affect As removal in wetlands are: (1) pH, and (2) the presence of iron and sulfur (Lizama Allende et al, 2011a). Preliminary study by Lizama Allende et al

(2011b) has partly demonstrated the effect of the first factor. Regarding the second factor, iron hydrochemistry has been found to control As aqueous mobility in acid ferruginous mine waters when pH is below 4 (Williams, 2001). The interaction between Fe and As in wetland environment can have a significant effect on the removal of both pollutants. This is a phenomenon that needs to be further investigated, because Fe and As are so commonly found together, and optimising the treatment of one will typically require consideration of the other.

The aim of this study is therefore to investigate the use of subsurface flow wetlands to remove As and Fe from a synthetic acidic wastewater that simulates polluted water in the Azufre River. The efficiencies of four wetland media are studied: cocopeat, zeolite, limestone, and gravel, with the aim of evaluating the pollutant removal efficiency. A range of environmental factors, including pH, Eh, temperature and $SO_4^{-2}$ levels, are monitored alongside As and Fe removal rates, to explain the factors that must be taken into account when optimising constructed wetlands for heavy metal and arsenic removal from acidic wastewaters.

## MATERIALS AND METHODS

**Acidic Wastewater:** Synthetic wastewater was prepared using deionised water with the following reagents added per litre of water: 3 mL 1,000 mg/L arsenic standard solution (arsenic acid $As_2O_5$ in $H_2O$), 3 mL 10,000 mg/L boron standard solution (boric acid $H_3BO_3$ in $H_2O$), 0.5 g $FeSO_4 \cdot 7H_2O$, and 0.425 mL $H_2SO_4$ (95-97% Merck ISO grade). As a result, the concentrations of three main pollutants in the synthetic feed were (average ± standard deviation): 3.08±0.25 mg/L As, 32±2.19 mg/L B, and 107.33±6.53 mg/L Fe. The resulting pH value was 2.0±0.1. Under such acidic condition, the metals were mostly dissolved, consistent with how they are naturally found in the Azufre River.

**The Wetland System:** Twenty vertical flow wetland columns were built using PVC pipes. Each column was 1 m tall and 100 mm in internal diameter, as illustrated in Figure 1.
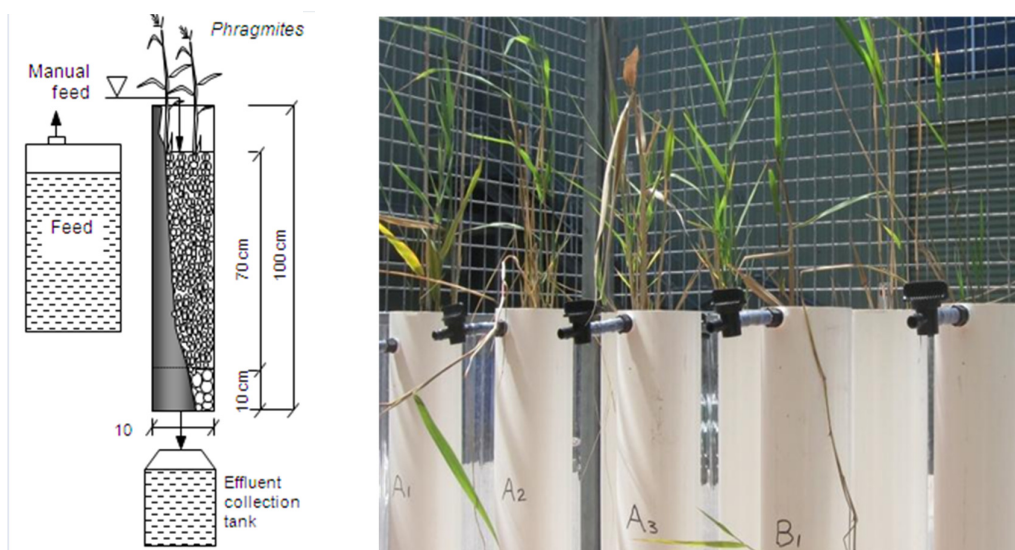


**FIGURE 1. A schematic diagram (left) and photo (right) of the wetland columns**

The wetland columns, placed in a greenhouse, were divided into four groups; each employing gravel, cocopeat, zeolite and crushed limestone as the main substrate. Each group had five identical replicate columns that were operated as individual treatment units. Packed porosities of the media are 40%, 55%, 25% and 30% in gravel, cocopeat, zeolite, and crushed limestone columns, respectively. Each column had a 0.1 m deep drainage layer of 20-40 mm gravel at base. The drainage layer was overlain with a single 0.7 m deep layer of main substrate (gravel, cocopeat, zeolite or limestone), resulting in a total depth of 0.8 m (the main layer plus the drainage layer). In each column, a single common reed, *Phragmites australis*, from the root-cuts of mature plants was planted.

During the experiments, the synthetic wastewater was stored in a 230 L continuously-stirred feed tank. From the tank, two litres of synthetic wastewater were collected and dosed manually onto the top of each wetland column. The wastewater was freshly prepared each week before the first dosing, and it was kept to the next dosing day on the same week. The water passed by gravity through the wetland media during the dosing, as the outlet was non-restricted. Effluent from each column was collected underneath in an effluent collection tank. The manual dosing was carried out twice per week, giving a hydraulic loading rate of 4 litres per week ($0.073 \ m^3/m^2d$) to each column. The dosing lasted for thirteen weeks.

**Sampling and Analysis:** Water samples were collected from the inlet (feed tank) and outlet (effluent collection tank) of each column in week 1, 4, 7, 9, 11 and 13. Analyses were carried out for As, B and Fe concentrations, and Sulfate ($SO_4^{-2}$), suspended solids (SS), pH, dissolved oxygen (DO), redox potential (Eh), and conductivity values. Separate samples were taken for total and dissolved metal analysis, with analysis undertaken according to standard methods. For the measurement of dissolved pollutants, the samples were filtered through 0.45 µm cellulose acetate papers and acidified (with nitric acid) immediately after sampling. The analyses of As, B and Fe concentrations were carried out for both unfiltered and filtered samples, to give total and dissolved values; only dissolved values are discussed in this paper. Other parameters were analysed for the unfiltered samples only.

**Pollutant Mass Removal Rates:** To compare the removal efficiencies of a specific pollutant in different systems, or under different conditions, the most appropriate parameter to use is kinetic or equilibrium coefficients at fixed temperature. When such coefficients are unavailable (for example: kinetics or equilibrium is unknown), pollutant mass removal rate is often used as an indicator of efficiency. Here the mass removal rate ($M_R$) for dissolved arsenic is calculated as:

$$M_R = (C_{in} - C_{out}) \times Q / V_{wetland} \tag{1}$$

Where: $C_{in}$ (mg/L) corresponds to the dissolved concentration of As in the inflow; $C_{out}$ is dissolved concentration in the outflow; Q (L/d) is daily flow rate; and $V_{wetland}$ ($m^3$) is the superficial volume of a single wetland column.

**RESULTS AND DISCUSSION**

**Overall Performance:** Boron concentrations were analysed, but the results are not presented in this paper, as discussion is primarily focused on arsenic and iron. Table 1 gives the average concentrations of dissolved As and Fe in the inflow and outflow of each wetland column. Significantly different As levels in the outflows demonstrate that the nature of media had a major impact on As removal, as well as pH and Eh values, in the wetland columns.

**TABLE 1. Mean values of dissolved As, Fe, and other parameters in inflows and outflows**

| | Influent | Effluent from | | | |
|---|---|---|---|---|---|
| | | G columns | C columns | Z columns | L columns |
| $As_{(aq)}$, mg/L | 3.0 | 1.7 | 2.7 | 0.25 | 0.01 |
| $Fe^{2+}_{(aq)}$, mg/L | 105.3 | 112.8 | 54.0 | 14.8 | 0.11 |
| SS, mg/L | 4.9 | 26.3 | 8.1 | 1.1 | 25.9 |
| $SO_4^{2-}$, mg/L | 907 | 939 | 954 | 1022 | 1126 |
| pH | 2.0 | 2.0 | 1.9 | 2.7 | 6.9 |
| Eh, mV | 452.8 | 501.5 | 501.6 | 497.9 | 198.0 |
| Temperature, $^0C$ | 19.4 | 18.8 | 18.8 | 19.0 | 19.0 |
| DO, mg/L | 9.2 | 9.3 | 8.5 | 9.0 | 8.7 |

On average, the mass removal rate ($M_R$) of dissolved As in G, C, Z and L columns reached 119, 27, 251 and 273 mg/m³d, respectively. In terms of As removal efficiency, limestone was clearly the media of choice among the four media studied.

Why did limestone media enable greater As removal efficiency during the experiment? As shown in Table 1, the removal of As and Fe took place simultaneously in the L columns, as $CO_3^{2-}$ and $HCO_3^-$ supplied by the crushed limestone increased pH of the wastewater. This result is consistent with report by Wang et al (2003) that more effective removal of arsenic can be expected with increased pH. The following reaction equilibrium demonstrates that increased pH stimulated arsenic-iron co-precipitation in the wetland columns.

**Fe-As Coprecipitation:** Iron hydroxide is known to be a strong reagent to remove arsenic from contaminated water. The route of As coprecipitation is either that: (a) As is adsorbed onto iron hydroxide precipitates, and then trapped with the precipitates inside the wetland columns; or (b) As is chemically bonded and enmeshed into complex $Fe(OH)_3$ molecule aggregates. Regardless of the exact route, the coprecipitation process can be quantified in the following formula:

$$nAs_{(aq)} + Fe^{2+} + 0.25O_2 + 2.5H_2O \leftrightarrow Fe(OH)_{3(s)} \cdot nAs + 2H^+ \tag{2}$$

In Eqn (2), n represents a fractional number of arsenic molecule that coprecipitates with an iron molecule. It is beyond the scope of this study to verify whether or not n is a fixed stoichiometric value, which only applies if As is chemically bound to iron hydroxide molecules. As such, in this study n should be seen as a value that may vary with the ratio of influent Fe to As concentrations. At equilibrium, and low solute concentrations (when the activity of each solute is equal to its molar concentration), the reaction product can be written as:

$$\frac{[H^+]^2}{[As]^n[Fe^{2+}][O_2]^{0.25}} = Cons\tan t \tag{3}$$

Considering that DO level is relatively stable in the water, and reaction equilibrium is much less sensitive to DO than the other three ions, Eqn 2 can be simplified as:

$$\frac{[H^+]^2}{[As]^n[Fe^{2+}]} = Cons\tan t \tag{4}$$

Thus
$$2\log[H^+] = \log[Cons\tan t] + n\log[As_{(aq)}] + \log[Fe_{(aq)}^{2+}] \tag{5}$$

$$2pH + \log[Fe_{(aq)}^{2+}] = C - n\log[As_{(aq)}] \tag{6}$$

Where C is a constant; $[Fe^{2+}]$ and $[As]$ are molar concentrations of dissolved iron and arsenic, respectively.

Equations (4)-(6) show that: (a) in theory, Fe precipitation (and As coprecipitation with Fe) is highly sensitive to pH value, and (b) if coprecipitation is indeed the predominant As removal route, a linear relationship can be expected between $2pH+\log[Fe_{(aq)}]$ and $-\log[As_{(aq)}]$. Figure 2 presents the plot of $2pH+\log[Fe_{(aq)}]$ vs. $-\log[As_{(aq)}]$ values, which have been calculated using As and Fe concentrations in the outflow from individual wetland columns. A liner relation is clearly shown in Figure 2. Thus, experimental data from this study match theoretical predictions by equation (6).

A cautious note should be made here that the nature of coprecipitated As-Fe particles is unknown, and value n in equation (6) must not be taken as stoichiometric constant without further experiment and analysis on the characteristics of settled solids in the wetland columns. In addition to iron hydroxide, calcium arsenates can also precipitate in oxidising environments, with the presence of Ca and As. Geochemical modelling and the use of advanced analytical techniques are required to further investigate the As speciation in the precipitates.

$$2pH + log[Fe_{(aq)}] = 0.73 - 1.98log[As_{(aq)}]$$
$$R^2 = 0.78$$
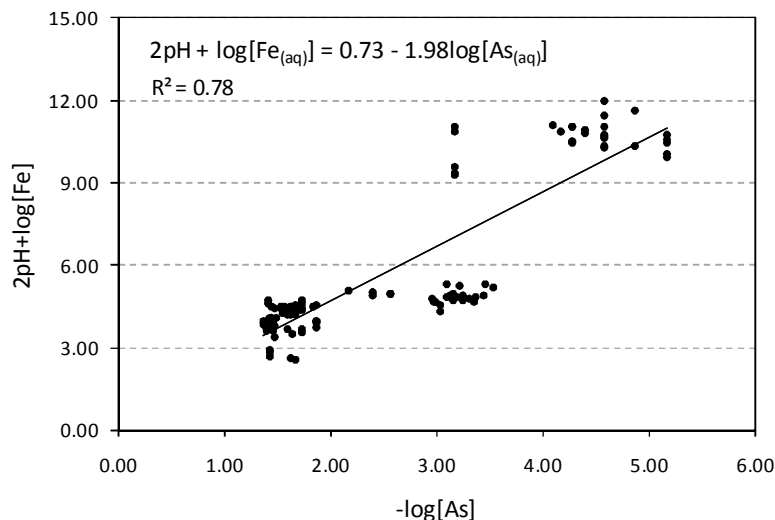
**FIGURE 2. Correlation between the values of 2pH+log[Fe$_{(aq)}$] and -log[As$_{(aq)}$]
for effluents from twenty wetland columns.**

**Arsenic Removal Routes in Wetland Columns:** Combined with a previous experiment under neutral pH condition (Lizama A et al, 2011b), this study gives further indication of arsenic removal routes in vertical flow wetland columns. As summarised by Lizama A et al (2011a), under oxidising or slightly oxidising condition (Eh>0) the following routes can all contribute to As removal.

Compared with As-Fe coprecipitation, other As removal routes, such as adsorption on media and assimilation into organic molecules, were less effective for removing arsenic in the experiment. Nevertheless these routes also contributed to As removal.

In G columns, no Fe precipitation took place (Table 1), indicating that 45% arsenic removal achieved in these columns was not due to As-Fe coprecipitation. Binding to humic acids is also unlikely, due to the lack of organic matter. It is postulated that As may have been removed by sorption onto protonated alumina sites, as suggested by Clifford and Ghurye (2002). It is also possible that the As may have been exchanged by Si anions, as suggested by Arai et al (2005), as silicate ions readily absorb onto mineral surfaces, and other oxyanions (such as arsenate) may replace the surface-absorbed Si anions.
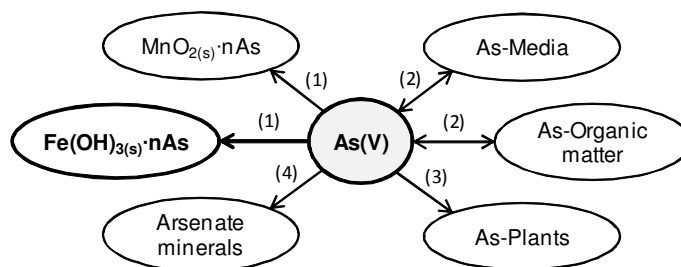


**FIGURE 3. As removal routes in a vertical flow constructed wetland under oxidising condition.
(1) coprecipitation; (2) sorption; (3) plant uptake; and (4) direct precipitation
to form soluble As compounds.**

In C columns, cocopeat was chosen to demonstrate how organic matter in the wetlands may affect As, Fe and B removal. Organic media, such as peat, have been reported to retain As (Cloy et al, 2009), Fe (Brown et al, 2000), and B. As shown in Table 1, cocopeat-based columns gave low As removal (9.7%), but higher Fe removal (47%). Although the sorption of As(V) onto organic matter has not been studied at pH level around 2, it has been found that the ability of humic acids to bind with As(V) improves when pH value increases from 4.6 to 8.4, with the maximum binding capacity occurring at pH 7 (Buschmann et

al, 2006). In this study, As(V) sorption onto humic acids appears to have been negatively affected by the presence of $H^+$, suggesting a preference of cocopeat to bind with Fe, instead of As, at low pH (around 2.0).

Zeolite is well known for its very high cation exchange capacity. Zeolite-based (Z) wetlands provided considerable removal of As and Fe at low pH, despite that in theory low pH adversely affects metal removal by zeolite due to competition between cations and $H^+$. A possible removal mechanism for As and Fe is postulated to be: $H^+$ and Fe cations are exchanged by other cations (such as Ca, Na, K) present on zeolite surfaces, resulting in increase in pH and decrease in dissolved Fe concentration (Table 1); and as this process progresses, As removal increases, attached to Fe on the zeolite sites (Payne and Abdel-Fattah, 2005). Advanced analytical technique is needed to investigate the mechanisms of arsenic removal in zeolite-packed wetland columns.

## CONCLUSIONS

The effects of four types of media on the removal of arsenic in vertical flow wetlands were studied. Arsenic-iron coprecipitation was found to be the predominant As removal route. A simple equilibrium model was developed to provide correlation between Fe and As concentrations in the outflow from a wetland; the model was verified by experimental data. Results from this study suggest the use of fine limestone chippings or grains in a constructed wetland, if arsenic removal is the main objective for the treatment of contaminated water.

## REFERENCES

Arai, Y., D.L. Sparks, and J.A. Davis. 2005. "Arsenate Adsorption Mechanisms at the Allophane - Water Interface". *Environ. Sci. Technol.*, 39: 2537-2544.

Brown, P.A., S.A. Gill, and S.J. Allen. 2000. "Metal Removal from Wastewater Using Peat". *Water Res.*, 34: 3907-3916.

Buddhawong, S., P. Kuschk, J. Mattusch, A. Wiessner, and U. Stottmeister. 2005. "Removal of Arsenic and Zinc using Different Laboratory Model Wetland Systems". *Eng. Life Sci.* 5:247-252.

Buschmann, J., A. Kappeler, U. Lindauer, D. Kistler, M. Berg, and L. Sigg. 2006. "Arsenite and Arsenate Binding to Dissolved Humic Acids: Influence of pH, Type of Humic Acid, and Aluminum". *Environ. Sci. Technol.*, 40: 6015-6020.

Clifford, D.A., and G.L. Ghurye. 2002. "Metal-Oxide Adsorption, Ion Exchange, and Coagulation-Microfiltration for Arsenic Removal from Water". In W.T. Jr. Frankenberg (Ed.), *Environmental Chemistry of Arsenic*, pp. 217-245, Marcel Dekker Publishers, New York.

Cloy, J.M., J.G. Farmer, M.C. Graham, and A.B. Mackenzie. 2009. "Retention of As and Sb in Ombrotrophic Peat Bogs: Records of As, Sb, and Pb Deposition at Four Scottish Sites". *Environ. Sci. Technol.*, 43: 1756-1762.

Lizama A., K., T.D. Fletcher, and G. Sun. 2011a. "Removal Processes for Arsenic in Constructed Wetlands". *Chemosphere* 84: 1032-1043.

Lizama A., K., T.D. Fletcher, and G. Sun. 2011b. "Enhancing the Removal of Arsenic, Boron and Heavy Metals in Subsurface Flow Constructed Wetlands using Different Supporting Media". *Water Sci. Technol.*, 63(11): 2612-2618.

Mohan, D., and C.U. Pittman Jr., 2007. "Arsenic Removal from Water/Wastewater using Adsorbents-A Critical Review". *J. Hazard. Mater.*, 142: 1-53.

Payne, K.B., and T.M. Abdel-Fattah. 2005. "Adsorption of Arsenate and Arsenite by Iron-Treated Activated Carbon and Zeolites: Effects of pH, Temperature, and Ionic Strength". *J. Environ. Sci. Heal. A*, 40: 723-749.

Romero, L., H. Alonso, P. Campano, L. Fanfani, R. Cidu, C. Dadea, T. Keegan, I. Thornton, and M. Farago, 2003. "Arsenic Enrichment in Waters and Sediments of the Rio Loa (Second Region, Chile)". *Applied Geochem.*, 18(9): 1399-1416.

Wang, J.W., D. Bejan, and N.J. Bunce. 2003. "Removal of Arsenic from Synthetic Acid Mine Drainage by Electrochemical pH Adjustment and Coprecipitation with Iron Hydroxide". *Environ. Sci. Technol.*, 37: 4500-4506.

Williams, M. 2001. "Arsenic in Mine Waters: International Study". *Environ. Geol.*, 40:267-278.

Ye, Z.H., Z.Q. Lin, S.N. Whiting, M.P. de Souza, and N. Terry. 2003. "Possible Use of Constructed Wetland to Remove Selenocyanate, Arsenic, and Boron from Electric Utility Wastewater". *Chemosphere*, 52: 1571-1579.

# SOLIDIFICATION, IMMOBILIZATION AND SEPARATION OF HEAVY METAL IN SOIL WITH NANO-Fe/Ca/CaO DISPERSION MIXTURES

*Srinivasa Reddy Mallampati*, Yoshiharu Mitoma, Shogo Sakita and Mitsunori Kakeda (Department of Environmental Sciences, Faculty of Life and Environmental Sciences, Prefectural University of Hiroshima, Shobara City, Hiroshima, Japan)

Tetsuji Okuda (Environmental Research and Management Center, Hiroshima University, Higashi-Hiroshima, Hiroshima, Japan)

**ABSTRACT:** At the present study, we developed for the first time, a nano-Fe/Ca/CaO dispersion mixture based solidification method for the immobilization of heavy metal (As, Cd, Cr and Pb) and their separation from contaminated soil. With simple grinding, about 79-86% of heavy metal immobilization could be achieved, and after grinding with nano-Fe/Ca/CaO dispersion mixtures about 95-99% of enhanced heavy metal immobilization was achieved in three different soils (decomposed granite, industrial clay and agriculture field). After treatment, about 25-44 wt% of magnetic and 75-56 wt% of non-magnetic fractions of soil were separated, and their condensed heavy metal concentration were about 85-95% and 10-20%, respectively. It was also clearly seen that the leachable heavy metal concentrations in non-magnetic fractions of soil are much lower than the Japanese soil leachate regulatory standard limits (< 0.01 mg/L for As, Cd and Pb and 0.05mg/L for Cr). By SEM semi-quantitative analysis, it was observed that the amounts of As, Cd, Cr and Pb detectable on soil particle surface decreased after nano-Fe/Ca/CaO treatment. The reduction of As, Cd, Cr and Pb amounts on particle surface by the covering with $Ca(OH)_2/CaCaO_3$ layer in soil surface is a possible explanation of the increase of immobilization efficiency after nano-Fe/Ca/CaO treatment. Furthermore, by magnetic separation, encapsulated nano-Fe particles in solidified media can also be separated; through this contaminated soil volume could be reduced. Therefore, this technology is considered having the ability to immobilization of heavy metal and reduce their volume by separation. These results appear to be very promising and the simple grinding with the addition of nano-Fe/Ca/CaO may be considered potentially applicable for the remediation and separation of heavy metal from contaminated soil.

## INTRODUCTION

The remediation of contaminated soil follows a rapid upward trend in Japan, especially after the proclamation of Soil Contamination Countermeasures Law in 2002 and its enforcement in 2003 (Ministry of Environment Government of Japan, 2002). Heavy metal contaminated sites pose a serious hazard to public health and the environment. Heavy metal contaminated soil are notoriously hard to remediate. Hence, its remediation is recognized to be one of the most difficult problems to be solved by taking advantage of suitable technologies. Typical remediation techniques for heavy metal in soil are constituted by extraction and immobilization processes. Extractive techniques may involve inorganic acids (Tessier et al. 1979) or organic acids and surfactants (Macauley and Hong 1995). Ex-situ extractive technologies are rarely adopted because of high risks and costs related to the use of hazardous extractants, the consequent need of treating secondary wastewater and shortage of landfill sites. On the other hand, in-situ extractive technologies are constituted mainly by phytoextraction and electrokinetic extraction (Reddy et al. 2001). Phytoextraction, may require extremely long time. The efficiency of electrokinetic extraction may be strongly affected by soil type and the removal of contaminant species.

Considering the limitations of the extractive techniques described above, immobilization processes are generally preferred for treating heavy metal contaminated soil (Paff and Bosilovich 1995). Immobilization is typically performed by mixing the contaminated soil with suitable binders, which are able to reduce heavy metal leachability through pH and alkalinity control to minimize their solubility, or by increasing adsorption, ionic exchange and precipitation of pollutants (USEPA 1982). A variety of binders (mainly with hydroxyapatite, zeolites, calcium hydroxide, phosphates and inorganic and organic

wastes) were investigated to immobilize heavy metal in soil. On the other hand, cement based stabilization/solidification treatment process for immobilizing hazardous substances that contain heavy metal is well known (USEPA 1993). Unfortunately, these immobilization treatment processes are carried out in wet condition, forming secondary effluents, requiring additional cost for treatment and the use of cement is also expensive. Therefore, the treatment under dry and water free conditions should be considered.

Our recent investigations showed that the nano-metallic Ca/CaO mixture was the most effective for hydrodechlorination of about 98% of PCDDs, PCDFs and PCBs in contaminated fly ash, and also, for cesium immobilization of about 96% in soil by ball milling treatment (Mitoma et al., 2011; Srinivasa Reddy et al., 2012). The high PCDDs, PCDFs and PCBs hydrodechlorination and cesium immobilization with the addition of nano-metallic Ca/CaO may be caused by the high reduction potentials and high surface area produced by ball milling. In case of cesium immobilization, Ca/CaO and sodium phosphate ($NaH_2PO_4$) can also make immobile salts with moisture and $CO_2$ in atmosphere, including pozzolanic cement and hydraulic property, cesium would be brought into the immobile $Ca/PO_4$ salts (Srinivasa Reddy et al., 2012). We assumed, that the addition of the nano-metallic Fe/Ca/CaO would effectively reduce the heavy metal leaching potential from contaminated soil by its high reduction potential and high surface area with simple grinding. On the other hand, nano-metallic Ca/CaO on the surface of soil can bind with the As, Cd, Cr and Pb metal elements in the presence of moisture due to its electron sources therefore, the $Ca(OH)_2/CaCO_3$ layer in soil surface could be produced. Further, encapsulated nano-Fe particles in solidified media can also be separated by magnetic separation, this way heavy metal contaminated soil volume can be reduced. Therefore, in the present work, the effect of nano-Fe/Ca/CaO dispersion mixture on to solidification, immobilization and its separation of Cd, Cr, Pb and As in three different (decomposed granite, industrial clay and agriculture field) contaminated soil was studied. Further, the degree of metal immobilization was evaluated by analyzing the leachable fraction of heavy metal obtained through the Japan soil elution standards.

## MATERIALS AND METHODS

**General experimental condition:** In a typical experiment three different samples are considered: decomposed granite soil (DG) containing 7% moisture and 0.52% organic substances; industrial clay soil (ORS) containing 18% moisture and 4.5% organic substances; and agricultural field soil (KSO) containing 18% moisture and 17% organic substances. Heavy metal contamination in soil samples were prepared in laboratory, sodium arsenate ($HAsNa_2O_4$), cadmium nitrate tetrahydrate (Cd $(NO_3)_2$ $4H_2O$), chromium (III) nitrate ($CrN_3O_9$ $9H_2O$) and lead nitrate (Pb $(NO_3)_2$) of each 0.1 g was dissolved in 5 ml water next, solutions was spread to 1 kg of each DG, ORS and KSO soil in a plastic bottle and mixed thoroughly for 24 hr to obtain desired concentrations. Nano-Fe/Ca/CaO (dry system) was prepared with iron (Fe), metallic Ca and CaO through planetary ball milling process. Granular particles of metallic calcium were purchased from Kishida Chemicals (99%, particle size distribution: 1.0-2.5 mm, surface area: 0.43–0.48 $m^2$/g). Fine grade CaO and iron powder (size 0.15 mm) was also commercially obtained with 98 % purity from Kishida Chemicals. Iron powder, metallic Ca and dry CaO (dried at 825°C for 2h) composition Fe/Ca/CaO of 2/2/5 were introduced in planetary ball mill (Retsch PM-100; 20 pieces SUS, 32g/ball) at room temperature, under Ar atmosphere. Stirring was carried out for 1 hr at 600 rpm to a rotation-to-revolution ratio of 1:2. Stirred samples were collected in glass bottles, filled with Ar gas and stored to be used in the succeeding treatment experiment. The maximum measured particle size distribution of Fe/Ca/CaO was about 206 nm.

Heavy metal contaminated individual DG, ORS, KSO, soil alone and mixtures of soil and nano-Fe/Ca/CaO (1.0/0.1) were mixed/grinded for 2hr with tumbling mill (500 mL ceramic pot, 10 ceramic balls of 10 mm diameter). After treatment, magnetic and nonmagnetic fractions of soil were separated using a magnetic plate. Acid digestion method was employed to analyze the total As, Cd, Cr, and Pb concentrations in DG, ORS and KSO soil before and after treatment with nano-Fe/Ca/CaO (Baker and Amacher (1982). On the other hand, elution/leaching test was carried out (liquid-to-solid ratio of 10/1 with 6 hr shaking) in accordance with Japanese standard methods (Ministry of Environment Government of Japan, 2003). Heavy metal concentrations in content and eluted solutions were measured using with inductively coupled plasma optical emission spectrometry (ICP-OES; Varian, 720-ES). These experiment were repeated three times and the results obtained were similar. In order to elucidate

immobilization mechanisms, to verify if soil alterations occurred during the treatment, and to analyze As, Cd, Cr and Pb distribution within the solid matrix, scanning electron microscopy combined with electron dispersive spectroscopy microanalysis and semi-quantitative analysis were carried out (SEM-EDS; JEOL, JSM6510A equipped with a Si (Li) probe with a resolution of 138 eV).

## RESULTS AND DISCUSSION

**Heavy metal immobilization and separation:** The concentration of As, Cd, Cr, and Pb in total contents and solutions leached during the elution test of three different DG, ORS and KSO soil by sole grinding and grinding with nano-Fe/Ca/CaO are presented in Table 1.

**TABLE 1.** Content and eluted heavy metal (As, Cd, Cr and Pb) concentrations in DG, ORS and KSO soils before and after treatment with nano-Fe/Ca/CaO.

| Soil Type | As (mg/L) | Cd (mg/L) | Cr (mg/L) | Pb (mg/L) |
|---|---|---|---|---|
| **DG Soil** | | | | |
| *Before treatment content* | 1.147 | 1.425 | 1.214 | 0.952 |
| *Elution* | | | | |
| Only mixing | 0.232 | 0.240 | 0.238 | 0.202 |
| Nano-Fe/Ca/CaO treated | 0.008 | 0.002 | 0.006 | 0.002 |
| Nano-Fe/Ca/CaO treated (magnetic fraction) | 0.007 | 0.002 | 0.005 | 0.005 |
| Nano-Fe/Ca/CaO treated (non-magnetic fraction) | 0.001 | 0.000 | 0.002 | 0.002 |
| **ORS Soil** | | | | |
| *Before treatment content* | 0.690 | 0.711 | 1.402 | 0.787 |
| *Elution* | | | | |
| Only mixing | 0.102 | 0.127 | 0.193 | 0.149 |
| Nano-Fe/Ca/CaO treated | 0.006 | 0.008 | 0.005 | 0.009 |
| Nano-Fe/Ca/CaO treated (magnetic fraction) | 0.002 | 0.006 | 0.002 | 0.005 |
| Nano-Fe/Ca/CaO treated (non magnetic fraction) | 0.007 | 0.000 | 0.001 | 0.001 |
| **KSO Soil** | | | | |
| *Before treatment content* | 0.925 | 0.780 | 1.666 | 0.925 |
| *Elution* | | | | |
| Only mixing | 0.194 | 0.140 | 0.193 | 0.202 |
| Nano-Fe/Ca/CaO treated | 0.011 | 0.010 | 0.015 | 0.011 |
| Nano-Fe/Ca/CaO treated (magnetic fraction) | 0.008 | 0.007 | 0.002 | 0.009 |
| Nano-Fe/Ca/CaO treated (non magnetic fraction) | 0.001 | 0.000 | 0.001 | 0.001 |

All these values are the average of three replications. By sole grinding, As, Cd, Cr and Pb eluted concentrations decreased to 0.232, .240, 0.238 and 0.202 mg/L from 1.147, 1.1425, 1.1214 and 0.952 mg/L respectively in DG soil. Similar trend was observed in ORS and KSO soils. On the other hand, when nano-Fe/Ca/CaO was added during grinding, heavy metal concentration decreased significantly in three different soil samples (Table 1). These eluted concentrations of heavy metal correspond to intrinsic heavy metal immobilization efficiencies of about 95-99 % with nano-Fe/Ca/CaO treatment (Figure 1).

After treatment with nano-Fe/Ca/CaO, about 25, 44 and 40 wt% of magnetic and about 75, 56 and 60 wt% of non-magnetic fractions were separated in three different DG, ORS and KSO soil samples, respectively (Figure 2). Results, indicated that, ORS and KSO soil have the higher magnetic separated fraction, when compared to DG soil. This can be due to the moisture content differences 17 % moisture for ORS, KSO; 7% moisture for DG soil. Further, about 85-95 % of initial heavy metal content concentrations were condensed in magnetic fraction and only 10-15 % of heavy metal concentration remained in nonmagnetic fractions (Figure 3). It is also clearly seen that the leachable heavy metal

concentrations in nonmagnetic fractions in DG, ORS and KSO soils are much lower than the Japanese soil leachate regulatory standard limits (< 0.01 mg/L for As, Cd and Pb and 0.05 mg/L for Cr) (Ministry of Environment Government of Japan 1991). These results appear to be very promising and the addition of nano-Fe/Ca/CaO mixture with simple grinding technique may be considered potentially applicable for the remediation and volume reduction of contaminated soils by heavy metal.
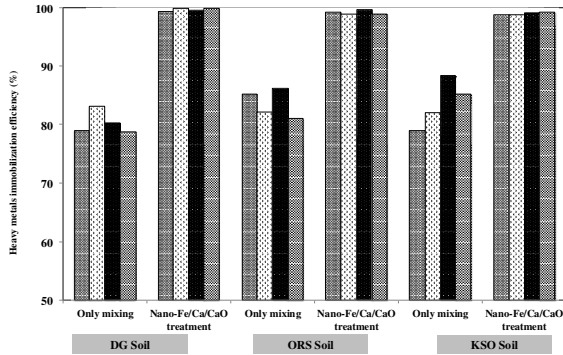


**FIGURE1.** Heavy metal immobilization efficiencies in DG, ORS and KSO soils after nano-Fe/Ca/CaO treatments.
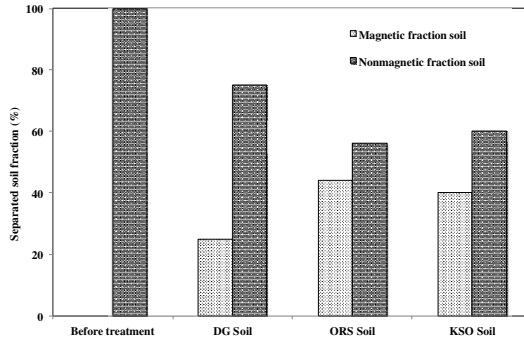


**FIGURE2.** Magnetic and nonmagnetic separated fractions in DG, ORS and KSO soils after nano-FE/Ca/CaO treatment.

**Immobilization and separation mechanism of heavy metal:** By SEM microstructure analysis, blending the heavy metal contaminated DG, ORS and KSO soils with nano-Fe/Ca/CaO decreased the production and development of the core particles and would cause the hydration products to coat the aggregates extremely, as shown in Figure 4. This fact probably indicates that a certain amount of heavy metal was entrapped inside the new aggregates produced during the nano-Fe/Ca/CaO treatment. With semi-quantitative SEM–EDS analysis, it is also clear that the mass and atoms percent of As, Cd, Cr and Pb in soil surface decreases after nano-Fe/Ca/CaO treatment. The decreased mass percent reached 99% for Cd, Cr Pb and 100% for As. While, about 74 % mass percent and 76 % of atoms percent increased for Ca and Fe about 13.9 to 4.9 % respectively (Table 2). The reduction of As, Cd, Cr and Pb amounts on particle surface by the covering with Ca and its compounds is a possible explanation of the increase of immobilization efficiency after nano-Fe/Ca/CaO treatment.
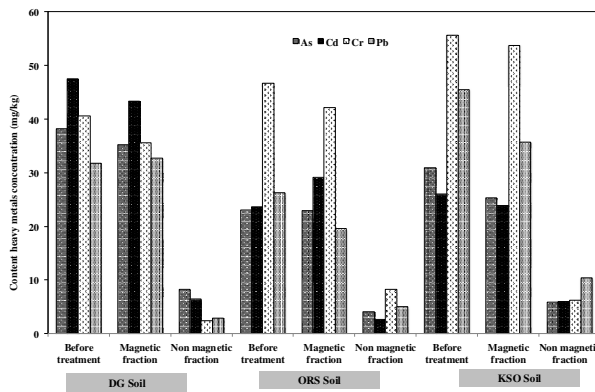


**FIGURE3.** Heavy metal concentrations in before treatment, magnetic and non-magnetic separated fractions in DG, ORS and KSO soil after nano-Fe/Ca/CaO treatment.
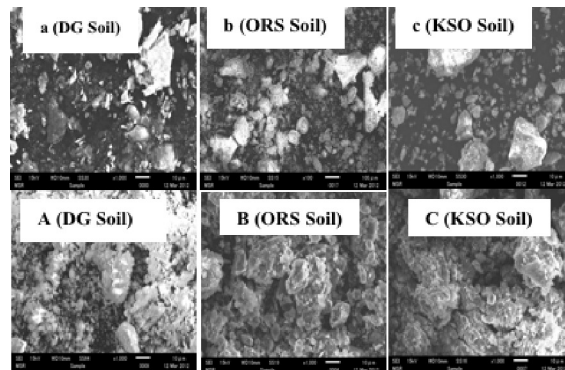


**FIGURE4.** SEM microstructure for heavy metal contaminated DG, ORS and KSO soil at 1000× magnitude: (a, b and c) before treatment and (A, B and C) after nano-Fe/Ca/CaO treatment.

The most probable mechanism for the enhanced heavy metal immobilization capacity with nano-Fe/Ca/CaO treatment may be probably ascribed to phenomena such as adsorption and entrapment of

heavy metal into new formed aggregates due to enclosed/bided with Ca associated immobile salts and its separation. It is possible to assume that when soil is contaminated, heavy metals are adsorbed onto soil particles through a surface coordination process (Montinaro et al. 2007). By simple grinding, coarser sand or gravel soil particles decrease to fine clay or silt particles, hence, the particle surface area increases and the heavy metal mobility decreases because adsorption area increases.

**TABLE 2.** Semi-quantitative SEM-EDS analysis of DG soil before and after treatment with nano-Fe/Ca/CaO.

| Elements | Before treatment | | After nano-Fe/Ca/CaO treatment | | % of removal/decreased on soil surface | |
|---|---|---|---|---|---|---|
| | Mass (%) | Atoms (%) | Mass (%) | Atoms (%) | Mass (%) | Atoms (%) |
| Si | 60.70 | 75.04 | 36.92 | 48.73 | 14.3 | 35.1 |
| Ca | 9.50 | 8.21 | 37.10 | 34.31 | 74.3* | 76.1* |
| Fe | 21.10 | 1.36 | 24.55 | 0.43 | 13.9* | 4.9* |
| Cr | 2.03 | 13.15 | 0.60 | 1.30 | 99.0 | 90.1 |
| As | 2.16 | 1.00 | 0.00 | 0.00 | 100.0 | 100.0 |
| Cd | 3.47 | 1.07 | 0.57 | 0.19 | 99.4 | 82.2 |
| Pb | 1.06 | 0.18 | 0.27 | 0.05 | 99.7 | 72.2 |

* Increased value

On the other hand, wher grinding with nano-Fe/Ca/CaO additives, the soil particles are subjected to collisions that may promote aggregation. When aggregation occurs in the presence of nano-Fe/Ca/CaO, the amount of heavy metal adsorbed on the surface of two overlapping particles may be entrapped within the new-formed aggregates. Furthermore, nano-metallic Ca/CaO could make immobile salts with moisture and $CO_2$ in atmosphere, including pozzolanic cement and hydraulic property, hence the heavy metal (As, Cd, Cr and Pb) would be brought into the immobile Ca salts, therefore, the surfaces of soil might enclosed/bided with Ca associated ($CaCO3/Ca(OH)_2$) salts. Moreover, the magnetic properties of nano-Fe facilitate the rapid separation of nano-Fe from soil, through a magnetic field (Yavuz et al. 2006). By this way, encapsulated nano-Fe particles in solidified soil fractions can also be separated. Furthermore, the controlling mechanism is a function of the standard redox potential of the contaminant metal in the presence of nano-Fe. Heavy metal are either reduced at the nano-Fe surface (e.g., $Cu^{2+}$, $Ag^{2+}$) or directly adsorbed to the nano-Fe surface where they are rendered immobile (e.g., $Zn^{2+}$, $Cd^{2+}$, $Cr^{6+}$, $Cu^{2+}$, $Pb^{2+}$, $As^{3+}$, etc.) (Boparai et al. 2011). The standard redox potential of zerovalent iron is ($-0.41$ V) which is very close to those of $Cd^{2+}$ ($-0.40$ V), $Cr^{3+}$ ($-0.42$ V), $Pb^{2+}$ ($-0.13$ V) and $As^{3+}$ ($-0.23$ V). Thus, the removal of As, Cd, Cr and Pb ions by nano-Fe is due to sorption (Boparai et al. 2011). In this way, the amount of heavy metal exposed to the leaching completion is reduced thus determining a high immobilization capacity in three different types of soil. Therefore, this technology is considered to have the ability to insoluble heavy metal as well as their separation and volume reduction.

**CONCLUSIONS**

This study was conducted to evaluate the nano-Fe/Ca/CaO dispersion mixture as suitable binder for the immobilization of heavy metal (As, Cd, Cr and Pb) and their separation from contaminated soil. With simple grinding, about 79-86 % of heavy metal (As, Cd, Cr and Pb) immobilization could be achieved, and after grinding with nano-Fe/Ca/CaO dispersion mixtures about 95-99% of enhanced heavy metal immobilization was achieved in three different soils. After treatment, about 25-44 wt% of magnetic and 75-56 wt% of non-magnetic fraction of soils were separated, and their condensed heavy metal concentrations were about 85-95% and 10-20%, respectively. It was also clearly seen that the leachable heavy metal concentrations in nonmagnetic fraction of soil are much lower than the soil leachate

regulatory standard limits (< 0.01 mg/L for As, Cd and Pb and 0.05mg/L for Cr). By SEM semi-quantitative analysis, it was observed that the amounts of As, Cd, Cr and Pb detectable on soil particle surface decrease after nano-Fe/Ca/CaO treatment. The addition of nano-Fe/Ca/CaO dispersion mixtures that immobilize heavy metal in soil at natural moisture condition is an innovative approach for the remediation and separation of soil polluted with heavy metal.

## ACKNOWLEDGEMENTS

## REFERENCES

Baker DE, Amacher M. C. 1982. "Nickel, copper, zinc, cadmium". In: Miller RH, Keeney DR, *Methods of Soil Analysis*, Part 2. ASA-SSSA, pp 323.334. Madison, WI, USA.

Boparai H.K, Joseph M, Carroll D. M. O. 2011. "Kinetics and thermodynamics of cadmium ion removal by adsorption onto nano zerovalent iron particles". *Journal of Hazardous Materials* 186:458–465.

Macauley E, Hong A. 1995. "Chelation extraction of lead from soil using pyridine-2,6-dicarboxylic acid". *Journal of Hazardous Materials* 40:257–270.

Ministry of Environment Government of Japan. 1991. "Environmental Quality Standards for Soil". *Notification No.46. http://www.env.go.jp/en/water/soil/sp.html.*

Ministry of Environment Government of Japan. 2003. "Matters providing for measurement method of soil elution test". *Notification No. 18.*

Mitoma Y, Miyata H, Egashira N, Simion A, Kakeda M, Simion C. 2011. "Mechanochemical degradation of chlorinated contaminants in fly ash with a calcium-based degradation reagent". *Chemosphere* 83:1326–1330.

Montinaro S, Concas A, Pisu M, Cao G. 2007. "Remediation of heavy metal contaminated soil by ball milling". *Chemosphere* 67:631–639.

Paff S. W, Bosilovich B. E 1995. "Use of lead reclamation in secondary lead smelters for the remediation of lead contaminated sites". *Journal of Hazardous Materials* 40:139–164.

Reddy KR, Xub CY, Chinthamreddy S. 2001. "Assessment of electrokinetic removal of heavy metal from soil by sequential extraction analysis". *Journal of Hazardous Materials* 84: 27–296.

Srinivasa Reddy M, Mitoma Y, Okuda T, Sakita S, Kakeda M. 2012. "High immobilization of soil cesium using ball milling with nano-metallic $Ca/CaO/NaH_2PO_4$: implications for the remediation of radioactive soil". *Environ. Chem. Lette.* 10:201–207.

Tessier A, Campbell PGC, Bisson M. 1979. "Sequential extraction procedure for the speciation of particulate trace metal". *Anal Chem* 51:844–851.

USEPA. 1982. "Guide to the disposal of chemically stabilized and solidified waste, SW-872". Office of water and waste management, Washington DC.

USEPA. 1993. "Technology resource document-solidification/stabilization and its application to waste materials". *EPA/530/R- 93/012.*

Yavuz C. T, Mayo J. T, Yu W. W, Prakash A, Falkner J. C, Yean S, Cong L. L, Shipley H. J, Kan A, Tomson M, Natelson D, Colvin V. L. 2006. "Low-field magnetic separation of monodisperse $Fe_3O_4$ nano crystals". *Science* 314:964–967 .

# MIGRATION BEHAVIOR OF ARSENIC AND COPPER DURING QUICK ELECTROKINETIC REMEDIATION PROCESS

*Hafiz Ahmad* and Korhan Adalier (Florida State University, Panama City, FL, USA)
Danuta Leszczynska (Jackson State University, Jackson, MS, USA)
Mario Oyanader (Geneva College, Beaver Falls, PA, USA)

**ABSTRACT:** This study presents a comparative analysis of the transient behavior of arsenic (toxic metal) and copper (non-toxic metal) during electrokinetic (EK) remediation process. The migration of arsenic, which can exists in various complex states (e.g. various species, oxidation states, absorbed or desorbed forms) was compared with the mobility of the simple and less-complex copper during a short duration (25 hours) EK remediation. A systematic bench-scale laboratory study was conducted for arsenic as well as copper-spiked soil to better understand and compare the ionic mobility of arsenic with copper. Various migration-enhancement chemicals were purged (using electroosmotic flow) through the arsenic and copper-spiked soil. Besides tap-water (baseline), the chemicals purged through the spiked soils included alkaline solution (NaOH), oxidative solution ($H_2O_2$) and acidic solution (HCl). The study confirmed that arsenic migration can be enhanced by many times when a basic condition is created in the soil that results arsenic desorption. Results showed that up to six (6) times more arsenic can be removed from the contaminated soil by purging alkaline solution (NaOH) instead of using conventional tap-water. On the other hand, copper migration is best performed in normal (base-line) condition. About three (3) times more copper was removed by purging conventional tap-water rather than using alkaline solution (NaOH).

## INTRODUCTION

Arsenic is a hazardous material due to its high toxicity and carcinogenicity to human beings. Arsenic contamination in soil results as a consequence of industrial or agricultural activities, such as spills or leaks from wood impregnating plants, mining, smelting activities or application of the arsenic-rich herbicides and pesticides (Khalequzzaman et al., 2005; Kim et al., 2005; Yuan and Chiang. 2007 and 2008; Wang and Mulligan., 2006). Removal of arsenic in a safe, non-destructive way *has become a challenge in recent years.*

In electrokinetic (EK) soil remediation process, principle mechanisms leading to removal of metals from soil are electroosmosis and electromigration (Acar and Alshawabkeh, 1993). Electromigration expresses movement of ions toward opposite charged electrodes; transport by advection due to electroosmosis is typically towards cathode. At the end of the remedial process, contaminants that accumulate at the electrodes due to movements described above are collected and disposed above ground.

During EK process, the contaminant migration is highly dependent on phenomena such as sorption/desorption, precipitation, and dissolution (Puppala et al., 1997). The migration of arsenic is complex as it can exist in various oxidation states, species and also it can be retained by adsorption onto clays. On the other hand, migration behavior of copper in contaminated soils during EK process is less complex and a better understood phenomenon. In this study, initially EK removal of arsenic and copper is compared to assess the level of difficulty of arsenic remediation under conventional field situation, where water is purged during the remediation process. Additionally, removal efficiency of arsenic is improved by soil-conditioning with the help of purging chemicals.

## MATERIALS AND METHOD

Kaolin (Imerys Kaolin Inc., Georgia), a low buffering soil was used for all experiments. Two batches of spiked soils were prepared: batch 1 soils were spiked with copper; and batch 2 soils were spiked with arsenic. Soil spikes were prepared with standard solutions of copper sulfate and arsenic trioxide, according to the Standard Methods (Greenberg et al. 1992) to achieve a target concentration of copper 500 mg/kg (batch 1) and arsenic 50 mg/kg (batch 2). The spiking solution was added to the soil yielding the desired concentration of each tested element and water content of 35%. The purging solutions were prepared separately by mixing tap-water with appropriate chemicals to obtain the chosen concentration shown in Table 1.

### TABLE1: Experimental program

| Parameters | Tests | | | | | |
|---|---|---|---|---|---|---|
| | Cu (Test-1) | As (Test-2) | Cu (Test-3) | As (Test-4) | Cu (Test-5) | As (Test-6) |
| Initial soil pH | 7.621 | 5.726 | 7.017 | 6.234 | 7.469 | 6.267 |
| Initial contaminant in spiked soil (mg) | 515.0 | 51.5 | 515.0 | 51.5 | 515.0 | 51.5 |
| Initial concentration of spiked soil (mg/kg) | 500 | 50 | 500 | 50 | 500 | 50 |
| Soil Redox potential (mV) | 382.7 | 1260 | 428.0 | 970 | 417.3 | 1059 |
| Initial Soil conductivity ($\mu$S/cm) | 391.4 | 469.4 | 1099.0 | 464.3 | 309.2 | 509.9 |
| Purging Inlet solution | tap-water | tap-water | NaOH (0.1N) | NaOH (0.1N) | HCl (0.01N) | $H_2O_2$ (3%) |
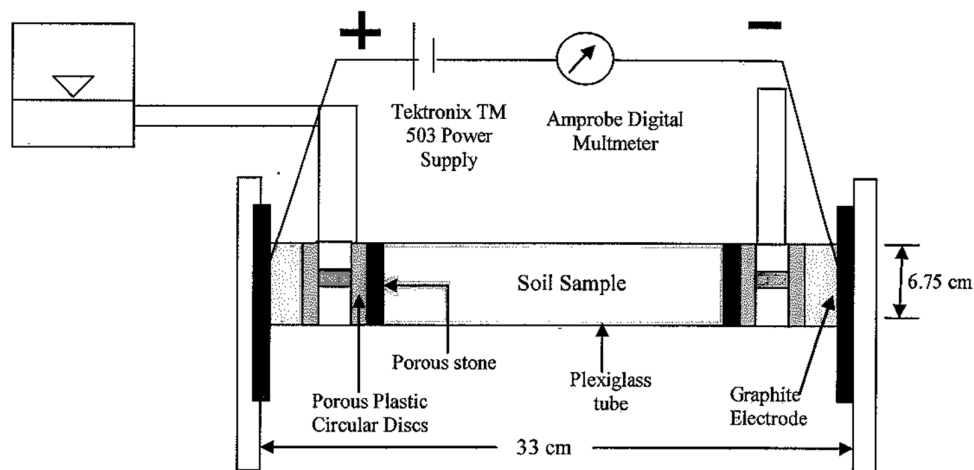


**FIGURE1.** Electrokinetic cell.

The experimental program consisted of six electrokinetic remediation tests. Table 1 presents a summary of the tests. First two tests (Test-1 and 2) were conducted as baseline tests. Tap water was purged through the spiked soils to evaluate copper and arsenic migration during most common field condition. The second pair of tests (Test-3 and 4) were conducted to see if the alkaline soil condition can enhance the migration of copper and arsenic. For this purpose, alkaline NaOH was used as purging chemical. In the final pair of tests (Test-5 and 6), two purging chemicals were used: (i) HCl was used to

find if acidic condition can enhance migration of copper and (ii) $H_2O_2$ was used to determine if an oxidizing soil environment can improve arsenic removal from contaminated soil.

The electrokinetic cell shown in Figure 1 was fabricated using a Plexiglas tube. The actual length of the soil specimen inside the Plexiglas tube ranged from 22 to 23 cm. This spiked soil specimen was compacted inside the cell in 2.54 cm (1 inch) layers. Depending on the test (Table 1), fluid compartment was filled with either tap-water or appropriate solution. Tap-water was selected as a baseline, because it is the most likely source of replenishing fluid at field/contaminated sites (Reddy and Chinthamreddy, 2003). In all tests, fluid levels at cathode and anode compartments were maintained at the same level to avoid any hydraulic gradient. The graphite electrodes were connected to a D.C. electric power supply (Tektronix TM503 PS503A Dual Power Supply). The voltage gradient used for all tests was maintained 1.0 Volt/cm. The system was kept horizontal throughout the experiment. During the experimental period electroosmotic flow was determined. At the end of 25-hour EK treatment, arsenic and copper concentration in the anode, cathode fluids and in the soils were determined.

## RESULTS AND ANALYSIS

**Electroosmotic flow.** Electroosmosis flow (EOF) normally drags fluid from anode to cathode. Hence, EOF is necessary to carry enhancement chemicals for proper soil conditioning and washout of non-charged dissolved species. The cumulative volume of electroosmotic flow collected at cathode is presented in Figure 2. Effluent collected during the experiment Test 2 and 4 (where tap-water and NaOH were purged respectively through arsenic contaminated soil) was relatively higher than Test 1, 3, 5 and 6 (all copper contaminated soils and $H_2O_2$ purged through arsenic contaminated soil). Decreased electroosmotic flow rate due to purging of oxidizing agent (e.g. Test 6) was also reported by (Isosaari et al., 2007). It is believed that charge-carrying ions were eliminated as they formed precipitations (Yukselen and Kaya, 2003) after certain time resulting reduced electroosmotic flow (Test 1, 3, 5).
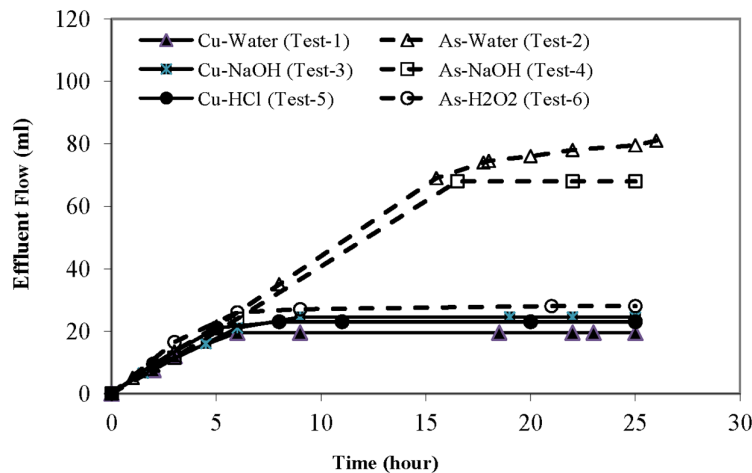


**FIGURE2.** Volume of effluent vs. time.

**Copper migration to anode and cathode chamber.** Figure 3 and 4 shows the percentage of accumulated total copper and arsenic deposition in anode and cathode chamber. Comparing the six tests, it was found that increased copper (32%) (Test 1 in Figure 3) deposited (compared to arsenic) in anode chamber. Most of the copper migrated to anode which is believed to be the effect of mainly electromigration. Besides this, significant amount (1%) of copper migrated to cathode (Test 1 in Figure 4) mainly due to the effect of electroosmosis. Most of the copper migrated when the purging liquid was tap water indicating that the migration of copper is best achieved by base-line condition (tap-water) rather than using enhancement chemicals such as NaOH, and HCl (Test 3 and 5).
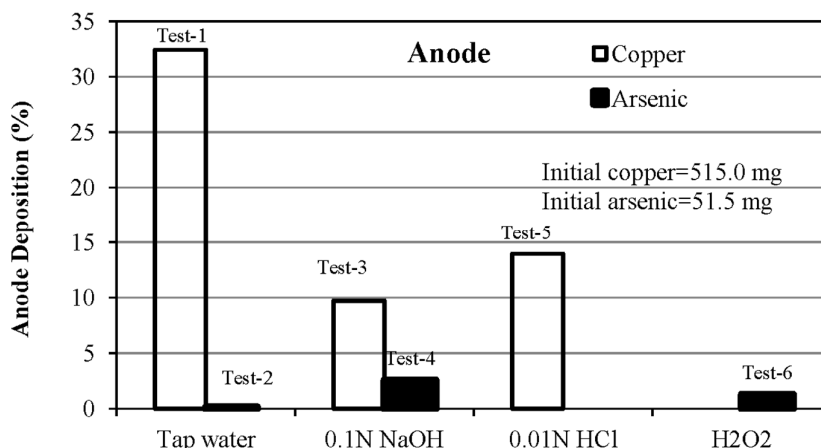
**FIGURE3.** Copper and arsenic deposition in anode.
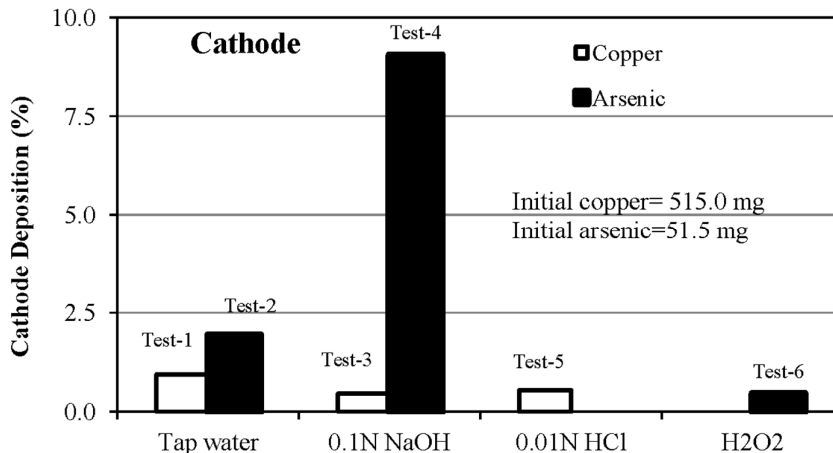


**FIGURE4.** Copper and arsenic deposition in cathode.

**Arsenic migration to anode and cathode chamber.** The migration behavior of arsenic was found completely different than copper. While copper migration was best achieved by tap-water, arsenic migration was not significant with water (Test 2 in Figure 3 and 4). The migration of arsenic was enhanced by many times by purging of alkaline solution, NaOH (pH 11~13). In cathode, increased amount (9%) of arsenic deposited when the purging liquid was NaOH (Test 4 in Figure 4). The amount of arsenic deposited in anode was 2.5% with the same purging liquid (Test 4 in Figure 3). On the other hand, arsenic removal with tap-water in anode and cathode was only 0.1% and 1.9% (Test 2 in Figure 3 and 4) respectively. It is believed that high soil pH condition caused arsenic to exist in aqueous form leading to enhanced migration. It was found that arsenic deposition in cathode was higher than that of anode. This suggested that electroosmosis of species (e.g., $H_2AsO_3$, $HAsO_4$ etc.) were significant phenomenon for the enhanced migration of arsenic to cathode. Besides electroosmosis, it is believed that electromigration of ions (e.g., $H_2AsO_3^-$, $HAsO_3^{-2}$, and $AsO_3^{-3}$ etc.) resulted in significant deposition of arsenic in anode. Arsenic removal with oxidizing agent ($H_2O_2$) was achievable (1.3% in anode 0.5% in cathode) but the removal is very small as seen in Test 6 of Figure 3 and 4.
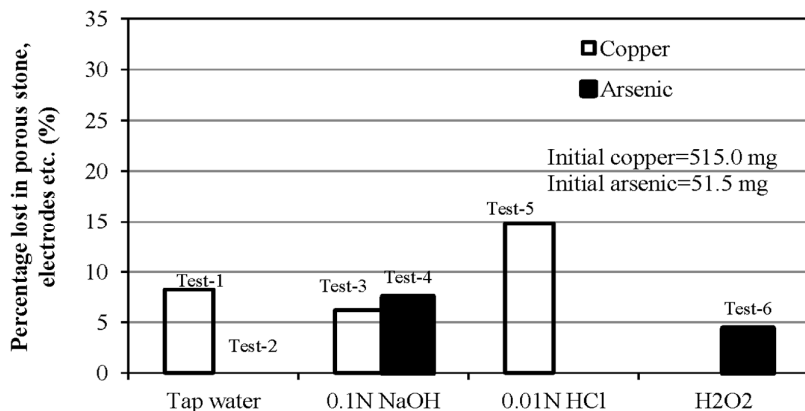
**FIGURE5.** Copper and arsenic adsorbed in porous stone, electrodes.
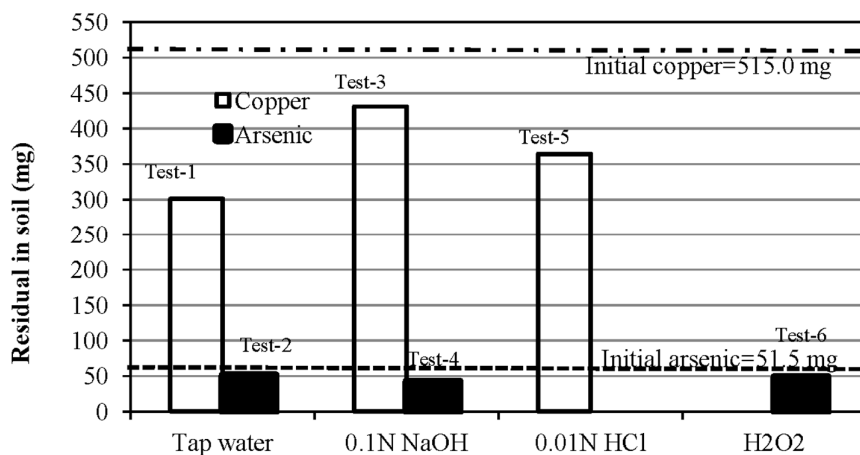


**FIGURE6.** Residual copper and arsenic after treatment.

**Copper and arsenic migration to electrodes and porous stone.** The migrated total copper and arsenic to the porous stones and graphite electrodes located at the end of soil column was determined by performing mass balance in each of the tests (Test 1-6). Figure 5 shows copper and arsenic adsorption on to the porous stones and graphite electrodes due to their migration from the contaminated soil. Again, it was found that arsenic and copper migration in porous stones and graphite electrodes is 0% (Test 2) and 8% (Test 1) respectively when tap-water was used as purging agent. This indicates that purging of tap-water to remove arsenic is not as effective as cooper. Comparing Test 4 and 3, it is evident that NaOH is more effective to remove arsenic compared to other purging agents such as Tap-water (Test 3) or $H_2O_2$ (Test 6).

*Residual copper and arsenic in treated soil.* Figure 6 shows results of residual copper and arsenic in the soil at the end of the quick (25 hour) electrokinetic treatment. Comparing Test 1, 3 and 5, it is seen lowest copper residual (300 mg) is in the soil of Test 1 (where tap-water was used as purging agent). In other words, maximum copper (215 mg) was removed when tap-water was used. This copper removal (215 mg) in Test 1 is far more than Test 3 (84 mg removed with NaOH) and Test 5 (151 mg removed with HCl). Approximately three (3) times more copper was removed by purging conventional tap-water rather than using alkaline (NaOH).

Arsenic residuals in Test 2, 4 and 6 were 50 mg, 42 mg, 49 mg respectively. In other words, arsenic removed with tap-water, NaOH and $H_2O_2$ were 1.5 mg, 9.5 mg and 2.5 mg respectively. This

again shows that arsenic is best removed when NaOH is used as purging agent (six times more than that of tap-water).

**CONCLUSIONS**

The feasibility of quick arsenic remediation with various purging solutions was investigated using electrokinetic technology. The study demonstrates that it is possible to remove a hazardous material like arsenic from a low permeable soil in a safe manner avoiding the potential risk of contact with the contaminated soil. The study shows that unlike copper remediation, soil-conditioning is necessary for arsenic remediation. Purging of conventional tap-water will not work for arsenic removal from the contaminated soil. Application of alkaline solution (e.g. NaOH) as purging agent will significantly enhance arsenic remediation and quicken the process.

**REFERENCES**

Acar, Y.B. and A.N. Alshawabkeh. 1993. "Principles of electrokinetic remediation". *Environ. Sci. Technol.* 27:2638–2647.

Greenberg, A.E., L.S. Clesceri, A.D. Eaton. 1992. "Standard Methods for the Examinations of Water and Wastewater", 18th ed., APHA, Washington DC,

Isosaari, P., R. Piskonen, P. Ojala, S. Voipio, K. Eilola, E. Lehmus and M. Itävaara, 2007. "Integration of electrokinetics and chemical oxidation for the remediation of creosote-contaminated clay". *J. Hazard. Mater.* 144(1-2):538-548.

Khalequzzaman, M., F.S. Faruque and A.K. Mitra. 2005. "Assessment of arsenic contamination of groundwater and health problems in Bangladesh". *Int. J. Environ. Res. and Public Health.* 2(2):204-213.

Kim, S.-O., W.-S. Kim and K.-W. Kim. 2005. "Evaluation of  electrokinetic  remediation of arsenic-contaminated soils". *Environ. Geochem. Health.* 27:443–453.

Puppala, S.K., A.N. Alshawabkeh, Y.B. Acar, R.J. Gale, M. Bricka. 1997. "Enhanced electrokinetic remediation of high sorption capacity soils". *J. Hazard. Mater.* 55:203–220.

Reddy, K. R., S. Chinthamreddy. 2003. "Sequentially Enhanced Electrokinetic Remediation of Heavy Metals in Low Buffering Clayey Soils", *J. Geotech. Geoenviron. Eng.* 129(3):263-77.

Wang, S., C. N. Mulligan. 2006. "Occurrence of arsenic contamination in Canada: Sources, behavior and distribution". *Sci. Total Environ.* 366: 701–721.

Yuan, C. and T.-S. Chiang. 2007. "The mechanisms of arsenic removal from soil by electrokinetic process coupled with iron permeable reaction barrier". *Chemosphere.* 67:1533–1542.

Yuan, C., T.-S. Chiang. 2008. "Enhancement of electrokinetic remediation of arsenic spiked soil by chemical reagents". *J. Hazard. Mater.* 152:309-315.

Yukselen, Y. and A. Kaya. 2003. "Zeta potential of kaolinite in the presence of alkali, alkaline earth and hydrolysable metal ions". *Water Air Soil Pollut.* 145:155–168.

# REMOVAL OF CHROMIUM (VI) IONS BY USING BIOFILM-BIOMASS OF YARROWIA LIPOLYTICA

*Ashok Bankar[1],* Prajakta Vishe[1], Priyanka Mitra[1], Ameeta Ravikumar[1], Balu Kapadnis[1], Mark Winey[2] and Smita Zinjarde[1]
(University of Pune, Pune, Maharashtra, India[1]; University of Colorado Boulder, USA[2])

**ABSTRACT:** Biofilm formation by two marine strains of *Yarrowia lipolytica* (NCIM 3590 and NCIM 3589) in the presence or absence of Cr (VI) ions was compared. The morphology of the yeast biofilms under stress of metal ions was studied by scanning electron microscope (SEM) and light microscope observations. Biofilm-mediated removal of Cr (VI) ions from aqueous solutions with respect to pH, temperature, biomass, contact time and initial concentration of metal ions was studied. Maximum Cr (VI) biosorption was observed at pH 2.0 and at a temperature of 35°C. Increase in biomass resulted in a decreased metal uptake. With an agitation speed of 130 rpm, equilibrium was observed within 2 h. Under optimum conditions, biosorption was enhanced with increasing concentrations of Cr (VI) ions. Biofilm-biomass of NCIM 3590 and NCIM 3589 displayed specific uptake values of $500 \pm 5.53$ mg/g and $424 \pm 5.3$ mg/g at 500 ppm, respectively. The adsorption data fitted well to the Langmuir, Freundlich isotherms and followed the pseudo-second-order kinetics. The surface sequestration of Cr (VI) by *Y. lipolytica* was confirmed by SEM-energy dispersive spectrometer (SEM-EDS) observations. Presence of metal ions was also demonstrated by a transmission electron microscope (TEM). Fourier transform infrared (FTIR) spectroscopy revealed the involvement of different functional groups such as hydroxyl, carboxyl, and amide groups on the yeast cell surfaces in Cr (VI) binding.

## INTRODUCTION

Hexavalent chromium [Cr (VI)] ions are widely used in dyes, pigments, galvanometric devices, films, photography, plating, electroplating, leather and mining industries (Costa, 2002; Bankar et al., 2009a). Cr (VI) ions are harmful to animals and human health due to the neurotoxicity, genotoxicity, dermatotoxicity, carcinogenicity, immunotoxicity and general environmental toxicity that they display (Bagchi et al., 2002). Cr (VI) ions persist in marine food chains also as they are accumulated by aquatic plants and animals (Wen-Xiong et al., 2002). Thus, removal of this toxic pollutant from the contaminated wastewater is of prime importance in environmental restoration and protection initiatives. Physicochemical methods for removal of Cr (VI) ions have certain limitations and are often not economically viable (Ho and Poddar., 2001).

In such a scenario, bioremediation is suitable in managing heterogeneous environments, such as ground water, soil sludge, and industrial wastes (Boopathy, 2000). Microbial interactions with heavy metals are mediated via enzymatic reactions, bioaccumulation and biosorption. On account of these properties, microbial systems have become significant in the removal of metal ions (Srinath et al., 2002). Bioaccumulation is a slower, metabolism-dependent process performed by living organisms. On the other hand, biosorption is rapid, a metabolism-independent process and thus can be performed by both living as well as dead microorganisms (Gadd, 2004; Malik, 2004). Bioaccumulation and biosorption by fungi for metal remediation have been reported earlier (Aguilar et al., 2008; Bankar et al., 2009b). Metal sorption studies on planktonic cells of *Aspergillus niger*, *Aspergillus oryzae*, *Penicillium crysogenum*, *Mucor rouxii, Rhizopus arrhizus* and *Yarrowia lipolytica* have been studied earlier (Bishnoi and Garima, 2005; Bankar et al., 2009b). However, such studies on the biofilm-form are very few.

In this study, we selected *Y. lipolytica,* the dimorphic oleaginous hemiascomycetes yeast with several applications as a model system. The fungus is routinely isolated from oil-polluted environments or lipid containing effluents and is used in the bioremediation of polluted environments (Barth and Gaillardin, 1997; Bankar et al., 2009a). The organism inherently forms biofilms (Dusane et al., 2008). Since biofilms are surrounded by a heterogeneous matrix composed of the extracellular polymeric substances (Hullebusch et al., 2003), they play an important role in bioremediation (Decho et al., 2000).

Biofilms have been effective in removing heavy metals from wastewaters (Quintelas et al 2008; Lameiras et al., 2008). In the present study, biofilms formed by two marine strains of *Y. lipolytica* were used for removal of Cr (VI) ions from aqueous solution.

## MATERIALS AND METHODS

### Maintenance of Microorganisms.

Both the strains of *Y. lipolytica* were maintained on MGYP slants (malt extract, 3.0; glucose, 10.0; yeast extract, 3.0; peptone, 5.0; agar, 25.0 g $l^{-1}$ of distilled water) and sub-cultured at monthly intervals. Pre-inoculum for experiments was grown in YNB medium (yeast nitrogen base 0.7%, dextrose 1%). The growth temperature for NCIM 3590 and 3589 is 20 and 30$^o$C, respectively.

### Biofilms Formation by *Y. lipolytica* NCIM 3589 and 3590.

Standardized cell suspensions (4 x $10^9$cells/ml) of *Y. lipolytica* NCIM 3590 and 3589 were added into 50 ml YNB liquid medium containing different concentrations of Cr (VI) ions and mixed properly. The mixture (200µl) was added into the wells of pre-sterilised polystyrene, 96 well microtitre plates.Yeast cells inoculated into YNB medium without Cr (VI) ions served as controls. All these plates were incubated at optimum conditions for 24, 48, 72, 96 and 120 h. Quantitative estimation of biofilms was carried out by the crystal violet assay (Dusane et al., 2008). Effect of Cr (VI) concentrations on biofilm formation on glass surface was also studied. The *Y. lipolytica* cultures were grown for 48 h under optimum conditions and inoculated into sterile Petri plates (with glass slides) containing 20 ml of sterile YNB liquid medium and different concentrations of Cr (VI) ions. The plates without Cr (VI) were served as control. Biofilms formed on glass surfaces with or without Cr (VI) ions were analyzed by light and SEM.

### Effect of pH, Temperature, Contact Time, Biomass and Initial Metal ion Concentrations.

Standardized cell suspension (4x$10^9$ cells/ml) of *Y. lipolytica* NCIM 3590 and NCIM 3589 were individually inoculated into small-sized sterile plastic Petri dishes (60 mm) containing YNB glucose medium. All plates were incubated at optimum temperature for 48h. The planktonic cells were discarded and cells in the biofilm form were scraped from the base of the plates. The scraped wet biofilm-biomass was washed thrice and weighed. The wet biomass was added into reaction mixture to adjust 2g dry weight of biomass per litre. For all experiments, the source of Cr (VI) was provided as $K_2Cr_2O_7$ in distilled water. Dry weight of the biofilm-biomass was determined for each set and this was used during further calculations. All biosorption assays were carried out in tubes containing 5 ml of metal solution (200 mg/l) unless otherwise mentioned. The pH of metal solutions was adjusted to 2.0, 3.0, 4.0, 5.0, 6.0 and 7.0 by using 1N $HNO_3$ or NaOH. Standard cell suspension of both yeasts (100 µl) were added to each tube separately and incubated at optimum temperature. The effect of temperature on biosorption of Cr (VI) was determined at pH 2.0. The reaction mixtures were incubated at 4, 20, 30 and 37$^o$C. The residual Cr (VI) in the supernatant was determined after 2 h of interval. To study effect of contact time on biosorption, aliquots were taken out at different time intervals and the residual Cr (VI) ion in the supernatant was determined. Effect of biomass concentrations on biosorption was studied by adding different volume of standard yeast suspensions. The effect of initial metal ion concentrations on biosorption was studied by varying Cr (VI) concentrations from 50 to 500 ppm. Cr (VI) was determined spectrophotometrically by the diphenylcarbazide method. Cells were harvested by centrifugation for 5 min at 5000 rpm and the Cr (VI) ion in the supernatant was estimated after adding 6N $H_2SO_4$, a solution of 1,5-diphenyl carbazide in acetone and measuring the absorbance at 540 nm (Balasubramanian and Pugalenthi, 1999). The biosorption capacities ($q_{eq}$) at equilibrium were calculated using equation (1). The Langmuir isotherm and Freundlich isotherm model in linearized form are given as equation (2) and (3) respectively. The linearized form of the pseudo-second-order is given as equation (4).

$$q_{eq} = \frac{(C_0 - C_{eq})}{X} \times V$$ ................ (1)

where $C_0$ was the initial Cr (VI) concentration (mg/1); $C_{eq}$ the Cr (VI) concentration at equilibrium (mg/1); V the volume of solution used; $X$ was biosorbent mass (g/1).

$$\frac{1}{q_{eq}} = \frac{1}{b_m} \frac{1}{C_{eq}} + \frac{1}{q_m} \quad .................. (2)$$

where $b_m$ is a coefficient related to the affinity between the sorbent and sorbate, and $q_m$ is the maximum sorbate uptake under the given condition.

$$\ln q_{eq} = \ln K_F + \frac{1}{n} \ln C_{eq} \quad .........(3)$$

where $q_{eq}$ is metal ions sorbed (mg/g) and $C_{eq}$ equilibrium metal ion concentration, respectively. $K_F$ and n are adsorption isotherm parameters.

$$\frac{t}{q_t} = \frac{1}{K^2 q_{eq}^2} + \frac{1}{\left(\frac{1}{q_{eq}}\right) t} \quad .....................(4)$$

where $K^2$ (g/mg/min) is the rate constant of the second-order equation, $q_t$ (mg/g) the amount of metal adsorbed at time t (min) and $q_{eq}$ is the amount of biosorption equilibrium (mg/g).

## RESULTS AND DISCUSSION

**Biofilm Formation by *Y. lipolytica* NCIM 3590 and 3589 Under Stress of Cr (VI).** As shown in Figure 1(A, B) biofilms of *Y. lipolytica* NCIM 3590 and NCIM 3589 were monitored at different time intervals with or without stress Cr (VI) ions. Maximum growth of biofilm formation by NCIM 3590 and NCIM 3589 were observed at 60 h and 48 h, respectively. Biofilm formation decreased with increasing concentrations of Cr (VI) ions. Thus, Cr (VI) ions had inhibitory effect on biofilm formation. It was noticed that biofilm formation was further increased with increasing incubation time. These results indicated that biofilms were resistant to Cr (VI) ions after adaption within certain time. Metal resistance in *Candida* biofilms has been reported earlier. This resistance was due to metal absorption by biofilm (Harrison et al., 2006). Figure 2 shows SEM images of *Y. lipolytica* NCIM 3590 and NCIM 3589 biofilms on glass surfaces without (Figure 2A and D) or with Cr (VI) ions (Figure 2B, C, E and F). Biofilms were formed on the glass surfaces after 60 h of incubation without Cr (VI). Biofilms were slightly inhibited in presence of 0.05mM and 0.1 mM Cr (VI). Cells in biofilms were increased in size due to stress of Cr (VI). Light microscopy revealed in comparison with the control biofilms that showed uniform growth, (Figure 3 A and D, respectively, for NCIM 3589 and NCIM 3590) a distinct microcolony-like structure of the biofilms in the presence of the Cr (VI) ions (Figures 3 B, C, E and F). Such morphological changes in biofilms are observed may be due to stress of Cr (VI) on biofilm and their response towards adaptation.
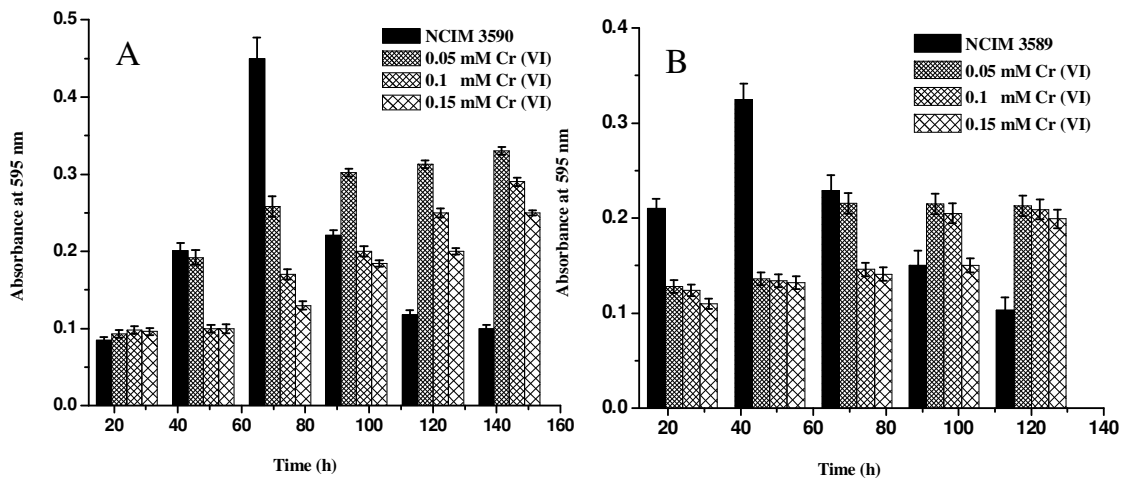


**FIGURE 1** Effect of Cr VI on Biofilm Formation of *Y. lipolytica* NCIM 3590 and NCIM 3589

**Effect of pH, Temperature, Contact Time, Biomass and Initial Metal ion Concentrations Cr (VI) Biosorption.** As shown in Figure 4A, the optimum pH for the Cr (VI) biosorption by biofilm-biomass was 2.0. Increasing pH of solution was result into decreased uptake of Cr (VI). At pH 7.0, uptake of Cr (VI) by NCIM 3590 and NCIM 3589 was $74.75 \pm 2.0$ and $51.16 \pm 4.0$ mg/g, respectively. At pH 2.0 this was increased to $97.95 \pm 4.0$ and 71.41 mg/g. Thus, biosorption was increased with decrease in pH for biofilm-biomass. Such observations on enhanced biosorption at acidic pH have been previously reported with fungal biomass (Özer and Özer, 2003; Bankar et al., 2009b). Figure 4B showed there was enhanced biosorption at higher temperatures. Similar results have also been reported earlier (Zhou et al., 2007, Bankar et al., 2009b).
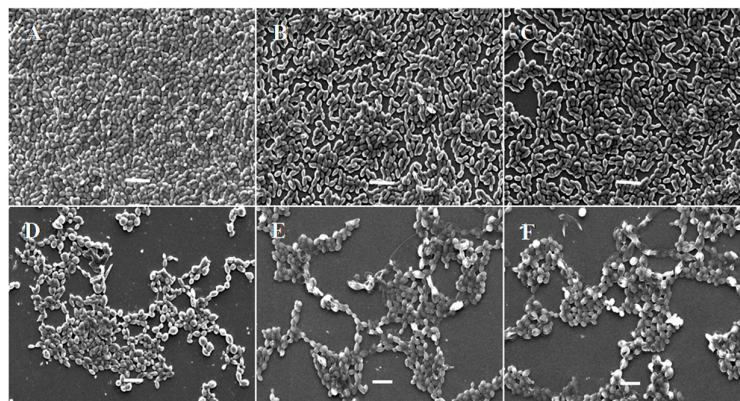


**FIGURE 2** Representative SEM Images of Biofilm Formation on Glass Surface (A, D) Control NCIM 3590 and NCIM 3589; in the presence of (B, E) 0.05mM; (C,F) 0.1mM Cr (VI) ions. Bar represents 10 μm at 1000 X magnification.
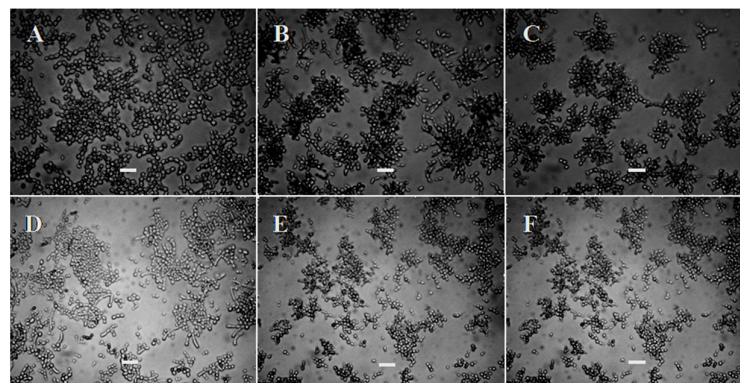


**FIGURE 3** Representative Light Microscopic Images of Biofilm Formation on Glass Surface (A, D) Control NCIM 3590 and NCIM 3589; in the presence of (B, E) 0.05mM; (C,F) 0.1mM Cr (VI) ions. Bar represents 10 μm at 100X magnification.

The specific uptake of Cr (VI) decreased with an increase in biomass (Figure 4C). This is due to the augmentation of electrostatic interactions that increase with larger quantities of biomass (Ferraz and Teixeira, 1999). The effect of contact time on biosorption of Cr (VI) by the biofilm-biomass was studied under optimal conditions (Figure 4D). Biosorption occurred rapidly within 5 to 15 minutes. The biosorption process became slower from 15 min to 2h and thereafter, there was no significant increment in metal uptake. Thus, equilibrium was reached within 2h. Similarly, rapid removal of Cr (VI) ions has been reported previously in planktonic biomass of *Y. lipolytica* (Bankar et al., 2009b). The initial concentration of Cr (VI) ions greatly influenced the biosorption capacities ($q_{eq}$). Figure 5E showed that Cr (VI) biosorption for biofilm-biomass of NCIM 3590 and NCIM 3589 increased from $97.95 \pm 5.0$ and

50.71± 4.0 mg/g to 500.91 ± 2.0 and 424.59 mg/g, respectively with an increasing metal concentration (50 to 1000 mg/l). Thus, adsorption of Cr (VI) ions was increased with increasing metal ion concentration in the solution.
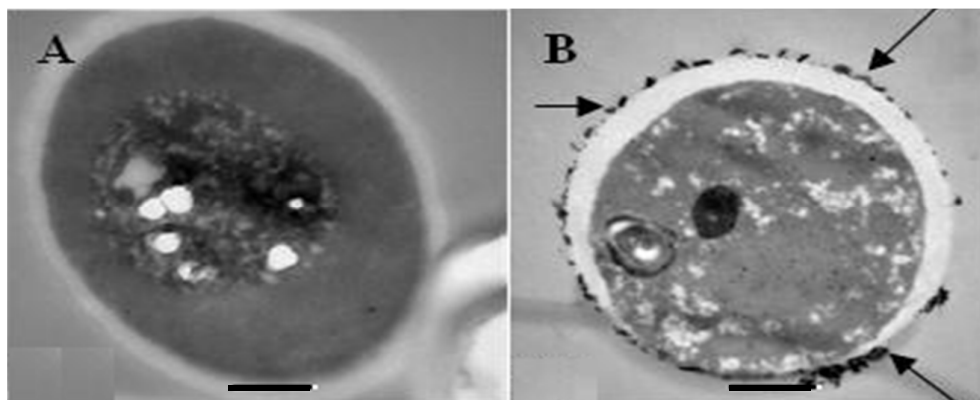


**FIGURE 4** Representative TEM images of (A) *Y. lipolytica*NCIM 3589  cells without Cr (VI) (B) with 0.15mM of  Cr (VI) ions Bar represents 0.5µm at 25000X magnification.

**Adsorption Isotherms and Kinetics.** The experimental data of metal ions adsorption by the biofilm biomass of both the strains was analysed by the Langmuir and Freundlich isotherms. All parameters are listed in table 1. Figure 5 (F, G) shows that high determination coefficient ($r^2 = 0.99$) of the Langmuir and Freundlich isotherms, respectively. High correlation coefficients, $r^2$ values for the Langmuir and Freundlich isotherms suggested that monolayer adsorption as well as heterogeneous conditions under the experimental conditions maybe playing an important role. The plots of ln ($q_{eq}$-$q_t$) versus t for the pseudo-first-order model (not shown as a Figure) showed that coefficients ($r^2$) for Cr (VI) adsorption onto biofilm biomass was 0.70. This suggested that the experimental data did not fit well to the pseudo-first-order rate equation. The linear plots of t/$q_t$ versus t of the pseudo-second-order for the adsorption of Cr (VI) ions onto biofilm- biomass are shown in Figure 5H. The rate constants ($K^2$), the $q_{eq}$ and the $r^2$ values are given in Table 1. The determination coefficients ($r^2$) obtained for Cr (VI) adsorption onto biofilm biomass surfaces were 0.99. The high $r^2$ values suggested that the adsorption of metal ions onto biofilm-biomass surfaces fitted well to the pseudo-second-order kinetic equation.

These results indicated that chemical processes may be affecting the overall rate of the metal ion adsorption (Ho and McKay, 1999). Figure 4A is a representative TEM image of *Y. lipolytica* NCIM 3589 control cells. After interaction with Cr (VI) ions, cells showed electron dense regions (indicated by black arrows in Figure 4B) thereby suggesting the uptake of the metal. FTIR studies revealed role of functional groups such as amino, carboxylic and hydroxylic etc (figure not shown) in biosorption of Cr (VI). Thus, it is concluded that biofilm of *Y. lipolytica* has potential for removal of Cr (VI) ions from aqueous solution and that this study can be useful for development of technology for removal of Cr (VI) from wastewater.

**TABLE 1** Adsorption Isotherm and Kinetics Parameters for Cr (VI) Ions on biofilm-biomass of *Y. lipolytica* NCIM 3590 and 3589.

| Metal Cr (VI) | Langmuir isotherm | | | Freundlich isotherm | | | Pseudo-second-order | | |
|---|---|---|---|---|---|---|---|---|---|
| | $q_m$ | $b_m$ | $r^2$ | $K_F$ | $n$ | $r^2$ | $K_2$ | $q_{eq}$ | $r^2$ |
| NCIM 3590 | 1000 | 3.03 | 0.99 | 1.83 | 0.54 | 0.99 | 5.55 | 111.1 | 0.99 |
| NCIM 3589 | 1000 | 2.5 | 0.99 | 2.5 | 0.53 | 0.99 | 1.53 | 76.92 | 0.99 |
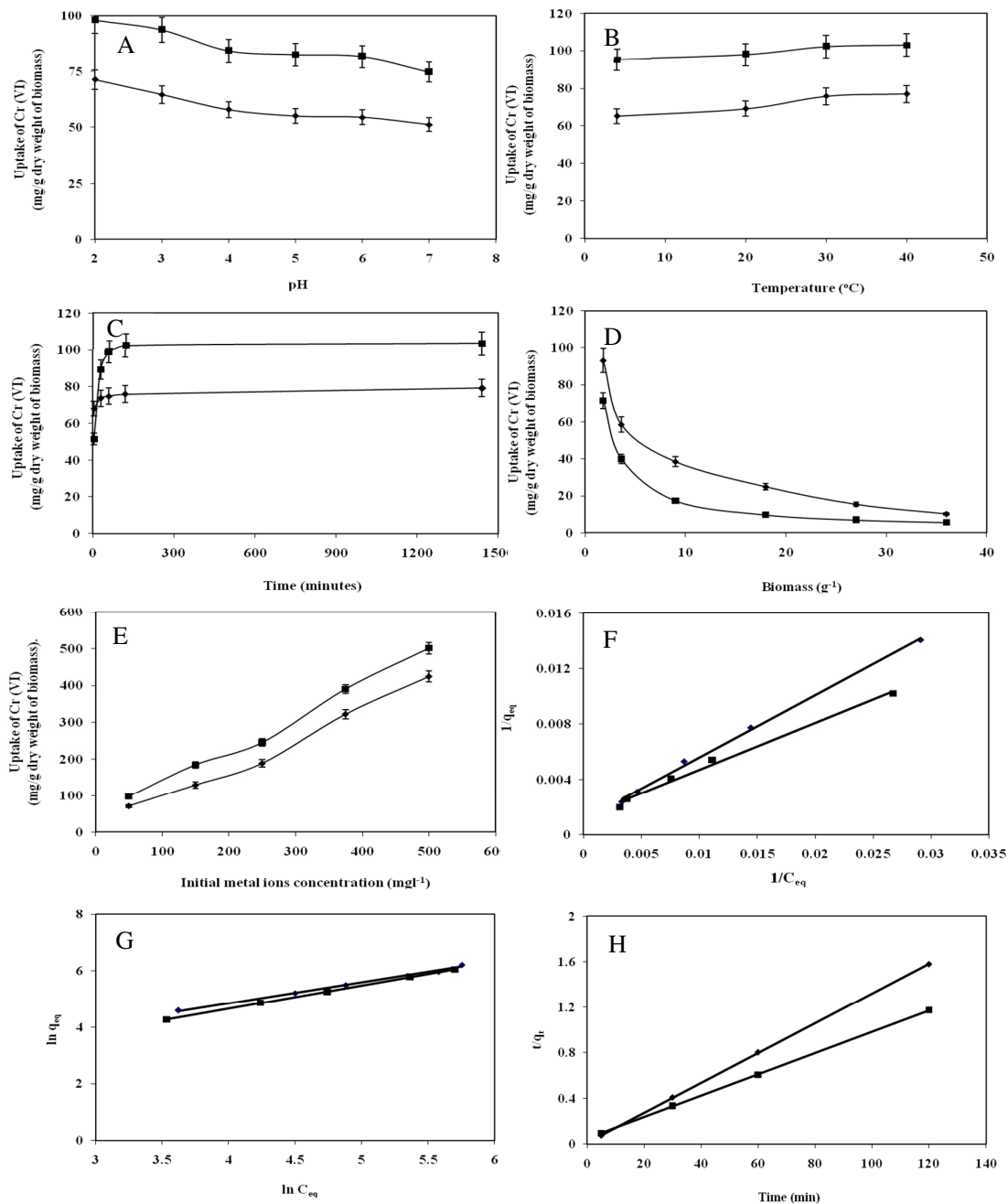
**FIGURE 5** Effect of pH (A), Temperature (B), Time (C), Biomass (D) and Metal Initial Concentration (E) on Cr (VI) Biosorption by *Y. lipolytica* NCIM 3590 (■) and NCIM 3589 (▲)and Langmuir (F), Freundlich (G) and pseudo-second-order (H).

## ACKNOWLEDGMENTS

## REFERENCES

Aguilar, F.J.A., K. Wrobel, K. Lokits, J. A. Caruso, A. C. Alonso, J. F. G. Corona and K. Wrobel, 2008 "Analytical speciation of chromium in in-vitro cultures of chromate resistant filamentous fungi," *Analytical and Bioanalytical Chemistry*, 392 (1-2) : 269-276.

Bagchi, D., S. J. Stohs, B. W., Downs, Bagchi, M., and H. G. Preuss, 2002. "Cytotoxicity and oxidative mechanisms of different forms of chromium". *Toxicology*, 180: 5-22.

Balasubramanian, S., and V. Pugalenthi, 1999. "Determination of total chromium in tannery waste water by inductively coupled plasma-atomic emission spectrometry, flame atomic absorption spectrometry and UV–visible spectrophotometric methods." *Talanta*, 50: 457-467.

Bankar, A.V., A.R. Kumar and S.S. Zinjarde, 2009. "Removal of chromium (VI) ions from aqueous solution by adsorption onto two marine isolates of *Yarrowia lipolytica*". *Journal of Hazardous Materials,*170: 487- 494.

Bankar, A.V., A. R. Kumar, and S. S. Zinjarde, 2009. "Environmental and industrial applications of *Yarrowia lipolytica*". *Applied Microbiology and Biotechnology,* 84 (5) : 847-865.

Barth, G. and C. Gaillardin, 1997. "Physiology and genetics of the dimorphic fungus *Yarrowia lipolytica*". *FEMS Microbiology Reviews*, 19 (4): 219-237.

Bishnoi, N. R. and Garima, 2005. "Fungus an alternative for bioremediation of heavy metal containing waste water: A review". *Journal of Scientific and Industrial Research*, 64: 93-100.

Boopathy, R. 2000. "Factors limiting bioremediation technologies". *Bioresource Technology*, 74: 63-67.

Costa, M. 2003. "Potential hazards of hexavalent chromate in our drinking water". *Toxicology and Applied Pharmacology,* 188:1-5.

Decho, A.W. 2000. "Microbial biofilms in intertidal systems: an overview." *Continental Shelf Research*, 20: 1257-1273.

Dusane, D. H., Y. V. Nancharaiah, V. P. Venugopalan, A. R. Kumar, and S. S. Zinjarde, 2008. Biofilm formation by a biotechnologically important tropical marine yeast isolate, *Yarrowia lipolytica* NCIM 3589". *Water Science and Technology,* 58 (6):1221-1229.

Ferraz, A. I. and J. A. Teixeira, 1999. "The use of flocculating brewer's yeast for Cr (III) and Pb (II) removal from residual waste waters." *Bioprocess Engineering*, 21: 431-437.

Gadd, G. M. 2004. "Microbial influence on metal mobility and application for bioremediation". *Geoderma*, 122: 109-119.

Harrison, J. J., M. Rabiei, R. J. Turner, E. A. Badry, K. M. Sproule and H. Ceri, 2006. "Metal resistance in *Candida* biofilms." *FEMS Microbiology Ecology*, 55:479-491.

Ho, W. S. W., and T. K. Poddar, 2001. "New membrane technology for removal and recovery of chromium from waste waters". *Environmental Progress*, 20:44-52.

Hullebusch, E. D. V., M. H. Zandvoort and P. N. L. Lens, 2003. "Metal immobilization by biofilms: mechanisms and analytical tools". *Reviews in Environmental Science and Biotechnology*, 2: 9-33.

Lameiras, S., C. Quintelas and T. Tavares, 2008. "Biosorption of Cr (VI) using a bacterial biofilm supported on granular activated carbon and on zeolite." *Bioresource Technology,* 99: 801-806.

Malik, A. 2004. "Metal bioremediation through growing cells". *Environment International*, 30: 261-278.

Quintelas, C., B. Fernandes, J. Castro, H. Figueiredo, and T. Tavares, 2008. "Biosorption of Cr (VI) by a *Bacillus coagulans* biofilm supported on granular activated carbon (GAC)." *Chemical Engineering Journal*, 136:195-203.

Özer, A. and D. Özer, 2003. "Comparative study of the biosorption of Pb (II), Ni (II) and Cr (VI) ions onto *S. cerevisiae*: determination of biosorption heats." *Journal of Hazardous Material* B 100: 219-229.

Srinath, T., T. Verma, P. W. Ramteke, and S. K. Garg, 2002. "Chromium (VI) biosorption and bioaccumulation by chromate resistant bacteria". *Chemosphere*, 48: 427-435.

Wen-Xiong, W. 2002. "Interactions of trace metals and different marine food chains". *Marine Ecology Progress Series*, 243: 295-309.

Zhou, M., Y. Liu, G. Zeng, Li Xin, W. Xu and T. Fan, 2007. "Kinetic and equilibrium studies of Cr (VI) biosorption by dead *Bacillus licheniformis* biomass." World Journal of Microbiology and Biotechnology, 23; 43-48.

# BIOLOGICAL LEACHING OF HEAVY METALS FROM CONTAMINATED SEDIMENT BY HETEROTROPHIC MICROORGANISMS

*Shen-Yi Chen* and Sheng-Ying Wang

(National Kaohsiung First University of Science and Technology, Kaohsiung, Taiwan)

In the remediation strategies of contaminated rivers, besides controlling pollution sources and building sewer systems, the contaminated sediment may need dredging from the contaminated rivers. Most of sediments dredged from contaminated rivers often contain substantial amount of heavy metals and thus can not be disposed of on the land and in the water body without any treatment. In future, there are two typical and important problems will be faced: increasing volumes of contaminated sediment and high concentrations of toxic substances in sediment. It is very important to develop the techniques for treatment of the large quantity of dredged sediments in the remediation of contaminated rivers. Bioleaching for metal removal from sediment, sludge and soil using chemolithoautrophic bacteria such as sulfur-oxidizing bacteria is a well-known process. It was observed that besides the well-know autotrophic bacteria also heterotrophic microorganisms play an important role in the bioleaching process. This biotechnology is environmentally sound and it may be lower operational cost and energy requirement than conventional physico-chemical technologies. However, bioleaching of heavy metals from contaminated sediments by heterotrophic microorganisms has received little attention to date. The purposes of this study are to develop a metal bioleaching process by heterotrophic microorganisms for contaminated sediments, and to investigate the effects of operational parameters on this biotechnology. An adapted and mixed culture of *Aspergillus niger* and *Penicillium simplicissimum* was used as the inoculum in bioleaching process in this study. The results showed that the rate of pH reduction decreased with increasing sediment solid content, whereas it increased as the sucrose concentration increased during the bioleaching process. The maximum efficiencies of metal solubilization were 65-69% for Zn at the 8th day and 43-57% for Ni at the 6th day, respectively. However, after 14 days of reactor time, 53-55% of Zn and 21-47% of Ni were leached from sediments in this bioleaching process. The efficiencies of metal leaching were found to increase with a decrease in sediment solid content and an increase in sucrose.

# ENHANCEMENT OF HEAVY MEATLS MOVEMENT BY CAPILLARY FORCES BY ADDITION OF CHELATE SOLUTION IN POLLUTED SOIL

*AL-Oud S.S.* Soil Sciences. Dept., College of Food and Agricultural Sciences, King Saud University, P.O. Box 2460, Riyadh 11451, Kingdom of Saudi Arabia

In metal-contaminated soils, reducing soil volume would reduce the cost of remediation. Dissolved organic compounds could form soluble complexes with heavy metals and enhance their transport upward and possibly reduce the contaminated soil volume. The aim of this study was to evaluate the efficiency application of dilute chelate solutions to mobilize heavy metals, namely Cd, Pb, Cr, and As upward by capillary force in a soil under greenhouse conditions. The soil sample a Sultan silt loam soil (Aquandic Xerochrept) used in this study were incubated prior to use with the following concentration: 3ppm Cd, as CdCl2; 20ppm As, s $As_2O_3$; 150 ppm Pb, as $PbCl_2$; and 150ppm Cr as $K_2Cr_2O_7$ . Portions of 148.46 g of the treated soil sample were packed to a height of 15 cm PVC columns of (25 cm height and 4.5 cm internal diameter). Columns were provided with a tub for solution injection from the bottom. Leaching solutions EDTA (0.1 mM,1.0 mM) and distilled $H_2O$, were added to the soil columns from the bottom. The result showed that EDTA solutions were more capable in mobilizing specially Cd and Pb upward to the surface layer. Out of the total Cd added less than 2% remained in the bottom of the column (12 to14 cm), whereas greater than 50% of the Cd added was transported to the surface layer (0 to 2 cm). For Pb, out of the total added less than 3% remained in the bottom layer, whereas greater than 35% of the added Pb was accumulated in the surface layer in the soil. For Cr, and As the results showed these metals were less mobilized.

# MICROWAVE ASSISTED PRE-TREATMENT OF BLACK SHALE FOR REMOVAL OF CARBONACEOUS MATTER

*O.P. Karthikeyan*, Raghu Betha, A.Rajasekar, S. Manivannan and R.Balasubramaniam (National University of Singapore, Singapore)

Black shale, a low grade copper ore, from a mining site in Poland was collected for this work. This ore contains the valuable metal fractions (64 %) and sulfide mineral phases along with carbonaceous matters (2-15%). The carbon matter mainly comprises alkanes and polycyclic aromatic hydrocarbon (PAHs) which tends to interfere with the selective bioleaching of valuable metals such as copper (Cu). Therefore, it is necessary to pre-treat the black shale for the removal of the carbonaceous matters such as that the bioleaching efficiency for metals of interest can be maximized. In the present study, the microwave-assisted pre-treatment (MWAP) technique was explored for effective removal of carbonaceous matter, especially alkanes and PAHs. The MWAP technique has been used for a range of environmental applications, especially for the monitoring of metals and PAHs in sediments and airborne particulate matter. However, little is known about its potential for decontamination of the black shale, which is a refractory material.

For the present study, the black shale collected from the mining site was pre-treated using a microwave oven under a range of irradiation conditions (100 to 800 W) for different time intervals (1 to 25 minutes). Untreated and pre-treated black shale samples were subjected to simple solvent extraction with organic solvents of different polarity. The extracts were then concentrated using a rotary evaporator and then with nitrogen purging followed by GC-MS analysis to quantify a range of alkanes and PAHs of different molecular weights and account for their removal from the black shale ore. The metal leachability of the ore was examined before and after pre-treatment. In addition, bioleaching experiments were conducted with the pre-treated black shale using the mixed acidophilic bacteria namely *Leptospirillum ferrooxidans, Leptospirillum ferriphilum,* and *Sulfobacillus thermosulfidooxidanse* (DSMZ isolates) in 9K medium with a pulp density of 2% at 37$^o$C for 15 days. Results showed that the MWAP technique effectively removed more than 80 % of alkanes and PAHs from the black shale and thus improved the bioleaching efficiency for Cu significantly. Further insights into the pre-treatment method and its effectiveness for the bioleaching of Cu from the refractory ores will be discussed at the conference.

# REMOVAL OF CHROMIUM (III) AND LEAD (II) BY USING YARROWIA LIPOLYTICA: YEAST-METAL INTERACTIONS

*Ashok Bankar*, Soumitra Marathe, Ameeta Kumar and Smita Zinjarde
(IBB, University of Pune, Pune, India)
Balu Kapadnis (D M, University of Pune, Pune, India)
Mark Winey (MCDB, University of Colorado, Colorado, USA)

Two marine strains of *Yarrowia lipolytica* were evaluated for their minimum inhibitory concentration (MIC) values of heavy metals on solid YPD agar media. Effect of heavy metal ions on growth kinetics of yeasts was also studied. Morphological changes in yeasts under stress of heavy metals were observed using light and scanning electron microscope (SEM). Bioaccumulation of Pb (II) and Cr (III) by *Y. lipolytica* was demonstrated by using a transmission electron microscope (TEM). Metal ion accumulation in *Y. lipolytica* cells was determined by atomic absorption spectroscopy (AAS).

The removal of Pb (II) and Cr (III) ions from aqueous solutions by the biomass of two marine strains of *Y. lipolytica* was studied with respect to pH, temperature, biomass, contact time and initial concentration of metal ions. The adsorption data is well fitted to the Langmuir and Freundlich isotherms. The surface sequestration of Pb (II) and Cr (III) by *Y. lipolytica* was investigated with a scanning electron microscope equipped with an energy dispersive spectrometer (SEM-EDS). Fourier transform infrared (FTIR) spectroscopy revealed the involvement of carboxyl, hydroxyl and amide groups on the yeast cell surfaces in metal binding.

# ARSENIC MOBILIZATION AND PLANT UPTAKE FROM AN INDUSTRIAL CONTAMINATED SOIL IN TUSCANY (ITALY). CROP PLANTS VS PTERIS VITTATA

Meri Barbafieri[1], Virginia Giansoldati[1], Francesca Pedron[1], Gianniantonio Petruzzelli[1], Irene Rosellini[1], Roberto Bagatin[2], Elisabetta Franchi[3]

[1] National Research Council, Institute of Ecosystem Study, Section of Pisa, Via Moruzzi 1, 56124 Pisa, Italy

[2] Research Center for Non-Conventional Energy,  Istituto ENI Donegani, Via Fauser 4, 28100 Novara, Italy

[3] Research Center for Non-Conventional Energy,  Istituto ENI Donegani, Via Maritano 26, 20097 San Donato Mil.se, Italy

**ABSTRACT:** We evaluated the phytoextraction capacity of crop plants (*Helianthus annuus, Brassica juncea* and *Lupinus albus*) and the As hyperaccumulator (*Pteris vittata),* in arsenic contaminated soil. Phosphate application to maximize the efficiency of arsenic removal was tested for crop plant and *P. vittata*. Arsenic uptake by crop plants was determined after 60 days of growing while *Pteris* plants were monitored at different times in a 9 months experiment. Results showed an increase of As uptake in crop plants of about 10 times after phosphate addition. *H. annuus* had the highest As accumulation up to 500 mgkg$^{-1}$. *P. vittata*, during the growing period, progressively increased the As uptake reaching the maximum content of about 3000 mg/kg in fronds. In the phosphate treated pot, *Pteris* increased the As uptake faster than that in non-treated pot. In terms of phytoextraction capacity, at the end of the experiment treated and not treated plants showed the same ability in the As phytoextraction. The As mobile species were determined by a simplified chemical extraction ($H_2O$ and $K_2HPO_4$).

## INTRODUCTION

Phytoextraction, a plant-based alternative and/or complementary technology to remedies contaminated soil has been receiving renewed attention for its potential utilization in brownfields area. Phytoremediation applicability was evaluated  on a soil from brownfield site contaminated by As.

Different strategies are being used for the phytoextraction of toxic metals: (i) use of hyperaccumulator plants, which are able to accumulate high metal concentrations in shoots (natural phytoextraction); (ii) use of high biomass crops which are induced to take up large amounts of bioavailable metals by means of chemical treatments in soil (chemically assisted phytoextraction). Hyperaccumulator plants have a natural capacity for accumulating large quantities of metal quantities (for example, more than 1000 mg Ni kg-1 dry leaves) but, in general, produce a relatively small shoot biomass with low growth rate and long life cycle.

Compared to hyperaccumulator plants, the biomass of crop plants is significantly higher and can compensate for the difference in metal accumulation (1-3 orders of magnitudes higher in hyperaccumulator plants). Several crop plants with elevated and rapid biomass production (such as indian mustard, sunflower, maize) can be induced to accumulate large quantities of metals in their upper parts. Assisted phytoextraction strategy for reducing heavy metal contamination generally involves addition of chelates (such as EDTA or NTA) or a weak acid (as citric acid) which render the heavy metals soluble in soil solution and increase their bioavailability, thus enhancing the crop plants uptake (Gleyzes et al. 2001, Pedron et al. 2009). The possibility to plan repeated growing cycles with harvesting metal-rich biomass may be more advantageous than using hyperaccumulator species. In this case, particular attention should be paid to the depth of ground-water and the possible risk of metal leaching into the soil profile must be considered. Thus, it is advisable to monitor metal movement in soil with the use of appropriate water controls, in order to prevent downward displacement and/or impact of soluble metals on water resources.

Arsenic and phosphorus are in the same periodic family and it is known that, due to its chemical and physical similarities to arsenic, phosphorus competes the arsenic fixation sites in soil. Studies reported that the application of phosphate-containing fertilizers can displace arsenate from soil, increasing arsenic solubility and phytoavailability (Tassi et al. 2004, Caille et al. 2003, Wang et al. 2002)

Considering that arsenic uptake by plants occurs primarily via the same route as phosphorus (Wang et al 2002; Cao et al. 2003) or via an altered phosphate uptake system; our purpose in this work was to take advantage of this situation to render it a means for assisted phytoremediation action.

We evaluated the phytoextraction capacity of the As hyperaccumulator (*Pteris vittata*) and of the crop plants (*Helianthus annuus, Brassica juncea* and *Lupinus albus*) in arsenic contaminated soil collected from industrial site in Avenza (Tuscany, Italy). Phosphate application to maximize the efficiency of arsenic removal was tested for crop plants and *P. vittata*.

## MATERIALS AND METHODS

**Soils Used.** Four samples with different As content collected from an industrial area in Avenza (Tuscany, Italy) were used. The source of as contamination were from chemical plant. Soil characteristics were: pH 8.26, OM 3.53% CSC 17.5(cmol(+) kg$^{-1}$). Arsenic content and speciation in the different used samples are shown in table 1. Soils were collected from the plough layer (0-20 cm), air dried and sieved through an 5mm sieve.

TABLE 1. Arsenic content and speciation in used soils. Data expressed as mgkg$^{-1}$.

| Sample | Total | Extractable (NH$_4$)$_2$SO$_4$ | Extractable KH$_2$PO$_4$ |
|--------|-------|------------------|------------------|
| N. 409 | 1064  | 4.1              | 24.9             |
| N. 117 | 581   | 0.3              | 1.8              |
| N. 443 | 2595  | 1.4              | 30.1             |
| N. 434 | 878   | 3.5              | 23.6             |

**Plant Growth:** For *Pteris vittata* growth, soils were placed in 500mL plastics pots (8 replicates for each soils). In each pots were transplanted one Pteris vittata plant at four frond stage. Phosphate addition was performed once time at the second month of plant growing. The experiment lasted 9 month. Fern plant grown in growth chamber under controlled condition for its best grown (28-23 ° C for day/nights periods, humidity 70%, light 200umolm-2 s-1 for 14 h/day). For crop plants experiment (*Helianthus annuus, Brassica juncea* and *Lupinus albus*), soil were placed in five Kg pots (20 pots for each plant species). The experimented lasted 60 days. Phosphate addition was performed in five diluted doses after 30 days of plant growing. At the end of each experiments plants were collected washed, dry and registered the dry weight. Data related N°443 soil are reported. Plants grown in green house under controlled condition for their best grown (24-19 ° C for day/nights periods, humidity 70%, light 200umolm$^{-2}$ s$^{-1}$ for 14 h/day).
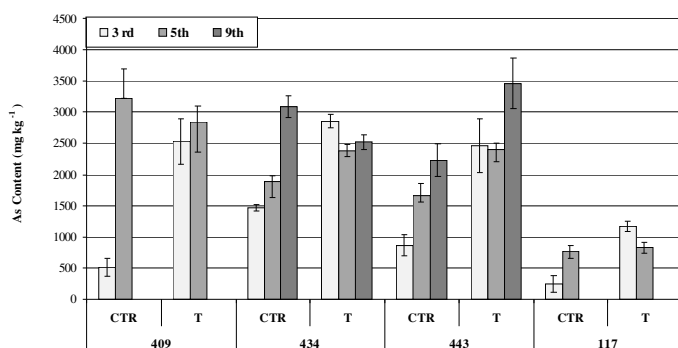


FIGURE 1. As content in *Pteris vittata* fronds at the 3 rd, 5th and 9 th month after phosphate treatment. CTR: control, T: treated.

**Chemical Analysis:** Total soil As were determined by the digestion of finely ground soil using HNO$_3$/HClO$_4$. Extractable As was determined by two step sequential extraction with: 1) (NH$_4$)$_2$SO$_4$; 2) KH$_2$PO$_4$ (modified by Wenzel et al. 2001). For plant material the dried fine plant powder were used for As analyses by acid digestion. Arsenic in solution was measured by Inductively Coupled Plasma (ICP-OES Liberty158 Axial Varian, Torino, Italy).

## RESULTS AND DISCUSSION

**Arsenic phytoextraction by *Pteris vittata*.** *P. vittata*, were grown in all soils with different As content (Table 1). Arsenic uptake by *Pteris* plants were monitored three times in a 9 months experiment. During the growing period, progressively increased the As uptake reaching the maximum content of about 3000 mg kg$^{-1}$ in fronds. In the soil N°117 fronds reached the maximum content of about 1000 mg kg$^{-1}$. In the phosphate treated pot, *Pteris* increased the As uptake faster that in non-treated pot (Figure1). In fact at the 3$^{rd}$ month plants reached the highest As content.

In the Figure 2 are reported data on plant biomass, As content in fronds and As phytoextraction. Phosphate treatment showed its beneficial effects increasing the plant biomass in all tested soils except for the soil117. The biomass increased is particularly evident in the soil N°443 and 117.

In terms of phytoextraction capacity treated plants showed the highest ability in the As phytoextraction.
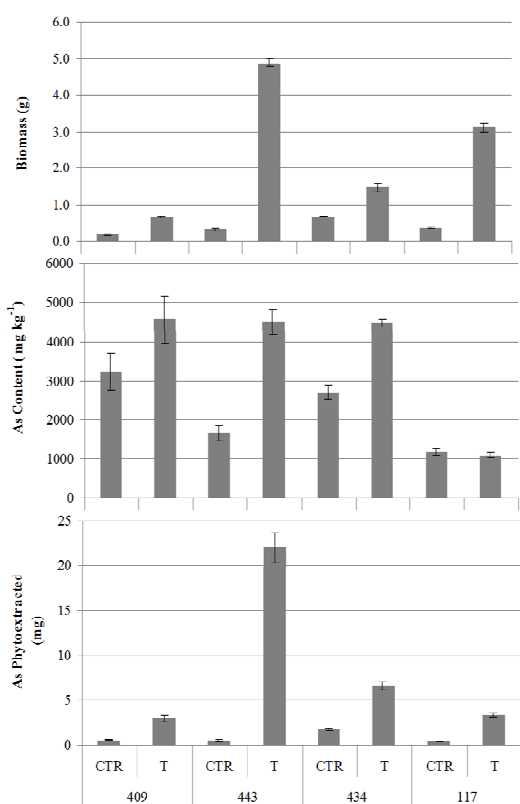


**FIGURE 2. *Pteris vittata* biomass, As content and As phytoextraction in the tested soils.**
**CTR: control, T: treated.**
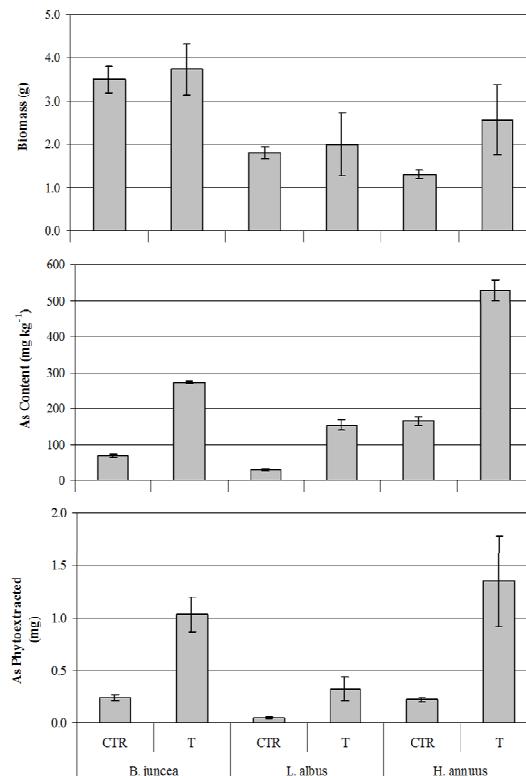
**FIGURE 3. Crop plants biomass, As content and As phytoextraction in the N° 443 tested soil.**
**CTR: control, T: treated.**

**Arsenic phytoextraction by crop plants:** For crops plants results are shown in Figure 3. For an example are reported data on the soil N° 443. The biomass was not affected or slightly increased (*H.annuus*) with the phosphate treatment. All the tested plants increased the As uptake of about 10 times after phosphate addition. *H. annuus* had the highest As accumulation up to 500 mgkg$^{-1}$. The phytoextraction resulted increased for all the tested plants. *L. albus* showed the lowest potential in As phytoextraction in comparison with *B juncea* and *H. annuus*.

Comparing phytoextraction potential between As hyper accumulator and crop plants, in the adopted experimental condition, *Pteris* is most effective as it removed up to 20 mg of As (in soil 443) while the highest As removal in crop plants is about 1.5 mg by *H annus*. The fern has a phytoextraction power about 13 fold higher.

**CONCLUSIONS**

Phosphate treatment positively affects the As phytoextraction for both plants typology (hyper accumulator and not) but with different rate. The hyper accumulator further increases its potential increasing both biomass and As content. In crop plants phosphate tratement increased the As content and biomass production (in particular for *H. annuus*). *Pteris* plants showed the highest phytoextraction potential even if the lowest biomass production and the longer time required to growth. Moreover remain to verify its adaptability and growth rate in the field. Fern plant usually required specific environmental condition. While the tested crop plants are well known and adapt for Mediterranean climate condition.

Following this experiment, field test need to be performed to verify the effectiveness and potentiality efficiency of fern hyper accumulator and crop plants.

**ACKNOWLEDGEMENTS**

**REFERENCES**

Gleyzes C., Tellier S., Sabrier R., and Le Cloirec P. 2001. Arsenic characterization in industrial soils by chemical extractions. *Environ. Technol.* 22: 27–39.

Pedron F., Petruzzelli G., Barbafieri M., Tassi E. 2009. "Strategies to use phytoextraction in very acidic soil contaminated by heavy metals". *Chemosphere,* 75: 808-814.

Tassi E., Pedron F., Barbafieri M., and Petruzzelli G. 2004. "2Phosphate-assisted phytoextraction in As-contaminated soil". *Eng. Life Sci.,* 4: 341-346.

Wenzel W.W., Kirchbaumer N., Prohaska T., Stingeder G., Lombi E., Adriano D.C. 2001. 2Arsenic fractionation in soils using an improbe sequential extraction procedure". *Anal. Chim. Acta*, 436: 309-323.

Cao X., Ma Q.L., Shalipuour A. 2003. "Effect of compost and phosphate amendments on arsenic mobility, in soils and arsenic uptake by the hyperaccumulator *Pteris vittata* L." *Environmental Pollution* 126: 157-167

Caille N., Swanwich S., Zhao F.J., and Mc Grath S.P. 2003. "Arsenic hyperaccumulation by Pteris vittata fern from arsenic contaminated soils and the effects of liming and phosphate fertilization". *Environmental Pollution* 132: 1113-1120.

Wang J., Zhao F.J., Meharg A., Raab A., Feldman J., and Mc Grath S.P. 2002. "Mechanism of arsenic hyperaccumulation in *Pteris vittata*. Uptake kinetics, interactions with phosphate, and arsenic speciation". *Plant physiology* 130: 1552-1561.

# PROTECTION BY *CLERODENDRUM PHLOMIDIS* AGAINST MANGANESE TOXICITY

*Ram* Prakash

(Department of Zoology, Dr. A.G.D. Bendale Mahila Mahavidyalaya JALGAON-425001, India)

Manganese is an essential trace element and involves widely in biological reactions. It activates numerous enzymes such as , kinases, esterases , mutases ,peptidases ,dehydrases etc.. However higher intake of manganese was recorded hazardous to cell/tissue. It was recorded in our laboratory that manganese cause hepatic cell necroses ,fibro-proliferation, binucleated cells, pycnosis of nuclei, glomerulo-nephritis, glomerular damage and disturbances in the plasma membrane of PCT and DCT. Manganese also decreased activity of some key enzymes such as alkaline and acid phosphatases, cholinesterase and glucose - 6-phosphatase. Recently we designed experiments on rats as first they were treated with manganous chloride for thirty days and than post treated with the leaf extract of *Clerodendrum phlomidis* for further fifteen days. The observations were made on liver and kidney for similar histological and histochemical parameters .It was recorded that most lesions were reversed towards their normal conditions. Therefore it was concluded that *C. phlomidis* has therapeutic value against manganese toxicity in liver and kidney of rats .The observation on other parameters also support present data.

# ARSENIC INTAKE FROM WATER, RICE AND VEGETABLES IN BANGLADESH

***Mohammad Mahmudur Rahman*** and Ravi Naidu (Centre for Environmental Risk Assessment and Remediation (CERAR), University of South Australia, Mawson Lakes Campus, Mawson Lakes, South Australia, SA 5095, Australia and Cooperative Research Centre for Contamination Assessment and Remediation of the Environment (CRC-CARE), P O Box 486, Salisbury South, SA 5106, Australia)

Inorganic As compounds are identified as human carcinogens and intake of inorganic As was also recognized as a cause of cancers in skin and other internal organs such as bladder, kidney and lung. The accumulation of As in crops especially rice and vegetables irrigated with geogenic As-contaminated groundwater is well established in Bangladesh and West Bengal in India. Arsenic contaminated groundwater is widely used for agricultural irrigation in many countries, and as a result, crops may contain considerable concentration of As. This study reports concentrations of total and inorganic arsenic (As) in drinking water and foods (rice and vegetables) in an arsenic-contaminated area (Noakhali) of Bangladesh and daily intake of total As from these sources. The levels of total As in drinking water, rice and vegetables were 328 μg/L, 153 μg/kg and 113 μg/kg, respectively. Arsenic speciation shows that on average 73% and 87% of total As were present as inorganic form in raw rice and vegetables samples, respectively. The daily estimated average As intake from food was 90 µg whereas the total As intake from food and drinking water was 1041 µg for adults. The study shows that high percentage of inorganic As consumption poses at risk to the local inhabitants. Drinking water alone contributes 91% of As to the daily As consumption to adults.

# ENHANCED PHYTOREMEDIATION OF HEAVY-METAL CONTAMINATED SOILS BY FUNCTIONAL ENDOPHYTIC BACTERIA

*Liang Chen*, *Sheng-lian Luo*, Chen-bin Liu, Jue-liang Chen and Yong Wan
(Hunan University, Changsha, Hunan, China)

**ABSTRACT:** Phytoremediation is emerging as an ecologically sound and safe method for *in situ* treatment of heavy-metal contaminated soils. However, this plant-based technology is often inefficient due to the phytotoxicity for the plants and low metal bioavailability in soils. A clever solution is to combine the advantages of plant-endophyte partnerships within the plant rhizosphere or endosphere into an effective cleanup technology. In this study, inoculation of cadmium hyperaccumulator *Solanum nigrum* L. with a heavy metal resistant-plant growth-promoting endophytic bacterium, *Serratia* sp. LRE07, has resulted in a remarkable decrease in cadmium phytotoxicity and a maximum increase of 53.3% in cadmium accumulation in the plant root. The present observations demonstrated that the use of functional endophytic bacteria for improving the efficiency of phytoremediation may be a promising strategy to restore heavy-metal polluted soils.

## INTRODUCTION

Soil pollution by heavy metals has received much attention in recent years because of its significant threat to the natural ecosystem and human health. To avoid or neutralize the toxicity associated with these heavy metals, several technologies and methods have been developed to remove them from polluted soils. Compared with chemical or physical means, phytoremediation of metals is a cost-effective "green" technology based on the use of specially selected hyperaccumulating plants to extract metals from soils. However, this approach also has its drawbacks, as the phytoremediation efficiency is often limited by the bioavailability of the metal in soil, plant root development, and the level of tolerance of the plant to each particular metal (Pilon-Smits, 2005).

Recently, various studies have demonstrated that metals phytoremediation (as well as plant growth) can be facilitated by some plant-associated microbes. These microbes often possessed high metal tolerances and have exceptional ability to promote the growth or metal accumulation of plant by various mechanisms such as production of indole-3-acetic acid (IAA), siderophores and 1-aminocyclopropane-1-carboxylic (ACC) deaminase, solubilization of minerals, and mobilization of metals (Rajkumar et al., 2009). As plant-associated microbes, endophytes colonized to internal of the plant and are known for their beneficial effects on growth and health of the host plant (Sturz et al., 2000). However, studies devoted to plant-endophyte partnerships in metal remediation are rather scarce, and little is known about the mechanisms of the interactions between endophytes and hyperaccumulators under condition of metal toxicity. Consequently, the aim of this work was to application of plant growth-promoting endophyte (PGPE) isolated from Cd-hyperaccumulator plant *Solanum nigrum* L. for phytoremediation of Cd-contaminated soils. In addition, the mechanisms of plant-endophytes interactions were also discussed.

## MATERIALS AND METHODS

**Isolation and characterization of Cd-resistant PGPE:** The endophytic bacteria was isolated from a Cd-hyperaccumulator plants *S. nigrum* L. which were collected from the sewage discharge canal bank of Zhuzhou Smeltery, Hunan Province, China (27°52′ N, 113°05′ E), previously described by Xiao et al. (2010). In order to obtain the Cd-resistant PGPE, all the bacterial isolates were check the extent of Cd resistant and the ability to grow on salts minimal medium with ACC as the sole source of nitrogen.

Several plant growth-promoting features of the selected endophytic bacterium were characterized as follow. The ACC deaminase activity of cell-free extracts was determined by monitoring the amount of α-ketobutyrate generated by the enzymatic hydrolysis of ACC according to Penrose and Glick (2003). Production of siderophore by the bacterial strain was detected and quantified by the "universal" chrome

azurol-S (CAS) analytical method (Schwyn and Neilands, 1987). IAA production was measured according to Sheng et al. (2008). The phosphate solubilizing activity was measured according to Ma et al., (2011).

**Pot experiments:** The soils were firstly collected from the bed of Xiangjiang River near the Hunan University. The soils were air-dried and sieved (4 mm) to remove plant materials and stones, and then equally divided into three parts. The three parts of soils were amended with increasing amounts of $CdCl_2$ to achieve the final Cd concentration at 12.1, 63.7, 116.5 mg/kg soil, respectively. The accurate Cd concentration was determined using flame atomic absorption spectrometer (Z-2000, Hitachi). Before used, the amended soils were left in the greenhouse for a month to stabilize metal.

Seeds of *S. nigrum* L. were surface-sterilized with a mixture of ethanol and 30% $H_2O_2$ (1:1) for 20 min and washed with extensive sterile water. The seeds were then placed in blotters filled with sterilized vermiculite which moistened with sterilized half-strength Hoagland's nutrient solution, and were allowed to germinate at 25 °C and a 16/8 day/night regime. For inoculation of the seedlings, bacterial cultures were grown for 20 h, harvested by centrifugation (6000 rpm, 10 min), washed twice with sterile distilled water, and resuspended in biological saline (0.85% KCl). Twenty-day-old equally developed seedlings were soaking for 2 h in an actively growing bacterial culture (about $1 \times 10^9$ CFU/ml) and transplanted in plastic pot containing 300 g of three different levels of Cd-contaminated soil, respectively. Seedlings were soaked in sterile water as a control. Each treatment was performed in three replicas. The plants were grown in a glasshouse at 25 °C and a 16/8 day/night regime. The soil was moistened with sterile water and maintained at 60% of its holding capacity.

After six weeks, whole plants were carefully removed from the pots and the soil was removed from the roots. Plant roots were immersed in 10 mM EDTA for 30 min, and then rinsed thoroughly with deionized water to remove surface adsorbed metal. The dry weight of the plants was measured after oven dried at 80 °C for 24 h. The concentration of Cd in root, stem and leaf tissue of plant were also quantified following the method of Dell' Amico et al. (2008).

## RESULTS AND DISCUSSION

The metal-tolerant bacteria which survive in habitats with high metal pressure could be isolated and selected for their potential application in the bioremediation of contaminated sites (Piotrowska-Seget et al., 2005). Idris et al (2004) deemed that hyperaccumulator accumulated high concentration of heavy metals, which provided a specific niche for bacterial endophytes, and in that study he found that endophytes generally tolerated higher Ni levels than rhizosphere bacteria. Moreover, during the long period of evolution with plants, some bacterial endophytes have formed a beneficial mutualistic symbiosis relationship with their host plants. Bacterial endophytes profit from host plants because of the enhanced availability of nutrients, and plants can also receive benefits from bacterial endophytes by growth enhancement or stress reduction (Hardoim et al. 2008). In this study, a strain isolated from the root of *S. nigrum* L., designated as LRE07, showing a high degree of Cd-resistant (Table 1) and can utilized ACC as the sole N source in DF salts minimal medium, was selected for further studies. The strain LRE07 was characterized as *Serratia* sp. based on its 16S rDNA sequence homology (100%) and the sequences was deposited at GenBank under accession number GU270854. The strain was further assayed for a number of properties which were important for plant growth-promoting activity (Table 1). The presence of more than one PGP trait in this bacterial endophyte can facilitate the growth of plant by utilizing one or more above mechanisms at different times during the life cycle of host plant.

Under conditions of metal stress, most of the commonly known hyperaccumulators have a slow growth rates and low biomass which will limit the efficiency of heavy metal phytoremediation (Raskin et al., 1997). Plants inoculated and non-inoculated LRE07 were subjected to three levels of Cd-contaminated soil for 6 weeks responded differently plant growth. The results of biomass (dry weight) measurement showed that the Cd-contaminated soils (especially the high Cd-contaminated soil) substantially inhibited the growth of *S. nigrum* L. However, inoculation with this Cd-resistant PGPE bacterium lightened the inhibitory effects and stimulated the growth of *S. nigrum* L. to some extent (Figure 1). Compared to the non-inoculated control, the dry weights of bacterial inoculated plants grown in the three levels of Cd-contaminated soil were enhanced by 37.8, 22.1 and 18.6%, respectively. LRE07 had the capacity of facilitating the growth of plants, which might be relevant to its ability to produce IAA, siderophore and

ACC deaminase, agreement with the other reported results (Sheng et al., 2008; Ma et al., 2011).

**TABLE 1** Characteristics of the selected Cd-resistant PGPE strain.

| PGPE strain | ACC deaminase ($\mu$m $\alpha$-KB mg$^{-1}$ h$^{-1}$) | IAA synthesis (mg L$^{-1}$) | Siderophore production ($\lambda/\lambda_0$)[a] | Phosphate solubilization (mg L$^{-1}$) | Cd-resistance (mM)[b] |
|---|---|---|---|---|---|
| *Serratia* sp. LRE07 | 0.45 ± 0.03 | 58.30 ± 2.78 | 0.433 | 258.56 ± 5.44 | 3 |

±, standard deviation
[a] Siderophore production: little, 0.8-1.0; low, 0.6-0.8; moderate, 0.4-0.6; high, 0-0.4.
[b] The data are reported as minimal inhibitory concentrations of $Cd^{2+}$ in mineral salt medium.
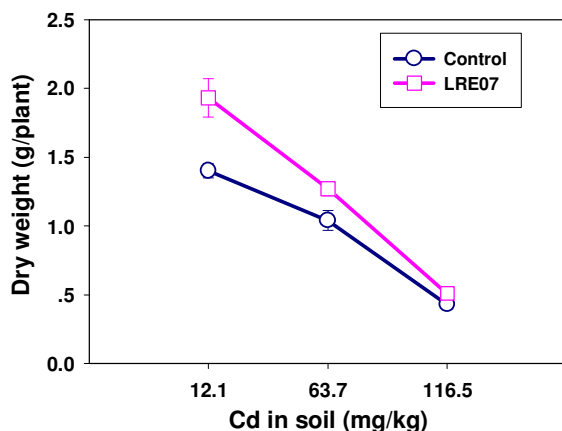


**FIGURE 2** Influence of LRE07 on plant biomass. Error bars represent standard deviation (n = 3).

The limiting factor of phytoextraction is often the availability of metals to plants rather than the maximal amount of metal that a plant can extract (Lebeau et al. 2008). The effects of LRE07 on Cd concentration in *S. nigrum* L. root, stem, and leaf tissues growing in three levels of Cd-contaminated soil are shown in Figure 2. In low Cd-contaminated soil, the Cd concentration in each tissue was no different between the inoculated and non-inoculated plant. However, in the moderate and high Cd-contaminated soil, the concentration of Cd was increased in plant tissues under the condition of inoculating endophytes, which enhance the concentration of Cd in root, stem and leaf by 21.3%, 15.6% and 11.9%, and by 53.3%, 10.6% and 17.6%, respectively compared with the control. The mechanism of LRE07 inoculation influence Cd accumulation by *S. nigrum* L. might be in several different ways. First, the bacterium with PGP traits has beneficial effects on root growth and hair production; this growth promotion could increase the Cd uptake by increasing the functional surface area of its roots. Moreover, the bacteria can facilitate the solubilization of non-labile forms of Cd in the soil and mobility to the plant, through acidification, redox changes and siderophores production. In addition, the presence of bacteria in the rhizosphere or internal of the host plant might increase the transport of Cd from soil to root or aboveground.

**CONCLUSIONS**

The results of the present study were demonstrated that utilizing the symbiotic plant-endophyte system to lighten heavy-metal contamination was a feasible and effective method for bioaugmentation-assisted phytoextraction. Inoculation with PGPE did not only achieve a significant aboveground biomass harvest, but also greatly influence the Cd concentrations in plant tissues, thus resulting in higher Cd removal. A further understanding of the role of PGPE in reduce metal toxicity for host plant and increase metal translocation to the aerial parts is essential for the development of effective phytoextraction of metal-polluted soils.
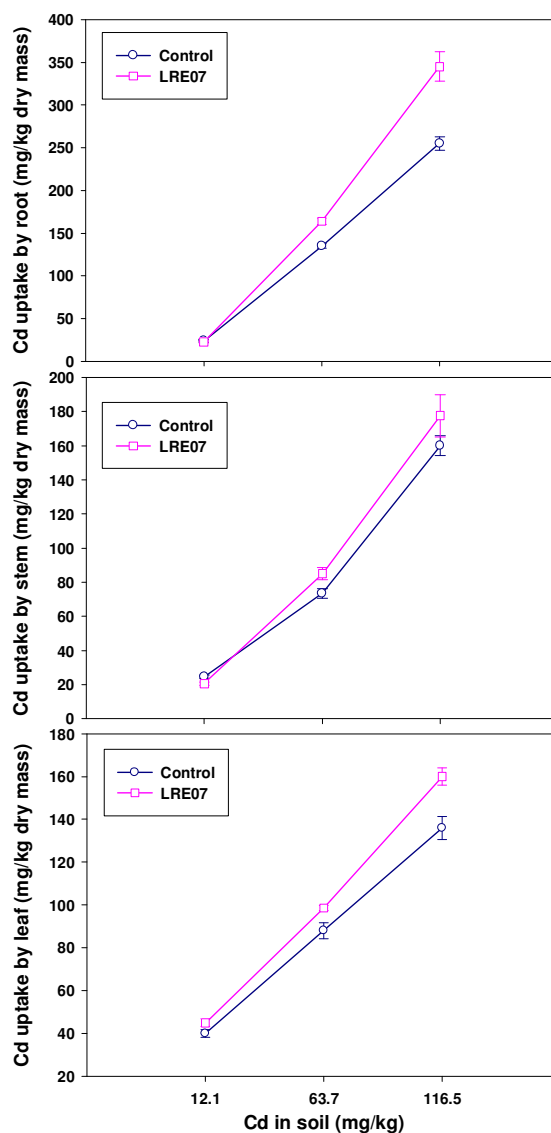
**FIGURE 2** Effects of inoculation with LRE07 on Cd concentration (mg/kg) in the root (a), stem (b) and leaf (c) of *S. nigrum* L. Error bars represent standard deviation (n = 3).

**REFERENCES**

Dell'Amico, E., L. Cavalca, and V. Andreoni, 2008. "Improvement of *Brassica napus* growth under cadmium stress by cadmium-resistant rhizobacteria". *Soil. Biol. Biochem.* 40: 74-78.

Hardoim, P.R., L.S. van Overbeek, and J.D. van Elsas. 2008. "Properties of bacterial endophytes and their proposed role in plant growth". *Trends. Microbiol.* 16: 467-471.

Lebeau, T., A. Braud, and K. Jézéquel. 2008. "Performance of bioaugmentation-assisted phytoextraction

applied to metal contaminated soils: A review". *Environ. Pollut.* 153: 497-522.

Idris, R., R. Trifonova, M. Puschenreiter, W.W. Wenzel, and A. Sessitsch. 2004. "Bacterial communities associated with flowering plants of the Ni hyperaccumulator *Thlaspi goesingense*". *Appl. Environ. Microb.* 70: 2667-2677.

Ma, Y., M. Rajkumar, Y.M. Luo, and H. Freitas. 2011. "Inoculation of endophytic bacteria on host and non-host plants-Effects on plant growth and Ni uptake. *J. Hazard. Mat.* 195: 230-237.

Penrose, D.M., and Glick, B.R., 2003. Methods for isolating and characterizing ACC deaminase-containing plant growth-promoting rhizobacteria. *Physiol. Plant* 118: 10-15.

Piotrowska-Seget, Z., M. Cycon, and J. Kozdrój. 2005. "Metal-tolerant bacteria occurring in heavily polluted soil and mine spoil". *Appl. Soil Ecol.* 28: 237-246.

Pilon-Smits, E. 2005. "Phytoremediation". *Annu. Rev. Plant Biol.* 56: 15-39.

Rajkumar, M., N. Ae, and H. Freitas. 2009. "Endophytic bacteria and their potential to enhance heavy metal phytoextraction". *Chemosphere* 77: 153-160.

Raskin, I., R.D. Smith, and D.E. Salt. 1997. "Phytoremediation of metals: using plants to remove pollutants from the environment". *Curr. Opin. Biotech.* 8: 221-226.

Sheng, X.F., J.J. Xia, C.Y. Jiang, L.Y. He, and M. Qian. 2008. "Characterization of heavy metal-resistant endophytic bacteria from rape (*Brassica napus*) roots and their potential in promoting the growth and lead accumulation of rape". *Environ. Pollut.* 156: 1164-1170.

Schwyn, B., and J.B. Neilands. 1987. "Universal chemical assay for detection and determination of siderophores". *Anal. Biochem.* 160: 47-56.

Sturz, A.V., B.R. Christie, and J., Nowak. 2000. "Bacterial endophytes: potential role in developing sustainable systems of crop production". *Crit. Rev. Plant Sci.* 19: 1-30.

Xiao X., S.L. Luo, G.M. Zeng, W.Z. Wei, Y. Wan, L. Chen, and H.J. Guo. 2010. "Biosorption of cadmium by endophytic fungus (EF) *Microsphaeropsis sp*. LSE10 isolated from cadmium hyperaccumulator *Solanum nigrum* L." *Bioresour. Technol.* 101: 1668-1674.

# PHYTOREMEDIATION AS BIOAVAILABLE CONTAMINANT STRIPPING TOOL: A CASE STUDY OF HG CONTAMINATED SOIL

*Meri Barbafieri*, Gianniantonio Petruzzelli, Luca Cassina, Francesca Pedron, Eliana Tassi, Virginia Giansoldati, Irene Rosellini

(National Research Council, Institute of Ecosystem Study, Section of Pisa, Via Moruzzi 1, Pisa, Italy)

**ABSTRACT:** The Bioavailable Contaminant Stripping (BCS) efficiency was evaluated analyzing the labile-Hg residue in the soil after the plants growing. Combined treatments with a plant hormone (cytokinine) and a thioligand (ammonium thiosulfate, TS) to strengthen Hg uptake by two crop plants (*Brassica juncea* and *Helianthus annuus*) were tested. Plant biomass, evapotranspiration, Hg uptake and distribution following treatments were compared. Results indicate the plant hormone foliar treatment, increased the evapotranspiration rate in both tested plants. The Hg uptake and translocation in both tested plants increased with simultaneous addition of CK and TS. *B. juncea* was the most effective in Hg uptake; application of CK to plants grown in TS-treated soil led to an increase in Hg concentration of 232% in shoots and 39% in roots with respect to control. *H. annuus* gave a better response in plant biomass production and the application of CK to plants grown in TS-treated soil led to an increase in Hg concentration of 248% in shoots and 185% in roots with respect to control plants. Plants grown with CK and TS in one growing cycle significantly affected labile-Hg pools in soil characterized by sequential extraction, but did not significantly reduce the pseudototal metal concentration in the soil.

## INTRODUCTION

Phytoremediation is a broad term that comprises several technologies to clean up water and soil. Despite the numerous articles appearing in scientific journals, very few field applications of phytoextraction have been successfully realized. To overcome the imbalance between the technology's potential and its drawbacks, there is growing interest in the use of plants to reduce only the fraction that is the most hazardous to the environment and human health, that is to target the bioavailable fractions of metals in soil.

Bioavailable Contaminant Stripping (BCS) would be a remediation approach focused to remove the bioavailable metal fractions. In this study, BCS has been used in a mercury contaminated soil from an Italian industrial site. Soil samples polluted by mercury from a petrochemical plant in southern Italy were used to test the hypothesis that cytokinine (CK) application could alleviate Hg phytotoxicity symptoms and increase Hg uptake and translocation.

In previous studies we observed an increase in transpiration rate of about 40% in H. annuus plants (Tassi et al. 2008) and of 58% in the Ni hyperaccumulator Alyssum murale plants (Cassina et.al 2011) after the application of CKs to leaves of plants growing in heavy metal-contaminated soil. Recently, Zhao et al. 2011, showed the effectiveness of exogenous kinetin in increasing stress tolerance to Cr toxicity and Cr uptake and translocation from roots to shoots of Mexican Palo Verde plants.

To check this hypothesis, we conducted a semi-closed system with low soil quantity (microcosm, MC) growing two crop plants (*Helianthus annuus* and *Brassica juncea*), selected for their rapid growth, high biomass production and adaption to the Mediterranean area. We combined the assisted phytoextraction using ammonium thiosulfate (TS) as soil amendment and exogenous CK spraying on leaves. The experimental scale and the controlled conditions of growth allowed us to better quantify the dynamics of metal solubilization and plant uptake, which could be less evident in field tests due to the heterogeneity of soil contamination.

## MATERIALS AND METHODS

**Soil Sampling:** The soil samples were collected in a contaminated industrial area (petrochemical plant) located near Brindisi, in southeastern Italy. All soil samples were collected from the top layer (0-20 cm), air-dried at room temperature to constant weight, and well-mixed to homogenize possible different levels of Hg contamination. The soil was sieved in two separated size-classes: 2 mm for laboratory analysis and 5 mm for microcosm setup. Soil samples for Hg analysis were further ground into finer particles (< 1 mm) in an agate mortar. Soil pH, cation exchange capacity (CEC), particle size analysis (sand, silt and clay percentages), organic matter (OM) and macro-nutrient concentrations were determined according to procedures in Methods in Soil Analysis (1996). The soil collected had a pH (H2O) value of 7.9 and a CEC of 20.6 meq 100 g-1. The OM and total N concentration (%) were 1.6 and 0.06, respectively, whereas the available P and K concentrations (mg kg-1) were 11.3 and 193, respectively. According to percentages of sand (66.9%), silt (14.1%) and clay (19.0%) of the matrix collected, it could be classified as a sandy loam soil (USDA classification). Total Hg concentration in the replicated microcosms was $16.4 \pm 1.1$ mg kg-1.

**Microcosm Experiment:** Microcosms were set up in 250 mL capacity beakers filled with 200 g of contaminated soil. A total of 24 microcosms was prepared where one half was sown with *Helianthus annuus* cv. Paola (4 seeds per microcosm) and the other half with *Brassica juncea* cv. Scala (0.3 g of seeds per microcosm). Four groups of microcosms per species were set up: a control group (no treatment in soil or plants), a group with CK treatment in leaves, a group with TS addition in soil and a group with both treatments CK and TS. Plants were grown in controlled light exposure (approximately 12 h of light a day), temperature ($22 \pm 2$ °C) and humidity (70%) in a growth chamber. Microcosms were watered daily with deionized water. Cytokinin treatments in plants were performed using the commercial product CYTOKIN consisting of a mix of three different vegetal CKs (Miller Chemical & Fertilizer Corporation, Hanover, PA, USA). *H. annuus* and *B. juncea* were treated with diluted product at a rate of 20 mg kg-1 of CKs; foliar applications started 34 days after plant germination and were performed three times at 5-day intervals each, spraying both the adaxial and the abaxial surfaces of leaves [Tassi et al 2008]. Soil treatments were carried out adding 2 mL of 0.27 M TS solution for 5 consecutive days, starting from the day after the first foliar treatment.

**Plant and Soil Analysis of Hg:** *B. juncea* and *H. annuus* plants were harvested 50 days after seed germination. vegetal samples were oven-dried at 40 °C to constant weight and ground into fine particles for Hg analysis. In soil, mercury bioavailable fractions (nominally water soluble- and exchangeable fraction) were determined by a two-steps sequential extraction procedure according to Millán et al. [2006]. Briefly, 0.5 g of soil were suspended in 25.0 mL of deionized water and constantly shaken for 1 h. The supernatant was separated from soil after centrifugation at 15,000 rpm for 15 min. The residue was resuspended in 25.0 mL of 1 M NH4Cl, shaken for 1 h and then centrifuged at 15,000 rpm for 15 min. Samples of plant tissues, soil and soil extracts were analyzed for Hg concentration using an Atomic Absorption Spectrophotometer with an Automatic solid/liquid Mercury Analyzer AMA 254 (FKV, Bergamo, Italy), without any further sample preparation.

**TABLE 1. Shoots plant biomass, Hg content and Hg phytoextracted in plants grown in microcosm trials.**

| | *Plants* | **Ctr** | **CK** | **TS** | **CK+TS** |
|---|---|---|---|---|---|
| **Biomass (g MC⁻¹)** | *H. annuus* | 0.49a | 0.63b | 0.63b | 0.75b |
| | *B. juncea* | 0.36a | 0.37a | 0.35a | 0.39a |
| **Hg concentration (mg kg⁻¹)** | *H. annuus* | 1.55b | 0.74a | 2.90c | 5.41d |
| | *B. juncea* | 3.28b | 2.76a | 7.90c | 10.89d |
| **Hg phytoextracted (µg MC⁻¹)** | *H. annuus* | 0.76b | 0.47a | 1.84c | 4.08d |
| | *B. juncea* | 1.18a | 1.03a | 2.74b | 4.30c |

## RESULTS AND DISCUSSION

**Effect of treatment on Hg phytoextraction.** The amount of Hg phytoextracted was calculated as the product of biomass yield and Hg concentration in plant tissues (Table 1).

*Helianthus annuus* grown in TS-treated soil showed an increase in phytoextracted Hg, 142% and 165% higher than control in shoots and roots, respectively. The amount of Hg phytoextracted was even higher when both treatments (CK and TS) were performed, showing an increase of 435% and 324% of the Hg extracted by shoots and roots, respectively. CK-treated plants showed a decrease in phytoextracted Hg (38% in shoots and 52% in roots) compared to control plants.

In *Brassica juncea*, considering the above-ground tissues, phytoextracted Hg increased by 132% in TS-treated soil and by 264% in (CK + TS) treatments, compared to control plants. CK-treated plants did not differ significantly from control plants and no difference in Hg phytoextracted in roots was observed with all the treatments.

These data show a significant tendency to have higher phytoextraction values in the combined treatment (CK + TS).

**Effects of treatments on BCS** Table 2 shows the extractable Hg concentrations in soil after plant harvest. The pattern is similar in both plants (*B. juncea* and *H. annuus*) for all treatments. CK-treatment alone did not produce any difference in the residual Hg extractable fraction compared to control microcosms. The addition of TS decreased the extractable Hg by an order of magnitude, mainly in the water-soluble fraction. These results reflect the extraction of Hg from soil by plants able to reduce the fraction of Hg present in soil water extraction, i.e., the Hg-TS soluble complexes. The simultaneous treatments (CK + TS) resulted in a 33% and 45% lower extractable fraction in *H. annuus* and *B. juncea* respectively, with respect to TS-treated soil. The reduction of extractable Hg was in agreement with the increase of Hg phytoextracted in TS and (CK + TS).

**TABLE 2. Extractable Hg in soils after microcosm trials of different treatments.**

| | | Extractable Hg ($\mu$g kg$^{-1}$) | | |
| --- | --- | --- | --- | --- |
| | | H$_2$O | NH$_4$Cl | Total extractable |
| *H. annuus* | Ctr | 59.6 d | 3.9 ab | 63.5 c |
| | CK | 65.1 c | 3.8 a | 68.9 c |
| | TS | 7.6 b | 4.0 bc | 11.7 b |
| | CK+TS | 5.1 a | 4.1 c | 9.2 a |
| *B. juncea* | Ctr | 56.1 c | 4.5 c | 60.6 c |
| | CK | 57.1 c | 4.4 c | 61.2 1 c |
| | TS | 7.7 b | 3.4 b | 11.1 b |
| | CK+TS | 4.2 2 a | 3.0 a | 7.2 a |

We then calculated the amount of Hg phytoavailable in soil (HgPA-S, $\mu$g) as the sum of the total extractable Hg in the soil (HgTE-S, $\mu$g) after plant harvest (Table 2) and Hg extracted by plants (HgPHY, $\mu$g) (Table 1) in the four different groups of microcosms for both plants as shown in the following equation:

$$HgPA\text{-}S = (HgTE\text{-}S \cdot 0.2) + HgPHY$$

where the factor 0.2 is a multiplier to obtain the amount of total extractable Hg ($\mu$g) in each microcosm (200 g of soil).

Comparing the values obtained for HgPA-S (data not shown) it was not possible to observe any significant difference (p = 0.05) between the four different groups for each plant. This comparison indicates that the sum of HgTE-S and HgPHY is constant and the plants grown in thiosulfate-treated soil thus led to a reduction in total extractable Hg, i.e., a reduction in residual phytoavailable Hg. This reduction is even more marked in the combination treatment (CK + TS).

We can therefore hypothesize that no significant loss of volatile Hg via the plants occurred, in agreement with previous studies on other crop plants (Greger et al. 2005) and TS as Hg-mobilizing agent (Moreno et al. 2005). Our experimentation also indirectly supports the hypothesis that CKs have no influence on Hg volatilization process.

**CONCLUSIONS**

This study demonstrates that plants grown with CK and TS in one growing cycle significantly affected labile-Hg pools in soil characterized by sequential extraction. Moreover, if properly optimized, the use of a coupled phytohormone/thioligand system may be a viable strategy to strengthen Hg uptake by crop plants.

**REFERENCES**

Cassina L., Tassi E., Morelli E., Giorgetti L. , Remorini D., Chaney R. L. and Barbafieri M.. 2011. "Exogenous cytokinin treatments of a Ni Hyper-Accumulator, Alyssum murale, grown in a serpentine soil: implications for phytoextraction". *Int. J. Phytoremediat*. 13 90-101.

Greger, M., Wang, Y., and Neuschutz, C. 2005. "Absence of Hg transpiration by shoots after Hg uptake by roots of six terrestrial plant species. " *Environ. Pollut.* 134: 201-208.

Millán, R., Gamarra, R., Schmid, T., Sierra, M.J. , Quejido, A.J., Sánchez, D.M., Cardona, A.I., Fernández, M., and Vera, R. 2006. "Mercury content in vegetation and soils of the Almadén minig area (Spain)." *Sci. Total Environ.* 368:79-87.

Moreno, F.N., Anderson, C.W.N., Stewart, R.B., Robinson, B.H., Ghomshei, M., and Meech, J.A. 2005. "Induced plant uptake and transport of mercury in the presence of sulphur-containing ligands and humic acid." *New Phytologist* 166:445-454.

Tassi, E., Pouget, J., Petruzzelli, G., and Barbafieri, M. 2008. "The effects of exogenous plant growth regulators in the phytoextraction of heavy metals." *Chemosphere* 71: 66-73.

SSSA Book Series, 1996. *Methods of soil Analysis – Part 3* – Chemical Methods, Soil Science Society of America, Inc., D.L. Sparks (Ed.), Madison, USA.

Zhao Y., Peralta-Videa J.R., Lopez-Moreno M.L, Ren M., Saupe G., Gardea-Torresdey J.L. 2011. "Kinetin increases chromium absorption, modulates its distribution, and changes the activity of catalase and ascorbate peroxidise in Mexican Palo Verde." *Environ. Sci. Technol.* 45:1082-1087.

# DO RHIZOSPHERIC PROCESSES LINKED TO PHOSPHORUS NUTRITION PARTICIPATE TO SOIL URANIUM PHYTOAVAILABILITY?

*Antoine Tailliez* and Pascale Henner (IRSN, St Paul lez Durance, FRANCE)
Catherine Keller (CEREGE, Aix en Provence, FRANCE)

Our research focuses on uranium (U) phytoavailability at the soil - plant interface. Solubilization processes in soils are of major interest in the understanding of phytoavailability mechanisms. Modification of rhizospheric soil conditions by root activity, often linked with plant nutrition, is expected to be one of the probable mechanisms that govern U soil phytoavailability, through enhancement of solubilization processes. In this study, we tested to what extent the modifications in rhizospheric soil solution chemistry would lead to influence U available concentrations (i.e. U effective uptake by plants). In this purpose, we chose the white lupine (*Lupinus albus cv. amiga*) as a model species for its peculiar physiological response to low phosphorus (P) conditions. It exudates huge amounts of citrate during P starvation via specifically induced roots called proteoid roots, to solubilise and acquire P. As U is often associated to P-bearing phases in soil and since citrate is a strong U chelator, then varying P-controlled lupine physiology should also vary U uptake capacity.

The behaviour of white lupine was characterized under different hydroponically controlled P and U regimes, so as to evaluate the effect of U on lupine metabolism (root growth, proteoid root induction, exudation) and consequences on U accumulation in plants roots and shoots. We combined U exposure (0 or 20 µM) and inorganic P nutrition (1 or 100 µM for Pi-deficient and Pi-sufficient) during 15 or 30 days after proteoid roots apparition to measure phenotypic traits and U accumulation, to collect roots exudates and to study the repartition of accumulated U in the plants. The pH of the nutrient solution was not buffered since exudation is linked with variations of rhizospheric pH. We also observed ultra-thin plastic root sections using Transmission Electron Microscopy coupled to an Energy-Dispersive X-ray (TEM-EDX) on root sections to localize internalized U and visualize cell damage. All results were compared to control plants (100 µM P and 0 µM U).

During P starvation (1 µM), we observed important effects of U on development: the production of biomass and the number of leaves decreased significantly whereas number of proteoid roots increased. Citrate exudation was strongly impacted and root development was anarchic. TEM-EDX analysis revealed the presence of U precipitates (mainly associated with K) in numerous cells of the cortex. The precipitates were observed both in the cytoplasm and the apoplasm, at least in the first 5 cells layers. Furthermore, we observed numerous damaged cells.

The same exposure with proper P nutrition hardly affected the integrity of white lupine: development was similar to control conditions and a lower U accumulation was recorded in the roots. Citrate exudation was higher than in controls, as expected despite a slight increase in the number of proteoid roots. TEM-EDX analysis showed that U was mainly associated with K, P and Ca outside the root surface. U was sometimes found in the apoplasm of the first cortical cell layer.

The simulation of U chemical speciation in the nutrient solution using specialized software (CHESS software with an updated thermodynamic database for U) was consistent with our observations. In the presence of P, the formation of low soluble U-P complexes may limit the availability of U for root uptake which consequently limits toxic effects. The colocalization of U and P outside the cell combined with the lower effects observed suggest that those chemical forms are less harmful than free U in solution during P starvation. These results support the importance of the identification of available forms of U in an environment to understand its toxicity. Our study addresses the question of whether exudation will finally favour (by solubilizing solid phases) or limit (by formation of secondary non available forms in soil solution) U transfer. Additional soil experiments designed for bioavailability issues would be of a great interest to test these hypotheses in more realistic conditions.

# CHLORINATED
# AND
# OTHER PERSISTENT ORGANIC COMPOUNDS

# A SIMPLE AND CONVENIENT DECHLORINATION OF PCDD/Fs IN SOIL USING NANO-SIZE CALCIUM DISPERSING AGENT

*Yoshiharu Mitoma,* Shogo Sakita and Srinivasa Reddy Mallampati (Department of Environmental Sciences, Faculty of Life and Environmental Sciences, Prefectural University of Hiroshima, Shobara City, Hiroshima, Japan)

Tetsuji Okuda (Environmental Research and Management Center, Hiroshima University, Higashi-Hiroshima, Hiroshima, JAPAN)

**ABSTRACT:** A new process for chemical degradation of 7 PCDDs and 10 PCDFs for practicable disposal of dioxins under mild conditions, using nano-size metallic calcium in dispersing CaO under atmospheric condition at room temperature was investigated. We found that the dechlorination of dioxins recorded good efficiencies from 61.4 to 99.0% under atmospheric conditions at room temperature, in solid state with nano-size metallic calcium in calcium oxide dispersing agent without mechanochemical treatment such as planetary ball milling processes. Further, the good efficiencies have been retained when using three different decomposed granite, clay, and field soil.

## INTRODUCTION

Substantial soil pollution caused by persistent organic pollutants (POPs) has emerged as a serious issue in various regions of Japan (Ministry of Environment Government of Japan, 2002). In japan, the soil contamination countermeasures act went into effect in February 2003, with the purpose of preventing adverse effects on public health caused by soil contaminated with toxic substances (Ministry of Environment Government of Japan, 2002). POPs contaminated soil are notoriously hard to remediate and its remediation is recognized to be one of the most difficult problems to be solved even with the use of suitable technologies. The dechlorination processes are widely investigated class of chemical reactions with direct application in depollution treatments of various contaminated substrates with harmful chemicals such as polychlorodibenzodioxins (PCDDs), polychlorodibenzofurans (PCDFs), or polychlorobiphenyls (PCBs) (Miyoshi et al., 2004; Ukisu and Miyadera, 2003; Knox, 2005; Kawai, 2005). The past few years saw, along with the development of the classic types of activation for carbon-chlorine bond (chemical (Miyoshi et al., 2004; Ukisu and Miyadera, 2003), thermal (Knox, 2005), or photochemical (Kawai, 2005)), one of useful applications of mankind's oldest technology, a new type grinding, in what came to be known as mechanochemical processes. In the dechlorination field, these new activation-type methods started to make their own little niche, becoming the mechanochemical dechlorination processes (MDP) (Monagheddu et al., 1999; Mitoma, 2011). These are a series of procedures that are using, along with the contaminated substrate, a dechlorination additive, both being introduced in a planetary ball mill. Among calcium species used in such MDP, the preferred reagent is by far CaO, but $Ca(OH)_2$, $CaCO_3$ or $CaH_2$ were also used. Unfortunately, those methods present unfavorable aspects of low degradation rates and low efficiency. Our goal is to reduce energy consumption for dechlorination of dioxins to the conventional technology involving heating process while maintaining the same processing efficiency. Therefore, in the present work, the use of nano-metallic Ca and CaO dispersion mixture toward decomposition of PCDDs and PCDFs in three different (decomposed granite, clay and field soil) was investigated under mild conditions (simple grinding) at room temperature.

## MATERIALS AND METHODS

**General experimental conditions:** In a typical experiments, three different decomposed granite (DG) soil (0~10% moisture, 0.52% organic substances), clay (ORS) soil (18% moisture, 4.5% organic substances) and field (KSO) soil (18% moisture, 17% organic substances) samples are used. Nano-metallic Ca/CaO (dry system) was prepared with metallic Ca and CaO through planetary ball milling

process. Granular particles of metallic calcium were purchased from Kishida Chemicals (99%, particle size distribution: 1.0-2.5 mm, surface area: 0.43–0.48 $m^2$/g). Fine grade CaO was also commercially obtained with 98 % purity from Kishida Chemicals. Metallic Ca and dry (825°C for 2h) CaO composition Ca/CaO of 2/5 were introduced in the planetary ball mill (Retsch PM-100; 20 pieces SUS, 32g/ball) at room temperature, under Ar atmosphere. Stirring was carried out at 600 rpm to a rotation-to-revolution ratio of 1:2. Stirried samples were collected in glass bottles, filled with Ar gas and stored to be used in the succeeding treatment experiments. Mixture of nano particle metallic calcium in CaO (2.80 mmol of metallic Ca/g-mixture) and average particle size of nano-metallic Ca/CaO was 206 nm. PCDDs and PCDFs contaminated soil was prepared with standatd solutions; ten gram of polluted decomposed granite soil showed average PCDDs and PCDFs concentration of 19,000 and 23,100 pg⁻TEQ respectively.

PCDDs and PCDFs contaminated individual (DG, ORS and KSO) soil and nano-metallic Ca/CaO (10:1) were grinded into a ceramic mortar at 100 rpm for 24 hr at room temperature. After treatment the reacted mixture was poured into 1 M nitric acid and extracted twice-using dichloromethane under vigorous shaking. The separation from the aqueous layer, the combined organic phases were washed with distilled water until the pH of the aqueous layer became neutral. The dichloromethane layer was dried on anhydrous $MgSO_4$, then filtered and concentrated to 10 ml. PCDDs and PCDFs determination were performed according to Japanese Industrial Standard (JIS) methods (JIS, 1999). PCDDs and PCDFs analysis was performed by a gas chromatograph (GC-17A; Shimadzu Co.) equipped with a 60 m BPX-5 (i.d. 0.25 mm, 0.25 µm film thickness) (SGE) and QP-5000 series (Shimadzu Co.). These experiments were repeated for three times and the results obtained were similar.

## RESULTS AND DISCUSSION

**Decomposition treatment for PCDDs and PCDFs in soil with nano-metallic Ca/CaO:** Initially, PCDDs and PCDFs contaminated decomposed granite soil was grinded with nanno-metallic Ca/CaO for 24hr. As presented in Table 1, after treatment PCDDs concentration in 0% moisture soil, reduced from 19,600 to 1,660 pg. On the other hand, PCDFs concentration, reduced forms 23,100 to 227 pg. This value corresponds to intrinsic decomposition efficiencies of 99%. The decomposition of PCDDs/PCDFs is sensitive to moisture content, since its efficiency decreases along with the increase in soil moisture (Figure 1).

Table 1. Dechlorination of PCDDs and PCDFs in soil using a nano-metallic Ca/CaO aystem at room temperature.

| Entry | Polluted source | Conditions[1] | | Initial Quantity in 10g soil (pg) | Final total quanity (pg) |
|---|---|---|---|---|---|
| | | Grinding | Moisture (%) | | |
| 1 | PCDDs | Mortar[2] | 0 | 19,600 | 1,660[3] |
| 2 | | | 0 | | 227 |
| 3 | PCDFs | Mortar | 4.36 | 23,100 | 5,930 |
| 4 | | | 9.61 | | 8,920 |

[1]1.12 wt% of metallic Ca in mixture of Ca/CaO and polluted soil, [2]Mortar-typed mill at 100 rpm for 24hr, [3]Initial polluted soil : Ca/CaO = 10g : 1g.

Further, in order to check the treatment efficiency at different soil conditions, PCDDs/PCDFs contaminated clay (ORS) and field (KSO) soil were grinded with addition of different nano-metallic Ca and CaO compositions. The experimental results as shown in Figures 2, with 6 and 8 g of CaO addition during grinding, PCDDs/PCDFs concentrations for the treatment of KSO soil decreased from 2,400pg⁻TEQ to 847 and 675 pg⁻TEQ respectively. Instead, the efficincy for ORS decreased in the addition of 8g CaO. It shows the decrease of collision number between nano-metallic Ca and small particles of soil. When the input of same rate of metallic Ca to CaO was added in to the bottle, the efficiency recovered. Similarly, as shown in Figure 3, at 1 g of nano-metallic Ca (4g CaO) showed the better PCDDs/PCDFs decomposition. In addition, higher PCDDs/PCDFs efficiency by preliminary drying of soil was observed (0% moisture). The use of excess metallic Ca as a drying agent was effective for the reduction of PCDDs/PCDFs. The decomposition of PCDDs/PCDFs is sensitive to moisture content, since its

efficiency decreases along with the increase in moisture.
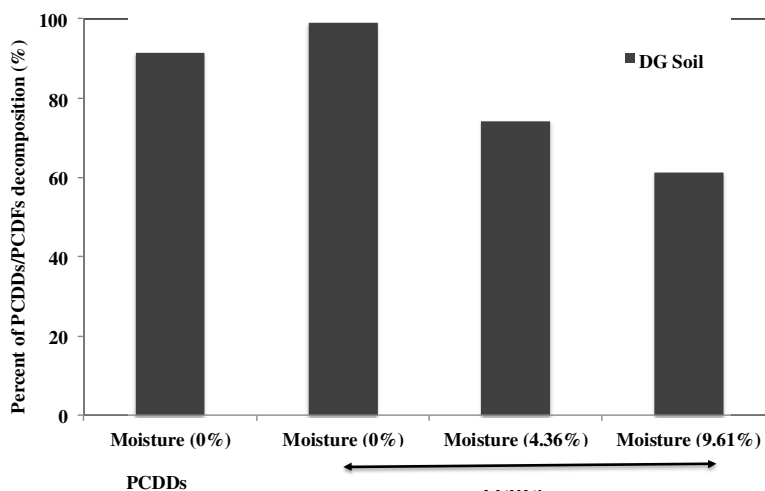


**FIGURE1.** Dechlorination efficiency of PCDDs/PCDFs in DG soil (different moisture contents) using with nano-metallic Ca/CaO.
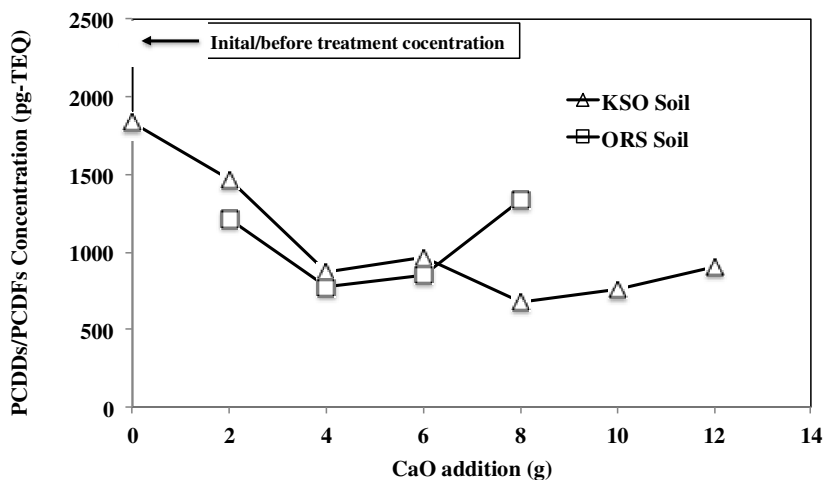


**FIGURE2.** PCDDs/PCDFs concentration in contaminated ORS and KSO soil with different CaO composition treatment (nano-metallic Ca 1 g).

## CONCLUSIONS

In the present work, a new process for chemical degradation of PCDDs and PCDFs for practicable disposal of dioxins under mild conditions, using nano-size metallic calcium in dispersing CaO under atmospheric condition at room temperature was investigated. We found that the dechlorination of dioxins in different soils recorded good efficiencies from 61.4 to 99.0% under atmospheric conditions at room temperature, in solid state with nano-size metallic calcium in calcium oxide dispersing agent without mechanochemical treatment such as planetary ball milling processes. The dechlorination treatment process does not require external heating, organic solvents, fancy catalysts or expensive reagents, and it does not generate exhaust gases. On the contrary, it only requires water, electricity and commercially available cheap reagents. Therefore, this treatment process is considered to be an environmental friendly depolluting technique.
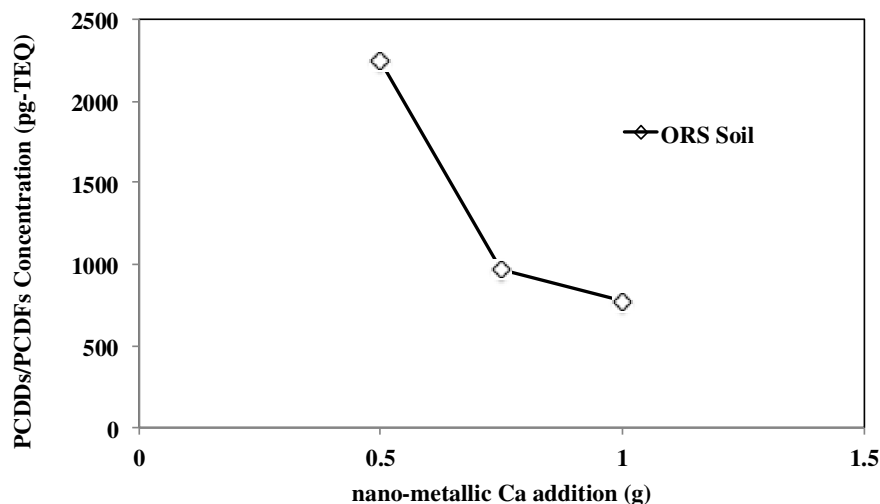
**FIGURE3.** PCDDs/PCDFs concentration in contaminated ORS soil with different nano-metallic Ca composition (CaO 4 g).

## ACKNOWLEDGEMENTS

## REFERENCES

JIS K 0312-1999, *Measuring method of dioxins and coplanar PCBs in industrial water and industrial liquid waste*; Japanese Industrial Standards Committee: Tokyo, 1999.

Kawai, T. 2005. Decontamination and detoxification technologies for persistent organic pollutants. *Kobelco Eco-solutions Engineering Reports* 1: 28–38.

Ministry of the Environment, Government of Japan, 2001. "*Law Concerning Special Measures for Promotion of Proper Treatment of PCB Wastes*".

Ministry of Environment, Government of Japan, 2002. "*Soil Contamination Countermeasures Law Enforcement Regulation*", Ordinance No. 29, Tokyo.

Mitoma Y., H. Miyata, N. Egashira, A. Simion, M. Kakeda, C. Simion. 2011. "Mechanochemical degradation of chlorinated contaminants in fly ash with a calcium-based degradation reagent". *Chemosphere* 83: 1326–1330.

Monagheddu M., G. Mulas, S. Doppiu, G. Cocco, S. Racanelli. 1999. "The reduction of polychlorinated dibenzo-dioxins and dibenzofurans in contaminated muds by mechanically induced combustion reactions". *Environ. Sci. Technol.* 33, 2485–2488.

Miyoshi, K., T. Nishio, A. Yasuhara, M. Morita, T. Shibamoto. 2004. "Detoxification of hexachlorobenzene by dechlorination with potassium–sodium alloy". *Chemosphere,* 55, 1439–1446.

Ukisu, Y., S. Kameoka, T. Miyadera. 1998. Rh-based catalysts for catalytic dechlorination of aromatic chlorides at ambient temperature. *Applied Cat. B* 18, 273–279.

Knox, A. 2005. *Overview of incineration, An overview of incineration and EFW technology as applied to the management of municipal solid waste (MSW).* University of Western Ontario.

# OZONATION OF TERTIARY TREATED MUNICIPAL WASTEWATER FOR THE REMOVAL OF PERSISTENT ORGANIC POLLUTANTS - RESULTS AND TOXICOLOGICAL EVALUATION

*Norbert Kreuzinger* and Heidemarie Schaar
(Vienna University of Technology, Vienna, AUT)

**ABSTRACT:** The case study presented in this paper investigates the removal potential of  activated sludge based wastewater treatmentprocesses with different sludge retention times and a subsequent ozonation step at a municipal wastewater treatment plant (4,000,000 p.e). In a first step the removal performance of the former high loaded full scale plant (C removal only) was monitored. Later on, the plant was upgraded to a low loaded nitrogen removal (nitrification & denitrification) plant. A new assessment of the removal capacity showed a significant increase of the removal capacity for pollutants such as bisphenol-A, 17α-ethinylestradiol and the antibiotics erythromycin and roxithromycin that were only removed after the upgrade of the WWTP. Nevertheless, a number of organic pollutants were not removed. Thus, a pilot scale ozonation plant ($O_3$ production capacity of 1,000 g/h) was installed for additional treatment of the effluent. The application of $0.6 – 0.9$ g $O_3$ g $DOC_0^{-1}$ increased the removal of most of the pollutants, especially for compounds that were not degraded in the previous biological process, as for example carbamazepine and diclofenac. Additionally, standardized ecotoxicity tests were applied to assess the toxicity of the tertiary treated wastewater before and after ozonation for green algae, daphnids, and fish eggs. Endocrine and general health effects on fish were tested using a OECD 21-day fish assay. Enzyme immunoassays considering both unconjugated estrogenic (E-Assay) and androgenic (T-Assay) activity were applied as well as three different standardized mutagenity tests (Salmonella/microsome assay; SCGE - comet assay, Allium cepa micronucleus test).

## INTRODUCTION

The application of BAT (best available technology: nitrification and denitrification) in wastewater treatment does not provide complete elimination of micropollutants and subsequently, residues of the above mentioned substances enter the aquatic ecosystem. Several technologies for further micropollutant removal from wastewater such as ozonation (Huber et al., 2005), advanced oxidation (Huber et al., 2003), activated carbon (Westerhoff et al., 2005) and filtration (Poseidon, 2004) have been investigated and proved to be able to further remove PPCPs and EDCs. Especially the application of ozone is expected to be a suitable technology for the removal of micropollutants in laboratory, pilot and full scale experiments (Ternes et al., 2003; Poseidon, 2004; Bahr et al., 2005; Huber et al, 2005, Bahr et al., 2007, Nakada et al., 2007; Hollender et al., 2009). On the other hand it has been postulated that ozonation of waters may cause adverse effects in the environment (Paraskeva and Graham, 2002; Stalter et al., 2010) and it was also reported in a few studies that it may increase the genotoxic activity of waters (for reviews see Noot et al., 1989; Paraskeva and Graham, 2002).

The presented paper summarizes the impact of the sludge retention time on the removal of organic pollutants by comparing removal rates before and after the upgrade of a full scale municipal wastewater treatment plant for 4,000,000 population equivalent (p.e.) from a high loaded C-removal only towards a low loaded plat with full nitrification and denitrification. Additionally the potential of a subsequent post treatment step by ozonation is presented as well as results from toxicological investigations.

**MATERIAL AND METHODS**

**Full scale wastewater treatment plant:** Experiments were conducted at the location of a two-stage activated sludge plant in Austria being upgraded from a high loaded WWTP with carbon removal only to a low loaded, nutrient removing WWTP in 2005. 80 % of the incoming wastewater is collected by a combined sewer system and 20 % by a separate sewer system. Solids retention time normalized to 10°C ($SRT_{10°C}$), hydraulic retention time (HRT) and the food to microorganism ratio (F/M) before (high loaded) and after the plant upgrade (low loaded) are listed in Table 1. In Table 2 typical effluent concentrations for carbon (COD, BOD), nitrogen (Total Nitrogen TN, Ammonia Nitrogen $NH_4$-N, Nitrate Nitrogen $NO_3$-N) and phosphorus (Total Phosphorous TP) are given for two operation conditions.

**TABLE 1**: Characteristics of the investigated WWTP before and after the upgrade

|  | $SRT_{10°C}$ (d) | HRT (h) | F/M (g COD gTSS$^{-1}$d$^{-1}$)* |
|---|---|---|---|
| high loaded | 2 | 2 | 1.7 |
| low loaded | 17* | 22 | 0.15-0.2 |

**TABLE 2:** Typical effluent characteristics at the WWTP before and after the upgrade

|  | COD (mg L$^{-1}$) | BOD (mg L$^{-1}$) | TN (mg L$^{-1}$) | $NH_4$-N (mg L$^{-1}$) | $NO_3$-N (mg L$^{-1}$) | TP (mg L$^{-1}$) |
|---|---|---|---|---|---|---|
| high loaded | 139 | 49 | 33 | 27 | 2.3 | 0.9 |
| low loaded | 34 | 4 | 9.8 | 0.6 | 6.9 | 0.9 |

**Ozonation pilot plant:** The pilot plant situated at the location of the then low loaded plant included an ozone generator (Wedeco, type SOM 7) with a production capacity of 1,000 g h$^{-1}$ and a 2,670 m$^3$ storage tank for liquid oxygen for the feed gas supply (Messer Austria). The reactor unit consisted of two cylindrical reactors with a working volume of 5 m$^3$ each. The two reactors were operated in series with the first reactor (R1) in downflow, counter current mode. Ozone was dosed to R1 via two fine bubble plate diffusers (Aquaconsult Anlagenbau). The diffuser plates were made of silicone and polyurethane, respectively, in order to test the stability of the material during ozonation. No ozone was supplied to the second reactor (R2) which acted as a decay unit operated in upflow mode.

The results on micropollutant removal during ozonation were obtained during three sampling campaigns. Ozone was dosed to the first reactor (R1) at a gas flow rate of 2.5 m$^3$ h$^{-1}$. The tested ozone concentration in the feed gas ranged between 86 and 153 g Nm$^{-3}$. The specific ozone consumption ($z_{spec}$, transferred ozone dose normalized to $DOC_0$) for the sampling campaigns ranged between 0.6 – 0.9 g $O_3$ g $DOC_0^{-1}$. Relevant parameters for the three campaigns such as the total HRT, temperature (T), the transferred ozone dose ($O_3$), the liquid ozone concentrations in the two reactors ($O_3$ R1, $O_3$ R2), the $DOC_0$ in the influent to the pilot plant (effluent of the low loaded WWTP) and a detailed description of the experimental setup can be obtained from Schaar et.al. 2010.

**Substances investigated:** A broad range of substances such as one antiepileptic (CBZ), one tranquilizer (DZP), two analgesics (DCF, IBP), one lipid regulator (BZF), four antibiotics (SMX, ROX, ERY, TMP), one iodated contrast media (IPM), seven endocrine disrupters (E1, EE2, BPA, NP, $NP_1EO$, $NP_2EO$, OP),two musk fragrances (HHCB, AHTN), five organotin compounds (DBT, TBT, DPT, and TPT), the pesticide DIU and two complexing agents (EDTA, NTA) were selected in this work. Substances and their abbreviation are summarized in table 3.

**Analytical Methods**: The chemical analyses of the selcected micropollutants were performed at the Austrian Umweltbundesamt GmbH. Unfiltered samples were analyzed. Details of the analytical methods can be found in Clara et al. (2005a, 2005b). Limits of detection (LOD) and limits of quantification (LOQ) for the individual substances are summarized in Schaar et.al. (2010).

**TABLE 3**: Analyzed compounds, CAS number, limit of detection (LOD) and quantification (LOQ)

| Substance | Abbr. | CAS No. | Substance | Abbr. | CAS No. |
|---|---|---|---|---|---|
| 17α-ethinylestradiol | EE2 | 57-63-6 | Galaxolide | HHCB | 1222-05-5 |
| Bezafibrate | BZF | 41859-67-0 | Ibuprofen | IBP | 15687-27-1 |
| Bisphenol-A | BPA | 80-05-7 | Iopromide | IPM | 73334-07-3 |
| Carbamazepine | CBZ | 298-46-4 | Nitrilotriacetic acid | NTA | 139-13-9 |
| Diazepam | DZP | 439-14-5 | Nonylphenol | NP | 25154-52-3 |
| Diclofenac | DCF | 15307-86-5 | Nonylphenol monoethoxylate | NP1EO | 104-35-8 |
| Di-n-butyltin | DBT | 1002-53-5 | Nonylphenoldiethoxylate | NP2EO | 20427-84-3 |
| Di-n-phenyltin | DPT | 1135-99-5 | Octylphenol | OP | 1806-26-4 |
| Diuron | DIU | 330-54-1 | Roxithromycin | ROX | 80214-83-1 |
| Erythromycin | ERY | 114-07-8 | Sulfamethoxazole | SMX | 723-46-6 |
| Estrone | E1 | 53-16-7 | Tonalide | AHTN | 1506-02-1 |
| Ethylenediaminetetra-acetic acid | EDTA | 60-00-4 | Trimethoprim | TMP | 738-70-5 |
| | | | Tri-n-butyltin | TBT | 56573-85-4 |

**Ecotoxicological tests:** Standardized biotests with green algae (DIN, 2004), daphnids (DIN, 1996), and zebrafish eggs (DIN, 2003) were employed to assess the aquatic ecotoxicity of the tertiary treated wastewater before and after ozonation. The microbioassays included Toxkit® MicroBioTests (Mariakerke, Belgium) with *Pseudokirchneriella subcapitata* (*Selenastrum capricornutum*, Algaltoxkit F) and *Daphnia magna* (Daphtoxkit F). Eggs for the fish egg test with *Danio rerio* were from a laboratory stock maintained at the Department of Biomedical Sciences of the Vetmeduni Vienna. Investigations on fish reproductive output, external morphology, histology and immunohistochemistry were conducted with the fish exposed to the OECD-21-day fish screening assay (see next chapter). A detailed description of the methodology can be found in Altmann et al. (2012).

**Endocrinology:** Endocrine effects in fish were analyzed following the OECD 21-day fish screening assay for estrogenic and androgenic activity, and aromatase inhibition (OECD, 2009). The fish treated in this study were 5-6 months old, sexually mature, male and spawning female wild-type Japanese medaka (*Oryzias latipes*). Competitive enzyme immunoassays (EIA) using biotin linked steroids as labels and streptavidin-peroxydase as detection system were performed to measure immunoreactive 17ß-hydroxyandrogens using testosterone as standard (Palme and Möstl, 1993) and immunoreactive unconjugated estrogens (estrone, 17ß-estradiol, 17α-ethinylestradiol and estriol, as described by Möstl et al. 1987) using estrone as standard. Because of the group specificity of the assays used the results have to be considered as estrone or testosterone equivalents. A detailed description of the methodology can be found at Altmann et al. (2012).

**Mutagenity tests:** Three different standardized mutagenity tests were investigated. The Salmonella/microsome assay is based on the detection of the induction of back mutations in different strains of Salmonella typhimurium which lead to histidine auxotrophy (Maron and Ames, 1984). The samples were tested with the three strains, namely TA98, TA100 and TA102 and the experiments were carried out as plate incorporation assays as described by Maron and Ames (1984), in presence and absence of metabolic activation mix. The SCGE - comet assay was carried out with primary rat liver cells. The impact of the samples on DNA migration was tested in single cell gel electrophoresis assay (SCGE, also known as "comet assay"). This technique is based on the detection of DNA migration in an electric field (Singh et al., 1988). The Allium cepa micronucleus (MN) is based on detection of clastogenic and aneugenic effect via formation of micronuclei in meristematic cells. In the present study the most widespread protocol of MN tests by Ma et al. (1995) was applied. A detailed description of the methodology can be found at Mišík et.al (2011).

## RESULTS AND DISCUSSION

**Removal of organic pollutants**: The results obtained during sampling campaigns before and after the upgrade of the investigated WWTP from carbon to nutrient removal emphasize the role of the sludge retention time (SRT) for the elimination of micropollutants. The degrees of removal for high and low loading conditions as well as for low loading conditions with a subsequent ozonation step at a specific ozone consumption of 0.6 g $O_3$ g $DOC_0^{-1}$ are shown in figure 1. The micropollutants are sorted according to the removal percentage under high loading conditions. The method of mass balance was used to determine the degree to which each micropollutant was removed by the biological treatment process. Details on the method are described in Clara et al. (2005b). The influent samples were flow proportional daily composite samples. Effluent samples and samples of the ozonation pilot plant were grab samples.
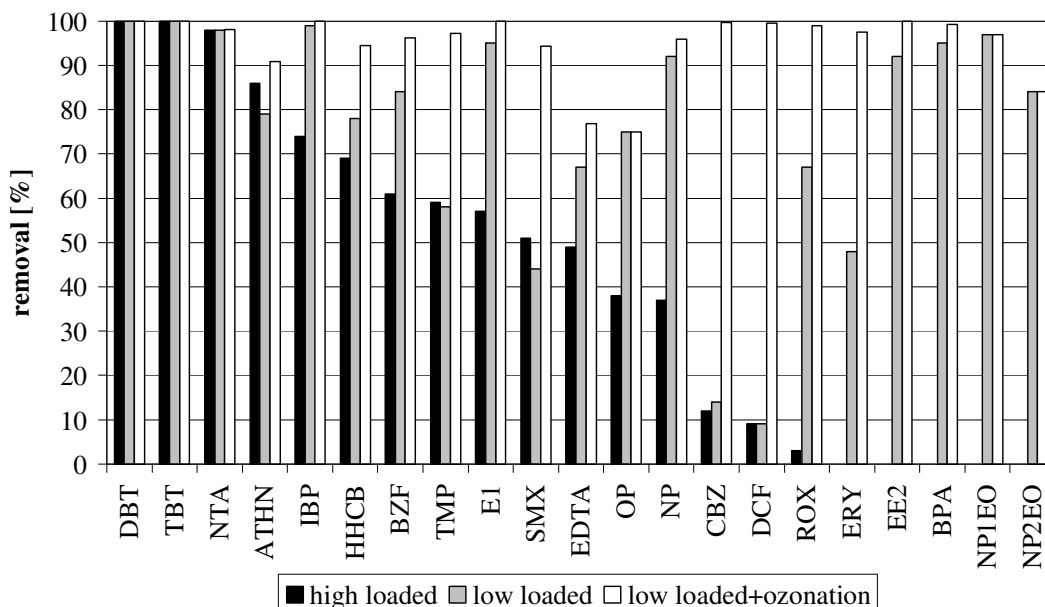


**Figure 1:** Removal of selected micropollutants under high and low loading and under low loading conditions with a subsequent ozonation at 0.6 g $O_3$ g $DOC_0^{-1}$

Especially Substances with high adsorption potential to the organic matrix of the activated sludge show high removal rates even in the high loaded activated sludge plant (figure 1). The removal of sorbing

substances in wastewater treatment is a function of the specific excess sludge production which decreases with decreasing sludge load (F/M ratio) and consequently with higher sludge retention time. The removal observed under high loading conditions can be described by the adsorption potential of substances and the excess sludge production (Clara et al. 2005b). As a consequence it can be concluded, that for wastewater treatment plants under high loading condition and low SRT, adsorption to primary and secondary sludge is the most significant pathway for the removal of organic trace pollutants, whereas biological degradation is secondary. At an F/M ratio or SRT respectively that is required for nitrification and denitrification, biological transformation is more significant. Especially EDCs like EE2, BPA, NP or NPnEOs are removed by a far higher extend by low loaded systems compared to the high loaded systems (figure 1). However, persistent substances as CBZ or DCF that show low adsorption potential and high stability against biological transformation, are removed to an equally low level in both, the highloaded and the low loaded plant. Only the application of chemical oxidation by a subsequent ozonation step is able to remove those substances significantly (figure 1).

**Ecotoxicology**: None of the ecotoxicity tests revealed acute toxicity in the WWTP effluent before and after the ozonation step (Data not shown).

**Fish Reproductive Output and External Morphology**: Neither the reproductive output nor the gross morphological examination of the fish exposed to the effluents before and after ozonation showed indication of estrogenic or androgenic endocrine effects. These results are consistent with the scarce pertinent literature. Thorpe et al. (2009) observed no effects of WWTP effluents (UK) on survival, growth and condition (CF) in fathead minnows (*Pimephales promelas*) but a significant reduction in egg production in undiluted and 50% diluted effluent samples. Also no effects in survival, growth or condition of fathead minnows (*P. promelas*) exposed to effluents (UK, Derbyshire) before and after advanced treatment (granular activated carbon, ozone or chlorine dioxide) were reported by Filby et al. (2010) whereas again a significant reduction in egg production in undiluted and 50% effluent before and in undiluted samples after granular activated carbon treatment was observed. Growth suppression and a significant decrease of reproductive output were described by Ma et al. (2005) for secondary treated WWTP effluent (China, Beijing) below 20-fold dilution. In none of the mentioned studies exposure to effluent increased reproductive output. A detailed description and discussion of the results can be found at Altmann et al. (2012).

**Histology and Immunohistochemistry:** Neither changes of the gonadal stage nor other histological alterations indicating estrogenic or androgenic endocrine disruption in the gonads and livers of both sexes of fish exposed to the WWTP effluents before and after ozonation for almost three weeks were observed. Comparable results were reported by Nichols et al. (1998) for fathead minnow (*P. promelas*) exposed to municipal WWTP effluents (USA, Michigan) for three weeks where no effects in gonad histology were observed. Contrasting results of EDC effects of WWTP effluents (China, Beijing) were reported by Ma et al. (2005) for medaka where from concentrations of 5 % effluent a significant increase of VTG plasma levels in males was observed. A significant increase in VTG plasma levels of male fathead minnows (*P. promelas*) was also documented by Thorpe et al. (2009) and Filby et al. (2010) in undiluted and 50% diluted WWTP effluent samples (UK). A detailed description and discussion of the results can be found at Altmann et al. (2012).

**Endocrinology**: The results of the enzyme immunoassays indicated a decrease of endocrine binding activity in the ozonated effluent depending on the specific ozone consumption (table 4). The concentration of the immunoreactive steroids decreased by a factor of more than hundred and sixty to seventy, respectively, which was mainly attributed to the decrease in estrogens. The androgenes only declined by factors ranging from two to ten. Taken together, the results of the enzyme immunoassays

clearly indicated a dominance of estrogenic activity in the effluent of the WWTP, while androgenic activity dominated in the effluent of the ozonation pilot plant. A detailed description and discussion of the results can be found at Altmann et al. (2012).

**TABLE 4:** Estrogenic (E-Assay) and androgenic (T-Assay) activity in the effluent before and after the ozonation step during three sampling campaigns at 0.6 and 0.9 g $O_3$/g DOC

|  | **E-Assay** [ng $L^{-1}$ equivalents] | | | **T-Assay** [ng $L^{-1}$ equivalents] | | |
| --- | --- | --- | --- | --- | --- | --- |
|  | 0.9 g $O_3$ / g DOC | 0.6 g $O_3$ / g DOC | 0.6 g $O_3$ / g DOC | 0.9 g $O_3$ / g DOC | 0.6 g $O_3$ / g DOC | 0.6 g $O_3$ / g DOC |
| Effluent low loaded WWTP | 37.9 | 17.7 | 13.6 | 10.0 | 3.0 | 2.2 |
| Effluent subsequent ozonation step | 0.2 | 0.3 | 0.2 | 1.0 | 1.4 | 0.9 |

**Mutagenity**: Results of the Salmonella/microsome assay - Ames test for undiluted samples show that all samples are devoid of mutagenic activity in the *Salmonella*/microsome assay. With concentrated samples however, mutagenic effects were found in the effluent of the WWTP. The mutagenic effects were decreased by 39% after ozonation of the samples in strain TA98 without metabolic activation, while no effect was seen in the base-substitution strain (TA100). Results of the SCGE assays indicate significant induction of DNA migration for the effluent of the WWTP and for the effluent of the ozonation reactor, compared to the control. The effluent of the pilot plant showed a lower extent of DNA damage compared to the untreated effluent and the effluent of the ozonation reactor. In the MN test exposure no increase of the MN frequencies was observed. This indicates that the ozonation of tertiary wastewater does not cause MN induction in *Allium cepa* roots. A detailed description and discussion of the results can be found at Mišík et.al (2011).

## CONCLUSIONS

The SRT plays a significant role for micropollutant removal during biological treatment as especially natural hormones are removed to a significant higher amount in low loaded plants with a high SRT compared to a high loaded plant with low SRT (see figure 1 and Clara, 2005b). But even at high SRT WWTPs are not able to remove micropollutants completely from the wastewater. If further removal is required advanced treatment is needed. Even though there are groups of compounds such as iodated contrast media that are not removed, a subsequent ozonation step at 0.6 g $O_3$ g $DOC_0^{-1}$ proved to be a suitable technology to decrease the emission of micropollutants as well as estrogenic and androgenic effects to the aquatic ecosystem.

Effluents before as well as after ozonation did not show any adverse effects in the basic set of the short term exposure biotests employed for aquatic ecotoxicity screening. Furthermore, adult medaka fish did not show external signs of detrimental effects during the almost three-week continuous exposure to the undiluted WWTP effluents before and after ozonation. In the quantitative E- and T-Assay, ozonation decreased both the estrogen and - to a lesser extent - testosterone immunoreactivity of the WWTP effluent. The absence of female specific VTG expression in the liver and gonads of male fish and the absence of male specific external sex characteristics in the female fish along with no changes in reproductive output of female fish and of the gonadal tissues of both sexes indicated no observable estrogenic and androgenic effects of the WWTP effluents in the fish screening assay.

Our results show that ozonation reduces the genotoxic effects of tertiary treated urban waste water which in the frameshift strain TA98. Furthermore, this is the first study which indicates that the treatment reduces also the extent of DNA-damage in primary liver cells possessing xenobiotic metabolic enzymes. These observations, and the lack of acute toxicity seen in experiments with bacterial, mammalian and plant derived indicator cells can be taken as an indication that $O_3$ treatment does not cause adverse effects but leads to destruction of DNA reactive toxins in treated urban water.

**ACKNOWLEDGEMENTS**

**REFERENCES**

Altmann, D., H. Schaar, C. Bartel, D.L. Schorkopf, I. Miller, N. Kreuzinger, E. Möstl, and B. Grillitsch. 2012. "Impact of ozonation on ecotoxicity and endocrine activity of tertiary treated wastewater effluent." *Water Research* 46(11): 3693-3702

Bahr, C., M. Ernst, and M. Jekel. 2007. Pilot investigations covering the combined oxidative and biological treatment of sewage works effluents aiming at the removal of trace organics and active agents and at achieving enhanced disinfection (PILOTOX). Project report, *Schriftenreihe Kompetenzzentrum Wasser Berlin* 5.

Bahr, C., M. Ernst, T. Reemtsma, B. Heinzmann, F. Luck, and M. Jekel, 2005. Pilot scale ozonation of treated municipal effluent for removal of pharmaceutical compounds and pathogens - The Berlin study. Proceedings of the 17th IOA World Ozone Congress, 22-25 August, Strasbourg.

Benotti, M.J., R.A. Trenholm, B.J. Varnderford, J.C. Holady, B.D. Stanford, and S.A. Snyder. 2009. "Pharmaceuticals and Endocrine Disrupting Compounds in U.S. Drinking Water". *Environmental Science and Technology* 43: 597-603.

Clara, M., B. Strenn, O. Gans, E. Martinez, N. Kreuzinger, and H. Kroiss, 2005a. "Removal of selected pharmaceuticals, fragrances and endocrine disrupting compounds in a membrane bioreactor and conventional wastewater treatment plants." *Water Research*. 39: 4797-4807.

Clara, M., N. Kreuzinger, B. Strenn, O. Gans, and H. Kroiss, 2005b. „The solids retention time – a suitable design parameter to evaluate the capacity of wastewater treatment plants to remove micropollutants." *Water Research* 39, 97-106.

DIN, 1996. Water quality - Determination of the inhibition of the mobility of Daphnia magna Straus (Cladocera, Crustacea) - Acute toxicity test. DIN EN ISO 6341.

DIN, 2003. Standard methods for the examination of water, waste water and sludge - Subanimal testing (group T) - Part 6: Toxicity to fish; Determination of the non-acute-poisonous effect of waste water to fish eggs by dilution limits (T 6). DIN 38415-6.

DIN, 2004. Water quality - Freshwater algal growth inhibition test with unicellular green algae. DIN EN ISO 8692.

Filby, A.L., J.A. Shears, B.E. Drage, J.H. Churchley, and C.R. Tyler, 2010. "Effects of Advanced Treatments of Wastewater Effluents on Estrogenic and Reproductive Health Impacts in Fish." *Environmental Science and Technology* 44: 4348-4354.

Hollender, J., S.G. Zimmermann, S. Koepke, M. Krauss, C.S. McArdell, C. Ort, H. Singer, U. von Gunten, and H. Siegrist, 2009. „Elimination of Organic Micropollutants in a Municipal Wastewater Treatment Plant Upgraded with a Full-Scale Post-Ozonation Followed by Sand Filtration". *Environmental Science and Technology* 43: 7862-7869.

Huber, M.M., A. Göbel, A. Joss, A., N. Hermann, D. Löffler, C.S. McArdell, A. Ried, H. Siegriest, T.A. Ternes, and U. von Gunten, 2005. „Oxidation of Pharmaceuticals during Ozonation of Municipal Wastewater Effluents: A Pilot Study." *Environmental Science and Technology* 39: 4290-4299.

Huber, M.M., S. Canonica, G.Y. Park, and U. von Gunten, 2003. „Oxidation of Pharmaceuticals during Ozonation and Advanced Oxidation Processes." *Environmental Science and Technology* 37: 1016-1024.

Ma, T.H., Z. Xu, C. Xu, H. McConnell, E.V. Rabago, G.A. Arreola, H. Zhang, 1995. "The improved Allium/Vicia root tip micronucleus assay for clastogenicity of environmental pollutants." *Mutat Res* 334: 185-195.

Maron, D.M., and B.N. Ames, 1984. Revised methods for the Salmonella mutagenicity test, in: Kilbey, B.J., Legator, M., Nocols, W., Ramel, C. (Eds.), Handbook of Mutagenicity Test Procedures. Elsevier Science Publishers BV, New York, pp. 93-140.

Mišík, M., S. Knasmueller, F. Ferk, M. Cichna-Markl, T. Grummt, H. Schaar, and N. Kreuzinger 2011. „Impact of ozonation on the genotoxic activity of tertiary treated municipal wastewater." *Water Research*. 45(12): 3681-3691

Möstl, E., H.H.D. Meyer, E. Bamberg, and G. von Hegel, 1987. "Oestrogen determination in faeces of mares by enzyme immunoassay on microtiter plates." Proceedings of the 3rd Symposium on the Analysis of Steroids, Sopron, Hungary, 1987, 219-224.

Nakada, N., H., Shinohara, A. Murata, K. Kiri, S. Managaki, N. Sato, and H. Takada, 2007. "Removal of selected pharmaceuticals and personal care products (PPCPs) and endocrine-disrupting chemicals (EDCs) during sand filtration and ozonation at a municipal sewage treatment plant." *Water Research* 41: 4373-4382.

Nichols, K.M., S.R. Miles-Richardson, E.M. Snyder, and J.P. Giesy, 1999. "Effects of Exposure to Municipal Wastewater in situ on the Reproductive Physiology of the Fathead Minnow (Pimephales promelas)." *Environmental Science and Chemistry* 18(9): 2001-2012.

Noot, D.K., W.B. Anderson, S.A. Daignault, D.T. Williams, and P.M. Huck, 1989. "Evaluating treatment processes with the ames mutagenicity assay". *J Am Water Works Assoc* 81: 87-102.

OECD. 2009. 21-day Fish Assay: A Short-Therm Screening for Oestrogenic and Androgenic Activity, and Aromatase Inhibition. Guideline No. 230. Adopted 7 September 2009.

Palme, R. and E. Möstl, 1993. "Biotin-Streptavidin enzyme immunoassay for the determination of oestrogens and androgens in boar faeces". In: Advances of Steroid Analysis ´93, S. Görög (ed.), Akademiai Kiado Budapest 94, Proc. 5th Symp.Anal. Steroids, Szombathely, Hungary, 111-117.

Paraskeva, P., and N.J. Graham, 2002." Ozonation of municipal wastewater effluents." *Water Environ Res* 74: 569-581.

Poseidon, 2004. Assessment of Technologies for the Removal of Pharmaceuticals and Personal Care Products in Sewage and Drinking Water Facilities to Improve the Indirect Potable Water Reuse. EU project report Contract No. EVK1-CT-2000-00047.

Schaar, H., M. Clara, O. Gans, and N. Kreuzinger, 2010. „Micropollutant removal during biological wastewater treatment and a subsequent ozonation step." *Environmental Pollution* 158: 1399-1404.

Singh, N.P., M.T. McCoy, R.R. Tice, and E.L. Schneider, 1988. "A simple technique for quantification of low levels of DNA damage in individual cells." *Exp. Cell. Res.* 175: 184-191

Stalter, D., A. Magdeburg, and J. Oehlmann,. 2010. „Comparative toxicity assessment of ozone and activated carbon treated sewage effluents using an in vivo test battery." *Water Research* 44(8): 2610-2620.

Ternes, T.A., J. Stüber, N. Herrmann, D. McDowell, A. Ried, M. Kampmann, and B. Teiser, 2003. „Ozonation: a tool for removal of pharmaceuticals, contrast media and musk fragrances from wastewater?" *Water Research* 37: 1976-1982.

Thorpe, K.L., G. Maack, R. Benstead, and C.R. Tyler, 2009. "Estrogenic Wastewater Treatment Works Effluents Reduce Egg Production in Fish." *Environmental Science and Technology* 43: 2976-2982.

Westerhoff, P., Y. Yoon, S. Snyder, and E. Wert, 2005. „Fate of Endocrine-Disruptor, Pharmaceutical, and Personal Care Product Chemicals during Simulated Drinking Water Treatment Processes." *Environmental Science and Technology* 39: 6649-6663.

# THE ROLE OF METHANOGENS IN DEGRADATION OF CHLOROPHENOLS UNDER ACIDIC CONDITION

*JIANG X.*, ZHOU Y. and NG W.J.

(Nanyang Technological University, Singapore)

An anaerobic sequencing batch reactor (anSBR) was set up to investigate feasibility of acidic dechlorination of chlorophenols and the consequent microbial community involved. The anSBR was acclimated with monochlorophenols (MCPs) and pH was reduced in a step-wise manner at pH 0.5 per week from pH 7.5. The final working pH was controlled at $5.5\pm0.1$. The reactor was mixed by re-circulating the produced biogas to the bottom of the anSBR. After about 80 days acclimation, the biomass was capable of *ortho*-dechlorination. *Ortho*-chlorines were removed from 2-MCP, 2,4,6-trichlorophonel (TCP), and pentachlorophenol (PCP) at significant loading rates of 200 μM/L·day, 100 μM/L·day and 10 μM/L·day respectively. Due to the toxicity of PCP, the process was inhibited when PCP loading exceeding 10 μM/L·day, and recovery took around 100 days before the process fully recovered. Quantitative PCR results showed that the copy number of *Methanosarcinaceae* (the only acetate-utilizing methanogen) was reduced over 1000 times during the inhibition period. The percentage of this family in the total methanogens decreased to only 0.01% from more than 1.6% before inhibition. The counts of *Methanosarcinaceae* gradually resumed to its original level after dechlorination capability of the system recovered. To investigate the role of methanogens in the dechlorination process, methanogenic-specific inhibitor 2-Bromoethanesulfonate (BES) was dosed into the biomass to inhibit methanogen activity. It was found that dechlorination of 2-MCP was completely stopped at 25 mM BES although acetate was at 10 mM. 70-100% of 2-MCP was removed in the control reactor without BES. The step-wise reduction of pH and recirculation of produced biogas may preserve or enhance certain methanogenic activities under acidic conditions. The above results indicate that the acetate-utilizing methanogens *Methanosarcinaceae* played an important role in the dechlorination process under acidic conditions.

# ENHANCED BIODEGRADATION OF ENDOSULFAN AND ITS METABOLITE-ENDOSULFATE BY A BIOSURFACTANT PRODUCING BACTERIUM

*Greeshma Odukkathil** and Namasivayam Vasudevan
(Centre for Environmental Studies, Anna University, Chennai, India)

Endosulfan is a broad spectrum contact insecticide and acaricide registered for use on a wide variety of vegetables, fruits, cereal grains, and cotton, as well as ornamental shrubs, trees, vines, and ornamentals in agriculture. This insecticide is one of the widely used and most problematic insecticides used in India. Its low water solubility of 0.03 mg/L had resulted in persistence of endosulfan residues in Indian soil. The present study aims to enhance the bioavailability of this pesticide and its metabolites for bacterial degradation.

A consortium of bacteria was isolated from endosulfan contaminated soil for the degradation of endosulfan. The mixed bacterial culture was able to degrade about 80% of α-endosulfan and 75% β-endosulfan in five days.

Individual bacterial strain in the consortium degraded endosulfan as a sole carbon in the range of 30% to 99%. Among the different strains, a biosurfactant producing bacterium was isolated from endosulfan degrading mixed culture enriched from pesticide contaminated soil. Among the isolates screened four strains (ES-34, ES-36, ES-40, and ES-47) were found to produce biosurfactant on endosulfan. ES-47 showed better emulsification of endosulfan and degraded endosulfan upro 99% and 94% of endosulfate formed during endosulfan degradation. Biosurfactant produced was characterized quantitavely and qualitatively. The strain reduced the surface tension up to 37 dynes/cm. The study revealed that the strain was capable of degrading endosulfan and its metabolite with simultaneous biosurfactant production. A detailed study on the biodegradation of endosulfan in soil by using this isolate will be also presented during the conference.

# DEGRADATION OF CARBON TETRACHLORIDE USING THE MODIFIED PERSULFATE OXIDATION

*Yong-jae Kwon*, Moon-ho Kang, Su-jin Bang, Sil-hee Hong and Sung-ho Kong
(Hanyang University, Seoul, Republic of Korea)

The concerns for carbon tetrachloride ($CCl_4$) in environment are widespread due to its refractory nature. Even though the advanced oxidation processes, which are generally with UV radiation, are tested for their effectiveness, a common degradation pathway of $CCl_4$ is reduction (e.g. reductive dechlorination using ZVI). Recently, persulfate oxidation has been modified and evaluated to expand its applicability. UV radiation (254 nm) with persulfate ion ($S_2O_8^{2-}$) can produce sulfate radicals ($SO_4\bullet^-$) and hydroxyl radicals ($OH\bullet$) with superoxide anion ($O_2\bullet^-$) as minor. At the same time, those radicals (i.e. sulfate or hydroxyl radical) subsequently react with methanol to generate hydroxymethyl radicals ($\bullet CH_2OH$). Therefore, the expected reactive species to reduce $CCl_4$ can be superoxide anion or hydroxylmethyl radicals.

In this work, the modified persulfate oxidation (i.e. $S_2O_8^{2-}$/methanol/UV system) to remove $CCl_4$ was investigated. First of all, the concentration effects of persulfate (i.e. from 0.5 to 10 mM) and methanol (i.e. from 0.1 to 100 mM) were evaluated at pH 7. As a result, the highest $CCl_4$ degradation was achieved when the ratio of $S_2O_8^{2-}$ and methanol was 10:1 (i.e. 10 mM persulfate: 1 mM methanol) and the apparent first-order rate constant in this optimum condition was 17 $h^{-1}$. As a cost-effectiveness point of view, the ratio of $S_2O_8^{2-}$ : methanol as 5:1 could satisfy the effluent standard in Korea (i.e. 0.04 mg/L).

Reaction mechanism and the optimum conditions for a continuous stirred tank reactor (CSTR) to treat chlorinated contaminants will be investigated.

## TOXICITY OF NONYLPHENOL COMPOUNDS IN ANAEROBIC DIGESTERS

Hande Bozkurt and **F. Dilek Sanin**

(Middle East Technical University, Ankara, Turkey)

Nonylphenol compounds constitute about 80% of the alkylphenols being used in our daily activities. Due to their surface active properties nonylphenols have high commercial, industrial and domestic uses. Their widespread use and disposal cause them to exist in different compartments of environment at high concentrations including municipal wastewaters. In addition to their toxic, carcinogenic and persistent characteristics, they have drawn the attention of scientists lately due to their endocrine disrupting properties. Nonylphenol(poly)ethoxylates are degraded by microbial action and lose their ethoxylates to NP2EO (nonylphenol diethoxylate), NP1EO (nonylphenol monoethoxylate) and NP (nonylphenol). Since they are highly persistent and hydrophobic, they accumulate mostly on biosolids. Therefore, scientifically the presence and fate of these compounds during sludge treatment systems should be monitored.

In this study using Anaerobic Toxicity Assay (ATA) tests, the toxicity of NP and NP2EO in the anaerobic digestion of sludge was determined. The test bottles were dosed with NP and NP2EO in acetone, with concentrations ranging from 30 mg/L to 1 mg/L. During the tests, gas productions and compositions in terms of methane and carbondioxide were observed. Moreover, TS and VS reductions were determined in addition to COD analysis. As a result, it was observed that methane production and VS reduction decreased with the increasing chemical concentrations. On the other hand, inhibition of NP or NP2EO was not observed throughout the test. In addition, to be able to judge about the fate, the target compounds were extracted from water and sludge and analyzed using GC/MS.

# CHEMICAL COMPOSITION OF ESSENTIAL OILS FROM THE LEAVES OF MENTHA LONGIFOLIA

*O. O. Okoh* and A. J. Afolayan (Phytomedicine Research Centre, Faculty of Science and Agriculture, University of Fort Hare, Alice 5700, South Africa).

The effects of hydrodistillation (HD) and solvent free microwave extraction (SFME) methods on the chemical composition and toxicity of *Mentha longifolia* subsp. *capensis* leaves were studied. Oil yields of 1.52 and 1.63% (w/w) were obtained from HD and SFME methods, respectively. Analyses of the two oils revealed a total of 21 components. The HD oil was found to be characterized by monoterpenoids with oxygenated monoterpenes, such as menthone (41.9%), α-pinene (5.4%), pulegone (34.2%), β-pinene (2.4%) and 1, 8-cineole (6.5%). Other identified constituents, include cis-sabinene hydrate (0.4%), linalool (1.0%), piperitenone (1.3%), β-caryophyllene (0.4%), germacrene D (0.5%) and isomenthone (0.4%). Also, the HD oil showed the presence of 3-octanol (0.2%), bicyclogermacrene (0.1%) and caryophyllene oxide (0.1%) which were not found in the SFME oil. The SFME oil was characterized by menthone (28.0%), α-pinene (3.6%), pulegone (23.0%), β-pinene (1.0%) and 1, 8-cineole (5.4%). Other identified constituents, include cis-sabinene hydrate (0.1%), linalool (0.5%), piperitenone (0.1%), β-caryophyllene (0.3%), germacrene D (0.2%) and isomenthone (0.3%). *In vitro* cytotoxicity test revealed that the oils were minimally toxic at 40 μg/ml, and maximally toxic at 200 μg/ml for both HD and SFME oils. Both extraction methods do not appear to significantly affect composition and toxicity of the essential oils from *Mentha longifolia* subsp. *capensis* leaves.

# MODELING

# A NUMERICAL APPROACH TO QUANTYFY SELECTIVE SORTING OF HEAVY - MINERAL ASSEMBLAGES

*Gerhard Bartzke* and Katrin Huhn
(Marum – University of Bremen, Bremen, Germany)

**ABSTRACT:** The enrichment of heavy minerals causing placer formation has been explained as selective grain entrainment using laboratory experiments. However, the validation, in particular, the quantification of grading processes in the sediment bed is difficult using such techniques. For quantification of selective grain entrainment, we used a 3D high resolution numerical 'flume tank' based on a coupled Finite Difference Method (FDM) and Discrete Element Method (DEM) model. For the quantification of processes occurring at the bed surface and in the interior we designed four suites of experiments: (1) deposition of a single 'quartz' grain on top of a 'magnetite' bed, and (2 – 4) deposition of the 'quartz' grain at depths with respect to the bed. All samples were tested at flow velocities ranging from 10 – 30 cm/s. Further measurement routines, such as fluid profiles, transport distances, and coordination numbers (nearest neighbors) were extracted. The results showed that an exposed light mineral is entrained more easily than a heavy mineral grain. In contrast, with increasing burial depth, erosion resistance of the light mineral increased. We conclude that for placer formation, higher flow velocities (e.g., storm events) are needed to 'wash-out' the lighter fractions in the deeper part of a sediment bed.

## INTRODUCTION

Heavy minerals (e.g., Magnetite, Ilmenite, Zircon and Garnet) play an important role in the mineral industry due to their high economic value. In general, such heavy minerals differ from light minerals (e.g., Feldspar and Quartz) based on mineralogical composition, grain size, and also in hydrodynamic susceptibility according to their differing densities (e.g., 4 - 6 g/cm³ for heavy minerals and 2.5 - 2.8 g/cm³ for light minerals). Due to their higher densities, heavy minerals are more resistant to erosion by flowing water (Komar, 1987). Therefore, the light mineral fractions can be 'washed-out' more easily due to differing density-related threshold conditions. This process of hydrodynamic sorting, understood as selective grain entrainment, can lead to the formation of heavy mineral placers (Komar, 2007). The position and distribution of such placers is interesting for the industry, because they are easier to mine. So within the marine environment beach placer deposits are very common, where heavy minerals can be found in high concentrations. These are defined as deposits of residual or detrital mineral grains in which a valuable mineral has been concentrated by a natural process (Komar, 1987; Peterson et al., 1989).

Prior studies, attempted to determine the formation of placers by the process of selective grain entrainment used analogue, mechanical models (e.g., flume tanks). Here, research focused on interaction between fluid forces and resulting particle motion by testing a variety of particle mixtures differing in grain size, density, and weight. An excellent review of these experiments can be found in Komar (2007). However, it is difficult to validate the process of selective grain entrainment on exposed or buried light minerals in a heavy mineral bed (Komar, 2007). Hence there is a clear lack in knowledge about the role of sediment texture or granular skeleton besides hydrodynamic forcing on heavy mineral enrichment, and placer formation (Komar, 2007). In consequence, further studies are required, for a better understanding of mineral enrichment processes, and to develop conceptual models dealing with 'wash-out' processes on a grain-scale level. Additionally, this information will improve numerical simulations, to simulate the physical processes controlling selective sorting at the surface and in the interior of a sediment bed. This can assist in the detection of heavy mineral accumulations and can concurrently reduce expensive and time consuming exploration activities for mining heavy mineral placers in the marine environment.

Our study shows the quantification of the physical processes controlling selective grain entrainment to understand the formation of heavy mineral placers. Therefore, a 3D numerical model approach was designed by coupling two simulation techniques – the Finite Difference Method (FDM)

with the Discrete Element Method (DEM). This 3D model parameterized general settings of laboratory flume tanks to investigate selective grain entrainment as the main factor for heavy mineral accumulation. In order to quantify the 'wash-out' processes, four suites of experiments were designed, wherein different grades of exposure of light minerals within a heavy mineral bed were tested under different flow velocities: starting with an exposed 'quartz' grain (Experiment 1, z = 0.4 mm) deposited on top of a 'magnetite' bed, and ending with a fully buried 'quartz' grain (Experiment 4, z = 0.2 mm). Hence, exposure (z) is defined as the distance of the 'quartz' grain to the model base (Table 1). Analyses of these experiments indicated that the erosion resistance of the light fraction increases with burial depth, which is caused by a decreased inflow to the 'magnetite' bed. Therefore, it should be considered that the quantity of 'washed-out' light minerals, located in deeper parts of a sediment bed, might also contribute to the enrichment of heavier minerals in a placer. The resultant higher erosion thresholds of the buried lighter fractions suggest that their entrainment would be more likely in high energy flow events, such as during episodically occurring extreme storm events.

## NUMERICAL METHODS

We developed a high resolution, 3D numerical 'flume tank' (Figure 1) for the simulation of light and heavy mineral transport through a fluid. Therefore, we coupled a FDM model with a DEM model by an input - output routine. These are two independent numerical simulation techniques, wherein the FDM simulation creates the flow conditions and flow velocities (fluid model) and the DEM model simulates the 'sediment' matrix (sediment matrix model, Figure 1). The 3D FDM fluid model was generated using the commercial software (FLAC3D, Itasca). It is based on the spatial discretization of the study domain by a finite number of three-dimensional, rectangular, polyhedral elements. These elements can be assigned with broad physical property spectra e.g., fluid density, pore pressure, and flow velocities, to mimic natural conditions. Hence, this FDM model calculates fluid forces and solves the differential flow equations by partial integration in defined time steps based on given boundary conditions e.g., inflow velocity. Simultaneously, we used the PFC 3D software (Itasca, 2004), which is based on the DEM theory by Cundall and Strack (1978), to simulate the 'sediment' matrix. This granular model consists of ideal spherical particles which interact according to physical contact laws. Hence, these granular assemblages mimic the 'sediment' bed (i.e. numerical 'magnetite' and 'quartz' grains), in particular the internal structure and porosity. DEM enables to investigate the mechanical behavior, deformation processes and hence, the 'sediment' grain interactions caused by applied, defined boundary conditions, e.g. fluid forcing (Figure 1). Physical properties are assigned adopting natural conditions, such as e.g., grain density, friction, and stiffness. For a detailed review of PFC and FLAC refer to Itasca, 2004.

In order to couple both models, the fluid model and the sediment matrix model have identical geometries, dimensions, material properties, as well as boundary conditions (Figure 1). Initially, the grain or 'sediment' model was generated. The spatial parameters of this sediment matrix model (x, y, z coordinates and the particle radii) were then sent to the FDM model. Based on these data representing the grain distribution in the DEM model, the fluid model is discretized into a high resolution finite difference grid wherein each grain is represented by at least 8 elements. The resulting FDM model consists of elements, where fluid streaming was either allowed (fluid zones) or not allowed (particle / solid matrix zones). Therefore, the FDM model and the DEM model, showed identical porosity distributions within the 'sediment' filled areas (compare 'sediment' beds in Figure 1).

After the 'sediment' bed was generated (Figure 1), a flow field streaming into X-direction was initiated above the bed, by an inflow boundary condition in the FDM model. In the following step, all flow velocities were calculated based on the initial porosity distribution. After the flow field reached stable conditions, all fluid forces were extracted around each element and sent to the sediment matrix model to be assigned to all particles at their corresponding X-Y and Z coordinates. If the added fluid forces are larger than the resisting force of the particles and their inter-particle friction respectively, the particle contacts break up and the grains are transported (Cundal and Strack, 1978). Hence, 'sediment' transport was initiated at the sediment matrix model, which caused new porosities within the DEM model. Those were sent back to the fluid model, and subsequently a re-meshing of the FDM model grid was initiated. This calculation cycle between both models was repeated until constant flow and transport conditions were reached. Hence, high resolution information about e.g., particle distribution, porosity, texture, and fluid velocities at the 'sediment' surface as well as in the interior of the 'sediment' matrix are

capable in space and time. This approach yields a deeper insight into grain-fluid interactions on a micro-scale level and provides a fundamental understanding of physical processes occurring during selective grain entrainment.
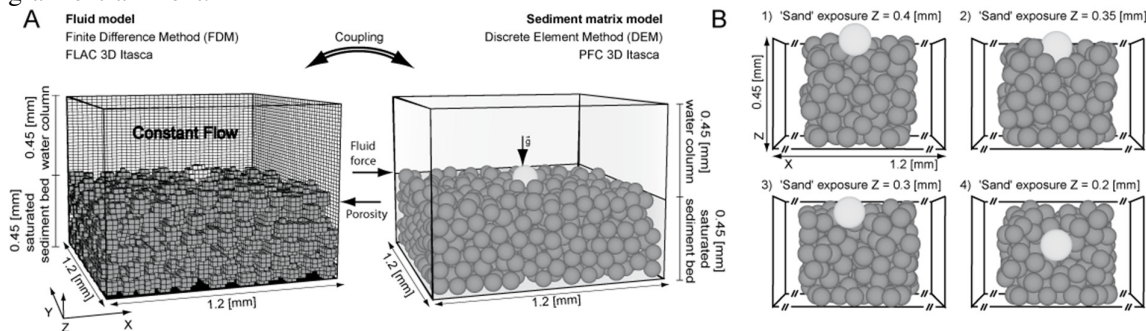


**FIGURE1.** A) Schematic of the coupled fluid model (FDM) and sediment matrix model (DEM) for simulation of particle transport by a fluid. B) Experimental setup, 'quartz' deposited on top or within a 'magnetite' bed at increasing the particle depths or respectively reducing the exposure (z).

## EXERIMENTAL SETUP

Both the FDM and DEM models had identical dimensions (1.2 x 1.2 x 0.45 mm), which were designed to isolate a micro-scale section of the sediment surface from a laboratory flume tank, to focus on the quantification of the physical processes controlling selective grain entrainment at the surface and in the interior of the 'sediment' bed. The grain sizes, and physical properties of all grains, as well as the flow velocities, were chosen to ensure conditions known from natural environments of heavy mineral placers (Allen 1970; Table 1, 2). Therefore, two end-members of heavy- and light-mineral fractions, which are significantly differing in their hydrodynamic and physical properties (Table 1), were tested as a simplified 'sediment' bed of smaller, heavier, numerical 'magnetite' grains ($D_{50} = 0.08$ mm, $\rho_m = 5.6$ g/cm³) and larger numerical 'quartz' grains ($D_{50} = 0.14$ mm, $\rho_q = 2.65$ g/cm³,). Within all DEM model experiments the 'sediment' bed consisted of 1000 'magnetite' particles, which were randomly distributed and deposited under applied gravity into the numerical 'sediment' box (Figure 1B). Here, the generated 'magnetite' bed filled always half of the box. To validate the effect of selective grain entrainment and the influence of exposure (i.e. z = distance from the 'quartz' grain to the box base) between of light/larger and heavy/smaller minerals under different flow velocities, we designed four suites of experiments: 1) a single 'quartz' grain was deposited on top of a heavy 'magnetite' bed (z = 0.45 mm; Experiment 1; Figure 1B). In order to reach a deeper burial position of the 'quartz' grain within the 'magnetite' bed, i.e. Experiment 2 - 4 (Figure 1B), we removed 'magnetite' particles out of the matrix at those locations where 'quartz' grains should be embedded. Then we deposited the single 'quartz' grain there (Figure 1B).

Starting from these initial stable conditions, a constant free-stream in positive X-direction above the fully saturated 'sediment' bed was calculated at the beginning of each model run in all FDM models (grid space: 48 x 48 x 40 elements). To investigate the erosional behavior, flow velocities were stepwise increased, ranging from 10, 15, 20, 25 to 30 cm/s, within each Experiment 1 - 4. These flow velocities were chosen to mimic the environment of tidal sand flats (Leeder, 1999).

In order to validate the effect of selective entrainment within all experiments, we extracted fluid profiles, coordination numbers, and transport distances from the fluid and sediment matrix models (Figure 2). To quantify changes in the flow field above and in the 'magnetite' bed, we generated X-Z slices (fluid profile slice in Figure 2), which were sliced exemplarily at 0.06 mm (Y-direction) through the fluid model. The exact flow velocities were extracted from each cell and are illustrated as a contour plot (Figure 2). Furthermore, we processed single fluid profiles to highlight velocity differences in more detail. Within the sediment matrix model we recorded the exact position and speed of the 'quartz' grain, and all 'magnetite' grains, to compare and quantify both 'quartz' and 'magnetite' transport. Therefore, particle transport was defined as a transport distance greater than the radius of each individual particle. Furthermore, we measured the coordination numbers of the 'quartz' grain and the nearest 'magnetite' neighbors.

In addition, we compared the ratio of exposure, and coordination number with respect to transport distance, to understand the relationship between the transport distances of the light minerals, the burial depth of 'quartz' grain, and the coordination number (Figure 3).

<table>
<tr><td colspan="5" align="center"><b>TABLE 1</b></td></tr>
<tr><td colspan="5" align="center"><b>Particle properties</b></td></tr>
<tr><td><b>Properties</b></td><td><b>Exp. 1</b></td><td><b>Exp. 2</b></td><td><b>Exp. 3</b></td><td><b>Exp. 4</b></td></tr>
<tr><td>'Quartz' diameter $D_{50}$ [mm]</td><td>0.14</td><td>0.14</td><td>0.14</td><td>0.14</td></tr>
<tr><td>'Magnetite' diameter $D_{50}$ [mm]</td><td>0.08</td><td>0.08</td><td>0.08</td><td>0.08</td></tr>
<tr><td>Particle number: 'quartz'</td><td>1</td><td>1</td><td>1</td><td>1</td></tr>
<tr><td>Particle number: 'magnetite'</td><td>1000</td><td>1000</td><td>980</td><td>975</td></tr>
<tr><td>Normal stiffness [N/m]</td><td>$1\times10^8$</td><td>$1\times10^8$</td><td>$1\times10^8$</td><td>$1\times10^8$</td></tr>
<tr><td>Shear stiffness [N/m]</td><td>$1\times10^8$</td><td>$1\times10^8$</td><td>$1\times10^8$</td><td>$1\times10^8$</td></tr>
<tr><td>Density $\rho_s$ 'quartz' [kg/m³]</td><td>2650</td><td>2650</td><td>2650</td><td>2650</td></tr>
<tr><td>Density $\rho_m$ 'magnetite' [kg/m³]</td><td>5640</td><td>5640</td><td>5640</td><td>5640</td></tr>
<tr><td>'Quartz' friction $\mu_s$</td><td>0.5</td><td>0.5</td><td>0.5</td><td>0.5</td></tr>
<tr><td>'Mineral' friction $\mu_m$</td><td>2</td><td>2</td><td>2</td><td>2</td></tr>
<tr><td>'Quartz' exposure z [mm]</td><td>0.4</td><td>0.35</td><td>0.3</td><td>0.2</td></tr>
</table>

<table>
<tr><td colspan="5" align="center"><b>TABLE 2</b></td></tr>
<tr><td colspan="5" align="center"><b>Fluid properties</b></td></tr>
<tr><td><b>Fluid properties</b></td><td><b>Exp. 1</b></td><td><b>Exp. 2</b></td><td><b>Exp. 3</b></td><td><b>Exp. 4</b></td></tr>
<tr><td>Fluid density $\rho_f$ [kg/m³]</td><td>1000</td><td>1000</td><td>1000</td><td>1000</td></tr>
<tr><td>Pore pressure $\psi$ [mbar]</td><td>250</td><td>250</td><td>250</td><td>250</td></tr>
<tr><td>Fluid saturation $\varphi$ [%]</td><td>100</td><td>100</td><td>100</td><td>100</td></tr>
<tr><td>Fluid velocity u [cm/s]</td><td colspan="4" align="center">10, 15, 20, 25 and 30</td></tr>
</table>

## RESULTS AND DISCUSSION

All experiments showed that a continuous free stream developed above the 'sediment', which decreased from the top of the water column (0.9 mm in height) towards the 'sediment' surface (0.45 mm height) in a logarithmic shape (Figure 2, fluid profiles). Towards the deeper parts of the 'magnetite' bed the flow velocity was further decreased in all experiments and ranged from 12 to 2 cm/s. Considering the results from all experiments in terms of the exposure of the 'quartz' particle, it was observed that the deeper the position of the particle within the 'magnetite' bed, the lower the surrounding fluid flow. In addition, it was shown that at a 30 cm/s free stream velocity, the 'quartz' particle in Experiment 1, was encountered to higher flow velocities as compared to the buried 'quartz' grain. Further, the flow velocity above the 'quartz' particle in Experiment 1 was higher as compared below, whereas the flow velocities of the deeper buried case of Experiment 4, were more constant above and below the particle.

The model results showed that transport speeds seem to depend on the 'quartz' particle exposure (see speed vectors in the top view slice of Figure 2). Within all models 'sediment' transport at the surface was imitated at 10 cm/s for 'quartz' and 15 cm/s for 'magnetite'. Therein, the most exposed 'quartz' particle of Experiment 1 was transported with fastest speeds at 3 cm/s, compared to the deepest positioned particle of Experiment 4, which was transported at relatively low speeds (~0.2 cm/s). This corresponds to the findings of the velocity profiles, where the flow velocities decreased with increasing depth (top view slice in Figure 2). In addition, it was observed that in Experiment 1, the exposed 'quartz' grain was transported faster as the 'magnetite' particles of the bed. In contrast, the experiments with deeper embedded 'quartz' particles (Experiment 3 and 4) showed that the heavy mineral fractions were transported at higher speeds than the buried 'quartz' grain.

To quantify the individual transport distance of the 'quartz' particles differing in exposure, in relation to their nearest adjacent 'magnetite' neighbors (coordination number), we compared Experiments 1 - 4 for 30 cm/s in more detail (Figure 3). It was observed that the exposed 'quartz' grain was transported a greater distance (Experiment 1, 0.19 mm total distance) than the embedded 'quartz' grains of Experiments 2 - 4 (Figure 3; Experiment 2, 0.07 mm, Experiment 3, 0.03 mm and Experiment 4, 0.002 mm total distance). This finding was also confirmed by the coordination number measurements, where the 'quartz' grain of Experiment 1 showed 4 contacts and the deeper buried grain of Experiment 4 had 7 contacts. In comparing the ratio of exposure, and coordination number to the transport distance it was

shown that an increase of burial depth of the particle in the 'magnetite' bed caused an increase of coordination number and subsequently a lowering in the transport distance (Figure 3).
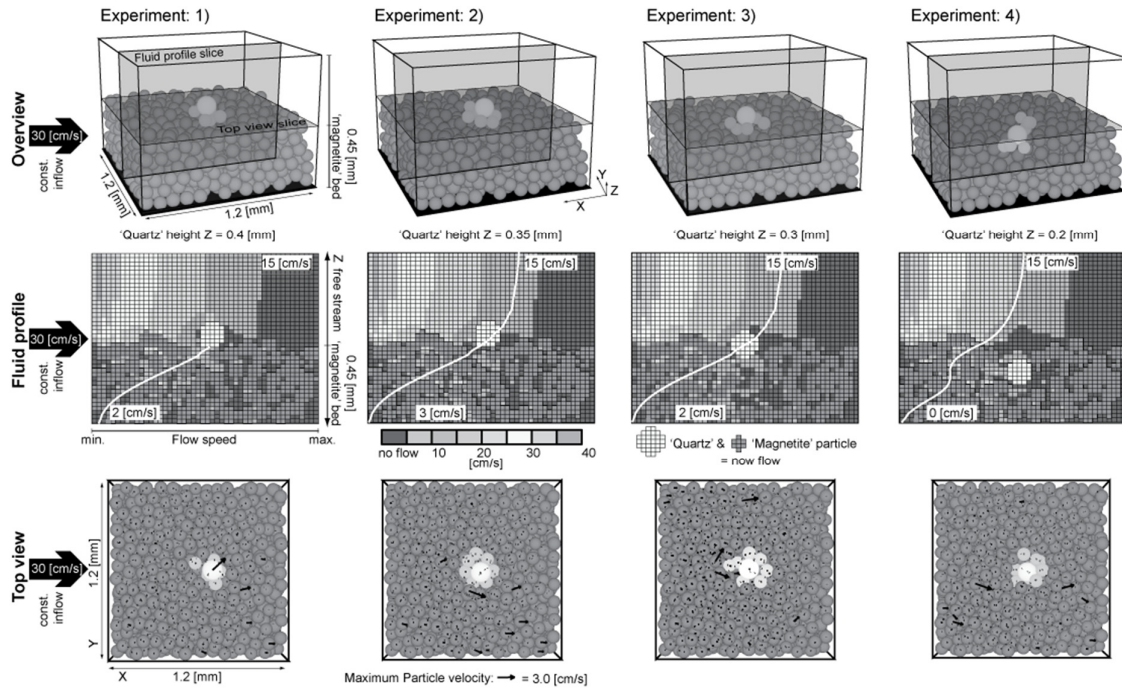


**FIGURE2.** Overview of the processed experiments at 30 cm/s flow velocity, showing the fluid profiles (fluid profile slice), transport velocities and coordination numbers (top view slice)
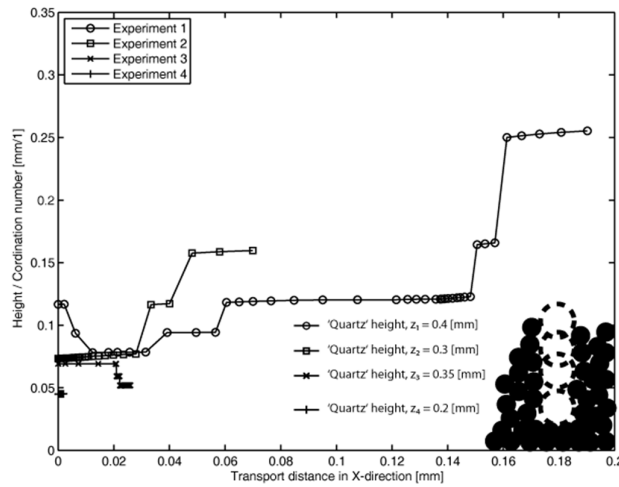


**FIGURE3.** Processed transport distances in x-direction of all experiments with respect to 'quartz' exposure and coordination number

Our 3D numerical 'flume box' experiments are capable to quantify selective grain entrainment and 'wash-out' processes, which cause heavy mineral placer formation. The experiments showed that the enrichment of heavy minerals by the 'washing-out' of light minerals is controlled by the exposure of the light 'quartz' grains. It was identified, that a single 'quartz' grain deposited on top of a 'magnetite' bed was transported preferentially due to their lower density over the bed (Figure 3). By decreasing the

exposure of a 'quartz' grains with respect to the 'magnetite' bed it was validated that the deeper buried 'quartz' minerals were not, or to a minor extend transported. This finding for exposed grains in our study corroborate, those from previous laboratory flume experiments (Komar 2007), which showed that heavy minerals, especially magnetite, are harder to entrain as the pure quartz fraction. However, the quantification of selective grain entrainment by those analogue models was limited in their validation of the processes occurring in the sediment bed, and hence in their ability of measuring the transport of buried grains (Komar, 2007).

In analyzing the flow properties in interior of the 'sediment' bed numerically, a decrease of the flow velocities was shown, and hence, decreasing threshold velocities with depth. In addition, coordination number measurements indicated that 'quartz' particles located deeper in the bed were surrounded by more 'magnetite' neighbors, which mechanically prevented the 'quartz' grain from moving. In addition, the increase in coordination number implicates that more particle contacts have to break up to 'wash-out' the larger lighter minerals. This indicates that much higher flow velocities are required to 'wash-out' particles located in the deeper parts of a 'magnetite' bed, which causes the accumulation of heavy minerals in placer deposits. Such extreme velocities, influencing deeper depth levels in the 'sediment' bed, could occur during cyclic storm events. In this case, the deeper buried sediments are perfused with higher flow velocities, effecting a higher potential to 'wash-out' quartz fractions located in deeper parts of the bed (Leeder, 1999). We hypotheses that only such an extreme event is able to 'wash-out' all light fractions with respect to the heavy mineral fraction, which possibly causes the establishment of a pure placer deposit. However, a detailed quantification of this effect influencing selective grain entrainment requires further investigations testing multiple grain spectra and heavy mineral compositions.

## CONCLUSION

A new high resolution 3D numerical model approach to simulate particle transport by fluid forcing has been developed. Hence, it is possible by this numerical 'flume tank' to quantify the physical processes of selective sorting of heavy and light minerals fractions and explains the formation of placers with high economical values. Through our experiments it was validated that selective grain entrainment is causing a 'wash-out' of the light minerals above a heavy mineral deposit at the sediment-water interface, which is directly linked to grain exposure. By decreasing the burial depth of light minerals i.e. 'quartz' within the heavy mineral bed i.e. 'magnetite', it was quantified that the exposure has an important influence on the threshold conditions and therefore, on the erosion resistance of the light minerals. This is caused by a reduced flow velocity reaching the light minerals located deeper in the bed, which prevents a 'wash-out'. This coincides that the greater the number of heavy mineral neighbors, the greater the required velocity for transport. We conclude that higher flow velocities are required, such as those caused by cyclic storm events, to 'wash-out' light mineral fractions in the deeper parts of the bed, which cause an enrichment of heavy minerals and the formation of placer deposits. Based on that, extreme events have to be taken into account particular in large scaled sediment transport models to study evolution of heavy mineral placer deposits.

Our numerical approach can be used as a prototype characterizing selective grain entrainment at the sediment-water interface, but also for quantification of processes acting in the sediment bed, which may be useful to the heavy mineral industry.

## ACKNOWLEDGEMENTS

## REFERENCES

Allen, J.R.L. 1970. *Physical processes of sedimentation*. Unwin University Books, London.

Cundall, P.A. and O.D.L., Strack, 1979. "A discrete numerical model for granular assemblies." *Géotechnique*. 29(1): 47-65.

Itasca 2004. *FLAC 3D 3.1 Manual*. Itasca Consulting Group, Inc., Minneapolis.

Leeder, M.R. 1999. *Sedimentology and sedimentary basins: From turbulence to tectonics*. 3rd ed., Blackwell Science, Oxford.

Komar, P.D. 1987. "Selective grain entrainment by a current from a bed of mixed sizes: A reanalysis." *J. Sediment. Petrol.* 57(2): 203-211.

Komar, P. D. 2007. "The entrainment, transport and sorting of heavy minerals by waves and currents." In M.A. Mange, and D.T. Wright (Ed.), *Heavy minerals in use*, pp. 3-48. Elsevier, Amsterdam.

Peterson, C. D., P. D. Komar and K. F. Scheidegger. 1989. "Distriburion, Geometry, and Origin of heavy mineral placer deposits on oregon beaches." *J. Sediment. Petrol.* 56(1): 67-77.

# MODELING THE FATE AND TRANSPORT OF RESIDUAL CHLORINE AND CHLORINE BY-PRODUCTS (CBP) IN COASTAL WATERS OF THE ARABIAN GULF

Venkat Kolluru, Shwet Prakash (Environmental Resources Management, Inc., Exton, Pennsylvania) and Eric Febbo (ExxonMobil Research Qatar, Doha, Qatar)

**ABSTRACT:** A 3-dimensional hydrodynamic modeling assessment was undertaken to simulate a thermal mixing zone and predict the fate of residual chlorine and chlorination by-product (CBP) formation for industrial cooling water discharged to the Arabian Gulf. Field surveys and data collection along with laboratory study of chlorine decay and transformation kinetics were accompanied by the development of a hydrodynamic, thermal and chlorine model. Kinetic relationships for chlorine consumption and by-products formation were developed based on field surveys and laboratory analyses. The study developed these relationships using pH, temperature, initial chlorine dosage and natural organic matter (NOM) as independent variables. Decay of residual chlorine and production of CBPs are modeled as a combination of two first order reaction terms that account for fast reacting and slow reacting NOMs. Parameterization of these reaction terms (kinetic rates) was done using regression analyses on the laboratory data. Based on these regression analyses, kinetic relationships were developed for residual chlorine, bromoform, dibromoacetic acid (DBAA), dibromoacetonitrile (DBAN), and monochloroacetic acid (MCAA) as a function of elapsed time since the seawater sample was dosed with a known initial chlorine concentration. Calibration and validation data available from the field data programs were used to test the kinetic relationships and the model's ability to reproduce field measured behavior.

## INTRODUCTION

Several Liquefied natural gas (LNG) production facilities located at the Ras Laffan Industrial City (RLIC) in northeastern Qatar use significant quantities of Arabian Gulf seawater for their non-contact, once-through cooling systems. These cooling systems utilize sodium hypochlorite to prevent biofouling in the pipe system. The chlorinated seawater is returned back to the Gulf after it has circulated through the cooling system. The returned cooling water may contain elevated temperatures, residual chlorine and some chlorine by-products (CBPs). ExxonMobil Research Qatar (EMRQ) and ERM undertook a comprehensive research study to develop an understanding of the transport and fate of residual chlorine and chlorination by-products. The study included extensive field data collection and testing of seawater samples for CBPs, laboratory experiments to quantify the kinetics of CBP formation, and development of a numerical modeling tool that can be used to study transport and fate of the various constituents in the coastal area near Ras Laffan. This paper focuses on the model application including model calibration and validation, and formulations representing CBP kinetics.

## MODEL SETUP

The region of RLIC is highly industrialized with recent expansions of the LNG terminal. The waters off the shores of RLIC in northeastern Qatar receive cooling water discharge from two Liquefied Natural Gas (LNG) operators and a utility company. FIGURE 1**FIGURE 3** shows the location of these discharges in relation to the LNG terminal.

The modeling system employed for the study is the **G**eneralized **E**nvironmental **M**odeling **S**ystem for **S**urfacewaters (GEMSS®). GEMSS® is an integrated system of 3-D hydrodynamic and transport models embedded in a Geographic Information System (GIS) and environmental data system, grid

generator and editor, control file generator, 2-D and 3-D post processing viewers and additional tools such as meteorological and time-varying data generators to aid the modeling process. Three GEMSS® modules: hydrodynamic module (HDM), thermal analysis module (TAM) and chlorine kinetics module (CKM) were used for the study. Additionally, a new atmospheric diffusion module (ADM) was developed to model the volatilization of chlorine and CBPs.
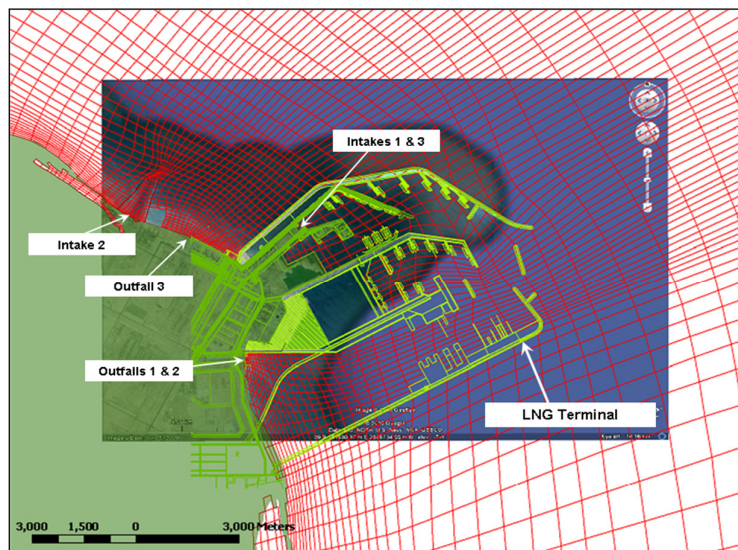


**FIGURE 3     Locations of the LNG terminal and the three outfalls and intakes**

## CHLORINE KINETICS

An extensive literature survey showed that the mechanistic and empirical approaches were normally used in estimating the formation of CBPs from residual chlorine. In the mechanistic approach, a detailed analysis of chemical structure of natural organic compounds in seawater is established to identify which compounds take part in the reactions with chlorine to produce CBPs (McClellan et al., 2000). In the empirical approach, chlorine decay and CBP formation reaction kinetics are established through use of laboratory data interpreted on an assumption of a series of first order reactions (Mok et al., 2005). In the current analysis, empirical formulation methodology was used since the mechanistic approach necessitates the estimation of numerous reaction rates along with substantial field data on water quality as inputs to the model.

The kinetics of chlorine consumption and by products formation reactions are known to depend on the initial residual chlorine concentration, pH, water temperature, and the nature and concentration of natural organic matter in the water (Buttrick, 2005). The significance of each of these factors on the reaction kinetics was investigated in a series of laboratory experiments conducted as part of the overall EMRQ Residual Chlorine Study. The results of those experiments were then analyzed to estimate the values of the various parameters in the empirical kinetic rate equations assumed for the reactions.

Addition of chlorine gas or other chlorine substitutes (e.g. hypochlorite of sodium or calcium, chloramines, chlorine dioxide etc.) to seawater results in a rapid hydrolysis forming hydrochloric acid (HCl) and hypochlorous acid (HOCl) according to equation (1) or (2).

$$Cl_2 + H_2O \rightarrow HCl + HOCl \tag{1}$$

$$NaOCl + H_2O \rightarrow NaOH + HOCl \tag{2}$$

HOCl then reacts with various chlorine demands present in the water, such as natural organic matter (NOM) to produce CBPs as shown in equation (3)**Error! Reference source not found.**.

$$HOCl \quad + \quad Chlorine\ Demand \quad \rightarrow \quad CBPs \tag{3}$$

Several empirical (Haas et al., 1984; Clark and Sivaganesan, 1998; Gang et al., 2003) and mechanistic (Mills et al., 1998: McClellan et al., 2000; Mok et al., 2005) kinetic models have been developed to predict or estimate residual chlorine consumption and CBP production in hydrological systems. An empirical formulation has been used in this study to model the residual chlorine consumption and CBPs formation. A typical empirical model uses a first-order decay model as shown in equation (4) and assumes that there are two types of chlorine demand:

- Shorter-time chlorine demand (SCD) or fast reacting labile NOM
- Longer-time chlorine demand (LCD) or slow reacting refractory NOM

$$C(t) = C_0 \left\{ A e^{-k_1 t} + (1 - A) e^{-k_2 t} \right\} \tag{4}$$

Where $C(t)$ = concentration of free residual oxidant at time $t$;

$C_0$ = initial chlorine (oxidant) concentration or chlorine (oxidant) dosage;

$A$ = fraction of sites on the natural organic matter that are involved in fast reaction (*>0 and <1*)

$k_1$ = first order free residual oxidants decay constant for the fast reaction sites;

$k_2$ = first order free residual oxidants decay constant for the slow reaction sites.

Similarly, the equation for the estimate of CBP concentrations is given in equation (5).

$$C'(t) = C_0 \left\{ A_T \left( 1 - e^{-k_1 t} \right) + B_T \left( 1 - e^{-k_2 t} \right) \right\} \tag{5}$$

The corresponding derivative form of equation (5) is $\dfrac{dC}{dt} = k_{1T} C + k_{2T} C$

Where $k_{1T}$ and $k_{2T}$ are derived growth rates defined by $k_{1T} = \dfrac{A_T k_1}{A}$ and $k_{2T} = \dfrac{B_T k_2}{(1 - A)}$

These relationships formulate decay and formation in terms of parameters that are functionally related to the variables pH, initial concentration of residual chlorine (Co), water temperature (T) and abundance of naturally occurring organic matter (NOM). This parametric relationship can be expressed as shown in equation (6).

$$Parameter = a (pH)^b (C_0)^c (T)^d (NOM)^e \tag{6}$$

Where *Parameter* refers to the decay and formation rates defined in equation (4) and (5) and a, b, c, d and e are coefficients that are obtained using multivariate regression analysis.

Levels of NOM are not easily measurable and, thus, a surrogate should be used for parameterization. This surrogate could be the measurable levels of TOC, DOC or UV254. Usually a combination of these parameters can not be used as it may lead to poor conditioned coefficient estimation (Chowdhury and Champagne, 2008). The surrogate DOC can be estimated using a first-order loss term for oxidation. Carbonaceous Biochemical Oxygen Demand (BOD) in a waterbody is the same as DOC.

However, BOD (or CBOD) is usually defined in terms of oxygen consumption units while DOC is defined in terms of carbon units. Since BOD and DOC refer to the same waterbody property, the two can be used as surrogate for each other. BOD was modeled as part of a water quality module (WQM) which was then converted to DOC for use in chlorine kinetics module. Since BOD concentrations at the open ocean boundaries were not available, a correlation between DOC and salinity was used since discrete measurements were available on these two variables at the ocean boundaries. A study aimed at estimating water column organic carbon in Strait of Georgia, Canada (Johannessen et al., 2008) found that DOC was inversely related to salinity. This relationship was also observed in the Mediterranean Sea (Doval et al., 1999). The relationship obtained from Strait of Georgia modified to represent the salinity ranges in the Gulf is shown in equation (7)

$$DOC = -5.3326 \times S \text{ (ppt)} + 336.92 \tag{7}$$

## CALIBRATION AND VALIDATION

The field study program covered two separate periods: September 3, 2006 to September 12, 2006 and November 26, 2006 to December 4, 2006. The field data collected during September were used to calibrate the model while the field data collected during November/December were used for model validation. Data available for model calibration and validation consisted of continuous monitoring of tidal elevation, currents, temperatures and salinities along with discrete measurements of temperatures, salinities, free residual chlorine and CBPs. These discrete measurements were made during two separate tidal phase: flood and ebb.
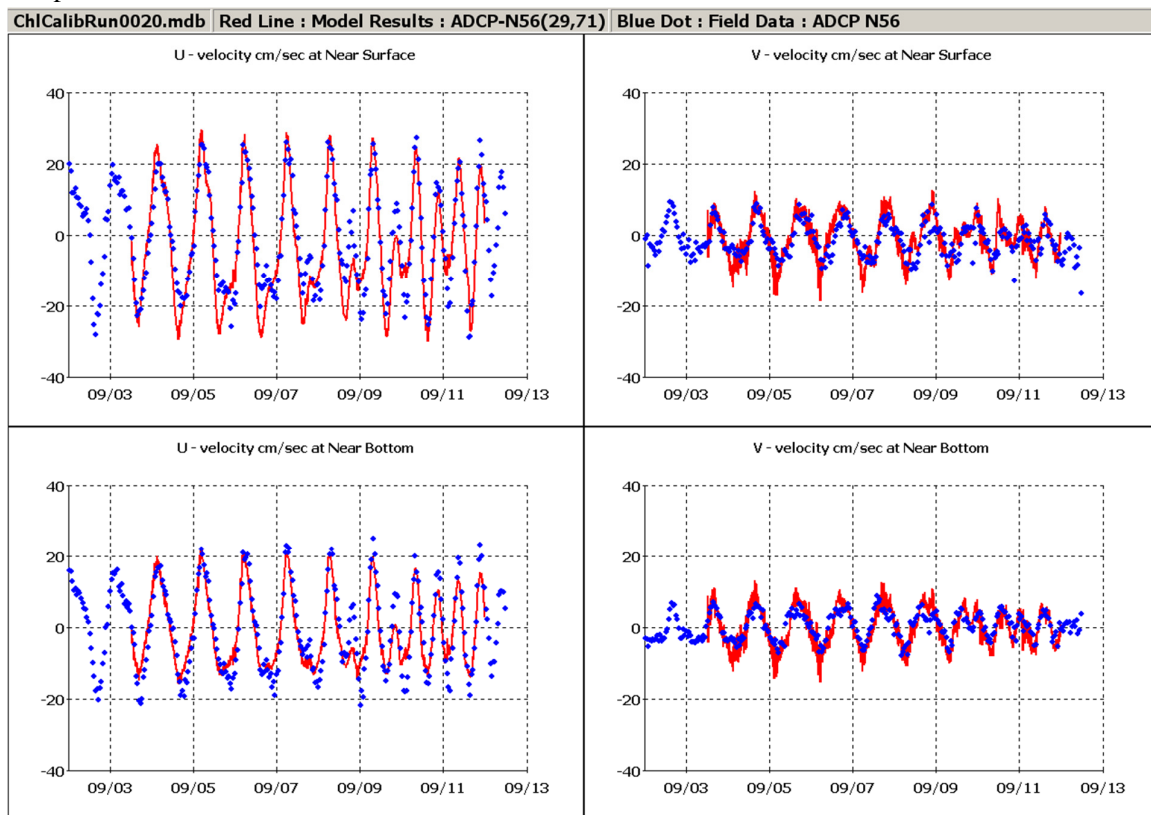


**FIGURE 4**    **Computed (red lines) versus field-measured (blue dots) near-surface and near bottom water velocity components at an ADCP station.**

The model calibration effort involved several steps. The hydrodynamic aspects of the system were the first ones to be calibrated. Next, the model was calibrated against temperature and salinity (variables which affect the water density); and finally, the model was calibrated for free residual chlorine and CBPs. FIGURE 2 shows a comparison of the modeled versus field measured currents at a near-field station where ADCP was installed. The comparison shows good agreement between the model results and field data. Both velocity phase and magnitude match closely with the field observed conditions. Similar agreement was found between modeled results and field measurements at other near-field and far-field stations to suggest that the model is calibrated.

After the model was calibrated for hydrodynamics (currents, temperatures and salinities), it was calibrated against the residual chlorine and CBP data. Measurements for both residual chlorine and CBPs were available at discrete times corresponding to different tidal phases. It was essential to match the concentration predictions from the model to the field observed conditions for the model to be useful. FIGURE 3 shows a comparison of model computed CBP (bromoform and dibromoacetic acid) concentrations with field measurements overlaid. The model performs well in reproducing field observed conditions.

Following the model calibration, model validation was carried out. Same set of comparisons (continuous measurements of tidal elevation, currents, temperatures and salinities and discrete measurements of temperatures, salinities, residual chlorine and CBPs) as calibration were done during the model validation. FIGURE 4 shows the statistical comparison of model computed concentrations for residual chlorine and CBPs compounded at different stations categorized by three regions (region near outfalls 1 and 2, region near outfall 3 and the far-field which covers the entire model study area). The model performs well in reproducing the range of field observed conditions with the exception of dibromoacetic acid where the model over-predicts the concentrations.
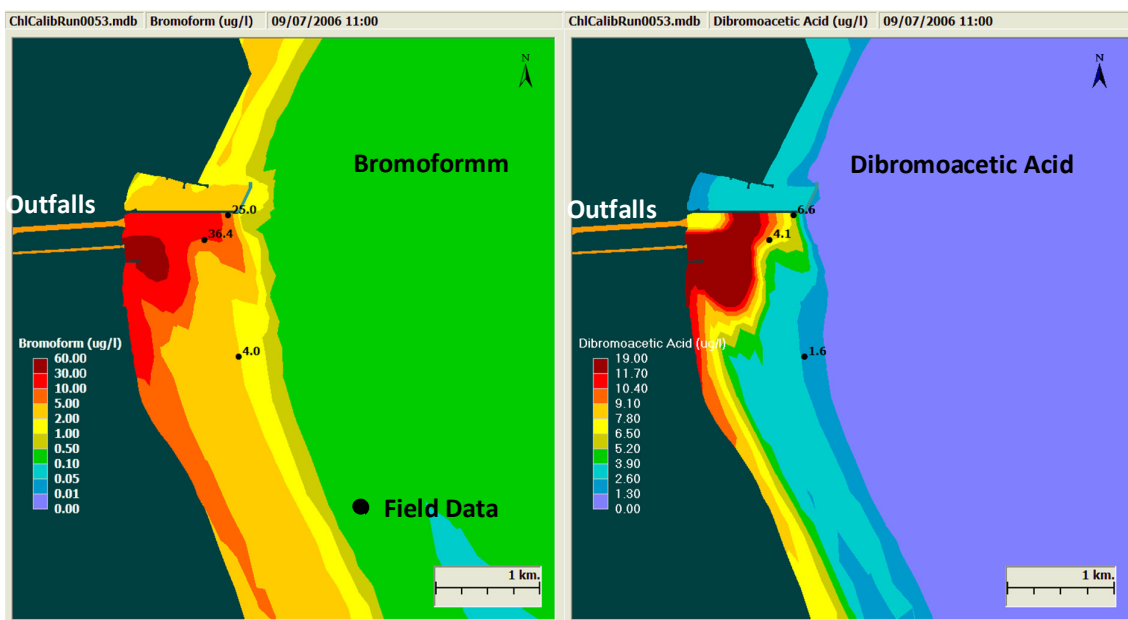


**FIGURE 5      Model computed (colored contour) versus field measured bromoform and dibromoacetic acid on September 7, 2006 at 1100 hours (flood tide)**
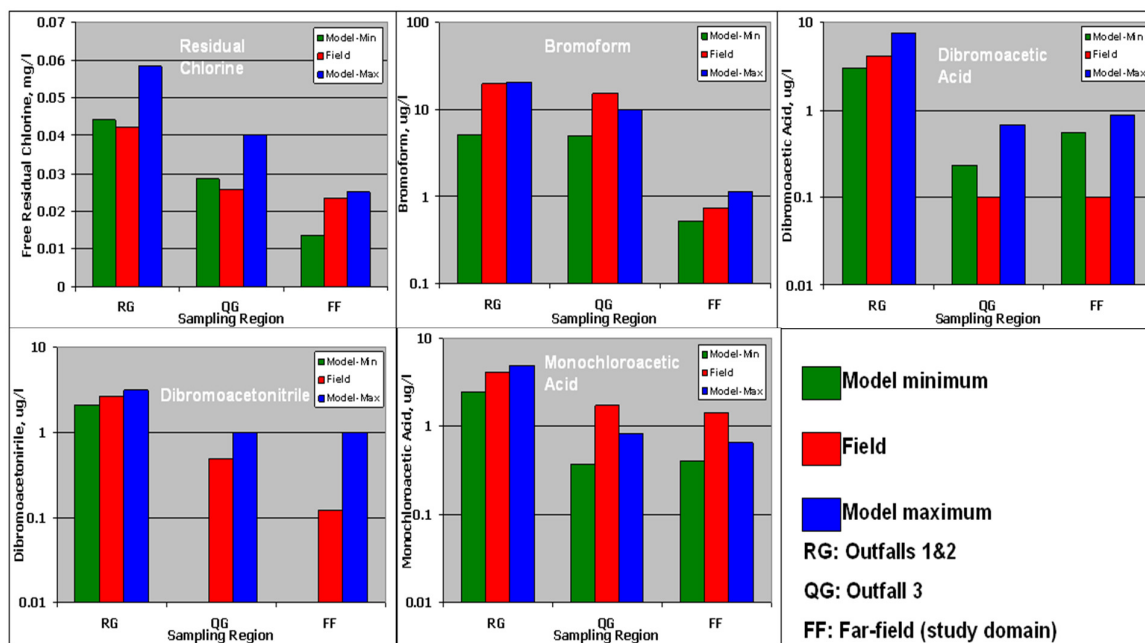
**FIGURE 6** **Comparison of model computed minimum and maximum concentrations (residual chlorine and CBPs) against actual field measurements for validation period during ebb tide.**

## CONCLUSIONS

A numerical computer model was developed to assess transport and fate of free residual chlorine and chlorination by-products (CBPs) associated with discharged cooling water in the Arabian Gulf off the northeastern coast of Qatar. In addition to being able to model hydrodynamics and heat transport, GEMSS-CKM is able to simulate transport of residual chlorine, transformation of free residual chlorine into chlorination by-products, as well as transport of the by-products including their volatilization. Two sets of field data covering two different time periods: September 3 - 13, 2006, and November 24 - December 4, 2006 were used to calibrate and validate the model.

The simulations performed during this study are useful in improving the understanding of circulation and mixing offshore Ras Laffan, and how these affect transport and fate of the chemical constituents in the discharged cooling water. Overall the model performed well in reproducing the field-observed conditions. The calibration and validation simulations produced results that matched field hydrodynamic conditions.

ERM and EMRQ's future research and development plans include extending the model over a longer simulation period (multiple years) to develop eco-risk capabilities. The model could be used to estimate organism exposure to CBPs at documented toxic levels based on laboratory analyses. Similar assessments are being explored for known sensitive ecosystems, including corals. The model also provides the framework to evaluate thermal effects on aquatic habitat based on avoidance temperatures and Upper Incipient Lethal Temperature (UILT). These new ecological risk tools could be used to evaluate environmental impacts from individual, combined or new releases in the study region in the future.

## REFERENCES

Buttrick, D., Tobiason, J.E. and Ahlfeld, D.P. 2005. "Modeling as an Operational Tool for an Unfiltered Surface Water Supply". Proceedings of the American Water Works Association Annual Conference.

Chowdhury, S and P. Champagne, 2010. "An Investigation on Parameter for Modeling THMs Formation". *Global NEST Journal*, Vol. 10, No. 1: 80-91.

Clark, R.M., Sivaganesan, M., 1998. "Predicting chlorine residuals and formation of TTHMs in drinking water". *Journal of Environmental Engineering-ASCE*. 124 (12): 1203–1210.

Doval MD, Pérez FF, Berdalet E. 1999. "Dissolved and particulate organic carbon and nitrogen in the Northwestern Mediterranean". *Deep-Sea Research*. 46:511–527

Gang, D. C., Clevenger, T.E. and S.K. Banerji. 2003. "Modeling Chlorine decay in surface water". *Journal of Environmental Informatics*. Vol 1(1): 21-27.

Hass CN, Karra SB, 1984. "Kinetics of wastewater chlorine demand exertion". *Journal of Water Pollution Conference*, 56(2): 170-173.

Johannessen, S. C, G. Potentier, C.A. Wright, D. Masson and R. W. Macdonald, 2008. "Water Column Organic Carbon in a Pacific Marginal Sea (Strait of Georgia, Canada)". *Marine Environmental Research:* 549-561.

McClellan, John N., David A. Reckhow, John E. Tobiason, James K. Edzwald and Darrel B. Smith, 2000. "A Comprehensive Kinetic Model For Chlorine Decay and Chlorination By-Product Formation". *American Chemical Society, Washington D.C. :* 1-23.

Mills, William B., Christine S. Lew and John Y. Loh, 1998. "Predictions of Potential Human Health and Ecological Risks From Power Plant Discharges of Total Residual Chlorine and Chloroform into Rivers". *Environmental Science and Technology*, v. 32: 2162-2171.

Mok, K.M., H. Wong, X. J. Fan, 2005. "Modeling Bromide Effects on the Speciation of Trihalomethanes Formation in Chlorinated Drinking Water". *Global NEST  Journal* Vol. 7, No 1: 1-16.

# MODELING HYDROLOGICAL IMPACTS OF CLIMATE CHANGE IN DIFFERENT CLIMATIC ZONES

*Fasil Ejigu Eregno* (Norwegian University of Life Sciences, Ås, Norway)
Chong-Yu Xu (University of Oslo, Oslo, Norway)

**ABSTRACT:** Recent advances in hydrological impact studies points that the response of specific catchments to climate change scenario using a single model approach is questionable. This study was aimed at investigating the impact of climate change on three river basins in China, Ethiopia and Norway using WASMOD and HBV hydrological models. Responses were evaluated in terms of runoff, actual evapotranspiration and soil moisture change for incremental precipitation and temperature change scenarios. First, hydrological model parameters were determined using current hydro-climatic data inputs. Second, the historical time series of climatic data was adjusted according to the climate change scenarios. Third, the hydrological characteristics of the catchments under the adjusted climatic conditions were simulated using the calibrated hydrological model. Finally, comparisons of the model simulations of the current and possible future hydrological characteristics were performed. This study demonstrated that the sensitivity of catchments in response to climate change scenario was varied in different climatic regions. The change detected by the two models for the same basin and scenario was also wide-ranging. Our findings thus support a concern that climate change analysis using single hydrological model may lead to unreliable conclusion. In this regard, conducting multi model analysis seems a better approach.

## INTRODUCTION

Climate change can cause significant impacts on water resources by changing the hydrological cycle. The increasing trend of temperature will alter the hydrologic cycle through raising the amounts of water vapour in the atmosphere and as a result, the hydrological cycle will intensified with more precipitation. However, the extra precipitation will be unequally distributed around the globe. Some parts of the world may see significant reductions in precipitation, or alterations in the timing of wet and dry seasons and would lead to increases in both floods and droughts (Seino, Kai et al. 1998). Hydrological models provide a conceptual framework to investigate the relationships between climate, and water resources (Xu 1999). Many studies of the impact of climate change on the hydrology of specific geographic regions using hydrological model had been reported (Dvorak, Hladny et al. 1997; Xu 2000; Jiang, Chen et al. 2007; Steele-Dunne, Lynch et al. 2008). This study attempts to place the hydrological consequences of climate change in three different climate zones using two hydrological models.They are HBV-light, daily water balance model described in (Seibert. J. 1998) and WASMOD, monthly water balance model described in (Xu 2002). The potential of the models for studies of climate change impact on hydrological regimes of river basins is presented in (Xu 1999; Xu 2005).The main objective of this study is to test the magnitude differences one can expect when using different hydrological models in different regions to predict hydrological impact of climate change.

## MATERIALS AND METHODS

**Study Areas and Data.** The study was conducted on three river basins in different continent representing a range of geographic and climatic conditions. 1) Dongjiang river basin, a tributary of the Pearl River in southern China. The area of the river basin is 25,555 Km$^2$ and flows from north-east to south-west direction.2) Didessa river basin, a tributary of upper Blue Nile River in south western Ethiopia.The drainage area of the river basin is 9981 Km$^2$ up to the river gauge near Arjo.3) Elverumbasin, a part of Glomma basin, located in the middle part of Norway. The drainage area of the basin up to Elverum river gauge station is 15449 Km$^2$. In order to evaluate the models performance at different catchment scale, small nested catchments of Shuntian, Dembi, and Hummelvoll which are found within Dongjiang, Didessa, and Elverum basins respectively were also examined. The current climate is represented by

observed climatic data and for Dongjiang basin, areal rainfall was calculated from the records of the 51 stations using the Thiessen polygon method, mean daily temperature from 8 stations and evaporation data from 5 stations for the period of 1978–1988 were organized. For Didessa basin, rainfall data obtained from 10 stations mean daily temperature from 11 stations and evaporation data from 6 stations for the period 1987–1998 were prearranged. For Elverum basin, rainfall data from 13 stations mean daily temperature from 12 stations and evaporation data from 7 stations for the period 1985-1997were organized in order to use as model input.

**Approach.** As it is discussed in (Xu 1999; Xu 2005), this study also follow four steps. 1) The parameters of hydrological models were determined in the study basins using current climatic inputs and observed river flows for model calibration and validation. 2) The historical time series of climatic data was adjusted according to the climate change scenarios. 3) The hydrological characteristics of the catchment under the adjusted climate were simulated using the calibrated hydrological model. 4) Comparisons of the model simulations of the current and possible future hydrological characteristics were performed.

**Climate Change Scenarios.** In order to cover a wide range of possible change in climate variables, ten hypothetical climate change scenarios were derived from combinations of two absolute temperature changes and five relative precipitation changes.

Table 1. Hypothetical climate change scenarios

| Scenarios | 1 | 2 | 3 | 4 | 5 | 6 | 7 | 8 | 9 | 10 |
|---|---|---|---|---|---|---|---|---|---|---|
| $\Delta T$ ($^oC$) | 2 | 2 | 2 | 2 | 2 | 4 | 4 | 4 | 4 | 4 |
| $\Delta P$ (%) | -20 | -10 | 0 | +10 | +20 | -20 | -10 | 0 | +10 | +20 |

**Hydrological Models.** For this study, WASMOD lumped conceptual hydrological model and HBV semi-distributed conceptual models were preferred for their simplicity and flexibility in running with limited data set

*HBV Model:* HBV model was first developed at the Swedish Meteorological and Hydrological Institute and HBV model version used in this study is HBV light (Seibert. J. 1998). As described by Seibert (1998), the HBV model runs on daily time step to simulate daily discharge using daily rainfall, temperature and potential evaporation as inputs. The model has in total 10 parameters and the principal equations are indicated in Table 2.

Table 2.Principal equations of HBV model

$$Melt = CFMAX * (T(t) - TT) \tag{1}$$

$$Refreezing = CFR * CFMAX * (TT - T(t)) \tag{2}$$

$$\frac{recharge}{p(t)} = \left[\frac{SM(t)}{FC}\right]^{BETA} \tag{3}$$

$$E_{act} = E_{pot} * \min\left[\frac{SM(t)}{FC * LP}, 1\right] \tag{4}$$

$$Q_{GW}(t) = K_2 * SLZ + K_1 * SUZ + K_0 * \max(SUZ - SLZ, 0) \tag{5}$$

$$Q_{aim}(t) = \sum_{i=1}^{MAXBAS} C(i) * Q_{GW}(t - i + 1)$$

$$where, c(i) = \int_{i-1}^{i} \frac{2}{MAXBAS} - \left|u - \frac{MAXBAS}{2}\right| * \frac{4}{MAXBAS^2} du \tag{6}$$

*WASMOD Model:* The <u>W</u>ater <u>A</u>nd<u>S</u>now balance <u>MOD</u>eling system (WASMOD) is a conceptual lumped modeling system. The model version used in this study was developed by (Xu 2002). WASMOD is monthly water balance model that requires monthly values of areal precipitation, potential evapotranspiration and air temperature as inputs. The principal equations for the parameters are presented in Table 3.

Table 3 Principal equations for the parameters of WASMOD model

| Snowfall | $st = pt\{1 - \exp[-(ct - a)/(a1 - a2)]2\}+$ | $a1 \geq a2$ | (7) |
|---|---|---|---|
| Rainfall | $rt = pt - st$ | | (8) |
| Snow storage | $spt = spt-1 + st - mt$ | | (9) |
| Snowmelt | $mt = spt\{1 - \exp[-(ct - a2)/(a1 - a2)]2\}+$ | | (10) |
| Potential evapotranspiration | $ept = [1 + a3(ct - cm)]epm$ | | (11) |
| Actual evapotranspiration | $et = \min\{wt[1 - \exp(-a4ept)], ept\}$ | $0 \leq a4 \leq 1$ | (12) |
| Slow flow | $bt = a5(sm+t-1)2$ | $a5 \geq 0$ | (13) |
| Fast flow | $ft = a6(sm+t-1)2 (mt + nt)$ | $a6 \geq 0$ | (14) |
| Water balance | $smt = smt-1 + rt + mt - et - bt - ft$ | | (15) |

$w_t = r_t + sm^+_{t-1}$ is the available water; $sm^+_{t-1}$ is the available storage; $n_t = r_t - ep_t(1 - \exp(r_t/ep_t))$ is the active rainfall; $p_t$ and $c_t$ are monthly precipitation and air temperature respectively; and $ep_m$ and $c_m$ are long-term monthly averages. $a_i (i = 1, \ldots, 6)$ are the model parameters. The superscript plus means $x^+ = \max(x,0)$.

**Model Calibration and Validation**. For HBV model, Monte Carlo procedure was used to investigate the best parameter values using the results of a large number of model runs with randomly generated parameter sets. Using the best parameter, the first one year used as a warm up period to initialize the model before actual calibration and the remaining periods were divided in such a way that two-third of the data was used for the calibration and one-third of the data was used for validation. In the case of WASMOD, an automatic optimization is used. After the specification procedure, two-third of the data was used for calibration and the remaining one-third of the data for validation. It is a common practice to make use of some statistical criteria to evaluate model performance. Among the many model performance indicators, the Nash–Sutcliffe model efficiency coefficient (E), root mean square error (RMSE), relative volume of error (RVE) were performed. Which are defined as:

$$E = 1 - \frac{\sum (Q_{obs} - Q_{sim})^2}{\sum (Q_{obs} - \overline{Q_{obs}})^2} \tag{16}$$

$$RMSE = \sqrt{\frac{\sum_{t=1}^{n} (Q_{obs_t} - Q_{sim_t})^2}{n}} \tag{17}$$

$$RVE(\%) = \frac{\sum (Q_{obs} - Q_{sim})}{\sum (Q_{obs})} \times 100 \tag{18}$$

Where $Q_{obs}$ and $Q_{sim}$ represent observed and simulated discharge respectively, $\overline{Q_{obs}}$ is observed mean discharge and n is a number of observations..

**RESULT AND DISCUSSION**

**Evaluation of Model Performance.** Statistical analysis was conducted to evaluate the performance of the models. In order to compare the statistical performance of the two models, the daily time step result of HBV model is aggregated into monthly values. The result of statistical analysis for the calibration and validation period is presented in Table 4. The value of Nash–Sutcliffe coefficient (E) indicates that both models are performed quite well in all catchments and it ranges from 0.88 to 0.96 for calibration period and from 0.80 to 0.95 for validation period. The corresponding low error (RMSE and RVE) increased the confidence of the models performance to simulate the historical records at acceptable accuracy. Also, the statistical result shows that no significant difference exists between the two models in reproducing the historical records.

**Comparison of Model Simulation.** Four scenarios a) scenario-1, b) scenario-5, c) scenario-6, and d) scenario-10 were selected to discuss the seasonal variability of the change. The results were plotted as a percentage of change for the simulated long-term monthly water balance components. Due to the limit of pages, all the figures cannot be displayed.

Table 4. Model performance statistics obtained during the specified calibration and validation period

| Basins and sub-basins | Model | Calibration | | | | Validation | | | |
|---|---|---|---|---|---|---|---|---|---|
| | | Period | E | RMSE | RVE (%) | Period | E | RMSE | RVE (%) |
| Dongjiang | HBV | 1978-1983 | 0.91 | 15.87 | 1.64 | 1984-1988 | 0.84 | 15.44 | 8.98 |
| | WASMOD | 1978-1983 | 0.91 | 15.57 | -1.09 | 1984-1988 | 0.83 | 16.24 | 4.04 |
| Shuntian | HBV | 1978-1983 | 0.96 | 16.37 | 0.95 | 1984-1988 | 0.95 | 15.53 | -4.42 |
| | WASMOD | 1978-1983 | 0.94 | 21.6 | -2.24 | 1984-1988 | 0.90 | 2.23 | -8.59 |
| Didessa | HBV | 1987-1992 | 0.89 | 11.59 | -0.38 | 1993-1996 | 0.87 | 11.18 | -11.36 |
| | WASMOD | 1987-1993 | 0.89 | 11.6 | -1.2 | 1993-1996 | 0.90 | 11.14 | -5.32 |
| Dembi | HBV | 1987-1993 | 0.88 | 27.55 | 2.38 | 1994-1998 | 0.85 | 25.19 | -16.22 |
| | WASMOD | 1987-1993 | 0.88 | 30.00 | -3.85 | 1994-1998 | 0.87 | 24.5 | -0.88 |
| Elverum | HBV | 1985-1992 | 0.90 | 10.8 | 0.40 | 1993-1997 | 0.90 | 11.40 | -15.5 |
| | WASMOD | 1985-1992 | 0.92 | 11.49 | 2.65 | 1993-1997 | 0.85 | 16.21 | -1.28 |
| Hummelvoll | HBV | 1980-1988 | 0.90 | 12.58 | 0.90 | 1989-1995 | 0.90 | 12.2 | -0.80 |
| | WASMOD | 1980-1988 | 0.89 | 14.93 | -1.87 | 1989-1995 | 0.80 | 17.45 | -8.40 |

*Change in Mean Monthly Runoff:* Fig. 1shows that the magnitudes of change in mean monthly runoff detected by the two models for each scenario are different. However, the patterns of change of the two models result are mainly consistent. In Elverum basin, seasonal variability of runoff change predicted by both WASMOD and HBV models have similar pattern. During late spring, runoff increases in both model prediction and the magnitude of change is higher in WASMOD as compare with HBV model. In April, the spring peak runoff is predicted using both models and in the case of scenario ($\Delta T=+4^o$C $\&\Delta P=+20\%$), the runoff change reached 187% with WASMOD and 120% with HBV models, this reflecting the fact that the temperature increase sufficiently enough to cause snowmelt and the combination of snowmelt with 20% precipitation increase results higher runoff. In Didessa basin, seasonal variability of runoff change predicted by both WASMOD and HBV models have different pattern. Summer runoff (July to September) seems to be more sensitive to precipitation change than temperature change. In Dongjiang basin, the seasonal variation of runoff change is less as compare with the other basins with both models prediction. The pattern of change is similar and the magnitude of change is not large between the two models.

*Change in Mean Monthly Soil Moisture Content:* Mean monthly soil moisture content changes detected by the two models were plotted in Fig. 3and the figure shows that, the patterns of change as well as the magnitude of change between the two models are quite different. Seasonal variation of change is relatively less in Dongjiang basin as compare with the other two and during summer season, the magnitude of change is relatively high in Elverum in both models predictions.

*Change in Mean Monthly Evapotranspiration:* Fig. 4 illustrates changes in mean monthly actual evapotranspiration (AET) and indicates that there is a remarkable difference between the two model prediction and also between the regions. For extreme condition of climate change scenario ($\Delta T = +4^o$C $\&\Delta P = -20$ %), the mean monthly actual evapotranspiration increase up to 4.9 % (October), 20.1 %

(September), and 53.9 % (April) using WASMOD and 9.1 % (May), 40.3 % (November), and 100.7 % (October) using HBV model for Dongjiang, Didessa, and Elverum basins respectively. The seasonal variability of mean monthly actual evapotranspiration change in Dongjiang basin is relatively less as compare with Didessa and Elverum basins for all scenario cases using both models.
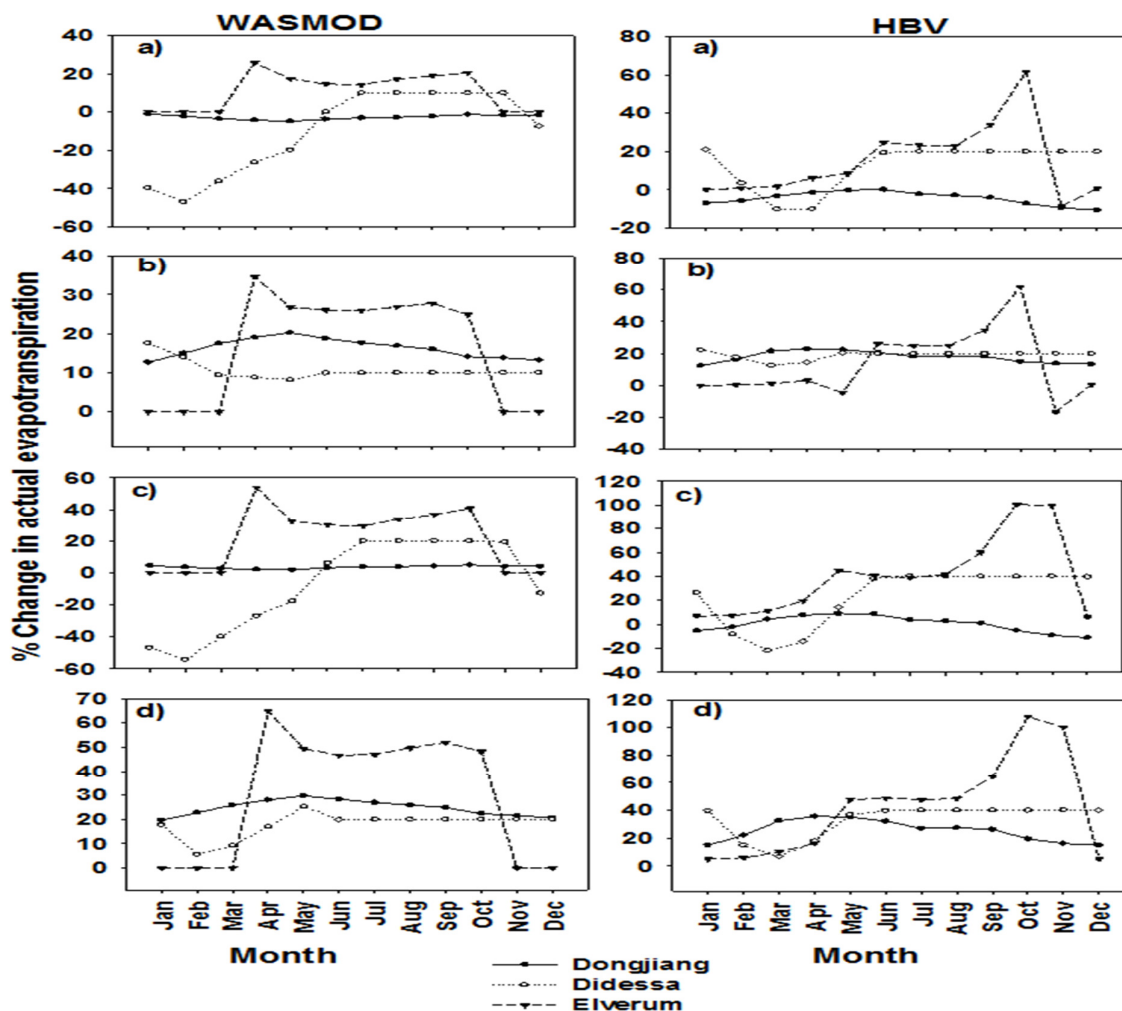


Fig. 1.Comparison of change in mean monthly runoff simulated by WASMOD (left) and HBV (right) for scenarios 1(a), 5(b), 6(c), 10(d).

*Change in Mean Annual Runoff:* Annual runoff is more sensitive for change in precipitation in Didessa basin as compare with other basins under both model predictions (Fig. 4). On the other hand, the annual runoff change in Elverum basin is less sensitive for precipitation change with HBV mode but not observed with WASMOD. Elverum basin is more sensitive for temperature change as compare to the other basins underboth model simulations.

*Change in Mean Annual Evapotranspiration:* Similar to the change in seasonal distribution of actual evapotranspiration, the change in annual evapotranspiration also vary between the regions when climate change scenarios are used to drive the two models. The variation in prediction of annual actual evapotranspiration change between the two models are large under $+4^{o}C$ temperature change scenarios in Dongjiang basin relative to the other basins.

*Change in Mean Annual Soil Moisture Content:* Annual soil moisture content in Didessa basin is more sensitive for precipitation change scenario using WASMOD model as compare to HBV model

simulation. Elverum basin is less sensitive for precipitation change under both model simulations. The magnitude of change between the two models are vary in each basins according to the scenario applied.
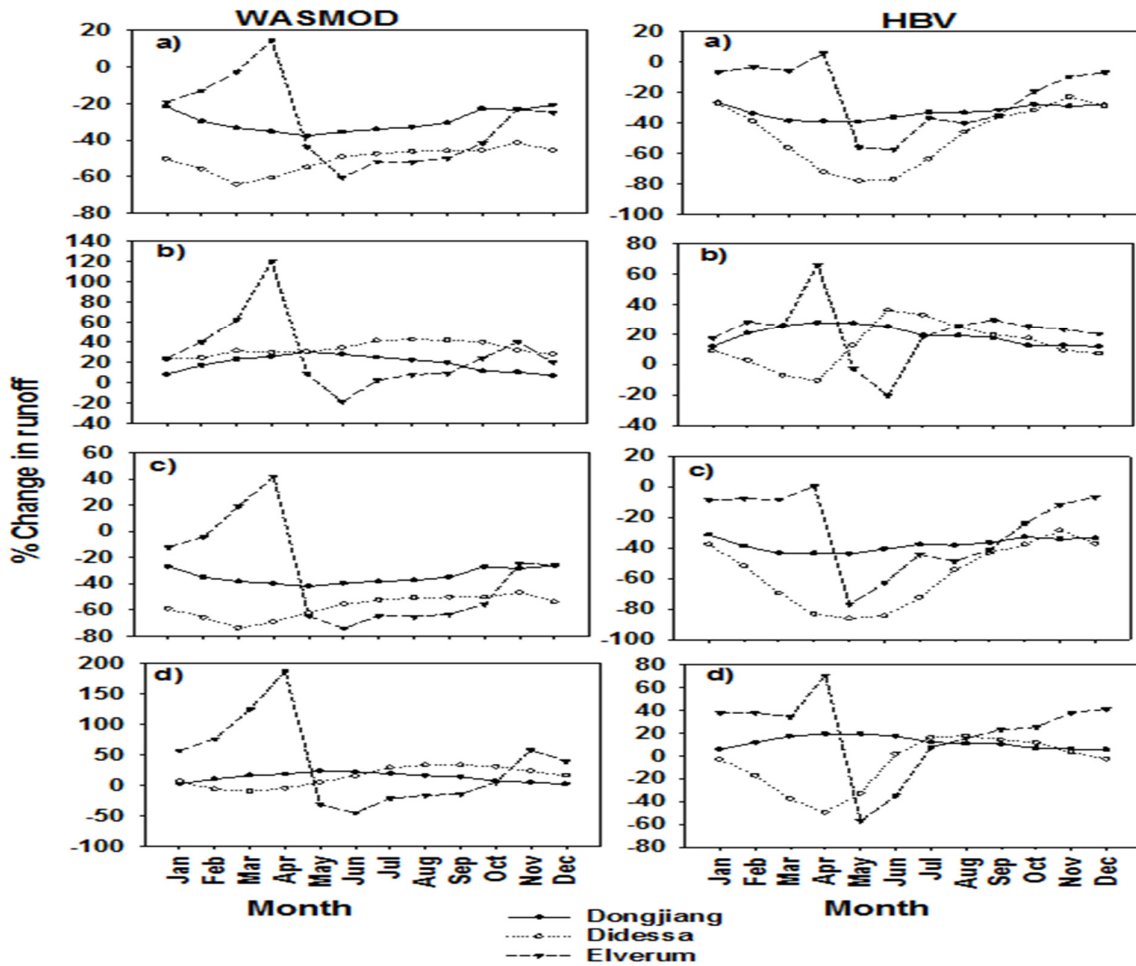


Fig. 2.Comparison of change in mean monthly actual evapotranspiration simulated by WASMOD (left) and HBV (right) for scenarios 1(a), 5(b), 6(c), 10(d).

**CONCLUSION**

The main focus of the study is to test the magnitude differences one can expect when using different hydrological models to simulate hydrological response of climate changes in different climate zones as compared to their capacities in simulating historical water balance components. The result of statistical analysis for calibration and validation shows that both models can reproduce the runoff with acceptable accuracy for each basin. Even though the model performance to simulate the historical time series are within the range of acceptable accuracy, large differences exist between the two models under climate change condition when climate change scenarios incorporated to predicted runoff, actual evapotranspiration and soil moisture. The differences depend on the models, climate change scenarios, the seasons, the region where the study is conducted and the hydrological variables under examination.The result of this study demonstrates that, hydrological impact of climate change predicted by any particular hydrological model represent only the result of that model for the specific region where the study is conducted.Beside to that, this study support concern that hydrological impact of climate change analysis using single hydrological model may lead to unreliable conclusion. In this regard, conducting multi model analysis is one way to give an idea about such uncertainty. Therefore, we recommend further research in this area in order to exhaustively explore hydrological impact of climate change using hydrological models in different regions.
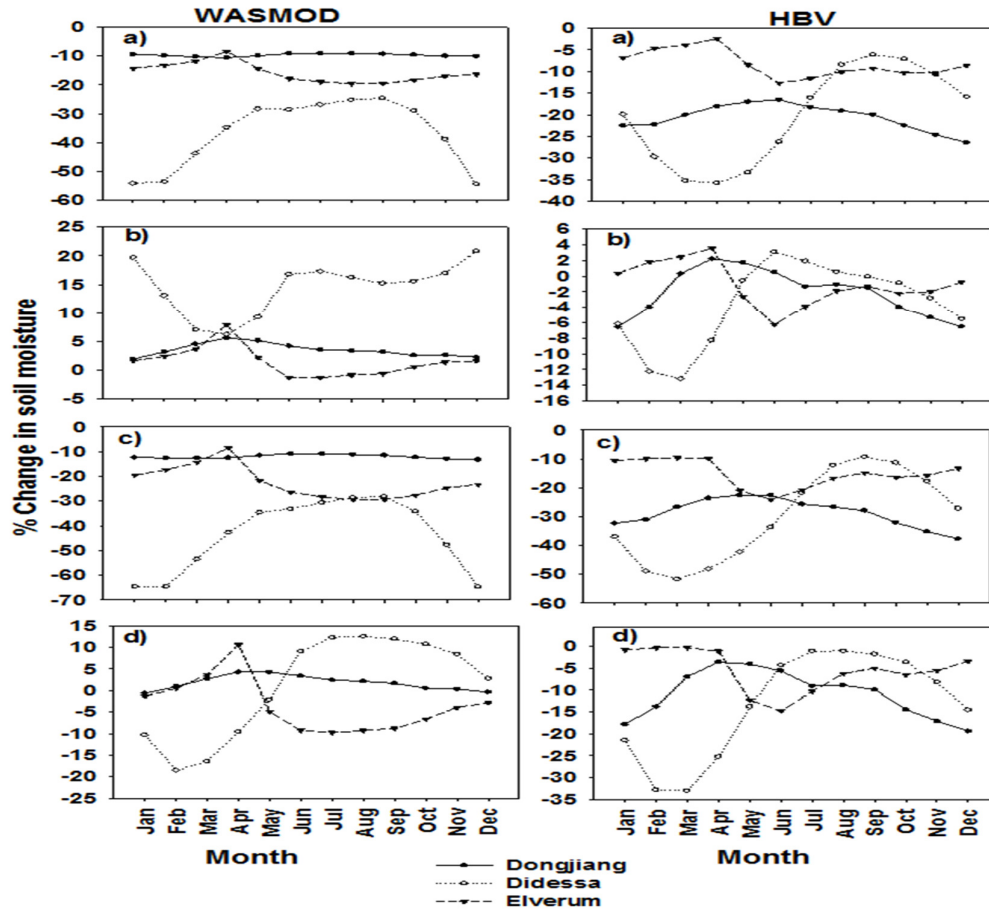
Fig. 3.Comparison of change in mean monthly soil moisture content simulated
by WASMOD (left) and HBV (right) for scenarios 1(a), 5(b), 6(c), 10(d).
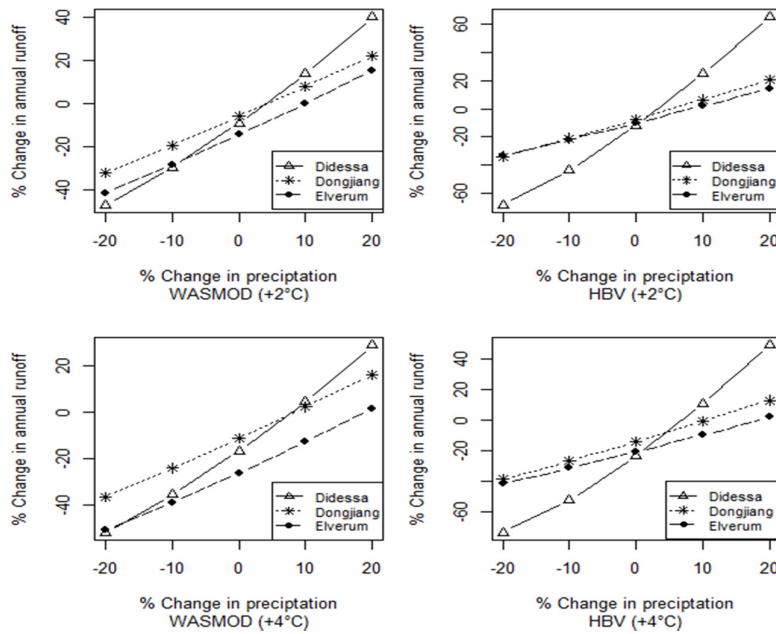


Fig. 4.Comparison of change in annual runoff simulated by WASMOD (left) and HBV (right) models

**ACKNOWLEDGEMENTS**

**REFERENCES**

Dvorak, V., Hladny, J. and Kasparek, L. 1997. "Climate change hydrology and water resources impact and adaptation for selected river basins in the Czech Republic." *Climatic Change*. 36(1-2): 93-106.

IPCC, 2007. *Climate Change 2007*: Synthesis Report, Valencia, Spain.

Jiang, T., Chen, Y.Q.D., Xu, C.Y.Y., Chen, X.H., Chen, X. and Singh, V.P. 2007. "Comparison of hydrological impacts of climate change simulated by six hydrological models in the Dongjiang Basin, South China." *Journal of Hydrology*. 336(3-4): 316-333.

Seibert. J., 1998. *HBV light User's Manual*. Uppsala University, Department of Earth Sciences, Hydrology, Uppsala, 3-16 pp.

Seino, H., Kai, K., Ohta, S., Kanno, H. and Yamakawa, S. 1998. "Concerning the IPCC report (1996): General remarks of research group for impacts of climate change (ICC)." *Journal of Agricultural Meteorology*. 54(2): 179-186.

Steele-Dunne, S., Lynch, P., McGrath, R., Semmler, T., Wang, S.Y., Hanafin, J. and Nolan, P. 2008. "The impacts of climate change on hydrology in Ireland." *Journal of Hydrology*. 356(1-2): 28-45.

Xu, C.Y. 1999. "Climate change and hydrologic models: A review of existing gaps and recent research developments". *Water Resources Management*, 13(5): 369-382.

Xu, C.Y. 2000. "Modelling the effects of climate change on water resources in central Sweden." *Water Resources Management*. 14(3): 177-189.

Xu, C.-Y., 2002. "WASMOD - The Water And Snow balance MODelling system." In: V.P.a.F. Singh, D. K. (Editor), *Mathematical Models of Small Watershed Hydrology and Applications*. pp. 443-476. Water Resources Publications, Colorado, USA.

Xu, C.Y., Widen, E., and Halldin, S. 2005. "Modelling Hydrological Consequences of Climate Change – Progress and Challenges." *Advances in Atmospheric Sciences*. 22(6): 787-797.

# NUMERICAL MODELING OF THE PERFORMANCES FOR HORIZONTAL AXIS TIDAL STREAM TURBINE

Ai Choong Loh, *Yongson Ooi*, Dirk Rilling (Multimedia University, Malacca, Malaysia)
Mohd. Zulkifly Abdullah (Universiti Sains Malaysia, Penang, Malaysia)

**ABSTRACT:** Tidal stream turbines are usually installed in the sea with high tidal currents velocity. Tidal current flows are predictable and therefore it gives a great advantage for power generation, unlike the other renewables, such as wind energy and solar energy, which are more dependent on the weather conditions. The power output of a horizontal axis tidal stream turbine can be obtained by predicting its hydrodynamic performances. A numerical code base on Reynolds-averaged Navier-Stokes equations has been used to analyze the hydrodynamics of the blades for the tidal stream turbine. The three dimensional meshing around the blades with structured and unstructured meshes have been presented. The pressure distributions at various cross-sections of the blade with various tip-speed-ratios have been shown. Separations are observed at certain tip-speed-ratios and it serves as an evident of reducing the coefficient of performance. The results of the numerical models are compared and validated with experiments and they are in good agreement.

## INTRODUCTION

At present, the world energy consumptions are mainly relying on fossil fuel due to its large amonut of energy resources. However, with the decline of fossil fuel reserves, the renewable energies are playing more important role in energy generation, in particular the clean renewables. Among the clean renewables, wind energy, wave energy, and etc., many are greatly dependent on the respond toward the random weather conditions, which are unpredictable. The uncertainty of the amount of energy available is obviously a huge challenge for power generation, where the energy storage will be an additional problem to overcome. Unlike the other renewables, tidal energy is predictable and this is obviously the great advantage for power generation. There are several methods to harvest the tidal energy from the ocean. This paper will focus on harvesting the tidal energy, in particular the harvesting the kinetic energy of the tidal current using the tidal stream turbine. The tidal stream turbine is rather easy to install and lower cost of investment in comparison with its counter part, the tidal dam. The tidal stream turbine is environmental friendly as it is safe for the fishes to pass through owing to its low rotating speed. The tidal stream turbine presented in this paper is the horizontal-axis turbine and this turbine also known as marine current turbine. The analysis of the hydrodynamic performance is crucial to maximize the power output of tidal stream turbine in response to the local tidal stream currents. Numerical analysis using commercialized CFD code has been used to predict the hydrodynamic performances of the tidal stream turbine. The data has been validated with existing experimental results. Local tidal or ocean current data has been used for prediction of the amount of power generated.

## LITERATURE REVIEW

The power generations in Malaysia are mainly depending on natural gas and coal. These fossil fuels are making up the total of more than ninety percent of power generation [1]. With the decline of fossil energy reserves in Malaysia, a long term solution is required to ensure the energy security. Apart from fossil fuels, the hydroelectric power is taking up about five to seven percent of power generation in Malaysia, while the other power generation methods are taking up less than one percent [1]. However the hydropower-dam projects are constantly under criticism due to its impact to the environment. To provide a substantial amount of electrical power and at the same time protect the local environment, more attention has been given to tap the energy from alternative energy sources, in particular from renewables

such as wind, solar, wave and tidal resources. Among the renewables, ocean energy has invaluable energy resource as the peninsular of Malaysia and the two states in East Malaysia has extensive coastline. The forms of ocean energy are tides, surface waves, ocean circulation, salinity and thermal gradients. Among the energies, the kinetic energy of the tidal currents and the surfaces wave energy are the potential energies for power generation [2]. The predictability of tidal current has provided a great advantage for power generation compared to other renewables. Some studies were carried out to identify the potential harvesting the ocean energy for power generation in Malaysia. The Princeton Ocean Model was used to create a three-dimensional numerical ocean model for Malaysia. With the data of tidal speed and tidal elevation available, the potential areas of installing the tidal stream turbines and the amount of power generated can be estimated [3]. Tables of tides forecasting and observation published by the Department of Survey and Mapping Malaysia can be used as the reference for tidal currents data prediction [4].

At present, the methods used to harvest the kinetic energy of ocean current are adopted from well-established wind turbine technology where the experimental data as well as the numerical models are widely available. The Unsteady Aerodynamics Experiment (UAE) has provided information of the full scaled three-dimensional aerodynamics of the horizontal axis wind turbine. These data can be used to validate numerical models for designing and developing advanced wind energy turbines [5]. Numerical models of the effect of various wind speeds at a fixed blade pitch angle using unsteady Reynolds-Averaged Navier-Stokes (RANS) and Detached Eddy Simulation (DES) have been evaluated and both models showing minor differences in the averaged forces and moments [6]. Although the basic principles of aerodynamics and hydrodynamics are similar, however a practical large scaled system for harvesting the kinetic energy of ocean current designed in a cost-effective way has yet to be developed [7]. Tidal current data from Race of Alderney in Channel Islands has been used to run simulations of the tidal stream turbine over various flow regimes and produced the energy capture with time [8]. In Raz de Sein (Brittany, France), Matlab Simulink is used to model the tidal stream turbine system. With the rotors placed strategically in the regions of high velocity flow, the extractable power can be evaluated [9].

Flows over the tidal stream turbine are three dimensional and unsteady. The experimental studies are time consuming and costly. The numerical modeling is the solution of the time and the cost constraints of the experimental methods. The numerical approaches typically are Reynolds Average Navier-Stokes (RANS), Large Eddy Simulation (LES), Direct Numerical Simulation (DNS), and etc. There is no single turbulence model is universally accepted as being superior for all classes of problems [10]. The numerical models developed are useful for the investigation of the hydrodynamic performances for the newly designed tidal stream turbines. Numerical models are required to be validated by experimental results. For example, the numerical model is compared with experiment data obtained from a tested prototype of 800 mm diameter rotor carried out in a cavitation tunnel [11]. A study on the power, thrust and cavitation characteristics of 1/20 scaled model of a 16 m diameter horizontal axis tidal turbine has been carried out in a cavitation tunnel for different blade pitch settings. The results have been compared with the simulations based on blade element momentum theory [12], [13]. In addition, the tidal stream turbines placing in the form of array in the tidal current farm have been investigated by placing multiple turbines behind one another. The inflow conditions of the downstream turbines are depending on the wake and blockage effects of the upstream turbines [14], [15].

## TURBINE BLADE DESIGN AND NUMERICAL MODELS

There are several areas in Malaysian, most likely in Sabah and Sarawak have relatively high tidal current velocity, as high as reaching 2.0 m/s for a significant number of hours base on the data published by the Department of Survey and Mapping Malaysia and the tidal current modeling results from local researchers. The tidal current velocity is the important parameter for power generation as the amount kinetic energy in the tidal stream is proportional to the power of three of the stream velocity. As such, the power generation of the tidal stream turbine is optimized by designing the turbine at the higher site of the local tidal current velocity rather than the average velocity. The diameter of the turbine rotor will be limited by the depth of the sea water. The hydrodynamics performances of the turbine were predicted by numerical models. In order to validate the numerical models, two-dimensional flow experiments have been carried out in the flow channel at National Hydraulic Research Institute of Malaysia. In addition, the three-dimensional experimental data from literature [12] were used to validate the numerical models. Therefore, the blade of 400 mm is selected for the modeling and the designed blade for the tidal stream

turbine is shown in Figure 2. The blade has the sectional profile interpolated from NACA 63-812, 63-815, 63-818, 63-821, and 63-824. The geometry of the turbine blade is shown in Table 1.
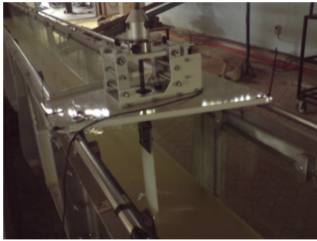


**FIGURE 1.** Two-dimensional experiment setup in the flow channel at NAHRIM
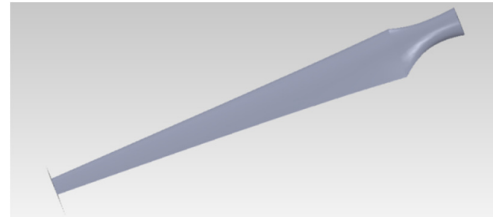


**FIGURE 2.** Blade design of the tidal stream turbine

**TABLE 1.** Geometry of the designed turbine blade

| Radius ratio, r/R | Chord ratio, c/R | Twist angle, $\Theta$ (°) | Radius ratio, r/R | Chord ratio, c/R | Twist angle, $\Theta$ (°) | Radius ratio, r/R | Chord ratio, c/R | Twist angle, $\Theta$ (°) |
|---|---|---|---|---|---|---|---|---|
| 0.20 | 0.1250 | 15.0 | 0.50 | 0.0969 | 3.9 | 0.80 | 0.0688 | 0.9 |
| 0.25 | 0.1203 | 12.1 | 0.55 | 0.0922 | 3.1 | 0.85 | 0.0641 | 0.6 |
| 0.30 | 0.1156 | 9.5 | 0.60 | 0.0875 | 2.4 | 0.90 | 0.0594 | 0.4 |
| 0.35 | 0.1109 | 7.6 | 0.65 | 0.0828 | 1.9 | 0.95 | 0.0547 | 0.2 |
| 0.40 | 0.1063 | 6.1 | 0.70 | 0.0781 | 1.5 | 1.00 | 0.0500 | 0.0 |
| 0.45 | 0.1016 | 4.9 | 0.75 | 0.0734 | 1.2 | | | |

The rotor of the tidal stream turbine consists of three blades. Since the blades are symmetry, only one-third of the flow region is consider for modeling in order to save computation time. The flow region is approximately one-third of a cylinder consists boundary conditions illustrated in Figure 3. The far field distance is double the radius of the rotor to eliminate the wall effect. The inlet velocity is set as 1.73 m/s as it is close to the selected site of interest, Tanjung Karang, Malaysia. The SST $k - \omega$ turbulence model has been selected as it gives a good behavior for separation of the boundary layer. The simulations were carried out using the commercial CFD codes (ANSYS CFX).
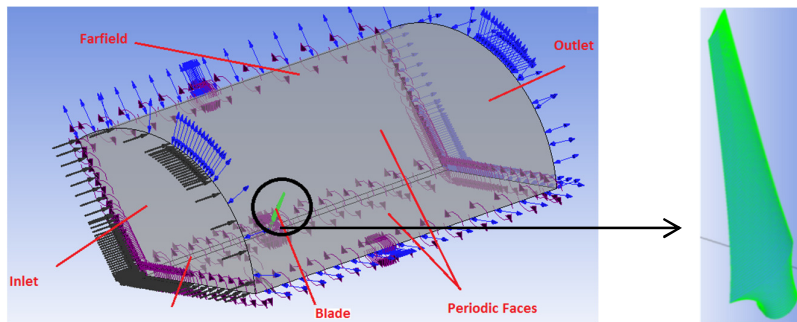


**FIGURE 3.** Flow region and the boundary conditions of the numerical model and the enlarge view of the blade with the surface meshing

The flow region is discretized by structural meshes. The surface meshing of the blade and the hub are shown in Figure 4 and Figure 5 respectively. In the earlier stage, the mesh was constructed using tetrahedron elements or unstructured mesh. The tetrahedron elements are able to accommodate well with complex curvature without much difficulty, however the resolution of the tetrahedron elements in the boundary layer on the blade is the main drawback. In the boundary layer, the variation of velocity in the direction perpendicular to the blade surface is much greater than the variation along the blade surface. For this reason, the structural mesh is selected and constructed with the aid of commercial CFD meshing tool (ANSYS ICEM CFD 12.1). The sectional view of meshing around the blade at the tip is shown in Figure 6. The boundary layer meshing of the blade near the leading and tailing edge are shown in Figure 7 and Figure 8 respectively. The structural meshes consist of 4,2820,078 hexahedron elements ranging from

very small boundary layer elements near the turbine blade and coarse elements toward the far field away from the blade. In general, the meshes quality is acceptable since 99% of the elements having equiangular skewness of above 0.30.
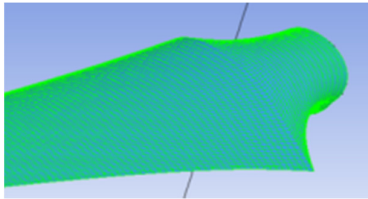


**FIGURE 4.** Structural surface meshing of the blade
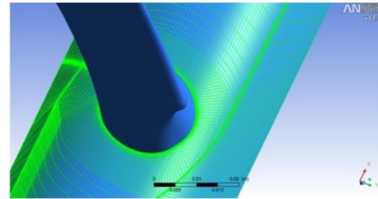


**FIGURE 5.** Surface meshing of the hub
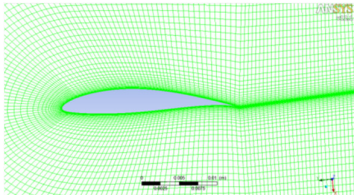


**FIGURE 6.** Sectional view of meshing around the blade at the tip
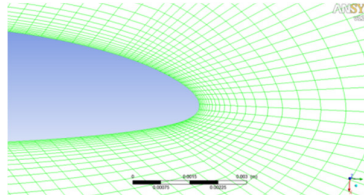


**FIGURE 7.** Boundary layer meshing of the blade nears the leading edge
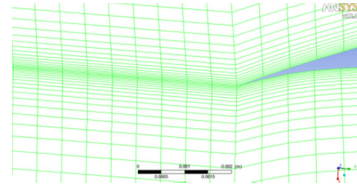


**FIGURE 8.** Boundary layer meshing of the blade nears the trailing edge

## HYDRODYNAMICS PERFORMANCES

Numerical models are important to predict the hydrodynamics performances of the tidal stream turbine and hence to determine some important design parameters. As such, the pressure distributions, velocity vectors, and the streamlines at the blade section are observed. The convergence criteria are set as $10^{-2}$ for monitored torque value while other criteria are set as $10^{-6}$.
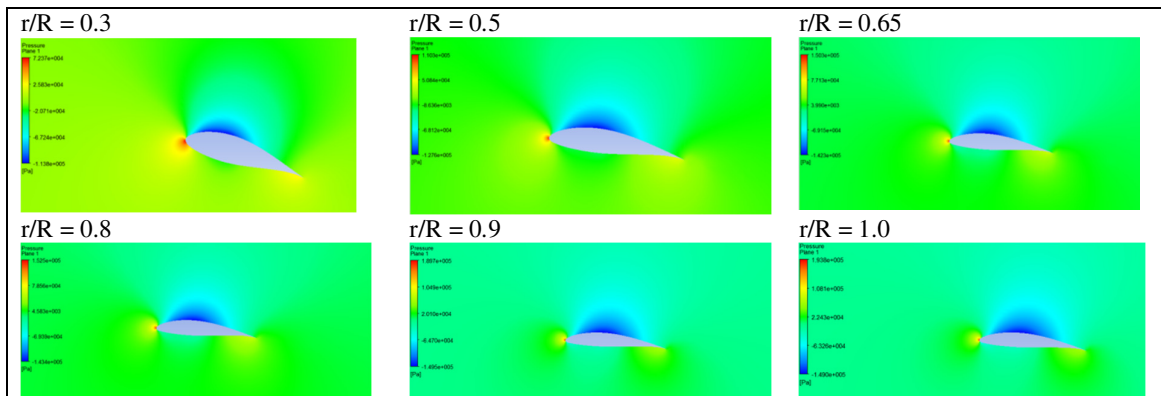


**FIGURE 9.** Blade section pressure distribution at various locations for TSR 5
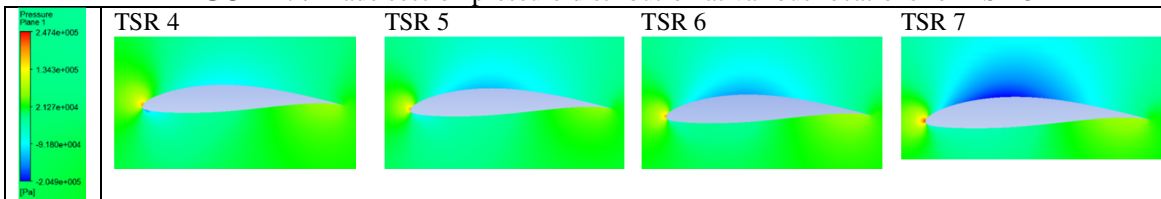


**FIGURE 10.** Pressure distributions at the tip for various tip speed ratio

The pressure distribution chart in Figure 9 and Figure 10 show that the pressure is lower on the upper side of the blade compared to the lower side. Therefore, upward lift force is acting on the blade. At various locations along the blade, the pressure distribution changes and at location closer to the hub (r/R = 0.3), the blade experience the greatest pressure different compared to the other locations shown in the

figure. Referring to Figure 10, the pressure has greatest different at higher tip-speed-ratio. Therefore, the total lift force applied on the blade increases when the turbine is rotating faster. However, the lift force reduces when separation occurred. The pressure distribution can be used for analyzing the stresses on the blade, and hence determine the material selection of the blade. However, the stress analysis of the turbine blade will not be discussed in this paper.

The pressure distributions in the radius direction of the blade are shown in Figure 11. Along the radius direction, the pressure increase toward the tip of the blade on the upper surface while not much variation is observed on the lower surface of the blade.
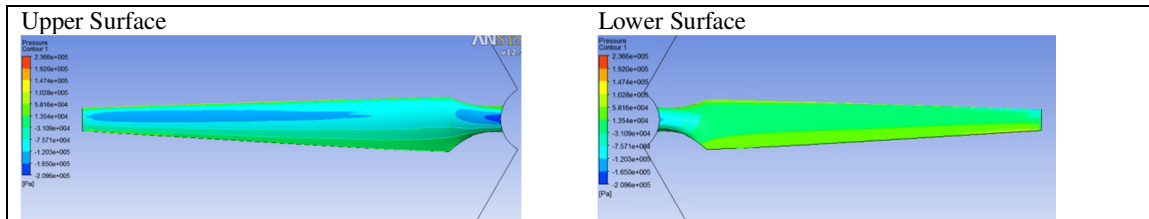


**FIGURE 11.** Blade surface pressure distributions at TSR 5

The streamlines of the blade section show that no separation occurs for the four observed tip speed ratio at the tip as shown in Figure 12. However, moving further away from the tip toward the axis of rotation along the direction the radius of the rotor, separations are observed at all the four selected tip speed ratio. The variation of velocity vector field for TSR 5 is illustrated in Figure 13. At the tip speed ratio of 5, the separation is observed at r/R = 0.65, which is very similar to the results obtained from the simulated model of the wind turbine [16]. The separations are occurring at the radius ratio between 0.65 and 0.70 for the selected tip speed ratio, (TSR 4 - TSR 7).
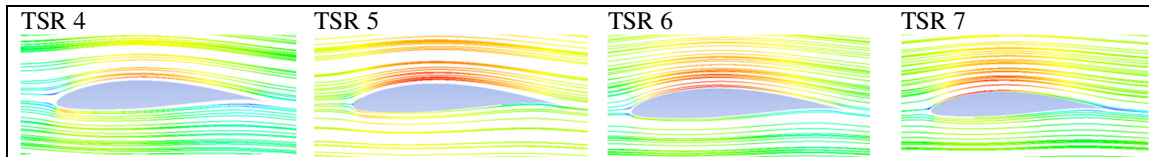


**FIGURE 12.** Streamlines of the blade section at the tip for various tip speed ratio
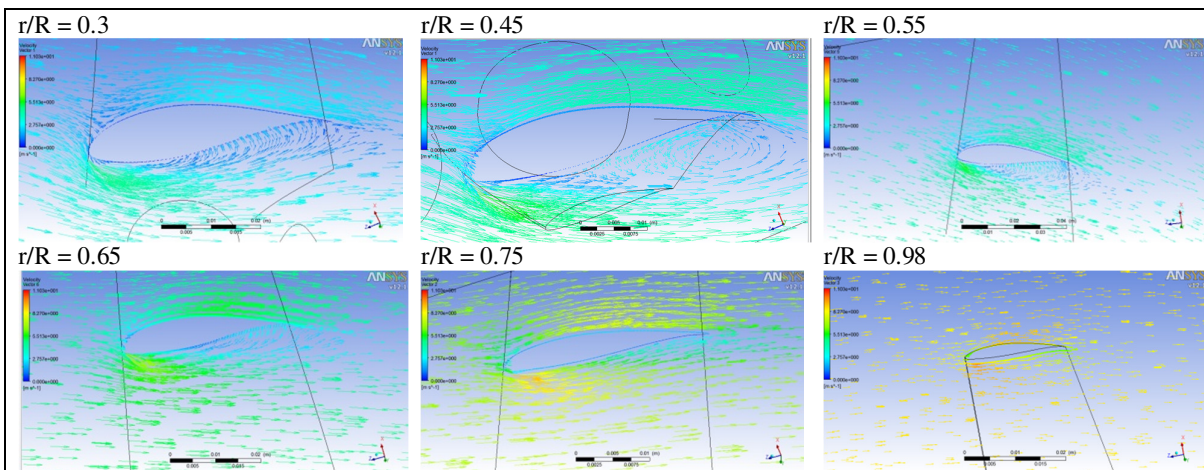


**FIGURE 13.** Velocity vector field near the blade at various locations for TSR 5

The torque exerted on the blade is computed by integrating the pressure force and the viscous force across the blade. The contribution of viscous force is much smaller than the pressure force. The power coefficient is obtained by

$$C_p = \frac{\tau\omega}{\frac{1}{2}\rho A U^3}$$

where $\tau$ is the torque, $\omega$ is the angular speed of the rotor, $\rho$ is the density of sea water, $A$ is the sweep area of the rotor, and $U$ is the tidal stream velocity. The torque exerted on the blade and the power coefficient at various tip speed ratio are shown in Table 2. The power coefficient for TSR 7 is 0.46841 and it is quite close to the Betz limit.

**TABLE 2.** Torque and power coefficient at various tip speed ratio

|  | $\tau$ (Nm) | $C_p$ |  | $\tau$ (Nm) | $C_p$ |
|---|---|---|---|---|---|
| TSR 3 | 4.13421 | 0.041538 | TSR 6 | 14.9800 | 0.30102 |
| TSR 4 | 7.03782 | 0.094282 | TSR 7 | 19.9800 | 0.46841 |
| TSR 5 | 10.6588 | 0.178488 |  |  |  |

The hydrodynamics performances of the actual scale model can be obtained easily by up scaling the numerical models. The amount of available energy resource from a specific location by installing the tidal stream turbine can be predicted. With these data, the returns of the tidal stream turbine power plant investment can be measured. On the other hand, the threat of tidal stream turbine to the marine wildlife may be the main environmental issue to be addressed.

## CONCLUSIONS

The separation location is observed to be independent from the tip speed ratio. The power coefficient is close to the maximum at tip speed ratio of 7. Hence, the amount of power generated using the designed rotor can be estimated for the selected site.

## ACKNOWLEDGEMENT

## REFERENCES

[1] Energy Commission (2011). The Energy Commission Annual Report 2010, Energy Commission, Malaysia.

[2] A. S. Bahaj (2011). Generating electricity from the oceans. *Renewable and Sustainable Energy Reviews 15*, 3399-3416.

[3] Y. S. Lim, S. L. Koh (2010). Analytical assessments on the potential of harnessing tidal currents for electricity generation in Malaysia. *Renewable Energy 35*, 1024-1032.

[4] Department of Survey and Mapping (2011). The Table of Tides Forecasting and Observation in Malaysia 2011. Department of Survey and Mapping, Malaysia.

[5] M. M. Hand, D. A. Simms, L. J. Fingersh, D. W. Jager, J. R. Cotrell, S. Schreck, S. M. Larwood (2001). Unsteady Aerodynamics Experiment Phase VI : Wind Tunnel Test Configurations and Available Data Campaigns. National Renewable Energy Laboratory, US Department of Commerce, Springfield.

[6] Y. Li, K. J. Paik, T. Xing, P. M. Carrica (2011). Dynamic overset CFD simulations of wind turbine aerodynamics. *Renewable Energy 37*, 285-298.

[7] P. L. Fraenkel, (2002). Power from marine currents. *Proceedings of The Institution of Mechanical Engineers Part A - Journal of Power and Energy 216*, 1-14.

[8] L. E. Myers, A. S. Bahaj (2005). Simulated electrical power potential harnessed by marine current turbine arrays in the Alderney Race, *Renewable Energy 30*, 1713-1731.

[9] S. E. B. Elghali, R. Balme, K. L. Saux, M. E. H. Benbouzid, J. F. Charpentier, F. Hauville (2007). A Simulation Model for the Evaluation of the Electrical Power Potential Harnessed by a Marine Current Turbine, *IEEE Journal of Oceanic Engineering 32*, 786-797.

[10]   J. H. Ferziger, M. Peric (2001). Computational Methods for Fluid Dynamics. Springer. New York.

[11]   W. M. J. Batten, A. S. Bahaj, A. F. Molland, J. R. Chaplin (2008). The prediction of the hydrodynamic performance of marine current turbines, *Renewable Energy 33*, 1085-1096.

[12]   A. S. Bahaj, A. F. Molland, J. R. Chaplin, W. M. J. Batten (2007). Power and thrust measurements of marine current turbines under various hydrodynamic flow conditions in a cavitation tunnel and a towing tank, *Renewable Energy 32*, 407-426.

[13]   W. M. J. Batten, A. S. Bahaj, A. F. Molland, J. R. Chaplin (2007). Experimentally validated numerical method for the hydrodynamic design of horizontal axis tidal turbines, *Ocean Engineering 34*, 1013-1029.

[14]   L. Myers, A. S. Bahaj (2007). Wake studies of a 1/30th scale horizontal axis marine current turbine, *Ocean Engineering 34*, 758-762.

[15]   S. R. Turnock, A. B. Phillips, J. Banks, R. F. N. Lee (2011). Modelling tidal current turbine wakes using a coupled RANS-BEMT approach as a tool for analysing power capture of arrays of turbines. *Ocean Engineering 38*, 1300-1307.

[16]   Yuwei Li, Kwang-Jun Paik, Tao Xing, Pablo M. Carrica (2012). Dynamic overset CFD simulations of wind turbine aerodynamics. *Renewable Energy 37*, 285-298.

# A NOVEL MATHEMATICAL 'SUSTAINABLE UNIVERSITY MODEL'. THE BARCELONA INDUSTRIAL ENGINEERING SCHOOL CASE

*Yolanda Bolea* and Antoni Grau, (Technical University of Catalonia at Barcelona, Spain)

In front the serious environmental crisis is crucial to adopt measures to face the sustainability issue and to change the present unsustainable actions in the world. Education, and specifically the University, plays an important role in such a task. For this reason, the University must adopt the compulsory competence in "Sustainability and Social Commitment" in the teaching (its Degrees) and research as well as in the campus life. The Technical University of Catalonia (UPC) is leading a process of teaching future professionals that adopt sustainable solutions in their working and personal life. To build a Sustainable University, administrators must take actions, decisions and policies in this direction, and they need some assessment tools that indicate them the right path.

In this work we present such a tool, a simulator, able to forecast the sustainable behavior of the Institution. The tool is based on a novel mathematical model that will be used to study and analyze how sustainable is the University, and it could be used as an indicator (quantifiable) of sustainability. Depending on the value of this indicator, University administrators can take decisions and manage efficiently resources in order to achieve the excellence in sustainability.

This model has been validated at the Barcelona Industrial Engineering School with historical data with satisfactory results. Different cases have been studied for this School with the objective of a suitable sustainable management.

The developed mathematical model is based in considering the University as a system in which the results of its actions are its inputs, that is, considering it as an autoregressive system AR. The variables taken into account are:

   * Students: they are divided into 2 groups: those with a sustainable behavior and with an unsustainable behavior.
   * Education for the Sustainability. This variable is formed with two parts: the sustainable curricular education, and sustainable infrastructures that influence the university community.
   * Unsustainable capital, it refers to the infrastructures, services and budgets that are assigned to the University in an unsustainable manner.

To realize the model different parameters have been considered such as the number of subjects that takes into account the sustainability in their syllabus, the ratio of students that have sustainable conducts in front other students and faculty, the recovery in infrastructure investments and many others. All these parameters have been experimentally and heuristically obtained.

Finally, a 4-Ordinary Differential Equations system has been obtained and implemented using an specific simulation software (Easy Java Simulation); the results of the simulation have been successfully validated with data of previous years and we can conclude that the simulation can be valid to forecast the Sustainable behavior of our institution for the next years.

# EVALUATING COMBINED TOXICITY OF MULTI-COMPONENT MIXTURE USING A COMPREHENSIVE MODEL

*Li-Tang Qin*, *Shu-Shen Liu*, and Qing-Sheng Wu

(Tongji University, Shanghai, PR China)

It is commonly accepted that the effect of chemicals on human health mainly comes from exposures to mixtures rather than from individual chemicals. Despite the huge amount of effort made for the determination of chemical mixtures, an accurately estimation and prediction of mixture toxicity remain a challenging objective. Currently, two reference models, concentration addition (CA) and independent action (IA), have been employed to predict the potential combined effects of chemicals. The accuracy of mixture toxicity predictions using the CA and IA models, however, need to be resolved before their use in risk assessments. We had built a new comprehensive model (ICIM), which combines CA with IA based on the multiple linear regression, for predicting the toxicities of multi-component mixtures. The aim of this study is to examine the applicability of the ICIM in evaluate the toxicity of mixtures.

The microplate toxicity analysis was used to determine the concentration-response curve (CRC) of 46 individual chemicals and their 77 mixtures causing acute toxicity to freshwater photobacterium, *V. qinghaiensis* sp.-Q67. 77 mixtures include four antagonism mixtures of nine heavy metal compounds, seven noninteractive and two interactive mixtures consisted of six pesticides, 13 noninteractive mixtures of five herbicides and four heavy metal compounds, 11 noninteractive mixtures and two interactive mixtures of ten substituted phenols, ten noninteractive mixtures of six organophosphorus insecticides, and 28 noninteractive mixtures of 12 substituted phenols and ten substituted amines. The experimental designs of mixtures were designed by uniform design concentration ratio and equivalent-effect concentration ratio method. Toxicity tests and relative light units of all chemicals and mixtures were performed on the VeritasTM luminometer (Turner BioSystems Inc., USA) or the SpectraMax M5 reader (Molecular Devices Inc., USA) with a 96-well microplate. The CRCs of all single-compound and mixtures were modeled by fitting the experimental data to a Weibull or Logit function. 77 ICIM models were developed using the effect concentrations of the 77 mixtures calculated from CA and IA. The correlation coefficient ($r2$) values are higher than 0.99 and leave-one-out cross-validation correlation coefficient ($q2$) values are higher than 0.97 for all models. The results showed that the ICIM model can accurately evaluate the toxicities of the 77mixtures, and its evaluated ability appears to be better than CA and IA. In addition, the ICIM model is available to evaluate not only the response at EC50 (effect concentration of the mixture provoking 50% effect) but also those at the other EC*x*s. It can be said that the ICIM model is a powerful tool to evaluate the mixture toxicity, and maybe offer an important approach in risk assessment of chemical mixture.

# ESTIMATION OF MISSING VALUES WITH DIFFERENT MISSINGNESS MECHANISM

*Fadhilah Yusof*, Ho Ming Kang  and Ismail Mohamed
(Universiti Teknologi Malaysia, Johor , Malaysia)

In this study data-sets with different missingness mechanism namely Missing Completely At Random (MCAR), Missing At Random (MAR) and Missing Not At Random (MNAR) were simulated accordingly. To treat the missing data from these three missingness mechanism two methods were used namely Expectation maximization (EM) algorithm and mean imputation (MI). The performances are evaluated by using the mean absolute error (MAE) and root mean square error (RMSE) values obtained. The results showed that EM was able to estimate the missing data with minimum errors as compared to mean imputation (MI) for the all the three missingness mechanisms. However the graphical results showed that in actual situation EM was unable to estimate the missing values in the missing quadrants when the missingness mechanism is MNAR. Hence, the MNAR missingness mechanism would require other methods other than EM or MI to treat the missing data problem.

# REGIONAL DATA HUB AND TIME SERVICES TO SUPPORT FLASH FLOOD SITUATIONAL AWARENESS

Stefan Fuest (KISTERS AG – Aachen, Germany)
Matt Ables, **Phil Stefanoff** (KISTERS North America, Citrus Heights, CA, USA)
David Maidment (University of Texas at Austin, Austin, TX USA)

Emergency management is an interdisciplinary field dealing with strategic organizational management processes that rely on timely information, situational awareness, and quick decision making. Flood emergency management, in particular, is very often organized on a regional level to provide the necessary scope for getting information, understanding the situation, making decisions, and providing information about the status and decisions to others. However, other regional decision makers need to also take advantage of the information provided by the flood warning centre, as well as from other sources. This process results in a mesh of dependencies which is not strictly hierarchical anymore, and can lead to delays and errors in decisions, potentially causing loss of life.

KISTERS and the University of Texas at Austin (UTA) have teamed up to develop a regional data hub to support the situational awareness for flash flooding in the Capital Area Council of Governments (CAPCOG) area surrounding Austin, Texas. This regional data hub is using KISTERS' new Web Interoperability Solution (KiWIS) to create a network of networks using web services for water and geospatial data to acquire and display data from multiple sources. This new data hub is being engineered to integrate with 911 services, web mapping and advanced modelling systems used by UTA which can live "in the cloud" and may eventually become global in extent.

The project that is described here shows that:

- data acquisition is a complex process since data sources are sometimes standardized, and other times provided in custom formats
- mediation of measurement information is important to be able to develop homogenous information (e.g "Waterlevel", "Stage", "Level")
    - algorithms to classify the current status can continuously be run to provide additional indicators for decision makers
- data dissemination should follow standards like web services, but should provide multiple formats and service types to allow all existing client software to interface in a smooth and easy manner

# NUMERICAL MODELING ON TOXIN PRODUCED UNDER NUTREINT LIMITED DOMINANT CYANOBACTERIA IN LAKE KASUMIGAURA, JAPAN

***Md. Nazrul Islam*** (The University of Tokyo, Japan)
Daisuke Kitazawa (The University of Tokyo, Japan)
Ho-Dong Park (Shinshu University, Japan)

A three dimensional hydrodynamic ecosystem coupled model was employed to simulate the toxin produced ability under the nutrients limited e.g. phosphorus (P)*,* Nitrogen (N) and co-limited (P and N) dominant species of cyanobacteria *(Microcystis aeruginosa, Microcystis viridis and Microcystis ichthyoblabe*) in shallow and eutrophic Lake Kasumigaura (sampling stations e.g. off Tomoe, off Takei and off Kamaya) in Japan. Toxin production is generally the result of two major factors-natural processes and human interferences. Both factors have an extreme influence on the generation of cyanobacteria toxins within lake ecosystems. The numerical model was calibrated by tuning toxin decay coefficient, half saturation constant of phosphorus and nitrogen and other input parameters for achieving a good agreement between the observation and the prediction. The phosphorus, nitrogen and co-limited cyanobacteria those are conducive to generating the dominant species of *Microcystis* spur blooms and their toxin. The model results of the N, P and co-limited cyanobacteria conditions are shown high, medium and low discrepancy, respectively. The simulation and observation results also show that total toxin as *Microcystin-(Leucine+Arginine:MC-LR), Microcystin-(Arginine+Arginine: MC-RR)* and *Microcystin-(Tyrosine+Arginine: MC-YR)* concentration rate is very high at the station off Tomoe in the month of July 2005. It might be occurred due to the concentration of dissolved oxygen is low for a longer period with stronger stratification in summer. Low dissolved Oxygen (DO) enhances the release of nutrients from sediment and increase dissolved inorganic phosphorus (DIP) concentration. Another reason could be the inflow nutrients come from Tomoe River and connecting Lake Nishiura and Sotonasakura by Wani River. The timing and duration of the cyanobacteria bloom depends on the ability to make scum or colonies, stratification, buoyancy regulation, sinking and floating, presence of nitrogen and phosphorus limited cyanobacteria and others environmental factors.

# DEVELOPING A SYSTEM DYNAMIC MODEL OF ECOSYSTEM SERVICES FOR ASSESSING CONSERVATION SCENARIOS

*Yu-Pin Lin*, Wei-Chi Lin, Li-Chi Chiang, and Yen-Lan Liu
(National Taiwan University, Taipei, Taiwan)

Wetland ecosystems generate a diverse array of goods and services important for human well-being. Such services include surface water supply, water regulation, soil retention, soil accumulation, carbon storage, and biodiversity. Despite its importance, this natural capital is poorly understood, scarcely monitored, and often undergoes rapid degradation and depletion. This study develops a system dynamic simulation model of wetland ecosystem services for AOGU area included the largest wetland in Taiwan. According to investigations of the Council of Agriculture (COA) in Taiwan, 221 bird species, 10 mammal species, 18 fish species, 22 crustacean species, 17 amphibian species and 346 insect species were investigated. Therefore, COA has designated 665 hectares of AOGU Wetland Forest Park as an important wildlife habitat, rendering legal protection to the area and banning development there. The system dynamic model is used to assess and compare ecosystem services including water resources, crop production, environmental purification, and flood control based on various conservation scenarios included the AOGU wetland Forest Park. The results shows that the total values of the above ecosystem services increased from 13.43 million to 179.79 million after developing the Wetland Forest Park. Moreover, the total values of the food focus scenario (increased 10% of the crop area) and the conservation scenario (increased 10% of the wetland area) are 14.30 million and 18.17 million, respectively. However, as a decision support system, the ecosystem services based model can be successfully used to assess and predict ecosystem services of planning policies and scenarios.

# ANALYSIS OF LID TECHNOLOGY EFFICIENCY IN URBAN SUB-WATERSHED USING SWMM-LID MODEL

*Tae Seok Shon*, Ji Ye Im, Sang Gu Lee, *Hyun Suk Shin* (Pusan National University, Busan, Korea)
Bong Gwon Kang (K-water, Busan, Korea)
Jong kyoung Jang (E-matrix, Anyang, Korea)

Urban watershed management has been settled as pending issues to control water balance, non-point source pollutant and urban flash flood according to severe human civilization. However, the conventional storm water management focuses on "end-of-pipe control" which concentrates on peak rate control according to detention and retention basin while paying little attention to the increased volume of urban runoff. Storm water has been routed on impervious surfaces to the outside of the urban watershed. Indeed, it has been occurred different pattern of hydrologic cycle according to development condition. In view of these aspects, LID (Low Impact Development) has been arisen as new alternative to mimic predevelopment hydrologic condition recovering infiltration, evapotranspiration and natural storage into soil and vegetation. On top of that, LID is a land planning and storm water management approach that seeks to control runoff as close as possible to its source. There are many on-going researches all over the world to develop LID practice and technology which will be functional to control storm water and NPS pollutant. The purpose of this study is to verify efficiency and applicability of the LID technology in urban watershed using SWMM-LID model. In order to examine whether LID can recover predevelopment hydrology, EPA SWMM was constructed based upon a proposed development in Dong-Rae watershed. The study area represents highly packed residential area and faces on frequent inundation problem. The newest version of SWMM contents LID control module so that this study would suggest how LID can be designed in a detail and which parameter SWMM-LID model should consider when LID is applied to study area. Several different scenarios were evaluated including: continuous simulation using historic rainfall during 2005 to 2010 and design storm 2, 10, 30, 50, 100-year; and BMPs combinations. Each model was then analyzed following in sight of runoff volume reduction and pollutant reduction. The LID BMPs that were modeled include Green Roof, permeable interlocking concrete pavement(PICP). The results show several advantages in use of LID technology in urban area, which indicated the efficient measure of recovering urban water cycle and reducing floods and NPS pollutants. In future, the process and result of this study might be deeper on more applications and real urban management.

# EVO: A VIRTUAL OBSERVATORY TO BRIDGE ENVIRONMENTAL DISCIPLINES USING CLOUD COMPUTING

*Yehia El-khatib*, Gordon S. Blair (The School of Computing & Communications, Lancaster University, Lancaster, UK)
Alastair Gemmell, Robert Gurney (Reading e-Science Centre, Reading, UK)
John W. Watkins (Centre for Ecology & Hydrology, Lancaster, UK)
Gwyn Rees (Centre for Ecology & Hydrology, Wallingford, UK)

Providing answers to many environmental questions is a complex matter which almost always involves the bringing together of expertise from different scientific user communities, together with inputs from government bodies and the general public. The Environmental Virtual Observatory pilot (EVOp), a NERC[128]-funded project, aims to provide a step in this direction by fostering integration between different domains of environmental science through the use of cloud computing. The Environmental Virtual Observatory (EVO) is a bespoke cloud-based infrastructure and associated collection of web-based tools designed to enable users from different backgrounds to access data concerning different environmental issues. The EVO is accessible by domain specialists (without any programming prerequisites) wishing to compose workflows, and also by non-specialist users through a feature-rich web portal. In doing so, the EVO supports a wide user base beyond the scientific community. The EVO facilitates the use of established and emerging scientific techniques and datasets in the wider discussion within and between policy makers, the education sector, the commercial sector, and local communities. The project also brings together people from the areas of environmental science and computer science (in particular, distributed computing). For the pilot phase which ends in December 2012, the project focuses on water related environmental disciplines (including hydrology, land cover management, and diffused pollution) with a view to expand this to other areas (such as soil science and biodiversity) in the future. The EVO architecture is built using cloud computing technologies. These, along with other associated technologies, offer a number of advantages that translate to low operational costs at the infrastructure level and very high flexibility at the application level. One of the pillars of clouds (and service-oriented architectures in general) is the concept of 'everything as a service' where all resources have a uniform view. This offers versatile resource management, allowing the EVO to support data assets of different origins: from in situ gauging stations, warehoused data stores, user provided, and external sources. The management of such resources is also transparent, i.e. details of where and how the data is held are hidden from the user without affecting his/her experience. Moreover, this design concept supports sharing between scientists (e.g. workflows) which in turn promotes a culture of collaboration. It also allows for the data to be used in models and simulations without necessarily giving it away to the users, thus avoiding some of the delicate aspects of data ownership. 'Infrastructure as a service' is an extension of the 'everything as a service' concept to include tangible resources, which means that hardware arrangements could be obtained as and when required. This provisioning of hardware resources as a utility introduces elasticity, whereby the EVO infrastructure is allowed to scale to meet user demand and maintain a minimum quality of service. This is made possible by handing over some of the key distributed systems management functions to a cloud provider. The return is assured levels of reliability, performance, and security which lets us focus on solving domain-specific problems. Furthermore, virtualisation technologies are used to dynamically deliver environments that are specifically customised to execute user workflows (e.g. GIS models).

In this presentation, we will discuss the potential benefits the EVO holds for tackling grand challenges in environmental science and how we will evaluate them. We will also reflect on our experiences in assembling the EVOp infrastructure. Finally, we will demonstrate the working prototype web interface through two case studies, the first of which relates to forecasting local floods while the other studies the flux of pollutants to coastal waters.

# MODELLING SPATIAL AND TEMPROAL DYNAMICS IN FLOODPLAINS: EXTENT, NUTRIENT LOADS AND RETENTION

*Stephanie Natho*, Markus Venohr,
(Leibniz-Institute of Freshwater Ecology and Inland Fisheries, Berlin, Germany)

**ABSTRACT:** This study extends and improves the recently introduced approach of Natho & Venohr (2012) to calculate the extent of flooded riparian wetlands and share of nutrient load entering the floodplain as discharge dependent variables. The new approach does not only take the results of the Software FLYS 2.1.3 into account, as the former approach, but also flow velocities. Since the new approach was successfully validated by means of reference discharges provided by the gauges along the rivers (Elbe, Rhine and Main) this model can be used as an appropriate tool for predicting incoming nutrient loads depending on actual discharge and river characteristics. The new database allows the application of yearly and monthly nutrient retention models from literature for phosphorus and nitrogen in comparison to the riverine retention for the years 1997-2004. Maximum cumulative nitrate retention of 14% of the river nitrate load and 13% of the total phosphorus load could be calculated for the floodplains of the considered river stretch of the Elbe during August floods in 2002, whereas riverine retention contributed only 5.6% and 6% respectively. With this approach it is possible to calculate nutrient retention depending on the dynamics of flooded riparian area and incoming nutrient load.

## INTRODUCTION

The role of riparian floodplains for nutrient retention (e.g. nitrogen and phosphorus) is widely accepted (Mitsch & Gosselink 2000, Verhoeven *et al.* 2006). As main processes denitrification and sedimentation are identified on yearly basis for nitrogen retention (Saunders & Kalf 2001, Venohr 2006) and phosphorus retention respectively (Behrendt & Opitz 2000). On a monthly basis also aquatic plant uptake has to be considered (Venohr et al. 2011). There are several case studies (Trepel & Palmeri 2002) concerning measurement and modeling of nutrient retention in constructed floodplains (Mitsch et al. 2000). However, from what we know, there is no broad approach available for nutrient retention on landscape scale, since appropriate input data are hardly available. The reason for this are spatial and temporal dynamics, which result from changing hydrologic conditions on daily or even hourly basis. Thus total floodplains are inundated only seldom, but parts more often. Although the extent and the frequency of inundation are currently not known, the potentially active floodplain has decreased regarding the total floodplain. This was found out by a German wide inventory on recent floodplains, carried out for large rivers (Brunotte et al. 2009). Therefore Natho & Venohr (2012) applied the Software FLYS 2.1.3. Based on statistical values the authors empirically derived a first approach that enables the calculation of river loads entering the floodplain (incoming loads) as well as floodplain extents depending on actual discharges. This for the first time available dataset was subsequently applied on nitrate retention models taken from the literature. But Natho & Venohr (2012) considered too high incoming loads, due to a high degree of simplification of morphometrics and due to a disregard of flow velocity differences in river and floodplain. Furthermore yearly calculations did not reflect seasonal changes which are necessary to estimate the effect of floodplains in nutrient retention properly.

Hence the present study is addressed to improve this recently introduced approach which enables a more reliable prediction of incoming nutrient loads. The improved approach is capable to also be applied to phosphorus and nitrate retention models on a monthly basis.

## MATERIALS AND METHODS

For the present study, some hundred kilometer of main river sections were considered for each of the rivers Elbe, Main and Rhine, respectively (for details see Natho & Venohr 2012). Whereas in the recently developed approach of Natho and Venohr (2012), time independent volumes were considered in river and floodplain, flow velocities were now taken into account. Detailed land-use information was

obtained from digital maps in 10m resolution (of the federal states Saxony, Saxony-Anhalt, North Rhine Westphalia and Rhineland Palatinate) and intersected with FLYS 2.1.3 model results on inundated floodplains at certain discharges (for details see Natho & Venohr 2012). Additional land-use data were processed from the cooperation with the Helmholtz Centre of Environmental Research (for details see Natho et al. n.d.). On these intersected areas land-use induced roughness ($k_{st}$) was estimated according to Schneider (2009). The hydraulic radius ($r_{hy}$) describes the ratio of water surface are to sediment-water-surface which is crucial for the empirical Gauckler-Manning-Strickler equation (Eq. 1) to estimate flow velocities.

$$v = k_{st} \cdot r_{hy}^{\ 2/3} \cdot \sqrt{I_{So}} \qquad \text{Eq.1}$$

To calculate $r_{hy}$ information on water depths is needed. The Software FLYS 2.1.3 calculates inundated floodplain extents (A) and water depths ($d_{water}$) for given discharges. The linear difference of two gauging heights relative to N.N. was considered to estimate mean slopes ($I_{So}$) between two gauges. Following general hydrologic equations, this flow velocity was multiplied with the mean cross section area ($A_{cross\ section}$) to obtain the discharge (Q), whereby the mean cross section results from multiplication of water depth and surface area and the division by the length of river stretch (Eq. 2).

$$Q = v \cdot A_{cross\ section} = v \cdot \frac{A \cdot d_{water}}{l_{riverstretch}} \qquad \text{Eq.2}$$

For the river Elbe and the river Main one equation was sufficient to describe the relationship between the ratio of long-term mean discharge and daily discharge as a function of the incoming load expressed as share of volume in floodplain. Instead for the river Rhine three different sections could be identified with three different equations for each of them (see Figure 1). These characteristically differences can also be found considering land-use and elevation.
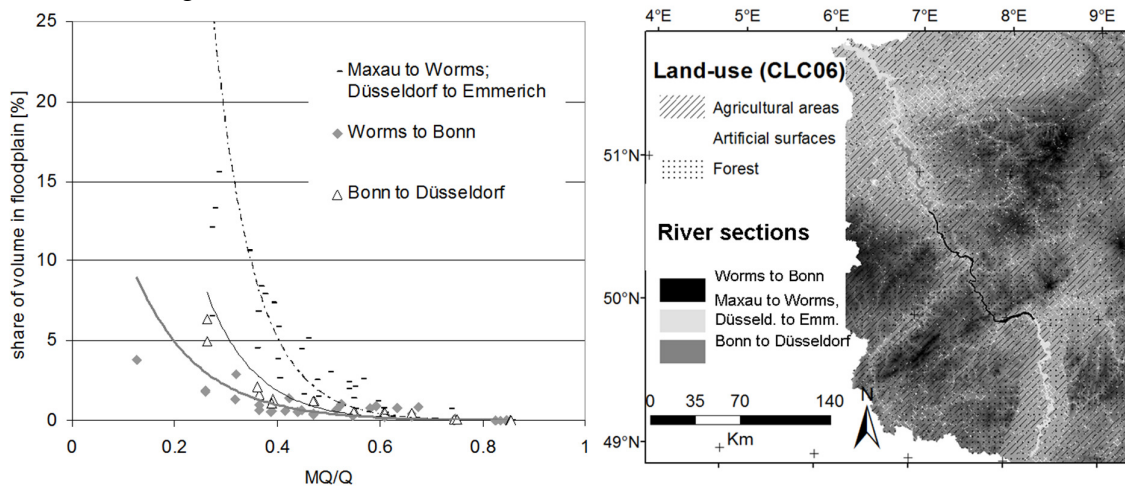


**Figure 7: Relations of volume to discharge, characterizing different sections of the river Rhine (left); illustrated by a land-use map (CORINE Land Cover 2006) underlain with a SRTM 90m (USGS 2000) as well as floodplains provided by FLYS 2.1.3 (right).**

It is assumed, that nutrients are evenly mixed transported in the discharge, so that the share of volume equals the share of load that enters the floodplain. Daily discharges were applied for calculating daily incoming loads according to the relation between long term discharge and daily discharge (Figure 1). Then, the daily incoming loads were averaged on a monthly basis and on yearly basis. Similarly, inundated areas were derived on a monthly and on a yearly basis, respectively. Based on these input data, different retention models taken from the literature were applied for phosphorus and nitrogen retention calculation for the years 1997 to 2004 (see Table 1).

**Table 1: Overview of applied retention models. Beside the necessary incoming nutrient load, following parameters are considered: HL = hydraulic load (discharge/area), T = temperature, R = global radiation, HRT = hydrologic retention time (area, discharge and shape dependent), c= concentration.**

| | Temporal Resolution | Considered Nutrient | Considered Process | Main Parameter |
|---|---|---|---|---|
| **Venohr 2006** | yearly | nitrogen | denitrification | HL, T |
| **Dortch & Gerald 1995** | yearly | nitrogen | denitrification | HRT, $c_{TN}/c_{NO3-N}$ |
| **Venohr et al. 2011** | monthly | nitrogen | denitrification & uptake by aquatic organisms | HL, T, R |
| | monthly | phosphorus | sedimentation | HL |
| **Behrendt & Opitz 2000** | yearly | phosphorus | sedimentation | HL |

## RESULTS

In the first part of the present study the former approach of calculating incoming loads could be reduced: whereas the former approach calculated up to 80% of the load entering the floodplain, this value is reduced to only maximum 35% according to the new approach. These values are found along the river Elbe, where floodplains are relatively natural. Smaller values (15%) are found for the river Main, which has small floodplains. For smaller floods, also for the river Elbe, less than 20% of the river load enters the floodplain and underlies retention.
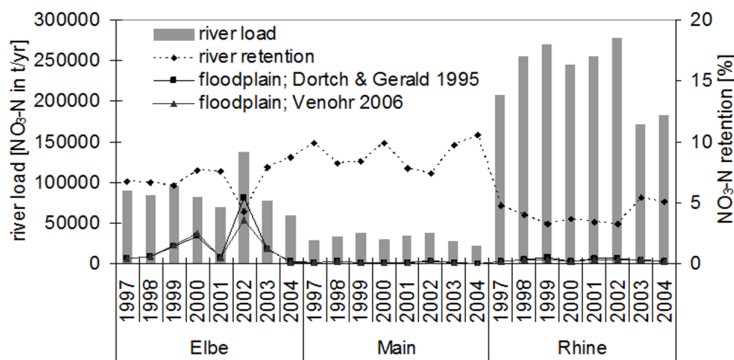


**Figure 8: Comparison of yearly NO₃-N retention calculations (in floodplains and rivers); yearly river loads are also shown.**
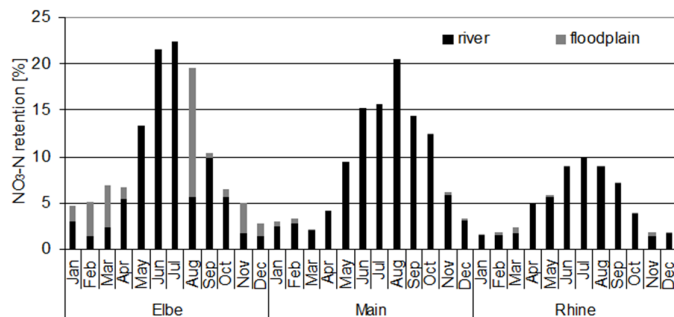


**Figure 9: Comparison of monthly nitrogen retention results in 2002, calculated according to Venohr et al. (2011).**

Considering nitrate retention on yearly basis, the results of the two retention models are similar (Figure 2). River retention decreases when river loads increase due to floods. However, deviation between the models can be found along the Elbe for the year 2002.

On a monthly basis the approach proposed by Venohr et al. (2011) reveals the influence of water temperature: floods in August lead to extremely high retention rates in the floodplain, exceeding the cumulative nitrate retention in the river by a factor of 2.5.

Generally nutrient retention is higher for the river Elbe than for the river Rhine of for the river Main. Total phosphorus retention is only shown for the river Elbe in Figure 4, where floodplain retention is highest in August 2002. As sedimentation is not water temperature dependent, floodplain retention in August does not exceed river retention as pronounced as for nitrate. Nevertheless, the contribution of floodplain retention on phosphorus retention in the whole river can be demonstrated.

After this general observation, area specific retention rates can be derived. On a yearly basis the calculated nitrogen and phosphorus retention rates range between 50 and 930 kg NO₃-N/ha/yr and 2 and 70 kg TP/ha/yr, depending on hydrologic condition and river.
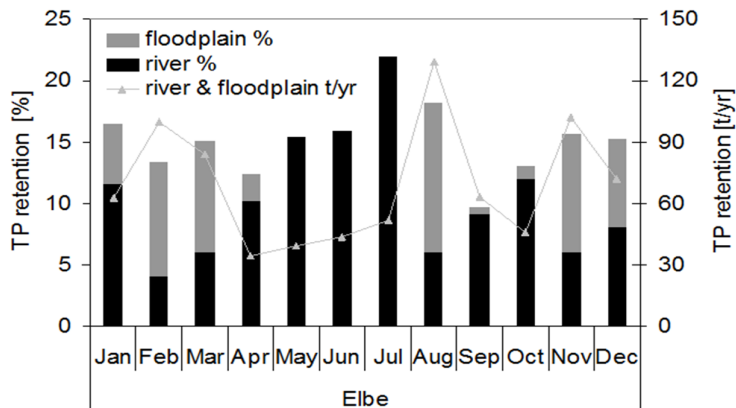
**Figure 10: Cumulative TP retention in 2002; calculated according to Behrendt & Optiz (2000).**

Again highest values can be found for the river Elbe, with average retention rates of 455 kg $NO_3$-N/ha/yr and 44 kg TP/ha/yr for the years 1997 to 2004. Along the river Main the lowest retention is calculated (with mean values of 186 and 18 kg/ha/yr), whereas for the river Rhine floodplains between 310 and 64 kg/ha/yr are calculated respectively.

**DISCUSSION**

Flow velocities are crucial for the amount of discharge and thus load entering the floodplain. Compared to the former approach, with the new approach the incoming load could be reasonably reduced. On a yearly basis the calculated nitrogen and phosphorus retention rates are within the range of reported values (Mitsch et al. 2000). Nutrient retention is higher for rivers with relative well connected floodplains like the river Elbe than for rivers without intact floodplains (Mitsch & Gosselink 2000). Although parts of the river Rhine possess large floodplains, their contribution to nutrient retention is relatively low, because retention is only accounted for flooded floodplains. In the considered years, most of the floodplains were not inundated and thus not active. Reconnection und hence more frequent inundation of floodplains can contribute to nutrient retention, if connection is similar to the connection of the floodplains of the river Elbe.

Inter annual variation of the retention is high due to variation in hydrology and due to potential floodplain extent. With respect to the modelling, this leads to a variation of the inundated floodplain extent in the current year. Usually floods occur in early spring, leading to inundation of floodplains and thus retention in all rivers. The model of Venohr et al (2011) captures the effect of summer floods, since water temperature increases which in turn leads to higher denitrification rates. The consideration of temperature based effects explains the difference in nitrate retention calculation between the model given by Dortch & Gerald (1995) and Venohr (2006) for the year 2002. Nevertheless on a monthly basis nitrogen retention might still be overestimated, since the model was developed for riverine retention. It is assumed that aquatic plant uptake occurs in summer time only. Terrestrial plants, as existent on floodplains, might have a slightly different effect on nitrogen transformation and thus nutrient retention processes.

The additive nutrient retention effect of floodplains is very important, since floodplain and river retention behave conversely: river retention is high, when discharge is low, whereas floodplain retention is high, when flood conditions are low. The latter occurs, when the biggest share of nutrient loads is transported as was shown in Figure 4 (Johnes 2007, Ouerng et al. 2010). Hence, under flooded conditions retention in floodplains is higher than in rivers (Saunders & Kalff 2001).

**CONLUSION**

This study presents an improved approach for calculating incoming nutrient loads for riparian floodplains of three German rivers, depending on flow velocities in river and floodplain. According to the naturalness of the floodplains, up to 35% of the river load for very high flood events and under normal conditions less than 20% of the river load enters the floodplain.

This approach is applicable for creating a reliable database for monthly and yearly retention models, since variation in hydrology and thus floodplain extent can be modelled.

Using different retention models the significant contribution of floodplains to nitrogen and phosphorus retention could be shown on landscape scale, which even exceeds river retention under wet hydrologic conditions, leading to several flooding events: In floodplains, nitrate retention of up to 14% of the transported load could be found for the river Elbe, a relative natural river. This indicates the retention potential of existing floodplains when reconnection is possible.

## ACKNOLWEDGMENT

## REFERENCES

Behrendt, H. & D. Opitz 2000. Retention of nutrients in river systems: Dependence on specific runoff and hydraulic load. *Hydrobiologica* 410, 111-122.

Brunotte, E., E. Dister, D. Günther-Diringer, U. Koenzen & D. Mehl 2009. *riparian wetlands in Germany, Inventory and Evalution of the conditions of floodplains "Flussauen in Deutschland - Erfassung und Bewertung des Auenzustandes"*. Bonn - Bad Godesberg.

CORINE Land Cover 2006 (CLC2006), Federal Environment Agency, DLR-DFD 2009. URL: http://www.corine.dfd.dlr.de/datadescription_2006_en.html; day of access: 06/09/12

Dortch, M. S., and Gerald, J. A. 1995. Screening-level model for estimating pollutant removal by wetlands Technical Report WRP-CP-9, U.S. Army Engineer Waterways Experiment Station, Vicksburg, MS., NTIS No. AD A302-097.

Johnes, P.J. 2007.Uncertainties in annual riverine phosphorus load estimation: Impact of load estimation methodology, sampling frequency, baseflow index and catchment population density, *Journal of Hydrology* 332, 241– 258.

Mitsch, W. J. & J. G. Gosselink 2000. The value of wetlands: importance of scale and landscape setting; *Ecological Economics* 35, 25-33; special issue: the values of wetlands: landscape and institutional perspectives.

Mitsch, W. J., A. J. Horne & R. W. Nairn 2000. Nitrogen and phosphorus retention in wetlands-ecological approaches to solving excess nutrient problems. *Ecological Engineering* 144, 1-7.

Natho, S. & M. Venohr 2012. Nutrient retention in riparian floodplains on landscape scale, the necessity for a monthly retention approach; manuscript submitted for publication

Natho, S., M. Venohr, M. Scholz, K. Hänle, C. Schulz-Zunkel n.d. Nitrogen retention in floodplains of great lowland rivers; manuscript in preparation.

Oeurng, C., S. Sauvage & J.-M. Sanchéz-Pérez 2010 Temporal variability of nitrate transport through hydrological response during flood events within a large agricultural catchment in south-west France. *Science of the Total Environment* 409, 140-149.

Saunders, D. L., & J. Kalff 2001. Nitrogen retention in floodplains, lakes and rivers. *Hydrobiologia* 443, 205-212.

Schneider, S. 2010. V*egetative resistance value of succession dominated riparian forest systems "W*i*derstandsverhalten von holzigen Auenpflanzen"*; Dissertation, Karlsruhe Institute of Technology.

Trepel, M. & L. Palmeri 2002. Quantifying nitrogen retention in surface flow floodplains for environmental planning at the landscape-scale. *Ecological Engineering* 19, 127-140.

USGS 2000. SRTM-3; 90m resolution. URL http://srtm.usgs.gov/ day of access: 06/09/12

Venohr, M. 2006. *Modelling the influence of temperature, discharge and hydromorphology on nitrogen retention in river system "Modellierung der Einflüsse von Temperatur, Abfluss und Hydromorphologie*

*auf die Stickstoffretention in Flusssystemen"* Berliner Beiträge zur Ökologie 14, Weißensee Verlag, Berlin, 193 pages. Thesis

Venohr, M., U. Hirt, J. Hofmann, D. Opitz, A. Gericke, A. Wetzig, S. Natho, F. Neumann, J. Hürdler, M. Matranga, J. Mahnkopf, M. Gadegast & H. Behrendt 2011. „Modelling of nutrient emissions in river systems - MONERIS: methods and background"; *International review of hydrobiology*. 96(5), 435-483.

Verhoeven, J. T.A., B. Arheimer, C. Yin, & M. M. Hefting 2006. Regional and global concerns over floodplains and water quality. *Trends in Ecology and Evolution* 21(2), 96-103.

# HOW CAN GERMAN RIVER BASINS CONTRIBUTE TO REACH THE NUTRIENT EMISSION TARGETS OF THE BALTIC SEA ACTION PLAN?

*U. Hirt[1]*, J. Mahnkopf[1], M. Venohr[1], P. Kreins[2], C. Heidecke[2], Schernewski[3]

[1] Leibniz-Institute of Freshwater Ecology and Inland Fisheries; Dept. of Lowland Rivers and Shallow Lakes; Müggelseedamm 310; 12587 Berlin; Germany; Tel.: +49 30 6392 4086; Email: hirt@igb-berlin.de
b Institute of Rural Studies, Federal Research Institute for Rural Areas, Forestry and Fisheries, Bundesallee 50, 38116 Braunschweig, Germany
[3] Leibniz-Institute for Baltic Sea Research, Biological Oceanography, Seestrasse 15, D-18119 Rostock, Germany

**ABSTRACT:** Since the 1900s, the Baltic Sea has changed from an oligotrophic clear-water sea into an eutrophic marine environment. The currently high nutrient emissions into the Baltic sea lead to intense algal growth, oxygen depletion and lifeless sea bottoms. To reduce the high nutrient emissions, the Baltic Sea Action Plan demands a reduction of nutrient loads. For the German catchments the reduction target is about 5,620 t for nitrogen and 240 t for phosphorus. Measures have to be taken to reduce the high nutrient emissions into rivers and seas. To identify the most effective measures, the sources and pathways of nutrient emissions into rivers have to be quantified. Furthermore, the reduction potential of different measures has to be assessed and measure packages have to be composed.

The MONERIS model is applied, a semi-empirical, conceptual model, which has gained international acceptance as a robust meso- to macro scale model for nutrient emissions. MONERIS quantifies nitrogen and phosphorus emissions into river basins, via various point and diffuse pathways, as well as the retention and the nutrient load in rivers. For 172 subcatchments of the german Baltic Sea river basins nutrient emissions were calculated and the pathways and sources were defined. The effect of measures can be quantified with the 'management alternative tool' in MONERIS. Therefore, on one hand the effect of agricultural measures and on the other hand measures concerning urban sources and waste water treatment plants can be assessed. Furthermore, the cost efficiency of those measures will be evaluated with a newly developed tool 'CEA' (cost-effectiveness-analysis) in MONERIS.

Currently, most nitrogen emissions come from tile drainages (63%), groundwater flow (19%), and point sources (5%), whereas most phosphorous emissions come from point sources (29%), groundwater flow (23%) and tile drainages (16%). Due to the high impact of tile drained areas, measures to reduce diffuse nitrogen emissions from tile drainages will be in the focus of our study. For phosphorous measures focus especially point sources. Results presented at the Conference will show the most cost effective measure packages for this region to reach the reduction targets of the Baltic Sea Action Plan.

## INTRODUCTION

Since the 1900s, the Baltic Sea has changed from an oligotrophic clear-water sea into a eutrophic marine environment. The currently high nutrient emissions into the Baltic Sea lead to intense algae growth, oxygen depletion and lifeless sea bottoms. To reduce the high nutrient emissions, the Baltic Sea Action Plan (BSAP) demands a reduction of nutrient loads. For the German catchments the reduction target is about 5,620 t (27%) for nitrogen (N) and 240 t (45%) for phosphorus (P). Therefore, the current emission situation has to be assessed and measures have to be taken into account to reduce the high nutrient emissions into rivers discharging into the Baltic sea. To identify the most effective measures, the sources and pathways of nutrient emissions into these rivers have to be quantified. Furthermore, the reduction potential of different measures has to be assessed and packages of measure have to be composed.

Humborg et al. (2007, 2011) and Hägg et al. (2010) calculated the effect of nutrient emission into the Baltic Sea and simulated scenarios concerning changes in point and non-point emissions and the possible effects of climate change. They used emission factors (e.g. for humans and animals), specific runoff and atmospheric deposition data to calculate the nutrient emissions. Mewes (2006) calculated the cost-effectiveness of water protection measures in the German Baltic Sea catchments using nutrient emissions calculated with the model MONERIS. Voss et al. (2011) simulated the effect of nutrient emissions and climate change on the eutrophication state of the Baltic Sea. They used emission results from the Odra river basin derived from the model MONERIS. Furthermore, Krämer et al. (2011) simulated different scenarios for landuse changes in the Oder catchment and their consequences for the Oder lagoon using MONERIS.

Nevertheless, a comprehensive study analysing the recent state of nutrient emissions and measures to reach the goals of the BASP for the German catchments have not been assessed. Furthermore, the packages of measures were adapted to the current emission situation and the demands of the BSAP. Because in the last decades measures focused mainly on point sources, today the share of diffuse emissions on total emissions is dominant (Behrendt et al. 2000, Fuchs et al. 2010). For nitrogen agricultural measures are basically effective in short term, only for the groundwater pathway high nitrogen emissions will be relevant for the next decades. For phosphorus agricultural measures will have an impact on the water quality only in middle to long term, due to the accumulation of phosphorus in the soil. The question is how far different measures could contribute to reach the goals of the BSAP.

## MATERIALS AND METHODS

The MONERIS model is applied, a semi-empirical, conceptual model, which has gained international acceptance as a robust meso- to macro scale model for nutrient emissions. MONERIS calculates nitrogen and phosphorus emissions and loads in the surface waters for (1) six diffuse pathways: atmospheric deposition on surface waters, erosion, surface runoff, tile drainages, groundwater / interflow, and urban areas, and (2) two point pathways: municipal waste water treatment plants (WWTP), and direct industrial dischargers. Furthermore, MONERIS calculates in-stream retention and resulting loads for nitrogen and phosphorus, which can be directly compared with measured loads (Venohr 2006; Behrendt and Opitz 2000, Fig. 1). Analytical units (which are subcatchments in a river basin are the basis of the spatial resolution, the temporal resolution for the calculation of scenarios is yearly. The basis for the model are data on runoff and water quality for the studied river catchments and a Geographical Information System (GIS) integrating digital maps as well as extensive statistical information for different administrative levels. Input data are: meteorological data, soil characteristics, land use, population, degree of urbanisation, connection to sewer systems and degree of waste water treatment, nitrogen surplus on agricultural soils, phosphorus accumulation in soils and atmospheric deposition.

During the last years MONERIS was applied for many European river systems (e.g., Axios, Elbe, Danube, Daugava, Po, Rhine and Vistula, Odra, and the total area of Germany (Behrendt et al. 2000, 2002, 2003a,b; Behrendt and Dannowski 2005; Schreiber et al. 2005) as well as currently in river catchments in Canada, Brazil, Mongolia and China (Hofmann et al. 2010).

For 172 subcatchments of the German Baltic Sea river basins nutrient emissions were calculated and the pathways and sources were defined. Due to the best data availability a time period from 1983 to 2005 was chosen. Nutrient surpluses in the German Baltic Sea catchments are calculated with the model RAUMIS and provided by the 'von Thünen-Institute' (Henrichsmeyer et al. 1996; Kreins et al. 2007). The effect of measures can be quantified with the 'management alternative tool' in MONERIS. To exclude the influence of temporal variations in hydrology for the management scenarios,

To analyse the necessary reductions the following scenarios were calculated with MONERIS:

1. The demands of the EU-urban waster water treatment directive (EU UWWT Directive, 1991) are fulfilled (effective for N and P).

2. All farms fulfil the demands of the new German fertilizer ordinance (DÜV 2009), which allows a surplus on arable land up to 60 kg N ha$^{-1}$ yr$^{-1}$ per farm. Further fertilizer use reductions scenarios are calculated, if necessary. Here, P emissions are not calculated, because the decrease would be negligible due to the long-lasting P accumulation in the soil, which only could be educed in a long term perspective.

3. 25% of all tile drained areas are equipped with a retention pond, which is installed between the tile drainage outlet and the rivers (N and P).

4. Buffer strips are introduced beside 30% and 100% of the rivers. Retention effect for P is assumed to be 100% (P).

5. Soil conservation agriculture is introduced in all areas with > 4% soil slope (P).
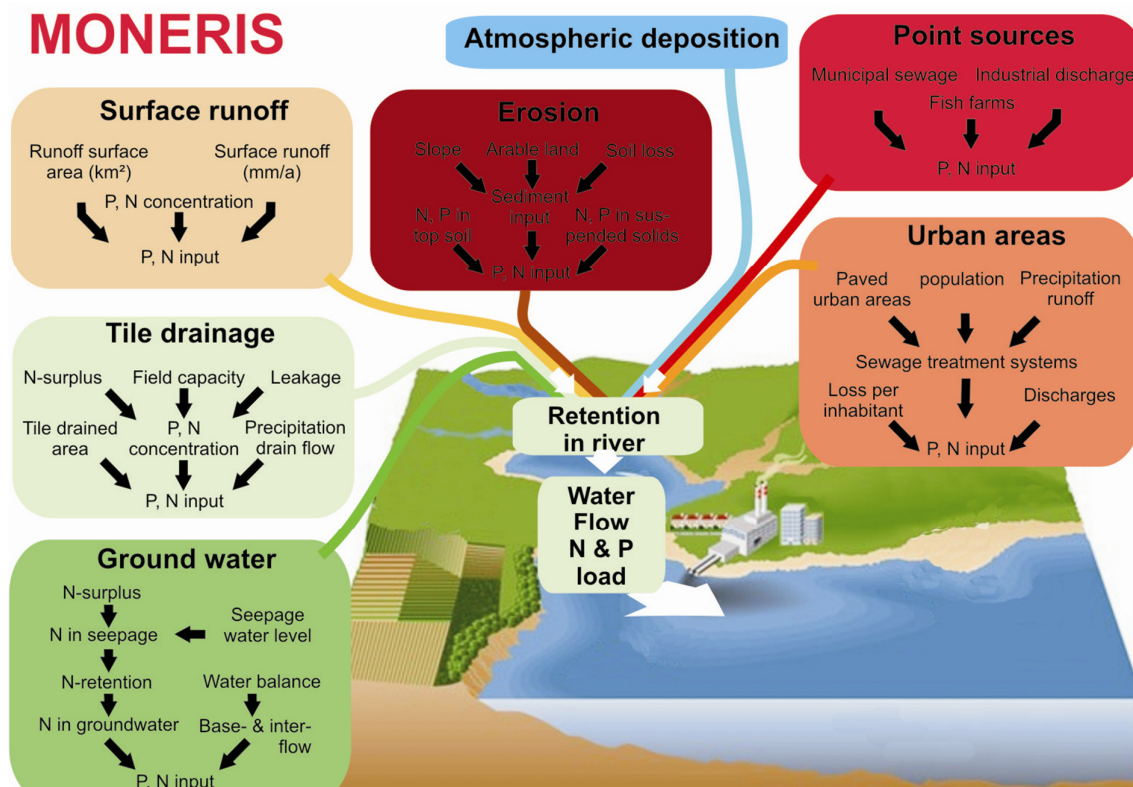


Figure 1. Pathways and processes for nutrient emission into surface waters (background picture modified after LOICZ, TURNER *et al.,* 1998).

Combinations of these measures are calculated, if they are necessary to reach the targets of the BSAP (27% for N and 45% for P). Scenarios are calculated under mean hydrological conditions (mean values for the period 1983 to 2005) to avoid the effect of extreme hydrologic situations and the nutrient sources of the year 2005.

## RESULTS

**Nutrient emissions.** Fig. 1 presents the annual nitrogen emissions via the different pathways from 1983 to 2005. Nitrogen emissions dropped from ~ 50,000 t/yr in 1983 to slightly more than 30,000 t/yr in 2005. The sharp reduction in 1990 is due to the German unification in 1990 and the following break-down of the agricultural structure in the New Federal States. In 2005, most nitrogen emissions come from tile drainages (63%), groundwater flow (19%), and point sources (5%, Fig. 2), whereas most phosphorous emissions (not shown) come from point sources (29%), groundwater flow (23%) and tile drainages (16%). Especially the catchments near the coast are those with the highest pollution due to the high share of tile drained areas. Calculated loads deviate from those declared by the BASP.

**Reduction scenarios.** The following results are calculated for the scenarios (Fig. 3 and Fig. 4):

- The standard of the EU UWWT Directive is almost fulfilled; emissions decline only insignificantly.
- If all farms fulfill the demands of the DÜV (2009) N emissions will drop about 16%. A 27% reduction of N emission could be reached with a maximum N-surplus of 40 kg N ha$^{-1}$ yr$^{-1}$.
- If 25% of all tile drained areas are equipped with a retention pond, emissions will decrease about 9% (N) and 6% (P). A combination of this measure with a maximum N-surplus of 50 kg N ha$^{-1}$ yr$^{-1}$ would also achieve a reduction of 27%.
- If buffer strips are introduced beside 30% and 100% of the rivers a reduction of 5% and 17% of the P emissions are visible. Soil conservation agriculture has a comparable effect to P emissions (reduction: 16%).
- A combination of 100% buffer strips with the installation of retention ponds in 25% of the tile drained area and the compliance with the EU UWWT Directive would lead to a reduction of 33%.
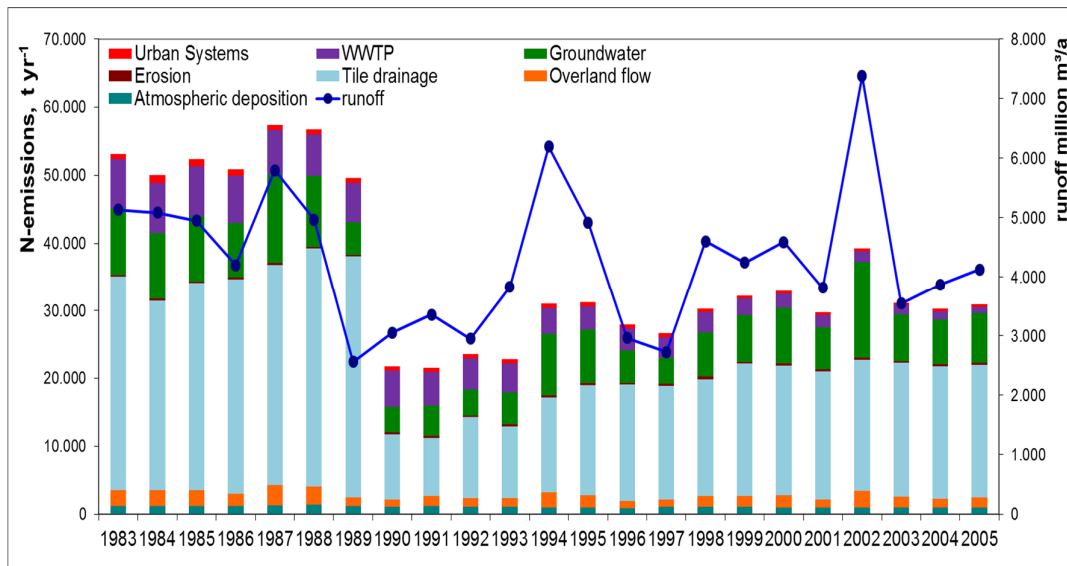


Figure 2: Annual nitrogen emissions via the different pathways
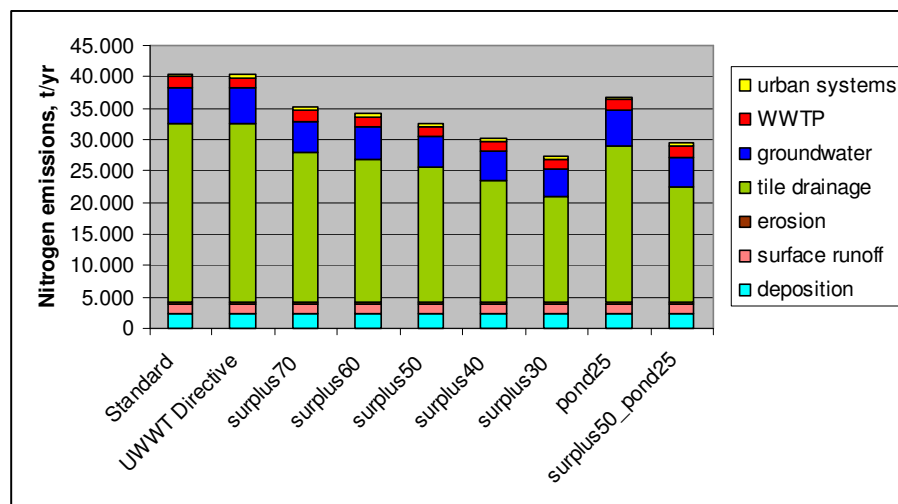


Figure 3: Reduction of N emissions due to scenarios settings
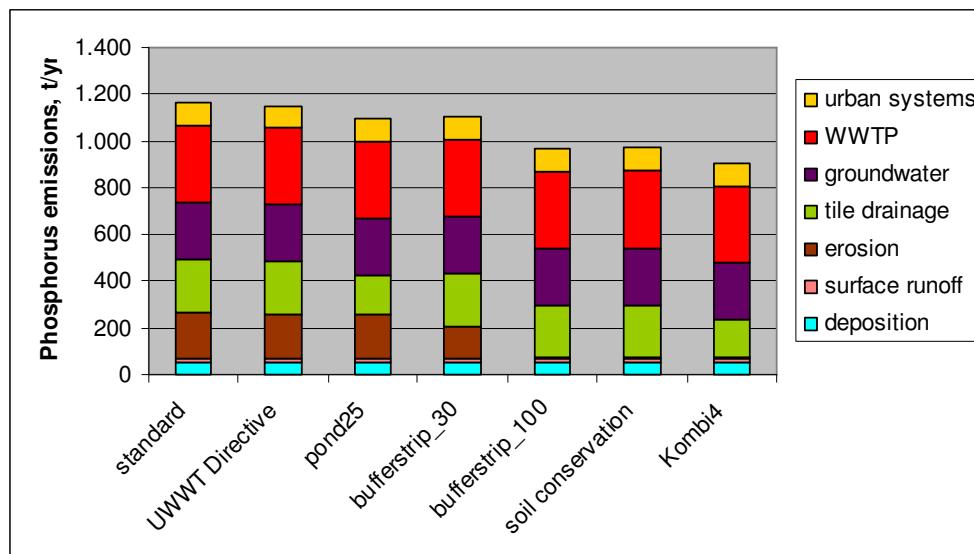
Figure 4: Reduction of P emissions due to scenarios settings

## CONCLUSION

The WWTP´s in the catchment fulfil the standards of the UWWTD. Therefore, the reduction of emissions from agricultural land has to be proved. The standards of the DÜV (2009) lead only to a moderate reduction (16%). A N-surplus of 40 kg N ha$^{-1}$ yr$^{-1}$ would be necessary to introduce a 27% reduction of N-emissions (acc. to the BSAP). The political intention for a further fertilizer reduction after the implementation of the DÜV (2009) seems not to be realistic. Further reduction potential lays in the pathway tile drainage, e.g. in the installation of retention ponds to enhance the retention capacity of the landscape. If these systems are installed in e.g. 25% of the tile drained area and additionally a maximum N-surplus of 50 kg N ha$^{-1}$ yr$^{-1}$ would also lead to a 27% reduction of N-emissions.

The P reduction of retention ponds is less effective as the N reduction. Because P fertilizer reduction would have an effect only in long term, a further reduction of emissions in short term is only possible with erosion protection or the P reduction of point sources. Even a combination of buffer strips of 100% beside of the rivers, retention ponds in 25% of the tile drained areas and the compliance with the EU UWWT Directive would reach only a reduction of 33%. Only with further measures concerning point sources targets seem to be achievable.

## ACKNOWLEDGEMENTS

## REFERENCES

Behrendt, H., P. Huber, M. Kornmilch, D. Opitz, O. Schmoll, G. Scholz, and R. Uebe. 2000. Nutrient emissions into river basins of Germany. UBA-Texte 23/00.

Behrendt, H., and D. Opitz. 2000. "Retention of nutrients in river systems: Dependence on specific runoff and hydraulic load." *Hydrob.*(410): 111-122.

Behrendt, H., P. Huber, M. Kornmilch, D. Opitz, O. Schmoll, G. Scholz, and R. Uebe. 2000. *Nutrient emissions into river basins of Germany*. UBA-Texte 23/00.

Behrendt, H., M. Kornmilch, D. Opitz, O. Schmoll, and G. Scholz. 2002. "Estimation of the nutrient inputs into river systems - experiences from German rivers." *Reg. Environ. Change*(3): 107-117.

Behrendt, H., M. Bach, R. Kunkel, D. Opitz, W. G. Pagenkopf, G. Scholz, and F. Wendland. 2003a. *Quantifizierung der Nährstoffeinträge der Flussgebiete Deutschlands auf der Grundlage eines harmonisierten Vorgehens.* UBA-Texte 82/03.

Behrendt, H., R. Dannowski, D. Deumlich, F. Dolezal, I. Kajewski, M. Kornmilch, R. Korol, W. Mioduszewski, D. Opitz, J. Steidl, and M. Stronska.2003b. *Point and diffuse emissions of pollutants, their retention in the river system of the Odra and scenario calculations on possible changes.* Weissensee Verlag, Berlin.

Behrendt, H., and R. Dannowski. 2005. Nutrients and heavy metals in the Odra River system. Weißensee Verlag, Berlin.

DÜV (Düngeverordnung). 2009. Legal ordinance for usage of fertilizers, soil auxiliary material, after the principle of good technical practice with manuring. http://www.gesetze-im-internet.de/bundesrecht/d_v/gesamt.pdf, online access: 20.2.2012.

European Parliament and Council of the European Union (Ed.). 2000. "Directive 2000/60/EC of the European Parliament and the Council of the European Union of 23 October 2000." *Off. J. of the Eur. Commun.*327: 1-73.

Fuchs, S., U. Scherer, R. Wander, H. Behrendt, M. Venohr, D. Opitz, T. Hillenbrand, F. Marscheider-Weidemann, and T. Götz. 2010. *Calculation of Emissions into Rivers in Germany using the MONERIS Model Nutrients, heavy metals and polycyclic aromatic hydrocarbons.* Federal Environment Agency (Umweltbundesamt), ISSN 1862-4804.

Hägg, H. E., C. Humborg, C. M. Mörth, M. Rodriguez Medina, and F. Wulff 2010. "Scenario Analysis on Protein Consumption and Climate Change Effects on Riverine N Export to the Baltic Sea." *Environ. Sci. Technol.* 44(7): 2379–2385.

Henrichsmeyer W., Cypris C., Löhe W., Meudt M., Sander R., Sothen Fv., Isermeyer F., Schefski A, Schleef K.-H., Neander E., Fasterding F., Helmcke B., Neumann M., Nieberg H., Manegold D., Meier T. (1996). „Entwicklung eines gesamtdeutschen Agrarsektormodells RAUMIS96". Endbericht zum Kooperationsprojekt, Forschungsbericht für das BML (94 HS 021), Bonn/Braunschweig.

Hofmann, J., M. Venohr, H. Behrendt, and D. Opitz. 2010. "Integrated Water Resources Management in Central Asia: Nutrient and heavy metal emissions and their relevance for the Kharaa River Basin, Mongolia." *Water Sci. and Technol.* 62(2): 353-363.

Kreins P., Behrendt H., Gömann H., Hirt U., Kunkel R., Seidel K., Tetzlaff B., Wendland F. 2010. Analyse von Agrar- und Umweltmaßnahmen im Bereich des landwirtschaftlichen Gewässerschutzes vor dem Hintergrund der EG-Wasserrahmenrichtlinie in der Flussgebietseinheit Weser – AGRUM Weser". Landbauforschung - vTI agriculture and forestry research, Sonderheft 336, Braunschweig, pp 342

Krämer I., J. Hürdler, J. Hirschfeld, M. Venohr, and G. Schernewski. „Nutrient Fluxes from Land to Sea 2011: Consequences of Future Scenarios on the Oder River Basin – Lagoon – Coastal Sea System." *Internat. Rev. Hydrobiol.* 96(5): 520–540.

Humborg, C., C. M. Mörth, M. Sundbom, and F. Wulff. 2007. "Riverine transport of biogenic elements to the Baltic Sea – past and possible future perspectives." *Hydrol. Earth Syst. Sci. Discuss.* 4: 1095-1131.

Humborg, C., C. M. Mörth, M. Sundbom, and F. Wulff. 2007. "Riverine transport of biogenic elements to the Baltic Sea – past and possible future perspectives." *Hydrol. Earth Syst. Sci.* 11: 1593–1607.

Schreiber, H., H. Behrendt, L.T. Constantinescu, I. Cvitanic, D. Drumea, D. Jabucar, S. Juran, B. Pataki, S. Snishko, and M. Zessner. 2005. "Point and diffuse nutrient emissions and loads in the transboundary Danube River Basin. – I. A modelling approach." *Arch. Hydrobiol. Suppl.* 158: 197-220.

Venohr, M. 2006. *Modellierung der Einflüsse von Temperatur, Abfluss und Hydromorphologie auf die Stickstoffretention in Flusssystemen.* Berliner Beiträge zur Ökologie, 14, Weissensee.

Venohr, M., U. Hirt, J. Hofmann, D. Opitz,, A. Gericke, A. Wetzig, K. Ortelbach, S. Natho, F. Neumann, and J. Hürdler. 2010. *The model system MONERIS 2.14.1vba Manual.* Leibniz Institute of Freshwater Ecology and Inland Fisheries, Berlin, Germany.

Venohr, M., U. Hirt, J. Hofmann, D. Opitz, A. Gericke, A. Wetzig, S. Natho, F. Neumann, J. Hürdler, M. Matranga, J. Mahnkopf, M. Gadegast, and H. Behrendt. 2011. „Modelling of nutrient emissions in river systems - MONERIS: methods and background." *Int. Rev. Hydrobiol.* 96(5): 435-483.

Voss, M., J. W. Dippner, C. Humborg, J. Hürdler, F. Korth, T. Neumann, G. Schernewski, and M. Venohr. 2011. "History and scenarios of future development of Baltic Sea eutrophication." *Estuarine, Coastal Shelf Sci.* 92(2011): 307-322.

# ROBUST MODELING OF NUTRIENT DYNAMICS IN LARGE WATER BODIES A CASE STUDY IN THE GULF OF FINLAND

*Safeyeh Sofie Soltani* (Royal Institute of Technology, Stockholm, Sweden)
Benoît Dessirier (Stockholm University, Stockholm, Sweden)

**ABSTRACT:** The high level of nutrients in large water bodies causes adverse effects like algae blooms, degraded habitat and drinking water, and compromised biological productivity. Quantitative projections of these various effects require an understanding of the flow field and the biogeochemical nutrient pools and pathways. We have created a simple carbon-based water quality, box model for the eutrophied Gulf of Finland. We tested different modeling strategies for the biogeochemical transformations. The new criterion determines the occurrence of anoxic events, based on the amount of fresh carbon detritus in the sediments. It compared well with the classical oxygen-based modeling approach. Different parameterizations of the release of iron-bound phosphate from the sediments under anoxia were also cross-tested. We have found that the use of time-averaged hydrodynamics over longer periods than daily intervals hinders the capture of rapid mixing events, which compromises water quality simulations. One could calibrate both modeling strategies to capture seasonal features and reach reasonable performance levels. However, the new carbon-based criterion for anoxia shows the best dynamic response when associated with a net-provider sediment phosphate flux and is less sensitive to its internal parameters. We believe our proposed model could be applicable to similar cases.

## INTRODUCTION

Water bodies are attractive environments that are subject to high environmental pressures. One such threat is critical nutrient enrichment in the water due to anthropogenic releases like agriculture, industrial effluents or municipal sewage. A significant excess of nutrients (Nitrogen and Phosphorus) can disrupt the balance of aquatic ecosystems and trigger an ecological shift called eutrophication (Ansari, 2010). Common features of a eutrophied environment are massive summertime green algae blooms, depletion of oxygen, increased water turbidity, and reduced fish populations (Ansari, 2010). To address these problems there is a need for reliable and robust control systems and management schemes.

Nutrients sources could be both from external loadings from rivers, land runoff, and atmospheric deposition or internal latent sources like buried nutrients in the sediment bed underlying the water body. An effective approach is to control external sources by enforcing adequate environmental legislation on admissible nutrient releases.

A good understanding of the local eutrophication process is the first step in the design and successful implementation of effective management schemes. The latter requires a combined field study and hydrodynamic-water quality modeling approach. Complicated 3D fine resolution models exist that can resolve the hydrodynamics coupled with the ecosystem (Kiirikki et al., 2006; Neumann and Schernewski, 2008; Eilola et al., 2011). However, the use of these models are limited by the long CPU times and the need for extensive data for model calibration and validation. One alternative is to use a simple box model structure that captures important processes affecting the water quality, given the scarcity of the available data. An example is the simple box model developed and successfully applied to the Lake Erie (Lam et al., 1987). Engqvist and Andrejev (2003) and Gustafsson (2003) developed similar models for the different basins in the Baltic Sea. Compared with the 3D models, the box models can yield reasonable and comparable results (Eilola et al., 2011) and thus serving as effective tools for flexible decision-making support (Gustafsson and Savchuk, 2010).

Regarding Nutrient cycling, the classical understanding is that the oxic state, i.e. the presence of electron acceptors, here mainly dissolved oxygen, determines the biogeochemical processes in the water column and at the underlying sediment interface. Most models tend subsequently to rely on the oxygen budget to trigger the appropriate set of reactions (Stigebrandt and Wulff, 1987; Cerco and Cole, 1995;

Neumann et al., 2002; Gustafsson, 2003). However, oxygen demand within the sediments can produce steep oxygen concentration gradients close to the bottom that are hard to render accurately in the models. To overcome this difficulty, Kiirikki et al. (2006) proposes an indirect estimation of the oxic state based on the organic carbon balance.

The focus of our study is on the Gulf of Finland (GoF). In spite of the Baltic Sea agreement in 1974 the state of Baltic Sea has become worse (http://www.helcom.fi/home/en_GB/welcome/). Nutrient levels in the water and sediments are high, and poor oxygen conditions and "dead bottoms" exist in large archipelago areas in both Sweden and Finland. Kiirikki et al. (2001) attribute the problem to the sustained internal loading phenomenon. We have emphasized the latter phenomenon.

We aim at developing a simple water quality model as well as identifying the sensitivity of the two alternative biogeochemical models in terms of parameterization and input data. We believe acquiring knowledge on the robustness of the models, especially to the rendition of high frequency variations in the flow system mostly wind-driven, is a crucial step towards integrating them with low frequency climate scenarios. To test our proposed model we have selected the (GoF) which is one of the sub-basins of the Baltic Sea (Fig. 1) and has some serious water quality problems.

## MATERIAL AND METHODS

The Gulf of Finland (GoF) is the easternmost extension of the Baltic Sea, a brackish enclosed sea in Northern Europe. The GoF has an area of 300 000 km$^2$ and flow depths in the range of 3m-120m with a mean depth of 38 m. It is fed by 10 rivers among which the river Neva supplies 70% (mean flow 2500 m$^3$/s) of the total freshwater inflow (Fig. 1). We also had data at several stations on various water quality parameters, water temperature, salinity, and solar radiation (Fig. 1).
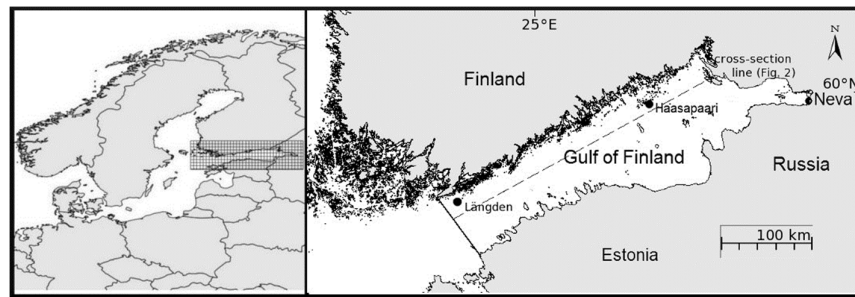


**FIGURE 111 Map of the Baltic Sea and the Gulf of Finland (GoF) with the data stations**
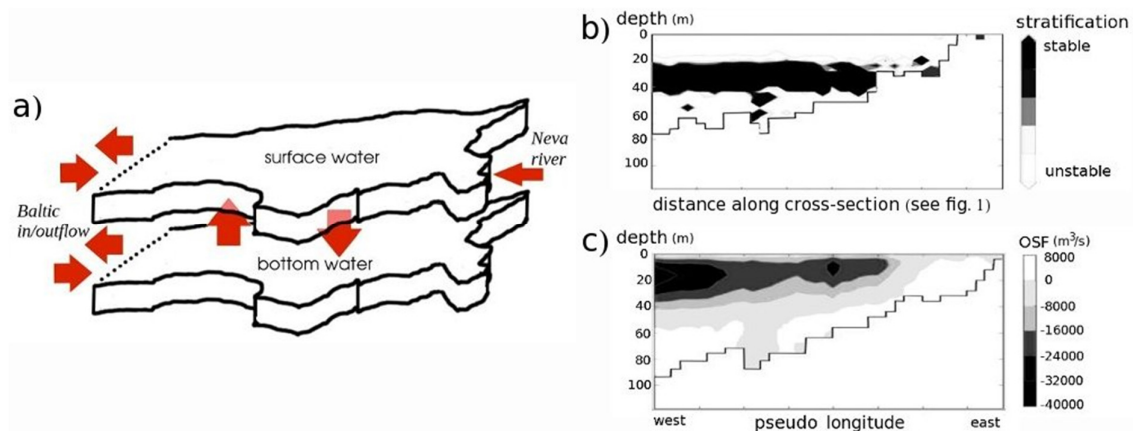


**FIGURE 2 12 a) Two layer box model b) Stratification by Richardson gradient number: Ri>10 stable, Ri<0 unstable c) yearly-averaged overturning stream function: negative poles indicate clockwise motion and positive poles, anti-clockwise**

We are proposing a new water quality model that subdivides the GoF into two boxes representing surface and bottom water layers (Fig. 2a). The motivation for this approach is our understanding of the hydrodynamic processes in the Gulf of Finland. We analyzed the output of a calibrated 3D hydrodynamic model for the Baltic Sea (Dargahi, 2012, in publication) for the period 2000-9 at 2 days intervals. He created the detailed hydrodynamic model using the Generalized Environmental Modeling System for Surface waters (GEMSS) with a spatial grid resolution of 10 km and 46 vertical layers ranging from 4m-14m. Our simplified hydrodynamic model consisted of two boxes of same area taken as the surface area of the GoF. The surface box was 20m deep and the bottom box 18m, which agree with the average depth of 38 m reported by Schiewer (2008). The fluxes between the two boxes allow simultaneous up- and down welling and exchange with the Baltic Sea in both directions at a resolution of 2 days. We also examined monthly averaged versus daily velocity values. We extracted the grid and the velocity vectors for the GoF from the detail Baltic Sea model for the period 2000-7. Using these data, we calculated the Richardson gradient number (Ri) and the Overturning Stream Function (OSF) (Döös et al., 2004) (Fig. 2b & 2c). We obtained the volumetric exchange between boxes (Fig. 2a) by integrating the flow rates across the horizontal plane at 30 m depth that represent the halocline and across the boundaries above and below 30 m.

The details of the verified basic hydrodynamic characteristics of the GoF and the water quality model are available from Dessirier and Soltani (2011). We coupled the oceanic phytoplankton model suggested by Tyrrell (1999) and implemented by Kiirikki et al. (2001) with two different sediment modules. A classical module derived from Neumann and Schernewski (2008) and a new module from Kiirikki et al. (2006). By this, we could simulate redox sensitive biogeochemical processes. The classical approach is based on the oxygen concentration in the bottom water. The new module delineates anaerobic conditions by applying a recently proposed criterion based on the amount of $CO_2$ gas formation due to oxidization of fresh carbon detritus in the sediments. Kiirikki et al. (2006) state the main advantage is the ability of capturing the occurrence of anoxic events in the sediments while the near-bottom water remains oxygenated.

Figs. 3a and 3b give a schematic view of the main processes at the lower layer. Two groups of phytoplankton species compete: nitrogen-fixing cyanobacteria (C) and other algae (A). C and A take up dissolved inorganic nitrogen (DIN) and dissolved inorganic phosphorus (DIP) and turned into detritus ($C_{det}$, $N_{det}$, $P_{det}$) both according to the Redfield ratio (C:N:P=41:7.2:1 by weight) (Redfield, 1958). Being mineralized while sinking at 1 m/s along, the water column they form volatile sediments ($P_v$, $N_v$, $C_v$) through sedimentation process. Internal loading takes place when iron-trapped phosphorus ($PFe_v$) releases DIP back to the bottom water under anoxic conditions (Fig. 3a).
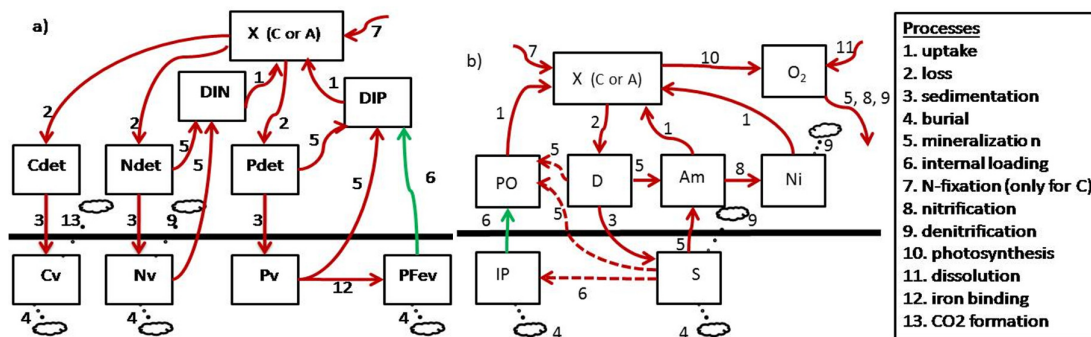


**FIGURE 3 a) Scheme of the new carbon-based model b) Scheme of the classical oxygen-based model and the main processes**

Neumann and Schernewski (2008) subdivide DIN into ammonium $A_m$ ($NH_4$) and nitrate $N_i$ ($NO_3$). DIP is taken equivalent to Phosphate PO ($PO_4$). The Dead biomass is accumulated in a detritus pool (D) similar to previous $N_{det}$ (the Redfield ratio could give the corresponding $P_{det}$). Nitrogen detritus reaching the sediment bed turn into volatile nitrogen (S). The iron minerals could bind to phosphorus under aerobic conditions, which is then noted as $I_P$ ($\approx PFe_v$). Produced by photosynthesis and dissolved from the atmosphere oxygen ($O_2$) drives the model by moderating redox reactions (Fig. 3b).
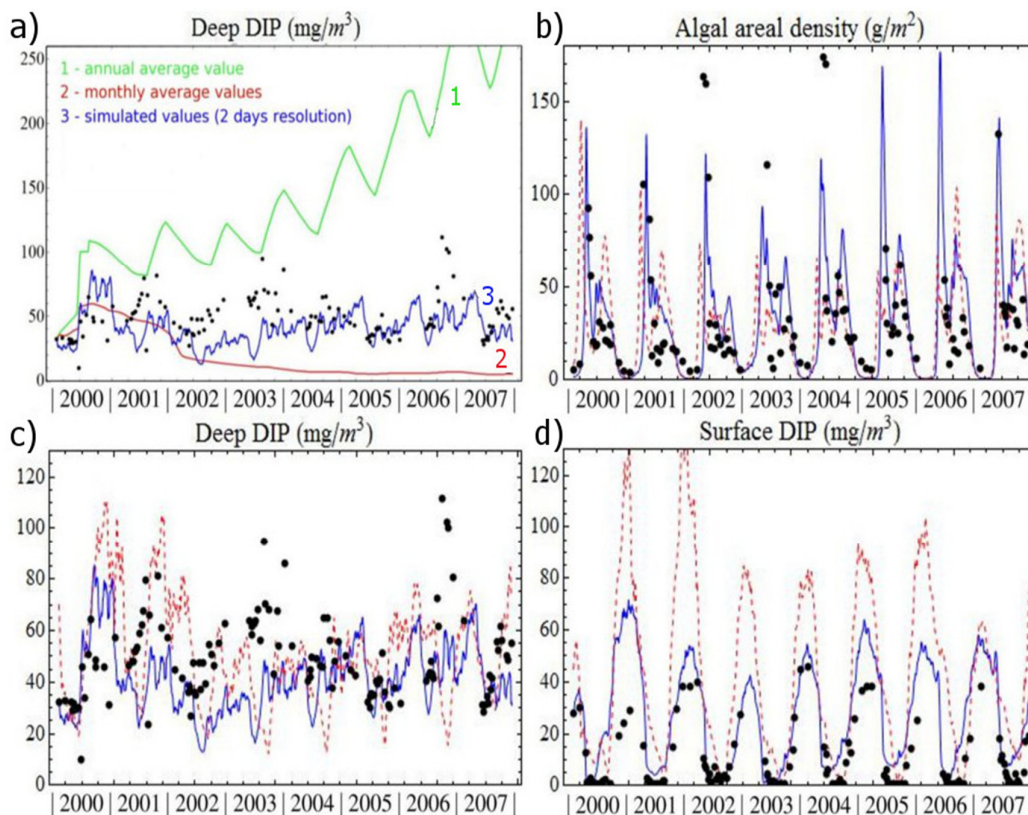
**FIGURE 4  a) Deep water DIP under flow with various time resolution; b-d) Model
results, oxygen-based (dashed line) and carbon-based (plain line), for the total biomass
(b), the deep water DIP (c) and the surface water DIP (d), dots field data**

We modified Neumann and Schernewski's (2008) formulation to enable a net source of phosphorus in the sediments for internal loading, which was similar to the approach used by Kiirikki et al. (2006). We designed a combination of two threshold conditions to trigger anoxic processes, in order to adapt the distributed classical model to our coarse box approach: $O_2 < O_{2T} = 8.5$ g/m$^3$ and $\partial O_2 /\partial t < 0$. The switch to anoxic conditions in the carbon-based model is activated when $CO_2$ formation in the sediments reaches a critical value $C_{Cr}$.

To drive the water quality model we used the simplified flow values from the GEMSS model, the temperature time series recorded in the Finish monitoring stations Haasapaari (Fig. 1) and the estimated averaged solar radiation. We supplied the external loading from the annual values given by (Schiewer, 2008). Interpolation of the records at the monitoring station Längden (Fig. 1) provided continuous boundary conditions. To initiate the model, we used literature values and the data at Haasapaari monitoring station. We first calibrated the models' internal parameters for the year 2004 and validated for the period 2000 to 2007 against the records at the Haasapaari station. To evaluate the model performance and its sensitivity to anoxia triggers we investigated the robustness of models by using the Nash–Sutcliffe model efficiency coefficient ($E_{NS}$) and running a Monte Carlo procedure. The internal parameters, i.e. critical carbon ($C_{Cr}$) and oxygen threshold ($O_{2T}$) for the Baltic Sea were uniformly distributed, over two ranges of 200-470 mg C m$^{-2}$.d$^{-1}$ (Kiirikki et al., 2006) and 7-12 g.m$^{-3}$, respectively.

## RESULTS AND DISCUSSION

We obtained an extensive set of results, here we only show some representative plots (Fig. 4a-4d, and Fig. 5a and 5b).The main features were the existence of a stable halocline at mid-depths (Fig. 2a). The values of Ri >10 confirm the existence of a stable stratification in the GoF. We also identified two circulation patterns using the OSF (Fig. 2b). The foregoing result support our assumption  that the two

circulation cells could be modeled as two fully mixed boxes embodying surface water and deep water separated by the halocline. Our analysis also showed that vertical mixing and transport were dominated by advection rather than dispersion (i.e., Peclet number) >1). Thus, we could neglect dispersion across the halocline. A calibrated biogeochemical model where all species are subject to the physical transport described by the simplified hydrodynamic model yielded values in the range of the collected data (Fig. 4a), which validates the spatial basin aggregation and the vertical layering. However, if we decreased the 2 day resolution of the hydrodynamics to monthly or yearly, the water quality simulation deteriorated significantly. It could become unstable or the ecosystem could die out completely (Fig 4a), for further details the reader is referred to Dessirier and Soltani (2011).
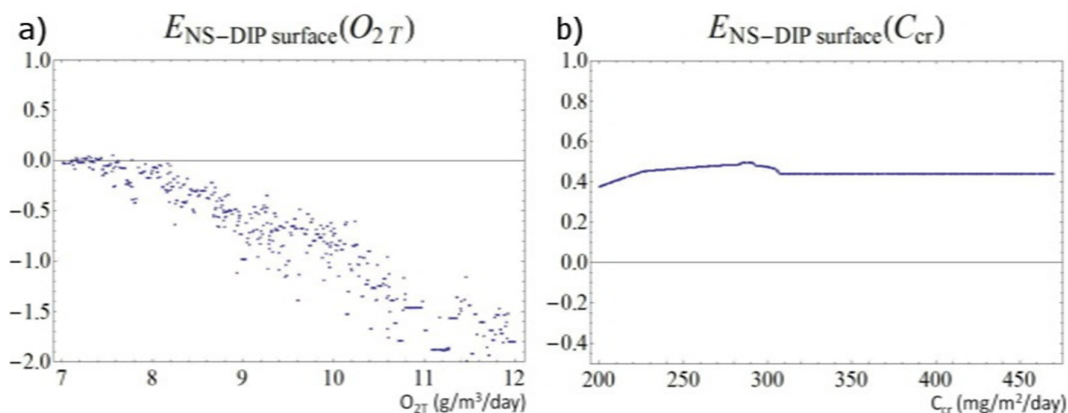


**FIGURE 5 a) Sensitivity of the oxygen-based model to $O_{2T}$; b) Sensitivity of the carbon-based model to $C_{Cr}$**

Both models forecasted summer algal blooms comparably well (Fig. 4b). Algal dynamics were effectively captured by the carbon-based model and peak values were well aligned with the measurements in spring time. The classical model did not render spring peak values as accurately but yielded a better average (Fig. 4b). The yearly averaged primary production values obtained from classical and carbon based simulations were respectively, 102 g C/ $m^2$/ year and 134 g C/ $m^2$/ year. Schiewer (2008) reported a typical yearly primary production of 75-110 g C/ $m^2$/ year. Both modules showed reasonable capabilities of modeling DIP accumulations in the surface in winter times whereas during summer periods excessive DIP concentrations were present in the classical model (Fig. 4d). DIP concentration in deep water or the so-called internal loading which was the main focus of the present study, was simulated with an up to standard accuracy in comparison to the measured data (Fig. 4c). The daily averaged phosphate release predicted by carbon-based model was 4.8 mg P / $m^2$ / day whereas Schiewer (2008) presents 5.5 mg P / $m^2$ / day. Both models showed that the ecosystem was Nitrogen-limited which complied with the published literature (Schiewer, 2008).

We found the DIP-$E_{NS}$ of carbon-based model to be close to 0.5 (ideal value: 1.0) (Fig. 5b). Parametric uncertainty on $C_{cr}$ did not impair the model performance (Fig. 5b). Therefore spatial variability of $C_{Cr}$ did not affect the results and only a limited tuning of internal parameters was required. On the contrary the oxygen-based model, showed high sensitivity to the oxygen threshold (Fig. 5a). The robustness of the carbon-based model enhances its applicability to the basins in the Baltic Sea or similar basins. Sensitivity to oxygen threshold and steep gradients of oxygen concentrations in near-bottom water and volatile sediments remain otherwise sources of uncertainty.

Both models gave better results when the sediments acted as a net source of Phosphorus for the studied years.

## CONCLUSIONS

We have successfully calibrated and validated a simplified water quality model for the Gulf of Finland. Our study has enabled us to draw the following conclusions.

1. The mean hydrodynamic characteristics of the GoF could be modeled using a two-box approach.
2. Our simple water quality box model for the eutrophied Gulf of Finland gives good results in comparison with more complex models that are oxygen-based.
3. The new carbon-based criterion for anoxia is less sensitive to its internal parameters.
4. The model shows the best dynamic response when associated with a net-provider sediment phosphate flux.
5. The main merits of our model are the simplicity of application and significantly less demanding data requirement.
6. We believe our model could be applied to similar cases.

## ACKNOWLEDGMENTS

## REFERENCES

Ansari, A.A., 2010. *Eutrophication: Causes, Consequences and Control.* Springer.

Cerco, C.F., Cole, T., 1995. *User's Guide to the CE-QUAL-ICM Three-dimensional Eutrophication Model: Release Version 1.0.* US Army Engineer Waterways Experiment Station.

Dessirier, B., Soltani, S., 2011. *Dynamics of internal nutrient sources in the Baltic Sea, a comparative modeling study of the Gulf of Finland.* M.S. Thesis, KTH, Stockholm, Sweden.

Döös, K., Meier, H.E.M., Döscher, R., 2004. "The Baltic Haline Conveyor Belt or The Overturning Circulation and Mixing in the Baltic." AMBIO: A Journal of the Human Environment 33, 261–266.

Eilola, K., Gustafsson, B.G., Kuznetsov, I., Meier, H.E.M., Neumann, T., Savchuk, O.P., 2011. "Evaluation of biogeochemical cycles in an ensemble of three state-of-the-art numerical models of the Baltic Sea." Journal of Marine Systems 88, 267–284.

Engqvist, A., Andrejev, O., 2003. "Water exchange of the Stockholm archipelago—a cascade framework modelling approach." Journal of Sea Research 49, 275–294.

Gustafsson, B.G., 2003. *A time-dependent coupled-basin model of the Baltic Sea.* Earth Sciences Centre. Göteborg University, Göteborg. Sweden.

Gustafsson, B.G., Savchuk, O.P., 2010. "BALTSEM - A computationally efficient model of the eutrophication of the Baltic Sea designed for decision support purposes." In: AGU Ocean Sciences Meeting. Presented at the AGU, np.

Kiirikki, M., Inkala, A., Kuosa, H., Pitkänen, H., Kuusisto, M., Sarkkula, J., others, 2001. "Evaluating the effects of nutrient load reductions on the biomass of toxic nitrogen-fixing cyanobacteria in the Gulf of Finland, Baltic Sea." Boreal Environment Research 6, 131–146.

Kiirikki, M., Lehtoranta, J., Inkala, A., Pitkanen, H., Hietanen, S., Hall, P.O.., Tengberg, A., Koponen, J., Sarkkula, J., 2006. "A simple sediment process description suitable for 3D-ecosystem modelling–Development and testing in the Gulf of Finland." Journal of Marine Systems 61, 55–66.

Lam, D.C.L., Schertzer, W.M., Fraser, A.S., 1987. "A Post-Audit Anaylsis of the NWRI Nine-Box Water Quality Model for Lake Erie." Journal of Great Lakes Research 13, 782–800.

Neumann, T., Fennel, W., Kremp, C., 2002. "Experimental simulations with an ecosystem model of the Baltic Sea: a nutrient load reduction experiment." Global Biogeochemical Cycles 16, 7–19.

Neumann, T., Schernewski, G., 2008. "Eutrophication in the Baltic Sea and shifts in nitrogen fixation analyzed with a 3D ecosystem model." Journal of Marine Systems 74, 592–602.

Redfield, A.C., 1958. "The biological control of chemical factors in the environment." American Scientist 46.

Schiewer, U., 2008. *Ecology Of Baltic Coastal Waters.* Springer.

Stigebrandt, A., Wulff, F., 1987. "A model for the dynamics of nutrients and oxygen in the Baltic proper." Journal of Marine Research 45, 729–759.

Tyrrell, T., 1999. "The relative influences of nitrogen and phosphorus on oceanic primary production." Nature 400, 525–531.

# WATER QUALITY PLANNING USING A RISK-BASED PROGRAMMING MODEL

*Qin Xiaosheng* and Xu Tianyi

(CEE & EOS, Nanyang Technological University, Singapore)

**ABSTRACT:** A genetic algorithm (GA) based chance-constrained programming (GACCP) model was proposed for supporting river water quality management under uncertainty. A risk-based framework was developed to assess the reliability of waste load allocation strategies in compliance with the water quality management goal. A coupled GA and Monte Carlo simulation (MCS) technique was used to seek the optimal solution of the management model by progressively evaluating the performance of individual waste-removal alternatives. A river section, with the need to do a waste allocation planning considering both minimum treatment cost and uncertainty in the water quality processes, was used to demonstrate the applicability of the proposed method. The studied system had a total of 12 decision variables and 30 random variables. The study results indicated that GACCP could effectively communicate uncertainties associated with water quality parameters into the optimization process. Decision alternatives could be obtained by analyzing tradeoffs between the wastewater treatment cost and the failure risk of violating the related environmental standards. Generally, GACCP could be widely used for many environmental management problems, where simulation and optimization models are coupled together under an uncertain environment.

## INTRODUCTION

With an increasing concern on total maximum daily load (TMDL) control in recent years, the multi-point-source waste reduction (MWR) model has been widely used for limiting the amount of waste discharged into water bodies (Loucks et al., 1981; Tung and Hathhorn, 1990). The MWR model generally integrates a water quality simulation model within an optimization framework to provide analysis on relationships that describe the stream water quality and the cost of each management alternative as functions of design and operating policy variables. However, water-quality planning efforts are complicated with a variety of uncertainties, which may affect optimization solutions and the associated decision making processes. The complexity of the river pollution control problem necessitates the development and use of a variety of inexact optimization models that explicitly incorporate uncertainty into the regional characteristics of the pollution problems (Sasikumar and Mujumdar, 1998; Stijnen et al., 2003; Revelli and Ridolfi, 2004).

Among various alternatives of inexact optimization methods, chance-constrained programming (CCP) model has been extensively used for minimizing total effluent treatment costs while maintaining violation of water quality standards within maximum allowable probability levels (Dupacova, 1991; Huang, 1998; Qin and Huang, 2009). However, in most of the previous studies, the chance constraints had to be converted to their crisp equivalents through a series of mathematical manipulations (Huang, 1998). Such a treatment was only applicable to a limited number of special cases. In recent years, genetic algorithms (GAs) have gained their popularity in solving many water quality management problems due to their suitability for complex, discontinuous, and nonlinear problems (Burn and Yulianti, 2001; Cho et al., 2004). Hence, this study attempts to demonstrate the applicability of using a genetic algorithm (GA) based chance-constrained model to a river water quality management problem. GA will be coupled with MCS for identifying the optimal solution of the management model. An explicit risk-based framework will be used to address the propagation of uncertainty effects that are originated from the simulation model.

## METHODOLOGY

**Framework of Solving a Probabilistic Model Based on Genetic Algorithm:** A chance-constrained programming with random parameters can be written as follows (Dupacova et al., 1991):

$$Min\ f(\mathbf{x}, \xi) \tag{1a}$$

Subject to:

$$\Pr\{\xi \mid g_i(\mathbf{x}, \xi) \leq 0\} \geq 1 - ARL_i, \quad i = 1, 2, ..., k, \tag{1b}$$

$$h_j(\mathbf{x}) \leq 0, \quad j = 1, 2, ..., p, \tag{1c}$$

$$\mathbf{x} \geq 0 \tag{1d}$$

where $g_i$ are the constraint functions with random parameters, $i = 1, 2, ..., k$; $k$ is the number of uncertain constraints; $h_j$ are the deterministic constraint functions, $j = 1, 2, ..., p$; $p$ is the number of deterministic constraints; $\mathbf{x}$ is a vector of decision variables; $\xi = (\xi_1, \xi_2, ..., \xi_m)$ is a $m$-dimensional stochastic vector; $ARL_i$ is the allowable risk level for the $i$th uncertain constraint. The objective of model (1) is to accomplish the balancing with minimum value of objective function so that the probability of the inequalities being met should stay under the predetermined limits. The fundamental idea is to use GA to search optimal solutions, with stochastic simulation (i.e. MCS) being employed to check the feasibility of an individual solution. The detailed procedures of GA components are described as follows (Pelletier et al., 2006):

*Step 1: Initialization.* The individuals (i.e. chromosomes, denoted as $\mathbf{x}^{(1)}$) in the first generation of population are initialized, with each one being randomly generated within a pre-specified interval.

*Step 2: Evaluation.* Each individual is evaluated by a fitness function. For a constraint programming model, the fitness function is defined as follows:

$$F = f(\mathbf{x}, \xi) + M_1 + M_2 \tag{2}$$

where $M_1$ is a penalty factor for reflecting violation of deterministic constraints; it is defined as a large real number when $h_j(x) \leq 0$ is not met. $M_2$ is a penalty factor for reflecting violation of stochastic constraints at a certain probability level; it is defined as a large number when the estimated real risk level is larger than the allowable risk level; and as zero when it is lower.

Let $RRL_i = 1 - \Pr\{\xi \mid g_i(\mathbf{x}, \xi) \leq 0\}$ ($i = 1, 2, ..., k$), where $RRL_i$ is the real risk level for stochastic constraint $g_i$. For any given $\mathbf{x}$, MCS is used to estimate $RRL_i$. Totally, $NT$ independent random vectors $\xi^{(r)}$ = ($\xi_1^{(r)}, \xi_2^{(r)}, ..., \xi_m^{(r)}$), $r = 1, 2, ..., NT$, will be generated based on their probability distribution functions. Let $NY_i$ be the number of occasions when $g_i(\mathbf{x}, \xi) \leq 0$ is satisfied. Then, $RRL_i$ can be approximated by $RRL_i \approx (NT - NY_i) / NT$ (Liu and Iwamura, 1998):

*Step 3: Selection, Crossover and Mutation.* In this study, tournament selection with elite protection is used. One or two elites (i.e. individuals with the best fitness values) in the current generation will be guaranteed to survive to the next generation. One-point crossover with probability $p_{cross}$ (i.e. crossover rate) and Gaussian mutation with probability $p_{mut}$ (i.e. mutation rate) are used.

*Step 4: Stop Check.* The GA iteration will be terminated either after the maximum generation number is exceeded or the change of the fitness function value is lower than a specified value (i.e. termination tolerance). The chromosome with the lowest fitness value becomes the final optimal solution. If the termination criterion is not met, go to *Step 3* and continue iterations. Figure 1a shows the overall framework of the study methodology.

**Formulation of GACCP for Water Quality Management:** A CCP model for a multiple-point-source water quality management system can be formulated as follows (Qin and Huang, 2009):

$$Min\ f = \sum_{t=1}^{ND} Q_t^{k_{2t}} \left[ k_{1t} + k_{3t} H_t^{k_{4t}} \right] \tag{3a}$$

Subject to:

$$H_t = \left( \frac{L_{c0t}\eta_{ct} + L_{N0t}\eta_{Nt}}{L_{c0t} + L_{N0t}} \right), \quad t = 1, 2, ..., ND \tag{3b}$$

$$L_{c0t}(1-\eta_{ct}) + L_{N0t}(1-\eta_{Nt}) \le DS_t, \quad t = 1, 2, ..., ND \tag{3b}$$

$$\Pr\left[ \sum_{t=1}^{ND}\left[ U_{cst}L_{c0t}(1-\eta_{ct}) \right] + m_{cs} + \sum_{t=1}^{ND}\left[ U_{Nst}L_{N0t}(1-\eta_{Nt}) \right] + m_{Ns} \le SS_s^\omega \right]$$
$$\ge 1 - ARL_{s,\omega}, \quad s = 1, 2, ..., NS; \omega = BOD \text{ or } DO \tag{3c}$$

$$\eta_{at}^{\min} \le \eta_{at} \le \eta_{at}^{\max}, \quad a = c \text{ or } N; t = 1, 2, ..., ND \tag{3e}$$

where $f$ represents the total operational cost, [RMB]; $t$ is the index of wastewater discharge sources, $t = 1$, 2, …, $ND$; $ND$ is the total number of discharge sources; $s$ is the index of river segment, $s = 1, 2, …, NS$; $NS$ is the total number of river segments; $H_t$ is the averaged treatment efficiency at discharge source $t$; $\eta_{ct}$ and $\eta_{Nt}$ are treatment efficiencies of CBOD and NBOD at discharge source $t$; $Q_t$ is the wastewater flow rate at the source $t$ [ML$^{-3}$]; $k_{1t}$, $k_{3t}$, and $k_{4t}$ are the cost-function coefficients ($k_{1t}$, $k_{3t} > 0$, $k_{4t} > 1$) for the discharge source $t$; $k_{2t}$ is the economy-of-scale index for the discharge source $t$ and normally ranges from 0.7 to 0.9; $L_{c0t}$ and $L_{N0t}$ are the initial concentrations of CBOD and NBOD at discharge source $t$, [ML$^{-3}$]; $DS_t$ is the effluent discharge standard for the discharge point $t$; $SS_s^\omega$ is the standard for surface water quality indicator $\omega$ at the river segment $s$; $U_{cst}$, $U_{Nst}$, $V_{cst}$, and $V_{Nst}$ are the stochastic elements at the $s$th row and the $t$th column ($s = 1, 2, …, NS; t = 1, 2, …, ND$) of the water-quality transformation matrices (U$_c$, U$_N$, V$_c$, and V$_N$), respectively; $m_{cs}$, $m_{Ns}$, and $n_s$ are the stochastic element at the $s$th row of water-quality transformation vectors (m$_c$, m$_N$, and n); $ARL_{s,\omega}$ is the acceptable risk level of violating standard of $\omega$ at the $s$th river segment; $\eta_{at}^{\min}$ and $\eta_{at}^{\max}$ are the minimum and maximum treatment efficiencies for either CBOD ($a = c$) or NBOD ($a = N$), respectively, at the discharge point $t$.

**Generation of Stochastic Transformation Matrices and Vectors:** For each river segment, O'Connor model will be used for supporting quantification of surface water quality, and is described as (O'Connor and Dobbins, 1958):

$$L_c = L_{c0}e^{-(k_d+ks)x/u_x} \tag{4a}$$

$$L_N = L_{N0}e^{-k_N x/u_x} \tag{4b}$$

$$O = O_s - (O_s - O_0)e^{-k_a x/u_x} - \frac{k_d L_{c0}}{k_a - (k_d + k_s)}\left[ e^{-(k_d+k_s)x/u_x} - e^{-k_a x/u_x} \right] - \frac{k_N L_{N0}}{k_a - k_N}\left[ e^{-k_N x/u_x} - e^{-k_a x/u_x} \right] \tag{4c}$$

where $L_{c0}$, $L_{N0}$, and $O_0$ are initial ultimate CBOD, NBOD and DO loads in stream, respectively; $L_c$ is the ultimate CBOD concentration, [ML$^{-3}$]; $L_N$ is the ultimate NBOD concentration, [ML$^{-3}$]; $k_d$ is the CBOD decay rate in river streams, [T$^{-1}$]; $k_s$ is the CBOD decay rate due to sedimentation, [T$^{-1}$]; $O$ is the DO concentration, [ML$^{-3}$]; $O_s$ is the saturated DO concentration, [ML$^{-3}$]; $k_N$ is the nitrification rate (NBOD decay rate in river), [ML$^{-3}$]; $k_a$ is the reaeration rate, [ML$^{-3}$]; $u_x$ is the average stream flow rate, [L/T]; $x$ is the flow distance, [L]. The stochastic transformation matrices and vectors are predetermined based on MCS coupled with a water quality prediction model. Based on mass balance, flow continuity and rate, and BOD equilibrium under a steady-state water flow regime, the following relations in light of uncertainties can be derived (Qin and Huang, 2009):

$$L_{c2} = \bar{U}_c(\chi, \xi)L_c + \bar{m}_c(\chi, \xi) \tag{5a}$$

$$L_{N2} = \bar{U}_N(\chi, \xi)L_N + \bar{m}_N(\chi, \xi) \tag{5b}$$

$$O_2 = \bar{V}_c(\chi, \xi)L_c + \bar{V}_N(\chi, \xi)L_N + \bar{n}(\chi, \xi) \tag{5c}$$

where $\bar{U}_c$, $\bar{U}_N$, $\bar{V}_c$, and $\bar{V}_N$ are stochastic water-quality transformation matrices; $\bar{m}_c$, $\bar{m}_N$, $\bar{n}$ are stochastic water-quality transformation vectors; $\chi$ is a vector of deterministic parameters; $\xi$ is a vector of stochastic parameters; $L_c$ and $L_N$ are vectors of CBOD and NBOD loadings of various discharge sources, respectively; $L_{c2}$ and $L_{N2}$ are predicted CBOD and NBOD levels at different river segments, respectively.

## RESULTS

**Case Background:** A short section of a river system in China with 25 km length will be used as a study case to demonstrate the applicability of the proposed method (Figure 1b). The study case has been reported by Qin et al. (2007, 2009). The river section receives the majority of wastewater discharged from six industrial discharging sources, including a Leatheroid Plant, a Hospital, a Paper Mill, a Wastewater Treatment Plant, a Textile Plant and a Chemical Plant. Based on the locations of discharge sources, six river segments are considered. Water quality in these segments should meet the national surface water quality standard. Raw wastewater at each discharge source contains high concentrations of BOD, and must be treated before discharge. Meanwhile, the total treatment cost is desired to be as low as possible. The objective of this study case is then to minimize the operating cost and satisfy the national environmental standard. Table 1 shows the related water quality parameters.



(a)                                                      (b)
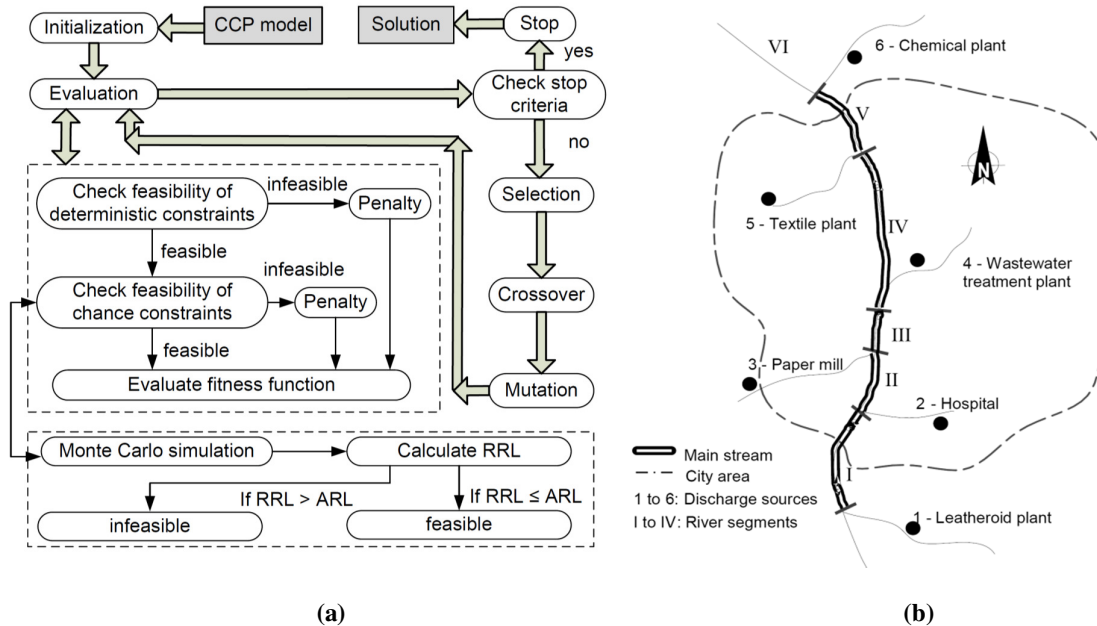
**FIGURE 1.** Framework of methodology and study case.

**Result Analysis:** Figure 2 shows the relationships between the system cost and ARL under various scenarios. The three scenarios are designed based on different levels of China national surface water quality standards. Under Scenario 1, the Class II standards for BOD and DO will be used (3 and 6 mg/L); under Scenarios 2 and 3, Class III (4 and 5 mg/L) and IV (6 and 3 mg/L) standards will be applied, respectively (CEPA, 2002). It is indicated that the system costs are inversely proportional to ARLs under Scenarios 1 and 2. Under Scenario 3, the cost would keep relatively constant (around $2,136 \times 10^4$ RMB) at various ARLs, showing that the effluent constraints (i.e. deterministic constraints) are strict enough to

ensure the Class IV water quality standard being met. The ARLs represent a set of probabilities at which the constraints would be violated. Thus, the relationship between the system cost and ARL level exhibits a tradeoff between cost efficiency and constraint-violation risk. An increased ARL means a loosened requirement for the water-quality constraints, which may then result in a decreased system cost; a lower ARL would lead to an increased reliability in meeting the water quality standards but with a higher cost.

**Table 1.** List of parameters

| | Leatheroid Plant (t = 1) | Hospital (t = 2) | Paper Mill (t = 3) | Wastewater Plant (t = 4) | Textile Plant (t = 5) | Chemical Plant (t = 6) |
|---|---|---|---|---|---|---|
| $k_{dt}$ (d$^{-1}$) | $N(0.54, 0.06)^*$ | $N(0.35, 0.09)$ | $N(0.84, 0.09)$ | $N(0.84, 0.09)$ | $N(0.71, 0.09)$ | $N(0.71, 0.09)$ |
| $k_{st}$ (d$^{-1}$) | $N(0.30, 0.06)$ | $N(0.18, 0.06)$ | $N(0.34, 0.09)$ | $N(0.34, 0.09)$ | $N(0.31, 0.06)$ | $N(0.31, 0.06)$ |
| $k_{Nt}$ (d$^{-1}$) | $N(0.43, 0.09)$ | $N(0.30, 0.12)$ | $N(0.62, 0.06)$ | $N(0.62, 0.06)$ | $N(0.58, 0.12)$ | $N(0.58, 0.12)$ |
| $k_{at}$ (d$^{-1}$) | $N(0.52, 0.12)$ | $N(0.45, 0.09)$ | $N(0.85, 0.14)$ | $N(0.85, 0.14)$ | $N(0.56, 0.10)$ | $N(0.56, 0.10)$ |
| $Q_t$ (m$^3$/s) | $U(0.35, 0.45)^{**}$ | $U(0.40, 0.50)$ | $U(0.10, 0.20)$ | $U(1.95, 2.05)$ | $U(0.55, 0.65)$ | $U(0.10, 0.18)$ |
| $k_{1t}$ | 396.09 | 408.71 | 379.69 | 451.59 | 374.65 | 362.66 |
| $k_{2t}$ | 0.8 | 0.8 | 0.8 | 0.8 | 0.8 | 0.8 |
| $k_{3t}$ | 4749.00 | 4909.50 | 4550.30 | 5416.00 | 4499.90 | 4360.80 |
| $k_{4t}$ | 5.0035 | 4.9999 | 5.0014 | 4.9979 | 4.9992 | 4.9996 |

**Notes**: $^*N(\mu, \sigma)$ = normal distribution; $^{**}U(a, b)$ = uniform distribution; source: modified from Qin et al. (2007).
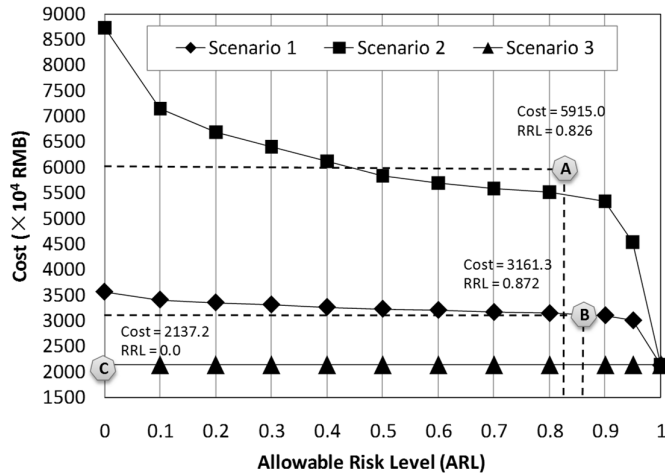


**FIGURE 2.** Solutions of GACCP model under various scenarios

The number of realization for Monte Carlo simulation is a critical factor that determines the time consumed for solving the management model. Figure 3 presents the absolute errors of RRL under different numbers of realizations for Monte Carlo simulation. The solutions at ARLs of 0.2 and 0.8 under Scenario 2 are used as known variables. The absolute error is calculated by $AE = (RRL_n - ARL) \times 100\%$, where $RRL_n$ is the real risk level obtained from MCS with $n$ realizations; ARL is the allowable risk level.

From Figure 3, it is indicated that the number of realizations for Monte Carlo simulation has significant impacts on the accuracy of calculating RRLs. Generally, the accuracy will increase with the increase of number of realizations. When the number is 10, the AE could reach $\pm 30\%$; when the number decreases to 5000, the AE could reduce to as low as $\pm 1\%$. Since the number of realizations is directly linked to the requirement of calculation amount, a tradeoff between the number of realizations and the accuracy of RRL calculations needs to be considered. It is recommended that a threshold AE level be defined for a specific problem based on discussions with different stakeholders and a test of AE levels under various conditions be implemented.
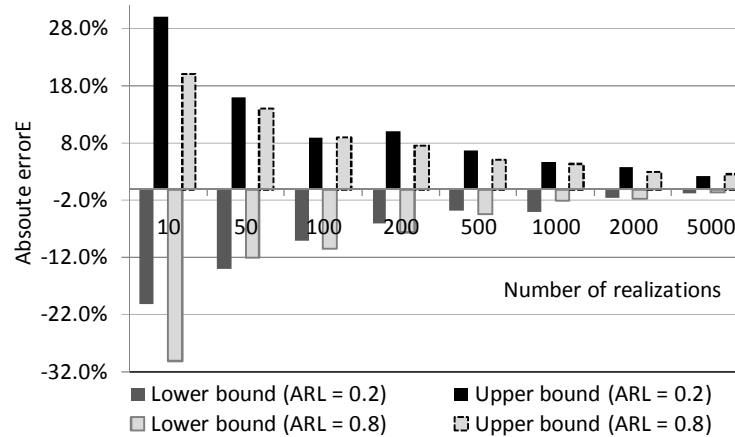
**FIGURE 3.** Absolute errors of RRL under different numbers of realizations of MCS

## CONCLUSIONS AND FUTURE WORKS

This study investigated the applicability of using GACCP model to support river water quality management problems under uncertainty. A river section, with the need to do a waste allocation planning considering both minimum treatment cost and uncertainty in the water quality processes, was used for demonstration. The study results indicated that method could effectively communicate uncertainties into the optimization process, and generate solutions that contain a spectrum of potential wastewater treatment options. Decision alternatives could be obtained by analyzing tradeoffs between the overall wastewater treatment cost and the system-failure risk due to inherent uncertainties. Considering that computing probability is only one part of solving the waste allocation problem, which requires solving a time-demanding GA-based optimization, it seems justified to test more computationally efficient methods in future studies.

## ACKNOWLEDGEMENT

## REFERENCES

Burn, D. H. and J. S. Yulianti. 2001. "Waste-Load Allocation Using Genetic Algorithms." *J. of Water Resources Planning and Management.* 127 (2): 121-129.

CEPA (China Environmental Protection Agency) (2002). Environmental quality standard for surface water (GB3838-2002), Beijing.

Cho, J. H., K. S. Sung, and S. R., Ha. 2004. "A River Water Quality Management Model for Optimizing Regional Wastewater Treatment Using a Genetic Algorithm." *Journal of Environmental Management.* 73 (3): 229-242.

Dupacova, J., A. Gaivoronski, Z. Kos, and T. Szantai. 1991. "Stochastic Programming in Water Management: a Case Study and a Comparison of Solution Techniques." *European Journal of Operational Research.* 52 (1): 28-44.

Huang, G. H. 1998. "A Hybrid Inexact-Stochastic Water Management Model." *European Journal of Operational Research.* 107 (1): 137-158.

Liu, B. D. and K. Iwamura. 1998. "Chance-Constrained Programming with Fuzzy Parameters." *Fuzzy Sets and Systems.* 94 (2): 227-237.

Loucks, D. P., J. R. Stedinger, , and D. A. Haith. 1981. Water resource systems planning and analysis. Prentice-Hall Inc., Englewood Cliffs, New Jersey.

O'Connor D. J. and W. E. Dobbins. 1958. "Mechanisms of Reaeration in Natural Streams." *Transactions of the American Society of Civil Engineers*. 123: 641–684.

Pelletier, G. J., S. C. Chapra, and H. Tao. 2006. "QUAL2Kw – A Framework for Modeling Water Quality in Streams and Rivers Using a Genetic Algorithm for Calibration." *Environmental Modelling & Software*. 21 (3): 419-425.

Qin, X. S. and G. H. Huang. 2009. "An Inexact Chance-Constrained Quadratic Programming Model for Stream Water Quality Management." *Water Resources Management*. 23 (4): 661-695.

Qin, X. S., G. H. Huang, G. M. Zeng, A. Chakma, and Y. F. Huang. 2007. "An Interval-Parameter Fuzzy Nonlinear Optimization Model for Stream Water Quality Management Under Uncertainty." *European Journal of Operational Research*. 180 (3): 1331-1357.

Revelli, R. and L. Ridolfi. 2004. "Stochastic Dynamics of BOD in a Stream With Random Inputs." *Advances in Water Resources*. 27 (9): 943-952.

Sasikumar, K. and P. P. Mujumdar. 1998. "Fuzzy Optimization Model for Water Quality Management of River System." *J. of Water Resources Planning and Management (ASCE)*. 124 (2): 79–84.

Stijnen, J. W., A. W. Heemink, and K. Ponnambalam. 2003. "Numerical Treatment of Stochastic River Quality Models Driven by Coloured Noise." *Water Resources Research*, 39: WR001054.

# HYDROGRAPH, POLLUTOGRAPH, AND THERMOGRAPH ANALYSIS
# OF DEICED HIGHWAY DRAINAGE

*David W. Ostendorf*, Erich S. Hinlein, and Camelia Rotaru
(University of Massachusetts, Amherst, MA, USA)

**ABSTRACT:** Precipitation, discharge, specific conductivity, and temperature have been measured at a gaging station in a highway right of way in eastern Massachusetts. Exponential decay constants successfully model the hydrograph as the linear superposition of systems for runoff from the closed highway drainage system, interflow from the vadose zone, and baseflow from the aquifer. A zero order source strength models deicing agent dissolution that generates the specific conductivity. The thermograph suggests a periodic contribution from the subsurface systems at a diurnal frequency. Summer and winter storms are analyzed with the coupled models, with plausible results.

## INTRODUCTION

The study variables have been measured by the USGS (United States Geological Survey) at a gaging station in the right of way of Interstate 95 in eastern Massachusetts (Figure 1). The station is at the outlet of a subbasin in the watershed of the principal reservoir of the CWD (Cambridge Water Department), and the highway is deiced by MassDOT (the Massachusetts Department of Transportation). UMass (the University of Massachusetts at Amherst) was asked to analyze these data to model the fluxes of water and deicing agents through the subbasin. Specific conductivity $\mu$ is a surrogate for dissolved deicing agent contamination (Granato and Smith, 1996) and requires temperature T to be measured, since $\mu$ is normalized to 298 deg K. Thus two federal and two state agencies are cooperating in an attempt to inform policy constrained by competing demands of drinking water quality, public driving safety, and expected levels of winter service. Since all data are measured, logged, and maintained online at 15 minute intervals, the hyetographs, discharge Q hydrographs, $\mu$ pollutographs, and T thermographs offer corroborating data sets at hourly, diurnal, and seasonal scales.

## MATERIALS AND METHODS

The USGS measured precipitation P at a meteorological station (01104430) near the Cambridge Reservoir (Smith, 2007), while Q, $\mu$, and T were measured at a gaging station (01104415) 80 m upstream of the Reservoir (Waldron and Bent, 2001). Figures 2 and 3 display data (as symbols) for a summer (June 2006) and winter (March 2006) storm at the research site. The data continue for several days into the interstorm period after each event.

The *hydrograph* is modeled as a superposition of single linear reservoirs for surface runoff $Q_R$ from the highway drainage system (Nash, 1959), interflow $Q_I$ from the vadose zone (Ostendorf et al., 2001), and baseflow $Q_B$ from the unconfined aquifer (Gelhar and Wilson, 1974)

$$Q = Q_B + Q_I + Q_R \tag{1a}$$

$$Q_I = (Q_O - Q_B)\exp(-\lambda_I t) + C_I A\lambda_I \int_{t_O}^{t} P(\tau)\exp[-\lambda_I(\tau - t_O)]d\tau \tag{1b}$$

$$Q_R = C_R A\lambda_R \int_{t_O}^{t} P(\tau)\exp[-\lambda_R(\tau - t_O)]d\tau \tag{1c}$$

with time t from the start of the calibration period. The baseflow is held constant, while $Q_I$ includes a recession from the prior interstorm period as well as contribution from the storm. The interflow decay constant $\lambda_I$ routes a fraction $C_I$ of this latter through the vadose zone. The surface runoff is similarly modeled, although its decay constant $\lambda_R$ is larger than its vadose zone counterpart, reflecting relatively

swift hydraulics of the closed highway drainage system. The precipitation data at the top of Figures 2 and 3 drive the hydrographs in Equations 1b and 1c along with the observed discharge $Q_O$ at t equals zero. A nested Fibonacci search optimizes the discharge fractions, $Q_B$, and depression storage thickness $\zeta$ (Linsley et al., 1982), which must be filled before the onset of runoff at time $t_O$

$$\zeta = \int_0^{t_O} P dt \tag{2}$$

The observed *specific conductivity pollutograph* is taken as the sum of advective fluxes from the baseflow, interflow $F_I$, and runoff $F_R$ systems

$$\mu = \frac{Q_B \mu_B + F_I + F_R}{Q} \tag{3a}$$

$$F_I = (Q_O - Q_B)\mu_{IO} \exp(-\lambda_I t) + Q_I \mu_I \tag{3b}$$

$$\mu_{IO} = \frac{Q_O \mu_O - Q_B \mu_B}{Q_O - Q_B} \tag{3c}$$

$$F_R = C_R A \lambda_R \int_{t_O}^{t} P(\tau)\mu_P(\tau) \exp[-\lambda_R(\tau - t_O)]d\tau \tag{3d}$$
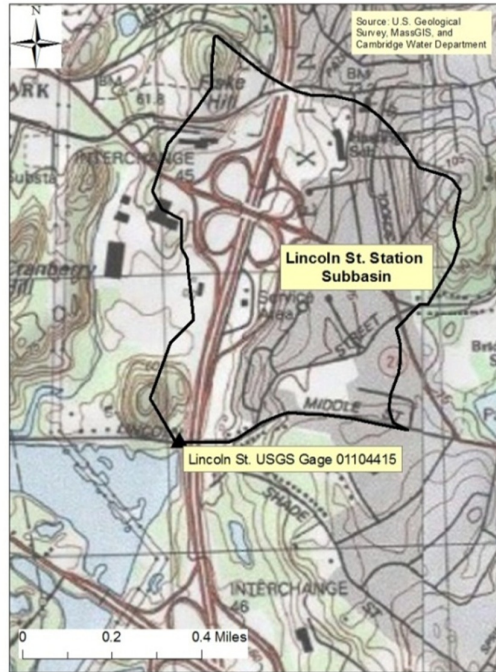


**Figure 1.** USGS gaging station in subbasin of Cambridge Reservoir and Interstate 95 right of way. The topographically defined subbasin area A is $1.07 \times 10^6$ m$^2$ (Waldron and Bent, 2001).

The baseflow specific conductivity $\mu_B$ is constant for the event, while the interflow flux adds an average event conductivity $\mu_I$ to the recession of the initial vadose zone conductivity $\mu_{IO}$. The observed initial specific conductivity $\mu_O$ sets the latter through Equation 3c, which couples the pollutograph and hydrograph calibrations, along with the common decay constant and discharge fractions. The dissolution of deicing agents into precipitation on the pavement generates the specific conductivity $\mu_P$ input to the

highway drainage system. Ostendorf et al. (2001) model the dissolution kinetics with a zero order source strength $\omega$ that depends in part on $\zeta$ and the solid deicing agent remaining in the texture of the pavement

$$\zeta \frac{d\mu_P}{dt} + P\mu_P = \omega \tag{4}$$
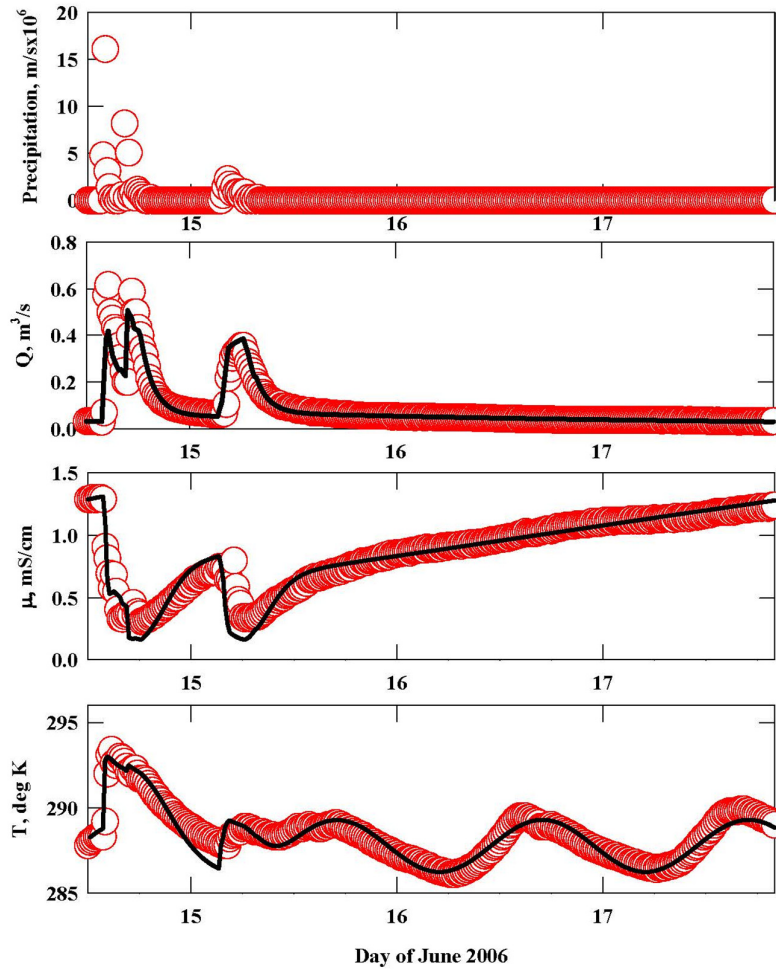


**Figure 2.** Observed (symbols) and calibrated (lines) hyetograph, hydrograph, pollutograph, and thermograph for summer storm.

The source strength is constant for the event, but varies seasonally as the deicing agent solid granules dissolve and shrink. A finite difference approximation of Equation 4 is programmed into the integrand of the convolution integral in Equation 3d. A nested Fibonacci search calibrates $\omega$, $\mu_B$, and $\mu_I$.

      The *thermograph* is simply modeled by adiabatic mixing of the runoff $T_R$, interflow $T_I$, and baseflow $T_B$ temperatures

$$T = \frac{Q_B T_B + Q_I T_I + Q_R T_R}{Q} \tag{5a}$$

$$T_I = T_B = T_S + \Delta T \sin(\Omega t + \phi) \tag{5b}$$

$$T_R = T_{RO} - \kappa(t - t_O) \tag{5c}$$

The runoff temperature varies linearly from its initial value $T_{RO}$, while the interflow and baseflow temperatures are sinusoidal with a diurnal frequency $\Omega$, amplitude $\Delta T$, and phase shift $\phi$. The steady subsurface temperature of $T_S$, though constant for the calibrating period, varies seasonally.
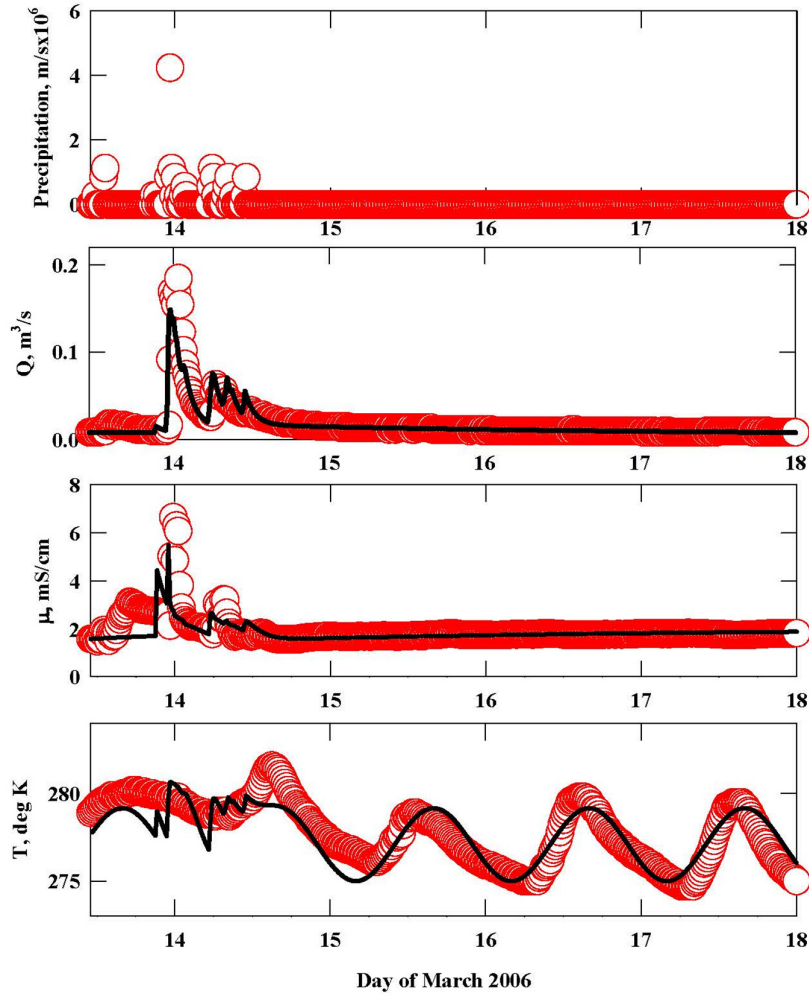


**Figure 3.** Observed (symbols) and calibrated (lines) hyetograph, hydrograph, pollutograph, and thermograph for winter storm.

## RESULTS AND DISCUSSION

The calibrations are the lines in Figures 2 and 3. The calibrated decay constants of $1.84 \times 10^{-4}$ s$^{-1}$ ($\lambda_R$) and $4.55 \times 10^{-6}$ s$^{-1}$ ($\lambda_I$) hold for both seasons, and imply an hourly response time for the drainage system and a diurnal response time for the vadose zone. Open channel (White, 2010) and subsurface hydraulics (Fetter, 2001) help elucidate these values

$$\frac{1}{\lambda_R} \approx \frac{3\nu L_R}{gh^2 S_R} \tag{6a}$$

$$\frac{1}{\lambda_I} \approx \frac{\nu L_I}{kgS_I} \tag{6b}$$

with gravitational acceleration g (10 m/s$^2$) and water kinematic viscosity $\nu$ ($10^{-6}$ m$^2$/s). Equation 6a compares $1/\lambda_R$ to the residence time in laminar sheet flow of pavement slope $S_R$ (0.01) and characteristic

length $L_R$ between catch basins of the drainage system. The Table 1 value implies a sheet flow depth h of 0.5 mm, comparable to the depression storage thickness. Runoff does not puddle on the pavement. The hydraulic head gradient $S_I$ (0.1) and lateral right of way distance $L_I$ of 100 m characterize vadose zone hydraulics, and imply a permeability k of $5 \times 10^{-10}$ m$^2$. This corresponds to sandy soil.

**TABLE 1.** Seasonally Varying Calibrated Parameter Values.

| Symbol | Definition | Summer | Winter |
|---|---|---|---|
| $\zeta$, mm | Depression storage thickness | 0.549 | 2.05 |
| $C_R$ | Runoff fraction | 0.341 | 0.144 |
| $C_I$ | Interflow fraction | 0.370 | 0.167 |
| $Q_B$, m$^3$/s | Baseflow | $7.78 \times 10^{-3}$ | $5.11 \times 10^{-3}$ |
| $\omega$, m-mS/cm-s | Source strength | $2.0 \times 10^{-5}$ | $4.9 \times 10^{-4}$ |
| $\mu_B$, mS/cm | Baseflow specific conductivity | 2.24 | 2.04 |
| $\mu_I$, mS/cm | Vadose zone specific conductivity | 0.062 | 1.24 |
| $T_S$, deg K | Steady subsurface temperature | 288 | 277 |
| $T_{RO}$, deg K | Initial runoff temperature | 293 | 281 |
| $\kappa$, deg K/s | Runoff cooling rate | $6.5 \times 10^{-5}$ | 0 |
| $\Delta T$, deg K | Amplitude of temperature fluctuation | 1.52 | 2.08 |

Table 1 summarizes summer and winter values for the seasonally varying parameters. The discharge fractions decrease from summer to winter for the drainage system and vadose zone, as does the baseflow. The latter is an order of magnitude smaller than the maximum Q displayed in Figures 2 or 3: the aquifer contribution though small, is perennial. The mm scale of the $\zeta$ calibration compares favorably to the pavement texture (Croney and Croney, 1998), as has been discovered by similar analyses of highway runoff (Ostendorf et al., 2001, 2006).

The calibrated pollutographs yield a winter source strength an order of magnitude larger than the summer source strength, due to application of deicing agents on the pavement. Indeed, monthly calibrations across entire periods of records support coupled models of specific conductivity and deicing agent solids on a seasonal basis at other highway sites (Ostendorf et al., 2001, 2006). The winter increase of the interflow specific conductivity is more than an order of magnitude larger than the summer value, while the baseflow value remains at the 2 mS/cm level year round. The baseflow, though small, continually discharges deicing agents to the Cambridge Reservoir. While winter storm runoff temporarily adds salinity to this discharge, summer storms dilute it. In the latter regard, Figure 2 shows a gradual rise towards the asymptotical specific conductivity of the groundwater under the highway in June.

The thermographs are nearly 10 deg K warmer in summer than winter, and exhibit diurnal periodicity during interstorm periods with a 1.5 to 2 deg K amplitude. Though the summer thermograph model does suggest aperiodic cooling of runoff, the winter model does not accurately describe the temperature of the surface drainage. Future study is certainly warranted before thermographic analysis can be viewed with confidence. Fortunately, Figures 2 and 3 suggest that the hydrographs and pollutographs are accurately described with the simple models of linear systems.

**CONCLUSIONS**

Classical linear theory accurately describes the hydrographs and specific conductivity pollutographs of a deicied highway drainage system with physically plausible parameter values. The highway drainage system delivers surface runoff with an hourly response time, the vadose zone response is diurnal, and the baseflow is seasonal. The surface runoff dilutes the specific conductivity during the summer and concentrates it during the winter, due to the continuous salinity of the baseflow. While thermographic analysis recovers the observed cooling of runoff during a summer storm, it does not describe winter temperatures at an hourly scale. Thermal periodicity is shown at diurnal and seasonal scales, however.

**ACKNOWLEDGMENTS**

## REFERENCES

Croney, P. and D. Croney, 1998. *The Design and Performance of Road Pavements.* McGraw Hill, New York, NY, 508 pp.

Fetter, C.W., 2001. *Applied Hydrogeology.* Prentice Hall, Upper Saddle River, NJ, 598 pp.

Gelhar, L.W. and J.L. Wilson, 1974. "Groundwater quality modeling". *Groundwater,* 12(6): 399-408.

Granato, G.E. and K.P. Smith, 1999. "Estimating concentrations of road salt constituents in highway runoff from measurements of specific conductance". *WRI Rept. 99-4077*. USGS, Northborough, MA, 22 pp.

Linsley, R.K., M.A. Kohler, and J.L.H. Paulhus, 1982. *Hydrology for Engineers.* McGraw Hill, New York, NY, 508 pp.

Nash, J.E., 1959. "Systematic determination of unit hydrograph parameters". *J. Geophys. Res.,* 64(1): 111-115.

Ostendorf, D.W., D.C. Peeling, T.J. Mitchell, and S.J. Pollock, 2001. "Chloride persistence in a deiced access road drainage system". *J. Environ. Qual.,* 30(5): 1756-1770.

Ostendorf, D.W., E.S. Hinlein, D.P. Ahlfeld, and J.T. DeJong, 2006. "Calibrated models of deicing agent solids, pavement texture, and specific conductivity of highway runoff". *J. Environ. Eng.,* 132(12): 1562-1571.

Smith, K.P., 2007. "Hydrologic, water quality, and meteorological data for the Cambridge, MA, drinking water source area, water year 2005". *OF Rept. 07-1049.* USGS, Reston, VA, 119 pp.

Waldron, M.C. and G.C. Bent, 2001. "Factors affecting reservoir and stream water quality in the Cambridge, MA drinking water source area and implications for source water protection". *WRI Rept. 00-4262.* USGS, Northborough, MA, 89 pp.

White, F.M., 2011. *Fluid Mechanics.* McGraw Hill, New York, NY, 862 pp.

# OIL SPILL TRANSPORT IN THE WAVE CHANNELS USING TWO- PHASE LAGRANGIAN MODEL

*Hanifeh Imanian*, Mahsa Jannati and Morteza Kolahdoozan
(Amirkabir University of Technology, Tehran, Iran)

One of the most important environmental problems in marine ecosystem is water pollution due to oil spill. Oil spills in marine waters experience different physical and chemical processes including advection, spreading, evaporation, emulsion, dissolution, dispersion, bio- degradation, photo- oxidation and hydrolysis. In the current study, a two- phase oil spill numerical model based on moving particle semi-implicit (MPS) method is developed to simulate oil transport in water body. This full lagrangian model, simulate both fluid and oil phases as particles, concurrently. Hydrodynamic part of developed model is validated by available experimental data in the literature. Oil slick spreading on water surface is simulated by developed model as well. Comparison of its results with empirical relationships indicates the accuracy of the model in oil location prediction. Finally, dispersion process of oil spill in water column is investigated by present model. Different sets of results are compared with empirical equations and the ability of the developed lagrangian numerical model in predicting oil spill transport is shown.

# INVESTIGATION OF OPTIMAL OPERATION ON IMPROVED IRRIGATION SYSTEM IN NILE DELTA

*Ahmed M. ALY* (Tottori University, Tottori, JP/National Water Research Center, Cairo, EG)
Yoshinobu KITAMURA, Katsuyuki SHIMIZU (Tottori University, Tottori, JP)
Taleet EL-GAMEL (National Water Research Center, Cairo, EG)

Climate change will significantly impact agriculture by increasing water demand, limiting crop productivity and by reducing water availability in areas where irrigation is most needed. The forms of agricultural water management in Nile Delta are important and will be impacted by climate change through it may be submerged by a sea-level rise are increasingly prone to flood and storm damage or experience salinity intrusion through surface and groundwater and/or rainfall will decrease and become more variable. The Nile Delta is home to one of the most ancient agricultural systems in the world, which is both vast and complex. So, the operation water distribution in the Nile Delta is the process of regulatory to maintain the available water resources and good use and that deliver it to the sites used in the quantities and the appropriate water levels in a timely manner without an increase or decrease threatened flawed. However, water becomes a highly valuable commodity, needs policies and strategies for its optimal use.

This study deals with the use of a hydrodynamic model to assess first of all the hydraulic behavior of the canal and hence to investigate the optimal discharge values apply it. Computer models are used widely for better management. One of such model is Hydrologic Engineering Center River Analysis System (HEC-RAS) is performing one-dimensional hydraulic calculations for a full network of natural and constructed channels. This model was applied to the improved irrigation system at Wasat command area. This area is located on the northern edge of the Nile Delta, and it is fed from the tail reaches of the main canal (Meet Yazid). Due to location at the tail of the feeder canal system, El-Wasat command area suffers from inadequate water supplies. This problem is exacerbated by the tendency of farmers who plant more paddy field than which government allowed (50%). This area is famous for its rice production, which contributes to 40% of rice production in Egypt.

The study illustrated that the chance to improve the hydraulic performance should be through reducing water losses downstream the lifting points as the conveyance losses are already small, and this should be achieved through better control of the water. The released water downstream the head regulator should be distributed between lifting points through the internal rotation "Motarefa". The evaluation results showed that the continuous flow was applied in the previous explained manner in any branch canals. Therefore, it is essential to change a revolutionary approach in water management, from the state being a central managing towards a greater participation of others, including local governments, non-governmental (organizations), and beneficiaries. Many governments are committed to sharing irrigation management responsibilities with water users and, in some cases, to hand them over completely to the privates.

# FATE AND TRANSPORT MODELING OF PCBS IN THE HOUSTON SHIP CHANNEL ESTUARY

*Nathan L. Howell* and Hanadi S. Rifai
(University of Houston, Houston, TX, USA)

The Houston Ship Channel (HSC) is a highly industrialized corridor both for commercial shipping and petrochemical activities.  As is the case with many such industrialized areas, there are high concentrations of persistent organic pollutants (POPs) such as polychlorinated biphenyls (PCBs).  This study brings together PCB data from five separate sampling events between 2002 and  2009 in several media (bed sediment, water, and tissue) to develop a hydrodynamic water quality model using Environmental Fluid Dynamics Code (EFDC).  The model incorporates specific known PCB sources from industry, urban runoff, and Superfund sediment sites to quantify external loads and internal PCB contaminant transport.

Two specific research objectives were in view concerning the model's development.  The first is to understand the role of the bed sediment in the overall contaminant picture.  It is fairly clear that a large repository of PCBs exists throughout the HSC, some in areas that are highly localized and others over a larger sediment region spanning an entire reach of the estuary.  But, due to complex pathways for the movement of bed sediment and the bioavailability of PCBs in the bed sediment, it is not as clear how important bed sediment is with regards to overall PCB loading and risk as compared with other sources.  The second research objective is to evaluate temporal trends in water and sediment PCB contamination in the HSC, especially with regard to the area of the HSC upstream of the San Jacinto River, which contains the highest concentration of industrial activities.  Though PCB contamination generally seemed to be decreasing from 2002-2008, the concentrations increased from 2008-2009.  Unusually long dry periods and Hurricane Ike are possible explanations for the increase.

Preliminary results indicate that a significant portion of the PCBs in bed sediments is not bioavailable due to the levels and type of organic carbon present in them (effectively reducing the bed sediment PCB risk to the aquatic food web) and that there are highly contaminated bed sediments in the upper reaches of the HSC that are not transported further downstream due to lower water velocities. These highly contaminated areas will only be mitigated through sediment burial and natural attenuation processes such as biodegradation.

# APPLICATION OF A FULLY DISTRIBUTED WASHOFF AND TRANSPORT MODEL FOR A GULF COAST WATERSHED

*Aarin Teague* (U.S Environmental Protection Agency, Gulf Breeze, FL, USA)
Philip Bedient (Rice University, Houston, TX, USA)

Advances in hydrologic modeling have been shown to improve the accuracy of rainfall runoff simulation and prediction. Building on the capabilities of distributed hydrologic modeling, a water quality model was developed to simulate buildup, washoff, and advective transport of a conservative pollutant throughout a watershed. Coupled with the physically based *Vflo*$^{TM}$ hydrologic model, the pollutant transport model was used to simulate the washoff and transport of total suspended solids for multiple storm events in the Cypress Creek Watershed, near Houston, Texas. The spatially explicit model output provides greater spatial information on the dynamics of pollutant movement during storm events as well as a greater density of temporal information than current resource limited sampling data.

The output of the distributed buildup and washoff model was compared with storm water quality sampling in order to assess the performance of the model. The model output was then analyzed to temporally and spatially characterize the storm events. This effort was the first step in developing a fully distributed water quality model. As such it provides the framework for the incorporation of more sophisticated pollutant dynamics and a spatially explicit evaluation of best management practices and land use change. Thus it is a step towards advancing the use of simulation to developing sustainable and healthy communities.

# GIS,
# DATABASE
# AND
# REMOTE SENSING

# WEST NILE VIRUS DISEASE PREDICTION MODELING USING GIS TECHNIQUES

Samuel Atkinson, Armin Mikler and *Abhishek K. Kala*
(University of North Texas, Denton, TX, USA)

West Nile virus is a serious infectious disease that has recently spread across the North America. Since first detected in the New York State in the year 1999, this disease infected thousands of people and hundreds have died. West Nile virus (WNV) is transmitted by mosquitoes and birds act as reservoirs of the disease. In this study different GIS techniques and simple statistical methods were used to develop the model. Results indicated that infected dead birds occurrence and infected human incidence data have strong positive correlation thus facilitating basis of the model and its validation approach. Spatial prediction of WNV in California was carried out by analyzing both static and dynamic environmental variables to estimate potential mosquito habitats. Modeling results estimated the areas of high risk for West Nile virus infection which was validated with the human incidence data for similar period of time.

# DESERTIFACTION ASSESSMENT IN NORTH SINAI USING REMOTE SENSING AND GIS

### *Elsayed Said Mohamed*
(National Authority for Remote Sensing and Space Sciences, Cairo, Egypt)

This study aims to use spatial analyses and Geographic Information System (GIS) to assess the environmental sensitivity for desertification in north Sinai Peninsula, Egypt. Based on the MEDALUS approach and the characteristics of study area a regional model developed using GIS. Five main factors or indicators of desertification including: soil, climate, erosion, plant cover, and management were considered for estimating the environmental sensitivity to desertification.Spatial analyst extinction Arc-GIS 10 software was used for matching the thematic layers and assessing the desertificatio index, of which the map of environmentally sensitive areas of north Sinai peninsula is produced. The obtained data reveals that 75 .5% of north Sinai  is characterized by very severe sensitivity to desertification, while the low sensitive one exhibits only 2 %. The moderately sensitive area occupies 22.5% of the study area. ETM+ and SPOT images are recommended to monitoring of sensitivity. The MEDALUS model developed may be used to assess desertification process and distinguish the areas sensitive to desertification in the other areasthat have the same conditions.

# PROTECTED AREAS IN A DYNAMIC FOREST LANDSCAPE: A LARGE SCALE CONNECTIVITY ANALYSIS

*Arvid Bergsten* and Örjan Bodin (Stockholm University, Stockholm, Sweden)
Frauke Ecke (Swedish University of Agricultural Sciences, Uppsala, Sweden)

This paper presents a connectivity analysis of boreal lichen forests in northern Sweden, which is a habitat type that hosts many red listed species. We evaluate connectivity of habitat in nature reserves using a network approach, and examine how areas subject to less strict or informal protection schemes supplement the reserve network. Our results show that the current spatial arrangement of protected areas favors certain species, determined by their specific habitat specialization and dispersal capacity. We then quantify the significance of mature forests in the surrounding unprotected landscape. Results show that unprotected mature forests provide large amounts of temporary habitat for species that can colonize and disperse further before logging occurs. Our analysis also indicates that unprotected areas increase the spatial resilience of sensitive species that mostly occur in protected natural forests, by providing connectivity to other protected areas in the event of disturbance in a reserve. The results are discussed with reference to the spatial planning of harvest and strategies of area protection.

# NEW TECHNIQUE IN FLOOD MITIGATION IN URBAN AREA, EXAMPLE FROM RIYADH SAUDI ARABIA

*Farhan AlJuaidi* (King Saud University, Riyadh, P O Box 2456, Riyadh, Saudi Arabia)
Ibrahim Almejadeah (Imam Mohammed Bin Saud University, Riyadh, Saudi Arabia)

State-of-the-art technique was applied using Liadar Mobile Mapping System (Lynx Mobile Mapper, Optech's mobile terrestrial lidar system) to generate contour lines for the actual elevation of the highways in the northern of Riyadh capital of Saudi Arabia. Unicom Lynx system captures 3D georeferenced spatial data (X, Y, Z points) of features within the floodplain and urban areas, such as bridges, buildings, barriers, lighting, and vegetation. These data were analyzed and compared with the contour lines and georeferenced spatial data (X, Y, Z points) generated from the topographical maps 1:50.000. These maps were produced before the development in late 1980s. However, the results shows that cut and fill process created a major problem in diverting the flow towards undesired area. This kind of process creates a flood risk area where the engineers should pay some attention to identify the old channel system pre-development.

# QUANTIFICATION OF PERCENT SHRUB CANOPY WITH LANDSAT ACROSS THE CONTERMINOUS UNITED STATES

*George Xian* (ARTS/USGS EROS Center, Sioux Falls, SD, USA), Collin Homer (USGS EROS Center, Sioux Falls, SD, USA), Debbie Meyer (SGT/USGS EROS Center, Sioux Falls, SD, USA), Brain Granneman (SGT/USGS EROS Center, Sioux Falls, SD, USA), Jon Dewitz (USGS EROS Center, Sioux Falls, SD, USA)

Shrub land ecosystems occupy a large portion of the terrestrial surface over the conterminous United States and provide unique ecosystem services especially in semiarid environments. These services are dependent upon the quality and quantity of the shrub land ecosystem. Most shrub lands are located in arid and semiarid environments and are vulnerable to external disturbances including livestock grazing, human development activities, wildland fire, and climate change. Good understanding of how shrub canopy distribution and density changes modify terrestrial ecosystems and affect environmental conditions is vital for both scientific research and land management. The main goal of this research is to develop a prototype approach for estimating the percent cover of shrub canopy at a 30 m scale across the conterminous United States. The approach contains three major procedures: creating training datasets by using field measurements and high resolution satellite imagery, extrapolating shrub distribution to a larger extent by incorporating the training datasets and medium resolution satellite imagery, and validating the final product. In the first procedure, both field measurements and multi-spectral high resolution satellite imagery from QuickBird or WorldView-2 are used to develop regression tree models to predict the shrub canopy over high resolution image footprints to provide a training base. In the second procedure, the training base dataset is rescaled to 30 m resolution and applied across medium resolution Landsat images with regression tree models to calculate the percent cover of shrub canopy over a much larger area. Finally, field measurements independent from training datasets are used to validate the model prediction. This method has been tested and validated at six locations across the conterminous United States in a variety of environments. Additional sensitivity experiments were also conducted to demonstrate the feasibility of implementing this prototype method to produce shrub canopy cover as part of the 2011 version of the USGS National Land Cover Database.

# COASTAL RESOURCE MONITORING WITH RADAR AND OPTICAL SATELLITE SENSOR DATA

*Amina Rangoonwala* (Five Rivers Services, LLC, USA), Elijah Ramsey III (U.S. Geological Survey, National Wetlands Research Center, LA, USA), Yukihiro Suzuoki (ASci Corporation, Inc., USA) and Terri Bannister (Five Rivers Services, LLC, USA)

Storm-surge flooding and marsh response throughout the coastal wetlands of Louisiana were mapped by using several types of remote sensing data collected before and after Hurricanes Gustav and Ike in 2008. These included Synthetic Aperture Radar (SAR) data obtained from the (1) C-band  Advanced SAR (ASAR) aboard the Environmental Satellite (EnviSat), (2) L-band Phased Array type SAR aboard the Advanced Land Observing Satellite (ALOS), and (3) optical data obtained from Thematic Mapper sensor aboard the Landsat satellite. Inundation, particularly sub canopy inundation was detected as a change in backscatter between pre–flood (reference) and post–flood (target) scenes. In estuarine marshes, results indicated that L-band and C-band SAR provided accurate flood extent maps when flood depths were high (>80 cm) but only L-band SAR provided consistent sub canopy detection when depths were shallow. Low performance of ASAR-based inundation mapping was attributed to an apparent inundation detection limit in tall *Spartina alterniflora* marshes and wind roughened water surfaces in flooded marshes where water-levels reached marsh canopy heights.  In addition, enhanced backscatter in the near-range portion of the pre- and post-flood ASAR scenes diminished differences related to subcanopy flooding resulting in lowered inundation mapping performance.

Sudden marsh dieback resulting from storm-surge flooding was mapped with a vegetation index (VI) based on Landsat Thematic Mapper (TM) images collected before and after Hurricanes Gustav and Ike.  Within the estuarine zone, intermediate-brackish marshes were most often the severest impacted while more shoreward estuarine marshes dominated by smooth cordgrass experiencing a similar inundation history exhibited lower impact.  This may indicate that under similar inundation scenarios, smooth cordgrass marshes are more tolerant to surge inundation than intermediate-brackish marshes.  In contrast, palustrine marshes in close vicinity to the ocean suffered the most severe impacts.  The more severe impacts of these near-shore palustrine marshes may have been more a consequence of direct exposure to elevated salinities than surge flood durations. The highest spatial agreement between the change-detected geographic extents of the storm-surge marsh dieback occurred in the western portion of the study area.  This region is also characterized by the least lag time between the storm-surge peak occurrence and after hurricane satellite data collection.  By contrast, the SAR-based surge and dieback areas in the eastern coastal region did not align as well.  In this case, the calculated residual flooding distribution was based on a PALSAR scene collected 167 hours after Gustav and an ASAR scene collected 115 hours after the Ike central storm-surge peak; 82 hour later than the storm-surge peak and ASAR collection lag time obtained in the west.

# ENVIRONMENTAL ANALYSIS
# AND
# MEASUREMENTS

# SURFACE-ENHANCED RAMAN SCATTERING DETECTION OF ENVIRONMENTAL POLLUTANTS USING FE₃O₄@AG NANOPARTICLES

J. J. Du, S. Q. Liu, *C. Y. Jing*

(Chinese Academy of Sciences, Beijing, China)

Field in-situ rapid detection of environmental pollutants presents a great challenge. Most conventional identification and quantification analytical techniques require the sample pre-treatment and use of expensive equipments. Developing novel analysis method which is sensitive and easy-to-use with affordable equipments for routine environmental monitoring is an urgent need. This study developed a sensitive and functionalizable SERS substrate based on $Fe_3O_4$@Ag core-shell magnetic nanomaterial. SERS sensing of common environmental pollutants including Cr(VI), paraquat (PQ), diquat (DQ), simazine, aldrin, and eight PAHs was achieved using a portable Raman spectrometer. The selected pollutants belong to five different classes: heavy metal, herbicide, estrogen, OCPs, and PAHs. The surface morphology and structure of the substrate were characterized using multiple complimentary techniques including transmission electron microscopy, atomic force microscopy, and X-ray photoelectron spectroscopy. The SERS effect of the substrate was verified using rhodamine 6G (R6G) and crystal violet (CV). The enhancement factor was estimated to be $10^9$ for R6G and $10^7$ for CV, respectively. SERS spectra of Cr(VI) in water with a detection limit of 5 μg/L was obtained. The substrate is capable for trace detection of DQ and PQ, and SERS spectra of both herbicides with concentrations of $10^{-6}$ M were resolved. As electron acceptors, PQ can interact with silver surface, thus create intermolecular cavities inside the hot spot. Detection of aldrin and simazine was performed using the PQ modified $Fe_3O_4$@Ag as substrate. Comparison with the Raman and SERS spectrum of simazine revealed some differences due to its interaction with substrate surfaces. In the case of aldrin, intense bands in the low wavenumber region were attributed to the C-Cl stretching motions, which were actually fingerprints of aldrin. Finally, Benzene, naphthalene, anthracene, phenanthrene, flourene, pyrene, perylene, and BaP were chosen as probe molecules. With thiol monolayer embedding the analyte on the substrate surface, qualitative and quantitative determination of PAHs with good selectivity was achieved at μg/L level. The SERS signal was linearly correlated with the PAHs concentration. The sensitivity of this analytical method and the flexibility in the substrate modification have opened a new way towards a generalized use of our technique, not only in the laboratory but also in field assays with the availability of portable Raman spectrometer.

# A NEW GLOBALCONTAMINATION GENERATED FROM MARINE DEBRIS POLYSTYRENE

*Katsuhiko Saido,* Hideto Sato, Akifumi Okabe(Nihon University, Tokyo,Japan), Seon-Yong Chung(Chonnam National University, Gwangju,Korea)
Yasushi Kamaya, Naoto Ogawa(Shizuoka University, Japan), Kazuhiro Kogure(The Tokyo University, Japan)and Takashi Kusui.(Toyama Prefcture University,J apan)

Huge amounts of plastic wastes are scattered in the ocean from the land site. It was supposed many kinds of the chemicals generated from the marine debris plastic. For clarification of the causes of new global chemical contamination, 5g beach sand and 2.5L water taken from sites throughout the world were extracted with dichloromethane and analyzed by SIM-GC/MS. All samples were found to contain of the styrene oligomer which consists of phenylethylene 1: (styrene monomer, SM), 2,4-diphenyl-1-butene 2: (styrene dimer, SD) and 2,4,6-triphenyl-1-hexene :5 (styrene trimer, ST). To study the decomposition of polystyrene (PS), polyethylene glycol (PEG) was used as a heating medium. PS was found to decompose at 30°C to generate the styrene oligomer. The results clearly indicated the new global chemical contamination generated by PS decomposition in the ocean and the presence of any one of which may be considered to persist long into the future.

# A STUDY ON EXTREME WEATHER EVENTS IN JAPAN

*Masato Okabe* and Tadashi Yamada
(Chuo University, Tokyo, Japan)

The purpose of this study is to introduce a new statistical methodology for a rainfall analysis. Due to the climate change you are experiencing a strong rainfall comparing from the past. The river design in Japan is usually based on return period and every rainfall event is treated as unique event. Although there are many natural phenomena have periodicity. El Niño/La Niña is one example. From this study the observed rainfall data in Japan was used to clarify the recent trend of the weather in Japan. From analysis the mountainous areas in Japan has extreme rainfall almost every 10 years. This 10 years return period was found on 3-day total precipitation, and daily precipitation. This return period was also found at the lowland areas such as Tokyo with annual 10 minutes maximum rainfall and annual 1 hour maximum rainfall. From this study it was found that it is difficult to evaluate extreme rainfall using return period and it is also difficult to discuss periodicity if you have less than 1000(years) of data.

# OVERVIEW AND VALIDATION OF THE TRAINING RANGE ENVIRIONMENTAL EVALUATION AND CHARACTERIZATION SYSTEM

*Mark S. Dortch* and Billy E. Johnson
(U.S. Army Engineer R&D Center, Vicksburg, MS, USA)

**ABSTRACT:** The Training Range Environmental Evaluation and Characterization System (TREECS™) was developed to provide the Army with predictive modeling tools to assess the potential for migration of munitions constituents (MC) into surface water and groundwater systems in order to protect human and environmental health associated with off-range migration. Four validation applications of TREECS™ were conducted and summarized. TREECS™ compared reasonably well with measurements, but results for high explosives (HE) were more accurate than for metals due to complexities associated with metal dissolution and partitioning between sediment and water.

## INTRODUCTION

TREECS™ (http://el.erdc.usace.army.mil/TREECS™/) was developed for the Army to forecast the fate of and risk from MC, such as HE and metals, within and transported from firing/training ranges to surface water and groundwater. The objective is to provide tools to assess the potential for migration of MC into surface water and groundwater systems. There are two levels of capability. Tier 1 consists of screening-level methods that assume highly conservative, steady-state MC loading and fate. Tier 1 requires minimal input data requirements and can be easily and quickly applied. Tier 2 provides time-varying analyses and solves mass balance equations for both solid and non-solid phase MC mass with dissolution. Additionally, MC residue loadings to the range soil can vary from year-to-year based on munitions use. Thus, media concentrations computed with Tier 2 should be closer to those expected under actual field conditions. Four validation applications of Tier 2, as summarized in this paper, were conducted to determine the adequacy for predicting field conditions by comparing computed results to measured, or field observed, values.

## METHODS

This section provides an overview of the modeling methods used within Tier 2 of TREECS™. Figure 1 is a schematic of the Tier 2 model components and connectivity. The source zone for MC is the surface soil of the firing range and is referred to as the area of interest (AOI). The AOI could be the primary impact area of fired munitions for example. The MC residue loading to the AOI must be estimated or specified. In addition to the loading model, fate and transport models are included for the four media of AOI soil, vadose zone beneath the AOI, groundwater (aquifer), and receiving surface water including sediment. Potential environmental and human receptors could be exposed to MC that migrates to groundwater wells or receiving surface waters. Thus, the end point metrics are the predicted MC concentrations at target groundwater wells and/or surface water body down-gradient of the AOI. These concentrations are compared against Department of Defense-established, conservative, screening-level benchmarks for ensuring protection of human and environmental health. Each of the model components and the connecting framework within Tier 2 are briefly described below. TREECS™ Tiers 1 and 2 development is described in much greater detail within reports by Dortch et al. (2009 and 2011).

**AOI Loading Model**. There are three options within the AOI loading model: 1) estimate MC loadings within an impact area stemming from munitions items fired on range; 2) estimate MC loadings at range firing points; and 3) specify generic source loading that could represent any other scenario not pertaining to firing ranges. The latter option is simply a table of loading rates per year (g/yr) for each constituent of

concern, thus, this option could be used for applications that do not pertain to firing/training ranges. For each munitions item used on a range, the user first selects the munitions identification using the munitions type and the Department of Defense Identification Code (DODIC) or National Stock Number (NSN). For each munitions item fired into the impact area, the user provides the following for each year of input: number fired; percent of duds (no explosion); percent of low order detonations (partially exploded); percent yield (portion of MC used up when munitions explode) for low order detonations; percent of duds that are sympathetically exploded by another detonation; percent yield for sympathetic detonations; and percent yield for high order detonations. Guidance is provided within TREECS™ for estimating dud, low order rate and yields, and high order yields. The amount of MC mass in each munitions item must be known to compute the MC residue loading. This information can be obtained from the Munition Items Disposition Action System (MIDAS) (https://midas.dac.army.mil/) based on DODIC or NSN. However, extraction of information from MIDAS can be slow and tedious. A utility was developed for automatically pulling this information into the TREECS™ application. For firing points, the user must enter for each item the emission factor (mass deposited/item fired) or the percent of unexpended MC when fired as well as the numbers fired each year. The other inputs associated with the impact area are not required. Once the MC mass delivered to the impact area or firing point is known for each munitions item used and the other input parameters are entered, the calculation of residue mass loadings is a straightforward summation.
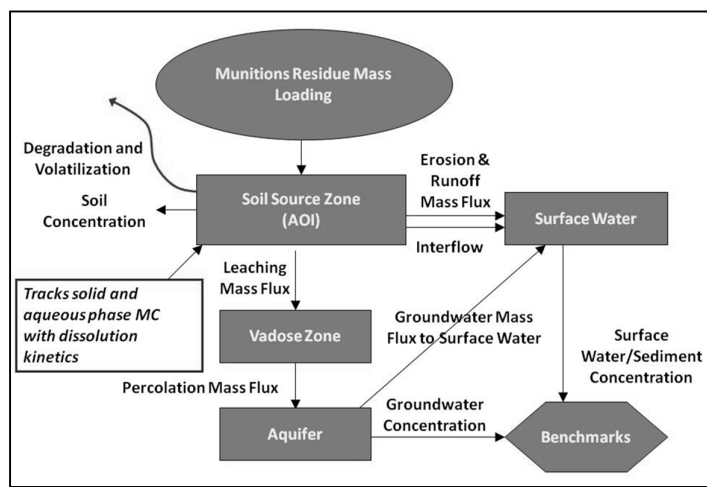


**Figure 1. Schematic of TREECS Tier 2 model components and connectivity.**

**AOI Soil Model**. All of the multi-media fate models are based on mechanistic mass balance principles. The AOI surface soil is treated as a homogeneous, fully mixed compartment of constant thickness and surface area. Each MC can exist in solid and non-solid (water-dissolved from solid) phases. The non-solid phase mass exists in equilibrium and distributed as dissolved in water within the water-filled soil pore spaces, as adsorbed from water to soil particles, and as a vapor in air within the air filled pore spaces. A time-varying mass balance is performed for both the solid and non-solid phases. The solid phase mass balance is stated as

$$\frac{dM_s}{dt} = L(t) - F_{dis} - F_{es} + F_{precip} \tag{1}$$

where $M_s$ is the solid phase MC mass (g), $t$ is time (yr), $L(t)$ is time-varying solid phase MC mass loading (g/yr), $F_{dis}$ is dissolution flux (g/yr), $F_{es}$ is the erosion flux of solid phase MC particles (g/yr), and $F_{precip}$ is

the precipitation flux (g/yr) of MC due to dissolved pore water concentration exceeding the water solubility limit. The formulation for $F_{dis}$ developed by Dortch et al. (2011) is a function of average annual precipitation, solid phase particle size, specific gravity, and water solubility.

The non-solid phase mass balance is stated as

$$\frac{dM_{ns}}{dt} = F_{dis} - F_r - F_e - F_l - F_{decay} - F_{vol} - F_{precip} \tag{2}$$

where $M_{ns}$ is non-solid phase constituent mass (g), $F_r$ is the rain-induced pore water ejection and runoff flux (g/yr), $F_e$ is constituent flux due to soil erosion (g/yr), $F_l$ is leaching flux (g/yr), $F_{decay}$ is degradation flux (g/yr), and $F_{vol}$ is volatilization flux (g/yr). Reversible, equilibrium partitioning is used within the soil-water-air matrix to distribute non-solid phase mass among water dissolved, soil particle adsorbed, and vapor in air.

The flux terms are expressed as functions of soil MC solid phase mass and non-solid phase concentrations, thus requiring the solution of the two coupled ordinary differential equations for the two unknowns. The auto adaptive stepping, fourth-order, Runge-Kutta-Fehlberg method is used to solve the equations. Once the equations are solved, the export fluxes can be computed and used as inputs for the down-gradient water models that are described next. There is an option to include soil interflow export flux when infiltration exceeds percolation rate. The fate processes are driven by average annual hydrology and erosion that are inputs.

**Vadose Zone and Aquifer Models**. These are legacy models originally used with the Multimedia Environmental Pollutant Assessment System, MEPAS (Buck et al. 1995). The MEPAS version 5.0 models (http://mepas.pnl.gov/mepas/maqu/index.html) compute fluxes through the vadose zone and aquifer and resulting aquifer concentrations at specified well locations. The vadose zone model solves the one-dimensional (1D), vertical, reactive, transport equation for partially saturated conditions. The aquifer model solves the reactive, transport equation for 1D, longitudinal advection and three-dimensional dispersion for saturated conditions. A detailed description of these models is not repeated here since the scientific documentation of the MEPAS groundwater models is provided by Whelan et al. (1996), and a more detailed description is provided by Dortch et al. (2011).

**Surface Water Models**. There are two options for modeling contaminant fate in surface water and sediments: RECOVERY (Ruiz and Gerald 2001) and the Contaminant Model for Streams, CMS (Fant and Dortch 2007), available at http://el.erdc.usace.army.mil/products.cfm?Topic=model&Type=watqual. RECOVERY is best suited for pooled surface water, such as ponds and lakes, while CMS is best suited for streams and rivers. These two models are briefly described here since detailed documentation of the models is given in the above references, and a more detailed overview of each model is provided by Dortch et al. (2011). Both models solve time-varying, mass balance equations for total (dissolved and particulate) contaminant mass in surface water and bottom sediments with reversible, equilibrium partitioning between dissolved and adsorbed particulate forms.

For the RECOVERY model, the water column is treated as a fully mixed single compartment. The bottom sediments are layered into two types: a single, mixed sediment layer at the sediment-water interface; and multiple, 1-cm thick, deep sediment layers below the mixed layer. This treatment results in three mass balance equations with three unknowns, which apply to the water column, the mixed sediment layer, and the deep sediment layers. Two coupled ordinary differential equations are solved for the surface water and the mixed sediment layer. A partial differential equation is solved for the deep sediment layers. Fate processes include: water column flushing; sorption partitioning in the water column

and benthic sediments; degradation in water and sediments; volatilization from water; water column sediment settling and bottom sediment resuspension; deep sediment burial; mass transfer of dissolved constituent between the water column and mixed sediment layer pore water; bioturbation between the mixed sediment layer and top layer of the deep sediments; and pore-water diffusion within the deep sediments. Loading boundary conditions include inflowing contaminant mass due to export from the soil model, which includes rainfall extraction and runoff, erosion, and soil interflow fluxes. There is also an option to enter user-specified constant external loadings. The model produces output for total and dissolved concentrations in the water column and bed.

The CMS is very similar to RECOVERY with the primary difference being the dimensionality and its orientation. CMS divides the stream into 1D longitudinal (stream-wise direction) segments. A single, fully mixed compartment is used to represent the benthic sediments underneath each 1D stream water segment. There is exchange between the sediment compartment and the overlying water just as in RECOVERY, but there is no longitudinal exchange between benthic sediment compartments except that associated with surface water fate and transport. The model solves a partial differential equation for the 1D, advection-diffusion-reaction (mass balance) equation of the surface water cells and an ordinary differential equation for each benthic sediment compartment. The CMS assumes steady, uniform flow. Stream flow can vary over time, but there is no hydraulic or hydrologic routing involved. There are various options for estimating the flow cross-sectional area and depth based on flow rate. The modeled fate processes are the same as those in RECOVERY except that bioturbation is not included since there is only one benthic layer. CMS formulations and verification are documented by Fant and Dortch (2007).

**Model Linkages**. The exchange of model outputs that are used as inputs to down-gradient models, such as soil export to vadose zone and surface water, are handled within TREECS™ via the file specification system used in the Framework for Risk Analysis in Multimedia Environmental Systems (FRAMES, http://mepas.pnnl.gov/framesv1/). FRAMES has been used by several U.S. Federal agencies to facilitate multi-media environmental modeling. For worst-case conservatism, mass fluxes exported from soil to the target surface water are transferred directly without attenuation, transport time delay, or mass loss. Thus, if the target surface water is a pond downstream of a range, and the stream connecting the range to the pond is not part of the surface water model, then mass fluxes from the range become input mass loadings to the pond without alteration in route through the connecting stream.

## VALIDATION RESULTS AND DISCUSSION

TREECS™ Tier 2 was applied to sites at four different Army installations. The installation names are withheld here due to sensitivity requiring lengthy Army approval. The four installations consisted of the conditions shown in Table 1.

**Table 1. Application conditions.**

| Installation No. | AOI | MC | Target Receiving Water |
|---|---|---|---|
| 1 | Demolition area | RDX | Groundwater |
| 2 | HE impact area including small arms ranges | RDX, TNT, lead, copper, perchlorate | Groundwater, lake |
| 3 | HE impact area and small arms ranges | RDX, lead | Pond |
| 4 | Small arms ranges | Lead, copper, zinc, antimony | Pond |

The applications at the above four installations are presented in detail by Dortch (2012), including descriptions of site characteristics, munitions usage and MC loading, soil and receiving water fate parameters, MC properties, and application results. In general, model inputs include: 1) selection of MC and their properties from one of three linked databases; 2) operational inputs (munitions use and related parameters); 3) protective health benchmark parameters (such as water alkalinity and sediment organic carbon); 4) AOI site dimensions, soil properties (water content, porosity, and bulk density), average annual hydrology (precipitation, rainfall, number of rainfall events, runoff depth, infiltration depth, and evapotranspiration) and soil erosion rate, MC fate/transport parameters (soil-water partitioning, $K_d$, half life, etc.), and MC properties (solid phase density, solubility, molecular weight, and Henry's constant as extracted from the MC database or user-specified); 5) vadose zone and aquifer soil composition (sand, silt, clay, organic carbon), media characteristics (water table depth, Darcy velocity, etc.), well locations, and MC fate/transport parameters ($K_d$, and half life); and 6) surface water morphometry and hydrology (surface area, depth, average annual water flow through rate, and total suspended solids concentration including fraction organic carbon), sediment properties (mixed layer and deep layer thicknesses, organic carbon content, porosity, and specific gravity), mean annual wind speed, sedimentation rates (enter two of the three for settling, resuspension, and burial, and the third is computed), MC initial conditions and any external loadings other than those from the AOI, MC fate parameters (degradation rates, $K_d$ for inorganic MC and metals; $K_d$ for organic MC are computed), and model control and output parameters. There are tools within TREECS™ for estimating soil properties, average annual hydrology, and average annual erosion rate.

**Table 2. Application Results.**

| Inst. No. | MC | Groundwater Concentration, µg/L | | Surface Water Concentration, µg/L | | Sediment Concentration, mg/kg | |
|---|---|---|---|---|---|---|---|
| | | Computed | Measured | Computed | Measured | Computed | Measured |
| 1 | RDX | 1.35 | 0.7 – 1.8 | NA | NA | NA | NA |
| 2 | RDX | 3.6E-4 | ND (<0.2) | 0.042 | ND (<0.2) | 3.8E-5 | ND (<0.15) |
| | TNT | 2.7E-3 | ND (<0.2) | 0.29 | ND (<0.2) | 3.3E-4 | ND (<0.15) |
| | Lead | 0.0 | ND (<1) | 1.05 | 0.25 | 3.35 | 6.0 |
| | Copper | 0.0 | ND (<8) | 0.49 | 0.32 | 1.71 | 2.9 |
| | Perchlorate | 1.2E-3 | ND (<0.2) | 2.3E-4 | ND (<0.2) | 2.0E-7 | NM |
| 3 | RDX | NA | NA | 0.035 | 0.023 | 7.7E-5 | ND |
| | Lead | NA | NA | 3.0 | ND(<1000) | 30.1 | 30.3 |
| 4 | Lead | NA | NA | 153 | ND (<68) | 1214 | 257 |
| | Antimony | NA | NA | 1.53 | ND(<246) | 3 | 32 |
| | Copper | NA | NA | 101 | ND(<274) | 88 | 92 |
| | Zinc | NA | NA | 31 | 123 | 105 | 95 |

NA = Not applicable; ND = Not detected; NM = Not measured

A comparison of the computed and measured results is presented in Table 2, where dissolved groundwater, total surface water, and total sediment concentrations are shown. Results for installation 1 are for 35 years after initiation of site use. Results for the other three installations are after 60 years of initiation of range use. The installation 2 application was a blind application since the measured results were not available until after the application had been conducted.

The predicted (computed) concentrations for HE and perchlorate were in good agreement with measurements (both detected and below detection). All but one metal concentration (lead at installation 4) was predicted to be below detection when the measurement was also below detection. Many of the metal concentrations that were predicted to be above detection were about the same order of magnitude as the measured values. Predicted sediment concentrations for copper and zinc were close to the measurements for installation 4, whereas predicted sediment lead and antimony concentrations were about an order of magnitude larger and smaller, respectively, than measured.

The computed surface water/sediment results for metals are particularly sensitive to water solubility and the sediment-water partitioning coefficient $K_d$, both of which are difficult to estimate since these parameters for metals are affected by the form of the weathered metal, ambient chemistry, and sediment characteristics. The relationships of these parameters to these ambient conditions are not fully understood and can be quite complex. Such uncertainties can be addressed within TREECS™ through a Monte Carlo simulation module for conducting sensitivity/uncertainty analysis. Another complexity associated with installation 4 is that the target receiving water (pond) is connected to the AOI by a relatively long creek that provided opportunity for deposition of metals (particularly lead) as well as background concentrations which were not available. Given these uncertainties, it is encouraging that the predicted metal concentrations for installation 4 sediments are within an order of magnitude or less of the measured values.

## CONCLUSIONS

This study showed that the applications of TREECS™ Tier 2 to the four Army installation sites resulted in relatively good agreement between computed results and measured field data. The results of these applications help validate TREECS™ and build confidence in its use for predicting export and fate of MC associated with munitions usage on firing and training ranges.

## ACKNOWLEDGEMENTS

## REFERENCES

Buck, J. W., G. Whelan, J. G. Droppo, Jr., D. L. Strenge, K. J. Castleton, J. P. McDonald, C. Sato, and G. P. Streile. 1995. *Multimedia Environmental Pollutant Assessment System (MEPAS) Application Guidance, Guidelines for Evaluating MEPAS Input Parameters for Version 3.1*. Tech. Report PNL-10395. Pacific Northwest Lab., Richland, WA.

Dortch, M.S., J. A. Gerald, and B. E. Johnson. 2009. *Methods for Tier 1 Modeling with the Training Range Environmental Evaluation and Characterization System*. Tech. Report ERDC/EL TR-09-11. U.S. Army Engineer Research and Development Center, Vicksburg, MS.

Dortch, M.S., B. E. Johnson, Z. Zhang, and J. A. Gerald, J.A. 2011. *Methods for Tier 2 Modeling within the Training Range Environmental Evaluation and Characterization System*. Tech. Report ERDC/EL TR-11-2. U.S. Army Engineer Research and Development Center, Vicksburg, MS.

Dortch, M.S. 2012. *Validation Applications of the Training Range Environmental Evaluation and Characterization System*. Tech. Report ERDC/EL TR-12-3 U.S. Army Engineer Research and Development Center, Vicksburg, MS.

Fant, S., and M.. S. Dortch. 2007. *Documentation of a One-Dimensional, Time-Varying Contaminant Fate and Transport Model for Streams*. Tech. Report ERDC/EL TR-07-01. U.S. Army Engineer Research and Development Center, Vicksburg, MS.

Ruiz, C. E., and T. Gerald. 2001. *RECOVERY version 2.0, a Mathematical Model to Predict the Temporal Response of Surface Water to Contaminated Sediments*. Tech. Report ERDC/EL TR-01-3. U.S. Army Engineer Research and Development Center, Vicksburg, MS.

Whelan, G., J. P. McDonald, and C. Sato. 1996. *Multimedia Environmental Pollutant Assessment System (MEPAS): Groundwater Pathway Formulations*. Tech. Report PNL-10907. Pacific Northwest National Laboratory, Richland, WA.

# RAPID LYSIS OF BACTERIAL CELLS IN A MICROFLUIDIC CHIP

Tsung-Ju Yang and *Shu-Chi Chang*
(National Chung Hsing University, Taichung, Taiwan)

Cell lysis or poration is a vital pretreatment step for a variety of cellular biological experiments and environmental microbial studies. Isolated treatment of each cell is the first step to gather information at single cell level. To envelop each cell in a single water microdroplet, *Escherichia coli* cells were exposed to mild probe sonication. Thus, each cell was dispersed in an oil phase with a small amount of water amended with propidium iodide (PI). Then, this suspension was sent into a microfluidic chip fabricated using soft lithography. Coupled with oil phase hydrodynamic focusing, the microelectrodes embedded in microchannels can effectively lyse more than 90% of the bacterial cells at a rate higher than100 cells per second. The cell lysis successful rate was determined by observing PI fluorescence under an epifluorescent microscope. After electrical lysis, each cell was still well isolated in its own water droplet. Thus, this technology has high applicability in the studies of microbial identification and microbial ecology.

# DEVELOPMENT OF MOLECULAR IMPRINTING POLYMERS FOR ENVIRONMENTAL PHTHALATE ESTERS ANALYSIS

Yu-Yin Liu and *Ta-Chang Lin*
(National Cheng Kung University, Tainan, TAIWAN)

Among the phthalate esters (PAEs), the di-(2-ethylhexyl) phthalate (DEHP) is a popular plasticizer used to improve the flexibility of polyvinyl chloride (PVC). DEHP easily leaches from the PVC products into the environment and may be transferred into water, air and food. Animal experiments indicated that DEHP is a toxicant to the reproductive system. In this study molecular imprinting polymers (MIPs), synthesized using DEHP as the template, were developed to improve the recovery and to reduce the interference in environmental matrice during sample pretreatment. Various MIP formulations were tested to obtain a good candidate MIP for PAEs adsorption. The result shows that the optimal formulation of MIP for DEHP is respectively 1: 4: 20: 0.2 for the template, function monomer, cross-linker and initiator. Five different formulations (M1-M5), a parallel set of NIPs (B1~B5, without template) were tested. From the dynamic adsorption tests, M5 revealed a maximum adsorption capacity of 427.4 µg/g at a concentration of 15 ppm, as well as M3 (imprinting factor: 7.93) and M4 (imprinting factor: 1.95 at trial 15 ppm) were adopted to proceed with the consequent molecular imprinting solid phase extraction for their high imprinting factors. Result of DEHP recovery of M5 reached 90.9 %.

# ASSESSMENT OF HEAVY METALS IN SOILS IN THE SURROUNDINGS OF A COAL-FIRED POWER PLANT

*Maria de Lurdes Dinis*, António Fiúza, Joaquim Góis, José Soeiro de Carvalho, Ana Meira Castro
(Geo-Environment and Resources Research Center (CIGAR), Porto University, Porto, Portugal)

**ABSTRACT:** This paper aims to survey metal concentrations in soils in the vicinity of a coal-fired-power plant located in southwest of Portugal. Two annual sampling campaigns were carried out to measure a hypothetical soil contamination around the coal plant. The sampling area was divided into two subareas, both centered in the emission source, delimited by two concentric circles with radius of 6 km and 20 km. About 40 samplings points were defined in the influence area. Metals measurements were performed with a portable analytical X-ray dispersive energy fluorescence spectrometer identifying about 20 different elements in each sampling point. The most relevant elements measured included As, Cu, Fe, Hg, Pb, Ti and Zn in both sampling areas. Considering the results obtained in the first sampling campaign, arsenic is predominantly higher within the 6-20 km sampling area. The second sampling campaign showed that both sampling areas presented relatively similar metal concentrations except for Fe, Mn, Sr and Zn which concentration is higher within the 6-20 km sampling area. Also, As, Fe, Mn and Ti concentrations decreased significantly from the first to the second sampling campaign and their concentration were predominately higher in the NE-E and E-SE directions.

## INTRODUCTION

Many hazardous air pollutants are associated with emissions from coal-fired power plants. During coal combustion metals and heavy metals such as Al, As, Be, Cd, Cr, Fe, Pb, Mn, Zn, Ra, Hg and V, are released to the atmosphere as dust components in the fly ashes. Coal-fired power plants are at the present time equipped with technological solutions such as electrostatic precipitators with high collection efficiency ($\cong$ 99%). However, considerable amounts of fly ash particles enriched in several hazardous elements are still discharged into the environment due to the high rate of coal consumption.

Fly ash consists of finer sized particles, ranging from 0.5 to 200 µm (Baba, 2002). Due to its relatively small size and hence large surface area, the ashes have a great tendency to absorb trace elements that are released from coal during combustion. As the fly ash particles have high atmospheric mobility they may be transported from their source over a wide range of distances and deposited on the ground. In addition, concern regarding soil metals concentration remains due to past fugitive emissions that could have contributed to the increasing metal concentrations in soil.

Atmospheric deposition from industrial activities can be a potentially source of atmospheric discharge of many metals inducing long-term changes in soil quality. In particular, heavy metals from fossil fuel combustion are a common source of pollution for surface soils. Thus, soil at those sites may potentially present higher concentrations in various pollutants depending upon the coal quality, the combustion and dust collection technology as well as on the local meteorological conditions.

Bityukova et al., (2000) observed that the levels of As, Cr, Mn and V were more than three times higher and the levels of Pb and Zn were more than five times higher than the background levels for industrial polluted soils resulting from fossil fuel combustion. Soils around a coal power plant are enriched in Ag, Cd, Co, Cr, Cu, Fe, Hg, Ni, Ti and Zn (Klein and Russell, 1973) and in Mo, As, Mn, Pb, Be, and V (Mandal and Segupta, 2006).

This paper aims to survey metal concentrations in soils in the vicinity of a coal power plant located in the southwest of Portugal (Sines). The purpose was to determine the extent and degree of soils contamination that may be related to the dispersion from the coal power plant stacks emissions. The contribution from meteorological conditions, in particular wind parameters, was also considered.

The present study has been focused in two main areas around the stacks of Sines coal-fired power plant. The design of the sampling area was based on the stack's emissions influence considering the

potential effect on soils contamination in the neighborhood of this coal plant up to distances of 20 km. Two annual sampling campaigns were carried out to measure soil contamination around Sines coal-fired-power plant. About 40 samplings points were defined in the influence area. Heavy metals measurements were performed with a portable analytical X-ray dispersive energy fluorescence spectrometer (XRF). Two measurements were done in situ and about 20 different elements were detected in the sampling area.

Metal contents in soils were compared with legal legislation limits for the maximum permissible concentration according to soil use: agricultural, residential or industrial. Arsenic was found to be the only element with an average concentration above the guidelines for all types of land use. Lead and zinc were found to be below the legislation limits for any types of land use.

## MATERIALS AND METHODS

**Study Area.** The present study was conducted in the vicinity of Sines coal-fired power plant located in the southwest coastline of Portugal, at 6 km south-east from the city of Sines and about 150 km south of the country's capital, Lisbon. It is located in an industrial area with more than 14 other industrial plants, including a petrochemical complex, a refinery and a resins plant.

Sines coal-fired power plant consumes bituminous coal as primary fuel, imported from many different countries. It has four units of 314 MW each and supplies about 20 to 25% of all electrical energy produced in Portugal. In 2009 the energy produced in this coal power plant was approximately 9516 GWh. The plant has two operational stacks with 225 m height. Coal is stored at open air in 4 active piles with 150 000 tons each and in one passive pile with 700 000 tons.

Data on this particular source emission is reported in the European database "European Pollutant Release and Transfer Register" (E-PRTR, 2010) for 2007, 2008, 2009 and 2010 (Table 1).

**TABLE 1 :** Pollutant releases to air from Sines coal-fired power plant (extracted from E-PRTR, 2010).

| Releases to air | 2007 | 2008 | 2009 | 2010 |
|---|---|---|---|---|
| Arsenic and compounds (as As) | 40.0 kg | 31.0 kg | 33.0 kg | - |
| Mercury and compounds (as Hg) | 107 kg | 209 kg | 95.0 kg | 54.7 kg |
| Nickel and compounds (as Ni) | 126 kg | 271 kg | 341 kg | 254 kg |
| Particulate matter ($PM_{10}$) | 587 t | 394 t | 130 t | 99.7 ton |
| Zinc and compounds (as Zn) | - | 265 kg | 349 kg | 220 kg |
| Chromium and compounds (as Cr) | 127 kg | - | - | - |

The historical data referent to the study area indicates that the prevailing wind direction is from the sector N-NW with the exception for the month of October when the prevailing winds direction is from SW and S. In autumn there is a significant decrease in wind directions blowing from NW indicating the prevailing winds to be from N with a frequency of 34.5%. Wind velocity is relatively constant during all year with long calm periods; stronger winds blow from N-NW and SW with maximum velocities during the winter season. The sampling periods were carried out during mid September to mid October 2010 and during the month of April 2011; the prevailing wind direction for these periods were from N-NW and from N-NE, respectively.

**Sampling and analysis.** Sampling was carried out in 2010 and 2011 in seasonal periods considering rainy or dry atmospheric conditions to evaluate soils contamination in the vicinity of Sines coal-fired power plant. The sampling area was defined by two concentric circles with a radius of 6 and 20 km centered in the plant stacks. The sampling area is approximately 688 km$^2$; a total of 40 samplings points were defined in both sampling areas: 13 sampling points in the inner area, with urban and sub-urban characteristics, and 27 sampling points in the outer area, mainly rural (Figure 1).

The sampling points more distant from the stacks (20 km) were selected as control representing the "zero" background concentration level, meaning theoretically without the influence of the power plant. Field measurements were carried out using a portable XRF spectrometer. Two measurements were carried out in each sampling point at surface soil level.

Element concentration detected in surface soils were compared with legal legislation limits values for the maximum permissible concentration according to soil use: agricultural, residential or industrial.

Fly ashes retained in the stacks' filters were also analyzed; the detected elements included As, Ba, Co, Cr, Cu, Fe, Hg, Mn, Mo, Pb, Rb, Se, Ti, Zn and Zr.
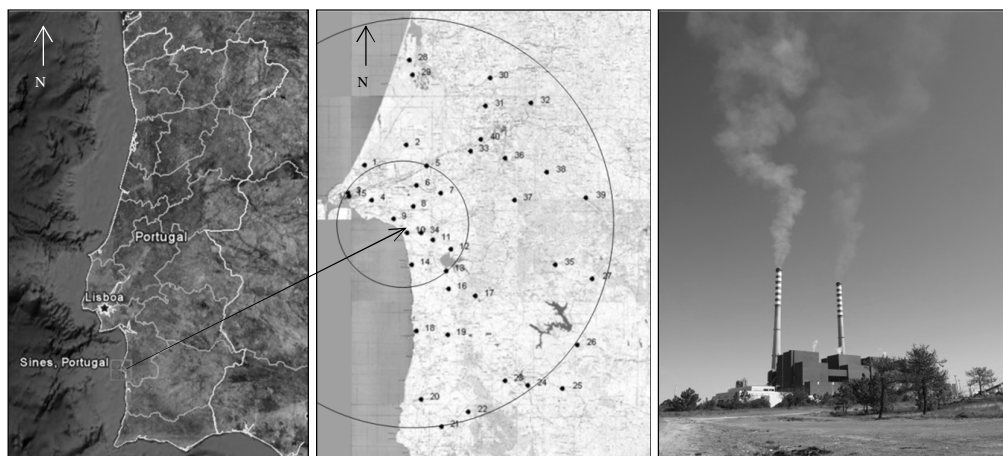


**FIGURE 1:** Sines location, sampling area around the coal-fired power plant and stacks.

## RESULTS AND DISCUSSION

Twenty elements were quantified in the measurements carried out with the portable XRF spectrometer: As, Ba, Ca, Co, Cu, Fe, Hg, K, Mn, Mo, Ni, Pb, Rb, S, Sb, Se, Sr, Ti, Zn, Zr. The average values and the statistical description of measurements carried out on total 40 sampling points for both sampling campaigns are presented in Table 2, Table 3 and Table 4. The number of cases for each detected element is also presented (N).

**TABLE 2:** Average values and statistical description of measurements carried out on 40 sampling points for sampling campaign Nº 1 (mg/kg).

| Element | Average | Median | S.D. | Skewness | Max. | Min. | N |
|---------|---------|--------|------|----------|------|------|---|
| As | 101.30 | 91.50 | 28.73 | 0.71 | 164.00 | 63.00 | 40 |
| Ba | 578.66 | 378.00 | 429.61 | 1.20 | 1713.00 | 144.00 | 32 |
| Ca | 19244.13 | 11213.00 | 19124.05 | 1.26 | 68411.00 | 1602.00 | 38 |
| Co | 387.00 | 368.50 | 75.66 | 0.92 | 487.00 | 324.00 | 4 |
| Cu | 56.56 | 62.00 | 16.04 | -0.22 | 79.00 | 31.00 | 9 |
| Fe | 30858.80 | 21097.50 | 28830.36 | 1.28 | 98306.00 | 5190.00 | 40 |
| Hg | 15.50 | 15.50 | 7.78 | - | 21.00 | 10.00 | 2 |
| K | 33830.39 | 30945.00 | 14791.74 | 0.94 | 78883.00 | 10988.00 | 3 |
| Mn | 1269.83 | 724.00 | 1943.53 | 4.59 | 12027.00 | 101.00 | 40 |
| Mo | 17.50 | 17.50 | 13.44 | - | 27.00 | 8.00 | 2 |
| Ni | 31.00 | 31.00 | - | - | 31.00 | 31.00 | 1 |
| Pb | 25.75 | 21.50 | 17.23 | 2.26 | 89.00 | 10.00 | 32 |
| Rb | 60.25 | 52.00 | 33.50 | 0.83 | 149.00 | 11.00 | 40 |
| S | 17809.60 | 11643.50 | 14484.61 | 2.24 | 63846.00 | 7944.00 | 20 |
| Sb | 115.00 | 115.00 | - | - | 115.00 | 115.00 | 1 |
| Se | 5.00 | 5.00 | - | - | 5.00 | 5.00 | 1 |
| Sr | 108.78 | 47.00 | 236.53 | 5.49 | 1498.00 | 11.00 | 40 |
| Ti | 7027.73 | 5754.00 | 6136.45 | 2.06 | 32977.00 | 800.00 | 40 |
| Zn | 69.18 | 35.50 | 92.43 | 4.09 | 552.00 | 10.00 | 38 |
| Zr | 116.83 | 96.00 | 82.18 | 1.12 | 378.00 | 10.00 | 40 |

Some of the selected elements were detected in very few sampling points: Co, Hg, Mo, Ni, Se and Sb in addition to Ba for sampling campaign nº 2. Elements content in soils were compared with legal legislation limits for the maximum permissible concentration according to soil use: agricultural, residential or industrial. The Canadian Soil Quality Guidelines for the Protection of Environmental and Human Health were used for comparison with the selected elements.

The concentration values obtained for As, Co, Sb and Se are above the respective limit for all types of land use but Cu, Pb and Sn are below the guidelines values. Barium, mercury and molybdenum

exceed the legislation limits for agriculture and residential soils. Nevertheless, it should be noted that some of these elements were detected in very few sampling points.

**TABLE 3:** Average values and statistical description of measurements carried out on 40 sampling points for sampling campaign N° 2 (mg/kg).

| Element | Average | Median | S.D. | Skewness | Max | Min | N |
|---------|---------|--------|------|----------|-----|-----|---|
| As | 71.50 | 71.00 | 13.33 | 0.27 | 101.00 | 52.00 | 40 |
| Ba | 1679.00 | 1679.00 | 195.16 | N.A. | 1817.00 | 1541.00 | 2 |
| Co | 330.75 | 252.00 | 183.52 | 1.87 | 603.00 | 216.00 | 4 |
| Cu | 41.33 | 39.00 | 12.42 | 0.75 | 61.00 | 29.00 | 6 |
| Fe | 18048.25 | 10162.00 | 17805.01 | 1.45 | 74805.00 | 829.00 | 40 |
| Hg | 12.00 | 12.00 | - | - | 12.00 | 12.00 | 1 |
| Mn | 515.83 | 280.00 | 659.26 | 2.81 | 3392.00 | 19.00 | 36 |
| Mo | 11.00 | 9.00 | 3.46 | N.A. | 15.00 | 9.00 | 3 |
| Pb | 24.91 | 19.00 | 26.01 | 4.84 | 162.00 | 8.00 | 33 |
| Rb | 57.29 | 57.00 | 31.37 | 0.59 | 138.00 | 10.00 | 38 |
| Sr | 72.78 | 53.00 | 78.78 | 2.65 | 386.00 | 10.00 | 40 |
| Ti | 3579.28 | 2961.00 | 3243.84 | 3.56 | 19616.00 | 647.00 | 36 |
| Zn | 53.69 | 38.50 | 61.78 | 3.46 | 351.00 | 9.00 | 36 |
| Zr | 110.60 | 102.00 | 71.38 | 0.51 | 259.00 | 16.00 | 40 |

**TABLE 4:** Average values and statistical description of measurements for selected elements for sampling campaigns N°1 and N° 2 (mg/kg).

| | Sampling Campaign N° 1 | | | | | | Sampling Campaign N° 2 | | | | | |
|----|---------|--------|------|------|------|----|---------|--------|------|------|------|----|
| | Average | Median | S.D. | Max. | Min. | N | Average | Median | S.D. | Max. | Min. | N |
| *Area within the 6 km circle* | | | | | | | | | | | | |
| As | 87.46 | 79 | 24.46 | 137 | 63 | 13 | 68.92 | 67 | 13.07 | 101 | 53 | 13 |
| Ba | 590.25 | 338.50 | 533.90 | 1713 | 195 | 12 | 1817 | 1817 | - | 1817 | 1817 | 1 |
| Cu | 57 | 64 | 13.89 | 66 | 41 | 3 | 35.50 | 35.50 | 9.19 | 42 | 29 | 2 |
| Fe | 23580.69 | 22644 | 20714.78 | 83843 | 5190 | 13 | 14557.31 | 8611 | 20092.39 | 74805 | 1847 | 13 |
| Hg | 15.50 | 15.50 | 7.78 | 21 | 10 | 2 | - | - | - | - | - | 0 |
| Mn | 1639.46 | 761 | 3157.26 | 12027 | 159 | 13 | 267.36 | 194 | 277.72 | 926 | 19 | 11 |
| Mo | 27 | 27 | - | 27 | 27 | 1 | 9 | 9 | - | 9 | 9 | 1 |
| Pb | 31.78 | 25 | 24.53 | 89 | 12 | 9 | 21.50 | 17 | 11.75 | 44 | 8 | 10 |
| Rb | 56.62 | 46 | 31.20 | 149 | 31 | 13 | 57.73 | 60 | 29.21 | 123 | 18 | 11 |
| S | 17868.38 | 11643.50 | 18710.17 | 63846 | 7944 | 8 | - | - | - | - | - | 0 |
| Sr | 202.62 | 65 | 401.16 | 1498 | 20 | 13 | 94.69 | 80 | 90.98 | 299 | 20 | 13 |
| Ti | 8013.23 | 5066 | 8434.19 | 32977 | 1614 | 13 | 4481.91 | 2559 | 5302.77 | 19616 | 1081 | 11 |
| Zn | 61.92 | 46.50 | 47.16 | 162 | 12 | 12 | 32.90 | 22 | 26.70 | 83 | 9 | 10 |
| Zr | 113.85 | 83 | 90.15 | 378 | 37 | 13 | 104.31 | 77 | 67.93 | 229 | 29 | 13 |
| *Area within the 6 and 20 km circles* | | | | | | | | | | | | |
| As | 107.96 | 104 | 28.63 | 164 | 72 | 27 | 72.93 | 75.50 | 13.31 | 95 | 52 | 28 |
| Ba | 571.70 | 535.50 | 368.74 | 1438 | 144 | 20 | 1541 | 1541 | - | 1541 | 1541 | 1 |
| Co | 387 | 368.50 | 75.66 | 487 | 324 | 4 | 330.75 | 252 | 183.52 | 603 | 216 | 4 |
| Cu | 56.33 | 55.50 | 18.28 | 79 | 31 | 6 | 44.25 | 43 | 13.96 | 61 | 30 | 4 |
| Fe | 34363.07 | 19551 | 31772.62 | 98306 | 5607 | 27 | 19211.32 | 12331 | 16652.47 | 60366 | 829 | 28 |
| Hg | - | - | - | - | - | 0 | 12 | 12 | - | 12 | 12 | 1 |
| Mn | 1091.85 | 717 | 981.83 | 3153 | 101 | 27 | 610.54 | 383.50 | 737.61 | 3392 | 59 | 26 |
| Mo | 8 | 8 | - | 8 | 8 | 1 | 12 | 12 | 4.24 | 15 | 9 | 2 |
| Ni | 31 | 31 | - | 31 | 31 | 1 | - | - | - | - | - | - |
| Pb | 23.39 | 20 | 13.36 | 70 | 10 | 23 | 26.39 | 21 | 30.33 | 162 | 9 | 23 |
| Rb | 62 | 53 | 35 | 123 | 11 | 27 | 57.04 | 53.50 | 32.14 | 138 | 10 | 28 |
| S | 17770.42 | 11725.50 | 11815.76 | 42951 | 8703 | 12 | - | - | - | - | - | 0 |
| Sb | 115 | 115 | - | 115 | 115 | 1 | - | - | - | - | - | 0 |
| Se | 5 | 5 | - | 5 | 5 | 1 | - | - | - | - | - | 0 |
| Sr | 63.59 | 46 | 55.83 | 281 | 11 | 27 | 60.79 | 43 | 70.72 | 386 | 10 | 28 |
| Ti | 6553.22 | 6394 | 4788.83 | 16612 | 800 | 27 | 3130.65 | 2983 | 1742.52 | 5954 | 647 | 26 |
| Zn | 72.54 | 35.50 | 107.83 | 552 | 10 | 26 | 61.69 | 42 | 69.62 | 351 | 9 | 26 |
| Zr | 118.26 | 116 | 79.84 | 299 | 10 | 27 | 112.32 | 102 | 73 | 259 | 16 | 28 |

The same variation pattern was observed in the second sampling campaign: Pb, Zn and Cu concentrations are below the guidelines limits and As and Co concentrations are above the legislation limit for all types of soil use. Barium, Hg and Mo concentration levels are above the respective limits for agricultural and residential soil use.

All concentration levels decreased significantly from the first to the second campaign. This variation may be a consequence of soil moisture content for sampling campaign nº 2, carried out after an intense rainy period. Excessive soil moisture is a limitation in using field XRF; the higher the soil moisture in a particular matrix, the lower the reported concentration relative to the actual concentration. The actual difference may vary significantly for all samples from a site (Hunter, 2011). Other factors could have indeed contributed to the lower results obtained in the second sampling campaign such as local and seasonal meteorological conditions that interfere with particulate matter dispersion and deposition on the ground, in addition to the fact that the coal plant was not working at full power during this sampling period which means less emission rates.

The concentrations of the selected elements according to the distance to the potential emitting source, within the 6 km area and from 6 to 20 km, are presented in
For both sampling campaigns, the obtained concentrations are higher in the outer sampling area (6-20 km) with the exception of Sr and Ti for sampling campaign nº 1 and Ba, Sr and Ti for sampling campaign nº 2.

The distance that particles travel depends on meteorological conditions, on particle size and on stack height; 6% of the emitted particles from a coal power plant with a 300 m stack fell within 5 km. In power plants equipped with electrostatic precipitators most particles emitted have less than 2 µm in diameter which can agglomerate accelerating the deposition near the source. Even though, smaller particles can travel between 100 and 1700 km (Keegan et al., 2006).

The height of the stacks and the dispersion by strong seasonal winds could explain the observed enrichment of the selected elements in the area between the 6 and 20 km. However, some of the typical heavy metals associated with coal combustion emissions such as Cd, Cr, Hg and Ni were not detected in the sampling area or at least in a significant number of cases. This may result from the limitations of field XRF, in particular high soil moisture; metals interference (Fe tends to absorb Cu X-rays, whereas Cr levels will be enhanced in the presence of Fe); lack of sensitivity due to peak overlapping (high detection limits demanding more field measurement time; Cd and Hg are not detected easily by XRF because of their detection limit) (Hunter, 2011).

Emissions dispersion from industrial processes and consequently the deposition on soils is mainly influenced by the wind parameters, rainfall, other sources of emissions, resuspension of dust from earth's surface, intensified agricultural activities and road traffic. In cases where none of these factors is present, the intensity of particles deposition and consequently the concentration on soil should decrease with the distance to the main source of pollution.

Iso-concentration maps have been made for some elements of the first sampling campaign: As, Mn, Pb and Zn (Figure 2). These elements were selected regarding to their relation with industrial contaminated soils, in particular soil contamination from coal combustion.
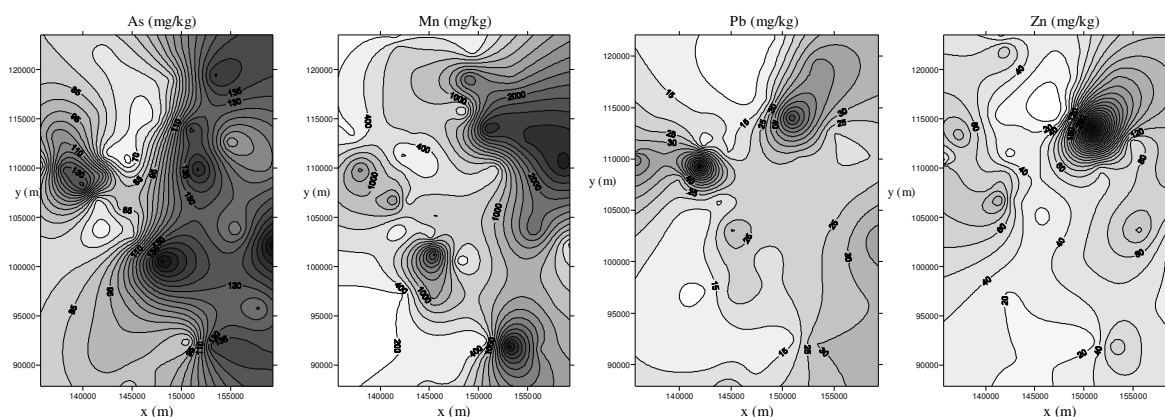


**FIGURE 2:** Iso-concentration maps for As, Mn, Pb and Zn (sampling campaign nº 1).

The iso-concentration maps for the selected elements showed a pattern concentration described by either marked element enrichment for distances between 6 and 20 km in the NE-E and E-SE sectors to the stacks and peak concentrations in the immediate area around the stacks. The stacks are locate at approximately 141 000 m (x) and 107 600 (y).

The distribution of the selected elements as well as other elements in surface soil (e.g. Fe and Ti) seems to follow a similar pattern observable in both sampling campaigns: As, Mn, Pb and Zn concentration decreased significantly from the first to the second campaign and the concentrations were predominately higher in the NE-E and E-SE directions. Nevertheless, no regular trends could be observed for elemental concentration and distance from the power plant.

During both sampling campaigns the prevailing wind directions were from N-NW and N-NE. This could explain at some extent the metals concentration pattern in soils, however, peak concentration suggests also the contribution from others sources. An important feature in atmospheric emissions is the influence of stack height in the dispersion and deposition patterns: about 25% of emitted particles from a 40 m stack fell within 5 km and 34% within 10 km (Keegan et al., 2006). We should have present that a huge coal deposit is located in the immediate area around the stacks and the contamination in the immediate vicinity of the power plant is likely to be predominately from local fugitive sources in the form of windblown ash and dust.

## CONCLUSIONS

The present study provides an analysis of metal concentration in soils around Sines coal-fired power plant, comparing the obtained results from seasonal sampling campaigns as well as their significance according to legislation limits. An analysis of the variation concentration pattern with the distance to the emitting source was done considering the influence of local meteorological parameters.

Sines coal-fired power has been a source of atmospheric emissions of metals and particulate matter for many years. In the last five years these emissions decreased substantially. Nevertheless, past historical emissions must have contributed to soil contamination.

Maximum concentration values were obtained in the dry season (end of summer) as well as a higher number of detected elements. Weather conditions strongly affect the dispersion and deposition of air dust as well as the fluctuations of emissions sources over the seasons. The obtained values for sampling campaign nº 2 were clearly affected by weather conditions and emission fluctuations, reflected in the XRF efficiency. Dried samples should be analyzed at laboratory for lower detection limit in order to measure Cd, Hg and Cr.

Average concentrations of several elements measured in soil (As, Ba, Co, Hg, Mo, Ni, S and Se) are above the Canadian guideline limit for agricultural and residential soils. Nevertheless, with the exception of As and Ba very few measurements were obtained for these elements.

No regular trend was observed for elemental concentration and the distance from the power plant. However, a similar concentration pattern was observed for both sampling campaigns: the average concentration is higher within the outer area (6 - 20 km). High concentrations were measured at NE, E and SE from the stacks influenced by the wind parameters; stacks height combined with wind patterns are expected to have transported the contaminated particulate matter and dust to relatively long distances from the emission source. Peak concentrations were measured in the soil around the stacks that could not fall from the plume vertically. This anomaly is directly related with the presence of a coal deposit in the vicinity of the stacks in addition to fugitive emissions from ground-level areas enriched in these elements by other means.

Though recent measures mean that stacks height is no longer a significant point source of pollution, the contribution from other sources related to the coal combustion or to the coal plant as well as past historical emissions, may increase exposure to the population living in the vicinity of the Sines coal plant. Even though for some elements the concentration was not substantially raised, emissions and environmental levels of these metals may have been higher in the past.

## REFERENCES

Baba A. 2000. "Assessment of radioactive contaminants in by-products from Yatagan (Mugla, Turkey) coal-fired power plant". *Environmental Geology Journal*, 41: 916-921.

Bitykova L., A. Shogenova, M. Brike 2000. "Urban Geochemistry: a study of element distributions in the soils of Tallinn (Estonia)". *Environmental Geochemistry Health*, 22: 172-193.

CCME 2011. Canadian Environmental Quality Guidelines, http://ceqg-rcqe.ccme.ca/.

Hunter D. 2011. "Field X-Ray Fluorescence Measurement". *USEPA*, SESDPROC-107-R2.

Keegan T. J., M. E. Farago, I. Thornton, B. Hong, R. N. Colvile, B. Pesch, P. Jakubis and M. J. Nieuwenhuijsen 2006. "Dispersion of As and selected heavy metals around a coal-burning power station in central Slovakia". *Sci Total Environ. 358(1-3):61-71.*

Klein D. and P. Russell 1973. "Heavy Metals: Fallout Around a Power Plant". *Env Sci and Tech*, 7, nº 4: 357-358.

Mangal A. and D. Sengupta 2006. "An assessment of soil contamination due to heavy metals around a coal-fired thermal power plant in Indis". *Environmental Geology Journal*, 51: 409-420.

# DEVELOPMENT OF DATABASE FOR MARINE OIL POLLUTION STUDY

*Nguyen Kim Anh* , Nguyen Dinh Duong
(Institute of Geography, Vietnam Academy of Science and Technology)

**ABSTRACT:** This paper provides a new methodology for developing database server for studying oil pollution in the sea. At the same time, the newly developed database that was developed for oil pollution study of Vietnam and East Sea will be useful to support the assessment and zoning oil pollution risk. The authors have developed the database based on GIS (Geographical Information System) and RS (Remote Sensing) technologies, where ArcSDE and ArcGIS Server software are used to accomplish the goals for building an open GIS database and which is able to sharing online data through web services. This word has meaningful for studying oil spill because, the oil spills will be updated continuously and the system will provide an overall of oil spill picture of this area. Then it can be easy to build oil spill density map and design the monitoring system for this area. By comparison between this system and other existing systems in the area, it can be clearly seen that there are two strong points of this system e.g.: the first thing, by IWS (Image Web Server) and ArcGIS Server software system which can be share fully two types of data format as vector and raster data which allows to transmit information to the related offices to solve urgent oil spills. The second thing is that it can be control sharing with many levels and the system allows as save or not save on server GIS through editing from users.

## INTRODUCTION

As can be seen from real situation on the oceans are that oil pollution has begun more and more seriously, especially to Vietnamese marine and East Sea. In the last few years, Vietnamese marine have to face to many oil spills with difference scales and levels. Oil pollution has its own particularities which is different from other types of pollution. To detect the sources of oil pollution, it needs to have a monitoring system, which is able to detect oil spill from satellite images, then that information need to be determined and calculated in very short period to fulfil the need of the users. Combining the obtained information with other supported information such as winds, waves and coastal areas conditions, report etc. about oil spill can be created and sent to relational users. Based on this information, necessary actions will be to take to solve oil spills problem. Thus, in order to satisfy all requirements, it needs to have an efficient monitoring system in which a server database have to build for pollution detection, zoning and transmission of oil pollution forecasting. So far, there are many studies which have shown through several methodologies for developing the database system for studying oil pollution in the sea through which some of the related projects can be listed below.

The first project is Oceanides by the European Commission Joint Research Centre. This project was built a Web server with a GIS management tools which ArcIMS is installed outside the firewall. The Web site includes several GIS functionalities such as Zooming, attribute query; Map combining and much more; Oracle database installed inside the firewall with ArcSDE for GIS capability communication by secure connection (but less flexibility). Oil spills data was built up for all European Seas Baltic Sea, North Sea, Mediterranean Sea and Black Sea from 2000 to 2005 with 17 650 oil spills collected by the end of the project. Additionally, many maps products such as sea depth (bathymetry); petroleum ports; ferry links; energy and other data, including political boundary; maritime boundaries; satellite image and bath Oil spill density maps, which is available in pdf format in Oceanides website http://serac.jrc.it/midiv/maps. This system allows users to download and edit data online. Products from this project is the most perfect and up-to-date in the world, because it provides a rule distributing of oil spills on seas belongs to the European countries.

The second project that needs to mention is Cearac which was established by NOWPAP (China, Russia, Korea and Japan). One of the final goals of WG4 is to establish marine environmental monitoring systems by remote sensing in the NOWPAP region. Moreover, it is important to collect data and

information, including satellite images to forecast the development and behaviour of eutrophication and oil spill and then to disseminate data and information in the present conditions of eutrophication and oil spill and then forecasting the results quickly. However, the data and information about the marine environment collected by remote sensing are actually scattered in different organizations in the NOWPAP region. In order to share their usability to share existing research and development resources and also to understand the future trends in marine environmental monitoring by developing remote sensing information network system which integrates the scattered information. It is the basic work to be implemented. This organization was built a website where contain reports about oil spills happened in their seas where images and maps database were built. More detail information about this project can be seen on website: http://cearac.poi.dvo.ru/en/main/about.

The third project is related to Kongsberg Company which is one of the most pioneers in building monitoring system of oil spills in the marine. This company has been building a perfect technical system for monitoring, detecting and warning oil spills where a modern database was built based on GIS and RS foundation and ArcSDE and Sensor WebGIS system were used. From this system, warning of oil spills will be sent to the related offices via messages, email and computer network system. Immediately, a report about oil spill will be created for necessary action. Further information can get from website: http://www.kongsberg.com.

Turn back to the case of the oil spill study in Vietnamese sea, it worth to mention to OILSAS project of Dr. Nguyen Huu Nhan. The author has built Oil Spill Assistant software and database server system for oil spills warning at Khanh Hoa province in which the Phase 1 of the project started since 2004. The outcomes of this project are: software server system for managing oil spills and database in MapInfo format include layers about meteorological and hydrography for calculating and transmitting oil pollution forecast data.

Project in national level named "Oil pollution on Vietnam and East sea", with the number code KC.09.22/06-10 was done by Dr. Nguyen Dinh Duong and other staffs during the period from 2008 to 2010, where the authors have built a database supports for forecasting and zoning oil spills. A lot of SAR images were purchased and were used to combine with other information in GIS environment after that gave out confident assessment reports about oil spills. Project reached necessary goals; however, it still contains some weak points: The first weak point is the system could not share vector data, all most it just provided images data throughout IWS software. The second weak point is the right to access to the system; it is difficult to control in different levels. In summary, authors have not built a perfect methodology and conclusions yet.

In this paper, the authors would like to discuss a better structure to provide out a new methodology to use and share better database was built. At the same time, the authors will introduce some results from study include database in ArcSDE environment and system sharing data via data sharing service and web application.

## MATERIALS AND METHODS

Data is collected from national project named: Oil pollution on Vietnam and East sea areas number code KC.09.22/06-10 which include the data is listed as follow: 110 SAR satellite images which cover ALOS PALSAR and ENVISAT ASAR; Data components of some data groups are: meteorological, hydrography, transportation, exploitation and processing of oil and gas, coastal development activities, damaged tankers sunk in the past and other support information.

In order to conduct this study five methods are combined. The first step is the review of the literature to have rough ideas of previous researches. What they did and assess for the strong and weak points of existing systems and how to improve it. The second step is data collection, which to collect the data and set up the research funding, this step is popular for building GIS database. Once we have enough data, it needs to analysis and systematic such as assess the accuracy of the data what should use edit. GIS is major goal of this study, where personal geodatabase structure and other techniques will be used, especially using the analysis tools to assess oil spill and build density oil spill maps. Finally, remote sensing data will be used to get information about oil spills in the past and real time to have overviewed picture about oil spills on East Sea. Sometimes, it can be detected other information as: wind, wave, vessel, etc from satellite imagery, which is really useful for analysis and forecast oil spill.

In addition to the implementation of goals outlined in the previous section, the choice of web GIS technology used is the other major goal of the research: utilize open source solutions rather than proprietary ones. The oil spill database application and sharing system was designed in the part as an attempt to significantly improve upon the user interfaces offered by other natural hazard web GIS system. Both systems are used as ArcServer and ArcSDE mapping software are from ESRI. Although intend to be comprehensive web applications, both are slow at displaying map features and are hindered with a somewhat dated user interface. Utilizing dynamic client-side web technologies such as Ajax combined with the popular Google Maps interface was deemed to be a desirable goal to make the oil spill easy to use, responsive, and appealing to look at.

As can be seen from figure-1, separate layers were rebuilt and organized following structure of Personal Geodatabase in Geodatabase Server SQL Express in ArcSDE software. Where each group of information is feature dataset SDE and each layer in each group is feature class SDE. Next step, maps were edited and saved in *mxd format after that reports about oil spills will be created in *PDF format and link to oil spills and image in geotiff format with ID code.

Group information that serves detecting oil spills early including: images data that the authors can extract information of oil spills and sometimes it allows restoring winds and stream flow directions where operation of vessels and drilling platform are available. Combining with the others supportive information such as maps of satellites orbits which are ALOS PALSAR, ENVISAT ASAR and RADARSAT. Finally, data about common oil spills characteristics: shape, colour, pattern, which are useful to reduce error in detecting oil spills with other information such as: rainfall, fishes oil, low winds and shadow.
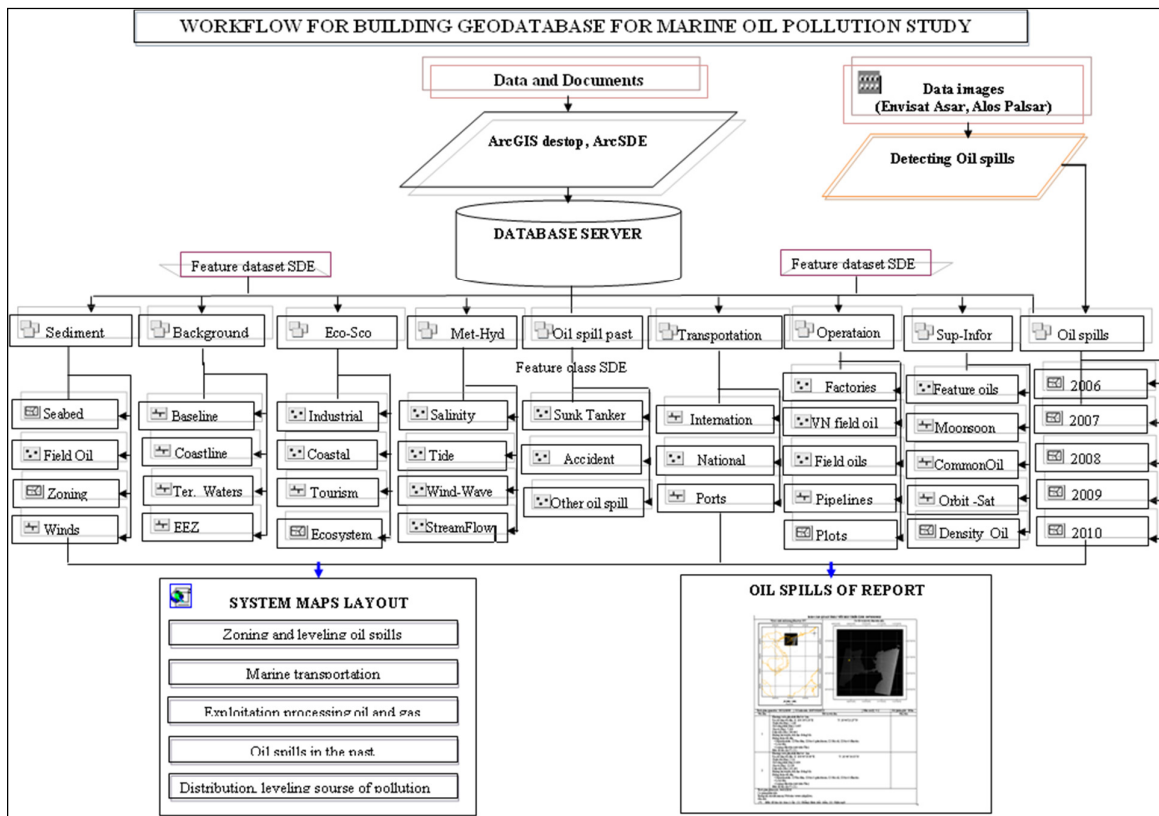


**FIGURE1.**Workflow for the generation of Geodatabase for oil pollution study

Group information that serves calculating and transmitting for forecasting oil spills information including: temperature of marine surface, conditions of meteorological environment, hydrography and properties of common different oil types.

Group information that serves calculating of damage and creating sensitive oil spill maps including: coastal development economic and social activities, ecosystem areas tourism.

Group information that serves zoning level according to difference sources including: data contain potentials that can bring out oil pollution such as: routes of transportation, field oils and exploitation and processing of oil and gas, coastal industrial, damaged tankers sunk in the past.

Background of Group information including: baseline, coastline, and outline 250 miles, national boundary, exclusive economic zone.

When the authors have already built geodatabase and need to take our GIS resources and make it available to others which are the maps, geodatabases and other tools that for others need for storing and using geographic information. ArcGIS Server gives us the advantages to take the GIS resources on our computer and make them available to a wider group of users throughout a network of computers. With ArcGIS server, the way we publish a GIS resources to others is throughout a service. In this study the authors have been using ArcGIS Server Manager belongs to ArcGIS Server dotnet 9.3 software to share GIS resources to users by the following two methods: The first method is that publishing GIS resources throughout tools as a service, users can connect to server computer throughout internet to use geodatabase. This level needs users have to install ArcGIS desktop software and they must to have password and username from manager. In additionally, the users need to have knowledge about GIS and know how to use ArcGIS software. The second method is that publishing GIS resources on the web application. This level does not need users have to know about GIS and how to use ArcGIS software just have some web browsers to open websites. Steps to share GIS resources can be summarized in a workflow as shown in figure 2 as below.
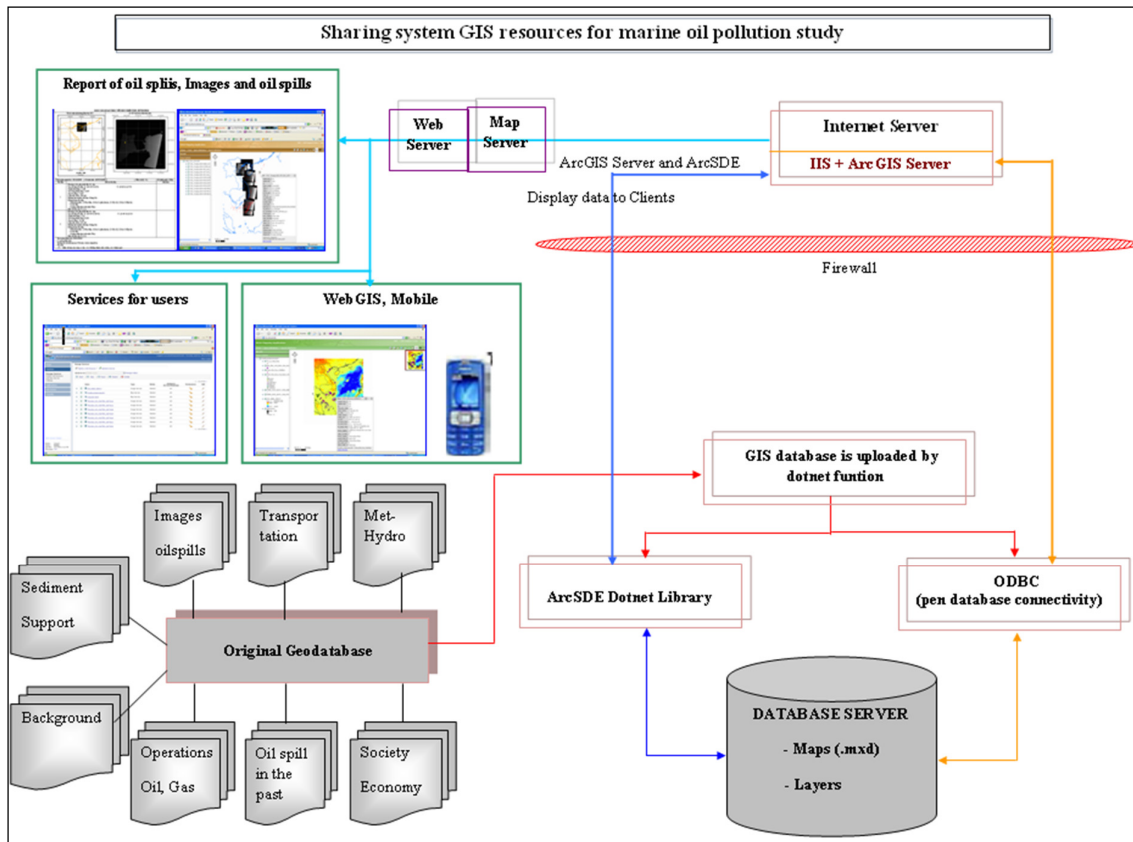


**FIGURE2.** Sharing system GIS resources for studying oil pollution on the sea

## RESULTS AND DISCUSSION

Based on the methodology that was above mentioned and after that an open Personal Geodatabase SDE has been building with named: CSDL_tonghop. There are two types to access to the database system: the first way the users will have username and password to connect to geodatabase by

GIS Server\Add ArcGIS Server tool to connect to the data on server GIS where users can use full data such as download, modify throughout publish services on ArcGIS Server manager. The second way is from other computers throughout web application, data has published on the web with tools such as: Editor, Print, and Query, Search and so on. The users can edit, update new data, download, etc. Especially, new oil spills data detected from satellite imagery will be updated to database through web application and the most important is the system can save or not save the new data which is updated from users through web application on server GIS. The work is very signification for studying about oil spill because from the oil spills will be updated continuously, the system will provide an overall of oil spill picture of this area, then we can build oil spill density map and design the monitoring system for this area. By comparison between this system and other existing systems in the area, it can be clearly seen that there are two strong points of this system e.g.: the first thing, by IWS (Image Web Server) and ArcGIS Server software system which can be share fully two types of data format as vector and raster data which allows to transmit information to the related offices to solve urgent oil spills. The second thing is that it can be control sharing with many levels and the system allows as save or not save on server GIS through editing from users.
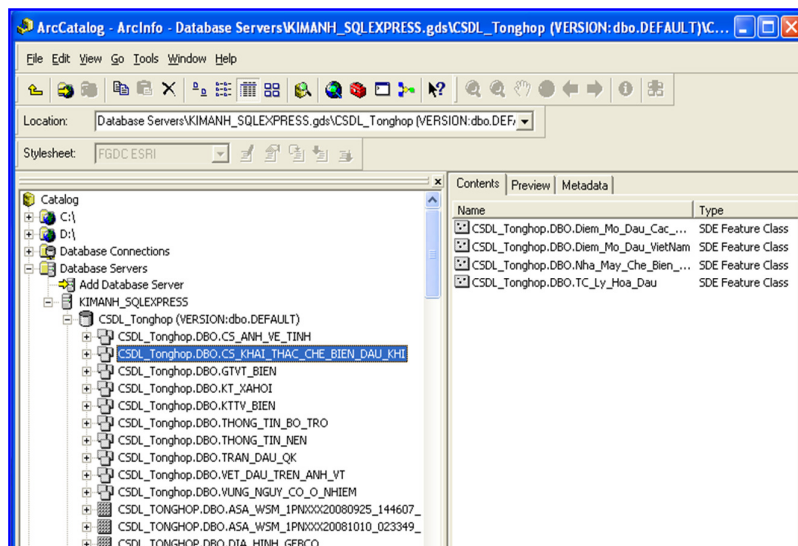


**FIGURE3.** Personal Geodatabase SDE was built for studying oil pollution on the sea
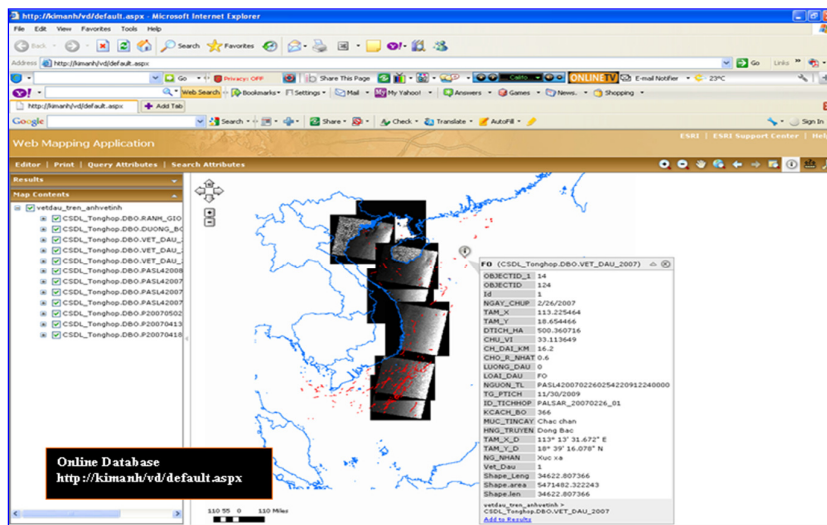


**FIGURE4.** Oil spills and images satellite were published on a web application

A service for sharing GIS database on ArcGIS server manager, system available in *mxd format is uploaded on that as a service. To have right to use data users need to have password and username from manager. Figure 4 below is a web service where oil spills were detected from images satellite and images satellite ALOS PALSAR and ENVISAT ASAR have been uploading. In this web users can download and edit data online with tools that were provided.
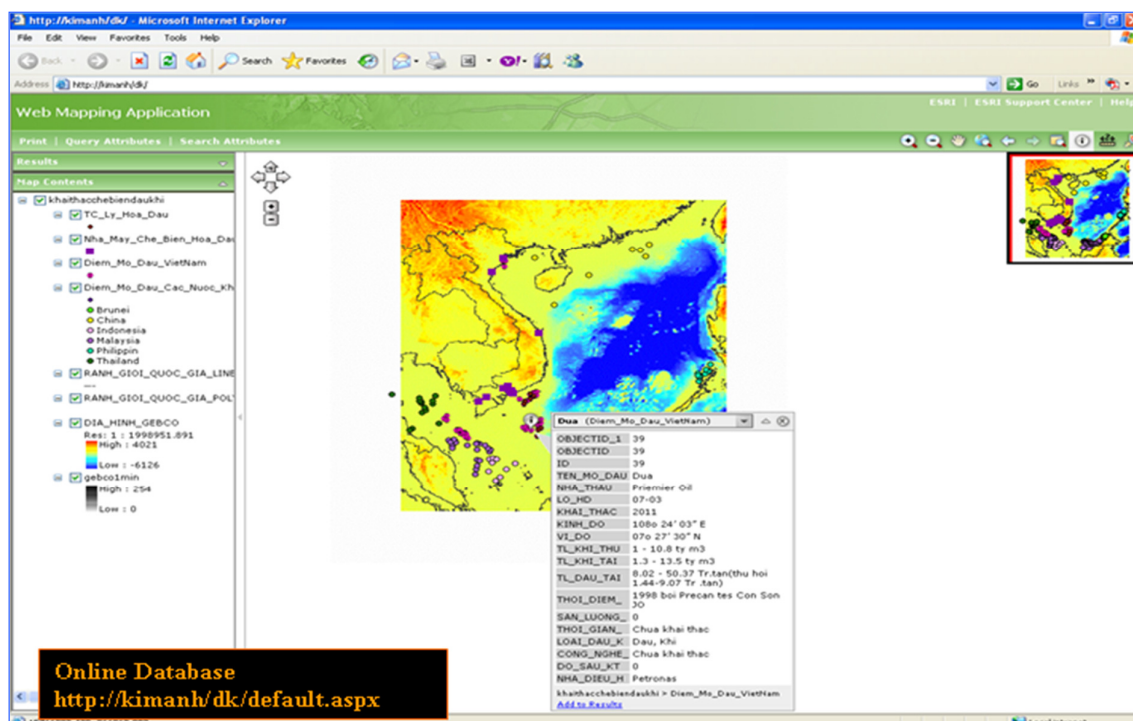


**FIGURE5.** Exploitation and processing of oil and gas and topographic data of Gebco

## CONCLUSIONS

The results of this study provide a methodology to support the study on oil pollution in the sea. In addition to, geodatabase and sharing system were built and have significant meaning in combination between related offices to implement the goals such as raising quality of management, monitoring and detecting oil pollution. With a system, open personal geodatabase that allows users to be able a group or individual use. In the other hand, the sharing of GIS resources system on the web transmitted information about oil pollution to users and provides tools that can be modified the data online.

The strong point of this system is by combination between Image Web Server and ArcGIS Server software to share two types of data format as raster and vector. In additionally, the system allows us to control and sharing in many levels. The system will be improved if the system is updated satellite images in real-time and the way to approaches methodologies to build database which compared with areas where contain conditions same as Vietnam and East sea.

## ACKNOWLEDGEMENTS

**REFERENCES**

JRC-Annalia Bernardini, European Commission, Joint Research, Institute for the protection and Security of the Citizen. 2005. "The way forward: Towards a European Atlas and Database". *Oceanides Final Workshop*.

Ispra. 2005. "Developping an harmonised oil spill reporting".*Oceanides Final Workshop*.

Philippe Careau (JRS). 2004. "User manual & Database description". *Oceanides Final Workshop*.

Nguyen Dinh Duong. 2010. "Oil pollution on Vietnam and East sea", number code KC.09.22/06-10 *Technologies and Marine Sciences for suitable development of society and economics*

Nguyen Huu Nhan. 2004. "Oil Spill Assistant system software and database server for oil spills warning at Khanh Hoa province of Vietnam". Phase 1.

# WHEN ONE GROUNDWATER MONITORING WELL IS ENOUGH

Neil S. Shifrin, and Aaron C. Chow
(Gnarus Advisors LLC, Waltham, MA, USA)

Monitoring groundwater during and after remediation can be costly. A perpetual (*e.g.*, 100-year) semiannual monitoring program consisting of 50 wells might cost about $10 million in constant dollars with a new present value of about $1.5 million at a real discount rate of 7 percent. Monitoring programs often rely on the network of wells left over from delineation sampling and, thus, result in oversampling for remediation effectiveness purposes. Once contaminant plume boundaries have been defined from delineation sampling and groundwater dynamics are understood from several rounds from sampling key wells, one or a few carefully selected wells usually will suffice for remediation purposes and for public health protection. An effective monitoring program must have clear and specific monitoring objectives as well as monitoring shutdown criteria in order to be technically and cost effective. This presentation will present a framework to consider remediation and post-remediation monitoring needs.

# SOCIETY
# AND
# THE ENVIRONMENT

# A SOCIO-DEMOGRAPHIC ANALYSIS OF BIOMASS ENERGY AND WASTE INCINERATOR FACILITY LOCATIONS IN THE UNITED STATES

*Robin Saha* (University of Montana, Missoula, MT, USA)
Michael Ewall (Energy Justice Network, Philadelphia, PA, USA)
Glenn S. Johnson (Clark Atlanta University, Atlanta, GA, USA)
Robert D. Bullard (Texas Southern University, Houston, TX, USA)

This study considers the environmental justice and policy implications related to the use of woody biomass and waste incineration technologies in the United States by providing a socio-demographic analysis of facility locations. Numerous environmental justice studies have examined the socio-demographic composition of neighborhoods and communities hosting a wide range of environmental hazards, including Toxic Release Inventory (TRI) facilities, Superfund sites, and hazardous waste facilities. Much less is known about areas with currently-operating biomass, municipal waste and sewage sludge incinerators, despite continued use of these technologies and calls for their expanded use in a carbon-constrained world. Using precise facility locations, 2010 Census data and Geographic Information Systems (GIS), this study examines current racial/ethnic and socioeconomic disparities associated with facility locations at national and sub-national scales. Renewable energy and climate policy implications of the findings are discussed.

# THE IMPLEMENTATION OF "THREE RED LINES" WATER MANAGEMENT SYSTEM IN BEIJING

***Xinxin Huang***, Xinyi Xu, and Hongrui Wang
(Beijing Normal University, Beijing, China)

In order to promote the strategy of sustainable development of water resources, the most stringent water management system is proposed by the Chinese government. Beijing has established an evaluation system which is called "Three red lines". The exploitation and utilization control of water resources is the first red line, aimed at the total water consumption; the second red line is on water use efficiency for the purpose of restraining water waste; as for the total pollution load control, limiting the contamination into water functional areas is the third red line. 15 indices are selected to compose the evaluation index system and the selection is based on Analytical Hierarchy Process. Through the establishment of the "Three red lines" index system, Beijing will achieve the target in three steps and implement the most stringent comprehensive water management system by 2020.

# PROTECTED AREA AND LIVELIHOODS OF ETHNIC COMMUNITY: EXPERIENCE FROM BANGLADESH

*Kazi Kamrul Islam* and Noriko Sato
(Kyushu University, Fukuoka, Japan)

Protected areas are an appropriate means for managing biodiversity and have become increasingly central to conservation approaches. However, declaring a natural resource to be protected has an immense influence on the livelihoods of forest dependent communities living in and around the protected area since long time. This study explores the role of protected Sal forests, namely Madhupur Sal Forests (MSF) of Bangladesh on the livelihoods of forest-dependent ethnic minorities, drawing empirical data from ethnic households. The results revealed that MSF has brought changes, most of which have had negative impacts on ethnic livelihoods. Now their livelihoods are not stable, as most do not have substantial sources of securing income. In spite of this, the ethnic community has experienced severe antagonistic relationships with park managers and faced social inequity; all these factors affect their livelihoods and forests. The study identified that the main challenge of MSF is establishing institutional alliances based on respect for the rights of different stakeholders including the ethnic community. Once clear rights are established and a basic institutional structure exists with clear rules for consensus-building and conflict resolution, there are several productive options available for improving livelihoods.

---

# REGULATING THE USE OF PLASTIC PACKAGING: A CASE STUDY IN THE PHILIPPINES

Raquel Rosario A. Reyes and Emelita C. Aguinaldo

(National Solid Waste Management Commission Secretariat, Quezon City, Philippines)

The Philippine Ecological Solid Waste Management Act (RA 9003) brought about the formulation of a National Solid Waste Management Framework built along three principles of dimensions of scope, critical actors and partners and means of implementing the concepts of ecological solid waste management with the view of generating greater multi-sectoral interest and partnership in addressing the solid waste management problem. The main actors are Local Government Units (LGUs) which the law empowered to manage a solid waste management system in their own locality. The law requires compliance with Section 21 (Segregation at Source), Section 23 (Segregated Collection), Section 33 (Recovery and Recycling Systems), Section 37 (The Closure of Open and Controlled Dumpsites and the adoption of final disposal systems or alternative technologies). However, even with waste diversion strategies, the volume of residual waste or those waste that remain after segregation, composting, recycling and other methods of resource recovery and waste reduction, may be as high as thirty (30) percent. With the high cost of implementing a solid waste management system, only a few LGUs have adopted technologies to address their residual waste and long-term strategies are still lacking. In Section 29 of RA 9003, the law provides for the prohibition of non-environmentally acceptable products and packaging (NEAP). On the local level, LGUs are also empowered to ensure the protection of the public's health and right to a healthful environment. This paper examines the country's land and water pollution caused by residual waste (primarily plastic packaging) as well as people's behavior particularly in disposing plastic packaging. Results of the study show that although plastic packaging is technically recyclable, functionally, it is not being recycled. Overcoming barriers to its recovery is the key to reduce its disposal and prevent its harmful impacts. This requires establishing unique and innovative recovery mechanisms thru regulatory instruments and education programs that are applicable to local settings.

# STUDY OF THE ROLE OF NON-GOVERNMENTAL ORGANIZATIONS IN NON-GOVERNMENTAL ENVIRONMENTAL EDUCATIONS IN IRAN

*Seyyed Mohammad Shobeiri*

(University of Payam Noor, Lashkarak Road, Tehran, 19569, Iran)

Sustainable development ties together concern for the carrying capacity of natural systems with the social challenges facing humanity. The increasing stress we put on resources and environmental systems such as water, land and air cannot go on forever. Environmental sustainability is the process of making sure current processes of interaction with the environment are pursued with the idea of keeping the environment as pure and perfect as naturally possible based on ideal-seeking behavior. The importance of environmental education, as the foundation for social, institutional, and economic well-being, is becoming globally recognized. Human organizations of environment are one of the most significant components that play a crucial and effective role in this challenge for assistance. Protecting the environment can not be accomplished without participation and responsibility of people, from personal and social aspects. Non-governmental organizations have tried to be effective in informing and developing environmental culture. Education is the most important component of sustainable development and primary bases for improving quality of Life and human welfare. The role of environmental organizations in expansion and organization of global movements which derive their power from philanthropy, have been effective and this power has been proved in season 27 of "Earth parent." In order to affect people one must educate the basics of protecting the environment using a functional method with permanent outcome. This survey is aimed to study the role of non-governmental organizations in development of knowledge and environmental culture through unofficial environmental education. In order to accomplish this survey, necessary information were gathered from books and magazines and also information were acquired from active non-governmental organizations in environmental education filed of Tehran. With the purpose of assessing the effectiveness of these educations, the questionnaires were designed. In the end of study, non- governmental organizations in field of environment were measured unofficially and obstacles and problems were specified and also suggestions and methods were offered.

# EDUCATING STUDENTS ABOUT COMPUTING APPLICATIONS IN ENVIRONMENTAL TECHNOLOGY

Anu A. Gokhale

(Illinois State University, Normal, IL, USA)

Our NSF-funded project aims to increase student awareness of information technology (IT) related applications in a variety of majors. IT is revolutionizing all types of disciplines, including environmental science and technology, especially enhancing ecosystem restoration. The first step in applying computational methods to ecosystem restoration is mapping—creating a database which includes maps and soil characteristics, distribution and restoration potential of threatened species. Mapping is enabled by GPS, ground sensors, and accompanying correlation analysis software that helps determine how two or more variables may relate to specific plant conservation. Geographic Information Systems provide the basis for which field data can be captured, stored, analyzed, and represented in map form, providing visual understanding. Students studying the ecosystem, biodiversity and plant conservation benefit significantly from learning computational modeling methods to enhance understanding of plant soil interactions. The presentation will include examples of mapping software and hardware, and their implementation. It is important to empower our students with computing-related applications within their majors.

# STEP, OR HOW TO INTEGRATE THE SUSTAINABILITY IN TECHNOLOGICAL DEGREES

*Antoni Grau* and Yolanda Bolea,
(Technical University of Catalonia at Barcelona, Spain)

Embedding Sustainability in technological curricula has become a crucial factor for educating engineers with competences in sustainability. The Technical University of Catalonia UPC, in 2007, designed the Sustainable Technology Excellence Program STEP 2015 in order to assure a successful Sustainability Embedding. This Program takes advantage of the opportunity that the redesign of all Bachelor and Master Degrees in Spain by 2010 under the European Higher Education Area framework offered. The STEP program goals are: to design compulsory courses in each degree; to develop the conceptual base and identify reference models in sustainability for all specialties at UPC; to create an internal interdisciplinary network of faculty from all the schools; to initiate new transdisciplinary research activities in technology-sustainability-education; to spread the know/how attained; to achieve international scientific excellence in technology-sustainability-education and to graduate the first engineers/architects of the new EHEA bachelors with sustainability as a generic competence.

The program has been structured in 4 phases. First, the curricula of all Schools have been analyzed within the UPC, and benchmarked with other technological universities in order to develop a feasible and effective program, those external universities are TU Delft (Holland), University of Chalmers (Sweden), Tokyo University (Japan) and ETH Zurich (Switzerland). Second, a pilot implementation of the STEP program in 4 schools has been carried out for a period of one academic year. These Schools participated voluntarily. Third, the program has been spread for implementation to 10 Schools of UPC taking advantage of the lessons learnt in the pilot experience. Fourth, the program is going to be applied to all UPC schools and departments. This paper explains the full process and shows only the results of the third phase, where the collected experience already covers ten technological schools of UPC (over 16 schools). The process has been undertaken by each school independently with its own specific goals, action plans and activities, organized internally and coordinated from the program. This participatory approach has shown to be very successful in terms of faculty involvement and creation of internal and global networks for embedding sustainability. This paper presents the STEP program, its implementation, development and evaluation and highlights the process recommendations to export the program to other Universities.

# THE URANIUM FUEL CYCLE AND RENEWABLE ENERGY ALTERNATIVES FROM A PEDAGOGICAL POINT OF VIEW

*Antoni Grau* and Yolanda Bolea
(Technical University of Catalonia at Barcelona, Spain)

More than ever, nuclear energy is at the centre of political debate and environmental discussions. These try to address the question of how to provide electricity for the world's needs and how to avoid damaging the planet's climate because of it. Within such circles, there is a growing feeling that contributions are needed from all fields of expertise, in fact, from society at large. The objective of this paper is to present an instrument which we believe can help in this respect, by making the existing information clearer and more attractive. The idea is to show the potential hazard of using nuclear energy with qualitative data and example and to promote the use of renewable energies.

When looking into the existing information related to the political and environmental debate around nuclear energy one finds a considerable number of official reports. They are mostly issued by agencies, such as, the IAEA (International Atomic Energy Agency), the World Nuclear Energy and the organisation "WISE" (with wise-uranium as one of its projects), among others. Besides, readers can also find published literature on this matter: books, journals.... However, as is obvious when reading the previous list of sources, it is not easy for the general public to access them: the information is not presented in a reader-friendly way, it is not attractive. An additional fact to be taken into account is that it is only within the agencies mentioned that there is a database large enough so that it allows us to obtain the general picture on this issue at once. In sum, although it is not difficult for anyone interested in nuclear energy to access crucial information on the matter, it is however difficult to both gain a general picture of the mechanisms determining the cycle of nuclear energy worldwide, and follow the details of it all.

Such a situation does not help to involve other parts of society in the debate. A solution to it may be to invest time and energy in analysing the existing information and making it readily available. This is what the authors seek to achieve, in order to fill the gap between very exclusive information and the general public.

The instrument presented uses a slide presentation format in order to integrate the existing information on nuclear energy and arms in a series of interactive maps which describe the cycle of uranium. These maps make it easier for the reader to get an idea of where uranium comes from, where it is mostly used for energy purposes or where it is used for nuclear arms, among other purposes. At the same time, we have tried to make them entertaining to consult by introducing as much visual animation as possible. They also offer the opportunity to analyze the uranium cycle from different knowledge fields: economy, political science and environmental science. They can also be used for other more academic purposes, for example: by simplifying the facts one can design a math exercise for the use of "differential equations".

The ultimate objective of this instrument is actually pedagogic: in order to help raise the students' awareness of sustainability. In fact, this was the initial reason we started working on it. This work, as well as other similar works, will be used as a pedagogical material to cover the compulsory transversal competence of "Sustainability and Social Commitment" at the Technical University of Catalonia, UPC, in different technological degrees. The aim of the project is to generate a number of "power points" on different topics so that they might be used in lectures.

# STUDY OF THE POTENTIAL OF POLITICAL MEASURES ON CITIZEN PARTICIPATION IN WASTE RECYCLING AND REDUCTION

*Yasuhiro MATSUI* and Haruka ITOH
(Okayama University, Okayama, JAPAN)

This study focused on the estimation of the potential of political measures on citizen participation in the household solid waste recycling and reduction in Okayama city. The authors implemented a questionnaire survey for citizens in Okayama city in 2009. One thousand households were selected for the questionnaire survey by the systematic sampling of Basic Resident Register. The authors designed the questionnaire to measure factors relevant to 3Rs behavior: 3Rs behavior, perception of information, behavioral intention, evaluation of trouble, pro-environmental attitudes. In this study, the degree of change in the citizen participation rate, which occurs when the contents of political measures such as the raising of environmental attitude, provision of information, strengthening of external pressure, and the conditions of collection services were changed, was estimated together with the effect on the waste recycling/reduction amounts. The authors developed predictive models on recycling behaviors for 8 recyclable categories and 7 waste reduction behaviors including home composting by logistic regression analyses, and sensitivity analyses of the models were carried out to estimate the increase in citizen participation rate achievable through the implementation of various political measures. The authors also implemented a waste measurement survey for 2 weeks at the same time of the questionnaire survey. Assuming that the population density was the representative indicator of the urbanization level, five levels by the percentile rank of the population density were defined; 10th, 30th, 50th, 70th, and 90th percentiles, and 20 households for each level, a total of 100 households, were selected. The generation amounts per capita of waste/recyclables in 30 categories were estimated. By multiplying the estimated increase of participation rates on recycling/reduction behaviors by the corresponding waste/recyclable amounts, the authors estimated the expected waste recycling/reduction amounts by implementing the political measures such as the raising of environmental attitude, provision of information, strengthening of external pressure, and the conditions of collection services.

# ENVIRONMENTAL PLANNING
# AND
# MANAGEMENT

# VULNERABILITY TO STORM SURGE OF THE HOUSTON SHIP CHANNEL IN TEXAS

### *Daniel W. Burleson*, Hanadi S. Rifai
(University of Houston, Houston, TX, USA)

**ABSTRACT:** The Houston Ship Channel (HSC) is one of the nation's largest and most active ports with many facilities that are vital to the economy and surrounding environment. This region has had a long history of severe storms and hurricanes. Understanding the vulnerability of the region to storm surge is vital to instituting appropriate mitigation measures, protection strategies, and re-entry protocols. While vulnerability analysis to date has focused on the location and elevation of the facilities in a "static" manner, this study includes an investigation of the "dynamic" vulnerability of HSC facilities to storm surge before, during, and after the landfall of a severe storm or hurricane. This study examined the spatial (static) vulnerability of the region and the environmental vulnerability where "dynamic" vulnerability was included in the analysis. The analysis performed utilizes results from ADCIRC modeling, Geographical Information Systems (GIS) in conjunction with information from Risk Management Plans (RMPs) and EPA's Toxic Release Inventory. The results from the study identified highly vulnerable regions along the HSC and created a framework for assessing the spatial and environmental vulnerability of the region.

## INTRODUCTION

The Houston Ship Channel (HSC) is a 530 feet wide by 45 feet deep by 50 miles long man made canal that originated in the early 1900s due to its proximity to the Texas oilfields. Since that time, the HSC has grown into one of the largest and most productive ports in the United States with many chemical and petrochemical facilities along the water way. The HSC contributes $7.7 billion to the economy of the Houston-Galveston area and according to the Hazard Exposure Information presented by the NOAA Coastal Services Center, 16% of critical facilities and 15% of road miles (3230 miles) are within the 100-year floodplain in Harris County. The study area identified in Figure 1 includes a highly industrialized segment of the Houston Ship Channel with many facilities that have significant economic impact locally, regionally, and nationally.

The Houston-Galveston region has had a long history of severe storms and hurricanes that have affected its evolution and development. Since 1854, for example, 61 tropical storms have hit the upper Texas coast. The 1915 Galveston Hurricane delayed the opening of the HSC by weeks causing millions in losses. Most recently in 2008, Hurricane Ike hit the region causing damage ranking it as the $3^{rd}$ most destructive hurricane at $27 billion in losses in four states. The Coast Guard estimates that $250 to $300 billion is lost each day the HSC is closed due to hurricane related precautions. Hence, identifying and managing vulnerabilities in this study area is a critical need that must be addressed to ensure the continued economic development of the region.

In order to accomplish the aforementioned goal, the vulnerability of the HSC must be understood. While efforts after Tropical Storm Allison, hurricanes Katrina, Rita and Ike, have gone a long way towards addressing the regional vulnerabilities along the Texas Gulf Coast, less focus has been placed on critical and specialized use areas such as the HSC. This paper aims to address this gap by developing a conceptual framework of vulnerability of the HSC given its specialized function, location, economic value, and potential to pollute Galveston Bay due to spills, leaks, and unintentional releases during severe storms and hurricanes.

Vulnerability is defined as a "flaw and weaknesses in the design, implementation, operation, and/or management of an infrastructure system (Zio and Kroger, 2009). Metzger et al. in 2008 described vulnerability as the "degree to which a system is susceptible to cope with adverse effects." Bowle in 2001 acknowledged the dual structure of vulnerability: (1) external vulnerability referring to the exposure to risk (2) and internal vulnerability referring to its capacity to anticipate or cope. These definitions provided a springboard for preparing the framework for vulnerability in the HSC.

Hurricanes bring strong winds and rain; however, storm surge has been found to be the most costly aspect of a storm due to the high levels of inundation and strong currents (Santella, Steinberg et al. 2010). Several studies have addressed the vulnerabilities associated with wind damage; however, the examination of the storm surge vulnerability has been limited. Vulnerability assessments, as mentioned previously, in the literature have focused mostly on large-scale or community level assessments. Initial studies relied mostly on a low, medium, or high rating of qualitative and quantitative aspects for a community. More recently, however, geographical vulnerability has become a starting point for most vulnerability assessments. One study used Geographical Information System (GIS) to assess the vulnerability of critical facilities in the Territory of American Samoa (Willmott, Robeson et al. 2011). Facilities were identified as vulnerable based on their location within the designated FEMA 100-year floodplain. More recent studies have created maps that represent storm surge inundation zones in frequent occurrence such as a 50-year return period, a likely scenario for global warming, and an extreme scenario for global warming (Rao, Chittibabu et al. 2007). However, previous assessments have failed to address the relationship between the two zones (100-yr floodplain and storm surge) and identify regions affected by storm surge that do not fall in the 100-yr floodplain and vice versa. This relationship is important in order to differentiate between vulnerabilities for areas that do not lie within a regulated floodplain and additional vulnerabilities that are not addressed for areas within a regulated floodplain. This research integrates this concept into the vulnerability framework that is developed for the HSC.

**METHODS**

Using the definitions of vulnerability described in the previous section, a framework for assessing vulnerability in the HSC was developed. Vulnerability, for this study, was categorized into: (1) static vulnerability and (2) dynamic vulnerability. Static vulnerability is defined as vulnerability due to inherent characteristics of a facility that cannot be changed in the case of a severe storm or hurricane. Dynamic vulnerability is defined as vulnerability due to actions that occur before, during, and after landfall of a severe storm or hurricane. The static vulnerability was considered when evaluating the spatial vulnerability (inundation with flood waters or storm surge) while both aspects of vulnerability were considered in evaluating the environmental vulnerability of the HSC region.
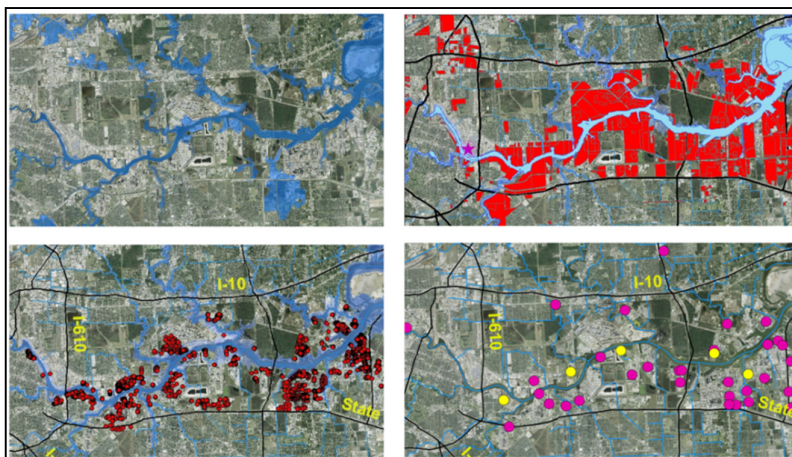


FIGURE 1. The Houston Ship Channel, located on the southeast corner of Texas in Harris County along the Gulf Coast. Starting with the top left corner and moving clockwise: 100-yr floodplain, industrial facilities, Risk Management Plan (RMP) facilities, and AST locations

In order to develop the vulnerability framework, a comprehensive geodatabase in ArcGIS was compiled using a variety a sources including the EPA and Texas Commission on Environmental Quality (TCEQ). The data collected was used to evaluate the spatial vulnerability by investigating the area of inundation outside the FEMA 100-yr floodplain and the environmental vulnerability using toxic release data, aboveground storage tank (AST) locations, and Risk Management Plans (RMP) for various facilities in the database. Figure 1 shows the four categories for analysis in relation to the HSC.

For spatial vulnerability, storm surge events ranging from 10-ft to 25-ft were created via the ADCIRC hurricane model (Dawson et al. 2011) using an Ike-like hurricane with various landfall locations along the Texas Gulf coast. The resulting inundated areas due to storm surge were mapped and compared with the existing floodplain using spatial analysis within ArcGIS. The total area (acres) of inundated land outside the 100-year floodplain was calculated for each given storm and compared to determine trend.

For environmental vulnerability, toxic release data was collected using the EPA's Toxic Release Inventory (TRI) database. Facilities were identified from their history of past releases and these facilities were evaluated for their potential inundation under the various surge scenarios described above. AST data was gathered using visual inspection of detailed aerial photography then evaluated based on their potential inundation for the various storm surge scenarios generated in the study. RMP were used to evaluate the dynamic aspect of a facility's environmental vulnerability to storm surge. A vulnerability score was determined based on quantity and proximity of chemical storage and processing to a waterway. These characteristics were compared to other facilities along the HSC and ranked from lowest to highest quantities and closest to farthest away from water. A higher vulnerability score represents a facility that is potentially more vulnerable to a storm surge event. A prevention score was determined based on the plans in place for the facility given scenarios related to severe storm surge events (hurricanes, flooding, etc.). The existence of these plans was quantified and compared to other facilities along the HSC. A higher prevention score indicates a facility with a better capacity to cope with a storm surge event.

## RESULTS AND DISCUSSION

Figure 2 shows the results of evaluating the area affected by given storm surge events outside the FEMA 100-yr floodplain.
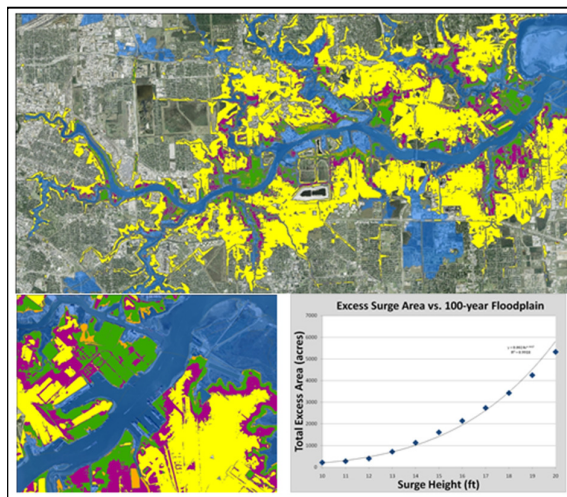


FIGURE 2. Surge inundated areas outside the 100-yr floodplain as a function of surge height.

As can be seen from the accompanying chart in Figure 2, the area affected by storm surge outside the 100-yr floodplain increases exponentially with an increase in storm surge height. This relationship is expressed mathematically by Equation 1.

$$Area\ Inundated\ Outside\ Floodplain\ (acres) = 0.0024e^{4.9(Surge\ Height\ (ft))} \quad R^2 = 0.992 \quad (1)$$

Figure 3 shows the TRI analysis results for a 13-ft, 18-ft, and 25-ft storm surge; a majority of TRI facilities would be inundated between 0 – 20% at 13-ft surge but with a 25-ft surge, inundation increases to between 60% - 100%. It should be noted that a 13-ft surge was the closest scenario to a 100-yr floodplain and to what occurred in the region during Ike. It is further noted that even with as little as 1 or 2 ft storm surge above the 100-yr floodplain, inundation becomes much more widespread and approaching catastrophic levels from a facility shut-down and recovery perspective. While the likelihood

that surge heights above 13 ft was not addressed in this research, it is not an inconceivable scenario given the history of severe storms and hurricanes in the region.
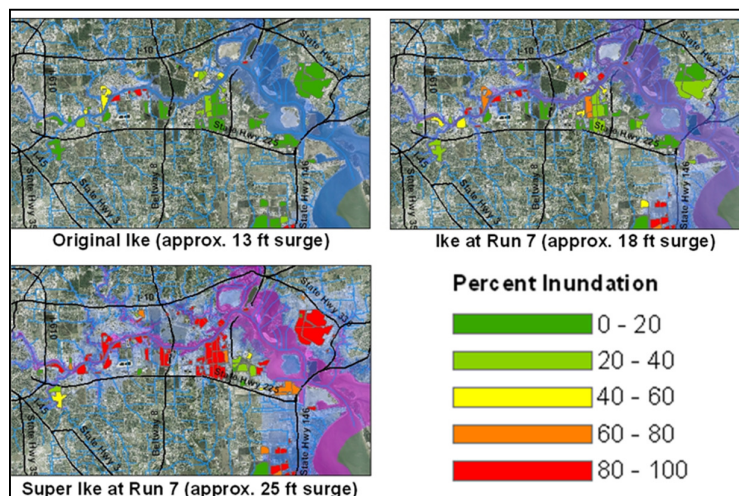


FIGURE 3. Percent of TRI facility inundation results by storm surge height:

A relationship was found based on the inundation within TRI facilities and storm surge height. This relationship is represented in Equation 2 and shown in Figure 4.

$$TRI\ Facility\ Inundation\ (acre) = 378.44e^{0.153(Surge\ Heigh(ft))} \qquad R^2 = 0.996 \qquad\qquad (2)$$
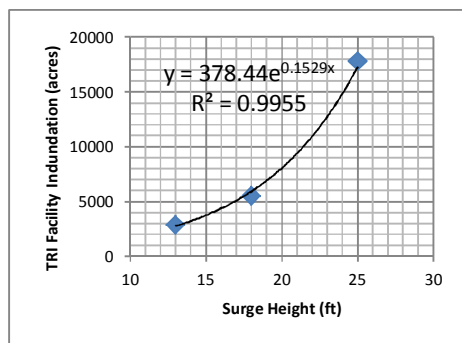


FIGURE 4. TRI facility inundation area in acres as a function of surge height in feet.

Equation 3 shows the relationship determined between the number of ASTs inundated given a storm surge event.

$$Number\ of\ Tanks\ Inundated = 116.65e^{0.136(Surge\ Heigh(ft))} \qquad R^2 = 0.983 \qquad\qquad (3)$$

Based on the analysis, when the storm surge increases from 13-Ft to 18-Ft, the number of tanks affected double (see Figure 5). The surge height will have a direct impact on tank containment failure and will increase the potential for environmental releases and displacement of large objects into waterways thus affecting safety and navigability of the waterway.

Table 1 shows the results of the Risk Management Plan analysis for five example facilities along the HSC. These facilities represent a variety of manufacturing, storage, and treatment facilities. The results indicate that the most vulnerable facilities typically have a higher prevention score in order to protect against more chemicals and proximity to open waterways. As can be seen in Table 1, Facility #5 is the most vulnerable but has the second highest prevention score and therefore is considered better at

coping with a storm event.  While Facility #3 has a median vulnerability score it is the weakest at coping with a storm event shown in the low prevention score.
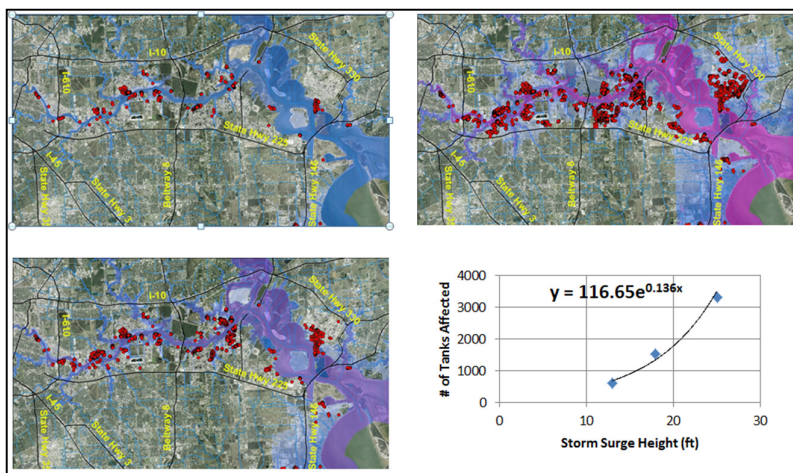


FIGURE 5. AST inundation results with the number of tanks affected as a function of storm surge height in feet.

TABLE 1. Facility assessment using Risk Management Plans (RMP) table titles go on top.

| Analysis | Facility #1 | Facility #2 | Facility #3 | Facility #4 | Facility #5 |
|---|---|---|---|---|---|
| Vulnerability Score | 1.94 | 1.6 | 1.91 | 1.6 | 2.4 |
| Prevention Score | 16 | 39 | 7 | 35 | 32 |

**CONCLUSIONS**

This study demonstrates a conceptual framework for understanding the vulnerability to storm surge of an industrial facility such as the Houston Ship Channel in Texas.  The framework uses modeled surge height to develop inundation potential and environmental vulnerabilities. The relationships found for area, facility, and tank inundation provide insight on the potential effect on the region given a surge event.  These relationships could also be used to assess the potential economical vulnerability of the region.  By valuating land, facility, and tank information and quantifying the amount of potential damage, a comprehensive economic vulnerability model can be implemented that incorporates facility and channel downtime and environmental cleanup.  The quantitative assessment of the facility RMP indicates an understanding by facilities to compensate for their characteristic vulnerabilities with prevention plans (coping capacity).  This can also be used to identify facilities that may have a high vulnerability but a low prevention score.

**ACKNOWLEDGEMENTS**

**REFERENCES**

Bohle, H. G. (2001). "Vulnerability and Criticality: Perspectives from Social Geography." Newsletter of the International Human Dimesions Programme on Global Environmental Change **1**(7).

Dawson, C., E. Kubatka, J. Westerink, C. Trahan, C. Mirabito, C. Michoski, N. Panda (2011). "Discontinuous Galerkin methods for modeling Hurricane storm surge." Advances in Water Resources 34(9): 1165-1176.

Metzger, M., D. Schröter, et al. (2008). "A spatially explicit and quantitative vulnerability assessment of ecosystem service change in Europe." Regional Environmental Change **8**(3): 91-107.

Rao, A., P. Chittibabu, et al. (2007). "Vulnerability from storm surges and cyclone wind fields on the coast of Andhra Pradesh, India." Natural Hazards **41**(3): 515-529.

Santella, N., L. J. Steinberg, et al. (2010). "Petroleum and Hazardous Material Releases from Industrial Facilities Associated with Hurricane Katrina." Risk Analysis **30**(4): 635-649.

Zio, E. and W. Kroger (2009). "Vulnerability Assessment of Critical Infrastructures." IEEE Reliability Society Annual Technoloby Report.

# GREEN BUILDING- FOR SUSTAINABLE DEVELOPMENT

## *C.V.R. Vaishnavi*
(G. Pulla Reddy Engineering College, Kurnool, A.P., India)

**ABSTRACT:** Shelter is one of the most important things which is essential for human beings. As the civilization developed construction evolved from caves to huge multi-storeyed buildings. In this realm of social and economic development environmental change has become inevitable and it compelled for new effective means of achieving new levels of efficiency and sustainability. This paper presents one of the most important Sustainable construction, Green Building, from its site to design, construction, operation, maintenance and also its economic aspects. To give more protected environment to the future generation, adopting methods of protective technologies is very important and here green building is one of the such technology which is very economical and useful.

**Key Words:** Green Building, Sustainable Development, Designing, Construction, Economical

## INTRODUCTION

Shelter is one of the fundamental needs of human beings. The need to own a place for living is also seen in animals and birds. In the beginning of human civilization man used to live in caves and on trees, gradually he has identified materials suitable for construction like clay, stone and timber. Basic purpose of these dwellings is to protect man from weather and predators. These houses made way for larger inhabitations like castles, forts and palaces which had built in mechanism for providing sunlight and fresh air. As the time went on, man with his knowledge invented latest technologies and materials which helped him in construction of different types of buildings. These buildings and the materials used for construction brought rapid changes in the environment. Limitation of space, growth of population and rapid urbanization lead to community dwelling culture which increased problems like CFC emissions, insufficient ventilation, increase of waste materials during construction and maintenance of house arouse.



Figure 1. Shelter of human beings in the early history

It is found that the building industry will consume 40% of total global energy and release about 3800megatons of $CO_2$ into atmosphere. They have harmful impact on the nature. According to a report the building industry has following impacts:

- Consumption of 40% of world's total energy.
- Consumption of 30% of raw materials.
- About 25% of timber harvest is going down.
- 35% of $CO_2$ emission.
- 16% of fresh water is being depleted.
- 40% of municipal solid waste is being generated.
- 50% of ozone depleting CFC's are still in use.

- 30% of the residents have sick building syndrome.

The above issues have forced man to think along the terms of sustainable development which gave solution for his problem through "green building" concept. Most of the people think that it is latest technology which has been invented in recent times. But a very few people know that this concept is being used since time immemorial. The Hawa Mahal in Jaipur Rajasthan in India is constructed in such a way that it has natural ventilation which is also one of the principles of green construction. Similarly many buildings were constructed using different principles of green construction unknowingly the concept.



Figure 2. Building of human beings in the morden history

The concept of sustainable development can be traced to the energy crisis and environmental pollution concern in the 1970s (1). In the US Green Building movement started from the need and desire for the more energy efficient and environment friendly construction practices. There are number of benefits from building green like environmental, economical and social. Environmental benefits protect biodiversity, ecosystems and also improve air and water quality, reduce wastes, conserve and restore natural resources. Economic benefits are reduction of costs and improvement in occupant productivity and optimize life-cycle economic performance. Social benefits enhance comfort and health of occupants by giving aesthetic quality.

A Green Building is the one whose construction and life time operation provides healthiest possible environment having the most efficient and least disruptive use of the land, water, energy and resources. Green Building is the one that preserves and restores the habitat which is vital for sustaining life by reducing negative environmental impact. Construction of Green Building minimizes on-site grading, saves natural resources by using alternative building material and recycles construction waste rather than dumping in landfill. Green Building's interior spaces have natural lighting, outdoor views while highly efficient heating, ventilating and air conditioning (HVAC) systems and low volatile organic compounds like paints, flooring and furniture create a superior indoor air quality. Most of the Green Buildings are designed

according to LEED (Leadership in Energy and Environmental Design). Green Buildings are more comfortable and easier to live with due to Row operating and owning costs. It is estimated by the year 2050, residential, commercial and institutional buildings consume about 38-40%global energy and release3800-4000 mega tones of carbon in to the atmosphere. Climate change by itself can also precipitate lager energy demand as people seek greater comfort levels in more extreme conditions (2, 3).

A report by US General Services Administration found that sustainably designed buildings cost less and have excellent energy performance and occupants are more satisfied than those living in normal commercial buildings. The market for green building materials and products is estimated to reach Rs.15000crores in India by 2012 (4). Though new technologies are constantly being developed to complement current practices in creating greener structures, the common objective is that Green buildings are designed to reduce overall impact of the built environment on human health and the natural environment(5). To build Green it is very important to select proper site, maintain energy efficiency, water conservation, storage of rain and storm water, material and resource management and construction waste management.

**NEED FOR GREEN BUILDINGS**

❖ The environmental impact of building design and construction industry is significant. Buildings consume more than 20% of electricity used in India.
❖ Normal construction deprives land usage from natural biologically diverse habitats.
❖ Green Building practices can substantially reduce or eliminate negative environmental impacts and improve existing unsustainable design, construction and operational practices.
❖ As an advantage greendesign measures help in reducing running costs and mitigate indoor air quality problems.
❖ Studies conducted on green buildings reported productivity gains up to 16%.
❖ As a matter of fact green building enhances environmental and economic benefit for occupants.

**PLANNING AND CONSTRUCTION OF GREEN BUIDING**

**Site efficiency**. It is very important for careful planning before a Green Building project is started. Though building greenhouse does need to be expensive or time consuming, final choice of type of green building will depend on the space desired, home architecture, available site and costs. Green building should be located in such a place where there is maximum sunlight. The first choice of location is either south or south eastern side. Sunlight all the day is best for proper lighting of the house and growing trees like maple, oak, neem and tamarind can efficiently shade the Green building from intense late summer afternoon. Good drainage system is another important requirement for the site. The Green building should be built above the ground level so that rain water and irrigation water will drain in to the soil. Evolve strategies to stockpile top soil for landscaping purpose. Consider adopting measures such as temporary and permanent seeding, mulching, dykes, silt fencing, sediment traps and sediment basins where ever required. Open areas can be landscaped and paved areas can be developed with permeable paving. For impermeable surfaces like concrete surfaces, direct entire runoff towards storm water collection pits.

It is necessary to select a site which is nearer to all basic amenities like grocery store, pharmacy, post office, police station, hospital, railway station, bus station. Site should have provision for parking and open space for growing plants.

**Heat Island effect:** Precautions are to be taken to reduce heat island effect i.e., thermal gradient differences formed between heat developed and undeveloped areas to minimize impact on micro climate.

Typical materials with high reflective properties like china mosaic, white cement tiles and paints should be used for reducing heat island effect.



Figure 3. Heat island effect in buildings

**WATER EFFICIENCY**

Reduction of water consumption and protection of water quality is other important factor for Green building. The conservation and protection of water throughout the life of a Green building can be accomplished by designing for dual plumbing that recycles water in toilet flushing. Waste -water may be minimized by using water conserving fixtures like ultra low flush toilets and low flow shower heads. Bidets may be used to reduce the usage of toilet papers, reduce load on sewers and increasing possibilities of reusing water on-site. Water treatment is a must for maintaining water quality. Usage of grey water for growing plants will also helpful for water conservation. There should be provision for rain water harvesting systems. Water efficient fixtures are to be used to minimize indoor water usage.

**Rain Water Harvesting System.** Reuse of harvested rain water in plumbing systems in commercial or residential setting proves to be environmentally and economically effective. It can reduce usage of drinking water for other purposes. In this system runoff water can be harvested from roofs via down pipes that are connected to water reservoirs and underground tanks. It will be easy to install this system for new dwellings with down pipes at one end and a cellar with a place for a low cost tank at other end. The harvested water can be used for washing clothes and toilet flushing.

The factors to be considered while designing rain water harvesting system are:

- ✓ Rainwater availability.
- ✓ Size based on average availability and consumption.
- ✓ Materials of cistern.
- ✓ Suitable location .

Basic Components include:

o Catchment Area
o Gutters and downspouts
o Leaf screens and roof washers
o Cisterns
o Conveying systems
o Treatment of water.

For the Operation and Maintenance of Harvesting System:

- Cleaning must be done at beginning of summer and winter rainfall to remove any foreign material.
- Filtering and distribution system should be maintained.
- Filtration is essential to prevent entry of contaminants.
- Preferred height of distribution line should be 30.48cm above bottom of tank or reservoir
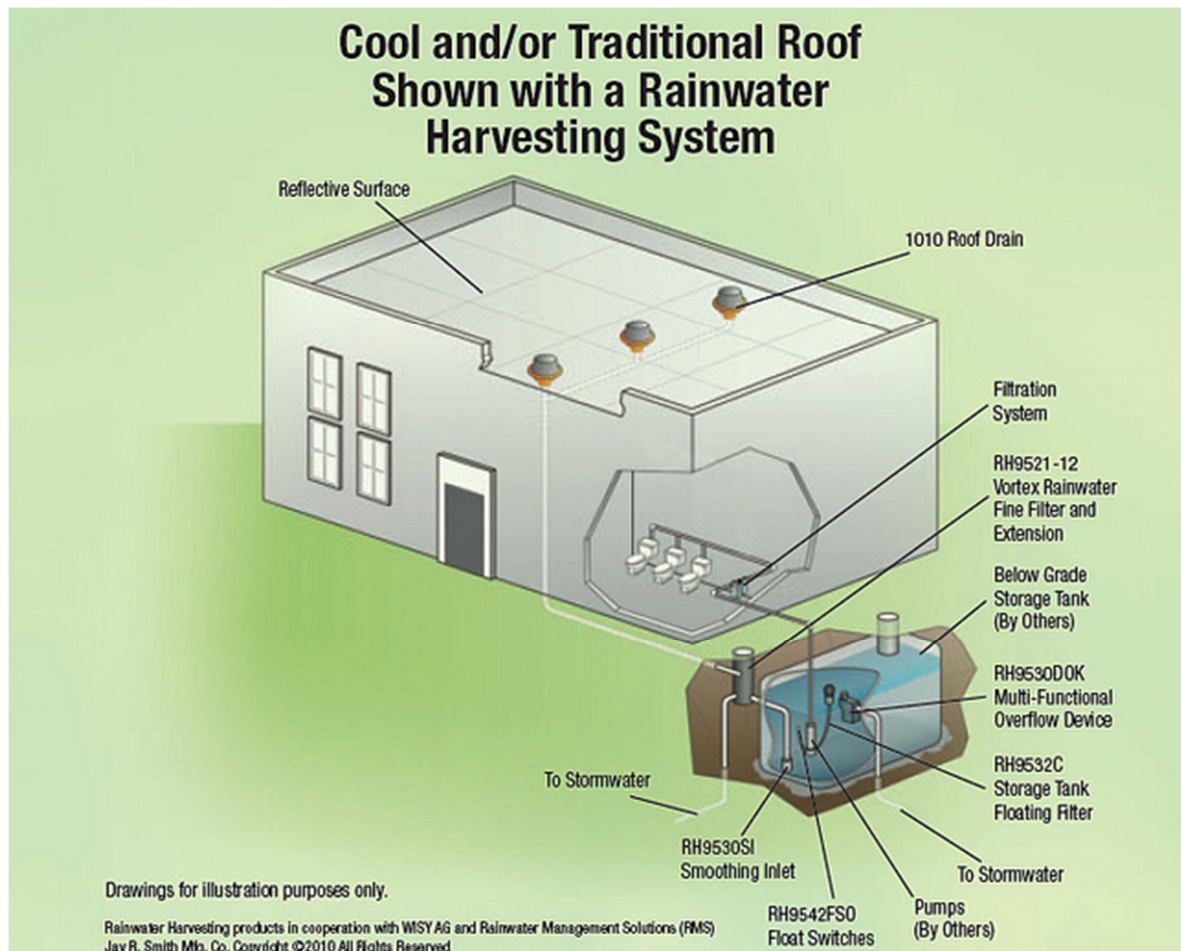


Figure 4. Cool and traditional roof shown with a rainwater harvesting system

**Water Efficient fixtures**. These are used to reduce indoor water usage. The water fixtures which are being used should be efficient. Fixtures are available with ultra high efficiency which can reduce substantial quantity of water consumption.

| SNo | Items | Base line | Units |
|---|---|---|---|
| 1 | Flushing | 6.3 | LPF |
| 2 | Faucets | 7.6 | LPM |
| 3 | Shower | 7.6 | LPM |

Landscape should be designed to ensure minimum consumption of water. It is applicable only for those projects which have at least 15% of area landscaped. Drought resistant species require less water for their supplemental growth hence these should be used considering xeriscaping as an for landscaping

**Grey water Use.** At least 50% of grey water generated can be used for landscaping,flushing and make-up water for air-conditioning. Treated grey water for reuse must conform to the quality standards as high lighted in the table below

| Parameter | Quality Standards for treated water |
|---|---|
| BOD 5 days @$20^0$C | 100mg/l |
| Suspended solids | 200mg/l |
| Oil and grease(after grease trap for canteen/kitchen) | 10mg/l |
| pH | 5.5-9.0 |

## ENERGY EFFICIENCY

Green buildings are also useful to reduce energy consumption. Higher performance buildings use less operating energy. Studies such as U.S. LCI Database Project(6) show buildings built primarily with wood will have a lower energy than those built with brick, concrete or steel(7). Usage of high efficiency windows and insulation in walls, ceiling and floors increase the efficiency of the energy envelope. Passive solar building design can also be used in low energy homes. Designers orient windows and walls, porches and trees to shade windows and roofs during the summer while maximizing solar gain in the winter(8). Apart from this proper window placement can provide more natural light and lessen the need for electric lighting during the day. Providing proper metering also saves energy. Solar water heating also reduces energy costs. Onsite generation of renewable energy through solar, wind, hydro or biomass energies can significantly reduce the environmental impact on the building.

Energy saving measures in various equipments:

To conserve energy we can use following equipment

1) Level controllers in overhead water tanks.
2) Energy efficient lifts.
3) Minimise 60% efficiency in water pumps
4) Minimise 75% efficiency in motors.

## MATERIALS EFFICIENCY

Building material is another criterion that should be selected carefully for Green building. Materials like bamboo, straw, dimension stone, recycled stone, recycled metal and other products that are nontoxic, reusable, renewable or recyclable can be used(9). Environmental Protection Agency EPA recommends using recycled industrial goods like coal combustion products, foundry sand and demolition debris of construction projects(10). Building materials are to be extracted and manufactured locally nearer to the building site to reduce the energy required for their transportation. Usage of green refrigerants (clorofluoro carbon free)is recommended.

Use of recycled and renewable material can reduce total cost by at least 5-10%. Some of materials with recycled content are fly ash block, tiles, steel, glass, cement, false ceiling, aluminium and composite wood.

## IN DOOR AIR QUALITY

Indoor Environmental Quality (IEQ) category in LEED standards (Leadership in Energy and Environmental Design) is the one which provides comfort, wellbeing and productivity of occupants of the Green buildings. The LEED IEQ addresses for the thermal quality, lighting quality and indoor air quality (11). Indoor air quality reduces volatile organic compounds and

other air impurities like microbial contaminants. Properly designed ventilation is required for proper recirculation of clean air. Another important thing is the control of moisture accumulation leading to mould growth and presence of bacteria viruses by proper insulation. Exhaust systems are to be provided in kitchens and bathroom for clean air. Green architecture reduces waste of energy, water and materials used during construction. Recycling is the other important process by which there can be reduction of wastage.

**Cross Ventilation**. Cross ventilation is another criterion which should be given lot of importance. While designing the building certain distance norms are to be followed:

* a minimum of 3m distance should be maintained between walls of two dwelling units

* a minimum of 2.4m corridor width separating dwelling units(12)

**Wind Towers.** These are traditional architectural elements mainly part of buildings. They were used since ancient time but after the advent of air conditioners and other mechanical ventilators the use of wind towers reduced. However in green buildings use of wind towers is very essential since they substantiate the use of artificial ventilation systems to a very great extent. The main function of this tower is to collect cool breeze that prevails at higher level above ground and direct it to the interior of the building. Now -a -days this feature has again gained a great prominence in many countries due to its advantages.

### ECONOMIC ASPECTS OF GREEN BUILDINGS

Generally the ecological properties of a building are considered as additional costs. In this view construction of green building is inevitably more expensive as it implies use of high quality materials, high efficiency materials and a more complex work flow. It also involves high cost of construction due to provision various additional facilities. All these increase the cost of green construction to a great extent. According to a report it was known that price premium of energy star buildings and LEED certified buildings is higher than that of a normal building. And report also showed that rents of ecological buildings are higher than rent of other buildings by about 3.5% (13). From the above studies we can say that economically green buildings may be more expensive than ordinary buildings but due to advantages like energy efficiency, good ventilation, reduction in maintenance cost over its life period and healthy atmosphere to the occupants people now a days are finding them more attractive and occupancy rate increased by about 6%. Since building owners are succeeding in assessing the benefits of green buildings more effectively and increasing number of projects will follow the path in near future.

Man can live on the Earth with minimal pollution by changing over to Green buildings. They are Economical cost wise and Environmentally sustainable design wise. A Green renovation includes everything from a green roof to more efficient HVAC and lighting systems, enlarged existing windows and low VOC paints and flooring. Hence future is GREEN.

### REFERENCES

1. Mao, X., Lu, H., & Li, Q., (2009) International Conference on Management and Service Science .

2. Environmental Building News (2002). www.buildinggreen.com.

3. Cole, R.J., Building Environmental Assessment Methods: Clarifying Intentions, Building Research and Information, Vol. 27 (4/5), pp.230-246, (1999)

4. Portland Energy Office, Portland Oregon(2000) Green Building Applying the LEED Rating System.

5. Sanjeeva Rayudu, E., & Murali, S.M., Building for Healthy Community,(2011) Proceedings of Green Technologies and Environmental Conservation (GTEC) Chennai 15-17 December 2011

6.    U.S. Life Cycle Inventory Database. http://www.nrel.gov/lci.

7.    Naturally Wood Building Green with Wood Module. 3&6 Energy Conservation & Health & Wellbeing.

8.    Simpson, J.R., Energy and Buildings, Improved Estimates of Tree-shade Effects on Residential Energy Use, Science Direct, February (2002)

9.    Time: Cementing the Future, http://www.time.com/time/magazine/article.

10.    http://www.epa.gov/greenbuildings/pubs/components.

11.    Lee, Y.S., & Guerin, D.A., Indoor Environmental Quality Differences between Office Types in LEED Certified Buildings in the U S, Building and Environment. (2009)

12.    Praveena,K., Planning, Analysis and Design of Green Building, Project Report Submitted to  S.K.University for the award of B.Tech.,in Civil Engineering.2009.

13.    Commercial and Institutional Green Building: Green Trends Driving Market Change, McGraw-Hill Construction and USGBC 2008.

# NIGERIA URBAN AND REGIONAL PLANNING LAW AND PROBLEMS OF URBAN GOVERNANCE IN LAFA TOWN, NASARAWA STATE, NIGERIA

Barau Daniel and Bashayi Obadiah

(Nasarawa State Polytechnic, Lafia, Nasarawa State, Nigeria, Email: baraudaneil@yahoo.com)

**ABSTRACT:** For the management of urban centres various legislations were developed successively. In Nigeria the most recent is the urban and regional planning law of 1992. The paper reviews previous legislations that relate to urban and regional planning up to the present planning law in Nigeria. By means of questionnaires, the paper used unstructured questions to obtain information from Lafia Local Government Council. The study reveals that rapid urban growth and lack of the establishment of local planning Authorities as required by the provision of the law create conflicts in urban governance. The study makes recommendations for improvement.

## INTRODUCTION

Local Governments exist to offer services to their communities (Seeley, 1978, Owera and Adewumi, 1985, Bello-Imam, 2004), National Governments, whether unitary as Britain, Australia, Israel, e.t.c. have forms of local governments for the purpose of service delivery (Appodorai 2004). In federalist structure of governments, each level of government is created with specific objectives. Assessing the performance or roles of any level will help to determine the efficiency of that level of government.

Populations of political states live in geographical space of cities and rural areas. Urban and Regional planning deals with the orderly organization of the physical settlements (Adedeji 1973, Aridil 1973, Mobogunje 1978, Udo 1978, Oyesiku 1995, Agbola 2005), Urban and Regional planning, often simply referred to as planning is broad in concept, emphasizing social, economic and environmental issues of a defined political and physical setting. The emphasis of planning has always depended on the social economic and environmental problems faced by a community at a given time. Oyesiku (1995) and Aduwo (2004) saw that the emphasis of planning in Nigeria was a response to environmental conditions. Later, planning emphasis was on the provision of infrastructure and services and manageability of cities.

Local authorities in urban areas are just one of the governing institutions that have the responsibility for managing urban development, providing services, redistributing revenue: making bye-laws on social and environmental issues on behalf of its citizens (Badcock 2002). In Nigeria, a federal State with three tiers of government like U. S. A., Germany, and Australia, the local government is the third tier of government with expected responsibilities. The Nigeria Constitution (1999), other national legislations (URP Law 1992) and long established practices to prescribe some specific roles to this third tier of government: the local government.

**Statement of problem.** In Nigeria, the 1963 census recorded settlements with 20,000 and above as urban. The number of such urban areas accounted for 19% of the total population (Adedeji, 1973). Over the years, settlements considered as urban have not only increased but those that have been in existence have continued to rise in population. By 1980, between 20-25% of Nigeria's population lived in urban agglomeration of a least 20,000 persons (Smile,1982). This trend of rising population, rising number of urban areas has been increasing so that about 50 million of Nigerians live in urban area, (Agbola, 2003). Politically and physically all the urban areas are within their respective local government areas. Thus, the local governments are expected to provide the services required of them to the citizens who live in the urban area of their respective local governments as enshrined in the constitution, national statutes and long accepted convections.

The concentration of large populations in physical geographical space as settlements requires that supportive public services for such populations be provided. The availability, adequacy and quality of urban public facilities and services like recreation, water supply, refuse management, commerce, health care etc. gives an indication of the quality of life and environmental quality of urban settlements. Public

facilities in cities in Nigeria are not only inadequate but in some cases lacking leading to physical and social urban decay (Dansan, 2008).

Though there are enabling statutes on the provision of urban public facilities the environmental quality and human support services in urban centres have continued to deteriorate (Anyanwu, Oyelusi, Oaihenan and Dimuro, 1997). Though local government administration has had a number of reforms in Nigeria, their expected roles have been basically the same. The problem of facilities has continued to increase. Assessing the role of local government in the provision of public facilities within the field of urban and regional planning will give an understanding to the cause of their inability and attempt to proffer solutions.

**Aim and objectives.** The aim of this work is to assess whether Local Governments in urban areas have been able to provide urban public facilities as an aspect of good governance. Lafia urban area within the Local Government, of Nasarawa State, Nigeria is used as a case study. This assessment was done by means of:

i.   Giving a background of Lafia town.
ii.  A review of legislations that relate to the provision of public facilities by Local Government.
iii. The state of some urban public facilities in Lafia urban area.
iv.  Some recommendations

## METHODOLOGY OF STUDY

The ministry for Local Governments Nasarawa State and Lafia Local Governments were visited several times. Unstructured questions were asked to relevant officer Mr. Sadiq administrative Officer Ministry for Local Government, Nasarawa State and the Officers in charge of town (urban planning in Lafia, Local Government).

## BACKGROUND TO THE STUDY AREA

**Origin and growth.** Present day Lafia has its origin as a multiple nuclei of the Migili and Alago market point, in the early 1700s, the arrival of Borno emigrants (beri-beri) late 1700s (Oyigbenu, 2005) and the establishment of a railway station in the mid 1800s. The beri beri who were accepted and permitted to settle by the Andoma of Doma were admonished to live in peace ( lafia in hausa language) with other ethnic groups. Hence, Lafia became the name of the settlement. The north/south Port-Harcourt, Maiduguri regional road that passes through the town, and agricultural rich hinterland reinforced the permanency of the settlement. The rapid growth of Lafia to its present size is attributed to political, social and national development. Regionally, after the civil war, (1968-1970) both soldiers and civilians settled in Lafia contributing to its growth. As a major railway station (when passenger and goods trains were in operation before the civil war and after, up to 1985), Lafia attracted and still attracts farm produce and passengers from the hinterland. Hence the location of the present Lafia market and commercial ribbons has physical links to Lafia railway station. Presently Lafia town is the administrative headquarters of Lafia local government and headquarters of Nasarawa State. Lafia local government was one of the local government in the then Benue- Plateau State in the 12 states structure of Nigeria between 1966 and 1976. Benue and Plateau were two provinces in northern Nigeria. And Lafia Native Authority (local government, as they were then called) was part of the Benue province. When Benue state was created from Benue Plateau state in 1976, the Lafia local government opted to remain in plateau state. The Lafia local government of 1976 was later split into Lafia, Awe, Doma, and Obi local governments of more states in the country in 1996, Nasarawa state was one of them with Lafia as the headquarters of the state.

**Regional setting.** Regionally, Lafia town is about 100km (straight distance) from the federal capital city Abuja and approximately south-east (SE) from federal capital territory (FCT). This means that Lafia town is within the 100km radius from the geographical centre of Nigeria. A regional trunk 'A' road passes through the city thus fostering inter-regional interaction. Cities that are of higher population size and higher order services that Lafia city interacts with are Makurdi (100km) south, Jos (190km) north east, and Abuja (180) see map 1, Lafia in National/Regional setting. All those cities have express roads linking them to Lafia. As a state capital and large city, Lafia serves as a higher order city in the provision of

consumer goods, administrative and other services to the immediate smaller towns that are directly linked to it. Such towns are, Nasarawa Eggon (20km and North of Lafia), Akwanga (60km, North) Doma (30km, South west) Kadarko (45km South) Asakio (40km Weast) and few other towns.

Lafia as the headquarters of Lafia local government has several towns and villages, some which have expanded and are mapped as independent uncleus of the larger Lafia area. Shabu, North of Lafia is physical part of Lafia metropolis, os is Kwandare. See map 2, map of Lafia LGA. Thses were small independent towns some years ago but are today part of the larger Lafia metropolis using the public facilities and services available to Lafia people.

**Physical features of Lafia.** Udo (1981) and Offordile (2002) all put Lafia as belonging to the Benue valley. The major stream, a river west of Lafia drains into river Mada which flows into Benue drainage basin. The soils are sandy making many untarred roads (most roads are unturned) difficult to use either by cars or motorcycle. Below the sandy soils are sedimentary formations that are easily eroded when there are heavy rains, creating gully's and floods on low lying roads that have no storm water drainages.

Geologically, Ofodile (2002) describes the metropolis as sitting on Lafia formation. This formation comprises essentially of sandstones which are brownish. The sandstones are described as fine to coarse grained friable and telepathic. The sandstone formation is not of even thickness, as the formation increases in thickness from south to north ranging between 10m to 150m.

The climate is characterized by, high temperatures, ranging between $27 - 30^{o}$C mean annual. The relative humidity is between 60-80%, with rainfall ranging from 1120mm to 1500mm spanning between late March to early November. The metropolis as any other large human settlement has greatly altered the natural vegetation. The natural common grassland savannah trees like shear butter, locus beans tree, Maje (Hausa) are hardly seen. These have been thinly replaced by mango, nymp, cashew, gmalina, eucalyptus, making the built up area naked vegetationaly.

**Literature review - Evolution of local government in Nigeria.** There was a form of local administration with various formal political institutions in Nigeria before the advent of British Colonial administration (Bello-Imam 2004). The indirect rule-ruling through existing traditional structures in the Northern region was the basic local administration centred on the traditional structure with a Resident (a White British Administrator), a Native Authority (N.A), a Native treasury and a Native Court. The cultural diversity even in the north especially the middle belt constituted a problem for the uniform acceptance of the indirect rule. The shortcomings of this local administration by indirect rule were that there was of long range of policy on democratization and development. In 1946, the Richardson constitution brought the whole structure of local administration into a critical review which leads to the transition from the NA to local government. Local Government became a regional affair in 1950, up to military rule in 1996 with each state designing its administrative structure up to 1970s local governments were regarded as agents of central administration at the periphery with the Divisional Office (D. O) serving as the; local field agent of the colonial administrations. This concept still lingers. There were a lot of experimentation in the structure of local government between 1966 and 1976 when there was a nationwide reform (Orewa and Adewumi 1983), abolishing variegated systems and the structures and the D.O. The 1976 reform stand above all previous reforms, it provided for a single tier multipurpose local government authority, but may have subordinate units. It could delegate its functions and powers. Other features in the 1976 reforms are:

i. A local government was recognized as a level government with defined boundaries, with clearly stated functions.
ii. A standardized forum of organization structure comprising of six departments: viz
- Department of finance, supplies planning and statistics
- Department of Education
- Department of Agriculture and natural Resources
- Department of works, land and surveys
- Medical and health department
- Administration and personnel department
iii. Local governments are to be incorporated in the planning process of their states through the state planning board, and the basic units of the perspective planning.
**iv.** Local governments are made to have a unified local government service scheme.

**The present state of affairs in Nigeria local government's administration and their roles.** The foregoing section discussed the evolution and the development of local government in Nigeria. There were several adjustments in the number, structure and functions of local government in Nigeria by military heads of state after the 1976 major reform. The 1976 reform created 301 local governments units. The criteria used were population between 150,000 and 800,000 population (except for continuous municipality) geographical continuity and financial viability. By 1983, the number of local governments rose to 1000, as States created them without federal recognition i.e. during civilian government of Alh. Shehu Shagari. But in between 1983 – 1985, the then military Head of State, Gen. Mohammed Buhari reduced them to the original 301, on the advice of Asuki report. The report was of the *opinion that the 1976 reforms had operational problems from persons to persons* and not the structure. The ministry for local Government in each State played the supervisory role and the sole Administrator – a civil servant was appointed as the Head of the local government, supported by supervisory councillors. The sole Administrator system was replaced with a five persons committee. Drawing from the experience of older federations like USA, Canada and Australia, the political Bureau advised that the local government should be the basic structural unit for administration and development of Nigeria (Bello-Imam, 2004). This view of local government being basic units for development is supported by Aronstein (2001), arguing that local government is important because plural actors can influence the outcome of policies and programmes that affect their lives. It is projected that local government will have an increasing important part of the new global order where public, private and non-profit sectors will work together in complex regimes.

The number of local government kept increasing as more states were created as depicted by Table 1.

**Table 1. Local government structure in relation to the other level of government***

|  | **Period** |  |  |  |
| --- | --- | --- | --- | --- |
| Level of Govt | 1976 | 1987 | 1991 | 1996 |
| Federal (Central Government) | 1 | 1 | 1 | 1 |
| State government | 19 | 21 | 30 | 36 |
| Local Government | 301 | 449 | 589 | 774 |
| Sub-ordinate | (Discretory) | (Discretory) | (Discretory) |  |
| Councils FCT | Nil | Mayoralty with 4 area councils | Mayoralty with 4 area councils |  |

*\*Imam-Bello (2004, p.30)*

The reforms and the existing structure in such local governments have executive and legislative arms all which are elective on ward basis and party platform. Despite these reforms to make local governments viable financially, and administratively, and become effective centres of development, local governments in Nigeria have been Able to propel much development.

Some typical problems or constraints are given by Eliagwu (2000 and bello-Imam (2004) are:

i. Lack of funds (finance) as there is dependency on external funds.
ii. Lack of and under-utilization of manpower and professionals in many fields.
iii. Over control, state governments have not realized that local governments are constitutionally guaranteed third-tier government and are therefore autonomous of state government.
iv. Policy conflicts and distortions in federal arrangement which most often make local government the sacrificial lamb.

The above listed are some of the constraints confronting local government system in Nigeria to the detriment of not fulfilling their expected roles. Lack of finance and over-control (for political patronage) has been the two major problems (Eminue 2000). Internal revenue sources are few-local tax, users fees and charges and rates on property which is unpopular politically, Hence, capital expenditure is not much. Because of psychological inferiority placed on this level of government, professionals like doctors, chartered engineers, town planners, etc are hardly found in the service of local government.

From the fourth schedule of the 1999 Nigerian constitution, and imam Bello (2004), some expected roles of the local governments which are of relevance to physical planning:

i. To promote economic development under the concept of development from below. The state House of Assembly is to provide legislative framework for this to take place.
ii. There is the need for small units to stimulate the provision of services nearer to the point of delivery. Area based consumer services nearer to the point of delivery. Area based consumer services like water supply, farm inputs etc help to redress the in-evitable imbalance between consumer and producer.
iii. The establishment, maintenance and regulation of slaughter houses, markets, motor' parks and public conveniences.
iv. The construction and maintenance of roads, streets, street lightings,drains and other public highroads, parks, gardens, open spaces, including naming of roads, streets and numbering of house.

**Legislations relating to the provision of urban public facilities in Nigeria.** The 1999 Nigeria's Constitution has its function schedule sections c, d, g, and k, having a wide variety function be performed by local governments from its citizens both urban and rural. As an example, section (d) has services like markets, motor arks and section (h) has roads, street rights, parks gardens including numbering, naming of streets and refuse disposal in section (g0 and (h) respectively. Apart from the 1999 constitution, some of the previous legislations that relate to the urban and regional planning are:

i. The own improvement ordinance of 1863.
ii. The cantonment proclamation of No 29. The planning of colonial housing Areas if 1904.
iii. Town and country planning ordinance of 1946 (Cap 134 in Western Nigeria).
iv. Land use decree of 1978.
v. Urban policy of 1992
vi. Housing policy of 1992
vii. Urban and repair planning Act of 1992.

Despite these successive acts good urban governance in the Area of the provision of Urban public facilities have elected many Nigeria urban centres Ndam (2001) and Imam-Bello (2004) reviewing Local government to urban areas.

**The concept of urban public facilities and services.** Orubu (2001), considers public services being the same as social services, arguing that the essential feature of social services is that it is difficult for the market to provide them efficiently. Other conceptual characteristics of public goods according to O'Sulivan (2000) and Orubu (2001) are:-

i. *The principle of non-execudability in provision.* A public is a commodity or service one which if supplied to one person can be made available to others at no extra cost. A public good is in the principles intended for share, joint or public use. Within the area of urban and regional planning examples are city beautification, street lighting, roads and environmental protection.

ii. *A public good also characterized by being non vital consumption.* This means that the consumption of a public good by one person does not reduce its availability to others. Admiring a water fountain or other street furniture by one person does not reduce another person's capability of admiring same.

iii. *A public good also has the characteristics of being confined to a relatively small geographical area e.g a city, local government, a neighbourhood etc.*An essential distinction is made between basic economic services and basic or local or Community services which are expected to be provided by local government or regional or national. A common economic consideration of a public good or service is that its consumption by one person does not diminish the consumption by another. O'Sullivan (2000) gives three characteristic of a local public good as being non-rivalries, non-excludable and confined to a relatively geographical area.

iv. This research adopts the immediate foregoing concepts which are an extension of Olowu's table. Earlier works in urban and regional planning, Farris and Sampson, 1973, Wilson, Rees and Leight, 1977, Barlow 1981) have applied similar understandings as it affects the concepts of public facilities and

services therefore and those facilities provided by an organization that is considered public for the purpose of enhancing the quality of life of the users.

**Table 2. FUNCTIONS OF THE LOCAL GOVERNMENT WITH IMPLICATIONS FOR URBAN AND REGIONAL PLANNING\***

| Functions | Relevant sections of the Constitution |
| --- | --- |
| Establishment and maintenance of cemeteries, burial ground and homes for the destitute or in firm. | Fourth Schedules 1 (c) |
| Establishment, maintenance and regulation of slaughter houses, slaughter slabs, markets, motor parks and public conveniences | Fourth Schedules 1 (d) |
| Contruction and maintenance of roads, streets, street lightings, drains and other public highways, parks gardens open spaces or such public facilities as may be prescribed from time to time by the House of Assembly of a state. | Fourth Schedules 1 (f) |
| Naming of roads and streets and numbering of houses | Fourth Schedules 1 (g) |
| Provision and maintenance of conveniences, sewage and refuse disposal | Fourth Schedules 1 (h) |
| Assessment of privately owned houses or tenements for the purpose of levying such rates as may be prescribed by the House of assembly of a state. | Fourth Schedules 1 (j) |
| Control and regulation of (i) outdoor advertising and hoarding. (ii) Movement and keeping of pets of all description. (iii) Shops and Kiosks. (iv) Restaurants, bakeries and other places for sale of food to the public. (v) laundries. (vi) Licensing, regulation and control of sale or liquor | Fourth Schedules 1 (k) |
| LG shall participate in (a) the provision and maintenance of primary, adult and vocational education (b) the provision and maintenance of health services. | Fourth Schedules 2 (a, d and e) |

*\*Nigeria 1999 Constitution*

Olowu (2005), in a tabular form utilizes the fore-going characteristics of the concept of a public good to distinguish the difference between public and privates goods (Table 3).

Earlier works in urban and regional planning, (Farris and Simpson 1973, Wilson, Rees and Leigh, 1977, Barlow 1981) have applied similarly understandings as it affects the concepts to public facilities and services.

**RESULTS/FINDINGS**

Local governments in Nigeria either under colonial or independent have not had a very effective role in physical planning. Even where there were local planning authorities, these were outfits of respective state governments and not part of the local governments (i.e decentralization and not devolution) several factors hinder effective role of local government in physical planning in Nigeria, some are discussed here as follows.

*The historical development:* The historical development of local government in Nigeria revealed that local government were seen as representatives of regional government (and later states) and not as

autonomous institutions to carryout planning (Imam Bello, 2004). Even though the 1916 planning law with regional versions cap 1.36 of laws of northern Nigeria (and later on states) made provisions for the establishment of local planning authorities, theses were not established except in some few states in the then Western region of Nigeria. The picture of local governments being outfit of state government was so pronounced in the military government in Nigeria especially the 70s and 80s so that state governments produced master plans for the development of local government Headquarters. In the plateau State (before 1996) master plans were prepared for Lafia, Akwaga, Obi, Keffi, Nassarawa Toto, Barikin ladi, Langtang and a few others. There was very little implementation done by local governments in the preparation and implementation of the plans. Local government functions and roles will continue to become important as there are always social and political concerns for local participation. (Arnstein, 2001) and Mollenkopt, (2001). The concern for greater participation is not only an American or Australian issues as (Doe, 2005) see local government as the strongest institution for achievement of millennium development growth in Ghana. The local government system of Ghana as enshrined in the 1992 Ghananaian constitution. Article 35 (5d) requires that the state should take appropriate measures to ensure decentralization in administrative structures and with a population of 115m (Kankwede, 2001) has a little over 2,000 professional town planners (Ichaba, 2005 while U.K with a population of 74m has over 12,000 professional town planners at work as early as 1990s (Healey and Williams, 1994). Omisore and Akande (2004) studied five local government councils in Ondo state, Nigeria and found that each local government lacked at least 4 staff out of 8 of various ranks from assistant town planning officer to Director of planning.

**Table 3. Differences between public goods and Private goods**

| PUBLIC GOODS | PRIVATE GOODS |
|---|---|
| Relatively difficult to measure quantity and quality | Relatively easy to measure quantity and quality |
| Consumed jointly and simultaneously by many people | Can be consumed by a single persons |
| Difficult to exclude someone who does not pay | Easy to exclude someone who does not pay |
| Generally on individual choice to consume or not | Generally individual choice to consume or not. |
| Generally on individual choice of kind and quality of goods | Generally individual choice of kind and quality of goods |
| Payment of goods not closely related to demand or consumption | Payment for goods closely related by political process |
| Allocation decisions made primarily by political process | Allocation decisions made primarily by political process |

*\*Olowu (2005) P.124*

*Rapid Urban growth:* The inadequacy of skilled manpower is made more acute with rapid urbn growth, Nigerians settlements have continued to rise both in physical size and population figures, with an average urban growth rate of 2.8% Thomas, 91999), Kankwede (2001), Jinadu (2004). It is projected that this tread will continue at an increasing rate reaching 4.23% per year by 2010 Agbola 92005). Local governments that have this kind of high growth rates will need strong support from the higher tiers of government in terms of finance for the development plans and implementing such plans Karu local government of Nasarawa State, Nigeria, because of its proximity to Abuja experiences a very high urban growth rate requiring studieste to a planned physical environment.

*Land use Decree.* The 1976 land use decree vested the power of the control of land of a state in the lands of a state governor: Since physical planning is done on land, state governments over stress this

provision of the Act to mean that all planning activities i.e problem identifications, projections, listing of aalternatives, implementation and monitoring are to be performed by that level state government with no strong participatory role. The land use Act also gives the state governor the power to set up a state land use and allocation committee.  An allocation by the state land use and allocation committee in any local government even when usage does not conform to the locality still stands because it is from a higher tier of government.   Local governments thus perform a function of land administration rather i.e acknowledging sales from customary ownership to take place as provided for the land use act.

*Conflicts of policies.* Inherent policy conflicts and distortion in federal arrangement which most often make local governments the sacrificial lambs is also a factor that does contribute to the ineffective participation of local governments in the planning process.  Local governments have either little or no say in the sitting of project within their jurisdiction, by either state or federal government even if such projects may have social or environmental impacts on the locality e.g highways, but the input of the local community through the local government is not sought.  As a result of the right of each of the three levels of government to certain functions either exclusively or concurrently, there  is often as inevitable conflict which multiple laws on the some issues usually generate (Imam-bello, 2004).

*Finance.* Finance is crucial and critical in the implementation of all planning proposals especially in the provision of facilities and services in urban areas (Barau, 1990).  The problem of inadequate finance is multidimensional. Local government are over depended on external funds, which endanger local autonomy and meaningful execution of plans and budgets.  Local governments themselves erroneously believe that whatever funds that are allocated or are generated should be spent especially on administration and to the detriment of capital development like facilities and services.  In the present (2006) 4th Republic, the joint account of local governments which state governments are to add to from internally generated  revenue, is withheld by many states to the detriment of local government being able to perform their functions.  Harsh (2006), that one of the greatest dilemmas facing many African cities is how to finance the development and maintenance of essential services such as waste removal and provision of clean water.

*Non Implementation of 1992 urban and regional Planning law.* The non implementation of the 1992 and regional planning law has not afforded the local governments of exercising their full planning functions SS3(c) of the law provides for the establishment of local planning Authorities (LPA) at all the local government levels to handle the administration of planning in their jurisdiction.  Many states (Nasarawa inclusive) have not done so.

## THE STATE OF SOME URBAN PUBLIC FACILITY IN LAFIA URBAN AREA

The provision and management of most urban public facilities and services is neither by the Local Government not by Local Planning Authority as prescribed by the urban planning Act.  In Lafia urban area many major streets do not have names and no numbers on buildings.  The situation of refuse removal and disposal is quite critical as generation of domestic and commercial based solid waste exceeds ability to present set up to contain.  The market is congested as it has not been expanded to meet the demands even with rapid and growing population.  Probably most deplorable is the service listed in section (f0 i.e the constitution and maintenance of roads, streets and drains.  Most of the function of service is carried out directly by state government or its organs, leaving the Local Government perpetually inexperience without knowing their responsibilities.  This is the situation in all urban areas in the state – Akwanga, Karu, Nasarawa, Keffi.  All these have populations of 100,000 and above (Abumere 2002).

## RECOMMENDATION AND CONCLUSION

Nigeria urban centres like all urban centres in the developing world are growing rapidly and the provision and management of urban public facilities is essential to improve the quality of life of urban residents.  The following recommendations will help the situation in Lafia and the urban area in the state.

1.      Federal and State government should set standards for the provision and management of urban facilities so that local governments can carry out the delivering and management of services.
2.      All funds meant for Local government should be released in proportion to the ability of their adherence to standards set for urban public service delivery.

3.      Local government should utilize the provisions in the contribution and other legislations to demand their proper roles in urban management.
4.      The provision in the statutes provides for local governments to have various forms of revenue base like tenement rates which need to be explored.

**REFERENCES**

Abumere, I . S. (2002) *Urbanization, In Alas of Nigeria. Ed. Jagguar.*

Adedeji A. and Rowland, I. Ed (1973) *Management Problems of Rapid Urbanization in Nigeria;* University of Ife Press, Nigeria.

Agbola. T. (2005)   *Urbanization, physical and Development in West Africa; In proceedings of Commonwealth Association of planners (CAP) West African Region, workshop Nov. 4-5, 2005.*

Appadorai, A. (2004) *The Substance of politics 4th Impression* Oxford University press, India.

Arnstein, S. (2004) *'A Ladder of Citizen participation'* in the City Reader 2nd Ed, Le Gates, RT and Stad F (Ed), Routledge, New York.

Abumere, S. (2003), *Urbanization,* in Alas of Nigeria, Pans France.

Anyanwu, J. C., Oyefusi, A. Oaikenau, H; Dimiro, F. A., (1997), *The structure of Nigerian Economy, Journal Educational* Publishers Ltd Onisha Nigeria.

Barau D. (1990) *Planning for Urban Facilities and Services: A Case study of Akwanga, Plateau State. An Unpublished M. Sc Thesis URP ABU Zaria 1990.*

Badcock, B. a. (2002) *Unfairly structured cities ,*London, Blackwell

Barlow, I. M. (1977) *Spatial Dimensions of Urban Government,* Research Studies Press, New York.

Bello-Imman, I. B. (2004) *Local Governement in Nigeria, Evolving a third Tier of Government* Heinemann Educational Books (Nigeria) Plc Ibadan.

Dausan, p. k (2008), Arresting Urban Decay in Nigeria: The calabar experience, In the 39th Nigerian institute of Town planners conference, 22nd -25th October, 2008, Yola, Nigeria.

Dansan, P.K. (208), arresting Urban Decay in Nigeria: The Calabar Experience, in the 39th Nigerian Institute of Town Planners Conference, 22nd – 25th October 2008, Yola, Nigeria.

Doe, B. (2005),   *Achieving the Millennium Development Goals in the City- Ghana Experience' :*In proceeding of CAP West African Region Nov. 14th- 15th 2005, Abuja.

Farris, T. M. and Sampsan R J. (1977) Public utilities regulation management and ownership: Houghton, Mifflin coy Boston

Healey, P, and Williams, R. (1994) *European Urban planning system:* Diversity and Convergence in International Perspectives in Urban Studies (2), *Paddison, R. Money J. and Leaver, B. ( Ed)* Jessica Kingley Publishers, Pennsylvania.

Ichaba, (2005) *Speech Delivered, (President NITP)* at the Government House, Lafia Nasarawa State on July 27th, 2005 during a Courtesy Visit.

Imam – Bello (2004), Local government in Nigeria, Ibadan Nigeria

Jinadu, (2004) *Urban Expansion and Physical Development problems in Abuja. Implications for the National Urban* Development, Adequacy and Limitations, Policy in Journal of the NITP Vol. xvii, October, 2004.

Kankwedo, M. (2001) *United Nations System in Nigeria,* Nigeria Common Country Assessment, United Reactions.

Mabonguje, A. L. (1973) *Systems Approach to a theory of Rural Urban Migration in Man, Space and Environment,* English, P. W. and May Field R. C. (Ed) Oxford University Press, Inc. London.

Ndam J. (2001) local government reforms.

Orewa, G. O. And Adewumi, J. B. (1983) *Local Government in Nigeria.* The Charging Scene Ethiopia Publishing Corporation Benin City.

Oyesiku, K. (1998) *Modern Urban and Regional Planning Law and Administration in Nigeria. Kraft Books Ltd Ibadan.*

Offodile, M. E. (2002) *Ground water study and Development* in Nigeria.

Oyeigbenu (2005) *The story of Agwatashi,* Evans Press

Savanna Lausult (998), Great Lafia Master Plan.

Udo, B. K. (1981) *Geographical Regions of Nigeria* London Herinemaan, Ibadan

Wilson, Rees, and Leigh (977), models of urban and regional planning London

# THE EMPATHY, UNDERSTANDING, EMPOWERMENT (EUE) MODEL OF ENGAGEMENT IN ENVIRONMENTAL DECISION MAKING

*Daniel Ducker* and Dr Kepa Morgan
(University of Auckland, Auckland, New Zealand)

**ABSTRACT:** It is now well understood that historical processes for resolving complex environmental issues have been inadequate. At best they have helped to slow down local and global environmental problems; at worst, measures have exacerbated or transformed problems into more intractable forms. This paper identifies common, although rarely acknowledged environmental problem solving issues influencing the viability and success of proposed solutions. A psychosocial approach to interpreting these common problems is adopted, thereby recognising the critical role of psychological and inter-subjective processes which affect problem solving success. This approach in particular recognises the importance of empathy, understanding, and empowerment at both an individual and organisational level. It thus provides a new formulation for environmental problem solving and a means of questioning the organisational "silos" which currently exist for addressing environmental issues. A comparison between the traditional and proposed approaches is exemplified using an environmental cleanup project as a case.

## INTRODUCTION

In a time of fiscal pressures, austerity measures and economic stagnation questions of environmental health appear at best a low priority and at worst wholly irrelevant. However, what is also apparent is that substantial destabilizing large-scale environmental changes are now well under way (Vitousek et al. 1997; Brown et al. 2000). Increasingly apparent environmental changes - global warming, loss of biodiversity, worldwide land degradation, depletion of fresh water, disruption of the elemental cycles of nitrogen and sulphur, and the global dissemination of persistent organic pollutants-have great consequences for the sustainability of ecological systems, for food production, for human economic activities, and for human population health (McMichael et al. 2003). We have begun to understand that, even in the modern, affluent, urbanising world, humankind is dependent on intact ecosystems that support the flourishing of life. For decades, many concerned scientists and "green" politicians have warned that unless societies opt for social institutions, technologies, and conservationist behaviours that sustain the natural resource base, the life-supporting capacity of ecosystems – then the long-term health of global populations may be compromised (McMichael, Butler et al. 2003). While significant efforts at collaboration between scientists, politicians, economists, environmental and social groups have been made to attain these lofty visions, to date their success has been mixed.

This paper posits that the barriers to successful collaboration stem from individual ideologies and the constructed systems which serve to facilitate those ideologies. We briefly examine a case of environmental problem solving – an environmental cleanup, then examine the two chief ideologies present. Can the differences between these ideologies be reconciled? We suggest through reframing the issues reconciliation is possible.

## CASE STUDY: FORMER FRUITGROWERS CHEMICAL COMPANY REMEDIATION, MAPUA, NEW ZEALAND

We begin with a case study of environmental cleanup. The Fruitgrowers Chemical Company formed in 1931 producing a variety of organochlorine pesticides such as DDT, DDD and dieldrin. FCC began as a highly revered operation. By the late 1970s the plant was making 84 different pesticides, herbicides, insecticides and fungicides, however, with increased awareness of the toxicity and persistence of these compounds a band of dissenters formed opposing the operation. By the mid 1980's the environmental lobby had gained sufficient strength to enforce closure of the plant in 1988.

In the early 1990s the scale and consequences of the toxic site became increasingly evident. However, no party was willing to accept responsibility for the contamination – the owner believed that

the operation had been permitted by the government, and the Crown believed that the polluter should pay. This stalemate lasted for nearly 10 years until the Crown took over responsibility for the land. The site then became an "orphan contaminated site", meaning no party was identified as capable of funding the remediation of the site. The site was classified as New Zealand's most contaminated.

Two separate remediation attempts were developed for the site. In 1996, with very little public consultation, an engineering (bund) solution was proposed and consents were granted. Although most neighbours were satisfied that finally something was being done, a national environmental group appealed the decision on the grounds that it did not represent the most effective long-term solution and the risk of failure was high. The appeal was sufficient to halt the plan. In 1999, the Ministry for the Environment allocated funding to a decontamination programme. Following a series of trials a remediation contract was awarded to a local novel technology – Mechanochemical Dehalogenation (MCD). Consents were again appealed by the environmental group, this time on purely safety concerns – the plant was novel and largely untested. In November 2003 consents were granted.

Proof of Performance (POP) testing occurred in early 2004. During one of the four trials, a mechanical breakdown led to the formation and release of contaminants that included small quantities of dioxin from the POP plant. An independent scientific advisory team considered that the dioxin emissions did not represent emissions during normal operating conditions, and that the problem could be eliminated. Citizens were not directly informed of this event.

Following POP trials the main contractor withdrew from the project. Rather than allowing the project to fail, consents for operation was transferred from the contractor to the Ministry for the Environment. Remediation eventually began in September 2004. Ongoing problems occurred with the soil dryer and with the emissions control system. Although the scientific advisory panel was aware of the problems, they did not inform affected or interested parties. Ongoing issues lead to substantial time and cost overruns.

The remediation was completed in 2008, nearly three times longer than originally anticipated. Yet concerns remained about the effectiveness and safety of the cleanup. In mid 2008 a report from the Government's environmental watchdog, the Parliamentary Commissioner for the Environment, raised serious flaws in the process. Government sanctioned reports tried to damper community fears and claim the cleanup was an overwhelming success, however further health and worker safety reports (most recently 2012) have only increased community anxiety and distrust. Although the cleanup achieved nominal remediation goals, it did little to alleviate community safety concerns, as such it cannot be described as wholly successful.

In similarity to many other large scale environmental cleanups, the remediation of the FCC site proved to be far more complex and costly than originally anticipated. Although on a world scale, the volumes treated were moderate, cleanup of the Mapua site took nearly 20 years and cost (not counting administrative overheads) in excess of NZ$13 million. Contrary to some reports published on the clean-up which highlight the uniqueness of the technology employed, the unusual scale of the problem, and the difficulties encountered while clean-up occurred, the most fascinating aspect of Mapua is, quite simply, how beautifully ordinary it is. Common to many environmental problem solving measures, the Mapua cleanup encountered a range of socio-political, technical and economic hurdles which were overcome, with varying degrees of success. As such, Mapua proves to be a typical case of environmental problem solving.

## A PSYCHOSOCIAL APPROACH TO ENVIRONMENTAL PROBLEM SOLVING

Mental models colour the way we perceive, think and act in the world. Our brains are hard wired for learning and over time, we grow to form particular perspectives, or ideologies which help us to make sense of, and function in the world. Ideologies form the basis for differences of opinion in environment matters and can be so ingrained that they elicit automatic and habitual responses (van den Bergh et al. 2000). A range of factors is thought to influence ideological development, significant influences include intrinsic genetics, hormone levels, gender, upbringing, access to education, affluence. Many of these factors are of course inter-related, and there is strong evidence for interdependencies between intrinsic (biological) mechanisms, and extrinsic (social) influences.

In a world with considerable genetic and cultural diversity, a wide variety of environmental ideologies may be anticipated. However, a broad body of diverse literature suggests there are chiefly two disparate orientations which conflict during environmental problem solving.

**Table 1. Comparison of Imperial and Arcadian Orientations
(following Cotgrove 1982; Pepper 1996; Miller 1999)**

| IMPERIAL | ARCADIAN |
|---|---|
| **Human Nature** | |
| Humans are wholly self interested | Humans can be altruistic |
| Humans are naturally aggressive and competitive | Humans are naturally cooperative |
| We are capable of only limited caring | We are capable of widespread concern |
| Risks should be taken to attain rewards | Caution should be exercised |
| Individuals should look after themselves | We should take care of each other |
| Rational thought is more important than intuition and emotion | Emotion and intuition are at least as important |
| Fact and reasoning can be separated from value and feeling | Fact and reasoning cannot be separated from value and feeling |
| **Nature of Society** | |
| Human societies are naturally hierarchical | Social hierarchies are naturally egalitarian |
| Decisions should be made by experts: Politicians advised by scientists | We should all be involved in decision making |
| The way forward is through representative democracy | The way forward is through direct democracy |
| Material acquisition underlies social progress | Spiritual quality of life and loving relationships are of utmost importance |
| Separation of spirituality and life, church and state | Spirituality integrated within all aspects of life |
| Economic growth is desirable and can go on forever | Indiscriminate economic growth is bad and should not continue |
| Trade should be increased to further economic development | Trade should be reduced to foster local self-sufficiency |
| Large scale production and central control are desirable | Small scale production locally controlled is more desirable |
| Current socio-political arrangements are ok | There needs to be fundamental socio-political change |
| The best societies are efficient | The best societies are resilient |
| Private ownership is valued | Public ownership is valued |
| Justice based on adversarial process | Justice based on natural law |
| Justice enacted by 'impartial' judges | Justice enacted by esteemed peers |
| Future focused | Past, present and future acknowledged |
| Short-term goals | Long-term goals |
| Reverence toward youth | Reverence toward aged |
| **Nature** | |
| Nature is hostile and neutral | Nature is benign |
| Mechanistic | Complex and chaotic |
| The natural world contains ample reserves | Earth's resources are limited |
| Ecosystems are resilient | Ecosystems are delicately balanced |
| Humans are separate from nature | Humans are part of nature |
| Nature should be exploited for human material benefit | We must respect and protect nature, nature has intrinsic value |
| Environmental problems can be solved by analytic/scientific reasoning and technology | Environmental problems can only be solved by holistic approaches. |

Although called by various names, for example competitive/cooperative, dominant/indigenous, reductionist/holistic, contemporary/alternative, these two orientations provide a useful entry point into understanding why environmental decision making is so challenging, and often intractable. Following Worster (1993) and Miller (1999), these are subsequently referred to as Imperial and Arcadian ideologies (Table 1).

The Imperial ideology views life an individual struggle for existence. The overwhelming emphasis of the Imperial ideology is individualism thus, competition is inevitable and natural. For Imperialists, human beings are chiefly self-interested creatures competing for power. This primal competitive drive can generate predispositions of aggression; however, Imperialists also contend that self-interest drives humans to be ingenious, creative and innovative. Thus, the Imperial ideology merges core values of individual self-interest, intrinsic talent and creativity, domination and utilitarianism with strategic or detached reasoning. The culmination of these factors is a hierarchical society focused on economic growth and personal advancement (Miller 1999, p. 15).

In contrast to the Imperial ideology, the Arcadians emphasise that humans are social animals. Rather than purely individualistic traits, Arcadians focus on pro-social parts of human nature and cooperative pursuits, although they accept that competitiveness is also evident. Arcadians contend that a decentralised partnership society, in harmony with nature, which discourages self-aggrandizement, ought to be societal goals. The Arcadian ideology diverges strongly from the current social model.

Conflict among these two rationalities is commonplace and was aptly demonstrated in our cleanup case. At first sight, the two paradigms appear to have little in common, environmental problem solving thus appears to represent an intractable dilemma. However, when dilemmas dominate, it is time to reframe (Laws and Rein 2003; Innes and Booher 2004).

## AN INTEGRATED MODEL FOR ENVIRONMENTAL PROBLEM SOLVING – THE EMPATHY, UNDERSTANDING, AND EMPOWERMENT (EUE) MODEL

Environmental problem solving has many analogies with conflict resolution, perspectives are frequently entrenched and challenges lie fundamentally in an ability (or lack thereof) to reframe issues. The dual concern model of conflict resolution is a widely acclaimed conceptual perspective that contends the preferred method of dealing with conflict is based on two underlying dimensions (Forsyth 2009):

1. A concern for self; and
2. A concern for others.

According to the model, group members balance their concern for satisfying personal needs and interests with their concern for satisfying the needs and interests of others in different ways. The intersection point between these two dimensions ultimately lead individuals towards exhibiting different styles of conflict resolution. The dual concern model of conflict resolution provides a useful conceptual foundation for environmental problem solving. However, as we have seen from the Mapua case example, environmental problem solving appears to be a complex process of collaboration and compromise in technical, political and socioeconomic spheres. To encapsulate the full range of attributes associated with environmental problem solving the dual concern model appears inadequate. Deriving from our case, and generalised from other environmental decision making situations, it is possible to discern three primary themes of empathy, understanding and empowerment divided along two dimensions of self and others (Figure 11).

Empathy pertains to the general concern one has for wellbeing - for oneself and for others. Deeply rooted in the old, affective regions of our brains (Iacoboni 2009), empathy is often thought to be a rapid, automatic process which involves little conscious consideration (e.g. Evans 2008), however, more recent studies have demonstrated that situational influences can affect the concern for others and for oneself – capacity for empathy is innate, but it is also learned. Strong empathic concern for oneself without concern for others can lead to strong willed, uncompromising individuals, archetypal Imperial individuals. In contrast, those with overwhelming concern for others are more closely aligned with the Arcadian paradigm, commonly displaying altruistic, self-sacrificing or selfless behaviours which can easily become overly burdensome. Those with low levels of empathy for oneself and for others demonstrate affective avoidant behaviours ("hiding one's head in the sand"). Individuals with both high levels of self-concern and high concern for others exhibit more compassionate behaviour.

Understanding pertains to effective knowledge of ourselves, others and the world around us. High external understanding is typical of the materialistic techno-scientific paradigm which emphasises

systematisation. Paradoxically, while proffering scepticism, a high level of external understanding can lead to an increasing need for certainty – as exhibited by the stubbornness of adherence to dominant scientific customs and traditions (Kuhn 1962). Self-understanding is largely neglected by the Imperial ideology but highly regarded by the Arcadian. High levels of self-understanding can lead to self-awareness, but may also accompany a certain level of conceitedness and intolerance. Low levels of both self and external understanding are tantamount to ignorance, and conversely, high levels of both may be correlated with humility, tolerance, "healthy" scepticism and wisdom.

A) Empathy

| | Low toward Others | High |
|---|---|---|
| **High** (toward Self) | Imperial Selfishness Strong willed Individualistic | Compassion |
| **Low** | Affective Avoidance | Arcadian Selflessness Sacrifice Altruistic Over-burdening |

B) Understanding

| | Low Of Others | High |
|---|---|---|
| **High** (of self) | Arcadian Self-awareness Conceitedness Intolerance | Wisdom Humility Tolerance "Healthy" scepticism |
| **Low** | Ignorance | Imperial Systematisation Cynicism/Doubt/ Need for certainty |

C) Empowerment

| | Low of others | High |
|---|---|---|
| **High** (of self) | Imperial Dominance Action "Getting things done" | Compromise/ Collaboration Trust |
| **Low** | Stagnation Resignation | Arcadian Naivety / Oppression |

Figure 1. The three themes and two dimensions of environmental problem solving

Empowerment pertains to agency, the ability to act. Comparatively, Imperialists exhibit high desires for self agency whereas Arcadians are more likely to help others. High levels of self empowerment can lead to action, to "getting things done", but may be accompanied by domineering

behaviour and the exercise of power. High levels of helping others can encourage pro-social behaviours, but may also cater to oppressive regimes or be considered naive and ineffective. Low levels of both self and other empowerment leads to stagnation and resignation, whereas high levels of both can generate sensible compromise solutions, collaboration and trust.

Together, high levels of self and externalised empathy, understanding and empowerment present the most effective means of solving environmental problems. We term highly developed levels of empathy, understanding and empowerment whole person environmental decision making (Figure 2). In contrast, largely Imperial typologies were exhibited in the Mapua case, which placed a high emphasis on fiscal accountability, high empowerment of the technoscientific paradigm, and low engagement and empowerment of other parties. Minimal empathy was demonstrated toward those most affected. But the Mapua case also demonstrated some Arcadian attributes, particularly in relation to the environmental lobby which closed the original plant and blocked what they considered to be an unsustainable solution.
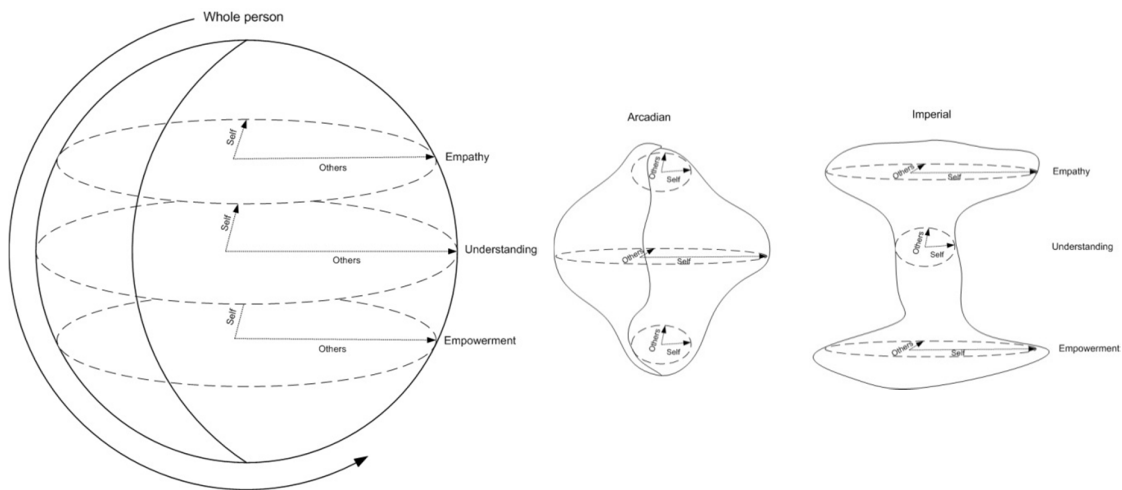


Figure 2. Comparison of Whole person decision making with Arcadian and Imperial decision making in environmental problem solving

**CONCLUSION**

Environmental problem solving has traditionally been divided into two strongly contrasting perspectives, which we have termed Arcadian and Imperial. Historically, these perspectives have been considered competing, non-overlapping paradigms. However, we suggest that such reasoning is misguided and that the dogmatism surrounding apparently disparate worldviews has largely hampered efforts to peacefully resolve environmental problems. In contrast, taking a psychosocial approach, we contend that the three principal themes of empathy, understanding and empowerment are evident in any environmental problem and only through consideration of self, and others in each of these themes can we hope to devise solutions which are widely accepted and readily implemented. Therefore, to maximise opportunities for peaceable resolution of long-term environmental dilemmas, educational, financial, and sociotechnical systems will need to be transformed.

**REFERENCES**

Brown et al. (2000). State of the world : a Worldwatch Institute report on progress toward a sustainable society. New York, Norton.

Cotgrove, S. (1982). Catastrophe or cornucopia: The environment, politics and the future. Chichester, Wiley.

Evans, J. S. B. T. (2008). Dual-processing accounts of reasoning, judgment, and social cognition. Annual Review of Psychology. **59:** 255-278.

Forsyth, D. R. (2009). Group dynamics. Belmont, CA, Thomson/Wadsworth.

Iacoboni, M. (2009). Imitation, empathy, and mirror neurons. Annual Review of Psychology. **60:** 653-670.

Innes, J. E. and D. E. Booher (2004). "Reframing public participation: Strategies for the 21st century." Planning Theory and Practice **5**(4): 419-436.

Kuhn, T. (1962). The structure of scientific revolutions. Chicago, University of Chicago Press.

Laws, D. and M. Rein (2003). Reframing practice. Deliberative Policy Analysis: Understanding Governance in the Network Society. M. Hajer and H. Wagenaar. Cambridge, Cambridge University Press**:** 172-206.

McMichael, A. J., C. D. Butler, et al. (2003). "New Visions for Addressing Sustainability." Science **302**(5652): 1919-1920.

Miller, A. (1999). Environmental problem solving : psychosocial barriers to adaptive change. New York, Springer.

Pepper, D. (1996). Modern environmentalism: An introduction. London, Routledge.

van den Bergh, J. C. J. M., A. Ferrer-i-Carbonell, et al. (2000). "Alternative models of individual behaviour and implications for environmental policy." Ecological Economics **32**(1): 43-61.

Vitousek, P. M., H. A. Mooney, et al. (1997). "Human domination of earth's ecosystems." Science **277**: 494-499.

Worster, D. (1993). The wealth of nature: environmental history and the ecological imagination, New York : Oxford University Press.

# SPATIAL AND TEMPORAL PATTERNS OF ROAD TRAFFiC NOISE POLLUTION IN RIYADH, SAUDI ARABIA

**A. O. Al-Jasser** (Civil Engineering Department, College of Engineering, King Saud University, P.O. Box 800, Riyadh 11421, Saudi Arabia)
**Saad M. Mogren** (Department of Geology & Geophysics, King Saud University, PO Box 2455, Riyadh, 11451, Saudí Arabia)

The large and rapid expansion of the city of Riyadh, the capital of Saudi Arabia, during the past decades was accompanied by improved standard of living and increased population and associated with activities and services such as transportation. As a result of such development, noise pollution became an important issue for the city. Sound intensity level measurements at different location, including residential, commercial, and industrial areas as well as main intersections, was designed and collected. It was found that noise levels in some areas were higher than the acceptable levels and could cause serious annoyance according to the World Health Organization (WHO) outdoor noise guidelines. Additionally, noise levels were found to be affected by different factors including time of the day and season of the year.

# MODELING ADOPTION OF ENERGY EFFICIENT DEVICES IN INDIAN URBAN HOUSEHOLDS

*S. Somashekar* (S.J. College of Engineering, Mysore, Karnataka, India)
N. Nagesha (UBDT College of Engineering, Davanagere, Karnataka, India)

**ABSTRACT:** Human-imposed threats to global sustainability have two fundamental dimensions: 'population growth' and 'increasing per capita demand for goods and services', particularly material needs and energy. Presently, the share of direct energy use of households in India is about 40% of the total direct indigenous energy use which goes up to 70%, if the indirect energy of all goods and services purchased by households is taken into account. Thus, study of residential sector energy consumption assumes significance from both supply-side and sustainability considerations. In this backdrop, the current paper discusses the findings of a research on factors influencing adoption of energy efficient devices in Indian urban households. The survey data of 270 households in the south Indian city of Mysore is used for the purpose. Principal Component Factor analysis is adopted to reduce the number of variables involved. Factor scores are subsequently employed in modelling the adoption of energy efficient devices, through multiple regression analysis. The study revealed 'financial status' as the most important and 'government efforts' and 'owner qualification' as the least important factors influencing the adoption of energy efficient devices. These results underscore the need for massive information campaign about energy efficient devices and to revamp the subsidy policy.

## INTRODUCTION

The energy use in the residential sector is an important area for campaigns to conserve energy. The primary purpose of major research works focused on household energy consumption and conservation is to understand the factors influencing energy consuming behaviors (Brent Ritchie J. R., et al, 1981). The underlying rationale is to bring about energy conservation by stimulating behaviors that are more energy efficient and/or by stimulating a reduction of energy consuming behaviors. Debates over key questions regarding consumers' rational behavior in making decisions regarding energy use and energy efficiency have continued unabated for more than two decades, becoming more intense in recent years due to growing concerns over the environmental impacts of energy use. The behavioral literature quotes some empirical regularities, each of which is thought to promote the over utilization of energy in households (Alan H. Sanstad and B. Richard Howarth, 1994). They include, 'use of high implicit discount rates in evaluating energy-efficiency investments', 'use of incorrect units in calculating energy consumption and related costs', 'salience effects' and 'incorrect use of technology'.

Though there are numerous studies of energy use in the residential sector, very few have investigated energy consumption based on awareness about energy efficiency, conservation and environmental implications. An attempt has been made in this paper to fill this vacuum. The primary data collected from the survey of 270 households in the south Indian city of Mysore is used for this purpose. At present, the share of direct energy use of households in India is about 40% of the total direct commercial and noncommercial indigenous energy use (Shonali Pachauri, 2004). If, in addition, one takes into account the indirect or embodied energy in all goods and services purchased by households, then about 70% of the total energy use of the economy can be related to the household sector.

The concept of energy efficiency and the introduction of renewable energy technologies can be widely viewed as important elements of economic and environmental policy, as improved access to modern energy carriers alone cannot ensure development (Sudhakara Reddy B, 2004). The Kyoto Protocol objectives and more recently, emerging constraints on energy supply have raised the significance attached to energy efficiency policies (World Energy Council, 2008). Energy efficiency scenarios are developed in the national and international context using conventional energy modeling tools. This takes into account and represent decentralized microeconomic decision-making frameworks only to a limited extent (Lena Neij, et al, 2009). However, microeconomic decision-making frameworks for energy-efficient technologies are far more complex and depend on multiple parameters, in reality. Energy can be

an instrument for sustainable development with an emphasis on more efficient use, and increased use of renewable sources (Amulya K.N. Reddy, 2000).

Human-imposed threats to global sustainability have two fundamental dimensions: population growth and the ever-increasing per capita demand for goods and services, particularly material needs and energy (Shobhakar dhakal, 2004). The energy usage of a household is influenced by energy related behaviors viz., purchase, usage and maintenance related behaviors (Fred Vaanraaij W. and M. M. Theo Verhallen, 1983). Energy use is already high in industrialized countries and is increasing rapidly in developing countries as they industrialize. Being a developing economy, India is at the acceleration stage of urbanization (Pranati Dutta, 2006). The increase in energy use of households is also attributed to TEDIC factors: Technological developments, Economic growth, Demographic factors, Institutional factors and Cultural developments (Wokje Abrahamse et al., 2005). In turn, these TEDIC factors shape individual factors such as motivational factors, abilities and opportunities.

Several strategies can be used to reduce household energy consumption. First, a distinction can be drawn between behavioral and technical energy-saving measures, which have different psychological properties (Wouter Poortinga, et al, 2003). Technical measures are generally seen as an expensive way to reduce energy use, but in the long run, technical measures may be cost saving. On the other hand, behavioral measures are often associated with additional effort or decreased comfort. Therefore, there may be differences in acceptability of technical and behavioral energy-saving measures. Second, a distinction can be drawn between the reduction of direct and of indirect energy use. Traditionally, measures aimed at reducing direct energy use have attracted most attention. However, more than half of households energy use is consumed in an indirect way. Substantial energy savings could be achieved through this route.

## MATERIALS AND METHODS

**Questionnaire design:** After extensive literature survey and in-depth discussions with experts, a list of five broad areas relevant in the adoption of energy efficient technologies in the context of Indian urban households was made. These areas include: demographic and economic background, possession and awareness of energy efficient technologies, personal/behavioral factors, financial factors and, government policies. Under each broad area, several variables were included amounting to a total of 32 variables. A questionnaire was then designed to collect relevant data regarding these variables.

**Variable Measurement:** Because of the nature of information being collected, it was decided to use Likert scale for measuring the intensity of the respondents' answers. This scale is considered to be more discriminating and reliable (Harper w. Boyd et al., 1985). For ease of analysis a score ranging from five to one was selected for each variable (five being the most favorable and one the least.). It was also decided to obtain the responses through researcher administered personal interview using a structured questionnaire.

**Income stratification and sampling:** The study uses expenditure and ownership of assets to arrive at income classes. According to NSSO (National Sample Survey Organisation) $62^{nd}$ round household expenditure data (NSSO, 2008), 120 households out of the top 291 (41.24%) households of urban Karnataka in India had MPCE (Monthly Per Capita Expenditure) of `1380-1880 (Household Expenditure (HE) of `5520-7520) and were treated as Middle Income Group (MIG). 75 households (25.77%) had MPCE of `1880-2540 (HE `7520-10160) and were treated as Upper Middle Income Group (UMIG). Remaining 32.99% had MPCE above `2540 (HE above `10160) and were treated as High Income Group (HIG). Hence out of 270 households surveyed, 111 were selected from MIG, 70 from UMIG and the remaining 89 households from HIG. The households were selected randomly from different localities within the corporation limits of the south Indian city of Mysore.

**Establishing validity and reliability of the questionnaire:** Questionnaires as measuring instruments must be valid and reliable, if they are to produce useful measurements. Validity indicates the degree to which an instrument measures what it is supposed to measure. Validity can be determined by using a panel of experts who shall judge how well the measuring instrument meets the standards (Kothari C.R., 2007). Accordingly, the questionnaire is validated here with a panel of five experts. The reliability of a

measure indicates the stability and consistency with which the instrument measures the concept and helps to assess the 'goodness' of a measure. Cronbach's alpha is a reliability coefficient that reflects how well the items in a set are positively correlated to one another (Krishnaswamy K. N., et al, 2006). The closer the Cronbach's alpha is to unity, the higher is the internal consistency or reliability. In this case, a reliability test using SPSS 14.0 yielded a Cronbach alpha value of 0.7, which is considered satisfactory in these kinds of studies (SPSS manual, 1990).

## RESULTS AND DISCUSSION

The main objective of the study is to analyze the factors which influence the adoption of energy efficient devices amongst Indian urban households and subsequently to prioritise them. As 32 variables were used in the questionnaire, it is necessary to establish an appropriate group of variables for proper interpretation. Hence, it is felt that factor analysis (principal component type) could be adopted effectively for this purpose. Factor analysis is used for data reduction and to identify a small number of factors that explain most of the variance that is observed in a much larger number of manifest variables (SPSS manual, 1990). However, it is necessary to ascertain the suitability of the data for factor analysis. Two statistics are used to decide the factorability of the data: Barlett's test of spherecity (significance < 0.05) and KMO (Kaiser-Meyer-Olkin) index (> 0.6, SPSS manual, 1990). For the survey data of 270 households Barlett's test of spherecity significance is at 0.000 and KMO index is at 0.739 and hence it is decided that the data is suitable for factor analysis. The analysis is carried out using SPSS version 14.0. The solution is then rotated for ease of interpretation using varimax rotation. Only those components with Eigen values greater than one are considered and accordingly first ten components are extracted. These ten components explain 60% of the variability in the original 32 variables as shown in Table 1. Hence, the complexity gets reduced greatly by these components with only 40% loss of information.

**TABLE 1 Results of factor analysis (Variance explained by the extracted components)**

| Component | Extraction Sums of Squared Loadings | | | Rotation Sums of Squared Loadings | | |
|---|---|---|---|---|---|---|
| | Eigen values | % of Variance | Cumulative % | Total | % of Variance | Cumulative % |
| 1 | 4.390 | 13.718 | 13.718 | 3.585 | 11.204 | 11.204 |
| 2 | 3.378 | 10.556 | 24.274 | 2.059 | 6.434 | 17.639 |
| 3 | 1.991 | 6.222 | 30.496 | 1.996 | 6.238 | 23.877 |
| 4 | 1.829 | 5.717 | 36.213 | 1.881 | 5.880 | 29.756 |
| 5 | 1.604 | 5.012 | 41.225 | 1.853 | 5.790 | 35.546 |
| 6 | 1.411 | 4.410 | 45.635 | 1.838 | 5.744 | 41.290 |
| 7 | 1.236 | 3.864 | 49.499 | 1.786 | 5.582 | 46.872 |
| 8 | 1.149 | 3.592 | 53.091 | 1.761 | 5.503 | 52.374 |
| 9 | 1.093 | 3.417 | 56.508 | 1.194 | 3.730 | 56.104 |
| 10 | 1.045 | 3.267 | 59.775 | 1.174 | 3.670 | 59.775 |

**Modelling the adoption of Energy Efficient Technologies** The factor scores obtained in principal component analysis are used in multiple regression, with the number of energy efficient technologies owned by the households as the dependent variable. The resulting equation is:

$$N = 2.389 + 0.336 * F1 + 0.088 * F2 + 0.230 * F3 + 0.118 * F4 + 0.030 * F5 + 0.201 * F6 + 0.068 * F7 - 0.054 * F8 + 0.111 * F9 - 0.057 * F10$$

Where N is the number of energy efficient technologies owned by the household and F1 to F10 are the factor scores.

The Adjusted $R^2$ of 0.613 and F statistic significance at 0.000 shows the usefulness of the model. R (Multiple correlation coefficient) value of 0.792 indicated a strong relationship between the dependent variable and the considered factors. The ranking of factors based upon the beta values is shown in Table 3. The negative Beta values for Government efforts and Qualification need a bit of explanation. The questions asked under Government efforts were: 'Is the government providing enough incentives for owning EETs?', 'Is the government putting sufficient effort to facilitate EETs?', and 'Is the information provided by the various agencies adequate?'. 69% of the respondents were not at all satisfied with the government incentives and 38% of them own more than average number of EETs. Similarly 53% of the respondents feel that very little information is available about EETs. This clearly indicates that either the government efforts are really poor or the information is not being disseminated properly.

**TABLE 2 Factor loadings and names**

| Component | Variables | Factor Loadings | Name |
|---|---|---|---|
| 1 | Annual income, Ownership of energy consuming assets, Monthly expenditure, Size of the house, Number of Energy Efficient Technologies (EETs) owned, Type of residence | 0.875, 0.842, 0.833, 0.711, 0.530, 0.521 | Financial status |
| 2 | Ego factor, Tech savvy | 0.764, 0.693 | Attitude towards EET |
| 3 | Awareness about EETs, Energy consumption, and Environment | 0.638, 0.618, 0.607 | Awareness about energy and environment |
| 4 | Energy conservation habits, Concern for environment, Maintenance cost, Purchase cost. | 0.659, 0.653, 0.589, 0.446 | Cost driven concern for environment |
| 5 | Attitude towards change, Willingness to adopt, Willingness to invest. | 0.780, 0.639, 0.516 | Willingness to adopt EETs |
| 6 | Ownership of residence, Degree of satisfaction. | 0.689, 0.636 | Dwelling characteristics |
| 7 | Risk coverage, Government subsidies, Government regulations. | 0.764, 0.743, 0.539 | Attitude towards risk |
| 8 | Government incentives, Government efforts, Adequacy of information. | 0.696, 0.683, 0.672 | Government efforts |
| 9 | Family size. | 0.776 | Family size |
| 10 | Qualification. | 0.853 | Qualification |

These components are named appropriately considering their correlations with the variables as shown in Table 2.

The case of qualification revealed another interesting fact. Table 3 shows that the 'financial status' of the household exerts the greatest influence over the ownership of efficient energy devices. The qualification of heads of majority of households (64%) is a bachelor's degree and 51% of these households are in high income group (Annual income of more than `7 lakhs). Whereas only 33% of the heads of the households have a qualification of Post Graduation and above and 47% of these households are in HIG. It would be wrong to conclude that higher qualification is associated with lower income. It is just that households with bachelor's degree qualification and belonging to HIG have not felt the need to

pursue higher qualifications. As higher qualification is given a higher Likert scale rating in the questionnaire, this explains the negative Beta value of 'qualification' component.

**TABLE 3 Rankings of factors based on the beta values**

| Factor | Beta value | Ranking |
|---|---|---|
| Financial status | 0.336 | I |
| Attitude towards EET | 0.088 | VI |
| Awareness about energy and environment | 0.230 | II |
| Cost driven concern for environment | 0.118 | IV |
| Willingness to adopt EETs | 0.030 | X |
| Dwelling characteristics | 0.201 | III |
| Attitude towards risk | 0.068 | VII |
| Government efforts | -0.054 | IX |
| Family size | 0.111 | V |
| Qualification | -0.057 | VIII |

**CONCLUSIONS**

The task of understanding energy-consuming behaviours presents substantial complexities. The complexities involve determining both the factors that influence energy-consuming behaviours and the nature of their influence. This paper has attempted to do this by using the results of a recently concluded survey of 270 households in the south Indian city of Mysore. The major objective of the study was to determine the factors which are influencing energy efficiency and conservation behaviours in the urban households of India and also to determine the strength of their influence. Factor analysis was first carried out on the survey data to reduce the number of variables to manageable proportions, which resulted in 10 factors. The factor loadings of each factor on closely correlated variables were considered to appropriately name these factors. The factor scores were saved to carry out regression to determine the strength of the relationship between these factors and the number of energy efficient technologies owned by the households. Accordingly the 'financial status' of the household turned out to be the most important factor and 'willingness to adopt EETs', the least important one. Also of particular interest is the fact that, two factors had negative beta values. The implications of these findings to national government policy in general, and Karnataka State policy in particular, are summarized as follows: The continuous growth in the demand for electricity has resulted in multi dimensional crises for the state: economic slowdown, huge letdown for those who depend on it, fast depletion of ground water table, environmental concerns etc. Whereas the recent philosophy all over the world has been to maximize the efficiency of operation of the existing electricity infrastructure, Karnataka continues to think that addition of generating capacity will solve the problem even though this policy has failed since many decades. The recent report of Inter Governmental Panel on Climate Change (IPCC, 2007) has provided enough indications that such a policy is not suitable for a sustainable lifestyle. Hence there is a need for thorough review of the power sector in the future. This study shows that the 'financial status' is the most important factor influencing the adoption of energy efficient devices. 48% of the households have an annual income of above `7 lakhs and 55.4% of these households have above average number of energy efficient devices. Hence, there is an urgent need on the part of the government to do away with untargeted and unscientifically based subsidies. The high income group households don't need subsidies and the only energy efficient device that most of the lower income group households have is solar water heater. None of these households have said that subsidy is the motivating factor for them but have cited savings in electricity bill and convenience as the main reasons for possessing the solar water heaters. The second and the fourth most important factors, namely 'Awareness about energy and environment' and 'Cost driven concern for environment' and the possible reasons for the negative beta value of 'government efforts' (as discussed under analysis of results) indicate the need for massive information campaign about the government

efforts and economies of energy efficient devices (something on the lines of family planning campaign that the central government undertook several years back which paid rich dividends).

**REFERENCES**

Alan H. Sanstad and B. Richard Howarth, 1994. "Consumer Rationality and Energy Efficiency", Proceedings of the ACEEE 1994 Summer Study on Energy Efficiency in Buildings.

Amulya K.N. Reddy, 2000, *Energy and Social Issues*, Chapter 2, World energy assessment, Energy and the Challenge of sustainability, United Nations Development Programme, pp 39-60.

Brent Ritchie J. R., H.G. Gordon McDougall and D. John Claxton, 1981, "Complexities of Household Energy Consumption and Conservation", *The Journal of Consumer Research,* Vol. 8, pp. 233-242.

Energy Efficiency Policies around the World: Review and Evaluation, 2008, World Energy Council.

Fred Vaanraaij W. and M. M. Theo Verhallen, 1983, "A Behavioral model of Residential Energy Use", *Journal of Economic Psychology*, Vol 3, pp 39-63.

Harper WB, Ralph Westfall and Stanley F. Stasch, 1986, "*Marketing Research, Text & cases*", V Kumar, Arya publishers, Delhi, India.

Household Consumer Expenditure in India 2005-06, 2008, NSS 62nd round, National Sample Survey Organisation (NSSO).

Intergovernmental Panel on Climate Change (IPCC), 2007, Fourth Assessment Report on Climate change.

Kothari C.R., 2007, "*Research Methodology, Methods and Techniques*", New Age International Pvt Ltd, India.

Krishnaswamy K. N., Appa Iyer Sivakumar and M. Mathirajan, 2006, "*Management Research Methodology, Integration of Principles, Methods and Techniques*", Dorling Kindersley (India) Pvt Ltd.

Lena Neij, Luis Mundaca and Elvira Moukhametshina, 2009, "Choice-decision determinants for the (non)adoption of Energy-Efficient (EE) technologies in households", European Council for EE Economy, *Summer study*, 687-695.

Pranati Dutta, 2006, "Urbanization in India", European Population conference.

Shobhakar dhakal, 2004, "Urban energy use and greenhouse gas emissions in Asian mega-cities- policies for sustainable future", *Urban environmental management project*, Institute for global environmental strategies.

Shonali Pachauri, 2004, "An analysis of cross-sectional variations in total household energy requirements in India using micro survey data", *Energy Policy*, Vol 32, pp 1723–1735.

SPSS manual, 1990, SPSS Inc.

Sudhakara Reddy B., 2004, "Economic and social dimensions of household energy use: a case study of India", Proceedings of IV Biennial International Workshop "*Advances in Energy Studies*", pp 469-477.

Wokje Abrahamse, Linda Steg, Charles Vlek and Talib Rothengatter, 2005, "A review of intervention studies aimed at household energy conservation", *Journal of environmental psychology,* Vol 25, pp 273-291.

Wouter Poortinga, Linda Steg, Charles Vlek, and Gerwin Wiersma, 2003, "Household preferences for energy-saving measures: A conjoint analysis", *Journal of Economic Psychology,* Vol 24, pp 49-64.

# LEARNING FROM VERNACULAR ARCHITECTURE OF CITIES OF IRAN TO SAVE ENERGY

*Shahryar shaghaghi G*., Eshagh Rasuli S., Hamidreza Zamani

(Islamic Azad University, Shabestar branch, Shabestar, Iran)

**ABSTRACT:** The subject of the climatic design has been vastly discussed for decades. The discussions are primarily fueled by issues surrounding global warming, environmental pollution, and energy conservation for the next generations. This is now considered as sustainable development. Analysis of applied strategies in designing vernacular and traditional buildings in each region can help solve a significant portion of the problems caused by local climatic issues. Additionally, these analyses can help optimum designing new buildings, as well. Iran is a multi climate country. As it is evident in regional designs of buildings in various regions in Iran, each region has its own unique climatic design. This has brought diversity and unique identity to regional urban fabric. For instance, comparison of two cities one located in a hot and dry climate and the one in a cold and dry climate could clearly reflect the unique strategies applied in designing buildings in each region. The same strategies can be still used in designing new buildings and settlements to not only reduce energy consumption, but also help decrease air pollution and global warming, which ultimately would help conserve the fossil energy resources for next generations. Iran's climate can be divided in two categories; "hot and dry" and "cold and dry". There are some similarities and differences between these two climates, which is why I have selected them for my discussions and analysis.

## INTRODUCTION

In recent decades, the issues of economizing energy consumption and usage of renewable energies are widely debated. Notification to vernacular and tradition architecture can potentially help discover many strategies to save energy in old buildings, that didn't have cooling and heating technologies to conserve energy and protect against energy losses. In Iran, a vast majority of the country is impacted by two distinct climates in which major energy consumption strategies have been historically applied in designing of buildings. The "cold and dry" climate can be seen in North West, North East, and West regions of the country and "hot and dry" climate are spread out in the central part, Eastern, and South Eastern regions. Study of the vernacular architecture and urban fabric of cities in these areas can help us learn how the local buildings have been designed to hedge against their regional climates and help conserve energy. The results of these studies can help architects properly design new buildings and urban districts to save significant amount of energy in the future.

In this article, two large cities, Yazd, located in the "hot and dry" region and Tabriz, located in the "cold and dry" climates are selected for further analysis and discussions. These are two large and highly populated cities, which have some similarities and differences in their unique architectural designs for energy conservation.

## MATERIALS AND METHODS

The data for this research was collected from books, articles, and local studies in Yazd and Tabriz by the authors. Additionally, some climatic data was obtained from departments of meteorology of the two cities.

---

**Climatic Conditions of Yazd City.** Yazd is located in center of Iran near the central desert of the country. The humidity rate is very low for its distance from sea, while the alteration of temperature between seasons and day/ night is quite high. Winter is very short, cold, and dry and summer is very long, hot, and dry. These characteristics have resulted in such harsh climatic conditions that require specific designs for buildings and urban fabric.(Table1)

**TABLE1.** Average monthly temperature of Yazd city

| MONTHS | MAXIMUM | MINIMUM | DAILY AVERAGE |
|--------|---------|---------|---------------|
| Jan. | 11.9 | -0.9 | 5.5 |
| Feb. | 15.3 | 1.8 | 8.5 |
| March | 20.4 | 6.6 | 13.5 |
| Apr. | 25.7 | 11.7 | 18.7 |
| May | 31.9 | 17 | 24.4 |
| June | 37.4 | 21.8 | 29.6 |
| July | 39.2 | 23.9 | 31.6 |
| Aug. | 37.6 | 21.4 | 29.5 |
| Sep. | 33.9 | 16.9 | 25.4 |
| Oct. | 27.3 | 10.3 | 18.8 |
| Nov. | 19.3 | 4 | 11.7 |
| Dec. | 13.5 | -0.3 | 6.6 |

**Specifications of Buildings and Urban Fabric of Yazd.** The aforementioned climatic conditions in Yazd have shaped the unique urban fabric of the city. The architectural responses to these conditions are as follow:

*Interior inclined pattern of buildings.* The buildings have been built with a central yard, where each building is surrounded its yard. All openings are toward the central yard; there are no other openings to the outside of building except for the entrance. This pattern is called interior inclined and makes two major parts in the buildings; the summer parts and the winter parts. These two parts can have equal areas or, alternatively, in some cases the summer parts may have bigger because summer seasons are long. (Ghobadian,2000)

*Usage of cubic forms.* The cube has a big inner space and a small surface area, where the proportion is 8 to 1. This indicates that a cube is a most suitable volume for this climate, as it has the lowest surface area countered to the outside. During the winter or summer this causes low air convection between inside and outside of the building. It must be mentioned that in the cubic form, the southern side must be bigger than all other sides, especially the eastern and the western sides. This is because sunlight absorption in the winter has canopies against the summer light. The southern side usually is 1.3 times bigger than the other sides.

*Color of materials.* The color, especially in the summer is white or light colors to reflect the summer light. The material is usually white plaster in this side. (Mofidi,1998)

*Type of materials.* The materials used are insulations and have high thermo capacity to absorb energy at day time and give it back to the inner spaces at night. This property especially used in the winter to save more heat during the winter nights. All buildings in Yazd have outer walls built by brick, which are up to one meter thick to prevent air convection.

*Height of ceilings.* In the summer part, the buildings have high ceiling while in the winter parts the height is standard; in the winter parts the areas must get warm rapidly. This property can help accomplish that, while in the summer parts, the inner spaces must remain cool, hence, high ceilings are essential.

*Type of ceilings.* In this climate, most ceilings are flat or dome shaped. The dome shape has advantage to the flat, because these types of ceilings always create shade in one half of their own surface. Additionally, a dome makes chimney effect, which make air ventilation in inner spaces.(Figure1)



**FIGURE1.** Dome shaped ceilings in Yazd city

*The pit yards.* Most buildings of the City, have two level yards in ground and underground levels. This means that, underground floor also has a yard that called pit yard. The underground floor has the warmest area in the winter for its winter sunlight and coldest area in summer for the shade.(Figure2)



**FIGURE2.** A pit yard in Yazd city

*Usage of underground floors.* As previously mentioned, buildings of the City have an area called cellar or underground floor so that one floor of the buildings buried into the ground. This floor has minimum air transition to outside, because the ground is the best insulation.

*Usage of windward in summer parts.* The summer part shave elements called windward, which are little spires mostly in cubic form and can lead the wind to the inner spaces at daytime, while it make chimney effect at night. (Figure3)



**FIGURE3.** Wind wards of Yazd city

*Rotation of buildings.* The southern sides of buildings are rotated about 17º to the South West or South East to get maximum sunlight in the winter and maximum prevailing wind in the summer. (Kasmaee,1995)

*Urban fabric.* The city has a compact urban fabric and narrow alleys with high walls to create shade in the summer. The alleys have arcades and porticos to make more shade in the summer.(Figure4)



**FIGURE4.** Fabric of Yazd city

**Climatic Conditions of Tabriz City.** This city is located in North West of Iran in a mountainous region. So it has a low humidity rate and a high temperature alteration. Summers are short and mild, while winters are long, cold, dry, and snowy.(Table2),(Meteorology department of Tabriz city)

**TABLE2.** Average monthly temperature and snowing/ raining rates of Tabriz:

| PARAMETER MONTH | AVERAGE TEMPERATURE (˚c) | AVERAGE RAINING &SNOWING(mm) |
|---|---|---|
| Jan. | -2.3 | 29 |
| Feb. | zero | 25.5 |
| Mar. | 5.3 | 47 |
| Apr. | 11.2 | 53.2 |
| May | 16.4 | 44.7 |
| June | 21.7 | 17.5 |
| July | 26 | 4.4 |
| Aug. | 25.6 | 3.3 |
| Sep. | 21.4 | 8.8 |
| Oct. | 13.8 | 26.9 |
| Nov. | 6.9 | 29.3 |
| Dec. | 1.2 | 18.7 |

**Specifications of Buildings and Urban Fabric of Tabriz City.** Major specifications of the City, which differentiates it from other cities, are as follow:

*Interior inclined pattern for buildings.* Most buildings have central yards, which the summer parts are quite small. In many buildings summer yards have been eliminated altogether as the summer seasons are only about two months, while, the winter parts are quite large, as the winters are quite long.(Figure5&Figure6),(Soltanzadeh,1995)

**FIGURE5.** A house in Tabriz with central yard
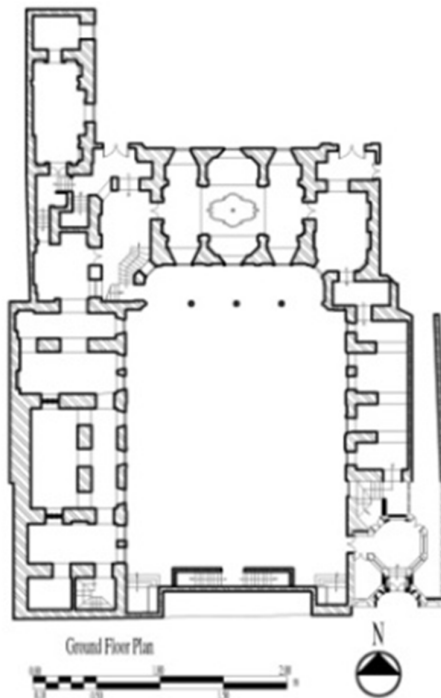


**FIGURE6.** Plan of a house with central yard in Tabriz, which is built in u-shape.

*Usage of cubic forms in buildings.* Similar to the Yazd's buildings, most buildings in Tabriz are made in cubic form for pretty much the same reasons. (Large inside and little surface area). (Ghobadian,1997)

*Color of materials.* The colors are mostly dark to help absorb maximum solar energy in the winter. (Mofidi,1998)

*Type of materials.* Similar to materials used in Yazd's buildings, materials used in buildings in Tabriz have high thermo capacity to absorb solar energy during the day and give it back to inner spaces at night. This help prevent air convection between inside and outside.(Shaghaghi,2005)

*Height of ceilings.* All parts of buildings have standard height to help inner spaces get warm rapidly.

*Type of ceilings.* Most buildings have flat ceilings and roofs to keep snow on it, as snow is a good insulation and don't let heat loss from the ceiling.(Shaghaghi,2011)

*Underground floor.* Similar to Yazd's buildings, buildings in Tabriz have also underground floor to decrease surface area.

*Building rotation.* The southern side of buildings are mostly rotated to south east about 12º to get maximum sunlight in winter mornings. (Kasmaee,1995)

*Urban fabric.* The urban fabric is completely compact with medium width alleys having low height walls to get maximum sunlight in winter days. Most alleys have organic shape to prevent wind blow. (Figure7)



**FIGURE7.** Fabric of Tabriz city

*Exterior inclined pattern of buildings.* There are other building patterns in Tabriz that called exterior inclined pattern. In these types of buildings northern and eastern sides have fewer windows to encounter to polar and winter wind with maximum width of walls, while, southern sides have large windows with canopies to get maximum sunlight during the winter. (Figure8), (Shaghaghi,2004)



**FIGURE8.** A house with exterior inclined pattern in Tabriz

**CONCLUSIONS**

The following table outlines differences and similarities of the two cities:

As it is detailed in this table, there are some similarities and differences in the architectural structure of these two cities. The differences are primarily driven by differences in winter and summer seasons ( in terms of duration, temperature, humidity, etc) in these cities. If these strategies are used in new buildings and urban contexts, it can potentially have significant impact on economization in fuel and energy consumption in the country, because most major cities in Iran are located in these two climates. Furthermore, if these strategies are extended in other cities, it can decrease a great deal of energy consumption. These strategies can be used in other countries which have similar conditions.

**TABLE3.** Total comparison of the two cities

| TITLE | Tabriz | Yazd | |
|---|---|---|---|
| Building pattern | Interior & exterior inclined | Interior inclined | |
| Buildings volume | Cubic | Cubic | |
| Color of materials | Dark | Light | |
| Type of materials | Insulation/ thermo capacity | Insulation/ thermo capacity | |
| Height of ceilings | Low | High in summer part/ low in winter part | |
| Roof coverage | Flat | Flat/ dome | |
| Yard | Ground yard | Pit yard | |
| Underground | Underground floor | Underground floor | |
| Wind ward | No wind wards | Wind wards in summer parts | |
| Building rotation | 12º to southeast | 17º to southeast or southwest | |
| Urban fabric | Compact | Compact | |
| Width of alleys | Medium | Narrow | |
| Height of outer walls | Low | high | |

**ACKNOWLEDGEMENTS**

**REFERENCES**

Kasmaee, M. 1995. *Climate & Architecture(*in Persian*)*, Kaktus publishers, Tehran, Iran.

Ghobadian, V. 1997. *Climatic design*(in Persian*)*, University of Tehran, Tehran, Iran.

Ghobadian, V. 2000. *Climatic analysis of vernacular buildings of Iran(*in Persian*)*, University of Tehran, Tehran, Iran.

Soltanzadeh, H. 1995. *Tabriz a stable brick in traditional Arch. of Iran(*in Persian*)*, Cultural researches press, Tehran, Iran.

Mofidi, M. 1998.*Climatic urban design.* Ph.D. Thesis , Sheffield University, Sheffield, England.

Shaghaghi, Sh. 2005. *Strategies of sustainable development in urban fabric(*in Persian*)*, Ph.D. thesis, Islamic Azad University, Science & research branch, Tehran, Iran.

Shaghaghi, Sh. 2004." Clear energy at home, a strategy to reduce fuel consumption"(in Persian), Journal of  Shahrdariha,70(6):45-51,Tehran,Iran.

Shaghaghi, Sh., and P.V. Shakiba, 2011. "Analysis of climatic strategies in designing of residential buildings in cold dry climate of Tabriz metropolis to reduce air pollution in urban environment" , pp.497-500.  International conference on building science and engineering (ICBSE), Venice, Italy.

# PEAK OIL: KNOWLEDGE, ATTITUDES, AND PROGRAMMING ACTIVITIES IN PUBLIC HEALTH

*Sammi L. Tuckerman* (The Ohio State University)
*J. Mac Crawford* (Clinical Public Health Environmental Health Sciences at the Ohio State University)
Robyn S. Wilson (Environmental Decision Science and Risk Analysis at The Ohio State University)
W. Berry Lyons (The Byrd Polar Research Center at the Ohio State University)

Peak oil is the point at which the production rate of conventional crude oil can no longer be increased; and globally, annual petroleum production goes into irreversible decline. It has great implications on the future of US as well as global energy resources and policy. Will we run out of oil before infrastructure advancements can be put in place? Will we turn to coal or tar sands to replace oil, in turn increasing our carbon footprint and hastening the intensification of anthropogenic climate change? These questions are largely unanswered. With increasing concern on how peak oil will impact human health, public health agencies and medical centers must prepare to address the impacts predicted to affect their jurisdiction.

This project seeks to identify the most effective ways to move the public health system to adopt strategies aimed at reducing the carbon footprint on a population scale. A research project at The Ohio State University sought to identify what factors lead Environmental Health and Nursing Directors to address peak oil mitigation and adaptation in their jurisdictions. A web-based questionnaire was completed by a national sample of approximately 200 environmental public health directors and 175 public health nursing directors eliciting knowledge, attitudes, and programmatic activities around the issue of peak oil. Multivariable regression methods will be used to evaluate the influence of knowledge, attitudes and socio-demographic variables on the likelihood of health departments engaging in peak oil mitigation planning and programming. The presentation will discuss the project's results (analyses are in progress) and will suggest solutions to help increase the number of Environmental Health and Nursing Directors addressing the issue of peak oil. As with many public agencies, local and state health departments are struggling with budgetary constraints. To the extent these directors see the need for this programming and would like to engage their constituent populations in peak oil mitigation, their ultimate success will depend on funding and effective communication.

# A SUITABLE FOOD WASTE DISPOSER SYSTEM IN KOREA

*Yong-Woo JEON*, Hae-Min YOO, and Jong-Woo KANG(Korea Testing Laboratory, Seoul, Republic of Korea)
Dong-Hoon LEE (The University of Seoul, Seoul, Republic of Korea)

**ABSTRACT:** A food waste disposer is a device, electrically powered, installed under a kitchen sink between the sink's drain and the trap which shreds food waste into pieces small enough to pass through plumbing. Use of this unit is convenient and hygienic for discharging food waste in kitchen. Nevertheless, it has been illegal until now in Korea because of a conflict with the government's policy-resource recovery from food waste-and a perceived threat of damage to the city's sewer system. Kitchen waste disposer units increase the load of organic carbon that reaches sewage treatment plant, which in turn increase the consumption of oxygen. But there is a growing need to introduce this unit in Korea lately for manhattanization and ageing society, etc. So an attempt was made to introduce the food waste disposer system of 'treatment type before discharging to sewer', but it was not appropriate for Korean situation. In this study, we suggest a suitable disposer system in Korea based on a proper disposer technology followed by an innovative solid-liquid separation technology. After grinding and solid-liquid separation using these technologies, less than 20 percent solids were discharged as wastewater. This novel food waste disposer system can allow satisfaction with the government's policy and more high-quality resource recovery from food waste in the facilities.

## INTRODUCTION

The amount of food waste generated per day in Korea reaches approximately 14,000 tons (based on 2010 data), and it accounts for 28% of the total domestic waste, which is the highest portion among the domestic waste types (MoE, 2012). This is a significantly high amount compared to the U.S., where food waste accounts for 10% of the total domestic waste. Most of the food waste generated (95.5%) is turned into compost or feed in a recycling facility, but this has causes for concerns due to the following reasons: cost related to separation, discharge and collection, heterogeneity of food waste, foreign substances and salt contained in food waste, occurrence of odor during the treatment process, and disposing large amounts of highly concentrated wastewater generated during the treatment process in accordance with the prohibition of ocean dumping, etc.

Due to the problems arising from the existing treatment process for food waste, introduction of the food waste disposer system is being reviewed in Korea. The food waste disposer, which is a device developed by John W. Hammes in the U.S. in 1927, grinds food waste generated in the kitchen to be discharged into the sewer (K. S. Kim et al., 2010). This is a highly hygienic and convenient device in terms of the discharge, storage and collection of food waste as it quickly processes food waste, prevents unpleasant odor occurring during the storage process, and eliminates the need for a separate collection container or bag. However, it poses concerns for an increased pollutant load in the sewer system, soil and groundwater contamination in areas without a well-maintained sewer system, suspension of sewage flow due to deposition of shredded food waste within the sewer system, and occurrence of odor from decomposition. For these reasons, the use of the food waste disposer system is currently prohibited in Korea.

In Korea, research and pilot projects for the distribution of disposer system were conducted, centering on the 'treatment type before discharging to sewer', in which the ground food waste and wastewater from the kitchen pass through the wastewater treatment system to be treated into a form that

does not increase the pollutant load before being discharged into the public sewer system. However, the 'treatment type before discharging to sewer' has a disadvantage in that the facility and treatment costs are too high, and still poses the fundamental problem of being in conflict with the food waste recycling policy of the Ministry of Environment. Thus, the aim of this study is to propose a new food waste separation and discharge system that can collect and recycle solid materials from the ground food waste using the liquid-solid separation technology, through which commercialization of the food waste disposer in Korea is expected.

## MATERIALS AND METHODS

**Experimental Equipments (Disposer System):** Figure 1 shows the configuration of the experimental system, which consists of a food waste disposer, a storage and service tank, a solid-liquid separation unit, and solid and liquid collectors connected in series. The disposer applied to this system is equipped with hammer mill and cutter as a dual-grind feature, and is characterized by the forced transport function of the impeller structure that reduces the problem of deposition of ground food waste and blocked plumbing. Also, in order to use less water during grinding, it is equipped with a separate container to store wastewater generated during cooking and dish-washing, which is another feature that differentiates this disposer from the existing disposer.

The solid-liquid separation unit installed in the latter part of the disposer is a device to ensure efficient separation of solid and liquid materials in the ground food waste, and it is designed to collect solid materials in a solid collector using the solid delivery pump, and allow liquid (wastewater) to pass through the internal filter and be discharged into the liquid collector.

For convenience in the long-term experiment, a storage and service tank was installed in between the disposer and the solid-liquid separation unit, and the ground materials from the disposer were automatically supplied in a designated quantity to the solid-liquid separation unit using the volumetric pump. With the total capacity of the storage and service tank being 500 L, a five-day amount of ground materials from the disposer could be stored. In order to minimize the decomposition and destruction of food waste during storage and feeding, a chiller was installed to keep the internal temperature of the tank cool, and the pump and agitator were operated in conjunction only during feeding by using a timer.
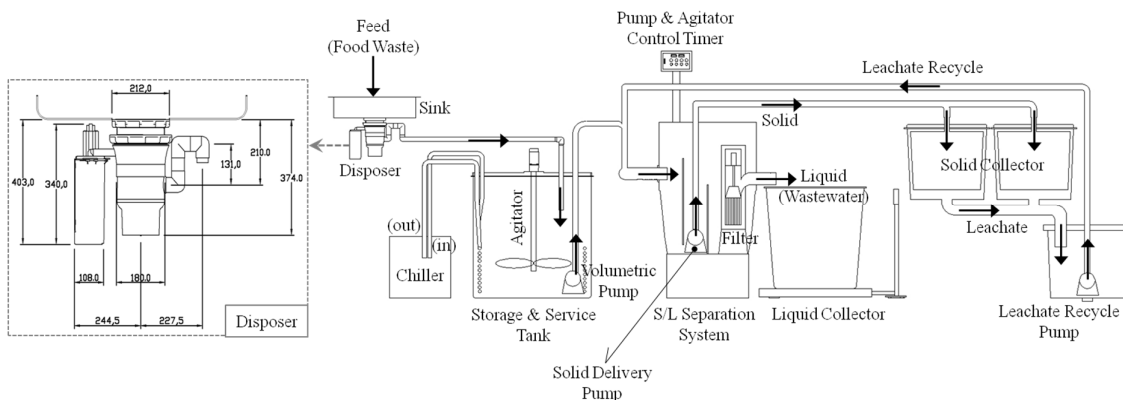


**FIGURE 1.** Schematic diagram of the experimental system coupled with food waste disposer and solid-liquid separation apparatus.

**System Operation and Experimental Method.** Food wastes generated from a variety of Korean restaurants around the laboratory were used in this study, and the average proportions of the food types are shown in Table 1. In comparison with the general food waste composition in Korea, the food wastes used in this study are characterized by the relatively high amount of grains and low amount of fruits.

**TABLE 1.** Average food waste composition used in the experiment.

| Category | Grain | Vegetable | Fruit | Fish & Meat | Foreign Substance | Total |
|----------|-------|-----------|-------|-------------|-------------------|-------|
| Experiment | 35.9% | 40.8% | 4.1% | 17.5% | 1.6% | 100% |
| Standard food waste composition in Korea | 16±2% | 51±5% | 14±2% | 19±2% | - | 100% |

The amount of food waste fed into the disposer system was equivalent to the daily amount of food waste generated from 30 households living in apartment units, which was calculated to be 14.44 kg/day based on the statistics of Korea (average number of members in 1 household in an apartment housing: 3.1 persons/household, daily amount of food waste generated per person living in an apartment housing: 155.3 g/person·day). The average amount of food waste fed into the disposer system was 14.58 kg/day, and the amount of water used during grinding was 5 L/kg of food waste based on the results of previous studies.

The total operation period was 25 days, during which the feeding of food waste was conducted for 23 days and collection of solid and liquid materials took place without the feeding of food waste in the last 2 days prior to the completion of the operation. Ground materials were fed into the solid-liquid separation unit 3 times a day in the morning, during lunch hour and at night, in accordance with the times when food waste is generated in reality. Collection of solid materials was performed automatically 1 hour after the feeding. In order for the performance assessment and establishment of mass balance of the system, the amounts of food waste fed into the system, collected solids, and discharged wastewater were measured and the total solid (TS) was analyzed, through which the solid recovery rate and solid discharge rate were calculated. In addition, the wastewater's BOD, $COD_{Mn}$, SS, T-N, T-P and so forth were analyzed.

## RESULTS AND DISCUSSION

The average amount of food waste fed into the system during the operation period was 14.58 kg/day with an average moisture content of 80.99%, and the average amount of solids collected from the food waste was 2.82 kg/day (Figure 2).

The behavior of solids from the fed food waste, collected solids, discharged wastewater and remnants during the operation period is shown in Figure 3. Based on the cumulative amount of solids, 40.06% of the solids fed into the system were recovered as solid matter, while 16.09% were discharged as wastewater and 43.85% remained inside the system. The solid discharge rate was under 20%, which satisfied the 'standard solid discharge rate (under 20%) for the wastewater discharge-type food waste disposer' of Korea. However, the solid recovery performance of the system was found to be slightly poor as only half of the remaining solids, excluding the solids discharged as wastewater, were recovered, with the rest of the solids remaining inside the system.

On the other hand, Figure 3 shows that in the first 7 days of the operation, the amount recovered as solids is relatively low, with a large amount of the fed materials remaining inside the system. This could be explained by the fact that clean water was filled into the solid-liquid separation unit before operation, requiring a stabilization period of approximately 7 days. Thus, excluding the stabilization period, i.e. 7 days after the start of operation, 49.60% of the solids fed into the system were recovered as solids, with 21.23% discharged as wastewater and 29.17% remaining inside the system.
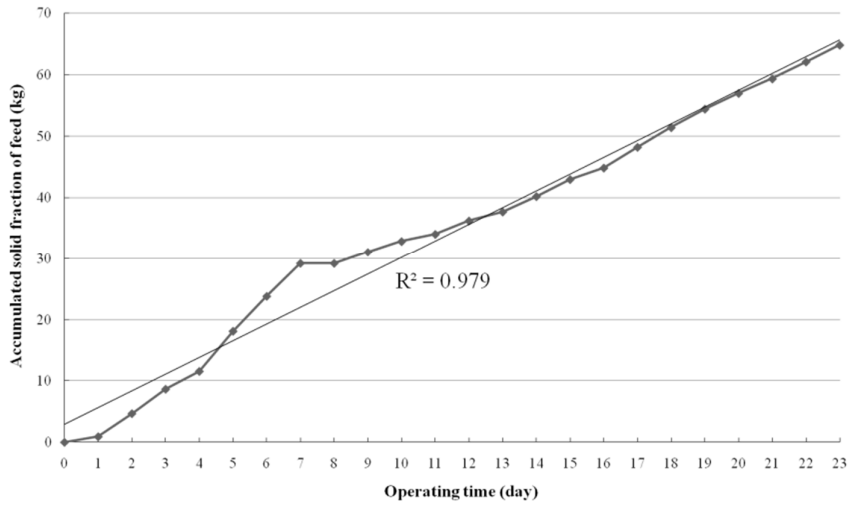
**FIGURE 2.** Accumulated solid fraction of feed (food waste).
Average solid fraction of feed was 2.82 kg/day ($R^2 = 0.979$).
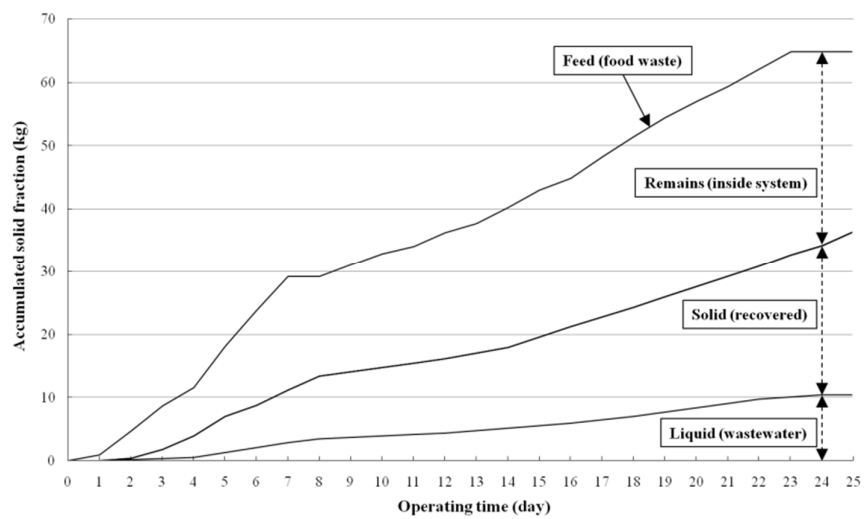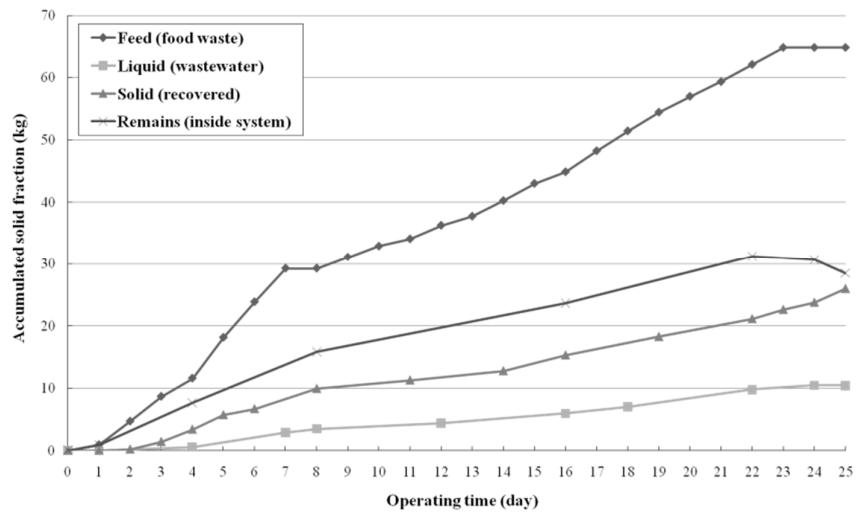




**FIGURE 3.** Accumulated solid fraction of feed, liquid, solid, and remains.

The results of the analyses of BOD, COD, SS, T-N and T-P of wastewater according to the operating time are shown in Figure 4. The overall concentration of wastewater does not significantly exceed the concentration levels of the actual domestic wastewater. Also, since this experiment ignored the inflow of wastewater other than the ground materials from the disposer, the concentration levels of the discharged water are expected to be lower with an inflow and mixture of domestic wastewater such as wastewater from the kitchen and to stay within the present concentration range of domestic wastewater.
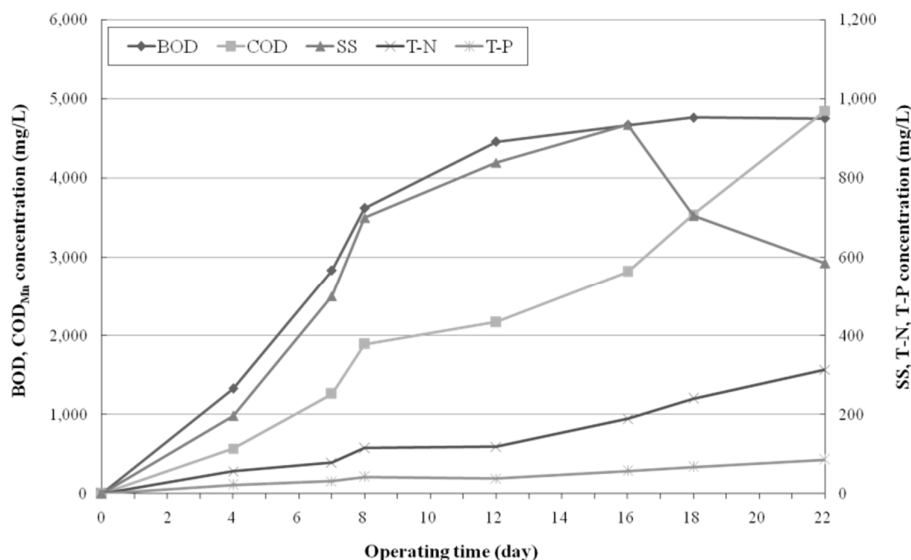


**FIGURE 4**. Concentration of water pollutants in the discharged water according to operation time.

**CONCLUSION**

Based on the final cumulative amount of solids, 40.06% of the solids fed into the system were recovered as solid matter, while 16.09% were discharged as wastewater and 43.85% remained inside the system. After the stabilization period, i.e. 7 days after the start of operation, 49.60% of the solids fed into the system were recovered as solids, with 21.23% discharged as wastewater and 29.17% remaining inside the system. The amount of solids discharged as wastewater was under 20%, which was satisfactory, yet the solid recovery rate was poor at less than 50%. Thus, there is a need to design and operate a system with a higher solid recovery rate in future research.

**ACKNOWLEDGEMENTS**

**REFERENCES**

Environmental Statistics Portal. 2012. Current Status of Waste Production in Korea. Ministry of Environment (Republic of Korea). http://stat.me.go.kr/nesis/index.jsp (assess date : May 16, 2012).

K. S. Kim, and K. Y. You. 2010. Food Waste Disposer, Kwangmoonkag, Korea.

Enforcement Regulations of the Wastes Control Act. Article 10. Ministry of Environment (Republic of Korea). http://www.me.go.kr

# ASSESSMENT OF CLEANER PRODUCTION OPTIONS FOR ELECTROLYTIC MANGANESE METAL INDUSTRY OF CHINA

***Zhigang Dan***, Xiuling Yu and Fan Wang
(Chinese Research Academy of Environmental Sciences, Beijing, China)

**ABSTRACT:** The electrolytic manganese metal (EMM) industry in China has a proportion of 97% of global output makes an important contribution to national and world economy. However, the rapid growth of EMM industry has resulted in heavy environmental pollution as it generates large amount of solid waste and wastewater with high manganese and chromium content. This study explored the applicability of clean technology options to improve the environmental performance of EMM plants in China. Three options proposed from screened, survey, expert questionnaires and integrated assessment mainly involved technology modification in the pressure filtration process, recycling of valuable elements in waste water, and recycling of manganese mud. An integrated cleaner production system based on the proposed options was formed and then implemented in the factory. Results showed that a reduction of 50% manganese loss in mud, recycling 95% of manganese in wastewater and recycling manganese mud can be achieved. This study verified that application of cleaner production technologies is effective environmental policy to solve heavy environmental pollution in the EMM industry of China.

**KEYWORDS:** Manganese pollution reduction, Manganese mud recycle, Cleaner production, Electrolytic manganese metal

## INTRODUCTION

As an import basic material industry, electrolytic manganese metal (EMM) industry provides products ,which are widely used in non-ferrous metallurgy, electronics, chemical industry, environmental protection, food hygiene, welding, aerospace industry and other fields. The Chinese EMM industry has grown at a dramatic speed since the first EMM production facility was established in 1956 (Tan, 2005). After more than 50 years of development, China now has a dominant role in global EMM production, and accounted for 97.4% of the total world annual production and 98.6% of the total world annual production capacity in 2008 (Manganese Metal Company, 2009; Tan, 2009). With rapid development of the Chinese economy in recent years, the rise in EMM output in China maintained an average rate of 30% from 2000 to 2009 (Fig. 1). As indicated in Fig. 1, the annual Chinese EMM production output in 2009 expanded 78-fold compared with that in 1990. It is remarkable that both the annual output and capacity in 2007 increased more than in previous years, and for the first time China's annual output of EMM exceeded 1 million tons.

The EMM industry as a whole is generally known as an industry with high level of resource consumption and large quantities of waste discharge. In China, on average, to produce 1 ton of EMM, 6–9 tons of solid waste and 1–3 tons of waste water are discharged into the environment. In addition 0.9–1.9 kg of selenium is consumed to produce 1 ton of EMM and selenium pollution cause a worldwide concern (Lemly, 2004; Reilly, 2006). The situation has become worse as the grade of manganese ores gets lower due to depletion of mineral resources, which means more and more waste will be generated due to EMM production (Yu, 2006).

With the increasing concern on environmental problems, issues on the pollution caused by EMM industry have been considered in the government agenda. To effectively control such pollution becomes an urgent task for researchers and managers. Cleaner production (CP) has been widely recognized as a useful approach to mitigate pollutions during industrial production (Boyle,1999; Frijns,1999). With the technologies of CP being introduced into Chinese industry since 1990, remarkable improvement has been achieved in pollution reduction (Duan, 2007; Li, 2008). The emphasis of such reduction has transferred from the terminal treatment to the beginning cut and the whole-procedure control. After two decades practices on CP, tremendous benefits on social, economic and environmental aspects were obtained.

However, for EMM industry in China, the evolution process is relatively slow and more effective CP systems are needed. To improve the efficiencies of reduction on pollutants discharge and resources consumption, effective assessment and optimization of CP systems for EMM industry are desired.
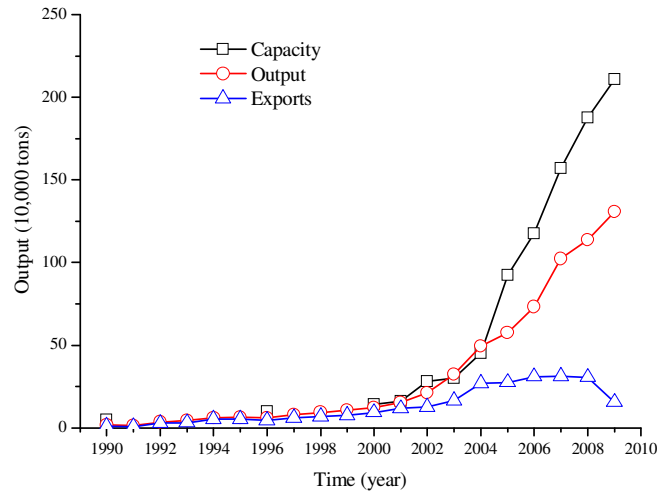


**FIGURE 1 Chinese EMM output, exports and capacity from1990 to 2009**

The objective of this study is to assess the CP options and design an optimum production system for the EMM industry in China. The objective entails as follows: (a) to propose a series of optimized options of CP system for EMM production; (b) to apply the proposed options for a real-world case, which will be targeted on the Woning EMM Factory (WEF) in Southwest China; (c) to assess the proposed options by evaluating their effects on waste reduction; and (d) to identify the optimum CP system which will be recommended for implementation in the EMM industry of China.

## OVERVIEW OF THE STUDY FACTORY

**Basic status** The Woning EMM Factory (WEF) was one of biggest company, founded in 2004. This factory is situated in Xiushan County Chongqing City, Southwest China, and occupies a large land area of 30000 $m^2$. It has a production capacity of 30,000 tons of EMM per year and single process lines producing 10,000 tons of EMM per year. In 2007 and 2008, the EMM output of WEF was 29,000 tons and 28,000 tons, respectively. WEF is technologically and managerially advanced in China.

As shown in Fig. 2, the production process of WEF, using manganese carbonate ore as raw material, is a traditional hydrometallurgical process (Zhang, 2007). The EMM production process is described briefly as follows: Step 1: Sulfuric acid, $MnO_2$ and ammonia are added to crushed ores to leach manganese ions from the ores, and to obtain theMnSO$_4$-contained slurry; Step 2: The slurry is pressed and purified to produce electrolyte by filter equipment; Step 3: The electrolyte is pumped into electrolytic cells and manganese is deposited on cathode plates; Step 4: The cathode plates with manganese metal are pulled out from the cells for passivation in potassium dichromate solution; Step 5: The cathode plates are washed and dried, manganese is stripped from the plates and final products are obtained.
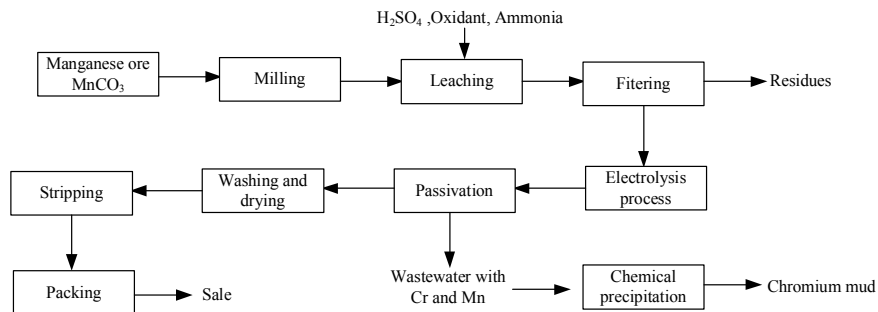


**FIGURE 2 Flow diagram of principle procedures for EMM Factory**

**Analysis of wastes generation and discharge** Wastewater and sludge which once result in serious environmental pollution are the main environmental problems in EMM industry.

Firstly, huge potential ecological and environmental risks on large number of landfill sites in manganese mud. Manganese mud containing manganese, ammonium sulfate, etc. not only pollute the environment but also waste resources. Producing 1 ton EMM has 6- 9 tons manganese mud emissions currently, our stock of manganese mud reached 44.69 million tons, and an annual increase of more than 800 million tons. Almost all of existing landfill field stacked with simple treatment such as using local stone as dam material, overloading fill, without seepage control measures, improper location. All of these bring serious environmental security risks, once the collapse would be disastrous. In addition, the manganese mud with 3.0-4.0% Mn (total manganese content of 18-25% in ores) is not being used.

Secondly, large volume, high concentration and chromium-containing are characteristics of wastewater from EMM industry. The dense wastewater generating from electrolysis process has an average of manganese 1500mg/L, hexavalent chromium 200mg/L, respectively. Currently, simple chemical methods were applied to treat the chromium-containing wastewater treatment. The shortcomings of this approach are listed as high operating costs; unstable operation; high value of the hexavalent chromium converting into low-value trivalent chromium, manganese and chromium precipitating in sludge; producing hazardous waste residue, secondary pollution.

## DESIGNS OF CP OPTIONS

The CP system is an integrated technology group, which is expected to be composed of a series of individual techniques. Based on the survey on 43 typical EMM factories and questionnaires of related experts/engineers/technicians, three groups of CP technologies were screened for designing the proposed CP options and then the integrated CP system. The principle screening processes and related criteria are illustrated in Fig. 3 and Table 1 (Yu, 1999), respectively.

**TABLE 1 Criteria for screening CP options**

| Economy | Environment | Technology |
|---|---|---|
| Gross investment | Water saving | Equipment modification |
| Operation cost saving | Energy saving | Equipment purchase/installation |
| Increased cash flow | Wastewater discharge | Workers training |
| Inner rate of return | Manganese mud discharge | Technology transformation |
| Net present value | Chromium mud discharge | Productivity |
| Net income | manganese utilization ratio | Product quality |
| Pollution treatment cost | | Flexibility/feasibility |
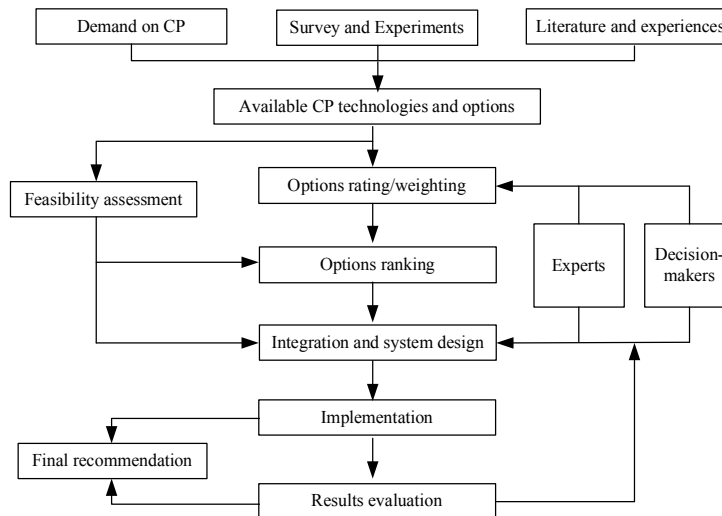


**FIGURE 3. The screening process for CP options**

According to the criteria, CP options can be came from use of raw materials and energy, technology transformation, maintenance and renewal of equipment, optimum of process control, change and improvement of product, reuse and recycle of waste, strengthening management, improvement on staff skills. A series of possible CP solutions will help create a more integrated and effective CP system. After the screening procedure based on consideration of environmental impacts and economic benefits, three integrated CP options for promoting CP in WEF, increasing resource utilization ratio, reducing pollutants emission and recycling solid waste are suggested as Table 2.

**TABLE 2 Introduction of three CP options**

| Option No. | Option 1 | Option 2 | Option 3 |
|---|---|---|---|
| Name | Reducing Mn-containing in manganese mud | Recovering and reusing Cr and Mn ions from wastewater | Producing building materials with manganese mud |
| Effect | Decreasing Mn-containing in residues, increasing manganese utilization ratio | Reusing manganese ions and bichromate, no chromate mud and manganese mud during wastewater treatment | Harmless treatment of manganese mud, recycling utilization |
| Type | Technique reformation | Waste reusing | Waste recycling |
| Equipment | Multi-function membrane pressure filter | High performance adsorption materials, exchange pole, control system | Pretreatment and press forming equipment |
| Benefit （1,000$） | 437 | 158 | 576 |

**CP option 1: Reducing Mn-containing in residues** After leaching, the mixed liquid containing high concentration $Mn^{2+}$（$C_{Mn}^{2+}$:32-36g/L）need to be separated by press filter to prepare qualified electrolyte. Under current process, the residue pressed by filter still has 30% water, an aqueous solution with high concentration $Mn^{2+}$. 3.0-4.0% of total Mn in ores are loss in residue resulting a lower manganese utilization ratio about 70%. In tradition, the residue with high concentration $Mn^{2+}$ was sent to stockyard for stacking and many environmental problems are generated due to seepage. At this stage, Mn in the residue becomes pollutants as for environment, and for process, big in Mn loss.

Technology on reducing Mn-containing in manganese mud use multi-function membrane pressure filters to leach filter cake secondly, then wash it with little flesh water to decrease Mn residue. Compared with original process, this option only needs to modify the press filter and control system. The modified process is quiet easy and does not require extra training for workers. The gross investment of this CP option is close to 1.03 million USD for a 350m$^2$ line. The flow diagram of principle processes of this option is illustrated in Fig. 4.
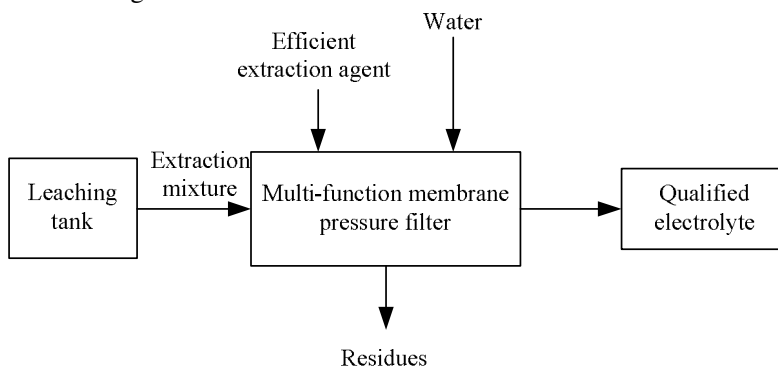


**FIGURE 4 The principle process flow diagram of option 1**

**CP option 2: Recovery and reusing Cr and Mn from wastewater** As previous statement, high concentration wastewater in EMM industry has high recovery values. Enterprises desire new advanced technology recycling valuable resources to overcome shortcomings of traditional technology in treated

wastewater.

Technology on recovery and reusing Cr and Mn from wastewater were developed successfully. It pretreated the wastewater firstly with precipitating in manganese highly. Then the pretreated wastewater with a lower Mn-bearing was exchanged by high performance adsorption materials which can enrich Mn and dichromate ions with different materials separately. The Mn-bearing precipitation and enriched dichromate can be directly returned to the main production process, avoiding the generation of hazardous waste. As a result, recycling rate of manganese and chromium was 95%. The total investment of this CP option at a 30,000t/a capacity is about 0.88 million USD. The flow diagram of principle processes of this option is illustrated in Fig. 5.
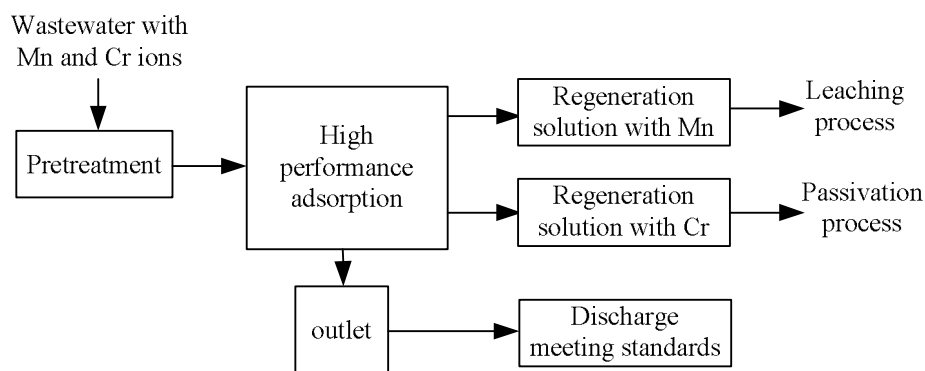


**FIGURE 5 The principle process flow diagram of option 2**

**CP option 3: Producing building materials with manganese mud** Manganese mud, large quantity and containing large number of dense pollutants, is the largest source of pollution in EMM industry as it is difficult to solve easily. From another perspective, manganese mud is also a kind of resources. Recycling utilization is root to solve pollution and environmental hazards due to manganese mud.

Technology on producing building materials with manganese mud brings a way to resolve problems in manganese mud. Harmless pretreatment is essential to recycling utilization to solidify soluble manganese and heavy metals, remove ammonia nitrogen. Pretreated residues and other raw materials with mixed are fabricate by press forming equipment to get final building materials. The keys to this technology are that not only solution to containing manganese sulfate residue, ammonia and other chemical ingredients affect product performance issues, but also ensure the environmental safety of products. It features as big adding capacity, low costs, and large market. The gross investment of this CP option is near to 1.18 million USD for adding residues 3 0,000t/a capacity.

**EVALUATIONS OF CP OPTIONS**

To identify the optimum CP system for the WEF, a comprehensive assessment of the proposed CP options was conducted. The expected option should be the one containing advanced CP techniques and being friendly to the environment, as well as bringing attractive economic benefits. In this study, the three proposed options were evaluated from multiple aspects of technology, economy and environment as follows.

**Technology aspect** Compared with existing technology, the option 1 used multi-function membrane pressure filters as a reactor on secondly acid leaching to achieve extraction of solvent and washing for residue. The manganese content in manganese mud can decrease from the traditional 3% down to 1.5%. The technique involved in this option are relatively mature and technically sound, several large-scale plants in China have applied it by demonstration line. No additional workers and impact on production quality result from implementation of this option. Approximately 600 tons soluble Mn in mud could be recovered annually, contributing to an increase about 10% of utilization ratio. The discharge of Mn and other associate pollutants is decreased significantly.

Option 2 recovering Cr and Mn from wastewater have been adopted in demonstration line in

China. Both $Mn^{2+}$ and $Cr^{6+}$ in the wastewater could be adsorbed by high performance adsorption material reaching at a proportion of 95%. And its concentration $Mn^{2+}$ and $Cr^{6+}$ would be recycled and increase to 30g/L and 7g/L, respectively, a suitable value used in main process of EMM industry directly. By employing this option, over 60 tons Mn and 25 tons bichromate can be reclaimed per year.

In option 3, producing building materials with manganese mud, is a practical technology. Environmental safety of using manganese mud is ensured with pretreatment by ammonia removal and solidification of soluble metal. Quality, leaching toxicity and radioactivity of building materials with 30% manganese mud meet the requirement of corresponding national standards. The annual emission reduction is about 20,000 tons of manganese mud. This option may be a feasible and attractive CP technology as it gives good solution to environmental risks on manganese mud stacking.

**Environment impact** In CP option 1, the discharge of Mn in mud is decreased by using second acid leaching and washing technology. Due to Mn-bearing in mud reduction, utilization ratio of Mn is increased, which contributes to ore consumption during the process. With an annual output of 30,000 tons of EMM plant, for example, it has a reduction of 3,000 tons manganese pollution annually, equivalent to saving manganese 20,000 tons.

By employing CP option 2, the discharge of chromium waste is greatly reduced during recovery and reusing Cr and Mn from wastewater. The reduction rate of Cr and Mn is up to 97%. As for an annual output of 30,000 tons of EMM plant, reduction in chromium waste, controlled as a dangerous waste in China, reaches 360 tons, and also 437 tons of manganese mud emissions.

Through CP option 3, manganese mud is used as raw material for bricks. The adding proportion is up to 30%. Recycling weight of residues will achieve 200,000 tons for an annual output of 30,000 tons of EMM plant, which find a key way on solution to manganese mud emissions.

**Economic benefit** In this study, the evaluation indices include a set of economic parameters, such as gross investment, net present value, net profit, operation cost saving, and inner rate of return. All the three CP options are compared (Fig. 6). Among them, the gross investment and the rate of return are the most critical factors, which strongly affect the decision of stakeholders and managers on the CP option choice of the factory. All options have sound financial indicators. If reviewed from economic return and net profit aspects, option 3 is better than options 1 and 2. However, option 3 presents a disadvantage of relative high capital investment for it requires purchase of new equipment and worker training, also for uncertainty of product sales. Options 1 and 2 have a similar profile for the five indicators, but option 1 has higher gross investment and lower operation cost saving. While, the economic return of option 2 is the lowest.
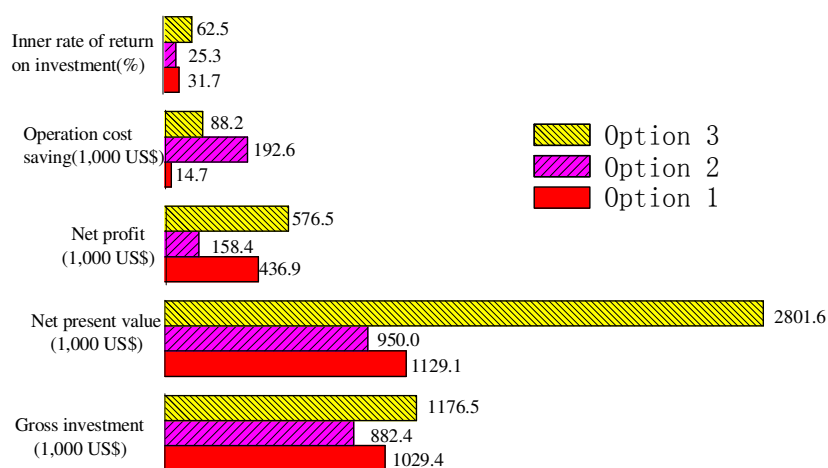


**FIGURE 6. Alternatives comparison of economic benefit**

**Integrated assessment** In terms of technical level, the three options are all involved with advanced CP technologies. They are feasible to implement and easy to operate. In terms of environment protection, all options reduce pollutant discharge and perform friendly to the environment. Among them, option 1 is the

best choice because it not only reduces Mn pollutants in mud, but also returns Mn to leaching process. In terms of economic benefits, each of the three options has strong points and can provide significant benefits. In general, the three options all satisfy the comprehensive requirements of technology, economy and environment. However, option 3 is not currently recommended for implementation because new equipment and worker training are needed and the investment is relatively high. In addition, uncertainty of product market in bricks might decreased benefits from its sale in China is another cause for removing option 3.

**Effects of implementation** Based on the evaluation, a two-stage implementation plan was designed. In the first stage, an integrated CP system combined with options 1 and 2 was implemented in the WEF in 2009. In the second stage, part of the profits obtained from the first stage was used for the implementation of option 3. The gross investment of the first stage was 1.91 million USD.

According to the statistic analysis from November, 2009 to June, 2010, the average Mn content in residues was about 1.8%, with 10% lower than planned value, which were decreased 50% compared with traditional process. Chromium and manganese ions in wastewater are recycled more than 97%. The consumption of ores per ton EMM was 6.94 tons (18% grade ore). The amount of pollutants generated by residues was reduced by over 50% and the pollution burden of chromium waste was eliminated. After the implementation of the proposed integrated CP system, the quality of the surrounding environment has been improved and the cost of pollution treatment has been dramatically decreased.

## CONCLUSIONS

To improve the pollution reduction for EMM industries in China, an integrated system combined with a series of advanced CP technologies was proposed in this study. Based on the survey and questionnaire of related experts, a number of technologies were grouped and screened. After the consideration of environmental impacts and economic efficiency, three CP options integrated with various advanced technologies were proposed.

To verify the proposed options, a case study was conducted in the EWF, Southwest China. The effects of three options were evaluated from the technical, environmental, and economic aspects, respectively. After the assessment, the two-stage integrated CP system based on the proposed options was recommended to implement in the factory. Through the application, significant results were obtained. A reduction of 50% manganese loss in residues, recycling 95% of manganese in wastewater and recycling manganese mud can be achieved. The utilization ratio of Mn was improved due to reusing of Mn in residues. The goals of elevating economic benefits and improving environmental quality were achieved through the integrated CP system.

In this study, the current situation of CP technology implementation in EMM industry in China was analyzed. The development potential of such technologies in EMM industry was assessed by a case study. A series of CP technologies involved in the proposed system have been verified to be suitable for EMM industries through the practices in WEF. Furthermore, the results provide reliable theoretical and technological support for improving CP in the EMM industries of China. However, more studies and longer practice in quantify effects of applying the proposed integrated system on other Chinese EMM factories are needed.

## ACKNOWLEDGEMENTS

## REFERENCES

Boyle C. 1999. "Cleaner production in New Zealand." *Journal of Cleaner Production* 7(1):59-67.

Duan N., Zhou C.B. 2007. "Research and analysis of the formation process of compulsory regulation and policy of cleaner production audit. (in Chinese)" *China Population, Resources and Environment* 17(4):107-110.

Frijns J., and Vlient B.V. 1999. "Small-scale industry and cleaner production strategies." *World*

*Development* 27(6):967-983.

Wei C.H., Lu Y.C. 1998. "Cleaner production evaluation of brewage industry in Huaihe River. (in Chinese)" *Food and Fermentation Industries* 24(4):47-52.

Lemly A.D. 2004. "Aquatic selenium pollution is a global environmental safety issue." *Eco-toxicol. Environ. Saf.* 59:44–56.

Li X.M. 2008. In-depth study and practice the scientific concept of development of key enterprises do cleaner production audit. Available from: *Website of National Centre of Cleaner Production in China*. http://www.cncpn.org.cn/ReadNews.asp?NewsID=1577, Beijing: [ 2009-04-15 ]

Manganese Metal Company (MMC). 2008. "IMnI annual review." *International Manganese Institute*, Available from: http://manganese.org/, Paris: 2009-10-21

Reilly C. 2006. *Selenium in food and health*. Springer Science & Business Media, NY.

Song S.W., Xue J.Y. 1999. "Elementary study on the integrated evaluation methods of cleaner production alternatives. (in Chinese)" Environmental Protection Science 25(1):16-21.

Tan, Z.Z., and Mei G.G. 2005. *Metallurgy of manganese*. Press of Central South University of Technology, Changsha, CN.

Tan Z.Z. 2009. "Retrospect of 2008 Chinese electrolytic manganese industry circumstances and responding measures in 2009. (in Chinese)" In: *International forum on electrolytic Mn products*. pp. 44–52.

Yu X.L. 1999. *Investigation on the cleaner production practices of China alcohol industry*, Institute of Environmental Science, Beijing, CN

Yu Q., and Luo J. 2006. "Pollution and its treatment during EMM production. (in Chinese)" *China's Manganese Industry* 24(3):42–45.

Zhang W.S., and Cheng C.Y. 2007. "Manganese metallurgy review. Part II. Manganese separation and recovery from solution." *Hydrometallurgy* 89:160–77.

## PARTNERSHIP APPROACH IN ENVIRONMENTAL MANAGEMENT: A STRATEGY TO SOLVING URBAN PROBLEMS IN LAFIA TOWN, NIGERIA

Bashayi Obadiah and Barau Daniel (Nasarawa State Polytechnic, Lafia, Nasarawa State, Nigeria. Email: tplobedcrown@yahoo.com)

**ABSTRACT:** The environment is increasingly characterized in terms of a crisis situation. The unique and complex characteristics of the environment entail social, political, and economic implications in its management. This paper describes the responsibilities of urban management institutions toward an efficient management of the environment in accordance with the constitution and national policies on the environment but in practice, their operations are limited due to weak finances and little expertise in environmental management. Therefore, the community seems to have taken over the management of their environment in terms of water supply and sanitation service in a disorderly manner. The paper highlights the current state of these services and their institutional framework in Lafia town, and calls for a partnership approach in managing these urban problems. The paper also describes the existing policies that were developed in support of partnership in line with good governance norms and illustrates this with an account of the experience of best practices in the world to evolve a partnership approach for environmental management in Lafia town. This paper then examined the potentials benefits and challenges of the partnership and recommends ways of addressing the challenges.

### INTRODUCTION

As urban centers continue to grow, the need to meet increasing water demand for the population has become a major problem of concern to Urban Managers. One of the objectives of National Policy on Water supply and Sanitation (NPWSS), 2000 and the MDG's goals is to provide adequate and quality water to the urban and rural population by the year 2015. The crucial issues on this paper is that government of Nigeria alone cannot provide most of urban services to the people and the agencies created with a responsibility to manage these services are been faced with the problems of inadequate finance and corruption.

To achieve the national and state water supply and sanitation policy objectives major institutional reforms must be carried out in our water and sanitation sectors, since most of the agencies are faced with the challenges of institutional development to provide water and sanitation facilities for the needs of urban population. Therefore, government have resorted into privatization and commercialization of his companies which are widely considered as social goods than as economic goods in most developing and socialist countries. The World Bank and UN-Habitat on the other side are promoting private sector participation through partnership since these public services cannot longer be provided by the government.

Partnership is seen as the core of these two concepts is therefore a shift in balance away from the public sector towards the private sector and a shift towards sharing tasks and responsibilities (Kooiman, 1993). Mitchell (1997, 156) defined partnership as: ...a mutually agreed arrangement between two or more public, private or non-governmental organizations to achieve a jointly determined goal or objective, or to implement a jointly determined activity, for the benefit of the environment and society. As such, partnership could mean government working together with a wide range of social partners at the national and local level to plan, implement and evaluate policy and actions for socio-economic development. The Sustainable Cities Programme (SCP) developed by the UNCHS/UNDP is a recent attempt at involving people in the management of their cities through the partnership approach.

Therefore, this paper presentation is aimed at reviewing the existing water supply and sanitation conditions, institutional policies, existing partnership management and also some case studies with a view of making recommendations to straightening and improving partnership approach in Lafia town, Nasarawa State.

### BACKGROUND OF THE STUDY

Nasarawa State was created in 1996 with Lafia town as the State capital. The State is located in North central near the Federal Capital Territory (FCT), Nigeria in West Africa. Lafia town is situated on

Longitudes 08º 30¹ East and Latitude 08 º 31¹ north. The area is located in the middle climatic belt that is generally very warm and humid with dry and rainy seasons. It has a mean temperature range of 26 º C to 30 º C, a mean rainfall of 1120mm to 1500mm relative humidity of 60-80% and falls within the guinea savannah kind of vegetation; (Meteorological dept, 2009). Greater Lafia master plan

The final results of 1991 population census obtained from National Population Commission put the population of Lafia town as 78,247 with an estimated annual growth rate of 2.5%. When projected to 1996 the population stands at about 103,590 and this was further projected to 2009 as 203,790 people. The 2006 national population census for Lafia town is still being awaited for.

## MATERIALS AND METHODS

The study first, source for information from official's reports, published and unpublished source, internet source and the author's personal knowledge to examine the concept of the study. The study appraised water and sanitation situations in Lafia town with the projected population of 263,998. The survey investigation was based on a three-stage clustered sampling framework in which a sample of 230 households (representing about 1.0% sample size of the 20,308 total households) was drawn across the three districts (Sabon pegi district, Bukan sidi district and Gayam district as the first stage). The second stage cluster was that the three districts were divided into sets of four clusters of neighbourhoods, giving rise to a total of 12 sampling areas from which street blocks as the third stage cluster were identified and a systematic random sampling was used to administer questionnaires.

## URBAN ENVIRONMENTAL PROBLEMS IN LAFIA TOWN: AN OVERVIEW

**Water supply and urban sanitation condition.** For quite some time now, most Nigerian cities are grossly underserved with pipe borne water. By 1995, only about 30% of urban households were served with underground pipes (Onokerhoraye, 1995), causing those who could afford them to spend considerable household revenue on capital intensive deep wells, electric pumps and overhead tanks. Sanitation in most of the cities is poorly maintained. Sanitary facilities like sewers, sewage treatment facilities, septic tanks and toilets for homes are known to be grossly inadequate in Nigerian cites and have worsened over the years because of the rapid rate of urbanization in the country.

## DATA RESULTS

The statistics of the urban water and sanitation in Lafia town are presented below:

**Table 1. Type of water supply and sanitation facility used by the households***

| Water supply use | Percentage served | Sanitation facility | Percentage served |
|---|---|---|---|
| House connections | 13.4 | Public sewers | 0.0 |
| Yard taps | 15.2 | WC with septic tank | 0.7 |
| Public standpipes | 4.1 | Simple Pit latrines | 54.6 |
| Boreholes with hand pumps | 5.1 | Pour flush | 18.9 |
| Water tanker | 6.5 | VIP Latrines | 6.2 |
| Water vendor | 8.2 | Public toilet | 0.4 |
| Boreholes | 19.5 | No facility | 14.7 |
| Community well | 6.5 | Other | 4.5 |
| Yard well | 26.7 | | |
| River/stream | 1.3 | | |
| Total | 100 | | 100 |

*Source: Field survey, 2011*

**Table 2. Satisfaction with current water supply and toilet system\***



**People satisfied with water supply**

Yes 21%
No 79%

**People satisfied with toilet system**

Yes 36%
No 64%
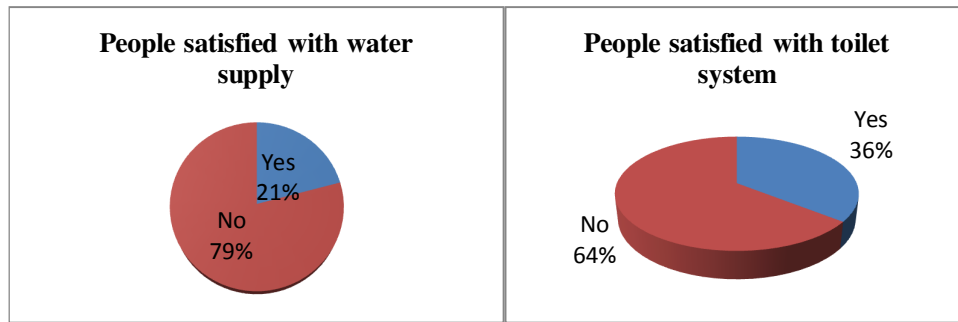
*\*Source: Field survey, 2011*

**Table 3. Opinion on present state of water supply and sanitation\***

| Variables | **Frequency** | **(%)** |
|---|---|---|
| **State of water supply and sanitation** | | |
| Very poor | 90 | 37.5 |
| Poor | 89 | 37.1 |
| Fair | 51 | 21.2 |
| Good | 10 | 4.2 |
| Total | 240 | 100.0 |

*\*Source: Field survey, 2011*

**Table 4. Desire for change in provision**

| People want to change to improved water system | Frequency | percentage |
|---|---|---|
| Yes | 218 | 95.0 |
| No | 12 | 5.0 |
| Total | 230 | 100 |
| **People want to change to improved sanitation system** | | |
| Yes | 174 | 75.8 |
| No | 56 | 24.2 |
| Total | 230 | 100 |

*Source: Field survey, 2011*

**RESULT DISCUSSIONS**

The results in Table 1 show that the water supply situation in Lafia town is very poor. Less than 30% have access to safe water and others may be depending on other sources of water supply that may be polluted. The water services available in Lafia town include household dug wells (which constitute the major source up to 60% in the rainy season), community concrete wells provided by local governments, boreholes with hand-pumps provided by the State Government, public stand posts and water selling kiosks using water from NSWB, privately owned borehole water systems, hawkers and house connection from NSWB pipelines.

The sanitation situation is also generally poor with 15% of the people interviewed saying that they have no sanitation facility at all. Pit latrines (54.6%), Pour Flush, VIP latrines (6.2%), San-plats and Bush (no facility). The serious environmental sanitation problem in Lafia town consists of the unhygienic city landscape in both the residential and commercial areas. They are found along some of the streets, particularly the back streets, where they often impact negatively on city transportation. There are several toilets built by private individuals in public places like markets and motor parks where people pay to use the service. This has implications for public health and urban development in Lafia town.

Table 2 shows only 21 % of the households expressed satisfaction with their current water supply systems. This is not surprising, given the above analysis about quality, distance and regularity of water supply, coupled with the cost of water. Reasons given for dissatisfaction with their current water supply system include: poor quality of water, inconvenience and irregular water supply.

Only 35.5 % expressed satisfaction with their present toilet systems. Only 30 % thought their toilet was good in terms of privacy, 22 % considered their toilets good in terms of cleanliness and 14 % thought their toilets were convenient to use. Further analysis shows that households with no toilet facility were least satisfied with their present human waste/excreta disposal systems (5.2 % satisfied). This is perhaps understandable given the problems of inconvenience, lack of privacy and distance to alternative facilities.

From the opinion survey respondents (Table 3) gave their opinion on the present state of water supply as very poor 37.5%, while some said water supply is poor 37.1. About 21.2% said is fair and 4.2% said is good. The present level of water supply is described as very poor.

From Table 4, the viability and sustainability of improved facilities in the Lafia town depend on the desire of the people for change. Respondents were thus asked about their desire to change their existing water supply systems to improved systems. The overwhelming majority (95 %) of the households had considered changing to an improved system of water supply for various reasons, including shorter distance to collect water which 83 % considered to be an important factor, the possibility of using more water 93 % and safer drinking water 96 %. Other reasons mentioned include: improved health and hygiene factors, convenience, regular supply and possibly cheaper water.

Most (75.8 %) of the households had considered taking necessary steps to change their human waste/excreta disposal system to an improved system for various reasons, including: improved health or hygiene reasons, cleaner environment, avoidance of smell and rats, convenience and proximity to the house. Households with no toilet facility are most likely to have considered changing to an improved human waste disposal system (92 %), 87 % of households with other types of toilet facility had thought of changing to an improved system, public toilet 79 %, pit latrine 74 %, VIP latrine 50 % and WC connected to septic tank 46 %.

**Existing partnership strategy for water supply and sanitation in lafia town.** The community participation exit because neither the NSMWR, NSWB, NASEPA, NUDB, nor the local government councils could meet the water supply demand and sanitation services of these communities, a community committees were formed which have assumed a major role in filling up this important gap. In the study area various communities has formed Water Supply and Sanitation committees (WASCOMs) since 1996 which partner with the NSWB, NASEPA, NUDB, Ministry of Health and Municipal council, Police and Civil Defence as stakeholders in the management. This was to provide water supply and essentially enforced NUDB and NASEPA's regulations on sanitation and solid waste disposal. The Nasarawa State Community and Social Development Agency (NSCSDA) was established by law No. 78 2009 as an agency to carry community and social development project assisted by World Bank. It adopts the community driven development (CDD) approach in solving community problems. The CDD approach is participatory approach that enhances accountability, improves efficiency, effectiveness and delivers projects at a much lower cost.

Various community organizations, including Water and Sanitation Committees (WASCOMs) are progressively being involved in community management of water infrastructure and State Government appointed Task Forces on Environmental Sanitation who utilize equipment from various Government and private organizations to remove and dispose of such refuse damps on monthly basis. In this case Community Self Help Groups assist the Task Force with the manual labour required.

Increasingly, NGOs are becoming more interested and committed to actively participate in the sub sector. An association of NGOs has been formed that seeks to collaborate with state to improve on delivery of water supply and sanitation services in Lafia town. The arrangement was further enlarged in 2005 with the admission of NGO and private organizations which were involved in water supply, sanitation, drainage construction, road repair and security, among other social services.

**Evaluation of the partnership strategy.** Below is an evaluation of the existing partnership strategy in Lafia town.

**Table 5. Evaluation of existing partnership strategy in the study area**

| S/No. | Participant | Functions Assigned | Level of performance |
|---|---|---|---|
| 1 | WASCOM | 1. Collection of waste in the town | Irregular |
| | | 2. Construction of waste collection bunkers | Poor |
| | | 3. Health and sanitary inspection | Irregular |
| | | 4. Provision of community well/hand pump | Poor |
| | | 5. Repair and maintenance of facilities | Poor |
| | | 6. Enforcement sanitation laws | Regular |
| 2 | Municipal council | 1. Assisting the CBOs with working implements | Poor |
| | | 2. Enlightenment campaigns through ward heads | Irregular |
| | | 3. Payment of certain fee monthly to WASCOM | Irregular |
| | | 4. Sanitary inspection | Irregular |
| 3 | NUDB | 1. Monitoring and enforcing non-movement during sanitation exercise with police | Regular |
| | | 2. Invest in policy making- regulatory framework | Poor |
| | | 3. Enforce compliance of sanitary law | Poor |
| | | 4. Provision of funds | Poor |
| | | 5. Provision of vehicles during sanitation | Irregular |
| 4 | NSWB | 1. Construction of boreholes | Poor |
| | | 2. Installation of water facilities | Poor |
| | | 3. Collection of water bills | Regular, but ineffective |
| | | 4. Expert advice | Based on request from WASCOM |
| 4 | NASEPA | 1. public enlightenment campaign- seminar and workshops | Irregular |
| | | 2. enforcement of environmental laws | Poor |
| 5 | CBOs/NGOs | 1. Direct investment in water and sanitation | Fair |
| | | 2. Provision of well and boreholes | Fair |
| | | 3. Awareness campaign | Regular, but ineffective |
| | | 4. Expert advice | Regular |
| | | 5. Protection of right of people to water | Effective |
| | | 6. Capacity building and stakeholder consultations | Poor |
| | | 7. Provision local/ simple equipments and Labour | Poor |
| 6 | NSCSDA | 1. Drilling and equipping of mechanical boreholes | Fair |
| | | 2. Sinking of cement wells | Fair |
| | | 3. Rehabilitation of existing cements wells | Good |
| | | 4. Construction of tube wells with hand pumps | Very good |

*Author evaluation, 2011*

**Challenges and problems of partnership.** The study has demonstrated how residents in Lafia town are coming up with innovative approaches for dealing with the environmental problems they face. With the assistance of some NGOs and other actors, the partnership approach seems to be having some

considerable success. It is clear that the residents of Lafia are now involved in improving the quality of their living environment. However, this approach has limitations because it is not supported by a policy or legal framework. The roles of different partners/actors are often not well-defined and so do not address the issue of who will be responsible when things do not work.

## SUMMARY AND CONCLUSIONS

The partnership approach holds good prospects for addressing many of the environmental problems which Lafia town currently faces due to her rapid urban growth. Government now realises that it has to work in conjunction with the private sector (e.g. NGOs and CBOs) in efforts to attain the goals of sustainable development. It is argued that policy thrust should not only be towards commercialization and or privatization as most of our countries in Sub-Saharan Africa are still developing  but on forging credible partnership between various stakeholders to tackle and manage various environmental problems (Dung-Gwon, 1999).

The case studies examined in the paper show that different types of partnership such as Contributory, Operational, Consultative and Collaborative partnerships could be forged to address different environmental problems at different; multiple and complex problems at city level to single environmental issues using different techniques of partnership. The range of problems tackled would differ as would the stakeholders involved. Partnership could be very formal and well structured or informal: contributory and collaborator as in Environmental management in UK, Sustainable Ibadan project (SIP) and community and social development project in Nasarawa State. The degree of success recorded will depend on the level of commitment by all the stakeholders to the project. Partnerships that adopt a collaborative model have better chances of success than those that do not.

The key argument in this paper is that, with the exception of smaller or specific situations, urban environmental management cannot successfully be achieved or sustained without cooperation and collective action between different actors and the need for open, transparent and accountable system of government based on accepted democratic norms and principles. Government institutions and agencies have to change their attitude in the way of doing things by forging cooperation, mutual understanding and trust with the private sector, NGOs, CBOs and the people. The government needs to play a greater role in supporting these new initiatives by the local people. The partnership approach has a great deal of promise and might lead towards greater environmental sustainability. There is a need to monitor carefully these new initiatives, and detailed studies are required to examine the factors influencing the success and failures of the partnership approach.

## REFERENCES

Adebayo, A. and Rowland, L. 1973, Management problems of rapid urbanization in Nigeria. Carton press ltd, Ibadan.

Adepoju, A. A and Omonona, B. T. 2009, Determinants of Willingness to Pay for Improved Water Supply in Osogbo Metropolis; Osun State, Nigeria. Research Journal of Social Sciences , 4: 1-6, INSInet Publication.

Arnstein, S. A. 1969, A ladder of citizen participation, Journal of the American Institute of Planner, Vol.35 (4), pp 216-224.

Dale, W and etal 1989, Paying for urban services: Water vending and willingness to pay for  water in Onitsha. World Bank, N. W

Dung-gwon, J. Y. 1999, Partnership in planning and Environmental management in Nigeria: some case studies. Journal of Environmental Sciences, Faculty of Environmental Science, University of Jos, Nigeria. 3(1), pp 36-45.

Edi, M and E tal, 2006, Ecological Urbanization II: Journal of Environment and Urbanization, Vol. 18 No. 2, oct. 2006, pg 353-368. Sage publication, London.

Heilman, J. and Johnston, G. 1992, The Politics of Economics of Privatization, University of Alabama Press, p. 197.

Jane Nelson and Simon Zadek, 2000, Partnership Alchemy, The Copenhagen Centre.

Jiriko, K. G.: 1999, Effective urban management and governance for sustainable cities in Nigeria in the 21th century, Journal of NITP.

Mitchell, B. 1997, Resource and Environmental Management, Longman.

Oni, S. B. 1989, Managing the rapid growth of cities in Nigeria. Gaskiya press, zaria.

Owolabi, A. 2004 Public- Private sectors Linkage in water supply provision: Role of civil  society organizations in Lagos State. A paper presented at current trends in private sector participation in Lagos water supply. Boll foundation, Ikoyi, Lagos.

Samson, W. M. 2006, Partnerships in urban environmental management: an approach to solving environmental problems in Nakuru, Kenya.

Schiibeler, p. 1996, participation and partnership in urban infrastructure management, Washington D. C: They international Bank for reconstruction and development/ the World Bank.

Sani, M. 2006, Prospects and urban development implications of commercializing water supply. Unpublished PhD dissertation. Department of URP, ABU Zaria Republic of South.

Water Utilities Project. No. 5. March, 2000. Strengthening the Capacity of Water Utilities to Deliver Water and Sanitation Services, Environmental Health and Hygiene to Low Income Communities. Case Study for Kano (town), Nigeria.

Africa, Department of Finance, Strategic Framework for Delivering Public Services through Public- Private Partnerships, April 2000.

**APPENDIX 'A'**

Fig. 1 Proposed Partnership approach for environmental management in Lafia town
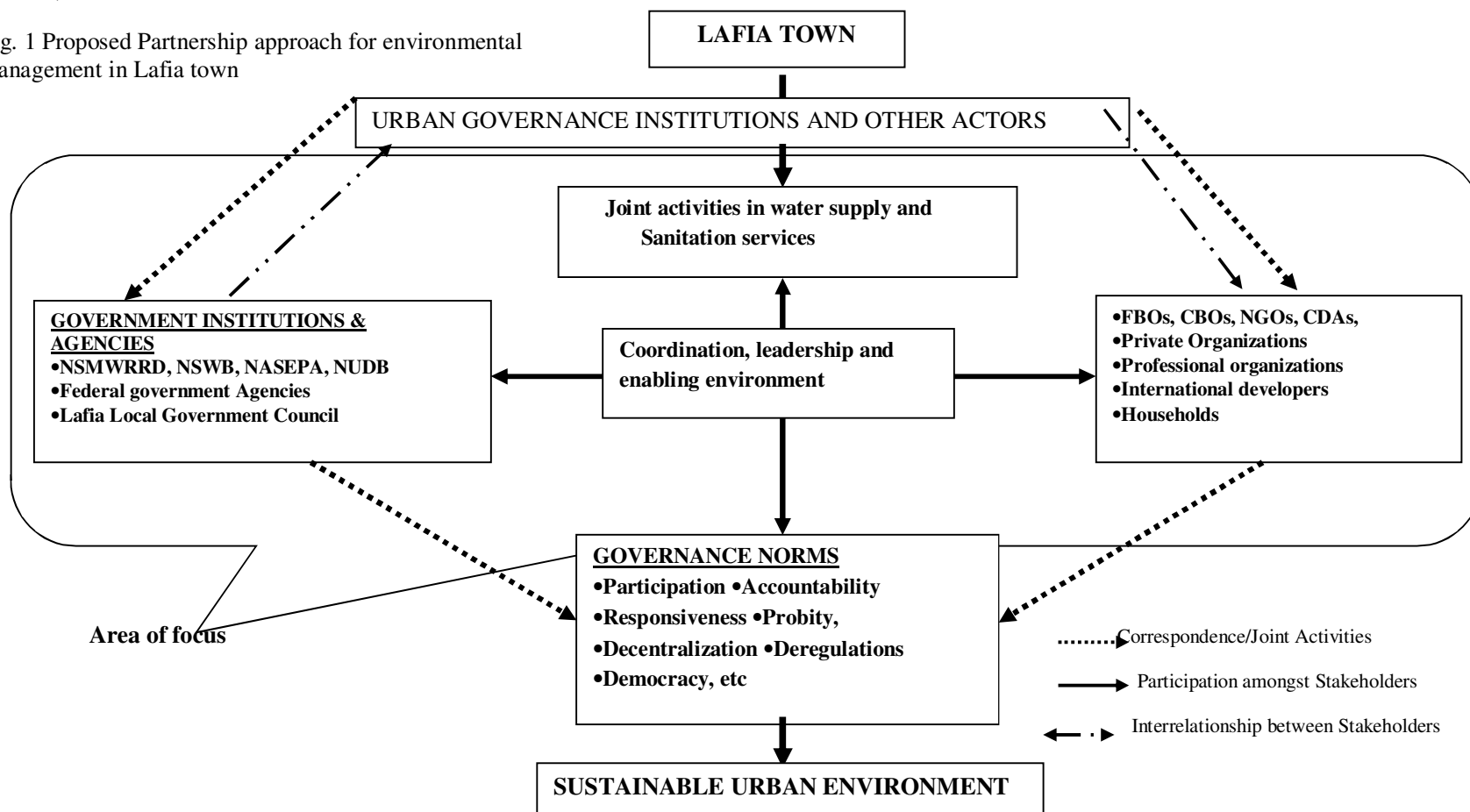


Figure 1 shows the various Actors involved in urban environmental management with the urban governance institutions. The linkages between these institutions provide a potential for strengthening partnerships for sustainable urban environment.

# INTEGRATED SAFETY AND ENVIRONMENTAL RISK SYSTEM FOR CIPS IN CHINA

*Yu Qian*, Jun Bi, Qiang Fang

(Nanjing University, Nanjing, Jiangsu Province, P.R.China)

With rapid economic development in China, environmental disasters have happened frequently in these years. The relationship between safety production and environmental risk is recognized more clearly after the Songhuajiang River pollution event, which could be regarded as a successful emergency response in the view of safety production, while leading to a water quality catastrophe in the view of environmental protection. Actually, there are two management systems controlling the uncertainty and risk of construction in China, one is ERA in environmental impact assessment (EIA) managed by State Ministry of Environmental Protection (SMEP), and the other is Safety Assessment (SA) supervised by State Administration of Work Safety (SAWS).

This paper compared these two kinds of management systems, and pointed out that many environmental pollution accidents in China were caused by the confusion of environment risk and working safety, and present emergency response process cannot coordinate different relevant departments and work efficiently. So it is distinguished between the two concepts and addressed about the coordination of the two systems in the occasion to accident happening. An integrated emergency response system for chemical industrial parks (CIPs) based on Decision Support System and Expert System was then introduced to improve the process and help decision-makers act correctly to prevent large-scale crisis in case of an accident.

Nanjing Chemical Industrial Park is a typical chemical industrial park along the Yangtze River. The emergency response system of this park was presented as a case. The system has a B/S structure and includes three parts named safety production subsystem, environmental risk subsystem, and public utility schedule subsystem. These three subsystems are constructed on a common database system and two sharing platforms. The one is command and control platform, and the other is simulation and exercise platform. Once an incident happened, the alarm information would transport in the public information channel of the system rapidly and reached all of the possible decision-making units immediately. Soon a systematic and scientific emergency response scheme would be formed automatically, and subsequent measures would be presented to the decision-maker. This emergency response system will surely guarantee the safety of Nanjing Chemical Industrial Park and all of the surroundings.

# A MISSED DIMENSION OF THE NEGLECTED PILLAR: THE CASE OF SOCIAL SUSTAINABILITY

*Tina Pujara*

(Indian Institute of Technology, Roorkee, India)

Asia has experienced rapid development and urbanization in the last half of the $20^{th}$ century. This rapid urbanization is distinctly linked to the challenge of sustainable development. 'Sustainable Development' being an extensively used term in the current century, its three pillars (environmental, economic & social) have featured in various debates, discussions & researches. However, the social dimension has commonly been identified as the weakest and relatively neglected 'pillar' of sustainable development, particularly when it comes to its analytical meaning. As social sustainability is the least developed of the oft-cited 'three pillars' of sustainability and there is a relative lack of understanding of the social pillar, it provides an opportunity for many researchers to contribute to defining and refining the term. Although various authors have attempted to define 'social sustainability', there has been little agreement as to what this constitutes and there has been no general agreement over its definition. The working paper explores the literature on the attempts to define social sustainability with particular reference to urban form, and further points out the missed dimension in the attempts. None of the current definitions explicitly incorporate the aspect of regional and cultural context.

This paper contributes to the advancing literature on social sustainability by exploring the various definitions put forward and highlights the missed dimension of region & culture in the definitions. The paper is not intended to provide conclusive answers about what 'social sustainability is' but rather to suggest the inclusion of regional and cultural context in the further development of the definition of social sustainability. It draws on work in progress on a broader project titled 'Assessment and Evolution of Sustainable Urban Form in the Indian Context' underway at the Department of Architecture & Planning, Indian Institute of Technology (IIT), Roorkee, India. [174]

# ENDOCRINE ACTIVITY OF DOMESTIC SEWAGE EFFLUENT FOLLOWING INDIRECT POTABLE REUSE TREATMENT

*Elizabeth Lawton*, Edwin Routledge and Susan Jobling (Brunel University, Uxbridge, UK)
Eve Germain and Martyn Tupper (Thames Water plc., Reading, UK)

The world's growing population is causing an ever increasing demand for clean safe drinking water. In some countries suitable sources of drinking water are becoming scarce and will not be able to satisfy future demand. In 2007, the Southeast of England was classified as experiencing 'serious' levels of water stress. Consequently, there is a need to find alternative sources of water that can be used for potable supply or to augment current sources. Modern water treatment methods are now being examined to investigate whether treated domestic sewage effluent can be treated to drinking water standards and discharged near a drinking water abstraction point; a process known as Indirect Potable Reuse. The pilot plant uses pre-filtration, microfiltration (MF), Advanced Oxidation Process (AOP), Reverse Osmosis (RO) and RO with the addition of AOP. Extensive chemical analysis from spot samples has been conducted on the treatment water at various points along the process to measure pharmaceuticals, natural and synthetic hormones, pesticides, metals and numerous organic industrial chemicals. Individual chemicals have been classified into groups based on their use and potential toxicological endpoints identified for each group. The variety and concentration of these contaminants has been clearly shown to be reduced by the stages of water treatments. In addition, passive samplers were deployed to provide a time-integrated sample of the mixture of contaminants present in the effluent and to allow further assessment of its biological activity. These samplers were placed in three ballast tanks receiving a constant flow of effluent that had undergone pre-filtration, micro-filtration and reverse osmosis. There were a total of eight deployments (August 2011 until March 2012), each lasting four weeks. Each of these deployments included Polar Organic Integrative Sampler (POCIS) devices and on two occasions (one summer and one winter) included Semi-permeable Membrane Devices (SPMD). The extracts from these devices will undergo yeast screen assays to determine their estrogenicity. This biological activity will be investigated as a progression along the treatment system and also compared to the time of year that the POCIS deployments took place.

# MEASUREMENT OF SUSTAINABLE DEVELOPMENT WITH REFERENCE TO A BACKWARD MINING REGION, INDIA

***Basanth Kommadth*** and Binayak Rath

**(**Indian Institute of Technology Kanpur, U.P., India)

After the Rio Convention, popularly known as the Earth Summit (1992) adopting the concept of *"Sustainable Development(SD)"* as a measure for attainment of economic development and the *Millennium Development Goal* (MDG) under Agenda 21[176] as the key instrument of development during the 21$^{st}$ century, a number scholars have taken of the task of measuring sustainability including the World Commission on measuring SD. Though a galore of definitions, frameworks and methodologies of sustainable development have emerged, showing a theoretical maturity of the concept over the years, still no unanimity is arrived at to cope of with the dynamics of frequent environmental changes. Thus, identifying a practical method to actualize this theoretical endeavour has become a central mission of the governments, industry and business. Specially, because of the complexities associated with the mining and minerals sector, the traditional sustainability models have failed to contain all aspects of their extraction and processing/ utilization. Owing to their distinct features it invalidates the idea of a 'one-fits-all' analysis. One of the main distinctiveness of the mining and mineral sector is its dichotomous nature which at one extreme creates substantial wealth from the land and improves the quality of life of its stakeholders; whereas at the other end, it disturbs the physical environment of land, water and air; and the community life associated with it through externalities. While the positive externalities of a mining are very often accrued to its proponents/owner and the national economy, but the negative externalities are generally borne by the local communities of the mining area. These specificities mining on environment, economy and society stresses the need for a sector specific framework to measure and monitor sustainable development of the sector at local level.

This paper is an attempt to develop a sector and regional specific sustainable development indicator by re-examining the scope of traditional models and to suggest a practical approach to SD measurement by using sector specific criteria, fuzzy logic and context-dependent economic, ecological, technological, societal and institutional sustainability indicators for the mining and minerals sector. The practicality of the proposed methodology is illustrated by using primary and secondary data of the iron ore mines of ***Bellary region*** of Karnataka State in India which is considered as one of the hotspots of the country because of its large iron ore and other mineral potentials and their massive exploitation after the mining boom during the first decade of the present millennium. In this study, we have reviewed all existing sustainable development models, and then suggested a renewed methodology with the help of demonstration of its application on real life situation. The results so derived can be useful internally for identification of 'hot spots' with the help of externalities like stakeholder engagements and is expected to facilitate estimating the degree of sustainability, and their monitoring. The results of our study are likely to provide guidance for government officials, policy-makers and mine operators to use sustainability frameworks in taking decisions and framing action regarding extraction and utilization mineral resources of a backward region and thereby to improve the degree of sustainability.

# RENEWABLE ENERGY DEVELOPMENT

# INVESTIGATION OF HYDROLOGICAL DROUGHT ON RUNOFF RIVER HYDROPOWER GENERATION IN DIFFERENT TIME SCALES

*Faeze Eghtesadi*, Abolfazl Shamsayi, and Bahram Saghafian (Research and Sience Islamic Azad University, Tehran, Iran), Moein Seyed Fakhari (Sharif University of Technology, Tehran, Iran)

**ABSTRACT:** In the present research, the relationship between hydrological drought of Mohamad-Abad river and the amount of electrical energy generation was investigated. The dependency on discharge of the river in electricity generation in run-off river hydropower plants, gives a high level of importance in hydrological drought studies. In this paper Streamflow Drought Index (SDI) is calculated in monthly, seasonal, and annual time scales. Using RETScreen software, the energies corresponding to the discharge in mentioned time scales are computed. The results showed that the longer time scale duration leads to the more correlation between SDI and generated energy. According to this, correlation between these two parameters are 0.68, 0.77, 0.83 In monthly, seasonal and annual time scales respectively.

Key Words: Hydrological drought, SDI, Hydropower, RETScreen Model, Generated Energy.

## INTRODUCTION

Descend in the level of available water during a significant time period in a vast region is defined as a natural phenomenon named drought. It is difficult to distinguish the major origin of drought due to the complexity of the hydrological cycle. However it is prevalent to consider the reduction of precipitation as the source of drought which leads to decrease in runoff or reserved water -in the shape of soil moisture or flowed water. With regard to American Meteorological Society (1997), drought can be grouped into three types including agricultural, hydrological, and meteorological and socioeconomic drought (Beran, 1985).

For each climate regime, there are some specially drought characteristics. For instance, in areas near Equator with a warm and humid climate, a decrease in the amount of rainfall in comparison with its annual average leads to a meteorological drought while having no significant effect on the water resources. In this situation hydrological drought is not observed in spite of meteorological drought. In the contrast, in an arid and semi-arid region, reduction in rainfall strongly affects on the water resources. Nevertheless, in most cases these two types of drought occurs coincidently (Dracup 1980)

What is called hydrological drought is a significant reduction in available water in all its shapes, such as streamflow, including snow melting and spring flow, lakes, reservoir level, and underground water.

Streamflow, among these parameters, is known as the most important factor considering volume of the available water which is assumed as the key index in express the streamflow. Bearing this point in mind hydrological drought can be simply defined as the reduction in the amount of streamflow in comparison with normal situation. A drought event is characterized using four major criteria including its severity, time and duration, region, and frequency (Ben-Zvi 1987, Bonaccorso 2003). Understanding the concept of drought, for using of energy resources efficiently can be achieved by engaging theoretical investigation however, it has limitations in monitoring and forecasting of drought. For studying the hydrological drought in this aspect, it is indispensable to employ an appropriate index to determine the severity of drought. This index should cover some conditions that are explained briefly as follows. A suitable drought index should convey a tangible and physical concept. Furthermore, it should include different kinds of drought conditions since it is independent on the study area. A suitable index can forecast the drought occurrence with the minimum delay using the available data. Generally, Streamflow Drought Index (SDI) can meet the requirement explained. SDI was introduced as a hydrological drought

index by Nalbantis and Tsakiris (2005) (Tsakiris 2005). Using this index the dependency of drought on severity, duration, frequency, and region is reflected to an index which is related on cumulative streamflow volume (Tsakiris 2006, Nalbantis 2008)

Electrical energy can be generated by using several methods so that one of which is engaging the potential of reserved water behind the dams by means of hydropower plants. This renewable type of electrical energy generation contains outstanding advantages such as durability, higher efficiency, lack of the need to fuel, no destroying effect on the environment and low maintenance and repair costs in addition to its flexibility in response to electrical system fluctuations. Using the hydropower plants, hazardous floods can be controlled and conducted to water supply systems. The most important point in designing the hydropower plant is the quantity of available water which is in a direct connection with the energy generation. The river flow directly affects on the amount of energy generation in runoff hydropower plants. Hence, occurrence of drought would reduce the amount of available water and consequently, will result in decreasing of hydropower generation.

## CASE STUDY AND DATA

The considered region is the Mohammad-Abad watershed located in Golestan, a northern province, of Iran. The study site, named Rigcheshme is located at 54º 49′ 00″ longitude and 36º 48′ 00″ latitude. The length of main river of Mohammad-Abad watershed to Rigcheshme site is 29 km with a drainage area of 362 square kilometers. The investigated region and its sites are illustrated in Figure 1.
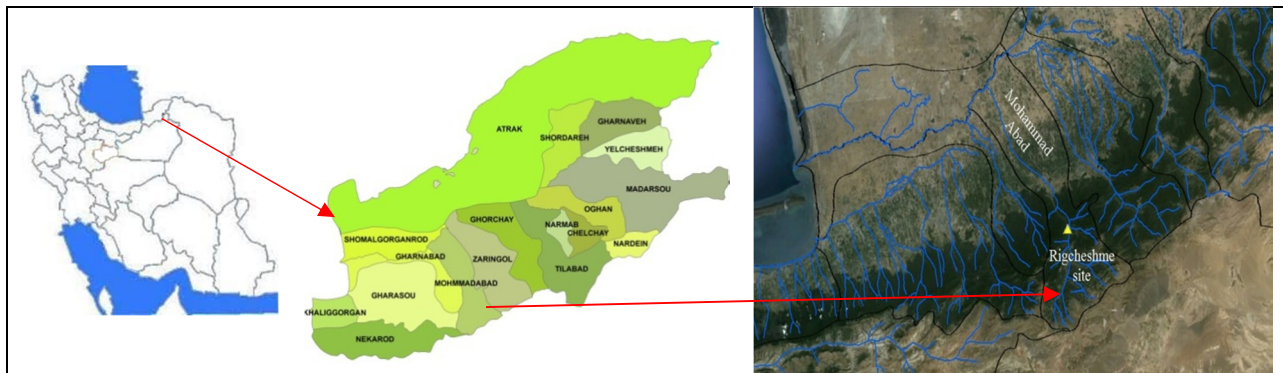


FIGURE 1. Location of Rigcheshme site on Mohammad Abad watershed and Iran map

In the first step, discharge data was fitted to different distribution functions for finding the best function using EasyFit software so that result showed that Lognormal distribution function could well fit with the data. In order to investigate the hydrological drought severity, SDI was calculated. SDI is normalized in time and space and can be used to compare different sites. It is also possible to calculate this index in various time scales such as one, three, or six months. In this paper SDI was calculated in monthly, seasonal and annual periods. In fact, this research is programmed to find what time scale can be more reliable on studding the relationship between drought hydrological and generated energy resulted from runoff river hydropower generation. Also, findings of the research will be helpful for policy and decision makers in order to impose an appropriate action on water resources and estimate the amount of energy can be generated under different hydrological drought intensities.

## METHODOLOGY

RETScreen software is used to calculate hydropower energy. This software provides the approximately achievable energy based on available discharge, design discharge, the amount of head, gross head, residual discharge, efficiency and losses.

RETScreen software is used for pre-feasibility and feasibility studies of small hydropower projects, which is proposed by a Canadian company in 1997. It also has the ability of risk analysis and can be utilized in feasibility studies supervision such as its cost aspect. Furthermore, in order to determine the percent of energy generation of dams which are not designed especially for hydropower plants, RETScreen is helpful. The RETScreen software is written in Visual Basic with iterative worksheets. The model addresses both run-off river and reservoir developments and calculates efficiencies of a wide variety of hydro turbines. In order to draw the flow duration curve which depicts the flow conditions in the river over a period of time hydrological data, such a design flow is required.

Design flow is defined as the maximum amount of flow that can be used by the turbine. The selection of design flow depends on the available flow at the site. Its calculation is based on frequency analysis of annual flow and varies by project conditions, hydro energy and economic studies. So a unique flow design should be considered for all months.

Initial inputting data required to the model consists of the project and turbine type and geographical situation of Rigcheshme hydropower. Other information such as resource assessment and hydro turbine properties are needed for the energy modeling step. The flow duration curve for the study river was drawn in order to calculate the energy. Flow duration curve displays the amount of flow over a period of time from larger to lower value that can be used to express the existing flows during the period and also available power and energy in a site.

Power calculation in the RETScreen is performed on basis of the following equation:

$$P = \rho g Q \left[ H_g - \left( h_{hydr} + h_{tail} \right) \right] e_t e_g \left( 1 - l_{trans} \right) \left( 1 - l_{para} \right) \tag{1}$$

（1）where $\rho$ is the density of water (1000 kg/m$^3$), g the acceleration of gravity (9.81 m/s$^2$), $H_g$ the gross head, $h_{hydr}$ and $h_{tail}$ are respectively the hydraulic losses and tailrace effect associated with the flow; and $e_t$ is the turbine efficiency at flow Q, $e_g$ is the generator efficiency, $l_{trans}$ is the transformer losses, $l_{para}$ the parasitic electricity losses; $e_g$, $l_{trans}$, and $l_{para}$ are specified by the user in the energy model worksheet and are assumed independent from the considered flow.

Hydraulic losses are adjusted over the range of available flows according to the following equation:

$$h_{hydro} = h_g l_{hydr,max} \frac{Q^2}{Q_{des}^2} \tag{2}$$

where $l_{hydr,max}$ is the maximum hydraulic losses specified by the user, and $Q_{des}$ the design flow. Similarly, the maximum tailrace effect is adjusted over the range of available flows with the following relationship:

$$h_{tail} = h_{tail,max} \frac{\left( Q - Q_{des} \right)^2}{\left( Q_{max} - Q_{des} \right)^2} \tag{3}$$

where $h_{tail,max}$ is the maximum tail water effect, i.e. the maximum reduction in available gross head that will occur during times of high flows in the river. $Q_{max}$ is the maximum river flow, and equation (3) is applied only to river flows that are greater than the plant design flow (i.e. when $Q \succ Q_{des}$ ) (RETScreen 2004).

The RETScreen output were displayed via power curves and compared with the SDI values calculated in different time periods including monthly, seasonal, and annual in order to determine the most efficient time interval in studding of SDI.

**RESULTS AND DISCUSSION**

Regression equation linking drought index and the amount of generated energy during different time intervals is calculated using SPSS software in order to extract the relation between drought and energy. Figure 2 shows the effect of drought on energy generation for June, and October as samples. Figure 3 and Fig.4 display the SDI and generated energy in seasonal (fall) and annual time scales over a period of 39 years from 1966 to 2004.

In addition to illustrating relationship between SDI and generated energy by graphs presented, their relation was explained using coefficient of determination ($R^2$). As seen in Tables 1 and 2, correlation between SDI as an accredited index for determining the amount of flow deviation from normal condition and the generated energy in monthly, seasonal and annual time scales were shown.
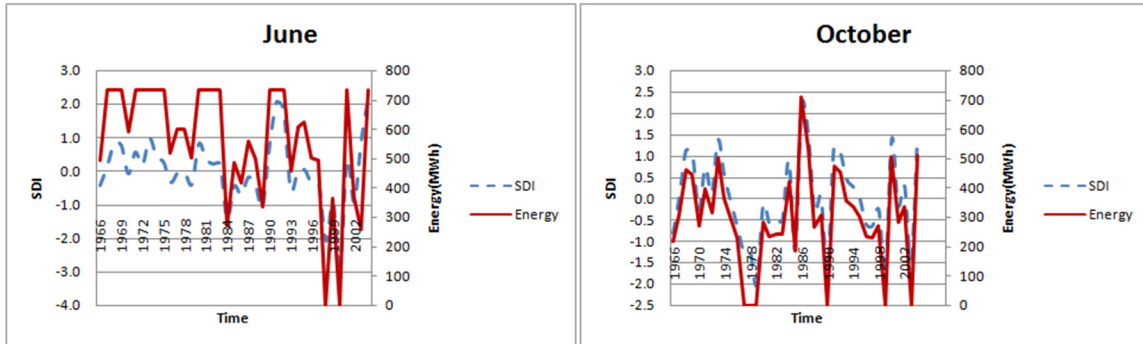


FIGURE 2.SDI and energy calculated for June and October
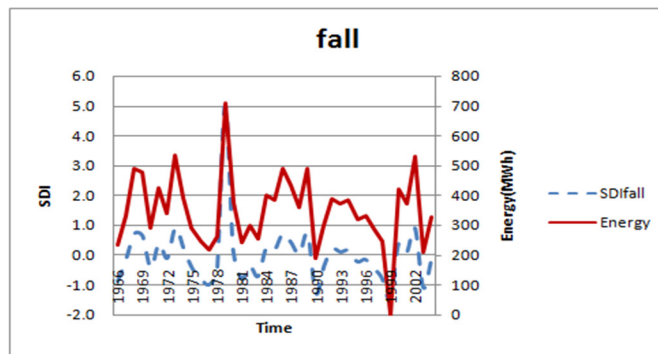


FIGURE 3.SDI and energy calculated for fall
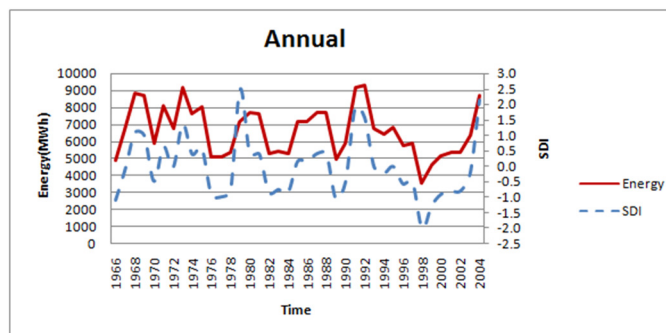


FIGURE 4.Annually computed SDI compared with annually generated energy over 39 years

According to the obtained relationships for different cases, $R^2$ is high which indicates the high level dependency of the generated energy on SDI. However, it can be inferred as duration of time scale enlarge, the relation between SDI and energy varies too. In the other words, more strong relation will be obtained if more duration time scales are used. This indicates that by increasing the duration of time intervals the effects of occurring the drought can be observed more vibrant. The reason can be explained by considering the full load capacity of the turbines. When time intervals is monthly during the months that the amount of river discharge is considerably more than design flow, all turbines will generate electrical energy with full capacity. In this situation, variation of river discharge and consequently the drought index has a negligible effect on energy generation as a result of the snowmelt and flood which

leads to an approximately constant value for the generated energy in a considerable percentage of the time and so the drought effects would be hidden. In the contrast in the investigation with longer time period this problem will be adjusted due to more diverse climate situations during the period of study. The $R^2$ values of various months were averaged in order to provide a sensible value to compare. The results are shown in Table.2 for different time periods.

TABLE 1. $R^2$ in different months

| Month | $R^2$ | Month | $R^2$ |
|---|---|---|---|
| October | 0.96 | April | 0.16 |
| November | 0.96 | May | 0.47 |
| December | 0.95 | June | 0.66 |
| January | 0.49 | July | 0.92 |
| February | 0.51 | August | 0.31 |
| March | 0.87 | September | 0.95 |

TABLE 2. $R^2$ in seasonal and annual intervals

| Time period | Spring | Summer | Fall | Winter | Annual |
|---|---|---|---|---|---|
| $R^2$ | 0.36 | 0.95 | 0.81 | 0.97 | 0.83 |

**CONCLUSION**

Variation of discharge and drought effects on hydropower generation of Rigcheshme dam with data over a period of 39 years from 1966 to 2004 was investigated in monthly, seasonal, and annual intervals. According to the obtained equations for different periods, the average of coefficient of determination between SDI and generated energy is 0.68, 0.77, and 0.83 for monthly, seasonal and annual intervals respectively. This indicates that by increasing the duration of study period the results of SDI can reflect the effects of drought on generated energy in a more efficient way.

**REFERENCES**

American Meteorological Society, 1997. *Meteorological drought –policy statement. Bull.* Amer. Meteorol. Soc. 78: 847–849.

Beran MA, Rodier JA. "Hydrological aspects of drought". *UNESCO–WMO Studies and Reports in Hydrology* 39:149, 1985.

Ben-Zvi A. "Indices of hydrological drought in Israel". J *Hydrol 92(1–2):*179–191, 1987.

Bonaccorso B, Bordi I, Cancelliere A, Rossi G, Sutera A. "Spatial variability of drought: an analysis of the SPI in Sicily". *Water Resour Manag* 17:273–296, 2003.

Dracup JA, Lee KS and Paulson EG "On the definition of droughts", *Water Resources Research*, vol. 16, pp. 297-302, 1980.

Nalbantis and Tsakiris,2008. "Assessment of Hydrological Drought Revisited Water Resource" .*Manage DOI* 10.1007/s11269-008-9305-1.

*RETScreen International, Small Hydro Project Analysis.* (2004-a) RETScreen Engineering and Cases Textbook.

RETScreen International, (2004-b) *RETScreen Software Online User Manual, Small Hydro Project Model.*

Tsakiris G, Vangelis H, 2005. "Establishing a drought index incorporating evapotranspiration". *European Water* 9/10:3–11.

Tsakiris G, Pangalou D, Vangelis H, 2006. "Regional drought assessment based on the Reconnaissance".

Nalbantis,2008. "Evaluation of Hydrological Drought Index". *European Water*23/24:67-77.

# EFFECTS OF BIOFUEL PRODUCTIONS IN THE OHIO RIVER BASIN'S WATER RESOURCES AND QUALITY

*Yonas Demissie*, Eugene Yan, and May Wu (Argonne National Laboratory, Argonne, IL, USA)

**ABSTRACT:** The use of biofuels as an alternative energy source has been widely pursued in the U.S. as a strategy to minimize dependency on fossil-fuel, decrease the greenhouse gas emission, and develop the rural economy. Supplying the emerging biofuels industry with enough conventional and cellulosic biomass may require changes in current land use and managements that can affect the water resources and quality at both regional and local scales. In this study, we have developed an integrated watershed hydrology model to study the potential consequences of the expected increase in the biofuel feedstock productions on the Ohio River Basin water resources. The basin is one of the six main drainage areas of the Mississippi River, which is expected to be greatly affected by the increased biofuel feedstock productions. It also currently contributes to the majority of the flow volume, nutrients, and sediments in the river that ultimately enter to the Gulf of Mexico. Several plausible future biofuel feedstock production scenarios including the DOE Billion Ton Study's projections were considered to assess the potential impacts on the region and its local streams discharges, evapotranspiration, soil moisture content, sediment erosion, nitrogen and phosphorus loadings. The results from these scenarios were compared with the results obtained from a baseline and business-as-usual scenarios. Depending on the change in land use and crop management associated with biofuel feedstock production, the potential impacts on the regional water resources and stream qualities can be mixed with considerable spatial and temporal variations, thus providing an opportunity to further optimize the biomass production by taking into account its potential implications on the basin water resources and quality.

## INTRODUCTION

As a continuing effort to assess the potential impacts of biofuel productions on the Mississippi River Basin (MRB) hydrology and water quality, this study has developed a Soil and Water Assessment Tool (SWAT) for the Ohio River Basin (ORB), which is one of the six USGS's 4-digit HUCs subbasins contributing to the Mississippi River (Figure 1). The basin has more than 422 thousand square kilometers area, partially covering eleven Eastern and Midwestern states in the United States. The U.S. Geological Survey divided the basin into 120 8-digit HUCs subbasins with an average drainage area of 3.5 thousand square kilometers. It is one of the primary sources of flow (49%), phosphorus (29%), and nitrogen (32%) to the greater MRB which eventually flow to the Gulf of Mexico (Goolsby et al., 1999). The land use in the region is predominantly forest followed by pasture, hay, and alfalfa, which account about 51% and 20% of the total basin area. The agricultures lands for corn, soybean, and wheat constitute about 17% of the region, while urban areas are about 10%. The current land use and agricultural practices in the region are expected to be affected as the demand for feedstock production for biofuel grows in the region over the near future. For example, the recent DOE and USDA joint study, also known as Billion-Ton Study (USDOE, 2011), estimated the region to supply significant amount of corn grain, stover and perennial grass biomass by 2022.

The main objective of this study is to develop an integrated water quality and quantity assessment tool using the SWAT watershed model to evaluate the ORB water resources and qualities under current and historical climate, land use, and management conditions as well as future biofuel feedstock productions. We have considered future change in corn rotation pattern and stover harvest for the biofuel

feedstock production scenarios. The basin responses to these changes were evaluated in terms of temporally and spatially varying evapotranspiration, soil moisture content, stream flow volumes, suspended sediment loading, total nitrogen and phosphorus loadings. The calibrated model result was used as a baseline or reference condition to evaluate the relative impacts of the future biofuel feedstock production on the basin water resources and qualities.



**FIGURE 1** The Ohio River Basin, covering parts of eleven states in the eastern and mid-western United States.

## MATERIALS AND METHODS

*SWAT Model*. The development of the ORB SWAT model (ORB-SWAT), which uses the modified SWAT 2009 version (Neitsch et al. 2011), specifically involves incorporating land use dynamics through four-year rotations of corn, soybean, wheat, and hay from 2006 to 2009, as well as utilizing recent data on agricultural activities and other model forcing data. In addition to improving representation of the basin current and historical conditions, the modeling objective also focus on providing flexible tool to test different combinations of future feedstock sources (including conventional and cellulosic) for biofuel production. The model simulates the basin daily physical and biological processes from 1987 to 2009. The first three years are used for tuning or warm up the model, while the rest is used to calibrate and validate the model. The model was discretized to 14,280 hydrologic response spatial units (HRUs).

*Input Data*. The four-year rotations among corn, soybean, wheat, and hay are determined using the method developed for the Upper Mississippi River basin SWAT model (Demissie et al., 2012). Commercial fertilizer and animal manure data, which are available at state and county levels, respectively, were distributed to the subbasin level using weighted average method based on crop areas. They are applied over the crop and hay lands using the heat unit scheduling techniques. The daily precipitation, minimum and maximum temperature data for the modeling period (i.e. 1987-2009) were interpolated from 3,514 precipitation and 2,480 temperature measuring NOAA weather stations in and around the basin. Tillage data, including no tillage, reduced tillage, and conventional tillage for corn, soybean, and wheat, were derived from the Conservation Tillage Information Center's (CTIC) 2004 county-level survey data. The country-level data were aggregated to the subbasins and then applied to crops using area weighted average method. Other detailed input data incorporated into the model include tile drains on

crops grown over flat regions, irrigation and consumptive water uses, major reservoirs along the mainstream of the Ohio River, point sources from industries and wastewater treatment plants.

## IMPACTS OF BIOFUEL PRODUCTIONS

In response to the growing feedstock demand for biofuel production, the corn rotation and stover harvest in the basin are expected to change (USDOE, 2011). This study has examined the potential impacts of these changes on the basin hydrology and stream quality. Currently, corn is grown mostly in rotation with soybean and wheat in order to maintain the soil productivity and decrease the need for supplemental fertilizer input. However, over the past decade the intensity of corn within a specific year of rotations have increased and are expected to increase further in this decade, mostly because of the increased demand for ethanol. In addition, the stover is also expected to be harvested from the field as the demand for the cellulosic based biofuel increases. Thus, our assessment of the potential impacts on regional and local water resources and quality can provide a much needed insight about the sustainability of increasing feedstock production for biofuel.
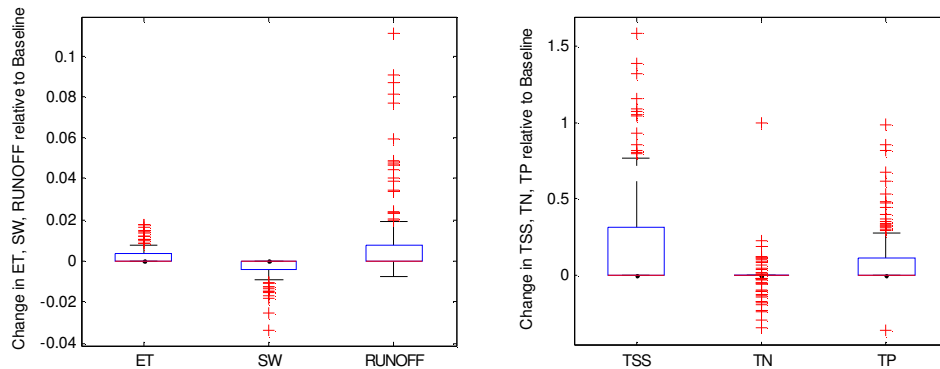


**FIGURE 2** Impacts of growing corn continuously, instead of in rotation with other crops, on the annual hydrology and water quality of the subbasins relative to the corresponding basin-average baseline values.

The corn rotation scenario was applied by changing all corn land uses which are currently in rotation to continuous corn. This resulted to conversion of about 6.0 million ha of corn which is grown in rotation with soybean, wheat and hay to continuous corn. The calibrated model was rerun using this new land use and adjusting the corresponding management operations. The resulting changes in discharge and water quality were analyzed at the subbasin and basin levels. Figure 2 shows the impacts on basin-average annual evapotranspiration (ET), soil moisture (SW), water yield (RUNOFF), suspended sediment loading (TSS), total nitrogen loading (TN), and total phosphorus (TP) loading relative to the corresponding baseline values. The box-plot results show that growing corn continuously instead of in rotation with other crops can slightly increase the annual ET in some of the subbasins, with few subbasins, out of the 120 subbasins in the ORB, having greater than 1% increase. Compare to soybean, wheat, and hay, corn has higher leaf area index which may lead to increase transpiration during the growing season. The runoff from the subbasins increased by up to 10% in some of the subbasins, but similar to the other impacts it shows no noticeable difference on the basin-average value. The soil moisture content is reduced by up to 3% in some of the subbasins, which might be attributed to the increase in ET and runoff from the subbasins. The change in rotation, however, has relatively higher impacts on sediment and total phosphorus loadings, with the loading in few subbasins increased by more than 50% from the baseline values. On the other hand, the nitrogen loading may slightly increase or decrease in some of the subbasins, suggesting that growing corn continuously might have mixed impacts on the subbasin contribution at least for a shorter period the analyses was based. The increase in sediment loading might be explained by

the increased in tillage and runoff from continuous corn field. The phosphorus is mostly transported attached with the sediment and may increase along with the sediment loading.
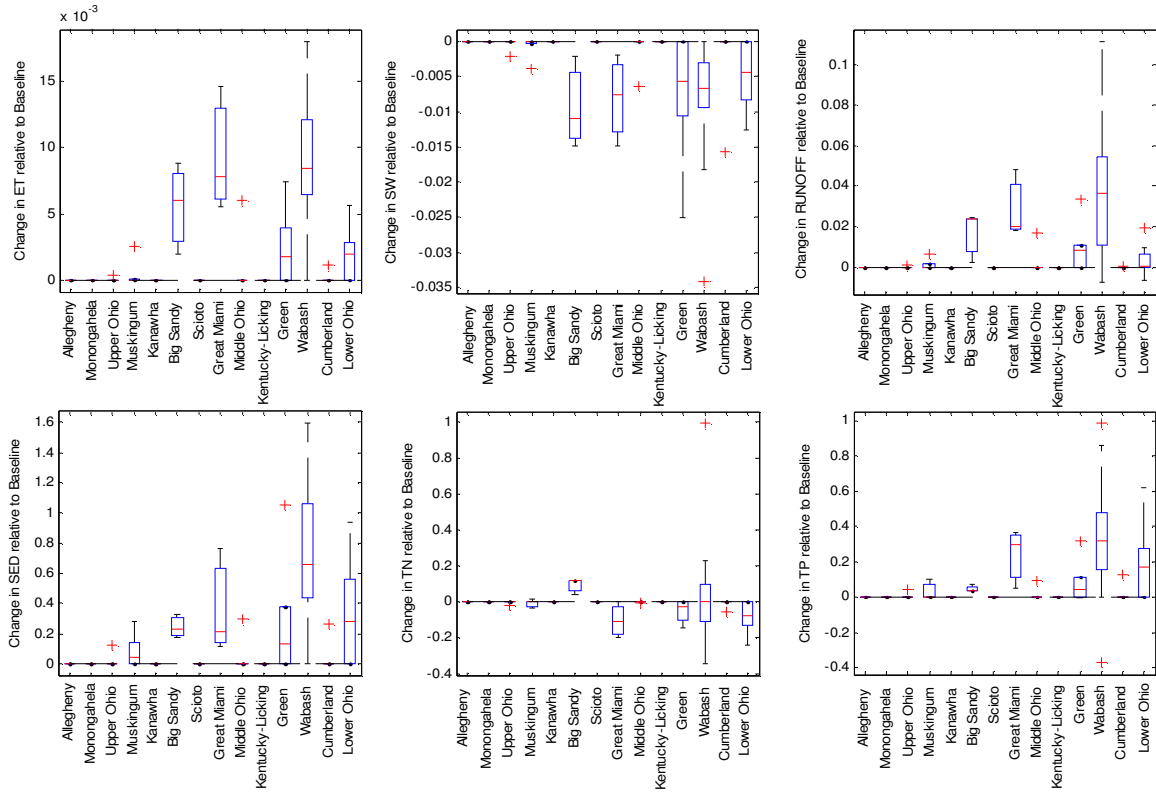


**FIGURE 3** Impacts of changing corn rotations to continuous corn at the major (6-digit HUC) watersheds within the ORB.
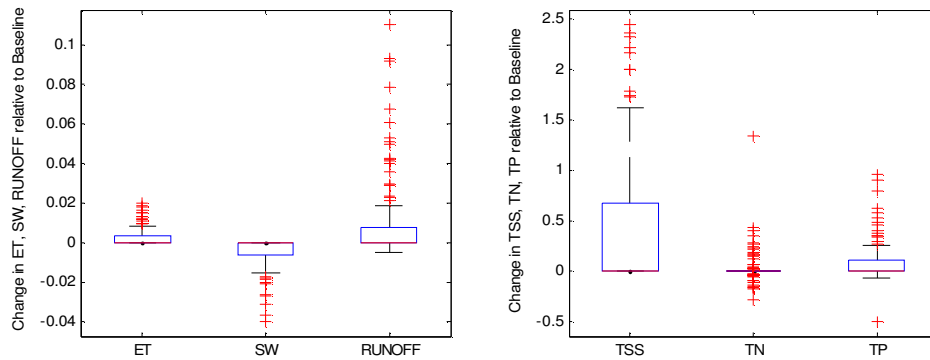


**FIGURE 4** Impacts of harvesting corn stover for cellulosic biofuel on the annual hydrology and water quality of the subbasins relative to the corresponding basin-average baseline values.

Figure 3 illustrates the impacts at the major (USGS's 6-digit HUC) watersheds locating within the ORB. Except for Wabasha, Big Sandy, Green, Great Miami, and Lower Ohio watersheds, majority of the watersheds show no impact to the change in corn rotation. As expected, the affected watersheds constitute relatively larger changes in corn areas.

The other scenario we considered in this study involves harvesting 75% of the stover from the corn yield each year. The corn harvest index parameter was modified to implement the scenario in the calibrated SWAT model. The water resource and quality impacts on the ORB and its major watersheds are illustrated in Figure 4 and Figure 5, respective. The results show that harvesting stover for cellulosic biofuel will increase the ET and runoff but decrease the soil moisture in some of the basins. The sediment and phosphorus loadings are also expected to increase in some of the subbasins, while the impact on nitrogen loading may vary across the subbasins. The impact patterns are similar to that of the rotation scenario, with the stover harvest scenario having relatively higher impacts.
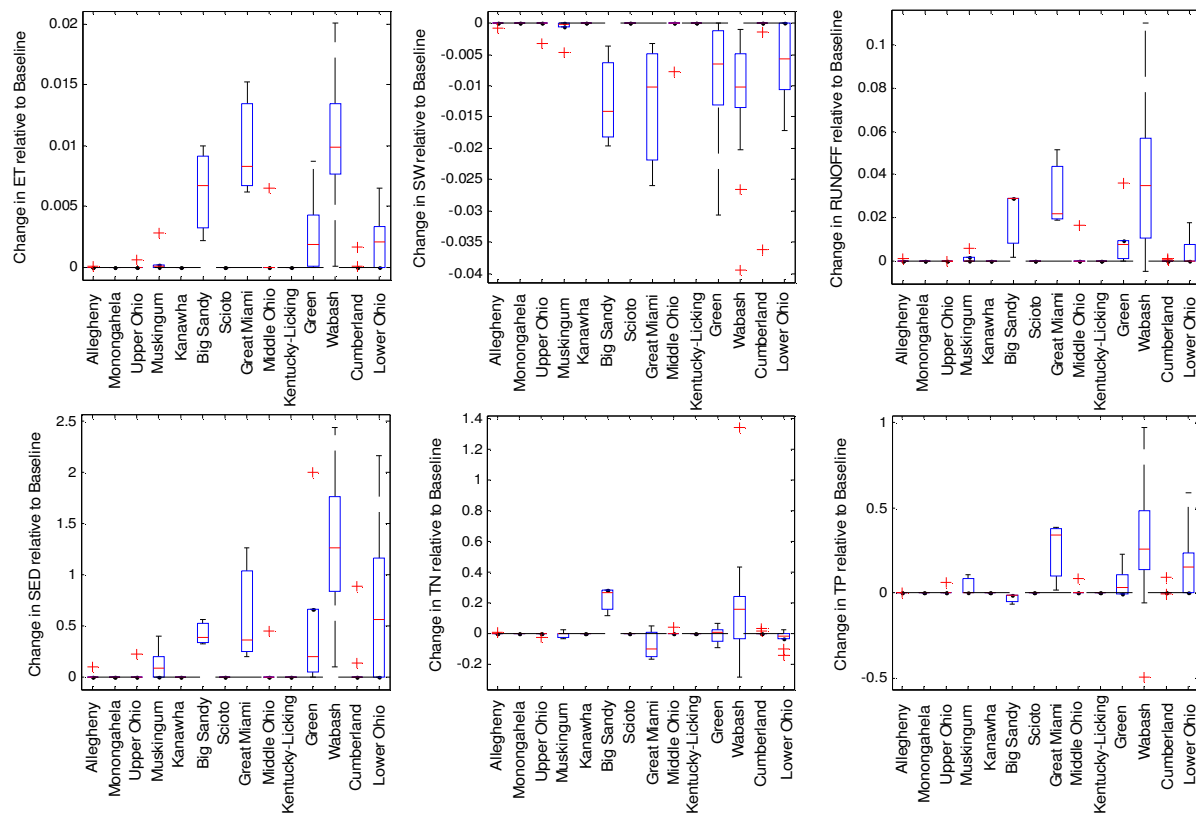


**FIGURE 5** Impacts of harvesting stover at the major watersheds within the ORB.

**CONCLUSION**

The study successfully developed a SWAT model application for the ORB to simulate the hydrology, water quality and biomass production under current and historical conditions of the basin as well as under the potential future changes in land use and management related to the expected increase in biofuel feedstock production. The model utilized detailed data on land use and management practices, and developed specifically to simulate different biofuel feedstock production scenarios. The calibrated model was applied for two potential future biofuel feedstock productions, namely growing corn continuously instead of in rotation with other crop and harvesting some portion of the stover. In both cases, the impact in hydrology was found to be moderate with increase in ET and runoff and decease in soil moisture content in some of the subbasins. However, the scenarios showed relative noticeable impact on sediment and phosphorus loading in some of the subbasins. The impact on nitrogen loading varies from subbasin to subbasin, with no noticeable trend.

**ACKNOWLEDGMENTS**

**REFERENCES**

Demissie, Y., E. Yan., M. Wu, and Z. Zhonglong. 2012. *Watershed modeling of potential impacts of biofuel feedstock productions in the Upper Mississippi River Basin.* ANL/EVS/AGEM/TR-12-07. Argonne National Laboratory Argonne, IL.

Goolsby D.A., W.A. Battaglin, G.B. Lawrence, R.S. Artz, B.T. Aulenbach, R.P. Hooper, D.R. Keeney, and G.J. Stensland. 1999. *Flux and sources of nutrients in the Mississippi-Atchafalaya River Basin - Topic 3 Report for the Integrated Assessment on Hypoxia in the Gulf of Mexico.* NOAA Coastal Ocean Program Decision Analysis Series No. 17. Silver Spring, MD.

Neitsch S.L., J.G. Arnold, and J.R. Kiniry. 2011. *Soil and Water Assessment Tool theoretical documentation version 2009.* Texas Water Resources Institute, TR-406-2011. College Station, TX.

U.S. Department of Energy. 2011, *U.S. Billion-Ton Update: Biomass Supply for a Bioenergy and Bioproducts Industry.* R.D. Perlack and B.J. Stokes (Leads), *ORNL/TM-2011/224.* Oak Ridge National Laboratory, Oak Ridge, TN.

# A WATER TURBINE GENERATOR AT A WASTEWATER TREATMENT PLANT

*Jonathan Gorman, Denis Guleiof*, Ashley Rivera, Theresa Perez, Arnoldo Ramirez, Daniel Guerra, Jianhong Ren, and Lee Clapp (Texas A&M University-Kingsville, Kingsville, TX, USA)

This paper presents a case study on converting energy contained in flowing wastewater effluent to electricity using hydropower technology. A water turbine generator that produces sufficient electricity to power a UV-light disinfection system at the north Kingsville wastewater treatment plant has been designed and will be implemented. The device is designed to have a capacity of 3 kW that can be used to fully power the UV-light system. It will be placed at the plant's outfall that has a static head measured at 5 feet and a flow rate of 2.7 ft3/s (0.076 m3/s). Preliminary design includes a vacuum head water turbine, in which the effluent wastewater is funneled and vertically directed through an impeller housed in a pressure casement. This design offers many advantages over other options for generating the required power. The turbine generator system design, performance and its associated uncertainties will be presented in this paper. The results of this project will contribute to solutions of reducing energy consumption in wastewater treatment industry.

# PHOTOACTIVITY OF NICKEL- CUPROUS-OXIDE-ON-COPPER ELECTRODE FOR HYDROGEN GENERATION

*Sangeeta*, Ashok N. Bhaskarwar
(Indian Institute of Technology, Delhi, Hauz Khas, New Delhi- 110016, India)

**ABSTRACT:** Photo-assisted electrolysis of water is a sustainable way of generating hydrogen, potentially a future fuel, from the most abundant substance on earth, i.e. water, using solar energy. Films of cuprous oxide on copper are examined for the photo-electrolysis of water using platinum (Pt) as a counter electrode and brine as an electrolyte in a photo-electrochemical cell illuminated by a halogen lamp. A maximum overall efficiency of 96.9 % is obtained for the process under a cathodic bias of 1.2 V vs. silver/silver chloride (Ag/AgCl) reference electrode. The effect of presence of nickel layer and its thickness on the photo-activity of cuprous oxide is also studied. Cuprous oxide shows the highest photocurrent. The presence of nickel on the oxide layer decreases the efficiency. Cuprous oxide with a layer of nickel of thickness of 6.75 µm shows the lowest photocurrent and also the lowest onset potential. Further, the increase in intensity of illumination decreases the overall efficiency of the process.

The performance of the photo-catalyst is related to the morphological structure of the photo-electrode which is studied by X-Ray Diffraction (XRD), Scanning Electron Microscopy (SEM) and Energy Dispersive X-Ray Spectroscopy (EDX). The plane of crystallinity, interfacial area of the semiconductor-electrolyte interface and surface area enhancement due to development of cracks play key roles in deciding the observed photo-efficiency of the photo-catalyst. There exists an optimum thickness of the nickel layer (of 5 µm) for this kind of photo-cathode.

## INTRODUCTION

Conversion of solar energy into chemical energy has been a topic of research for many decades. Photo-assisted electrolysis of water is a sustainable way of generating hydrogen, potentially a future fuel, from the most abundant substance on earth, i.e. water, using solar energy. In a pioneering work reported by Fujishima and Honda in 1972, water was electrolyzed for the first time at a potential lower than the minimum theoretical potential, by illuminating titanium-dioxide ($TiO_2$) photo anode with UV light (Fujishima, A. and K. Honda., 1972). Subsequent research in this area was concerned with improvement of efficiency of $TiO_2$ in different ways or with development of new photo-catalysts. Different semiconductors (metal-oxides, suplides, selenides, etc.) were used by researchers as photo catalysts in photo-electrochemical cells ( Nozik, A.J., 1978; Bard, A.J., 1979; Wrighton, M.S., 1979; Tomkiewicz, M. and H. Fay,1979; Memming, R., 1980).

All photo-catalysts studied so far can be classified into two groups: (i) photo-catalysts with a wide band gap (2.5-3.5eV) which are quite resistant to corrosion but have a very small range of absorption spectrum which results in a low efficiency of catalyst (Aroutiounian et al., 2005), and (ii) photo-catalysts with a low band gap (0.8-2eV) which have a broad range of absorption spectrum but give a low photo-voltage and are more prone to corrosion (Aroutiounian et al., 2005). Cuprous oxide with a band gap in visible region (2eV) is suitable for use in catalysis (Ortiz et al., 2001; Yang et al., 2006), gas sensors (Shishiyanu et al., 2006), and solar cells (Rai, B.P., 1988). The domain defect in cuprous oxide is copper vacancies, and hence it has p-type of conductivity. It is highly abundant (Tomkiewicz, M., and H. Fay., 1979), and perhaps has a limited toxicity (Somasundaram et al., 2007). The photo-activity of this material has been reported earlier (Khan, K.A., and J.F. Kos., 1986). The conduction and valence-band edges of cuprous oxide lie near the reduction and oxidation potentials of water, respectively, and hence it can be used for the photo-assisted electrolysis of water. Various methods are available in literature for the

preparation of different micro- and nano- structures of cuprous oxide, e.g. electro-deposition (Chen et al., 2007; Huang et al., 2002), gas-phase deposition (Reddy et al., 2006), wet-chemistry methods (Xu, et al., 2006), and thermal oxidation (Musa et al., 1998). Electro-deposition is a simple and economical method of preparing films which can control their crystalline nature. The crystallography of cuprous-oxide films deposited on TCO by the cathodic reduction of copper-lactate alkaline solution has already been studied (Wana et al., 2010). In the present work, films of cuprous oxide are prepared on copper substrate by electro-deposition. The proposed mechanism (Golden et al., 2006) is given below.

$$2Cu^{2+} + 2e^- + H_2O \rightarrow Cu_2O + 2H^+ \tag{1}$$
$$Cu^{2+} + 2e^- \rightarrow Cu \tag{2}$$
$$Cu_2O + 2H^+ + 2e^- \rightarrow 2Cu + H_2O \tag{3}$$

In an effort to increase the efficiency of photo-assisted electrolysis, various metals like Au, Pt, and Ni have been deposited on cuprous-oxide films on different substrates like TCO, FTO, and metals along with different electrolytes including sacrificial electron donors (Somasundaram, et al., 2007; Khan, et al., 1986; Khan, K.A., 2000 ).

In the present paper, we report the effect of Ni layer deposited by photochemical bath deposition on the efficiencies. The thicknesses of Ni layers are in turn regulated by the duration of deposition. The photo-activity of cuprous oxide and the effect of thickness of nickel layer are studied by photo-assisted electrolysis of brine in a photo-electrochemical cell

## MATERIALS AND METHODS

**Materials used**. Cupric sulphate, lactic acid, sodium hydroxide, deionised water, sodium chloride, phenolphthalein (as an indicator), Cu (10cm X 2 cm X 0.5 mm), nickel sulphate, and isopropyl alcohol have been used in the experiments for the preparation and testing of electrodes.

**Preparation of coatings of cuprous oxide on copper substrates.** Coatings of p-cuprous oxide on copper electrodes were prepared by electroplating. The film of p-cuprous oxide was grown on copper by the cathodic reduction of cupric-lactate solution (Somasundaram et al., 2007). It resulted in the formation of a brown layer of p-cuprous oxide on the cathode.

**Preparation of coatings of nickel on films of cuprous oxide.** The coatings of nickel were prepared by photo-chemical bath deposition (Somasundaram et al., 2007). The deposition of nickel was carried out for 1, 2, 3 and 4 hours to get different thicknesses of 1.65, 3.3, 5.0 and 6.8 µm, respectively, on cuprous-oxide substrate.

**Measurements.** The photocurrent for a photo-electrode  with Pt as a counter electrode and Ag/AgCl as a reference electrode was measured  by linear sweep voltammetry  (LSV) method using a potentiostat/galvanostat (of Gambry, 300B), 0.5M brine as the electrolyte and  halogen lamp (Details: Philips, Halolite, 500W, 240V~50)  as a source of illumination. The LSV was performed for cuprous oxide without and with nickel layers of different thickness under dark and illumination of two different intensities, viz $0.016W/cm^2$ and $0.025W/cm^2$. The crystallographic and morphological studies of the photo-electrodes were done by scanning electron microscopy (SEM), X-Ray diffraction (XRD).

## RESULTS AND DISCUSSION

**Physical Characterization.** The crystalline and cubic nature of cuprous oxide is confirmed by XRD.  It also confirms the presence of nickel on cuprous oxide (Figure 1). The cuprous oxide is mainly crystalline in 2 0 0 and 1 1 1 planes.  On deposition  of nickel, the crystallinity in 111 and 311 planes decreases, but as the  thickness of nickel  on cuprous oxide increases, the crystallinity in 111 plane increases. The

crystallinity in 311 plane decreases on deposition of nickel. SEM images confirm the cubic shape of particles of cuprous oxide deposited on copper (Figure 2). There are cracks in the layer of nickel and the cracks increase with the increase in the thickness of nickel layer on cuprous oxide layer.
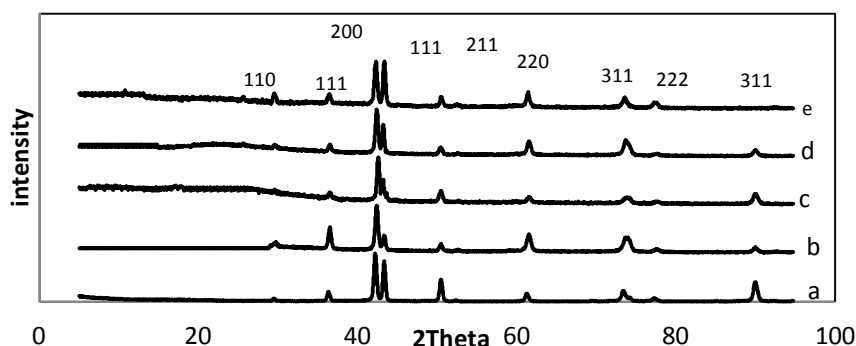


FIGURE 1. XRD of photocatalyst (a) Cuprous oxide (b) $Cu_2O$/Ni 1.5 µm (c) $Cu_2O$/Ni 3.3 µm (c) $Cu_2O$/Ni 5 µm (d) $Cu_2O$/Ni 6.8 µm.
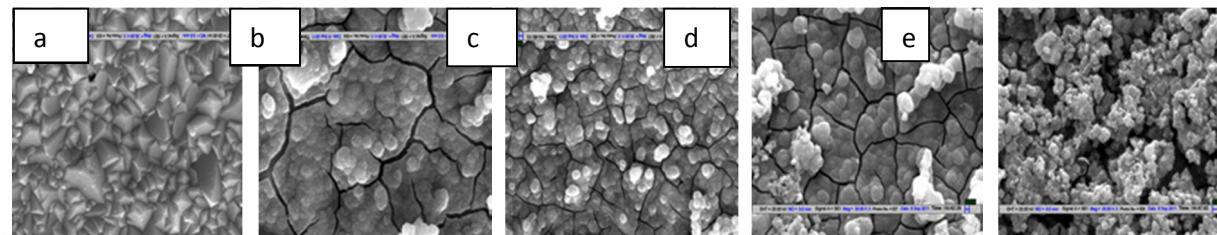


FIGURE 2. SEM images of (a) Cuprous oxide, (b) $Cu_2O$/Ni 1.5 µm, (c) $Cu_2O$/Ni 3.3 µm, (d) $Cu_2O$/Ni 5 µm, (e) $Cu_2O$/Ni 6.8 µm

**Electrochemical Analysis.** I-V curves are obtained by LSV and efficiency of the process is calculated from the expression given below (Varghese O.K., and C. A. Grimes, 2008).

$$\eta = \frac{1.229 \times I_P \times 100}{P_{total}} = \frac{1.229 \times I_P \times 100}{P_{illumination} + V_{bias} I_P}$$

(4)

Cuprous oxide on copper performs well as a photocatalyst. Under illumination, cuprous oxide shows the highest overall efficiency (Figure 3). When nickel is deposited on cuprous oxide, efficiency decreases; but upon increasing the thickness of nickel it increases to an extent and then decreases again. The same trend is observed under different intensities of illumination (Figure 4). For a thickness of 6.8µm the overall efficiency is lowest. A maximum efficiency of 96.9% is obtained at -1.2V vs. Ag/AgCl for cuprous-oxide electrode under illumination intensity of 0.016 W/cm$^2$. It is also observed that the increase in intensity of illumination decreases the overall efficiency of the process (Figure 4), perhaps as a result of the sub-linear increase of the output in the form of hydrogen. The presence of nickel on the oxide layer decreases the efficiency for both reported intensities of illumination (Figure 3 and 4).

When a semiconductor is immersed in an electrolyte, there is a charge transfer taking place at the interface. This charge transfer results in the formation of an electric field at the surface of semiconductor which may extend up to 5 to 200 nanometers (Bard, A.J., 1980). For a p-type semiconductor, direction of the electric field is from the interface to the bulk of semiconductor. Thus, if electron-hole pairs are generated in this region the electrons move towards the interface and these can reduce water while the

holes move towards bulk and are transferred to the other electrode where they oxidize the reductant present in the electrolyte.
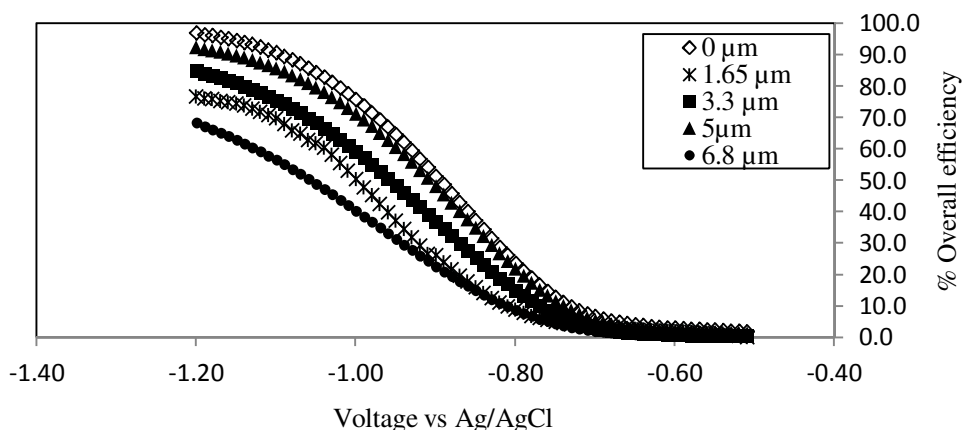


FIGURE 3. Comparison of overall efficiencies of photo-electrodes under illumination of power density 0.016W/cm2.
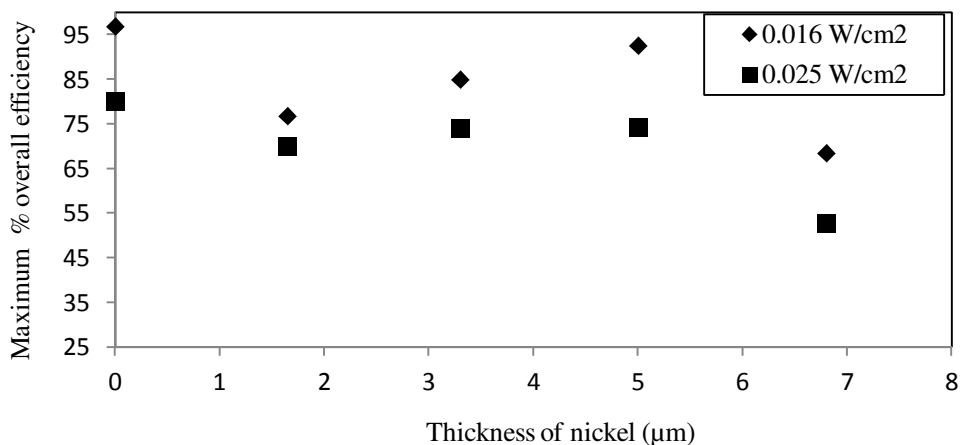


FIGURE 4. Effect of thickness of nickel on the maximum overall efficiencies of the photo-electrode under different intensities of illumination.

It is observed that on deposition of nickel some cracks developed in the coatings of cuprous oxide. The number of cracks increased with the increase in time of deposition of nickel on cuprous oxide (Figure 2). The following three factors play a role in this experiment in which the electrode acquires a sandwich- like structure with metal films on both sides and a semiconducting substance in between them.

- On increasing the thickness of nickel, the conductivity of electrode increases but at the same time the absorption of light decreases.
- On increasing the thickness of nickel on cuprous oxide, the number of cracks increases and the surface area of cuprous oxide film increases.
- On increasing the thickness of nickel, the crystallinity in 311 plane decreases.

A thin layer of nickel on cuprous oxide decreases the performance of the photo-electrode because of (i) the decrease in area of contact between the electrolyte and the semiconducting oxide, and (ii) the decrease in crystallinity in 111 plane. On increasing the thickness of nickel on cuprous oxide, the effect of increase in surface area becomes predominant and also the crystallinity in 111 plane increases. These two

factors collectively result in the improvement in the performance of the photo electrode. When the thickness of nickel layer reaches 6.75µm, nickel completely covers cuprous oxide and the indispensable electric field that is normally produced at the interface between the semiconductor and electrolyte does not form and therefore results in a quite low efficiency for large thicknesses of nickel layer.

## CONCLUSION

Cuprous oxide on copper is a promising photo cathode and gives a good performance with brine is used as the electrolyte. Photo-efficiency of cuprous oxide has been found to decrease with the presence of a metallic layer like of nickel on it which contradicts the earlier reported results for cuprous oxide on TCO coated glass. The semiconducting oxide thus shows a different behavior for a metallic substrate. With quite a thick layer of metal on the semiconducting oxide, there is no double charge layer in the absence of the semiconductor-electrolyte interface and the separation of electron-hole pairs does not occur and consequently the performance deteriorates.

*Notations*

$I_p$ = Photocurrent density, A/m$^2$
$P_{total}$ = Total power density supplied to photo-electrochemical cell, W/m$^2$
$P_{illumination}$ = Power density of the source of illumination W/m$^2$
$V_{bias}$ = Bias potential applied, Volts
$\eta$ = Overall efficiency, dimensionless

## ACKNOWLEDGEMENTS

## REFERENCES

Aroutiounian, V.M., V.M. Arakelyan, and G.E. Shahnazaryan. 2005. " Metal oxide photoelectrodes for hydrogen generation using solar radiation-driven water splitting."*Sol. Energy.* 78(5): 581–592.

Bard A. J. 1980. " Photoelectrochemistry." *Science.* 207 (4427) :139-144.

Bard, A.J. 1979. "Photoelectrochemistry and heterogeneous photocatalysis at semiconductor." *J. Photochem.* 10(1) : 59-75.

Chen, J.Y., P.J. Zhou., J.L. Li., and S.Q. Li. 2007. " Depositing Cu$_2$O of different morphology on chitosan nano-particles by an electrochemical method." *Carbohyd. Polym.* 67(4): 623–629.

Golden, T.D., M.G. Shumsky., Y.C. Zhou., R.A. VanderWerf., R.A.V. Leeuwen., and J.A.Switzer. 1996. " Electrochemical deposition of copper(I) oxide films." *Chem. Mater.* 8 (10): 2499–2504.

Huang, L., H. Wan., Z. Wang, A. Mitra., D. Zhao., and Y. Yan. 2002. "Cuprite nano wires by electrodeposition from lyotropic reverse hexagonal liquid crystalline phase." *Chem. Mater.*14 (2): 876–880.

Fujishima, A. and K. Honda. 1972. " Electrochemical photolysis of water at a semiconductor electrode." *Nature.* 238 (5358): 37-38.

Khan, K.A. 2000. "Stability of a Cu$_2$O photoelectrode in an electrochemical cell and the performances of the photoelectrode coated with Au and SiO thin films." *Appl. Energy.* 65(1) : 59-66.

Khan, K.A. and J.F. Kos. 1986. "Photocurrent characteristics in Cu$_2$O/Pt and Cu$_2$O/TiO$_2$ photoelectrochemical cells in aqueous and non-aqueous electrolytes." *Pramana. J. Phys.* 26 (3): 277 – 281.

Memming, R. 1980. "Solar energy conversion by photoelectrochemical processes." *Electrochim. Acta.* 25(1): 77-88.

Musa, A.O., T. Akomolafe., and M. J. Carter. 1998. " Production of cuprous oxide, a solar cell material, by thermal oxidation and a study of its physical and electrical properties." *Sol. Energ. Mat. Sol. C.* 51(3-4): 305–316.

Nozik,A.J. 1978. " Photoelectrochemistry: Applications to Solar Energy Conversion." *Ann. Rev. Phys. Chem.* 29(1): 189-222.

Ortiz, J.R., T. Ogura., J. Medina-Valtierra, S.E. Acosta-Ortiz., P. Bosch., J.A. Reyes., and V.H. Lara. 2001. "A catalytic application of $Cu_2O$ and CuO films deposited over fibreglass." *Appl. Surf. Sci.* 174(3-4): 177–184.

Rai, B.P. 1988. "$Cu_2O$ solar cells :A review." *Sol.Cells.* 25 (3): 265–272.

Reddy, A.S., G.V. Rao., S. Uthanna., and P.S. Reddy. 2006. "Structural and optical studies on dc reactive magnetron sputtered $Cu_2O$ films." *Mater.Lett.* 60(13-14): 1617–1621.

Shishiyanu, S.T., T.S. Shishiyanu., and O.I. Lupan. 2006. "Novel $NO_2$ gas sensor based on cuprous oxide thin films." *Sensor. Actuat.* B 113(1): 468–476.

Somasundaram, S., C.N.R. Chenthamarakshan., N.R. Tacconi., and K. Rajeshwar. 2007. "Photocatalytic production of hydrogen from electrodeposited p-$Cu_2O$film and sacrificial electron donors." *Int. J. Hydrogen Energ.* 32(18): 4661 – 4669.

Tomkiewicz, M. and H. Fay. 1979. " Photoelectrolysis of water with semiconductors." *J. Appl. Phys.* 18(1): 1-28.

Varghese O.K. and C.A. Grimes. 2008. "Appropriate strategies for determining the photoconversion efficiency of water photoelectrolysis cells: A review with examples using titania nanotube array photoanodes." *Sol. Energ. Mat. Sol. C.* 92(4):374–384.

Wana,L., Z. Wang., Z. Yang., L. Wenjun., L. Zhaosheng., and Z. Zhigang. 2010. " Modulation of dendrite growth of cuprous oxide by electrodeposition." *J. Cryst. Growth.*312 (21): 3085–3090.

Wrighton, M.S. 1979. "Photoelectrochemical conversion of optical energy to electricity and fuels."*Acc. Chem. Res.* 12(9): 303-310.

Xu, H., W. Wang., and W. Zhu. 2006. "Shape evolution and size-controllable synthesis of $Cu_2O$ octahedral and their morphology-dependent photocatalytic properties*." J.Phys.Chem.* B 110(28): 13829–13834.

Yang, H., J.Ouyang., A. Tang., Y.X. Xiao., Li, X. Dong., and Y. Yu. 2006. " Electrochemical synthesis and photocatalytic property of cuprous oxide nanoparticles." *Mater. Res. Bull.* 41(7): 1310–1318.

# WATER USE IN CELLULOSIC ETHANOL PRODUCTION

*Morten Moeller Klausen* and Gert Holm Kristensen
(DHI Group, Hoersholm, Denmark)

**ABSTRACT:** The interconnection between water use and energy production is a highly debated topic. Production of cellulosic ethanol from agricultural residues is an energy production technology, which does not require additional water for feedstock production. On the other hand, water is required for different processes and utilities at the ethanol plant. This study takes a detailed look at water use in the emerging cellulosic ethanol industry. Water consumption for cellulosic ethanol production is analyzed and discussed based on pilot scale and full scale design data on the water consuming processes for two commercial cellulosic ethanol production processes with plants in the construction or operational phase. The detailed analysis of the water consumption leads to identification of the most water intensive processes and investigates the possibilities for water use minimization as the industry matures. Furthermore, the water consumption in the two plants is compared with water consumption in process simulation optimized cellulosic ethanol processes as well as water consumption in conventional gasoline production. Besides looking at agricultural residues, the study also considers the water implications of using perennial energy crops for cellulosic ethanol production.

## INTRODUCTION

The pressure on global energy resources is intense and by 2030 the International Energy Agency (IEA) expects the global demand for oil to have grown by 41%. This has resulted in an increasing interest and need for renewable energy, in particular in the transport sector, and over the next 15 years the European Commission considers biofuels, to be the only way to significantly reduce oil dependency in the transport sector (COM, 2007). This has led to increased research, development, and commercialization of technologies and processes for the production of fuel based on biomass.

At the same time, critics have raised questions regarding the sustainability of biofuel production. For first-generation biofuels the sustainability has been questioned due to the competition for productive land and the competition with regards to food production (Naik et al., 2010). Second generation biofuels (cellulosic ethanol) based on waste biomass is generally considered more sustainable. The conversion of cellulosic biomass into ethanol requires a range of main process steps including: pre-treatment, enzymatic hydrolysis, fermentation, and distillation as well as wastewater treatment and residue utilization. Besides the main processes, a range of utility process steps is needed covering: cooling, steam generation, heat exchange, condensation and detoxification. Water is a necessary resource within all the process steps. Due to increasing global awareness on water scarcity, the impact on water resources of second generation technologies has been raised as an issue of possible concern in research and in the public debate. However, as the second generation technologies are at an early stage of development, only limited information about water consumption is available. Moreover, the available information does not reflect optimized industrial full scale facilities. The study presented here has analyzed the water consumption in cellulosic ethanol production based on literature data as well as information on a commercially developed process for cellulosic ethanol at the stage of implementation. The objective has been to establish solid near and long term water consumption data in cellulosic ethanol which can be compared with data on water consumption for gasoline production.

## MATERIALS AND METHODS

**Data framework and boundary conditions.** Initially, the basic framework and boundary conditions for the water consumption data were defined based on the terminology applied in the concept of Water Footprint(WFP) assessment which addresses direct and indirect consumption of blue, green and grey water resources to produce a product, measured over the full supply chain (Hoekstra et al., 2009). A full Water Footprint assessment was, however, not performed in the study. Instead, the boundary conditions for the water consumption data comprised: i) the direct blue water consumption allocated to production of the raw material – i.e. crude oil and biomass (corn stover/*Arundo Donax)* - for the cellulosic ethanol production; ii) the direct blue water consumption in the fuel production/refining process; and iii) the indirect water saving allocated to the exported surplus electricity through saved public electricity production. The study does not include the indirect water consumption relating to transport of raw materials, auxiliary chemicals, etc. However, for one of the data sources for cellulosic ethanol, enzymes for the process were produced onsite, and the water consumed for this was included in the total water consumption of the process. Consequently, the contribution of the externally supplied enzymes to the water consumption for the second data source for cellulosic ethanol was calculated for comparison. All water consumption data for cellulosic ethanol was calculated on the basis of gasoline equivalents to make direct comparison with gasoline straightforward.

**Data sources.** The assessment of water consumption in cellulosic ethanol production was based on data from two sources. The first data source was a detailed process simulation study on conversion of corn stover, conducted by the U.S. National Renewable Energy Laboratory (NREL) (Humbird et al., 2011). The other data source was a commercial process at the stage of implementation of a large scale facility in Crescentino Italy, by Chemtex Italia S.R.I. (Chemtex), the engineering subsidiary Mossi & Ghisolfi (M&G). The M&G/Chemtex process is based on conversion of a non-consumptive tall-growing perennial grass crop, *Arundo donax* (Giant Cane), which is a native to the Mediterranean region and grown on non-productive land. Design process diagrams with relevant data for the analysis were supplied by Chemtex.

The data used concerning water consumption in gasoline production included data reported in two recent studies (Wu et al., 2009; Wu and Chiu, 2011) where a detailed analysis of water consumption was conducted for US domestic crude oil supply, Saudi Arabian Crude oil and Canadian Oil Sands. Data for crude oil refining was supplemented with data reported in a recent draft of the BAT-Ref document for the Refining of mineral oil and gas, by the European IPPC Bureau (IPPC, 2012).

## RESULTS AND DISCUSSION

**Near term water consumption in Cellulosic ethanol**: For the two cellulosic ethanol processes, the ethanol conversion process itself is not a significant consumer of water and utility operation is responsible for practically all water consumption with 90-95% being consumed by cooling tower evaporation. Other water consuming losses include discharge of cooling tower blow-down, discharge of saline brine from the wastewater evaporation plant, water loss in steam generation and flue gas from the wet residue incineration.

In the NREL study, a range of water saving measures had already been implemented with a high degree of water recycling. The reported water consumption figures thus reflect a near term minimum for the conversion of corn stover. An analysis of the cooling needs of the plant showed that more than half of the water consumed through cooling tower evaporation could be allocated to the condensing turbine used to maximize the electricity production from the combustion of wet solid residues. Thus, a significant consumption of water could be attributed to the benefit of generating enough electricity to supply all users in the plant - plus a considerable surplus which is assumed to be sold to the grid, giving the cellulosic ethanol plant an indirect water saving through saved public electricity production. Summarizing the result of the NREL process simulation study yielded a near term minimum water consumption for conversion of corn stover, including credit for exported surplus electricity, of 6.8 gal water/gal gasoline equivalent.

With regards to the M&G/Chemtex Crescentino plant, the design data for unit processes to be installed at the large scale plant (60,000 ton ethanol/year) was analyzed and revised using input from the

NREL study as well as input from Chemtex on applied design safety factors and assumed operational conditions in order to develop a realistic operational scenario. The scenario was based on 30% dry matter content in the pre-treatment step (20% was used in the design), adjustment of the cooling of fermenters and wastewater treatment by chilled water to 3 months per year, i.e. the summer period (a full year operation was used in the design), and adjustment of the amount of water consumed to produce electricity from combustion of solid from the design value of 1.3 gal/kWh to the reference value applied in the NREL study and coal-fired electricity plants (0.46 gal/kWh). Based on this, the water consumption for realistic operation of the Crescentino plant, including export electricity credit, was calculated to 8 gal water/gal gasoline equivalent.

With additional input from the NREL study, a scenario for reduced water consumption was identified for the M&G/Chemtex Crescentino plant which in the very near term could be realized. In the The scenario involved recycling of cooling water blow-down through the wastewater treatment and desalination plant. In the design of the M&G/Chemtex Crescentino plant the blow-down from the cooling tower was discharged to a nearby creek. Recycling of cooling water blow-down is known in the chemical and petroleum industry (Byers, 2003). For the Crescentino plant, recycling of cooling tower blow-down resulted in a water consumption, including electricity credit, of 3.0 gal water/gal gasoline equivalent.

**Long term options for reduced water consumption in cellulosic ethanol**: Additional possibilities, which could be implemented in the longer term to minimize water consumption in cellulosic ethanol production, would require changes in cooling technology. This could be realized through improved integration of heat exchanging between different process streams and/or implementation of air cooling. Implementation of air-cooled condensers had already been implemented in the NREL study, however, the conclusion was that as air-cooled condensers have low capacity, many parallel units would be required at a significant capital expense, and the implementation of air-cooled condensers would not break even with their water savings (Humbird et al., 2011).
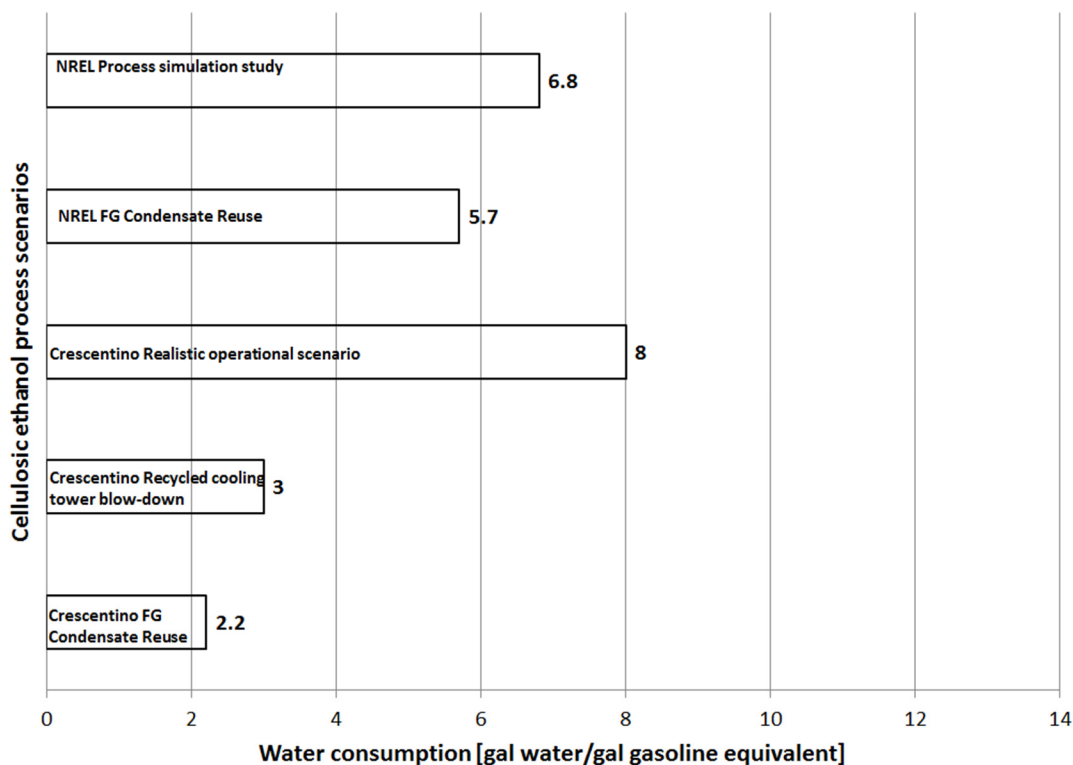


**FIGURE1.** Near term and long term water consumption in cellulosic ethanol processes.

Another more promising long term option for additional water savings in cellulosic ethanol production could be to reuse condensate from flue gas condensation after desulphurization. Flue gas condensate recycling is known from power plants using biomass feed (Loo and Koppejan, 2008). In both the presented designs this option could be implemented by pre-heating process water in the pre-treatment step with the flue gas. The resulting flue gas condensate can be recycled either through the boiler feed water preparation plant or via the wastewater treatment and evaporative water recovery plant. The amount of condensate depends on a number of factors and is thus difficult to assess. However, using a key figure of 132 gal condensate/MWh for relatively moist biomass (Loo and Koppejan, 2008), the potential water saving in the Crescentino case can be estimated to around 0.76 gal water/gal gasoline equivalent and for the NREL study the potential water saving can be estimated to around 1.1 gal water/gal gasoline equivalent. By taking the flue gas condensate recycling into account, the longer term optimized water consumption for the Crescentino plant is expected to be around 2.2 gal water/gal gasoline equivalent and in the NREL process simulation study to be around 5.7 gal water/gal gasoline equivalent. The near term and long term water consumption, including credit for electricity export, for the cellulosic ethanol process scenarios is summarized in the below figure.
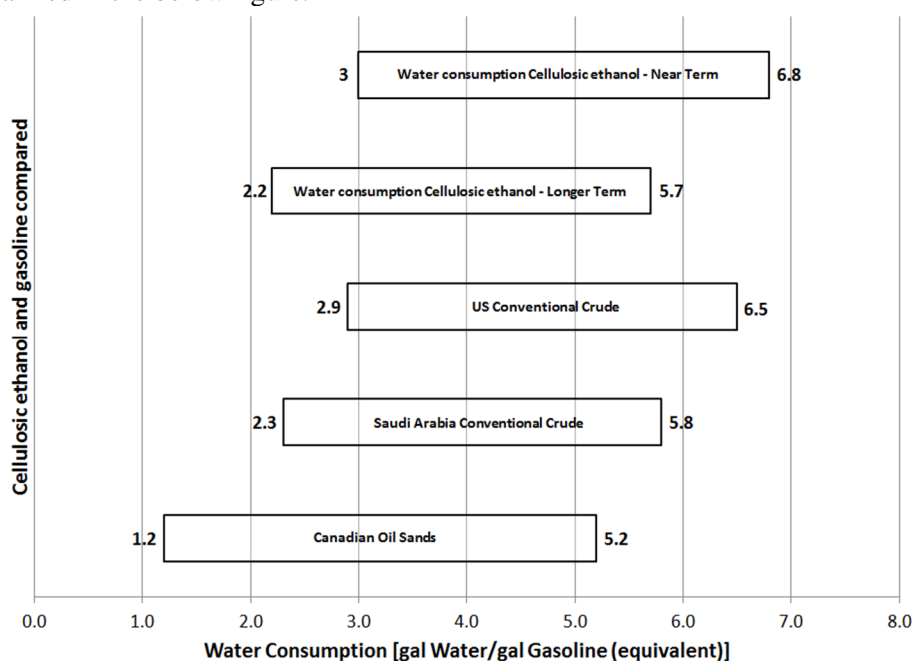


**FIGURE2.** Near term and longer term expected water consumption in cellulosic ethanol production compared to current water consumption in gasoline production.

The data shows that the near term direct water consumption for cellulosic ethanol production, including credit for electricity export, is in the range of 3-6.8 gal water/gal gasoline equivalent. In both the analyzed designs, the optimized water consumption is based on almost complete recycling of all liquid process water and heat integration. The differences in the actually achieved optimum water consumption between the two cellulosic ethanol processes are primarily governed by differences in the feedstock moisture content, which for corn stover is around 20%wt and for *Arundo donax* around 58%wt. In the longer term, additional water savings can be achieved through different measures, including air-cooling and flue gas condensate recycling. Flue gas condensate recycling seems like the most promising option. The long term water consumption for cellulosic ethanol production, including credit for electricity export, is expected to be in the range of 2.2-5.7 gal water/gal gasoline equivalent. It should be mentioned that in the Crescentino plant externally supplied enzymes contribute with an additional water consumption of 1.5 gal water/gal gasoline equivalent, which could be added to the above figures.

**Water consumption for gasoline production compared to cellulosic ethanol**: The data on fresh water consumption in crude oil extraction and refining was taken from Wu et al., 2009 and Wu & Chui, 2011 showing that the water consumption in crude oil extraction and refining yielded water consumption estimates in the range 1.2-6.5 gal water/gal gasoline. The comparison of the water consumption in gasoline extraction and refining with the near term and longer term water consumption figures for cellulosic ethanol obtained from the analysis is shown in the below figure.

As seen, the near and longer term expected water consumption in cellulosic ethanol production is comparable to or only slightly higher than the water consumption in gasoline production.

**CONCLUSIONS**

In the study presented, the water consumptions in cellulosic ethanol and gasoline production have been analyzed and assessed based on literature data and process data for a commercially developed cellulosic ethanol process being implemented at a large scale demonstration facility. The results show that the near and longer term expected water consumption in cellulosic ethanol production is comparable to the water consumption in gasoline production. As cellulosic ethanol production is an industry at the early stage of development, an expected unrealized potential for optimized water consumption through rapidly evolving production technologies and improved process integration exists.

**ACKNOWLEDGEMENTS**

**REFERENCES**

Byers, W., G. Lindgren, C. Noling and D. Peters. 2003. "Industrial Water Management: A Systems Approach – Chapter 5 Water Use in Industries of the Future", 2n*d Edition, Am. Inst. of Chem. Engineers.*

Commission of the European Communities. 2007. "An Energy Policy for Europe", *Communication from the commission to the European council and the European Parliament.*

Hoekstra, A.Y., A.K. Chapagain, M.M. Aldaya and M.M. Mekonnen. 2009. "Water Footprint Manual - State of the Art 2009", *Water Footprint Network*, Enschede, The Netherlands.

Humbird, D., R. Davis, L. Tao, C. Kinchin, D. Hsu, A. Aden, P. Schoen, J. Lukas, B. Olthof, M. Worley,

D. Sexton and D. Dudgeon. 2011. "Process Design and Economics for Biochemical Conversion of Lignocellulosic Biomass to Ethanol Dilute-Acid Pretreatment and Enzymatic Hydrolysis of Corn Stover", *Technical Report, US National Renewable Energy Laboratory.*

Integrated Pollution Prevention and Control (IPPC). 2012. "Best Available Techniques (BAT) Reference Document for the Refining of mineral oil and gas", *Draft. Joint Research Centre, Institute for Prospective Technological Studies, Sustainability Production and Consumption Unit.*

Naik, S.N., V.V. Goud, P.K. Rout and A.K. Dalaib. 2010. "Production of first and second generation biofuels: A comprehensive review". *Renewable and Sustainable Energy Reviews*, 14(2): 578-597.

Wu, M., M. Mintz, M. Wang and S. Arora. 2009. "Consumptive Water Use in the Production of Ethanol and Petroleum Gasoline", *Center for Transportation Research, Energy Systems Division, Argonne National Laboratory: Argonne, IL.*

Wu, M. and Y. Chiu. 2011. "Consumptive Water Use in the Production of Ethanol and Petroleum Gasoline – 2011 update", *Center for Transportation Research, Energy Systems Division, Argonne National Laboratory: Argonne, IL.*

# A FEASIBILITY STUDY OF MAKING BIODIESEL FROM TRAP GREASE: INVENTORY AS THE FIRST STEP

Qingshi Tu, Mark Schutte, Jingjing Wang, and *Mingming Lu*\*, School of Energy, Environmental, Biological and Medical Engineering, University of Cincinnati, 2600 Clifton Avenue, Cincinnati, Ohio, 45221
Ming Chai, Bluegrass Biodiesel, 175 David Pribble Drive, Falmouth, Kentucky, 41040
Ting Lu, Metropolitan Sewage District, 1600 Gest Street, Cincinnati, Ohio, 45204-2022
\*Corresponding author: Mingming Lu, Email: Mingming.lu@uc.edu

**ABSTRACT:** Trap grease is a major contributor to the overflow and pipeline corrosion issues in the US. Converting trap grease into biodiesel serves as a great opportunity for optimizing the management of trap grease and promotion of biodiesel industry. As the first step for creating a trap grease-to-biodiesel business, an inventory of trap grease generation and its usable portion for biodiesel production needs to be set up. This study adopted three methods for estimating the inventory for Greater Cincinnati area and the results indicated that around 10 million gallons of trap grease was generated every year and the usable FOG portion in Greater Cincinnati area was about 1.66 to 3.31 million pounds for biodiesel production.

## INTRODUCTION

The terms trap grease and brown grease have been used interchangeably. Brown grease, a term from the waste oil rendering industry, describes a waste oil with a free fatty acid (FFA) concentration of 15–50%, while trap grease loosely refers to the mixture of fat, oil, and grease (FOG), water, and solids that comes from the grease trap of commercial food services. A 2009 report by the U.S. Environmental Protection Agency (EPA) showed that 47% of sewer line blockages are related to FOG (US EPA, 2009). Trap grease clogging could cost communities billions of dollars to fix the problems (Parjus et al., 2011). To be more specific, only in San Francisco, the city spends more than \$3.5 million to clean out the grease-clogged pipes each year (San Francisco Water, Power, and Sewer, 2011). A total of more than 19 million gallons of sewer wastewater flowed back up from 1998 to September 2001 in the state of North Carolina (North Carolina, 2002). Most municipalities have coordinates that prevent the illegal dumping of FOG from commercial food sources, which is one of the major causes of pipe clogging. Restaurants and other food services should have a grease trap that separates grease from wastewater before discharging to the public sewers (see Figure 1, Tu et al., 2012). Periodically, the trapped grease is pumped by a specialized company at a cost to the restaurant and sent to wastewater treatment plants for disposal. Typically, the trapped grease is then incinerated, anaerobically digested, or landfilled. No regulations have been imposed for household cooking. Due to the cost involved in pumping and landfilling, trap grease has long been considered as a burden.

As mentioned earlier, FOG accumulation is the major cause of the overflow issues in combined sewer systems and sanitary sewer systems. Regulatory efforts have been put in preventing the illegal discharge of trap grease into the sewer pipes. 40 CFR 403.5 under National Pretreatment Program prohibits "solid or viscous pollutants in amounts which will cause obstruction" in the POTW and its collection systems. In addition, regional environmental protection agencies enforce regulations to control the FOG discharge from restaurants as well. For example, in Section 1004.5.5 (4102:2-65-04) of the Ohio Plumbing Code, *"Grease traps and grease interceptors shall be inspected frequently and cleaned as often as necessary to retain the grease wastes. The materials removed in cleaning shall be removed from the premises for disposal and not be deposited in the plumbing system or sewage system."* Cincinnati adopts

Ohio plumbing code 2007 and applies it to all plumbing work in Cincinnati. Besides the CSO/SSO issues, pipeline damage caused by $H_2S$ corrosion is also a vital problem to the infrastructure protection (US EPA, 2003). $H_2S$ forms when trap grease is decomposed by the anaerobic microorganisms. The $H_2S$ is then oxidized into $H_2SO_4$ in the wet environment by aerobic bacteria and long time exposure in the acidic environment will cause the corrosion of the sewer pipes (Burgess, 2010). Fixing and prevention of sewer pipe corrosion are very costly; for example, in County Sanitation Districts of Los Angeles County, a cost of about $9, 300 per mile sewer pipe was estimated based on the sulfide control technology with ferrous chloride and an annual cost of $2.5 million was projected if 90% of $H_2S$ was controlled. Another example is the control method with pure oxygen in Jefferson Parish, Louisiana, which approximately cost $200,000 per year for the entire system (US EPA, 1992).
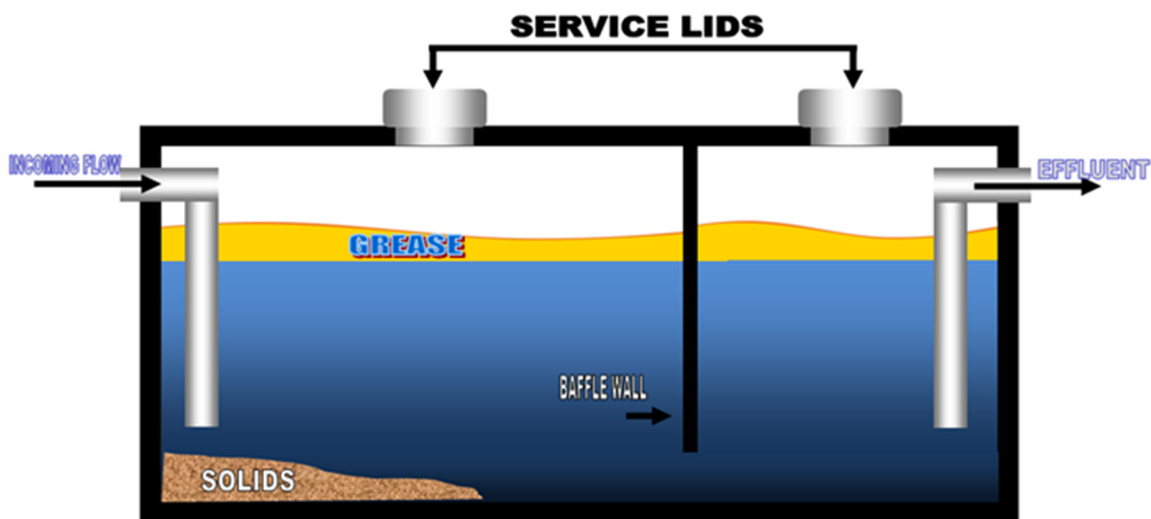


**FIGURE1.** Grease trap demonstration

Although regulatory tools already exist to prompt the food services to clean their grease trap/interceptor on regular basis, delay in practice occurs from time to time due to the economic concerns from the restaurants that are charged by the haulers with tipping fee for pumping their grease trap/interceptor. Once the timely clearance of the grease trap/interceptor becomes an economic burden for the restaurants, it will in turn increase the potential risk of trap grease overflow and FOG accumulation in the sewer pipes. One way to encourage the frequent cleaning of the grease trap/interceptor is to find the revenue for the restaurants to get rid of their trap grease. Biodiesel, a renewable fuel using FOG as the feedstock, can be a potential solution. Biodiesel is a mixture of esters made from the transesterification reaction between FOG and alcohol (typically methanol). Switching from petroleum diesel to biodiesel promotes the reduction in air pollutant emissions as well as the energy independence of the US. Currently, the US biodiesel industry has grown into a steady state with a productivity of hundreds millions gallons per year (NBB, 2012). This prosperity, however, poses several issues for the development of biodiesel industry. Firstly, the feedstock supply is tightening. The US currently consumes 51 billion gallons of diesel every year. If switching to B5 fuel (5% biodiesel blend with 95% diesel), it requires more than 2.5 billion gallons of biodiesel, which is more than twice of record-high biodiesel production. Also, the increasing feedstock prices have also urged the switch to low cost feedstocks, since the feedstock cost can account for up to 80% of the total biodiesel cost (Haas 2010). Last but not least, the sustainability concerns for the growth of biodiesel industry have brought up debates regarding using conventional oil crops, such as soybean, for biodiesel production. Therefore, under such a circumstance, finding the alternative feedstocks, such as waste-derived oil sources, can be a highly desirable solution to the above-mentioned issues. Converting trap grease into biodiesel is expected to benefit a variety of stakeholders: (1)

restaurants owners can sell the trap grease or get rid of them for free as the biodiesel feedstock; (2) biodiesel companies may reduce the total production cost by using trap grease as the low cost feedstock; and (3) wastewater treatment facilities will expect less overflow and pipeline corrosion issues due to reduced grease trap effluent. In the commercial aspect, there is limited number of biodiesel companies that are able to handle the trap grease as the feedstock, among which BlackGold biofuels is the most frequently mentioned one (McElroy, 2006). Formerly known as Philadelphia Fry-o-Diesel, this company has been recognized as the leading company in trap grease biodiesel production and gained opportunities to work with other organizations to promote the trap grease biodiesel. For example, San Francisco Public Utilities Commission (SFPUC) has initiated a city-based demonstration-scale brown grease (trap grease) biodiesel project with BlackGold (Voegele, 2009; Christiansen, 2009). Another trap grease to biodiesel project is by the Eastern Municipal Water District located in Perris CA (The press enterprise, 2011).

Before implementation of the trap grease to biodiesel plan, a trap grease inventory in the business area should be evaluated, with respect to the quantity, how the trap grease is collected and transferred, and physical/chemical properties, etc. . In this paper, an inventory study was performed to obtain the annual generation of trap grease and its usable part (FOG) in Greater Cincinnati area. The outcome of the study serves as the first step of the feasibility study for converting trap grease into biodiesel in a community-based scale.

## METHODOLOGY

There have been very limited studies on trap grease inventory, as it has always been a waste, whose potential value has just been brought up. Wiltsee (1998) conducted the first comprehensive survey on the urban waste grease resources in thirty metropolitan areas in the US. The resultant national average of 13.37 pounds/person/year is still being used by many municipalities to estimate their trap grease capacity. Here we call this national average method "method 1". Austic (2010) of Piedmont Biofuels LLC studied the feasibility of building a trap effluent dewatering facility in Raleigh, NC, and obtained his data by talking to the waste handling people in the service area. Chesebrough (2008) estimated the amount of trap grease in Columbia, SC. The results of those studies were summarized in Table 1.

**TABLE1.** Summary on trap grease inventory from literature review

| | Average Amount | | Study Area |
|---|---|---|---|
| | Grease Trap Waste (gallon/person/year) | Usable Grease (pound/person/year) | |
| Wiltsee (1998) | / | 13.37 | 30 Metropolitan Areas |
| Austic (2010) | 18.35-18.65 | 2.68-2.72 | Wake County, NC |
| Chesebrough (2008) | 2.83 | 1.13-2.26 | Columbia, SC |

Three methods were applied to estimate the inventory of trap grease in Greater Cincinnati area: (1) Estimation based on literature data. A careful literature review was conducted to understand the existing studies and methods/approaches in conducting trap grease inventory. The data retrieved was used as the factor for estimating the trap grease generation in Greater Cincinnati area based on the local population. (2) Estimation from wastewater treatment plant. The Metropolitan Sewer District of Greater Cincinnati (MSDGC) was contacted for their estimation of the annual generation of trap grease in the local area. (3) Industrial survey. 15 authorized grease haulers were interviewed for three major questions: the collection procedure, cost and waste amount. The collected data was analyzed and normalized to obtain estimation.

The results from three methods were compared and a representative one was selected as the inventory of trap grease in Greater Cincinnati area.

## RESULTS AND DISCUSSION

**Method 1**. Wiltsee's data was adopted considering its wide surveying area and the estimation of useable FOG was around 3.97 million lbs per year for Greater Cincinnati area.

**TABLE2.** Trap grease inventory for Cincinnati from individual haulers

| Waste Hauler Name | TP Inventory (gallons/year) |
|---|---|
| A.K. Butler Services, LLC | 200,000 |
| Ace Sanitation Service, LLC | 2,625,000 |
| Allied Plumbing and Sewer Service, Inc. | did not respond |
| Griffin Industries, Inc. | 1,300,000 |
| Gullet Sanitation Service, Inc. | 24,000 |
| Hack's Septic Service, Inc. | 5,000 |
| Kleenco Maintenance & Construction | 181,500 |
| Mahoney Liquid Environmental Solutions | 3,300,000 |
| Mike Hensley Plumbing, Inc. | 2,000,000 |
| Roto-Rooter Services Co. | 180,000 |
| Rumpke Transportation Company, LLC | did not respond |
| Saving's Liquid Waste, Inc. | 600,000 |
| Terminix International Compant Limited Partnership | did not respond |
| Triple A Sanitation | 240,000 |
| Tri-State Liquid Waste LLC | 500,000 |
| **Total** | **11,155,500** |

**TABLE3** Trap grease inventory for Cincinnati based on the data from three methods

| Data Source | Grease Trap Waste | | Usable Grease | |
|---|---|---|---|---|
| | Average Amount (gallon/person/year) | Total Amount (million gallon/year) | Average Amount (pound/person/year) | Total Amount (million pound/year) |
| Wiltsee | / | / | 13.37 | 3.97 |
| MSDGC | 12.5 | 3.71 | 5.00-10.00 | 1.48-2.97 |
| Haulers | 13.95 | 4.14 | 5.58-11.16 | 1.66-3.31 |

**Method 2.** In the Metropolitan Sewer District of Greater Cincinnati (MSDGC), trap grease is dumped at a receiving station by the haulers, mixed with the waste water from primary treatment process, skimmed, condensed, and placed in the holding tank. It is then mixed with the grit from the primary treatment process, and stays in a pit until going to landfill. MSDGC is a Hamilton County-owned sewer district collecting and treating 192 MGD of wastewater by operating seven major treatment plants and serving a community of more than 800,000 people. There are over 1,000 restaurants throughout the county and MSDGC receives approximately 10 million gallons of grease trap discharge annually (Tu et al., 2012) and the corresponding usable FOG was around 1.48-2.97 million lbs per year.

**Method 3.** For the industrial survey, 12 out of 15 haulers responded. The total amount of grease trap waste collected by the 12 out of the 15 grease haulers was 11.16 million gallons per year (Table 2), and

the range for the corresponding usable FOG was <u>1.66-3.31 million lbs per year</u>. <u>This number agrees well with the estimates provided by MSD.</u>

Results from the three methods are listed in Table 3 (all the values were converted to "<u>million lbs/year</u>"). This indicated that the potential capacity for biodiesel was approximately 20,000 gallons per year.

The results also indicated that the per person trap grease generated in Cincinnati was much lower than the national average, and therefore it is essential to conduct the inventory study as the basis for trap grease reuse. There is on going work to analyze the heating value, the elemental analysis and other physical/chemical properties of the trap grease.

## CONCLUSIONS

Converting trap grease into biodiesel can be a win-win solution for waste management and biofuel production. As the first step of a feasibility study, the development of trap grease inventory is essential. For Greater Cincinnati area, in this study, three methods were applied to estimate the annual trap grease generation. The estimate from Wiltsee's Report showed that based on the national average trap grease generation rate, the usable FOG inventory was about 3.97 million pounds per year. Based on the estimation given by the Metropolitan MSDGC, Cincinnati fell far below the national average, in a range of about 1.48 to 2.97 million pounds per year. This large difference indicated the necessity to conduct an estimation based on a third approach to verify the results. The outcome from interview with grease haulers indicated that the trap grease generation was around 10 million gallons per year and the usable FOG portion in Greater Cincinnati area was about 1.66 to 3.31 million pounds per year. This result agreed well with the estimates from MSDGC and thus was chosen as the representative value for the inventory of trap grease for Greater Cincinnati area.

## ACKNOWLEDGEMENT

## REFERENCES

Austic, G. 2010. "Feasibility study: Evaluating the profitability of a trap effluent dewatering facility in the Raleigh area". http://www.biofuels.coop/wp-content/uploads/2011/02/ECO Collectionstrap-grease-feasibility.pdf, accessed on March 2012.

Burgess, M.N. "What to do with brown grease?", *Plumbing System & Design magazine*, April Issue, 2010. pp 24-30.

Chesebrough, E.G. 2008. *From grease traps to bio-gold? An environmental and economic cost benefit assessment of converting trap grease to biodiesel.* M.S. Thesis, University of South Carolina at Columbia, SC.

Christiansen, R. C. 2009. "San Francisco to use BlackGold Biofuels technology". *Biodiesel Magazine*, March Issue. http://www.biodieselmagazine.com/article.jsp?article_id=3245, accessed on February 2012.

Haas, M. J. 2010. "Alternate feedstocks and technologies for biodiesel production." IN: G. Knothe, J. Krahl, and J. Van Gerpen (Ed.) *the Biodiesel Handbook*, pp. 47-66. 2nd edition, AOCS publishing, Urbana, IL.

McElroy, A. K. 2006. "Ultimate makeover." *Biodiesel Magazine*, June Issue. http://www.biodieselmagazine.com/article.jsp?article_id=946&q=&page=2, accessed on February 2012.

National Biodiesel Board (NBB). Http://www.biodiesel.org/, accessed on March, 2012.

National Pretreatment Program Parts 40 CFR 403.5

North Carolina. 2002. "Considerations for the Management of Discharge of Fats, Oil and Grease to Sanitary Sewer Systems." http://infohouse.p2ric.org/ref/20/19024/19024-1.pdf, accessed on January 2012.

Ohio Plumbing Code Section 1004.5.5 (4102:2-65-04)

Parjus, J.A., R. Larosa, and A. Gonzalez. 2011. "Grease trap waste treatment and fat, oil, and grease (FOG) recovery system." US Patent No. 7,967,985 B1.

San Francisco Water, Power, and Sewer. 2011. "Brown grease to biodiesel demonstration project." http://www.sfwater.org/modules/showdocument.aspx?documentid=1540, last accessed on January 2012.

The Press Enterprise, http://www.pe.com/local-news/riverside-county/hemet/hemet-headlines-index/20110307-perris-water-district-funds-grease-to-fuel-project.ece, accessed May, 2012.

Tu, Q., J. Wang, M. Lu, M. Chai, and T. Lu. 2012. "Feasibility and Practices of Making biodiesel Out of Low Quality Greases." *EM,* January Issue.

US EPA. 2009. "Oil and Grease Removal Technologies." Http://www.epa.gov/region8/water/pretreatment/pdf/W6_KyleSorenson_OilAndGreaseTechnology.pdf, accessed March, 2012.

US EPA. 2003. "EPA's National Pretreatment Program, 1973–2003: Thirty Years of Protecting the Environment." http://www.epa.gov/region8/water/pretreatment/pdf/EPAsNationalPretreatmentProgram.pdf accessed on April, 2012.

US EPA. 1992. "Detection, control, and correction of hydrogen sulfide corrosion in existing wastewater systems."

Voegele, E. 2009. "Biodiesel in the golden gate city." *Biodiesel Magazine*, February Issue, http://www.biodieselmagazine.com/article.jsp?article_id=3156, accessed on Dec. 2010.

Wiltsee, G. 1998. *Urban Waste Grease Resource Assessment*. NREL/SR-579-26141, National Technical Information Service, US Department of Commerce, or DOE information Bridge, Springfield, VA.

# ETHANOL PRODUCTION FROM FOOD CROP WASTES BY SIMULTANEOUS SACCHARIFICATION AND FERMENTATION PROCESS

*Itelima Janet,* Ikpe Charles and Pandukur Sunday
(University of Jos, Jos, Nigeria)

**ABSTRACT:** Most nations, whether economically advanced or at different stages of development are faced with the problem of disposal and treatment of wastes. Wastes could be treated in several ways (e.g. by reducing its bulk or by recovering and reprocessing it into useful substance) to meet sanitary standards. Ethanol fermented from renewable sources for fuel or fuel additives are known as bio-ethanol. In Nigeria, many food crops have been specifically grown for the production of bio-ethanol. However, bio-ethanol production from waste materials removed from food crops is very rare. In the present study, food crop wastes such as yam, potato and sweet potato peels, which are in abundance and do not interfere with food security were subjected to simultaneous saccharification and fermentation for 7days by co–culture of *Aspergillus niger* and *Saccharomyces cerevisiae*. Biomass yield, cell dry weight, reducing sugar concentration and the ethanol yield were determined at 24 hours interval. The results of the study showed that after 7 days of fermentation, sweet potato peels had the highest biomass yield of 4.65 (OD), followed by yam peels 3.50 (OD), while potato peels had the least 2.38 (OD). The microbial cell dry weights obtained from the wastes materials ranged between 6.04 –9.50 mg/cm$^3$, while their reducing sugar concentrations ranged between 0.10 – 0.72 mg/cm$^3$. The optimal ethanol yields were 10.89% v/v, 9.40 % v/v and 6.00% v/v for sweet potato, yam and potato peels respectively. These indicate that sweet potato and yam peels ethanol yields were significantly higher (P<0.05) than potato peel ethanol yield. The findings of this study suggest that food crop wastes that contain fermentable sugars can no longer be discarded into our environment, but should be converted to useful products like bio-ethanol that can serve as alternative energy source.

## INTRODUCTION

Yam, potato and sweet potato peels are agricultural by-products, which are available in abundance in Nigeria and presently constitutes a nuisance to the environment if not well disposed (Okonko *et al*., 2006). In the past, disposal of root and tuber crop peels by burning was an accepted practice. This practice is now being challenged due to concern over the health effect of sooths from burning them. These agricultural wastes are used as food supplement for livestock feeds. Recently agricultural wastes can be converted into useful materials such as bio-ethanol, biogas and single cell proteins (Kivaisi and Rubindamayugi, 1996; Joshi *et al*., 2001; Sun and Cheng, 2000; Akin-Osanaiye *et al*., 2008).

Ethanol is an aliphatic alcohol compounds composed of hydroxyl groups (-OH) linked to alkyl groups (CH$_3$). They can be considered as being derived from corresponding alkenes by replacing the hydrogen atoms with hydroxyl groups (Amadi *et al*., 2004). Ethanol is an alcohol fuel made by fermenting the sugars found in grains, such as corn and wheat as well as lignocellulosic feedstock, such as corn fiber, rice straw and saw dust (Pandey *et al*., 2000; Ashiru, 2005; Jimoh *et al*., 2008).

Ethanol is both essential solvent and fundamental feedstock for the synthesis of other products. Currently there is growing interest for ecological sustainable bio-fuels. In Nigeria, hydrolysis of raw tuber starches by amylases of *Aspergillus niger* AMO7 was studied by Omemu *et al*. (2005). Simultaneous saccharification and fermentation of lignocelluloses to alcohol by baker's yeast and a thermotolerant *K. marxianus* using industrial wastes as substrate was reported by Kadar *et al*. (2004).

Ethanol is also a safer alternative to methyl tertiary butyl ether (MTBE), the most common additive to gasoline used to provide cleaner combustion (Jimoh *et al*., 2008). The United States

Environmental Protection Agency (EPA) announced the beginning of regulatory action to eliminate MTBE in gasoline because it is toxic chemical compound and has been found to contaminate ground water (SECO, 2006). According to Jimoh *et al*. (2008) demand for ethanol could increase further if MTBE is eliminated from gasoline.

The objective of this study was to produce ethanol from food crop wastes such as yam, potato and sweet potato peels using co- culture of *Aspergillus niger* and *Saccharomyces cerevisiae*. These waste materials are reasonable rich in fermentable sugars and may serve as good substrates for ethanol production.

## MATERIALS AND METHODS

**Preparation of Yam, Irish Potato and Sweet Potato Peels for Ethanol Production:** Yam tubers, potatoes and sweet potatoes were washed, dried and their outer coats i.e. removed, dried under the sun ground into fine powder using hammer milling and stored at room temperature.

**Preparation of Growth Medium:** The growth medium used for preparing the *Aspergillus niger* inoculum consisted of 30g of yam peel, potato peel and sweet potato peel substrates separately, peptone, 0.1%; malt extract, 0.1% (w/v), yeast extract, 0.2% (w/v), calcium carbonate 0.2% (w/v); ammonium phosphate, 0.2% (w/v), and ferrous sulphate.$7H_2O$, 0.001% (w/v) respectively. *Saccharomyces cerevisiae* growth medium was prepared using yeast – malt broth at pH 5.5 (Abouzied`and Reddy, 1986).

**Preparation of Inocula and Fermentation Procedure:** *A. niger* inoculum was prepared in $250cm^3$ cotton–plugged conical flask containing $100cm^3$ of the different substrates growth media. The flasks were sterilized and inoculated with 0.11 (OD) *A. niger* spores. Each of the flasks was incubated on a shaker with agitation rate of 300rpm at $30^0C$ for five days. *S. cerevisiae* inoculum was prepared in the same way as the *A. niger* inoculum except that yeast malt broth was used. The growth medium was inoculated with 0.08 (OD) yeast cells and incubated for 24 hours. The fermentation medium used for ethanol production was identical to the growth medium as indicated above. Ethanol fermentation was carried out in $500cm^3$ conical flasks each containing $300cm^3$ of medium. The medium was sterilized and inoculated with 5% (v/v) growth media containing *A. niger* and *S. cerevisiae* and incubated on a shaker with an agitation rate of 300rpm at $30^0C$ for seven days.

**Analytical Procedure:** Thirty cubic centimeters ($30cm^{3)}$ of the sample was collected from each flask at 24 hours interval and $27cm^3$ was centrifuged at 400rpm for 30 minutes to remove the cells. The supernatant fluid was filtered through whatman filter paper No.1 and the filtrate was used for determining ethanol and reducing sugar concentration. The remaining $3cm^3$ was used to determine the cell density.

**Determination of Cell Density:** Three cubic centimeters ($3cm^3$)of the sample was used to determine the cell density at 690nm using CECILCE 1020 spectrophotometer. The spectrophotometer was blanked with an uninoculated fermentation medium.

**Determination of Cell Dry Weight:** The residue (cells) obtained after centrifugation was filtered using whatman filter paper No.1, washed with distilled water to remove the residual substrates and dried in the hot air oven at $70^0C$. The filter paper was pre–weighed before filtering and reweighing after drying until a constant weighed was obtained. Thus, the cell dry weights were determined as follows: **Cell dry weight = weight of filter paper and cell after drying – weight of filter paper only.**

**Qualitative and Quantitative Analysis of Reducing Sugar Present in the Samples:** The qualitative analysis was carried out using Benedict's solution (Amadi *et al*., 2004), while the quantitative analysis was carried out using 3, 5–dinitrosalicylic acid. The concentration of the reducing sugar present in the samples was determined by adding $1cm^3$ of 3, 5 – dinitrosalicylic acid to $1cm^3$ of each of the samples and

boiled for 5 minutes and $10cm^3$ distilled water was added. The absorbance of each of sample was determined at 540nm using JENWAY 6400 spectrophotometer. Thus, the concentration values were extrapolated from the glucose standard curve (Amadi *et al.*, 2004).

**Qualitative and Quantitative Analysis of Ethanol Present in the Distillate:** The filtrates were distilled at $70^0C$ using rotary evaporator. The qualitative analysis was carried out using ethanolic acid. Two cubic centimeters of ethanolic acid was added to $1cm^3$ of the distillate and heated in the water bath for 5 minutes until characteristics sweet smell of esters was perceived. The quantitative analysis was carried out by determining the densities of the distillates as follows.

**Density = <u>Weight of the density bottle + distillate – Weight of empty density bottle</u>**
**Volume of distillate**

Thus, concentrations of the distillates were extrapolated from the density standard curve. Furthermore, the pH, refractive index, and specific gravity values were extrapolated from the standard curves prepared from each parameter since the concentrations of the distillates were known (Amadi *et al.*, 2004).
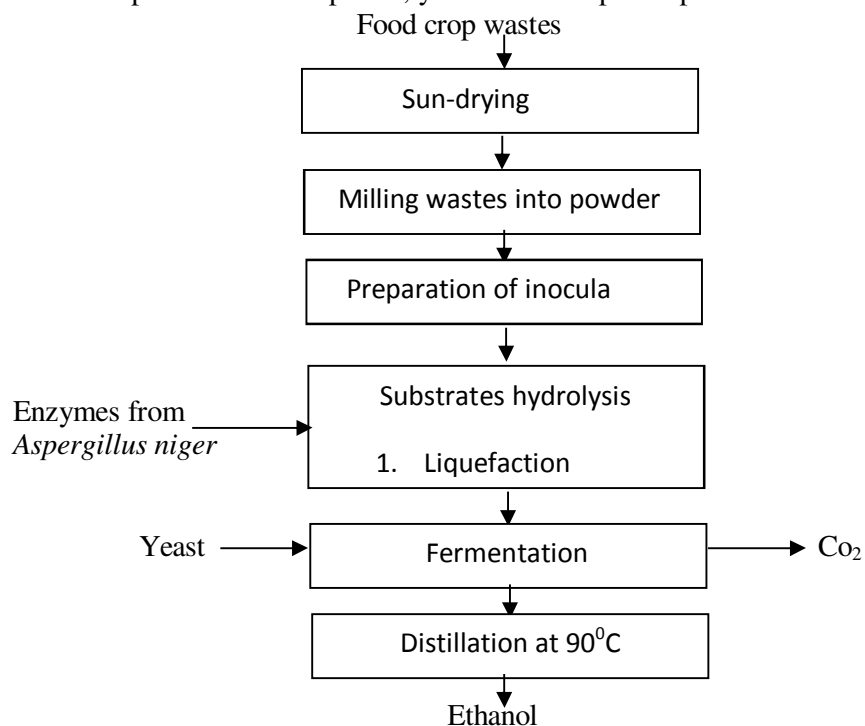The flow chart of Ethanol production from potato, yam and sweet potato peels are shown in Fig. 1

Food crop wastes

```
                    ┌─────────────────────────────┐
                    │        Sun-drying            │
                    └─────────────────────────────┘
                                 │
                    ┌─────────────────────────────┐
                    │  Milling wastes into powder  │
                    └─────────────────────────────┘
                                 │
                    ┌─────────────────────────────┐
                    │   Preparation of inocula     │
                    └─────────────────────────────┘
                                 │
                    ┌─────────────────────────────┐
 Enzymes from       │    Substrates hydrolysis     │
 Aspergillus niger ─►│                             │
                    │    1.   Liquefaction         │
                    └─────────────────────────────┘
                                 │
                    ┌─────────────────────────────┐
 Yeast ────────────►│        Fermentation          │──────► Co₂
                    └─────────────────────────────┘
                                 │
                    ┌─────────────────────────────┐
                    │    Distillation at 90⁰C      │
                    └─────────────────────────────┘
                                 │
                              Ethanol
```

**Fig.1: Bio- ethanol production from food Crop Wastes (Potato, Yam and Sweet potato peels)**

**RESULTS AND DISCUSSION**

The yeast and mould (biomass) yield was obtained by determining the absorbance of the samples at 690nm which represented the cell density (Table 1). The results show that from the first day to the seventh day of fermentation, the yeast and mould biomass yield obtained from sweet potato, yam and potato peels fermentation media increased from 0.37 to 4.65(OD), 0.29 to 3.50 (OD) and 0.15 to 2.38 (OD) respectively. On day seven of the fermentation period, the highest microbial cell dry weight was obtained from sweet potato peel $9.50 mg/cm^3$, followed by yam peel $7.32mg/cm^3$, while potato peel had the least $6.04mg/cm^3$ (Table 2).The ability of the amylase and cellulase secreted by *A. niger* to breakdown the 3 substrates into reducing sugar was determined in the study. The results are presented in Fig. 2 in terms of the amount of reducing sugars (mg/cm3) produced at 24 hours interval for seven days. The results show that in all the substrates the concentration of the reducing decreased gradually as the fermentation period increased. Thus, on day 7 of the fermentation period, the highest reducing

concentration (0.72mg/cm$^3$) was obtained from sweet potato peel. This was closely followed by yam peel (0.59mg/cm$^3$) while potato peel had the least (0.45mg/cm$^3$).

**Table 1: Yeast and Mould Biomass Yield obtained from Potato, Yam and Sweet Potato Peels fermentation Medium for Seven Days**

| Waste Material | Yeast and Mould Biomass (Cell Density at 690nm) for seven days | | | | | | |
|---|---|---|---|---|---|---|---|
| | 1 | 2 | 3 | 4 | 5 | 6 | 7 |
| Potato peel | 0.15 | 0.83 | 0.88 | 1.06 | 1.55 | 2.00 | 2.38 |
| Yam peel | 0.29 | 0.85 | 0.96 | 1.60 | 2.21 | 2.86 | 3.50 |
| Sweet potato peel | 0.37 | 0.93 | 1.43 | 1.98 | 2.75 | 3.34 | 4.65 |

**Table 2: Microbial Cell Dry Weight obtained from Potato, Yam and Sweet Potato Peels Fermentation Medium for Seven Days**

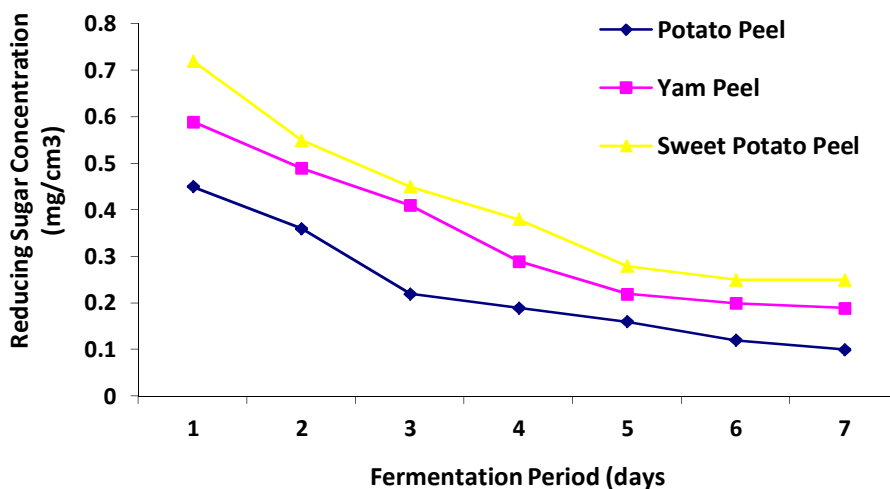| Waste Material | Microbial Cell Dry Weight ( mg/cm3) for seven days | | | | | | |
|---|---|---|---|---|---|---|---|
| | 1 | 2 | 3 | 4 | 5 | 6 | 7 |
| Potato peel | 0.52 | 0.97 | 1.59 | 2.43 | 3.74 | 5.15 | 6.04 |
| Yam peel | 0.75 | 1.10 | 1.96 | 2.85 | 4.50 | 6.28 | 7.32 |
| Sweet potato peel | 1.31 | 2.30 | 3.10 | 4.24 | 5.69 | 7.53 | 9.50 |



**Fig. 2: Reducing Sugar Concentrations obtained from Potato, Yam and Sweet Potato Peels fermentation Medium for Seven Days**

The results of the ethanol yield obtained from the three substrates are shown in Figure 3. During the fermentation period, the ethanol yield of the 3 substrates were found to increase gradually from the

first day to the seventh day with the sweet potato having the highest yield of 10.89% (v/v), followed by yam peel 9.40% (v/v), while the least was obtained from potato peel 6.00% (v/v).
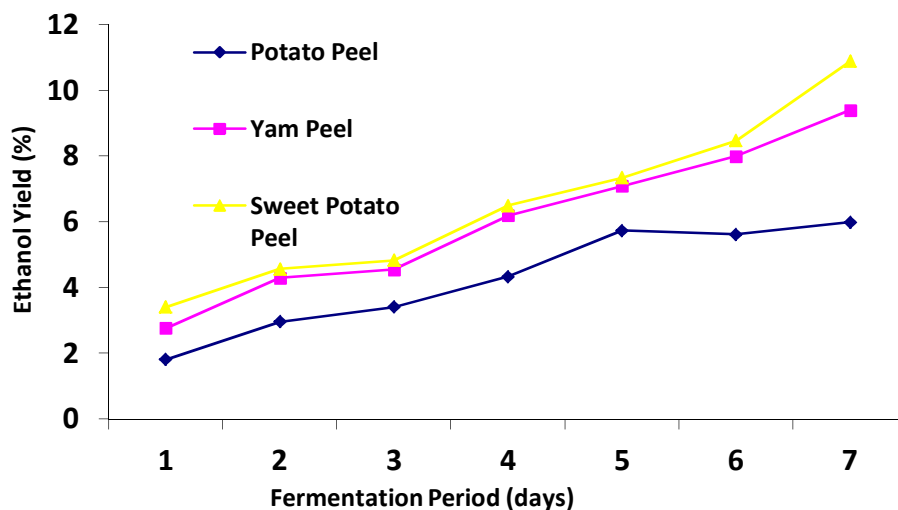


**Fig. 3: Ethanol Yield obtained from Potato, Yam and Sweet Potato Peels fermentation Medium for Seven Days**

Agricultural wastes rich in fermentable sugars have been found to be good substrates for ethanol production, a promising alternative energy source for limited crude oil. Ethanol derived from biomass feed stock which is one of the modern forms of biomass energy has the potential to be a sustainable transportation fuel as well as a fuel oxygenated that can replace gasoline (Puri, 1984; Wang, 2000). The gradual increase in cell densities of the 3 substrates from the day one to the day seven of the fermentation periods suggested that substantially more carbon was utilized for ethanol production instead of cell production and this due to the ability of yeast *S. cerevisiae* to ferment the sugar to ethanol (Table 1). The amount of biomass present in the substrates is directly proportional to quantity of ethanol production. Hence the sweet potato peel which had the highest biomass production had the highest ethanol yield. This suggests that the favourable region for bio-ethanol industrial production should have surplus biomass that would not affect food security.

The susceptibility of sugars obtained after hydrolysis of the substrates by *A. niger* to the fermentation activity of *S. cerevisae* is significantly depended on the composition of sugar (Fig. 1). This is because various mixture of hexoses (e.g. glucose, mannose) and pentoses (e.g. xylose, arabinose) are released from the hydrolysis of lignocellulosic materials (Park and Barrati 1991; Anon, 2006). The fermentation process is significantly dependent on the effectiveness of sugar transporters of *S. cerevisiae* cells on translocating different sugars across the cell membrane (Fig. 2). Sugar transporters are membrane bound proteins that take up sugars from the environment and deliver them to the metabolic pathways insides cells. The result of this study agrees with the report of Abouzied and Reddy (1986) that stated that most substrates are utilized for ethanol production in co-culture fermentation (Fig 3).

**CONCLUSIONS**

Conclusively, the present work has clearly shown that simultaneous saccharification and fermentation of yam, sweet potato and potato peels to ethanol by a mixture of starch digesting fungus *A. niger* and non starch digesting sugar fermenter (*S. cerevisae*) is feasible. Simultaneous saccharification and fermentation has been found to effectively remove glucose, which is an inhibitor to cellulase activity, thus increasing the yield and rate of cellulose hydrolysis. It is interesting to note that even though ethanol

is produce from renewable resource, economic factors such as land availability, labour, taxation, utilities, crop processing costs and transportation are to be put into consideration otherwise there will be no profit for its production.

## ACKNOWLEDGMENTS

## REFERENCES

Abouzeid, M. M., and A. Reddy. 1986. Direct Fermentation of Potato Starch to Ethanol by Co-Culture of *Aspergillus niger* and *Saccharomyces cerevisiae*. *J. of Appl. Microbiol.* 52:1055-1059.

Akin – Osanaiye, B. C., H. C. Nzelibe, and A. S. Agbaji. 2008. Ethanol Production from *Carica* papaya (pawpaw) Fruit Waste. *Asian J. of Biochemistry*. 3 (3):188-193.

Amadi, B. A., E. N. Agomuo, and C. O. Ibegbulan. 2004. *Research Methods in Biochemistry*. Supreme Publishers, Owerri, Nigeria. 93-99.

Anonymous.2006. http:// doegenomestlife. Org.

Ashiru, A. W. 2005. Production of Ethanol from Molasses and Corn Cobs Using Yeast and A Mould. In: The Book of Abstract of the 29th Annual Conference and General Meeting (Abeokuta, 2009) on Microbes As Agents of Sustainable Development Organized by Nigerian Society for Microbiology (NSM) University of Agriculture, Abeokuta, from 6-10th November, 2005. Pp.22.

Jimoh, S.O., S. A. Ado, and J. B. Ameh. 2008. Simultaneous Saccharification and Fermentation of Yam peel to Ethanol by Co-culture of *Aspergillus niger* and *Saccharomyces cerevisae*. *Biol. and J. for the Tropics.*

Joshi, S. S., R. Dhopeshwarker, U. Jadav, R. Jadav, L. D'souza, and D. Jayaprakash. 2001. Continuous Ethanol Production by Fermentation of Waste Banana Peels Using Flocculating Yeast. *Indian J. of Chem.Tech*. 40:325.

Kadar, Z. S., O. S. Szengyel, and K. Reckey. 2004. Simultaneous Saccharification and Fermentation of Industrial Waste for the Production of Ethanol. *J. of Industrial Crops and Products*. 20(1): 103-110.

Kivaisi, A. K., and M. S. T. Rubindamayugi. 1996. The Potential of Agro-industrial Residues for Production of Biogas and Electricity. *Renewable Energy*. (1-4): 917-921.

Okonko, I. O., O. P. Olabode, and O. S. Okeleji. 2006. The Role of Biotechnology in the Socio-Economic Advancement and National Development: A Review. *African J. of Biotechnol.* 5(19): 2354 – 2366.

Omemu, A. M., I. Akpan, M. O. Bankole, and O. D. Teniola. 2005. Hydrolysis of Raw Tuber Starches by Amylase of *Aspergillus niger* AMO7 Isolated from the Soil. *African J. of Biotechnol.* 4:19-25.

Pandey, A., C. R. Soccol, P. Aligam, D. R. Mohan, and S. Roussoss, 2000. Biotechnology Potential of Agro-Industrial Residues, part II. Cassava bagasse. *Biores. Technol.* 78: 81 – 87.

Park, S. C., and J. Barratti, 1991. Kinetics of sugar beet molasses fermentation by *Z. mobilis*. *J. of Biotech. and Bioeng.* 38: 304.

Puri, V. 1984. Effect of Crystallinity and Degree of Polymerization of Cellulose in Enzymatic Saccharification. *Biotechnol. Bioeng*. 26, 1219-1222.

SECO, State Energy Conservation Office (file://A:/Ethanol%20production%20. 2006. Ethanol Production in Texas in 20% Texas.htm). Retrieved 28.03.08

Sun, Y., J. Cheng, 2002. Hydrolysis of Lignocellulosic Material from Ethanol Production: A review. *Biores. Technol*. 83: 1-11.

Wang, M. 2000. Transport fuel–cycle mode. Argonne National Laboratory http://www.aginternetwork. net/-base. (Retrieved 03.11.2008).

# EFFECT OF HEAT-, ALKALI-, AND ULTRASONIC-PRETREATMENT ON ANAEROBIC DIGESTION OF CHICKEN MANURE

Funda Şentürk, Hasret Şahin and *Tuba Hande Erguder* (Middle East Technical University, Ankara, Turkey)
Eray Esendir (Istanbul Technical University, Istanbul, Turkey)

**ABSTRACT:** Two sets of anaerobic batch reactors were conducted to investigate the effect of pretreatment / type and TS contents (1 3, 6 and 8%) on anaerobic digestion of chicken manure. Increasing the TS contents increased the acclimation periods from 4 to 56 days during digestion of untreated manure. Pretreatment of low TS (1 and 3%) manure was found to be unnecessary. Among pretreatment types, alkali-heat and ultrasonic-alkali-heat treatments were found to improve the biogas production rates for TS contents of 8 and 6%, respectively. Despite the longer acclimation periods and slow rates, digestion of untreated manure (6 and 8%) with anaerobic sludge resulted in same and even higher biogas volumes compared to those of treated manures. Addition of anaerobic sludge was also found to significantly increase the degradation efficiency of both treated and untreated manure types.

## INTRODUCTION

Poultry, especially chicken husbandry, is the most developed husbandry in Turkey. The egg and chicken meat production has an increasing trend in Turkey, as it is also the worldwide case. The ninth-5 Year Development Plan Report of State Planning Organization indicates that egg and chicken meat production in Turkey is expected to increase to 823,900 and 1,483,000 tons in 2013, which approximates to 42% and 58% increase since 2004, respectively (SPO, 2007). Such an increase in egg and chicken meat production corresponds to the increased amounts of chicken manure to deal with.

Chicken manure, due to its high organic and nutrient contents, is a renewable source which can be converted to biogas and fertilizer by anaerobic digestion. Yet, the high solids and nitrogen contents of chicken manure and low C/N values might cause toxicity problems. C/N ratio of 30-40 was recommended as the optimum range promoting the proper digestion of chicken manure (Kayhanian, 1999). Free ammonia concentration of 45 mg/L and total ammonium nitrogen of 1500 mg/L at pH 7.2 were reported as inhibitory levels for anaerobic digestion (Kayhanian, 1999). COD/N (as TKN) ratio of 50 resulted in complete cessation of the process (Poggi-Varaldo et al., 1997).

Co-digestion, dilution and pretreatment of chicken manure are the methods used to increase the biogas production and volatile solids reduction (Kayhanian, 1999; Ward et al., 2008). Dilution to 4-6% TS or lower values resulted in optimum methane production (Bujoczek et al., 2000). Pretreatment methods such as thermal (heat), alkaline, acidic, and their combination are studied extensively to improve the hydrolysis of particulate matter, activated sludge as well as manures (Ward et al., 2008). Ultrasonication is also a pretreatment method usually studied for waste activated sludge, where the digestibility can be increased approximately by 40% (Khanal et al., 2007). Yet, to our knowledge, the researches on ultrasonication of manure are limited to the studies of Elbeshbishy et al. (2011) and Castrillon et al. (2011) for cattle and hog manures, respectively. Castrillon et al. (2011) reported 15% more solubilization compared to waste activated sludge and 28% increase in methane production with ultrasonicated hog manure. [185]

In this study, it was aimed to investigate the individual and combined effects of heat-, alkali- and ultrasonic-pretreatment, and initial manure TS content on anaerobic digestion of chicken manure. To our knowledge, this is the first study to investigate the effect of ultrasonic pretreatment on anaerobic digestion of chicken manure.

## MATERIALS AND METHODS

**Chicken Manure and Anaerobic Seed Sludge:** Chicken (broiler) manure was obtained from the chicken farm of Ankara University, Faculty of Agriculture. The broiler manure was thoroughly mixed and analyzed for its nutrient contents (Table 1). The manure was stored at $4^{\circ}C$ until its use in the experiments. Anaerobic seed sludge was obtained from the anaerobic digesters of Ankara Municipality Wastewater Treatment Plant. The total solids (TS) and volatile solids (VS) concentrations of the two-times concentrated seed sludge used in the experiments were $84777 \pm 2053$ and $34443 \pm 1106$ mg/L for Set-1, and, $53400 \pm 339$ and $21030 \pm 127$ mg/L for Set-2, respectively. The volume of the seed sludge used in both sets of experiments was 10 mL for all reactors.

**TABLE 1.** Characteristics of the original chicken manure

| Parameter | Set-1 | Set-2 |
|---|---|---|
| Total Solids (TS, %) | $29.4 \pm 0.6$ | $30.23 \pm 0.2$ |
| Volatile Solids (VS, % of TS) | $75.5 \pm 1.5$ | $70.6 \pm 1.5$ |
| Chemical Oxygen Demand (COD, mg/g of dry matter) | $943 \pm 160$ | $1390 \pm 172$ |
| Total Kjeldahl Nitrogen (TKN, mg N/g dry matter) | $43.9 \pm 12.8$ | $44.5 \pm 12.7$ |
| $NH_3$-N (mg N/g dry matter) | $5.9 \pm 0.4$ | - |

**Experimental Set-ups:** Biochemical Methane Potential (BMP) tests were conducted for two sets of anaerobic batch reactors, Set-1 and Set-2. For both sets, glass amber reactors of 250 mL with an effective volume of 100-110 mL were used. Each set was composed of control reactors (seed sludge+basal medium) and test reactors (manure+basal medium or manure+seed sludge+basal medium). Basal medium of 8-15 mL containing the macro- and micro-nutrients necessary for anaerobic growth was added to all reactors (Erguder et al., 2000). After seeding with the necessary constituents (seed sludge, basal medium, manure), the reactor contents were purged with 25% $CO_2$ and 75% $N_2$ gas mixture for 5 minutes and closed tightly with rubber septa. The reactors were incubated in a temperature-controlled room at $35 \pm 2^{\circ}C$ on a shaker at 175 rpm for several days.

Set-1 was conducted to investigate the effect of initial TS content on anaerobic digestion of chicken manure. Therefore, each test reactor was seeded with manure of different amounts leading to the initial TS contents of 1, 3, 6 and 8%. It was also aimed to obtain preliminary information on the effect of combined pretreatment methods on anaerobic digestion of chicken manure. Thus, for each initial TS %, reactors seeded with different manure types, namely, untreated manure, alkali-heat treated manure and ultrasonic-alkali-heat treated manure were conducted. TS content of 8% was not studied for the ultrasonic-alkali-heat treated manure. All reactor types (controls and tests -with different TS content and manure type-) were run in duplicates and the results were evaluated and demonstrated for average values.

Set-2 was conducted to investigate the effects of individual and combined pretreatment, and the addition of anaerobic seed sludge on anaerobic digestion of chicken manure. All test reactors were seeded with a different manure type such as untreated, heat-treated, alkali-heat treated, ultrasonic-treated, ultrasonic-heat treated or ultrasonic-alkali-heat treated manure. Each test reactor had the same initial TS content of 8%. To examine the effect of seed sludge on anaerobic digestion of treated and untreated chicken manure, seed sludge was not added to the half of the test reactors. All reactors, except the test reactors without seed sludge, were run in duplicates, and the results were demonstrated for average values.

**Pretreatment Methods for Set-1.** The original broiler chicken manure (Table 1) of 250 g was mixed with 2.5 L of distilled water. The manure mixture with new TS content of 2.6% and pH of 6.33 was further subjected to the following pretreatment methods.

   *Alkali-heat treatment.* Ca(OH)$_2$ pellets were added to the homogeneous manure mixture to increase pH to 10.7. The manure mixture was heated via TKN apparatus, which makes the ammonia stripping possible, for 1 hr at boiling temperature. After alkali-heat treatment, the TS content was measured as 10.33%.

   *Ultrasonication-alkali-heat treatment.* Ultrasonication was initially applied for 10 minutes at 42 kHz in an ultrasonic shaker. Alkali-heat treatment was further performed at initial pH of 10.5 at boiling temperature for 1 hr via TKN apparatus. The final TS content was measured as 9.17%.

**Pretreatment Methods for Set-2:** In order to minimize the water amount used for dilution of manure, the chicken manure (Table 1) of 1500 g was mixed with distilled water to a final volume of 4.5 L. The manure mixture with new TS content of 10% and pH of 7.63 was further subjected to the following pretreatment methods.

   *Heat-treatment*: In order to ease and control the heating operation and temperature, a different heat pretreatment method was performed in Set-2, instead of the application of TKN apparatus as in Set-1. Manure mixture was heated in an oven at 105$^o$C for 2 hr. The mixture was periodically mixed. The TS content of the heat-treated manure was 10.02%.

   *Alkali-heat treatment:* Manure mixture, where Ca(OH)$_2$ pellets were added to increase pH to 10.5, was heated in an oven at 105$^o$C for 2 hr. Final TS content after treatment was 12.27%.

   *Treatments involving Ultrasonication*: Ultrasonication treatment involved the application of ultrasonication for 10 minutes at 42 kHz. For ultrasonication-heat treatment, manure mixture was heated at 105$^o$C for 2 hr following the ultrasonication treatment. Ultrasonication-alkali-heat treatment was performed by initially ultrasonication for 10 minutes at 42 kHz, followed by addition of Ca(OH)$_2$ pellets to increase the pH of manure mixture to 10.5 and further heating the mixture in an oven at 105$^o$C for 2 hr. The final TS contents of the treated manures were in the range of 9.8-10.5%.

   The pH values of all the pretreated manures were finally adjusted to 7.0-7.2 by HCl or NaOH before their use as reactor content in Set-1 and Set-2.

**Analytical Methods:** Gas produced in each reactor was daily measured by a water displacement device (Erguder et al., 2000). Gas compositions of the reactors in Set-2 were analyzed by a gas chromatograph as mentioned by Ozkan et al. (2010). COD, TS, VS, TKN and NH$_3$-N analyses were performed according to the standard methods (APHA, AWWA, WEF, 2005). pH was analyzed by a pH-meter (model 2906, Jenway Ltd.) and a pH probe.

**RESULTS AND DISCUSSION**

**Results of Set-1.** The experiments lasted for 110 days. The cumulative gas productions of the reactors with varied initial TS contents are given in Figure 1. Control reactors including only seed culture and basal medium displayed negligible biogas production (30 mL in 110 days). All test reactors, either with treated or untreated manure, started gas production immediately after the start-up, followed by a lag period. This lag phase was attributed to the period required for hydrolysis of particulate solids and acclimation of the microorganism. For untreated manure, the lag phase or acclimation period increased with the increasing TS content, such as between Days 4-8 and Days 6-62 for TS contents of 1 and 8 %, respectively (Figure 1a, 1d). For treated manure types, almost same acclimation periods were observed, which were independent of the TS content and the pretreatment type.

   Figure 1 depicts, for each manure type studied (treated or untreated), that the total gas amounts increased with the increasing TS content. The highest cumulative gas volumes recorded at the end of the experimental period were 2660 mL and 2350 mL for untreated and alkali-heat treated manures of 8% TS, respectively. Yet, the total gas amounts obtained from digestion of both treated and untreated manures were still less than the theoretical biogas volumes. Considering the influent TS amounts and COD equivalences, the expected COD amounts corresponding to 1, 3, 6 and 8% TS are 0.94, 2.83, 5.66 and 7.54 g, respectively. If methane content of biogas is assumed to be 80%, the theoretical biogas

productions corresponding to the 1, 3, 6 and 8% TS are expected to be 466, 1397, 2794 and 3725 mL, respectively. However, the highest total biogas amounts of untreated reactors with 1, 3, 6 and 8% TS contents were 200, 689, 1722 and 2660 mL, respectively. This indicates the inhibition in all reactors even for the best scenario (i.e. 80% methane content). The inhibition might be due to the high initial COD/N ratio (21) and its unbalanced change during digestion, potential high ammonia concentrations as well as high TS manure/ VSS microorganism ratio (from 3 to 24.3 for 1 to 8% TS, respectively).
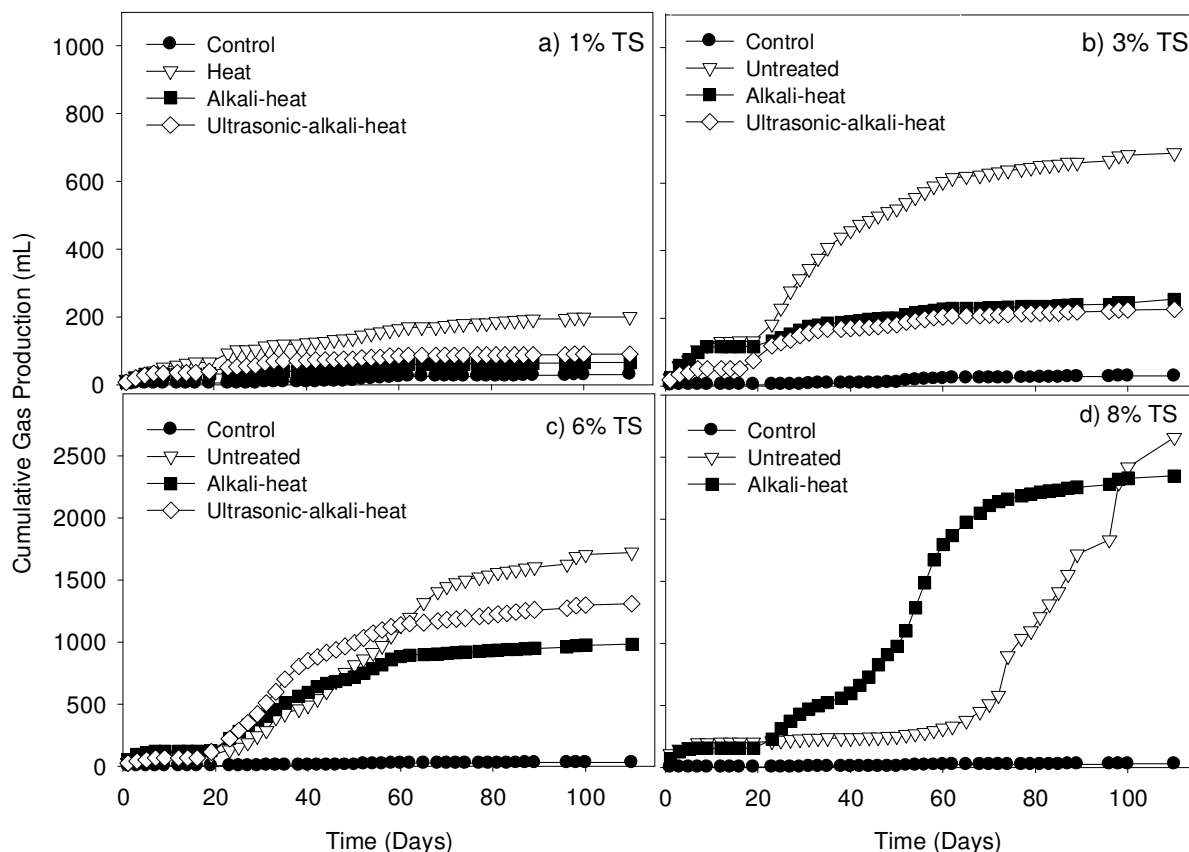


**FIGURE 1**. Cumulative gas production trends of the reactors in Set-1 with initial manure TS contents of a)1%, b) 3%, c) 6% and, d) 8%

Alkali-heat involving pretreatment was applied in this study to early solubilize the manure as much as possible, and strip $NH_3$-N content via volatilization at high temperature and pH. This early release and removal of ammonia, instead of accumulation during digestion process while COD is degraded, was an attempt to balance COD/N ratio and thus prevent the related-inhibition and increase the biogas production to expected levels. Yet, as mentioned before, pretreatment methods did not result in theoretical biogas values. Interestingly, pretreatment of 1 and 3% TS led to lower biogas production than that of the corresponding untreated manure (Figure 1a, 1b). For higher TS contents (6 and 8%), pretreatment increased the gas production rate, leading to higher volumes of gases produced in shorter incubation periods (Figure 1c, 1d). For untreated manure of 6 and 8% TS, despite the lower gas production rates and longer acclimation periods, the biogas production recovered and higher biogas volumes were obtained than those of the corresponding treated manures at the end of 110 days. The cumulative gas volumes obtained from digestion of untreated, alkali-heat treated and ultrasonic-alkali-heat treated manures of 6% TS were 1722, 983 and 1309 mL, respectively. In fact, for all TS contents studied, the highest biogas volumes were obtained from the digestion of untreated manures. This was attributed to the slow solubilization of COD and of organic nitrogen to ammonia in manure and better

acclimation of the microorganisms to the levels without inhibition during digestion. The pretreatment might provide early solubilization and partial removal of ammonia content during stripping. Yet, high amount of soluble COD at the beginning and its early degradation might lead to unbalanced COD/N ratio, and further inhibit and result in early cessation of the gas production as observed in treated manure-reactors. In addition, the pretreatment process, itself, might inhibit the intrinsic microorganisms in the manure. The decrease in the total amount of microorganisms in the reactor content might in turn decrease the tolerance and acclimation capacity to potential high ammonia concentrations and/or low COD/N ratios
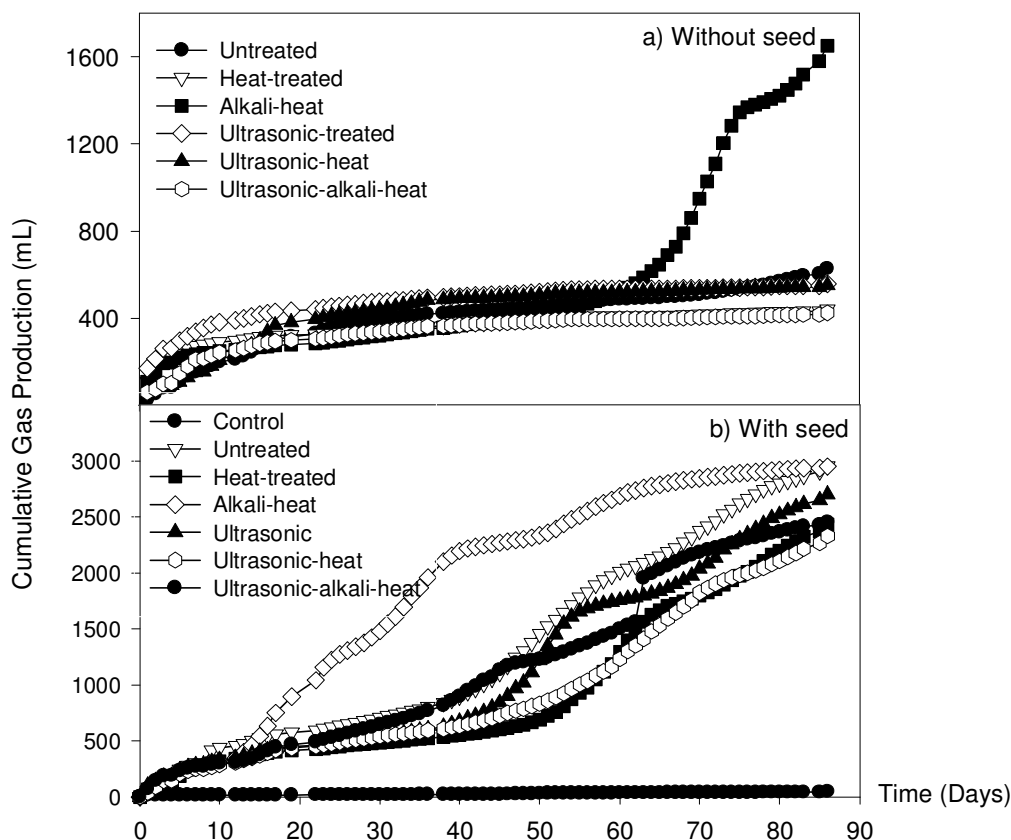


**FIGURE 2**. Cumulative gas production trends of the reactors in Set-2 (8% TS)

Ultrasonic-alkali-heat treatment resulted in slightly higher biogas production compared to alkali-heat treatment for 6% TS (Figure 1c). Yet, for lower TS contents studied, the effect of pretreatment type on biogas production was not significant. The similar acclimation periods independent of the treatment type also indicates the similar effects of both treatment types. In other words, application of ultrasonication in addition to alkali-heat treatment did not change the biogas production efficiency significantly for TS of 1 to 6%.

**Results of Set-2:** The experiments of Set-2 lasted for 86 days. The cumulative gas production of the reactors containing different manure types are given in Figure 2. GC analyses performed on Day 55 indicated that for reactors without seed sludge, $CH_4$ contents of the biogas were 34, 11, 32, 18, 18 and 9% for untreated, heat-treated, alkali-heat treated, ultrasonic-treated, ultrasonic-heat treated and ultrasonic-alkali-heat treated manures, respectively. For reactors seeded with anaerobic sludge, $CH_4$ contents of the biogas were 77, 76, 56, 80, 65 and 46% for untreated, heat-treated, alkali-heat treated, ultrasonic-treated, ultrasonic-heat treated and ultrasonic-alkali-heat treated manures, respectively. Figure 2 and GC analyses indicated that seed sludge addition significantly improves the biogas production and methane content of

the biogas for all manure types. For example, digestion of sole untreated manure produced 627 mL biogas, which increased to 2952 mL when anaerobic sludge was used. Anaerobic sludge addition increased the tolerance and shortened the acclimation periods to high TS contents and initial COD/N of 31 (Table 1) due to respectively lower food to microorganisms ratio (30 g dry TS/ g VSS seed)

Figure 2a revealed that the total biogas amounts produced from digestion of both treated and untreated manure did not differ significantly when seed sludge was not used. The total biogas production of all reactors without seed sludge (except the reactor with alkaline-heat treated manure) almost stopped after Day 30 and remained same till the end of the experiment. Early cessation of the gas productions was attributed to high ammonia levels and/or low COD/N values and further inhibition of the intrinsic methanogens which are probably low in number compared to seed sludge. These observations also indicated that manure pretreatment and the pretreatment type do not improve the biogas production when anaerobic sludge was not used. Digestion of the treated-manures (except alkali-heat treated manure) without seed sludge decreased the methane content from 34% to 9-18%. The reason of the decrease in methane content might be due to the inhibition of the intrinsic methanogens during pretreatment and/or digestion processes resultant of formation of inhibitory conditions. Figure 2a indicates the nearly cessation of the gas production after Day 30 and its further recovery after Day 60 for alkaline-heat treated manure (without seed sludge). Alkaline-heat treatment was found to be the best pretreatment method when manure is to be digested without seed sludge. Alkaline-heat treatment might have improved the stripping of ammonia, and the acclimation of the intrinsic methanogens.

When seed sludge was added (Figure 2b), alkaline-heat treatment resulted in higher biogas production rates and volumes. Yet, considering the $CH_4$ contents, the application of alkaline treatment in addition to heat and ultrasonication-heat treatments was found to decrease the methanogenic activities and in turn the methane percents (from 76-80 to 46-56%). Figure 2b also indicates the long acclimation period for untreated manure. Yet, as observed in Set-1 (Figure 1d), the digestion of untreated manure with seed sludge recovered in time and same amount of biogas as that of alkali-heat treated manure but with a higher $CH_4$ content (77%) was produced at the end of the experiment. Other pretreatment types resulted in more or less similar biogas production rates as that of untreated manure, but usually with lower $CH_4$ contents. Thus, despite the longer acclimation periods, digestion of high TS manure resulted in higher removal efficiencies when pretreatment was not applied.

Heat treatments applied in Set-1 and Set-2 were different. Figures 1d and 2b indicated that digestion of untreated and alkali-heat treated manure of 8% produced more or less same amount of biogas being slightly higher for Set-2. Thus, instead of using TKN apparatus to achieve boiling temperatures and ease stripping, heat treatment at $105^{o}C$ for 2 hr would be sufficient.

**CONCLUSIONS**

The use of anaerobic seed sludge improves the manure digestion efficiency and tolerance to high TS related potential inhibitory conditions. Yet, inhibition of gas production was observed for all TS contents and manure types studied, even if seed sludge was used. This was attributed to the unbalanced COD/N ratio and/or inhibitory levels of ammonia obtained during digestion. Manure pretreatment was not advantageous for low TS contents (1 and 3%). For higher TS of 6 and 8%, pretreatment especially alkali-heat treatment improves the biogas production rate. Yet, digestion of untreated manure resulted in same or even higher biogas volumes despite the low rates and long acclimation periods. Slow hydrolysis of untreated manure during digestion might be advantageous for microorganisms' acclimation. On the other hand, pretreatment improving the hydrolysis and biogas production rate is advantageous when digestion time and reactor volumes are of concern. Yet, unless the COD/N ratio and ammonia contents are controlled during or before digestion, pretreatment does not improve the digestion efficiency.

**REFERENCES**

APHA, AWWA, and WEF, 2005. *Standard Methods for the Examination of Water and Wastewater.* 21st ed., American Public Health Associaton Press, Washington, DC.

Bujoczeck, G., J. Oleszkiewicz, R. Sparling, and S. Cenkowski. 2000. "High solid anaerobic digestion of chicken manure." *J. Agric. Engng. Res*. 76: 51-60.

Castrillon, L., Y. Fernandez-Nava, P. Ormaechea, and E. Maranon. 2011. "Optimization of biogas production from cattle manure by pre-treatment with ultrasound and co-digestion with crude glycerin." *Biores. Technol*. 102:7845-7849.

Elbeshbishy, E., S. Aldin, H. Hafez, G. Nakhla, and M. Ray. 2011. "Impact of ultrasonication of hog manure on anaerobic digestability." *Ultrasonics Sonochemistry*. 18:164-171.

Erguder, T.H., E. Guven, and G. N. Demirer. 2000. "Anaerobic treatment of olive mill wastes in batch reactors." *Proc. Biochem*. 36: 243–248.

Kayhanian, M. 2007. "Ammonia inhibition in high-solids biogasification: an overview and practical solutions." *Environ.Technol*. 20:355-365

Khanal, S. K., D. Grewell, S. Sung, and J. V. Leewen. 2007. "Ultrasound applications in wastewater sludge pretreatment: A Review." *Critical Rev. Environ. Sci. Technol.* 37: 277-313.

Ozkan, L., T. H. Erguder, and G. N. Demirer. 2010. "Investigation of the effect of culture type on biological hydrogen production from sugar industry wastes." *Was. Manage*. 30: 792–798.

Poggi-Varaldo, H. M., R. Rodriguez-Vazquez, G. Fernandez-Villagomez, and F. Esparza-Garcia. 1997. "Inhibition of mesophilic solid-substrate anaerobic digestion by ammonia nitrogen." *Appl. Microbiol. Biotechnol*. 47:284-291.

SPO-State Planning Organization, 2007. *The Ninth-5 Year Development Plan-Special Expertise Area Committee Report on Animal Husbandry (2007-2013)*, Ankara.

Ward, A.J., P. J. Hobbs, P. J. Holliman, and D. L. Jones. 2008. "Optimisation of the anaerobic digestion of agricultural resources." *Biores. Technol*. 99: 7928–7940.

# CARBON FOOTPRINT ANALYSIS FOR ALGAE GROWN IN A PHOTOBIOREACTOR

*Jennifer Matczak,* Stephen Duda, Cody Edley, William Riddell (Rowan University, NJ, USA)
Tobey Kinkaid (AlgaeDyne)

**ABSTRACT:** Energy used to grow algae is a critical input for the overall lifecycle cost of biofuel derived from algae. This paper investigates the energy required to grow algae, and quantifies these values based on kg of $CO_2$ emissions per kg of algae harvested. Four cases are evaluated, covering cases with 2000 liter and 15,600 liter bioreactors; and with and without using waste heat combustion of methane gas resulting from anaerobic digestion to heat the photobioreactor facility. A value of 1.5 kg $CO_2$ per kg of algae grown was reduced to 0.81 kg $CO_2$ per kg of algae grown through the larger scale photobioreactor and utilization of waste heat.

## INTRODUCTION

Interest in the development of biofuels is growing due to the volatile prices and uncertain availability of fossil fuels, as well as environmental concerns. Algae is of particular interest as a potential biofuel for the future, as it produces a higher lipid yield per area than first generation bio crops such as corn, rapeseed, and soy (Schenk, *et al.* 2008). Furthermore, algae can be grown on land that is not suitable for most crops, so algae-derived biofuel will not cause competition with global food production. While promising as a potential source of biofuel, relatively little biofuel is produced from algae today. Additional research is needed in nearly all facets of production to allow for significant implementation of algae as a source of biofuel. In particular, further analysis is needed to determine that the carbon footprint of biofuels produced from algae is sufficiently low to allow for sustainable production.

Two different configurations that have been considered for the industrial-scale growth of algae are raceway ponds and closed photobioreactors (PBR). Previous lifecycle analyses have suggested that raceway ponds will result in significantly lower lifecycle costs for algae-produced biofuels than photobioreactors. However, PBR do have several features that are attractive. The closed systems allow for a particular species of algae to be grown under carefully-controlled conditions, greatly increasing the growth rates (in terms of mass of lipids produced per area per day). Photobioreactors can also produce algae year round in all climates. While lifecycle analyses performed to date have favored open ponds over PBR, the potential for reducing lifecycle costs through increased growth rates through carefully controlled conditions, as well as symbiotic operations with other facilities, such as an anaerobic digester, have not yet been fully accounted for. Therefore, it is conceivable that PBR can be developed that are significantly more efficient than those modeled to date.

This paper will investigate the effect of symbiotic operation with an anaerobic digester and scale of operation on the carbon footprint of algae grown in a PBR. The scope of this analysis will be limited specifically to the growth of algae. The requirements of harvesting and refining, while important, are not considered herein. However, the growth of algae itself is an important input for the total lifecycle cost of producing biofuel from algae. A 2000 liter PBR set in a small facility with efficient energy use is used as a baseline for comparison. Additional considerations include scaled up production in a 15,600 liter reactor, as well as the effect of using waste heat from combusting methane gas from an anaerobic digester to supply heat to the facility. First, assumptions made in the analysis of the baseline model are presented. Next, changes in the model to account for scale and symbiotic operation are presented. Finally, the results of the four scenarios are discussed.

## GROWTH OF ALGAE

The baseline for analyses is modeled after a 2000 liter PBR that is currently operational (Jossi 2012). Performance, operation and energy requirements for the PBR are assumed based on input from Algedyne, LLC. While exact details are considered proprietary, the values used are reasonable for a highly optimized system. The growth of an algae culture is typically modeled as having 5 distinct phases (ANACC 2006). In an initial lag phase very little algae growth occurs as the algae become acclimated to its new environment. The duration of the lag phase depends on the severity of the change in environmental conditions upon the start of developing the culture. Next comes a phase of exponential growth, where the algal concentration is described by equation 1

$$C = C_o e^{kt} \qquad\qquad (1)$$

where $C$ is the concentration at any given time, $C_o$ is the initial concentration, $t$ is the time in days, and $k$ is the growth parameter. Next comes a stationary phase, where the net growth rate of the algae is zero because the birth and death rates of algal cells go into equilibrium. Last is the declining growth phase where algae concentration collapses due to some deficiency in the environment (ANACC 2006).

Typically when algae are grown to produce biomass, it is desirable to keep an algae culture in the exponential growth phase. Under the exponential growth regime, the biomass produced is dependent on initial concentration, and the growth parameter, $k$. The growth parameter will depend on many variables, such as lighting level, water chemistry, temperature, and species. Algae growth can be kept in the exponential growth phase by carefully controlling the conditions, supplying nutrients over time and harvesting algae as mass increases to keep the concentration at a level that allows continued exponential growth.

A schematic growth cycle for algae growth and harvesting in a photobioreactor is summarized in Figure 1. For the system considered herein, an original culture is established at a density of 0.001 g/l. Following a relatively short lag phase, the culture enters the exponential growth phase with k $\approx$ 0.693 day$^{-1}$, which results in a doubling of concentration every day. The exponential growth continues until concentration reaches 4 g/l in 14 days. At this point, a harvesting phase begins, where 50% of the algal mass is harvested each day, which is replaced by growth over the next day. With careful monitoring, this phase can be maintained for approximately 60 days before the culture collapses. The result is an algal mass harvest of 120 g/l during a 74 day cycle, or an average of 1.62 g l$^{-1}$ day$^{-1}$. For the 2000 liter PBR, this results in 3.24 kg l$^{-1}$ day$^{-1}$.
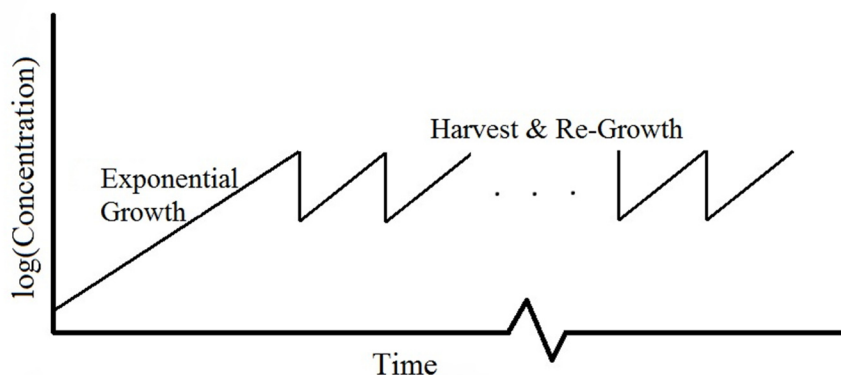


**FIGURE 1. Schematic of growth and harvesting cycle.**

## MODELING CARBON FOOTPRINT

The carbon footprint associated with the growth of algae is dependent on the footprint of the photobioreactor itself, a share of the footprint of the operating facility in which the photobioreactor is housed, and water that must be replaced following harvest of algae.

**Facility Footprint.** For the sake of this paper, the energy use in the facility that houses the PBR, excluding the PBR itself, is assumed to be similar to a highly efficient office (Thurmann, et al., 2009). The low end energy use index (EUI) for an office is 50,000 Btu ft$^{-2}$ yr$^{-1}$, of which approximately 50% is space heating, 25% air conditioning, 20% lighting, and 5% other. Heating is assumed to be by natural gas, with a carbon coefficient of 53 kg $CO_2$/MMBtu (EIA, 2012). All other uses are assumed to be by grid-supplied electricity, with a carbon coefficient of 0.6 kg $CO_2$/kWhr, or 178 kg $CO_2$/MMBtu (EIA 2002). A photobioreactor is assumed to account for 100 ft$^2$ of the facility. Therefore, a single PBRs share of the facility energy use during one 74 day growth cycle is 1.01 MMBtu. The results of these calculations are presented in the analysis and discussion section.

**Photobioreactor Footprint.** Within the photobioreactor, energy is required to supply the needs of the algae, such as light, heat, agitation, and maintaining appropriate water conditions. The model system includes a novel system (Jossi, 2012) for injecting light into the photobioreactor that requires 150 watts of LED lighting for 12 hours a day. This results in a total energy use of 1.8 kW-hours per day. The temperature of the photobioreactor is modeled as being the same as the facility temperature, so no energy use is assumed at this level. The model system will sparge gas into the photobioreactor to maintain appropriate $CO_2$ levels in the culture. A 100 watt pump, running for a total of 12 hours per day is assumed. This results in 1.2 kW-hours per day. The circulation induced by the sparged gas serves as agitation for the algae. Monitoring and control equipment use of 1.44 kW-hours per day is comparable to the CPU for a computer. The total for a 74 day growth cycle is 328.6 kW-hour per cycle, or 1.12 MMBtu per cycle. A $CO_2$ coefficient of 178 kg $CO_2$/MMBtu is used for this electricity. Finally, each harvest is assumed to require 20% of the water in the photobioreactor to be replaced, resulting in a total of 24 m$^3$ of water. For this aspect of operation, the $CO_2$ coefficients for drinking water are taken from the literature (Mo, et al., 2010). Energy required for harvesting is not considered in this analysis. Nutrients such as Nitrogen are assumed to be obtained as waste from agricultural processes, and are neglected in the $CO_2$ footprint calculations. The $CO_2$ that is consumed by the algal mass during photosynthesis is assumed to be taken from the atmosphere, and eventually re-released into the atmosphere upon combustion of the bio-fuel, resulting in zero net impact over time scales of interest. If the $CO_2$ utilized for the algae were produced by combustion (of natural gas, for example) this would need to be accounted for. However, it is not likely that algae would be grown in this manner.

## SYMBIOTIC OPERATION AND SCALE-UP

The baseline model considers a 2000 liter bioreactor. However, full scale production is envisioned as using 15,600 liter PBR operating symbiotically with methane combusted at an on-site anaerobic digester. Methane combustion will power an electric generator, which results in electricity, $CO_2$, and waste heat. The anaerobic digester is also a local source of nutrients for algae. Figure 2 shows a schematic symbiotic system. To account for symbiotic operation with the anaerobic digester, the $CO_2$ coefficient associated with heating the facility is set to zero. As methane has significantly greater impact on climate than $CO_2$, combustion of methane is actually beneficial. Therefore, electricity generated in this manner is considered to be a clean, renewable resource. However, for this study, the carbon coefficient for the national grid is used, as electricity is a fungible resource, and the clean electricity from the facility would otherwise be supplied to the grid. For the larger PBR, the energy for lighting and sparging pumps as well as water use are scaled linearly with volume, while monitoring and control use is kept constant. The larger PBR is assumed to take the same space (100 ft$^2$) in the facility.

## ANALYSIS AND DISCUSSION

The carbon emissions required for the baseline model, without consideration of the use on an anaerobic digester are summarized in Table 1. Similar calculations, but with adjusted values, were performed for each of the other three system considerations. For the systems with an anaerobic digester in place, the carbon coefficient associated with heating the facility was set to zero, assuming that waste heat from the methane combustion is used for heat. For the scale-up to the 15,600 liter tank, the facility values were kept constant, but the water and lighting in the photo-bioreactor were scaled up, the same ratio as the tank volume scale-up. Figure 3 shows the graphical results of Table 1 for each of the four system considerations. The carbon emissions are split into 3 categories: facility, photobioreactor, and water. The $CO_2$ emissions per kg of algae range from 1.5 to 0.8 kg $CO_2$ per kg of algae harvested. As the scale increases, the effect of the facility overhead is decreased.
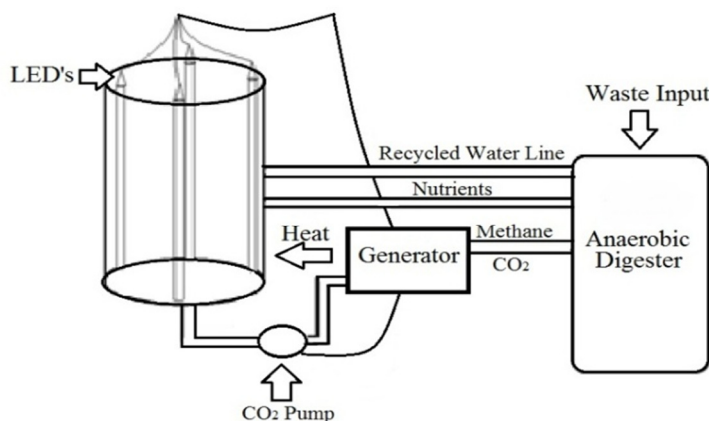


**FIGURE 2. Schematic figure of symbiotic system.**

**TABLE 1. Carbon footprint calculation for baseline scenario.**

| | Amount per growth cycle | Unit | Source | Carbon Emission Coefficient (kg $CO_2$/unit) | Carbon Emissions per growth cycle (kg $CO_2$) |
|---|---|---|---|---|---|
| **Facility** | | | | | |
| Space heating | 0.51 | MMBTU | Gas | 53 | 26.77 |
| Air Conditioning | 025 | MMBTU | Electric | 178 | 44.95 |
| Lighting | 0.20 | MMBTU | Electric | 178 | 35.96 |
| Other | 0.05 | MMBTU | Electric | 178 | 8.99 |
| **Subtotal** | **1.01** | **MMBTU** | | | **116.66** |
| **Photobioreactor** | | | | | |
| Light | 0.45 | MMBTU | Electric | 178 | 80.10 |
| Aeration and agitation | 0.30 | MMBTU | Electric | 178 | 53.40 |
| Monitoring and control | 0.36 | MMBTU | Electric | 178 | 64.08 |
| **Subtotal** | **1.11** | **MMBTU** | | | **197.58** |
| **Water** | **24** | **m$^3$** | | 1.7 | **40.8** |
| **Total** | | | | | **355.04** |
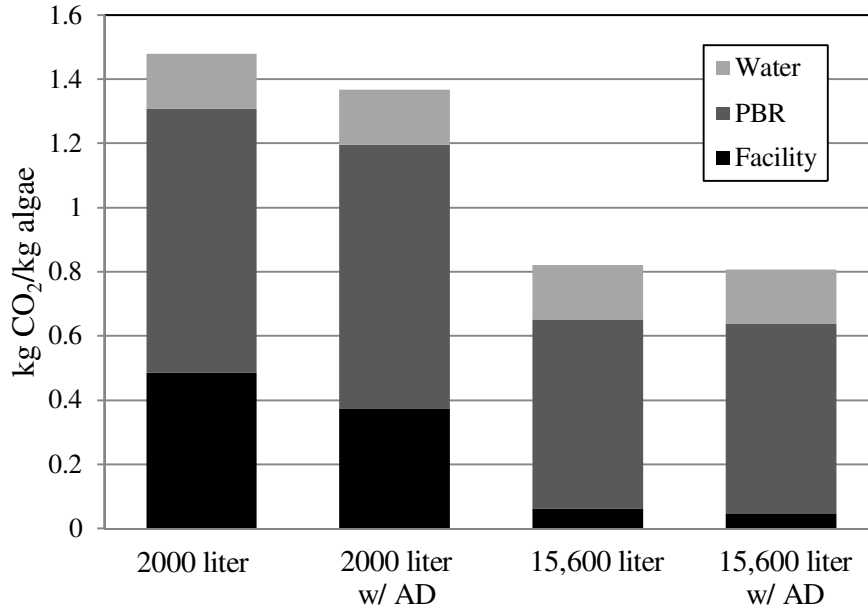
**FIGURE 3. Carbon emmissions resulting from growth
of 1kg algae under various conditions.**
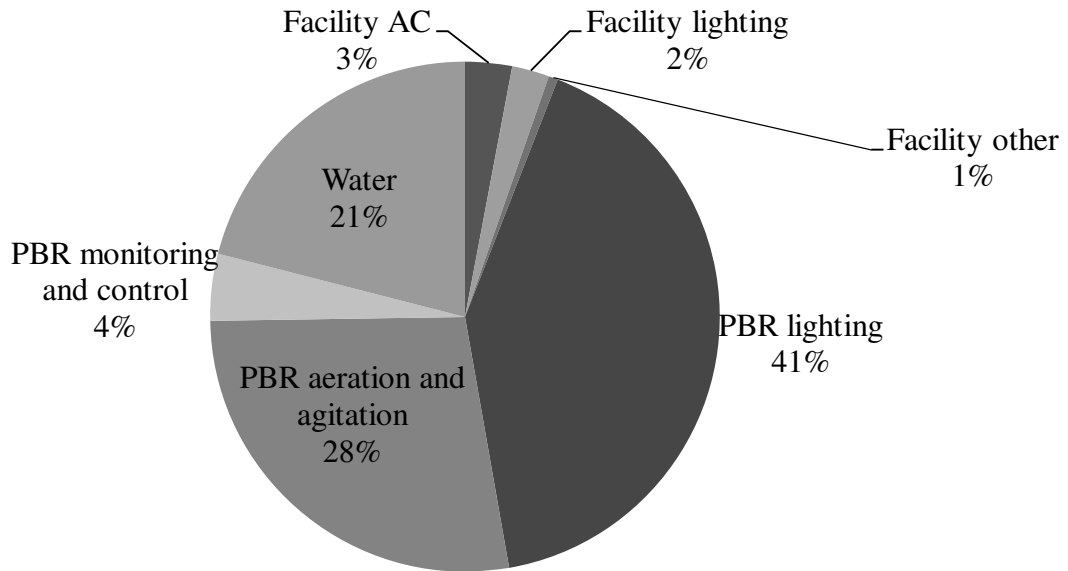


**FIGURE 4. Carbon emmisson distribution for
15,600 liter PBR using waste heat.**

For the best case scenario considered, a 15,600 liter PBR with waste heat from the methane combustion, the results are presented in a more refined manner in Figure 4. Here, contributions to the 0.8 kg $CO_2$ per kg algae are attributed to all of the categories listed in Table 1. Note that heating of the facility is not listed, as this is accomplished via waste heat, and results in zero $CO_2$ emissions. For this

case, the most significant contributions are lighting (41%), agitation and aeration (28%) and water replacement (21%).

## CONCLUSIONS

The energy required to grow algae for use as a biofuel feedstock was modeled, and quantified in terms of kg of $CO_2$ emissions per kg of algae harvested. Four cases were evaluated, covering cases with 2000 liter and 15,600 liter bioreactors; and with and without using waste heat combustion of methane gas resulting from anaerobic digestion to heat the photobioreactor facility. A value of 1.5 kg $CO_2$ per kg of algae grown was reduced to 0.81 kg $CO_2$ per kg of algae grown through the larger scale photobioreactor and utilization of waste heat. As the scale of the photobioreactor increases, the fraction of the total $CO_2$ emissions attributed to the facility overhead decreases. For the best case scenario considered herein, the most significant contributing factors to $CO_2$ emissions were lighting, agitation aeration; and water use in the photobioreactor, accounting for 41%, 28% and 21% of the total emissions, respectively.

## ACKNOWLEDEGEMENTS

## REFERENCES

Australian National Algae Culture Collection (ANACC.) 2006. "Algal Growth Phases Including Determination of the Growth Rate and Population Doubling Time" Dec 7, 2011. <http://www.marine.csiro.au/microalgae/methods/Growth%20rate.html.>

Mo, W., Nasiri, F., Eckelman, M. J., Zhang, Q., Zimmerman, J. B. 2010. Measuring the embodied energy in drinking water supply systems: A case study in the great lakes region, Environ. Sci. Technol. 44: 9516-9521.

Jossi, F., 2012. "Algaedyne plants a future for renewable fuels," Finance and Commerce, April 16, 2012, <http://finance-commerce.com/2012/04/algaedyne-plants-a-future-for-renewable-fuels/>

Schenk, P. M., Thomas-Hall, S. R., Stephens, E., Marx, U. C., Mussgnug, J. H., Posten, C., Kruse, O., Hankamer, B. (2008). "Second Generation Biofuels: High-Efficiency Microalgae for Biodiesel Production." *Bioenergy Resources.* pp. 20-43.

Thumann, A., Younger, W.J., Niehus, T. 2009. *Handbook of Energy Audits, Eighth Edition.* The Fairmont Press, Inc.

Energy Information Administration. 2002. "Updated State and Regional Level Greenhouse gas emission factors for electricity." <http://www.eia.doe.gov/oiaf/1605/e-factor.html>

# COMPLETE UTILIZATION OF SPENT COFFEE TO BIODIESEL, BIO-OIL AND BIOCHAR

*Brajendra K Sharma*[1], Derek Vardon[2], Bryan R. Moser[3], Wei Zheng[1], Katie Witkin[1], Roque Evangelista[3], and Nandakishore Rajagopalan[1]

[1]Illinois Sustainable Technology Center, University of Illinois at Urbana-Champaign, 1 Hazelwood Dr, Champaign, Illinois 61820, USA

[2]Department of Civil and Environmental Engineering, University of Illinois at Urbana-Champaign, Urbana, Illinois 61801, USA

[3]United States Department of Agriculture, Agricultural Research Service, National Center for Agricultural Utilization Research, 1815 N. University St., Peoria, Illinois 61604, USA

Energy production from renewable or waste biomass/material is more attractive alternative compared to conventional feedstocks, such as corn and soybean. The objective of this study is to maximize utilization of any waste organic carbon material to produce renewable energy. This study presents total utilization of a waste material, spent coffee ground, through a two-step process. The waste coffee ground was selected as a waste organic carbon material and then collected from local coffee shops and dried in oven to remove excess moisture.

In the first step, triacylglycerol oil was extracted from spent coffee ground using hexane soxhlet extraction. The extracted oil properties were studied and found suitable for producing biodiesel. This extracted coffee oil was transesterified using conventional alkaline-catalyzed methanolysis to prepare corresponding fatty acid methyl esters (biodiesel). This biodiesel and their 5 and 20% blends in ultra low sulfur diesel were studied for various fuel properties, such as oxidative stability, cold flow properties, kinematic viscosity, iodine value, acid value, free and total glycerol content, energy content and lubricity. While the FAMEs prepared from spent coffee oil are not compliant with biodiesel standards, their 5% blends did meet most of the specifications.

In the second step, the defatted spent coffee ground was converted into bio-oil and biochar using a thermochemical process (slow pyrolysis) at 450°C under nitrogen atmosphere. It was found that spent coffee ground produced more bio-oil and less biochar compared to defatted coffee ground. The bio-oils were analyzed for their physical properties, such as viscosity, density, elemental analysis, heating value, boiling point and molecular weight distribution. The spent coffee bio-oil approached the HHV of Illinois shale oil (41 MJ/kg), which falls within the range for conventional petroleum crudes (41-48 MJ/kg). Structural characterization of bio-oils was carried out using advanced spectroscopic and chromatographic techniques, such as NMR, FTIR, GPC, and GC-MS to provide insight on average structures, carbon and hydrogen distribution, functional groups, and major components present in bio-oils.

The biochars produced from spent and defatted coffee ground have potential to be used as fuel and also as soil amendment material. These biochars were characterized for their BET surface area, energy content, acid value, ultimate and proximate analysis. To demonstrate their soil amendment properties, these biochars were used in green house experiment to show how it can help to reduce the amount of chemical fertilizer. The implications of reduction of chemical fertilizers in field are improvements in the quality of agricultural runoff water, which will decrease nitrogen and phosphorus in streams and rivers and finally help to prevent gulf hypoxia. This will also reduce the energy input required to produce fertilizers.

# RENEWABLE BIO CRUDE OILS FROM THERMO-CHEMICAL CONVERSION OF WASTE LIPIDS

*Brajendra K Sharma*,1 Derek Vardon,2 and Nandakishore Rajagopalan1
1*Illinois Sustainable Technology Center, UIUC, 1 Hazelwood Dr, Champaign, Illinois*
2*Department of Civil and Environmental Engineering, University of Illinois at Urbana-Champaign, Urbana, Illinois 61801*

Two different thermo-chemical conversion processes were used to convert waste lipid, soapstock, into bio-oils with an objective to compare the process using dry feedstocks and another one using high moisture feedstock. In the first one, soapstock was dried and then converted into pyrolysis bio-oils through pyrolysis process at 450°C under nitrogen atmosphere. In the other one, soapstock was further diluted to prepare high moisture soapstock (20 % solids), which was then converted through hydrothermal liquefaction (HTL) to produce HTL bio-oil at 300°C. These bio-oils were analyzed for their physical properties, such as viscosity, density, elemental analysis, and heating value. Boiling point distribution was obtained using a high temperature GC simulated distillation method modeled after ASTM-7169-05 method, while molecular weight distribution was obtained using size exclusion chromatography. Structural characterization was carried out using advanced spectroscopic and chromatographic techniques, such as NMR for carbon and hydrogen distribution, FTIR for functional groups, TLC-FID for hydrocarbon class type distribution, and GC-MS to provide insight on major components present in it. The results were used to explain the influence of each process on bio-oil yield, composition and structures present in it. HTL process produced more bio crude oil compared to pyrolysis process. The higher heating values of bio crude oil produced using both processes are similar to that of the HHV of Illinois shale oil (41 MJ/kg), which falls within the range for conventional petroleum crudes (41-48 MJ/kg). Similar to FTIR, 1H-NMR spectra showed a high percentage of aliphatic functional groups (0.5-1.5 ppm) for pyrolysis bio crude oil (70%) compared to HTL bio crude oil (64%). The pyrolysis process has potential to produce 21% of low boiling distillates (boiling below 300°C, heavy naptha and kerosene) and 65% in the range of 300-500°C (mostly diesel and vacuum gas oil), while HTL is excellent for producing mostly diesel and vacuum gas oil range products (91%).

# AVAILABILITY AND PRODUCTION COSTS OF PINE-BASED BIOMASS AS A FEEDSTOCK FOR BIOETHANOL PRODUCTION

***Gustavo Perez-Verdin*** (Instituto Politecnico Nacional, Durango, Mexico)
Donald L. Grebner (Mississippi State University, Mississippi State, MS, USA)
Jose Navar-Chaidez (Instituto Politecnico Nacional, Durango, Mexico)

Forest biomass is a viable alternative to produce ethanol because is abundant, clean, renewable, and help mitigate greenhouse gas emissions. In this study, a methodology to estimate availability and production costs of pine-based biomass in the state of Durango, Mexico is presented. Forest periodic inventory and sawmill information were used to estimate forest residues and mill residues, respectively. Since a market for bioethanol from forest biomass is still not well defined, Monte Carlo simulations were conducted to estimate procurement, transportation, and stumpage costs. Results show that about 322,000 tons can be used to produce up to 38 million of liters of bioethanol per year. Of that amount, 66% is forest residues and the rest mill residues. Monte Carlo simulations indicated that the average cost of forest residues is $321 per ton ($2.67 $lt^{-1}$ bioethanol) while the cost for mill residues is $306 per ton ($2.55 $lt^{-1}$ bioethanol). The more important factors in the sensitivity analysis were stumpage costs, technological efficiency, and transportation. The study concluded that in the short term bioethanol development have to compete with industries that use similar raw material such as pulp, paper and wood-based panels. Alternatively, it is recommended the development of integrated biorefineries.

# PROMOTING JATROPHA PLANTATION: OPPORTUNITIES FOR BIOFUEL, FOR SOIL CONSERVATION AND WATER MANAGEMENT

*Tessema Bekele* (Emmanuel Development Association, Subcity Yeka, *CMC Road*, *Gurd Shola, Addis Ababa*, P.O.B. 908, *Ethiopia)*

*Jatropha* is a valuable multi-purpose plant which can contribute to alleviate soil degradation, desertification and deforestation, and be used for bio-energy replacing petro-diesel, for soap production. It can increase rural incomes, self-sustainability and alleviate poverty. *Jatropha* is a perennial plant which recently received much attention. Demand for vegetable oils as a source of biodiesel has increased recently due to a number of factors, including increased prices of petroleum, the desire to reduce CO2 emissions, and fuel security.

*Jatropha* will be one of the vast sources of biofuel and a key in reducing our dependence on fossil fuel and to bring significant environmental benefits. It can replace jet fuel and diesel without interfering with food crops and deforestation as a source of fuel. It is a plant that lives for a long time producing oil seeds, while it also absorbs lots of carbon dioxide from the atmosphere. Local production of bio fuel energy is projected to have a broad range of positive economic, social and environmental implications. Promoting *Jatropha* is significant since it upgrades eroded and deforested land, creates employment opportunity in rural farming and bio fuel production.

The other major benefit of promoting annual crops such as *Jatropha* and other oilseeds are their ability to store more carbon, maintain soil quality, and manage water and nutrients more conservatively since they have deeper root systems. *Jatropha* can be planted on marginal soils and recover the fertility of the soil.

Crop yields in sub-Saharan Africa are projected to fall by 20 percent under global warming. As yields fall and demand rises, Africa will become more dependent on expensive food imports. Already the poor in sub-Saharan Africa spend 60 to 80 percent of their total income on food. Famine due to climate change may displace more than 250 million people worldwide by 2050 (http://www.jatrophaworld.org/).

*Jatropha'*s benefits to developing countries like Ethiopia includes: - degraded lands recovery and aforestation; provide huge opportunities from new sustainable and renewable land resources; creating employment opportunities for its plantation and collection and oil extraction.

Ethiopia on average imports about 1 billion liters petrol diesel annually spending 86 % of its foreign earning per annum. (Ministry of Mining and Energy). Had 1.25 million farmers were engaged in Jatopha and other vegetable oilseeds for biodiesel production program the import of 1 billion liters petrol diesel would have been substituted with biodiesel.

With this perception, Emmanuel Development Association has been engaged in promoting sustainable farming for biodiesel production since 2010 in Kewot District in Northern Ethiopia. Thirty Six percent of Kewot District is ragged, hilly and mountainous, soil erosion caused by water runoff and land slide is very acute. Furthermore, the ever escalating price of fossil fuel has affected negatively the farmers' livelihood. The district has 17,916 hectare of marginalized land appropriate for *Jatropha* or for other bio fuel plants.

The pilot project and field experiences in Kewot District by Emmanuel Development Association objective is to contribute the national effort in ensuring environmental sustainability and bio fuel production program by empowering 2,000 rural women, girls and youth empowerment by the year 2015.

# PERFORMANCE AND MICROBIAL PROFILES OF 2-PAHSE ANAEROBIC DIGESTION OF FOOD WASTE LEACHATE

*Huang W H*[1,2], Wang Z Y[1,2], Zhou Y[1] and Ng W J[1,]\* (1, Nanyang Environment & Water Research Institute; 2, School of Civil & Environmental Engeering. Nanyang Technological University, Singapore)

A lab-scale two-phase anaerobic sequencing batch reactor system treating food waste leachate was investigated to enhance its biogas production. The initial seed sludge used was the same for the acidogenic and methanogenic reactors with phase separation occurring subsequently. In the acidogenic phase, a 210±30% increase in total VFAs (2-6 carbons) was achieved with pH controlled at 5.5, HRT of 2.5 d, and SRT of 25 d. In the methanogenic phase, 96±2% of the total VFAs was consumed with pH controlled at 7.5, HRT of 5 d, and SRT of 50 d. COD removal rate was 91±3%, and biogas production was about 0.6 L/g COD with CH4 content of 76±2%. qPCR was used to analyze the microbial communities in the acidogenic and methanogenic sludge. Results showed observable shifts in the microbial composition of the two sludges. In the acidogenesis phase, bacteria were more than 99% while in methanogenesis it was more than 90%. For the Archaea, hydrogen-utilizing methanogens were predominant in the acidogenic (97±3%) and methanogenic (90±4%) phase. About 10±6% of acetate-utilizing methanogen was detected in the methanogenic phase but these were not detected in the acidogenic phase.

# BUTANOL AND ABE SOLUTION AS THE ALTERNATIVE FUELS IN THE DIESEL ENGINE

*Yu-Cheng Chang* and Wen-Jhy Lee (National Cheng Kung University, Tainan, Taiwan)
Sheng-Lun Lin and Lin-Chi Wang (Cheng Shiu University, Kaohsiung, Taiwan)

Acetone-Butanol-Ethanol (ABE) solution (mean volume ratio of 4.0 : 15 : 1.0) is one of the major products from the hydrolysis and ABE fermentation processes of biomass. In this study, the engine performance and emissions of PM, NOx, and PAHs from a diesel engine generator were monitored and compared by using several diesel blends, D100 (100% regular diesel), B20 (80% regular diesel and 20% butanol), B20W0.5 (B20 and 0.5% water), ABE20 (80% regular diesel, and 20% ABE solution), and ABE20W0.5 (ABE20 and 0.5% water). At 3.2 kW power of diesel generator, the indicated specific fuel consumption (ISFC) were 493, 515, 502, 515 and 505 mL $kW^{-1}hr^{-1}$ by using D100, B20, B20W0.5, ABE20 and ABE20W0.5, respectively. The above results revealed that without water and by adding 20% butanol or ABE solution in the regular diesel did increase the ISFC by approximately 4.4% in the comparison with regular diesel; however, those of adding 0.5% water and 20% butanol or 20% ABE solution, the ISFC only increased by 2.1%. Due that the ABE solution is much cheaper than that of pure butanol, the ABE20W0.5 is suggested as the best fuel blend. As to the pollution emission, by using the ABE20W0.5 did reduce the PM, NOx and total PAHs by approximately 37.7%, 1.8% and 28.2%, respectively. By adding 0.5% water in the diesel fuel, not only decrease the ISFC, but also reduce the PM, NOx and PAH emission. ABE solution in certain fraction and small amount of water adding in diesel is a more green alternative fuel and has a highly potential for practical application.

# ENERGY DENSIFIED SOLID FUEL PRODUCTION: AN ALTERNATIVE APPROACH FOR BIOMASS UTILIZATION

*Ganesh K. Parshetti*, Akshay Jain, Rajasekhar Balasubramaniam and M. P. Srinivasan
(National University of Singapore, Singapore)

Depletion of fossil fuels and environmental concerns are prompting a search for alternative and renewable energy resources. Among various options, bioenergy derived from waste biomass has received increased attention in recent years.   The conversion of waste biomass to biofuels can be achieved using several technologies such as pyrolysis, gasification, fermentation and hydrothermal carbonization (HTC). Hydrogen, ethanol, organic acids, biofuels, and biochar are the key products obtained from the transformation of waste biomass using HTC. The advantages of HTC over other technologies are its ability to solubilize recalcitrant woody biomass under sub- and super-critical conditions with water (hydrothermal medium) such that high energy density solid fuels, liquid fuels and novel functional materials can be prepared for a variety of applications.

In this work, HTC of fruit shell of palm oil, a major energy crop in South-East Asia, was studied to produce densified biochar in a batch reactor at different temperatures (150, 250 and 350 $^{o}$C) with a residence time of 10 min. Proximate and ultimate analyses indicated a highly condensed nature of the biochar after the HTC treatment of the waste biomass. The biochars were characterized to identify their molecular structure by means of field emission scanning electron microscopy-energy dispersive spectroscopy (FESEM-EDS), Fourier transform infrared spectroscopy (FTIR), X-ray diffraction (XRD) and Brunauer–Emmett–Teller (BET) analysis.  The difference in the morphological features of the biochars obtained at different temperatures was examined by FESEM. Biochar products have a high degree of aromatization, and contain a large amount of oxygen-containing groups (i.e. carbonyl, carboxylic, hydroxyl, etc) as was revealed by FTIR.  Also, the micro-crystalline structure of cellulosic components present in fruit shell disappeared after the HTC treatment, and the biochar contained mainly amorphous fractions as confirmed by the XRD spectra.  BET analysis showed an increase in surface area and pore volume with an increase in the temperature of the HTC process. Overall, the results of this study indicated that the operating temperature of the HTC process plays an important role in the conversion of the waste biomass to biochar with a high energy density. Conventional thermal gravimetric analysis (TGA) parameters, activation energy and ignition index of different biochar and coal blends were also estimated. This preliminary work suggests that the HTC process has potential for the conversion of waste biomass to highly densified solid fuels and carbonaceous functional materials for use in a variety of applications.

# ENHANCEMENT OF LIPID ACCUMULATION IN *DUNALIELLA SALINA* IN RESPONSE TO CO$_2$ AERATION FOR BIODIESEL PRODUCTION

[1]Hanaa H. Abd El Baky, [2]Gamal S. El-Baroty and Abderrahim Bouaid[3]

[1]Plant Biochemistry Department, National Research Centre, Dokki, Cairo, Egypt

2 Biochemistry Department of, Faculty of Agriculture, Cairo University, Cairo, Egypt

[3]Chemical Engineering Department, Faculty of Science, Complutense University, Madrid, Spain

Microalgae can be used to convert CO$_2$ (through photosynthesis process) into potential biofuel biomass as well as food and high value fine chemicals. In this work, the effect of various levels of CO$_2$ (0.01, 0.03, 3, 9 and 12 %) aeration on the biomass production, lipid accumulation and its fatty acid profile as well as biodiesel properties of marine microalgae *Dunaliella salina* were investigated. The results show that the maximal biomass and lipid productivity (in parenthesis) in cultures aerated with different levels of 0.01, 0.03, 3.0, 9.9 and 12% CO$_2$ were 255 (5.36), 412 (15.10), 781 (25.32), 1451 (41.96) and 951 mg/L (59.23 mg L$^{-1}$d$^{-1}$), respectively, whereas, the lipid accumulation in the cells were 2.33, 5.62, 10.28, 28.36 and 40.65%, respectively. Moreover, the levels of CO$_2$ in culture medium had significant effect on fatty acid composition of *D. salina*. Linolenic and palmitic acids were identified as the major fatty acid in *D. salina* cells grown at different levels of CO$_2$. The quality of biodiesel produced from algal lipid by a transesterification reaction was located between the limit imposed by the European Standards (EU 14214) and ASTM (US D6751). Based on the results obtained, *D. salina* could be used for mass-cultured in outdoor ponds, as promising alternative to current CO$_2$ mitigation strategies and as a suitable feedstock for biodiesel production.

# CRUDE AND BIO-OILS PRODUCTION FROM APPLICATION OF LIQUEFACTION WITH PLANT RESIDUES

*JoungDu Shin*, Seung Gil Hong, Woo Kyun Park and Hyun Seon Shin (National Academy of Agricultural Science, Rural Development Administration, Suwon, Republic of Korea)

Agricultural biomass is a renewable energy source and provides the green and clean fuel energy. The plant residues contains 40~50% of cellulose, 25~35% of hemi-cellulose and 15~20% of lignin. Yields of rice straw and rice hull are 6.57 and 1.14 million tons per year, respectively in Korea. Objectives of this study were to estimate the calorific values of different crude oils based on feeding stocks and reaction temperatures, to evaluate the yield of liquefaction production with different crop residues, reaction temperature and solvents, and to investigate their chemical compositions.

The liquefaction of rice hull and rapeseed straw as an agricultural residue has been conducted with n-butanol of solvent at reaction temperatures ranging from 220℃ to 320℃ for the clean and green fuel production. As a result, it was found that biomass conversion rates were increased with increasing the reaction temperatures, especially for higher at 4.4% with rapeseed straw as compared to the rice hull at 320℃ of reaction temperature. Also it was considered that majority of extracted conversion products was 99% of bio-butanol. However, in case of using methanol as solvent, it was observed that its conversion rate was only 39.6% at 260℃ for 30 min. Furthermore, calorific values of bio-butanol produced from rice hull's conversion were ranged from 8,283 to 8,356 kcal $kg^{-1}$, especially for higher at 70 kcal $kg^{-1}$ in bio-butanol as relative to the solvent as n-butanol.

In GC analysis of soluble portions, it was observed that their retention times were different with fraction portions. The organic compounds in the crude oil were categorized 60 species into 8 classes of compounds such as acids, alcohols, aliphatic hydrocarbons, ethers, esters, ketones, phenol and aromatics and the other, especially for predominant at 32.0 and 19.2% of esters and ethers, respectively, in the crude oil compositions from rice hull's liquefaction. For analysis of bio-oil, the main chemical components were $C_5H_{12}O$, $C_7H_{14}O_2$, $C_8H_{16}O_2$ and $C_{12}H_{26}O_2$. Therefore, possibility of producing the clean and green fuel energy with plant biomass liquefaction was needed to investigate the upgraded oil through carbon cracking with catalysts.

# PRODUCTION OF FUEL PELLETS FROM CARBONIZED BIOMASS AND LIGNITE

*Serdar Yaman*, Hanzade Haykiri-Acma, Fulya Ulu
(Istanbul Technical University, Istanbul, Turkey)

Lignite is the most important national primary energy source in Turkey. Accordingly, a considerable amount of energy is produced in lignite-fired power plants that 8 % of world's lignite consumption is carried out in this country. However, Turkish lignites are very low quality coals with high sulfur and ash contents in addition to their very low calorific values. Also, dust forming characteristics of these lignites worsens their impacts on environment as well as economical losses.

Environmental problems due to firing of coal can be very serious around these power plants. Because of using pulverized-firing systems that are rather old technology, controlling the emissions of particulates, fly ash, SOx, NOx, VOC, PCDD, PCDF, PAH etc. from thermal plants is quite difficult. Also, high moisture content in these lignites is another factor enhancing the formation of some emissions. On the other hand, high temperatures which are typical in pulverized-firing combustors melts the inorganics, and further deposit problems such as slagging, fouling, and clinker formation that lead reduction in heat transfer and overall efficiency of the plant take place. Furthermore, disposal of ash which is as much as millions of tones is another negative perspective of this issue.

In contrast to the nature of fossil fuels, biomass is renewable, sustainable, and carbon dioxide-free energy resource. Some biomass species especially woody ones usually have even higher calorific value than high-ash lignites. Also, their sulfur content is generally negligible in comparison to coal. For an instance, sunflower seed shells offer good opportunity from these points of view, since its calorific value is 17.4 MJ/kg which is higher than that of the Turkish lignites in general. Besides, it has an ash content of 1.7 wt % on original basis, while its carbon and sulfur contents are 47.1 and 0.15 wt % on dry-ash-free basis, respectively. In fact, Turkey is among top-10 sunflower producing countries and very big amounts of sunflower seed shells are produced every year which present high potential of energy. On the other hand, high contents of moisture and volatiles, and low density are regarded the most important concerns to use such biomass species during co-combustion applications.

From these points of view, this paper focuses on production of environmentally-friend fuel by blending of a renewable energy source (biomass) with lignite. For this purpose, it is targeted to produce biomass-added lignite pellets using sunflower seed shell and a Turkish lignite from Soma-Denis region. This lignite is typical Turkish lignite which has 38.3 wt % of ash, 2.5 wt % of sulfur, and 12.5 MJ/kg of calorific value. Firstly, sunflower seed shells were carbonized in a tube furnace under nitrogen atmosphere at 600°C. This thermal treatment provided further improvement in the properties of biomass that its calorific value increased to 29.4 MJ/kg, also its moisture content and some of the volatiles could be eliminated. It is clear that the addition of this carbonized biomass into lignite provides increase in fixed carbon content as well as calorific value of lignite. In this context, lignite was blended with this carbonized biomass in different ratios that the ratio of biomass changed between 10-30 wt %. Then, the blends were subjected to pressures of 70-318 MPa in steel molds to produce fuel pellets with diameters of 2 or 3 cm. Falling stability and compressive strength tests of the produced pellets were performed to check their mechanical strength. Moreover, molasses was also used as a binding agent, and its effects on

pellets' strength were also interpreted. Combustion tests of the pellets were investigated by Thermogravimetric Analysis (TGA) and Differential Scanning Calorimetry (DSC) techniques.

It can be concluded that coal dusts that lead serious contaminations in surface- and underground-water reserves could be evaluated in this alternative way. The results of this study showed that carbonized biomass has superior properties than the parent biomass material, and blending of lignite dusts with carbonized biomass improves not only the combustion performance but also it reduces $CO_2$ emissions as well as $SO_2$. In addition, the compositions of the ashes from biomass and lignite show some differences and the presence of biomass also affects the ash composition.

# International Conference
# on
# Environmental Science and Technology

All information about the International Conference on Environmental Science and Technology can be found at http//:www.aasci.org/conference/env/index.html